

TREATISE ON INVERTEBRATE PALEONTOLOGY

Part H

BRACHIOPODA

Revised

Volume 1: Introduction

ALWYN WILLIAMS, C. H. C. BRUNTON, and S. J. CARLSON with
FERNANDO ALVAREZ, A. D. ANSELL, P. G. BAKER, M. G. BASSETT, R. B. BLODGETT,
A. J. BOUCOT, J. L. CARTER, L. R. M. COCKS, B. L. COHEN, PAUL COPPER, G. B. CURRY,
MAGGIE CUSACK, A. S. DAGYS, C. C. EMIG, A. B. GAWTHROP, REMY GOURVENNEC,
R. E. GRANT, D. A. T. HARPER, L. E. HOLMER, HOU HONG-FEI, M. A. JAMES, JIN YU-GAN,
J. G. JOHNSON, J. R. LAURIE, STANISLAV LAZAREV, D. E. LEE, SARAH MACKAY,
D. I. MACKINNON, M. O. MANCEÑIDO, MICHAL MERGL, E. F. OWEN, L. S. PECK,
L. E. POPOV, P. R. RACHEBOEUF, M. C. RHODES, J. R. RICHARDSON, RONG JIA-YU,
MADIS RUBEL, N. M. SAVAGE, T. N. SMIRNOVA, SUN DONG-LI, DEREK WALTON,
BRUCE WARDLAW, and A. D. WRIGHT

*Prepared under Sponsorship of
The Geological Society of America, Inc.*

*The Paleontological Society
The Palaeontographical Society*

*SEPM (Society for Sedimentary Geology)
The Palaeontological Association*

RAYMOND C. MOORE
Founder

ROGER L. KAESLER
Editor

JILL HARDESTY, KAREN RENTERIA
ELIZABETH BROSIUS, JACK KEIM, JANE KERNS
Assistant Editors and Editorial Staff

THE GEOLOGICAL SOCIETY OF AMERICA, INC.
and
THE UNIVERSITY OF KANSAS
BOULDER, COLORADO, and LAWRENCE, KANSAS

1997

© 1997 BY THE UNIVERSITY OF KANSAS
AND
THE GEOLOGICAL SOCIETY OF AMERICA, INC.

ALL RIGHTS RESERVED

Library of Congress Catalogue Card Number 53-12913
ISBN 0-8137-3108-9

Distributed by the Geological Society of America, Inc., P.O. Box 9140, Boulder, Colorado 80301, from which current price lists of parts in print may be obtained and to which all orders and related correspondence should be directed. Editorial office of the *Treatise*: Paleontological Institute, 121 Lindley Hall, the University of Kansas, Lawrence, Kansas 66045.

The *Treatise on Invertebrate Paleontology* has been made possible by (1) funding principally from the National Science Foundation of the United States in its early stages, from the Geological Society of America through the bequest of Richard Alexander Fullerton Penrose, Jr., and from The Kansas University Endowment Association through the bequest of Raymond C. and Lillian B. Moore; (2) contribution of the knowledge and labor of specialists throughout the world, working in cooperation under sponsorship of the Geological Society of America, the Paleontological Society, the SEPM (Society for Sedimentary Geology), the Palaeontographical Society, and the Palaeontological Association; (3) acceptance by The University of Kansas of publication without any financial gain to the University; and (4) generous contributions by our individual and corporate sponsors.

PART H, Revised
BRACHIOPODA

VOLUME 1

ALWYN WILLIAMS, M. A. JAMES, C. C. EMIG, SARAH MACKAY, M. C. RHODES, B. L. COHEN, A. B. GAWTHROP, L. S. PECK, G. B. CURRY, A. D. ANSELL, MAGGIE CUSACK, DEREK WALTON, C. H. C. BRUNTON, D. I. MACKINNON, and J. R. RICHARDSON

CONTENTS

INFORMATION ON TREATISE VOLUMES	vi
EDITORIAL PREFACE	vii
STRATIGRAPHIC DIVISIONS	xx
COORDINATING AUTHOR'S PREFACE (Alwyn Williams)	1
ANATOMY (Alwyn Williams, M. A. James, C. C. Emig, Sarah Mackay, and M. C. Rhodes)	7
General Characters	7
Mantles and Body Walls	9
Pedicle	60
Coelomic and Circulatory System	69
Muscular System	75
Digestive System	84
Excretory System	95
The Lophophore	98
Nervous and Sensory System	120
Reproduction	125
Embryology and Development	151
THE BRACHIOPOD GENOME (B. L. Cohen and A. B. Gawthrop)	189
Structure, Composition, and Organization of the Nuclear and Mitochondrial Genomes	189
Toward a Genealogical Classification of the Brachiopoda	191
Implications of the SSU rRNA Gene Comparison Results for Brachiopod Systematics	208
Future Prospects	209
Acknowledgments	210
PHYSIOLOGY (L. S. Peck, M. C. Rhodes, G. B. Curry, and A. D. Ansell)	213
Introduction	213
Sensory and Neuromuscular Physiology and Behavior	214
Body Size and Composition	215
Feeding	222
Digestion	228
Respiration	229
Excretion	233
Metabolic Pathways	236

Energy Partitioning	240
SHELL BIOCHEMISTRY (Maggie Cusack, Derek Walton, and G. B. Curry)	243
Introduction	243
Amino Acids in Brachiopod Shells	245
Proteins	250
Lipids in Brachiopod Valves	255
Carbohydrates in Brachiopod Valves	260
Immunology of Brachiopod Shell Macromolecules	261
SHELL STRUCTURE (Alwyn Williams)	267
Introduction	267
Periostraca	269
Primary Layer	271
Secondary Layer	275
Tertiary Layer	293
Shell Perforations	295
MORPHOLOGY (Alwyn Williams, C. H. C. Brunton, and D. I. MacKinnon)	321
Shell Form	321
Ornamentation	329
Modifications of Pedicle Opening	347
Articulation	360
Brachidia	372
Musculature	385
Mantle Canal Systems	410
MORPHOLOGICAL AND ANATOMICAL TERMS APPLIED TO BRACHIOPODS (Alwyn Williams and C. H. C. Brunton)	423
Glossary of Morphological and Selected Anatomical Terms	423
ECOLOGY OF ARTICULATED BRACHIOPODS (J. R. Richardson)	441
Substrate Relationships	441
Distribution	451
Demography	457
Predation and Parasitism	460
BIOGEOGRAPHY OF ARTICULATED BRACHIOPODS (J. R. Richardson)	463
Factors Concerning Distribution	463
Distribution of Families	464
Family Origins and Paths of Dispersal	470
ECOLOGY OF INARTICULATED BRACHIOPODS (C. C. Emig)	473
Introduction	473
Behavior	473
Ecology	482
BIOGEOGRAPHY OF INARTICULATED BRACHIOPODS (C. C. Emig)	497
Introduction	497
Patterns in Distribution	497
Distribution of Families and Genera	498
REFERENCES	503
INDEX	527

INFORMATION ON TREATISE VOLUMES

Parts of the *Treatise* are distinguished by assigned letters with a view to indicating their systematic sequence while allowing publication of units in whatever order each is made ready for the press. Copies can be obtained from the Publication Sales Department, The Geological Society of America, 3300 Penrose Place, P.O. Box 9140, Boulder, Colorado 80301.

VOLUMES ALREADY PUBLISHED

- Part A. INTRODUCTION, xxiii + 569 p., 371 fig., 1979.
- Part C. PROTISTA 2 (Sarcodina, Chiefly "Thecamoebians" and Foraminiferida), xxxi + 900 p., 5,311 fig., 1964.
- Part D. PROTISTA 3 (Chiefly Radiolaria, Tintinnina), xii + 195 p., 1,050 fig., 1954.
- Part E. ARCHAEOCYATHA, PORIFERA, xviii + 122 p., 728 fig., 1955.
- Part E, Revised. ARCHAEOCYATHA, Volume 1, xxx + 158 p., 871 fig., 1972.
- Part F. COELENTERATA, xvii + 498 p., 2,700 fig., 1956.
- Part F. COELENTERATA, Supplement 1 (Rugosa and Tabulata), xl + 762 p., 3,317 fig., 1981.
- Part G. BRYOZOA, xii + 253 p., 2,000 fig., 1953.
- Part G, Revised. BRYOZOA, Volume 1 (Introduction, Order Cystoporata, Order Cryptostomata), xxvi + 626 p., 1,595 fig., 1983.
- Part H. BRACHIOPODA, xxxii + 927 p., 5,198 fig., 1965.
- Part I. MOLLUSCA 1 (Mollusca General Features, Scaphopoda, Amphineura, Monoplacophora, Gastropoda General Features, Archaeogastropoda, Mainly Paleozoic Caenogastropoda and Opisthobranchia), xxiii + 351 p., 1,732 fig., 1960.
- Part K. MOLLUSCA 3 (Cephalopoda General Features, Endoceratoidea, Actinoceratoidea, Nautiloidea, Bactritoidea), xxviii + 519 p., 2,382 fig., 1964.
- Part L. MOLLUSCA 4 (Ammonoidea), xxii + 490 p., 3,800 fig., 1957.
- Part L, Revised. MOLLUSCA 4, Volume 4 (Cretaceous Ammonoidea), xx + 362 p., 2,070 illus. on 216 fig., 1996.
- Part N. MOLLUSCA 6 (Bivalvia), Volumes 1 and 2 (of 3), xxxvii + 952 p., 6,198 fig., 1969; Volume 3, iv + 272 p., 742 fig., 1971.
- Part O. ARTHROPODA 1 (Arthropoda General Features, Protarthropoda, Euarthropoda General Features, Trilobitomorpha), xix + 560 p., 2,880 fig., 1959.
- Part O, Revised. ARTHROPODA 1 (Introduction, Order Agnostida, Order Redlichiida), xxiv + 530 p., 309 fig., 1997.
- Part P. ARTHROPODA 2 (Chelicerata, Pycnogonida, Palaeoisopus), xvii + 181 p., 565 fig., 1955.
- Part Q. ARTHROPODA 3 (Crustacea, Ostracoda), xxiii + 442 p., 3,476 fig., 1961.
- Part R. ARTHROPODA 4, Volumes 1 and 2 (Crustacea Exclusive of Ostracoda, Myriapoda, Hexapoda), xxxvi + 651 p., 1,762 fig., 1969.
- Part R. ARTHROPODA 4, Volumes 3 and 4 (Hexapoda), xxii + 655 p., 1,489 fig., 1992.
- Part S. ECHINODERMATA 1 (Echinodermata General Features, Homalozoa, Crinozoa, exclusive of Crinoidea), xxx + 650 p., 2,868 fig., 1967 [1968].
- Part T. ECHINODERMATA 2 (Crinoidea), Volumes 1-3, xxxviii + 1,027 p., 4,833 fig., 1978.
- Part U. ECHINODERMATA 3 (Asterozoans, Echinozoans), xxx + 695 p., 3,485 fig., 1966.
- Part V. GRAPTOLITHINA, xvii + 101 p., 358 fig., 1955.
- Part V, Revised. GRAPTOLITHINA, xxxii + 163 p., 507 fig., 1970.
- Part W. MISCELLANEA (Conodonts, Conoidal Shells of Uncertain Affinities, Worms, Trace Fossils, Problematica), xxv + 259 p., 1,058 fig., 1962.

Part W, Revised. MISCELLANEA, Supplement 1 (Trace Fossils and Problematica), xxi + 269 p., 912 fig., 1975.

Part W, Revised. MISCELLANEA, Supplement 2 (Conodonts), xxviii + 202 p., frontis., 858 fig., 1981.

THIS VOLUME

Part H, Revised. BRACHIOPODA (Introduction), xx + 539 p., 417 fig., 40 tables, 1997.

VOLUMES IN PREPARATION

Part B. PROTISTA 1 (Chrysomonadida, Coccolithophorida, Charophyta, Diatomacea, etc.).

Part E, Revised. PORIFERA. Volume 2.

Part G, Revised. BRYOZOA (additional volumes).

Part H, Revised. BRACHIOPODA (additional volumes).

Part I. Introduction to MOLLUSCA (part).

Part J. MOLLUSCA 2 (Caenogastropoda, Streptoneura exclusive of Archaeogastropoda, Euthyneura).

Part L, Revised. MOLLUSCA 4 (Ammonoidea) (additional volumes).

Part M. MOLLUSCA 5 (Coleoidea).

Part O, Revised. ARTHROPODA 1 (Trilobita) (additional volumes).

Part Q, Revised. ARTHROPODA 3 (Ostracoda).

EDITORIAL PREFACE

From the outset the aim of the *Treatise on Invertebrate Paleontology* has been to present a comprehensive and authoritative yet compact statement of knowledge concerning groups of invertebrate fossils. Typically, preparation of early *Treatise* volumes was undertaken by a small group with a synoptic view of the taxa being monographed. Two or perhaps three specialists worked together, sometimes co-opting others for coverage of highly specialized taxa. Recently, however, both new *Treatise* volumes and revisions of existing ones have been undertaken increasingly by teams of specialists led by a coordinating author. This volume, Part H, Brachiopoda 1, Revised, the first of a series of volumes on the brachiopods, has been prepared by such a team of specialists whose work was coordinated by Sir Alwyn Williams. Editorial matters specific to this vol-

ume are discussed near the end of this editorial preface.

ZOOLOGICAL NAMES

Questions about the proper use of zoological names arise continually, especially questions regarding both the acceptability of names and alterations of names that are allowed or even required. Regulations prepared by the International Commission on Zoological Nomenclature (ICZN) and published in 1985 in the *International Code of Zoological Nomenclature*, hereinafter referred to as the *Code*, provide procedures for answering such questions. The prime objective of the *Code* is to promote stability and universality in the use of the scientific names of animals, ensuring also that each generic name is distinct and unique, while avoiding

unwarranted restrictions on freedom of thought and action of systematists. Priority of names is a basic principle of the *Code*, but under specified conditions and by following prescribed procedures, priority may be set aside by the Commission. These procedures apply especially where slavish adherence to the principle of priority would hamper or even disrupt zoological nomenclature and the information it conveys.

The Commission, ever aware of the changing needs of systematists, is undertaking a revision of the *Code* that will further enhance nomenclatorial stability. Nevertheless, the nomenclatorial tasks that confront zoological taxonomists are formidable and have often justified the complaint that the study of zoology and paleontology is too often merely the study of names rather than the study of animals. It is incumbent upon all systematists, therefore, at the outset of their work to pay careful attention to the *Code* to enhance stability by minimizing the number of subsequent changes of names, too many of which are necessitated by insufficient attention to detail. To that end, several pages here are devoted to aspects of zoological nomenclature that are judged to have chief importance in relation to procedures adopted in the *Treatise*, especially in this volume. Terminology is explained, and examples are given of the style employed in the nomenclatorial parts of the systematic descriptions.

GROUPS OF TAXONOMIC CATEGORIES

Each taxon belongs to a category in the Linnaean, hierarchical classification. The *Code* recognizes three groups of categories, a species-group, a genus-group, and a family-group. Taxa of lower rank than subspecies are excluded from the rules of zoological nomenclature, and those of higher rank than superfamily are not regulated by the *Code*. It is both natural and convenient to discuss nomenclatorial matters in general terms first

and then to consider each of these three, recognized groups separately. Especially important is the provision that within each group the categories are coordinate, that is, equal in rank, whereas categories of different groups are not coordinate.

FORMS OF NAMES

All zoological names can be considered on the basis of their spelling. The first form of a name to be published is defined as the original spelling (*Code*, Article 32), and any form of the same name that is published later and is different from the original spelling is designated a subsequent spelling (*Code*, Article 33). Not every original or subsequent spelling is correct.

ORIGINAL SPELLINGS

If the first form of a name to be published is consistent and unambiguous, the original is defined as correct unless it contravenes some stipulation of the *Code* (Articles 11, 27 to 31, and 34) or unless the original publication contains clear evidence of an inadvertent error in the sense of the *Code*, or, among names belonging to the family-group, unless correction of the termination or the stem of the type genus is required. An original spelling that fails to meet these requirements is defined as incorrect.

If a name is spelled in more than one way in the original publication, the form adopted by the first reviser is accepted as the correct original spelling, provided that it complies with mandatory stipulations of the *Code* (Articles 11 and 24 to 34).

Incorrect original spellings are any that fail to satisfy requirements of the *Code*, represent an inadvertent error, or are one of multiple original spellings not adopted by a first reviser. These have no separate status in zoological nomenclature and, therefore, cannot enter into homonymy or be used as replacement names; and they call for correction. For example, a name originally published with a

diacritical mark, apostrophe, dieresis, or hyphen requires correction by deleting such features and uniting parts of the name originally separated by them, except that deletion of an umlaut from a vowel in a name derived from a German word or personal name unfortunately requires the insertion of *e* after the vowel. Where original spelling is judged to be incorrect solely because of inadequacies of the Greek or Latin scholarship of the author, nomenclatorial changes conflict with the primary propose of zoological nomenclature as an information retrieval system. One looks forward with hope to a revised *Code* wherein rules are emplaced that enhance stability rather than classical scholarship, thereby facilitating access to information.

SUBSEQUENT SPELLINGS

If a subsequent spelling differs from an original spelling in any way, even by the omission, addition, or alteration of a single letter, the subsequent spelling must be defined as a different name. Exceptions include such changes as an altered termination of adjectival specific names to agree in gender with associated generic names; changes of family-group names to denote assigned taxonomic rank; and corrections that eliminate originally used diacritical marks, hyphens, and the like. Such changes are not regarded as spelling changes conceived to produce a different name. In some instances, however, species-group names having variable spellings are regarded as homonyms as specified in the *Code* (Article 58).

Altered subsequent spellings other than the exceptions noted may be either intentional or unintentional. If “demonstrably intentional” (*Code*, Article 33, p. 73), the change is designated as an emendation. Emendations may be either justifiable or unjustifiable. Justifiable emendations are corrections of incorrect original spellings, and these take the authorship and date of the original spellings. Unjustifiable emendations are names having their own status in nomen-

clature, with author and date of their publication. They are junior, objective synonyms of the name in its original form.

Subsequent spellings, if unintentional, are defined as incorrect subsequent spellings. They have no status in nomenclature, do not enter into homonymy, and cannot be used as replacement names.

AVAILABLE AND UNAVAILABLE NAMES

Editorial prefaces of some previous volumes of the *Treatise* have discussed in appreciable detail the availability of the many kinds of zoological names that have been proposed under a variety of circumstances. Much of that information, while important, does not pertain to the present volume, in which authors have used fewer terms for such names. The reader is referred to the *Code* (Articles 10 to 20) for further details on availability of names. Here, suffice it to say that an available zoological name is any that conforms to all mandatory provisions of the *Code*. All zoological names that fail to comply with mandatory provisions of the *Code* are unavailable and have no status in zoological nomenclature. Both available and unavailable names are classifiable into groups that have been recognized in previous volumes of the *Treatise*, although not explicitly differentiated in the *Code*. Among names that are available, these groups include inviolate names, perfect names, imperfect names, vain names, transferred names, improved or corrected names, substitute names, and conserved names. Kinds of unavailable names include naked names (see *nomina nuda* below), denied names, impermissible names, null names, and forgotten names.

Nomina nuda include all names that fail to satisfy provisions stipulated in Article 11 of the *Code*, which states general requirements of availability. In addition, they include names published before 1931 that were unaccompanied by a description, definition, or indication (*Code*, Article 12) and names

published after 1930 that (1) lacked an accompanying statement of characters that differentiate the taxon, (2) were without a definite bibliographic reference to such a statement, (3) were not proposed expressly as a replacement (*nomen novum*) of a preexisting available name (*Code*, Article 13a), or (4) for genus-group names, were unaccompanied by definite fixation of a type species by original designation or indication (*Code*, Article 13b). *Nomina nuda* have no status in nomenclature, and they are not correctable to establish original authorship and date.

VALID AND INVALID NAMES

Important considerations distinguish valid from available names on the one hand and invalid from unavailable names on the other. Whereas determination of availability is based entirely on objective considerations guided by articles of the *Code*, conclusions as to validity of zoological names may be partly subjective. A valid name is the correct one for a given taxon, which may have two or more available names but only a single correct, hence valid, name, which is also generally the oldest name that it has been given. Obviously, no valid name can also be an unavailable name, but invalid names may be either available or unavailable. It follows that any name for a given taxon other than the valid name, whether available or unavailable, is an invalid name.

One encounters a sort of nomenclatorial no-man's land in considering the status of such zoological names as *nomina dubia* (doubtful names), which may include both available and unavailable names. The unavailable ones can well be ignored, but names considered to be available contribute to uncertainty and instability in the systematic literature. These can ordinarily be removed only by appeal to the ICZN for special action. Because few systematists care to seek such remedy, such invalid but available names persist in the literature.

NAME CHANGES IN RELATION TO GROUPS OF TAXONOMIC CATEGORIES

SPECIES-GROUP NAMES

Detailed consideration of valid emendation of specific and subspecific names is unnecessary here, both because the topic is well understood and relatively inconsequential and because the *Treatise* deals with genus-group names and higher categories. When the form of adjectival specific names is changed to agree with the gender of a generic name in transferring a species from one genus to another, one need never label the changed name as *nomen correctum*. Similarly, transliteration of a letter accompanied by a diacritical mark in the manner now called for by the *Code*, as in changing originally *bröggeri* to *broeggeri*, or eliminating a hyphen, as in changing originally published *cornu-oryx* to *cornuoryx*, does not require the designation *nomen correctum*. Of course, in this age of computers and electronic databases, such changes of name, which are perfectly valid for the purposes of scholarship, run counter to the requirements of nomenclatorial stability upon which the preparation of massive, electronic databases is predicated.

GENUS-GROUP NAMES

Conditions warranting change of the originally published, valid form of generic and subgeneric names are sufficiently rare that lengthy discussion is unnecessary. Only elimination of diacritical marks and hyphens in some names in this category and replacement of homonyms seem to furnish basis for valid emendation. Many names that formerly were regarded as homonyms are no longer so regarded, because two names that differ only by a single letter or in original publication by the presence of a diacritical mark in one are now construed to be entirely distinct.

As has been pointed out above, difficulty typically arises when one tries to decide whether a change of spelling of a name by a subsequent author was intentional or unintentional, and the decision has often to be made arbitrarily.

FAMILY-GROUP NAMES

Family-group Names: Authorship and Date

All family-group taxa having names based on the same type genus are attributed to the author who first published the name of any of these groups, whether tribe, subfamily, or family (superfamily being almost inevitably a later-conceived taxon). Accordingly, if a family is divided into subfamilies or a subfamily into tribes, the name of no such subfamily or tribe can antedate the family name. Moreover, every family containing differentiated subfamilies must have a nominate subfamily (*sensu stricto*), which is based on the same type genus as the family. Finally, the author and date set down for the nominate subfamily invariably are identical with those of the family, irrespective of whether the author of the family or some subsequent author introduced subdivisions.

Corrections in the form of family-group names do not affect authorship and date of the taxon concerned, but in the *Treatise* recording the authorship and date of the correction is desirable because it provides a pathway to follow the thinking of the systematists involved.

Family-Group Names: Use of *nomen translatum*

The *Code* specifies the endings only for subfamily (-inae) and family (-idae) names, but all family-group taxa are defined as coordinate (*Code*, Article 36, p. 77): "A name established for a taxon at any rank in the family group is deemed to be simultaneously established with the same author and date for taxa based upon the same name-bearing

type (type genus) at other ranks in the family group, with appropriate mandatory change of suffix [Art. 34a]." Such changes of rank and concomitant changes of endings as elevation of a tribe to subfamily rank or of a subfamily to family rank, if introduced subsequent to designation of a subfamily or family based on the same nominotypical genus, are *nomina translata*. In the *Treatise* it is desirable to distinguish the valid alteration in the changed ending of each transferred family-group name by the term *nomen translatum*, abbreviated to *nom. transl.* Similarly for clarity, authors should record the author, date, and page of the alteration.

Family HEXAGENITIDAE Lameere, 1917

[*nom. transl.* DEMOULIN, 1954, p. 566, ex Hexagenitinae LAMEERE, 1917, p. 74]

This is especially important for superfamilies, for the information of interest is the author who initially introduced a taxon rather than the author of the superfamily as defined by the *Code*. The latter is merely the individual who first defined some lower-ranked, family-group taxon that contains the nominotypical genus of the superfamily. On the other hand, the publication that introduces the superfamily by *nomen translatum* is likely to furnish the information on taxonomic considerations that support definition of the taxon.

Superfamily AGNOSTOIDEA M'Coy, 1849

[*nom. transl.* SHERGOLD, LAURIE, & SUN, 1990, p. 32, ex Agnostinae M'COY, 1849, p. 402]

Family-group Names: Use of *nomen correctum*

Valid name changes classed as *nomina correcta* do not depend on transfer from one category of the family group to another but most commonly involve correction of the stem of the nominotypical genus. In

addition, they include somewhat arbitrarily chosen modifications of endings for names of tribes or superfamilies. Examples of the use of *nomen correctum* are the following.

**Family STREPTELASMATIDAE
Nicholson, 1889**

[*nom. correct.* WEDEKIND, 1927, p. 7, *pro* Streptelasmidae NICHOLSON in NICHOLSON & LYDEKKER, 1889, p. 297]

**Family PALAEOSCORPIDAE
Lehmann, 1944**

[*nom. correct.* PETRUNKEVITCH, 1955, p. 73, *pro* Palaeoscorpionidae LEHMANN, 1944, p. 177]

Family-group Names: Replacements

Family-group names are formed by adding combinations of letters, which are prescribed for family and subfamily, to the stem of the name belonging to the nominotypical genus first chosen as type of the assemblage. The type genus need not be the first genus in the family to have been named and defined, but among all those included it must be the first published as name giver to a family-group taxon. Once fixed, the family-group name remains tied to the nominotypical genus even if the generic name is changed by reason of status as a junior homonym or junior synonym, either objective or subjective. Seemingly, the *Code* requires replacement of a family-group name only if the nominotypical genus is found to have been a junior homonym when it was proposed (*Code*, Article 39, p. 79), in which case “. . . it must be replaced either by the next oldest available name from among its synonyms, including those of its subordinate taxa, or, if there is no such name, by a new replacement name based on the valid name of the former type genus.” Authorship and date attributed to the replacement family-group name are determined by first publication of the changed family-group name. Recommendation 40A of the *Code* (p. 81), however, specifies that for subsequent application of the rule of priority, the family-group name “. . . should be cited with its own author and date, followed by the date of the replaced name in paren-

theses.” Many family-group names that have been in use for a long time are *nomina nuda*, since they fail to satisfy criteria of availability (*Code*, Article 11f). These demand replacement by valid names.

The aim of family-group nomenclature is to yield the greatest possible stability and uniformity, just as in other zoological names. Both taxonomic experience and the *Code* (Article 40) indicate the wisdom of sustaining family-group names based on junior subjective synonyms if they have priority of publication, for opinions of the same worker may change from time to time. The retention of first-published, family-group names that are found to be based on junior objective synonyms, however, is less clearly desirable, especially if a replacement name derived from the senior objective synonym has been recognized very long and widely. Moreover, to displace a widely used, family-group name based on the senior objective synonym by disinterring a forgotten and virtually unused family-group name based on a junior objective synonym because the latter happens to have priority of publication is unsettling.

A family-group name may need to be replaced if the nominotypical genus is transferred to another family-group. If so, the first-published of the generic names remaining in the family-group taxon is to be recognized in forming a replacement name.

**SUPRAFAMILIAL TAXA: TAXA
ABOVE FAMILY-GROUP**

International rules of zoological nomenclature as given in the *Code* affect only lower-rank categories: subspecies to superfamily. Suprafamilial categories (suborder to phylum) are either not mentioned or explicitly placed outside of the application of zoological rules. The *Copenhagen Decisions on Zoological Nomenclature* (1953, Articles 59 to 69) proposed adopting rules for naming suborders and higher taxa up to and including phylum, with provision for designating a type genus for each, in such manner as not to

interfere with the taxonomic freedom of workers. Procedures were outlined for applying the rule of priority and rule of homonymy to suprafamilial taxa and for dealing with the names of such taxa and their authorship, with assigned dates, if they should be transferred on taxonomic grounds from one rank to another. The adoption of terminations of names, different for each category but uniform within each, was recommended.

The Colloquium on Zoological Nomenclature, which met in London during the week just before the 15th International Congress of Zoology convened in 1958, thoroughly discussed the proposals for regulating suprafamilial nomenclature, as well as many others advocated for inclusion in the new *Code* or recommended for exclusion from it. A decision that was supported by a wide majority of the participants in the colloquium was against the establishment of rules for naming taxa above family-group rank, mainly because it was judged that such regulation would unwisely tie the hands of taxonomists. For example, a class or order defined by an author at a given date, using chosen morphologic characters (e.g., gills of bivalves), should not be allowed to freeze nomenclature, taking precedence over another class or order that is proposed later and distinguished by different characters (e.g., hinge teeth of bivalves). Even the fixing of type genera for suprafamilial taxa would have little, if any, value, hindering taxonomic work rather than aiding it. No basis for establishing such types and for naming these taxa has yet been provided.

The considerations just stated do not prevent the editors of the *Treatise* from making rules for dealing with suprafamilial groups of animals described and illustrated in this publication. Some uniformity is needed, especially for the guidance of *Treatise* authors. This policy should accord with recognized general practice among zoologists; but where general practice is indeterminate or nonexistent, our own procedure in suprafamilial nomenclature needs to be specified as clearly as possible. This pertains especially to decisions

about names themselves, about citation of authors and dates, and about treatment of suprafamilial taxa that, on taxonomic grounds, are changed from their originally assigned rank. Accordingly, a few rules expressing *Treatise* policy are given here, some with examples of their application.

1. The name of any suprafamilial taxon must be a Latin or Latinized, uninominal noun of plural form, or treated as such, with a capital initial letter and without diacritical mark, apostrophe, diaeresis, or hyphen. If a component consists of a numeral, numerical adjective, or adverb, this must be written in full.

2. Names of suprafamilial taxa may be constructed in almost any manner. A name may indicate morphological attributes (e.g., Lamellibranchiata, Cyclostomata, Toxoglossa) or be based on the stem of an included genus (e.g., Bellerophontina, Nautilida, Fungiina) or on arbitrary combinations of letters (e.g., Yuania); none of these, however, can end in *-idae* or *-inae*, which terminations are reserved for family-group taxa. No suprafamilial name identical in form to that of a genus or to another published suprafamilial name should be employed (e.g., order Decapoda LATREILLE, 1803, crustaceans, and order Decapoda LEACH, 1818, cephalopods; suborder Chonetoidea MUIRWOOD, 1955, and genus *Chonetoidea* JONES, 1928). Worthy of notice is the classificatory and nomenclatorial distinction between suprafamilial and family-group taxa that, respectively, are named from the same type genus, since one is not considered to be transferable to the other (e.g., suborder Bellerophontina ULRICH & SCOFIELD, 1897 is not coordinate with superfamily Bellerophontacea MCCOY, 1851 or family Bellerophontidae MCCOY, 1851).

3. The rules of priority and homonymy lack any force of international agreement as applied to suprafamilial names, yet in the interest of nomenclatorial stability and to avoid confusion these rules are widely applied by zoologists to taxa above the family-group level wherever they do not infringe

on taxonomic freedom and long-established usage.

4. Authors who accept priority as a determinant in nomenclature of a suprafamilial taxon may change its assigned rank at will, with or without modifying the terminal letters of the name, but such changes cannot rationally be judged to alter the authorship and date of the taxon as published originally. A name revised from its previously published rank is a transferred name (*nomen translatum*), as illustrated in the following.

Order CORYNEXOCHIDA Kobayashi, 1935

[*nom. transl.* MOORE, 1959, p. 217, *ex* suborder Corynexochida KOBAYASHI, 1935, p. 81]

A name revised from its previously published form merely by adoption of a different termination without changing taxonomic rank is a *nomen correctum*.

Order DISPARIDA Moore & Laudon, 1943

[*nom. correct.* MOORE in MOORE, LALICKER, & FISCHER, 1952, p. 613, *pro* order Disparata MOORE & LAUDON, 1943, p. 24]

A suprafamilial name revised from its previously published rank with accompanying change of termination, which signals the change of rank, is recorded as a *nomen translatum et correctum*.

Order HYBOCRINIDA Jaekel, 1918

[*nom. transl. et correct.* MOORE in MOORE, LALICKER, & FISCHER, 1952, p. 613, *ex* suborder Hybocrinites JAEKEL, 1918, p. 90]

5. The authorship and date of nominate subordinate and supraordinate taxa among suprafamilial taxa are considered in the *Treatise* to be identical since each actually or potentially has the same type. Examples are given below.

Subclass ENDOCERATOIDEA Teichert, 1933

[*nom. transl.* TEICHERT in TEICHERT & others, 1964, p. 128, *ex* order Endoceroidea TEICHERT, 1933, p. 214]

Order ENDOCERIDA Teichert, 1933

[*nom. correct.* TEICHERT in TEICHERT & others, 1964, p. 165, *pro* order Endoceroidea TEICHERT, 1933, p. 214]

TAXONOMIC EMENDATION

Emendation has two distinct meanings as regards zoological nomenclature. These are alteration of a name itself in various ways for various reasons, as has been reviewed, and alteration of the taxonomic scope or concept for which a name is used. The *Code* (Article 33a and Glossary, p. 254) concerns itself only with the first type of emendation, applying the term to intentional, either justified or unjustified changes of the original spelling of a name. The second type of emendation primarily concerns classification and inherently is not associated with change of name. Little attention generally has been paid to this distinction in spite of its significance.

Most zoologists, including paleontologists, who have emended zoological names refer to what they consider a material change in application of the name such as may be expressed by an importantly altered diagnosis of the assemblage covered by the name. The abbreviation *emend.* then must accompany the name with statement of the author and date of the emendation. On the other hand, many systematists think that publication of *emend.* with a zoological name is valueless because alteration of a taxonomic concept is introduced whenever a subspecies, species, genus, or other taxon is incorporated into or removed from a higher zoological taxon. Inevitably associated with such classificatory expansions and restrictions is some degree of emendation affecting diagnosis. Granting this, still it is true that now and then somewhat more extensive revisions are put forward, generally with a published statement of the reasons for changing the application of a name. To erect a signpost at such points of most significant change is worthwhile, both as an aid to subsequent workers in taking account of the altered no-

menclatorial usage and to indicate where in the literature cogent discussion may be found. Authors of contributions to the *Treatise* are encouraged to include records of all especially noteworthy emendations of this nature, using the abbreviation *emend.* with the name to which it refers and citing the author, date, and page of the emendation. Examples from *Treatise* volumes follow.

Order ORTHIDA Schuchert & Cooper, 1932

[*nom. transl. et correct.* MOORE in MOORE, LALICKER, & FISCHER, 1952, p. 220, *ex suborder* Orthoidea SCHUCHERT & COOPER, 1932, p. 43; *emend.*, WILLIAMS & WRIGHT, 1965, p. 299]

Subfamily ROVEACRININAE Peck, 1943

[Roveacrininae PECK, 1943, p. 465; *emend.*, PECK in MOORE & TEICHERT, 1978, p. 921]

STYLE IN GENERIC DESCRIPTIONS

CITATION OF TYPE SPECIES

In the *Treatise* the name of the type species of each genus and subgenus is given immediately following the generic name with its accompanying author, date, and page reference or after entries needed for definition of the name if it is involved in homonymy. The originally published combination of generic and trivial names of this species is cited, accompanied by an asterisk (*), with notation of the author, date, and page of original publication, except if the species was first published in the same paper and by the same author as that containing definition of the genus of which it is the type. In this instance, the initial letter of the generic name followed by the trivial name is given without repeating the name of the author and date. Examples of these two sorts of citations follow.

Orionastraea SMITH, 1917, p. 294 [**Sarcinula phillipsi* MCCOY, 1849, p. 125; OD].
Schoenophyllum SIMPSON, 1900, p. 214 [**S. aggregatum*; OD].

If the cited type species is a junior synonym of some other species, the name of this latter also is given, as follows.

Actinocyathus D'ORBIGNY, 1849, p. 12
[**Cyathophyllum crenulate* PHILLIPS, 1836, p. 202; M; =*Lonsdaleia floriformis* (MARTIN), 1809, pl. 43; validated by ICZN Opinion 419].

In some instances the type species is a junior homonym. If so, it is cited as shown in the following example.

Prionocyclus MEEK, 1871b, p. 298 [**Ammonites serratocarinatus* MEEK, 1871a, p. 429, *non* STOLICZKA, 1964, p. 57; =*Prionocyclus wyomingensis* MEEK, 1876, p. 452].

In the *Treatise* the name of the type species is always given in the exact form it had in the original publication except that diacritical marks have been removed. Where other mandatory changes are required, these are introduced later in the text, typically in a figure caption.

Fixation of Type Species Originally

It is desirable to record the manner of establishing the type species, whether by original designation (OD) or by subsequent designation (SD). The type species of a genus or subgenus, according to provisions of the *Code*, may be fixed in various ways in the original publication; or it may be fixed subsequently in ways specified by the *Code* (Article 68) and described in the next section. Type species fixed in the original publication include (1) *original designation* (in the *Treatise* indicated by OD) when the type species is explicitly stated or (before 1931) indicated by n. gen., n. sp. (or its equivalent) applied to a single species included in a new genus, (2) defined by use of *typus* or *typicus* for one of the species included in a new genus (adequately indicated in the *Treatise* by the specific name), (3) established by *monotypy* if a new genus or subgenus has only one originally included species (in the *Treatise* indicated as M), and (4) fixed by *tautonymy* if the genus-group name is identical to an included species name not indicated as the type.

Fixation of Type Species Subsequently

The type species of many genera are not determinable from the publication in which the generic name was introduced. Therefore, such genera can acquire a type species only

by some manner of subsequent designation. Most commonly this is established by publishing a statement naming as type species one of the species originally included in the genus. In the *Treatise* such fixation of the type species by subsequent designation in this manner is indicated by the letters SD accompanied by the name of the subsequent author (who may be the same person as the original author) and the publication date and page number of the subsequent designation. Some genera, as first described and named, included no mentioned species (for such genera established after 1930, see below); these necessarily lack a type species until a date subsequent to that of the original publication when one or more species is assigned to such a genus. If only a single species is thus assigned, it automatically becomes the type species. Of course, the first publication containing assignment of species to the genus that originally lacked any included species is the one concerned in fixation of the type species, and if this publication names two or more species as belonging to the genus but did not designate a type species, then a later SD designation is necessary. Examples of the use of SD as employed in the *Treatise* follow.

Hexagonaria GURICH, 1896, p. 171 [**Cyathophyllum hexagonum* GOLDFUSS, 1826, p. 61; SD LANG, SMITH, & THOMAS, 1940, p. 69].

Mesephemera HANDLIRSCH, 1906, p. 600 [**Tineites lithophilus* GERMAR, 1842, p. 88; SD CARPENTER, herein].

Another mode of fixing the type species of a genus is action of the International Commission of Zoological Nomenclature using its plenary powers. Definition in this way may set aside application of the *Code* so as to arrive at a decision considered to be in the best interest of continuity and stability of zoological nomenclature. When made, it is binding and commonly is cited in the *Treatise* by the letters ICZN, accompanied by the date of announced decision and reference to the appropriate numbered opinion.

Subsequent designation of a type species is admissible only for genera established prior

to 1931. A new genus-group name established after 1930 and not accompanied by fixation of a type species through original designation or original indication is invalid (*Code*, Article 13b). Effort of a subsequent author to validate such a name by subsequent designation of a type species constitutes an original publication making the name available under authorship and date of the subsequent author.

HOMONYMS

Most generic names are distinct from all others and are indicated without ambiguity by citing their originally published spelling accompanied by name of the author and date of first publication. If the same generic name has been applied to two or more distinct taxonomic units, however, it is necessary to differentiate such homonyms. This calls for distinction between junior homonyms and senior homonyms. Because a junior homonym is invalid, it must be replaced by some other name. For example, *Callophora* HALL, 1852, introduced for Paleozoic trepostomate bryozoans, is invalid because Gray in 1848 published the same name for Cretaceous-to-Holocene cheilostomate bryozoans. Bassler in 1911 introduced the new name *Hallophora* to replace Hall's homonym. The *Treatise* style of entry is given below.

Hallophora BASSLER, 1911, p. 325, *nom. nov. pro Callophora* HALL, 1852, p. 144, *non* GRAY, 1848.

In like manner, a replacement generic name that is needed may be introduced in the *Treatise* (even though first publication of generic names otherwise in this work is generally avoided). An exact bibliographic reference must be given for the replaced name as in the following example.

Mysterium DE LAUBENFELS, herein, *nom. nov. pro Mysterium* SCHRAMMEN, 1936, p. 183, *non* ROGER, 1862 [**Mysterium porosum* SCHRAMMEN, 1936, p. 183; OD].

Otherwise, no mention of the existence of a junior homonym generally is made.

Synonymous Homonyms

An author sometimes publishes a generic name in two or more papers of different date, each of which indicates that the name is new. This is a bothersome source of errors for later workers who are unaware that a supposed first publication that they have in hand is not actually the original one. Although the names were separately published, they are identical and therefore definable as homonyms; at the same time they are absolute synonyms. For the guidance of all concerned, it seems desirable to record such names as synonymous homonyms. In the *Treatise* the junior of one of these is indicated by the abbreviation *jr. syn. hom.*

Not infrequently, identical family-group names are published as new names by different authors, the author of the name that was introduced last being ignorant of previous publication(s) by one or more other workers. In spite of differences in taxonomic concepts as indicated by diagnoses and grouping of genera and possibly in assigned rank, these family-group taxa, being based on the same type genus, are nomenclatorial homonyms. They are also synonyms. Wherever encountered, such synonymous homonyms are distinguished in the *Treatise* as in dealing with generic names.

A rare but special case of homonymy exists when identical family names are formed from generic names having the same stem but differing in their endings. An example is the family name Scutellidae RICHTER & RICHTER, 1925, based on *Scutellum* PUSCH, 1833, a trilobite. This name is a junior homonym of Scutellidae GRAY, 1825, based on the echinoid genus *Scutella* LAMARCK, 1816. The name of the trilobite family was later changed to Scutelluidae (ICZN, Opinion 1004, 1974).

SYNONYMS

In the *Treatise*, citation of synonyms is given immediately after the record of the type species. If two or more synonyms of differing date are recognized, these are ar-

ranged in chronological order. Objective synonyms are indicated by accompanying designation obj., others being understood to constitute subjective synonyms, of which the types are also indicated. Examples showing *Treatise* style in listing synonyms follow.

Mackenziophyllum PEDDER, 1971, p. 48 [**M. insolitum*; OD] [= *Zonastrea* TSYGANKO in SPASSKIY, KRAVTSOV, & TSYGANKO, 1971, p. 85, *nom. nud.*; *Zonastrea* TSYGANKO, 1972, p. 21 (type, *Z. graciosa*, OD)].

Kodonophyllum WEDEKIND, 1927, p. 34 [**Streptelasma Milne-Edwardsi* DYBOWSKI, 1873, p. 409; OD; = *Madrepora truncata* LINNE, 1758, p. 795, see SMITH & TREMBERTH, 1929, p. 368] [= *Patrophontes* LANG & SMITH, 1927, p. 456 (type, *Madrepora truncata* LINNE, 1758, p. 795, OD); *Codonophyllum* LANG, SMITH, & THOMAS, 1940, p. 39, obj.].

Some junior synonyms of either the objective or the subjective sort may be preferred over senior synonyms whenever uniformity and continuity of nomenclature are served by retaining a widely used but technically rejectable name for a genus. This requires action of the ICZN, which may use its plenary powers to set aside the unwanted name, validate the wanted one, and place the concerned names on appropriate official lists.

OTHER EDITORIAL MATTERS

BIOGEOGRAPHY

Purists, *Treatise* editors among them, would like nothing better than a stable world with a stable geography that makes possible a stable biogeographical classification. Global events of the past few years have shown how rapidly geography can change, and in all likelihood we have not seen the last of such change as new, so-called republics continue to spring up all over the globe. One expects confusion among readers in the future as they try to decipher such geographical terms as U.S.S.R., Yugoslavia, or Ceylon. Such confusion is unavoidable, as books must be completed and published at some real time. Libraries would be limited indeed if publication were always to be delayed until the political world had settled down. In addition, such terms as central Europe and western Europe are likely to mean different things to

different people. Some imprecision is introduced by the use of all such terms, of course, but it is probably no greater than the imprecision that stems from the fact that the work of paleontology is not yet finished, and the geographical ranges of many genera are imperfectly known.

NAMES OF AUTHORS: TRANSLATION AND TRANSLITERATION

Chinese scientists have become increasingly active in systematic paleontology in the past two decades. Chinese names cause anguish among English-language bibliographers for two reasons. First, no scheme exists for one-to-one transliteration of Chinese characters into roman letters. Thus, a Chinese author may change the roman-letter spelling of his name from one publication to another. For example, the name Chang, the most common family name in the world reportedly held by some one billion people, might also be spelled Zhang. The principal purpose of a bibliography is to provide the reader with entry into the literature. Quite arbitrarily, therefore, in the interest of information retrieval, the *Treatise* editorial staff has decided to retain the roman spelling that a Chinese author has used in each of his publications rather than attempting to adopt a common spelling of an author's name to be used in all citations of his work. It is entirely possible, therefore, that the publications of a Chinese author may be listed in more than one place under more than one name in the bibliography.

Second, most but by no means all Chinese list their family name first followed by given names. People with Chinese names who study in the West, however, often reverse the order, putting the family name last as is the Western custom. Thus, for example, Dr. Yi-Maw Chang, recently of the staff of the Paleontological Institute, was Chang Yi-Maw when he lived in Taiwan. When he came to America, he became Yi-Maw Chang, and his subsequent bibliographic citations are listed

as Chang, Yi-Maw. The *Treatise* staff has adopted the convention of listing family names first, inserting a comma, and following this with given names or initials. We do this even for Chinese authors who have not reversed their names in the Western fashion.

Several systems exist for transliterating the Cyrillic alphabet into the roman alphabet. We have adopted the American Library Association/Library of Congress romanization table for Russian and other languages using the Cyrillic alphabet.

MATTERS SPECIFIC TO THIS VOLUME

This volume is unlike most previous volumes of the *Treatise* in one important respect: it is devoted entirely to introductory material, having no systematic paleontology. This is true of Part A, Introduction (Robison & Teichert, eds., 1979), the introduction to the entire series. It is also true of Part T, Echinodermata 2(1), the first of three volumes on the crinoids, which, unlike the present series on brachiopods, were published simultaneously (Moore & Teichert, eds., 1978). All other volumes have included systematic paleontology, and this is the first so-called systematic volume to contain no systematics.

Each group of organisms, it seems, lends itself to different kinds of investigations or has attracted groups of investigators with special interests. The brachiopods are no exception. In spite of the fact that more than 95 percent of the brachiopod genera are extinct, the community of brachiopod specialists has made unprecedented progress in understanding the functional morphology, genetics, embryology, and anatomy of brachiopods, all topics that are discussed in detail in this introductory volume.

ACKNOWLEDGMENTS

The Paleontological Institute's Assistant Editor for Text, Jill Hardesty, and the Assistant Editor for Illustrations, Karen Renteria,

have faced admirably the formidable task of moving this volume through the various stages of editing and into production. In this they have been ably assisted by members of the other editorial team, Liz Brosius and Jane Kerns; by Jack Keim with photography; and by Jean Burgess with general support. Jill Krebs, the remaining member of the Paleontological Institute staff, is involved with preparation of PaleoBank, the paleontological database for future *Treatise* volumes, and has not been closely involved with the brachiopod *Treatise*.

This editorial preface and other, recent ones are extensive revisions of the prefaces prepared for previous *Treatise* volumes by former editors, including the late Raymond C. Moore, the late Curt Teichert, and Richard A. Robison. I am indebted to them for preparing earlier prefaces and for the leadership they have provided in bringing the *Treatise* project to its present status.

Finally, I am pleased to extend on behalf of the members of the staff of the Paleontological

Institute, both past and present, our most sincere thanks to Sir Alwyn Williams for the unwavering scholarship, dedication to the task, and scrupulous attention to detail that have marked his involvement with this project from the outset and, indeed, his entire career as a specialist on the Brachiopoda.

REFERENCES

- Moore, R. C., and C. Teichert. 1978. *Treatise on Invertebrate Paleontology*. Part T, Echinodermata 2(1). The University of Kansas and Geological Society of America. Lawrence & Boulder. 401 p.
- Ride, W. D. L., C. W. Sabrosky, G. Bernardi, and R. V. Melville, eds. 1985. *International Code of Zoological Nomenclature*. International Trust for Zoological Nomenclature. University of California Press. Berkeley & Los Angeles. 338 p.
- Robison, R. A., and C. Teichert. 1979. *Treatise on Invertebrate Paleontology*. Part A, Introduction. The University of Kansas and Geological Society of America. Lawrence & Boulder. 569 p.

Roger L. Kaesler
Lawrence, Kansas
July 15, 1997

STRATIGRAPHIC DIVISIONS

The major divisions of the geological time scale are reasonably well established throughout the world, but minor divisions (e.g., substages, stages, and subseries) are more likely to be provincial in application. The stratigraphical units listed here represent an authoritative version of the stratigraphic column for all taxonomic work relating to revision of Part H. They are adapted from the International Union of Geological Sciences 1989 Global Stratigraphic Chart, compiled by J. W. Cowie and M. G. Bassett.

Cenozoic Erathem

Quaternary System

- Holocene Series
- Pleistocene Series

Neogene System

- Pliocene Series
- Miocene Series

Paleogene System

- Oligocene Series
- Eocene Series
- Paleocene Series

Mesozoic Erathem

Cretaceous System

- Upper Cretaceous Series
- Lower Cretaceous Series

Jurassic System

- Upper Jurassic Series
- Middle Jurassic Series
- Lower Jurassic Series

Triassic System

- Upper Triassic Series
- Middle Triassic Series
- Lower Triassic Series

Paleozoic Erathem

Permian System

- Upper Permian Series
- Lower Permian Series

Carboniferous System

Upper Carboniferous Subsystem

- Stephanian Series
- Westphalian Series

Namurian Series (part)

Lower Carboniferous Subsystem

- Namurian Series (part)
- Visean Series
- Tournaisian Series

Devonian System

- Upper Devonian Series
- Middle Devonian Series
- Lower Devonian Series

Silurian System

- Pridoli Series
- Ludlow Series
- Wenlock Series
- Llandovery Series

Ordovician System

- Upper Ordovician Subsystem
 - Cincinnatian Series
 - Champlainian Series (part)
- Lower Ordovician Subsystem
 - Champlainian Series (part)
 - Canadian Series

Cambrian System

- Lower Cambrian Series
- Middle Cambrian Series
- Upper Cambrian Series

COORDINATING AUTHOR'S PREFACE

ALWYN WILLIAMS

[University of Glasgow]

The first edition of Part H, Brachiopoda, of the *Treatise on Invertebrate Paleontology* predated, by months rather than years, the publication of ZUCKERKANDL and PAULING's proposition (1965) that genetic macromolecules are "documents of evolutionary history" (p. 357), HENNIG's *Phylogenetic Systematics* (1966), and the results of the earliest electron microscopic studies of the brachiopod shell (SASS, MONROE, & GERACE, 1965; TOWE & HARPER, 1966; WILLIAMS, 1966). The limitations imposed on our understanding of the phylum by the unavailability of these revolutionary methods of classifying and studying organisms are well illustrated by the first edition itself. Cluster analysis had been used sporadically (WILLIAMS, 1965, p. 243; WILLIAMS & WRIGHT, 1965, p. 301) to identify trends in stratigraphic distributions of fossil assemblages and in the modal morphologies of orthidines. The structure of the shell in relation to its secreting mantle had also been widely studied to ascertain taxonomically important changes in the skeletal fabric of extinct and living species. Moreover, the section on shell composition (JOPE, 1965) is now hailed as a pioneer systematic exploration of the degradation of the organic residues (episemantic molecules of ZUCKERKANDL & PAULING, 1965, p. 358) of representative living and fossil shells of marine invertebrates. These methods, however, hardly compare with the sophisticated protocols afforded by computers, electron microscopes, and amino-acid analyzers, which are among the wide range of facilities used in the preparation of this revision.

Yet crucial as these facilities have been to the continuing advancement of the natural sciences as a whole, the prime source of upsurge in recent brachiopod research has been the first edition itself, which was the first comprehensive account of all brachiopod genera since the ZITTEL series (1880, *et seq.*).

Its publication in 1965 was most opportune, as the number of brachiopod genera had increased fivefold over those recognized by HALL and CLARKE (1892–1894) to nearly 1,700. Monographs and catalogues of the phylum appearing between 1894 and 1965 indicate that new genera were being proposed at a fairly steady rate of just under 20 per year, with new discoveries being described at about one-half the rate of those created by continual taxonomic revision (WILLIAMS, 1957). In contrast, between 1965 and March 1995 (the generally observed deadline for the retrieval of taxonomic data for inclusion in the revision) about 2,000 new genera were proposed. Even assuming an abnormally high proportion of invalid or synonymous genera, the annual rate of creation has been four to five times that obtaining prior to the publication of the first edition. Moreover, a casual scrutiny of post-1965 literature confirms that many of the new taxa were long-established species upgraded to generic rank to conform with the taxonomic practices of the first edition. However, significant numbers of new genera were also erected for specimens recovered from previously poorly known geological successions in Australia, North Africa, and especially Asia, where Chinese and Russian colleagues have not only collaborated in revising many brachiopod groups but also willingly provided all contributors with relevant translations and illustrations that would otherwise have remained inaccessible.

These extraordinary increases in new genera were not the only consideration prompting a thorough revision of the 1965 edition. Brachiopod evolution and biology have also attracted keen interest among scientists other than taxonomists. Brachiopods are probably unique among metazoans in the continuity and diversity of their geologic record. They were well represented among the earliest

Cambrian fossil assemblages and quickly dominated most ecological niches available for sedentary benthos. By Ordovician times, they had attained maximum diversity in those stem groups determining the main lines of phyletic descent and had reached the peak of generic proliferation by the Devonian. Thereafter, these ciliary suspension filter feeders, notwithstanding their lower oxygen consumption rates, were increasingly displaced by the more efficient, filter-feeding and deposit-feeding molluscs as the dominant shellfish of most benthic environments. There is some evidence that brachiopod diversity, as measured by fluctuations in the numbers of contemporaneous genera recorded throughout the geological column, has been increasing since the end of the Mesozoic. Even so, fewer than 4 percent of the genera currently assigned to the phylum are represented by living species.

Living brachiopods, however, are modest only in the number of described species as they are cosmopolitan in distribution and intertidal to abyssal in habit. Moreover, although they have been sidetracked within the protostomous mainstream of metazoan phylogeny, which accounts for their comparative neglect by biologists throughout much of the twentieth century, their ubiquity in time and space has stimulated multidisciplinary research into evolutionary aspects of many of the biological systems of brachiopods. Within the last two decades there have been significant new biochemical, ecological, embryological, genetic, and physiological investigations that have radically changed our understanding of the phylum. Accounts of brachiopod anatomy and embryology were included in the first edition. They were, however, largely based on the studies of the great Victorian naturalists in Europe and North America. Unsurprisingly, many of these classical investigations have stood the test of time; but they were necessarily limited in scope (especially at the cytological level) and selective in their coverage of the main groups of living species.

Anatomical studies in particular have been used by paleontologists to understand the biological significance of fossil morphology and thereby furnish reconstructions of ancient life forms. Such enterprise can, however, lead to a blurring of the distinction between observation and interpretation. Even BEECHER's classification (1892), based on the nature of the pedicle opening, was founded on a mixture of published accounts of the embryology of the living shell and assumptions on the anatomical significance of the delthyrial structures of long extinct stocks.

This widespread practice is understandable as the overwhelming weight of evidence for brachiopod evolution is the shell morphology of extinct groups. But it raises presentational problems when one is attempting to cover the natural history of the phylum as a whole. Should the fossilized shell and the inferred secreting epithelium of extinct strophomenides, for example, be discussed in the context of mantle anatomy or primarily as a chemicostructural variant of the biomineralized component of the integument? The issue was addressed during the preparation of the first edition. It was agreed that skeletal morphology, the variability of which is dominated by extinct features, should be described separately from the anatomy of the shell. This separation has been criticized as a "regrettable symptom of the divorce between neontology and palaeontology" (RUDWICK, 1970, p. 10), without any apparent awareness of the importance of distinguishing between fact and inference. The issue was reconsidered when the layout of the revision was being formulated and no overriding reason emerged to break with precedence.

In the broader perspective of affording brachiopodologists access to both neontological and paleontological methods, the range of specialties of current contributors should be reassuring. Only one of the 19 authors of the first edition was not a paleontologist-taxonomist compared with ten of the 45 contributors to the revision. These

transdisciplinary investigations of all aspects of the phylum have already made their mark even on a classification founded on shell morphology, with familial lineages as well as the broad-frame taxonomic hierarchy being reviewed in the light of genomic studies. Indeed the multidisciplinary nature of much recent research on the phylum and its constituent species can be shown in a brief review of the changes in content and topic of this *Treatise* compared with the 1965 edition.

The anatomy section has been entirely rewritten to include the main features of post-1965 investigations, which account for more than two-thirds of the cited references. Basic advances have been made in our understanding of most aspects of brachiopod anatomy, not least of which are the digestive system and gametogenesis. Especially noteworthy for their impact on phylogenetic studies, however, are the processes of mantle secretion and the elucidation of crucial phases in the development of the craniid larva.

The section on the brachiopod genome, not surprisingly, is even more modern in conception and execution. The earliest known paper on brachiopod genetics did not appear until 1975 (AYALA & others, 1975), and of the hundred or so cited references only one work earlier than 1965 merits special mention—DARWIN'S *Origin of Species* (1859b). Indeed, the research into the genetic constitution of 30 brachiopod species, which was undertaken and described by the authors of the section, was not conceived until 1987. It has, therefore, been a noteworthy feat to have obtained results in time for their use in the preparation of a broad-frame classification of the phylum as well as for inclusion in this first volume of the revision.

The section on physiology and metabolism is new, not through neglect of the topics in the first edition but as a result of a recent burgeoning interest in the way brachiopods live, as is confirmed by the fact that 90 percent of cited references were published in 1965 or later. Much of this interest

has been stimulated by a growing desire to know how extinct groups functioned. Accordingly, research has tended to concentrate on those activities such as physiology of growth, musculature, and feeding that are more readily recognized as indicators of the life-styles and habits of fossil species.

Skeletal biochemistry and shell structure, in contrast, were described in the first edition, although they, too, are essentially modern studies so that the reviews herein are based largely on research undertaken since 1965. The brachiopod exoskeleton is rich in a wide range of organic polymers occurring as intracrystalline and intercrystalline components of differently structured apatitic and calcitic shells. This chemicostuctural differentiation of the shell is now being chronicled throughout brachiopod phylogeny, as recounted in those sections of this volume.

The section on morphology has changed the least since its publication in 1965. The heart of the section is the glossary of morphological terms. When these terms were collated for the first edition, more than 700 were found scattered throughout the literature. Many of them were being used idiosyncratically, and a large number were redundant to our understanding of shell morphology and even obscured homologous relationships. Spurred (and stung) by the comment that it is "habitual with paleontologists to create a formidable terminology to cover every minute detail of extinct exoskeletons" (HYMAN, 1959b, p. 525), authors heavily pruned the list, although about 500 terms survived—almost as many words as in the basic English vocabulary! Moreover, a few contributors refused to accept any economy of jargon and continued to use a personal vocabulary, to the detriment of the first edition. In preparing the revision, four versions of a continually revised glossary were circulated in the largely realized hope of achieving unanimity on the definition and selection of approved terms. Even so, nearly 500 of over 800 terms have survived scrutiny and are used in this edition. With respect to

the general part of the morphology section, the most significant improvements include the scrapping of a labyrinthine terminology to describe the loop based on generic names and intelligible to only a few specialists; a rationalization of terms used for homologous parts of various articulatory devices; and the application of a better understanding of shell structure to elucidate the growth and function of various features.

In revising the section on ecology, an important policy decision had to be made. The 1965 review touched upon brachiopods in their past and present habitats with an emphasis on autecological aspects. At the time it was recognized that the almost total neglect by zoologists of brachiopod ecology had left paleoecological studies without any rigorous comparative standards. As a result, much of what was then being reported in this field was of "dubious validity" (RUDWICK, 1965a, p. 199) and would have to be discarded in due course. Since 1965, there has been a most welcome interest in the ecology of living species although accompanied by a disproportionate increase in paleoecological studies. Some of the latter will undoubtedly prove to be based on sound inferences. Most, however, have been founded on more tenuous speculation, and their merits have yet to be rigorously tested by further evidence. Such literature is, therefore, potentially ephemeral, and it would presently be fortuitous to single out those studies that will emerge as models for future investigations. In these circumstances it was decided to restrict the ecological section of the revision to those interpretations, mainly autecological, that are firmly upheld by field and laboratory observations of living inarticulated as well as articulated species.

The organization of the rest of the revision has been changed in line with the sequence of processing the taxonomic data. The remaining volumes of this revision will carry brief forewords. In addition, the systematic descriptions of Volume 2 will be prefaced by an account of the classification of the phylum as a whole, while those of the final vol-

ume will end with sections on evolution and stratigraphic distribution that cannot be completed until the diagnoses and geological ranges of all taxa are known. Such reviews will benefit from the many novel studies published over the last thirty years that have further clarified the scope and pace of phylogenetic diversification, proliferation, and extinction. On the other hand, the greatest challenge of the entire revision has been to produce a classification that is compatible with brachiopod genealogy while facilitating routine identification, one of the main aims of the *Treatise*.

The classification used in this revision is a hybrid device. When the revision was launched in 1989, contributors recruited for the project were assigned genera in groups delineated in the original volume. In effect, the empirical classification of 1965, based on morphological comparison at successive levels in the hierarchy, determined the taxonomic content and structure of assignments. At the time it was confidently believed that most of these suprageneric packages would prove to be monophyletic. In contrast, ordinal relationships within the Brachiopoda had already become controversial (HENNIG, 1966; ROWELL, 1982; GORJANSKY & POPOV, 1986). It was therefore decided to erect a classification in two stages. First, contributors would be responsible for grouping genera up to the superfamilial or subordinal rank. Second, the coordinating author and deputies (A. WILLIAMS, S. J. CARLSON, and C. H. C. BRUNTON) would provide a broad-frame classification for all higher taxa founded on genera. At the outset it was agreed that classifications at all hierarchical levels would be phylogenetically structured. With this in mind, an essay review of phylogenetic systematics was circulated in 1991 among all contributors by S. J. CARLSON in the hope that those who were unfamiliar with phylogenetic analysis would be encouraged to adopt such techniques in classifying and describing their assigned taxa.

The outcome has been mixed, with some contributors using phylogenetic methods

(PAUP, MacClade) in processing their data (CARLSON, 1993b; POPOV & others, 1993; WILLIAMS & BRUNTON, 1993) and others relying on qualitative procedures (BAKER, 1990; CARTER & others, 1994; RONG & COCKS, 1994). Such a cautious reaction is understandable, as many of the morphological features used in brachiopod classification have evolved repeatedly in the past and have, thereby, introduced a high level of homoplasy into the intraordinal classification of extinct groups. Even so, the information freely made available by all contributors was so comprehensive as to afford a unique opportunity to test the versatility of the revised, supraordinal classification (WILLIAMS & others, 1996). This broad-frame classification, which is mainly based on the anatomy and skeleton of living species, is compatible not only with orders erected on shell morphology for extinct groups throughout the geological record but also with the brachiopod genome as it is presently known. Whether new biological or paleontological evidence will prompt such profound reinterpretation of the homology or polarity of characters as to undermine this supraordinal classification remains to be seen. For the present, at least, the systematic descriptions presented in this revision of Part H on the Brachiopoda are set in a classification consistent with our current understanding of brachiopod phylogeny.

ACKNOWLEDGMENTS

This revision of Part H on the Brachiopoda was completed over a period of about eight years, by 45 contributors from thirteen countries. During that time all of us, almost without exception, enjoyed the support of various institutions—mainly our places of employment—universities, museums, marine stations, geological (and other) surveys and so on. We are indebted to such centers for providing the wide-ranging facilities that enabled us to complete our assignments. Most contributors have also benefitted from advice and gifts and loans of materials received from a host of experts and have had

access to type collections throughout the world. These invaluable sources of information are too numerous to be listed here. Specific acknowledgments will be made in the forewords to the remaining volumes and, with regard to illustrations and loaned specimens, at the appropriate places in the text of the systematic descriptions.

There are a few persons and institutions meriting special mention at this juncture for their notable contributions to the progression of the project as a whole. Pride of place goes to Mr. R. A. Doescher of the Smithsonian Institution, Washington, D.C. and Mrs. S. Ogden at the University of Glasgow. Rex Doescher maintained the unique, computerized database on brachiopod taxa and literature (SIBIC, Smithsonian International Brachiopod Information Center), which owes its origin to Dr. G. Arthur Cooper and his wife Josephine, who for decades translated Russian (and other) taxonomic descriptions of brachiopods for general use by any student of the phylum. The database has ensured that all contributors, directly or through Glasgow, have been provided with the essential data on every proposed brachiopod genus. Sue Ogden maintained a continually updated variant of SIBIC in Glasgow, with the genera grouped into families and superfamilies and packaged according to assignments. She compiled annual returns for four years as integrated reports for circulation among contributors, which gave snapshot views of the progress of work in all its aspects. The accuracy and expedition of this revision are a testament to the dedication of these two colleagues.

In addition to institutional support, many contributors have also been awarded grants by research councils, foundations, learned societies, philanthropic trusts, and industry to undertake research and to visit museums and universities at home and abroad in connection with their *Treatise* assignments. Among the awards made in support of research programs were National Science Foundation grants (BSR 8717424 and DEB 9221453) to S. J. Carlson; grants from the

Swedish Natural Science Research Council, the Royal Swedish Academy of Sciences, and the Swedish Institute to L. Holmer and L. Popov; a grant from the University of Kansas Paleontological Institute to E. Owen; grants from the Royal Society to G. B. Curry, M. Cusack, and A. Williams; a grant from Natural Sciences and Engineering Research Council of Canada to P. Copper; grants from the Natural Environment Research Council to B. L. Cohen, G. B. Curry, M. Cusack, and A. Williams; grants from the Leverhulme Trust (F 179Z) and British Petroleum plc to A. Williams; a grant from the Richard Lounsberry Foundation to G. B. Curry; and a grant from the International Science Foundation, Washington, D.C., to T. Smirnova.

Awards toward expenses of travel and

accommodation incurred during *Treatise* business included a grant from the Swedish Natural Science Research Council to M. Bassett, J. Laurie, and L. Popov; grants from the Natural Environment Research Council to nine British contributors; grants from the Royal Society of New Zealand to D. Lee; grants from the Royal Society of London to S. Lazarev, M. Mancenido, and A. Williams; grants from the University of Kansas Paleontological Institute and the Smithsonian Institution to N. Savage and from the latter source to L. Popov; and grants from the Consejo Nacional de Investigaciones Cientificas y Tecnicas of Argentina (CONICET) to M. Mancenido and the Royal Society of Edinburgh and the Carnegie Trust to A. Williams.

ANATOMY

ALWYN WILLIAMS¹, MARK A. JAMES², CHRISTIAN C. EMIG³, SARAH MACKAY¹, and
MELISSA C. RHODES⁴

[¹University of Glasgow; ²Ministry of Agriculture, Fisheries, and Food, London; ³Centre d'Océanologie de Marseille; ⁴Academy of Natural Sciences, Philadelphia]

GENERAL CHARACTERS

The soft parts of all living brachiopods (HANCOCK, 1859) are enclosed by a shell consisting of a pair of valves that typically are bilaterally symmetrical but dissimilar in size, shape, and even ornamentation. Posteriorly, the shell usually bears a variably developed fleshy stalk, the **pedicle**, which normally emerges from the **ventral** (or pedicle) valve (Fig. 1). The opposing valve, the **dorsal** (or brachial) valve, is generally smaller than the ventral valve. The body occupies the posterior part of the space inside the shell, and its wall is prolonged forward and folded as a pair of **mantles** that line the anterior inner surfaces of the valves to enclose the **mantle**

(or brachial) **cavity** (Fig. 2). The body space (**coelomic cavity**) accommodates the digestive, excretory, and reproductive organs as well as muscle systems, some of which are responsible for movements of the valves relative to each other, including the opening of the shell (**gape**). The mantle cavity is separated from the body by the **anterior body wall** and contains the feeding organ or **lophophore** (Fig. 1–2). A nervous system and a primitive circulatory system are present.

Although the Brachiopoda are well defined as a phylum, living species segregate into three groups differing fundamentally in their development, anatomy, and gross morphology. **Articulated brachiopods** have invariably calcitic shells, with valves

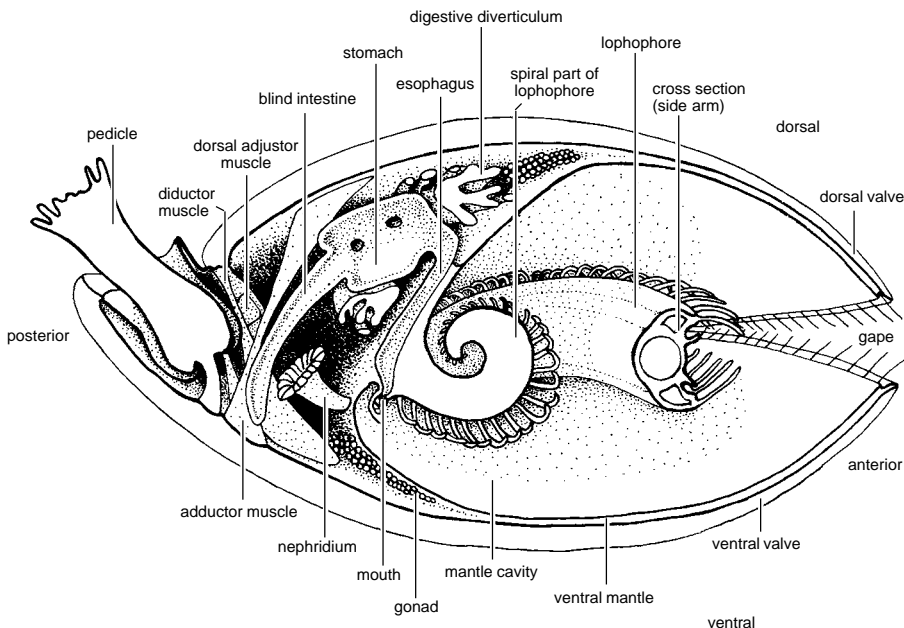


FIG. 1. Diagrammatic representation of the principal organs of the brachiopod as typified by *Terebratulina* (Williams & Rowell, 1965a).

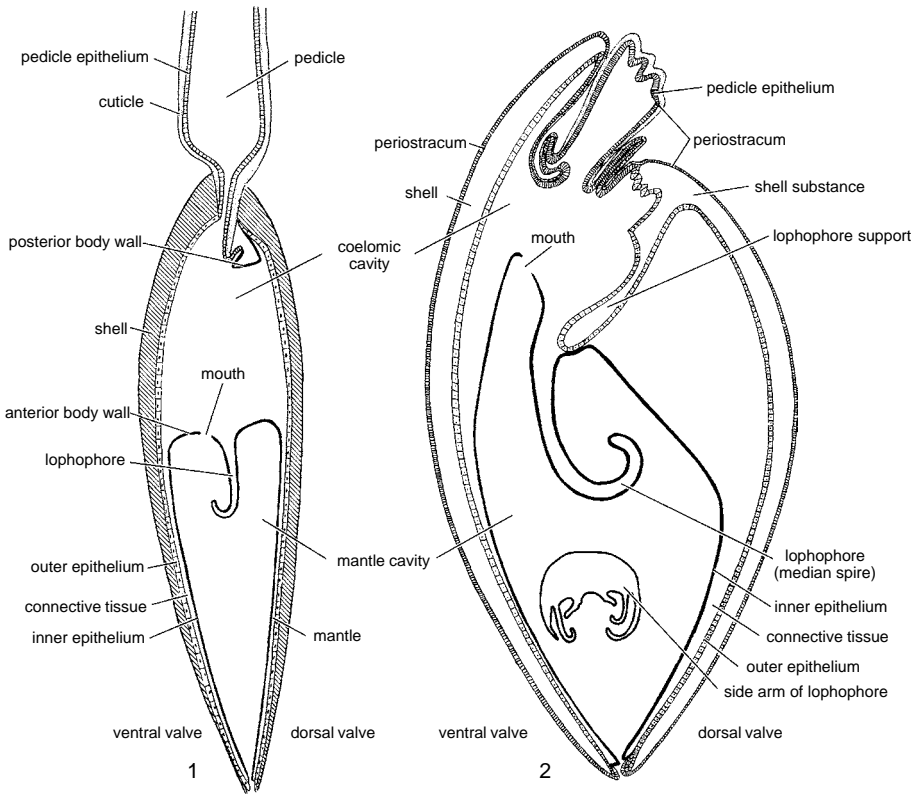


FIG. 2. Generalized representation of the distribution of epithelium 1, in lingulids (Williams & Rowell, 1965a) and 2, in terebratulids (Williams, 1956).

interlocking by **complementary teeth and sockets**; the dorsal valve is commonly equipped with outgrowths forming lophophore supports (Fig. 2.2). All organophosphatic-shelled brachiopods (lingulides and discinides) and the carbonate-shelled craniides are inarticulated with no biomineralized outgrowths developed for articulation or lophophore support. The lack of articulation permits rotation in the plane of the margins or **commissure**, and the musculature of inarticulated species is usually relatively complex. Other internal differences are even more profound. The pedicle of living articulated brachiopods develops from a primary segment of the larva, while that of the lingulides and discinides arises from evaginations of the ventral mantle. Living craniides lack even a rudimentary pedicle. The lingulides and discinides and the craniides are also distin-

guishable from one another as well as from articulated species in other respects. The biomineral constituents of their shells are apatite and calcite respectively with further significant differences in the organic content, especially the presence of chitin and collagen in the lingulide shell. Distinguishing features of the development and anatomy of the soft parts include differently disposed intestines (NIELSEN, 1991) and the loss of the anus among living articulated brachiopods.

In contrast to the wide diversity of most other anatomical features, the body wall of all brachiopods consists of an outer layer of ectodermal **epithelium** resting on a thin connective-tissue layer coated internally by a ciliated coelomic epithelium (peritoneum). In the mantles, coelomic epithelium is restricted in distribution, being limited to sinuses of the coelomic space permeating the

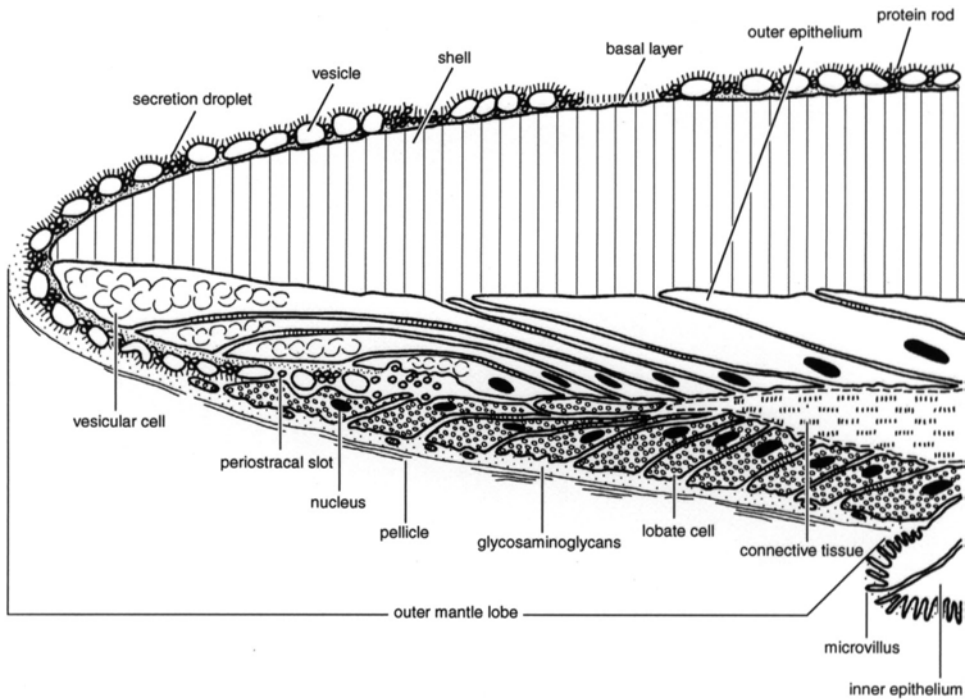


FIG. 3. Diagrammatic sagittal section of a valve of the terebratulide *Calloria* to show the outer mantle lobe in relation to the vesicles and basal layer of the periostracum and the underlying calcareous shell (adapted from Williams, 1990).

connective tissue (**mantle canals**) and unconnected marginal sinuses just within the mantle edges of organophosphatic brachiopods. The ectodermal epithelium is morphologically and functionally differentiated into a number of distinctive types. Posteriorly, it underlies and secretes a cuticular cover for the pedicle and is known as **pedicle epithelium** (Fig. 2). The zones responsible for the secretion of the biomineralized valves are referred to as **outer epithelium**. They are separated from the **inner epithelium** lining the mantle cavity by narrow strips of highly modified epithelium (**vesicular** and **lobate cells**) secreting various organic compounds, which occupy the hinge of the fold at the margins of both mantles. Within the mantle cavity, the inner epithelium is continuous with the selectively ciliated lophophore epithelium.

The adaptation of the ectoderm to secrete a biomineralized shell with outgrowths commonly of a complex nature occurred very

early in the Phanerozoic so that the brachiopod phylum is well represented by a more or less continuous, fossilized skeletal record. Accordingly, it seems appropriate to begin this account of brachiopod anatomy with a description of the morphology and function of the ectodermal epithelium.

MANTLES AND BODY WALLS

The outer epithelium, which underlies the brachiopod shell and envelops its outgrowths, is continuous with the inner epithelium along the mantle margin. The junction almost invariably lies in a groove between two asymmetrical mantle lobes just within the shell edge (Fig. 3) and is a reference-datum horizon in describing the differentiation of the mantle. These epithelial sheets are separated by a layer of connective tissue that is invaded to a varying degree by extensions (mantle sinuses or canals) of the coelom and further modified to facilitate storage and stiffening.

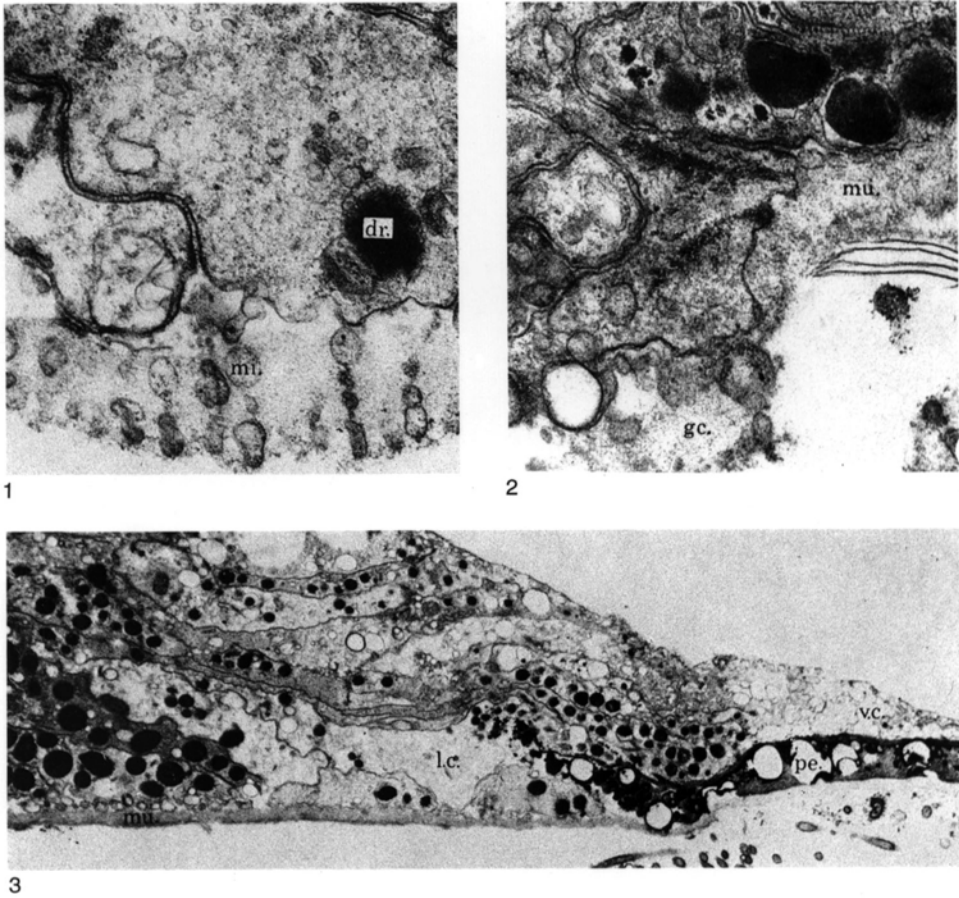


FIG. 4. TEM micrograph of mantle edge and periostracum of *Calloria inconspicua* (SOWERBY); 1, inner epithelial cells (adjacent to lobate cells) bearing short microvilli (*mi*) and electron-dense droplets (*dr*), $\times 36,000$; 2, detail of the inner epithelium-lobate cell junction showing the disappearance of microvilli from the lobate cell apical plasmalemma and the continuation of the glycocalyx (*gc*) into the GAGs film (*mu*) of the lobate cells with pellicles to the exterior, $\times 36,000$; 3, sagittal section of the mantle edge showing the periostracum (*pe*) emerging from a slot between the lobate cells (*lc*) secreting a GAGs film (*mu*) and the vesicular cells (*vc*), $\times 3,600$ (Williams & Mackay, 1978).

INNER EPITHELIUM AND CONNECTIVE TISSUE

The **inner lobe** at the mantle margin is a circumferential fold of inner epithelium. This layer typically consists of cuboidal, microvillous, monociliated cells with plasmalemmas disposed in folds especially adjacent to the basal lamina and well-developed, smooth endoplasmic reticulum, mitochondria, and Golgi complexes (Fig. 4.1). Vesicles and membrane-bound droplets of varying electron density, representing glycoproteins, lipids, and glycosaminoglycans (GAGs), are

common. These inclusions, together with the products of widely distributed mucous cells are constantly exocytosed so that the fibrillar coats of the microvilli are always impregnated with a glycocalyx of variable electron density. The columnar cells of the inner mantle lobe lack cilia and are commonly distended with crowded vesicles of mucus (the gland cells of *Lingula* and *Discinisca*) but are regularly microvillous and represent marginal folds of inner epithelium (Fig. 4.1).

The connective tissue, enclosed within the basal laminae of both inner and outer

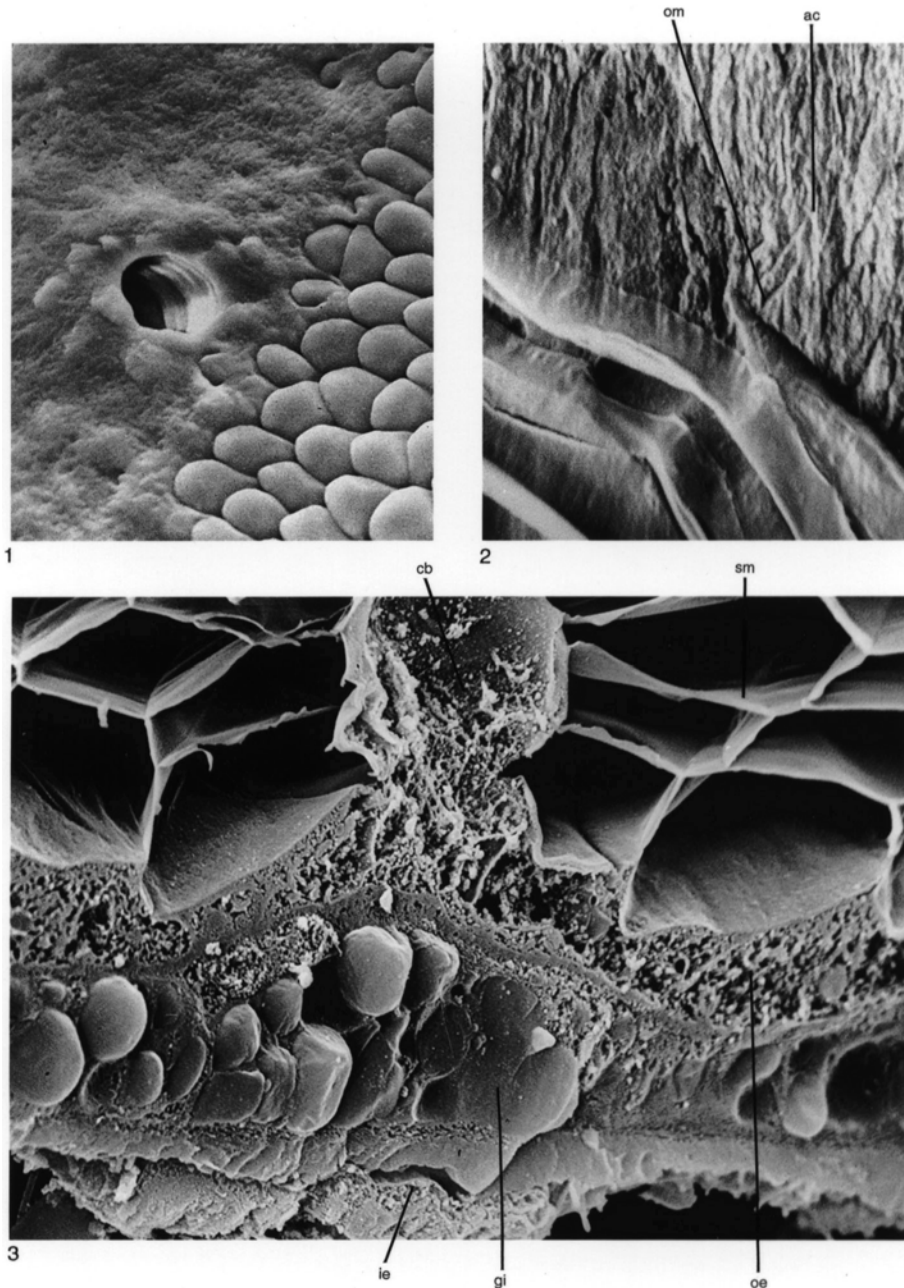


FIG. 5. Terebratulide secondary shell. 1, SEM micrograph of the internal edge of a dorsal valve of *Gryphus vitreus* (BÖRN) showing the primary-secondary shell junction with incipient fibers forming on the granular primary layer to the left, especially around the puncta, $\times 1,235$; 2, SEM micrograph of an etched submedian longitudinal section of the shell of *Liothyrella neozelanica* THOMSON showing acicular crystallites (*ac*) of the primary shell terminating at oblique, smooth boundaries representing the onset (*om*) of the membranes sheathing the secondary fibers below, $\times 6,840$; 3, SEM micrograph of cryoprotected and etched fracture surface of the mantle underlying a caecal base (*cb*) and the surrounding shell of *Calloria inconspicua*, showing interconnected membranes (*sm*) of the fibrous secondary layer and the collagenous storage zone with glycoprotein inclusions (*gi*), with the connective tissue between outer (*oe*) and inner (*ie*) epithelium, $\times 3,895$ (new).

epithelia, is the typical extracellular matrix composed mainly of GAGs and fibrous collagens. The alignment of collagens is normally determined by localized stresses set up, for example, by penetrating distributaries of the mantle canal systems or by biomineralized bodies (**spicules**) secreted by clusters of mesenchymous cells (scleroblasts). Distension by such cavities and bodies tends to pack collagens into concentric swarms; and, where large sinuses are developed (as in the *vascula genitalia*), the connective tissue is compacted into columns subtended between the bounding epithelia. The most distinctive feature of the connective tissue in the brachiopod mantle, however, is a highly collagenous zone beneath the outer epithelium (HARO, 1963). Numerous lacunae within this zone usually contain membrane-free glycoproteins, glycogen granules, and, in *Glottidia* at least, other granules of a biomineral nature (PAN & WATABE, 1988a). The zone is evidently an important storage site (Fig. 5.3).

OUTER EPITHELIUM: OUTER MANTLE LOBE

The **outer mantle lobe** is a fold of outer epithelium that underlies the edge of the valve and forms the circumferential hinge of the mantle. The lobe controls the expansion of the mantle that lines a valve and, therefore, the peripheral growth of the valve itself. An outer lobe is composed of variously specialized secretory cells that are best illustrated by describing how components of a terebratulide integument are deposited in successive layers by the outer mantle lobe of *Calloria*.

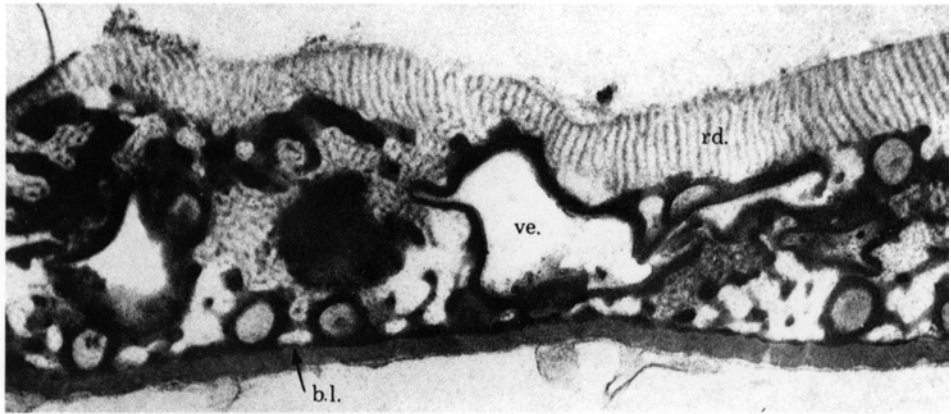
In *Calloria* (WILLIAMS & MACKAY, 1978) the proximal inner surface of the outer mantle lobe is composed of a band of lobate cells, 10 to 12 deep in sagittal section. The

lobate cells are distinguishable from adjacent inner epithelium: their secretory plasmalemmas are not regularly microvillous but disposed as irregular folds and protuberances, up to 0.5 μm long (Fig. 4.2–4.3; 6.2). They contain small and large vesicles, well-developed Golgi systems, and an increased number of electron-dense, membrane-bound droplets that are prominent among the constituents exocytosed at the apical plasmalemmas as a film of mucus bounded externally by impersistent, lightly fibrillar sheets lying in parallel packs. The film rolls forward to the edge of the outer mantle lobe and covers the **periostracum** proper.

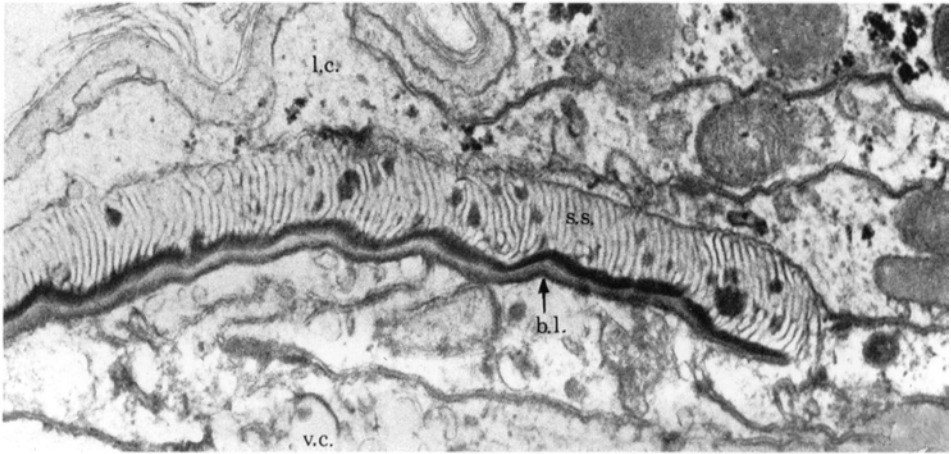
The periostracum arises in a slot, up to 20 μm deep, separating the more distant lobate cells from four or five elongate vesicular cells that occupy the hinge of the outer mantle lobe (Fig. 4.3; 6.3). These cells overlap one another as tongue-like extensions and are distinguishable from the lobate cells in being crowded with vesicles that usually culminate in one, large structure immediately beneath the apical plasmalemma. In other respects, lobate and vesicular cells are very much alike, being characterized by an abundance of glycogen, the folded and cylindroid extensions of their secretory plasmalemmas, and the rarity of tight junctions between crudely fitting adjacent cells.

The **periostracal slot** is variably developed in other brachiopod groups. It is deeply inserted between vesicular and lobate cells in thecideidines (WILLIAMS, 1973) but is only a superficial indentation separating the vesicular and lobate cells of the rhynchonellide outer mantle lobe (WILLIAMS, 1977). The unarticulated lingulids also lack a periostracal slot but have previously been described as having a few lobate cells (WILLIAMS, 1977). In fact, these lobate cells are distinguishable

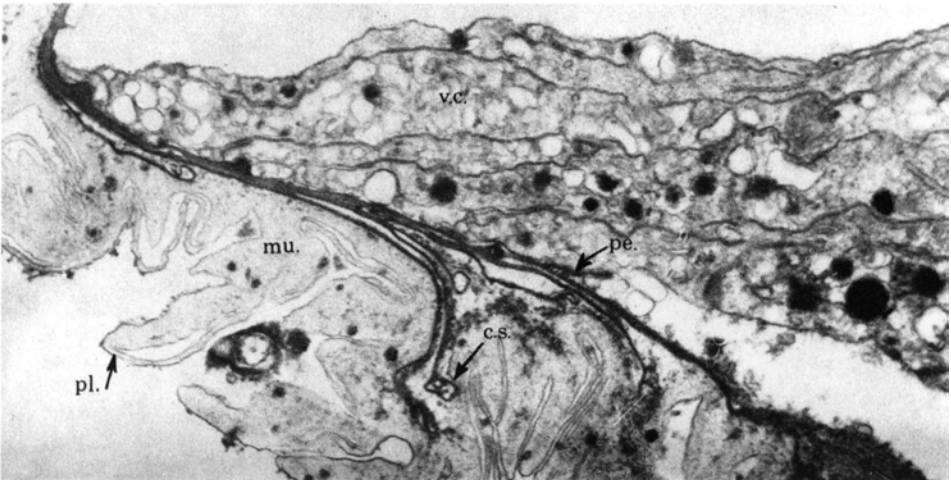
FIG. 6. TEM micrographs of the periostraca of various terebratulide brachiopods; 1, periostracum of young *Calloria inconspicua* showing the basal layer (*b.l.*), vesicle (*ve*) surrounded by amalgamated droplets and the outer fringe of electron-dense rods (*rd*), $\times 36,000$; 2, periostracum of *Gwynia capsula* (JEFFREYS) arising between lobate cells (*l.c.*) and vesicular cells (*v.c.*) and consisting of a basal layer (*b.l.*) and an isoclinally folded, sheeted superstructure (*s.s.*), $\times 36,000$; 3, vesicular cells (*v.c.*) at the mantle edge of *Terebratulina retusa* (LINNE) bounded externally with periostracum (*pe*) extended into curled sheets (*cs*), within folds of a film of GAGs (*mu*) with an external polymerized pellicle (*pl*), $\times 9,000$ (Williams & Mackay, 1978).



1



2



3

FIG. 6. (For explanation, see facing page.)

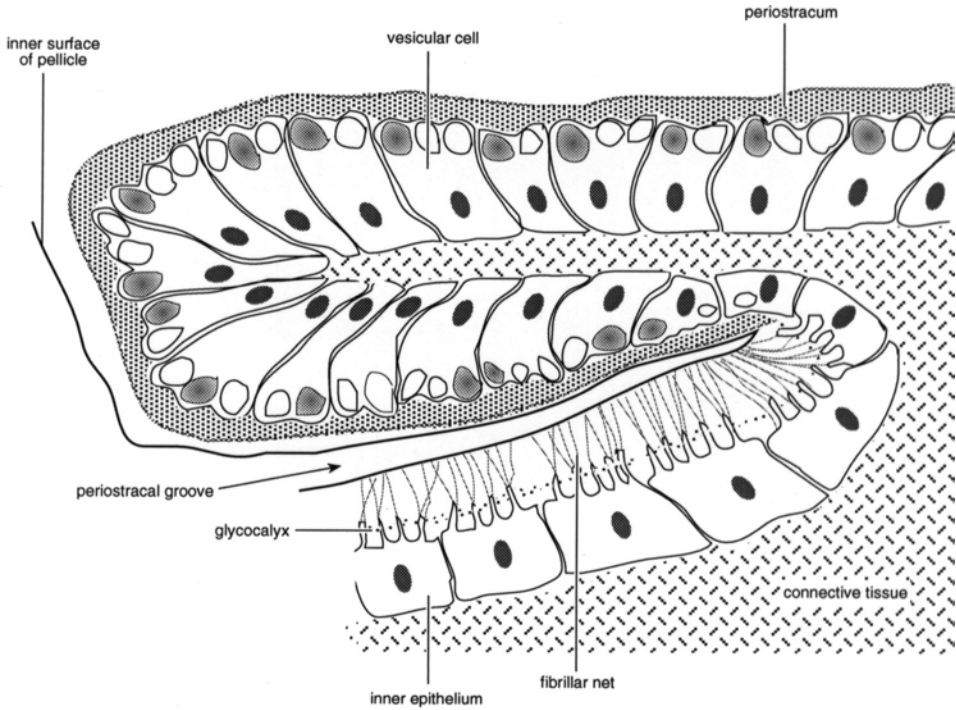


FIG. 7. Diagrammatic sagittal section of the edge of a valve of *Glottidia pyramidata* (STIMPSON) illustrating the differentiation of the periostracal lobe in relation to the inner epithelium (new).

from inner epithelium only in having shorter microvilli. Moreover, in discinids as well as lingulids, these cells act in unison with the inner epithelium in secreting the external surface of the pellicle, which is made up of fibrous constituents streaming from all microvillous plasmalemmas (Fig. 7–8). On balance, they are probably a modified fringe of inner epithelium along the junction with vesicular cells. This is also true of the inarticulated craniids (WILLIAMS & MACKAY, 1979).

The periostracum is a highly variable structure. In *Calloria*, the vesicular cells secrete a basal, electron-dense layer that thickens anteriorly away from its zone of origin by accretion on its proximal surface, which is consequently more irregular and less sharply defined than the distal surface (Fig. 3; 4.3). Indeed, the distal surface tends to be delineated as an electron-dense boundary underlain by a light layer to simulate a unit mem-

brane about 20 nm thick. The entire layer ultimately attains a thickness of 100 nm before its proximal surface becomes the seeding sheet for the first-formed calcite crystallites of the primary carbonate layer of the shell.

As this basal layer is being exuded, large vesicles and clusters of smaller droplets accumulate on the inner surface (Fig. 6.1). The vesicles, which may be up to 1 μm in diameter, are usually stacked in densely packed groups so that they assume distorted outlines in sections. They are exocytosed through the plasmalemmas of the lobate cells forming the inner boundary to the periostracal slot. As the periostracum matures, the accumulating droplets tend to be emptied of their contents, which form accretionary layers of variable thickness around the vesicles and the droplets to give a labyrinthine aspect to these amalgamated bodies. In addition, the labyrinths are filled by an exudation that quickly polymerizes into regular, closely packed hex-

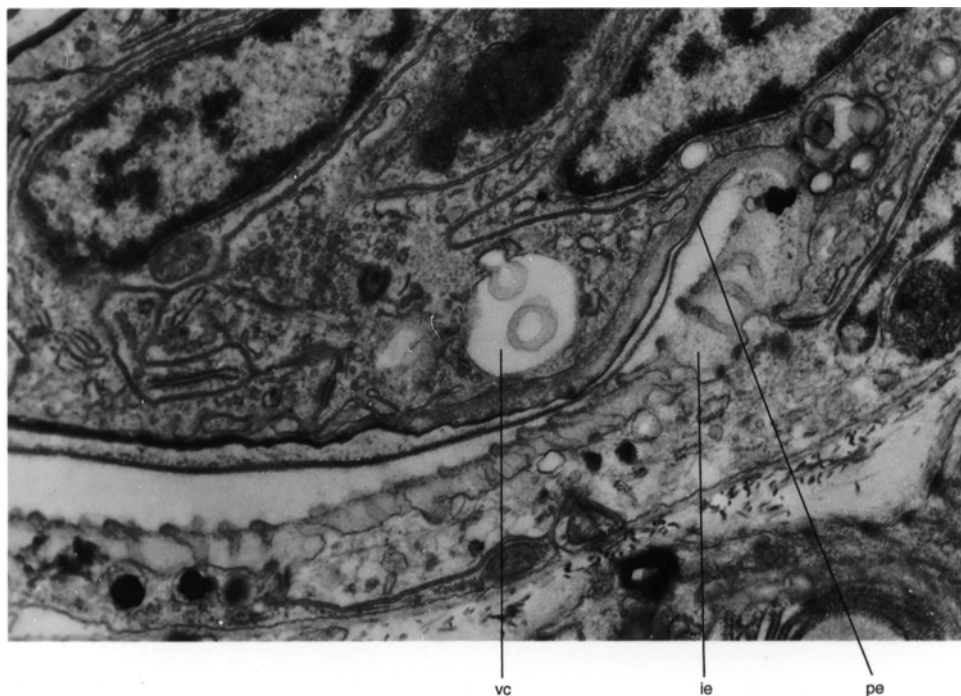


FIG. 8. TEM micrograph of the periostracal groove of *Lingula anatina* LAMARCK showing the origin of the double-layered pellicle (*pe*) secreted by inner epithelium (*ie*) and vesicular cells (*vc*), and the underlying periostracum, $\times 24,000$ (new).

agonal rays of medium, electron-dense rods. The rods bear signs of being spirally constructed and of being joined to one another by fine fibrillar webs. This fibrillar matrix seems to be exuded by lobate cells in adults (WILLIAMS & MACKAY, 1978), but STRICKER and REED (1985a) have not ruled out the possibility that it can also be secreted (as can some vesicles) by vesicular cells, at least in juveniles.

Either way, a periostracum of varying complexity is continuously built up beneath the outer mucous film and is conveyed forward to the very edge of the outer mantle lobe. In *Calloria* and other terebratelloids, the periostracal succession is, therefore, a diachronous one consisting of a labyrinthine superstructure and a thickening basal layer that are secreted simultaneously on the outer and inner surfaces of the first-formed membranous component by the lobate and vesicular cells respectively (Fig. 9). It is note-

worthy, however, in view of the limited variability of the periostracum of living species, that the terebratelloid labyrinthine superstructure, although characteristic of adult *Terebratalia*, is absent from the protogular periostracum, which is nothing more than a thin, amorphous, basal layer bearing a few electron-dense spheroidal bodies (STRICKER & REED, 1985b).

The terebratelloid periostracal succession is among the most complex so far known in living brachiopods as both superstructure and basal layer have been found to be variable (Fig. 9), although not below superfamilial rank (WILLIAMS & MACKAY, 1979). Thus, the superstructure may be absent as in the lingulids, craniids, rhynchonellids, and thecideidines. It is also absent from the periostracum of *Terebratulina*, which consists essentially of successions of sheets of the basal layer (Fig. 6.3), although in *Liothyrella* small, electron-dense secretion droplets are

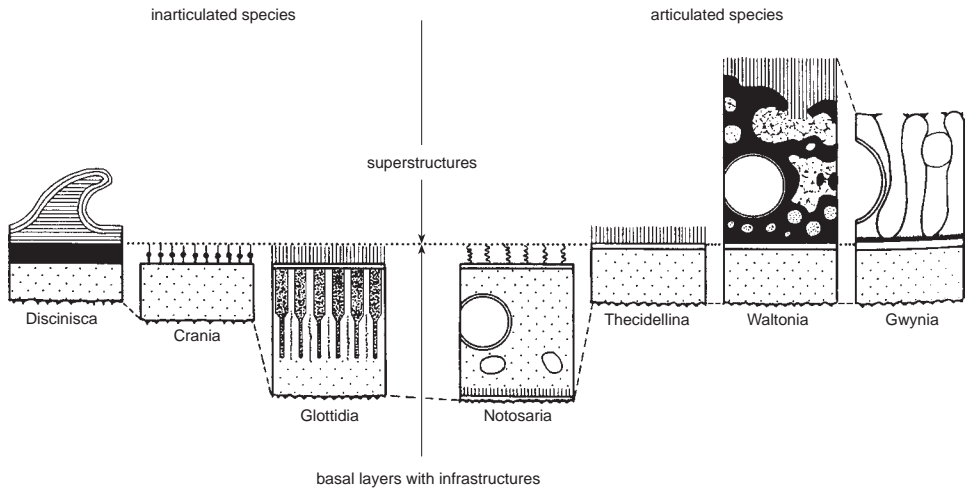


FIG. 9. The main types of periostraca characterizing inarticulated and articulated brachiopods (Williams & Mackay, 1979).

sporadically distributed on the external surface (comparable with the protegular periostracum of *Terebratalia*) and are secreted by lobate cells in the same way as the elaborate superstructure of *Calloria*. Moreover, both the enigmatic terebratulide *Gwynia* and the organophosphatic discinids have complex superstructures consisting respectively of folded proteinaceous sheets disposed normal to the basal layer (Fig. 6.2) and of concentric bands with thickened bases composed of up to 100 or so, electron-dense, fibrillar sheets disposed almost parallel with the basal layer (Fig. 10.1).

The basal layer can also consist of a variety of proteinaceous compounds, which, when banded, form chronological successions. The basal layer of the thecideidines consists of a simple, thickened membrane. That of the craniids is also essentially little more than a membrane with an outer coat of bulbous-tipped, fibrillar rods up to 30 nm high. In lingulids the distal surface of the basal layer polymerizes almost immediately after exudation into a coarsely fibrillar, unit membrane bounding a gradually thickening, medium, electron-dense, finely textured layer. When this inner layer attains a thickness of about 250 nm, internal differentia-

tion takes place (Fig. 10.2). Linear arrangements of electron-dense bodies disposed at high angles to the external surface polymerize out of the matrix and, as polymerization spreads inwardly, the thickening periostracum becomes three layered. In a fully developed periostracum, which may be 5 or 6 μm thick, the outer layer consists of hexagonally stacked, electron-dense rods separated by partitions, while a medium, electron-dense layer shares an irregular, interdigitating boundary with an inner, electron-light, somewhat fibrillar layer. The composition and distribution of these different components have not yet been determined although the lingulid periostracum is reported as being mainly a glycine-poor protein with some traces of chitin and hydroxyproline (JOPE, 1965). The basal layer of the rhynchonellid *Notosaria*, which may be up to 1 μm thick, is also differentiated. It consists of an outer, bounding, unit membrane with coiled fibrils in rhombic arrays; a main layer composed mainly of GAGs with scattered membrane-bounded vesicles; and vertically arranged fibrils and an inner bounding membrane.

In calcareous-shelled brachiopods, secretion of the periostracum is completed by the time it has been conveyed to the edge of the

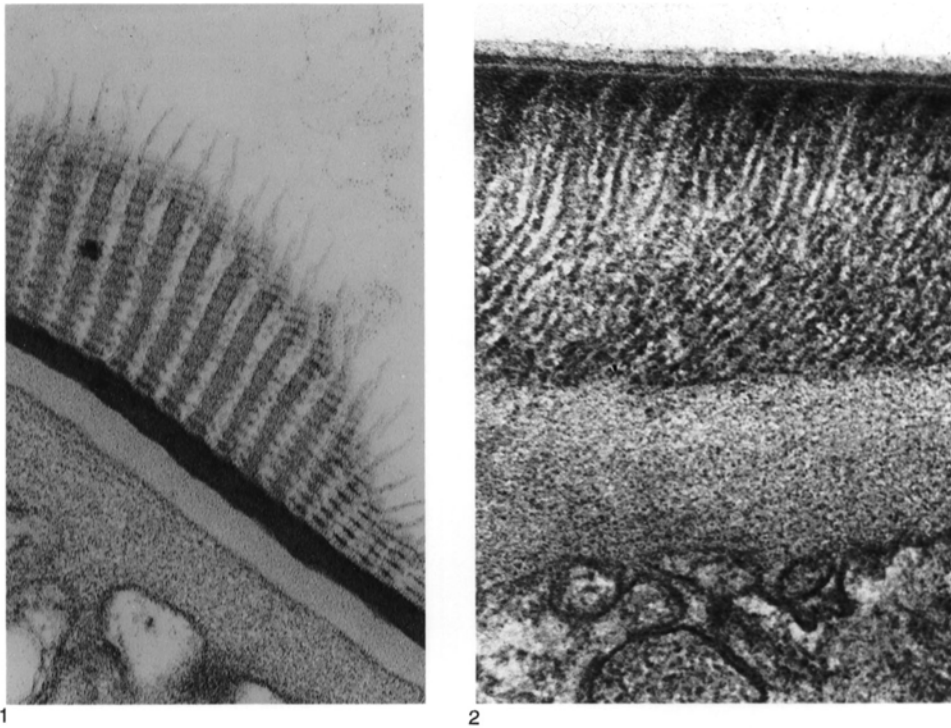


FIG. 10. TEM micrographs of the periostraca of organophosphatic brachiopods; 1, periostracum of *Discina striata* (SCHUMACHER) consisting of a sheeted superstructure and thickened, electron-dense basal layer underlain by the beginnings of a mainly organic primary layer secreted by protuberances of the apical plasmalemma, $\times 32,550$; 2, periostracum of mature *Glottidia pyramidata* showing the outer (top) layer of hexagonally stacked, electron-dense rods separated by partitions becoming less well defined internally and sharing an irregular boundary with an inner, electron-light layer being secreted by protuberances of the apical plasmalemmas (bottom), $\times 98,580$ (new).

outer mantle lobe. As it rotates around the hinge of the mantle to become an integral part of the expanding shell, isolated calcite rhombs are secreted on the proximal surface of the basal layer. The subsequent sequence in the secretion of the brachiopod integument is well known through the studies of the craniids (WILLIAMS & WRIGHT, 1970), the thecideidines (WILLIAMS, 1973), terebratulides including *Calloria* (WILLIAMS, 1968b; WILLIAMS & MACKAY, 1978; STRICKER & REED, 1985a, 1985b), and especially the rhynchonellide *Notosaria*, which, on account of the simplicity of the succession, may be taken as the standard sequence (WILLIAMS, 1968d).

As calcite rhombs continue to increase in number and size through further nucleation

and accretion, they amalgamate with one another to form a layer of inclined crystallites with sporadic lenticular patches (Fig. 11). This is the **primary shell layer**, which is featureless except for **growth banding** and high-angled breaks presumably corresponding to intercellular spaces in the secreting plasmalemmas. No organic traces other than those related to the retraction and advance of the mantle edge have yet been seen, but that does not preclude the existence of intracrystalline, water-soluble compounds. The cells responsible for the secretion of this layer form a well-defined band transitional between the elongate vesicular cells and the typical cuboidal cells of outer epithelium. In addition to being less elongate than the vesicular cells, those underlying the primary

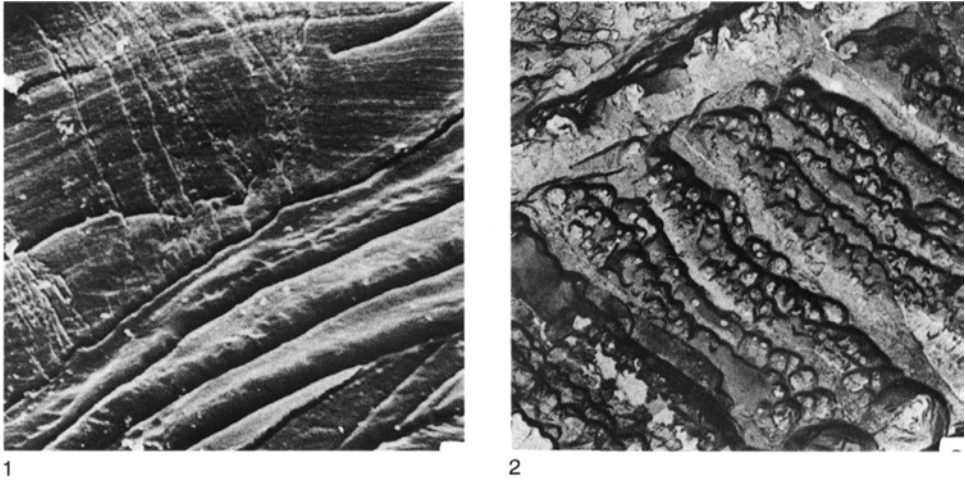


FIG. 11. SEM and TEM micrographs of the primary layer of *Notosaria nigricans* (SOWERBY); 1, section showing the growth banding in the primary shell and its junction with secondary fibers, $\times 2,500$; 2, external surface immediately below the periostracum, $\times 6,800$ (Williams, 1971a).

shell have fewer membrane-bound vesicles and smoother secretory plasmalemmas (Fig. 12).

OUTER EPITHELIUM OF CALCITIC SHELLS

As deposition of the primary layer proceeds, the secreting cells become increasingly separated from the periostracum. At a given distance behind the edge of the outer mantle lobe, however, the outer epithelial cells start secreting the organocalcitic secondary layer. The distance within the valve margin, at which secretion of the secondary layer is initiated, determines the thickness of the primary layer. The thickness varies not only from one species to another but also during ontogeny. In *Notosaria* the maximum thickness of the primary layer has been calculated as increasing more or less steadily from the umbo by about $12\ \mu\text{m}$ per mm of surface length (WILLIAMS, 1971a).

The first sign of **secondary shell** deposition on the internal surface of a valve is the occurrence of impersistent membranous strips adhering to the carbonate surface (Fig. 5.1). Each strip is the first-formed part of a membrane, about $10\ \text{nm}$ thick, exuded along an arcuate anterior zone of the secret-

ing plasmalemma of a cell. The membrane acts as a seeding sheet for calcite being secreted by the posterior part of the plasmalemma. Moreover, the outer epithelium underlying the secondary layer consists of outwardly inclined, cuboidal cells regularly arranged in alternating rows. Consequently, the membranes, spun out by adjacent cells, join up with one another so that the calcite of the secondary cell becomes segregated into a series of **fibers** (Fig. 5.2), each ensheathed in interconnected membranes (Fig. 5.3) and with its terminal face contained by the posterior part of the apical plasmalemma. The fibers are usually inclined at about 10° to the diachronous interface with the primary layer. They each have a distinctive, anvil-shaped cross section reflecting the posterior concavity of the secreting plasmalemma and occur in characteristically stacked series. The microtexture of a fiber is typically granular with a rough, pitted terminal face in complement to the microscopic protuberances of the apical plasmalemma (WILLIAMS, 1968a; GASPARD, 1986) and with smoothed surfaces corresponding to enclosing membranous sheaths.

Fibers continue to lengthen so long as their controlling cells continue to secrete

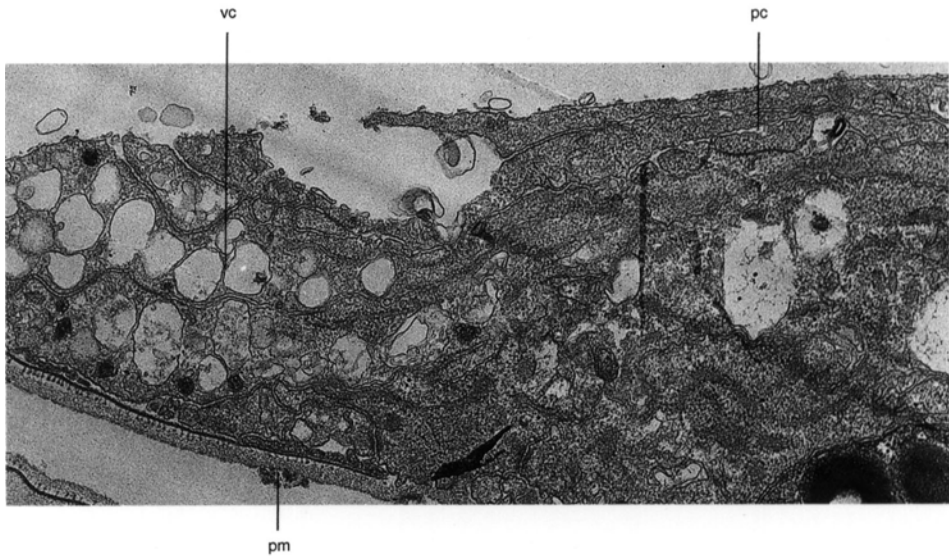


FIG. 12. TEM of the mantle edge of *Notosaria nigricans* showing the cells (*pc*) secreting primary shell (removed by decalcification of the section) in relation to vesicular vells (*vc*) and periostracum (*pm*), $\times 7,500$ (new).

protein and calcite (WILLIAMS, 1966, 1968a; GASPARD, 1986). Accordingly, the secondary layer is normally thickest posteromedially at the site of the oldest cells. All internal skeletal features (except spicules, described below) are composed of secondary shell.

The apical plasmalemma of a typical, outer epithelial cell, which secretes the secondary layer, is devoid of cilia and regular microvilli. It is, however, normally studded with an anterior arc of hemidesmosomes (Fig. 13). These are terminations of bundles of filaments extending to the basal lamina. Their fibrous constituents are probably incorporated into the proteinaceous membranes ensheathing the calcitic fibers, to which they are attached. Posteriorly, the apical plasmalemma is usually ruffled into low-lying protuberances, up to 150 nm long, with an adherent, discontinuous membrane. Membrane-bound droplets of glycoprotein and GAGs occur but less frequently than in the inner epithelium, while rough, endoplasmic reticulum is normally much more conspicuous than the smooth.

The skeletal succession and outer epithelium just described are characteristic of most

living brachiopods with calcitic fibrous shell. There are, however, two groups with significantly different secretory regimes, as revealed in changes in the outer epithelium as well as the integument.

The carbonate skeleton of the living thecididines, *Lacazella* and *Thecidellina*, mainly consists of a primary layer of acicular and granular calcite with growth banding bearing frequent signs of interrupted accretion or absorption and widely distributed microscopic features, such as tubercles and closely packed rhombic blocks, on the internal surfaces of mature shells (Fig. 14). The only traces of orthodoxly stacked secondary fibers with proteinaceous sheaths occur on the teeth and socket ridges and the tubercles (WILLIAMS, 1973). The outer epithelium secreting this persistent primary layer consists of flat, cuboidal cells with large composite inclusions of glycoprotein, and it varies greatly in thickness, being attenuated and thickened over tubercles and mantle canals respectively (Fig. 15.1). A conspicuous feature of the secretory surface of the outer epithelium is the presence of a medium electron-dense discontinuous layer about as

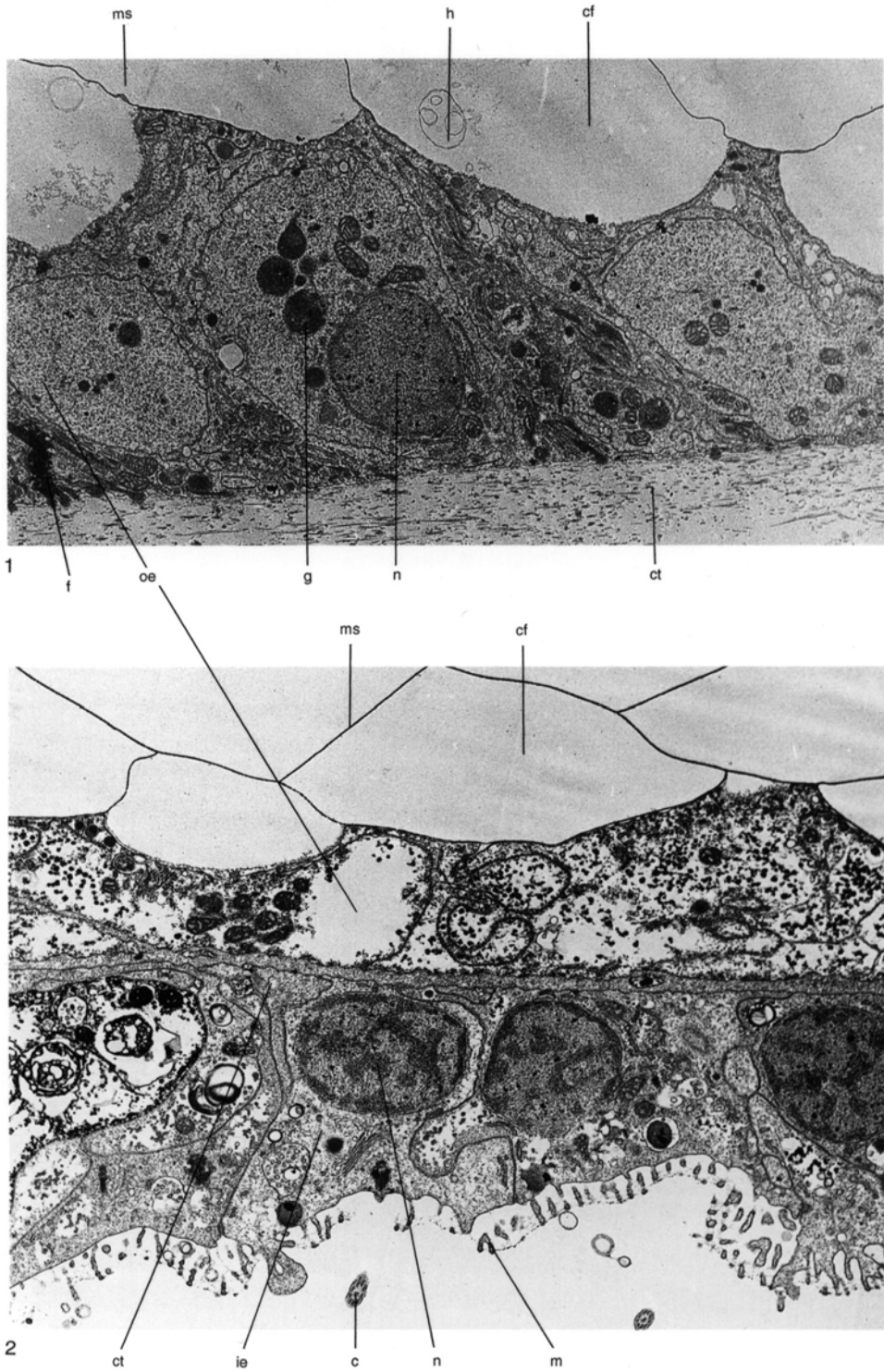


FIG. 13. (For explanation, see facing page.)

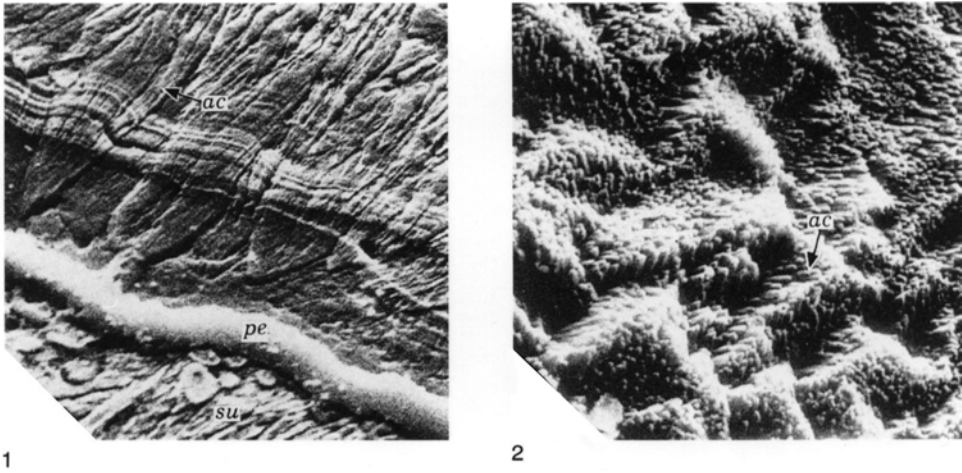


FIG. 14. SEM micrographs of the shell of *Thecidellina barretti* (DAVIDSON); 1, etched section showing the attachment of the periostracum (*pe*) to the substrate (*su*) with the overlying primary layer displaying growth bands and acicular crystallites (*ac*), $\times 1,500$; 2, internal surface of a dorsal valve showing acicular crystallites (*ac*) in rhombic arrays, $\times 3,000$ (Williams, 1973).

thick as the underlying plasmalemma to which it is attached by hemidesmosomes continuous with intracellular filaments (Fig. 15.2). As no comparable organic sheets are secreted within the carbonate shell, this discontinuous layer possibly represents a persistent organic mesh marking the external limit of a liquid film, about 100 nm thick, saturated with Ca^{2+} and HCO_3^- . The discontinuous layer may be a general feature of the epithelium responsible for the secretion of the primary layer as it is also well developed in the terebratulid *Liothyrella*, and traces of it have been found in *Notosaria*.

In contrast to the virtual suppression of the secondary layer in living thecideidines, such terebratulids as *Liothyrella* and *Gryphus* (MACKINNON & WILLIAMS, 1974) develop a continuous, tertiary layer. This consists of discrete units (prisms) that represent terminal faces of fibers growing normal to the surface of accretion (see Fig. 255). Sections of decalcified mantle show that the epithelium

secreting the tertiary layer is like that underlying the secondary shell except that it does not exude proteinaceous sheets between prisms (Fig. 16.1). A continuous proteinaceous sheet, up to 10 nm thick, however, persists about 20 nm external to the secreting plasmalemma to which it is attached by septate and fibrillar hemidesmosomes (Fig. 16.2). This monolayer, like that associated with the outer epithelium secreting the primary layer or the calcitic face of the secondary fiber, is interpreted as the outer boundary to a film of extracellular fluid sustaining carbonate secretion. The reason the tertiary layer consists of discrete prisms instead of one continuous sheet like the primary layer is presently unknown. Amalgamation of prisms may be inhibited either by sheets of water-soluble, organic compounds or by crystallographic incompatibility through the nonalignment of lattice structures. Shell sections normally show depositional continuity from the acicular primary shell through the

FIG. 13. TEM micrographs of *Calloria inconspicua* showing the relationship of outer epithelium (*oe*) with the membranous sheaths (*ms*) enclosing secondary calcitic fibers (*cf*) and with the underlying connective tissue (*ct*) and inner epithelium (*ie*); cilia (*c*), filaments (*f*), glycoprotein inclusions (*g*), hemidesmosomes (*h*), microvilli (*m*), and nuclei (*n*) are prominent; sections of 1, decalcified integuments of the shell, $\times 8,000$; and 2, descending lamella of the loop, $\times 17,000$ (new).

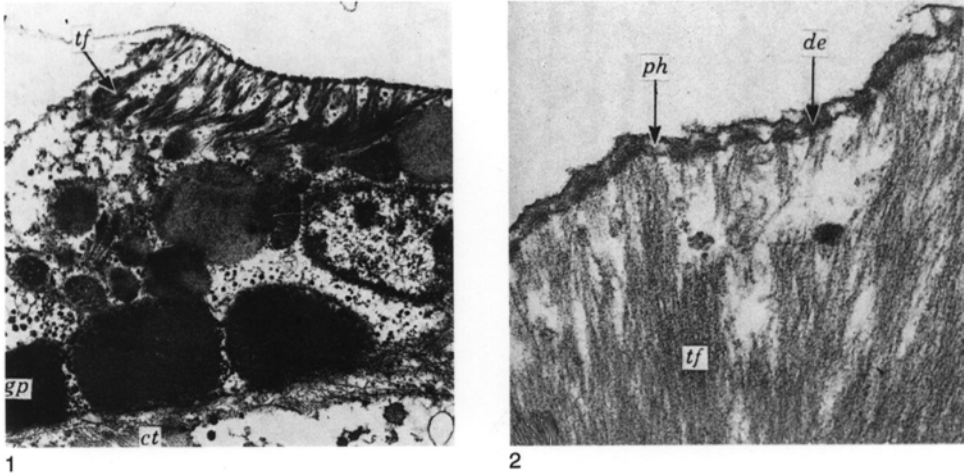


FIG. 15. TEM micrographs of sections of the outer epithelium of *Thecidellina barretti*; 1, bundles of filaments (*tf*) within the cell containing glycoprotein inclusions (*gp*); *ct*, connective tissue, $\times 11,000$; 2, their association with hemidesmosomes (*de*) attached to a discontinuous external membrane (*ph*) at the apical plasmalemma, $\times 68,700$ (Williams, 1973).

fibrous secondary layer to the tertiary prisms (WILLIAMS, 1968a; MACKINNON & WILLIAMS, 1974).

Although the calcitic shell of the craniids, as represented by living *Neocrania*, is separable into primary and secondary layers, both are different from those of the rhyngo-

nellides, the latter profoundly so (SCHUMANN, 1970; WILLIAMS & WRIGHT, 1970).

The primary layer normally consists of crystallites inclined at about 45° to the isochronous growth surfaces within the succession; here and there crystallites may amalgamate to form imperersistent lenticles of

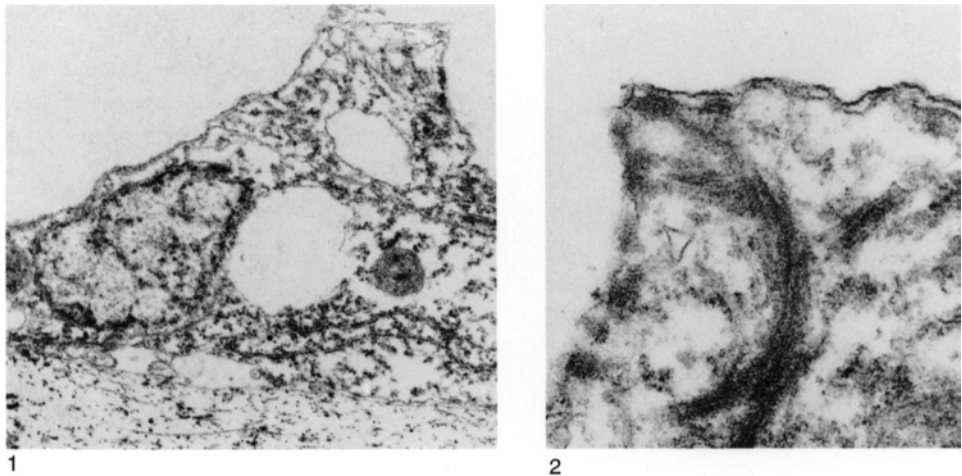


FIG. 16. TEM micrographs of decalcified sections of the outer epithelium underlying the tertiary shell of *Liothyrella neozelanica* showing 1, the absence of fibrous membranes distal of the apical plasmalemma, $\times 8,200$, and 2, a detail of the apical plasmalemma with an external membrane attached by hemidesmosomes at the distal ends of bundles of filaments, $\times 55,000$ (MacKinnon & Williams, 1974).

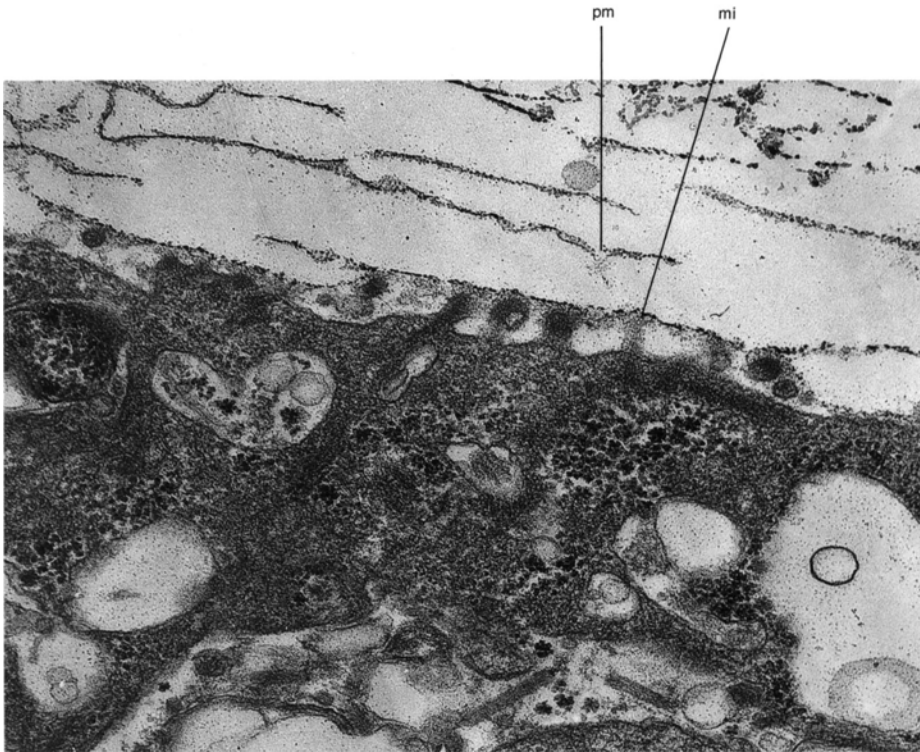


FIG. 17. TEM micrograph of decalcified section of the outer epithelium of *Neocrania anomala* (MÜLLER) showing the apical plasmalemma in relation to proteinaceous membranes (*pm*) covering calcitic laminae with short microvilli (*mi*), containing the ends of bundles of filaments extending through a zone presumably filled with extrapallial fluid; the zone occurs at different levels consistent with a section through spirally growing laminae, $\times 41,000$ (Williams, 1970b).

calcite. The main changes, however, occur in a narrow, transitional zone marking the boundary between the primary and secondary layers. Here the crystallites tend to form tabular aggregates that grade inwardly into uniformly thinner laminae. Both types form regular successions of overlapping tiles with comarginal edges scalloped in rhombohedral angles of 75° or 105° .

The secondary shell, which is not developed in the attached pedicle valve, is distinguishable from the transitional zone in that the laminae, about 250 nm thick and up to 15 μm across, are ensheathed in interconnecting proteinaceous sheets. The laminae are disposed as rhombohedral or dihexagonal tablets and are stepped in single- or double-screw dislocations (see Fig. 248) indicating that the secondary layer thickens by spiral

growth. An outer epithelial cell, contributing to the growth of secondary shell, contains numerous vesicles of glycoprotein and bundles of filaments (Fig. 17). At the secretory plasmalemma, groups of fibrils occupy cylindroid protuberances up to 200 nm long and become continuous through the membrane with clusters of hemidesmosomal fibrils. The fibrils pervade a narrow zone of variable electron density to connect with a membrane that represents the innermost proteinaceous sheet of the secondary shell. This zone intervenes everywhere between outer epithelium and shell and contains discarded vesicle membranes and finely divided particles. The zone presumably contains materials being used in the synthesis of proteinaceous membranes and a liquid saturated with Ca^{2+} and HCO_3^- ions that, on

precipitation, maintain the lateral expansion of laminae over newly forming membranes.

OUTER EPITHELIUM OF APATITIC SHELLS

The mantle and phosphatic integument of organophosphatic brachiopods are fundamentally different from those of carbonate-shelled species, micromorphologically, structurally, and biochemically. Recent research, however, has led to conflicting conclusions on the nature of the organophosphatic secretory regime so that no single model serves as a standard for comparison. The differences can be illustrated by comparing the studies of *Lingula*, *Glottidia*, and *Disciniscia* by IWATA (1981, 1982) with those of *Glottidia* and *Lingula* by WATABE and PAN (1984), of *Discina* by WILLIAMS, MACKAY, and CUSACK (1992), and of *Lingula* by WILLIAMS, CUSACK, and MACKAY (1994). The differences partly stem from using even such general terms as primary and secondary shell to mean different things. (In this account, the terminology is that of WILLIAMS, MACKAY, and CUSACK, 1992.) There are also disagreements on the structure and differentiation of the secreting epithelium and on the nature of the basic components of the skeletal successions. Accordingly, the lingulids and discinids will be separately described although it is evident that their secretory regimes are homologous and that the differences between them are likely to rest on misinterpretations.

PAN and WATABE (1988b) described *Glottidia* as having a thick, well-defined primary layer immediately underlying the periostracum within which crystal aggregates decrease in density toward the secondary shell. This layer is secreted by cuboidal cells containing calcium phosphate granules but relatively few organelles. The main components of the layer are apatitic spherulites consisting of acicular crystallites up to 200 nm long dispersed within a fibrous matrix consisting of proteins and GAGs.

In contrast, the inner part of the shell succession includes a number of secondary layers composed of amalgamated crystals,

which are separated from one another by thicker chitinous layers. These secondary mineralized and chitinous layers are, according to PAN and WATABE (1988a, 1988b), secreted by three kinds of squamous cells. Type I cells, with relatively smooth secretory plasmalemma, contain granule-bearing vesicles that are released into an extrapallial space to form the mineralized layer. Types II and III cells have short and small, irregular microvilli respectively connecting with intracellular bundles of filaments and the extracellular chitinous layers. A noteworthy feature of the chitinous layers of *Glottidia* is the presence of arrays of long, slender rods of apatitic spherulites set at acute angles to one another (see Fig. 238).

IWATA's studies of the skeletal successions of *Lingula* and *Glottidia* (1981, 1982) suggested that they differ in many respects. He was unable to differentiate the shell succession of *Lingula* into primary and secondary layers. Instead, he described the shell as consisting of alternations of organic and mineralized layers. A typical organic layer (also referred to as the chitin layer) is distinguishable from the organic matrix of a succeeding mineralized layer in being electron dense and composed of organic fibrils less than 10 nm long that are usually disposed in a reticulate mesh. Hexosamine and some proteins are the main constituents of the organic layer. The fully developed mineralized layer was zoned by IWATA (1981, p. 41) according to the size of apatitic components (Fig. 18). Overlying an organic layer with a sharply defined interface, a thin layer composed of apatitic granules about 50 nm in size is usually developed (designated the C zone). The mineral components of the succeeding A zone are acicular crystallites up to 150 nm long arranged more or less parallel to the boundaries of the zone. In the overlying B zone, which grades into the next organic layer, the apatitic components consist of coarse, acicular crystallites up to 200 nm long, which are irregularly disposed throughout the zone. The organic matrix of all three zones is comparable to collagen but has excessive concentrations of alanine. IWATA

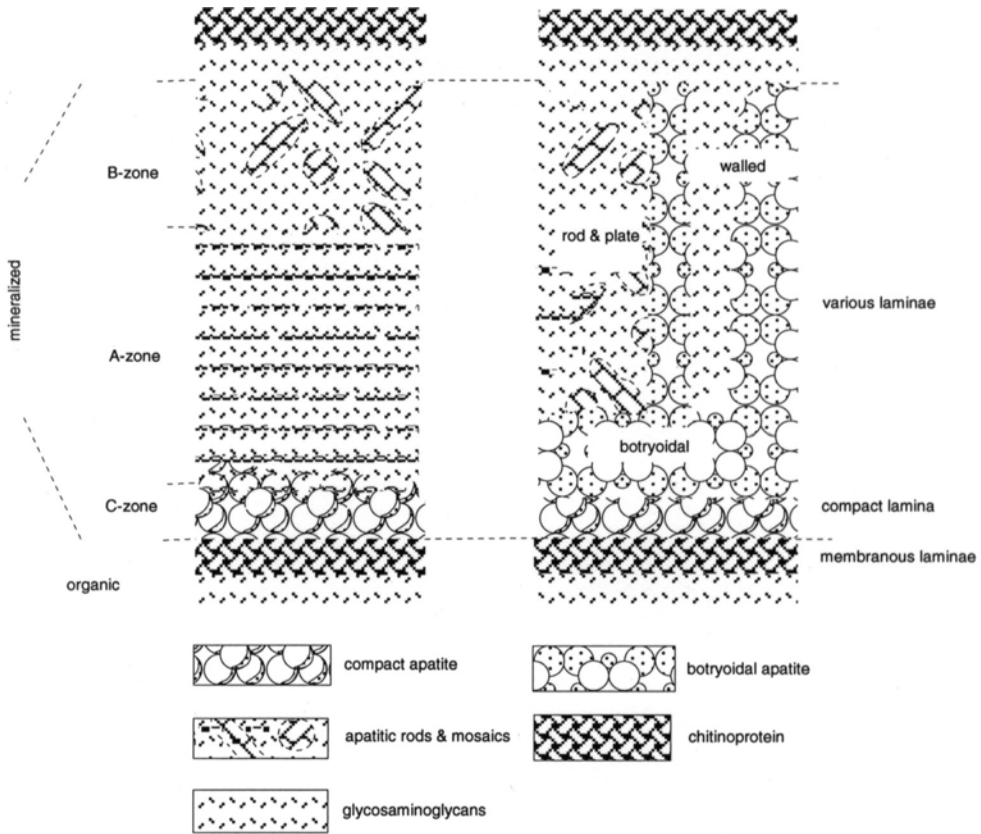


FIG. 18. A terminological correlation of a composite lamina set of the shell of *Lingula anatina* (right-hand side) as described herein with the mineralized and organic layers as understood by IWATA (1981, p. 41); laminae in the main part of the succession usually consist of botryoids, vertical walls, and rods and plates (see Fig. 235, 237 for SEMs of these lamina sets) of apatite in a GAGs matrix (adapted from Williams, Cusack, & Mackay, 1994).

(1981) noted that the *Lingula* could not be digested by chitinase and suggested that the chitin, which is known by other tests to be present, is masked by a scleroprotein.

IWATA (1981) did not find any differentiation of the outer epithelium secreting the *Lingula* shell, which consists of columnar cells with the secreting plasmalemmas forming irregular projections accommodating terminations of bundles of internal filaments. Some micrographs (IWATA, 1981, pl. 14/2) have been interpreted as showing the presence of extrapallial fluid.

IWATA (1982) confirmed that the succession of *Glottidia* consists of alternations of organic and mineralized layers but did not identify a primary layer. The mineral layers

are described as being composed of rods and needlelike crystallites of apatite aligned sub-parallel to the shell surface. The mineral components of the organic layer, on the other hand, are slender, mineralized fibrils that are disposed within the layer in a latticelike manner. With respect to the distribution of the biomineral components in the *Glottidia* shell, IWATA drew a closer comparison with *Discinisca* rather than *Lingula*. He additionally noted that the basic apatitic component of *Discinisca* is an extremely fine granule aggregated into acicular crystallites. All three genera have a collagen-like protein as a dominant organic constituent.

In describing the skeletal succession of *Discina*, a stratiform terminology was

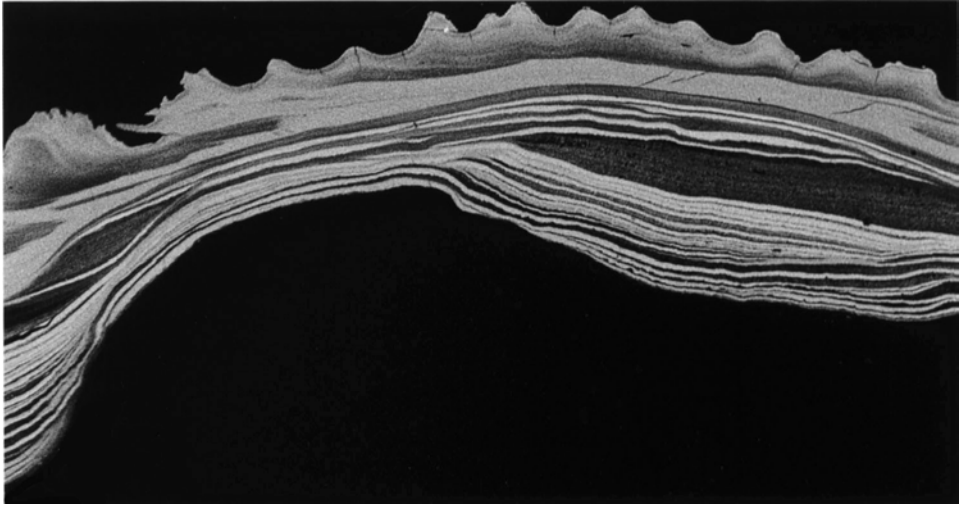


FIG. 19. Backscattered electron micrograph of a section near the dorsal umbo of *Discina striata*, digested in chitinase and papain and coated with carbon, showing the distribution of apatite (white) and organic (grey to black) components of the shell succession, $\times 40$ (Williams, Mackay, & Cusack, 1992).

introduced (WILLIAMS, MACKAY, and CUSACK, 1992) in an attempt to standardize definitions of the various distinctive structural and biochemical units secreted by the outer epithelium (Fig. 19). A subperiostracal primary layer no more than a few microns thick is normally well defined, especially in backscattered scans for phosphate because finely granular apatite is distributed throughout the layer. The succeeding secondary layer consists of a variety of organophosphatic sheets (*laminae*) that, although normally impersistent and subject to lateral as well as vertical changes, can be categorized as one of five distinctive types. All are composed of the same basic unit: an apatitic granule between 4 and 8 nm in size with an organic coat. The units are assembled and aggregated into spherules up to 200 nm in diameter within the outer epithelium. During exocytosis, spherules are further aggregated into discooidal or spheroidal mosaics up to 1 μm or so in size, which are added incrementally to the shell succession more or less in their final, polymerized and crystallized states. The distinctiveness of each type of lamina depends on the relative proportions of its organic and

biomineral components and on the aggregation of its apatitic mosaics. Typically, there is a discernible rhythmic sedimentation from a predominantly or exclusively organic to a mainly apatitic deposition, which reflects a recurrent cycle of secretion by the same group of cells.

The outer epithelium depositing these rhythmic successions consists of inclined cuboidal cells with secretory plasmalemmas prolonged as a series of prostrate tubes, 150 nm or so in diameter, which tend to form a layer up to three or four deep (Fig. 20.1–20.2). Within the cell, membrane-bound vesicles are common, and glycogen is densely distributed especially in the basal parts. Apatitic granules with medium electron-dense coats are usually distributed in varying size within and between the prostrate tubes. Such aggregates may be drawn out into rod-like structures (*baculi*) (Fig. 20.3–20.4). In fact, the main components of every type of lamination occur in what appears to be their final crystalline or polymerized states at the interface between the shell and outer epithelium. This kind of secretion precludes the existence of a film of extrapallial fluid

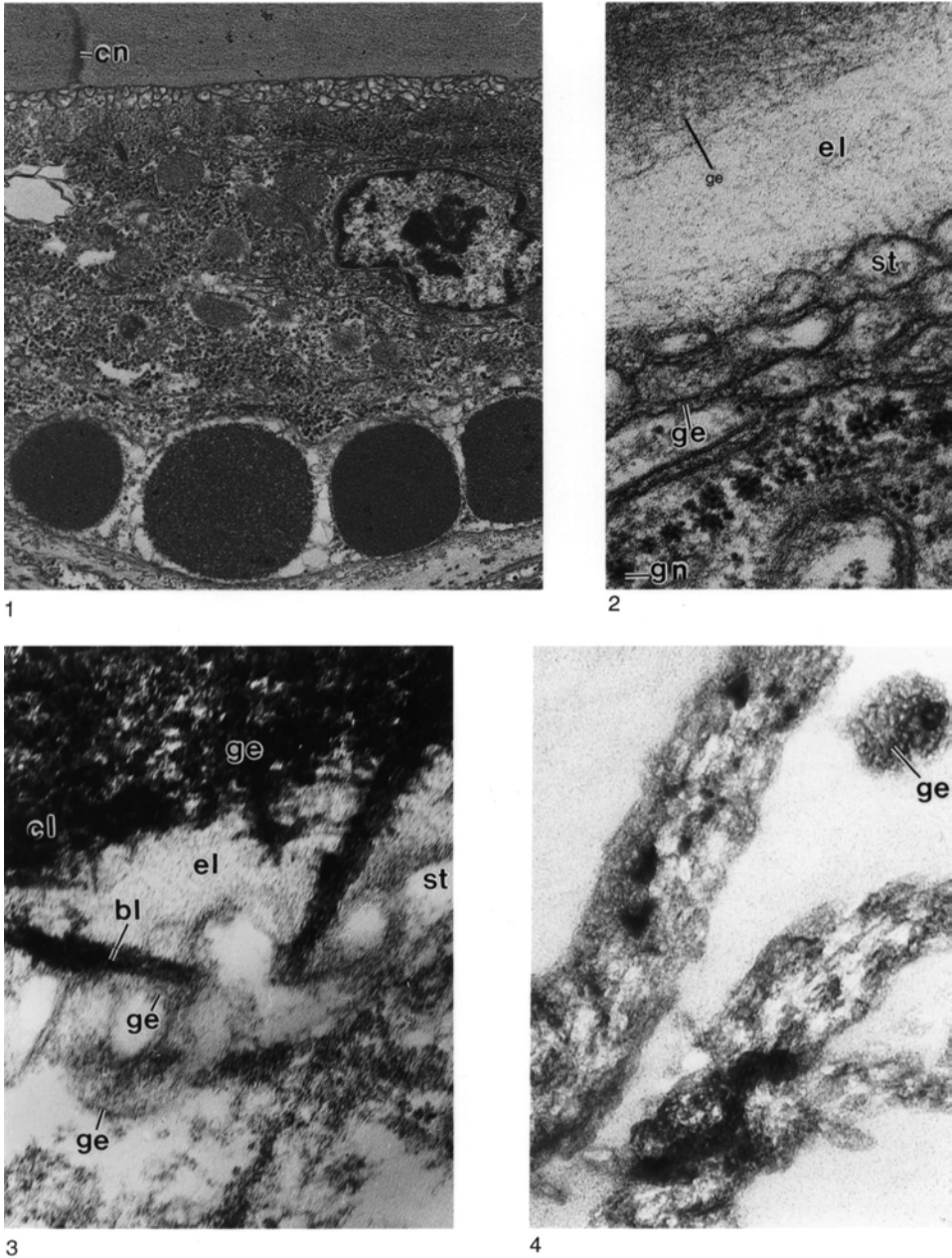


FIG. 20. TEM micrographs of shell and outer epithelium of dorsal valves of *Discina striata*; 1, general view ($\times 9,000$) and 2, detail ($\times 80,000$) of decalcified sections of cells showing apical plasmalemmas disposed as a series of low-lying tubes (*st*), a canal (*cn*) underlying mainly organic (1) and stratified (2) laminae with apatitic granules with coats (*ge*), glycogen (*gn*), and an electron-lucent (*el*) zone with fibrils and aggregates of apatite; 3, $\times 80,000$, and 4, $\times 130,000$, sections of shell (with secreting epithelium in 3) showing the origin of mineralized rods (baculi) and the structure of so-called acicular crystallites respectively with rods (*bl*) arising from a compact lamina (*cl*), within an electron-lucent zone containing coated apatitic granules (*ge*) being exocytosed with fibrils from plasmalemma tubes (*st*) (Williams, Mackay, & Cusack, 1992).

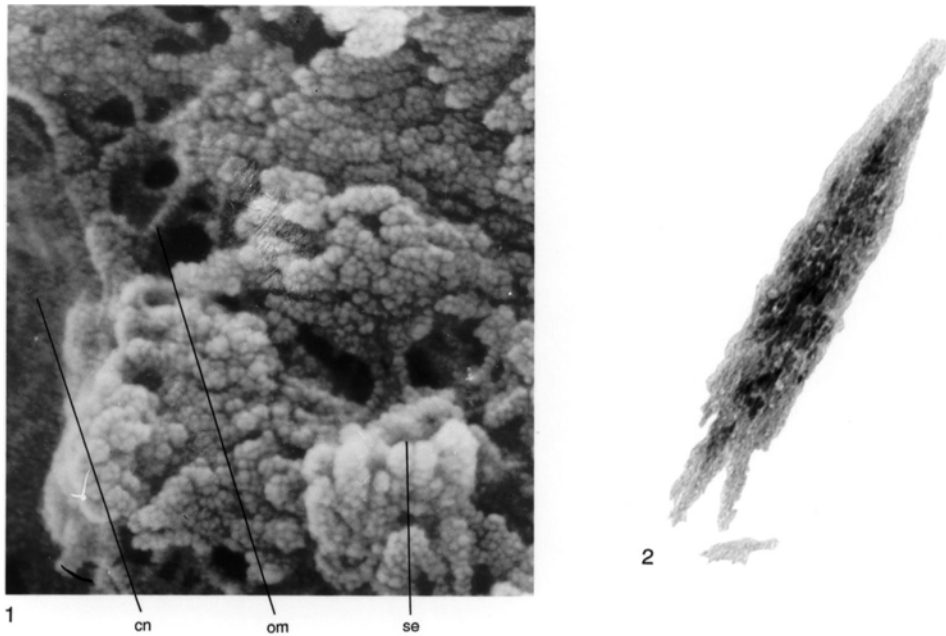


FIG. 21. Biomineral structures in the shell of *Lingula anatina*; 1, SEM micrograph of fracture section of a shell showing apatitic spherules (*se*) composed of granules adjacent to a canal (*cn*) and supported by an organic mesh (*om*) probably of chitin, collagen, or fibrous protein, $\times 150,000$; 2, TEM micrograph of original shell showing the structure of a so-called acicular crystallite with an electron-dense proteinaceous and chitinous matrix studded with granules, $\times 180,000$ (new).

between newly formed shell and mantle as has been reported in lingulid brachiopods (PAN & WATABE, 1988b; IJIMA, HIROKO, & others, 1991).

The previously reported differences in the structure and secretion of the lingulid and discinid shells also appear to be based on misinterpretations of ultrastructural features in shell and mantle (WILLIAMS, CUSACK, & MACKAY, 1994).

No evidence has been found of acicular (prismatic) crystallites constituting the basic apatitic unit in *Lingula*. The smallest apatitic unit is granular with dimensions comparable to that of the *Discina* shell (Fig. 21). This conclusion is not only at odds with the findings of IWATA (1981) and PAN and WATABE (1988b) but also appears to be incompatible with the X-ray diffraction studies of KELLY and others (1965), IJIMA and MORIWAKI (1990), and IJIMA, HIROKO, and others (1991). Both investigations explored

the orientation of apatite relative to the organic framework of the *Lingula* shell. KELLY and others (1965, p. 339) found that the *c*-axes of the apatitic crystals are normally aligned parallel to the plane of the shell but vary considerably in orientation relative to the shell margins and in strength of definition (Fig. 22). In the posteromedian zone, more or less coincident with the body cavity, the *c*-axis may be transverse or may be disposed in two directions and even tilted to the shell surface. In the lateral areas of a valve, the *c*-axes tend to be disposed normal to the valve margin; in the anteromedian sector of a valve, the *c*-axes are as disoriented as they are in the posteromedian area. The removal of apatite by EDTA showed that the β -chitin configuration is oriented in the same way as the apatite had been so that the polysaccharide chain lies parallel with the *c*-axis of the apatitic component. It was noted that the reflections are generally diffuse, indicat-

ing the presence of small crystallites of the order of 20 nm, but are sharper in the lateral areas suggesting larger crystallites up to 100 nm or so. The electron microscopy done by KELLY and others (1965) confirmed that the smallest particles, at about 5 nm, are rounded and enveloped by organic material. Fractionation of the mineral components suggested that three other grades existed: needle-shaped particles with organic envelopes about 30 nm long, closely packed acicular crystallites at about 100 nm in length, and larger, rectangular aggregations.

The diagrammatic representation of the findings of IIJIMA, HIROKO, and others (1991) is closely comparable with that of KELLY and others (1965) except that they ascribed the diffuse reflections of the median area to strong organic reflection and found that the orientation of the *c*-axes of apatite and the fiber axes of β -chitin were closely parallel with the growth vectors of the lateral areas (Fig. 22). IIJIMA, HIROKO, and others (1991) concluded that chitin fibers grow apatite on their surfaces.

Contrary to first impressions, the disposition of the apatitic *c*-axes and the relative sharpness of their diffraction patterns, as described above, are actually broadly consistent with recent ultrastructural studies of the *Lingula* shell. The basic biomineral unit is invariably a granule, presumably a flattened hexagonal prism, about 4 to 8 nm in diameter. In the anteromedian sector of a valve, the granules are usually widely dispersed in spherules or small mosaics (Fig. 21.1); in the posteromedian sector, larger mosaics are closely distributed and normally aggregate into botryoidal masses. The *c*-axes of the apatitic components in these sectors would accordingly have weak orientations with varying inclinations to the shell surface. In the lateral areas, spherules may be aggregated into rodlike structures (Fig. 21.2) up to 400 nm long as well as into mosaics. The rods usually have a preferred orientation more or less normal to the growing edge of the valve and lie parallel to anastomosing ridges, which probably accommodate volumetric

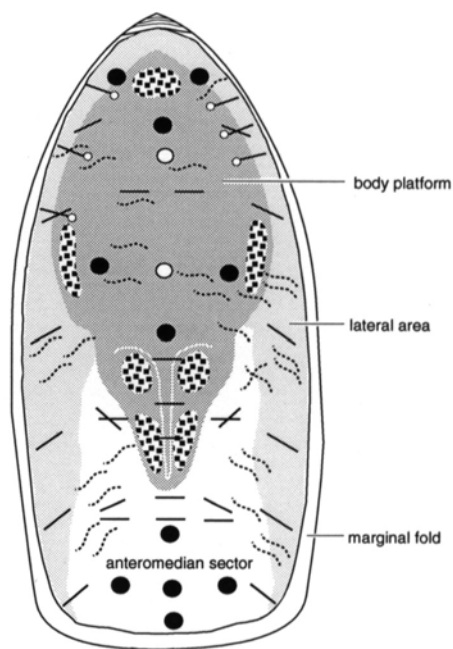


FIG. 22. The interior of a dorsal valve of *Lingula anatina* showing the orientation of apatitic crystallites, for which *c*-axis directions have been determined, relative to the trends of anastomosing ridges; the *c*-axes represented by lines ending in circles are those plotted by IIJIMA, MORIWAKI, and KUBOKI (1991b, p. 435), which were not coincident with those (plain lines) mapped by KELLY, OLIVER, and PAUTARD (1965, p. 339); the trends of the ridges are a compilation of observations of a number of interiors seen under the SEM; ●, disorientation areas; ○, strong organic reflection areas; wavy dotted lines, anastomosing ridge trends (Williams, Cusack, & Mackay, 1994).

changes in the mantle induced by the radial canal systems. The rods are not acicular crystallites but strings of granules that must be stacked in such a way as to have their *c*-axes aligned with the fiber axes of associated chitin.

As with *Discina*, the lingulid laminar succession is rhythmic as was first noted by IWATA (1982) although he did not describe its structural diversity (Fig. 18). The rhythm is initiated by the sudden bulk secretion of coated granules of apatite virtually to the exclusion of organic constituents that, however, become dominant toward the end of the cycle (Fig. 23). This increase in the organic content culminates in the secretion of

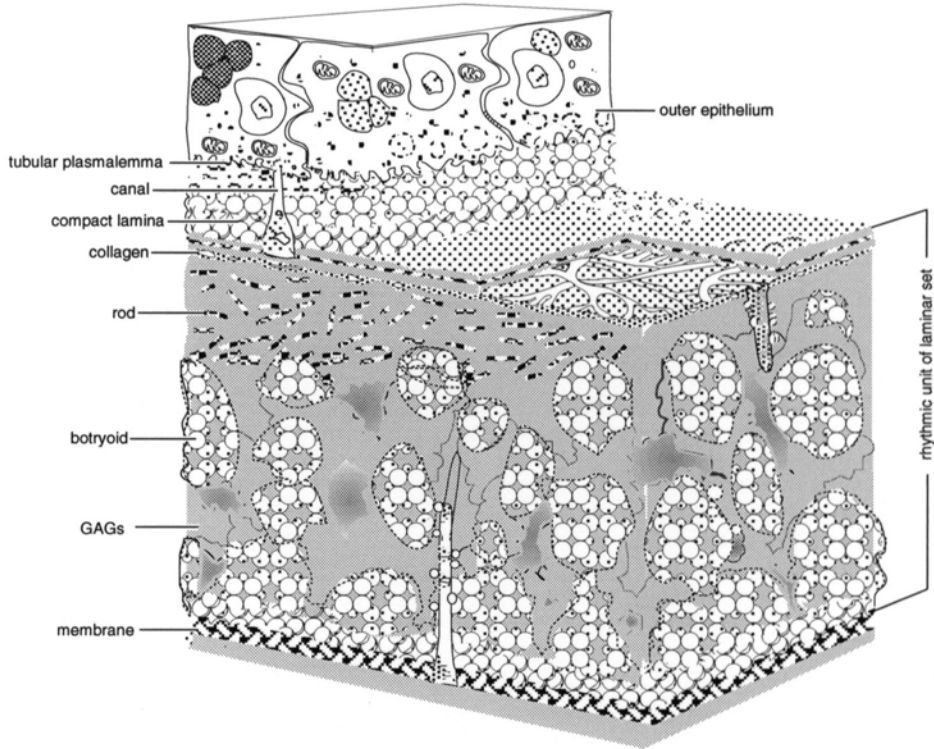


FIG. 23. Diagrammatic representation of a laminar set of the shell of *Lingula anatina* showing a complete rhythmic unit of secretion with the base of the compact lamina marking the onset of a decreasing cycle of apatitic secretion and the base of the botryoidal lamina marking the first exudation of an increasingly preponderant GAGs matrix (Williams, Cusack, & Mackay, 1994).

a chitinoproteinaceous membrane(s) that serves as the substrate for the next influx of apatite. At least ten proteins have been identified in the shell (WILLIAMS, CUSACK, & MACKAY, 1994). Some of these must be covalently attached to GAGs, the main organic matrix of the shell, while others must be associated with the chitin and fabricated into membranes and apatitic coats. Fibrillar collagens with a periodicity of about 45 nm occur mainly as sporadically developed mats within the body platform succession (Fig. 24) and as the core of the dorsal median septum. Elsewhere they appear sparingly as vertical and horizontal strands (WILLIAMS, CUSACK, & MACKAY, 1994).

The outer epithelium is normally anchored to the shell by canals (Fig. 25.1) so that a single cell can secrete in sequence that part of an entire rhythmic succession to

which it is attached. Consequently, the contents of cells attached to different successions vary according to whether the principal constituents of the laminae are organic or apatitic. Thus, the typical outer epithelial cell is cuboidal (Fig. 25), about 11 μm tall, with a basal nucleus and elaborately interdigitated lateral cell membranes. The cytoskeleton is normally well developed with bundles of filaments extending through the cytosol from hemidesmosomal plaques at the basal plasmalemma to tubular extensions of the apical plasmalemma, some of which are also attached by filaments to the lateral cell membranes. The Golgi apparatus is usually identified by trails of minute vesicles, while RER and mitochondria are variably distributed. Inclusions also vary in composition and distribution. Glycogen occurs widely, but lipid droplets tend to cluster in the basal

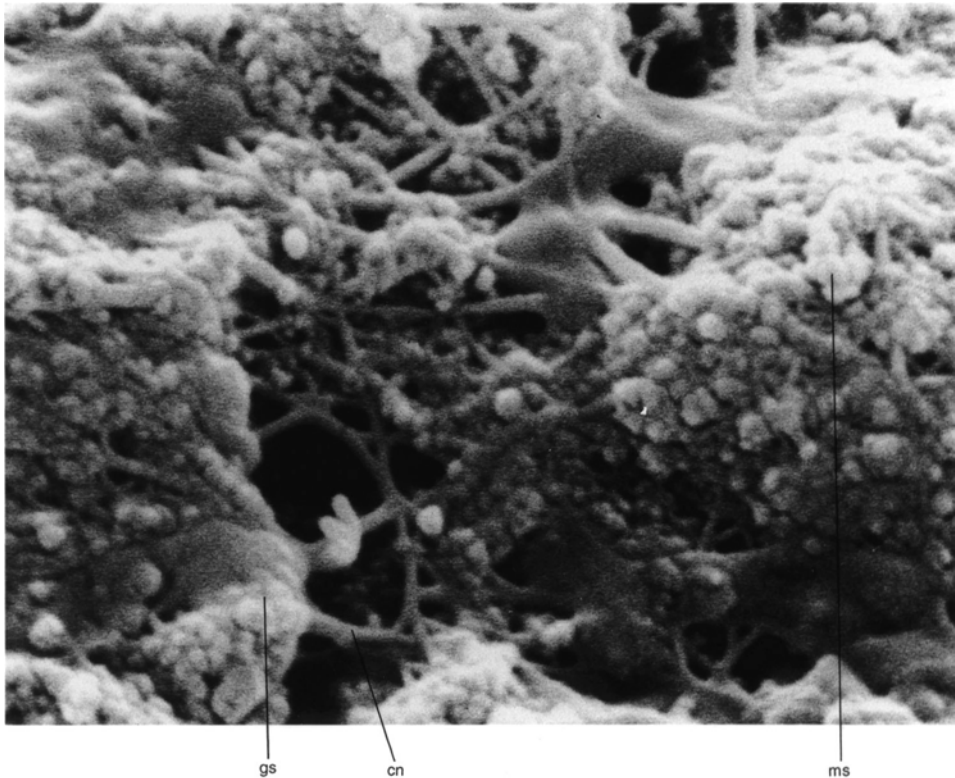


FIG. 24. SEM micrograph of an oblique fracture section of the shell of *Lingula anatina* showing the association of mosaics of apatite (*ms*) with glycosaminoglycans (*gs*) and a fibrous protein, possibly collagen (*cn*), $\times 24,500$ (new).

regions of all cuboidal cells that are normally distorted by large, closely packed aggregates ($10\ \mu\text{m}$ or so in size) of differently composed vesicles, up to $1.6\ \mu\text{m}$ in diameter. The large, membrane-bound vesicles in cells secreting mainly GAGs and other organic constituents, however, normally contain homogeneously electron-dense glycoprotein; mitochondria and RER are relatively rare and are much more common in the middle and basal regions of cells (Fig. 25.1). In contrast, the vesicles in cells secreting mainly apatite are mottled with electron-light granules in various stages of being reconstituted by RER; mitochondria with electron-light substrates are common within the apical region (Fig. 25.2; WILLIAMS, CUSACK, & MACKAY, 1994). It is evident that the different cell types previously observed (PAN & WATABE, 1988a, 1988b) represent phases in the secretory cycles of the basic outer epithelial cell.

MODIFICATIONS OF OUTER EPITHELIUM

The outer epithelium of brachiopods may be modified in many ways. Dense bundles of filaments attach the muscles to the floors of the valves. These traverse the outer epithelial cells to connect by hemidesmosomes proximally with basal lamina contiguous with the muscle base and distally with a proteinaceous membrane (*Thecidellina* WILLIAMS, 1973; *Liothyrella* MACKINNON, 1977; *Terebratalia* STRICKER & REED, 1985a) or a chitinous pad (*Neocrania* WILLIAMS & WRIGHT, 1970) intervening between the shell and the secretory plasmalemmas (Fig. 26–28). The emplacement of the muscle bases usually leads to partial or total suppression of secretion of the membrane within the secondary shell so that the biomineral components lose their identity and fuse into irregular plates (myotest). Even so, the epithelial cells between shell and

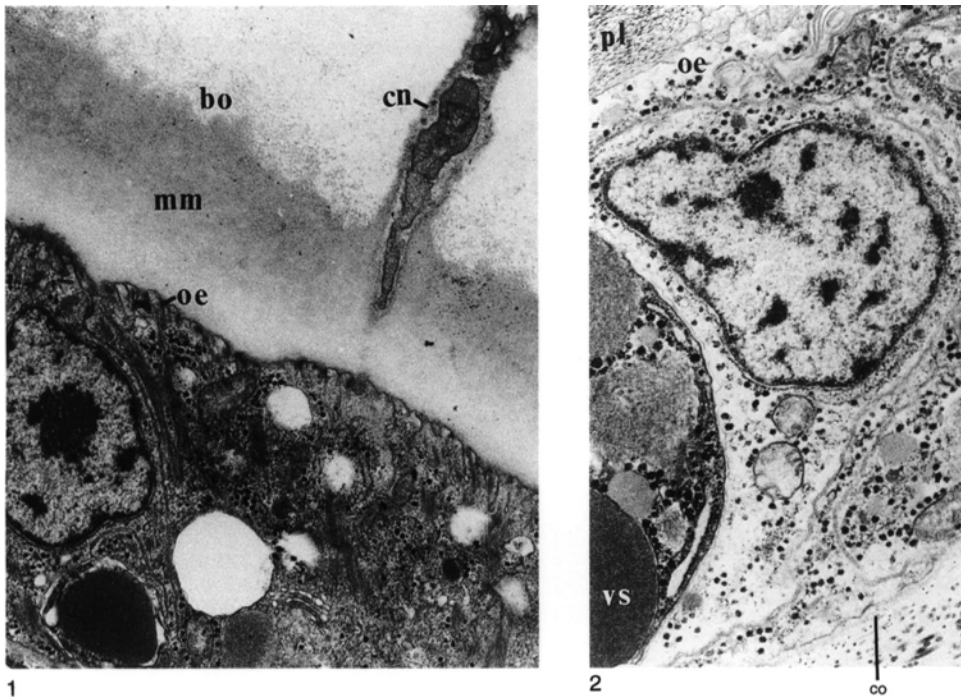


FIG. 25. TEM micrographs of sections of decalcified shell and outer epithelium of *Lingula anatina*; 1, canal (*cn*) penetrating laminae of apatitic mosaics clustered into botryoids (*bo*) and embedded in GAGs (*mm*), underlain by tubular extensions (*oe*) of the apical plasmalemmas, $\times 11,000$; 2, another outer epithelial cell that secreted dispersed apatitic rods (*pl*) through tubular extensions (*oe*), overlying connective tissue with fibrillar collagen (*co*) and adjacent to a cell bearing membrane-bound inclusions (*vs*), $\times 11,000$ (Williams, Cusack, & Mackay, 1994).

muscle bases usually retain their regular, cuboidal outlines, which are commonly impressed as closely packed hexagonal casts within the muscle scars of fossil as well as living species (Fig. 26.2; 28.2–28.3).

The outer epithelium also undergoes changes to accommodate the growth of all internal skeletal features arising directly from the floors of the valves. The main changes are localized proliferations of cells as only the teeth of the ventral valve appear as features of the primary layer (STRICKER & REED, 1985a). Many of these skeletal extensions in living articulated brachiopods, however, become modified during growth by differential secretion and resorption, which processes are controlled by morphologically distinctive cells. Thus, the lamella of the loop of *Calloria* is a two-layered structure (MACKAY, MACKINNON, & WILLIAMS, 1994) consisting of a

wedge of regularly stacked secondary fibers and an underlying thin layer of nonfibrous calcite (**brachiotest**) (Fig. 29). On one surface, secondary fibers predominate, but smooth, finely banded brachiotest occurs as a narrow, marginal lip upon which the secondary fibers proliferate and progressively overlap. This growing edge of the lamella is secreted by long, folded epithelial cells with fingerlike extensions to their apical plasmalemmas, which are distinguishable from the cuboidal epithelium secreting fibers and their membranous sheaths (Fig. 30.1). The other surface of the lamella consists entirely of roughened brachiotest. This surface is overlain by filamentary epithelium acting as a holdfast for the connective tissue frame of the lophophore (Fig. 30.2). The other edge of the lamella consists of truncated sections of both secondary fibers and brachiotest and

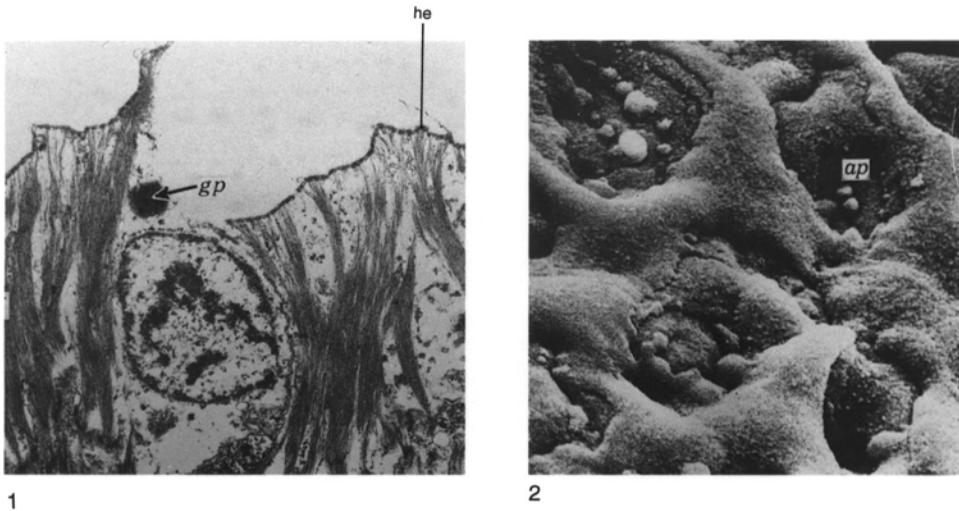


FIG. 26. Muscle attachment in *Thecidellina barretti* and *Lacazella mediterranea* (Risso); 1, TEM micrograph of a decalcified section of the outer epithelium permeated by bundles of filaments of a posterolateral adductor muscle showing hemidesmosomal attachment (*he*) to the apical plasmalemma and a glycoproteinaceous vesicle (*gp*), $\times 8,200$; 2, SEM micrograph of a muscle scar resulting from the attachment of the lophophore to the peribrachial ridge of a dorsal valve with adductor pits (*ap*) corresponding to the outline of the cuboidal outer epithelium, $\times 2,800$ (Williams, 1973).

bears signs of resorption consistent with the degenerated state of the associated epithelium.

MANTLE EXTENSIONS

The shell of all living brachiopods, except the rhynchonellides, is pierced by perforations that are either slender cylindroids less than $1\ \mu\text{m}$ in diameter (**canals**) or very much larger chambers up to $20\ \mu\text{m}$ or more in diameter (**punctae**), which respectively accommodate membrane-bound secretions of the outer epithelium or papillose outgrowths of the mantle (**caeca**).

The caeca of living terebratulides, which may be simple or branched, almost penetrate the calcareous shell to connect with the periostracum by a radiating **brush** of protein-lined tubes, each about $100\ \text{nm}$ in diameter (Fig. 31–32). The tubes permeate a canopy of primary shell about $1\ \mu\text{m}$ thick (Fig. 33–34) and, together with the space between the canopy and the distal head of the caecum, are filled with GAGs (OWEN & WILLIAMS, 1969). Mature caeca are differentiated into peripheral cells, which are a

flattened, cylindroid extension of the secretory outer epithelium and core cells hanging freely in a lumen occupying the basal part of the caecum. The core cells are full of inclusions of GAGs, glycoproteins, particulate glycogen, and minor lipids (Fig. 32). Their distal surfaces are extended into densely distributed microvilli (Fig. 32.1, 32.3). STRICKER and REED (1985a) have recently confirmed that, in the early stages of caecal generation at the mantle edge, microvilli give rise to the brush by being attached to the periostracum during secretion of the canopy (Fig. 35). The core cells act as storage centers for materials circulating within the mantle (OWEN & WILLIAMS, 1969).

The punctae and caeca of living thecideidines are homologous with those of the terebratulides, as is confirmed by the existence of a distal canopy penetrated by a brush of radiating canals averaging just under $300\ \text{nm}$ in diameter and by the differentiation of the proximal part of the caeca into peripheral and core cells. The core cells of mature caeca, however, are not microvillous and are restricted to the proximal part of the punctae

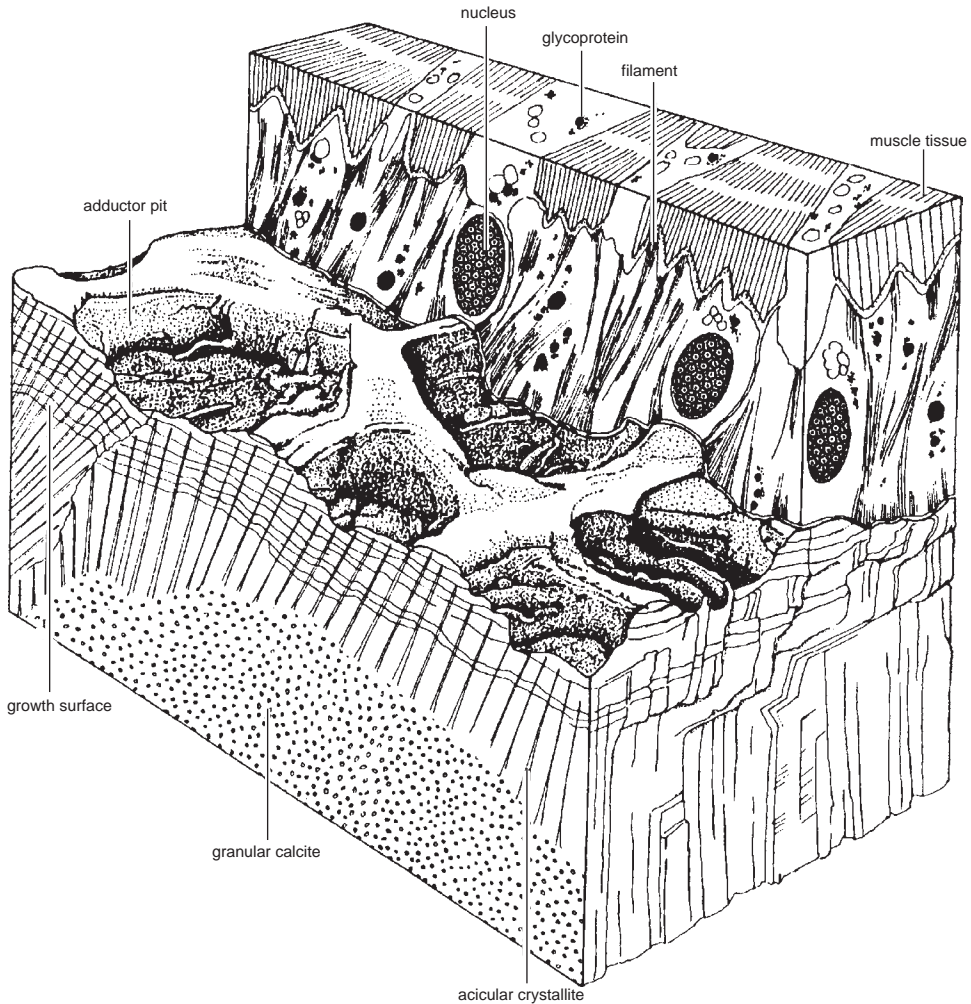


FIG. 27. Diagrammatic reconstruction of a pitted muscle scar in relation to the outer epithelium underlying the adductor muscle base of a typical thecideidine brachiopod, approximately $\times 3,000$ (Williams, 1973).

by proteinaceous partitions sealing off the more distal part of the punctae.

The shell of *Neocrania* is also penetrated by punctae accommodating papillose outgrowths of the mantle, which are conveniently referred to as caeca to distinguish them from the contents of the fine lingulide canals (Fig. 36–37). They differ fundamentally from the terebratulide and thecideidine caeca in many respects, however (WILLIAMS & WRIGHT, 1970). The craniid caecum is typically highly branched, especially distally

(Fig. 37.1) where fine, terminal tubules up to 150 nm in diameter and 2 μm long splay out radially within the primary layer and are connected to the periostracum, not through a well-organized brush but by filamentary trails. The trunk and main branches of a typical craniid caecum are lined by stretched, outer epithelial cells secreting the thickening secondary laminar layer. The axial lumen does not contain aggregated core cells but is normally charged (as are the finer branches and terminal tubules) with membrane-

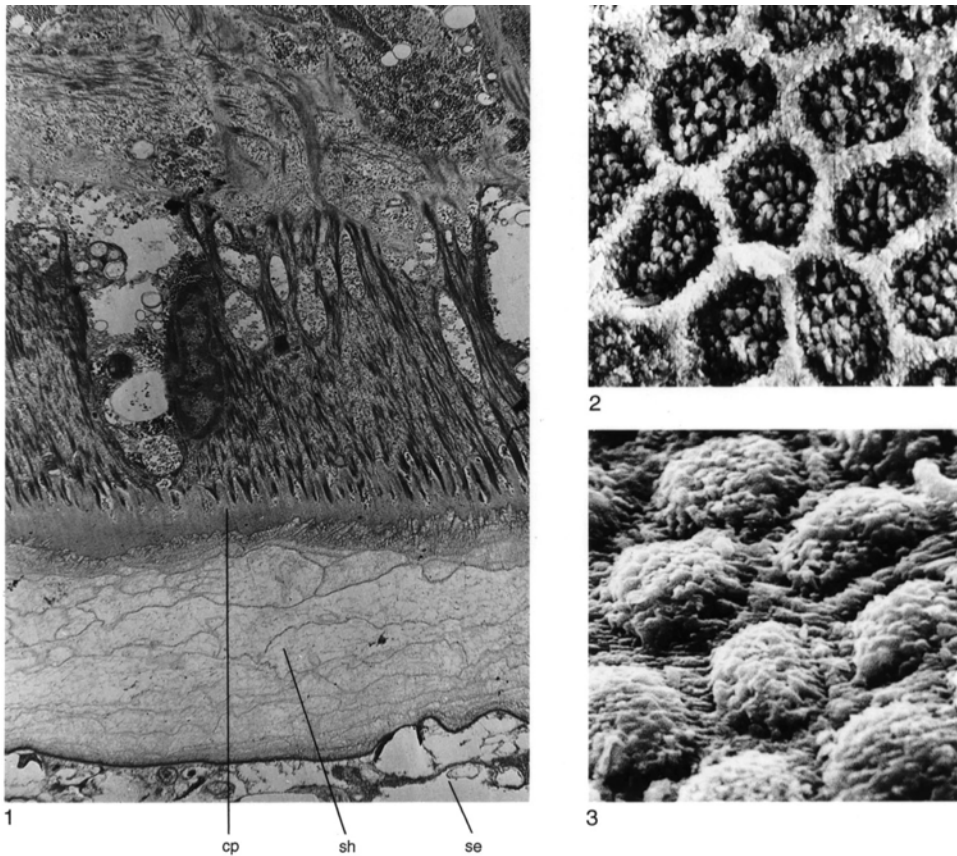


FIG. 28. Muscle attachment in *Neocrania anomala*; 1, TEM micrograph of a decalcified section of shell (*sh*), mantle, and adductor muscle base of a ventral valve, attached by folded periostracum to the substrate (*se*), showing densely distributed filaments permeating the outer epithelium and extending into a chitinous pad (*cp*), $\times 6,000$; 2, the raised ($\times 1,500$) and 3, depressed ($\times 1,400$) hexagonally close-packed boundaries of calcitic pads that underlie regular cuboidal epithelium in the medial area of a posterior adductor muscle scar (Williams and Wright, 1970).

bound droplets of GAGs, glycoproteins, and some lipids as well as crystalline proteinaceous rods and stellate glycogen particles (Fig. 37.2–37.3).

The canals permeating organophosphatic shells are not so much extensions of the mantle as repositories of various extracellular secretions (see Fig. 25.1). In both lingu-lids and discinids, they are densely distributed with as many as three or four originating at the secretory plasmalemma of a single cuboidal epithelial cell (Fig. 38.1). They are normally up to 300 nm in diameter but may rapidly thicken into short, vertical chambers or horizontal galleries up to a mi-

cro-meter or so across (Fig. 38.3–38.4). Many canals can be traced distally to slightly expanded terminal membranes situated sub-periostracally. They usually have slightly undulatory axes and commonly branch dichotomously into subparallel sets so that impersistent segments of canals of variable length can be found within any section of the secondary shell. Canals may also be temporarily terminated and sealed off by transverse membranes well within laminar successions (Fig. 38.2). Arrays of them may even be displaced for a micrometer or so along interfaces within the shell succession, usually between organic and mineralized laminae.

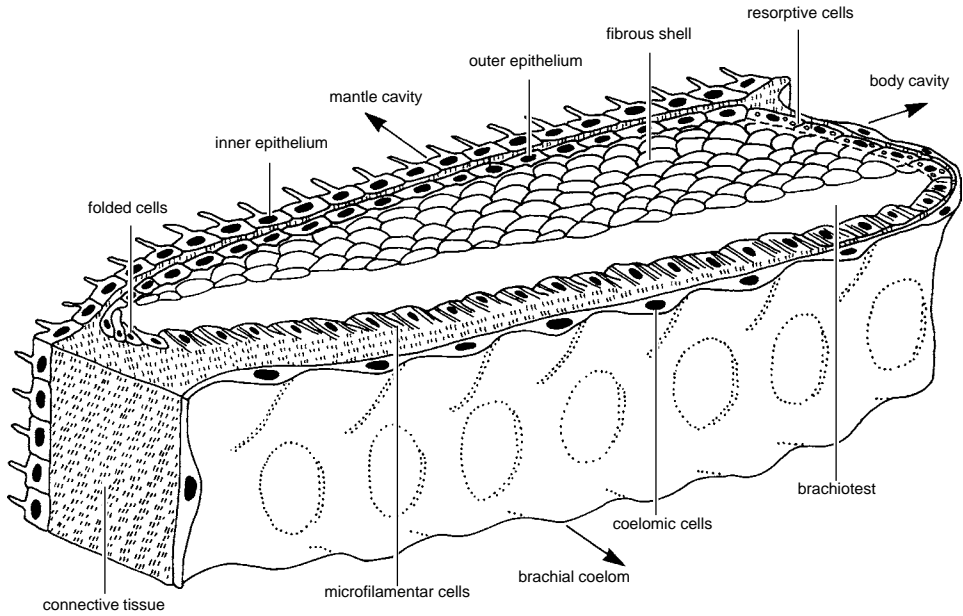
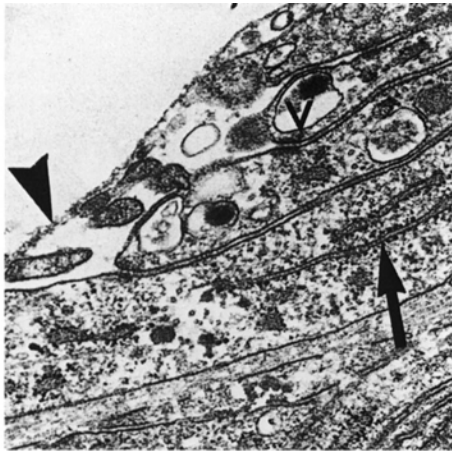


FIG. 29. Diagrammatic block section showing the differentiation of the outer epithelium enveloping a segment of the two-layered descending lamella of the loop of *Calloria inconspicua* (Mackay, MacKinnon, & Williams, 1994).

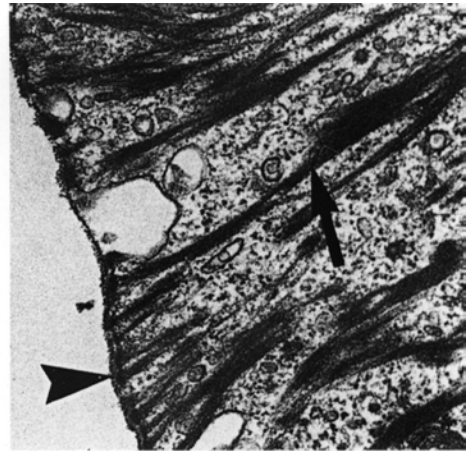
Accordingly, it is possible that some canals originate within the secondary shell. By far the most, however, must first appear beneath the periostracum and, although periodically interrupted during shell thickening, are

probably perpetuated by the same patches of secretory plasmalemmas throughout growth.

The canals of *Lingula*, which are sporadically traversed by membranes and proteinaceous strands, are variably filled with



1



2

FIG. 30. TEM micrographs through tissue associated with the descending lamella of the loop of *Calloria inconspicua*; 1, zone of elongately folded outer epithelium with arrow pointing to rough endoplasmic reticulum, arrowhead to electron-dense apical membrane and vesicles (V) in cells responsible for the secretion of the growing edge of the lamella, $\times 30,000$; 2, outer epithelium, with apical granular membrane (arrowhead), permeated by bundles of filaments (arrow) and attaching connective tissue to the lamella, $\times 30,000$ (Mackay, MacKinnon, & Williams, 1994).

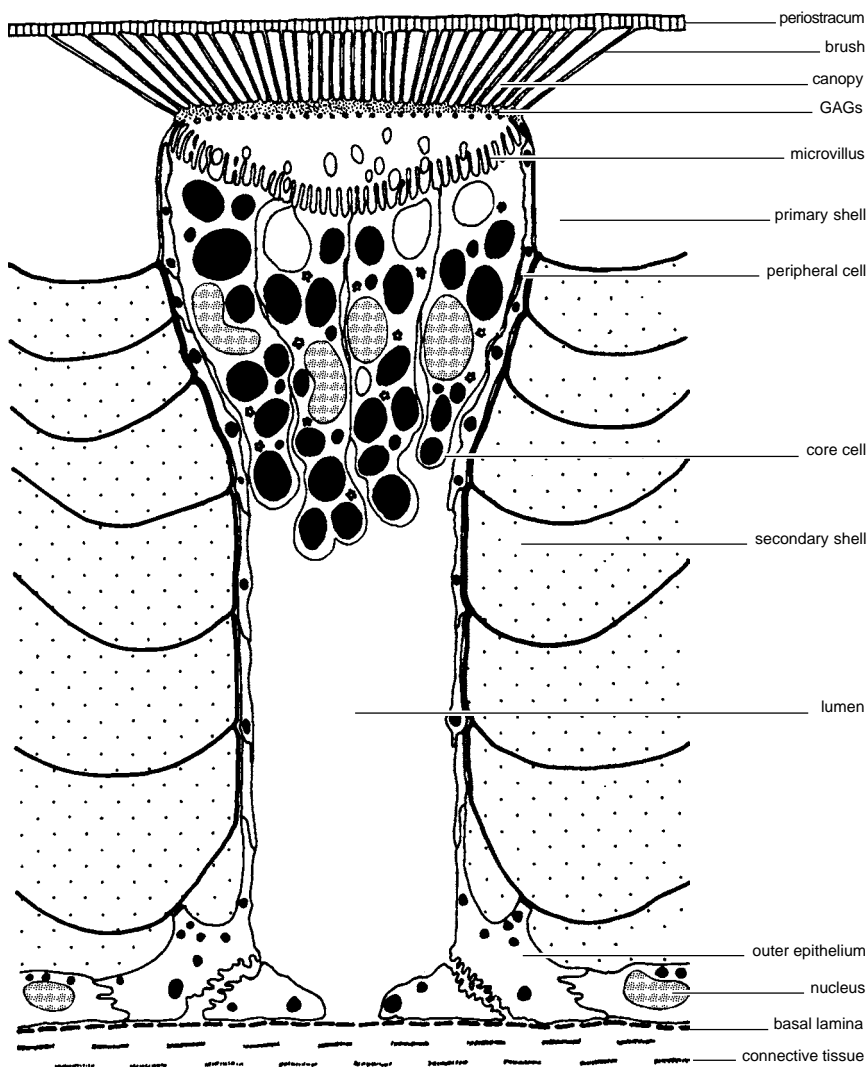


FIG. 31. Diagram of a medial longitudinal section of a terebratulide caecum showing its relation to shell and mantle (adapted from Owen & Williams, 1969).

electron-dense compounds, collapsed vesicle coats, and organically coated granules of apatite occasionally delineating ellipsoidal vacuoles. Sporadically occurring, enlarged chambers and galleries are formed around temporary, vertical and horizontal extensions of the tubular surface of the secretory plasmalemmas; but narrow canals can also be found contiguous with indentations in the plasmalemma surfaces, with which they may share a secreted infill of the same electron density. In effect, the organic constituents of

the vertical canal system are assembled independently of those incorporated into the shell.

The *Discina* canal system is comparable with that of *Lingula* in disposition and content. A distinctive suite of organic components found in the *Discina* canals, however, has not yet been seen in the *Lingula* shell. These components are exocytosed deep within the interdigitating tubes of the plasmalemma surface as a bulbous assemblage of medium and lucent electron-dense particles.

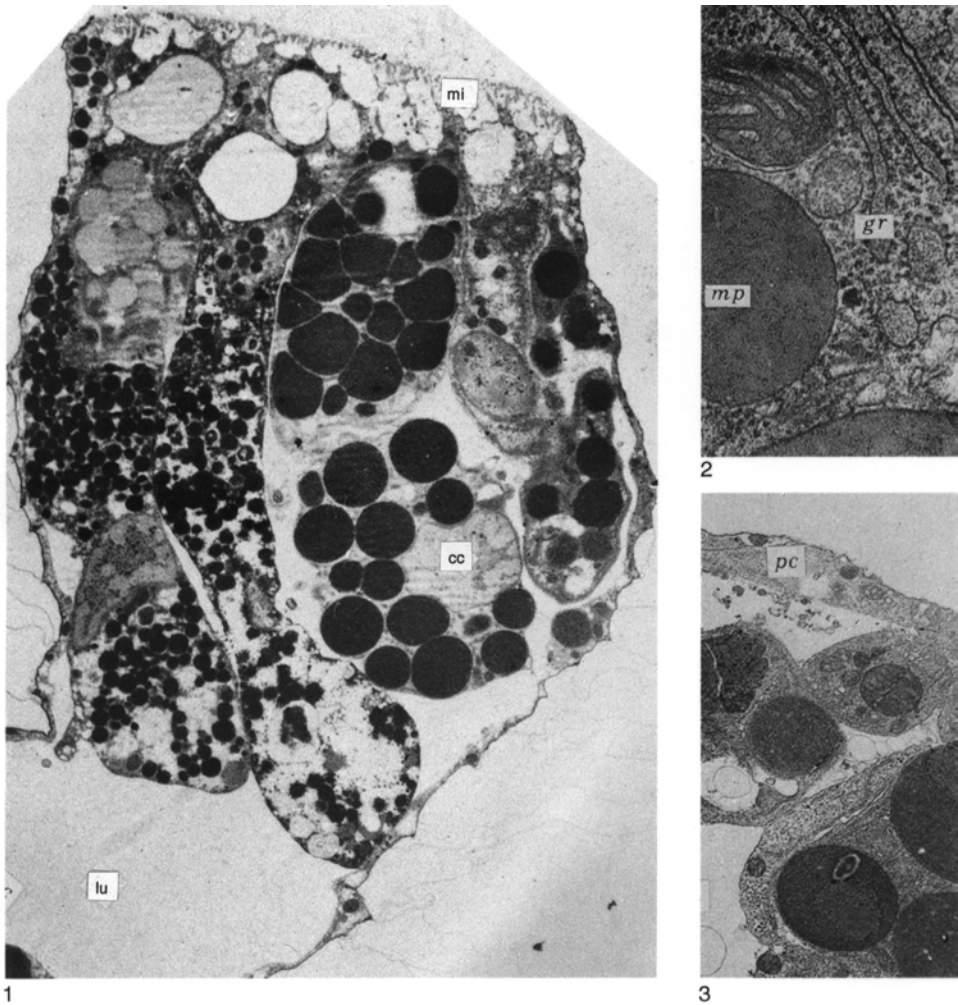


FIG. 32. TEM micrographs of decalcified sections of terebratulide caeca; 1, caecum of *Macandrevia cranium* (MÜLLER) showing the core cells (cc) with their microvillous apical surfaces (mi) and lumen (lu), $\times 55,000$; 2, details of core cells ($\times 55,000$) and 3, peripheral cells (pc) of *Calloria inconspicua* ($\times 8,000$) with conspicuous rough endoplasmic reticulum (gr) and glycosaminoglycans inclusions (mp) (Owen & Williams, 1969).

As these particles emerge from the apical surfaces of the secretory tubes, they polymerize into horizontally disposed alternating bands of electron-lucent and darker beaded lineations with a combined periodicity of 15 nm. This constituent appears to be a proteinaceous lining (with hydroxyproline) of at least part of the *Discina* canal system.

The concentric differentiation of cells at the mantle edge of living brachiopods, which can be correlated with the regular layering of

the integument and especially the incorporation within the shell of caeca and canals arising at the mantle edge, raises the controversial issue on how precisely cells are added to an expanding brachiopod mantle. An incremental expansion of the mantle can be sustained by uniformly distributed mitosis keeping pace with the areal increase in the shell so that the same cells or their replacements always secrete the same skeletal components in the same relative position on the

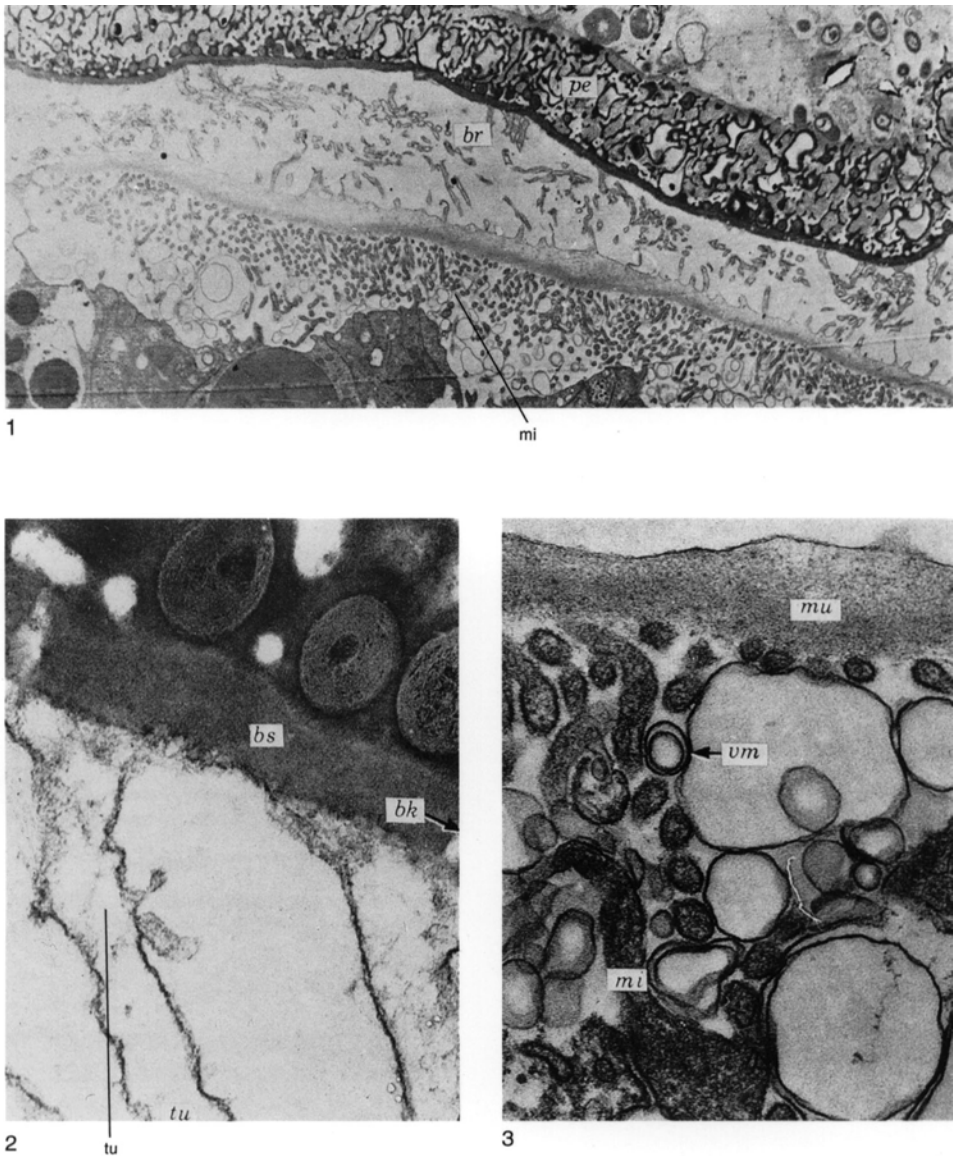


FIG. 33. TEM micrographs of decalcified sections of the caeca of *Calloria inconspicua*; 1, submedial section of the distal part of a caecum showing the composition of the caecal head with the microvillous surfaces (*mi*) of the core cells and their relationship to the brush (*br*) and periostracum (*pe*), $\times 6,000$; 2, detail of two tubules (*tu*) of the caecal brush showing their relationship to canal-like breaks (*bk*) in the basal layer (*bs*) of the periostracum, $\times 100,000$; 3, detail of the microvilli (*mi*) of the core cells showing their relationship to the GAGs layer (*mu*) and discarded vesicle membranes (*vm*), $\times 50,000$ (Owen & Williams, 1969).

internal shell surface. (This is the process favored by KNIPRATH, 1975, to explain the growth of the shell and mantle of the gastropod *Lymnaea*.) Alternatively, the mantle can grow by peripheral addition of cells prolifer-

ated from a relatively narrow generative zone in the outer mantle lobe. As each cell migrates around the outer mantle lobe to become incorporated in the outer epithelial layer, it secretes a variety of exoskeletal

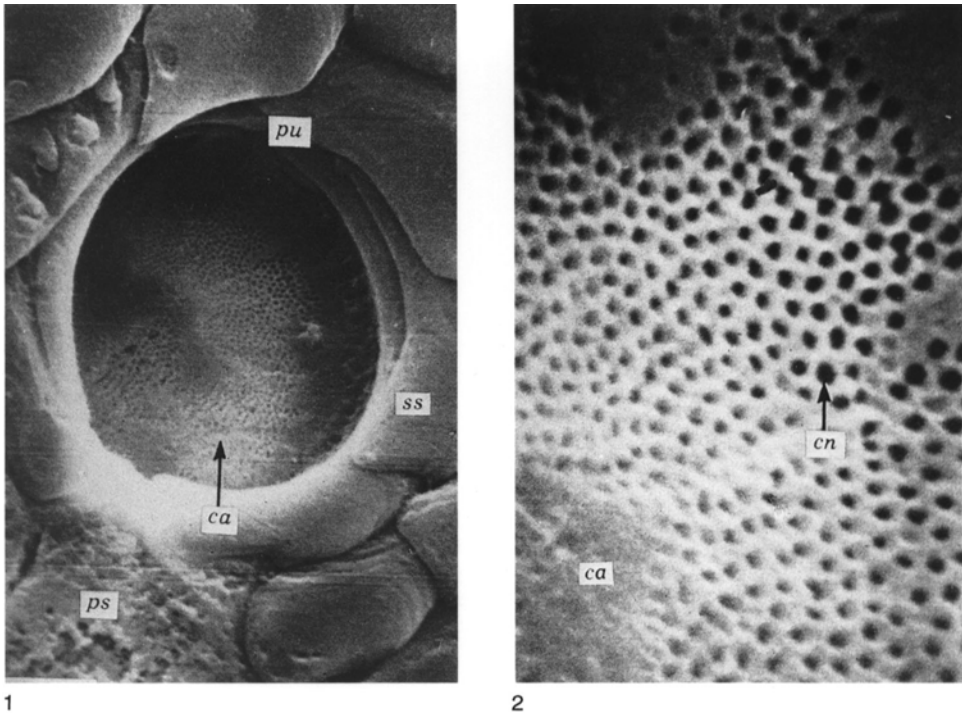


FIG. 34. SEM micrographs of a puncta (*pu*) of *Calloria inconspicua* at the internal junction between the primary (*ps*) and secondary (*ss*) shell; 1, internal view of canopy (*ca*), $\times 2,600$; 2, detail of canopy (*ca*) showing a meandriform array of canals (*cn*), $\times 13,000$ (Owen & Williams, 1969).

components in the same chronological order as their occurrence in the shell succession. In effect, except for adjustment during interphase (and minor, widely dispersed intramarginal mitosis), each cell of the mantle remains in proximity to that part of the shell it has secreted *ab initio*. The term conveyor-belt system has been applied to this mode of growth (WILLIAMS, 1968d).

The nature of the relationship between the outer epithelium and the shell succession of living brachiopods suggests that the growth of the mantle involves a continuous migration of cells from a mitotic zone at the outer mantle lobe. There is strong evidence for believing that the various constituents of organophosphatic shells are assembled intracellularly and, on exocytosis, become part of a thickening column of shell that has been secreted by the same patch of epithelium irrespective of structural and compositional

changes within the layers. The study by PAN and WATABE (1989) of the regeneration of periostracum and shell in *Glottidia* showed that repair progressed in the same order of secretion of constituents as is followed consecutively by vesicular cells and cuboidal outer epithelium.

Calcareous-shelled brachiopods, on the other hand, appear to be separated from the secreting plasmalemma of the mantle by a space that could be the main site for assembling shell constituents. The occurrences of caeca, however, which can arise only at the outer mantle lobe, must involve conveyor-belt growth throughout the postprotegeral shell of all punctate species (Fig. 35).

In accepting this mode of growth, account has to be taken of the secretory sequences of the cells making up the outer mantle lobe and the evidence for mitosis. Lobate cells, being responsible only for superstructural

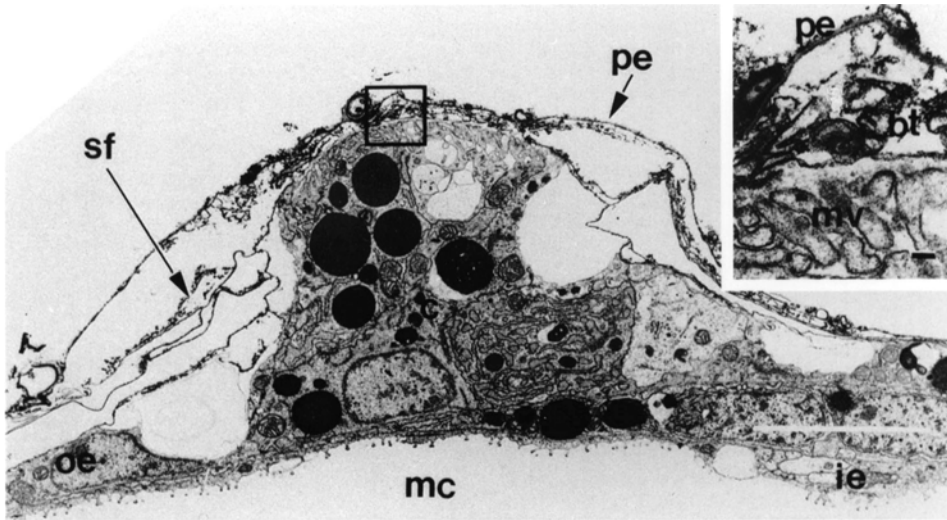


FIG. 35. TEM micrograph of a decalcified section of a juvenile caecum of *Terebratalia transversa* (SOWERBY) in relation to the periostracum (*pe*), membranes ensheathing secondary fibers (*sf*), and mantle consisting of outer (*oe*) and inner (*ie*) epithelium, $\times 5,000$; the box as an enlarged inset shows microvilli (*mv*) of the core cells immediately below brush tubes (*bt*), $\times 32,800$ (Stricker & Reed, 1985b).

embellishment of the periostracum, cannot be involved in migration into the position occupied by vesicular cells (WILLIAMS, 1973). Accordingly, any conveyor-belt movement would involve only the vesicular and cuboidal outer epithelial cells, in effect, the epithelial monolayer responsible for the secretion of the basal components of the periostracum and the succeeding shell succession. Moreover, the assumption that the mantle expands mainly by the addition of new cells at its margin prompts expectation that mitotic figures should be commonly found within that part of the outer mantle lobe delineated by the periostracal groove. Such evidence of active cell division has only been occasionally seen in margins of mature mantles (PAN & WATABE, 1989) and has not been found in the postlarval development of the mantle of *Terebratalia*, which has been subjected to an exhaustive scrutiny by STRICKER and REED (1985a, 1985b). Intercalation of new cells, however, must take place along the circumferential margin of an expanding epithelial monolayer, and the absence of evidence of significantly high mitotic activity does not

preclude an incremental addition of new cells, which is more likely to be at an unexceptional rate.

MANTLE-PEDICLE RELATIONSHIP

In the umbonal areas of a brachiopod, the mantle is normally associated with a pedicle, and their relationship is variable and can be topologically complex.

In lingulids, the pedicle is differentiated as an outgrowth of the ventral part of the embryonic inner epithelium, which later becomes the posterior body wall (YATSU, 1902a). In maturity, the junction between the wall and pedicle occurs along the dorsal arc of the circular pedicle base (Fig. 39.1). It is marked by a sudden change from microvillous, nonciliated inner epithelium secreting a glycocalyx to a pedicle epithelium distinguishable as a band of cells charged with electron-dense vesicles and exuding an electron-dense outer bounding membrane of the pedicle cuticle through irregular, cylindrical prolongations of the plasmalemmas. The dorsal boundary of the posterior body wall is the inner lobe of the mantle margin

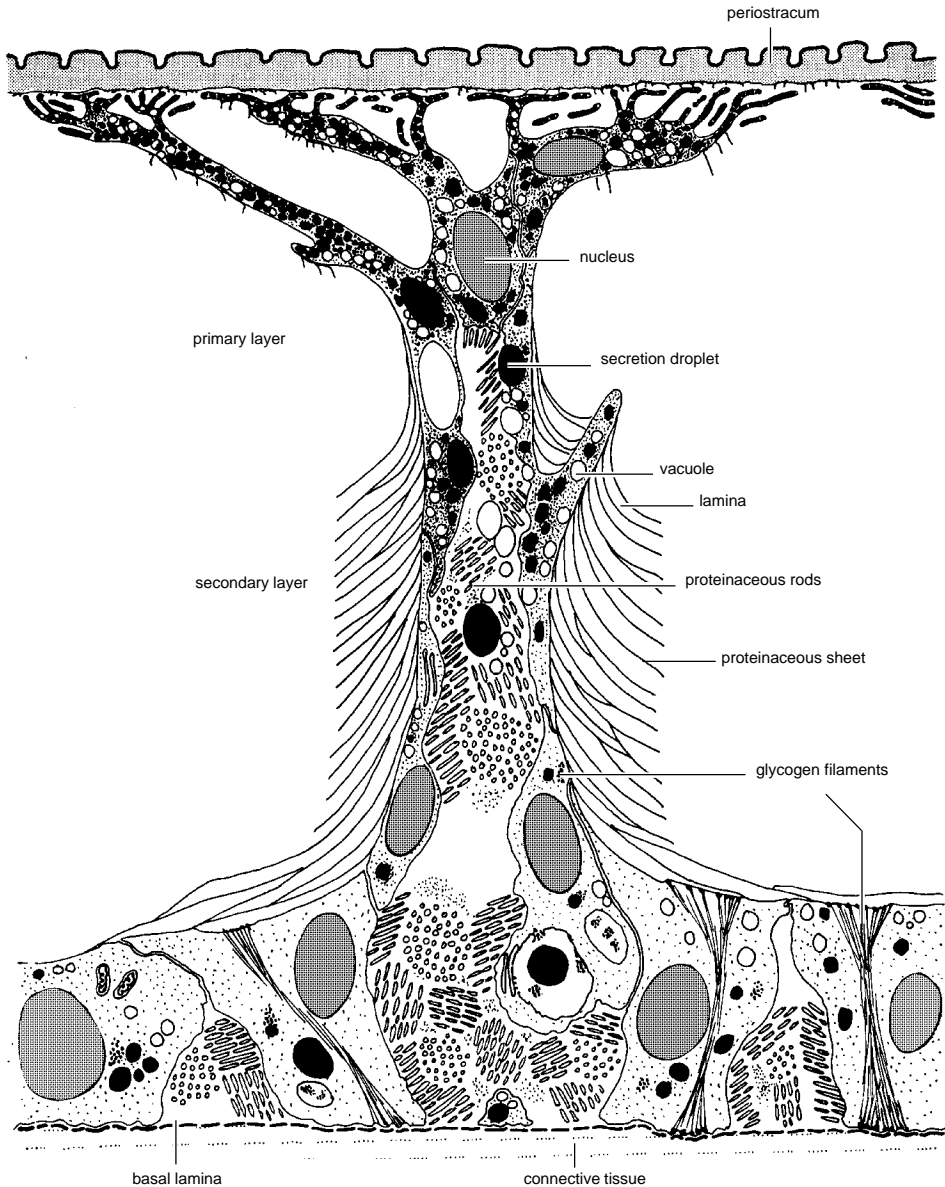


FIG. 36. Diagrammatic representation of a medial longitudinal section of a caecum showing its relationship to the periostracum and the dorsal mantle of *Neocrania anomala* (adapted from Williams & Wright, 1970).

underlying the posteromedian part of the dorsal valve. Here the junction between the inner and outer lobes is marked in the usual way by a marginal array of setae and their follicles (Fig. 39.1). The ventral sector of the pedicle base is also represented by a sharp junction, although between outer and

pedicle epithelia. The junction is marked by a thick, electron-dense sheet (pedicle sheet), intervening between cuticle and shell and secreted by a narrow band of vesicular columnar cells, which are assumed to be homologous with the vesicular cells of the outer mantle (Fig. 40).

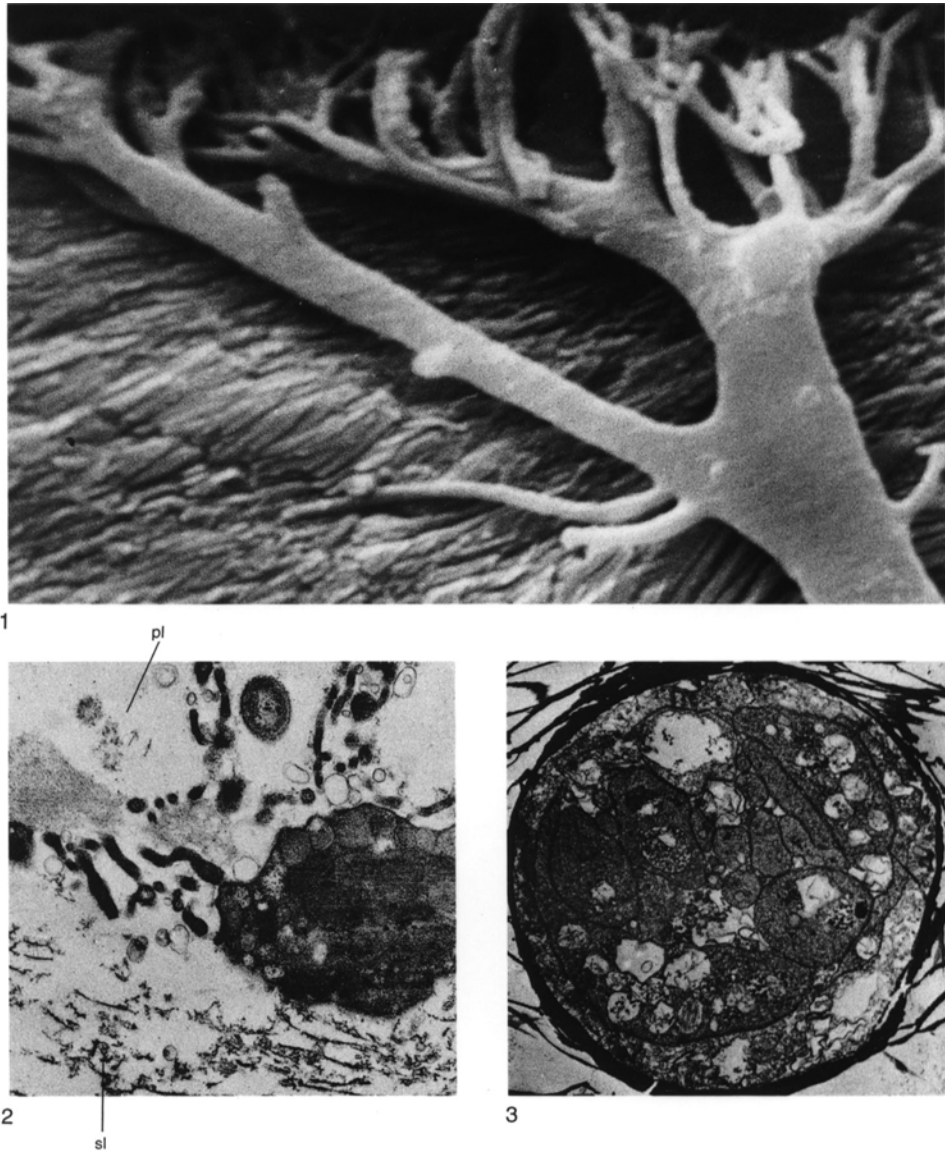


FIG. 37. Various aspects of the caeca and punctuation of *Neocrania anomala*; 1, SEM micrograph of an etched section of the primary layer of the dorsal valve showing the branches and tubules of a puncta filled with resin, $\times 5,200$; 2, TEM micrograph of a terminal branch of a caecum with branching tubules seen in transverse to longitudinal sections in the primary layer (*pl*) with proteinaceous sheets of the secondary layer (*sl*) beginning to appear at the bottom of the micrograph, $\times 15,000$; 3, transverse section of a caecal branch, surrounded by the proteinaceous sheets of the secondary shell, showing the highly vesicular inclusions forming the core to stretched outer epithelium at the periphery, $\times 8,000$ (Williams & Wright, 1970).

In lingulids the pedicle emerges between the umbones of both valves, but the pedicle of discinids is ventrally located relative to the commissural plane; and, although the early

stages in discinid development are unknown, the disposition of epithelial junctions in mature shells clarifies the relationship between mantle and pedicle (Fig. 39.2). In

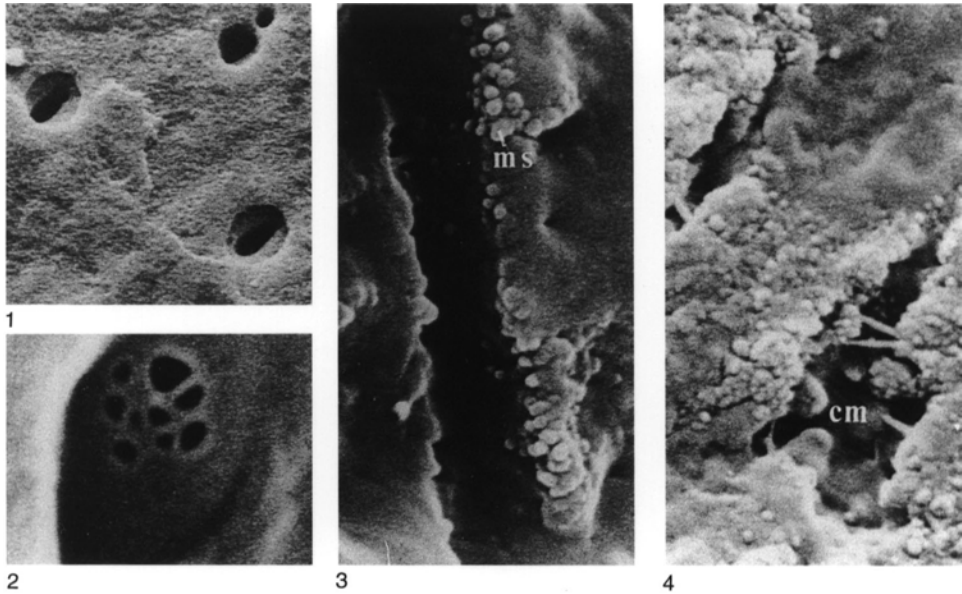


FIG. 38. Various SEM micrographs of canals and chambers in the shell of *Lingula anatina*; 1, canal apertures exposed on the internal surface of an apatitic lamina digested in chitinase, $\times 3,000$; 2, transverse membrane in a canal penetrating an apatitic lamina treated with Tris buffer, $\times 30,000$; 3, canal wall studded with apatitic mosaics (*ms*) penetrating a lamina of apatite and GAGs digested in endoproteinase Glu-C, $\times 14,000$; 4, vertical chamber (*cm*), intruded by apatitic mosaics, and branching canals all crossed by fibrous collagens in a lamina composed of botryoidal masses of apatitic mosaics and GAGs (especially in top right corner) treated with phosphate buffer, $\times 9,000$ (Williams, Cusack, & Mackay, 1994).

mature *Discinisca*, the pedicle epithelium along the ventral sector of the pedicle base is also contiguous with the outer epithelium responsible for the secretion of the ventral valve. The only difference from the lingulid arrangement is that the pedicle base and its surrounding cuticular sheet encroach anteriorly over a much greater area of the external surface (BLOCHMANN, 1900). The junction between the posterior body wall and the outer epithelium of the dorsal valve is also the same. That junction between the posterior body wall and the dorsal arc of the pedicle base, however, is indented to accommodate another array of marginal setae. Consequently, the discinid posterior body wall is fringed by two arrays of setae so that the array between the pedicle and inner epithelia is likely to be the homologue of the array along the margin of the ventral mantle (Fig. 39.2).

This relationship suggests that the pedicle originated entirely within the embryonic precursor to the ventral outer epithelium and not as an outgrowth of inner epithelium as in *Lingula*. The assumption explains why the posteromedian margin of a maturing ventral valve appears to grow dorsally around the pedicle, which becomes enclosed in an oval slit bridged by periostracum and primary layer only in *Discinisca* but by some underlying apatitic shell as well in *Discina*.

The various junctions between mantle and pedicle are similarly differentiated in lingulids and discinids so that those studied ultrastructurally in selected species are typical of the organophosphatic group as a whole.

The inner-outer epithelial junction at the pseudointerarea forming the posteromedian margin of the dorsal valve of *Glottidia* is like that at the anterior margin of the shell except

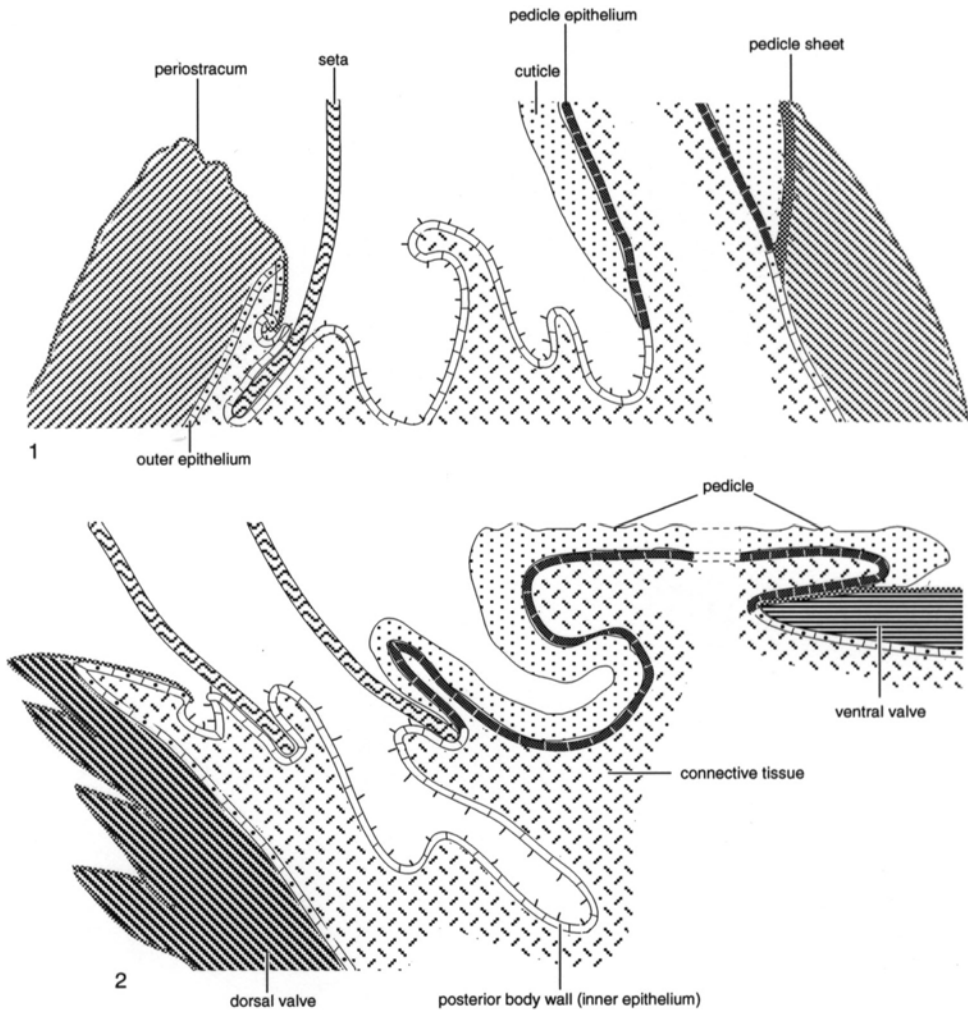


FIG. 39. Diagram of the inner, outer, and pedicle epithelia in relationship to the shell and pedicle of mature 1, *Lingula* and 2, *Discinisca* (new).

for the absence of the periostracal groove. Consequently, the microvillous, inner epithelium and periostracum-secreting outer epithelium, along the inner face of the outer lobe, are almost parallel to each other away from a deeply inserted, narrowly angled junction that is sharp (Fig. 41.1).

The junction between outer and pedicle epithelia in the posteromedian region of the ventral valve is also sharp with the short, microvillous apical plasmalemmas of the pedicle epithelium instantly distinguishable

from the irregularly extended ones of the outer epithelium. Vesicles with electron-dense contents are common in both types of epithelia and, at the junction, contribute to the expansion of the electron-dense sheet separating the base of the pedicle from the inwardly sloping posterior surface of the ventral valve (Fig. 40).

The junction between inner and pedicle epithelia is as sharp as those involving the outer epithelium. The inner epithelium secretes a thick, speckled glycocalyx that is

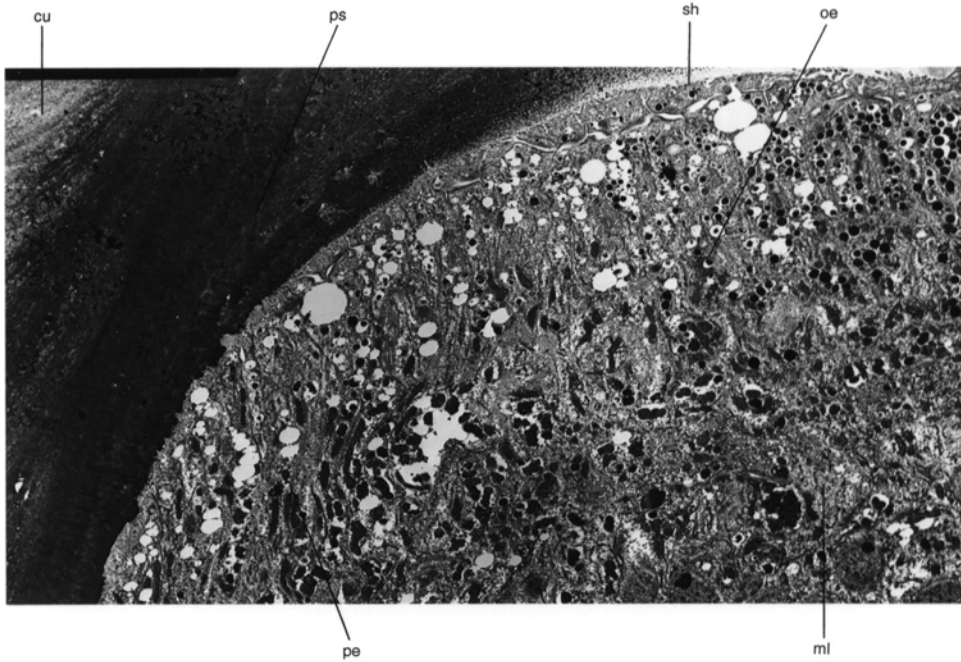


FIG. 40. TEM micrograph of a section of the posteromedian part of a decalcified ventral valve (with pedicle) of *Lingula anatina* showing the junction between outer (*oe*) and pedicle (*pe*) epithelium in relation to shell (*sh*), cuticle (*cu*), and pedicle sheet (*ps*) and the muscle layer (*ml*) lining the pedicle, $\times 3,000$ (new).

propelled across the junction by microvilli up to half a micrometer long. At the junction the inner epithelium gives way to a narrow band, one or two cells wide, that secretes beneath the glycocalyx a continuous sheet of electron-dense nodules that, within a micrometer or so, polymerize into an electron-dense, sparsely fibrillar coat about 15 nm thick and discrete nodules up to 150 nm in size (Fig. 41.2). The coat and nodules form the cover to the pedicle cuticle, which consists for the most part of a fibrillar mesh of chitin in an electron-light matrix; the chitinous fibrils interconnect with the nodules. The cells secreting the cuticular cover are more like pedicle epithelium although their apical plasmalemmas are extended as irregular protuberances up to 50 nm thick and are thereby distinguishable from the microvillous pedicle and inner epithelia.

In living craniides no pedicle is developed, and the ventral valve is cemented to the substrate by a posterior attachment area in the larval stage (NIELSEN, 1991) and additionally

by a film of adhesive mucin (Fig. 42), exuded as an external coat to the periostracum at the mantle edge in the mature shell (WILLIAMS & WRIGHT, 1970).

In articulated brachiopods, the relationship between the mantle lobes and between the pedicle and the mantle as a whole is fundamentally different from those of inarticulated species. In the former group, the pedicle is first differentiated, not as an outgrowth of the ventral mantle, but as a posterior pedicle rudiment continuous with a mantle rudiment that develops into both valves (see Fig. 63). Moreover, the mantle cavity contained by microvillous, inner epithelium is not continuous around the shell but restricted to the anterior part in the following way.

The mantle edges of both valves remain discrete around the gape of the shell as far as the cardinal extremities. Here at the lateral ends of the hinge line, the mantle edges join and simultaneously divide in another plane to accommodate the coelomic cavity. First,

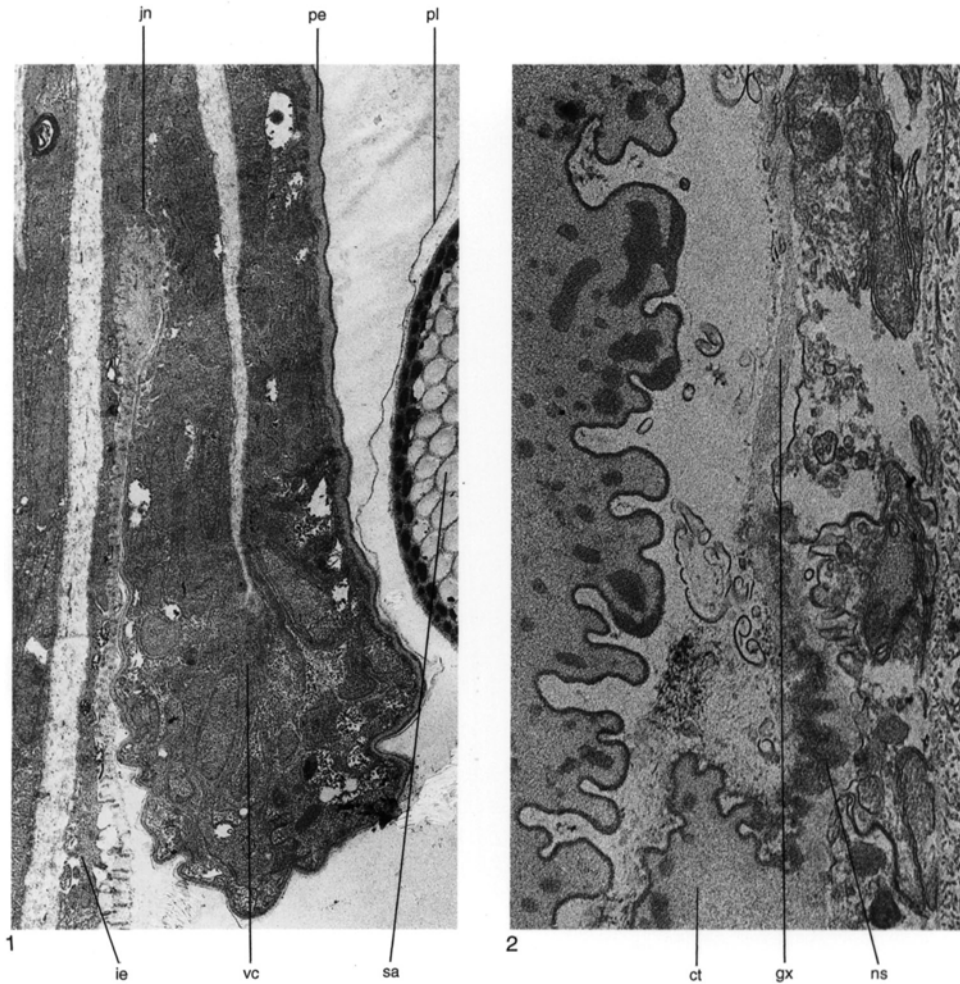


FIG. 41. TEM micrographs of sections of decalcified posteromedian regions of the shell of *Glottidia pyramidata*; 1, the junction (*jn*) between the vesicular cells (*vc*) of the outer mantle lobe secreting periostracum (*pe*) and the inner epithelium (*ie*) at the pseudointerarea of the dorsal valve with pellicle (*pl*) and seta (*sa*), $\times 5,250$; 2, the transition from cuticle-secreting (*ct*) pedicle epithelium to glycocalyx-exuding (*gx*) microvillous inner epithelium through cell(s) secreting electron-dense nodules (*ns*), $\times 17,750$ (new).

the inner mantle lobes of inner epithelium fuse into one layer, which falls away to become the anterior body wall. Then the outer lobes of both edges come together to form a complex of cells (Fig. 43). These constitute two strips of outer epithelium that secrete the carbonate ventral and dorsal interareas and their periostracal covers (WILLIAMS, 1956; WILLIAMS & HEWITT, 1977).

The posterior outer epithelial zone is well developed in *Thecidellina* but differs funda-

mentally from that of other living articulated brachiopods by lacking a pedicle. In living thecideidines, no pedicle develops from the caudal rudiment of the embryo (KOWALEVSKY, 1874). Instead, the periostracum of the pedicle valve is directly attached to the substrate, probably by a film of mucin. Accordingly, the hinge line is unbreached by such medial openings as the delthyrium and notothyrium and is underlain by a continuous strip of posterior epithelium extending from

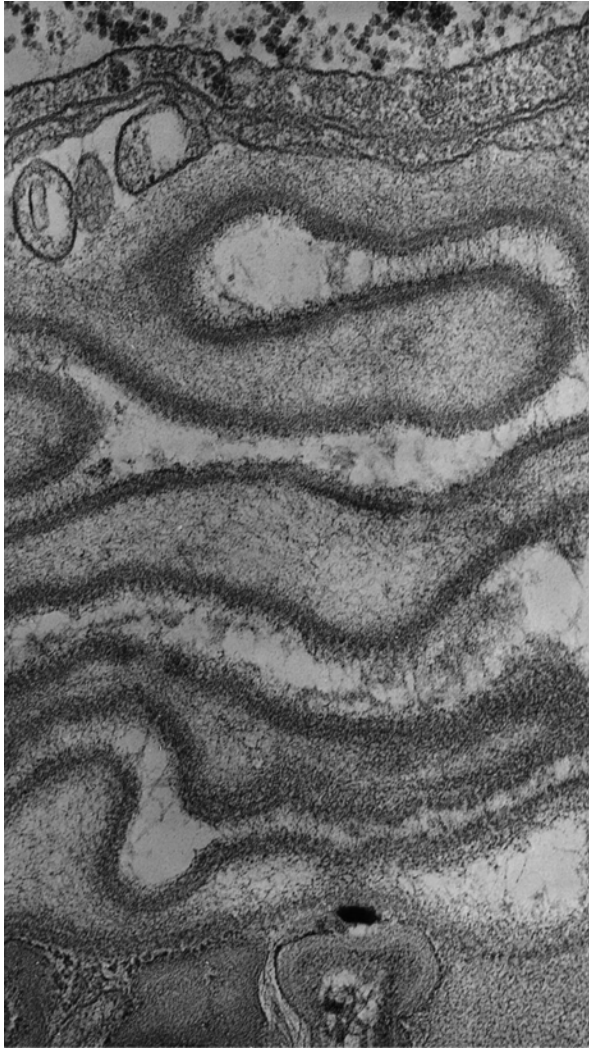


FIG. 42. TEM micrograph of a section of a decalcified ventral valve and mantle of *Neocrania anomala* showing a highly folded periostracum attached to the substrate (below) with tubular extensions of the plasmalemma of the secreting outer epithelium (above), $\times 40,000$ (new).

one cardinal extremity to another (WILLIAMS, 1973).

This strip consists of an inner row of six to eight, highly vesicular, columnar cells grouped around an infold of periostracum and an outer row of larger cells, continuous with cuboidal outer epithelium and probably also concerned with secreting carbonate shell, especially along the slowly growing faces of each interarea (Fig. 44). Secretion of the periostracum begins in the anteromedian

zone of the periostracal fold. Electron-dense granular material, probably comparable with the film of GAGs exuded at the outer mantle lobe, is secreted by two or three medially situated columnar cells along intercellular pathways as well as across the plasmalemmas. Within two micrometers of its deposition as a continuous mass, the exudation parts irregularly into two layers forming impermanent external coats of the ventral and dorsal interareas. The periostracum proper is

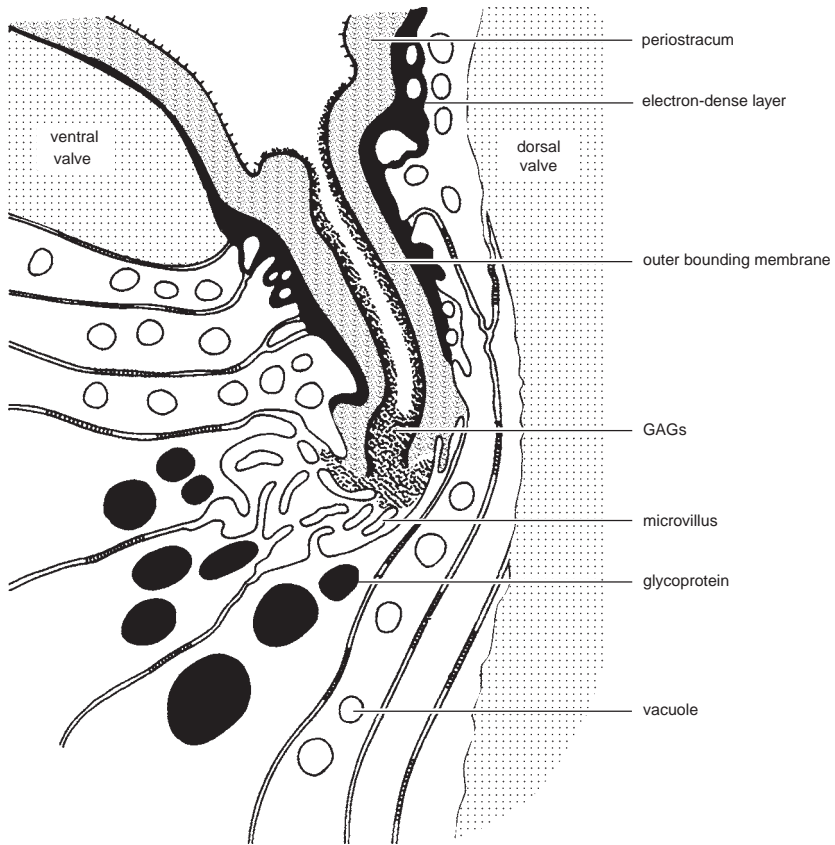


FIG. 43. Diagrammatic longitudinal section of the fused outer mantle lobes underlying the cardinal margins of a young *Notosaria*, approximately $\times 25,000$ (Williams and Hewitt, 1977).

secreted even within the fold as two discrete layers separated by the medial mass of the external coat. Each periostracal layer is banded and is deposited as a series of acutely disposed, overlapping wedges that become progressively younger toward the fold. Secretion of periostracum terminates at the edge of the fold with the exudation of a sealing membrane a few nanometers thick. The membrane acts as a seeding sheet for calcite crystallites representing the beginnings of the carbonate layer of the interarea.

In rhynchonellides and terebratulides, a posterior rudiment or lobe, which is non-ciliated (STRICKER & REED, 1985c), develops into a pedicle filling the larger, delthyrial and smaller, notothyrial openings in the ventral and dorsal interareas respectively of adult shells. The junction with the mantle, there-

fore, is shared with the outer epithelium responsible for the secretion of both valves and intersects the fused mantle lobes secreting the carbonate interareas and their periostracal covers. The junction between the microvillous epithelium secreting the pedicle cuticle and outer epithelium is sharp. It is marked by a narrow band of one or two cells that differ from pedicle epithelium in lacking microvilli and from outer epithelium in secreting granular calcite sealing off secondary fibers and their sheaths and a thin proteinaceous membrane, which acts as a bonding sheet for the folded cuticle (Fig. 45–46).

The ringlike junction can be distorted by differential growth of its biomineralized boundaries, but its circumference can only increase at its intersection with the fused mantle lobes underlying the hinge line. The

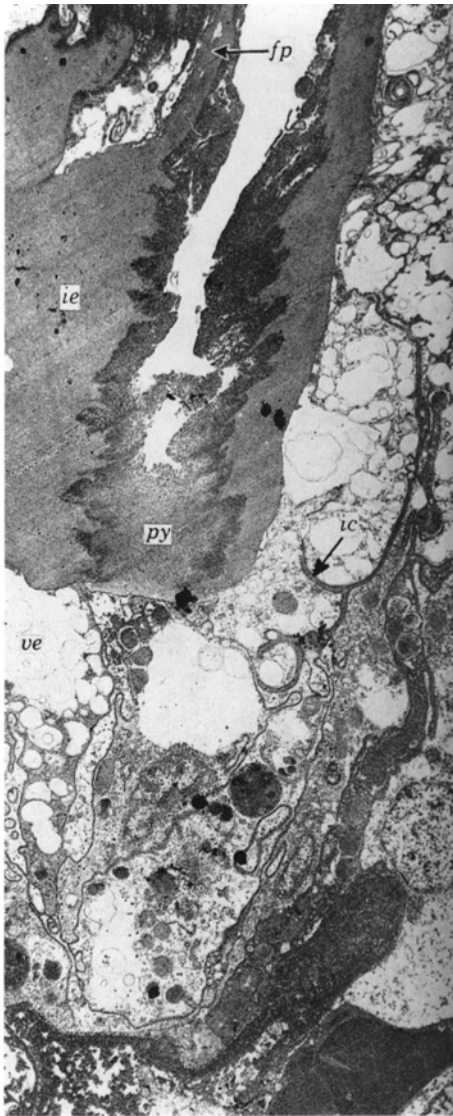


FIG. 44. TEM micrograph of a decalcified dorsoventral section of the periostracal fold and columnar cells at the hinge-line of *Thecidellina barretti* showing the periostracum consisting of an external flaplike layer (*fp*) and an internal layer (*ie*) of medium electron density, intercellular (*ic*) and medial (*py*) GAGs, and vesicular cell (*ve*), $\times 5,500$ (Williams, 1973).

fused mantle lobes of such rhynchonellides as *Notosaria* and such terebratulides as *Terebratulina* have been studied (WILLIAMS & HEWITT, 1977) and are structurally comparable with those described for the thecideidines.

The most striking deformation of the ringlike junction occurs when the ventral, outer-mantle lobes grow dorsomedially from their intersection with the pedicle-outer epithelial junction and secrete a pair of tetrahedral structures, the **deltidial plates**. The plates can extend medially only because they grow posterodorsally of the umbo of the dorsal valve. Further growth leads to a median conjunction of deltidial plates to form a **deltidium** and, in such genera as *Liothyrella*, to a median fusion of the paired ventral lobes to form a common secretory unit exuding both periostracum and underlying carbonate shell as a continuous structure (**symphytium**) across the delthyrium (see Fig. 317). The symphytium is frequently identified in such other terebratulides as *Gryphus* and *Laqueus*, but usually there is a well-developed median suture; and even in *Liothyrella*, transverse sections near the posterior margin of the symphytium will always show that the structure originated by fusion of ventral mantle lobes.

MARGINAL SETAE

Fine, chitinous bristles (*setae* or *chaetae*) occur in clusters at the epithelial surface of all brachiopod larvae and in closely spaced sets emerging from the mantle grooves of all adult brachiopods except for craniids, thecideidines, and megathyrids. A typical, mature seta within the mantle groove occupies a cylindroid invagination (**follicle**) of a single layer of cells with many characteristics of the inner epithelium (Fig. 47). In particular, they are covered with regular arrays of microvilli up to 500 nm long and contain abundant mitochondria with arcuate cristae, densely distributed glycogen, and filamentar bundles connected with the microvilli. The base of the follicle is formed of a specialized cell(s) (Fig. 48–49), the setoblast (GUSTUS & CLONEY, 1972; STORCH & WELSCH, 1972), with erect, apical microvilli up to 6 μm long in *Lingula* and in the larva of *Terebratalia*.

A seta occupying such a follicle, which may be several millimeters long, consists of closely packed cylindrical or prismatic canals with diameters of 600 nm or so medially but dwindling to less than 100 nm at the circum-

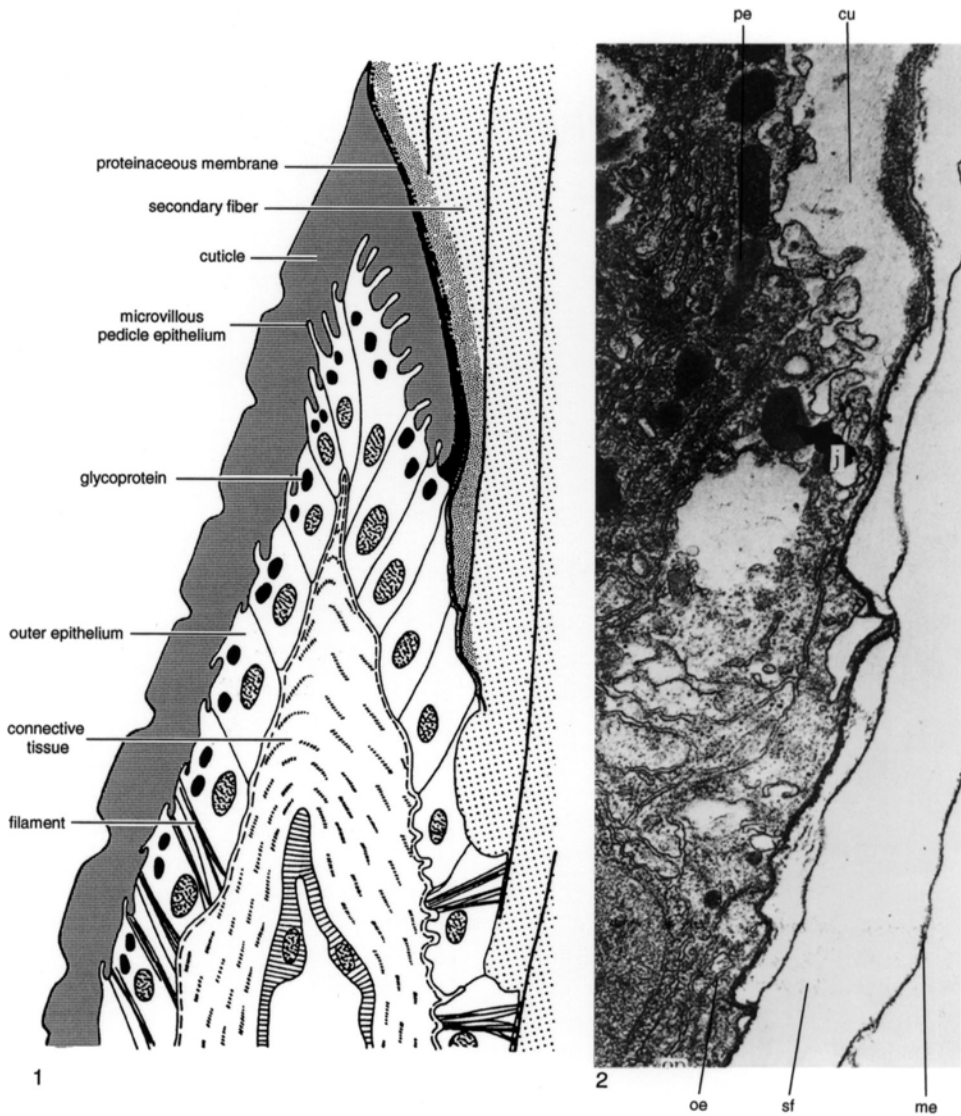


FIG. 45. Drawing and TEM micrograph of a decalcified longitudinal section of the ventral-pedicle mantle junction in young *Notosaria nigricans*; 1, relationship between the cuticular fold and the pedicle collar, approximately $\times 10,000$; 2, detail of junction (*j*) between pedicle epithelium (*pe*) secreting the cuticle (*cu*) and outer epithelium (*oe*) depositing secondary fibers (*sf*) with membranous sheaths (*me*), $\times 20,600$ (Williams & Hewitt, 1977).

ference (Fig. 47.1; 50.1). The walls defining the larger, medial canals are secreted by the setoblast as chitinous casts around but not over the long microvilli. The walls polymerize and, as secretion proceeds, move distally to form a seta that can eventually be composed of several hundred such canals. Although most of a seta is secreted by the setoblast, the outer layers of smaller canals,

which have thicker walls, are exuded by the cells lining the follicle (Fig. 50). In *Lingula*, electron-dense clots, composed of fibers and scattered throughout a loose mesh of branching chitinous fibers up to 300 nm long, migrate from the tips of the microvilli to become attached to and assimilated within the outer, cortical layer of the seta. Many such clots are emptied of their fibrous

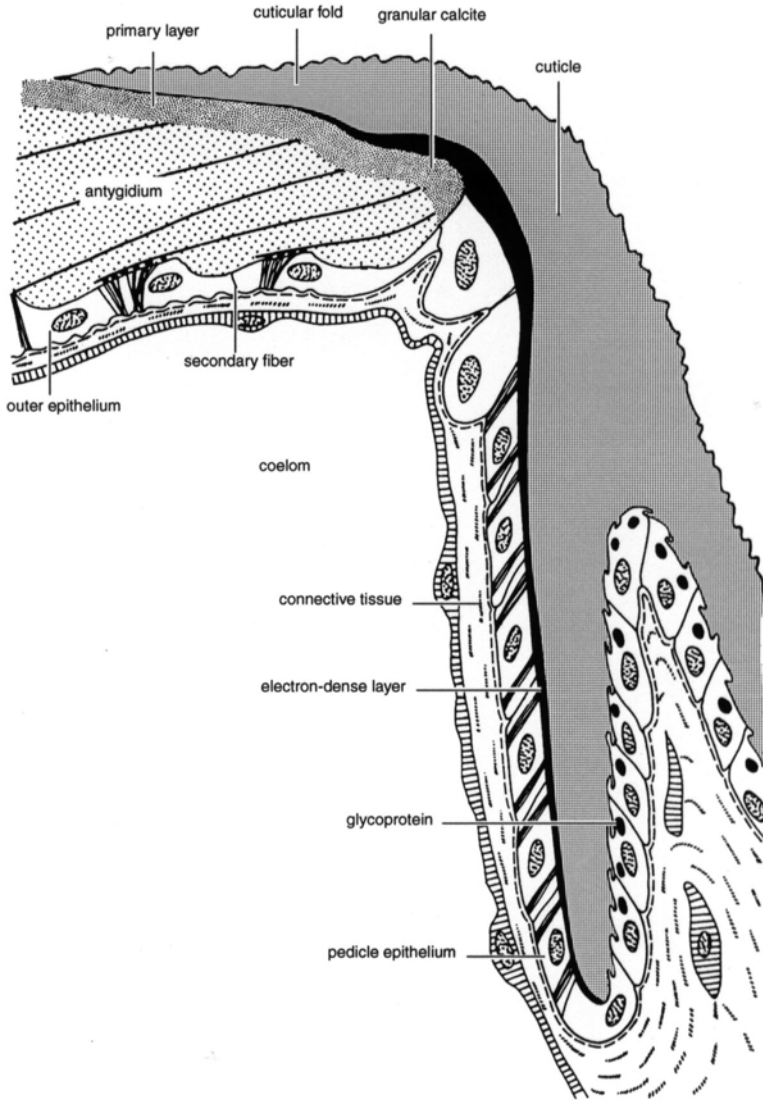
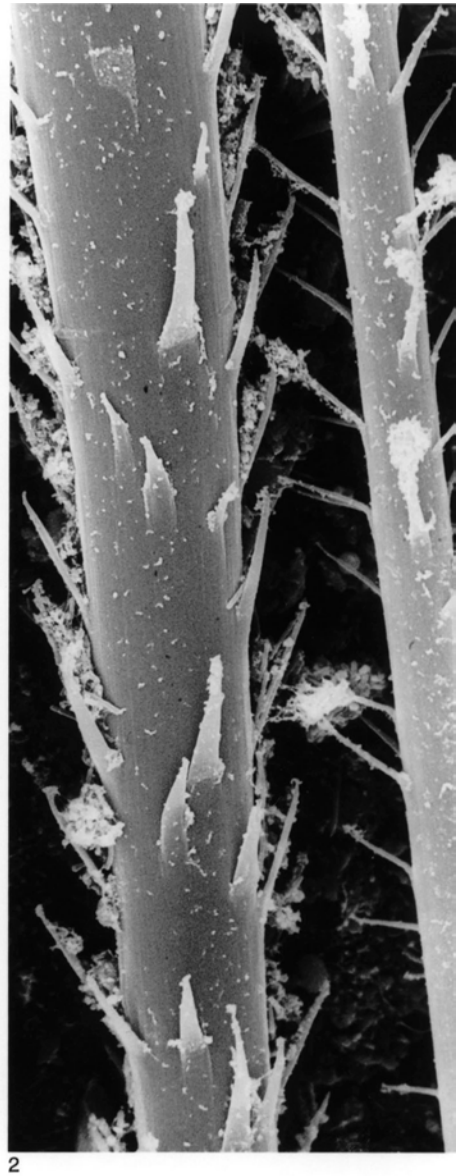
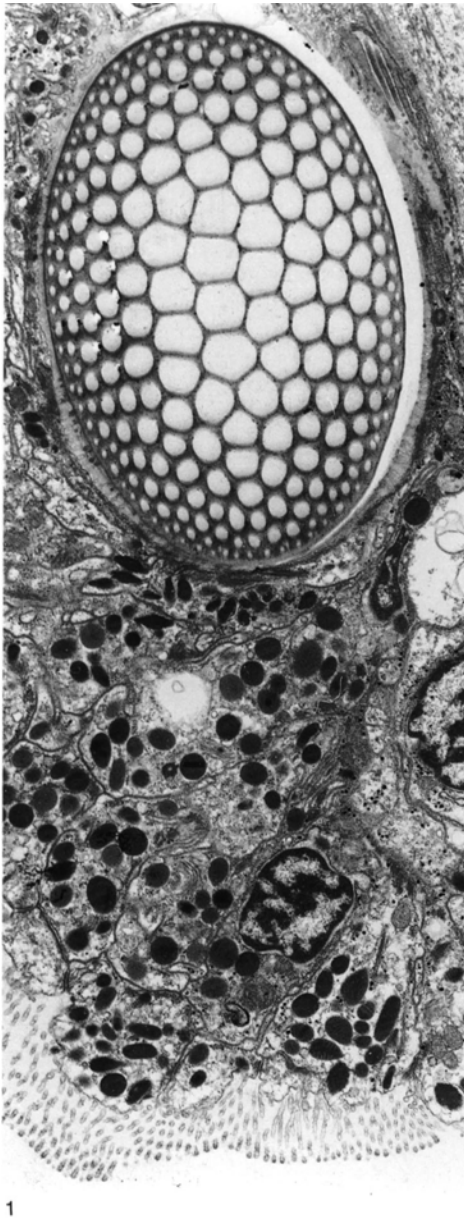


FIG. 46. Diagrammatic longitudinal section showing the relationship between the dorsal sector of the pedicle-outer epithelial junction and the antygidium of the dorsal valve of a young *Notosaria nigricans*, approximately $\times 10,000$ (Williams & Hewitt, 1977).

constituents presumably through their incorporation within the matrix of the cortical layer. This bounding layer is further differentiated so that, by the time the seta emerges from the follicle, it consists of a triple-layered membrane of contrasted electron density, about 60 nm thick, with an array of very short, erect fibers on the outer surface.

The larval setae of *Terebratalia* (GUSTUS & CLONEY, 1972) and *Terebratulina* (STRICKER

& REED, 1985a) are indistinguishable from those of adults except for diameter, as they are seldom composed of more than 50 canals. Setae of comparable delicacy are interspersed among more robust ones along the mantle edge of an adult valve and have evidently been secreted by newly formed follicles. Slender setae may also occupy the same follicles as mature ones; and this arrangement has been interpreted by RUDWICK



1

2

FIG. 47. TEM and SEM micrographs of a decalcified section and critical-point-dried mantle edges of *Discina striata*; 1, transverse section of a seta and its follicle with microvillous inner epithelium charged with glycoproteinaceous vesicles (below), $\times 3,990$; 2, setae with distally pointing barbs, $\times 1,900$ (new).

(1970) as the formation of new follicles by a process of budding. In such brachiopods as *Discina*, however, the occurrence of pairs of slender and robust setae in the same follicle (Fig. 47.2) is so common as to suggest that their association is a normal condition re-

lated to their function or to a periodic shedding of the older set of setae.

Setae have not been comprehensively studied, but those that are known show some variation from one species to another. The canals of the setae of *Terebratalia* larvae and

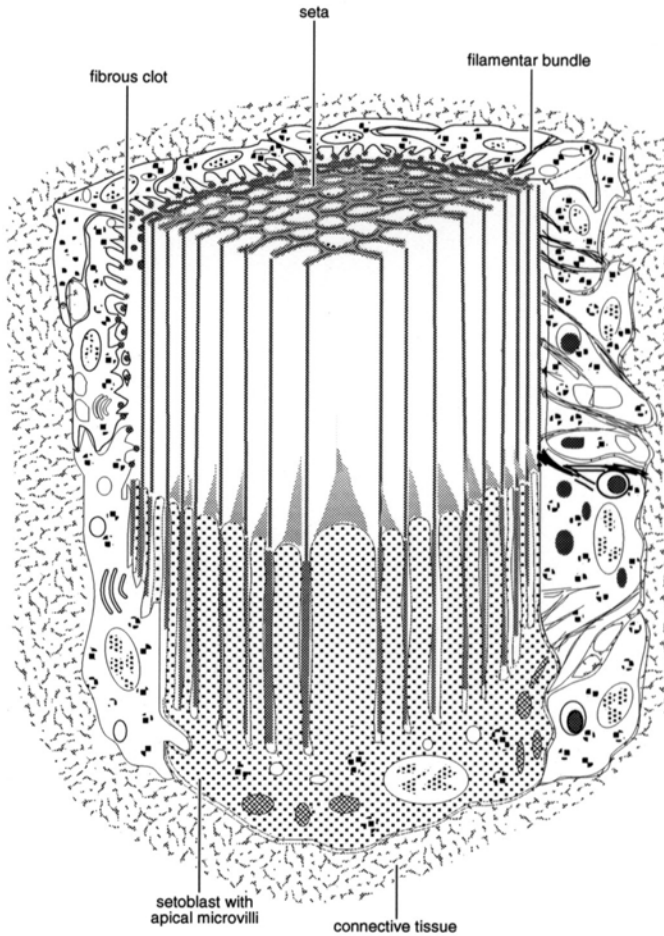


FIG. 48. Generalized diagram of the proximal part of a follicle of a lingulid showing the relationship of its seta to the apical microvilli arising from the setoblast (new).

of *Notosaria* adults (Fig. 51) have rounded transverse sections and relatively thick walls (up to 100 nm or so medially in *Notosaria*). The medial canals of the setae of the organophosphatic *Lingula* and *Discina* (Fig. 47.1) are normally hexagonal in cross section and thin-walled (about 30 nm). There are also differences in shape, with the setae of *Lingula* being more oval than those of *Notosaria* and *Discina*. The most distinctive variability, however, is in the external morphology. In many such genera as *Lingula* and *Notosaria*, setae are devoid of surface embellishments apart from some longitudinal striation and an occasional impersistent, thick-

ened ring marking variations in the rate of secretion, which very rarely may be extended as slivers up to 2 or 3 μm long along the setal axis. In the discinids, however, the setal surfaces are usually strongly striated at intervals of about 300 nm, and especially they are festooned with narrow, lanceolate, barblike outgrowths that may be up to 30 μm or so long (Fig. 47.2). The bars occur at intervals of up to 10 μm but are not distributed in any recognizable pattern along the surface although they tend to cluster at nodes between 30 and 50 μm apart. It is noteworthy that the larval setae of *Neocrania* are also embellished with short, acutely inclined barbs that

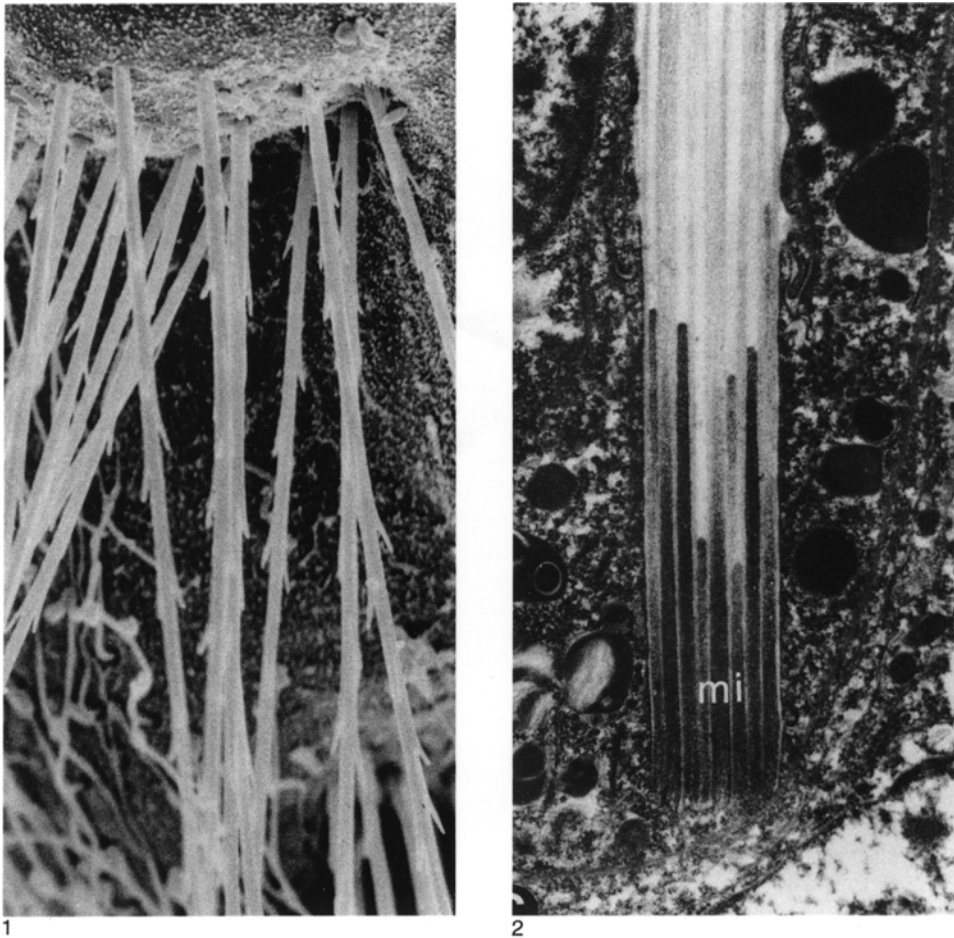


FIG. 49. SEM and TEM micrographs of larvae of *Neocrania anomala* showing 1, the proximal part of the first bundle of setae with their distally pointing barbs, $\times 2,500$, and 2, a section of the proximal end of a seta with the microvilli (*mi*) of the setoblast extending into the setal channels, $\times 16,000$ (Nielsen, 1991).

have been shown by NIELSEN (1991) to arise as terminations of peripheral canals (Fig. 49.1).

The close spacing and great length of most setae are related to their primary function as sensory grilles (RUDWICK, 1970). The setal fringe extending beyond the shell margin is normally longest anteromedially and posterolaterally and, in the planktonic genus *Pelagodiscus*, can exceed the length of a shell of several millimeters. In the related *Discina*, a fringe of some millimeters forms an effective sensory grille by supporting mucous curtains on the barbed outgrowths of the setae.

The shorter, simple setae of terebratulides (*Neothyris*) and rhychonellides (*Notosaria*) are also disposed to serve as a tactile safety sieve for the mantle cavity. The most extraordinary setal differentiation, however, occurs in *Lingula* (MORSE, 1902). The setae of this infaunal genus vary in size, attaining lengths of several millimeters posterolaterally and anteriorly where they are longest in a median and two lateral zones. The posterolateral and lateral setae, lubricated by mucus exuded by the inner mantle lobe, assist in the burrowing of *Lingula* into the substrate. The anterior fringe of setae cluster to form three

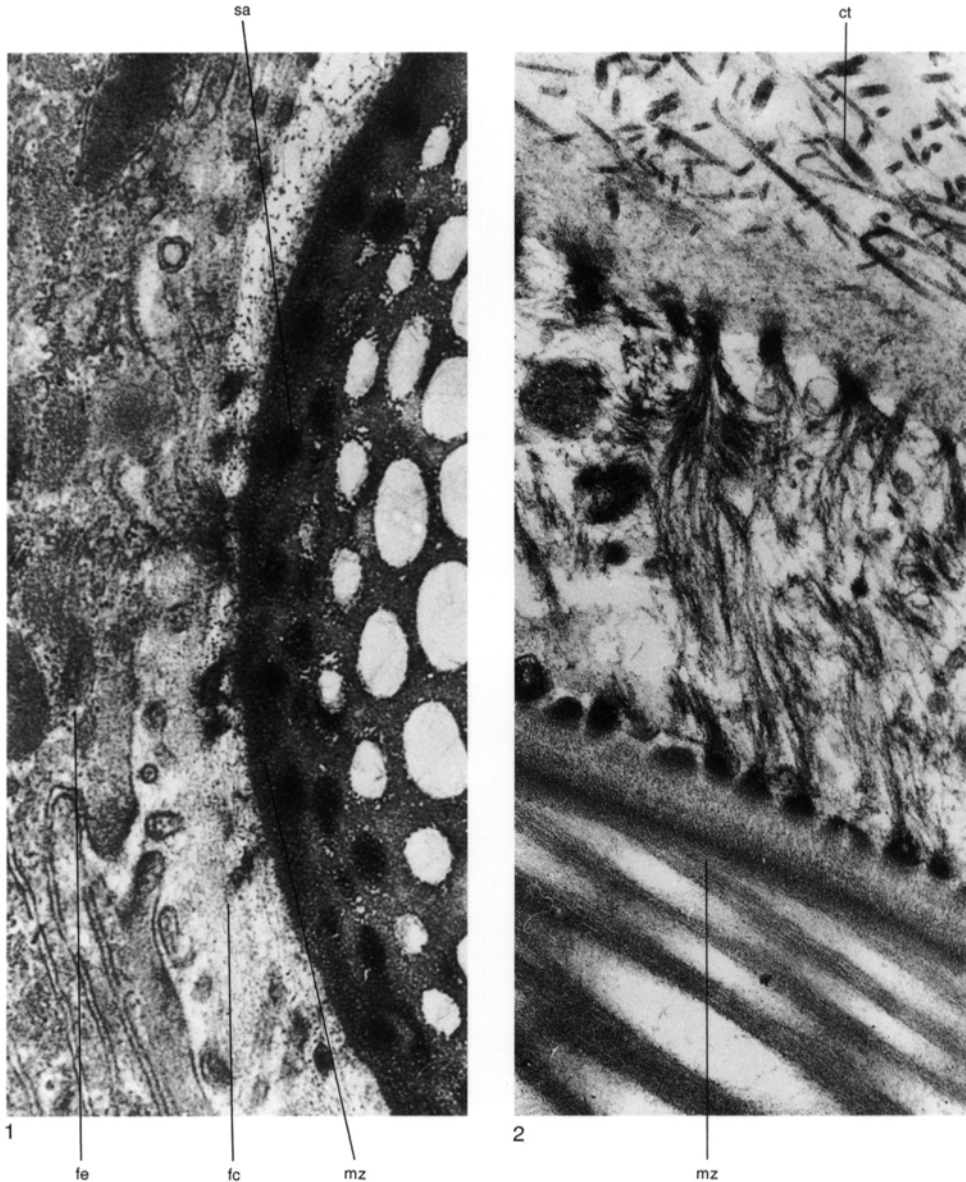


FIG. 50. TEM micrographs of sections of setal follicles in decalcified mantle edges; 1, edge of seta (*sa*) of *Glottidia pyramidata* showing the migration of fibrous clots (*fc*) secreted by follicular epithelium (*fe*) and incorporated into the electron-dense marginal zone (*mz*) of the seta, $\times 55,000$; 2, detail of follicular epithelium of *Discina striata*, between connective tissue (*ct*) and setal margin (*mz*), showing the filamentar bundles attached to hemidesmosomal plaques in the basal lamina and apical plasmalemma, $\times 40,000$ (new).

siphons through which the buried *Lingula* feeds by means of two lateral inhalant and one median exhalant currents.

All setae are mobile to a varying degree depending on the development of muscula-

ture controlling the follicles. In carbonate-shelled brachiopods, bundles of filaments within the connective tissue are attached to the follicles and are evidently responsible for some retraction of the setae as well as the

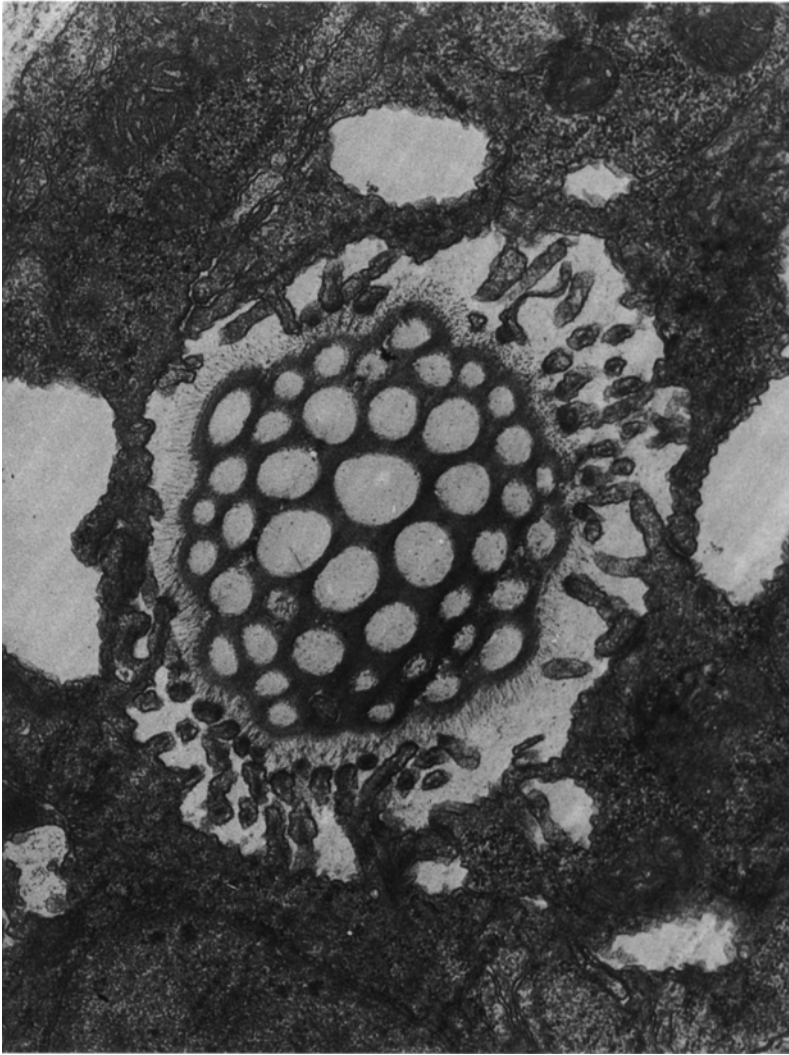


FIG. 51. TEM micrograph of the transverse section of a decalcified mantle edge of a young *Notosaria nigricans* showing the cylindroid nature of the canals and the microvillous apical plasmalemmas of the follicular epithelium, $\times 25,000$ (new).

mantle margin as a whole. The setal follicles of organophosphatic brachiopods (Fig. 52), however, are controlled by a highly organized muscle system (BLOCHMANN, 1900). In *Lingula* the muscle sets are located in the marginal mantle sinus and are capable of retracting, protracting, flexing, and elevating the setae and have been appropriately named.

The connective tissue immediately proximal of the mantle lobes of organophosphatic

brachiopods also contains two circumferential bands of circular fibers connected by diagonal bundles of filaments (BLOCHMANN, 1900). These are responsible for the retraction of the mantle edge, which occurs frequently and is indicated in shell successions by deep insertions of periostracal layers among the organophosphatic laminae. Despite the absence of comparable muscle sets in the mantles of articulated brachiopods,

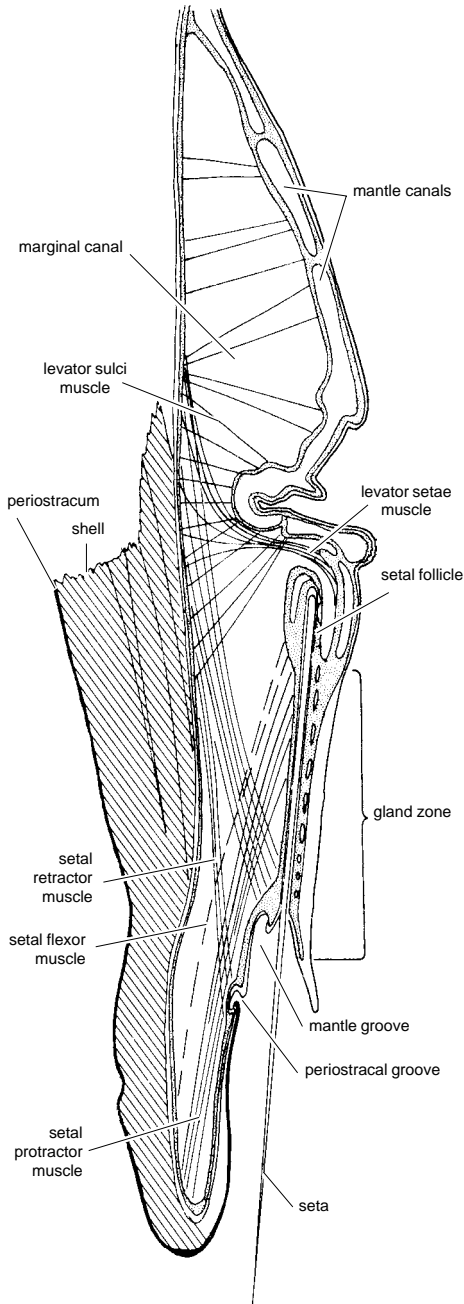


FIG. 52. Diagram of section through the mantle margin of *Lingula anatina* (Blochmann, 1900).

retraction of the mantle is commonly registered as variable regressions that are usually facilitated by the secretion of a proteinaceous membrane (see Fig. 279–280) between the

outer epithelium and the carbonate successions (WILLIAMS, 1971a). Following a regression, all cells resume shell deposition at that phase in the secretory regime where they left off. This phenomenon has been noted in the impunctate *Notosaria* and in such terebratulides as *Magasella*, in which punctae that had contained caeca before retraction took place are sealed by the membrane of regression.

MANTLE SPICULES

Although a biomineralized exoskeleton, secreted by outer epithelium, is characteristic of all brachiopods, calcitic bodies (**spicules**) also occur within the connective tissue and inner epithelium of terebratulides and terebratulidines and constitute an endoskeleton of variable solidity and continuity (see Fig. 339–340). In the heavily calcified mantle and lophophore of *Terebratulina*, the spicules are flattened to lie in the plane of the connective tissue (Fig. 53) so that segments of a spicule are lenticular in cross section and anastomose to form a sievelike, uniaxial structure with rounded perforations and curved peripheral horns. An outer, thin calcitic skin, which is patchily smooth, encloses highly inclined laminae (WILLIAMS, 1968d). SCHUMANN (1973) has shown that the laminae are composed of calcitic spherules about 200 nm in diameter.

Spicules are secreted as membrane-bound structures by mesenchymal cells (scleroblasts) that are attached to walls of cavities scattered throughout the connective tissue (JAMES & others, 1992). Accretionary growth of a spicule is indicated by the distension of the connective tissue so that collagen fibers in the vicinity of a well-developed scleroblast are streamlined parallel with the sides of the flattened scleroblasts (Fig. 54). Between adjacent scleroblasts, however, collagen fibers are aligned more or less normal to the connective tissue layer, while the immediately adjacent epithelia become folded inward toward each other within the rounded perforations of the spicular sieve. In other directions distension can be great enough to disrupt membranes and bring about an amalgamation of spicules to form a single struc-

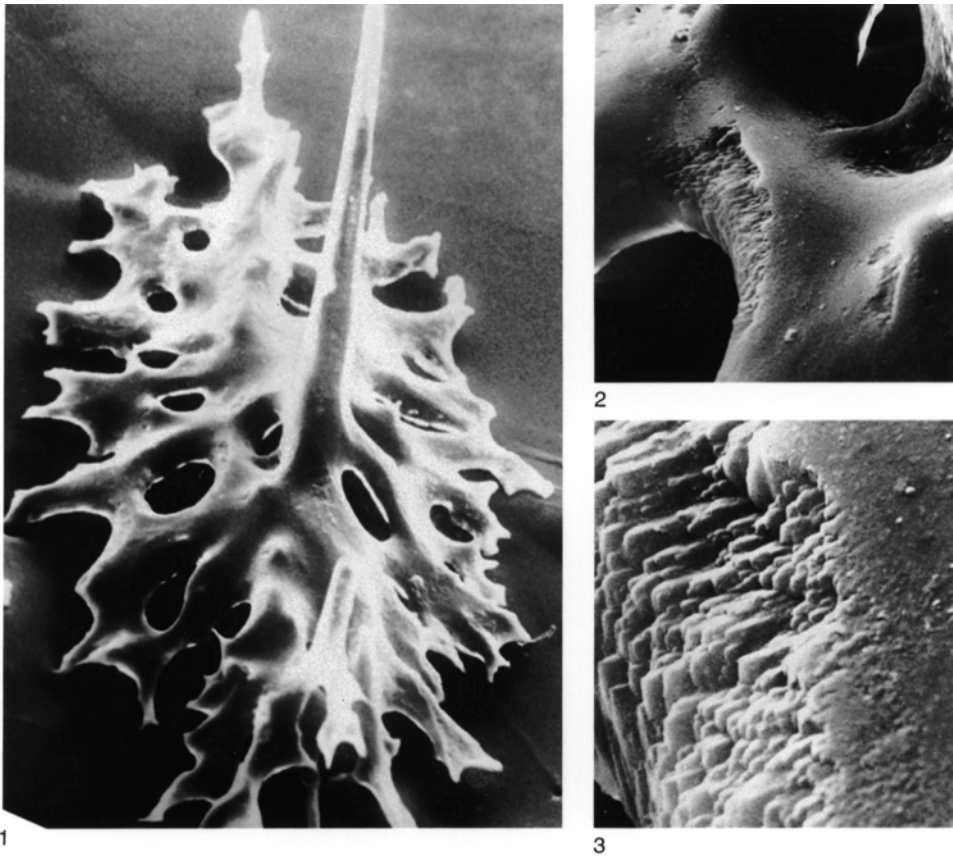


FIG. 53. SEM micrographs of a spicule in the mantle of *Terebratulina retusa*; 1, in general view, $\times 300$, and in progressive detail, 2, $\times 1,500$, 3, $\times 8,000$ (Williams, 1968d).

ture that is still contained within a proteinaeous sac but is now sustained by an encircling group of scleroblasts.

Spicular endoskeletons are not invariably characteristic of living terebratulides, being feebly developed in some families (Dallinidae) and unknown in others (Terebratulidae). Endoskeletal meshes are, however, strongly developed in the Terebratulidae, Platidiidae, and Krausiidae and have been well documented by SCHUMANN (1973). Spicular meshes are particularly conspicuous: as canopies over the lophophore and filaments of *Terebratulina*, within the main mantle canals of *Megerlia* (Fig. 55.1) where they form roofs over the gonads, and in association with the dorsal adductor bases of *Gryphus*. Spicule morphology is so specifi-

cally differentiated as to form part of the diagnosis of various groups. It can vary from the dispersed hook of *Gryphus* to the solid shield of *Platidia* (Fig. 55.2). Morphology of spicules is known to vary during the ontogeny of *Terebratulina*, however, and could well be related, in this genus at least, to facilitating a mechanical stiffening of the connective tissue (FOUKE, 1986).

Thecideidine spicules, as typified by those of recent *Pajaudina* (LOGAN, 1988), are predominantly platelike structures. According to LACAZE-DUTHIERS (1861), spicules are absent from the lophophore of *Lacazella* but are densely packed into a vaultlike structure covering the gonads in the ventral mantle. Loose spicules have been recorded in fossil shells (THOMSON, 1927), and this is their

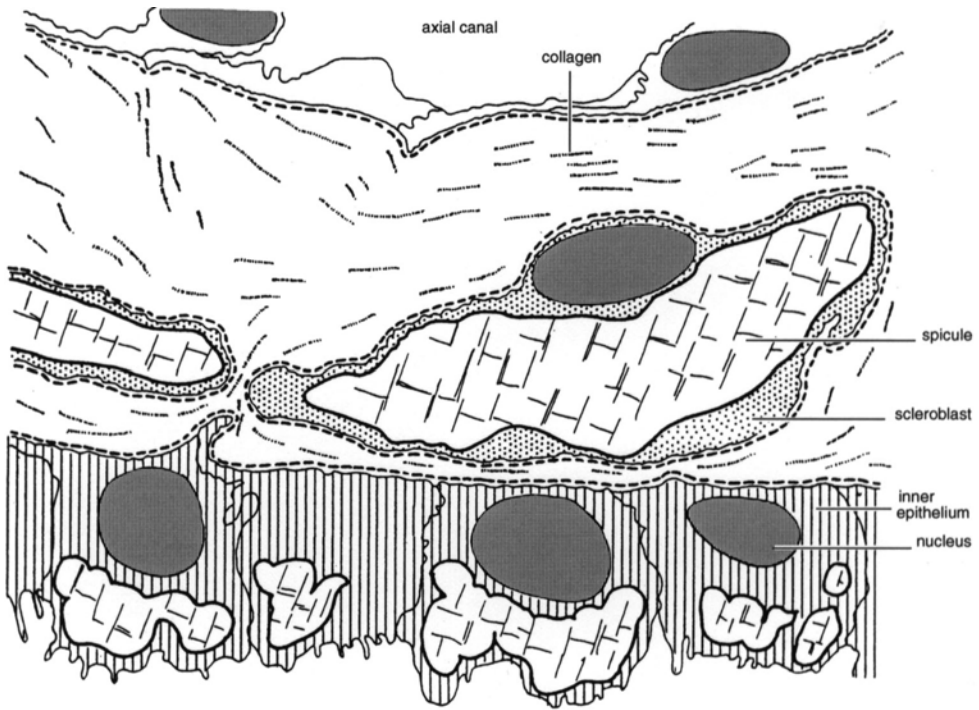


FIG. 54. Diagrammatic section of the lophophore filament of *Terebratulina retusa* showing the distribution of spicules in the inner epithelium and connective tissue (Williams, 1968d).

most common mode of occurrence in the shells of living species (Fig. 55.3).

PEDICLE

Most recent brachiopods are attached to their substratum by a pedicle. The pedicles of articulated and inarticulated brachiopods,

however, are only analogous organs, being of different origin and morphology (Fig. 56). The pedicle of inarticulated brachiopods develops as an outgrowth of the posterior body wall and is associated with the ventral valve only. In contrast, the pedicle rudiment of articulated brachiopods is continuous

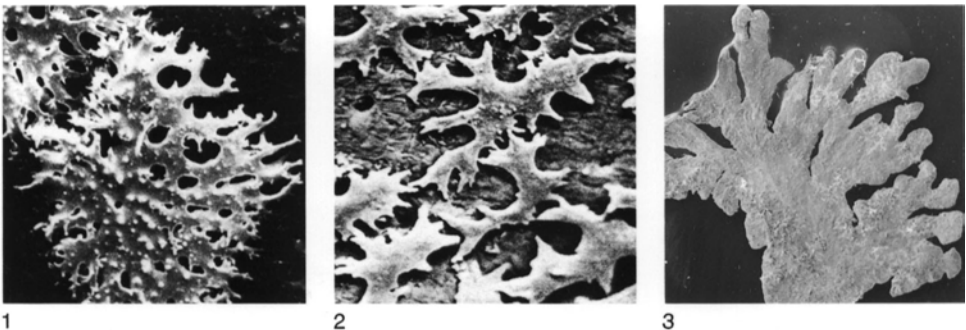


FIG. 55. SEM micrographs of various types of spicules; 1, from the lophophore of *Megerlia truncata* (LINNÉ), $\times 65$; 2, from the mantle of *Platidia anomioides* (SCACCHI & PHILLIP), $\times 140$ (Schumann, 1973); 3, from within the dead shell of *Pajaudina atlantica* LOGAN, $\times 50$ (Alan Logan, new).

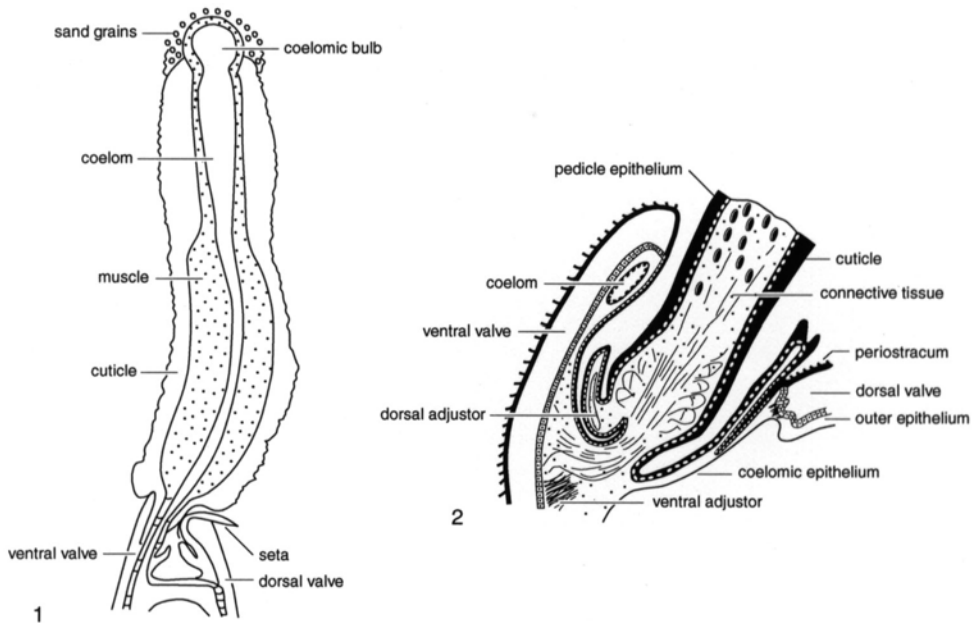


FIG. 56. Diagram showing generalized pedicle anatomy 1, of the representative inarticulated brachiopod, *Lingula* (adapted from Mackay & Hewitt, 1978; Yatsu, 1902a) and 2, articulated brachiopod, *Terebratulina* (Williams & Rowell, 1965a).

with the mantle rudiment, which produces both the ventral and dorsal valves; therefore the adult pedicle is continuous with the body wall of both valves.

An example of pedicle structure in inarticulated species is provided by a transverse section through that of *Glottidia pyramidata* (Fig. 57). There is a central coelomic cavity (pedicle cavity), an extension of the mantle canals present only in lingulids, which terminates distally in a small sac. The canal is filled with coelomic fluid containing erythrocytes and amoebocytes and is lined by coelomic epithelium about 5 μm tall with a microvillous border. The coelom is surrounded by a ring of muscle fibers running longitudinally along a spiral axis. Outside the muscle layer is a thin layer of connective tissue from 3 to 6 μm thick containing striated collagen fibers. This connective tissue layer supports the pedicle epithelium, which is found within the outer cuticle (MACKAY & HEWITT, 1978). The latter contains randomly oriented chitin fibrils arranged in concentric

layers (RUDALL, 1955) and is continuous with the periostracum.

The pedicle of *Lingula anatina* has a similar structure (Fig. 58) with a central coelomic cavity and an outer cuticle that is transparent in life. Circumferential muscle fibers of the body wall are antagonized by adductors and oblique fibers by means of the fluid skeleton formed by the perivisceral coelom, in a similar manner to the action of circular and longitudinal muscles in a classical hydrostatic skeleton. The mantle and brachial canals are closed during muscular activity so that the coelomic fluid is maintained at constant volume in the body cavity, but the canal to the pedicle remains open and its longitudinal muscle is part of the system (TRUEMAN & WONG, 1987). The basic structure of the *Discinisca* (Fig. 59) pedicle is also similar to that of *Glottidia* although the muscle layer in the wall of the pedicle is not as well developed, and three paired, principal pedicle muscles are found occupying the pedicle coelom. These principal muscles appear to

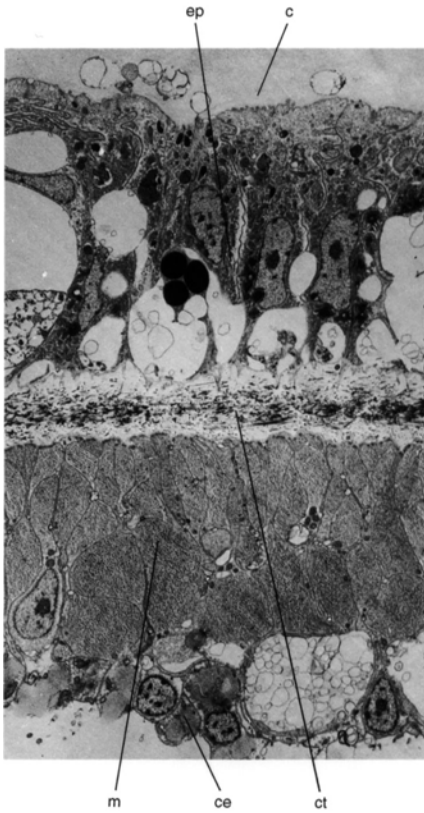


FIG. 57. TEM of a transverse section through the pedicle of a *Glottidia* showing the cuticle (*c*), pedicle epithelium (*ep*), connective tissue (*ct*), muscle layer (*m*), and coelomic epithelium (*ce*), $\times 2,300$ (new).

have been a late development in the evolution of the discinoid pedicle. Specimens of *Orbiculoidea* with pyritized soft parts, collected by Dr. W. H. Südkamp from the Lower Devonian Hunsrück Slate, were equipped with pedicles protruding for at least 1.5 cm beyond the shell margin (Fig. 60). Such a slender, cylindroid pedicle probably had a coelom, like that of lingulids, although it would have functioned as a hold-fast.

In structure, the pedicle of articulated species consists of a core of connective tissue, a pedicle epithelium, and an outer chitinous cuticle (Fig. 61). The pedicle trunk is enveloped by a thick cuticle, but this does not extend onto the surface in contact with the substrate (BROMLEY & SURLYK, 1973). Indeed, the structure of the pedicle rootlet

changes with distance from the pedicle trunk (MACKAY & HEWITT, 1978). First, the chitinous cuticle is replaced by a layer of fibrous tissue, and the connective tissue core shows less densely packed collagen fibers. Next, in more distal sections of the rootlets, collagen fibers disappear from the central core, being replaced by cellular processes, presumably from the pedicle epithelium, and aggregations of electron-lucent material.

The pedicle epithelial cells of *Terebratulina retusa* are cuboidal to columnar, measuring between 10 and 20 μm in height. Apical, cytoplasmic protrusions extend into a web of



FIG. 58. TEM showing a transverse section through the pedicle of *Lingula*; the pedicle epithelium (*ep*) can be seen below the cuticle (*c*), which has a dense exterior edge; note also the connective tissue (*ct*) and muscle (*m*) layers, $\times 4,000$ (new).

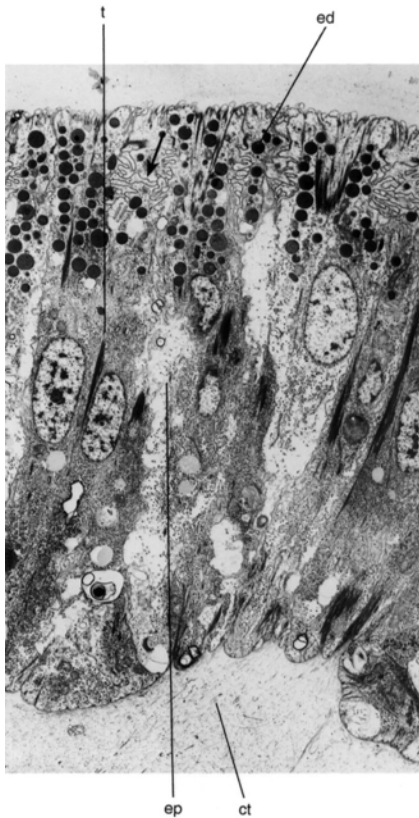


FIG. 59. Transverse section through the pedicle of *Discinisca* showing the pedicle epithelium (*ep*) supported by a layer of connective tissue (*ct*); note the characteristic features of the pedicle epithelium: folded lateral cell membranes (*arrow*), tonofibrils (*t*), and electron-dense droplets (*ed*), $\times 2,500$ (new).

finely fibrillar material. The basal cell membrane is irregular, and lateral cell borders are tightly folded, perhaps to allow expansion during changes of shape of the pedicle.

Typical organelles and inclusions at the ultrastructural level include tonofibrils; electron-dense, membrane-bound droplets; and clear vesicles. Free ribosomes, rough endoplasmic reticulum, and mitochondria are also found; the Golgi apparatus is not well developed. The pedicle epithelium of *Glottidia* is similar in shape and height and shows similar ultrastructural features, although apical cytoplasmic protrusions are larger and cell membranes are not as folded as in *Terebratulina*. The common ultrastructural features of cytoplasmic protrusions,

folded lateral cell membranes, tonofibrils, rough endoplasmic reticulum, electron-dense droplets, and clear vesicles are also present in the outer epithelial cells of the *Glottidia* mantle but not in those of *Terebratulina*. These common features may be related to the production of chitin.

In *Terebratulina*, pedicle epithelium, when followed into the pedicle rootlet, undergoes ultrastructural changes, with cell membranes becoming more regular in the absence of tonofibrils and rough endoplasmic reticulum. Electron-dense droplets are twice as large as those of the epithelium lining the pedicle trunk. Smaller, clear vesicles are found both apically and basally, the Golgi apparatus is more well developed, and glycogen is now present. As the epithelium is followed into the distal part of the rootlet, droplets of electron-dense material appear to be in the process of being extruded to the core of the rootlet, and fibrous material is



FIG. 60. External view of *Orbiculoidea mediorhenana* FUCHS with a pyritized, distal part of the pedicle protruding from beneath the left margin of the dorsal valve. Lower Devonian Hunsrück Slate, $\times 2.5$ (photograph courtesy of W. H. Südkamp).

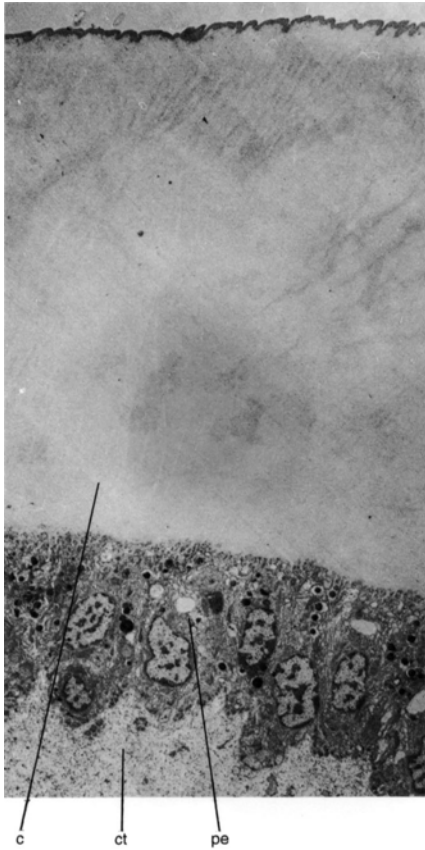


FIG. 61. Micrograph of a transverse section through the pedicle of *Terebratulina* showing connective tissue (ct), pedicle epithelium (pe), and cuticle (c), $\times 2,300$ (new).

produced at the free surfaces. Modifications of the pedicle epithelium are also seen at the *Glottidia* pedicle ending (Fig. 62). Some groups of pedicle epithelial cells bear microvilli, and there is an impersistent film of glycosaminoglycans (GAGs) apically. Ultrastructural features are similar to those of the pedicle trunk epithelium, although rough endoplasmic reticulum is more plentiful and is found in the folds of the lateral cell membranes. The cells also contain glycogen and large mucous droplets; these differences may be related to the ability of the pedicle ending to collect sand grains.

In *Terebratulina*, the central connective tissue of the proximal pedicle consists largely

of densely packed, longitudinal collagen fibers with fibroblasts and fat cells (MACKAY & HEWITT, 1978). It has been reported that brachiopod pedicles contain cartilage (HARO, 1963), but this has not been confirmed in more recent studies of *Terebratulina* and *Glottidia* (MACKAY & HEWITT, 1978), although a proximal mass of tissue resembling cartilage has been found in the pedicle of *Terebratalia transversa* (STRICKER & REED, 1985c). A study of pedicle development in the latter species (Fig. 63) showed that it is only the posterior half of the larval pedicle lobe that develops into the pedicle proper (from the distal part) and the pedicle capsule (from the proximal part). The connective tissue pedicle capsule lines the posterior end of the shell and forms a cuplike canopy around the pedicle. The anterior half of the pedicle lobe develops into the caudal end of the juvenile body. In young juveniles, the pedicle is continuous with and surrounded by the cuticle-covered epithelium and underlying pedicle capsule. Fibrils seen in the cuticle of adult specimens of *Terebratalia* may represent chitin. The pedicle epithelial cells show tonofibrils and hemidesmosomes as in *Terebratulina*. Although the pedicles of subadult and adult specimens are nonmuscular, at earlier stages fibers from pedicle adjustor muscles occur within the pedicle core. Furthermore, in subadult specimens, collagen fibers representing rudimentary tendons of the adjustor muscles extend into the pedicle (STRICKER & REED, 1985c). The adult pedicle bulb is attached to the posterior ends of the shell and body by sheets of dense connective tissue, the pedicle connectives (LABARBERA, 1978). Collagenous fibers, densely packed and oriented parallel to the long axis, are the most prevalent pedicle components.

Holdfast papillae of representatives of all major pedunculate groups (*Hemithiris psittacea*, *Terebratulina retusa*, *Macandrevia cranium*, and *Argyrotheca cistellula*) can dissolve carbonate substrates (EKMAN, 1896). The mechanism of boring remains unresolved except for a report that the pedicle rootlets of

Terebratulina contain vesicles similar to those associated with the resorption of bone by osteoclasts (MACKAY & HEWITT, 1978).

A study of borings made by both fossil and recent brachiopod pedicles showed pedicle form in articulated brachiopods to be much more variable than had previously been assumed (BROMLEY & SURLYK, 1973). Not only are different types of pedicle found among different higher taxonomic categories, but also, in many instances there is extreme variability in the pedicle of a single species. The pedicles of articulated brachiopods can be separated into a number of morphological groups (Fig. 64), depending on the size and length of the pedicle and adhesive processes sheathed with connective tissue (holdfast papillae):

i) massive pedicle of medium length with short, holdfast papillae that corresponds to a normal brachiopod pedicle of most textbooks;

ii) long, massive pedicle with long holdfast papillae;

iii) very long, massive pedicle with long, holdfast papillae that may be split distally into rootlets (processes with chitinous coverings);

iv) short massive pedicle with short holdfast papillae;

v) short massive pedicle divided distally into rootlets;

vi) very long pedicle with irregular lateral branches; and

vii) pedicle divided into rootlets immediately posterior to the pedicle opening.

Etched traces produced by pedicles of recent brachiopods vary with the nature of the substrate and the form of the pedicle. Furthermore, the pedicles of several recent brachiopods etch a very characteristic trace into hard calcareous substrates. A trace is a number of pits, closely spaced in brachiopods with solid unbranched pedicles, which correspond to holdfast papillae. The trace etched by brachiopods with divided pedicles consists of a series of more widely scattered pits corresponding to the rootlets of the

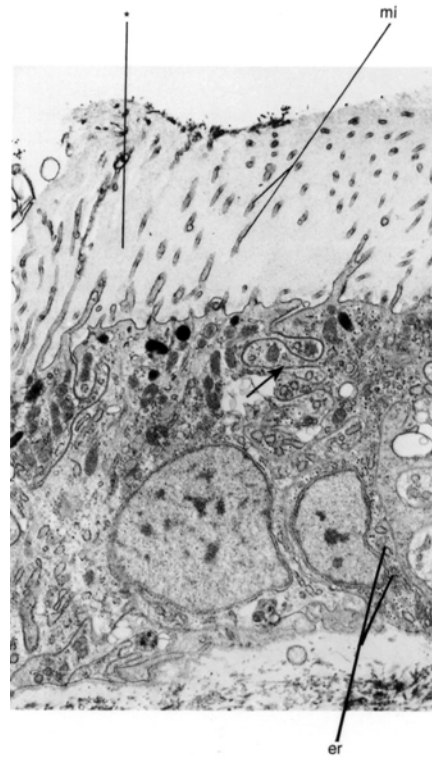


FIG. 62. Pedicle epithelium from the bulb of the pedicle of *Glottidia* in transverse section; note microvilli (*mi*), film of glycosaminoglycans (*), folds of lateral cell membranes (*arrow*), and rough endoplasmic reticulum (*er*), $\times 5,000$ (new).

pedicle. Here the scatter of pits can be recognized only as an individual entity where the substrate is extensive and flat. Similar traces can be found on fossilized substrates (BROMLEY & SURLYK, 1973).

The gross morphology of the pedicle can vary even within a single species, for example, within a population of the recent brachiopod *Terebratulina septentrionalis* living where little hard substrate is available. Most *Terebratulina* specimens in this habitat attach to the shells of living or dead scaphopods; others lie on the sea floor, enmeshed within a bushlike network of pedicle rootlets. Some larvae then settle on adult pedicle rootlets. In this way, constant refurbishment

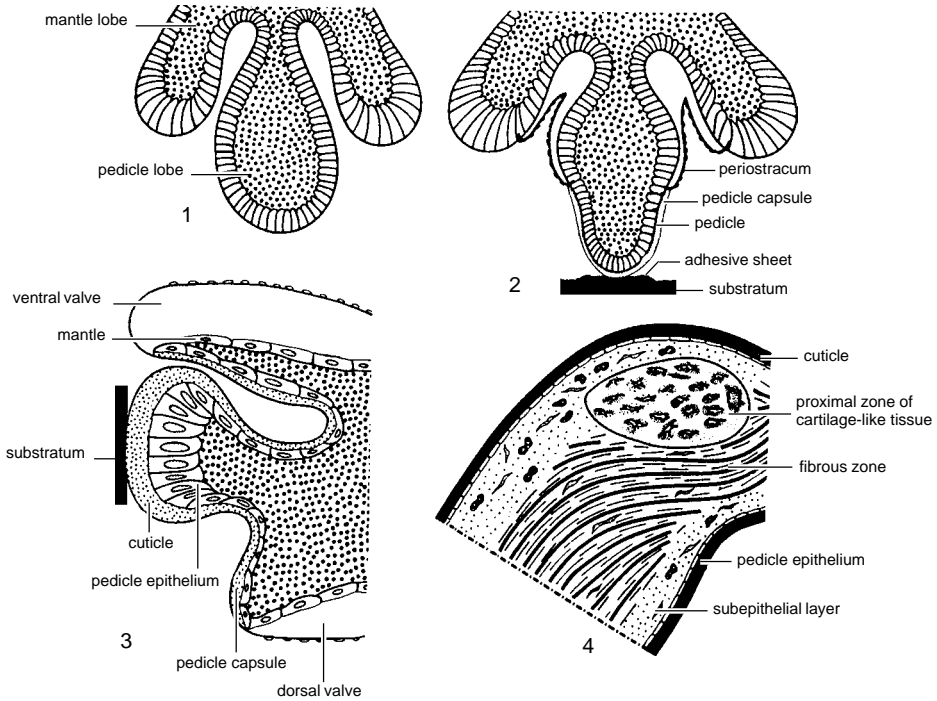


FIG. 63. Diagram showing longitudinal sections through the pedicle of *Terebratalia transversa* at different stages of development; 1, free-swimming larval stage, posterior half; 2, posterior half of a settled larva; 3, newly metamorphosed juvenile, pedicle, and surrounding tissues; 4, adult pedicle stalk; the distal end of the pedicle (below the dotted line) is not depicted (Stricker & Reed, 1985c).

of pedicle networks ensures survival; and, in effect, the brachiopods create their own substrate (CURRY, 1981).

The musculature of the pedicle of living articulated brachiopods varies greatly in size, position, and relation to the organ. Different pedicle types (immobile and rigid or muscular and flexible) can be related to differences in the disposition of pedicle muscles and in the form of the associated shell structures. The clearest guide to pedicle type in fossil forms is provided by the beak, since this houses the pedicle (RICHARDSON, 1979).

Paired ventral adjustor muscles pull the valves closer to the substrate in species with an inert pedicle (Fig. 65) but can also retract a muscular pedicle. Ventral, adjustor muscle fibers contribute to the shaft of the pedicle, and these may be contractile or tendinous. There is a greater muscle mass of ventral adjustors in species with muscular pedicles,

for example, *Notosaria* (Fig. 66). Median pedicle muscles (paired or single) of attached species consist predominantly of tendinous fibers and stabilize the pedicle, preventing its displacement when dorsal and ventral adjustors contract. In *Anakinetica cumingi*, however, homologues of the median pedicle muscles lie within the pedicle capsule and control withdrawal and extrusion of the pedicle. The motile pedicle of this species is used to adjust the animal to varying levels within the sediment (RICHARDSON & WATSON, 1975). When compared to that of an attached species, *Magadina flavescens*, differences in the pedicle and its muscles could be correlated with dissimilarities in the beak and cardinalia of these forms.

Paired, dorsal, adjustor muscles are usually attached to the ventrolateral surfaces of the pedicle. These muscles enable the shell to rotate and move laterally. Unilateral contrac-

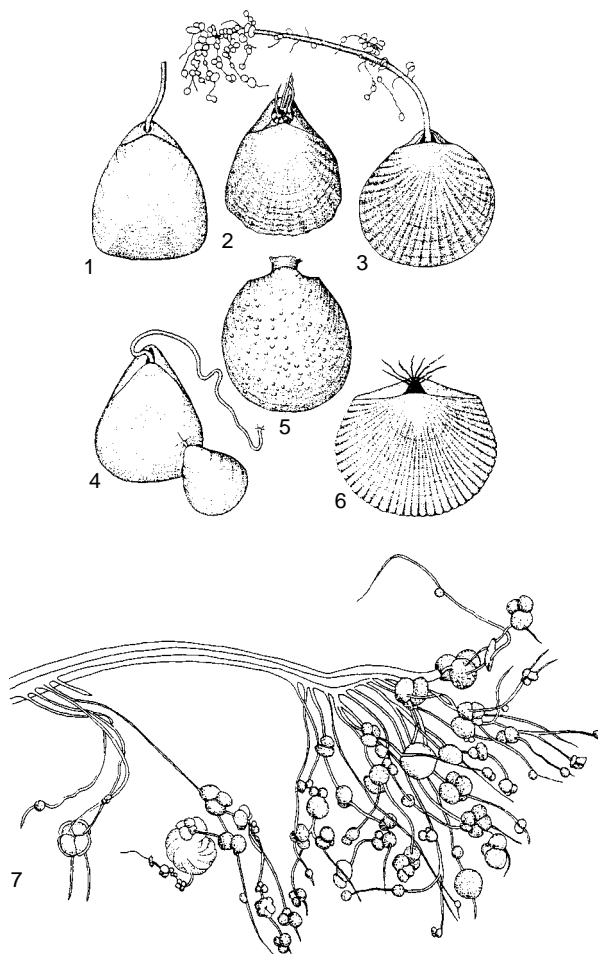


FIG. 64. Diagram showing different types of pedicle in articulated brachiopods: 1, *Macandrevia cranium*; 2, *Eucalathis murrayi*; 3, *Chlidonophora chuni*; 4, *Cryptopora gnomon*; 5, *Gwynia capsula*; 6, *Chlidonophora incerta*; 7, detail of pedicle of *Chlidonophora chuni* with penetrated and attached foraminifera (Bromley & Surlyk, 1973).

tion pulls the shell to the same side, while contraction of muscles on both sides pulls the pedicle down anteriorly, elevating the posterior part of the shell.

There appear to be two extremes of pedicle function. At one extreme, the pedicle is a relatively rigid organ for permanent attachment, acting as a pivot around which the shell moves due to the contraction and relaxation of the attached muscles. In this case, the shell rather than the pedicle moves, the pedicle acting as an intermediary between the muscles and the substrate. At the other

extreme, the pedicle is a contractile organ with muscle fibers continuous with those of the ventral adjustors and can adjust the position of the shell as a result of its own mobility. There is a graduation of intermediary types between these two extremes. All muscles (the median pedicle and the dorsal and ventral adjustor muscles) may contribute either tendinous or contractile fibers to the pedicle. Pedicles with few fibers (such as those of *Magadina*, *Cancellothyris*, and *Magellania*) are immobile and inflexible, while pedicles with a high, muscle-fiber

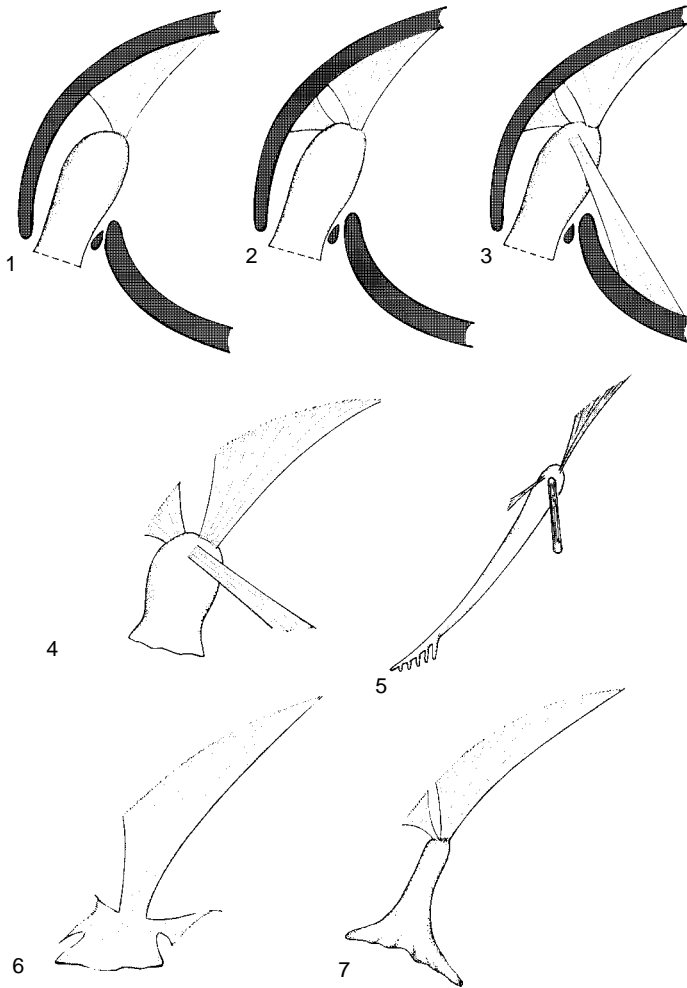


FIG. 65. Diagram showing the pedicle and muscles in articulated genera with different substrate relationships; 1-3, muscle arrangement common to *Magellania*, *Cancellothyris*, *Liothyrella*, and *Campages*; 1, ventral adjustor that pulls the valves close to the substrate, 2, adding the median muscle which acts as a stabilizer and 3, also including the dorsal adjustor which, acting with its partner, controls lateral and rotatory movements of the valves; 4-7, muscle arrangement in genera with a different substrate relationship than that seen in *Magellania*; 4, *Terebratalia*, 5, *Anakinetica*, 6, *Megerlina*, and 7, *Notosaria* (Richardson, 1979).

component, such as *Notosaria*, are contractile (RICHARDSON, 1979).

In *Terebratalia transversa*, the median pedicle muscles are absent, with only a ventral and a dorsal pair of pedicle adjustors present from the free-swimming larval stage to the adult form (STRICKER & REED, 1985c).

Little information is available on lingulid pedicle musculature. The principal pedicle

muscles of *Discinisca* consist of three pairs that nearly fill the pedicle coelom (Fig. 67). A large pair of rectus muscles runs dorsoventrally and is attached to the distal end of the pedicle and to the shell at the sides of the pedicle opening. There are two pairs of oblique muscles, the pedicle oblique median muscles and oblique external muscles. A sphincter is present at the proximal end of

the pedicle and controls the opening to the body cavity. A thick muscle layer is present in the *Lingula* pedicle, deep to the coelomic epithelium. Fibers run longitudinally along a helical spiral, coiled both clockwise and counterclockwise (WILLIAMS & ROWELL, 1965a). Similarly, a transverse section through the pedicle of *Glottidia* shows obliquely cut muscle fibers, some with a predominantly longitudinal and some with a predominantly transverse orientation (Fig. 68–69). Craniid inarticulated brachiopods lack a pedicle at all stages of development, being attached instead by cementation of the pedicle valve to the substratum, effected by adhesive properties of the mucus covering the periostracum.

The lingulid pedicle may be lost by breakdown and resorption, perhaps in response to stress (ROWLEY & HAYWARD, 1985; JAMES & others, 1992). Regeneration of the pedicle bulb of *Lingula anatina* after damage has been reported (TRUEMAN & WONG, 1987).

COELOMIC AND CIRCULATORY SYSTEM

As far as is known, all brachiopods possess an open circulatory system containing a colorless or faintly pigmented fluid that is coagulable and contains a variety of free cellular inclusions. The circulatory system is composed of a series of blood vessels that communicate with coelomic canals and sinuses (HYMAN, 1959b; WILLIAMS & ROWELL, 1965a; ROWLEY & HAYWARD, 1985).

COELOMIC SYSTEM

The coelom contains the main muscles, digestive tract, excretory organs, and reproductive structures. The part of the coelom that constitutes the main body (perivisceral) cavity occupies the posterior part of the shell. Coelomic canals and sinuses extend into the mantles, brachia, and tentacles and into the pedicle of inarticulated brachiopods. Parts of the coelom are subdivided by flat sheets or ribbons of connective tissue (mesenteries) or may be isolated during development. The

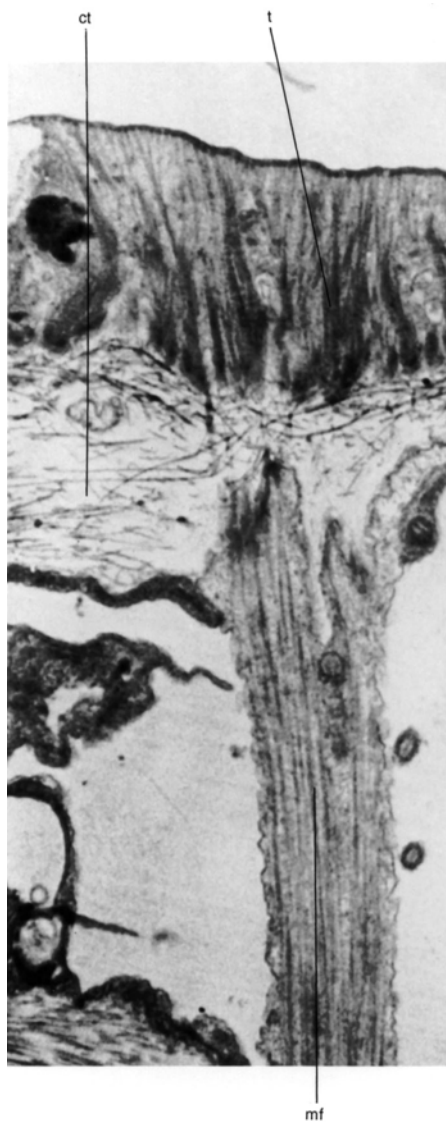


FIG. 66. TEM showing a ventral adjustor muscle fiber (*mf*) of *Notosaria* attaching to the ventral valve; note the extension of the muscle fiber through the connective tissue layer (*ct*) and the apparent continuity of myofibrils with the tonofibrils (*t*) of the outer epithelial cells providing a firm attachment point, $\times 26,500$ (new).

coelom and the tissues and organs it contains are lined with a flat, ciliated epithelium.

Mesenteries traverse the body cavity and contain fine muscle fibers. Dorsal and ventral mesenteries support and anchor the

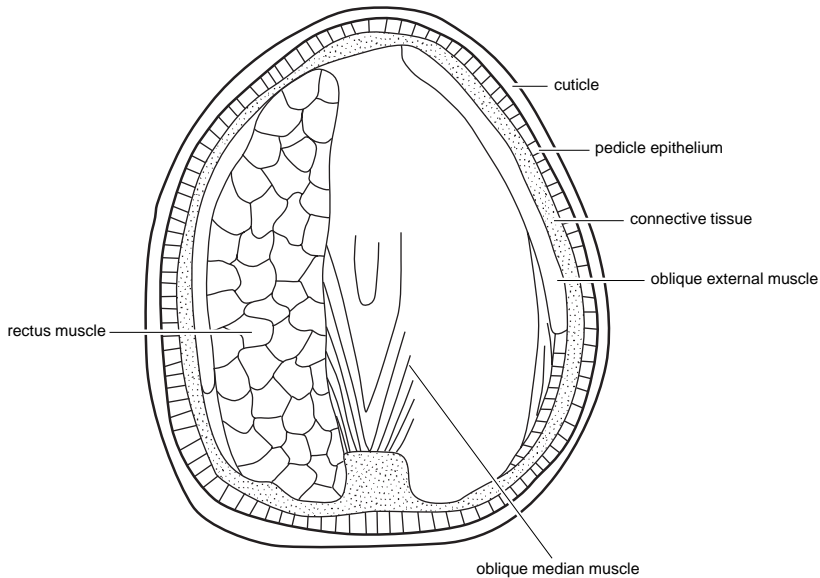


FIG. 67. Diagram showing the pedicle of *Discinisca* viewed ventrally after the ventral surface and left rectus muscle have been removed (Blochmann, 1900).

alimentary canal to the body wall. Only in *Neocrania* do the mesenteries completely divide the body cavity into two separate compartments (BLOCHMANN, 1892). Two lateral mesenteries, the gastro- and ileoparietal bands, also connect the alimentary tract and other organs in the body cavity to the body wall. Gastroparietal bands are absent in *Neocrania*, but in all other brachiopods they are relatively narrow, lie anteriorly to, and extend on both sides from the stomach, near the digestive diverticula, to the lateral body wall. The ileoparietal band is more complex, extending between the lateral body wall and the stomach, along which it may persist for some distance posterior to the gastroparietal band. The ileoparietal bands also support the posterior end of the excretory organs (metanephridia) extending anteriorly as a series of variably branched lamellae that carry the gonads (Fig. 70; see also Fig. 91).

Tubular extensions of the coelom penetrate the mantle to form a characteristic pattern of ciliated canals. In articulated brachiopods a thin layer of muscle underlies the coelomic epithelium of the inner mantle

membrane. In inarticulated brachiopods, two main mantle canals (*vascula lateralia*) emerge from the main body cavity through muscular valves and bifurcate distally to produce an increasingly dense array of blindly ending branches near the periphery of the mantle (Fig. 71.1–71.2). *Discinisca* has two additional mantle canals emanating from the body cavity into the dorsal mantle (*vascula media*). *Neocrania* lacks the muscular valve at the junction of the body cavity with the mantle canals. Unlike other inarticulated taxa, the primary canal of *Neocrania* gives rise to secondary and, only exceptionally, tertiary branches. In addition, these canals may also contain part of the gonads (Fig. 71.3).

Recent rhyntonellides and terebratulides possess two pairs of principal canals in each mantle (WILLIAMS, 1956), but the pattern may be complicated because some contain part of the gonads (Fig. 72). In rhyntonellides, for example, each mantle contains a pair of submedian canals (*vascula media*) curving posterolaterally and branching repeatedly toward the mantle edge. In *Hemithiris* the *vascula media* are flanked by a pair

of short, broad canals (*vascula genitalia*), which are unbranched extensions of the body cavity containing the gonads (Fig. 72.1). In *Notosaria* the pattern is identical except that the *vascula genitalia*, although still saclike proximally, branch repeatedly toward the mantle margin, and the *vascula media* are correspondingly abbreviated (Fig. 72.3). In living terebratulides the pattern is similar to that of *Notosaria*: the *vascula genitalia* are branched, and the *vascula media* are restricted peripherally (Fig. 72.2). In such genera as *Macandrevia*, *Pumilus*, *Fallax* (Fig. 72.4), and *Magellania*, however, gonads are also found in the *vascula media*. The fine distal branches of all canals that terminate just within the shell margins connect with the setal follicles in articulated brachiopods.

Circulation of Coelomic Fluid

Ciliated epithelium lining the coelomic canals circulate the coelomic fluid. In lingulids a defined pattern of circulation is maintained by rhythmically beating cilia. Aided by a median ridge, the cilia create separate outgoing and return currents within each coelomic canal (Fig. 73).

Similar medial epithelial ridges occur in *Discinisca* and *Terebratalia* on the inner side of the outer mantle membrane. The mantle canals have a respiratory function, facilitating the circulation of coelomic fluid. Gill ampulae are an unusual adaptation found only in the lingulid *Glottidia*. Small, thinly walled, tubular, saclike extensions of the mantle canals occur in the periphery of the anterior part of the mantle cavity, thereby increasing the surface area of the mantle canal system (MORSE, 1902).

VASCULAR SYSTEM

Comprehensive descriptions of the vascular system of inarticulated brachiopods are available (BLOCHMANN, 1892, 1900; SCHAEFFER, 1926), but no complete account exists for articulated species. It is generally accepted, however, that the open circulatory system is composed of a series of coelomic canals and a communicating vascular system.



FIG. 68. TEM showing the muscle layer of the pedicle of *Glottidia* cut in transverse section; note muscle fibers (*f*) with connective tissue between (*) and a supporting layer of connective tissue with circularly running collagen fibers (*co*), $\times 3,500$ (new).

The vascular system consists of a main dorsal vessel that contains one or more contractile appendages or hearts that are supported by a dorsal mesentery in the vicinity of the stomach (HYMAN, 1959b). Blood vessels, formed within the connective tissue, branch from the main dorsal vessel and communicate with sinuses in the digestive tract and with the small brachial and tentacular canals of the lophophore.

Posterior to the heart, the main dorsal vessel gives rise to two mantle vessels that divide, forming a network of vessels beneath the coelomic epithelia of the mantle membrane of the mantle canals. The vessels serve an extensive system of anastomosing sinuses

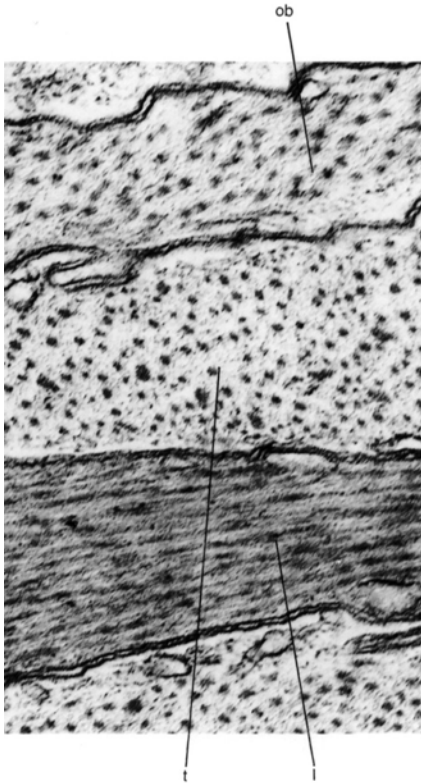


FIG. 69. Detail of a transverse section through the muscle layer of *Glottidia* showing adjacent muscle fibers; one fiber is cut obliquely (*ob*), while neighboring fibers are cut predominantly transversely (*t*) and longitudinally (*l*), $\times 35,000$ (new).

within the ileoparietal band, metanephridia, and gonads (see Fig. 133, 136; HYMAN, 1959b; WILLIAMS & ROWELL, 1965a). Accessory hearts have also been observed in *Liothyrella* as distended portions of the ileoparietal bands (FOSTER, 1974).

The heart of *Lingula* is a muscular chamber consisting of an outer coelomic epithelium covering a thick layer of circularly disposed muscle fibers but lacking an inner endothelial lining. In the main dorsal vessel, the muscles are disposed helically, but all the main vessels continue within the connective tissue. Subordinate blood vessels within the tentacles of the lophophore of the articulated *Terebratalia* (REED & CLONEY, 1977), the in-

articulated *Lingula* (STORCH & WELSCH, 1976), and probably all brachiopods are composed of a single layer of squamous myoepithelial cells, the basal lamina of which faces the blood space (Fig. 74). The course of the principal vessels is similar in *Neocrania* and *Lingula*, although in the former genus several contractile sacs fulfill the function of one or rarely more appendages in *Lingula* (Fig. 70). In front of the heart the main dorsal vessel runs forward dorsally of the esophagus and bifurcates to serve each brachidium of the lophophore. Inside the lophophore the branch runs ventrally and laterally in the central canals to the entrance of the brachial canal. At this point another branch arises and runs medially in the ventral part of the central canal to connect with the corresponding branch in the other brachium. In this way the circulatory systems of both the brachia are joined by a connective blood vessel ventral to the esophagus. The main branch in each brachium continues along the length of the small brachial canal. The lophophore circulatory system terminates as blind tentacular vessels arising from the small brachial or ventral connective vessels (see Fig. 110.1–110.2; BLOCHMANN, 1892, 1900).

Behind the heart, the main dorsal vessel splits into a left and right branch, each of which runs ventrally for a short distance before bifurcating into anterior and posterior branches; these two pairs of branches form the dorsal and ventral mantle vessels respectively. The two dorsal mantle vessels pass to the anterior body wall along the outer surface of the alimentary canal, on either side of the midline. They are then inserted into the dorsal mantle canal and send a branch that ends blindly in each branch of the mantle canal system. The ventral mantle vessels follow a more complex course before they reach the ventral mantle canals. The course of these vessels is different in *Neocrania* and *Lingula*, but they or their branches supply the ileoparietal bands and associated gonads in both genera and form a network of small vessels in

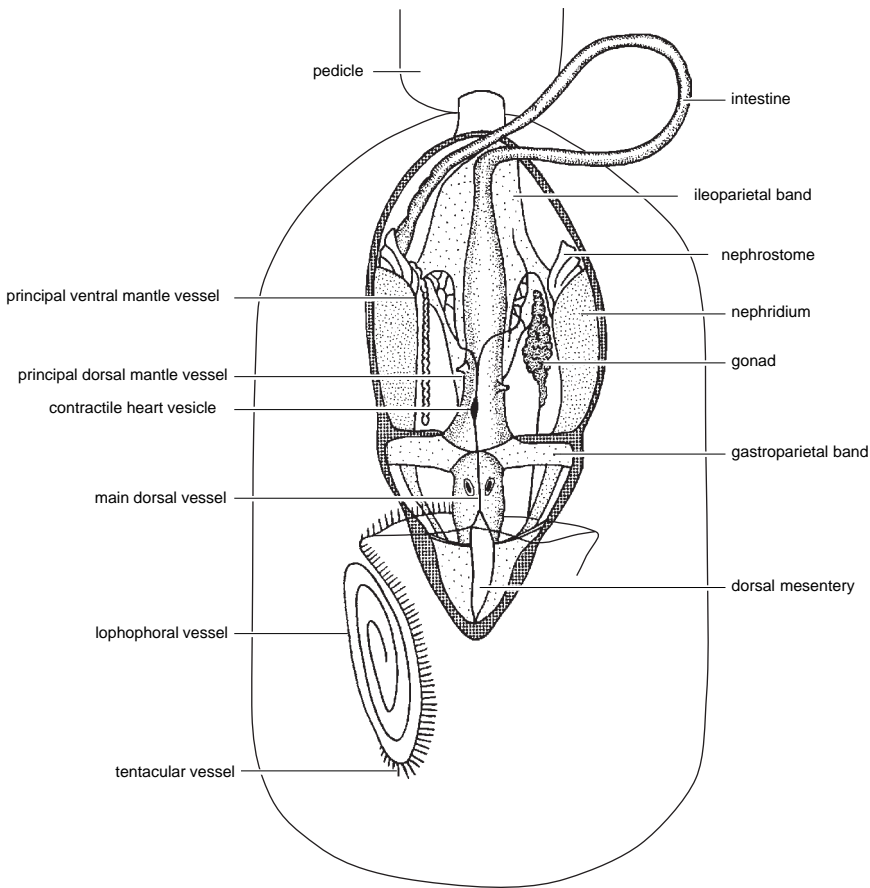


FIG. 70. Generalized diagram of the circulatory system of *Lingula* (adapted from Storch & Welsch, 1976).

this region. Both vessels then run anteriorly along their respective metanephridia and at the front turn laterally to be inserted in the ventral mantle canals, sending branches into the ramifications of the mantle canal system. *Discinisca* appears to have a poorly developed circulatory system (BLOCHMANN, 1892, 1900). The vessels in the lophophore are developed like those in *Neocrania* and *Lingula*, but the remainder of the system appears to be absent.

FREE CELLULAR INCLUSIONS

Free cellular inclusions may be classified as blood cells (erythrocytes), coelomocytes, and, in *Lingula*, spindle bodies.

Erythrocytes, which may carry a respiratory protein, occur throughout the circulatory system. The erythrocytes of *Lingula* impart a pale purple or violet color to the coelomic and vascular fluid (blood) (Fig. 75; 76.2–76.3; YATSU, 1902a; OHUYE, 1937). Lingulid blood cells are cowrie-shaped and have a central nucleus with few mitochondria (STORCH & WELSCH, 1976; ROWLEY & HAYWARD, 1985). The pigments present consist of two hemerythrins (KAWAGUTI, 1941; JOSHI & SULLIVAN, 1973). Erythrocytes are present in both the vascular and coelomic fluids, suggesting considerable interchange between the two systems (ROWLEY & HAYWARD, 1985). It is assumed that some of the

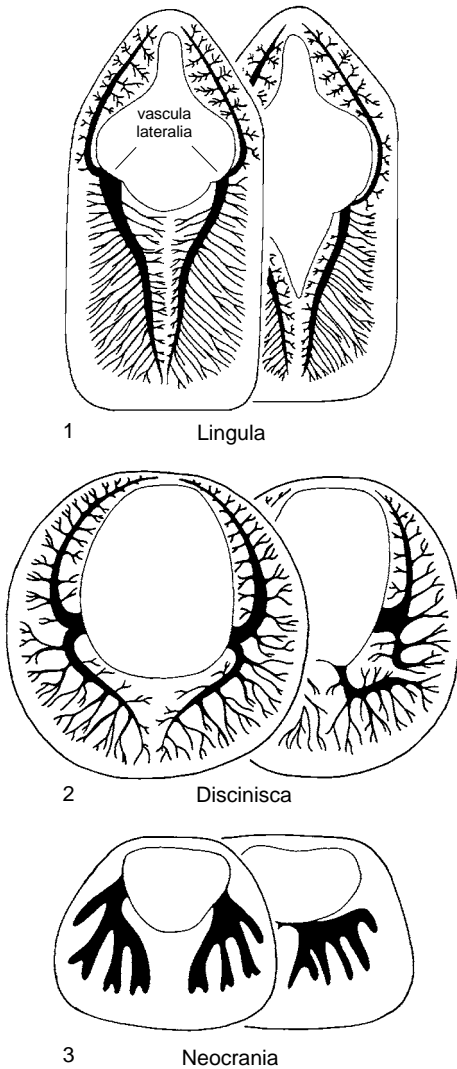


FIG. 71. Mantle canals; 1, *Lingula anatina*; 2, *Discinisca lamellosa*; 3, *Neocrania anomala* (adapted from Blochmann, 1892).

disciform or spherical cells found in articulated brachiopods (OHUYE, 1937) are similar to the erythrocytes of inarticulated species.

Brachiopod coelomocytes have been frequently and variously described (JAMES & others, 1992). At least two forms of coelomocytes exist, performing many diverse functions including immune responses (STORCH & WELSCH, 1976; ROWLEY & HAYWARD, 1985); the breakdown, recycling, and translocation of useful compounds as evidenced by oosorption (CHUANG, 1983a); the initiation of shell and mantle repair (PAN & WATABE, 1989); and hemostasis (ROWLEY & HAYWARD, 1985).

In *Lingula* several amoebocytes have been described (OHUYE, 1937) including hyaline eosinophilic and basophilic forms. Recent evidence suggests that only one population of variably granular cells exists, which is believed to be formed from the hyaline amoebocyte (ROWLEY & HAYWARD, 1985). The amoebocytes of *Lingula* contain large numbers of homogeneous granules, few mitochondria, alpha glycogen granules, free ribosomes, and debris-laden vacuoles, which are probably lysosomes (Fig. 76.1, 76.4–76.5). In life, the granules may be colorless or red, orange, or brown spherules or globules (HYMAN, 1959b). The cell membrane forms pseudopodia and is capable of ingesting bacteria (STORCH & WELSCH, 1976; ROWLEY & HAYWARD, 1985). Amoebocytes in a number of articulated genera occur as red to purple clumps along the distal margin of the genital lamella (JAMES, ANSELL, & CURRY, 1991b; JAMES & others, 1992). These cells produce pseudopodia and contain clusters of mitochondria often enmeshed with profiles of granular and agranular endoplasmic reticulum interspersed with lipid granules and vacuoles, some of which may be lysosomes (Fig. 77; JAMES & others, 1992).

The testes of some male brachiopods contain clusters of lipid-charged cells (SAWADA, 1973; JAMES & others, 1992). The cells are often present during the early stages of development, forming a band around the proliferating mass of gametes, and are believed to be trophocytes that nourish the proliferating gametes.

Spindle bodies have been described in the coelomic fluid of *Lingula*. Recent evidence has shown that lingulid spindle bodies are fragments of muscle fiber that have been broken down, probably by some form of stress-induced autolysis and shed into the coelomic fluid (ROWLEY & HAYWARD, 1985).

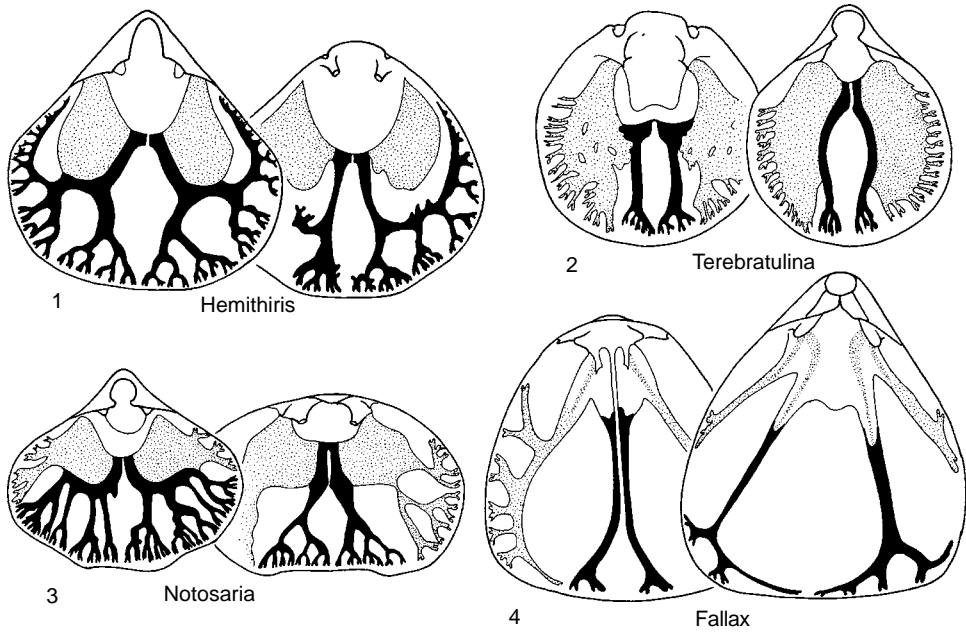


FIG. 72. Mantle canal systems; 1–2, recent rhynchonellids; 3, terebratulide (adapted from Williams, 1956); 4, terebratulide (adapted from Atkins, 1960a); *vascula media*, black; *vascula genitalia* and gonadal sacs stippled.

MUSCULAR SYSTEM

The brachiopod muscular system contains two main forms of muscular tissue. These exist as either discrete bundles of muscle fibers that control the movement of the valves or as myoepithelia (musculoepithelia), which are found on the inner side of coelomic epithelia, in the parietal bands, in mantle lobes, and in the lophophore. In turn, the muscular tissue contains either smooth or striated myofilaments, which impart different physiological and contractile properties to the muscle.

The principal valve muscles open, close, and rotate the valves relative to one another and to the pedicle. The absence of a hinge mechanism in the shell of inarticulated brachiopods also permits rotation of the valves and creates fundamental mechanical differences in the way in which muscles are disposed and operate.

Where the principal valve muscles are attached to the shell, the intervening outer epithelium consists of a series of striated cells

containing tonofibrils that penetrate the secondary layer (BLOCHMANN, 1892; YATSU, 1902a; PRENANT, 1928). These attachment areas are commonly seen on the inner side of the valve as muscle scars and result from the significantly slower rate of secondary shell secretion by the modified epithelium.

PRINCIPAL VALVE MUSCLES OF ARTICULATED BRACHIOPODS

The posterior hinge of articulated brachiopods permits valve opening (abduction) and closing (adduction) in a single plane. The adductor (occluser) muscles close the valves, and the diductor (divaricator) muscles open the valves. Adjustor muscles, generally a dorsal and ventral pair, extend between the pedicle and the valves, moving the entire shell relative to the pedicle. A median, sometimes paired, pedicle (peduncular) muscle has been reported in some older works, but the presence, extent, and functional properties of pedicle muscle fibers remain controversial (EKMAN, 1896; RICHARDSON, 1979).

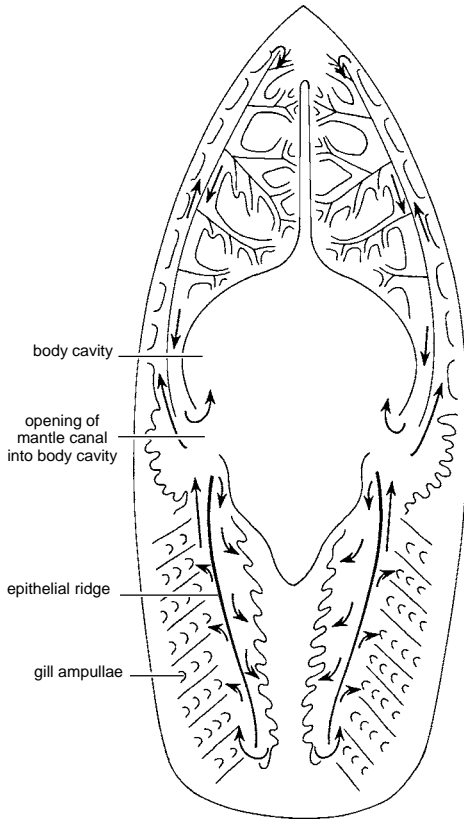


FIG. 73. Circulation in the dorsal mantle canals of *Glottidia* (adapted from Morse, 1902).

A set of adductor muscles extends from the dorsal to the ventral valve in front of the posterior margin, while a set of diductors is typically inserted into the dorsal valve posterior to the teeth and sockets that form the hinge axis or fulcrum about which the valves articulate (Fig. 78).

The adductor muscles are attached to the ventral valve posteromedially in two places. As the muscles pass between the valves, they bifurcate and attach anteromedially to the dorsal valve in four places (Fig. 79). In the thecideidines, the adductor muscles do not divide dorsally, but an extra set of adductor muscles occupies posterolateral positions in front of the hinge line. This arrangement, combined with highly developed teeth and sockets, presumably prevents lateral move-

ment that might arise from an articulation that is sufficiently flexible to allow the dorsal valve to open at right angles to the cemented ventral valve (Fig. 80).

The diductor muscles are inserted immediately in front of the beak of the dorsal valve either in or at the side of the cardinal process. From this position, the diductor muscles splay out to occupy a pair of extensive attachment areas in the ventral valve, usually on either side of the adductor bases. The dorsal attachment of the diductor muscles is posterior to the hinge axis of the shell and thus provides the mechanical leverage about the fulcrum to open the shell (Fig. 78). The dorsal umbo of some terebratulids (e.g., *Platidia*) is resorbed to accommodate the pedicle (Fig. 81). In such a valve, the dorsal attachment areas are in front of the hinge axis and the ventral areas are posterior, thus reversing the normal arrangement but maintaining the necessary moment about the hinge axis to open the valves. Commonly a pair of slender accessory diductors is also present, passing from the cardinal processes to become inserted into a small pair of attachment areas situated posterior to the ventral adjustors.

PRINCIPAL VALVE MUSCLES OF INARTICULATED BRACHIOPODS

The valves of the inarticulated brachiopod lack a hinge but possess a complex arrangement of muscles that make them capable of a wider range of valve movements than those of articulated shells. Generally there are two pairs of conspicuous anterior and posterior adductors (except in the lingulids, which have only one laterally placed posterior adductor), two pairs of oblique muscles (three in *Lingula*), an elevator, and three pairs of minor muscles: the lophophore protractors, retractors, and elevators (Fig. 82). The adductors pass dorsoventrally through the body cavity and are the largest sets in brachiopods. They have been given different names in different stocks, but all are concerned with the closure of the shell. The oblique muscles

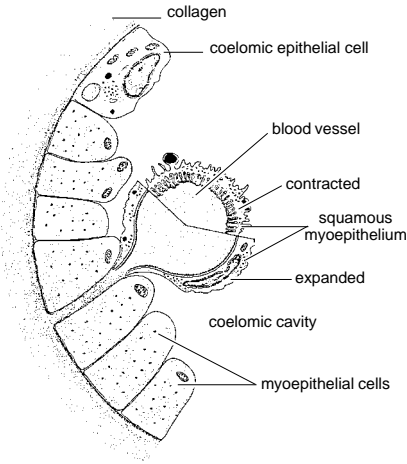


FIG. 74. Diagram of a transverse section through part of a tentacular canal, showing the coelomic epithelium and myoepithelial cells; the tentacular blood vessel is illustrated in both an expanded and contracted condition (adapted from Storch & Welsch, 1976).

control the rotation and sliding or longitudinal movements of the valves.

In *Lingula*, the shell is closed by a pair of medially located, central muscles and a third umbonal muscle, which is made up of two unequal bundles of muscle fibers (Fig. 82). The larger bundle of umbonal muscle fibers runs dorsoventrally. The smaller, flat bundle, which is inserted in front of the main bundle on the ventral valve, spirals around the main bundle, inserting posteriorly in the dorsal valve (BLOCHMANN, 1900). Both central muscles are double bundles of fibers passing dorsoventrally. Four pairs of oblique muscles are present, three of which (middle laterals, outside lateral, and transmedians) form a composite scar on the dorsal valve. The middle laterals arise between the central muscles in the ventral valve and pass obliquely backward to be inserted into the dorsal valve immediately in front of the scar outside the laterals. These outside lateral muscles converge slightly anteriorly from the dorsal valve and are inserted on the ventral valve lateral of the centrals. The third pair of muscles, the transmedians, are the largest of the oblique muscles and form the inner part

of the composite scars. The right transmedian muscle runs ventrally from the dorsal valve to become attached to the left side of the ventral valve. The left transmedian muscle splits just below the insertion on the dorsal valve, and the two branches cross over the right transmedian to become fixed to the right side of the ventral valve. This is the usual condition of the transmedians, but the left transmedian of a few species may be undivided (BULMAN, 1939). The fourth pair of muscles with an oblique course is the anterior laterals. These are inserted in the ventral valve posterolateral of the outside muscles and rise anteriorly to become attached to both the dorsal valve and the anterior body wall near the midline of the valve.

The muscular system of *Glottidia* is similar to that of *Lingula* (MORSE, 1902), but those of other recent inarticulated genera are generally less complicated with fewer oblique muscles. In the discinids (Fig. 83) two pairs of adductor muscles, a small posterior pair and a larger anterior pair, run directly dorsoventrally between the valves. Each anterior adductor consists of a small median and a much larger lateral bundle of muscle fibers. Three pairs of oblique muscles occur, all of them relatively long and thin in comparison with the adductors. The internal obliques arise from near the center of the ventral valve

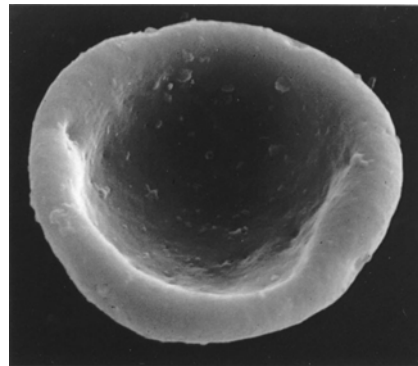
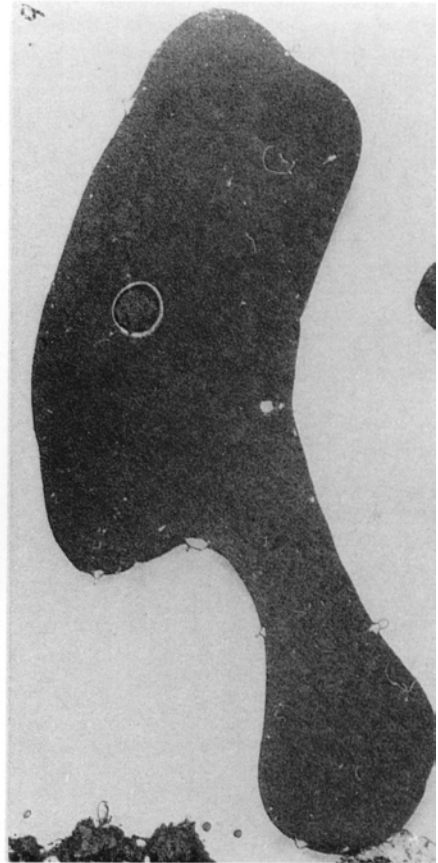


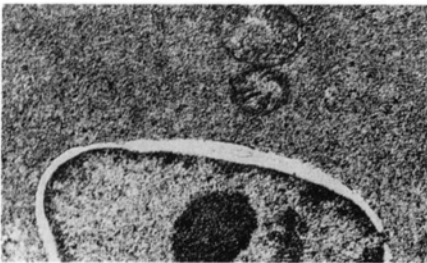
FIG. 75. SEM micrograph of a blood cell (erythrocyte) of *Lingula anatina*, $\times 2,700$ (new).



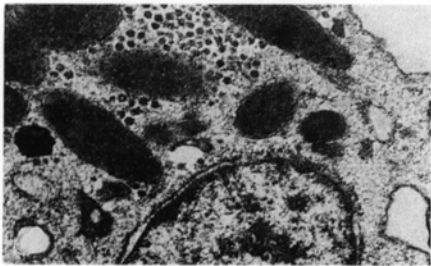
1



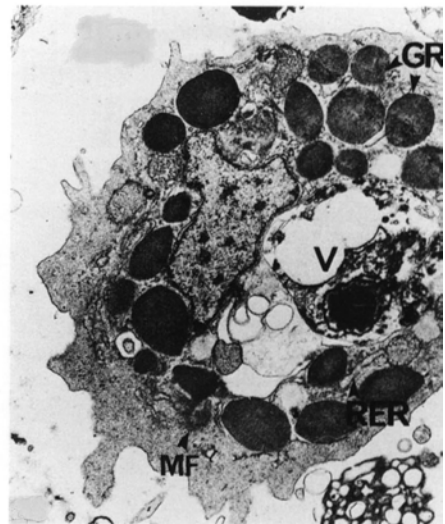
2



3



4



5

FIG. 76. For explanation, see facing page.

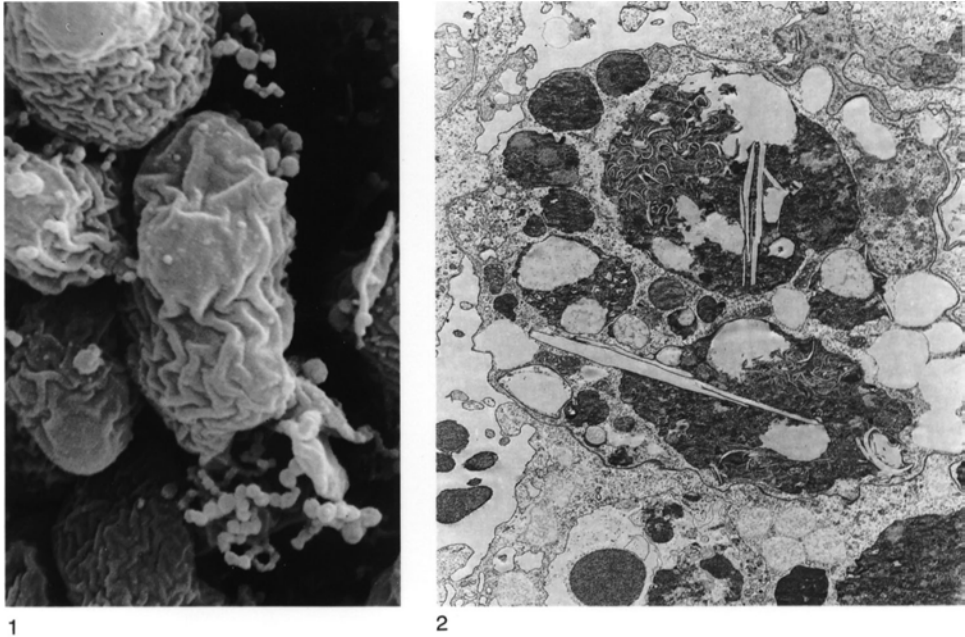


FIG. 77. 1, SEM, $\times 9,000$, and 2, TEM micrographs of an amoebocyte in *Calloria inconspicua*, $\times 1,350$; note vacuoles and heterogeneous granules in 2 with cytoplasm (new).

and diverge posteriorly to become inserted into the dorsal valve slightly anterolateral of the attachment of the posterior adductors. The third pair of oblique muscles, the posterior obliques, arise on the ventral valve slightly in front and median of the site of the attachment of the oblique laterals. They pass dorsally and converge posteriorly, becoming inserted into the dorsal valve close together near the midline, slightly in front of the posterior margin.

The principal muscles of *Neocrania* are similar to those of *Discinisca*. Two pairs of adductors occur, the anterior set consisting of two bundles of fibers. The oblique internals occupy a position similar to those of the discinids but follow a more S-shaped course. The oblique laterals originate on the ventral

valve on the side of the posterior adductors and are attached not to the dorsal valve but to the anterior body wall (Fig. 84).

The correlation of the muscles of the lingulids, discinids, and craniids is based on form, assumed function, and, more fundamentally, innervation (BLOCHMANN, 1892, 1900). The posterior and anterior adductors of the craniids and the discinids are considered to be homologous to the lingulid umbonal and central muscles respectively. The transmedian, outside, and middle lateral oblique muscles of the lingulids, which are attached only to the shell, may be correlated with the discinid oblique posterior, and oblique internal muscles with the oblique internals of *Neocrania*, all of which are similarly attached.

FIG. 76. TEM micrographs of the coelomocytes of *Lingula anatina*; 1, amoebocytes with granules, $\times 9,400$; 2, an erythrocyte in cross section, $\times 1,316$; 3, nucleus and mitochondria of an erythrocyte, $\times 28,200$; 4, nucleus and cytoplasm with glycogen and granules of an amoebocyte, $\times 28,200$ (Storch & Welsch, 1976); 5, amoebocytes with granules (GR), rough endoplasmic reticulum (RER), vacuole containing debris (V), and microfilament bundles (MF), $\times 8,460$ (Rowley & Hayward, 1985).

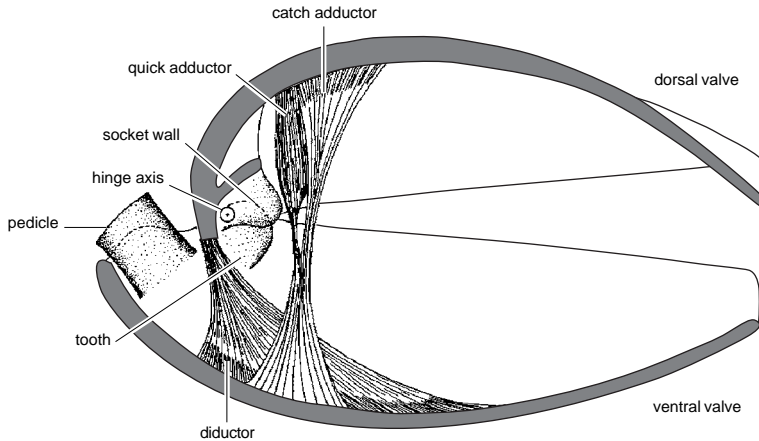


FIG. 78. Articulation and muscle system of the terebratulide *Calloria inconspicua* in median section showing the relationship of the muscles to the hinge axis (adapted from Rudwick, 1961).

STRUCTURE OF PRINCIPAL MUSCLES

Details of the ultrastructure of the adductor and diductor muscles of the articulated *Terebratalia* (ESHLEMAN, WILKENS, & CAVEY, 1982) and the adductor muscle of the inarticulated *Lingula* (KUGA & MATSUNO, 1988) are well documented, and both smooth and striated types are present (Fig. 85). Typically, articulated brachiopods possess one pair of striated and one pair of smooth adductors, originating as four separate muscles on the dorsal valve (the posterior is striated, while the anterior is smooth) and inserted by a common tendon (two tendons in some species) on the ventral valve (Fig. 79). In lingulids, each adductor muscle consists of smooth and obliquely striated components segregated into an anterior opaque and a posterior translucent portion that are constructed of smooth and obliquely striated muscles, respectively (Fig. 85.1–85.2; KUGA & MATSUNO, 1988). It is believed that the anterior adductor in the lingulid is responsible for the catch contraction. The smaller posterior adductors consist of quick, striated muscle fibers that snap the shell shut in response to various stimuli. The larger anterior adductors consist of unstriated catch fibers, which react more slowly and hold the shell

closed for long periods. The posterior and anterior adductors form separate bundles of fibers on the dorsal side, but they share a single attachment on the ventral side (Fig. 79; WILLIAMS & ROWELL, 1965a; ESHLEMAN, WILKENS, & CAVEY, 1982).

The muscular tissue of articulated brachiopods has been described only as smooth or striated, but three cell types have been identified in the anterior adductor of *Lingula* (KUGA & MATSUNO, 1988). These consist of striated (translucent) muscle and two types of smooth (opaque) muscle. In the striated adductor muscles of lingulids, cell organelles such as the sarcoplasmic reticular system are located in peripheral regions of the cell (KUGA & MATSUNO, 1988). There is no information regarding the sarcomeric construction of the striated cells of the inarticulated species. In the articulated *Terebratalia*, the striated muscle apparatus consists of sarcomeres of interdigitating thin and thick myofilaments in the ratio of 6:1 (Fig. 86.5–86.6; ESHLEMAN, WILKENS, & CAVEY, 1982).

Thin and thick myofilaments in an unregistered array form the contractile apparatus of the smooth adductor muscle of *Terebratalia* and are indistinguishable from those of the diductor muscles (Fig. 86; ESHLEMAN, WILKENS, & CAVEY, 1982). In *Lingula*, two

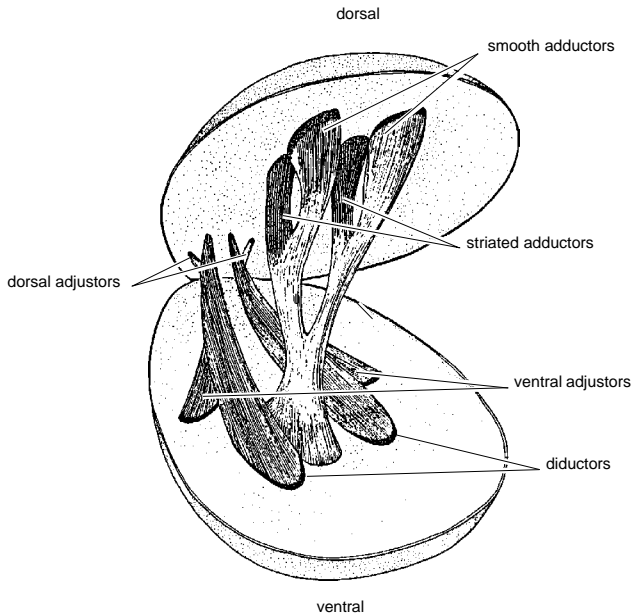


FIG. 79. Diagram of the musculature of *Terebratalia transversa*, with the anterior part of the shell cut away and the lophophore and viscera removed (adapted from Eshleman & Wilkens, 1979a).

populations of smooth muscle cells exist. Type A cells contain contractile fibers, which are relatively thin, thick myofilaments; type B cells contain thick myofilaments in addition to contractile fibers that are of similar size to those found in type A cells (Fig. 85.2–85.3; KUGA & MATSUNO, 1988).

Morphological and electrophoretic evidence suggests that, as in bivalve molluscs, paramyosin may be responsible for the catch contraction of the anterior adductor muscles in brachiopods (WILKENS, 1978a; ESHLEMAN, WILKENS, & CAVEY, 1982; KUGA & MATSUNO, 1988). In *Terebratalia* the presence of paramyosin has been demonstrated in both the smooth adductor and diductor muscles and to a lesser extent in the striated adductor muscle. The large fusiform myofilaments found within these muscles are morphologically characteristic of a paramyosin component and resemble molluscan smooth muscle and the very thick myoepithelial cells of brachiopod tentacles (REED & CLONEY, 1977). The structure of the smooth adduc-

tor of *Lingula* also suggests the presence of paramyosin (KUGA & MATSUNO, 1988).

MYOEPITHELIAL CELLS

Although the most conspicuous muscles within the brachiopods occur as well-defined bundles of muscular fibers or as muscular layers in contractile tissues, some specialized epithelial cells (myoepithelial cells) have been shown to contain contractile fibers. Myoepithelial cells have been described in tentacles of the lophophore of the *Lingula* (STORCH & WELSCH, 1974, 1976) and the articulated brachiopod *Terebratalia* (Fig. 87; REED & CLONEY, 1977). In the latter, striated and smooth myoepithelial cells occur in longitudinal rows that extend along each tentacle on opposite sides of the tentacular canal (see Fig. 106). A blind-ending blood vessel that penetrates each tentacle is formed from squamous, smooth myoepithelial cells (see Fig. 76). Myoepithelial cells have also been found in the mesentaria of *Lingula* (STORCH & WELSCH, 1974).

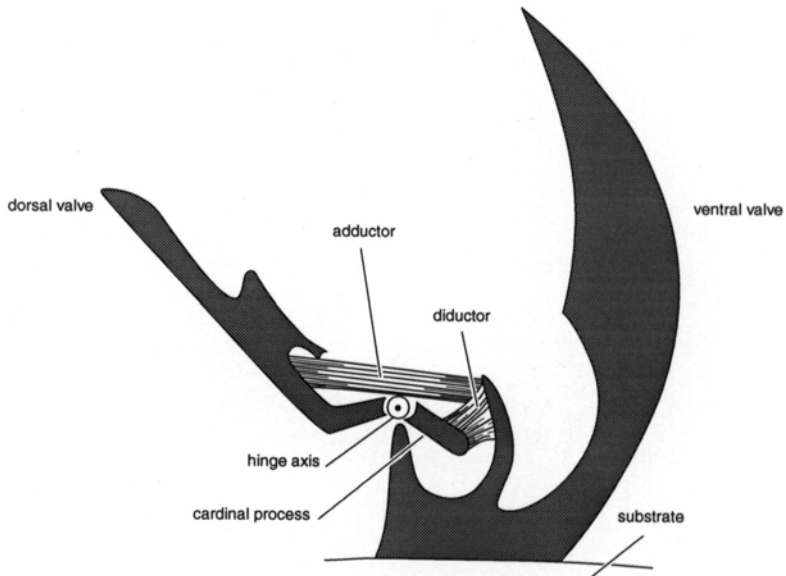


FIG. 80. Muscle system of the cemented thecideidine *Lacazella* showing the columnar muscles raised on a central platform (adapted from Lacaze-Duthiers, 1861; Rudwick, 1970).

The myoepithelial cells of both genera (STORCH & WELSCH, 1976; REED & CLONEY, 1977) appear to be similar. Occasionally ciliated, myoepithelial cells have a centroapical nucleus accompanying mitochondria and Golgi bodies. These organelles occur above a layer of thick and thin myofilaments, which

are inserted into basal extensions of the cell. Glycogen occurs in abundance throughout the cells, as alpha particles in *Lingula* and beta particles or rosettes in *Terebratalia*. Lipid inclusions are present in *Lingula* (STORCH & WELSCH, 1974). Attached to a basal lamina with numerous hemides-

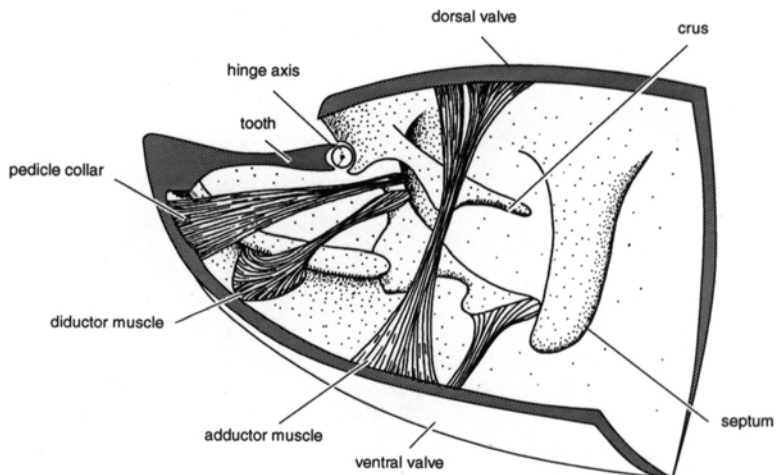


FIG. 81. Musculature of *Platidia annulata* (ATKINS) (adapted from Williams & Rowell, 1965a).

mosomes, the myoepithelia are joined to surrounding cells by *zonulae adhaerens* (Fig. 88; REED & CLONEY, 1977).

The fine structure of myoepithelial cells, myofilament fields, and sarcoplasmic reticulum are known only for *Terebratalia* (REED & CLONEY, 1977). The striated myofilament field (Fig. 88.1) is composed of interdigitating, thin and thick myofilaments, which combine to produce the characteristic striation or banding rendered visible by light microscopy. Each thick myofilament is surrounded by 12 thin myofilaments giving a thin to thick ratio of 6:1. The sarcoplasmic reticulum, which is peripheral to the myofilament field, is a smooth, membranous system of tubules that frequently form subsarcolemmal cisternae that couple peripherally with the lateral sarcolemma.

Smooth myoepithelial cells (Fig. 88.2) also contain thick and thin myofilaments that are of indefinite length and staggered throughout the myofilament field. Thick filaments are fusiform, surrounded by thin myofilaments, and resemble the paramyosin filaments of bivalve mollusc adductor muscles. The sarcoplasmic reticulum is reduced, and peripheral couplings are rare in comparison to the striated myoepithelial cells.

Functional Morphology of the Principal Valve Muscles

In articulated brachiopods when the adductor muscles relax and the diductor muscles contract, the anterior margin of the valves separate (gape). The gape is maintained by tonic contraction in the smooth diductor muscles. Closure of the shell occurs in two modes depending upon the stimulus and reflecting the physiological properties of the striated (quick) and smooth (catch) components of the adductor muscles. In articulated brachiopods, the anterior adductors are quick; the posterior adductors catch. A combination of slip, the rapid loss of tetanus in the diductors, and contraction of the striated portion of the adductors assures rapid shell closure. Closure of the valves is completed and maintained by the smooth portion of

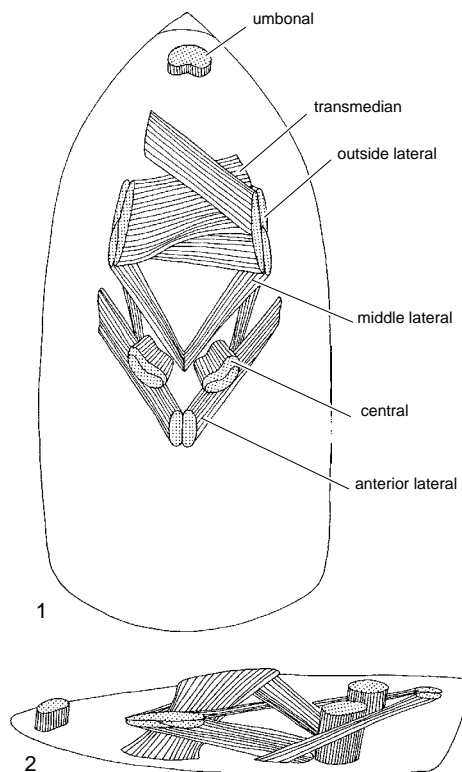


FIG. 82. Muscle system of *Lingula* viewed 1, dorsally and 2, laterally (adapted from Bulman, 1939).

the adductor contracting and achieving tetanus.

Pedicle muscles vary greatly in size, position, and relationship to the pedicle. The positions of these muscles are the most explicit guide to the pedicle type and function (RICHARDSON, 1979, 1981a, 1981b). During closure of the shell, contraction of the adjustor muscles pulls the proximal end of the pedicle deep into the body cavity, but it is believed that, since the diductors are intimately associated with the connective tissue around the base of the pedicle, their contraction during the opening of the shell assists in ejecting the pedicle, thus moving the shell forward into an erect position (WILLIAMS & ROWELL, 1965a).

It is thought that the contraction of the posterior adductors or the umbonal muscle

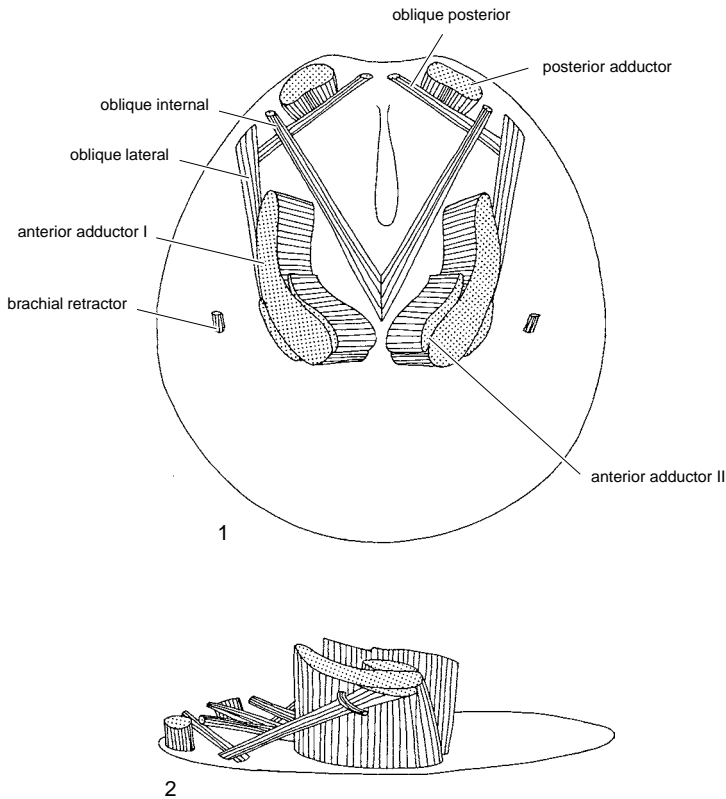


FIG. 83. Muscle system of *Discinisca* viewed 1, dorsally and 2, laterally (adapted from Bulman, 1939).

and relaxation of the anterior adductors or their homologues opens the valves of inarticulated genera. The action is probably assisted and partly controlled by the various oblique muscles and dermal muscles of the body wall.

DIGESTIVE SYSTEM

The brachiopod digestive system is composed of a continuous gut or alimentary tract, opening at the mouth and terminating with an anus or ending blindly in inarticulated and articulated species respectively. In both groups the digestive system consists of a mouth, pharynx, esophagus, stomach, digestive diverticula (liver), and a pylorus. In inarticulated brachiopods the gut continues beyond the pylorus through an intestine, terminating in an anus (Fig. 89).

ALIMENTARY CANAL

The mouth is a transverse slit that occurs medially in the brachial groove where the two arms of the lophophore (brachia) unite (see Fig. 103). The mouth opens to the pharynx, a short, dorsally curved, muscular tube embedded in the bases of the brachia. The gut continues as an esophagus, a relatively short tube leading to the stomach, which is a pouchlike distended portion of the digestive tract supported by mesenteries (the gastro- and ileoparietal bands). A number of ducts join the stomach to the digestive diverticula, which are formed from anastomosing clusters of blindly ending tubes (acini). A sphincter separates the stomach from the pylorus. In inarticulated brachiopods, the pylorus leads into an intestine that opens to the exterior (the mantle cavity) through the

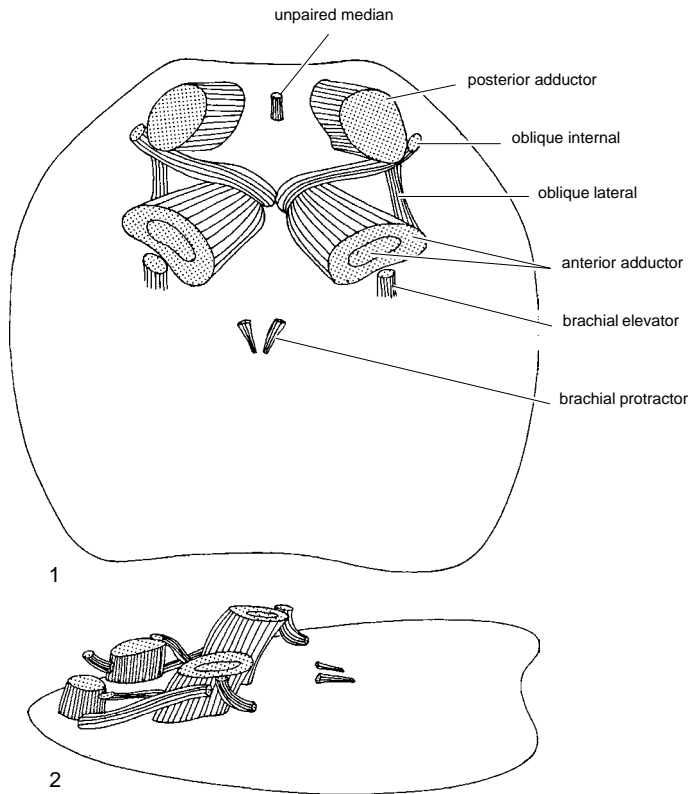


FIG. 84. Muscle system of *Neocrania* viewed 1, dorsally and 2, laterally (adapted from Bulman, 1939).

anus. The opening of the anus is also controlled by a sphincter (Fig. 90).

The esophagus of the inarticulated brachiopods is relatively short and leads to the stomach. In older literature, the stomach was described as being divided into posterior and anterior parts. These are now considered to be homologues of the stomach and pylorus respectively of articulated brachiopods (Fig. 89; CHUANG, 1960; STEELE-PETROVIC, 1976). The stomach extends posteriorly along the median line and in both lingulids and discinids is attached by part of the ileoparietal band to the posterior body wall. In *Neocrania* it curves ventrally forward toward the posterior end of the coelomic cavity. The stomach is separated from the pylorus by a sphincter, which is clearly visible in *Lingula* (BLOCHMANN, 1900) but less so in *Neocrania* (BLOCHMANN, 1892).

Digestive diverticula open through ducts into the stomach. There are four digestive diverticula in *Lingula* and *Discinisca* and two in *Neocrania* (JUBIN, 1886; BLOCHMANN, 1892). They open separately into the stomach and are subdivided into lobes, each comprising several bunches of short acini in lingulids and *Neocrania* (JUBIN, 1886; BLOCHMANN, 1892; MORSE, 1902; CHUANG, 1959b) but are long and tubular in *Discinisca* (JUBIN, 1886). Each of the four diverticula present in *Lingula* (three dorsal and one ventral) opens through a separate duct into the stomach. The three dorsal diverticula consist of an anterior diverticulum situated on the midline of the stomach and a posteriorly placed pair of diverticula on the left and right of the midline, slightly behind the point of attachment of the gastroparietal band. Diverticula of adults vary in size, the

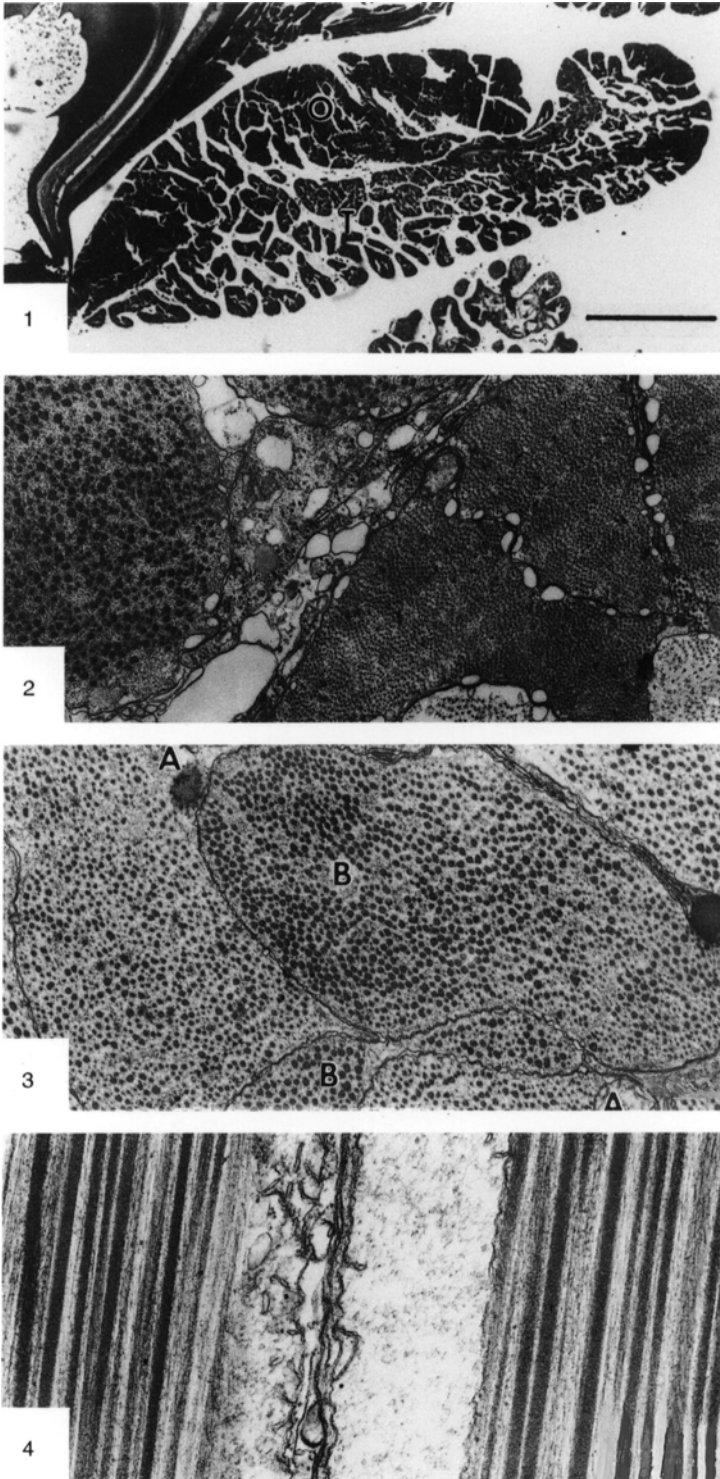


FIG. 85. (For explanation, see facing page.)
© 2009 University of Kansas Paleontological Institute

right posterior being the largest and the anterodorsal the smallest. All have a similar structure, with each diverticulum consisting of a fixed number of lobes, seven in the right posteroventral, two in the right postero-dorsal, and four in the ventral and antero-dorsal diverticula. The main duct of each diverticulum bifurcates shortly after leaving the stomach, and from the bifurcation a number of lobular ducts arise to serve the lobes. The lobes consist of repeatedly branching ducts terminating in bunches of acini (CHUANG, 1959b).

In *Neocrania* a pair of dorsal diverticula are separated by a mesentery. Each diverticu-

lum is divided into four lobes, which have a similar construction to those of *Lingula* (JOURBIN, 1886; BLOCHMANN, 1892). *Dis-cinisca* has three diverticula, all situated in front of the gastroparietal band as a dorsal pair and a single unpaired diverticulum. They open into the stomach by separate ducts but are apparently not divided into lobes, their terminal portions being long tubes (JOURBIN, 1886).

Both *Lingula* and *Neocrania* have a ciliated epithelial groove running along the stomach (CHUANG, 1959b, 1960). In *Lingula* it arises in the right postero-dorsal diverticula, traverses all the lobes of this organ, and

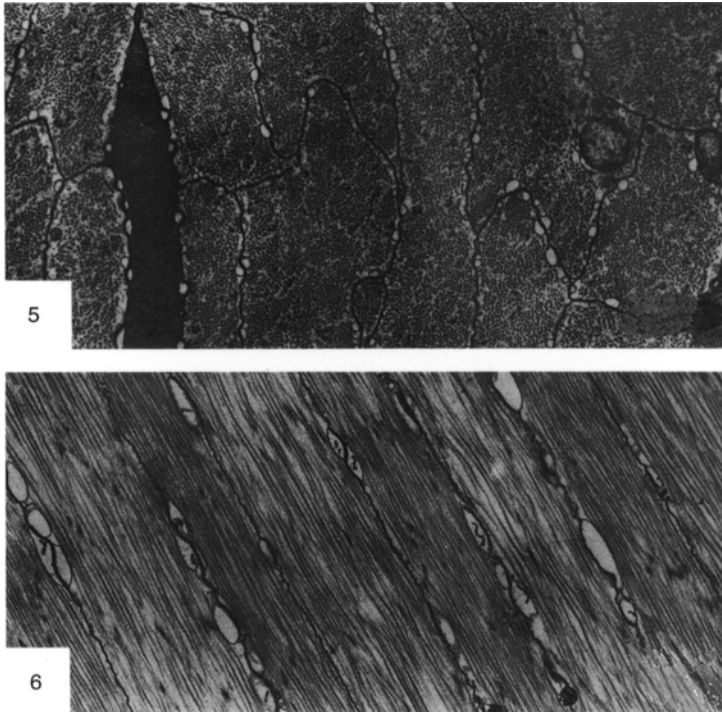


FIG. 85. The structure of muscles of *Lingula anatina*; 1, a light micrograph of a cross section of the anterior adductor of *Lingula anatina*. The dark area of the adductor (*O*) is the opaque (smooth) portion. The light area (*T*) is the translucent (striated) portion, $\times 15,75$; 2, TEM micrograph of a cross section of the opaque and translucent portions to the left and right respectively, $\times 7,290$; 3, TEM micrograph of a cross section of the opaque portion; cell organelles are located at the periphery of the cell, type A cells (*A*) have thinner-sized thick myofilaments. Type B cells (*B*) have two kinds of thick myofilaments, $\times 4,860$; 4, TEM micrograph of a longitudinal section of the opaque portion showing the differences in the size of the thick myofilaments in type A cell to left and type B cell to right, $\times 24,300$; 5, TEM micrograph of a cross section of the translucent portion with cell organelles located in the peripheral region of the cells; the thick myofilaments are gathered into units of 50 to 60, $\times 6,480$; 6, TEM micrograph of a longitudinal section of a translucent portion with thick myofilaments running parallel to the longitudinal axis of the cells, $\times 7,290$ (Kuga & Matsuno, 1988).

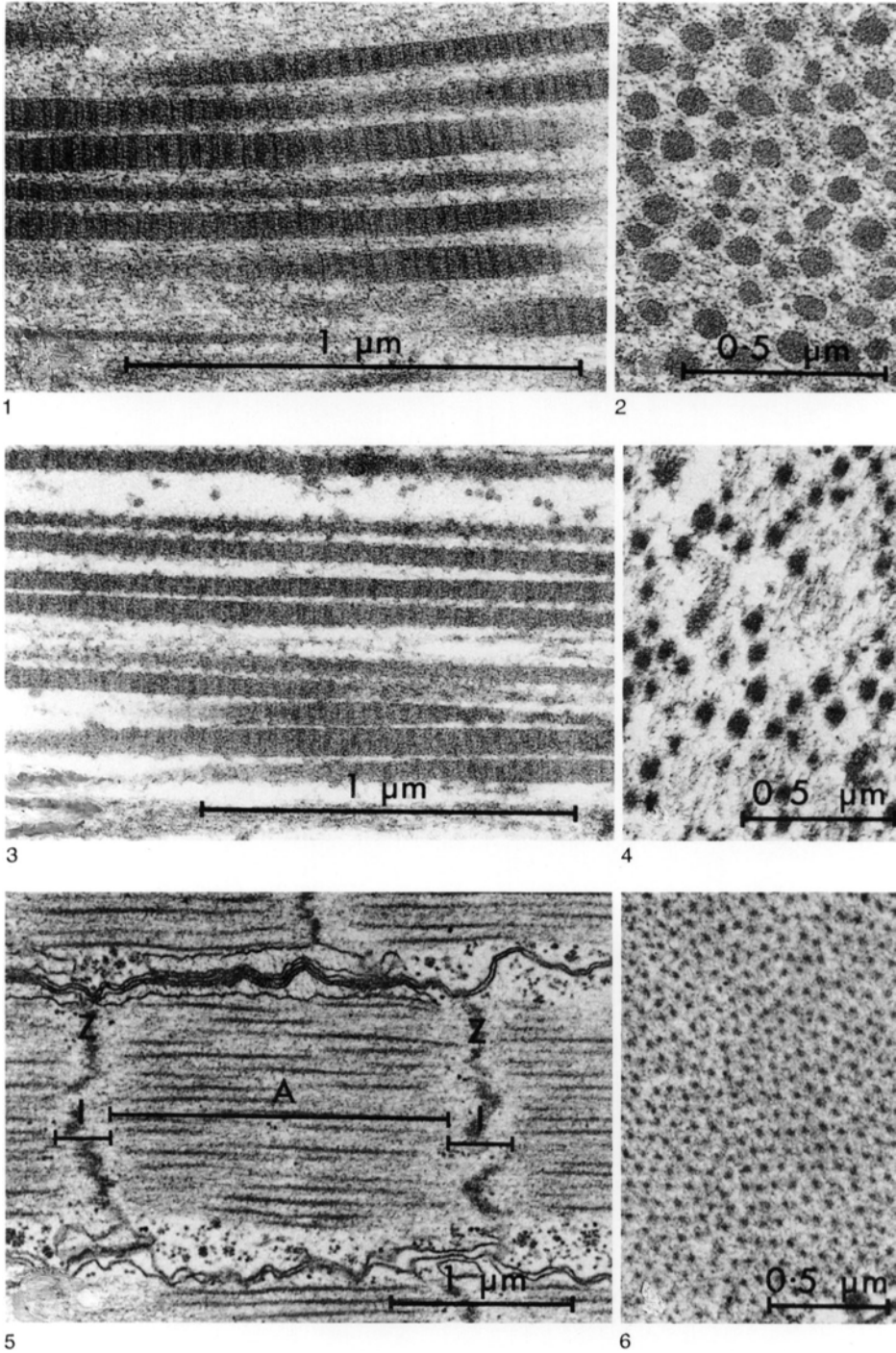


FIG. 86. TEM micrographs of myofilaments of *Terebratalia transversa*; 1, longitudinal section and 2, transverse section of smooth adductor cell; myofilaments of the diductor cells in 3, longitudinal section and 4, transverse section; myofilaments of the striated adductor cells (A, A-band; I, I-band; Z, Z-line) in 5, longitudinal section and 6, transverse section (Eshleman, Wilkens, & Cavey, 1982).

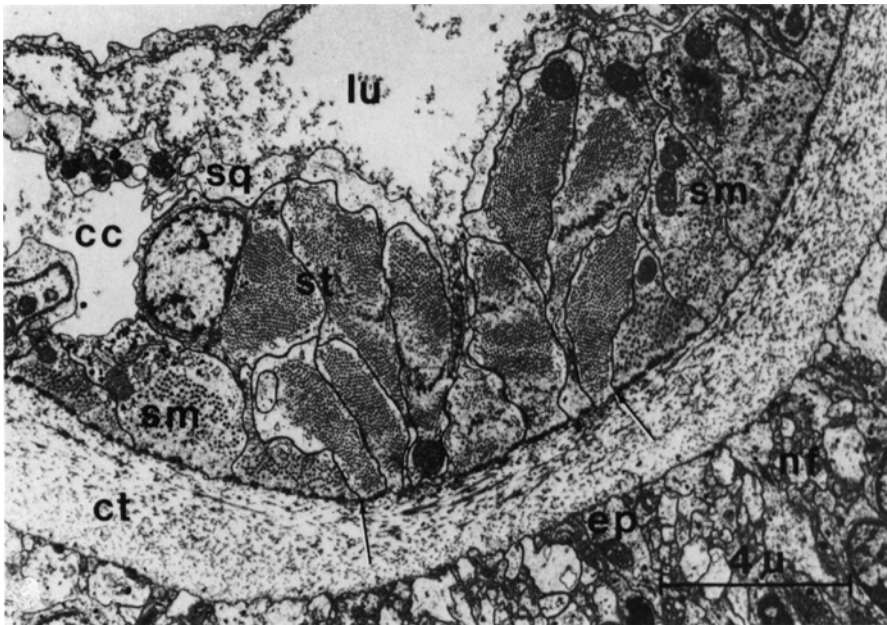


FIG. 87. TEM micrograph of a transverse section of the frontal contractile bundle near the distal end of the inner tentacle of *Terebratalia transversa*; about 10 striated myoepithelial cells (*st*) occupy the central part of the contractile bundle (between the *arrows*) and are bordered on either side by a group of three smooth myoepithelial cells (*sm*) (outside the *arrows*); striated fibers adjoin the squamous peritoneal cells (*sq*) of the tentacular blood vessel; the acellular connective tissue cylinder (*ct*) separates the myoepithelial cells from the epidermis (*ep*) and the neuronal processes (*nf*) at the bottom of the picture; also identified, lumen of blood vessel (*lu*) and tentacular canal (*cc*) (Reed & Cloney, 1977).

emerges to run along the dorsal surface to the pylorus. The epithelial groove in *Neocrania* lies longitudinally along the floor of the stomach and continues into the pylorus, rising dorsally from the floor to the roof of the pylorus by the right lateral wall.

Formally known as the posterior stomach, the pylorus of inarticulated brachiopods is narrower, has thicker walls, and is separated from the stomach by a constriction. Another, posterior sphincter separates the pylorus from the start of the intestine. The intestine in lingulids and discinids (Joubin, 1886; Blochmann, 1900; Morse, 1902; Chuang, 1960) is a slender tube, while in *Neocrania* (Joubin, 1886; Blochmann, 1892) it is dilated posteriorly.

In the lingulids, the thin-walled, tubular intestine bends to the left and forms a free loop before returning to the end of the coelomic cavity. It then turns right and follows an oblique course anteriorly to open at the anus

on the right body wall. The intestine of the discinids is shorter but similar to that of the lingulids, turning right from the stomach toward the lateral body wall and then obliquely forward in a dorsal direction, also opening on the right body wall at an anus. *Neocrania* differs considerably in possessing a V-shaped gut with the apex directed anteriorly. From the sphincter at the end of the stomach the intestine continues anteriorly and then bends back acutely to open at the anus, which is medially placed on the posterior margin. Although the anus is on the midline, it lies to the right of the attachment of the ventral and dorsal mesenteries to the intestine. As in other inarticulated brachiopods, the anus opens on the right side of the body but is posteriorly placed (Chuang, 1960).

In most articulated genera, the esophagus is divided into a relatively long anterior and a short posterior section, separated by a

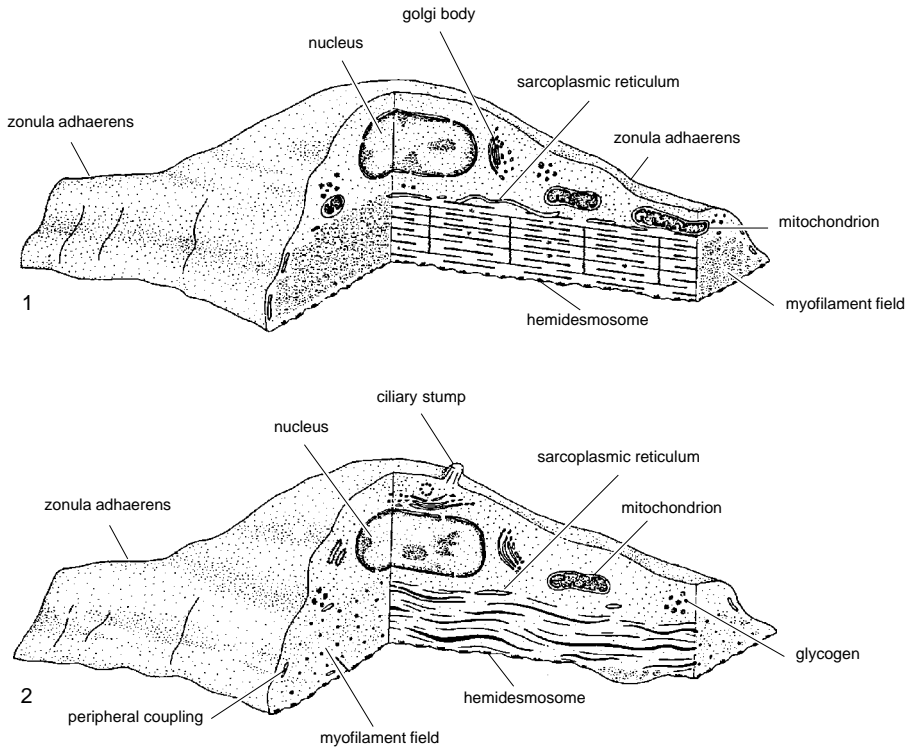


FIG. 88. Schematic diagrams of 1, a striated myoepithelial cell and 2, a smooth myoepithelial cell (adapted from Reed & Cloney, 1977).

valvelike thickening of the esophageal wall (MORTON, 1960). It is distinguished from that of inarticulated brachiopods in being strongly inclined anterodorsally before it bends abruptly to the relatively short stomach (Fig. 90).

The digestive diverticula of articulated species are not well known but commonly consist of a pair of posterior lobes that are symmetrically disposed around the dorsal mesentery and communicate with the stomach through 1 of 3 pairs of ducts. Different arrangements occur in *Argyrotheca* and *Lacazella*, where the diverticula consist of 6 to 8 pairs and 10 to 16 pairs of elongate tubules respectively.

The stomach passes middorsally into a tapering pylorus directed posteroventrally and terminating blindly as either a blunt end supported by a mesentery or exceptionally, as

in *Hemithiris*, as a bulbous end twisted upon itself and hanging free (Fig. 91; HANCOCK, 1859).

HISTOLOGY OF THE GUT

The histology of the gut in all brachiopods appears to be similar. The gut is essentially a variably elastic, connective tissue (collagen) tube encompassed by two layers of muscle, an inner, circular layer and an outer, longitudinal layer. These muscles appear to be smooth in the intestine and stomach of all brachiopods, but the esophageal muscles in some rhynchonelloids and terebratuloids are known to be striated. The gut is sheathed by a thin, ciliated, coelomic epithelium. The lumen of the connective tissue tube is covered by a basal lamina and columnar epithelium, the cells of which are modified in different parts of the gut to perform different

functions. Most of the lumen of the gut is covered by ciliated columnar cells interspersed with mucous (glandular) cells and wandering phagocytes (CHUANG, 1959b). Neurons pass along the axis of the gut between the bases of the columnar epithelial cells above the basement membrane (D'HONDT & BOUCAUD-CAMOU, 1982).

Each digestive diverticulum consists of acini connected to the stomach by a series of ciliated, branching ducts (Fig. 92; BLOCHMANN, 1892; STORCH & WELSCH, 1975; STEELE-PETROVIC, 1976; D'HONDT & BOUCAUD-CAMOU, 1982). Acini range in structure from the globular or tubular sacs in *Lingula* (CHUANG, 1959b) to the long, unbranched, digitate forms of a number of articulated brachiopods (Fig. 93; STEELE-PETROVIC, 1976; PUNIN & FILATOV, 1980; D'HONDT & BOUCAUD-CAMOU, 1982). Acini are constructed from a tube of collagen covered externally by a ciliated coelomic epithelium and musculoepithelial cells. Internally the acini are lined with an epithelium containing ciliated, glandular, and phagocytic cells.

The fine structure of columnar cells lining the lumen of the pylorus and stomach is known only for *Terebratulina* (D'HONDT & BOUCAUD-CAMOU, 1982), while the digestive diverticula have been documented for *Terebratulina* (D'HONDT & BOUCAUD-CAMOU, 1982), *Hemithiris* (PUNIN & FILATOV, 1980), and *Lingula* (STORCH & WELSCH, 1975). The fine structure of the digestive diverticula appears to be similar in all brachiopods so far investigated (*Hemithiris*, PUNIN & FILATOV, 1980; *Terebratulina*, D'HONDT & BOUCAUD-CAMOU, 1982; and *Lingula*, STORCH & WELSCH, 1975). A number of different types of cells line the acini, reflecting its role as the main site of intracellular digestion in the brachiopod (CHUANG, 1959b; STORCH & WELSCH, 1975).

Two kinds of cells have been noted in the digestive diverticula of the articulated genera, *Magellania*, *Notosaria*, *Terebratella* (STEELE-PETROVIC, 1976), and *Terebratulina*

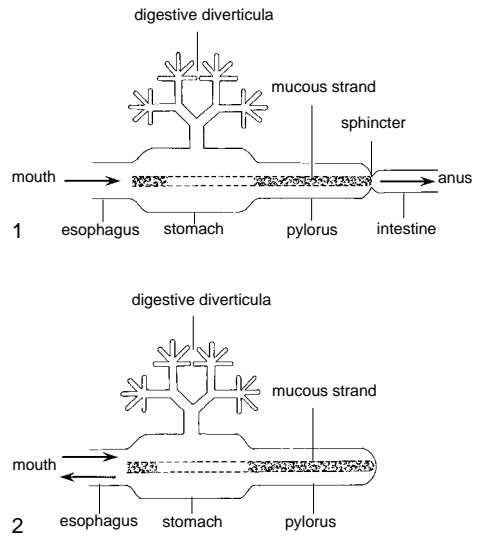


FIG. 89. Schematic diagrams of the guts of 1, inarticulated and 2, articulated brachiopods (adapted from Steele-Petrovic, 1976).

(D'HONDT & BOUCAUD-CAMOU, 1982); and, although three types of cells have been distinguished in *Lingula* (STORCH & WELSCH, 1975), at least two exhibit features common with those described in articulated brachiopods and probably function in the same way (Fig. 94; JAMES & others, 1992).

Although it is not presently possible to define unambiguously all the different types of cells forming the epithelial lining of the lumen of the gut and diverticula, broad categories can be recognized. They include ciliated cells, glandular cells, and digestive cells.

Monociliated columnar cells occur throughout most of the gut, and the available evidence suggests that they are similar in all living brachiopods (BOSI VANNI & SIMONETTA, 1967; STORCH & WELSCH, 1975; D'HONDT & BOUCAUD-CAMOU, 1982). Most of the columnar epithelial cells lining the gut possess an apical cilium surrounded by long, distal microvilli. In *Terebratulina*, many of these cells, especially in the stomach, contain paracrystalline inclusions, of unknown origin or function (D'HONDT & BOUCAUD-CAMOU, 1982).

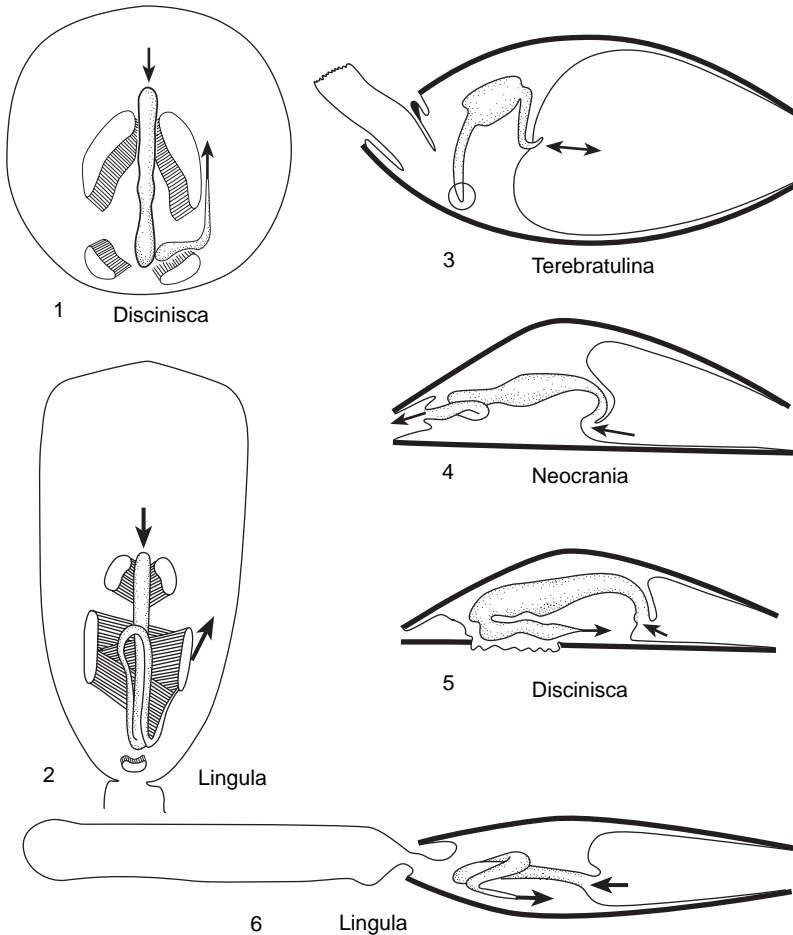


FIG. 90. 1–6, The position of the gut in relation to the major muscles between the valves in *Lingula* and *Discinisca* and comparisons between lateral views of the four main types of brachiopod gut arrangement. The end of the intestine is indicated by an open circle in *Terebratulina* (3) where the gut ends blindly. The position of the mouth and anus and the direction of movement of material are indicated by arrows (adapted from Nielsen, 1991).

Glandular cells are associated with the ciliated cells and two cell types, A and B, have been identified in *Terebratulina*.

Type A glandular cells are unciliated and distributed throughout the pyloric epithelium. The apical part of the cell contains vacuoles and glycogen granules and has a narrow basal region containing abundant mitochondria and reticulated vacuoles. A similar cell type also occurs in the digestive diverticula. These ciliated cells (cell type 1 in *Lingula* (Fig. 94–95; STORCH & WELSCH, 1975), with dense microvilli, extend into the

lumen of the acini and constitute the largest proportion of the parietal epithelium in *Terebratulina* and *Hemithiris*, where the cells are vacuolated and the vacuoles contain large numbers of glycogen granules. Some of these cells are packed with non-osmophilic globules with paracrystalline inclusions. Supranuclear Golgi give rise to secretory granules, which accumulate in the apices of the cells (D'HONDT & BOUCAUD-CAMOU, 1982).

Type B glandular cells differ from type A (D'HONDT & BOUCAUD-CAMOU, 1982) in possessing vacuoles with homogeneous con-

tents. They occur sporadically and do not seem to be present in the pylorus of *Terebratulina* (D'HONDT & BOUCAUD-CAMOU, 1982). A similar cell type (type 3 cell; Fig. 94, 96) occurs in *Lingula* (STORCH & WELSCH, 1975), which may be analogous to the type B cells of *Terebratulina*. The former occur mainly in the intestine and infrequently in the digestive diverticula; they are mucous-producing cells and contain electron-dense granules (STORCH & WELSCH, 1975).

Digestive cells (cell type 2 in *Lingula*, STORCH & WELSCH, 1975) occur in the acini of the digestive diverticula (Fig. 94, 97). These large, pleomorphic cells have been reported in various stages of growth and disintegration (CHUANG, 1959b, 1960; STORCH & WELSCH, 1975; STEELE-PETROVIC, 1976; PUNIN & FILATOV, 1980). During early stages of its development, the digestive cell of *Lingula* bears a cilium and is characterized by basally located lipid inclusions. As the cell matures, the apex of the cell bulges into the lumen of the acini. Digestive cells can absorb soluble material and ingest particulate material by both pinocytosis and phagocytosis at the bulging plasmalemma of the cell (STORCH & WELSCH, 1975; STEELE-PETROVIC, 1976). These cells also contain a well-developed lysosomal system; and in *Lingula*, algal cells and starch granules have been observed in their vacuoles (STORCH & WELSCH, 1975). Digestive cells are probably subject to cyclical disintegration following the completion of intracellular digestion (CHUANG, 1959b, 1960).

Basophil-like cells have been recorded in *Notosaria* and *Terebratella*. This type of cell is well known in bivalve molluscs, but their function is unknown (STEELE-PETROVIC, 1976).

FUNCTIONAL MORPHOLOGY OF THE DIGESTIVE SYSTEM

Details of the passage of food particles through the alimentary canal are well known only for *Lingula* (CHUANG, 1959b). Food particles, gathered by the lophophore, are entrapped by mucus in the food (brachial

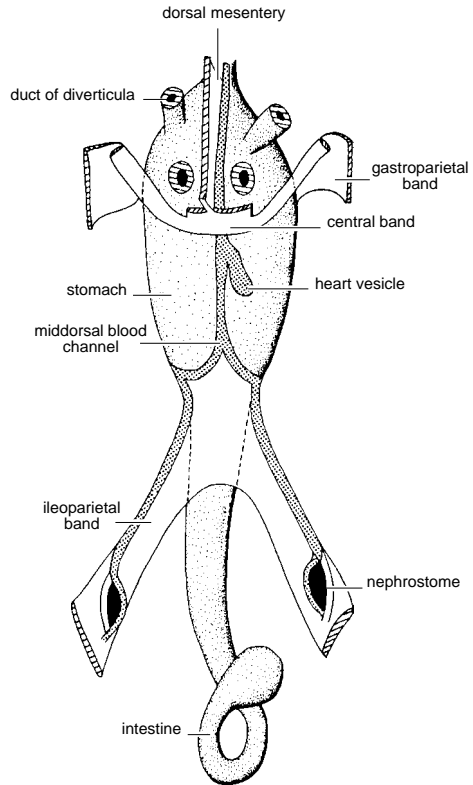


FIG. 91. View of part of the alimentary canal of *Hemithiris psittacea* (GMELIN) showing the distribution of the main mesenteries (adapted from Hancock, 1859).

groove and carried by ciliary currents into the mouth and pharynx, where the mucus becomes shredded. Posteriorly directed ciliary currents in the pharynx, esophagus, and intestine keep the food particles suspended. Movement of the particles through the gut is regulated and maintained by a combination of peristalsis, constriction, and pendular movements generated by the sequential contraction of the muscles surrounding the gut.

In *Lingula*, the stomach, pylorus, and digestive diverticula can be isolated from the rest of the digestive tract by the folded muscular pharynx, the esophagus, and the sphincter at the beginning of the intestine, thus creating a restricted area for the retention, agitation, and circulation of the ingested fluid and particles. Once food particles enter the stomach, ciliary action causes

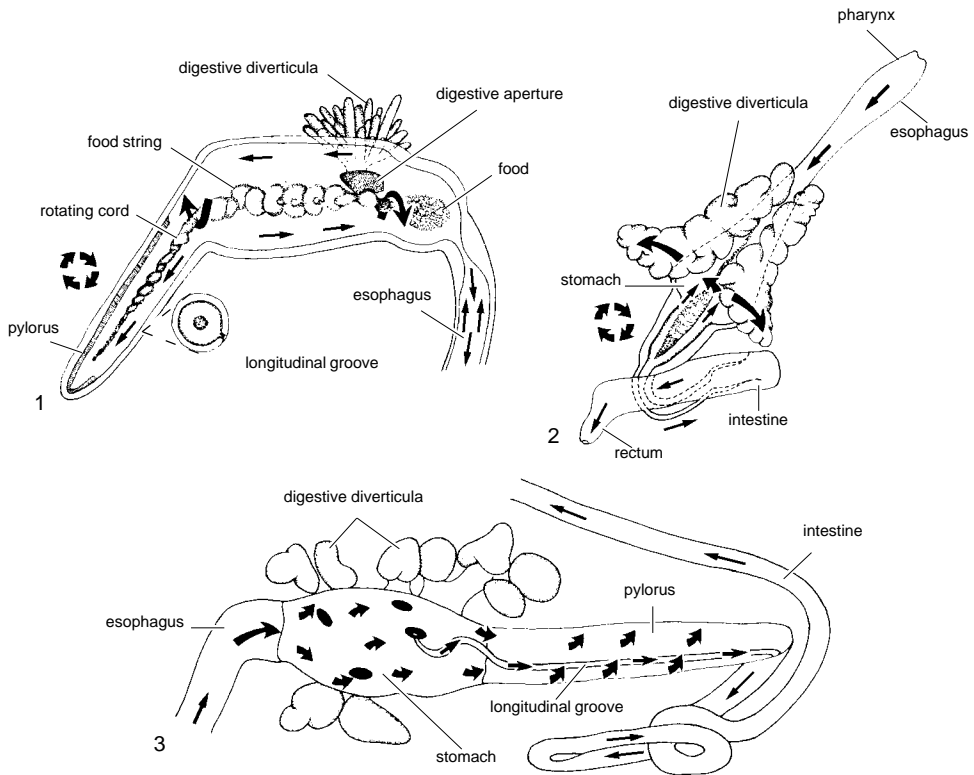


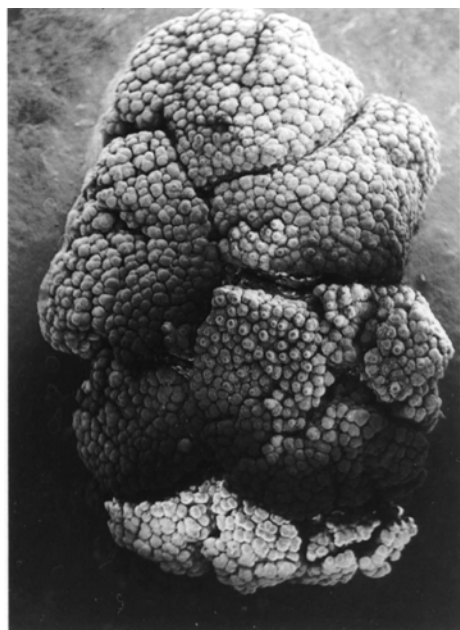
FIG. 92. Ciliary currents and direction of particle motion in brachiopod digestive tracts; 1, *Macandrevia*; 2, *Neocrania* (adapted from Morton, 1960); and 3, *Lingula* (adapted from Chuang, 1959b); note the clockwise rotation of mucus and food string; particles are passed back and forth between the stomach and the digestive diverticula in both articulated and inarticulated species during digestion; feces are expelled through the anus in 2 and 3 by peristalsis, constriction, and pendular motions; feces are disgorge through antiperistalsis in 1.

the suspended food particles to rotate, usually in a clockwise direction in *Lingula* (CHUANG, 1959b).

The acini of the digestive diverticula have an elastic and muscular sheath (STORCH & WELSCH, 1975) and are able to perform vigorous pulsations (MORTON, 1960). This action causes food particles to be drawn into the acini from the stomach. Relaxation of the acini and peripherally directed ciliary currents returns particles to the stomach. The rotation of particulate material in the stomach ceases during diverticular pulsations.

Most digestion in brachiopods is considered to be intracellular, and the digestive diverticula are the main sites of intracellular digestion (CHUANG, 1959b; STORCH & WELSCH, 1975). Strong carbohydrase activity in

the lumen of the digestive diverticula and the stomach of *Lingula* also indicates extracellular digestion (CHUANG, 1959b). Digestion is mainly the responsibility of the digestive cells in the acini of the digestive diverticula, which absorb soluble nutrients and phagocytose and pinocytose particulate food material. Wandering phagocytes are also found in the epithelium of the intestine, digestive diverticula, and esophagus. When intracellular digestion is complete, the digestive cells disintegrate into the lumen of the digestive diverticula. This appears to facilitate the elimination of undigested particulate material. The material discharged from the diverticula is gathered into a mucous rope that runs through the ventral, ciliated, epithelial groove from the duct of the right-posterior,



1



2

FIG. 93. SEM micrographs of the digestive diverticula of 1, *Lingula anatina*, $\times 12$, and 2, *Calloria inconspicua*, $\times 30$ (new).

digestive diverticula to the pylorus (Fig. 90). The residence time of food particles in the stomach and pylorus may be minutes; undigested material is retained and concentrated in the intestine for several hours. These processes are probably much the same for other inarticulated brachiopods (CHUANG, 1960).

The digestive process of articulated brachiopods appears to be similar, except that they have ventroanteriorly directed ciliary currents in the stomach (STORCH & WELSCH, 1975). Articulated brachiopods also have an epithelial groove running from the stomach to the pylorus, which generates a rotating mucous rope of particles (Fig. 92.1). It is suggested that the undigested remains are concentrated as fecal pellets and packed at the esophageal end of the stomach prior to elimination by antiperistalsis (MORTON, 1960; STORCH & WELSCH, 1975).

Possible digestive cycles of brachiopods are consistent with observations made on ventilating or feeding brachiopods in the laboratory (JAMES & others, 1992). Intermittent

feeding and ventilation are known to occur in brachiopods, which are constantly gaping (ATKINS, 1959; PUNIN & FILATOV, 1980; LABARBERA, 1984; RHODES, 1990; RHODES & THAYER, 1991).

EXCRETORY SYSTEM

The brachiopod excretory system consists of one or exceptionally, as in the rhynchonelloids, two pairs of metanephridia, which, during spawning, act as gonoducts and allow the discharge of gametes from the coelom into the mantle cavity. Although some solid waste may be ejected through the nephridiopore enmeshed in mucus (RUDWICK, 1970), the main excretory product, ammonia (HAMMEN, 1968), is probably voided by diffusion through the tissues of the mantle and lophophore. The metanephridia of *Calloria* are closed until the onset of sexual maturity toward the second year of life (PERCIVAL, 1944), which may indicate that, in this species at least, metanephridia serve primarily as gonoducts.

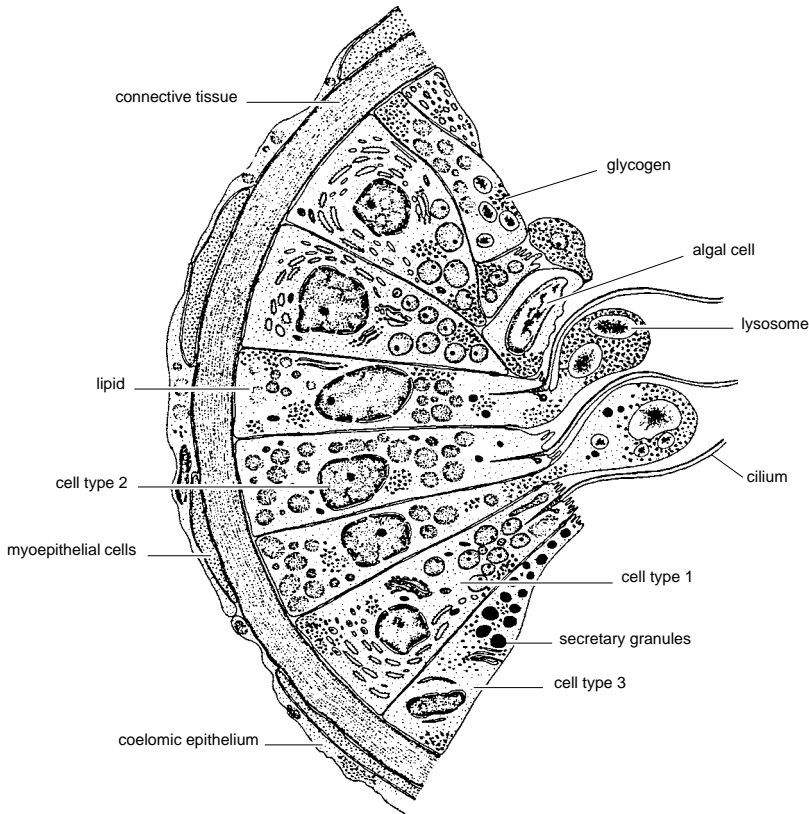


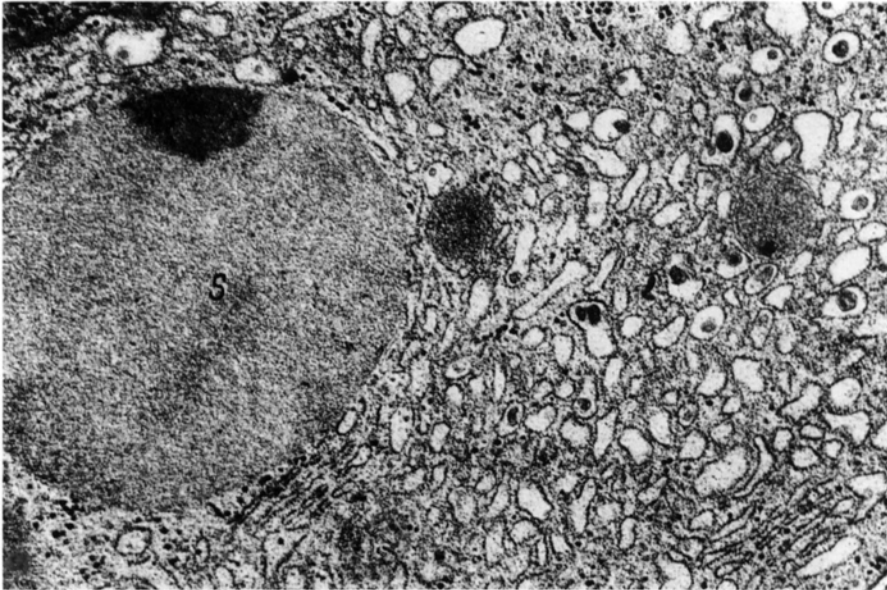
FIG. 94. Diagrammatic representation of a section through part of an acinus of the digestive diverticulum of *Lingula anatina* (adapted from Storch & Welsch, 1975).

Lingulid metanephridia are broad and relatively long, and the nephrostomes are turned laterally away from the midline to face the lateral body wall (Fig. 98). In the discinids and craniids, the metanephridia are relatively shorter, the nephrostomes facing dorsally and slightly medially in the discinids and medially in the latter. The nephrostomes of articulated brachiopods are generally oriented to face dorsally or dorsomedially.

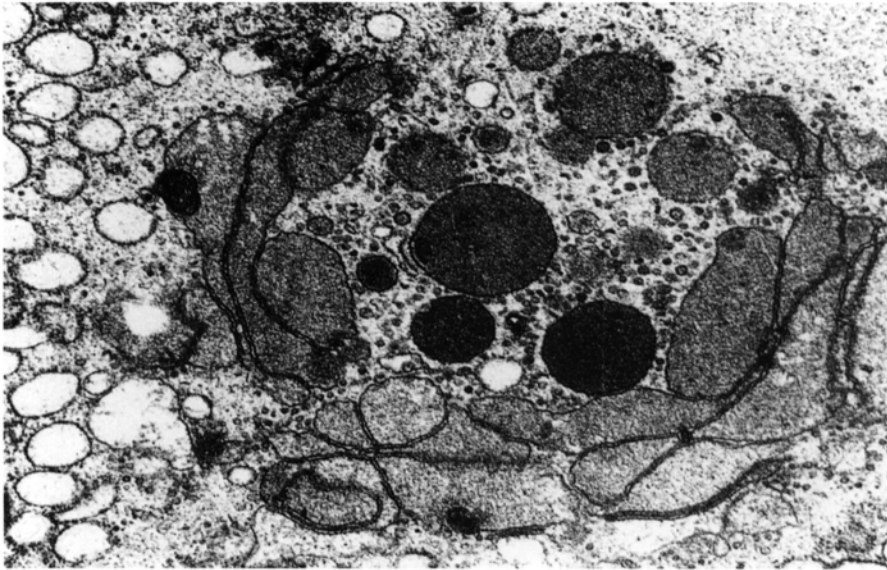
The structure of the metanephridia is similar in all brachiopods. Each metanephridium is essentially a ciliated funnel with a ruffled and densely ciliated inner surface. The widest aperture within the coelomic cavity consists of a broad funnel-shaped nephrostome that continues anteriorly as a narrow tube, usually ventrally placed against the lateral body wall and opening into the

mantle cavity through a small nephridiopore on the anterior body wall close to the midline and ventral to the mouth (Fig. 99–100). The ileoparietal bands support the nephrostomes of all brachiopods, including the posterior pair in the rhynchonellides. The anterior nephrostomes of rhynchonellides are supported by the gastroparietal bands.

The histology of the metanephridia is also similar in all brachiopods. The inner surface is covered by a highly microvillous, ciliated epithelium interspersed by secretory, probably mucous cells. The apices of these cells contain large vacuoles with coarse and variably granular contents. Beneath the vacuolated surface cells lies a much thicker layer consisting of a large number of nucleated cells with dense concentrations of glycogen and irregularly shaped, electron-opaque



1



2

FIG. 95. TEM micrographs of cell type 1 in the digestive diverticula of *Lingula anatina*; 1, granular endoplasmic reticulum and secretory granules (S), $\times 20,000$; 2, Golgi apparatus and granules, $\times 20,000$ (Storch & Welsch, 1975).

granules. The latter may be responsible for the pigmentation visible in the metanephridia of many species. The nature and function of the pigmentation is unknown, but it

could be an accumulation of metabolic waste products (JAMES, unpublished, 1991). This stratified epithelium overlies a differentially thickened layer of connective tissue that

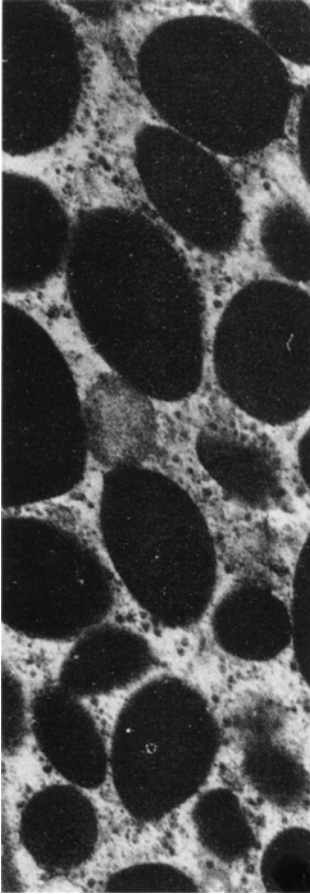


FIG. 96. TEM micrograph of the contents of a type 3 secretory cell in the digestive diverticula of *Lingula anatina*, $\times 20,000$ (Storch & Welsch, 1975).

creates the ruffled surface of the nephrosome. Coelomic epithelium covers the outer surface (Fig. 99).

THE LOPHOPHORE

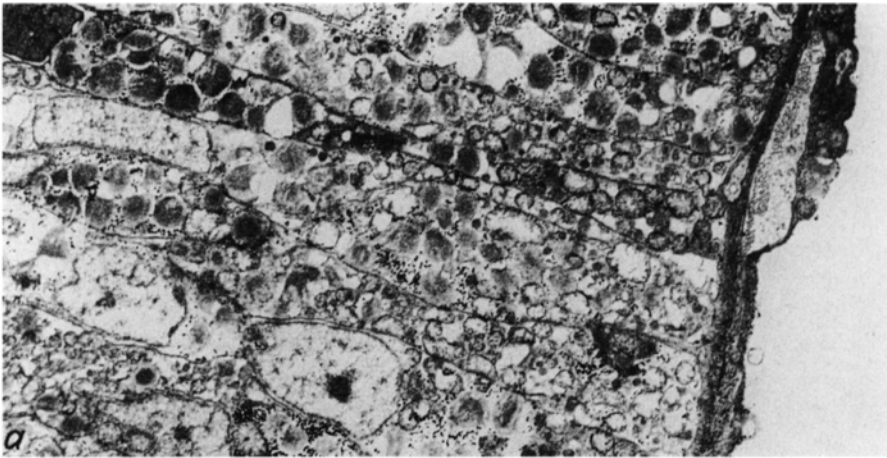
The lophophore has been described as a tentaculated extension of the mesosoma (and its cavity, the mesocoelom) that embraces the mouth but not the anus (HYMAN, 1959b; EMIG, 1976). The lophophore is ciliated and generates an inhalant and exhalant flow of water through the mantle (brachial) cavity, trapping particulate food material, allowing ventilation, and assisting in the removal of waste products.

GENERAL STRUCTURE

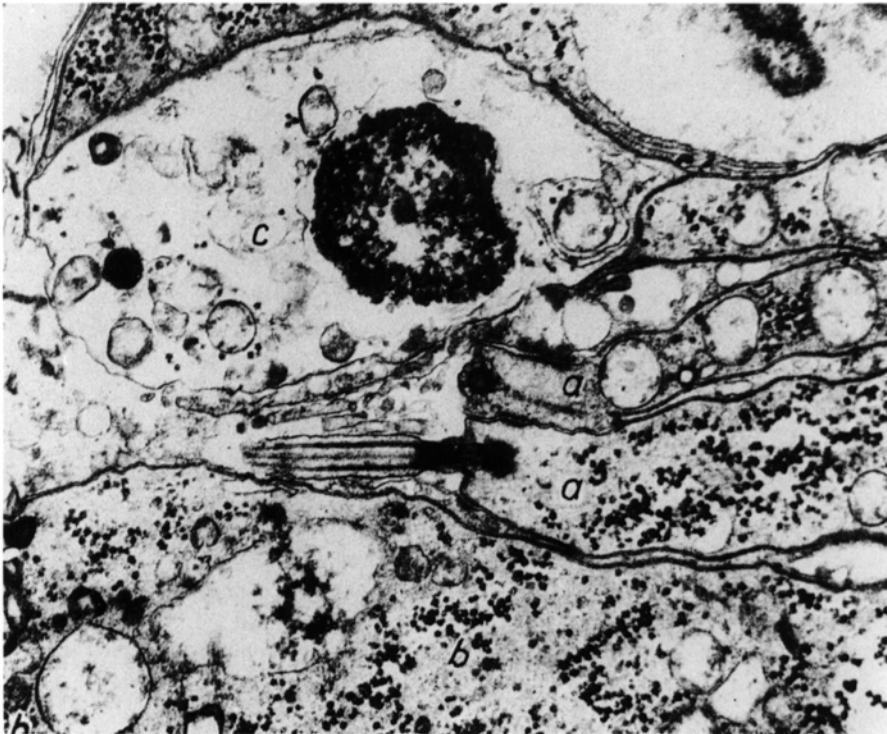
The lophophore is composed of two brachia (arms), disposed symmetrically about the mouth, attached to the anterior body wall, and extending into the mantle cavity. Brachia are fringed with one row of ciliated tentacles (filaments or cirri) in either a single or an alternating series. The brachial lip or fold runs perpendicular to the row of tentacles. The brachial (food) groove, created between the brachial lip and the base of the tentacles, is ciliated and runs along the entire length of the brachia, terminating at the slitlike mouth. Tentacles that are reflected toward the brachial groove are designated inner (adlabial), and those tentacles reflected away from the brachial groove are termed outer (ablabial) (Fig. 101–102; 103.2). Brachia are tubular with extensions of the coelom penetrating the main axes of the lophophore and giving off a branch into each tentacle. In inarticulated brachiopods, the form and position of the lophophore are maintained by a combination of muscles, connective tissue, and hydrostatic pressure created by muscle fibers in the brachial axis acting antagonistically against the incompressible fluid enclosed within the great brachial canal. In most articulated groups the support of the hydrostatic skeleton is commonly supplemented by the brachidium, a calcareous outgrowth of the secondary shell layer of the posterior part the dorsal valve. Calcareous spicules may also be secreted by scleroblasts within the connective tissue, thereby increasing the flexural stiffness of the brachia (FOUKE, 1986). The brachia may be partially fused to the dorsal mantle throughout and rest in brachial grooves in the inner surface of the dorsal valve, bounded on one or both sides by narrow ridges, as in the thecideidines (Fig. 104; LACAZE-DUTHIERS, 1861).

Coelomic Canals

Two, fluid-filled, coelomic canal systems, the great and small brachial canals, extend within the main axes of the brachia. The great brachial canal is closed off from the



1



2

FIG. 97. TEM micrographs of type 2 cells in the digestive diverticula of *Lingula anatina*; 1, base of cells, $\times 5,500$; 2, apices of cells, $\times 20,000$; a, ciliated cell; b, cell apex with glycogen and lysosomes; c, greatly enlarged cell apex (Storch & Welsch, 1975).

main body cavity, at least during the life of the adult, and in inarticulated brachiopods is divided into two separate cavities symmetri-

cally disposed about the midline. The small brachial canal gives off a branch into each tentacle (tentacular canal) that, except for

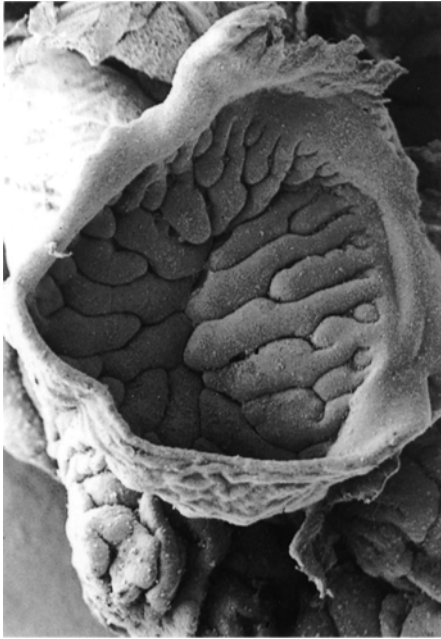


FIG. 98. SEM micrograph of the ruffled and densely ciliated nephrostome of *Lingula anatina*, $\times 30$ (new).

craniids and discinids, opens into the body cavity around the esophagus. In *Lingula* and, to a lesser extent, *Discinisca* the proximal ends of the great brachial canals are divided into several lobes (BLOCHMANN, 1900). Near the esophagus, infolding of the main body cavity creates narrow pouches and, where the lophophore is attached to the main anterior body wall, all small brachial canals contract abruptly. The coelomic canals then continue medially as narrow tubes, which, in *Neocrania* and *Discinisca*, open into a large, median, central canal developed in the connective tissue of the lophophore on the ventral side of the pharynx (Fig. 105). In *Lingula*, the central canal is poorly developed although the two, small, brachial canals are connected medially. In all inarticulated genera, connective tissue surrounding the pharynx contains a number of small, interconnected chambers (the periesophageal spaces) that connect with small brachial canals (BLOCHMANN, 1892, 1900). In *Discinisca* and *Lingula* a further extension of the small

brachial canal system is found in the coelomic spaces of the brachial lip (WILLIAMS & ROWELL, 1965a). The small, brachial canals of such articulated terebratulids as *Pumilus* are small, pouchlike extensions of the main body cavity and, although they have been called periesophageal sinuses (ATKINS, 1958), these canals are not infolded in the same way as in the inarticulated brachiopods. The body cavity is also prolonged as a pair of brachial pouches along the medially facing surfaces of the terebratulide side arms (Fig. 101). These pouches extend forward to more or less the same degree and are developed only incipiently in septate *Pumilus* but extend to the tip of the side arms in the long-looped *Macandrevia* (WILLIAMS & ROWELL, 1965a).

Musculature

Inarticulated brachiopods possess a pair of strongly developed brachial muscles that are attached to the connective tissue at the constricted proximal end of the small brachial canal and extend along the length of the canal in each brachium (Fig. 102). The discinids and the craniids also possess a pair of small brachial retractor muscles that appear to control the position of the lophophore relative to the dorsal valve and the anterior body wall. The retractor muscles are inserted in the dorsal valve lateral to the attachment of the anterior adductors. A further two pairs of muscles occur only in the craniids. A pair of stout, brachial elevator muscles, inserted on the dorsal valve anterolateral to the anterior adductors, are attached at their other extremity to the connective tissue at the base of the brachial muscle. A pair of small brachial protractor muscles placed anteromedially are also present (see Fig. 84). Calcified loops supplemented by calcareous spicules support the lophophore of terebratulide brachiopods. As a result, the muscles controlling the movement of the lophophore of articulated groups are less well developed than in inarticulated forms. Muscles are more numerous, however, in the spirally coiled, free brachia of the spirolophes of the rhynchonellides.

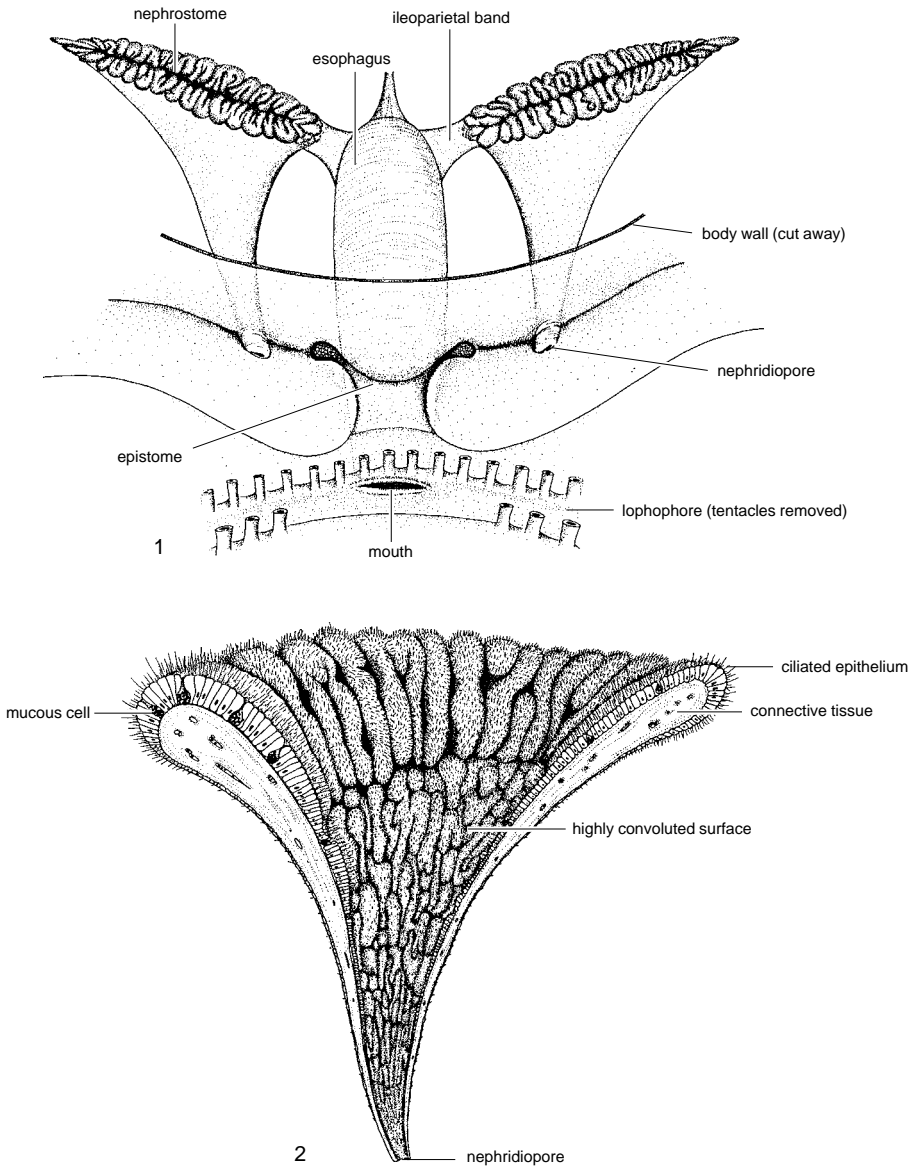


FIG. 99. Generalized diagrams of 1, the attitude of the metanephridia of *Terebratulina retusa* relative to the anterior body wall, mouth, and esophagus; 2, the structure of half a metanephridium in longitudinal cross section (new).

Tentacles

Rows of cilia on the tentacles are responsible for creating a flow of water past the tentacle and for diverting particulate material along the length of the tentacle to the brachial groove (see section on functional morphology of the lophophore, p. 116). There

are two distinct types of tentacle in most adult lophophores. The first-formed tentacles of the trochophore stage occur on either side of the mouth. The number of these tentacles, which, except in lingulids and discinids, are arranged in a single row, varies between genera relative to the size of the fully

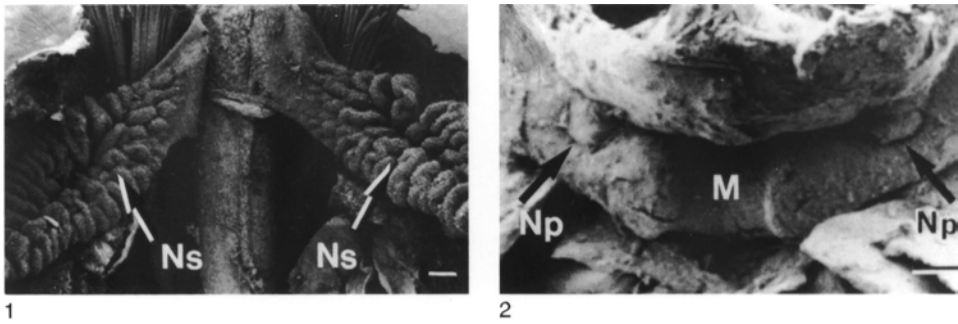


FIG. 100. SEM micrograph of *Terebratulina retusa*, showing 1, the metanephridia with ciliated nephrostomes (*Ns*), $\times 35.5$; 2, view from within the mantle cavity of the mouth and the nephridiopores (*Np*) laterally displaced on either side of the mouth (*M*), $\times 14.2$ (James, Ansell, & Curry, 1991b).

developed trocholophe (Fig. 103; WILLIAMS & WRIGHT, 1961). A few adult articulated brachiopods, such as *Argyrotheca* and *Dyscolia*, possess only this type of tentacle. The frontal surface (facing the brachial lip) of these outer tentacles forms two, rounded, laterofrontal epidermal ridges and a medial longitudinal groove, the latter bearing cilia that beat along the length of the tentacle. Two longitudinal tracts of longer cilia flank

the frontal cilia and beat across the length of the tentacle from the frontal to the abfrontal surface. Modification of the trocholophe into more complex forms of lophophore, however, results in the addition of an alternating set of inner tentacles. Typically, inner tentacles have paired lateroabfrontal epidermal ridges that also develop long lateral cilia (Fig. 106). The abfrontal surface of both types of tentacle appears to be sparsely cili-

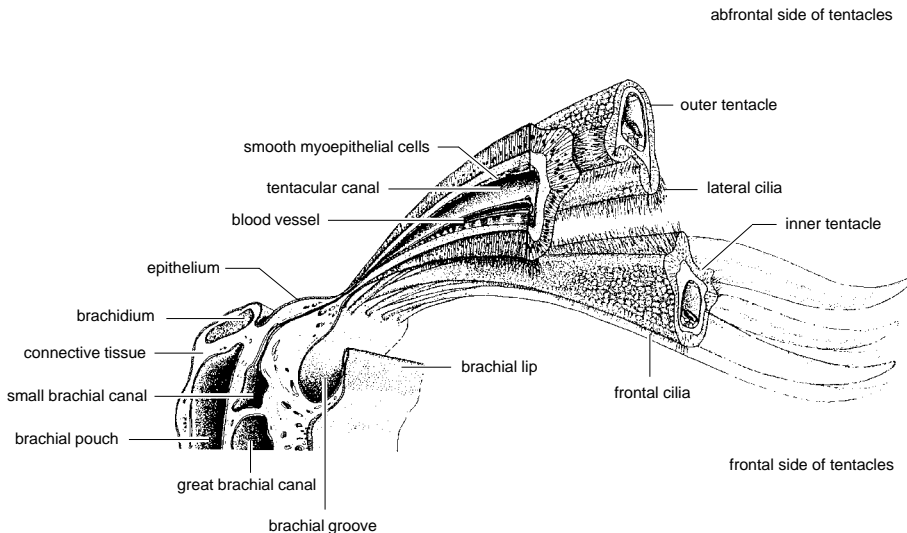


FIG. 101. Semidiagrammatic drawing of a cross section of part of the brachium and tentacles of an articulated brachiopod; the tentacles in the foreground are shown in transverse and longitudinal section (adapted from James & others, 1992).

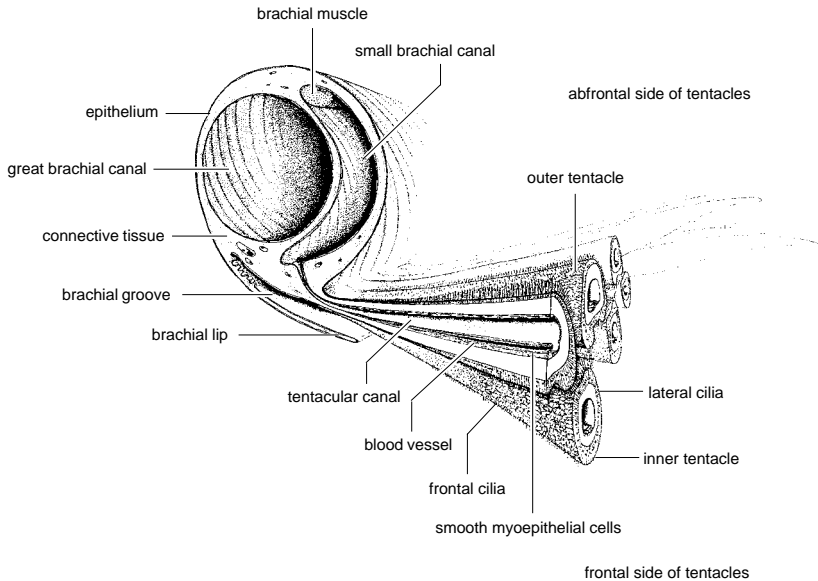


FIG. 102. Semidiagrammatic drawing of a cross section of the brachium and tentacles of the lophophore of *Lingula anatina*; the tentacles in the foreground are shown in transverse and longitudinal section (adapted from Pross, 1980).

ated in all brachiopods, with the exception of the lingulids, in which cilia are as densely distributed as on the frontal surface.

HISTOLOGY OF THE LOPHOPHORE

There are a number of accounts that feature the general histology of the brachiopod lophophore (HANCOCK, 1859; BLOCHMANN, 1892; RICHARDS, 1952; CHUANG, 1956; ATKINS, 1960a, 1960b, 1961a, 1961b, 1963). More recently, light microscopy and histochemistry have been used to study the lophophores of *Laqueus californicus*, *Terebratalia transversa*, *Hemithiris psittacea* (REYNOLDS & McCAMMON, 1977), and *Notosaria nigricans* (HOVERD, 1985, 1986). Ultrastructural details of the tentacles of *Lingula anatina* (STORCH & WELSCH, 1976), *Glottidia pyramidata* (GILMOUR, 1981), and *Terebratalia* (REED & CLONEY, 1977) are also available. Histologically the lophophore consists of three main elements: an epidermal cover of a selectively ciliated epithelium with basi-

epithelial nerves, a variably complex connective tissue tube, and an inner coelomic epithelium underlain by either muscle fibers, or in the tentacles, myoepithelial cells. These tissues are modified to accommodate the different functional requirements of the main axes of the brachia and the tentacles.

EPIDERMIS

Descriptions of the epidermis of the brachia and tentacles of *Hemithiris*, *Laqueus*, *Terebratalia* (REYNOLDS & McCAMMON, 1977), and *Lingula* (STORCH & WELSCH, 1976) generally agree with the most thorough description given by REED and CLONEY (1977) for *Terebratalia*. Only the tentacular epidermis, however, has been investigated in detail (STORCH & WELSCH, 1976; REED & CLONEY, 1977). The epidermis of the outer tentacles consists of an inner epithelium of columnar cells on the frontal side and cuboidal cells on the abfrontal side of the tentacle (Fig. 107). Inner tentacles are covered by a single layer of columnar epithelium. Ultrastructurally, four types of tentacular epidermal cell have been identified: microvillous

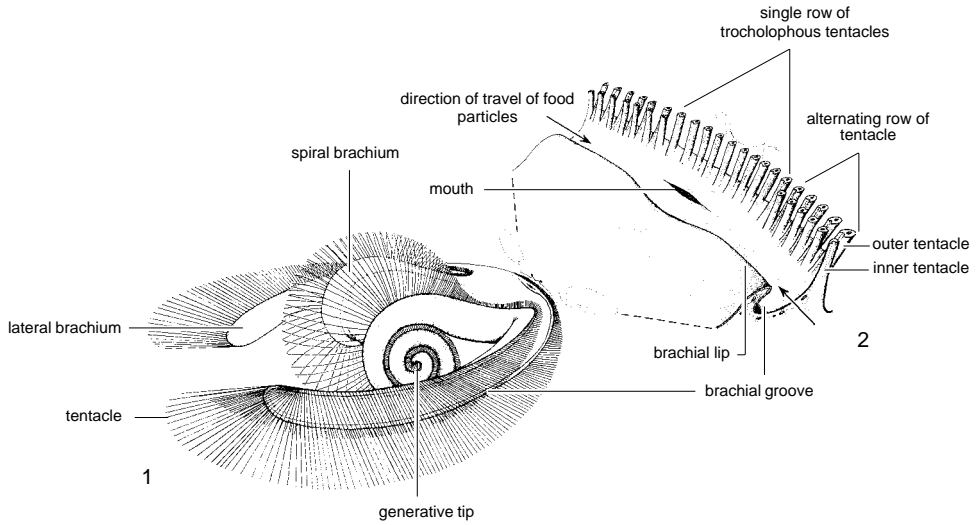


FIG. 103. Plectolophe of *Terebratulina retusa*; 1, general view and 2, with an enlargement of the trochophorous tentacles behind the mouth (new).

epithelial cells, monociliated epithelial cells with distal microvilli, secretory cells, and intra-epithelial cells.

Microvillous Epithelial Cells

The distal margin of each microvillous epithelial cell has a dense, microvillous border, which is consistent with the view that the lophophore is the primary site for gaseous exchange in brachiopods (HYMAN, 1959b) and may be capable of direct absorption of nutrients (MCCAMMON & REYNOLDS, 1976; REYNOLDS & MCCAMMON, 1977) and calcium (PAN & WATABE, 1988a). The microvillous cells of *Terebratalia* contain putative secondary lysosomes (REED & CLONEY, 1977), and the epithelium at the base of the tentacles and in the brachial groove appears to be secretory and possibly involved in lysosomal activity (REYNOLDS & MCCAMMON, 1977), which may be suggestive of hetero- or autophagy (REED & CLONEY, 1977). HOVERD (1985) found unusually long microvilli in *Notosaria* and alluded to their possible chemosensory role.

Monociliated Cells

All ciliated tentacular epidermal cells are monociliated, and each cilium has an acces-

sory centriole located on the downstream side of the ciliary root (ATKINS, 1958; STORCH & WELSCH, 1976; REED & CLONEY, 1977; NIELSEN, 1987). Reports of multiciliated cells in both *Laqueus* and *Glottidia* (GILMOUR, 1978, 1981) are considered to be erroneous (NIELSEN, 1987). The epithelium of *Terebratalia* is a simple, columnar structure (REED & CLONEY, 1977). Yet the frontal

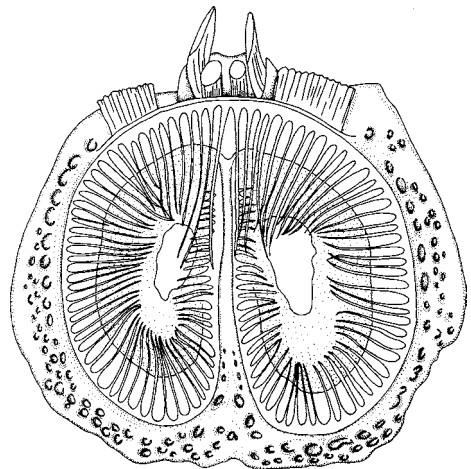


FIG. 104. Bilobed trocholophe of *Thecidellina* (adapted from Williams & Rowell, 1965a).

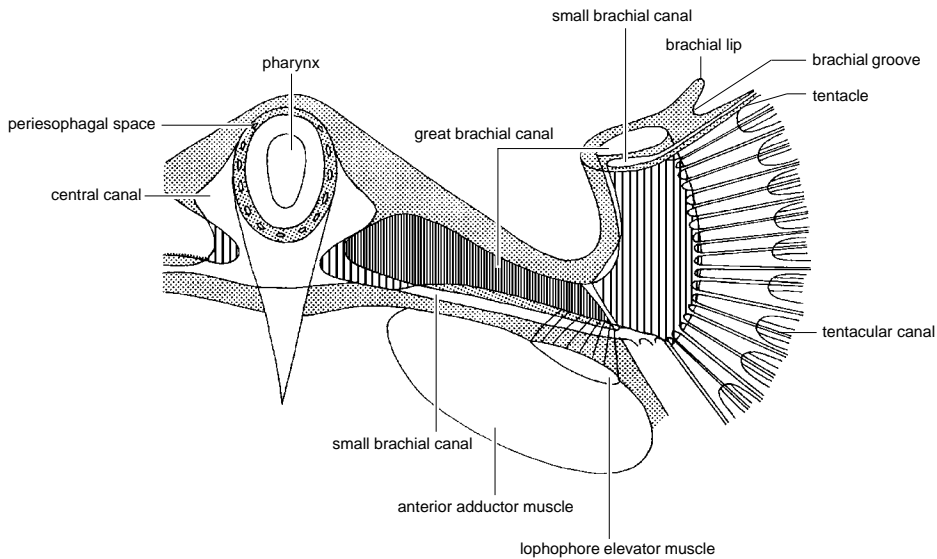


FIG. 105. Diagrammatic representation of canal systems in the lophophore of *Neocrania anomala* (adapted from Blochmann, 1892).

epidermis of the tentacles of *Laqueus* has been described as a stratified, columnar epithelium (REYNOLDS & MCCAMMON, 1977), while compound cilia have been described as forming part of a stratified, tentacular epithelium of *Lingula* (STORCH & WELSCH, 1976). Stratified epithelia are rare, however, in invertebrates (REED & CLONEY, 1977) and such observations may therefore be a misinterpretation of tangential sections. The knobbed, paddle, or disco cilia observed in *Notosaria* (HOVERD, 1985, 1986) are also considered to be artifacts (see SHORT & TAMM, 1991).

Secretory Cells

Mucous-secreting cells are commonly scattered throughout the epidermis and may be more numerous at the base of the tentacles (REED & CLONEY, 1977; REYNOLDS & MCCAMMON, 1977) particularly within the brachial groove. Some mucous cells are arranged in longitudinal rows along the tentacles of *Lingula* (Fig. 108; CHUANG, 1956). Ultrastructurally, two forms of secretory cell have been observed in *Lingula*, which contain large, electron-dense granules and may

be ciliated during the early part of their development (STORCH & WELSCH, 1976). One of these cell types probably corresponds to the mucous cells seen in studies using lower resolution microscopy.

Intraepidermal Cells

Clusters of round cells occur at the base of the tentacles in the *Terebratalia* (REED & CLONEY, 1977). Believed to be amoebocytes or coelomocytes, these cells may correspond to either similar cells found in the tentacular epidermis of *Lingula* (CHUANG, 1956; STORCH & WELSCH, 1976) or dark-staining aggregates that occur in the epithelium and connective tissue of some articulated brachiopods (REYNOLDS & MCCAMMON, 1977; HOVERD, 1985).

NERVES

Two main nerves innervate the lophophore: the principal nerve branches from the subenteric ganglion and extends along each brachium near the brachial lip; a second nerve forms branches (accessory and lower brachial nerves) that serve the brachia and tentacles (BEMMELEN, 1883; WILLIAMS &

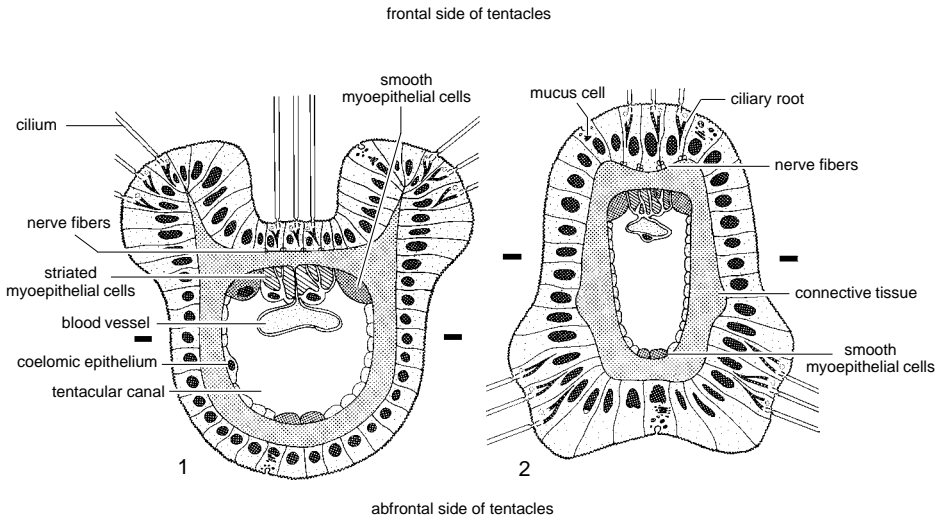


FIG. 106. Schematic diagrams of sections of tentacles of a brachiopod lophophore; 1, section of an ablabial (outer) tentacle; the epidermis is ciliated in longitudinal tracts on the frontal surface and on the laterofrontal surface and on the laterofrontal epidermal ridges; nerves extend longitudinally between the bases of the frontal epidermal cells; a thick layer of acellular connective tissue separates the epidermis from the peritoneum, consisting of myoeptithelial cells on the frontal and abfrontal sides of the tentacular coelomic canal; the frontal contractile bundle has both smooth (*stippled*) and striated (*slashed*) fibers, but the small abfrontal contractile bundle has only smooth fibers; a blood channel is formed by an involution of the frontal peritoneum; 2, transverse section of an adlabial (inner) tentacle. The ciliary tracts arise from the frontal epidermis and the paired lateroabfrontal epidermal ridges; the rest of the histological organization is similar to that of the ablabial tentacle (adapted from Reed & Cloney, 1977).

ROWELL, 1965a). Bundles of nerve fibers lie between the bases of the epithelial cells (basiepithelial nerves) above the basal lamina (see Fig. 130; BLOCHMANN, 1892, 1900; STORCH & WELSCH, 1976; REED & CLONEY, 1977; HOVERD, 1985). Detailed studies of the tentacles of *Terebratalia* did not reveal any nerve fibers traversing the connective tissue to form myoneural junctions or evidence of peritoneal nerves (REED & CLONEY, 1977). Laterofrontal cells of the tentacles of *Glottidia* make synapses with the nervous system, suggesting that cilia may have a sensory role (GILMOUR, 1981) or that these nerves innervate the laterofrontal cells (see HAY-SCHMIDT, 1992).

CONNECTIVE TISSUE

The connective tissue of the lophophore has been variously described as a noncellular matrix resembling hyaline cartilage (HANCOCK, 1859; HYMAN, 1959b; STORCH & WELSCH, 1976; REYNOLDS & MCCAMMON,

1977; HOVERD, 1985) and as a structureless supporting substance (ATKINS, 1961a, 1961b, 1963). According to HOVERD (1985) the hyaline matrix contains cells and bears no resemblance to vertebrate cartilage. CHUANG (1956) and REYNOLDS and MCCAMMON (1977) stated that the cartilaginous framework continues into the base of the tentacles. REED and CLONEY (1977), however, are the only authors to distinguish between the connective tissue of the tentacles and the main axes of the lophophore. The brachial axes of *Terebratalia* are constructed from a cartilaginous framework, which is a metachromatic matrix; the tentacles are an acellular, densely fibrous connective material.

The connective tissue in the tentacles contains two types of collagen fibers: a thick, longitudinal subepidermal layer and an inner, circumferential layer, subadjacent to the coelomic epithelium. This orientation of fibers creates a relatively stiff, inextensible

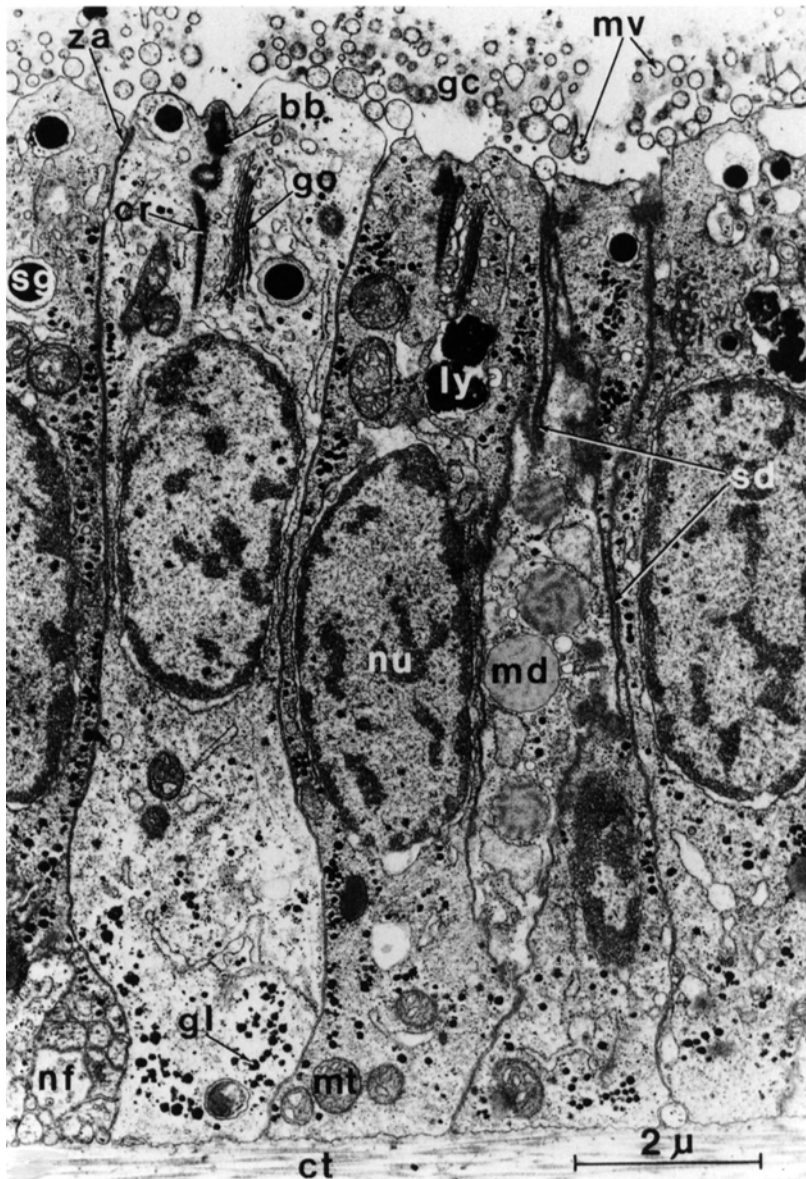


FIG. 107. TEM micrograph of a transverse thin section of the frontal epidermis near the base of an outer tentacle of *Terebratalia transversa*; columnar epidermal cells are joined apically by *zonulae adhaerens* and at the level of their nuclei by separate desmosomes; the apical plasmalemma of each cell bears a single cilium surrounded by sinuous microvilli perforating a faint glycocalyx; the apical cytoplasm in each cell is characterized by secretory granules, putative secondary lysosomes, and a supranuclear Golgi complex next to the basal body and the ciliary rootlet of the cilium; glycogen rosettes and occasional lipid droplets are also found dispersed throughout the cytoplasm; the section passes through part of a mucous cell containing large mucous droplets. A bundle of unsheathed nerve fibers is positioned between the bases of two epidermal cells in the lower left corner, scale bar: 2 μ m; *bb*, basal body; *ct*, connective tissue; *cr*, ciliary root; *gc*, glycocalyx; *gl*, glycogen particles or rosettes; *go*, Golgi complex; *ly*, putative secondary lysosome; *md*, mucous droplet; *mt*, mitochondrion, *mv*, microvilli; *nf*, nerve fibers; *nu*, nucleus, *sd*, septate desmosome; *sg*, secretory granule; *za*, zonula adhaerens (Reed & Cloney, 1977).

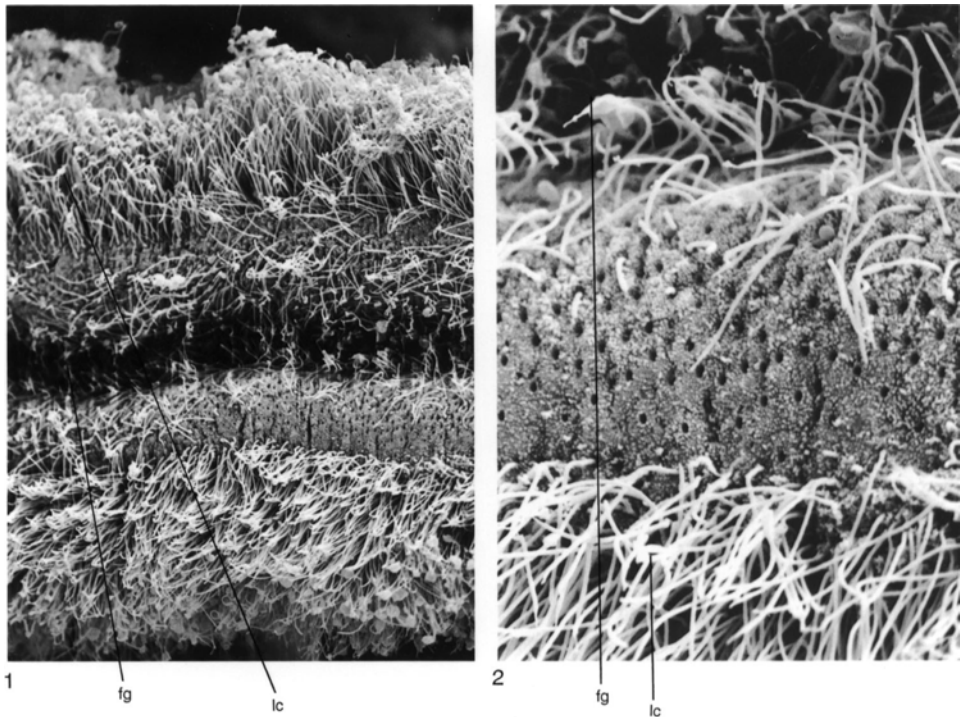
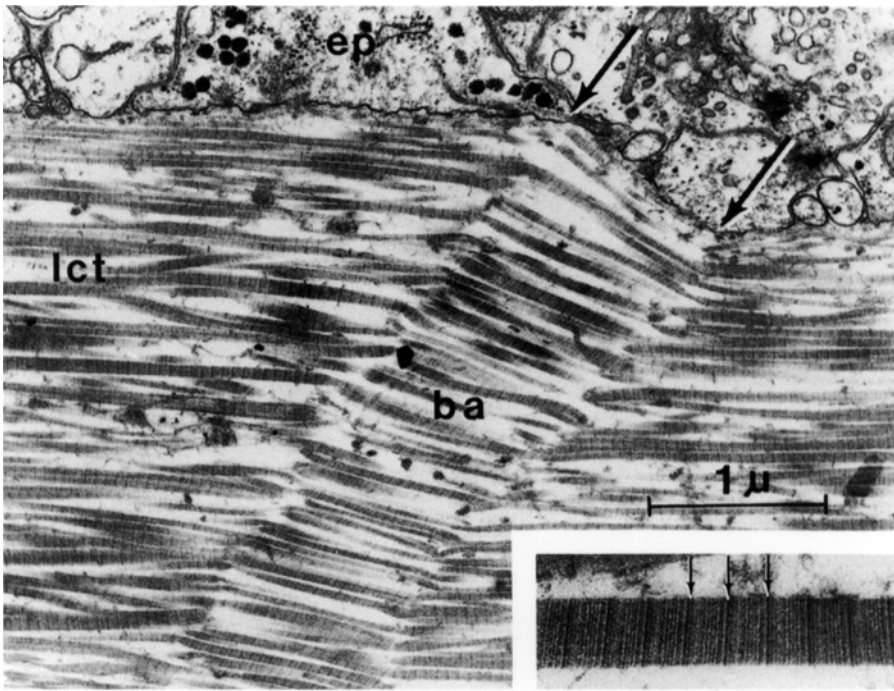


FIG. 108. SEM micrographs of the frontal surface of a tentacle of *Lingula anatina* showing 1, dense lateral cilia (*lc*) separated from the ciliated food groove (*fg*) by a sparsely ciliated band, $\times 660$; 2, note microvillous surface and numerous pores of sparsely ciliated band (shown in 1), $\times 2,500$ (new).

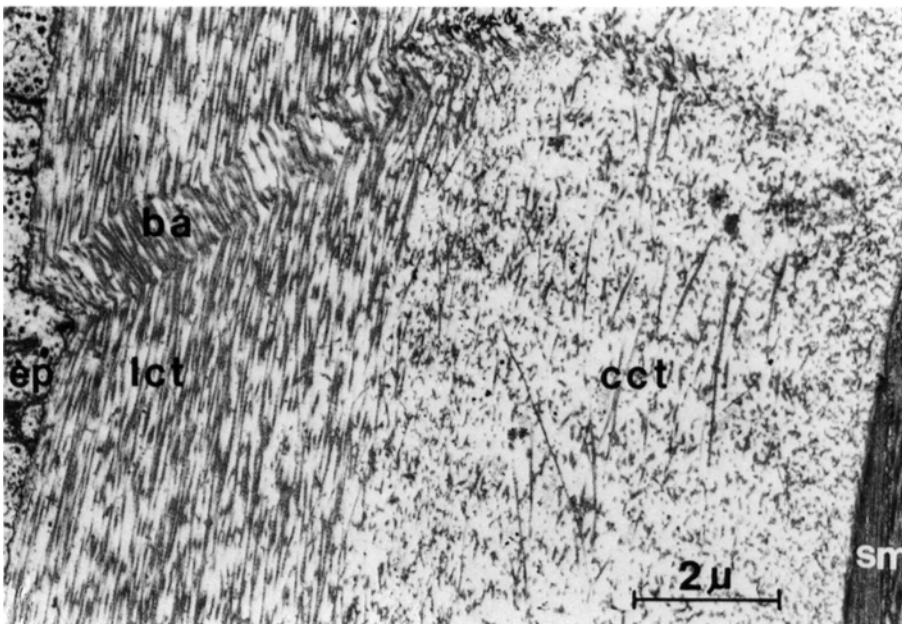
tube with the longitudinal layer resisting elongation and the circumferential layer resisting changes in diameter (STORCH & WELSCH, 1976; REED & CLONEY, 1977). In regions where the connective tissue cylinder of the tentacle buckles during flexion, the longitudinal collagen fibers of *Terebratalia* contain baffles consisting of zonulae of parallel, crimped collagen fibers (Fig. 109; REED & CLONEY, 1977). The connective tissue may contain a variety of other inclusions in addition to the cells secreting the connective tissue matrix. The connective tissue matrix of *Lingula* contains single or paired, ovule-shaped, nucleated cells (STORCH & WELSCH,

1976). *Notosaria* (HOVERD, 1986), *Hemithiris*, *Laqueus*, and *Terebratalia* (REYNOLDS & MCCAMMON, 1977) have lacunae or nests of membrane-bound cells containing globular inclusion bodies, which occur throughout the connective tissue matrix. Globular inclusions present in the connective tissue of a number of species, including *Lingula*, *Hemithiris*, and *Terebratulina*, closely resemble those found predominantly in the outer mantle epithelium of these species, where they appear to be storage material (CURRY & others, 1989; JAMES & others, 1992). REED and CLONEY (1977) did not, however, find cells in the connective tissue of the tentacles

FIG. 109. TEM micrographs of the connective tissue associated with the lophophore of *Terebratalia transversa*; 1, longitudinal section of the frontal side of the connective tissue cylinder in an inner tentacle, which consists of a subepidermal longitudinal layer and a subperitoneal circumferential layer of fibrils embedded in an amorphous matrix; a zone of crimped and displaced fibrils corresponds to the baffles, scale bar: 2 μm ; *ba*, baffles; *cct*, circumferential layer of connective tissue; *ep*, epidermis; *lct*, longitudinal layer of connective tissue; *sm*, smooth myoepithelial cells; 2, longitudinal section of the subepidermal connective tissue on the frontal side of the cylinder, with the region (Continued on facing page.)



1



2

FIG. 109. *Continued from facing page.*

between the *arrows* corresponding to the part of one of the baffles where the parallel fibrils are crimped and oriented at a different angle from those in the rest of the cylinder; the fibers have a major axis periodicity of 63 nm (inset: distance between *arrows*) that is diagnostic of native vertebrate collagen fibrils, scale bar: 1 μm (Reed & Cloney, 1977).

of *Terebratalia*. The connective tissue of many terebratulide species contains a closely-knit array of interdigitating calcareous spicules that increases the flexural stiffness of the lophophore and, in *Terebratulina*, supply the rigidity necessary to support the lophophore in regions anterior to the short-looped brachidium (FOUKE, 1986).

COELOMIC EPITHELIUM (PERITONEUM)

Brachial and tentacular canals are lined with ciliated coelomic epithelium (see, for example, REYNOLDS & MCCAMMON, 1977; HOVERD, 1985, 1986), which, in the former site, is underlain by a layer of muscle and in the latter by myoepithelia. The subepidermal (peritoneal) muscle has been described as smooth in *Notosaria* (HOVERD, 1985) or as a single, prominent layer of longitudinal, striated muscle around the great brachial canal in *Hemithiris* (REYNOLDS & MCCAMMON, 1977). The ultrastructure of the epithelial lining of the tentacular canal is known only for *Terebratalia*. The lining consists of four cell types: ciliated coelomic (peritoneal) cells, striated myoepithelial cells, smooth myoepithelial cells, and squamous smooth myoepithelial cells that form tentacular blood vessels (channels and capillaries) (see Fig. 76; REED & CLONEY, 1977). Both smooth and striated muscle fibers (myoepithelial cells) have been described in the tentacles of *Neocrania*, *Lingula*, and a number of articulated brachiopods (CHUANG, 1956; ATKINS, 1958, 1959, 1961a, 1961b; WILLIAMS & ROWELL, 1965a). The fine structure of myoepithelial cells, however, is known only for *Terebratalia* (REED & CLONEY, 1977) and *Lingula* (STORCH & WELSCH, 1976). In *Terebratalia*, longitudinal rows of fusiform myoepithelial cells extend the length of each tentacle on the frontal and abfrontal sides of the coelomic canal. A bundle of myofilaments is confined to the basal cytoplasm of each cell (see section on muscular system, p. 75; Fig. 88). The frontal myoepithelial cells consist of a central group of striated fibers and two lat-

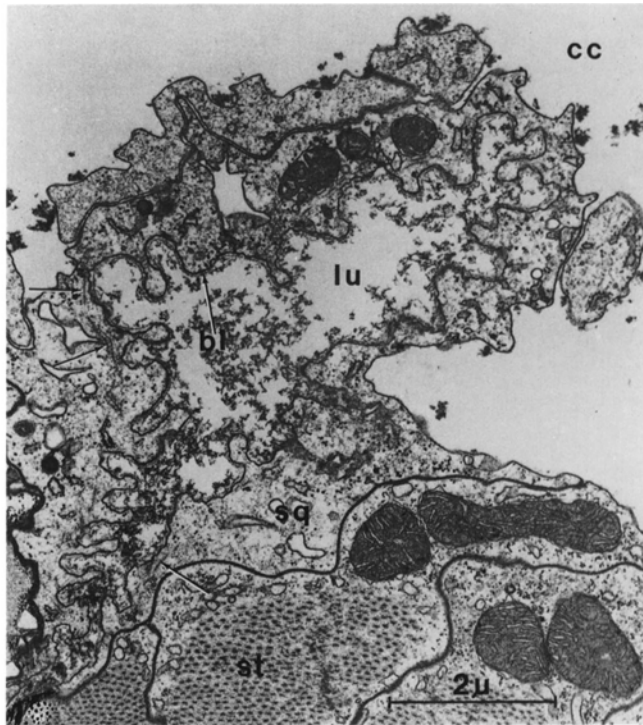
eral groups of smooth fibers. The striated myoepithelial cells are continuous with the squamous myoepithelial cells of the blood vessel and are oriented parallel to the longitudinal axis of the tentacle. Smooth myoepithelial cells occur on the abfrontal surfaces. The smooth myoepithelial cells are oriented at an angle of about 12 degrees from the longitudinal axis of the tentacle. These fibers and the small group of abfrontal myoepithelial cells are contiguous with the ciliated, coelomic cells.

Based on the structure of the connective tissue cylinders of the tentacles and the physiological implications of the observed morphologies of the different myoepithelial cells in *Terebratalia*, REED and CLONEY (1977) postulated that striated myoepithelial cells are responsible for flicking motions and for initial flexion of the tentacle, while smooth, frontal, myoepithelial cells hold the tentacle down for extended periods against the resilience of the cylinder of connective tissue. Smooth, abfrontal, myoepithelial cells initiate the return of the tentacle to the extended position. In *Terebratalia* the tentacles of subtidal specimens possess striated myoepithelial cells, while intertidal specimens contain only smooth myoepithelia (REED & CLONEY, 1977). In *Lingula* only smooth, myoepithelial cells occur (STORCH & WELSCH, 1976).

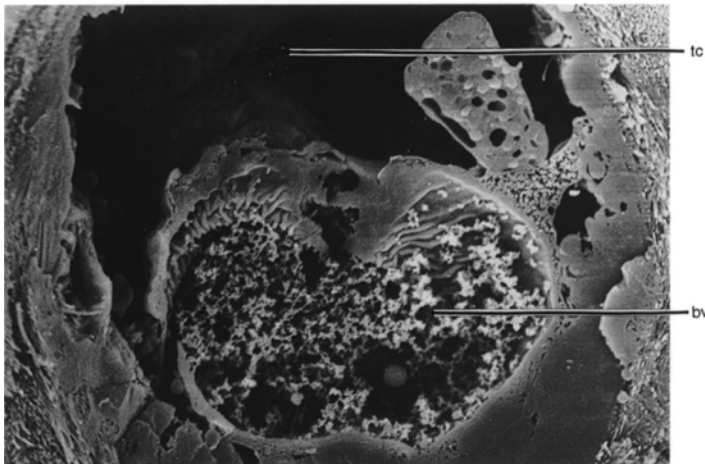
A blind-ending blood vessel extends the length of each tentacular canal along the surface of the frontal coelomic epithelium. The vessel is composed of a single layer of squamous myoepithelial cells, with parallel myofilaments that are oriented circumferentially and a basal lamina that faces the lumen of the blood vessel (Fig. 110; see section on coelomic and circulatory system, p. 69; see also Fig. 74; STORCH & WELSCH, 1976; REED & CLONEY, 1977).

DEVELOPMENTAL PATTERNS OF THE LOPHOPHORE

The effective surface area of the adult lophophore is one of the main physiological



1



2

FIG. 110. Blood vessels in the tentacles of lophophores; 1, TEM micrograph of transverse section of a tentacular blood (channel) vessel of *Terebratalia transversa*; squamous cells with myofilaments in their juxtaluminal cytoplasm (arrows) comprise the walls of the blood vessel with their basal (luminal) plasmalemmata thrown into folds, indicating that the cells have fixed in a contracted state; the blood vessel is laterally contiguous with the striated myoepithelial cells of the frontal contractile bundle; *cc*, tentacular coelomic canal, *lu*, lumen of blood vessel, *bl*, basal lamina, *sq*, squamous myoepithelial cell, *st*, striated myoepithelial cell, scale bar: 2.0 μ m (Reed & Cloney, 1977); 2, SEM micrograph of transverse section through the tentacular canal (*tc*) and blood vessel (*bv*) of *Lingula anatina* with the fibrogranular substance within a blood vessel, $\times 5,300$ (new).

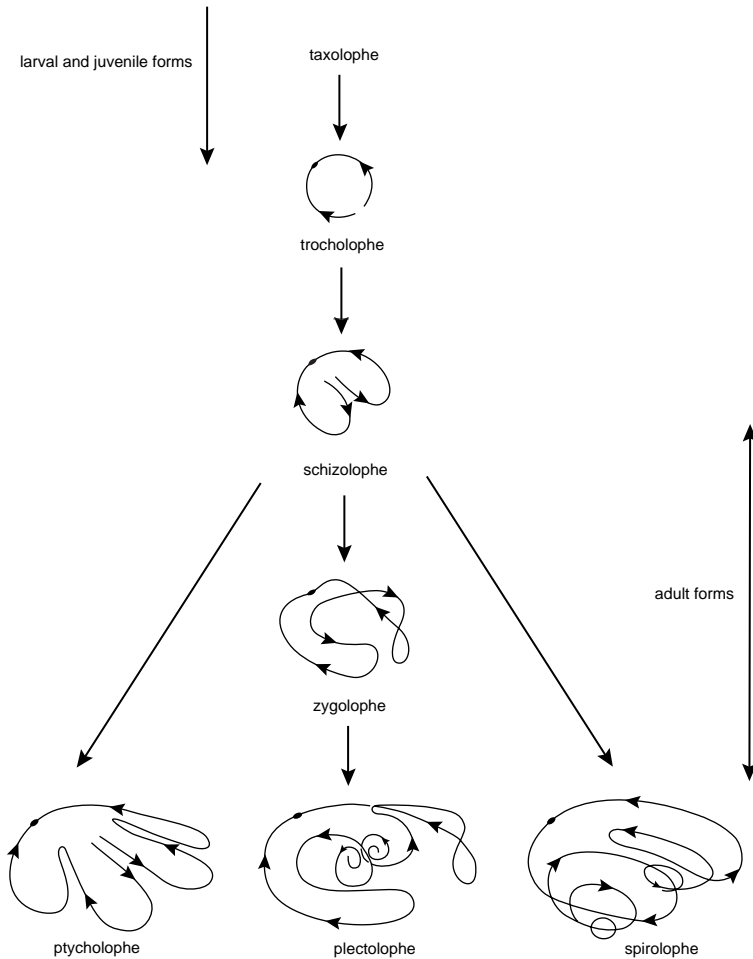


FIG. 111. Diagram showing three ontogenic pathways in the growth of the lophophore in living brachiopods; each drawing shows a perspective view of the course of the brachial axis (tentacles omitted), with *arrows* on the axis indicating the direction of transport of food particles toward the mouth (adapted from Rudwick, 1962a, 1970).

constraints governing the size of the brachiopod. As the brachiopod grows, the volume of body tissue increases. To supply the increase in metabolic requirements, the lophophore must undergo a commensurate increase in surface area. Given that the lophophore must also be arranged to create an efficient flow of water through the mantle cavity, evolution has provided several distinctive functional solutions to the problem of lophophore scaling, ranging from the simple crescent-shaped lophophore of larval or juvenile stages to the complex coils or spirals of some larger adults

(Fig. 111; RUDWICK, 1962a; LABARBERA, 1986b; EMIG, 1992).

Trocholophe

The **trocholophe** is the simplest functional lophophore and is a stage shared by all larval and small, juvenile brachiopods. It also characterizes the adults of the genera *Gwynia* (CHUANG, 1990), *Dyscolia* (BEECHER, 1897), and *Goniobrochus* (EMIG, 1992). The lophophore first appears in the larval or early juvenile stages as a few pairs of ciliated tentacles arranged in a crescent around the preoral

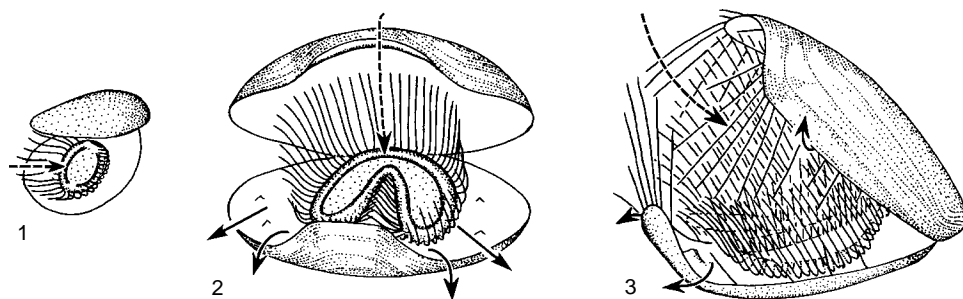


FIG. 112. Ontogeny of the lophophore and its current system in the small terebratulide *Pumilus antiquatus*; 1, the lophophore does not develop from the trocholophe, 2–3, beyond the schizolophe condition; setae shown only in 3; ventral valve above; *dashed arrows*, unfiltered (inhalant) water; *lined arrows*, filtered (exhalant) water (adapted from Rudwick, 1962a, 1970).

lobe and mouth on the anterior body wall or dorsal mantle surface. The crescent represents the first-formed brachia. Tentacles are added in pairs at the distal ends of the brachial axes on the dorsal or anterior side of the crescent. The frontal surface of all the tentacles faces inward. Although the number and length of the tentacles increase progressively, the spacing between tentacles remains constant (RUDWICK, 1970). The tentacles project forward, forming a bell-like aperture enclosed between two widely gaping valves. Water is drawn posteriorly through the mouth of the bell and is expelled laterally between the tentacles (Fig. 112.1; 113.1; 114.1).

Schizolophe

An involution of the brachial tips of the trocholophe forms the two lobes of the **schizolophe** and represents an increase in both structural complexity and surface area of the lophophore. Like the trocholophe, the schizolophe may be a transitional stage in the early growth of the lophophore, and for a few genera the schizolophe is the final form of the organ. Such genera include the discinid *Pelagodiscus*, such thecideidines as *Thecidellina*, and terebratulides including *Argyrotheca*, *Pumilus*, *Amphithyris*, *Thaumatostia*, and *Simplicithyris* (BEECHER, 1897; THOMSON, 1927; ATKINS, 1958; EMIG, 1992). As the lophophore increases in complexity, the brachia require additional sup-

port. In the schizolophe, the great brachial canal is sealed off from the coelom and becomes effective as a hydrostatic skeleton. In addition, calcareous outgrowths of varying complexity are developed to support the adult lophophore of articulated brachiopods.

Structurally the schizolophe differs little from the trocholophe except that the tentacles, which form the median indentation of the bilobed lophophore, create a tunnel that receives water pumped by these tentacles and directs it anteriorly (Fig. 112.3; 113.2; 114.2).

Ptycholophe

The bilobed schizolophe is enlarged by the addition of lateral indentations of the brachial axes creating the multilobed **ptycholophe**. In *Lacazella* and *Megathiris* the ptycholophe is four lobed (Fig. 115; RUDWICK, 1970). In *Pajaudina*, however, secondary indentations of the four-lobed ptycholophe produce up to eight lobes (LOGAN, 1988). Typically, the lophophore is supported by one median and two lateral septa. Each of the two anterolateral indentations acts as additional exhalant tunnels to the median tunnel; the current system is otherwise similar to the schizolophe of articulated brachiopods (ATKINS, 1960b).

Spirolophe

Both the schizolophe and the ptycholophe remain completely fused to the body wall

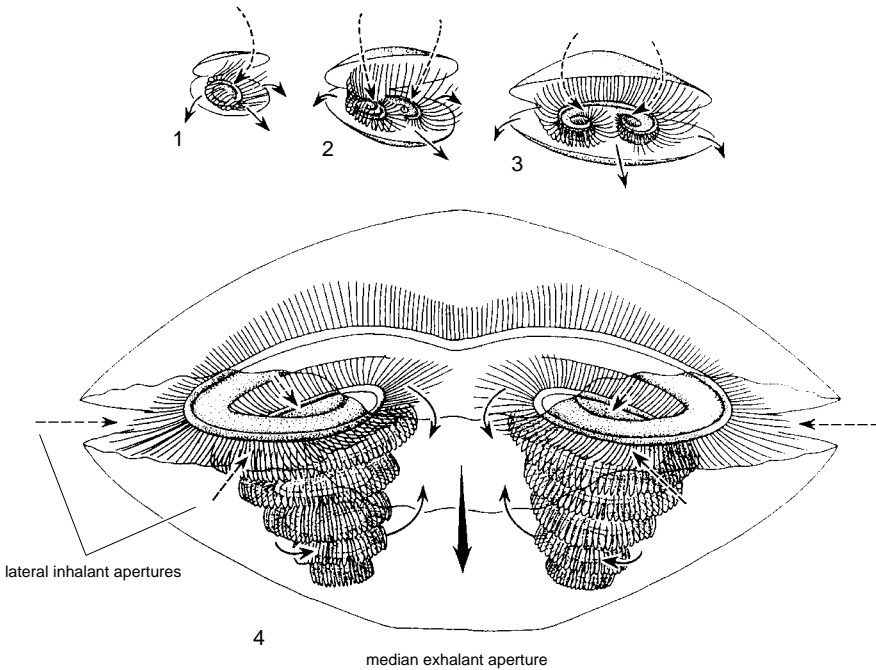


FIG. 113. Ontogeny of the lophophore and its current system in the rhynchonellide *Notosaria nigricans*; 1, trocholophe; 2, schizolophe; 3–4, spirolophes; valves in adult (4) are drawn as though transparent to show the full size of the spiral brachia; setae omitted; ventral valve above; dashed arrows, unfiltered (inhalant) water; lined arrows, filtered (exhalant) water (adapted from Rudwick, 1962a).

and the dorsal mantle so that any increase in the overall length of the lophophore lies in the same plane. In the **spirolophe**, the tips of the brachia diverge from each other and the mantle surface to form two, freely coiled spirals. The apices of the spirals converge toward one another and are generally oriented dorsally but point medially in the lingulids and ventrally in the discinids *Discina* and *Discinisca* (see EMIG, 1992). The spirolophe is characteristic of all inarticulated brachiopods (except the schizolophous *Pelagodiscus*) and rhynchonellides. *Leptothyrella* (possibly juvenile) is the only spirolophous terebratulide (MUIR-WOOD, 1965; MUIR-WOOD, ELLIOTT, & HATAI, 1965). The coiled brachia are supported principally by the hydrostatic skeleton of the brachial axes and, in the rhynchonellide spirolophe, by crura (Fig. 113).

In the spirolophe the tentacles of the proximal (first) whorl touch the mantle sur-

face. The tips of the median tentacles touch each other, dividing the mantle cavity into two separate inhalant chambers and a single exhalant chamber. At the margin of the shell, the lateral inhalant apertures form the median exhalant. The tentacles of successive whorls are reflected upward toward the preceding whorl, thus forming a cone that creates the main, exhalant current. Two posterolateral apertures exist in craniids and in the juvenile stages of rhynchonellides (ATKINS & RUDWICK, 1962; RUDWICK, 1962a; CHUANG, 1974) but not in discinids. *Crania californica* and *C. pourtelesi* have a median, incurrent flow (LABARBERA in EMIG, 1992). The discinid spirolophe is functionally similar to the schizolophe of *Pelagodiscus*. Discinids possess a large, median, inhalant compartment, which, at the shell margin, is delimited by long, anterior setae as an inhalant siphon, and two posterolateral exhalant gapes (PAINE, 1962a; LABARBERA, 1985). The

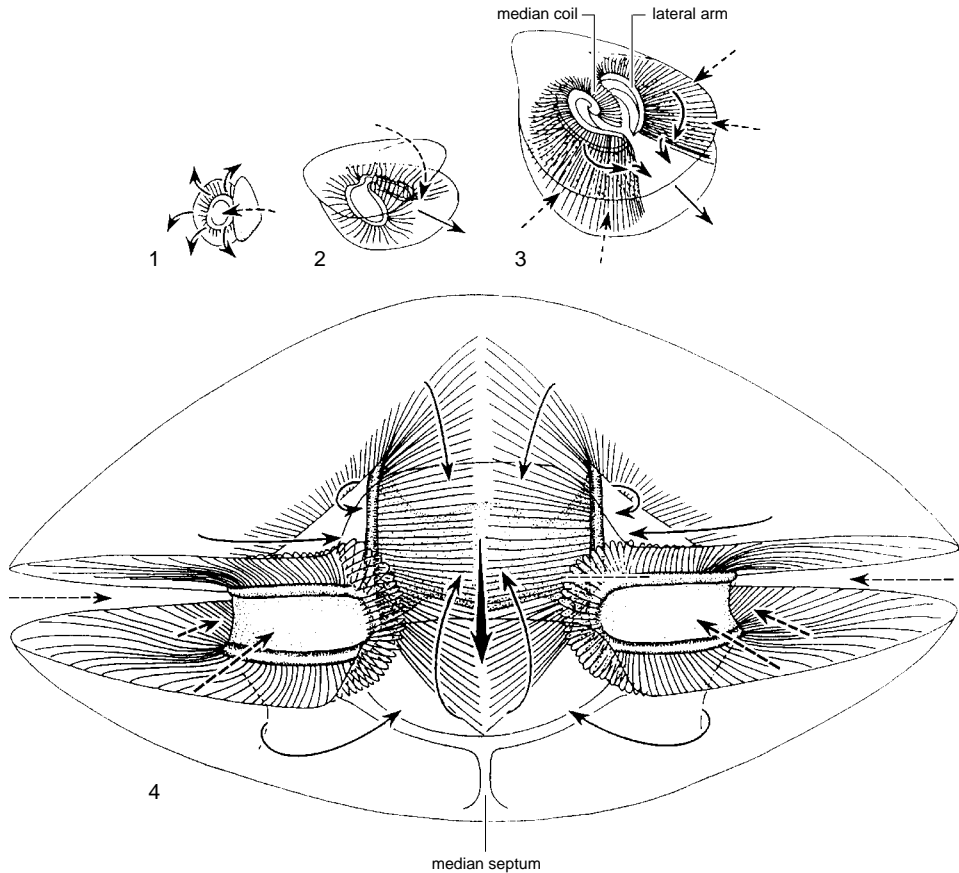


FIG. 114. Ontogeny of the plectolophe in the terebratulide *Calloria inconspicua*; 1, trocholophe; 2, schizolophe; 3, zygolophe; 4, plectolophe; all except 1, drawn as though the valves were transparent with ventral valve above; *dashed arrows*, unfiltered (inhalant) water; *lined arrows*, filtered (exhalant) water (adapted from Rudwick, 1962a).

reconstruction of *Discinisca* by ROWELL (1961) can therefore no longer be accepted (EMIG, 1992). In the sulcate rhynchonellides the exhalant aperture is shifted ventrally or dorsally, thus separating it from the lateral plane of the inhalant apertures (EMIG, 1992). Apertures are, however, never separated by fused or erected portions of the mantle edges except in the lingulids, where pseudosiphons are formed by the edges of the mantle and the arrangement of setae (EMIG, 1982).

Zygolophe and Plectolophe

Initially the lobes of the schizolophe twist laterally, away from the dorsal mantle surface and project freely into the mantle cavity.

Fusion of the two great brachial canals forms a supporting tube that allows the brachial axes to remain united across the floor of each lobe. The brachia are connected by a membrane forming a brachial gutter between the dorsal and ventral rows of tentacles. Although a precursor of the plectolophe, this transitional stage is recognized as the **zygolophe**. The tips of the zygolophe brachia develop anteriorly between the lateral lobes and rotate forward together to form a plane-spiral, median coil. A diaphragm of connective tissue connects the parallel coils across the median plane. The **plectolophe** derives support from modifications of the zygolophe brachidium. The plectolophe is

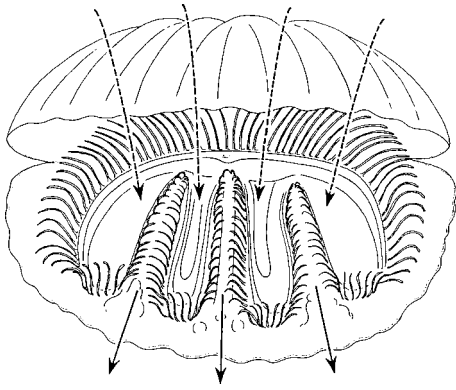


FIG. 115. Ptycholophe of *Megathiris detruncata*; dashed arrows, unfiltered (inhalant) water; lined arrows, filtered (exhalant) water (adapted from Atkins, 1960b).

characteristic of most adult terebratulides. The posterolateral inhalant apertures are defined by the tentacles of the lateral arms, which touch the mantle edges and, posteriorly, the mantle surface or body wall except anteriorly, where the tentacles separate these apertures from the median exhalant aperture (RUDWICK, 1962a). Water passes mainly through the tentacles of the lateral arms and partly through those of the median coil where the tentacles touch each other across the median plane. In many terebratulide genera, the exhalant aperture is deflected either dosally or ventrally by a median sulcus.

FUNCTIONAL MORPHOLOGY OF THE LOPHOPHORE

The brachiopod lophophore functions principally as a ciliary pump and feeding organ by creating water currents through the mantle cavity for the capture of food particles and the uptake of oxygen involved in respiration. These currents also assist in the elimination of metabolic waste products and undesirable particulate material from the mantle cavity. In a number of articulated species, the lophophore also functions as a brooding site for larvae (CHUANG, 1990).

The brachiopod lophophore is generally not capable of much extensive movement, even in the inarticulated brachiopods, where it has the best developed musculature. Some

apparent extensive motion has been reported, however, in the rhynchonellid *Notosaria*, and the extension can even result in self-amputation of portions of the coils. The reasons for this activity are unclear and may be the result of oxygen deprivation. Damaged lophophores of *Notosaria* appear capable of at least partial regeneration (HOVERD, 1985, 1986).

Currents

The lophophore creates water flow into and out of the mantle cavity, which is divided into inhalant and exhalant regions by the extension of the tentacles and their contact with the mantle. This flow facilitates metabolic exchanges with the environment, such as oxygen uptake, feeding, nitrogen excretion, and elimination of feces or undesirable particles. This water flow is generally continuous, although some individuals may stop pumping for short periods of time either due to disturbance or for no obvious reasons (LABARBERA, 1977, 1985; RHODES & THOMPSON, 1992, 1993).

Water movement through the mantle cavity of articulated brachiopods is generally slow and laminar, thus minimizing the energy dissipation involved in turbulent flow regimes (LABARBERA, 1977, 1981). The lateral cilia on the tentacles generate the currents passing through the lophophore, and their activity is complemented by ciliary activity on the mantle (WESTBROEK, YANAGIDA, & ISA, 1980; THAYER, 1986a). Laminar flow has been observed directly by mapping the pathways of fluorescein dye through the lophophore in the plectolophous species *Laqueus californianus*, *Terebratalia transversa*, and *Terebratulina unguicula* (LABARBERA, 1981). The flow lines do not cross, even when the dye makes a right-angle bend while entering the median coil from the lateral arms. A number of other plectolophous and spirolophous species have exhibited laminar flow (JAMES & others, 1992).

Although brachiopods must use metabolic energy to produce currents for ventilation and feeding, some species including those of

Laqueus, *Terebratulina*, *Hemithiris*, *Megathiris*, *Argyrotheca*, and *Gryphus* orient themselves to external water currents such that their ciliary pumping activity is augmented by the hydrodynamics of the ambient flow regime (SCHULGIN, 1885; ATKINS, 1960a, 1960b; LABARBERA, 1977, 1981; EMIG, 1992). They use the pressure differences from favorable orientations to external water currents to assist their ciliary pumps. Species that are capable of rotating about their pedicles in the adult stage tend to orient themselves with their anterior-posterior axes perpendicular to the prevailing flow or the substratum in their environments. The ptycholophous thecideids orient themselves with their anterior-posterior axis facing the current; the ventral valve is cemented to the substrate while the dorsal valve opens to a 90-degree angle relative to the substrate during feeding (LACAZE-DUTHIERS, 1861; NEKVASILOVA & PAJAUD, 1969; EMIG, 1992). Species such as *Terebratalia transversa*, which cannot reorient themselves in the adult stage, are often found in field observations to occur in favorable orientations due to preferential settlement by the larvae (LABARBERA, 1977).

Zygoplectolophous and spirolophous articulated groups may not assume a preferential position if the velocities of the ambient bottom currents are lower than the velocities of the excurrents of the brachiopods. As the speed of the bottom current increases, however, the incidence of preferential orientation also increases (data from McCAMMON, 1965, 1973; LABARBERA, 1977, 1978, 1981; RICHARDSON, 1981d, 1986; EMIG, 1987, 1992).

Orientation relative to the bottom currents maximizes the effects from Bernoulli's principle and viscous entrainment. When brachiopods orient themselves with their anterior-posterior axes perpendicular to the external flow, a low-pressure region is created near the anterior portion of the gape where the exhalant current exits, and relatively higher pressure is present on either side of the gape in proximity to the inhalant currents (Fig. 116). Thus brachiopods minimize

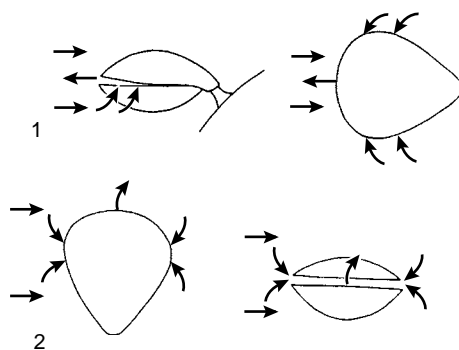


FIG. 116. Use of ambient external currents to assist in pumping water through the lophophore; straight arrows represent the current direction, with the velocity of the current proportional to the length of the arrows; smaller curved arrows indicate the inhalant and exhalant currents of the brachiopod; 1, most unfavorable orientation as a brachiopod must work against high pressure in order to produce an exhalant current. Since the flow is moving parallel to the incurrent region, low pressure regions will occur because of viscous entrainment and will increase the effort required by the brachiopod to draw water into its shell; 2, most favorable orientation as the excurrent region will be a low pressure zone because of viscous entrainment and the Bernoulli effect; the incurrent regions will be relatively higher pressure zones because the current decelerates on the upstream side as it approaches the brachiopod. The downstream side will have ambient hydrostatic pressure. This orientation enhances the pumping activity of the brachiopod (adapted from LaBarbera, 1977).

the energy needed for creation of feeding and respiratory currents and avoid recirculation of previously filtered water (LABARBERA, 1977, 1981).

Some species, however, such as *Liothyrella neozelanica*, *Calloria inconspicua*, and *Notosaria nigricans*, live in dense, conspecific clusters, where the water pumped by one individual may include water already filtered by other individuals or epibionts, resulting in a decrease in food intake relative to the total energy needed for pumping water to obtain food.

The hydrodynamics of water flow through epifaunal inarticulated brachiopods has yet to be studied intensively (LABARBERA, 1985), but the similarities of configurations and areas of the lophophore and pumping velocities to those of articulated species suggest that flow through epifaunal inarticulated

species is also slow and laminar (see Fig. 411.1, section on ecology of inarticulated brachiopods).

Discinids orient the lophophore relative to the current so that it functions as a basket facing the current (see Fig. 411.1, section on ecology of inarticulated brachiopods; EMIG, 1992). In craniids that have cemented shells, orientation to external currents may occur only upon larval settlement and metamorphosis. Thus the anterior region faces the ambient flow regime, while the excurrent region is perpendicular. This orientation is functionally equivalent to that seen in articulated species that orient themselves to ambient flow, but it is anatomically perpendicular to orientation of articulated forms (M. LABARBERA, personal communication to C. EMIG, 1992).

Due to the experimental difficulties involved in studying infaunal animals, there are no published studies on the fluid mechanics of currents through infaunal, inarticulated brachiopods, although current pathways have been described in general qualitative terms (CHUANG, 1956; EMIG, 1976, 1982, 1992; WESTBROEK, YANAGIDA, & ISA, 1980; GILMOUR, 1981). The infaunal lingulides create separate inhalant and exhalant tubes within their mucous-lined burrows by the arrangement of their marginal setae and edges of the mantle (see Fig. 411.1, section on ecology of inarticulated brachiopods). As in articulated, spirolophous species, the mantle cavity of the lingulides is separated into inhalant and exhalant regions by the fully extended lophophore. Water currents drawn into the anterolateral inhalant setal tubes, however, may not remain laminar; they appear to diverge as they enter the inhalant region of the mantle cavity (CHUANG, 1956). Lingulides do not orient themselves toward ambient currents because they live in burrows (EMIG, 1982, 1992).

Respiration

The lophophore is the main respiratory organ in both articulated and inarticulated brachiopods (PECK, MORRIS, & CLARKE,

1986a). Due to its large surface area, it is ideally suited for gaseous exchange. Weight-corrected respiration rates of brachiopods are generally much lower than those of other marine invertebrates (JAMES & others, 1992).

Feeding

All living brachiopods are suspension feeders, and, although brachiopod lophophores occur in a number of configurations, species possessing different types of lophophores feed in essentially the same manner. When the tentacles of the lophophore are fully extended for feeding and respiration, the mantle cavity is separated into inhalant and exhalant chambers. Weak, through-going currents are created by the lateral cilia of the tentacles, while the frontal cilia transport food particles along the length of the grooved, outer tentacles toward the brachial groove for transportation to the mouth (Fig. 117).

Particle Capture

The mechanisms brachiopods use in capturing particles have been a subject of much debate since recent aerosol models have demonstrated the improbability of the cilia acting as sieves (RUBENSTEIN & KOEHL, 1977; LABARBERA, 1984). Additionally, there is no evidence that brachiopods use mucus to capture particles and move them down the tentacles toward the brachial groove, although once the particles enter the groove they are transported in mucus toward the mouth. One set of observations of *Laqueus* suggests that particles passing close to or within one particle radius of the cilia exert a drag force that induces a local reversal of the ciliary beat. This local reversal of lateral cilia captures the particles and their surrounding parcels of water and prevents them from wandering off the frontal cilia of the tentacle as they are moved toward the food groove (STRATHMANN, 1973; LABARBERA, 1984).

A second hypothesis to explain the capture of particles emphasizes possible adhesive properties of both cilia and particles due to electrostatic charge and suggests that par-

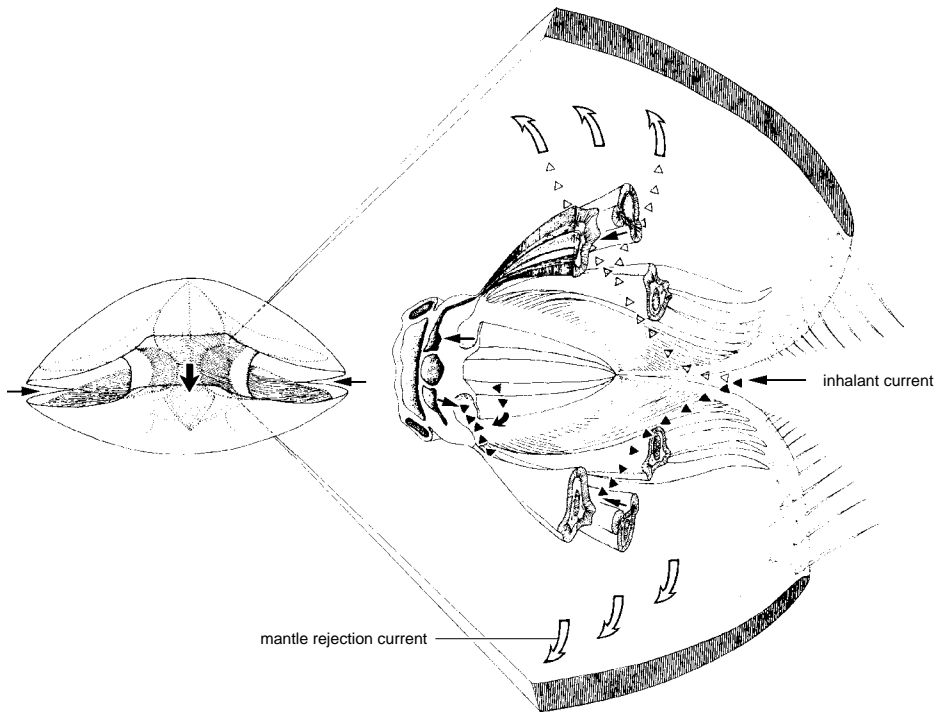


FIG. 117. Particle acceptance and transport down the frontal grooves of the outer (ablalial) tentacles to the food groove in a plectolophous brachiopod; *black triangles* represent the particles that are captured; *white triangles* represent the particles that pass through the tentacles and into the exhalant chamber; particles not intercepted are swept away in the exhalant current or by rejection currents on the mantle (adapted from James & others, 1992).

ticles approaching the cilia will be attracted by short-range, London-van der Waals forces and subjected to hydrodynamic retardation due to the viscosity of the fluid being squeezed out between the particles and the cilia (LABARBERA, 1984). A third hypothesis suggests that particles are extracted from suspension by steep velocity gradients created when the through-going currents meet currents perpendicular to them (JØRGENSEN, 1981), such as those potentially occurring when the through-going currents created by the lateral cilia on the tentacles encounter currents moving down the frontal ciliary tracts.

Finally, observations on the inarticulated species *Glottidia* and the articulated species *Laqueus*, using stroboscopic-interference-contrast optics, suggest that heavier and thus biologically undesirable particles impinge

directly upon the frontal surfaces of the lophophore tentacles for rejection (BULLIVANT, 1968), while lower density, potential food particles are filtered through the lateral cilia of the tentacles without the use of ciliary reversals for acceptance (GILMOUR, 1978, 1981). The fluid mechanics of such an impingement mechanism operating in a flow regime where viscous forces predominate over inertial forces have yet to be understood (JAMES & others, 1992).

Particle Sorting and Rejection

Undesirable or excess particles are generally bound in mucus and eliminated by a variety of mechanisms (RUDWICK, 1970; THAYER, 1986a; JAMES & others, 1992; THOMPSON, WARD, & RHODES, 1992). Mantle cilia commonly assist the lophophore in rejection and the exchange of water

through the mantle cavity, as noted in *Neocrania anomala*, *Lingula anatina*, *Coptothyris grayii*, and *Terebratalia transversa* (CHUANG, 1974; WESTBROEK, YANAGIDA, & ISA, 1980; THAYER, 1986a).

Articulated species use several mechanisms to reject particles. In the presence of unwanted particles or particles in dense concentrations, many species reverse the beat of the frontal cilia to transport mucous-bound particles away from the food groove toward the tips of the tentacles (ATKINS, 1956, 1959, 1960a, 1960b; RUDWICK, 1962a, 1970). Particles to be rejected may become concentrated on the inner (adlabial) tentacle series (where present), while particles to be accepted become concentrated on the outer (ablabial) tentacle series, thus allowing simultaneous feeding and rejection (GILMOUR, 1978). Additional rejection mechanisms noted in studies on the species *Terebratalia transversa* include lifting of a single tentacle to permit removal of particles by mantle currents, a spiralling motion between two adjacent tentacles that rolls particles into a mucous string and moves it distally, wholesale rejection where the lophophore coils tightly to allow the mantle to remove excess matter (RUDWICK, 1970; THAYER, 1986a), and a wiping motion where one, outer tentacle passes its abfrontal surface over the frontal surfaces of a whole series of neighboring tentacles, thus transferring strings of mucous-bound particles directly into the rejection current (Fig. 118; THOMPSON, WARD, & RHODES, 1992). Occasionally, *Terebratalia* reverses its entire current system, with water and mucous-bound particles exiting the normally inhalant regions (RHODES & THAYER, 1991; THOMPSON, WARD, & RHODES, 1992). These rejection mechanisms are likely to be used by many species, especially those living in areas with high loads of suspended particles.

Lingula is capable of simultaneous feeding and rejection of particles due to the action of adjacent tracts of frontal cilia on the same tentacles. The individuals accept or reject particles by suppressing the action of one set

of tracts while amplifying the opposite set. Reversals of frontal cilia have not been observed in this genus (CHUANG, 1956). Simultaneous feeding and rejection are particularly advantageous for the infaunal inarticulated groups because of the proximity of their anterolateral incurrents to the interface between water and unstable sediments. *Neocrania* is capable of reversing its frontal cilia to reject unwanted particles (ATKINS & RUDWICK, 1962; CHUANG, 1974).

Brooding in the Lophophore

Brooding of larvae in the lophophore appears to be quite common among articulated brachiopods, although it has not been found to occur in inarticulated groups (CHUANG, 1990). *Pumilus* broods its embryos using its schizolophous lophophore as a natural basket (RICKWOOD, 1968). The spirolophous species *Notosaria* and *Hemithiris* brood larvae using the coils and tentacles of their lophophores as baskets (Fig. 119; PERCIVAL, 1960; LONG, 1964, in CHUANG, 1990; HOVERD, 1985). The plectolophous species *Terebratulina unguicula* broods larvae between the tentacles on its lateral arms (LONG, 1964, in CHUANG, 1990), while the Antarctic species *Liothyrella*, which is also plectolophous, broods them within the median coil (PECK & HOLMES, 1989a; PECK & ROBINSON, 1994). The ptycholophous *Lacazella* species provides an attachment site behind the mouth by inserting modified lophophore tentacles with collars and swollen tips into a single median pouch (see Fig. 173; RUDWICK, 1970; CHUANG, 1990). The small trocholophous *Gwynia capsula* broods in a similar manner (SWEDMARK, 1967). Brooding in the lophophore protects the larvae, while allowing them maximum exposure to fresh seawater.

NERVOUS AND SENSORY SYSTEM

All brachiopods possess a central nervous system, but there are few detailed anatomical studies and little new neurophysiological data. *Gryphus vitreus* is the best documented

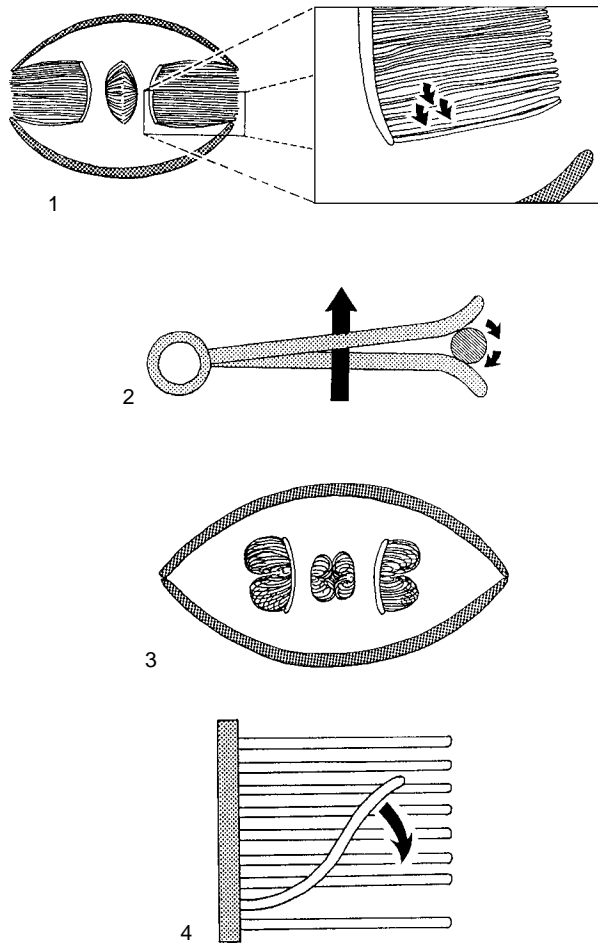


FIG. 118. Particle rejection mechanisms in brachiopods; 1, rejection of a particle by the lifting of a single tentacle; the enlarged region shows particle rejection by spiralling activity around pairs of tentacles; 2, construction of a mucous string by two tentacles to bind undesirable particles for rejection; 3, wholesale rejection of high particle loads by the lophophore tentacles remaining coiled until the mantle currents sweep away excess particles (adapted from Thayer, 1986a); 4, wiping motion of a single tentacle sweeping its ablabial surface across a region of neighboring tentacles and transferring mucous-bound particles directly into the excurrent region (new).

of the articulated brachiopods (BEMMELEN, 1883), while *Lingula anatina*, *Disciniscia lamellosa*, and *Neocrania anomala* are the most widely cited examples among the inarticulated species (BLOCHMANN, 1892, 1900). The ultrastructure and immunocytochemistry of the nervous systems of the larvae of *L. anatina* and *Glottidia* sp. have also been studied (HAY-SCHMIDT, 1992).

The nervous system of articulated brachiopods is considered to be typified by

Gryphus (Fig. 120). The main body of nervous tissue is found around the esophagus near its junction with the anterior body wall. Nerves emanate laterally from two ganglia, a larger subenteric ganglion and a smaller supraenteric ganglion, which lie above and below the esophagus respectively. One or more circumenteric nerves innervate the lophophore. The brachial lip is activated by a pair of nerves arising laterally from the subenteric ganglion. Branches of the

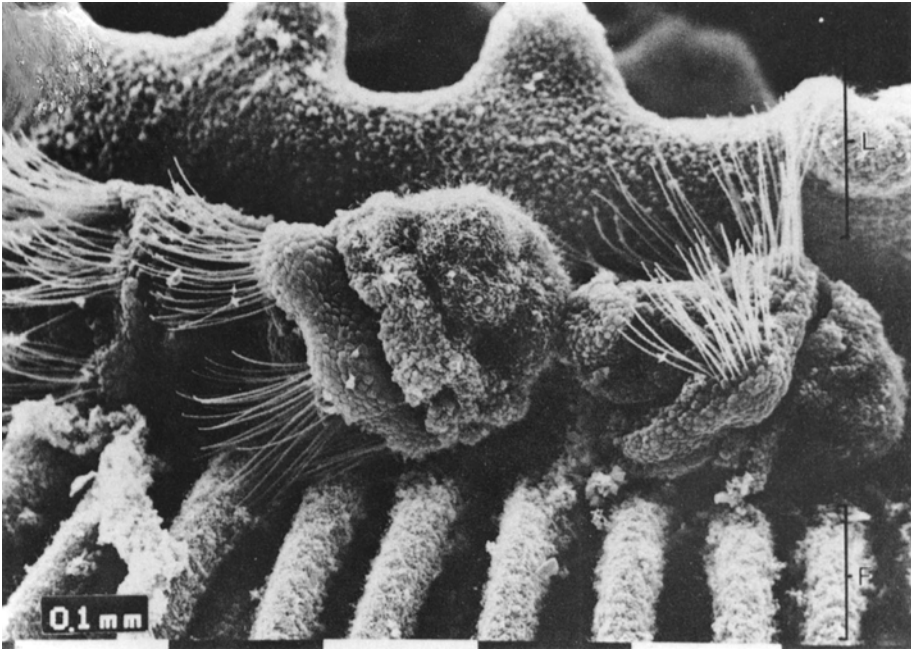


FIG. 119. SEM micrograph of the larvae brooded in the spirolophous lophophore of *Notosaria nigricans*, scale bar: 0.1 mm; L, lip of food groove; F, tentacle (Hoverd, 1985).

circumenteric nerves, accessory and lower brachial nerves, serve the brachia and tentacles. The dorsal mantle is innervated by two main nerves and a number of ancillary branches, which also arise from the subenteric ganglion. Similarly a pair of thick, subparallel branches, arising from the subenteric ganglion, serve the ventral mantle, adductor muscles, and pedicle. Mantle nerves radiate, splitting distally into ever finer branches that terminate close to the mantle margin at relatively regular intervals (Fig. 121; RUDWICK, 1970).

In the planktotrophic larvae of *L. anatina* and *Glottidia* sp., the nervous system appears to be divided into dorsal and ventral parts. The primary dorsal system consists of part of an apical ganglion, dorsal lophophore nerves, and a ventral ganglion. The second system is essentially ventral and includes part of an apical ganglion and ventral lophophore nerves. The dorsal lophophore nerves are believed to innervate the muscles (*musculus lophophoralis* and *m. brachialis*), and the ven-

tral lophophore nerves and lateral processes innervate the ciliary band. The known physiological function of detected neurotransmitters supports this pattern of innervation (Fig. 122; HAY-SCHMIDT, 1992). As with many other invertebrates, the planktotrophic larvae of *Glottidia* contain serotonin-like (5-HT), catecholamines (CA), and neuropeptide FMR-like neurotransmitters (Fig. 123–125; HAY-SCHMIDT, 1992).

The nervous system of adult inarticulated brachiopods lacks a supraenteric ganglion. In *Discinisca* and *Neocrania* the circumenteric nerves emanate laterally from the subenteric ganglion and from a ring around the esophagus. In *Neocrania*, however, the subenteric ganglion is also divided into two parts that occur in the epidermis of the lateral body wall lateral to the anterior adductor muscles. Brachial nerves serving the lophophore and tentacles arise from the branches of the circumenteric nerves (Fig. 126–128).

A network of finely divided nerves originating from the subenteric ganglion ramifies

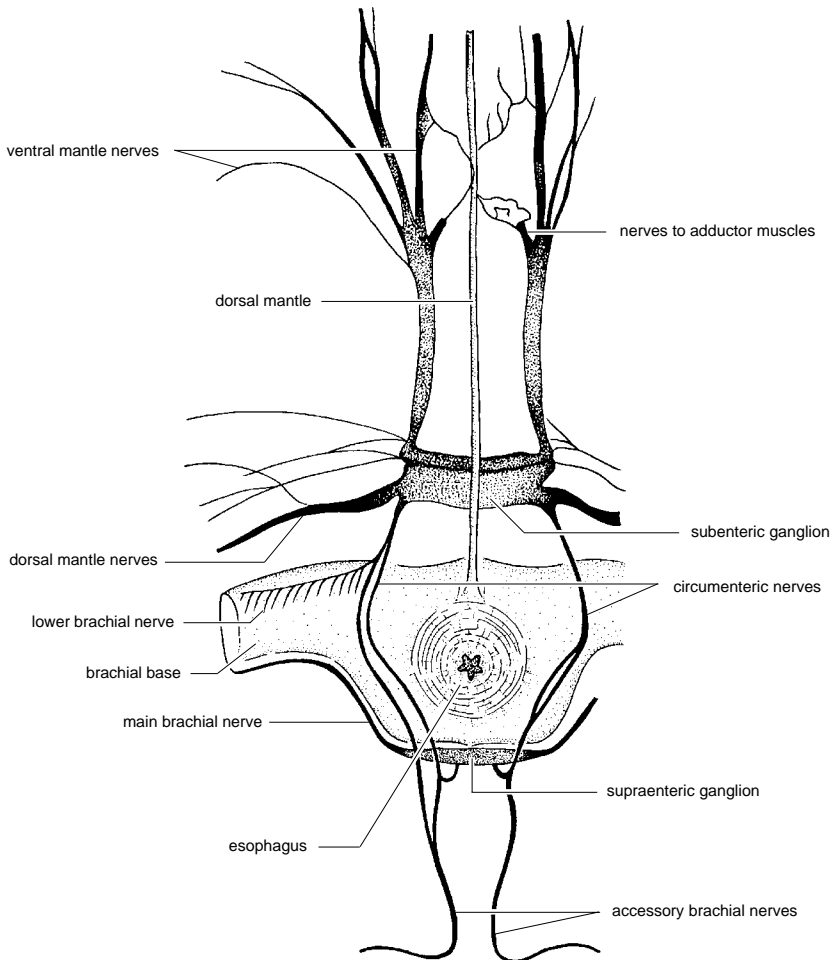


FIG. 120. Nervous system of *Gryphus vitreus* (adapted from Bemmelen, 1883).

throughout the dorsal and ventral mantles. In both *Discinisca* and *Lingula* the branches of the mantle nerves are joined distally to form dorsal and ventral marginal nerves. These peripheral nerves are found on the inner side of the setal follicles that occur around the edge of the mantle. Both follicles and marginal nerves are absent from *Neocrania*.

The pedicles of *Discinisca* and *Lingula* are each provided with a pair of nerves that branch from the subenteric ganglion or form ring-shaped, lateral nerves located in the body wall. The diagrams (Fig. 126–128) illustrate the course of the nerves that serve

the more complex inarticulate musculature. A nerve plexus in the base of the epithelium lining the alimentary canal has also been identified (BLOCHMANN, 1900).

Although there may be differences within the phylum, current evidence suggests that bundles of unsheathed nerve fibers are generally located between the bases of the inner mantle epithelium covering the lophophore and lining the alimentary canal above the basement membrane (Fig. 129–130; PERCIVAL, 1944; GILMOUR, 1981; SAVAZZI, 1991). Bundles of neurons have also been found in the connective tissue of the pharynx of *Calloria* (Fig. 131). The neurological gap

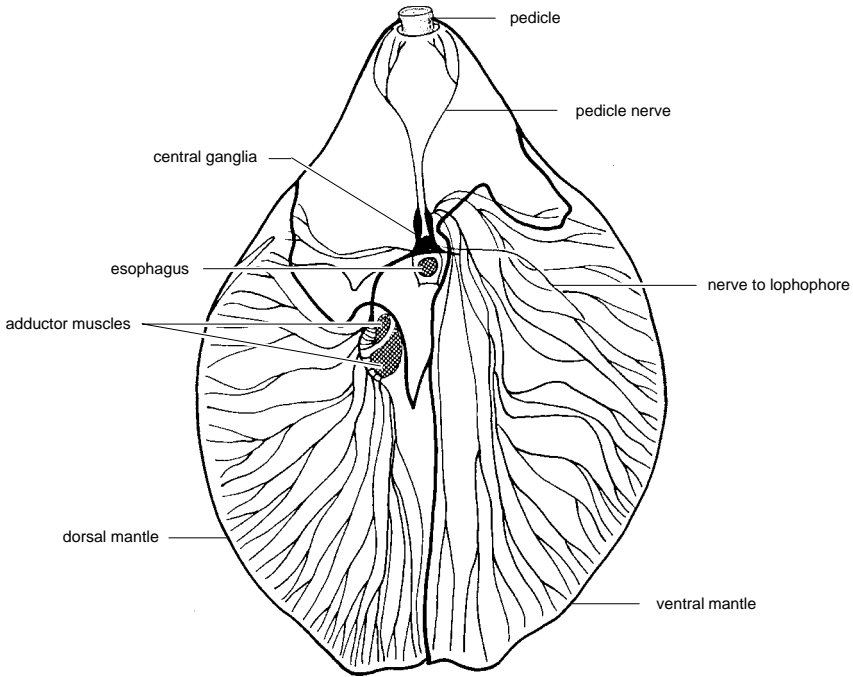


FIG. 121. Nervous system of *Magellania australis* QUOY & GAIMARD; dorsal view of decalcified specimen, with the dorsal mantle removed on one side; the sensory nerves terminate around the mantle edges and motor nerves are connected to the adductor muscles (adapted from Hancock, 1859).

junctions found between the nerves of the terebratulides *Calloria* and *Terebratella* have now been characterized as P-type junctions, which are also known to exist in the molluscs and bryozoans. The type of septate junction present, however, is identical to that found in many other lower invertebrate phyla and differs from the molluscan septate junction (FLOWER & GREEN, 1982).

FUNCTIONAL MORPHOLOGY OF THE NERVOUS AND SENSORY SYSTEM

Brachiopods show little evidence of differentiated sense organs. Although no rigorous experimental data exist, it is generally accepted that their responses to light and a range of chemical and physical stimuli indicate sensitivity.

The behavioral repertoire of the brachiopod, although limited, provides clues to their sensory capabilities. The most obvious sensory mechanisms appear to be confined to

the edge of the mantle lobes and possibly the pedicle. No special receptor organs have been found, but the mantles are richly supplied with nerves leading to the central ganglia, through which there is a simple reflex circuit to the adductor muscles.

A dramatic response to unfavorable conditions is the rapid and tight closure of the valves by contraction of the adductor muscles. Closure may be accompanied by movement of the whole shell on the pedicle, drawing the shell nearer to the substratum or, in lingulids, into its burrow or merely rotating the shell into a different orientation.

A sudden decrease in light intensity initiates a shadow reflex resulting in rapid closure of the shell. The mantle seems to be capable also of detecting water that is highly turbid, brackish, or poorly oxygenated (RHODES & THAYER, 1991).

The behavior of some brachiopod larvae may change during ontogeny with respect to light, gravity, and possibly the physical or

chemical nature of the substratum (JAMES & others, 1992). Immediately prior to settlement, the behavior of such brachiopods as *Terebratulina* and *Neocrania* suggests selection of the substrate, emphasized by patchy distribution and apparently gregarious settlement. Such behavior suggests mediation by some sort of sensory capability.

Setae

With few exceptions, notably craniids, thecideidines, and megathyrids, living brachiopods possess chitinous setae that develop in follicles along the margin of the mantle, project beyond the edges of the valves, and extend tactile sensitivity beyond the mantle (see section on mantles and body walls, p. 9). As no direct neurological connection with the setae has been reported, it is assumed that their tactile properties are transmitted mechanically to the mantle (RUDWICK, 1970).

Statocysts

A pair of statocysts occur in larval or juvenile inarticulated brachiopods. According to YATSU (1902a) and MORSE (1902) these persist in adult *Lingula*. MORSE (1902) did not find them in *Glottidia*. Statocysts occur in the gastroparietal bands near the anterior adductor muscles and consist of a sac of tall epithelial cells containing about 30 statoliths (SAVAZZI, 1991). They are assumed to allow the sensation of orientation and enable the animal to maintain an optimal position in the soft sediments it inhabits, which would accord with the ability of lingulids to burrow (WORCESTER, 1969; THAYER & STEELE-PETROVIC, 1975; SAVAZZI, 1991).

Particle Selection

The lophophore appears to be capable of particle selection based on size, specific gravity, charge, and other chemical properties (RHODES & THAYER, 1991). The ciliated laterofrontal cells of the tentacles of *Glottidia* make synapses with the nervous system, and it has been suggested that the cilia serve as detectors of high densities of heavy waste particles in the feeding current (GILMOUR,

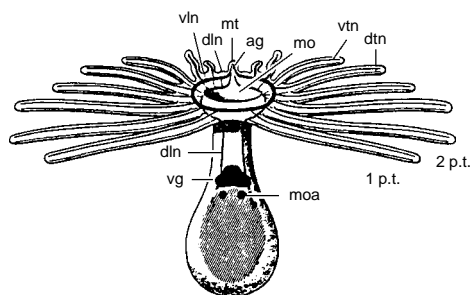


FIG. 122. Drawing of a planktotrophic brachiopod larva showing the course of the major nerves with the shell removed but the connection to the body wall (*oblique lines*) and *musculus ocludens anterior* (*moa*) indicated; the median tentacle (*mt*) represents the prosoma and contains the apical ganglion (*ag*); the lophophore represents the mesosoma and consists of a ring of tentacles numbered according to their appearance during development (1 p.t., 2 p.t.; see section on embryology and development, p. 154); the major nerves are the ventral and dorsal lophophore nerves (*vln* and *dln*), and the ventral and dorsal tentacle nerves (*vtn* and *dtn*); the dorsal lophophore nerve is connected to the ventral ganglion (*vg*); *mo*, mouth (Hay-Schmidt, 1992).

1981). In contrast, ultrastructural studies of *Terebratalia* did not reveal any nerve fibers traversing the connective tissue to form myoneuronal junctions or any evidence of peritoneal nerves (REED & CLONEY, 1977). The tentacles of the lophophore often react to adverse conditions by curling toward the brachial groove, presumably by contraction of their frontal group of myoepithelial cells.

Eyespots

There are numerous reports of the existence of eyespots (ocelli) and pigment granules in various larvae (see section on embryology and development, p. 151), but the anatomy and sensory potential of these structures is largely unknown (JAMES & others, 1992). *Argyrotheca* larvae possess eyespots that consist of cuplike invaginations of the ectoderm with underlying nerve fibers and vitreous humor (PLENK, 1913). The structure suggests photosensitivity.

REPRODUCTION

Most brachiopods occur as separate sexes (gonochoristic), although some are

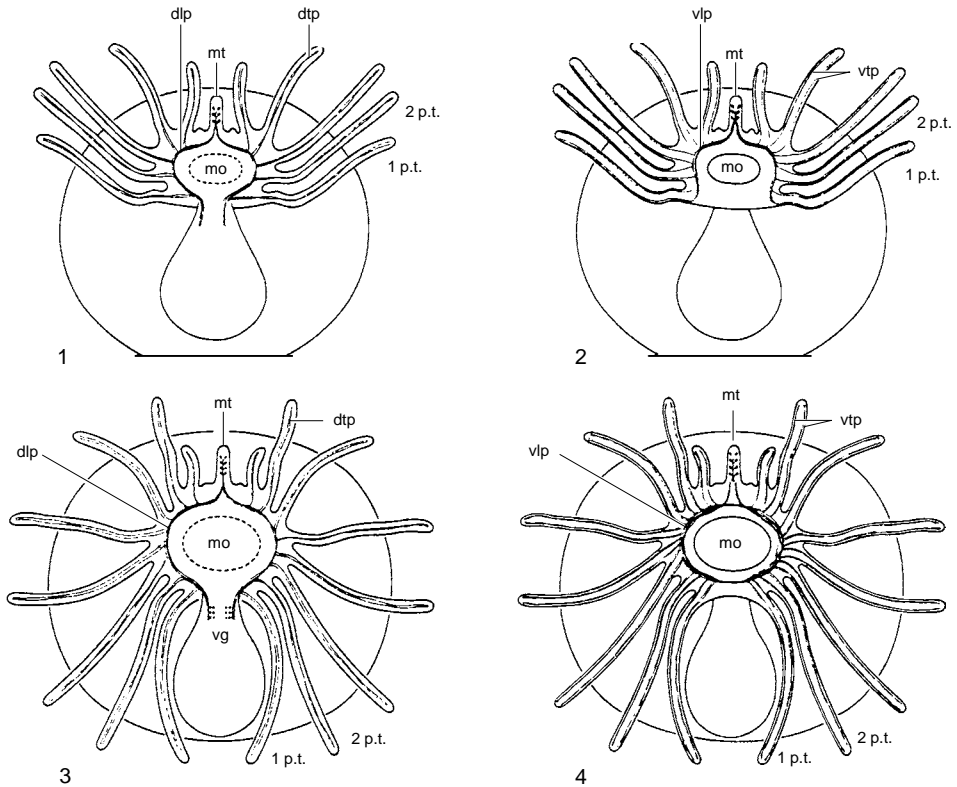


FIG. 123. Diagram of serotonin (5-HT) containing cells in a brachiopod larva; 1, dorsal and 2, ventral view of a 6 p.t. larva showing the dorsal lophophore processes continuing along the esophagus before the formation of the ventral ganglion; 3, dorsal and 4, ventral view of a 9 p.t. larva with the dorsal lophophore processes (*dlp*) connected to the ventral ganglion (*vg*) and the ventral lophophore processes (*vlp*) continuous between the 1 p.t.; *dtp*, dorsal tentacle process; *mo*, mouth; *mt*, median tentacle; *vtp*, ventral tentacle process (Hay-Schmidt, 1992).

hermaphroditic. Those factors influencing sex determination in brachiopods are unknown (LONG & STRICKER, 1991), but body size and the degree of isolation of the population may exercise some influence over the mode of reproduction. Micromorphic brachiopods tend to be hermaphroditic and brood their larvae. All gonochoristic nonbrooding brachiopods are relatively large. For the few species that have been studied, an approximately 1:1 sex ratio exists (PERCIVAL, 1944; PAINE, 1963; DOHERTY, 1979; CURRY, 1982), although greater variation has been reported in *Notosaria nigricans* (PERCIVAL, 1960). Sexual dimorphism has been reported only in *Lacazella mediterranea* (LACAZE-DUTHIERS, 1861), in which the ventral valve of the female is distended to incorporate a brood

pouch. The sex of mature gonochoristic brachiopods can sometimes be determined externally by the color of the gonads, observed either through the valve (ROKOP, 1977) or more reliably through the translucent, inner mantle membrane. Testes are usually white, cream, pink, or blue, while ovaries tend to be yellow to orange-brown. Hermaphroditic species such as three species of *Argyrotheca* (SENN, 1934), *Pumilus antiquatus*, *Platidia davidsoni* (ATKINS, 1958), *Lacazella* sp., and *Thecidellina barretti* (JAMES, unpublished, 1987) contain both ovary and testes simultaneously. *Fallax dalliniformis* possibly alternates between sexes (WILLIAMS & ROWELL, 1965a), and *Calloria inconspicua* may be predominantly male or predominantly female (JAMES & others, 1992). Some specimens of

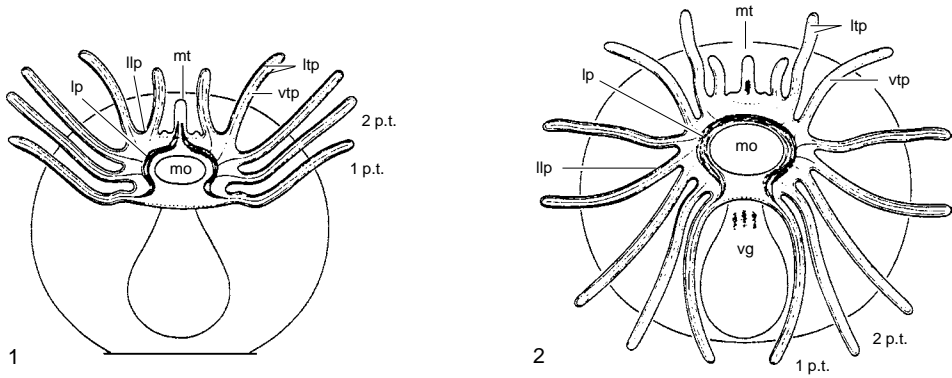


FIG. 124. Diagram of CA (catecholamine) containing processes in a brachiopod larva; 1, 6 p.t. larva ventral view; from the median tentacle (*mt*) extend the lophophore processes (*lp*), from which project the ventral tentacle processes (*vtp*), with the lateral lophophore processes (*llp*) extending into the tentacles as the lateral tentacle processes (*ltp*); 2, as for 1, but at the 9 p.t. larval stage, the neurophil of the apical ganglion seems to be separated from the lophophore processes (*lp*), while the ventral ganglion (*vg*) consists of three separate neurophils; *mo*, mouth (Hay-Schmidt, 1992).

Lingula anatina and *Glottidia pyramidata* (GRATIOLET, 1860; BEYER, 1886; CULTER, 1980; CULTER & SIMON, 1987) have also been recorded as containing both male and female reproductive tissue in the same gonad.

GONAD MORPHOLOGY

Brachiopods have one or, more usually, two pairs of gonads with the largest gonads developing ventrally in articulated groups

(Fig. 132). Some species of *Argyrotheca* possess only a dorsal pair of gonads (SENN, 1934), while only a ventral pair of gonads develops in *Lacazella mediterranea* (LACAZE-DUTHIERS, 1861). The gonads of inarticulated brachiopods are usually confined to the relatively large visceral cavity. The gonads of articulated brachiopods are only partially housed in the relatively smaller visceral cavity, with most of the gonad extending anteriorly into extensive mantle canals, the

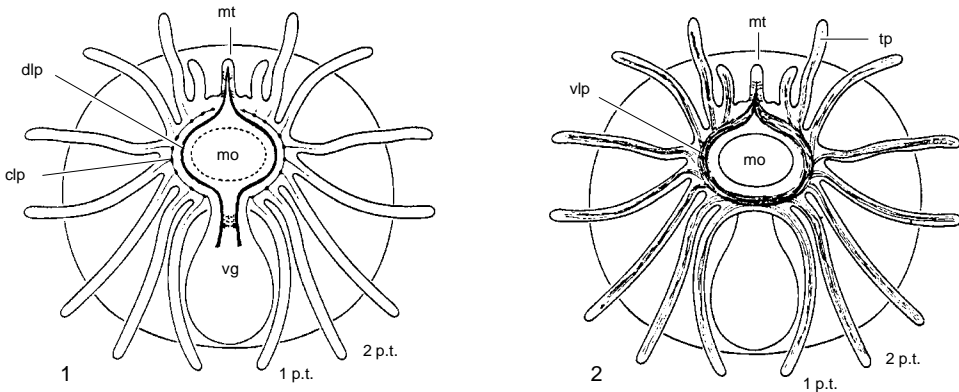


FIG. 125. Diagram of the distribution of FMRamide containing cells and processes in a 9 p.t. brachiopod larva; 1, dorsal view with the apical ganglion in the median tentacle (*mt*) consisting of two cell groups; the dorsal lophophore processes (*dlp*) continue to the ventral ganglion (*vg*), the central lophophore processes (*clp*) give rise to processes into the tentacles; 2, as for 1, but in ventral view, the ventral lophophore processes (*vlp*) give rise to processes into the tentacles as the tentacle processes (*tp*); *mo*, mouth (Hay-Schmidt, 1992).

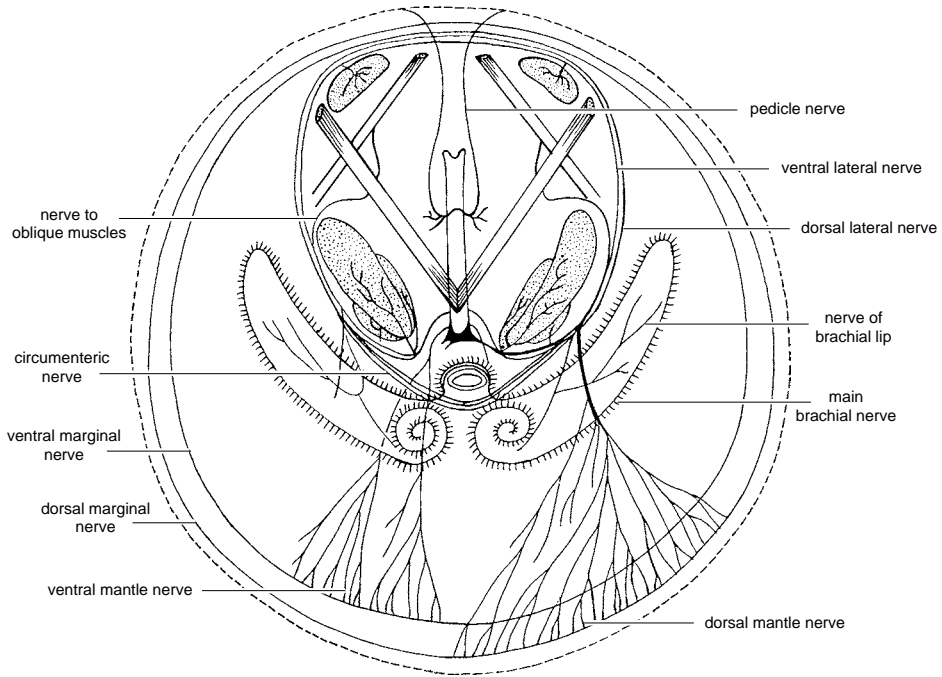


FIG. 126. Diagram of the nervous system of *Discinisca lamellosa* (mante nerves shown only anteriorly) (adapted from Blochmann, 1900).

vascula genitalia, and in some species with arborescent gonads, the *vascula media* (Table 1, p. 134; see also Fig. 71). The craniids are the only inarticulated brachiopods with gonads partially inserted into the mantle canals (HANCOCK, 1859; MORSE, 1873; SCHAEFFER, 1926; SENN, 1934). The disposition of the gonads may be influenced by the flow of water through the mantle cavity (EMIG, 1992) as determined by the architecture of the shell and mantle and the type of lophophore.

The construction of the gonads appears to be similar in all brachiopods and consists of a folded ribbon of connective tissue, the genital lamella, which develops from the membranes supporting the stomach (gastro-parietal bands) and the intestine (ileoparietal bands). Each fold is covered by a germinal epithelium from which the sex cells develop (Fig. 133–134).

The inarticulated *Discinisca lamellosa* possesses two portions of gonad that lie on the

lower surface of the two gastroparietal bands, two more on the triangular ileoparietal bands, and a fifth free in the posterior region of the visceral cavity (JUBIN, 1886). In

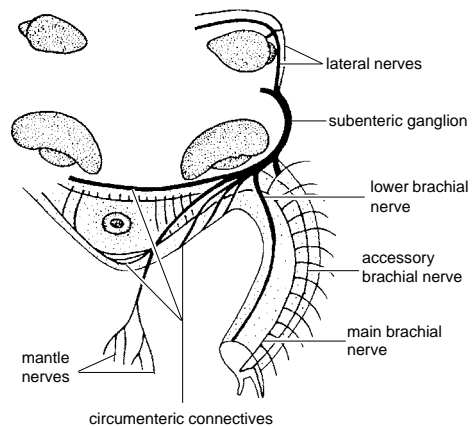


FIG. 127. Diagram of the nervous system of *Neocrania anomala* (mante nerves shown only anteriorly) (adapted from Blochmann, 1892).

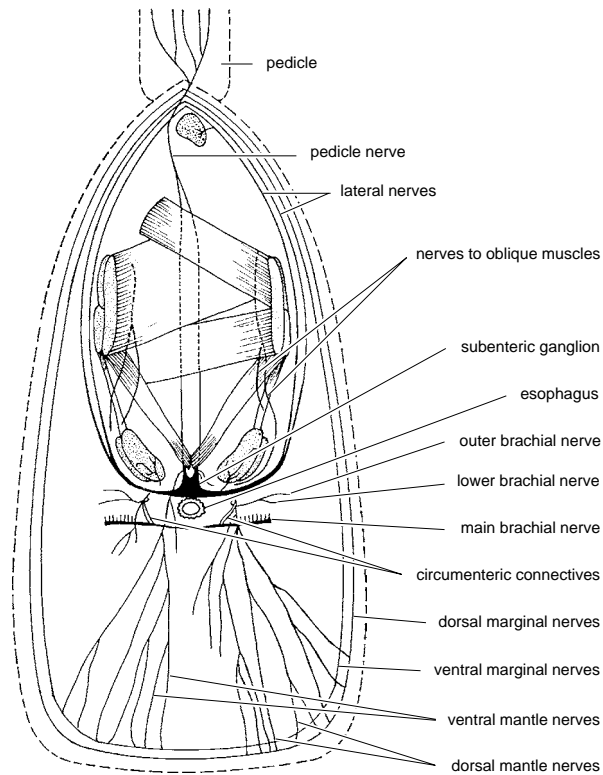


FIG. 128. Diagram of the nervous system of *Lingula anatina* (mantle nerves shown only anteriorly) (adapted from Blochmann, 1900).

young males of *D. laevis*, however, besides the two gonad portions on the lower surface of the gastroparietal bands, a single U-shaped portion of gonad lies on the ventral surface of the ileoparietal bands (CHUANG, 1983b). In adult *Lingula*, in which the germinal epithelium has developed into tufted lobes and lobules, the muscles crossing the body cavity partly separate each gonad into a dorsal mass of lobes in the ileoparietal band anchored to the sides of the stomach, while ventral masses on the same side of the visceral cavity remain connected by a small strand of apparently sterile ileoparietal band (CHUANG, 1983a, 1983b). Consequently *Lingula* has been reported as having four gonads (JOUBIN, 1886) or gonads in four groups (SCHAEFFER, 1926; SENN, 1934). Because of the physical continuity of the connective tissue band, all of the folds of the

genital lamella on one side of the body are regarded as constituting a single gonad (CHUANG, 1983a, 1983b). In *Lingula* the posterior part of the gastroparietal band is a flat ribbon of connective tissue attached along its medial edge to the lateral wall of the stomach, its lateral edge hanging freely in the dorsal region of the visceral cavity. Posteriorly the band of connective tissue bifurcates into medial and lateral bands. The medial band fuses with its counterpart from the other side of the stomach to form a single horizontal membrane that proceeds posteriorly from the ventral body wall of the posterior end of the stomach and becomes attached to the posterior body wall. The lateral band on each side curves ventrally and continues anteriorly and has its lateral edge fused to the medial wall of the metanephridium. The medial edge of this band lies free in the

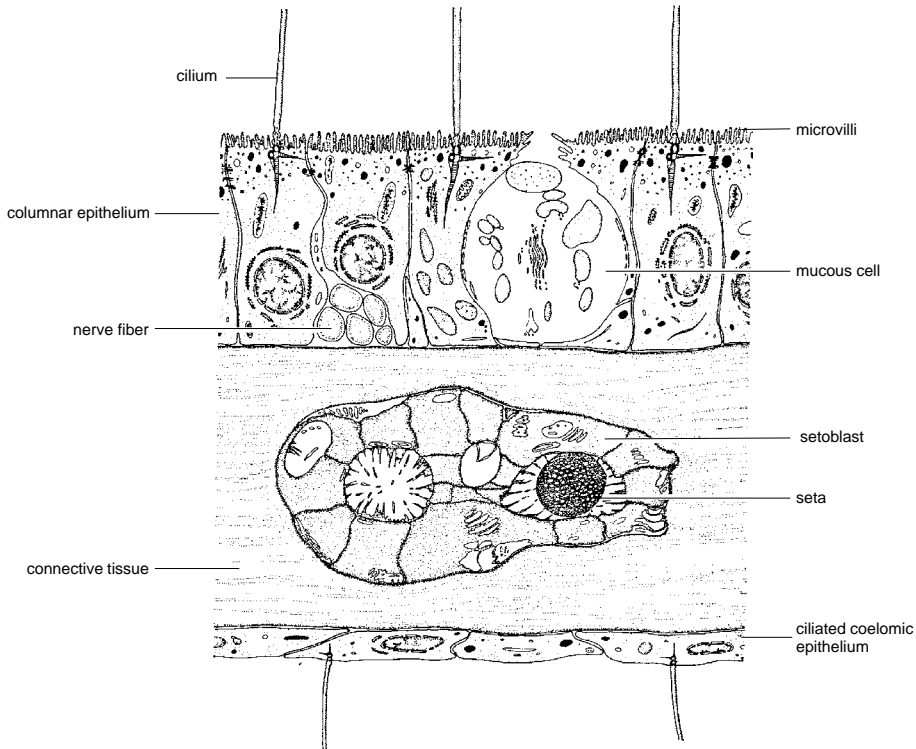


FIG. 129. Diagrammatic cross section through the periphery of the inner mantle membrane of *Terebratulina* (adapted from James & others, 1992).

ventral region of the visceral cavity (CHUANG, 1983a, 1983b). *Glottidia albida* and *G. pyramidata* also have right and left gonads, which occur along the continuous ileo-parietal bands (CHUANG, 1983a, 1983b).

In *Neocrania anomala* the gonads occur in six portions, two in the visceral cavity and a pair in each mantle (Joubin, 1886). Genital lamellae develop only on the inner mantle membrane of the mantle canals of articulated brachiopods and the inarticulated *Neocrania*. The connective tissue fold of the parietal band is fused throughout its length along one margin to the inner mantle membrane, with the remainder of the tissue fold projecting into the mantle canal or *vascula genitalia* (Fig. 135).

In articulated brachiopods and *Neocrania* the genital lamella is sacciform proximal to

the point of fusion with the inner mantle membrane, but in more distal regions adjacent folds are knit together with strands of connective tissue. The distended portions of the genital lamellae (Fig. 133, 136) form an anastomosing network that is traceable to the heart above the stomach and is believed to form part of the vascular (circulatory) system (CHUANG, 1983a; see section on coelomic and circulatory system, p. 69).

The morphology of the gonads ranges from the lobes of pleated ribbons of genital tissue found in *Lingula* (Fig. 137.4) to the complex reticular patterns that occur in some articulated brachiopods (Table 1, p. 134; Fig. 137.1–137.2). In those articulated species where the *vascula genitalia* are extensive and the genital lamellae form palmate reticulate lattices, the inner and outer mantle

membranes are periodically joined by pillars of connective tissue (Fig. 133; JAMES, ANSELL, & CURRY, 1991b). The genital lamellae of less complex genital morphologies may simply be separated by bands of connective tissue that unite the inner and outer membranes (JAMES & others, 1992). In *Neocrania* each extension of the genital lamella is contained in a separate canal within the mantle (Fig. 137.3).

The construction of the genital lamella is relatively uniform throughout the phylum, but the distribution of the germinal epithelium differs between the sexes. Male genital lamellae tend to be ruffled along the distal margin, increasing the surface area for production of gametes. Proliferating clusters of spermatogonia occur at the base of the genital lamella (JAMES, ANSELL, & CURRY, 1991b; JAMES & others, 1992). Subsequent stages in the development of spermatozoa occur more distally and are ultimately displaced by the proliferation of underlying cells, thus forming bands of cells at different developmental stages. Mature spermatozoa occur around the periphery of masses of spermatogenic and spermiogenic cells (Fig. 135.1–135.2; 138; JAMES & others, 1992).

The female genital lamella tends to be columnar with oogonia proliferating at the base of the genital lamella. As vitellogenic oocytes differentiate and enlarge through the accumulation of yolk, they occur on progressively distal regions of the lamella (JAMES, ANSELL, & CURRY, 1991c; LONG & STRICKER, 1991). The apparent migration of these cells is probably caused by elongation of the genital lamella. Eventually the oocytes become detached from the genital lamella and float freely in the coelomic fluid of the *vascula genitalia* where they complete their development prior to spawning. Once the oocytes have been released, it is assumed that the extended lamellar region is phagocytosed, along with any other necrotic material remaining in the gonad after spawning (JAMES, ANSELL, & CURRY, 1991c).

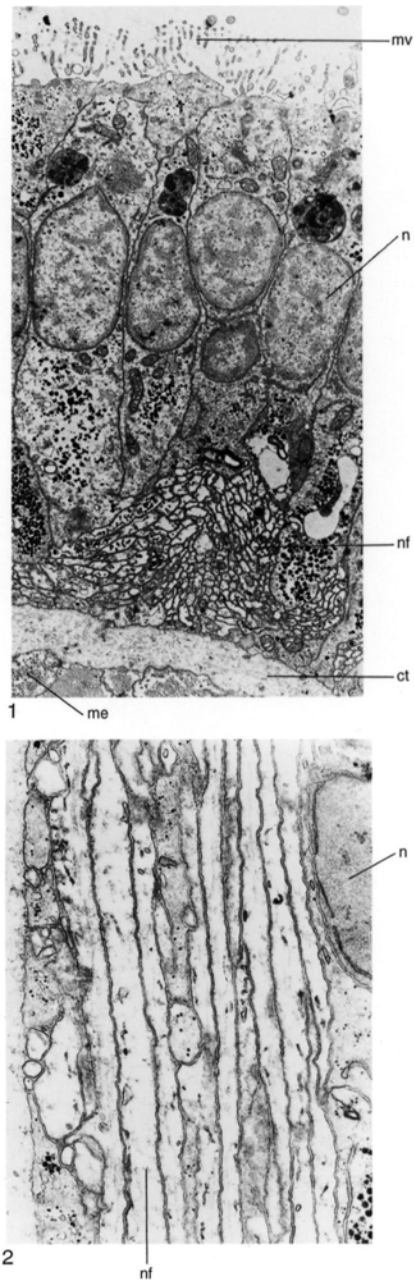


FIG. 130. TEM micrographs of unsheathed bundles of nerve fibers in the tentacles of *Calloria*; 1, transverse section showing the nerve fiber (*nf*) at the base of the epidermal cells with microvilli (*mv*); *n*, nucleus; *ct*, connective tissue; *me*, myoepithelium; 2, longitudinal section of nerve fibers (*nf*); *n*, nucleus, $\times 16,600$ (new).

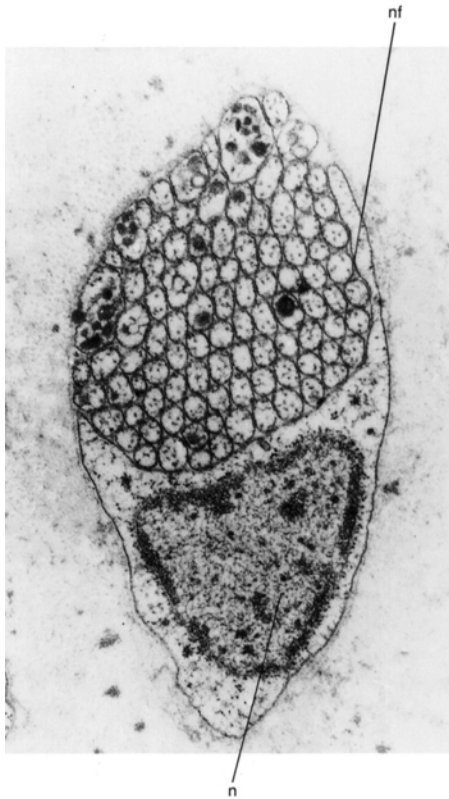


FIG. 131. TEM micrograph of a transverse section of a bundle of unsheathed nerve fibers (*nf*) and nucleated accessory cell in the connective tissue of the pharynx of *Calloria*; *n*, nucleus, $\times 20,000$ (new).

Development of hermaphroditic gonads in brachiopods is well known only for *Calloria* (JAMES, unpublished, 1992). This species generates sperm and eggs on the same genital lamella although the lineage of the germ cells remains unclear. As in gonochoristic species, the germinal cells tend to occur at the base of the genital lamella, with more advanced stages occurring distally. *Calloria* shows considerable reproductive plasticity and appears to be male or female or to display a predominance of male or female reproductive tissue in gonads that are clearly hermaphroditic (Fig. 139; JAMES, unpublished, 1992).

SPERMATOGENESIS

Spermatogenesis in brachiopods is poorly documented, but accounts of the inarticulated *Lingula* (SAWADA, 1973; CHUANG, 1983b) and the articulated *Terebratulina* (JAMES & others, 1992), together with observations of *Calloria* and *Notosaria* (JAMES, unpublished, 1993), suggest that spermatogenesis is similar in these brachiopods.

Spermatogonia generally contain a large, distinct nucleus with condensed chromatin and proliferate from the germinal epithelium at the base of the genital lamella. Spermatogonia give rise to primary spermatocytes that are conspicuously larger than neighboring somatic cells and are attached to the genital lamella. The nucleus of each primary spermatocyte lacks nucleopores and contains sparsely granular chromatin, much of which is condensed against the inner side of the nuclear envelope. The cytoplasm contains clusters of mitochondria, granular and agranular endoplasmic reticulum, and ribosomes. Primary spermatocytes undergo meiosis to produce secondary spermatocytes that have extremely condensed cytoplasmic and nuclear material (Fig. 140).

Secondary spermatocytes undergo a second meiotic division to form spermatids. In the two spermatocyte divisions the various cytoplasmic inclusions are usually distributed equally to the four spermatids, which seems to result from the tendency of such inclusions to be grouped so that cytokinesis separates them equally. Spermatids have less electron-dense cytoplasm than the preceding stage, a spherical nucleus, two centrioles, a Golgi complex, and, posteriorly, one or more pyriform mitochondria, depending on the species.

SPERMIOGENESIS

Spermatids undergo a series of morphological changes as they develop into spermatozoa. Spermatozoa have a head consisting of

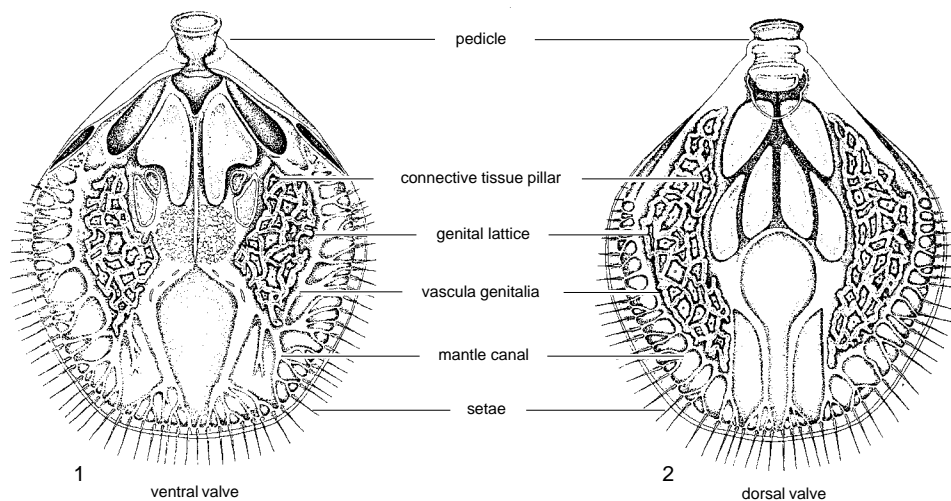


FIG. 132. Diagrammatic surface view of the mantle of the ventral (pedicle) and dorsal (brachial) valves of *Terebratulina retusa*, illustrating the mantle canals and the position and extent of the genital lattice (James, Ansell, & Curry, 1991b).

an acrosome and nucleus, a middle piece containing one or more mitochondria and two centrioles, and a tail (flagellum) (Fig. 141–142).

In *Lingula* (SAWADA, 1973) and probably *Terebratulina* (JAMES, unpublished, 1989), the Golgi complex or smooth endoplasmic reticulum gives rise to the acrosome. In *Lingula*, electron-dense granules are produced by the Golgi complex or smooth endoplasmic reticulum. These granules fuse to form the acrosomal vesicle, which migrates to the definitive pole of the spermatid (SAWADA, 1973). The acrosomal vesicle of *Terebratulina* contains a sparse, finely granular material (JAMES, unpublished, 1989), while in *Lingula* the acrosome contains dense, granular bands (SAWADA, 1973; CHUANG, 1983a). Acrosomes range in size and shape from the subapical, buttonlike acrosome found in *Terebratulina* (AFZELIUS & FERRAGUTI, 1978; JAMES & others, 1992) to the extremely elongate and conical acrosome of *Notosaria* (Fig. 141–142; JAMES, unpublished, 1992).

As spermatozoa mature, the nucleus is transformed from a spherical shape, normal

in spermatocytes and young spermatids, to a more compact body (AFZELIUS & FERRAGUTI, 1978; JAMES & others, 1992). During the later stages of spermiogenesis the nuclear material undergoes condensation accompanied by a reduction in nuclear volume, and residual cytoplasm is discharged (SAWADA, 1973; CHUANG, 1983b; JAMES & others, 1992). The chromatin of spermatozoa is generally homogeneous but finely granular in later stages and may include a small but distinct empty space (Fig. 142.4; FRANZEN, 1987). The nuclear envelope also appears to be differentially thickened wherever it is modified to accommodate other organelles within the head of the sperm.

The mitochondrion of *Terebratulina*, *Calloria*, *Notosaria*, and *Terebratella sanguinea* enlarges to form an asymmetrical, doughnut shape. *Lingula* and *Neocrania* usually possess six and four spherical mitochondria, respectively, which develop around the base of the nucleus. Both of the centrioles come to lie to the posterior of the cell in the center of the mitochondrial ring. Most invertebrate spermatozoa have two centrioles, the

TABLE 1. Summary of the shapes of gonads of articulated brachiopods (adapted from Chuang, 1983b).

Gonad shape	Family	Species	
Unbranched	L-shaped	Megathyridae	<i>Argyrotheca johnsoni</i>
			<i>A. baretti</i>
Arborescent	U-shaped	Terebratulidae	<i>Terebratella sanguinea</i>
			<i>Magellania australis</i>
			<i>M. macquariensis</i>
			<i>Terebratella dorsata</i>
			<i>Calloria inconspicua</i>
		Gyrothyris	<i>Gyrothyris mawsoni</i>
		Neothyris	<i>Neothyris lenticularis</i>
		Dallinidae	<i>Frenulina sanguinolenta</i>
			<i>Macandrevia cranium</i>
			<i>Terebratalia transversa</i>
	Laqueidae	<i>Laqueus californianus</i>	
	Cranidae	<i>Neocrania anomala</i> ¹	
Reticulate	Hemithyridae		<i>Hemithyris psittacea</i>
			<i>Notosaria nigricans</i> ¹
		Frieleidae	<i>Frieleia halli</i>
		Terebratulidae	<i>Liothyrella blochmanni</i>
			<i>L. notocardensis</i>
		<i>L. neozelanica</i> ¹	
		<i>Abyssothyris elongata</i>	
		<i>Terebratulina retusa</i> ¹	
Ovoid	Basiloliidae	<i>Neorhynchia profunda</i>	

¹adapted from James & others, 1992

proximal or anterior and the distal or posterior (FRANZEN, 1987). In *Terebratulina* the proximal centriole is in approximately the

same longitudinal axis as the distal one, whereas in *Neocrania* and *Lingula* it is transverse (CHUANG, 1983b). The nucleus may be modified posteriorly by invagination of the nuclear membrane to accommodate the proximal centriole. The distal centriole is oriented longitudinally and associated with the tail (Fig. 143).

The distal centriole of *Terebratulina* is suspended in a complex, fiber-anchoring apparatus with nine primary branches that bifurcate and fuse with their neighbors to form a stellate, satellite-like figure (AFZELIUS & FERRAGUTI, 1978). *Lingula* and *Neocrania* appear to have similar but less complex structures that consist of a series of tubules radiating from the distal centriole (SAWADA, 1973; CHUANG, 1983b). The fiber-anchoring complex is generally thought to be an anchor for the basal body of the tail. It enables the centrioles to resist the torque generated by the movement of the tail. The satellite complex may also transport ATP from the mitochondria to the tail (SUMMERS, 1970). The sperm of *Lingula* contain deposits of glycogen (SAWADA, 1973; JAMES, unpublished, 1993), whereas in *Terebratulina* this storage compound is absent (JAMES & others, 1992). It has been suggested that the energy necessary to drive the swimming activity of sperm that lack glycogen is derived from the oxida-

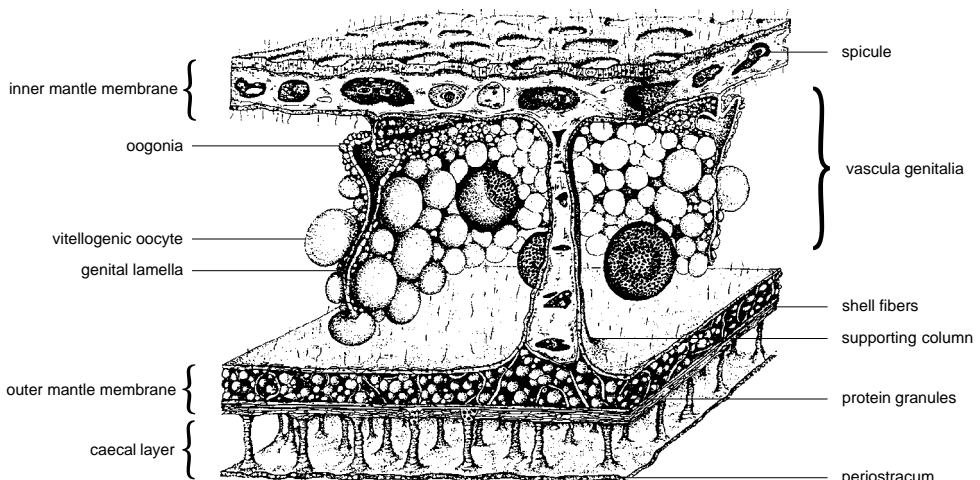


FIG. 133. Diagrammatic representation of a vertical section through the mantle of *Terebratulina retusa* showing part of an ovary and the mantle membranes (James, Ansell, & Curry, 1991b).

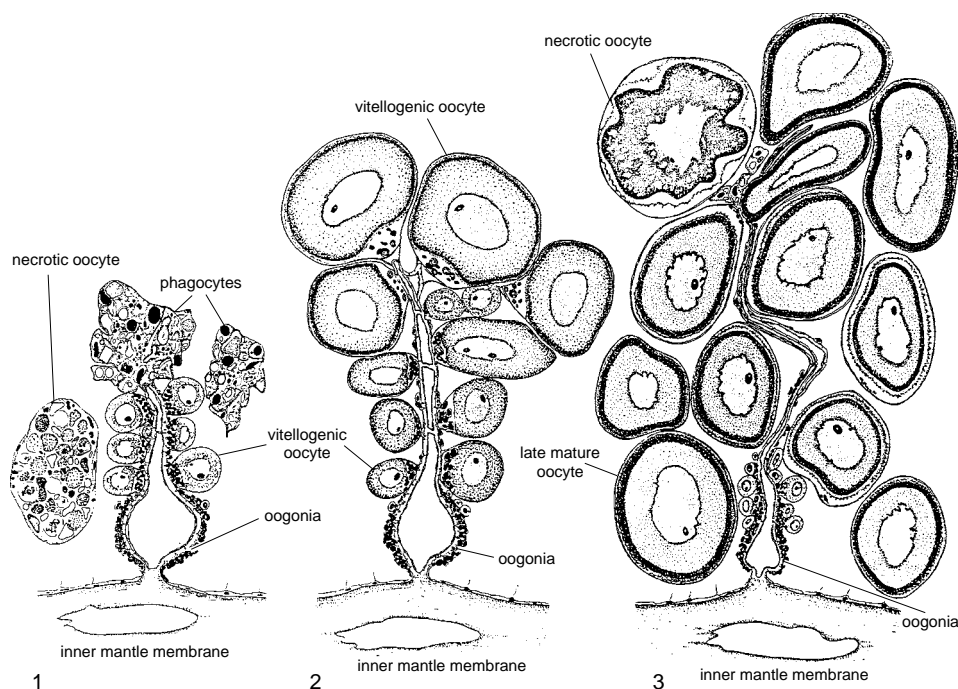


FIG. 134. Diagrammatic series illustrating the changes that occur during the development of the genital lamella and associated oocytes of *Terebratulina retusa*; 1, recently spawned individual; unspawned oocytes and necrotic genital tissues are phagocytosed, while the next generation of vitellogenic oocytes develop beneath; 2, the genital lamella extends as the vitellogenic oocytes increase in size; 3, a mature genital lamella; late stage vitellogenic oocytes have separated from the genital lamella and float freely in the *vascula genitalia* where they complete their development prior to spawning (James, Ansell, & Curry, 1991b).

tion of mitochondrial phospholipids (AFZELIUS & MOHRI, 1966).

The tail of the sperm issues from this anchoring complex, initially as peripheral microtubules, the central doublet appearing to originate from a more distal region. Tails of brachiopod sperm contain the familiar 9+2 arrangement of axonemes, but in *Neocrania* the tapering distal portion of the tail contains 9+2 single microtubules (AFZELIUS & FERRAGUTI, 1978).

Spermatozoan structure is generally related to the physiological demands of the fertilization environment (FRANZEN, 1956; AFZELIUS, 1979). Brachiopods have sperm of the ectoaquasperm type (ROUSE & JAMIESON, 1987), which is typical of animals that engage in external fertilization (FRANZEN, 1982). The shape and size of the head of brachiopod sperm, however, vary considerably (Fig. 143; Table 2, p. 144).

OOGENESIS

Precocious germ-cell determination due to the localization of a morphologically distinct germ plasm has been reported in the eggs of a number of invertebrates including brachiopods (see WOURMS, 1987). Primary germ cells are distinguishable by their large size from the coelomic epithelium of the ileoparietal band in *Lingula* larvae at the stage of eight pairs of tentacles (abbreviated p.t. hereinafter) (YATSU, 1902a, used the term: pairs of cirri—p.c.). In *Terebratulina*, *Calloria*, *Notosaria* (JAMES, unpublished, 1993), *Lingula* (SCHAEFFER, 1926), *Frenulina*, and other brachiopods studied by CHUANG (1983a), no transitional forms between germ cells and coelomic epithelium have been found, which suggests that primordial germ cells are differentiated early in ontogeny (Fig. 144; YATSU, 1902a; SCHAEFFER, 1926; CHUANG, 1983b; JAMES, ANSELL,

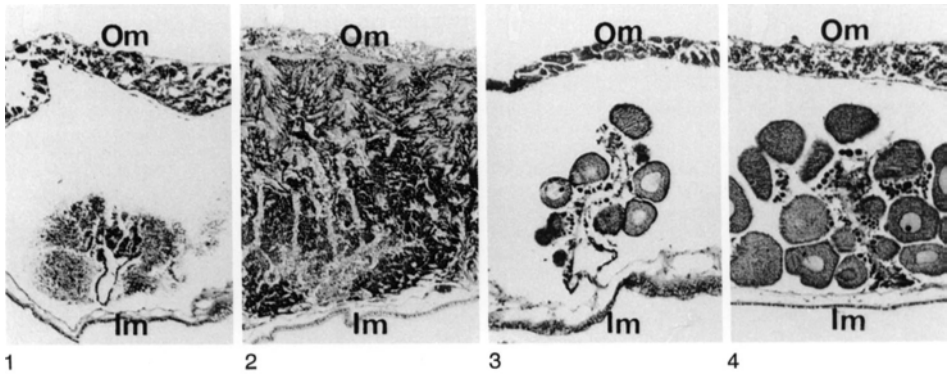


FIG. 135. Light micrographs of transverse sections of *Terebratulina retusa*; 1, immature testis; 2, mature testis; 3, immature ovary; 4, mature ovary, scale bar: 50 μ m; *Im*, inner mantle; *Om*, outer mantle (James, Ansell, & Curry, 1991b).

& CURRY, 1991c). A number of earlier reports, however, are contradictory and suggest that germ cells are derived from coelomic epithelium (BEMMELEN, 1883; JOUBIN, 1886; BLOCHMANN, 1892; LONG, 1964).

Primary oogonia occur at the base of the genital lamella proximal to the inner mantle membrane and contain cytoplasm and a nucleus of homogeneous electron density and relatively indistinct organelles (Fig. 145.1; JAMES, ANSELL, & CURRY, 1991c; JAMES, unpublished, 1993). Each cell is separated from its neighbor by the fine cytoplasmic processes of the coelomic epithelial cells. Primary oogonia undergo mitotic division to produce secondary oogonia that in turn divide meiotically to become primary oocytes (JAMES, ANSELL, & CURRY, 1991c). The early prophase changes of meiosis in brachiopod oocytes have not been observed, but all of the oocytes so far studied have been at the diplotene stage, an arrested stage of development, during which the oocyte undergoes vitellogenesis (the accumulation of yolk) (LONG, 1964; JAMES, ANSELL, & CURRY, 1991c; LONG & STRICKER, 1991).

The processes of vitellogenesis have been interpreted for the articulated *Terebratalia transversa* (LONG, 1964), *Frenulina* (CHUANG, 1983a), *Terebratulina* (JAMES, ANSELL, & CURRY, 1991c), *Calloria*, and *Notosaria* (JAMES, unpublished, 1993) and

for the inarticulated *Lingula* (SAWADA, 1973; CHUANG, 1983a), *Discinisca*, and *Neocrania* (CHUANG, 1983a). Vitellogenesis has been divided into a series of stages, which have been defined according to the occurrence and distribution of yolk granules (Fig. 146; LONG, 1964; CHUANG, 1983a; JAMES, ANSELL, & CURRY, 1991c) and ultrastructural development of the vitellogenic oocyte and associated cells (Fig. 145; JAMES, ANSELL, & CURRY, 1991c; see summary by JAMES & others, 1992).

Vitellogenic oocytes are usually enveloped by a single layer of several extremely thin follicular cells (JAMES, unpublished, 1993) that are assumed to be modified coelomic epithelial cells (CHUANG, 1983a) and, in some species, may be highly modified (JAMES, unpublished, 1993). CHUANG (1983a) reported the occurrence of several layers of follicular cells in some species. The vitellogenic oocyte is identifiable from an early stage and possesses a nucleus containing condensed chromatin and a conspicuous nucleolus. The ooplasm of early vitellogenic oocytes contains discrete and evenly distributed ribosomes with organelles such as mitochondria and endoplasmic reticulum proliferating in what appear to be defined areas (CHUANG, 1983a; JAMES, ANSELL, & CURRY, 1991c). Small numbers of lipid and membrane-bound, electron-dense (proteina-



FIG. 136. SEM micrograph of a transverse section through the base of the genital lamella of the ovary of *Dallina septigera*, $\times 480$; *bv*, blood vessel; *gl*, genital lamella; *ime*, inner mantle epithelium; *vg*, vascula genitalia; *vo*, vitellogenic oocyte (new).

ceous) granules may also be present. In regions where the follicle cells are not in close apposition to the surface of the oocyte, sections of the oocyte plasmalemma (oolemma) form simple digitate microvilli. While the order in which these events occur may vary, this pattern of early vitellogenesis has been observed at the ultrastructural level in a number of species, including *Terebratulina*, *Calloria*, *Notosaria* (JAMES, unpublished, 1993), and *Frenulina* (CHUANG, 1983a).

Currently available evidence, however, suggests that brachiopods have at least three distinct modes of vitellogenesis, follicular, nutritive, and mixed, which broadly define the mechanisms used to accumulate yolk (SENN, 1934; JAMES, unpublished, 1993) in the following way.

(1) Follicular vitellogenesis has been reported in *Neocrania*, *Lacazella*, *Macandrevia*

cranium, *Argyrotheca cuneata*, *Terebratalia*, and numerous other brachiopods (SENN, 1934; LONG, 1964; LONG & STRICKER, 1991). The ultrastructure of follicular vitellogenic oocytes is unknown, but light microscopy indicates that the follicular cells are unmodified, and the oocyte develops a microvillous surface. Follicular vitellogenic oocytes are not directly associated with nurse or accessory cells (see below).

(2) Nutritive vitellogenesis occurs in *Lingula* (SENN, 1934), *Calloria*, *Notosaria* (JAMES, unpublished, 1993), and *Frenulina* (Fig. 147.1; CHUANG, 1983a). Vitellogenic oocytes are surrounded by a variably complex follicular envelope that is closely associated with large somatic cells, particularly during the early stages of development. The somatic cells contain a diminutive nucleus and few organelles but are packed with

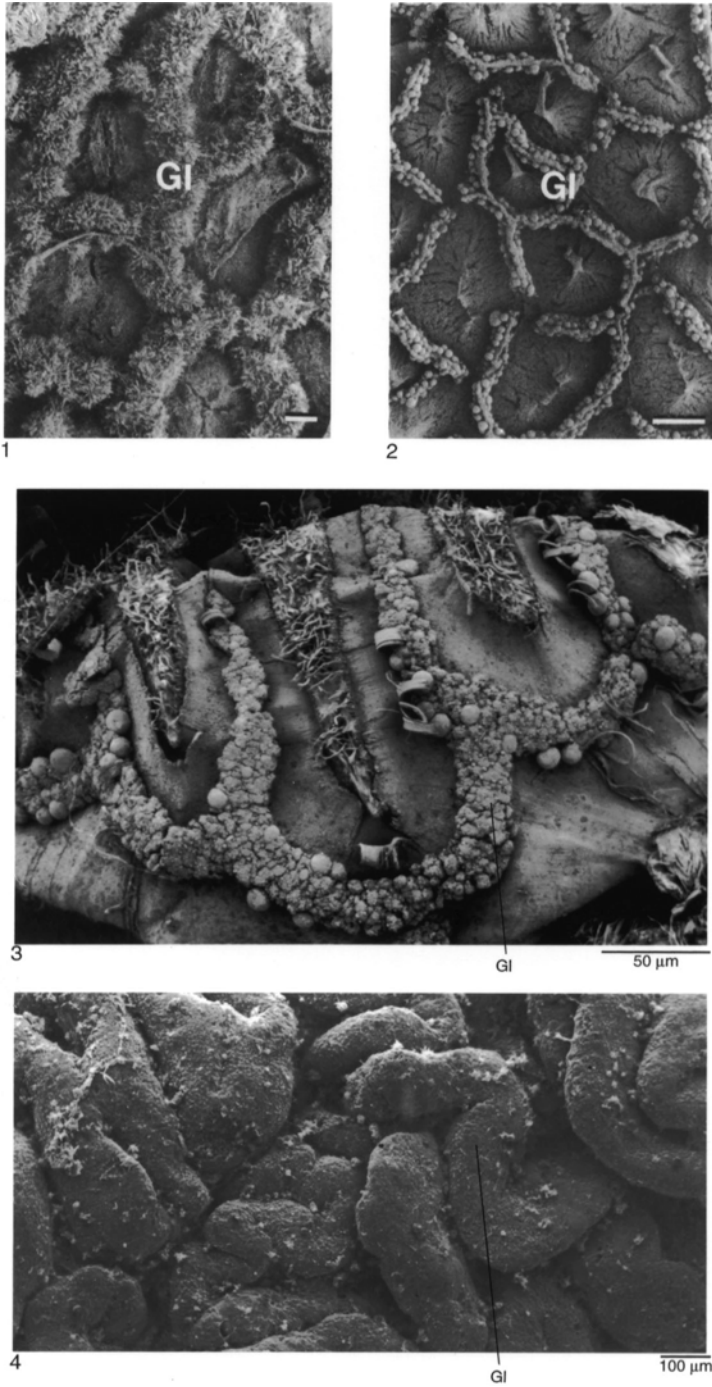


FIG. 137. SEM micrographs of surface views of the genital lamellae (*Gl*) of 1, *Terebratulina retusa*, testis, scale bar: 200 µm, 2, ovary, scale bar: 200 µm (James, Ansell, & Curry, 1991b); 3, *Neocrania anomala*, ovary, scale bar: 50 µm; 4, *Lingula anatina*, ovary, scale bar: 100 µm (new).

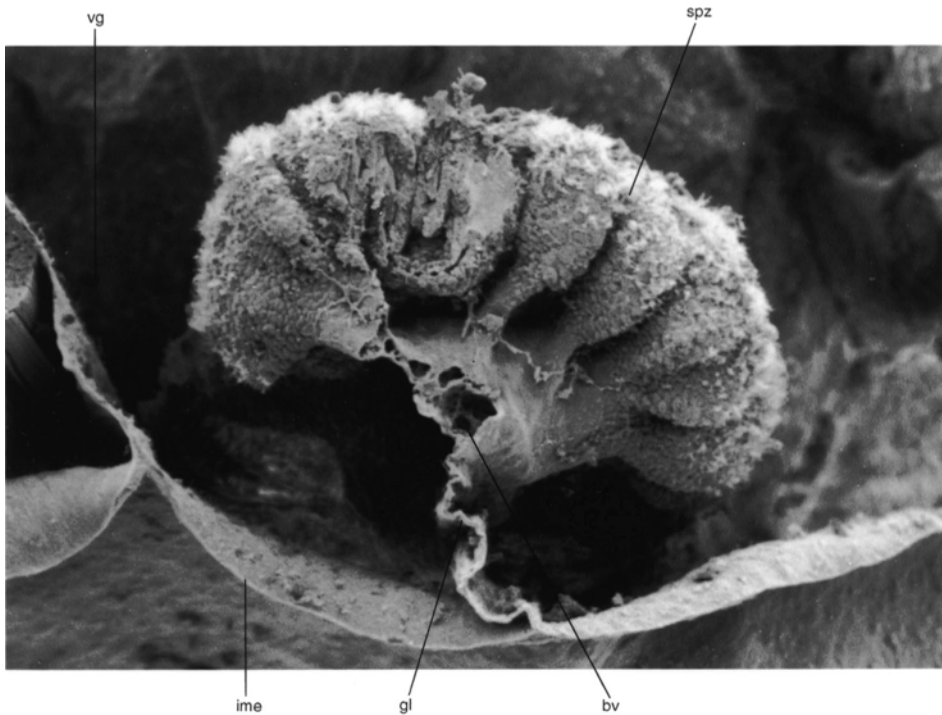


FIG. 138. SEM micrograph of a transverse section through the genital lamella of a male *Dallina septigera*, $\times 130$; *bv*, blood vessel; *gl*, genital lamella; *ime*, inner mantle epithelium; *spz*, spermatozoa; *vg*, vascula genitalia (new).

profuse quantities of glycogen and large, electron-dense granules. These nurse or nutritive cells can be seen most prominently in *Lingula* and *Calloria* where they form a distinctive palisade covering the surface of the genital lamella (Fig. 148).

The oocytes produce dense but simple branched or digitate microvilli of uniform length (Fig. 149). The follicular cells, however, may be modified. In *Calloria*, *Notosaria*, *Terebratella* (JAMES, unpublished, 1993), and *Lingula* (SAWADA, 1973), the follicular cells produce papillose extensions of their inner plasmalemma, which attach to the surface of the oocyte with desmosome-like gap junctions (Fig. 147.1; 149.1). Dense concentrations of glycogen may occur both within the follicular cells and between the microvilli of the oocyte and the follicular cells. Oocytes of this type, however, have not been observed to engage in pino- or endocytosis (CHUANG, 1983a).

In addition to papillose connections between the follicular cells and the vitellogenic oocyte, *Lingula* has serially banded strands that pass between the microvilli of the oocyte and the surrounding follicular cells (SAWADA, 1973). These strands form a fibrous matrix around the oocyte, but their function is unknown (Fig. 150).

Based on morphological evidence, the complex follicular cells are presumed to play a role in the synthesis of heterosynthetic yolk precursors or to regulate the transfer of these materials to the vitellogenic cell.

(3) Mixed vitellogenesis has been observed only in the terebratulids *Terebratulina* (JAMES, ANSELL, & CURRY, 1991c) and *Gryphus vitreus* (Fig. 147.2; BOZZO & others, 1983). Vitellogenic oocytes of *Terebratulina* develop in association with a series of accessory cells within an envelope of follicular cells, the follicular capsule (Fig. 145, 151).

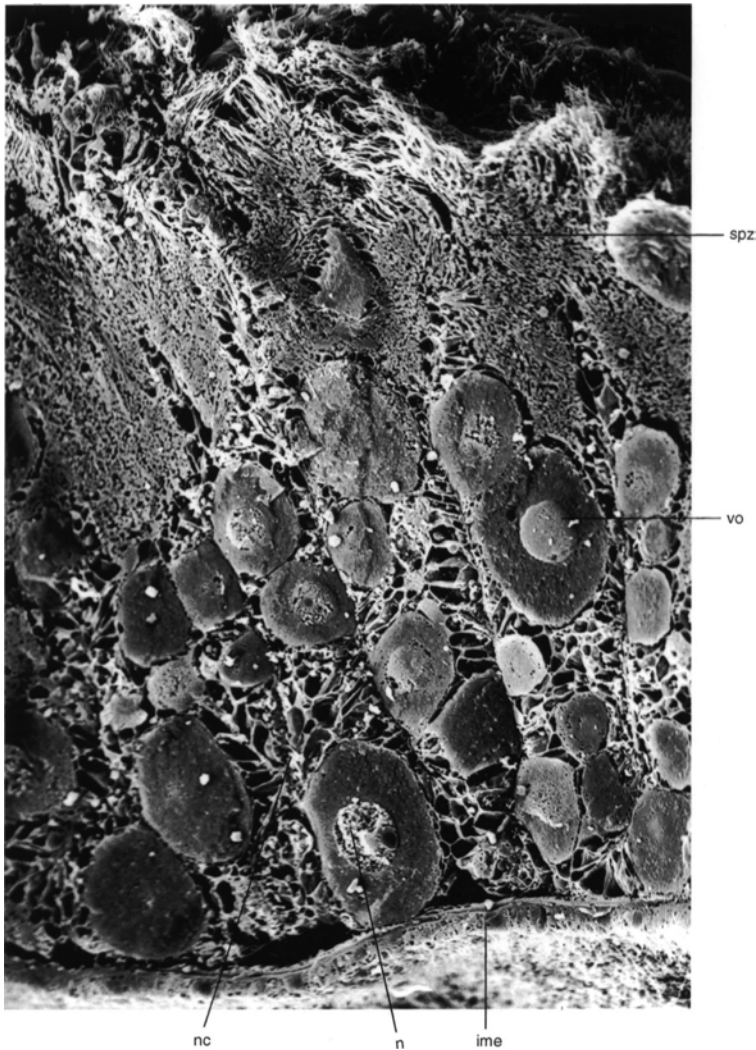


FIG. 139. SEM micrograph of a transverse section through the hermaphroditic gonad of *Calloria inconspicua*, $\times 300$; *ime*, inner mantle epithelium; *n*, nucleus; *nc*, nutritive cells; *vo*, vitellogenic oocyte (new).

The origin of accessory cells is unclear, but they are capable of proliferation and resemble small, vitellogenic oocytes. Accessory cells communicate with other accessory cells and the vitellogenic oocyte via desmosome-like gap junctions. Cytoplasmic bridges may also occur between accessory cells (JAMES, ANSELL, & CURRY, 1991c).

The function of accessory cells appears to be to supply the vitellogenic oocyte with nutrients, probably low-molecular-weight yolk precursors, which are first synthesized in

the accessory cell. In contrast to the less complex microvillous surface of oocytes engaged in follicular or nutritive vitellogenesis, the surface of the mixed vitellogenic oocyte is elaborated into a series of troughs and crests covered in highly modified microvilli (Fig. 152). Beneath the modified microvilli, the oolemma endocytoses yolk precursors. The enveloping follicular capsule consists of simple, follicular cells that make no connection with the vitellogenic oocyte. During the initial stages of vitellogenesis, accessory cells

proliferate and begin to accumulate small numbers of yolk granules, while the surface of the vitellogenic oocyte becomes sparsely microvillous. As vitellogenesis proceeds, the density and complexity of the microvilli increase until the microvilli effectively dissociate from the surface of the cell to form a characteristic pattern of crests and troughs (Fig. 152.2–152.3). The accessory cells gradually diminish in both size and number. Eventually the follicular capsule containing the vitellogenic oocyte and the remaining accessory cells is released from the genital lamella (JAMES, ANSELL, & CURRY, 1991c).

YOLK

Invertebrate carbohydrate yolk reserves include glycogen, galactogen, and various polysaccharide-protein complexes. Lipid reserves include fatty yolk globules, phospholipids, and triglycerides. Protein accumulations occur in the form of membrane-bound inclusions or platelets, lipoproteins, phosphoproteins (e.g., vitellogenins), and protein

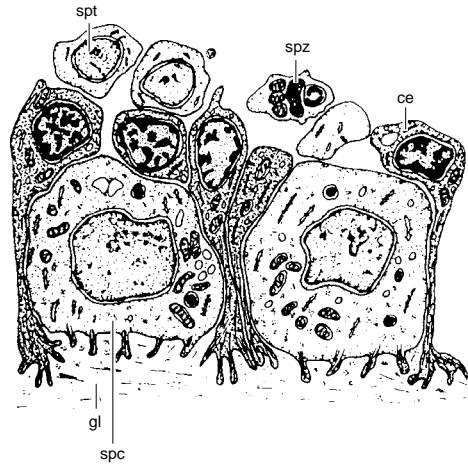
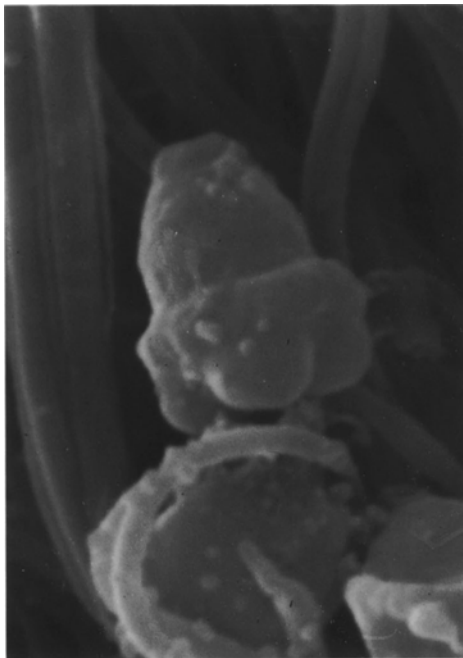
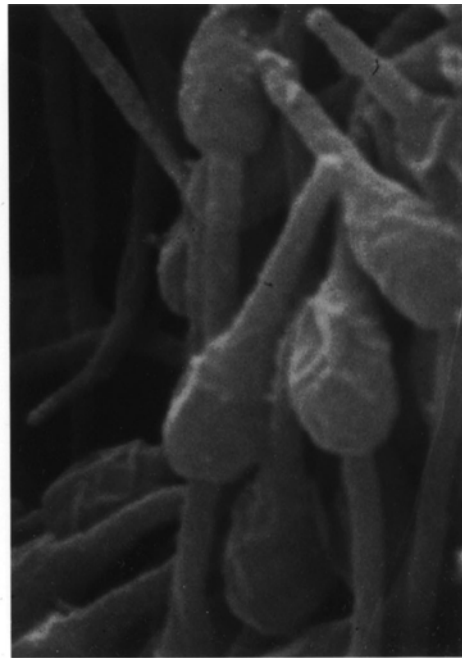


FIG. 140. Drawing of the genital lamella (*gl*) with coelomic epithelium (*ce*), spermatocyte (*spt*), spermatid (*spz*), and spermatozoon (*spz*). Note the pedal processes of cells attached to the genital lamella (adapted from Chuang, 1983b).

polysaccharide complexes (WOURMS, 1987). The biochemical nature and synthesis of brachiopod yolk is not well known.



1

1.0 μ m

2

1.0 μ m

FIG. 141. SEM micrograph of sperm heads of 1, *Lingula anatina*, scale bar: 1.0 μ m; 2, *Notosaria nigricans*, scale bar: 1.0 μ m (new).

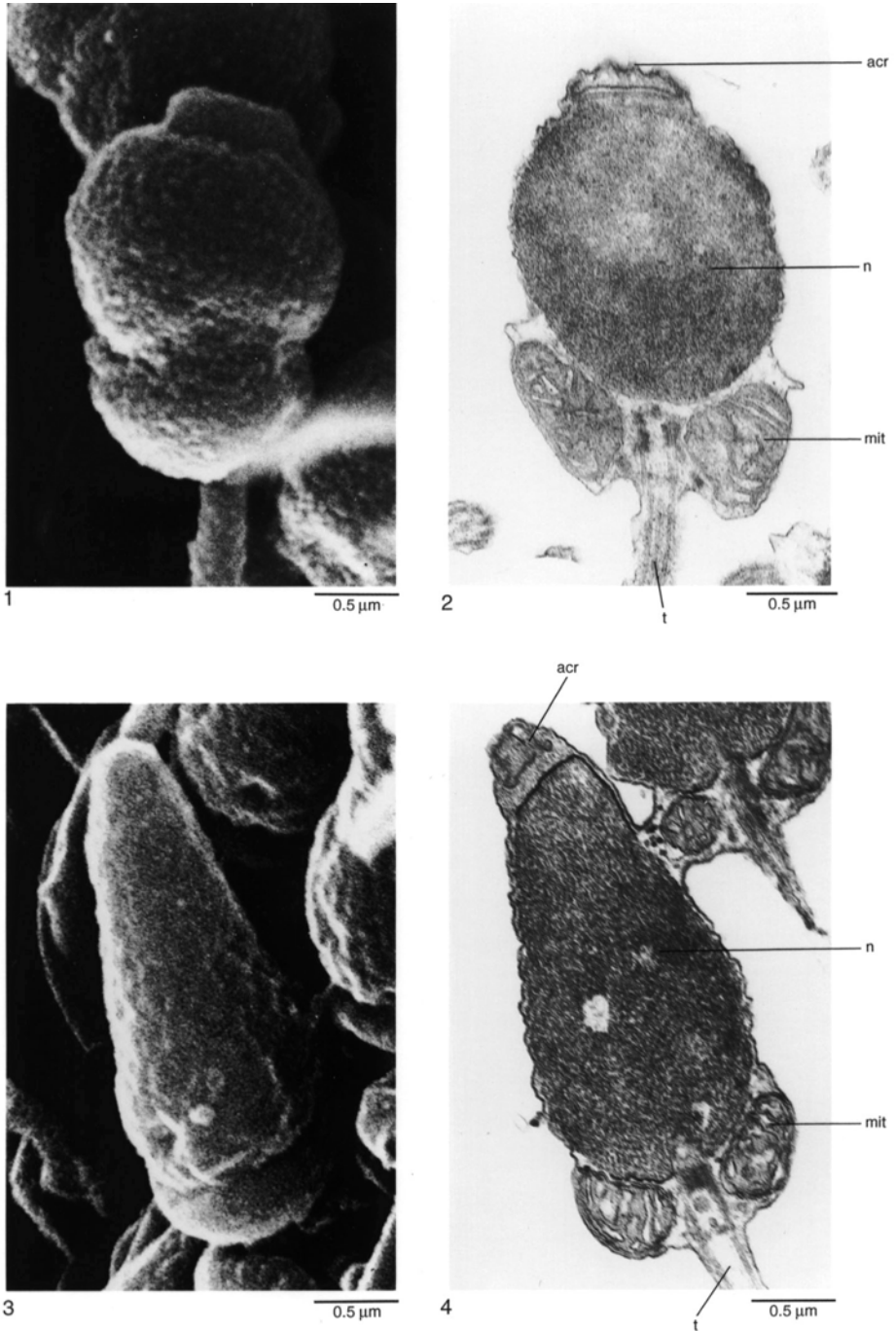


FIG. 142. SEM and TEM micrographs of sperm heads of 1–2, *Terebratulina retusa*, scale bar: 0.5 μm; 3–4, *Calloria inconspicua*, scale bar: 0.5 μm; *acr*, acrosome; *mit*, mitochondrion; *n*, nucleus; *t*, tail (new).

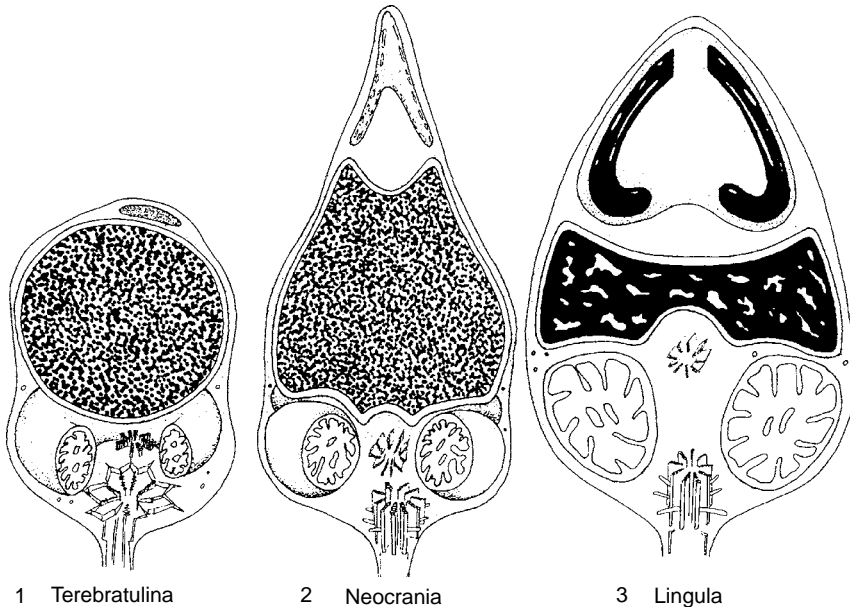


FIG. 143. Drawings of the spermatozoa of 1, *Terebratulina retusa*, 2, *Neocrania anomala*, and 3, *Lingula anatina* (adapted from Afzelius & Ferraguti, 1978; Chuang, 1983b).

Typically, yolk contains lipid droplets or granules, proteinaceous membrane-bound granules, cortical granules, glycogen, and a suite of cellular organelles that, if not involved directly in yolk synthesis, are stored for use after the egg has been fertilized. Glycogen is a prominent constituent of the ooplasm of *Terebratulina* (JAMES, ANSELL, & CURRY, 1991c), *Calloria*, *Notosaria*, and *Lingula* (JAMES, unpublished, 1993).

Lipid droplets or granules form a significant proportion of the volume of the yolk of brachiopods (LONG, 1964; CHUANG, 1983a; JAMES & others, 1992). In *Terebratalia* this lipid is believed to be neutral and not phosphorylated (LONG, 1964). Lipid granules or droplets lack a limiting membrane and are often enveloped by profiles of endoplasmic reticulum (Fig. 153; JAMES, ANSELL, & CURRY, 1991c).

As brachiopod oocytes mature, cortical granules form a distinctive band at the periphery of the oocyte. Cortical granules are membrane bound with either uniformly

electron-dense contents, as in *Terebratulina*, or a structured, internal matrix, as seen in *Terebratella* and *Gryphus* (Fig. 154; BOZZO & others, 1983). The cortical granules of *Terebratalia* contain tyrosine, basic amino acids, and sulphhydryl groups (Chevremont method) but do not stain for nucleic acids or with Periodic Acid Schiffs (PAS) (LONG, 1964). In *Terebratulina*, cortical granules have a proteinaceous component and give a positive reaction with PAS. Other proteinaceous yolk granules, which are distributed throughout the ooplasm, are also bounded by a continuous membrane. It has been suggested that some of these proteinaceous granules undergo a process of maturation and migration to become cortical granules (JAMES & others, 1992). Cortical granules are usually involved in the formation of a fertilization membrane at the time of penetration by the sperm. The function of cortical granules in brachiopods, however, is unclear. The cortical granules of *Terebratalia* (LONG & STRICKER, 1991), for example, are

TABLE 2. Summary of data of spermatozoan morphology (new).

Species	Head shape	Head length (μm)	Tail length (μm)	Number of mitochondria	Type of mitochondria	Authority
<i>Terebratulina retusa</i>	bullet	2.3	50	1	doughnut	Afzelius & Ferraguti, 1978
<i>T. unguicula</i>		1.9	30			Long, 1964
<i>Notosaria nigricans</i>	elongate	3.8		1	doughnut	James, unpublished
<i>Hemithiris psittacea</i>	elongate	4.3 ¹	30			Long, 1964
<i>Calloria inconspicua</i>	conical	3.0		1	doughnut	James, unpublished
<i>Terebratella sanguinea</i>	bullet	2.0		1	doughnut	James, unpublished
<i>Terebratalia transversa</i>		2.1	30			Long, 1964
<i>Neocrania anomala</i>	conical	3.0		4–5	spherical	Chuang, 1983
<i>Lingula anatina</i>	conical	2.0	40	5–7	spherical	Senn, 1934

¹4.3 μm long using light microscopy; noted a 2.2 μm acrosomal so-called filament in addition to the 2.1 μm head.

not discharged during fertilization but are retained near the surface of the ectodermal cells until late in the life of the larva. The origin, biochemical composition, and func-

tion of these nonsecretory, cortical granules are unknown (SCHEUL, 1978).

Ribosomes are also conspicuous components of the ooplasm, particularly during the

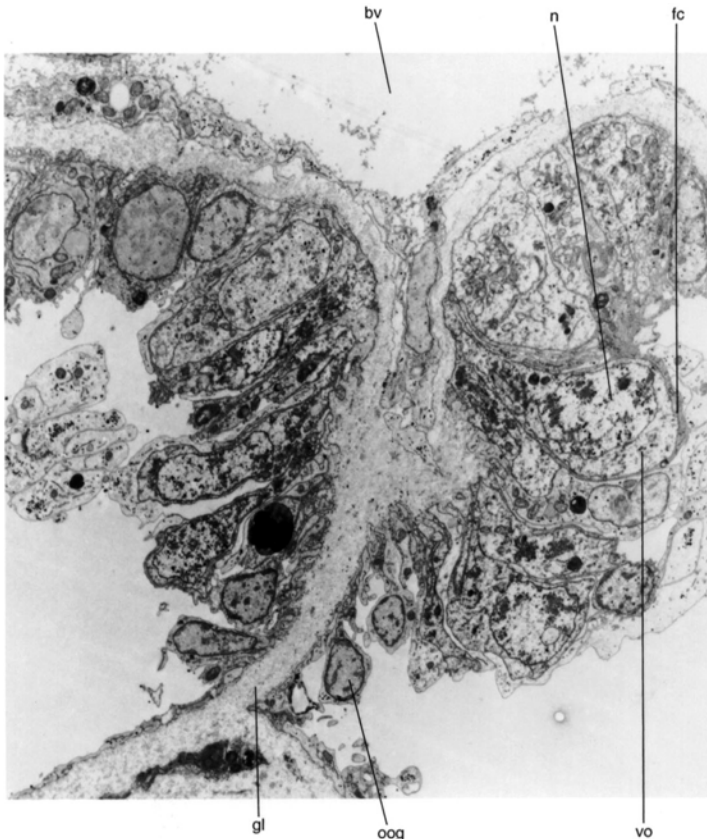


FIG. 144. TEM micrograph of the base of the genital lamella of *Notosaria nigricans* showing the discontinuity between the coelomic epithelium and the mass of proliferating gametes, $\times 2,184$; *bv*, blood vessel; *fc*, follicular cell; *gl*, genital lamella; *n*, nucleus; *oog*, oogonia; *vo*, vitellogenic oocyte (new).

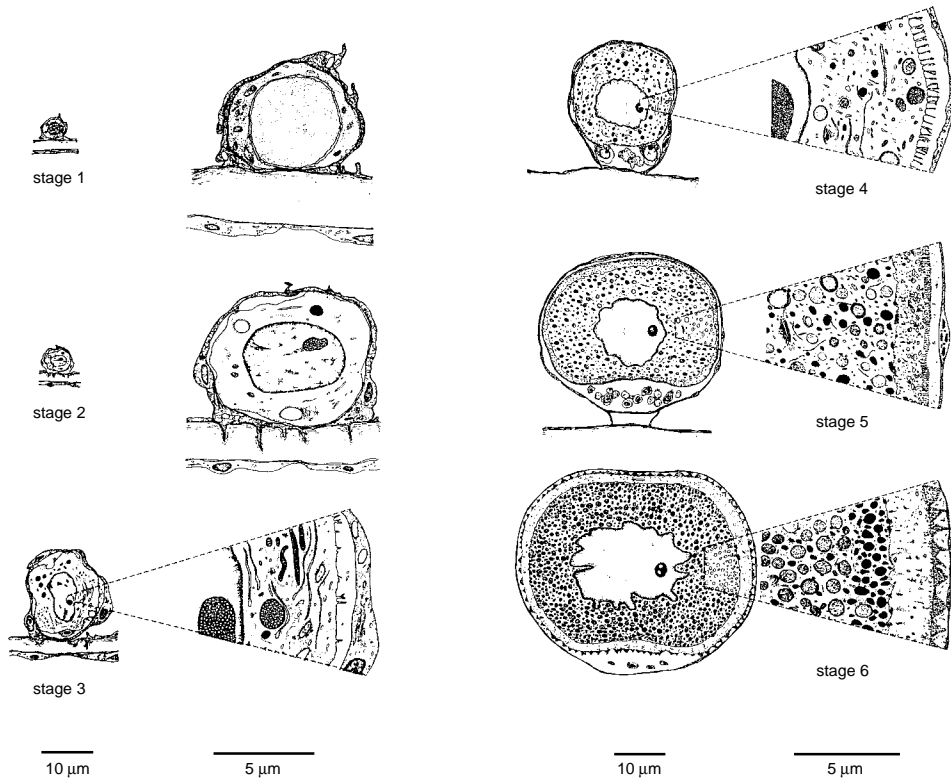


FIG. 145. Diagrammatic representation of stages 1 to 6 of vitellogenesis in *Terebratulina retusa* with all or a portion of each stage on the right enlarged to show features of the ooplasm and the microvillous fringe. Stages 1 to 5 are attached to the genital lamellae; stage 6 oocytes float freely in the *vascula genitalia*, and continue to increase in size; all stages are enveloped by follicular cells and each stage is marked by increasing complexity of the microvillous border of the vitellogenic oocyte; at stages 3 and 4, accessory cells appear and begin to proliferate; darker granules in the ooplasm represent proteinaceous and ultimately cortical granules in stage 6 oocytes; lightly shaded granules represent lipid granules (adapted from James, Ansell, & Curry, 1991c).

early stages of vitellogenesis (LONG, 1964; CHUANG, 1983a; JAMES, ANSELL, & CURRY, 1991c).

COELOMOCYTES

In addition to the complement of nurse and accessory cells found in the gonads of many brachiopods, coelomocytes also occur. Coelomocytes, in the form of phagocytes and trophocytes, play an integral role in the process of gametogenesis, resorbing necrotic tissue and supplying the gametes, particularly developing sperm, with nutrients (SAWADA, 1973; CHUANG, 1983b; JAMES & others, 1992). Dense concentrations of coelomocytes periodically occur along the distal edge of the genital lamella of articu-

lated brachiopods (JAMES, ANSELL, & CURRY, 1991b; JAMES & others, 1992) or may become invested among developing gametes (Fig. 155). Coelomocytes appear to be most abundant in the gonads immediately after spawning and during the early stages of gametogenesis (SAWADA, 1973; CHUANG, 1983a; JAMES, ANSELL, & CURRY, 1991c) but are often present throughout gametogenesis (CHUANG, 1983a). The distal margins of the genital lamella of *Terebratulina* and a number of other species can be traced by the presence of a concentration of droplets or granules, often pigmented red to orange in *Terebratulina*. These cells are highly pleomorphic and often contain conspicuous, probably digestive vacuoles, suggesting their ability to

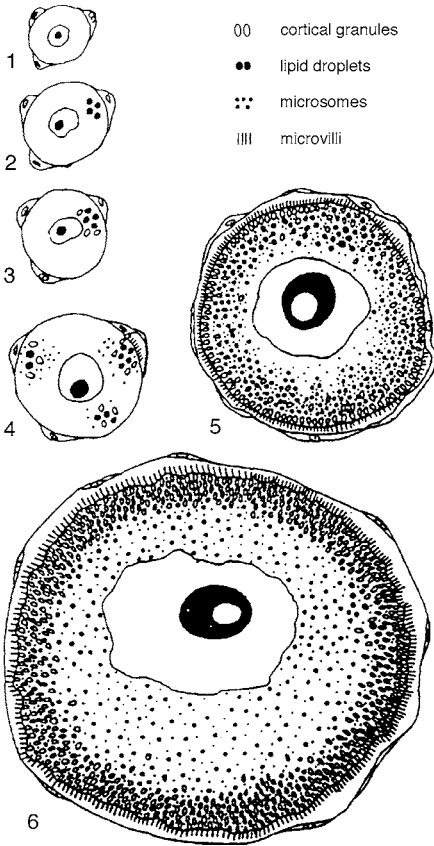


FIG. 146. Six stages of oogenesis in *Frenulina sanguinolenta*; 1, stage 1, oocytes without any lipid droplets or cortical granules; 2, stage 2, oocyte with a few lipid droplets; 3, stage 3, oocyte with a few lipid droplets and cortical granules; 4, stage 4, oocyte with several groups of lipid droplets, cortical granules, and microsomes; 5, stage 5, oocytes with random distribution of lipid droplets, cortical granules, and microsomes; 6, stage 6, mature oocyte (adapted from Chuang, 1983a).

phagocytose necrotic tissue and perhaps act as part of an immune system (Fig. 155). Mature ova that are not spawned become necrotic and are resorbed in the ovary. Absorption of oocytes in *Frenulina* has been observed to occur in flattened cells that engulf small spheres of fragmented oocyte and large subspherical cells (CHUANG, 1983a). In *Terebratulina*, degradation of oocytes occurs while the oocyte is contained within the fol-

licular capsule. The first sign of necrosis in the mature oocyte is that the nuclear envelope becomes highly convoluted and breaks down. Necrosis proceeds, producing an uneven distribution of ooplasm with regions devoid of inclusions. Finally the ovum breaks down into a number of unaltered but condensed fragments of ooplasm, and the follicular envelope degrades (JAMES, ANSELL, & CURRY, 1991c).

Trophocytes (nutritive cells) are common in the testes of many species of brachiopods and appear to supply the masses of spermiogenic and spermatogenic cells with nutrients (SAWADA, 1973; JAMES, ANSELL, & CURRY, 1991c; JAMES & others, 1992). In *Lingula*, nutritive cells are distinguished by the presence of lipid droplets of low electron density and granules of greater electron density (SAWADA, 1973). The nutritive cells of *Terebratulina* and *Calloria* contain glycogen and aggregations of lipid granules. Spermatis and spermatozoa can often be found with their heads touching the trophocyte or are oriented with their heads pointing toward the trophocyte (Fig. 156).

Spawning and Reproductive Strategies

Mature gametes are no longer attached to the genital lamella, having completed their development within the coelomic fluid of the *vascula genitalia* or body cavity. During spawning mature gametes are transported in coelomic fluid by strong ciliary currents generated by the metanephridia into the nephridial funnel where they leave the body cavity via the nephridiopores (HANCOCK, 1859; MORSE, 1873; CHUANG, 1983a, 1983b; JAMES, ANSELL, & CURRY, 1991b). The release of gametes is presumed to be assisted by increased pressure of the visceral fluid caused by muscular contractions (CHUANG, 1983a, 1983b).

Free-spawning brachiopods discharge their mature gametes via the densely ciliated metanephridia into the mantle cavity from which the gametes are expelled into the sur-

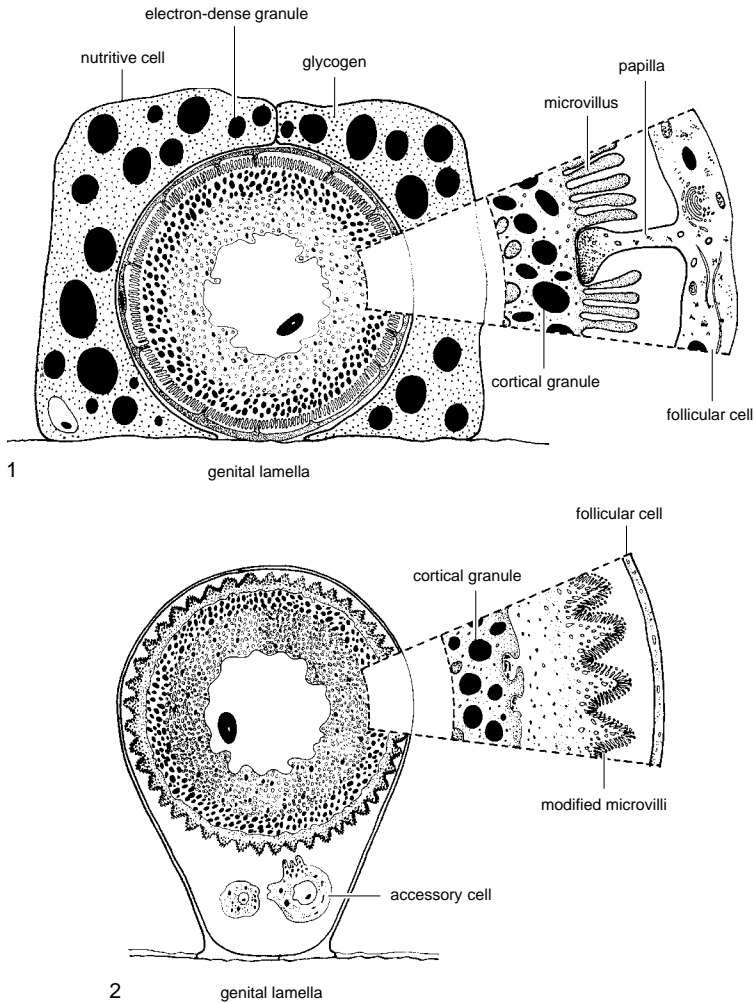


FIG. 147. Diagrammatic representation of oocytes undergoing 1, nutritive vitellogenesis, and 2, mixed vitellogenesis; to the right of each diagram is an enlarged portion to show the relationship between the follicular cell and the surface of the vitellogenic oocyte (new).

rounding water in the exhalant current generated by the lophophore. In *Lingula* (CHUANG, 1959a) and *Glottidia* (PAINE, 1963), spawning occurs in bursts, and females may release several thousand eggs per day. In *Terebratulina retusa*, spawned eggs are more dense than seawater and are deposited close to the female (JAMES & others, 1992). CHUANG (1959a) reports that *Lingula* will spawn in isolation, but *T. retusa* spawn syn-

chronously (JAMES & others, 1992). Little is known of those factors that initiate spawning in brachiopods, but spawning could be mediated by such environmental time cues as spring tides (PAINE, 1963), day length (KUME, 1956; PAINE, 1963), or temperature (CURRY, 1982). Ripe specimens of *T. retusa* can be induced to spawn *in vitro* by the introduction of sperm (CURRY, 1982; JAMES & others, 1992).

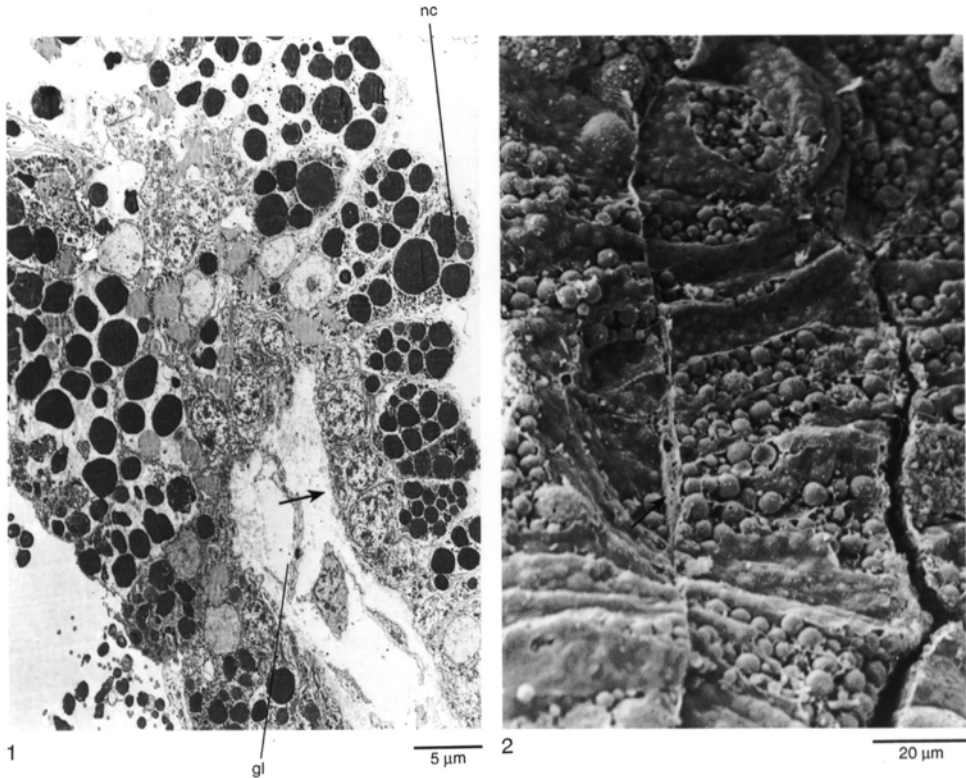


FIG. 148. TEM and SEM micrographs of the genital lamella (*gl*) and nurse cells (*nc*) in 1, *Calloria inconspicua*; arrow indicating an early stage vitellogenic oocyte, scale bar: 5.0 μm ; 2, *Lingula anatina*; arrow indicating genital lamella, scale bar: 20 μm (new).

Liothyrella uva antarctica (BLOCHMANN, 1906), *Pumilus* (RICKWOOD, 1968), *Calloria* (PERCIVAL, 1944), *Notosaria* (PERCIVAL, 1960), *Hemithiris psittacea*, *Terebratulina unguicula* (LONG, 1964), and *T. septentrionalis* (WEBB, LOGAN, & NOBLE, 1976) retain their eggs within the mantle cavity where larval development takes place within the confines of the lophophore (see section on embryology and development, p. 151). Other brooding species deliver their eggs into specialized brood chambers. *Lacazella* possesses a single median pouch behind the mouth where modified tentacles with collars of large cells at the base of the swollen tip are

inserted, thus providing an attachment site for the larvae (Fig. 173; LACAZE-DUTHIERS, 1861). Similar brooding occurs in *Gwynia capsula* (SWEDMARK, 1967). Some *Argyrotheca* have brood pouches formed from modified metanephridia (SHIPLEY, 1883; SCHULGIN, 1885; ATKINS, 1960b; KOWALEVSKY, 1974).

Few accurate accounts of brachiopod reproductive cycles exist. Most reports rely upon superficial analysis of the gonads or the detection of planktonic larva or juveniles. A summary of brachiopod reproductive cycles together with relevant corroborative information is provided in Table 3, p. 158–159.

FIG. 149. SEM and TEM micrographs of transverse sections 1–2, of the margin and 3, surface view of a vitellogenic oocyte of *Calloria inconspicua*, scale bars: 2.0 μm ; *cg*, cortical granule; *fc*, follicular cell; *mv*, microvilli; *pa*, point of attachment of follicular cell papilla; *pp*, papilla (new).

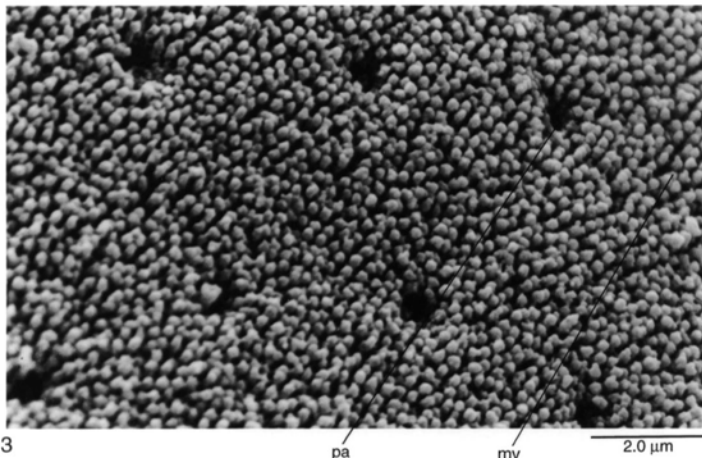
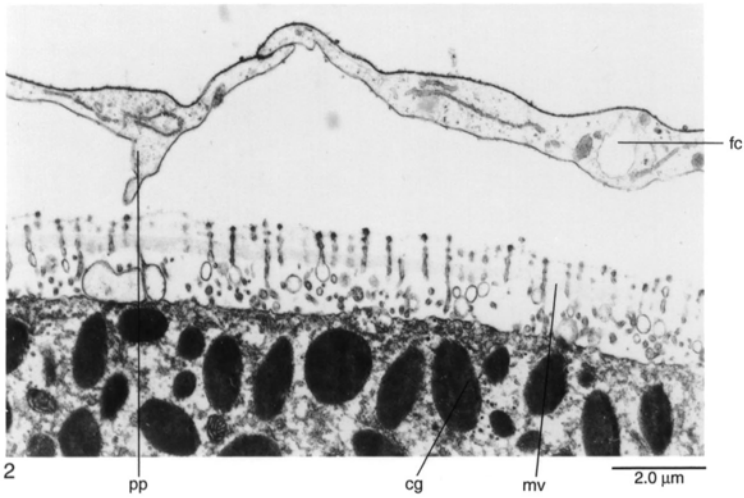
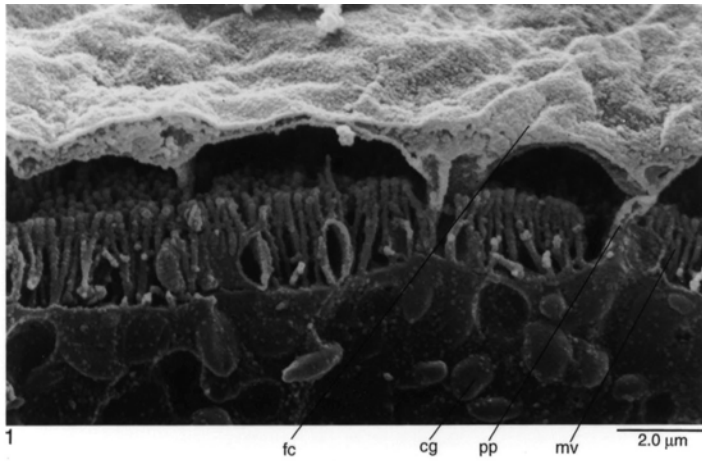


FIG. 149. For explanation, see facing page.

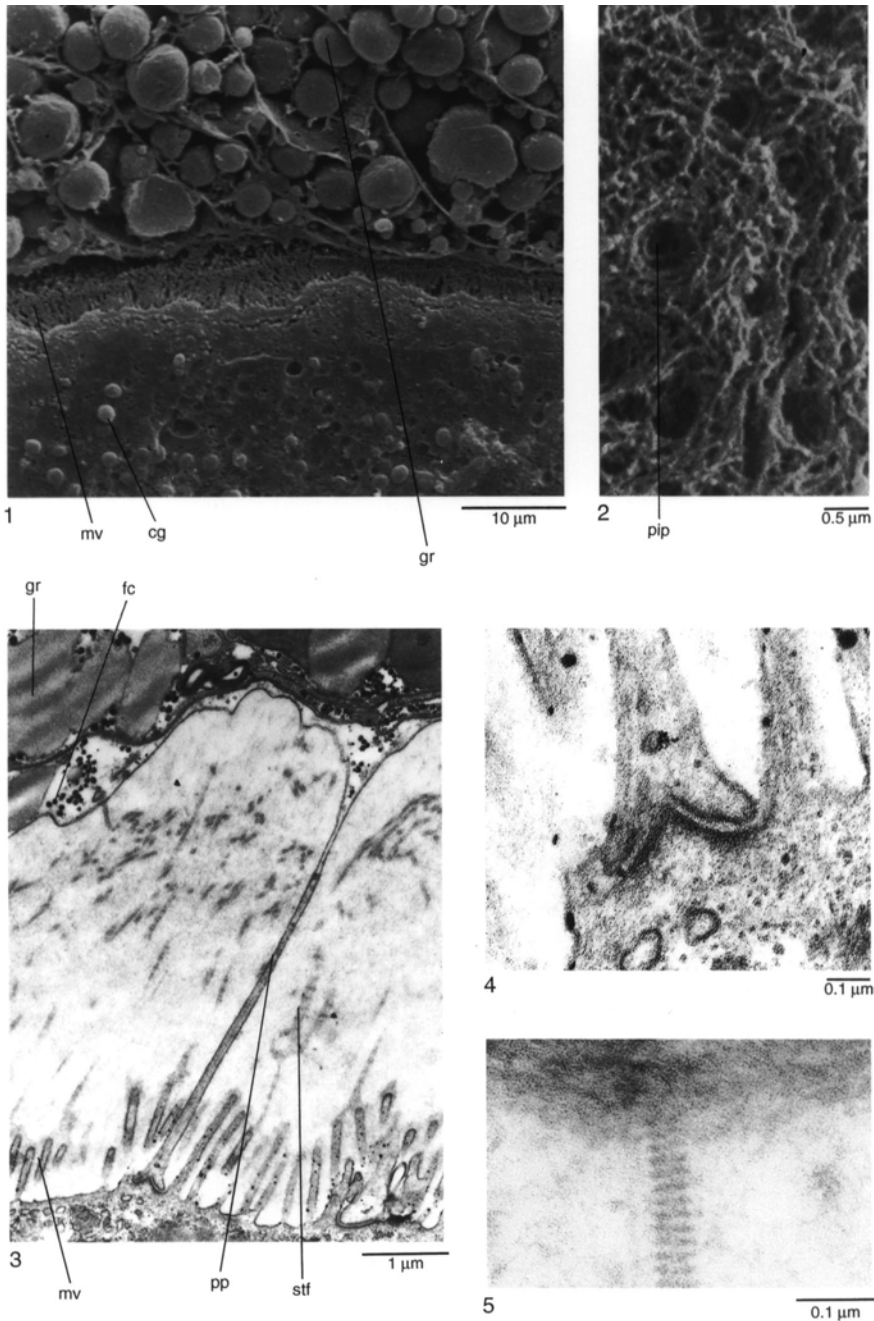


FIG. 150. SEM and TEM micrographs of 1, 3–5, transverse sections of the margin and 2, surface view of a vitellogenic oocyte of *Lingula anatina*; 1, the oocyte is surrounded by nutritive cells containing electron-dense granules, scale bar: 10 μm ; 2, the surface of the oocyte is covered with a dense fibrous matrix, scale bar: 0.5 μm ; 3, the follicular cell produces papillae that attach to the surface of the oocyte, scale bar: 1 μm ; 4, desmosome-like junctions form between the follicular cell papillae and the oocyte, scale bar: 0.1 μm ; 5, striated fibers appear to form a matrix around the vitellogenic oocyte (shown in 2), scale bar: 0.1 μm ; *cg*, cortical granules; *fc*, follicular cell; *gr*, electron-dense granules; *mv*, microvilli; *pip*, point of insertion of papilla; *pp*, papilla; *stf*, striated fibers (new).

The size of mature oocytes is relatively conservative within species (Table 4, p. 160), but fecundity may vary (see JAMES, ANSELL, & CURRY, 1991a), possibly because of disparity in the size of the individuals censused, genetic variation, or perhaps differences in availability of food. *Neocrania* and articulated brachiopods produce eggs that give rise to lecithotrophic larvae and, in this respect, have adopted a conservative reproductive strategy. Compared to other sessile marine invertebrates, they produce relatively small numbers of well-provisioned, lecithotrophic eggs, with the duration of the free-swimming larval phase ranging from hours to a few days (Fig. 157; see also section on embryology and development below). Micromorphic brachiopods produce very few eggs, which are retained within the adult and brooded; and well-developed motile larvae are released, which probably settle close to the adult. Larger species of brachiopods are more fecund, and both free-spawning and brooding strategies may occur even within genera: *Terebratulina retusa* is free spawning (CURRY, 1982; JAMES, ANSELL, & CURRY, 1991a, 1991b, 1991c), but *T. septentrionalis* (WEBB, LOGAN, & NOBLE, 1976) and *T. unguicula* (LONG, 1964) brood. Hermaphroditism tends to be a reproductive strategy that results from the isolation of a population or a size constraint on fecundity (GIESE, PEARSE, & PEARSE, 1987). All those brachiopods known to be hermaphrodites also brood their larvae (Table 4, p. 160; Fig. 157). *Calloria* displays a remarkable degree of reproductive plasticity, with individuals having apparently separate sexes or containing a predominance of either male or female reproductive tissue. Similar flexibility in the mode of reproduction can also be found within genera: *Lacazella* sp. and *Thecidellina* from Jamaica are hermaphroditic (JAMES, unpublished, 1987), while *L. mediterranea* from Naples is gonochoristic (LACAZE-DUTHIERS, 1861). *Argyrotheca jacksoni* from Jamaica is gonochoristic (JAMES, unpublished, 1987), but *A. cuneata* and *A. cordata* from Naples are hermaphroditic (SENN, 1934). *Lingula* and *Glottidia* in particular produce relatively

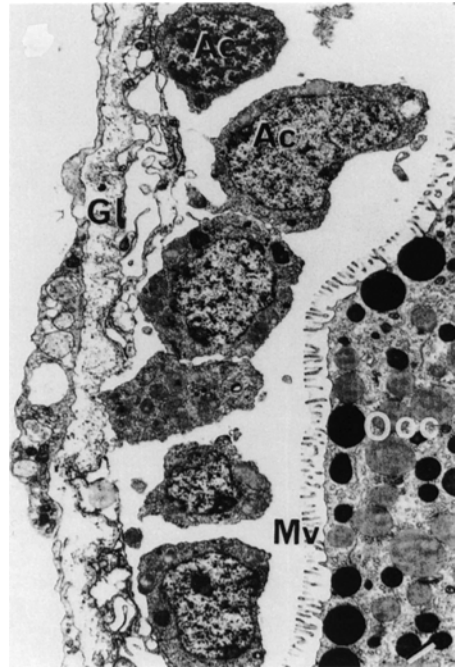


FIG. 151. SEM and TEM micrographs of accessory cells within the follicular capsule of a vitellogenic oocyte in *Terebratulina retusa*; accessory cells (*Ac*) proliferate during the early stages of vitellogenesis between the oocyte (*Ooc*) and genital lamella (*Gl*); early vitellogenic oocytes produce simple digitate microvilli (*Mv*), scale bar: 1.0 μ m (James, Ansell, & Curry, 1991c).

large numbers of eggs. Lingulids and discinids produce eggs that develop into planktotrophic larvae, which may persist in the plankton for prolonged periods and travel over considerable distances (see section on embryology and development below).

EMBRYOLOGY AND DEVELOPMENT

The embryology of the Brachiopoda is pivotal to understanding their phylogeny. Apart from resolving basic questions of affinity, embryological studies should clarify many misconceptions including the view that the brachiopods represent the dichotomy between two fundamental lineages of animal development, the Protostomia and the Deuterostomia. The embryological development of a number of inarticulated and articulated brachiopods has now been

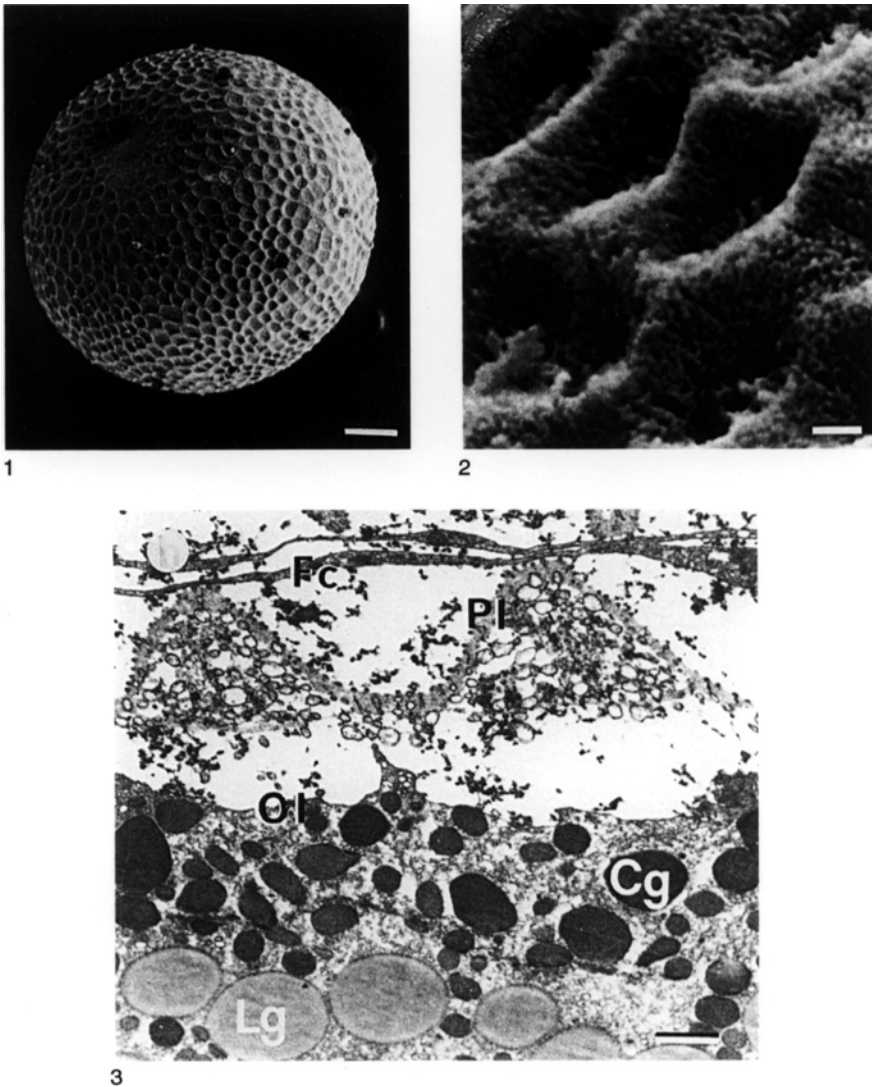


FIG. 152. SEM and TEM micrographs of a late-stage vitellogenic oocyte of *Terebratulina retusa*; 1, entire oocyte covered in follicular cells, scale bar: 20 μm ; 2, surface view of the mature oocyte without follicular cells, scale bar: 10 μm ; 3, periphery of late mature vitellogenic oocyte with convoluted microvillous fringe and containing membrane-bound microdroplets, scale bar: 1.0 μm ; Cg, cortical granules; Fc, follicular cell; Lg, lipid inclusions; Ol, oolemma; Pl, glycocalyx (James, Ansell, & Curry, 1991c).

studied in varying detail, producing conflicting reports and introducing somewhat confusing and inconsistent terminology. In the following sections an attempt will be made to rationalize this terminology, and the salient developmental features will be reviewed.

Among inarticulated brachiopods, the embryology and development of *Lingula anatina* (YATSU, 1902a), early stages of *Glottidia pyramidata* (PAINE, 1963), and the craniid *Neocrania anomala* (NIELSEN, 1991) have been studied in detail, although a number of descriptions of planktonic larvae also

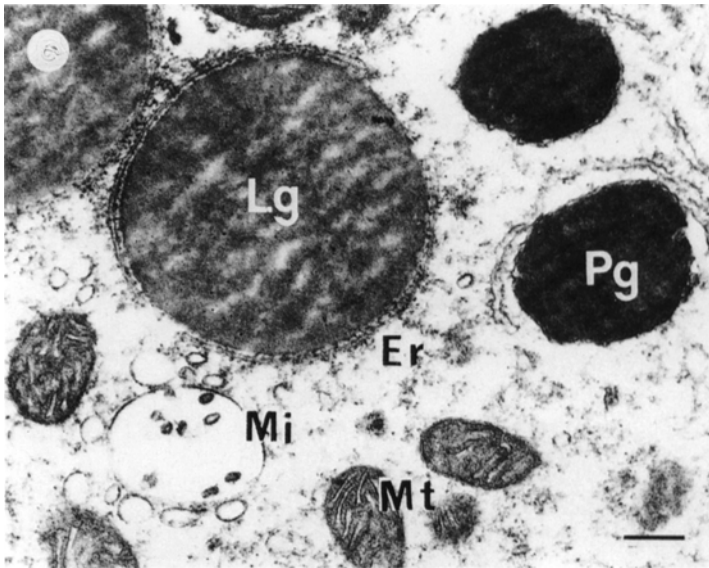


FIG. 153. TEM micrograph of yolk in a vitellogenic oocyte of *Terebratulina retusa* with mitochondria (*Mt*) and agranular endoplasmic reticulum (*Er*) in close association with lipid inclusions (*Lg*) and protein granules (*Pg*); coalescent microsomes (*Mi*) also occur, scale bar: 0.25 μm (James, Ansell, & Curry, 1991c).

exist (see Table 3, p. 158–159). Among the articulated groups, the embryology of *Terebratulina septentrionalis* (CONKLIN, 1902), *Calloria inconspicua* (PERCIVAL, 1944), *Notosaria nigricans* (PERCIVAL, 1960), *Terebratulina retusa* (FRANZEN, 1969), and *Terebratalia transversa* are best known (LONG, 1964; LONG & STRICKER, 1991).

MAIN FEATURES

Prior to fertilization, a number of structural and chromosomal changes of the gametes must take place in order for fertilization to be successful. The union of a mature ovum and a spermatozoon results in the formation of a zygote, which develops a fertilization (vitelline) membrane.

The zygote subsequently undergoes cleavage. Repeated cell divisions create a hollow ball of cells, the blastula (coeloblastula), which by a process of gastrulation by invagination (emboly) forms the gastrula. At this stage, the invaginated cells become the endoderm and the outer cells the ectoderm. The endoderm of the gastrula forms a chamber or

archenteron, which gives rise to a third cell line, the mesoderm, within which a cavity or coelom is created. The archenteron opens to the exterior through the blastopore, which eventually closes.

In articulated brachiopods, closure of the blastopore has been used to define the transition from embryo to larva and, for lingulids, the escape of the embryo from the fertilization membrane (hatching or eclosion) (Fig. 158; CHUANG, 1990). In the free-swimming planktonic phases of the lingulids, the widely accepted term larva has also been replaced by juvenile (LONG & STRICKER, 1991). For comparative and practical purposes, however, it is desirable to standardize the terminology for both articulated and inarticulated developmental stages. Although the free-swimming stages of lingulids and discinids can quite legitimately be defined as precocious juveniles (LONG & STRICKER, 1991), the free-swimming stages of *Neocrania* and articulated brachiopods have also been described as embryos. Herein, all stages of development that occur within

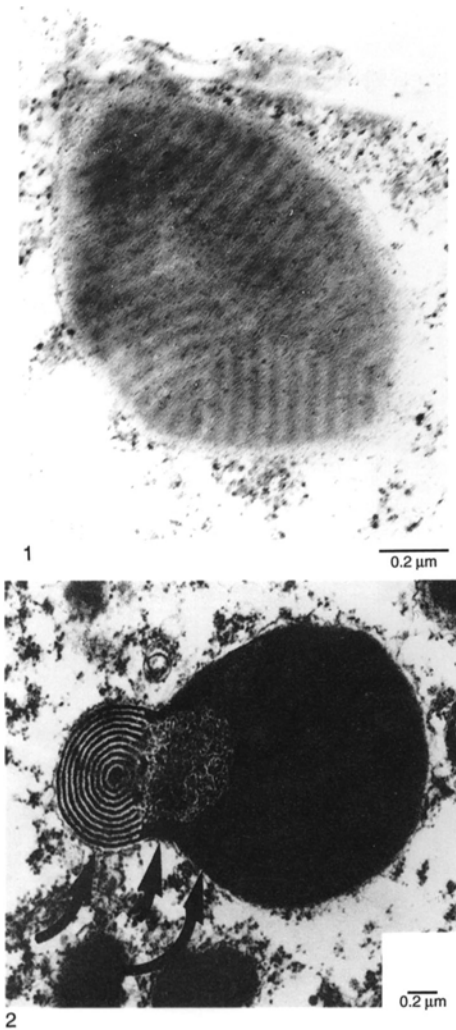


FIG. 154. TEM micrograph of cortical granules of 1, *Terebratella sanguinea*, scale bar: 0.2 μm (new); 2, *Gryphus vitreus*, scale bar: 0.2 μm ; arrows indicate three distinct regions of cortical granule (Bozzo & others, 1983).

the fertilization membrane prior to hatching will be referred to as embryos, and subsequent presettlement stages will be regarded as larvae, which may include free-swimming or brooded stages. Early settled stages are referred to as postlarvae or juveniles (Fig. 158).

Size alone is an unreliable measure of development (YATSU, 1902a; CHUANG, 1990),

and larval stages are defined in inarticulated species and to some extent in articulated species by the number of pairs of lophophoral tentacles.

Larval stages of articulated groups are less well defined. The lophophore is a postlarval development in articulated groups, and the formation of anterior, mantle, and pedicle lobes, the closure of the blastopore, and the occurrence of setal bundles are all used to define the stage of larval development. The larval stage terminates at settlement (CHUANG, 1990), when the postlarval or juvenile stage begins, involving growth and ultimately the attainment of sexual maturity.

The manner in which the cells or blastomeres cleave during early embryonic development, the origins of the mesoderm, formation of the coelomic cavities, and the position of the definitive mouth relative to the position of the closed blastopore determine embryological classification for protozoans and deuterostomes. Reports of brachiopod embryology refer to both enterocoelic and schizocoelic development (NIELSEN, 1991), and until more information is available no review can resolve this ambiguity.

GAMETE MATURATION

In studied articulated species, the oocyte is spawned as a primary oocyte at the prophase I stage of maturation with an intact germinal vesicle (nucleus) (CHUANG, 1990; LONG & STRICKER, 1991). Formation of the first polar body occurs soon after spawning, and fertilization takes place when the oocyte reaches metaphase of the second meiotic division. The germinal vesicle breaks down prior to the addition of sperm in *Hemithiris psittacea* (LONG, 1964), *Terebratalia coreanica*, and *Coptothyris grayii* (HIRAI & FUKUSHI, 1960) but after the addition of sperm in *T. transversa* (LONG, 1964) and *Calloria* (PERCIVAL, 1944). Only after fertilization, however, does the first polar body form in *T. coreanica*, *Coptothyris* (HIRAI & FUKUSHI, 1960), *Hemithiris*, and *T. transversa* (LONG, 1964). In *Terebratulina septentrionalis* (CONKLIN, 1902), *T. retusa* (JAMES & others,

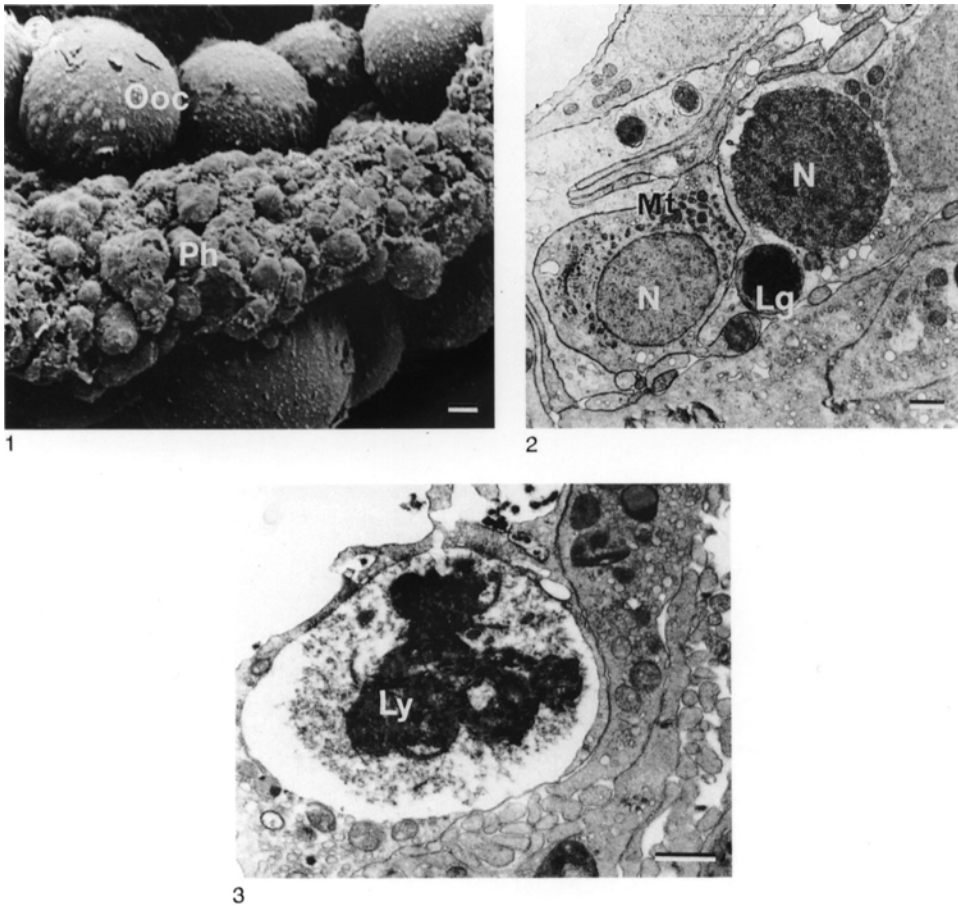


FIG. 155. SEM and TEM micrographs of coelomocytes of *Terebratulina retusa*; 1, the distal margin of the genital lamella in a recently spawned female showing vitellogenic oocytes (*Ooc*) and globular material that probably consists of phagocytes (*Ph*), scale bar: 10 μ m; 2, phagocytic matrix showing lipid granules (*Lg*), mitochondria (*Mt*), and nucleus (*N*), scale bar: 1.0 μ m; 3, putative lysosome (*Ly*) in a phagocyte, scale bar: 10 μ m (James, Ansell, & Curry, 1991b).

1992), and *Neocrania* (NIELSEN, 1991), two polar bodies are formed after fertilization; and in *Lingula* the first polar body may be produced while the oocyte is in the body cavity or immediately after spawning (YATSU, 1902a). The only report of the division of the first polar body is for *T. septentrionalis* in which the polar bodies do not remain attached to the blastula after the 16-blastomere stage (CONKLIN, 1902).

In *Lingula* (YATSU, 1902a), *Terebratalia* (LONG, 1964), and *Terebratulina* (JAMES, ANSELL, & CURRY, 1991c) the follicular cells are

shed sometime after spawning. The follicular cells of *Calloria* reportedly are not lost until fertilization has occurred and the fertilization membrane has formed (PERCIVAL, 1944). In *Neocrania* the follicular cells are shed prior to spawning (NIELSEN, 1991). Loss of the follicular cells that constitute the follicular envelope in *Terebratulina* reveals the highly convoluted and microvillous surface topography of the oocyte. The follicular cells retreat from the pole of the oocyte, which is diametrically opposite the region of accessory cell proliferation and the original

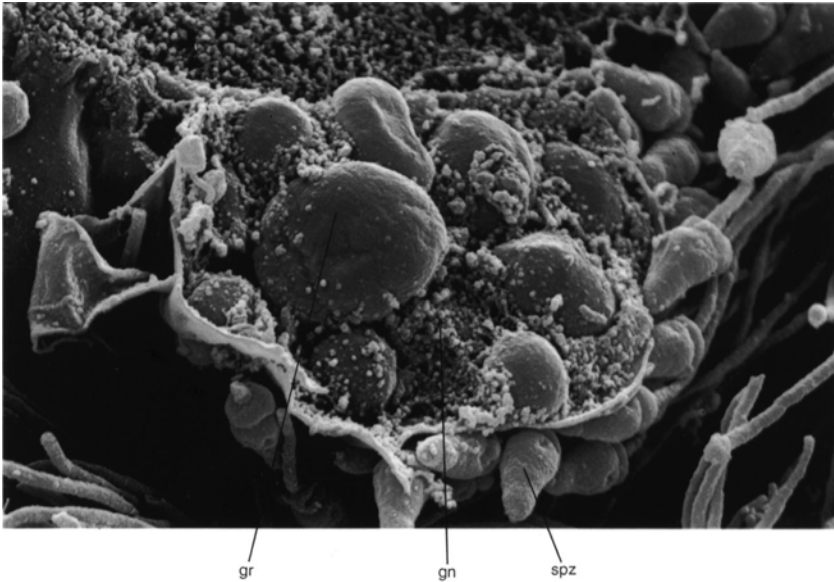


FIG. 156. SEM micrograph of a trophocyte in the gonad of *Calloria inconspicua*, which has been fractured to reveal glycogen granules (*gn*), large electron-dense granules (*gr*), and the heads of the spermatozoa (*spz*) touching the surface of the cell, $\times 5,800$ (new).

point of attachment to the genital lamella (JAMES, ANSELL, & CURRY, 1991c).

Ultrastructural studies of the oocytes of *Lingula* (CHUANG, 1990) and *Terebratulina* (JAMES, ANSELL, & CURRY, 1991c) show that loss of the follicular cells exposes the surface of the oocyte, which retains its microvilli embedded in a filamentous or granular layer, probably some form of glycocalyx. The layer has been described in light microscopic studies as a mucoid (CHUANG, 1990) or a jelly layer (NIELSEN, 1991).

Typically, once an ovum has been fertilized, a fertilization membrane is formed to prevent penetration by other sperm. In *Lingula* and probably other brachiopods the observed increase in density of the filamentous and granular matrix surrounding the ovum and the production of large numbers of transversely striated, radial fibrous strands of varying diameter are assumed to indicate the development of a fertilization membrane (CHUANG, 1990). Formation of the fertilization membrane probably occurs rapidly after successful penetration by sperm. In *T.*

coreanica and *Coptothyris* (HIRAI & FUKUSHI, 1960) and *Calloria* (PERCIVAL, 1944), the fertilization membrane is formed within 5 minutes of the addition of sperm.

Little information exists on the maturation of sperm in brachiopods. Spermatozoa appear to undergo no obvious morphological changes within the testes, although they probably become motile before being spawned. The acrosome filament, which is formed immediately prior to the penetration of the ovum, has been observed in *Hemithyris*, *Terebratulina unguicula*, and *Terebratalia* (LONG, 1964).

It is unknown whether any chemical stimulants are released by the ovum to attract sperm. Penetration by sperm has been observed only in *Lingula* in which the sperm enters the ovum at a point diametrically opposite the second polar body during the metaphase of the second meiotic division of the ovum (YATSU, 1902a). Typically, the ovum will respond to the penetration of the sperm by producing the fertilization membrane, thus excluding other sperm. In *Lin-*

gula, YATSU (1902a) reported the presence of a membrane prior to fertilization and assumed that a micropyle in the membrane facilitates penetration by sperm. The successful sperm sheds its tail, and, in *Lingula*, a thick nuclear membrane forms around the sperm nucleus and the female nucleus respectively, to form the (haploid) male and female pronuclei (YATSU, 1902a).

EMBRYOLOGY

In *Lingula* the male and female pronuclei migrate toward the center of the ovum, the pronuclear membranes break down, and the pronuclei fuse to form a zygote (Fig. 159.1; 160.1; YATSU, 1902a). Sperm penetration and fusion of the pronuclei have not been observed in detail for any other brachiopod.

The pattern of early cleavage of the zygote appears to be similar in all brachiopods. Cleavage into blastomeres is total (holoblastic), equal, and radial (Fig. 159.2–159.3; 160.2–160.3). Early reports of spiral cleavage are viewed with scepticism (NIELSEN, 1991). For all brachiopods studied, the first two divisions are meridional and at right angles to each other. Equal cleavage, relatively homogeneous distribution of ooplasm, and the loss or resorption of the polar bodies early in development have, however, confounded attempts to orient the blastomeres and trace the progress of a given cell lineage relative to any clearly recognizable cytological feature (YATSU, 1902a; CHUANG, 1990; LONG & STRICKER, 1991). Further descriptions of development will be divided into lingulids and discinids, craniids, and articulated groups.

Lingulids and Discinids

Nothing is known about the early stages of discinid development. Aspects of the early development of the lingulid *Glottidia* have been described (PAINE, 1963), but the most detailed account is that of YATSU (1902a) for *Lingula*. In *Lingula* the third cleavage is equatorial, and further cleavages tend to be biradial (KUME & DAN, 1968). According to

YATSU (1902a) the fourth cleavage occurs simultaneously in two parallel planes, whose relationship to the previous plane has not been determined and gives rise to 16 blastomeres, which enclose a spacious blastocoel (Fig. 159.4–159.5). The fourth cleavage may, however, be retarded, giving rise to a 12-blastomere stage. Cell division continues until a hollow, thin-walled, and ciliated blastula (coeloblastula) is formed (Fig. 159.7–159.8). A similar course of events produces the coeloblastula of *Glottidia* (PAINE, 1963).

Gastrulation in *Lingula* occurs at about the 30- to 40-cell stage and is initiated by flattening of the pole of the blastula that has the tallest blastomeres. These cells invaginate to form an endomesodermal cell mass that almost occludes the blastocoel. The invagination forms the archenteron and its communication with the exterior, the blastopore. Endomesodermal cell masses form two groups of mesodermal cell masses, one on either side of the archenteron. Each mesodermal cell mass hollows out to form a coelomic cavity, and the lining cells flatten out to line the endoderm on one side and the ectoderm on the other. The coelom of *Lingula* is thus formed by schizocoely (YATSU, 1902a; MALAKHOV, 1976). Soon after, the blastopore closes, and the anterior parts of the mesodermal masses become mesenchymetous and extend into the anterior part of the embryo, where the lophophore begins to develop (Fig. 159.11; YATSU, 1902a; LONG & STRICKER, 1991).

At this stage, proliferation of the ectoderm at the posterior end of the embryo forms a horizontal, ringlike mantle fold that grows forward to surround much of the remainder of the embryo, the anterior lobe (Fig. 159.12; LONG & STRICKER, 1991). The mantle lobe subsequently becomes constricted into a semicircular form with a straight, posterior margin separating the mantle into a dorsal and a ventral half. The shell appearing at this stage is a very thin cuticle (protegulum) secreted over the entire

TABLE 3. Table summarizing known brachiopod reproductive cycles; *BL*, brooding larvae; *GC*, gonad condition index; *PH*, plankton hauls; *PSP*, partially spawned; *RG*, ripe gonad; *RS*, recently spawned; *SF*, population size frequency analysis; *SP*, spawning (adapted from Long & Stricker, 1991; James & others, 1992).

Species	Author	Locality	Observation type	Month	
Northern Hemisphere					
Inarticulated brachiopods					
<i>Lingula anatina</i>	Yatsu, 1902a	Japan	SP, PH	July–Aug	
	Sewell, 1912	Southern Burma	PH	Feb–Mar; Dec–Jan	
	Ashworth, 1915	Indian Ocean: Red Sea	PH	May–Sept	
	Helmcke, 1940	West Africa; Indian Ocean	PH	Feb–Mar; Apr–May; Jun–Jul; Nov–Dec	
	Kume, 1956	Japan	SP	June–Aug	
	Chuang, 1959b	Singapore	SP	all year	
	Sundarsan, 1968	Western India	PH	Jan–Feb	
	Sundarsan, 1970	Western India	PH	Dec–Jan	
	Chuang, 1973	Indian Ocean	PH	all year	
	<i>Glottidia pyramidata</i>	McCrary, 1860	South Carolina	PH	June–July
		Brooks, 1879	Chesapeake Bay, USA	PH	July–Aug
		Davis, 1949	Southern Florida	PH	all year
		Paine, 1963	Northern Florida	PH	Mar–Apr; May–July; Nov–Dec
<i>Neocrania anomala</i>	Joubin, 1886	Southern France	RG	Apr–Oct	
	Rowell, 1960	Scotland	RS, RG, SF	April–Oct	
<i>Discinisca</i> sp.	Chuang, 1968	Singapore	PH	May–Oct	
<i>D.</i> sp.	Yamada, 1956	Western Japan	PH		
Articulated brachiopods					
<i>Argyrotheca</i> sp.	Atkins, 1960b	Mediterranean Sea	BL	Jan–Feb; Oct–Jan	
<i>A. jacksoni</i>	Jackson, Goreau, & Hartman, 1971	West Indies	SF	all year	
	Hirai & Fukushi, 1960	Japan	SP	Oct–Nov	
<i>Dallina</i> sp.	Lankester, 1873	Naples	RG	Nov–Dec	
<i>Frenulina sanguinolenta</i>	Mano, 1960	Japan	BL	all year	
<i>Frieleia halli</i>	Rokop, 1977	California	RG	Jan–Apr	
<i>Gryphus</i> sp.	Lankester, 1873	Naples	RG	Dec–Jan	
<i>Hemithiris psittacea</i>	Long, 1964	Washington	BL	Jan–Feb; Dec–Jan	
<i>Platidia</i> spp.	Atkins, 1959	Western France	RG	Feb–Mar; Jun–Jul; Aug–Sept	
<i>Terebratalia coreanica</i>	Hirai & Fukushi, 1960	Japan	SP	Oct–Nov	
<i>T. transversa</i>	Long, 1964	Washington	SP	Jan–Feb; Nov–Dec	
<i>Terebratulina</i> sp.	Morse, 1873	Maine	SP	April–Aug	
<i>T. unguis</i>	Long, 1964	Washington	BL	Feb–Mar	
<i>T. septentrionalis</i>	Webb, Logan, & Noble, 1976	Bay of Fundy, Canada	BL	Jan–Mar; Dec–Jan	
	Franzen, 1969	Western Sweden	RG	Nov–Dec	
<i>T. retusa</i>	Curry, 1982a	Scotland	SF	Apr–May; Oct–Dec	
	James, Ansell, & Curry, 1991a	Scotland	GC, SP	Jan–Feb; Nov–Jan ¹	
	James, 1991a & Curry, 1991a	Scotland	GC, SP	Jan–Feb; Apr; Jun; Nov–Jan ¹	
<i>Thecidellina barretti</i>	Jackson, Goreau, & Hartman, 1971	Jamaica	SF	(single spawning)	
<i>T. congregata</i>	Jackson, Goreau, & Hartman, 1971	Guam & Saipan	SF	(single spawning)	

TABLE 3. Continued.

Species	Author	Locality	Observation type	Month
Southern Hemisphere				
Inarticulated brachiopods				
<i>Lingula anatina</i>	Kechington & Hammond, 1978	Queensland, Australia	RG, PH	Nov–Mar
<i>Disciniscia</i> sp.	Hammond, 1980	Queensland, Australia	PH	Feb–May
<i>Pelagodiscus</i> sp.	Müller, 1860, 1861	Brazil	PH	Feb–Apr
	Blochmann, 1898	Indonesia	PH	July–Aug
	Eichler, 1911	Antarctic Ocean	PH	Feb–Apr
	Ashworth, 1915	Indian Ocean	PH	Oct–Nov
	Helmcke, 1940	Eastern Africa	PH	Dec–Jan; Feb–Mar
Articulated brachiopods				
<i>Liothyrella</i> sp.	Eichler, 1911	Antarctica	BL	Feb–Mar
<i>L. neozelanica</i>	Tortell, 1981	New Zealand	PSP	Feb–Mar
<i>Neothyris lenticularis</i>	Tortell, 1981	New Zealand	RG	Feb ² –Mar
<i>Notosaria nigricans</i>	Percival, 1960	New Zealand	BL	Apr–Jul
	Tortell, 1981	New Zealand	RG	Feb ³ –Mar
<i>Pumilus antiquatus</i>	Rickwood, 1968	New Zealand	BL	Sept–Nov
<i>Terebratella sanguinea</i>	Tortell, 1981	New Zealand	RG	Apr–Jul ²
<i>Calloria inconspicua</i>	Percival, 1944	New Zealand	BL	Apr–Jun ¹
	Doherty, 1979	New Zealand	SP	Jul–Sept ¹

¹same species taken from different localities; ²specimens collected between January and March; gonads appeared to be ripe but could not be induced to spawn; ³specimens collected between January and March; males released sperm when water temperature was slightly increased.

external surface of the mantle (Fig. 159.13; YATSU, 1902a). The anterior lobe is formed from a central area of the gastrula that is raised into a mound subsequently giving rise to the lophophore. An invagination marks the future median part of the brachial (arm) ridge. Proceeding dorsally and posteriorly, it forms the stomodaeum (the embryonic mouth). Interrupted on the ventral side by this invagination, the brachial ridge adopts a dorsally directed U-shape. Eventually, the stomodaeum opens into the archenteron. The stomodaeum is believed to invaginate at the site where the blastopore closed, but the exact derivation of the mouth is uncertain. Meanwhile, the mantle lobes rapidly increase in size especially along the anterior margin, and the brachial ridge becomes densely ciliated (Fig. 159.13).

As development proceeds, the brachial ridge forms a circular disc and projects from the anterior. The mouth becomes clearly visible, and the brachial apparatus is raised up on a stalk (Fig. 159.14–159.15; YATSU,

1902a). The brachia assume a triangular outline with the two posterior angles forming the first pair of rudimentary tentacles and the anterior apex the earliest manifestation of the median tentacle. A second pair of tentacles are added on either side and adjacent to the median tentacle. At the same time the mouth shifts into a central position where it becomes flanked anteriorly by the epistome, arising as a preoral transverse ridge. Additional pairs of tentacles arise from the generative zones on either side of the median tentacle, eventually forming a trocholophe. Embryos with three pairs of tentacles bear the rudiments of the ventral muscle. A few muscle fibers are embedded among the mesenchyme cells of the brachial canal (arm-sinus). In addition, the archenteron also becomes differentiated into a thickly walled esophagus and a thinly walled stomach (Fig. 159.16; YATSU, 1902a).

At hatching, lingulid embryos are much more advanced in their development than the embryos of craniids and articulated

TABLE 4. Summary of known sizes of brachiopod eggs and reproductive strategies; *G*, gonochoristic; *H*, hermaphrodite; *L*, lecithotrophic; *P*, planktotrophic; *FS*, free spawning; *BL*, lophophore brooding; *BC*, brood chamber (new).

Species	Sex	Development type	Fecundity	Egg diameter (µm)	Strategy
<i>Neocrania anomala</i>	G	L		120 ^{2,13} 125 ¹¹	FS
<i>N. californica</i>					FS
<i>Lingula anatina</i> ^{1,21}	G	P	17,250 ¹	95, 130 ⁷	FS
<i>Glottidia pyramidata</i>		P	60,000 ¹²		FS
<i>Pumilus antiquatus</i>	H	L	50–100 ¹⁵	200 ¹⁵	BL
<i>Argyrotheca cuneata</i>	H	L		95 ¹⁸	BC
<i>A. cordata</i>	H	L		100 ¹⁸	BC
<i>A. jacksoni</i>	G	L	3,000	90 ⁸	
<i>Megathiris detruncata</i>	H	L		90 ¹⁸	
<i>Calloria inconspicua</i>	H ⁸	L	18,000 ¹⁶ 22,000 ^{5,9}	180 ^{20,13}	BL
<i>Terebratella sanguinea</i>	G			100 ²⁰	
<i>Neothyris lenticularis</i>	G			85 ²⁰	
<i>Gryphus vitreus</i>	G			70 ¹⁸	
<i>Lacazella</i> sp.	H	L	150 ⁸	20 ⁸	BC
<i>L. mediterranea</i>	G ²²	L			BC
<i>Thecidellina barretti</i>	H	L	150 ⁸	20 ⁸	BC
<i>Terebratulina unguicula</i>	G			170 ¹⁰	BL
<i>T. septentrionalis</i>	G	L		160 ⁴	BL
<i>T. retusa</i>	G	L	8,000–15,000 ⁸	120 ⁶ 130 ⁸ 160 ³	FS
<i>Laqueus californianus</i>	G		35,000 ⁹	140 ⁹ 170 ¹⁹	FS
<i>Frieleia halli</i>	G		<1,000 ¹⁷	112 ¹⁷	
<i>Frenulina sanguinolenta</i>				130 ²	
<i>Terebratalia transversa</i>	G	L		150 ^{10,19}	FS
<i>Notosaria nigricans</i>	G	L	8,680 ¹⁴ 14,000 ²¹	160 ¹⁴ 200 ²⁰	BL
<i>Hemithiris psittacea</i>	G	L		190 ¹⁰	BL
<i>H.</i> sp.			22,000 ⁹	90 ⁹	
<i>Liothyrella antarctica</i>		L			BL
<i>Gwynia capsula</i>		L			BC

¹CHUANG, 1959a; ²CHUANG, 1983a; ³CLOUD, 1948; ⁴CONKLIN, 1902; ⁵DOHERTY, 1979; ⁶FRANZEN, 1969; ⁷HAMMOND, 1982; ⁸JAMES, ANSELL, & CURRY, 1991a; JAMES, unpublished data, 1989; ⁹LAW & THAYER, 1991; ¹⁰LONG, 1964; ¹¹NIELSEN, 1991; ¹²PAINE, 1962a; ¹³PERCIVAL, 1944; ¹⁴PERCIVAL, 1960; ¹⁵RICKWOOD, 1968; ¹⁶RICKWOOD, 1977; ¹⁷ROKOP, 1977; ¹⁸SENN, 1934; ¹⁹REED, 1987; ²⁰TORTELLI, 1981; ²¹YATSU, 1902a; ²²LACAZE-DUTHIERS, 1861.

brachiopods. The embryo essentially forms two lobes; an anterior lobe from which the lophophore develops, and a posterior mantle lobe. These constrict to form the ventral and dorsal mantle lobes, which grow to envelop much of the anterior lobe. The mantle lobes secrete the protogulum before the embryo hatches from the fertilization membrane and becomes a free-swimming larva (Fig. 158.3; 159.13).

Craniids

After the first three cell divisions, the embryological development of *Neocrania* differs significantly from other inarticulated brachiopods, sharing similarities with the develop-

ment of articulated groups (Fig. 161–162). The fourth cleavage results in two tiers of cells oriented perpendicular to each other, with the 16 blastomeres arranged as two, curved, double rows of cells forming a cross. Further cell divisions are irregular and asynchronous. The blastulae develop cilia and begin to swim. Gastrulation by invagination of the blastoporal pole occurs at about the 40- to 50-cell stage. In the postgastrulation stage, the larva of *Neocrania* remains fairly spherical even after the blastocoel has been occluded (Fig. 161.1; 162.1). Thereafter, it becomes somewhat flattened and elongate, with the blastopore located at the posterior end of the ventral side (Fig. 161.2; 162.2).

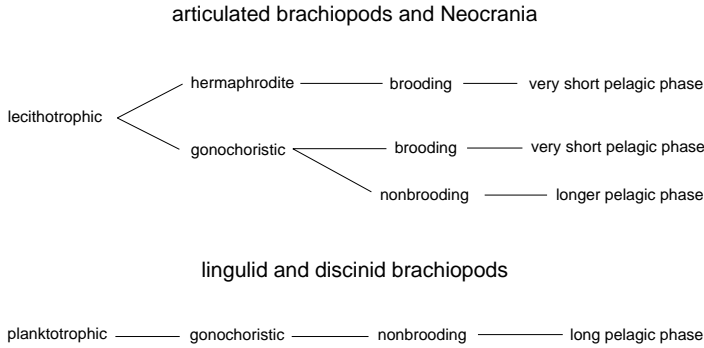


FIG. 157. Summary diagram of brachiopod reproductive strategies (new).

Endodermal and mesodermal cells occupy the anterodorsal and posteroventral sides of the archenteron wall respectively. The mesodermal layer expands anteriorly between the ectoderm and the endoderm as a single cell layer, while the endoderm elongates as a narrow sac (Fig. 161.3; 162.3). At a somewhat

later stage while the blastopore is still open, mesoderm covers both lateral surfaces of the ectoderm and starts to differentiate into four plates on each side of the ectoderm. The periphery of each plate curls medially and constricts, creating a series of four pouches on each side of the larva and finally the

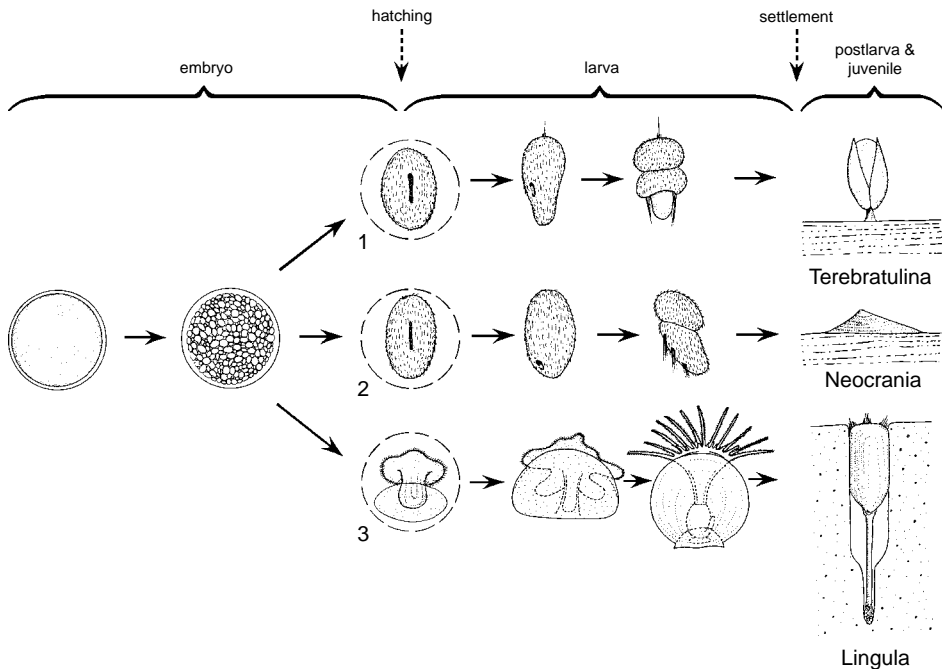


FIG. 158. Schematic diagram showing the approximate stages at which embryos of 1, *Terebratulina retusa*, 2, *Neocrania anomala*, and 3, *Lingula anatina* hatch from their fertilization membranes and become free-swimming larvae; the transition from the free-swimming larva to the postlarval (juvenile) stage occurs at settlement (new).

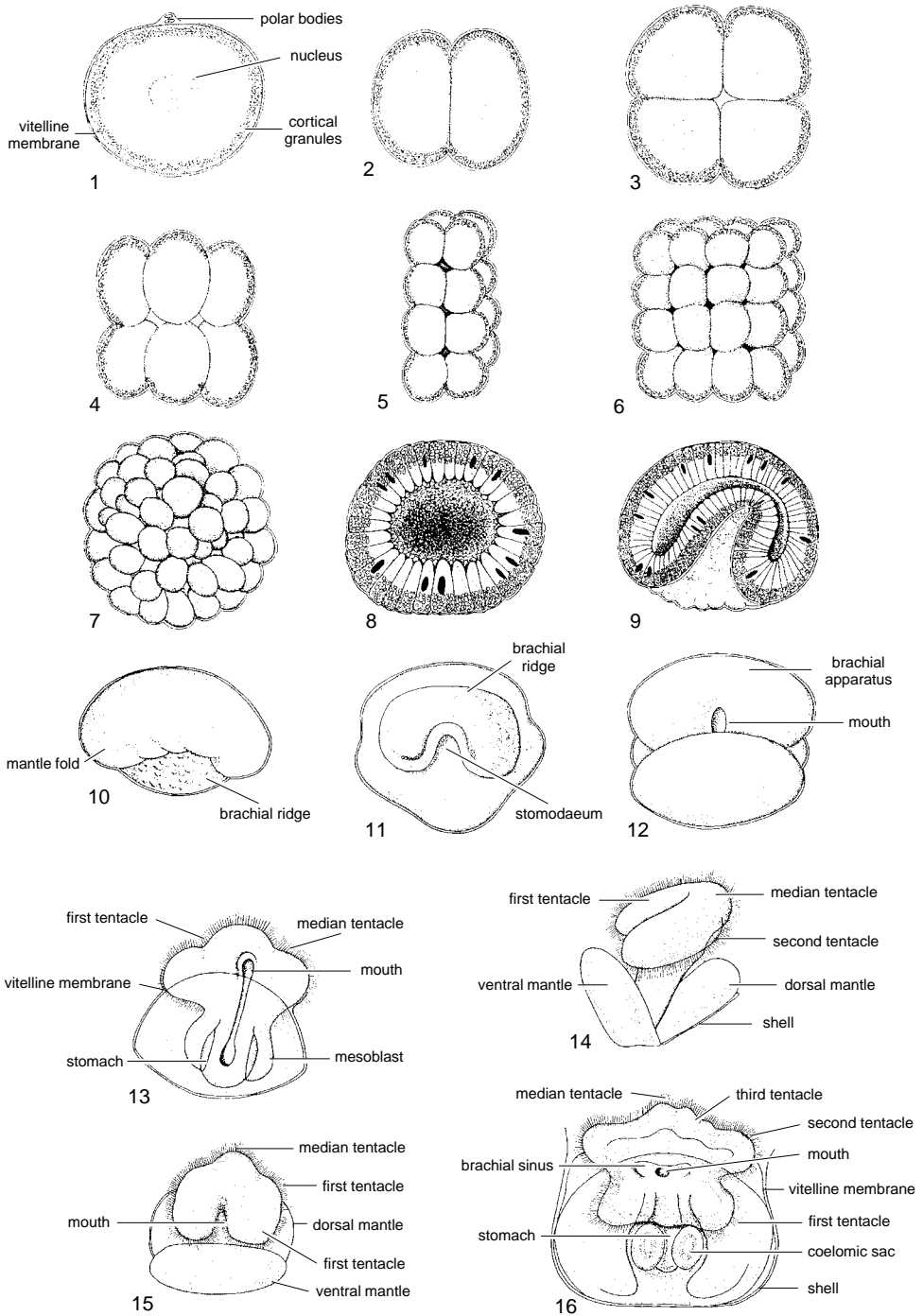


FIG. 159. For explanation, see facing page.

blastopore closes (Fig. 161.4; 162.4). Hence, the coelom of *Neocrania* is formed through modified enterocoely (NIELSEN, 1991).

In the *Neocrania* larva only one major constriction is apparent, which separates the rounded anterior lobe from the rest of the dorsoventrally flattened larva (Fig. 163.3; NIELSEN, 1991).

Articulated Groups

The development of the articulated brachiopods follows a similar course for all those species studied (LONG & STRICKER, 1991). The most detailed accounts are of *Terebratulina septentrionalis* (CONKLIN, 1902) and *Terebratalia transversa* (LONG, 1964).

In *Terebratalia* the third cleavage is meridional or equatorial and forms a doughnut-shaped ring of eight cells or two tiers of four cells respectively (Fig. 160.6–160.7). The fourth division is equatorial or meridional, depending upon the previous cleavage, resulting in the formation of two tiers of eight cells (LONG, 1964). As in *Neocrania*, beyond the stage of 16 cells further cell divisions are often irregular and asynchronous, eventually forming a hollow blastula (Fig. 160.8–160.9; CONKLIN, 1902; LONG & STRICKER, 1991). Cells at the presumptive blastoporal (vegetal) pole of the blastula (the point farthest from the position of the original egg nucleus) become columnar (LONG & STRICKER, 1991), and gastrulation occurs by invagination (emboly) of this thickened layer of cells (the gastral plate), thus forming a blastopore (Fig. 160.10–160.11). The invaginated cells form the endodermal anlage and eventually oc-

clude the blastocoel. The chamber created by the process of invagination forms the archenteron. The only reported exception is in *Lacazella mediterranea* where gastrulation occurs by delamination (KOWALEVSKY, 1883).

Hatching of the embryo of articulated groups is not well documented, but rupture of the fertilization membrane and subsequent escape of larvae probably occur during the late blastula or early gastrula stage when embryos develop cilia and achieve motility (Fig. 158; CHUANG, 1990). An apical tuft of long cilia forms, and the surface of the embryo is ciliated (Fig. 160.12; LONG & STRICKER, 1991). At this stage, the larvae of *Terebratalia*, *Terebratulina*, and probably other calcareous-shelled brachiopods are capable of swimming. Those of *Terebratalia* (LONG & STRICKER, 1991) and *Terebratulina* (JAMES, unpublished, 1989) propel themselves through the water with their anterior end forward and in a clockwise direction, while the larva of *Notosaria* (PERCIVAL, 1960) spirals counterclockwise. The archenteron is elongated anteroposteriorly, and the anterior end of the embryonic gut forms a blind-ending pouch. More posteriorly, the archenteron opens ventrally via a blastopore that is elongated by the curvature of the larva.

It is generally agreed that the coelom of these larvae is formed by a modified form of enterocoely (MALAKHOV, 1976); reports of schizocoely in articulated groups have been largely discounted (NIELSEN, 1991). With minor variations, the following description of coelomic formation applies to *Hemithiris*, *Terebratalia*, and *Terebratulina unguicula*

FIG. 159. Diagrammatic series illustrating the development of *Lingula anatina*; 1, mature ovum and polar bodies; 2, 2-cell stage; 3, 4-cell stage; 4, 8-cell stage; 5, 16-cell stage; 6, 32-cell stage; 7, blastula; 8, cross section of late blastula prior to gastrulation; 9, gastrula; 10, embryo with brachial ridge and mantle fold; 11, anterior view of a slightly more advanced embryo in which the stomodaeum has appeared; 12, ventral view of a slightly older embryo in which the mantle lobes have formed; 13, ventral view of embryo at the next stage with the rudiment of the median and first pair of tentacles; the mesodermal cell masses are also visible and the vitelline membrane has ruptured; 14, ventral view of larva in which the rudiments of the second pair of tentacles have formed, the dorsal and ventral mantles are clearly divided, and the larval shell is visible; 15, anterior view of previous example showing the brachial apparatus attached to the dorsal mantle; 16, ventral view of a larva with a well-developed median tentacle and two pairs of tentacles; coelomic sacs are clearly visible (adapted from Yatsu, 1902a).

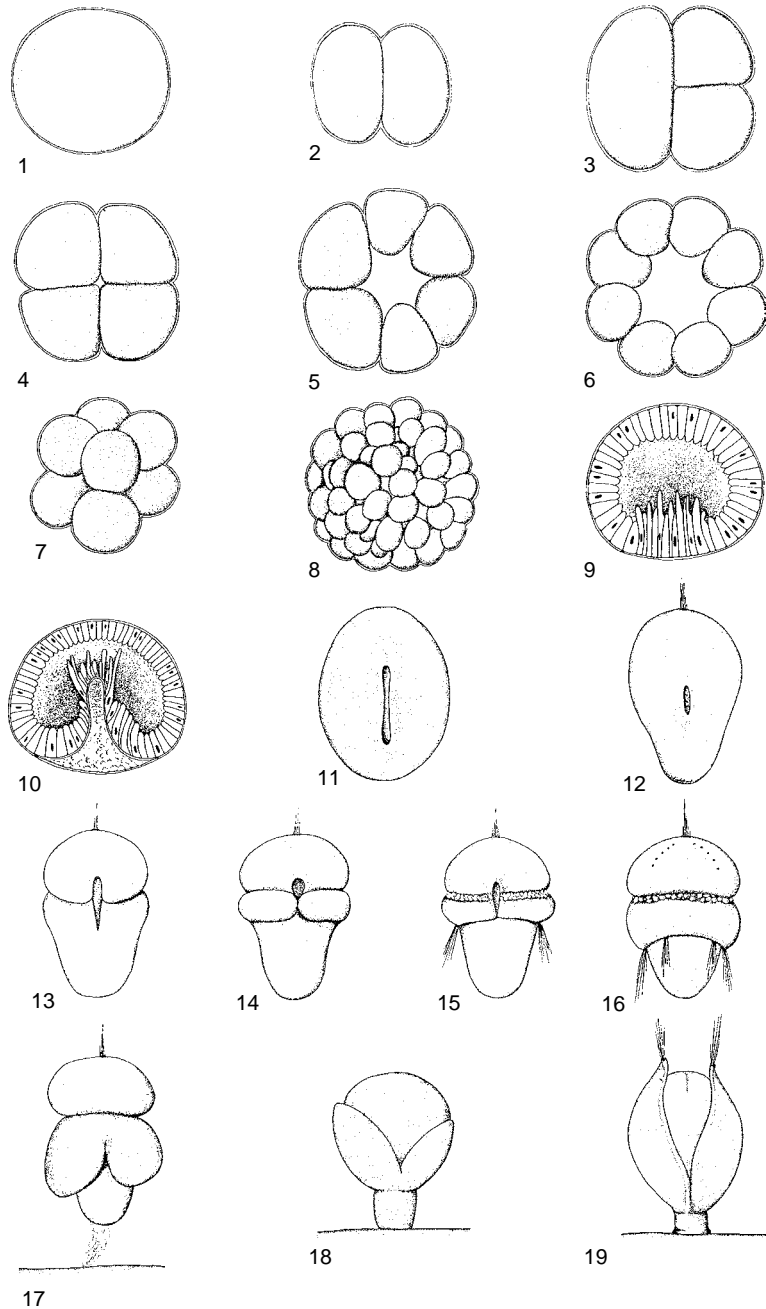


FIG. 160. Diagrammatic series illustrating the development of the articulated brachiopods; 1–16, *Terebratalia transversa* and 17–19, *Terebratulina retusa* in settlement and metamorphosis; 1, zygote; 2, 2-cell (blastomere) stage; 3, 3-cell stage; 4, 4-cell stage; 5, 6-cell stage; 6, 8-cell stage, flat ring; 7, 8-cell stage, two tiers of four blastomeres; 8, blastula; 9, cross section of late blastula with thickened gastral plate prior to gastrulation; 10, cross section of gastrulating blastula; 11, ventral view of a 35-hour-old larva showing the elongated blastopore; hatching has probably occurred; 12, ventral view of a slightly older larva with an apical tuft (adapted from Long & Stricker, 1991); (Continued on facing page.)

(LONG, 1964), *T. septentrionalis* (CONKLIN, 1902), *Calloria* (PERCIVAL, 1944), *Notosaria* (PERCIVAL, 1960), and *Argyrotheca cordata* (KOWALEVSKY, 1883; SHIPLEY, 1883; PLENK, 1913). The dorsal lining of the archenteron thickens, indicating the formation of mesoderm. Subsequently, a single layer of cells grows downward from the anterior and lateral parts of the roof of the archenteron to form a cellular curtain that eventually partitions elongated coelomic spaces (enterocoels) on either side of the archenteron. Almost simultaneously, the blastopore begins to close from its posterior end toward the anterior tip, but the exact manner in which the coelom becomes separated is unclear. Organogenesis in the larva of articulated brachiopods is heralded by a superficial, transverse constriction of the elongate gastrula into three lobes (CHUANG, 1990).

Constrictions may occur in several ways in different species (Fig. 163). In some, the embryo is first constricted into two lobes, one of which is divided by a second constriction. In others, division is achieved by an ectodermal folding around the middle of the embryo, which has also been interpreted as a simultaneous occurrence of two constrictions in front of, and behind, the ectodermal fold. Constriction of the embryos of *Terebratalia* (LONG, 1964) and *Argyrotheca* (KOWALEVSKY, 1883) first marks off the anterior lobe and then the mantle and pedicle lobe (Fig. 163.4). After marking off the anterior lobes in *Notosaria*, an ectodermal fold, first appearing on the dorsal side of the embryo, grows laterally downward on each side to encircle the embryo near the middle and forms the mantle lobe (Fig. 163.5; PERCIVAL, 1960). A

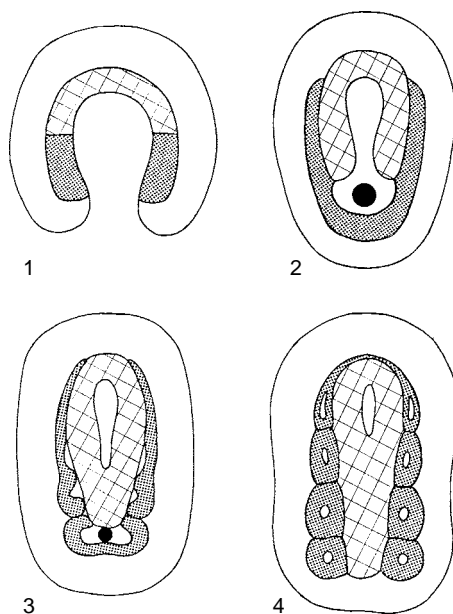


FIG. 161. Diagrams of four stages of development of the mesoderm (shaded) and the endoderm (crosshatched) of *Neocrania anomala*; black dot indicates position of the blastopore (adapted from Nielsen, 1991).

fold, with or without constrictions, forms around approximately the middle of the embryos of *Coptothyris*, *Terebratalia coreanica* (HIRAI & FUKUSHI, 1960), *Pumilus antiqualus* (RICKWOOD, 1968), *T. septentrionalis* (CONKLIN, 1902), and *Calloria* (PERCIVAL, 1944). The fold forms the mantle lobe between the anterior and the pedicle lobe (Fig. 163.6). In contrast, the first constriction in *T. septentrionalis* (MORSE, 1873), *T. unguicula* (LONG, 1964), *Argyrotheca* (SHIPLEY, 1883), and *Lacazella* (LACAZE-DUTHIERS, 1861) delineates the pedicle lobe from the

FIG. 160. *Continued from facing page.*

13, ventral view of a 40-hour-old larva in which the apical lobe has formed; 14, ventral view of a 42-hour-old larva with the mantle lobe forming; 15, ventral view of 48-hour-old larva; the blastopore is closing, the setal bundles have formed at the mantle margin, and vesicular bodies are evident at the base of the anterior lobe; 16, dorsal view of larva at 70 hours, showing apical tuft, eye spots, vesicular bodies, setae, and a posterior band of cilia on the apical lobe (adapted from Long & Stricker, 1991); 17, approximately 72-hour-old, trilobed *Terebratulina retusa* larva; separate ventral and dorsal mantle lobes are present and the pedicle lobe has secreted a mucous strand that adheres to the substrate; 18, the pedicle attaches and metamorphosis takes place, the mantle lobes reverse to envelope the anterior lobe, and the apical tuft is lost; 19, the shell is secreted and long marginal setae extend beyond the mantle of the postlarva (new).

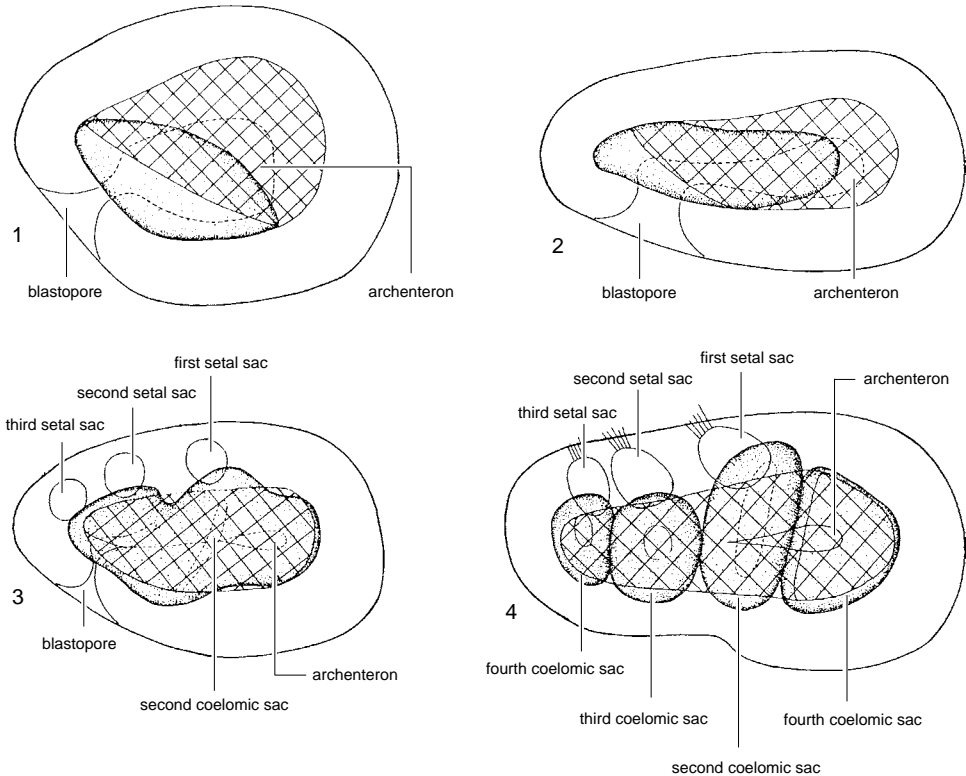


FIG. 162. Reconstructions of developmental stages of *Neocrania anomala* (based on serial sections) showing the differentiation of endoderm (crosshatched) and mesoderm (stippled); 1–4, free-swimming larva; 1, stage at 38 hours after fertilization; 2, 46 hours after fertilization; 3, 54 hours after fertilization; 4, 67 hours after fertilization; (Continued on facing page.)

rest of the embryo, which is soon divided into the mantle lobe and the anterior lobe by a more anterior constriction (Fig. 163.7).

LARVAL DEVELOPMENT

Lingulids and Discinids

The free-swimming larvae of *Glottidia* (PAINE, 1963) and *Lingula* (YATSU, 1902a; SEWELL, 1912; ASHWORTH, 1915; CHUANG, 1959a, 1977) have been well described, as have discinid larvae, mainly of the cosmopolitan species *Pelagodiscus atlanticus* (WILLIAMS & ROWELL, 1965a). All are planktotrophic.

The trocholophe of *Lingula* is first formed at the 3 p.t. stage and persists during the entire larval stage. Rupture of the fertiliza-

tion membrane occurs at this stage; further extensions of the coelom and tentacular canals have also been formed; and myoepithelial cells are present in the tentacles.

A functional gut with rudimentary intestine and anus may differentiate in the embryo at the stage when the embryonic lophophore is only present as five lobes (YATSU, 1902a). The transition from the embryonic lecithotrophic to the larval planktotrophic mode of life disrupts secretion of the protogulum and results in a disturbance ring on the umbo of the larval shell (CHUANG, 1977). Further development of the gut occurs during the early larval stages. The intestine and statocysts may first appear at the 3 p.t. stage but in some larvae may not be differentiated until the 5 and 6 p.t. stages respectively.

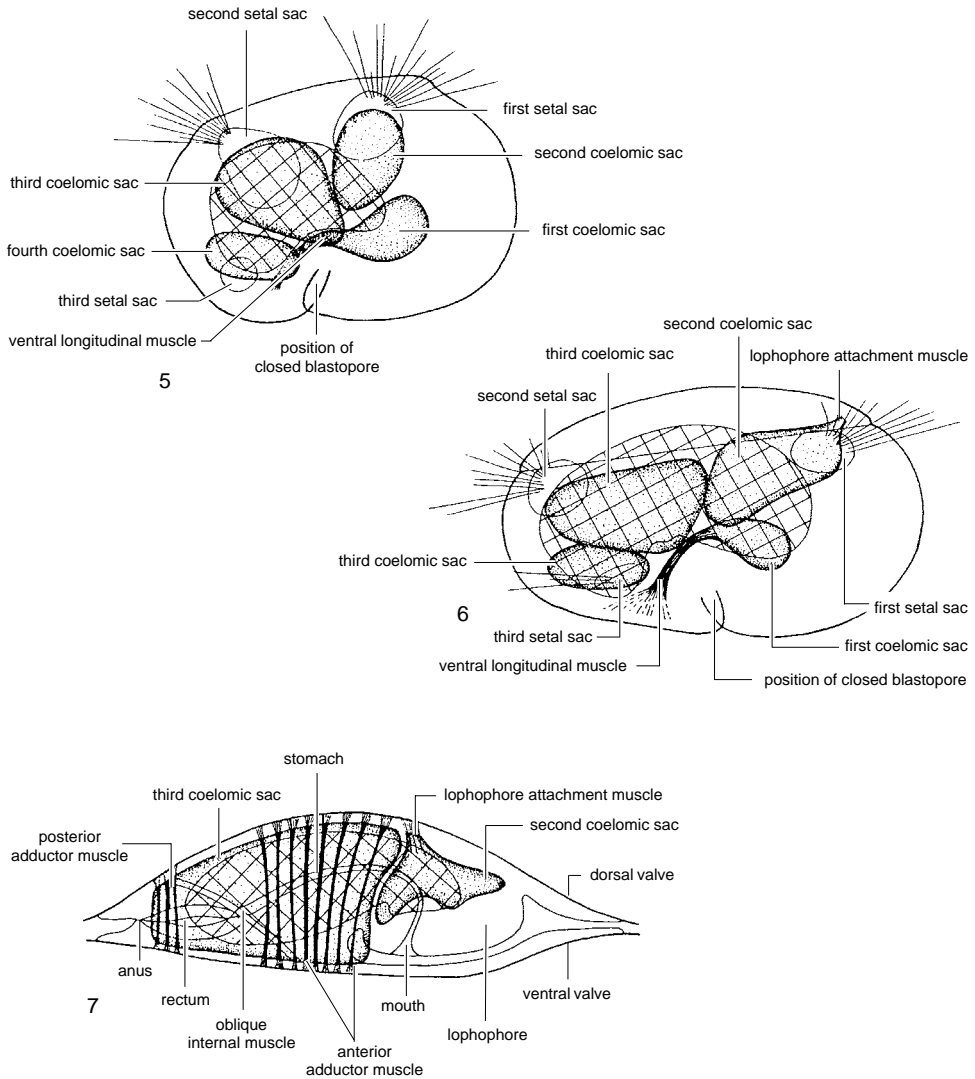


FIG. 162. *Continued from facing page.*

5, newly settled larva; 6, a later metamorphosis stage; 7, juvenile stage (adapted from Nielsen, 1991).

Rudimentary statocysts appear to be vesicular structures that, by the 6 p.t. stage, contain a few widely separated statoliths in rapid motion. The esophagus, digestive diverticula, stomach, and intestine begin to differentiate at about the 4 p.t. stage. Many of the main organ rudiments first become apparent at the 5 to 6 p.t. stage. Digestive diverticula become constricted into pouches; rudiments

of the metanephridia are present; and the parietal muscle fibers and ganglia are formed. Four pairs of muscles are also found at this stage: the anterior occlusor; the internal oblique; the dorsal and ventral muscles. The ventral muscles are larval muscles and characteristic only of the free-swimming stage, since they degenerate after the animal becomes attached. External oblique muscles

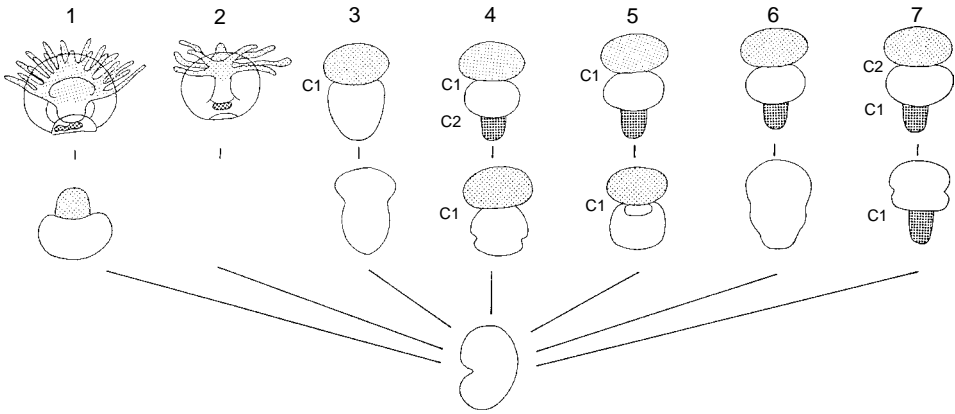


FIG. 163. Diagram of lobe formation during brachiopod development; 1, lingulids; 2, *Disciniscia*; 3, *Neocrania*; 4–7, articulated groups identified in text; anterior lobe and lophophore, *stippled*; mantle lobe, *plain*; pedicle lobe and pedicle bud, *shaded*; C1, C2, first and second constriction respectively (adapted from Chuang, 1990).

appear at the 6 p.t. stage, and an unpaired posterior occlusor is formed at the beginning of the 7 p.t. stage (Fig. 164).

A pedicle appears at the 6 p.t. stage, developing as an outgrowth of the ventral mantle and containing an extension of the main body coelom. This is lined with coelomic epithelium underlain by a layer of slightly oblique longitudinal muscle that is one fiber in thickness (YATSU, 1902a). At the 7 p.t. stage, the pedicle is circular. With age, it increases in length, attaining the form of a twisted sausage at the 7 to 9 p.t. stage. In both lingulids and discinids, the pedicle is initiated as an evagination of the inner surface of the ventral mantle immediately behind the posterior body wall, the juvenile mantle continuing on the posterior side of the pedicle to the margin of the valve. Prior to settling of the juvenile, the pedicle assumes a position entirely posterior to the tissue that formed the posterior sector of the juvenile ventral mantle. The change in relative position is assumed to be associated with the transformation of the ventral mantle lobe of the juvenile, for in adults the tissue immediately in front of the pedicle comprises a single layer of outer epithelium lining the body cavity. After settling, the ventral mantle of discinids and lingulids is intact. With the loss of the posterior sector of the juvenile

mantle, a flap of epithelium is developed that is continuous anterolaterally with the remainder of the ventral mantle. This sector of the adult mantle can only have developed from or have been proliferated by the tissues that initially formed the posterior body wall of the larva prior to settling. It is separated by the pedicle from the tissue that was involved in the corresponding sector of the juvenile mantle (Fig. 165). The secretory behavior of this posterior sector of the ventral mantle of the adult is considered to be of fundamental importance in determining the form of the adult shell (WILLIAMS & ROWELL, 1965a).

Considerable changes also affect the lophophore as it becomes a schizolophe, and a partition develops that divides the brachial canal into two canals: the future great canal and small brachial canals.

Increase in the size of the mantle and shell is continuous throughout these early developmental stages. At the 3 p.t. stage the two valves are semicircular and still joined together. The ends of the hinge line project laterally as a pair of small ears (the teeth in YATSU, 1902a). At the 7 p.t. stage, the shell is almost circular, becoming elongate by the 8 to 9 p.t. stage and elliptical by the 15 p.t. stage. Setae develop at the mantle margin by the 7 p.t. stage. The thin cuticle that initially joins the valves is ruptured along the hinge

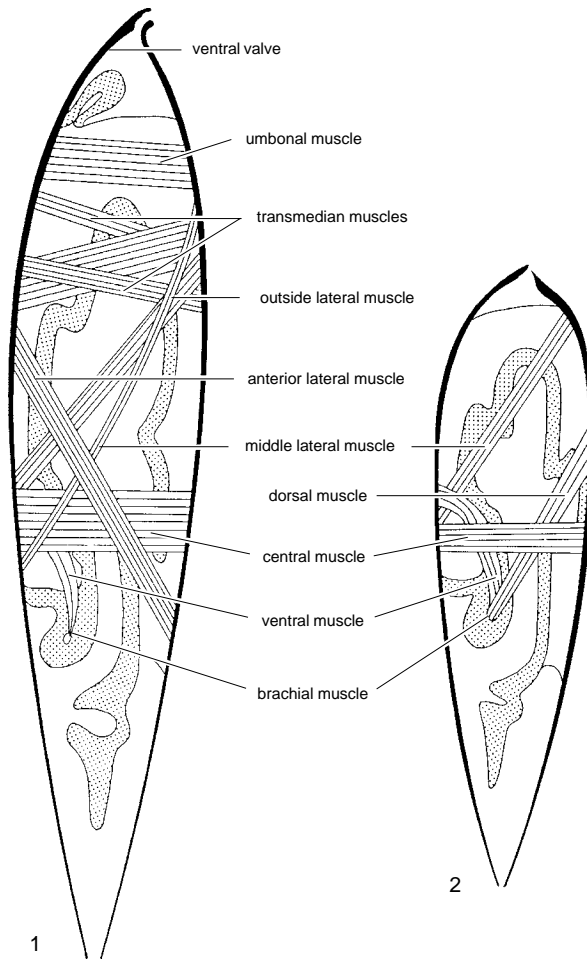


FIG. 164. Diagrammatic sections through *Lingula anatina* larva showing muscle development at 1, 5 p.t. and 2, 8 p.t. stages (adapted from Yatsu, 1902a).

line before the appearance of the 8 p.t. stage, and the transparent shell acquires a brownish tint along the margins. At the posterior end the superficial layers are bright green.

Statocysts at the 7 to 8 p.t. stage contain about 40 closely packed statoliths that move in unison within each enlarged statocyst. By the 8 to 9 p.t. stage, the digestive diverticula become progressively more lobulate, and the mantle canals start to appear.

The pedicle and setae develop during the later stages of the larva's planktonic life, unlike the differentiation of the gut, lophophore, and some elements of the muscular

system and protegulum, which are presumed to be necessary for planktonic life stages. Initiation of pedicle and setal development seems to be dictated by the availability of suitable settlement substrate. Lack of suitable substrate may have the potential to delay formation of the pedicle. Hence, the pedicle has been reported to develop as early as the 6 p.t. stage (YATSU, 1902a) and as late as the 11 p.t. stage (ASHWORTH, 1915), with settlement occurring at the 10 p.t. (YATSU, 1902a) and 15 p.t. (ASHWORTH, 1915) stages respectively. Setae develop along the entire mantle margin but extend beyond the shell only in

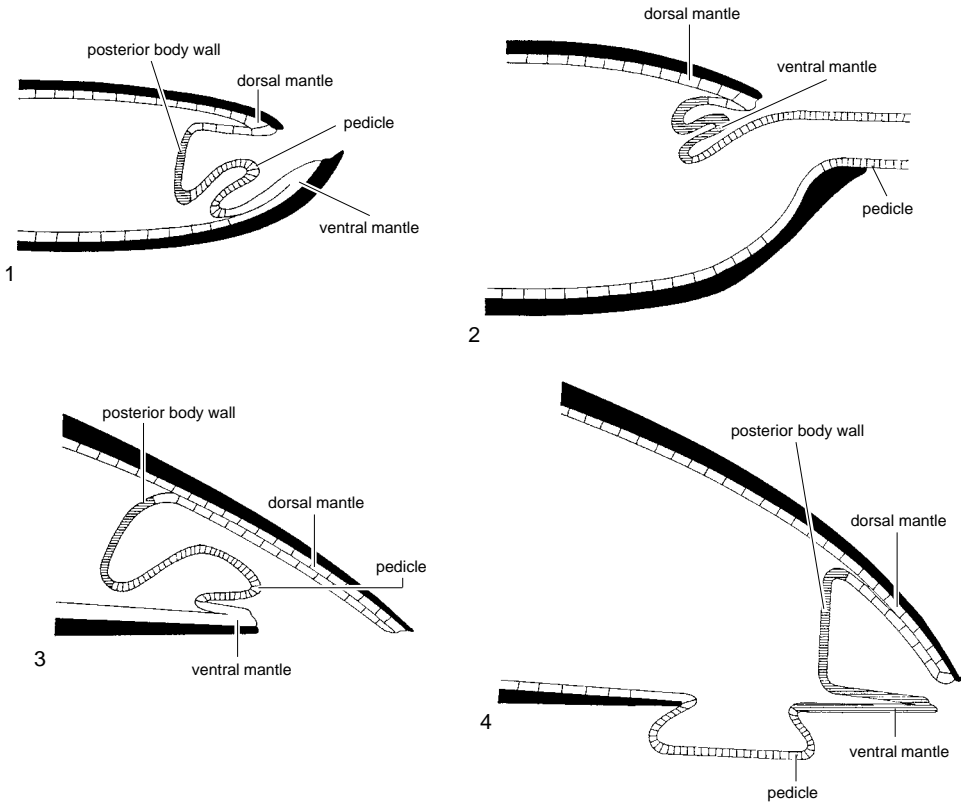


FIG. 165. Diagrammatic longitudinal sections; 1, young lingulid prior to settling; 2, adult lingulid; 3, young discinid prior to settling; 4, adult discinid (adapted from Williams & Rowell, 1965a).

posterolateral regions. In *Glottidia*, the pedicle is formed and the lophophore differentiated between the 2 and 9 p.t. stages (PAINE, 1963).

The earliest planktonic stage of *Discinisca lamellosa* is at the 2 p.t. stage and is characterized by two tufts of embryonic setae and a functional digestive system. The lophophoral tentacles are added in the same way as in *Lingula*, but the discinid larva is presumed to remain at the 4 p.t. stage throughout the planktonic phase, as no more developed, free-swimming stages have been observed. The shell is secreted at the 4 p.t. stage as a transparent, subcircular disc. Discinid larvae develop a complex succession of four different types of setae and may also possess statocysts and putative eyespots (Fig. 166;

HAMMOND, 1980). The shell-less larva swims with its trocholophe, tentacles, and median tentacle fully extended and the tentacles bent slightly inward or outward near the tip (Fig. 167). Older *Discinisca* larvae shed their setae and swim like *Lingula*, rotating in a clockwise direction when viewed from the anterior end (CHUANG, 1968, 1977). The larvae propel themselves mainly with the beating of the lateral cilia of the lophophore and tentacle.

All larvae of *Pelagodiscus atlanticus* have been taken in water less than 200 m deep, well above the range of adult *Pelagodiscus*; and earlier stages probably remain in deeper water. There is little information about settling, but it is assumed that the larvae become attached at the 4 p.t. stage after a free-

swimming period that lasts about five or six days (MÜLLER, 1860).

The two thin valves of the larvae are roughly circular with a width of about 400 μm to 500 μm and are held together by the body wall and muscles. Characteristically, there are five pairs of principal setae (Fig. 168). The anterior four pairs are attached to the ventral valve; those placed further back are much broader and larger than the others. The fifth pair of principal setae occurs posteromedially in the dorsal mantle where it is associated with about 30 pairs of minor setae developing along the lateral and anterior margins. The lophophore, which at this stage contains coelomic spaces and associated musculature, is similar to that of *Lingula*; but the tentacles are relatively thicker, and the median tentacle is only a broad projection of the anterior margin. Within the body cavity, the alimentary canal is functional, and the intestine opens to the right side of the body wall through the anus. The digestive diverticula are not developed, but the wall of the gut is already differentiated. Metanephridia and statocysts are present, and the musculature is well developed, although the posterior adductor muscles are not yet formed. A pedicle rudiment occurs, confined within the valves, and, as in *Lingula*, it projects from the inner surface of the ventral mantle (Fig. 169). A pair of larval eyespots is also developed on the lateral body walls.

At settlement, the pedicle is protruded from the valves through the notch at the posterior margin of the ventral valve. The eyespots are lost, larval setae are replaced by adult ones, and the median tentacle is reduced in size shortly after settling. There is no detailed information on the postlarval development of *Pelagodiscus*. Very little is known about the larval stages of other discinids, but *Discinisca laevis* have been observed already attached at the 6 p.t. stage; and morphologically they are similar to recently settled *Pelagodiscus* (WILLIAMS & ROWELL, 1965a).

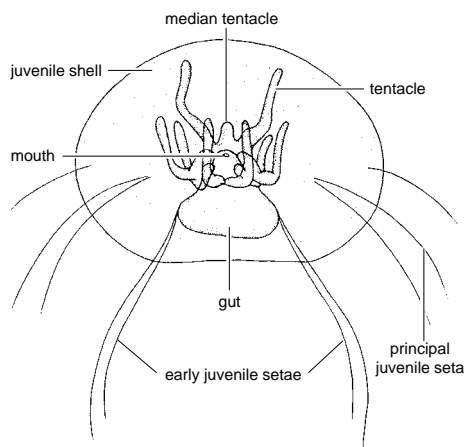


FIG. 166. Diagram of a free-swimming larva of *Discinisca* (adapted from Chuang, 1977).

Craniids

The larvae of *Neocrania* are lecithotrophic (NIELSEN, 1991). During the early, free-swimming stages of *Neocrania*, the endoderm occupies the anterodorsal part of the archenteron and the mesoderm occupies the posteroventral part (Fig. 162.1). The archenteron elongates with the blastopore at the posterior end of the ventral side. The endoderm elongates and narrows, while the mesoderm expands into a pair of lateral lobes (Fig. 162.2). Eventually, the endoderm constricts, and the archenteron persists anteriorly as a narrow lumen. Mesoderm still surrounds the narrow blastopore but extends to the anterior end of the endoderm and divides into a series of lateral plates. The setal sacs develop from three pairs of dorsal, ectodermal invaginations (Fig. 162.3). The posterior part of the endoderm becomes a solid cylinder, and the blastopore closes. Four pairs of coelomic sacs form from four pairs of plates of mesoderm, which fold up. The anterior pair of coelomic sacs surround the anterior part of the endoderm almost completely, while the three posterior pairs have a more restricted lateral position. In addition, small setae are formed from the setal sacs (Fig. 162.4; NIELSEN, 1991).

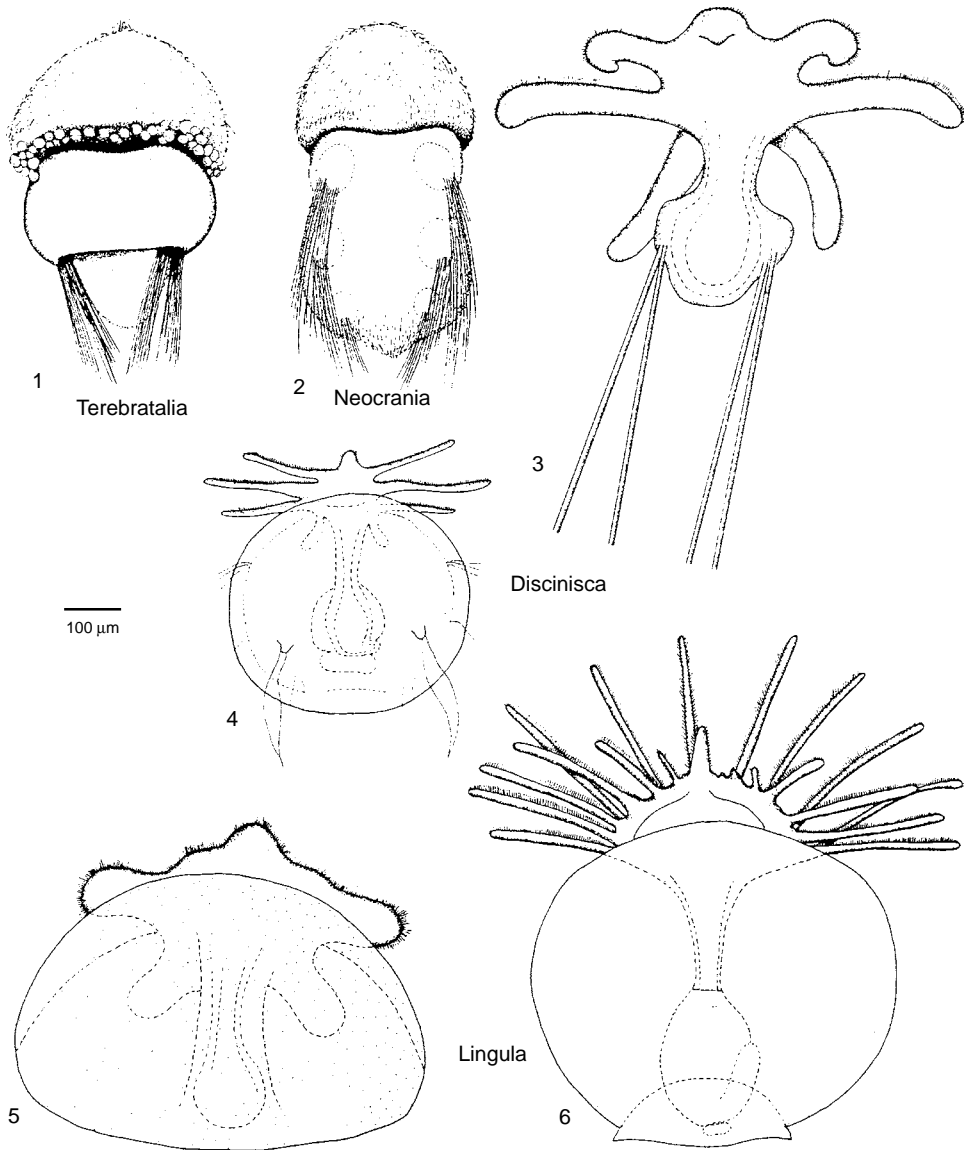


FIG. 167. Larvae of the four main types of brachiopods, dorsal views; 1, *Terebratalia transversa*; 2, *Neocrania anomala*; 3, early *Discinisca* larva; 4, full-grown *Discinisca* larva; 5, early *Lingula* larva; 6, the almost full-grown *Lingula* larva, scale bar: 100 μm (adapted from Nielsen, 1991).

Neocrania larvae, about 220 μm in length, appear to be fully developed approximately three days after fertilization (Fig. 170). The rounded anterior lobe and the lateral, ventral, and posterior sides are ciliated. Three

pairs of long, setal bundles occur laterally on the dorsal side. The larvae are light brown and have a pair of reddish, anterolateral pigmented spots that have been interpreted as eyespots (NIELSEN, 1991).

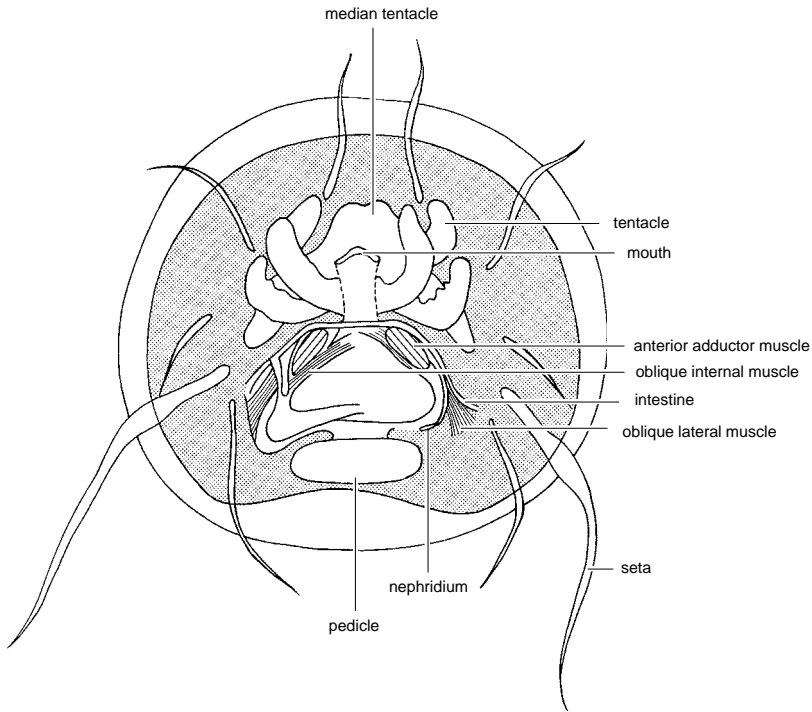


FIG. 168. Larval *Pelagodiscus* with 4 p.t. viewed ventrally, minor setae in dorsal valve omitted (adapted from Ashworth, 1915).

Articulated brachiopods

A fully developed, late stage larva of articulated brachiopods usually consists of the anterior, mantle, and pedicle lobes; it does not possess a functional gut and is lecithotrophic.

The anterior lobe is typically ciliated and bears a tuft of long apical cilia, supported on an apical plate. The apical cilia vary in length and in *Calloria* (PERCIVAL, 1944) and *Notosaria* (PERCIVAL, 1960) are lost prior to metamorphosis. In *Terebratalia*, the posterior margin of the anterior lobe supports a dense band of longer cilia (Fig. 171; LONG, 1964; STRICKER & REED, 1985a). The anterior lobe of many larvae possess putative eyespots (ocelli) or groups of small, usually red, pigment granules. Eyespots generally occur apically or subapically. *Argyrotheca* has four separate eyespots (KOWALEVSKY, 1883;

SHIPLEY, 1883; PLENK, 1913); *Lacazella* has two or four (LACAZE-DUTHIERS, 1861; KOWALEVSKY, 1883); *Pumilus* has four groups of two (RICKWOOD, 1968); *T. transversa* has two groups of five to eight granules (LONG, 1964); *Coptothyris* and *T. coreanica* have two groups of about 10 (HIRAI & FUKUSHI, 1960); and *Frenulina sanguinolenta* has two groups of about 20 (MANO, 1960). Pigment granules usually occur as spherical protuberances (vesicular bodies; LONG & STRICKER, 1991). *T. transversa* has a number of these outgrowths (Fig. 167, 171), and *Calloria* has about 60; they are arranged along the posterior margin of the anterior lobe in both species. Eyespots and pigment granules do not occur in the larvae of *Hemithiris*, *Notosaria*, *Terebratulina unguicula*, *T. septentrionalis*, or *T. retusa* (CHUANG, 1990). Descriptions of eyespots and pigment granules are often confused, but it is likely that these features are

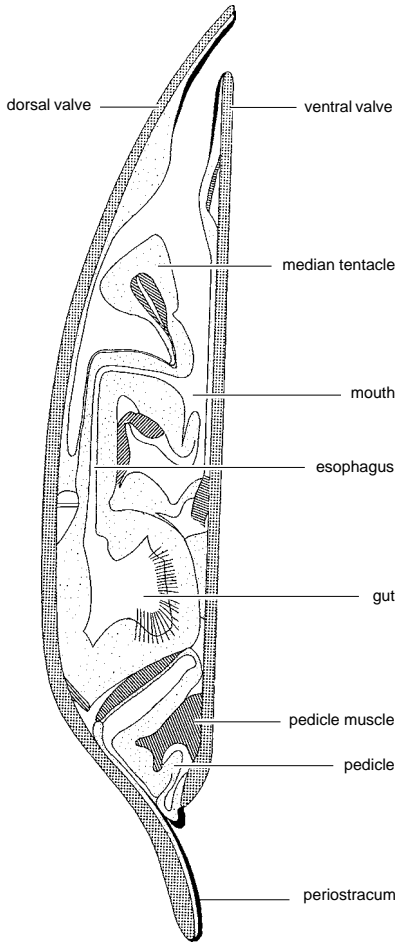


FIG. 169. Diagrammatic median longitudinal section of larval *Pelagodiscus* with four pairs of tentacles (not shown) located laterally from midline (adapted from Ashworth, 1915).

not homologous. Each of the eyespots of *Argyrotheca* consists of a cuplike invagination of the ectoderm with underlying nerve fibers and vitreous humor (PLENK, 1913), a neurological connection implying a sensory role. Pigment granules, however, lack any known connection with the nervous system and are assumed to be some form of metabolic waste (CHUANG, 1990).

The mantle lobes of the late-stage larva are clearly divisible into dorsal and ventral lobes. In *T. transversa* and probably other species a

mantle lobe comprises an outer layer of thin, flattened, ectodermal cells and an inner layer of tall, columnar cells. These two layers enclose a space containing mesodermal cells also arranged in two sheets with a coelomic space in between. The mantle lobe grows until it almost completely encloses the pedicle lobe (LONG, 1964). Both lobes extend posteriorly from the midriff of the larvae, progressively enveloping the pedicle lobe. The ventral lobe is the larger and in *T. retusa* has been observed to extend beyond the distal tip of the pedicle lobe in specimens with delayed settlement (JAMES, unpublished, 1989). The outer, ectodermal layer contains large vacuoles (LONG, 1964). A longitudinal band of cilia on the ventral side of the mantle lobe enables the larva of *Notosaria* to creep along the substratum (PERCIVAL, 1960). Similarly, in *T. transversa* only a mid-ventral band of cilia occurs on the mantle lobe (Fig. 171). Generally, two pairs of setal bundles are present and are formed in four separate ectodermal invaginations at the distal margin of the mantle lobe and disposed as two lateral and a pair of dorsal bundles. Each bundle contains from 4 to 20 setae in various larvae studied. The larva of *Lacazella* was reported as lacking setae (RUDWICK, 1970).

In the pedicle lobe, the ectoderm consists of a single layer of columnar cells that may be ciliated, although in *T. transversa* (LONG, 1964) and *T. retusa* (JAMES, unpublished, 1989) no cilia are present on the pedicle lobe. Some cells of the outer walls of the coelomic epithelium elongate and differentiate into smooth muscle cells to form a pair of pedicle adjustors. These extend from the base of the anterior (proximal) region of the mantle lobe into the pedicle lobe (FRANZEN, 1969; STRICKER & REED, 1985a, 1985b). Prior to settlement, the pedicle lobe of *T. transversa* develops a subequatorial constriction. The region to the posterior of the constriction tapers and eventually differentiates into the pedicle and the surrounding pedicle sheath of the metamorphosed juvenile. The anterior part of the pedicle is packed with

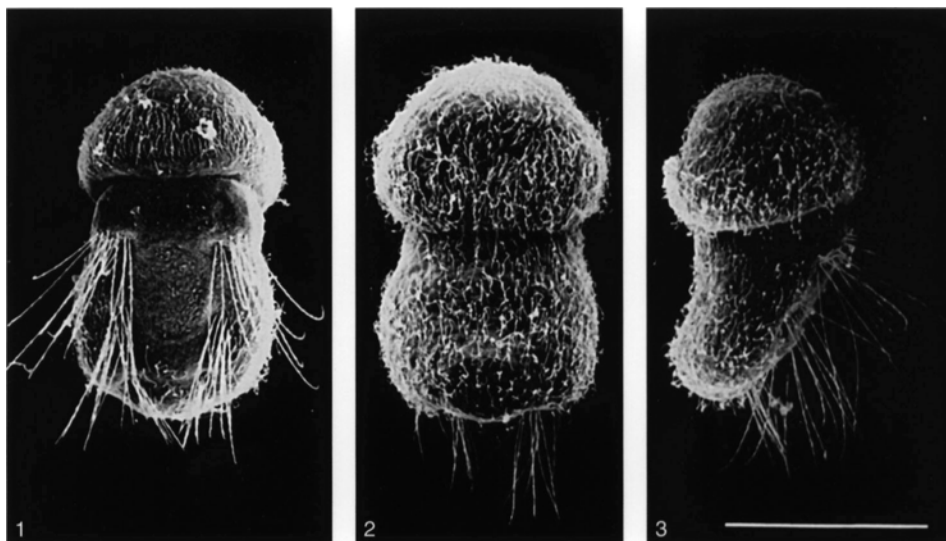


FIG. 170. SEM micrographs of full-grown larvae of *Neocrania*; 1, dorsal view, the circular dorsal area that will form the brachial valve recognizable; 2, ventral view; 3, lateral view, scale bar: 100 μm (Nielsen, 1991).

tissue that contains rudiments of some of the internal organs (see Fig. 63; LONG & STRICKER, 1991).

In contrast to the development of lingulids and discinids, the organs of the calcareous-shelled brachiopods are poorly differentiated during the free-swimming larval phase. Only the presumptive pedicle muscles, the incipient coelomic spaces, and the nonfunctional larval gut are present (Fig. 172.1; LONG & STRICKER, 1991). The presence of larval metanephridia, however, has been described in *Argyrotheca* (PLENK, 1913).

Larval Behavior

During the motile, planktonic larval phases, which may last from hours in articulated and craniid brachiopods to weeks in the lingulids and discinids, the larvae undergo morphological and behavioral changes. Accounts of larval behavior, particularly at settlement and metamorphosis, are rare (JAMES & others, 1992), and little information exists on the behavior of the planktonic larval stages of discinid and lingulid larvae.

When a brachiopod larva is capable of swimming freely, at hatching or upon liberation from a brood chamber, its behavior is likely to be influenced primarily by gravity or light. Positive phototaxis has been documented during the early, free-swimming larval stages of a number of articulated species, which become negatively phototactic prior to settlement.

The gametes of *T. retusa* are freely spawned, and the larvae first achieve motility at a stage that is presumed to be pregastrulation. The larvae, which are effectively revolving balls of cells, do not appear to move in a defined pattern until gastrulation has occurred. Postgastrulation larvae are slightly anteroposteriorly elongate and compressed dorsoventrally. Larvae at this stage rotate along the anteroposterior axis, usually in a clockwise direction when viewed anteriorly. Axial rotation and movement (anterior end forward) presumably allow the larvae to orient and swim in a trajectory. At this stage, larvae of *T. retusa* are negatively geotactic and swim away from the substrate. During early, free-swimming stages, such larvae exhibit no

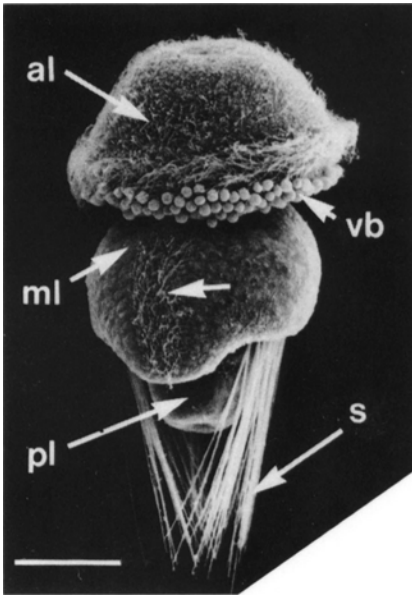


FIG. 171. SEM micrograph of a free-swimming larva of *Terebratalia* at 110 hours after fertilization; arrows mark an unlabeled band of cilia on the mantle lobe (*ml*), scale bar: 50 μ m; *al*, apical lobe; *pl*, pedicle lobe; *s*, setae; *vb*, vesicular bodies (Stricker & Reed, 1985a).

response to light, although positive phototaxis may occur for a short period later in development. Eventually, they become positively geotactic, and negative phototaxis may also be involved. The now characteristically three-lobed larva swims toward the substrate with the anterior lobe flexing and sweeping in a lateral arc whenever it, or the apical cilia, make contact with the substratum (JAMES, unpublished, 1989; JAMES & others, 1992).

Brooded articulated larvae that emerge from the parent at a later stage of development may behave differently. The larvae of *Frenulina*, for example, just after emerging from the mantle cavity of the brooding parent, show positive phototaxis that becomes negative within a few hours (MANO, 1960).

Like that of *T. retusa* (JAMES & others, 1992), the *Frenulina* larva (MANO, 1960) sinks and rubs its anterior lobe against the substratum (CHUANG, 1990). Likewise, larvae of *Notosaria* glide along the surface of the

substrate with the aid of a ventral band of cilia for several hours, the anterior lobe probing the substratum (PERCIVAL, 1960). *Neocrania* larvae that are competent to settle descend to the substrate and crawl, apparently seeking a suitable medium on which to settle (NIELSEN, 1991).

Most larvae possess a number of setal bundles that serve both a sensory and a defensive role. When the larva of *Argyrotheca*, for example, is disturbed, it contracts violently and projects its tufts of setae out in all directions (KOWALEVSKY, 1883). The larval setae of *Discinisca* are used in a similar defensive response (CHUANG, 1977). *T. transversa* larvae contract, bringing the anterior and posterior lobes closer together. The mantle lobe is raised from the pedicle lobe and the setae are erected perpendicular to the body to form a defensive circle around the middle of the body (LONG, 1964). The larva of *Neocrania* reacts in a similar manner. The undisturbed larva swims with the setae held close to the body. Irritation, however, stimulates contraction of the longitudinal ventral muscles, causing the body to curl up, bringing the anterior and posterior ends into contact and extending the setae in all directions (NIELSEN, 1991).

BROODING

Some articulated brachiopods brood their larvae in specialized pouches within the body cavity or in the mantle cavity. Species that brood are presumed either to draw sperm in with the inhalant current generated by the lophophore or, among simultaneous hermaphrodites, to effect self-fertilization (LONG & STRICKER, 1991). Fertilization probably occurs in the mantle cavity or within the brood pouch or chamber. Generally, small numbers of lecithotrophic embryos and larvae are brooded to an advanced state of motile larval development when settlement and metamorphosis may be possible soon after liberation from the parent.

Brooding within the mantle cavity occurs either by adherence of the larvae to the inner

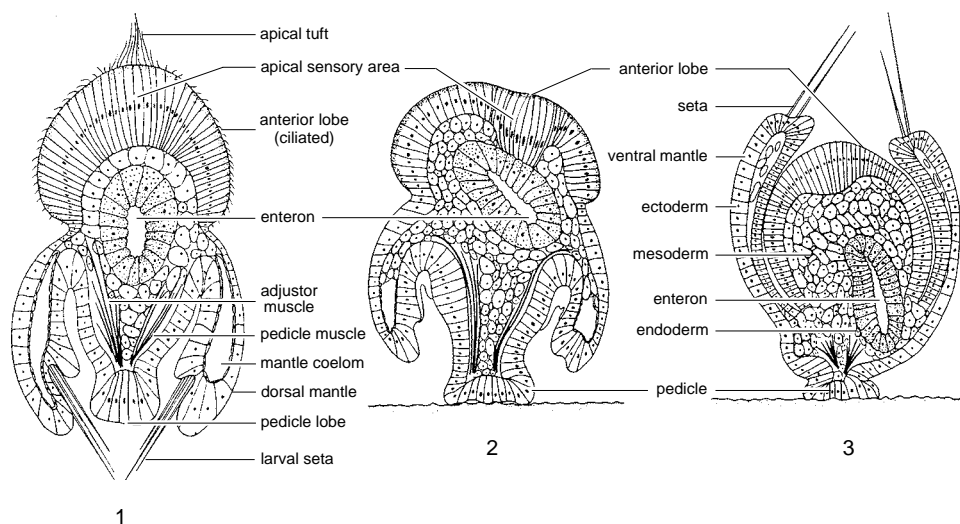


FIG. 172. Diagrams of longitudinal median sections of trilobed larva of *Terebratulina retusa*; 1, immediately prior to settlement; 2, after settlement; 3, after metamorphosis (adapted from Franzen, 1969).

mantle surface or within the confines of the tentacles of the lophophore. Early developmental stages of *Calloria* adhere to the mantle and develop into free-swimming larvae before discharge (PERCIVAL, 1944). The ova of *Frenulina* are spawned and adhere to longitudinal nurse ridges, one on each side of the midline of the dorsal mantle, where fertilization and development into free-swimming larvae take place (MANO, 1960).

Tentacles of the lophophore form a natural refuge in which a number of articulated species brood their larvae. *Pumilus* retains embryos and larvae within its schizolophe for at least nine days prior to the release of larvae, which are competent to settle (RICKWOOD, 1968). The rhychonellids *Hemithiris* (LONG & STRICKER, 1991) and *Notosaria* (PERCIVAL, 1960) retain their shed ova in a basket created by curling the distal ends of the lophophore tentacles. Larvae develop at the base of the tentacles and the brachial lip and are generally oriented with their anterior ends toward the mouth (see Fig. 119; HOVERD, 1985). The larvae of *Liothyrella uva antarctica* are similarly sequestered in the spirals of the lophophore (BLOCHMANN,

1906). *T. unguicula* broods several thousand larvae within the lateral arms of its plectolophe (LONG, 1964) as does *T. septentrionalis*. The larvae are retained beneath the lophophoral tentacles that enclose them against the wall of the main body cavity and the floor of the dorsal mantle, thus forming a basket (WEBB, LOGAN, & NOBLE, 1976).

Lacazella possess two median, lophophore tentacles that are modified for the attachment of the embryos and larvae. The specialized tentacles are longer and larger than other tentacles and possess a collar of cells at the base of the swollen, pyriform, and glandular tentacle tip. A cellular suspensory filament attaches individual embryos to these tentacles. The embryos suspended on the distal parts of the modified tentacles are inserted into a single median brood pouch behind the mouth, embedded in the posteroventral portion of the body cavity (Fig. 173; LACAZE-DUTHIERS, 1861). *Argyrotheca* (KOWALEVSKY, 1883; SHIPLEY, 1883; SCHULGIN, 1885) as well as *Thecidellina* are known to deliver their eggs into brood pouches (WILLIAMS & ROWELL, 1965a). In *Argyrotheca* that brood, each -

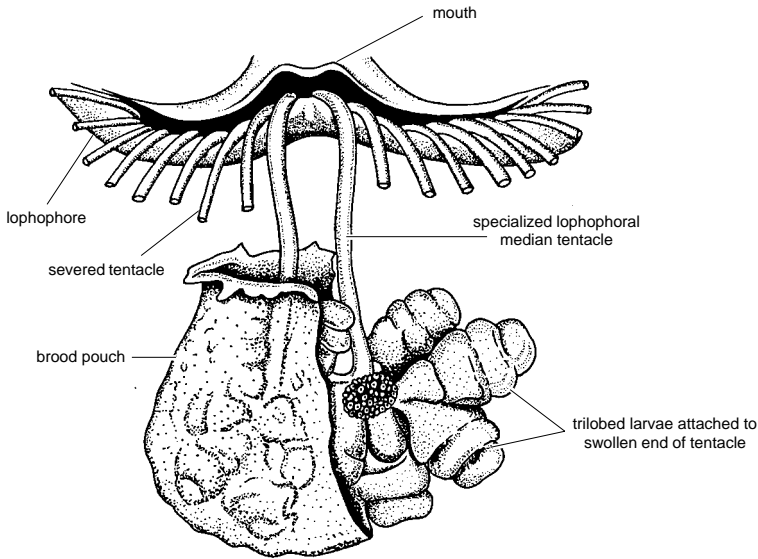


FIG. 173. Brood pouch and modified lophophoral tentacles of *Lacazella mediterranea*; part of the pouch has been removed to reveal the three-lobed larvae attached to a tentacle (adapted from Lacaze-Duthiers, 1861).

metanephridiopore opens to a separate brood pouch situated under the posterior border of the lophophore (SHIPLEY, 1883). Gametes are passed from the body cavity through the modified metanephridia directly into the brood pouches where the embryo develops, attached to the wall of the pouch by a fine filament (KOWALEVSKY, 1883; SHIPLEY, 1883). Brooding within the body cavity also occurs in *Gwynia capsula* where the larvae are retained to the three-lobed stage (SWEDMARK, 1967).

SETTLEMENT

Studies of substrate selection and the mechanisms involved in settlement and the subsequent survival and growth of the sessile and juvenile stages facilitate an understanding of brachiopod life history and distribution patterns.

Some authors report rugophilic behavior, preferential settlement on a particular type of substratum and on or near members of the same species. Inferences on behavior drawn from patterns of juvenile settlement neglect the impact of other processes such as grazing,

selective predation, substratum failure, and fluid dynamics near the substratum. Settlement of the larvae in the laboratory has been observed in *T. septentrionalis* (MORSE, 1873), *Argyrotheca* (SHIPLEY, 1883), *Calloria* (PERCIVAL, 1944; WISELY, 1969), *T. coreanica* and *Coptothyris* (HIRAI & FUKUSHI, 1960), *T. transversa* (LONG, 1964; STRICKER & REED, 1985a, 1985b), *Hemithiris* (LONG, 1964) and *Pumilus* (RICKWOOD, 1968). Data on selection of substrates are, however, sparse, and experimental evidence is inconclusive.

All brachiopod larvae are, to some degree, capable of delaying settlement until a suitable substratum has been located. For the planktotrophic lingulid and discinid larvae, competence to settle may last for several weeks; for the lecithotrophic larvae of articulated brachiopods and *Neocrania* the limit may be perhaps hours or a few days.

Lingulids and discinids

The larvae of lingulids and discinids, which pass through a relatively brief lecithotrophic embryonic phase before adopting a planktotrophic mode of life, may persist as

larvae for several weeks. Ambient water temperature, food, and suitable substrate availability may all have a profound influence on the rate of development of both embryo and larva. In temperate waters, it is estimated that the larvae of *Lingula* take approximately five to six days to achieve the 3 p.t. stage at which hatching occurs; and a further six weeks may be spent as plankton for the larva to reach the 15 p.t. stage (YATSU, 1902a). According to YATSU (1902a), in *Lingula* settlement is possible at the 10 p.t. stage. CHUANG (1959b) and BROOKS (1879), however, recorded settlement at the 9 p.t. stage in *Lingula* and *Glottidia* respectively. Given appropriate conditions it is estimated that *Lingula* may complete both embryonic and larval development in 31 to 32 days (CHUANG, 1990). The larval development of *Glottidia* is estimated to take 20 days at temperatures between 25 and 30°C (Table 5, p. 180; PAINE, 1963). The length of the larval stage in *Discinisca* is unknown, but the 4 p.t. stage is assumed to correspond to several p.t. stages in *Lingula* (CHUANG, 1990).

The pedicle protrudes from the valves, and the larvae burrow with the anterior end, using the setae to move the sand grains. The pedicle protrudes from between the valves, and the tip adheres to sand grains (PAINE, 1963). The larvae of *Discinisca* (CHUANG, 1977; HAMMOND, 1980) and *Pelagodiscus* (CHUANG, 1990) are presumed to settle at the 4 p.t. stage.

The larvae of lingulids and discinids can remain as plankton and become drift larvae. Drift larvae grow beyond the stage of development normally attained at settlement. In drift larvae of *Lingula*, the lophophore continues to grow by adding new pairs of tentacles, and the median tentacle persists. The epistome continues to enlarge and the shell valves continue to expand circumferentially. The mantle setae increase in number, and the pedicle increases in length but remains within the confines of the valves (CHUANG, 1990). Drift larvae of *Glottidia* also exhibit the characteristics of delayed

settlement, with both the pedicle and the setae appearing in much larger larvae (PAINE, 1963). In drift larvae of *Discinisca*, the valves continue to grow, setae continue to increase in length but not number, and the pedicle continues to increase in size while remaining within the valves; the flexible mantle setae also increase in number (CHUANG, 1990). Lingulid and discinid larvae do not, however, undergo true metamorphosis at settlement.

Craniids

Lecithotrophic larval development in *Neocrania* takes approximately 70 hours (Table 5, p. 180). The larva attaches when it is about 200 µm to 300 µm long. Newly settled larvae possess ventral muscles that extend from the first pair of coelomic sacs to the posterior end of the larva. These muscles constrict, causing the larva to curl up ventrally (Fig. 174). Likewise, the muscles around the coelomic sacs contract, spreading out the setae of sacs 1 and 2 (those of sac 3 having been shed and the cilia having disappeared) (Fig. 162.5; NIELSEN, 1991). The posterior part of the body of the larva and the apical part of the anterior lobe make contact with and adhere to the substratum. During the days following settlement the larval body of *Neocrania* gradually flattens and becomes more rounded. Glandular cells on the dorsal surface secrete the dorsal valve, which grows radially pressing out the mantle setae along the sides of the body (Fig. 175; NIELSEN, 1991).

Articulated groups

The fully developed, lecithotrophic larvae of articulated brachiopods descend to the substrate after a variably long, demersal phase that may last from hours to a few days in different species (Table 5, p. 180). Although substrate selection has not been demonstrated, accounts describe larvae exploring and probing the substrate, particularly with their anterior lobes. Eventually, the pedicle lobe secretes a sticky sheet (STRICKER &

TABLE 5. Times of appearance of identifiable embryological features during the development of brachiopods; (adapted from James & others, 1992).

Species	Egg diameter (μm)	Temperature ($^{\circ}\text{C}$)	Time (h)	Developmental stage	Authority
<i>Hemithiris psittacea</i>	190	10	23	blastula	Reed, 1987
			71	gastrula	
			117	mantle lobe appears	
			151	coelomic spaces present	
			187	setae develop	
			200	metamorphosis	
<i>Terebratalia transversa</i>	150	12	2–3	first cleavage	Reed, 1987
			4	second cleavage	
			18–14	blastula	
			22	gastrulation	
			33	coelomic partitioning	
			40	mantle lobe appears	
			48	setae appear	
			61	blastopore closes	
			92	mature larva	
			100	metamorphosis	
<i>Terebratulina unguicula</i>	170	10	3	second cleavage	Reed, 1987
			20	blastula	
			42	gastrulation	
			48	coelomic partitioning	
			66	mantle lobe present	
			102	short chaetae present	
<i>Terebratulina retusa</i>	130	10	2	first cleavage	James, unpublished data, 1989
			3	second cleavage	
			19–20	blastula	
			28–30	gastrula	
			50	mantle lobes present	
			60	short mantle	
<i>Neocrania anomala</i>	125	*	2	first cleavage	Nielson, 1991
			3	second cleavage	
			4	third cleavage	
			5	fourth cleavage	
			15	blastula (ciliated motile)	
			72	fully developed larva	
<i>Glottidia pyramidata</i>		27	0.5	first cleavage	Paine, 1963
			0.75	second cleavage	
			1	third cleavage	
			1.3	fourth cleavage	
			1.5	fifth cleavage	
			13	mantle lobes formed	
			19	cilia developed	
			24	median tentacle of lophophore formed	
			144–168	free-swimming 3 p.t. stage	
			264–408	5–8 p.t. stage	
480 (20 days)	9 p.t. stage; settlement				

*larvae cultured at ambient sea temperature ($\pm 1^{\circ}\text{C}$).

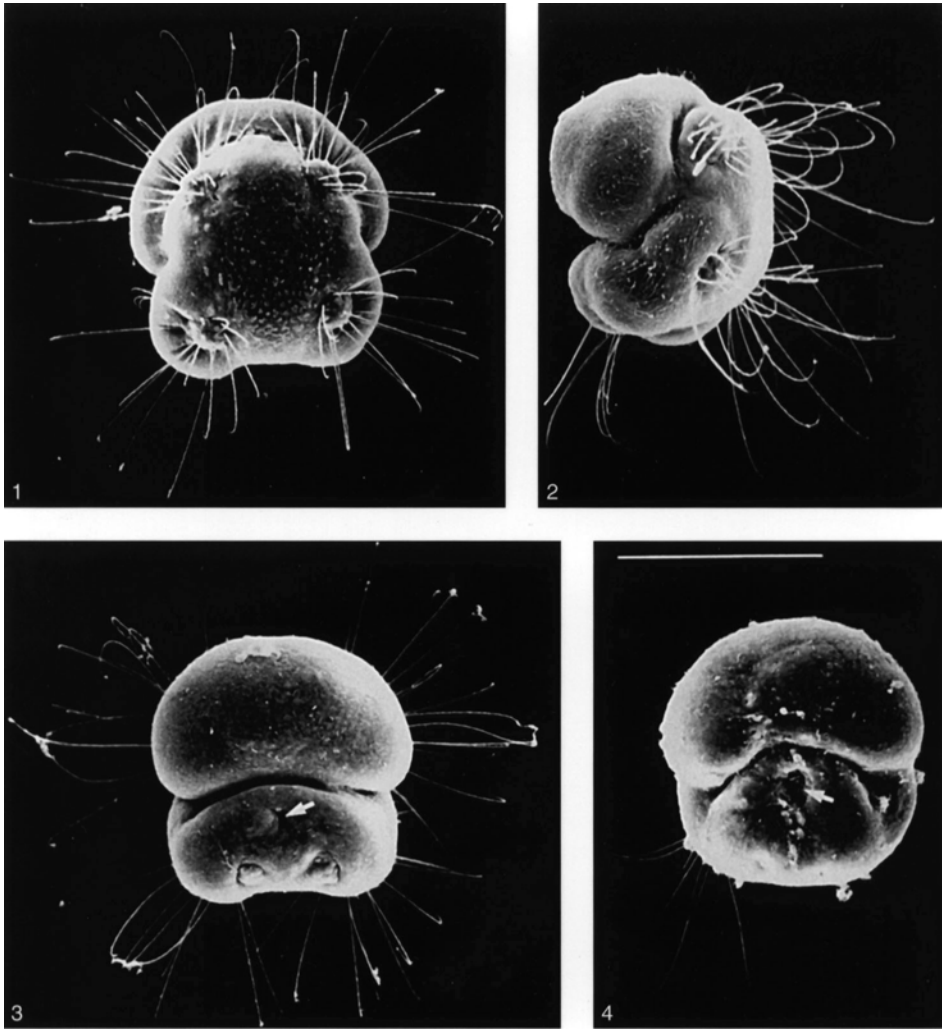


FIG. 174. SEM micrographs of contracted larvae and early settling stage of *Neocrania*; 1–3, contracted larvae in dorsal, lateral, and ventral views, respectively; 4, ventral view of the newly settled larva; arrows point to the retracted attachment areas, scale bar: 100 μm (Nielsen, 1991).

REED, 1985c) or mucous strand (KOWALEVSKY, 1883; JAMES & others, 1992) from the distal tip of the pedicle lobe (Fig. 160.17). By adopting an orientation perpendicular to the substrate, the mucous strand adheres to the substrate, anchoring the larva. The larvae of *T. retusa* displaced at this stage of settlement are capable of reattachment. Once attached, these larvae continue their

axial rotation, twisting the strand, effectively reducing its length and bringing the distal tip of the pedicle lobe into contact with the substrate (JAMES, unpublished, 1989). Subsequently, the pedicle lobe initiates a more stable form of substrate attachment.

When the larva of *T. retusa* is deprived of a suitable substrate, the mantle lobes continue to grow and may eventually extend

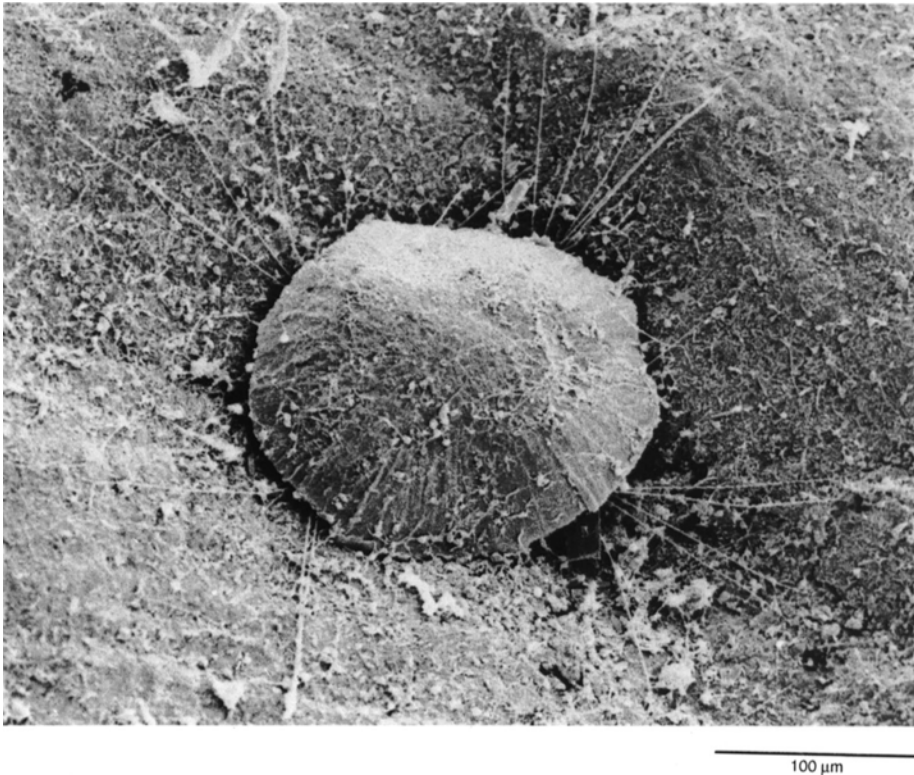


FIG. 175. SEM micrographs of a juvenile *Neocrania* about three days after settling, scale bar: 100 μm (Nielsen, 1991).

below the pedicle lobe. It is unknown if larvae in this condition remain competent to settle and metamorphose, but motile larvae were observed seven days after fertilization (JAMES, unpublished, 1989).

The process of metamorphosis has been described in detail for the terebratulides *T. retusa* (FRANZEN, 1969), *T. transversa* (STRICKER & REED, 1985a, 1985b), and *Calloria* (PERCIVAL, 1944). The general pattern of events appears to be similar in all articulated groups. Following attachment of the pedicle, the pedicle adjector muscles contract and thereby reverse the position of the mantle lobe, causing it to envelop the anterior lobe (Fig. 160.18–160.19). In addition, fluid pressure generated from the coelom (FRANZEN, 1969) and violent spasmodic contractions of the anterior lobe (PERCIVAL, 1944) may also facilitate reversal of the

mantle (CHUANG, 1990). Reversal of the mantle in the larva of *T. transversa* appears to be very rapid (LONG, 1964; STRICKER & REED, 1985a) but may require more than a day in other species (RICKWOOD, 1968). In the larva of *Calloria* the mantle lobe begins reversal at its base, forming a circular fold around the base of the anterior lobe, the free margin of the mantle lobe rolling anteriorly to envelop the anterior lobe (PERCIVAL, 1944). *Frenulina* combines settlement and metamorphosis. It stops swimming, lies on its side on the substrate, suddenly spreads the dorsal tuft of setae, and slowly lifts the dorsal mantle lobe. Simultaneously, the pedicle lobe protrudes and attaches to the substratum with a mucous secretion (MANO, 1960). As no reports exist of metamorphosis in unsettled larvae, it is assumed that settlement is a prerequisite of metamorphosis.

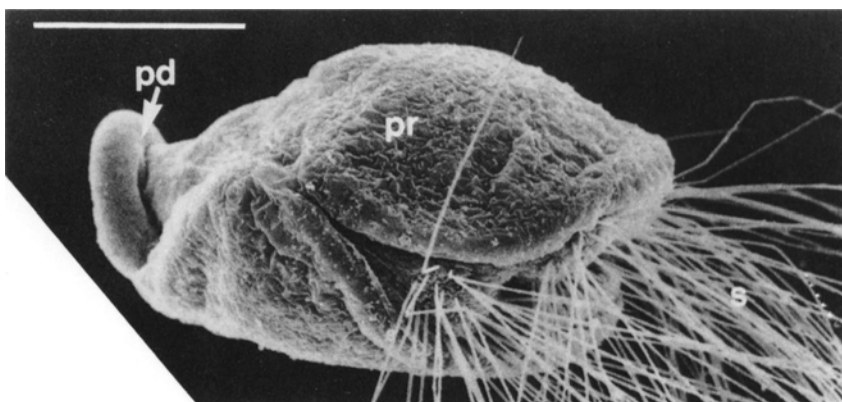


FIG. 176. SEM micrograph of a juvenile *Terebratalia* one day after metamorphosis, scale bar: 50 μ m; *pd*, pedicle; *pr*, protegulum; *s*, setae (Stricker & Reed, 1985b).

In the larva of *T. transversa*, the setae on the mantle lobe project anteriorly and are retained, at least during the early part of the juvenile stage. Although formation of the periostracum begins prior to reversal of the mantle in the larva of *T. transversa*, no larval or embryonic shell is deposited until metamorphosis has taken place (STRICKER & REED, 1985a). In the larva of *Calloria*, however, formation of the shell is initiated before the mantle lobe is reversed (PERCIVAL, 1944), and externally the metamorphosed juvenile resembles a small adult (Fig. 160.19; 176; STRICKER & REED, 1985a).

POSTLARVAL AND EARLY JUVENILE DEVELOPMENT

Lingulids and Discinids

Lingulid and discinid postlarval forms are effectively miniature adults at the time of settlement with most of the postlarval organs formed (Fig. 177; CHUANG, 1990).

During the entire larval stage of *Lingula* (YATSU, 1902a; CHUANG, 1959b), *Glottidia* (BROOKS, 1879; PAINE, 1963) and *Discinisca* (CHUANG, 1968, 1977), the trochlophore persists (CHUANG, 1990). After settlement at about the 9 p.t. stage (or later) in *Lingula* (CHUANG, 1959b) and *Glottidia* (BROOKS, 1879; CHUANG, 1959b) and at the 4 p.t.

stage in *Discinisca* (CHUANG, 1977), the median tentacle diminishes in size, becomes a small prominence in the epistome, and finally disappears. The two anterior, generative tips of the trochlophore, one on each side of the median tentacle, diverge, each developing into a curved brachium and giving rise to a series of tentacles. The lophophore is now a schizolophore, a condition that persists in the adult lophophore of *Pelagodiscus*.

In *Lingula*, *Glottidia*, and *Discinisca*, the trochlophore loses its locomotor function at settlement and is solely devoted to the role of circulating water through the mantle cavity for ventilation and feeding. For *Lingula*, this change in function coincides with atrophy of the two larval, lophophore retractor muscles before the 7 p.t. stage and the end of the larval stage respectively (YATSU, 1902a). An epistome forms, enlarges, and differentiates into the brachial fold to cover the mouth and the brachial groove.

The two generative zones at the tips of the pair of brachia of the trochlophore gradually move apart to define a median indentation, and the lophophore becomes a schizolophore. The epistome then undergoes lateral expansion concentric with the tentacle bases to form the juvenile brachial lip, which covers the brachial groove along its entire length. With further growth of the lophophore, the

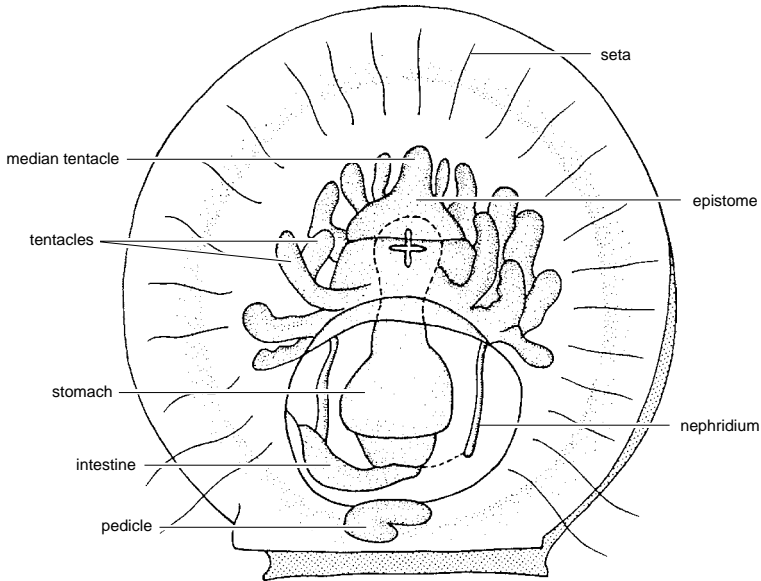


FIG. 177. Larval *Lingula anatina* with 8 p.t. viewed ventrally (musculature omitted) (adapted from Yatsu, 1902a).

generative zones are pushed away as the apices of the two ever-increasing spires, medially in the lingulids, ventrally in the discinids. Thus, the brachia form a series of whorls, eventually transforming the lophophore into a spirolophore; a chitinous brachial skeleton and the turgidity of the brachial canals provide the necessary support for the lophophore.

Craniids

Neocrania larvae are ciliated on the anterior lobe and the dorsal side of the body. At settlement, the cilia disappear, and the posterior pair of setal bundles are shed (NIELSEN, 1991). The newly settled *Neocrania* larva does not possess a functional gut, lophophore, or main organ rudiments and, like articulated forms, undergoes the most radical changes in morphology at settlement, adapting from a free-swimming, lecithotrophic larva to a sessile, suspension feeder. The dorsal valve forms within the first few days of settlement, and some of the attendant musculature appears to be present, as the valve

can be pulled down to the substratum when the animal is disturbed (NIELSEN, 1991).

A *Neocrania* juvenile at approximately two days after settlement possesses ventral muscles that extend from the first pair of coelomic sacs to the thickened posterior epithelium, which is, in turn, attached to the substratum (Fig. 162.6). The second and third pairs of coelomic sacs stretch longitudinally, and each sac of the second pair develops a small, dorsal extension that forms the attachment of the sac to the epithelium in the anterior region of the expanding valve. During the later stages of metamorphosis the growing valve also pushes the setae aside (Fig. 162.6). The fourth pair of sacs is situated below the expanding third pair. None of the coelomic sacs is fused in the midline, and at this stage the endoderm is compact with no trace of mouth or anus. Eventually the two valves completely cover the body. After about a month after settlement, three pairs of tentacles are present but there is no well-defined median tentacle. An open gut with a mouth has formed at the bottom of the un-

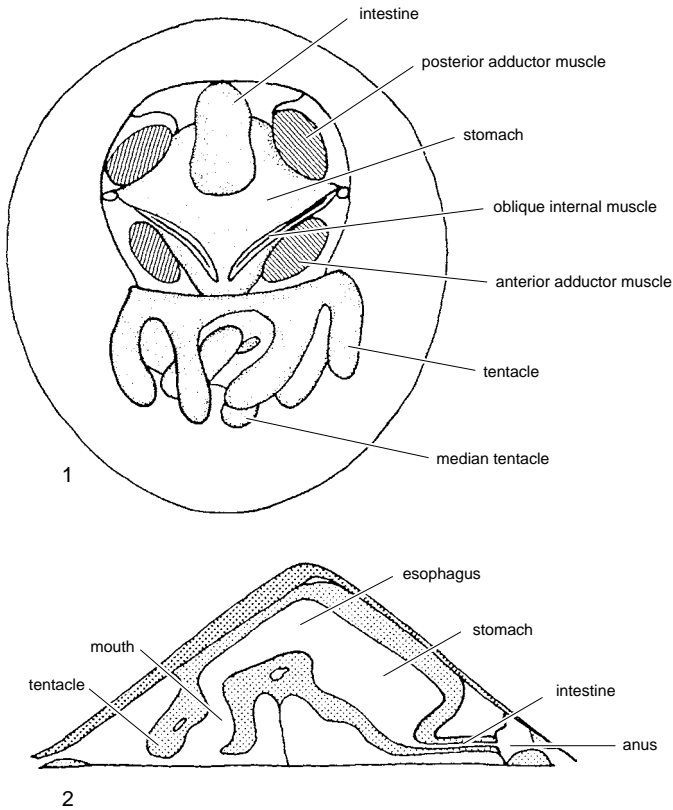


FIG. 178. Young *Neocrania anomala* recently attached, with 3 p.t. 1, viewed ventrally and 2, in diagrammatic median section (adapted from Rowell, 1960).

derside of the larval head, and the intestine is presumed to terminate at an anus at this stage (Fig. 162.7; NIELSEN, 1991).

At this stage the mantle has already secreted a thin calcareous shell covered by periostracum, but the ventral mantle is invested only in a periostracal layer that cements the animal to the substratum (WILLIAMS & WRIGHT, 1970). With the exception of the lophophore protractor and anal muscles, the adult muscle system is already present (Fig. 178).

The first and fourth pairs of coelomic sacs are no longer distinguishable, and the second pair fuses dorsally and ventrally, forming a ring around the secondary opening between the ectoderm and endoderm. Muscle fila-

ments are present in two extensions, which attach the coelomic sacs to the epithelium of the dorsal valve. The third pair of coelomic sacs extends and makes contact dorsally and ventrally to form thin mesenteria, dorsal and ventral to the stomach. There is a large anterior adductor muscle on either side of the anterior part of the stomach; each muscle cell is attached to the shell epithelia. A much smaller pair of posterior adductors develops somewhat later, lateral to the posterior end of the stomach. At the same time a pair of oblique, internal muscles develops (Fig. 162.7; NIELSEN, 1991).

Digestive diverticula first appear at about the 10 p.t. stage as pouchlike outgrowths of the anterodorsal stomach wall. The anus

originates at the 5 p.t. stage. Metanephridia first appear at the 9 p.t. stage as two rows of cells embedded in the lateral body walls. They do not develop a lumen or become fully functional until the 16 p.t. stage. At earlier stages of development, the lophophore possesses a median tentacle and is rather like that of juvenile *Lingula*. The median tentacle of the lophophore was reported as being lost during the 5 to 6 p.t. stage (ROWELL, 1960), the 10 p.t. stage, and as late as the 18 p.t. stage (CHUANG, 1974) in the postlarva of *Neocrania*. The brachia form a series of whorls, transforming the lophophore into a spirolophore; the turgidity of the brachial canals provides the necessary support for the lophophore.

Articulated groups

Articulated brachiopods have few specialized larval organs. The apical tuft of long cilia found on the anterior lobe of articulated larva is presumed to be sensory and is usually lost soon after or immediately before settlement. The eyespots of *Frenulina* disappear by the 2 p.t. stage and bundles of larval setae are replaced along the entire mantle margin by postlarval setae (MANO, 1960).

Externally, the settled, postmetamorphic juvenile of articulated brachiopods resembles a miniature adult. Internally, however, only the pedicle retractor muscles, an enclosed gut rudiment, and incipient coelomic spaces have been reported in early juveniles. In *T. transversa*, a bivalved protegulum is secreted over the entire surface of the mantle within the first 24 hours of metamorphosis. The protegulum is calcified, and by four days after metamorphosis the rudiments of a juvenile shell have been added to the anterior and lateral edges of the protegulum (STRICKER & REED, 1985b). An ectodermal invagination near the posterior margin of the apical lobe, assumed to be the former site of the blastopore, forms the stomodaeum (mouth) and the esophagus, which communicate with the anterior part of the gut rudiment.

The gut rudiment differentiates into two chambers. The anterior chamber forms the stomach, which gives rise to the digestive diverticula and is connected to the stomodaeum by the esophagus. The posterior chamber forms the blind-ending pylorus, as articulated brachiopods lack an anus or the equivalent of the intestine of inarticulated brachiopods (RUDWICK, 1970; CHUANG, 1990; LONG & STRICKER, 1991).

Little information exists on the formation of the excretory organs of articulated brachiopods, but strands of mesodermal cells near the inner surface of the body wall in postmetamorphic juveniles of *T. retusa* at about the 2 p.t. stage hollow out to form part of the metanephridia (FRANZEN, 1969).

In *T. transversa*, the pedicle adjustors are inserted into a solid core of connective tissue in the pedicle. Cartilage-like tissue occurs within the pedicle at later stages of development (STRICKER & REED, 1985c).

The lophophore of the articulated brachiopods is a postmetamorphic development of the anterior lobe (LONG, 1964) and is the best documented organogenesis of juvenile forms. After reversal of the mantle and following settlement, the anterior lobe flattens and fuses with the dorsal valve (CHUANG, 1990). The pattern of early development of the lophophore, however, varies. In *Calloria* (PERCIVAL, 1944), *Frenulina* (MANO, 1960), *T. transversa*, and *Hemithiris* (LONG, 1964; LONG & STRICKER, 1991) a subapical groove forms along the midline of the anterior lobe. Anteriorly, an ectodermal infolding forms the stomodaeum, and the lophophoral tentacles develop as two protrusions lateral to the stomodaeum. The tentacle rudiments form a crescent, to which subsequent tentacles are added anteriorly (dorsally) as bilateral pairs, thus forming the taxolophe (CHUANG, 1990; LONG & STRICKER, 1991). In *Frenulina* a thin fold or epistome appears anterior to the stomodaeum at the 4 p.t. stage (MANO, 1960). A number of juveniles of articulated species appear to bypass the

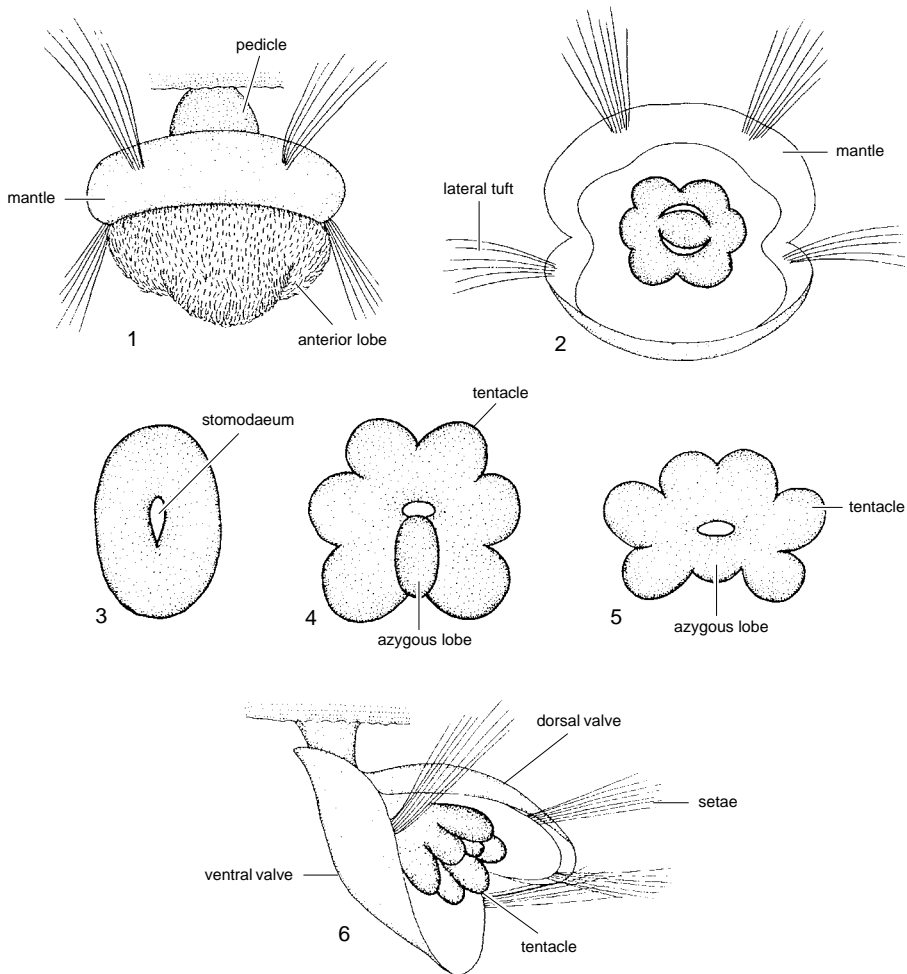


FIG. 179. Stages in the development of the lophophore of *Notosaria nigricans*, showing 1–4, the differentiation and migration of the azygous lobe, 3–4, breakthrough of the stomodaeum, and 2, 4–5, definition of the tentacle rudiments; 6, young adult viewed dorsally (adapted from Percival, 1960).

taxolophous stage of the trochophore by the simultaneous development of two or more pairs of tentacles. Four tentacles develop simultaneously in *Lacazella* (LACAZE-DUTHIERS, 1861), and *Argyrotheca* (KOWALEVSKY, 1883) and six develop in *Notosaria* (PERCIVAL, 1960).

In the juvenile of *Notosaria*, the surface of the apical lobe becomes modified into a low, central mound surrounded by a broad margin (Fig. 179). The outline of the margin

becomes hexagonal as the rudiments of the first three pairs of tentacles differentiate. The central mound becomes depressed, forming the stomodaeum; and an azygous lobe, which moves into a gap formed at the margin, forms the rudiment of the brachial lip. Additional tentacles are formed simultaneously at both ends of the row of tentacles on each side of the azygous lobe, and the brachial lip enlarges toward the tentacles to form a crescentic flap partially covering the

mouth. Meanwhile, the anterior lobe gradually shortens, flattens dorsoventrally, and spreads itself on the inner surface of the dorsal valve (PERCIVAL, 1960).

The first pair of tentacle rudiments of juvenile *T. retusa* are formed at about the same time as the stomodaeum connects with the stomach. A second pair of tentacles develops dorsally to the first and, when four pairs of

tentacles are present, they are arranged in a ring around the mouth to form the trocholophe (FRANZEN, 1969).

Although a few small articulated brachiopods retain the trocholophe in adult stages of growth, the lophophore of most articulated species develops into more complex structures (see the section on the lophophore, p. 98).

THE BRACHIOPOD GENOME

BERNARD L. COHEN and ANGELA B. GAWTHROP

[The University of Glasgow]

“Our classifications will come to be, as far as they can be so made, genealogies . . . we have to discover and trace the many diverging lines of descent in our natural genealogies by characters . . . which have long been inherited” (DARWIN, 1859a, p. 486).

STRUCTURE, COMPOSITION, AND ORGANIZATION OF THE NUCLEAR AND MITOCHONDRIAL GENOMES

INTRODUCTION

The genome is the complement of genetic material that an organism inherits from its ancestors; it is embodied chemically in deoxyribose nucleic acid (DNA). In most metazoans the genome consists of two components, nuclear and mitochondrial, that have separate evolutionary origins and distinct modes of inheritance. The nuclear genome, packaged in the chromosomes, typical of eukaryotes and of still-mysterious origin (GOLDING & GUPTA, 1994), is by far the largest component, being involved in the storage, transmission, recombination, and controlled expression of most of the genetic information. The mitochondrial genome (mtDNA), a relatively small element within the mitochondrion, is a relic of the genome of a prokaryotic endosymbiont (KARLIN & CAMPBELL, 1994) and is now responsible for only a limited number of essential functions, having lost most of its genes either to the chromosomes or completely. In metazoans, the mitochondrial genome is usually transmitted asexually by the maternal parent.

Investigation of genome functional anatomy may be thought of as proceeding at four levels characterized by use of different analytical approaches. At the organismal and population level, genetic markers (identifiable phenotype differences determined by allelic, homologous genes) are used to trace the transmission of the genome between individuals of successive generations or between populations. This approach may ei-

ther clarify the mechanism of heredity itself (e.g., show how a character is transmitted in a controlled mating), clarify the mechanism of heredity in relation to the life cycle (e.g., tell whether the organisms are haploid or diploid), or illuminate the genetic structure of populations (e.g., show whether there is gene flow between them). At the cellular and subcellular levels, microscopic techniques may be used to characterize the structural organization of the genome, especially to determine the size and number of chromosomes and the existence of special features such as sex chromosomes. Microscopy may also be used to characterize chromosome behavior in somatic and germinal cell divisions. At the third level, biochemical analyses of deoxyribose nucleic acid (DNA) or ribose nucleic acid (RNA) extracted in bulk enables some properties of the genome to be recognized and measured, such as the total quantity of DNA per nucleus, the genome complexity, or the existence of genome fractions composed of repeated sequences (BRITTEN & KOHNE, 1968). The fourth level of analysis involves determination of the organization, sequence, and modes of expression of individual genes and gene products, whether RNAs or proteins, using the techniques of molecular biology. Such sequence information provides the primary evidence for the reconstruction of phylogenetic history and for the identification of evolutionarily homologous structures and developmental functions (ZUCKERKANDL & PAULING, 1965).

Unhappily, no coherent program of research to characterize any brachiopod genome at any analytical level has been undertaken. All that exists are scattered observations at each level, together with the

beginnings of an attempt to use DNA sequence data to provide a molecular framework for brachiopod phylogeny (B. COHEN & A. GAWTHROP, unpublished work, 1995; COHEN, GAWTHROP, & CAVALIER-SMITH, in preparation) and work in progress on the complete DNA sequence of *Lingula* mtDNA (K. ENDO, personal communication, 1994). This chapter will briefly review the available, scattered information and will provide an account of results from the ongoing work on molecular phylogeny.

THE GENOME IN RELATION TO LIFE CYCLE AND POPULATION DYNAMICS

The organization of the brachiopod nuclear genome in relation to the life cycle is firmly established. Like most sexually reproducing metazoans, brachiopods are normally diploid (AYALA & others, 1975; VALENTINE & AYALA, 1975; HAMMOND & POINER, 1984; BALAKIREV & MANCHENKO, 1985; COHEN, BALFE, & CURRY, 1986), and gametes are produced by meiosis. Although brachiopod meiosis has not been fully described, evidence for its existence can be found in the pioneer cytological work of YATSU (1902a) and in recent studies of gametogenesis (JAMES & others, 1992). As would be expected of marine organisms that broadcast gametes of at least one sex, genetic markers indicate that sampled populations are large (*sensu* population genetics) and random mating (AYALA & others, 1975; VALENTINE & AYALA, 1975; HAMMOND & POINER, 1984; BALAKIREV & MANCHENKO, 1985; COHEN, BALFE, & CURRY, 1986). The limited available evidence is consistent with the anticipated matrilineal transmission of the brachiopod mitochondrial genome (COHEN & others, 1991; COHEN & others, 1993).

GENOME SIZE AND CHROMOSOME NUMBER

Despite the vast scope of animal cytology, there appears to be only a single report of brachiopod chromosomes: YATSU (1902a) clearly figured eight small, paired chromo-

somes in oogenesis of *Lingula anatina*. The range of variation in number, size, and architecture of brachiopod chromosomes remains unknown.

The DNA content of brachiopod genomes (nuclear plus mitochondrial) has been measured by HINEGARDNER (cited by BRITTEN and DAVIDSON, 1971). Using a fluorometric assay on DNA extracted from *Glottidia pyramidata* and *Lingula* sp., he estimated the haploid DNA content as 0.43 and 0.38 picograms, corresponding respectively to 4.15 and 3.67×10^8 nucleotide pairs per haploid genome. Since the estimated measurement error was 5 percent, the two species probably have different genome sizes (R. HINEGARDNER, personal communication, 1993). These genome sizes are comparable with the lowest values recorded for other metazoans and are about one-tenth the average sizes of molluscan, echinoderm, or mammalian genomes, implying that the brachiopod genome is probably not rich in repetitive sequences. If so, then these estimates of genome size are also good estimates of genome complexity, i.e., of the overall coding capacity. However, some evidence suggestive of repetitive nuclear sequence has been obtained (P. BALFE & B. COHEN, unpublished work, 1985).

The mitochondrial genomes of two species of *Terebratulina* are within the size range typical for metazoans (14 to 16 kb), but the mtDNA of *T. septentrionalis*, like that of several other organisms, contains a region that varies slightly in size in different individuals and perhaps also within individuals (COHEN & others, 1991). Although a quasi-complete mitochondrial genome of *T. retusa* has been cloned, the clone has not been sequenced, and only very preliminary evidence of gene order has been published (JACOBS & others, 1988). A mitochondrial genome of *Lingula anatina* has been cloned and is currently being sequenced; preliminary data indicate that this genome is atypically large, around 27 to 28 Kb (K. ENDO, personal communication, 1994). Sporadic examples of oversize mtDNAs have been observed in other phyla

(summarized by RAND, 1993), but the phenomenon appears to have no general significance. Determination of gene order in the mtDNA of a selection of brachiopods and other lophophorates is highly desirable, since the rate of rearrangement, except of tRNA (transfer RNA) genes, is low, and this character can strongly establish high-level phylogeny (SMITH & others, 1993; BOORE & BROWN, 1994).

GENOME BULK COMPOSITION

The overall base composition and nearest-neighbor base doublet frequencies of total DNAs from *Terebratulina retusa* and *Crania (Neocrania) anomala* have been determined. Base composition was unremarkable, around 33 percent G + C, and no density satellites were detected, suggesting that if repetitive DNA sequences exist they are not highly distinctive in base composition. Nearest-neighbor base doublet frequencies were not informative (RUSSELL & SUBAK-SHARPE, 1977). The base composition of *Lingula* DNA was not very different (SHIMIZU & MIURA, 1972).

TOWARD A GENEALOGICAL CLASSIFICATION OF THE BRACHIOPODA

INTRODUCTION

Publication of the first edition of Part H of the *Treatise* (MOORE, 1965) coincided with a watershed in genome studies when ZUCKERKANDL and PAULING laid the foundations for the study of molecular evolution by pointing out that the information-bearing molecules of the genome comprise the "documents of evolutionary history" (ZUCKERKANDL & PAULING, 1965, p. 357). At first, these documents could be read only indirectly and laboriously through the amino-acid sequencing of proteins. More recently, with the development of nucleic acid sequencing and especially of DNA sequencing based on the polymerase chain reaction (PCR), genomic sequences are more readily obtained, and our knowledge and understanding of the genealogical relation-

ships of many organisms has been revolutionized, although homoplasy remains a problem (HILLIS & MORITZ, 1990).

By pointing to the potential for genomic information to be used for the reconstruction of evolutionary history, ZUCKERKANDL and PAULING (1965) identified the key to satisfying DARWIN's prescient advice that the aim of taxonomists should be to create classifications that are "as far as they can be so made, genealogies" (DARWIN, 1859a, p. 486). Genealogy requires the genome; and, to the extent that the genomes of living brachiopods contain or retain phylogenetically useful information and that funds can be obtained to support the considerable work required to extract and analyze it, brachiopod taxonomists can look forward for the first time to being able to justify their classifications on genealogical grounds independent of morphology and of the fossil record. By determining genealogically validated sister groups it should become possible to confirm the evolutionary polarity of at least some morphological character-state transformations and hence to provide an independent, phylogenetically valid framework for classification. Unfortunately, the concerted application of DNA sequencing to the brachiopod genome started only in 1991, so relatively few results are yet available. Before we present a preliminary account of these new data, we shall first briefly review the scanty existing knowledge of the brachiopod genome obtained by inference from analyses of proteins and of RNA.

STUDIES OF PROTEINS

Properties of whole proteins may be treated as homologous characters and used for population genetic or phylogenetic studies. Alternatively, the amino-acid sequence of part or all of a protein may be determined chemically and used in phylogenetic comparison either directly or as a palimpsest of the genomic coding sequence. The comparison of brachiopod protein sizes and partial amino-acid sequences was pioneered by JOPE (1986), but such comparisons have yet to

prove phylogenetically useful. Similarly, the use of allelic variants of whole proteins (allozymes) is informative mainly in a population genetics context, and its few reported applications to brachiopods have already been noted (AYALA & others, 1975; VALENTINE & AYALA, 1975; HAMMOND & POINER, 1984; BALAKIREV & MANCHENKO, 1985; COHEN, BALFE, & CURRY, 1986).

Protein sequencing, both partial and complete, is still relatively cumbersome because of the need for purification. And because many expressed genes are represented in the genome by gene families resulting from duplication, the phylogenetic utility of amino-acid sequences may be limited unless parallel genomic studies establish that paralogy has been avoided. Nevertheless, studies of protein sequences are attractive because of the possibility that such knowledge might permit useful information to be recovered from residues in fossil or empty shells and for the light that might be shed on processes such as biomineralization (TUROSS & FISHER, 1989; CUSACK & others, 1992; COHEN, 1994; WILLIAMS, CUSACK, & MACKAY, 1994).

In an alternative approach, the taxonomic distribution of specific protein functions may be studied in the hope that phylogenetically useful markers will be discovered (LIVINGSTONE & others, 1983; HAMMEN & BULLOCK, 1991). This approach, however, has not been generally fruitful because of the universality of most biochemical processes and because it is not known whether the differential distribution of particular enzyme activities is due to differential gene expression or differential distribution of the corresponding genes. A similar difficulty applies to the oxygen-binding protein hemerythrin. The hemerythrin of *Lingula* appears to be the only brachiopod protein whose complete amino-acid sequence has been determined. It is a heteropolymeric protein comprising distinct alpha and beta polypeptides and it binds oxygen cooperatively, unlike the homopolymeric hemerythrins of polychaetes, priapulans, and sipunculans (KLIPPENSTEIN, 1980; SATAKE & others, 1990; YANO, SATAKE, UENO, KONDO, & TSUGITA, 1991; YANO,

SATAKE, UENO, & TSUGITA, 1991; ZHANG & KURTZ, 1991). The alpha and beta polypeptides show 65 percent amino-acid identity, while the corresponding subunits of *L. reevii* and *L. unguis* (= *anatina*) show 95 percent and 87 percent identity respectively (NEGRI & others, 1994). The existence of two distinct hemerythrin polypeptides in *Lingula* but not in polychaetes, priapulans, and sipunculans provides indirect evidence for a gene duplication event in brachiopod evolution, while recent evidence for two hemerythrins in a discinid suggests that this duplication antedated divergence of the lingulid and discinid lineages (M. CUSACK, personal communication, 1995). The distribution of hemerythrins in protostomes appears to be sporadic and apparently unrelated to phylogeny (Fig. 180–185). This probably indicates that one copy of this coding sequence is plesiomorphic in metazoans and that it is expressed only where the function of the hemerythrin gene product contributes to fitness. If so, the presence or absence of hemerythrin protein cannot be phylogenetically informative.

STUDIES OF NUCLEIC ACID SEQUENCES

Molecular Characteristics of RNAs

Because capability for the analysis, especially sequencing, of RNA developed before that for sequencing DNA, the earliest studies of brachiopod nucleic acids were on RNAs. Standing alone is the early work of ISHIKAWA (1977), who combined thermal dissociation with gel electrophoresis to compare the subunit sizes of ribosomal RNA (rRNA) in an explicitly phylogenetic study of all three phyla of lophophorates, including both an articulated and an inarticulated brachiopod. He concluded that their rRNAs were of the protostome type (ISHIKAWA, 1977).

RNA Sequences and Sequences of Genes Coding for RNAs

The smallest rRNA subunit, 5S rRNA (S = Svedberg unit, an indirect measure of mo-

lecular mass), was also the first to be extensively sequenced and many of these short sequences are available for comparison, including one from *Lingula* (KOMIYA & others, 1980; ERDMANN & others, 1985; HORI & others, 1985; HORI & OSAWA, 1986). It has become clear, however, that 5S rRNA sequences provide little useful phylogenetic information (HALANYCH, 1991; HILLIS & DIXON, 1991; STEELE & others, 1991).

The first attempt at a molecular phylogeny of the animal kingdom, using partial sequences of the nuclear-encoded 18S or small subunit (SSU) rRNAs, again employed *Lingula* to represent all brachiopods (FIELD & others, 1988). Despite some controversy over interpretation of the results, there was again the clear conclusion: "the lophophorate lineage represented . . . by a brachiopod, is solidly affiliated with the protostome group . . ." (FIELD & others, 1988, p. 749) (PATTERSON, 1985, 1989; GHISELIN, 1988; ADOUTTE & PHILIPPE, 1993). Extension of this work to other brachiopod lineages is described below, but, instead, sequencing quasicomplete SSU genes rather than parts of the RNA transcribed from them and aiming to build a comprehensive molecular framework for brachiopod systematics (COHEN, GAWTHROP, & CAVALIER-SMITH, in preparation). In addition to the SSU gene, the large nuclear-encoded rRNA subunit (28S or LSU) is also useful for phylogenetic comparison, and a number of brachiopod and other lophophorate sequences have been obtained, either from the gene or from the RNA transcript (A. CHENUIL, personal communication, 1994; K. HALANYCH, personal communication, 1994; B. COHEN & M. BURKE, unpublished work, 1995), but no publications using these sequences have yet appeared.

In all rRNAs and their genes, the number of accumulated sequence changes is at least roughly proportional to time (the molecular-clock hypothesis), and these sequences combine blocks that are highly conserved (because they are functionally constrained) interspersed with less strongly conserved regions. Also, the SSU (18S) gene generally

changes more slowly than the LSU gene (HILLIS & DIXON, 1991). Thus, both overall and regional rates of divergence differ. Moreover, since metazoan mtDNA generally accumulates base substitutions severalfold faster than nuclear DNA, the corresponding mitochondrial SSU (12S) and LSU (16S) genes further increase the divergence-time range over which useful results may be obtained. Thus, particular sequencing targets can be chosen to match expected divergence levels (HILLIS & DIXON, 1991). For example, the 18S sequence may not retain enough signal to resolve unambiguously events close to the protostome radiation (ADOUTTE & PHILIPPE, 1993; PHILIPPE, CHENUIL, & ADOUTTE, 1994), but it can be informative about more recent events in brachiopod evolution. Similarly, resolution of the most recent divergences may be limited by lack of signal in nuclear SSU or LSU, but adequate resolution of such events (e.g., those giving rise to taxa below the family level) may be obtained from comparison of mitochondrial sequences. Preliminary evidence indicates that the overall rate of brachiopod mtDNA evolution may be relatively low compared to other metazoans (COHEN & others, 1993), and this seems also to be true for the nuclear-encoded SSU gene (see below and COHEN, GAWTHROP, & CAVALIER-SMITH, in preparation).

Gene Sequence Comparisons: Work in Progress

The results to be presented here reflect the state of the literature and of work in progress in the authors' laboratory in May 1995. Brief details of materials and methods are given in the text and figure captions, and full details will be published elsewhere (COHEN, GAWTHROP, & CAVALIER-SMITH, in preparation). Nuclear-encoded SSU rRNA gene sequences, each approximately 1,790 nucleotides long, were obtained by the direct sequencing of DNA amplification products obtained by PCR (polymerase chain reaction) using oligonucleotide primers matching highly conserved terminal regions of eukaryotic rRNA genes. A notable advantage of

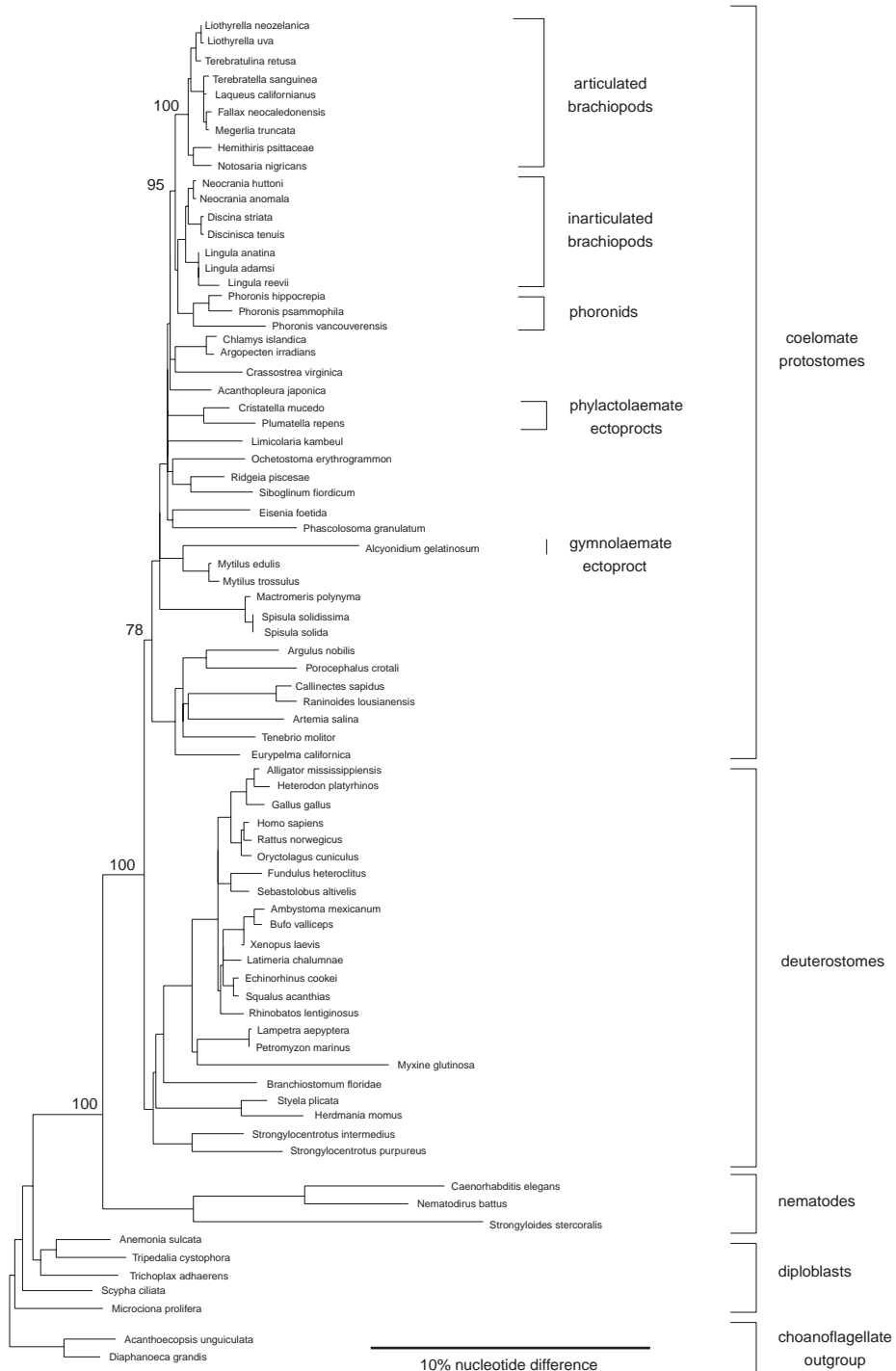


FIG. 180. For explanation, see facing page.

this approach is that the resulting sequence is a consensus, undistorted by divergence between the multiple genomic copies of this gene family or by gene cloning or PCR artifacts. Using this method we have determined sequences from 23 species of articulated brachiopods, 6 inarticulated brachiopods, 2 phoronids, and 1 ectoproct, while sequences from 1 articulated brachiopod, 2 inarticulated brachiopods (1 a partial sequence), 1 phoronid, and 2 ectoprocts are available from other sources (FIELD & others, 1988; B. WINNEPENNINCKX & R. DE WACHTER, personal communication, 1994; HALANYCH & others, 1995). The sequences analyzed are complete except for regions corresponding to the terminal primers (all cases), up to 18 undetermined nucleotides adjacent to 1 terminal primer (3 cases), and 2 large internal sections that are missing from the first brachiopod sequence to be determined (*Lingula reevii*, FIELD & others, 1988). The sequences were aligned manually with one another and subsequently with many protostome and other outgroup sequences obtained from databases (BENSON & others, 1994; MAIDAK & others, 1994) and other sources (B. WINNEPENNINCKX & R. DE WACHTER, personal communication, 1994; RUNNEGAR & others, in preparation; WINNEPENNINCKX, BACKELJAU, & DE WACHTER, 1995). In addition to the data and analyses

described here, mitochondrial SSU (12S rRNA) and cytochrome oxidase subunit I (COI) partial sequences are being obtained from selected taxa (S. STARK, C. THAYER, & B. COHEN, unpublished observations, 1993; B. COHEN & A. GAWTHROP, unpublished work, 1995) using primers that yield amplified fragments of approximately 400 and approximately 700 nucleotides respectively. These data will provide genetically independent tests of the nuclear gene phylogeny and should clarify relationships among relatively recently diverged brachiopods for which the nuclear SSU gene provides insufficient resolution. The COI gene may, in addition, help clarify unresolved deep branches (HILLIS & DIXON, 1991; FOLMER & others, 1994).

DNA was extracted from animals that had been freshly collected or had been preserved in alcohol (without prior formalin fixation) during the last 10 years. No full-length PCR amplification product has been obtained from DNA extracted from specimens preserved over 20 years ago. No attempt was made to amplify from fossils or dried specimens, except in the case of one sample vial that was crushed in transit and from which the alcohol had recently evaporated. These specimens of *Platidia anomioides* were recovered from the packaging using acid-washed forceps and an SSU gene of distinctive

FIG. 180. High-level phylogenetic relationships of phoronids, ectoprocts, and brachiopods. Neighbor-joining tree based on an alignment of conserved nucleotide sites. Representative ingroup and unpublished outgroup sequences were aligned manually with published sequences selected from the Ribosomal Database Project (release 3). The GCG program PLOTSIMILARITY (DEVEREAUX, HAEBERLI, & SMITHIES, 1984) was used to identify sites showing less than 60 percent similarity (as defined by the program), and these were then excluded, leaving 1,632 sites of which 1,361 were variable. The Kimura 2-parameter algorithm implemented in the program DNADIST (FELSENSTEIN, 1993) was used to obtain a distance matrix corrected for unseen multiple events, and the tree was constructed from this matrix using the program NEIGHBOR 81 (FELSENSTEIN, 1993). Alternative correction algorithms and taxon-addition orders did not alter tree topology. Bootstrap frequencies (%) based on 500 replicates obtained with SEQBOOT (FELSENSTEIN, 1993) are given for key nodes.

Key to nonlophophorate, coelomate protostome taxa: Annelida, Oligochaeta: *Eisenia foetida*; Annelida, Polychaeta: *Glycera americana*, *Lanice conchilega*; Arthropoda, Arachnida: *Androctonus australis*, *Eurypelma californica*; Arthropoda, Crustacea: *Argulus nobilis*, *Artemia salina*, *Branchinecta packardii*, *Berndtia purpurea*, *Callinectes sapidus*, *Philypis pismus*, *Porocephalus crotali*, *Pugettia quadridens*, *Raninoides lousianensis*, *Stenocypris major*, *Trypetasa lampas*, *Ulophyesema oeresundense*; Arthropoda, Insecta: *Tenebrio molitor*; Echiura: *Ochetostoma erythrogrammon*; Mollusca, Gastropoda: *Limicolaria kambeul*, *Onchidella celtica*; Mollusca, Aplacophora: *Epimienia australis*; Mollusca, Polyplacophora: *Acanthopleura japonica*; Mollusca, Bivalvia (filibranchs): *Argopecten irradians*, *Chlamys islandica*; *Crassostrea virginica*, *Placopecten magellanicus*; Mollusca, Bivalvia (eulamellibranchs): *Mactromeris polynyma*, *Mulinia lateralis*, *Mytilus edulis*, *Mytilus trossulus*, *Spisula solida*, *Spisula solidissima*, *Tresus capax*; Pogonophora: *Siboglinum fiordicum*; Priapulida: *Priapulius caudatus*, *Priapulius caudatus* 2; Sipuncula: *Phascolosoma granulatum*; Vestimentifera: *Ridgeia piscesae* (new).

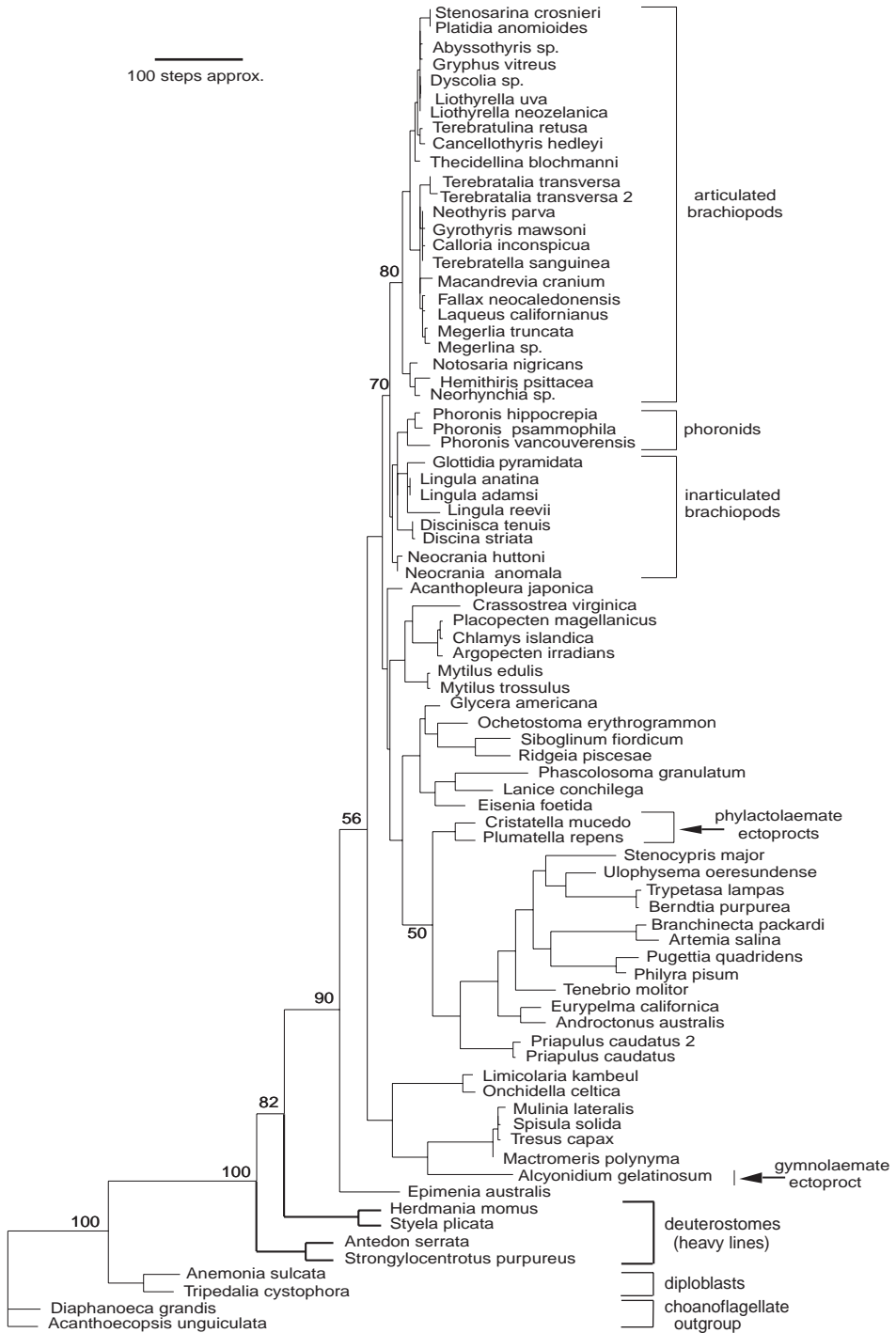


FIG. 181. For explanation, see facing page.

sequence was amplified from the resulting DNA preparations. Confirmation of the unexpected result obtained from these specimens should be sought.

Subject to obvious logistical constraints, we aimed to obtain nuclear-encoded SSU sequences from at least two taxa from every major, extant brachiopod lineage and from as many family-level taxa (*sensu* MOORE, 1965) as possible. Phoronids and an ectoproct were included so as to address the long-standing question of lophophorate relationships. We have used and will compare the results of three methods for phylogenetic reconstruction that have been reported to be among the most consistent, efficient, and robust under test conditions (HILLIS & MORITZ, 1990; HUELSENBECK, 1995). The parsimony method, with equally weighted (EP) or *a posteriori* weighted characters (WP), follows cladistic principles, permits the exclusion of plesiomorphic similarity by including only parsimony-informative sites, and lends itself to measurement of the support for each node. With *a posteriori* weighting based on the rescaled consistency index, homoplastic characters are proportionately downweighted and the number of equally most parsimonious trees reduced. WP will therefore be treated as the method of choice. The maximum likelihood method (ML) is less sensitive to artifacts due to base-composition and

evolutionary rate differences but is difficult to apply to large data sets because of computational intensiveness. Since parsimony and likelihood analyses use somewhat different models of the evolutionary processes, any result that is supported by both methods is likely to be a good estimate of the phylogeny represented by the data. The distance matrix method, particularly with the neighbor-joining tree construction program (NJ) is fast and convenient but possibly less reliable. Following common practice, we will generally treat the gene trees obtained as species trees; i.e., we shall describe conclusions in terms of the relationships of taxa.

Several well-known problems complicate the reconstruction of deep-branch protostome phylogeny from SSU rRNA gene sequence data. These problems, and strategies to deal with them, are as follows. The first arises from the great age and relative rapidity of the Cambrian or late Precambrian diversification that gave rise to the major lineages. Because most parts of the SSU gene evolve slowly, branches around deep divergence points are expected to be short, and nodes connecting high-level taxa of early origin may not (indeed, often do not) receive strong support. One solution to this problem is to add sequence data from other genes, but the total needed may be impractically high (PHILIPPE, CHENUIL, & ADOUTTE, 1994).

FIG. 181. High-level phylogenetic relationships of phoronids, ectoprocts, and brachiopods. Weighted parsimony tree based on an alignment of 80 complete SSU sequences from all available brachiopods, phoronids, and ectoprocts together with selected protostome and other outgroups. For list of organisms representing nonlophophorate, coelomate protostome taxa, see caption to Figure 180. Reliability of the alignment was maximized by starting with sequences from unarguably closely related brachiopod taxa, by minimizing the number of introduced gaps, and by nucleating alignment of the four most variable regions on conserved secondary structures (i.e., implied functional homologies of the transcribed rRNA molecules) inferred by means of a free energy minimization RNA folding program (JAEGER, TURNER, & ZUKER, 1989a, 1989b; ZUKER, 1989). The alignment contained 2,114 sites, of which 804 were parsimony-informative. The following heuristic search options (using PAUP; SWOFFORD, 1993) were invoked: collapse zero-length branches, no topological constraints, outgroup rooting, closest addition, no steepest descent, TBR, MULPARS, ACCTRAN. In trial analyses random addition, steepest descent, and DELTRAN did not alter tree topology. An initial search with equally weighted characters found 48 equally most parsimonious trees of length = 4,711 steps, RI = 0.604. Following three cycles of reweighting according to the worst fit of the rescaled consistency index (RCI, baseweight = 100) followed by heuristic search, the number of trees reduced to 6 of 86,565 weighted steps, RI = 0.717. These six trees differed only in the arrangement of the articulated brachiopod terminal taxa on the shortest branches, i.e., those whose relationships are most weakly resolved, and one of these trees is shown. Bootstrap % are given for key nodes based on 50 heuristic search replicates with reweighted characters. The limited number of replicates was dictated by computational constraints, which also precluded calculation of support indices (BREMER, 1988; KÄLLERSJÖ & others, 1992) (new).

Brachiopoda

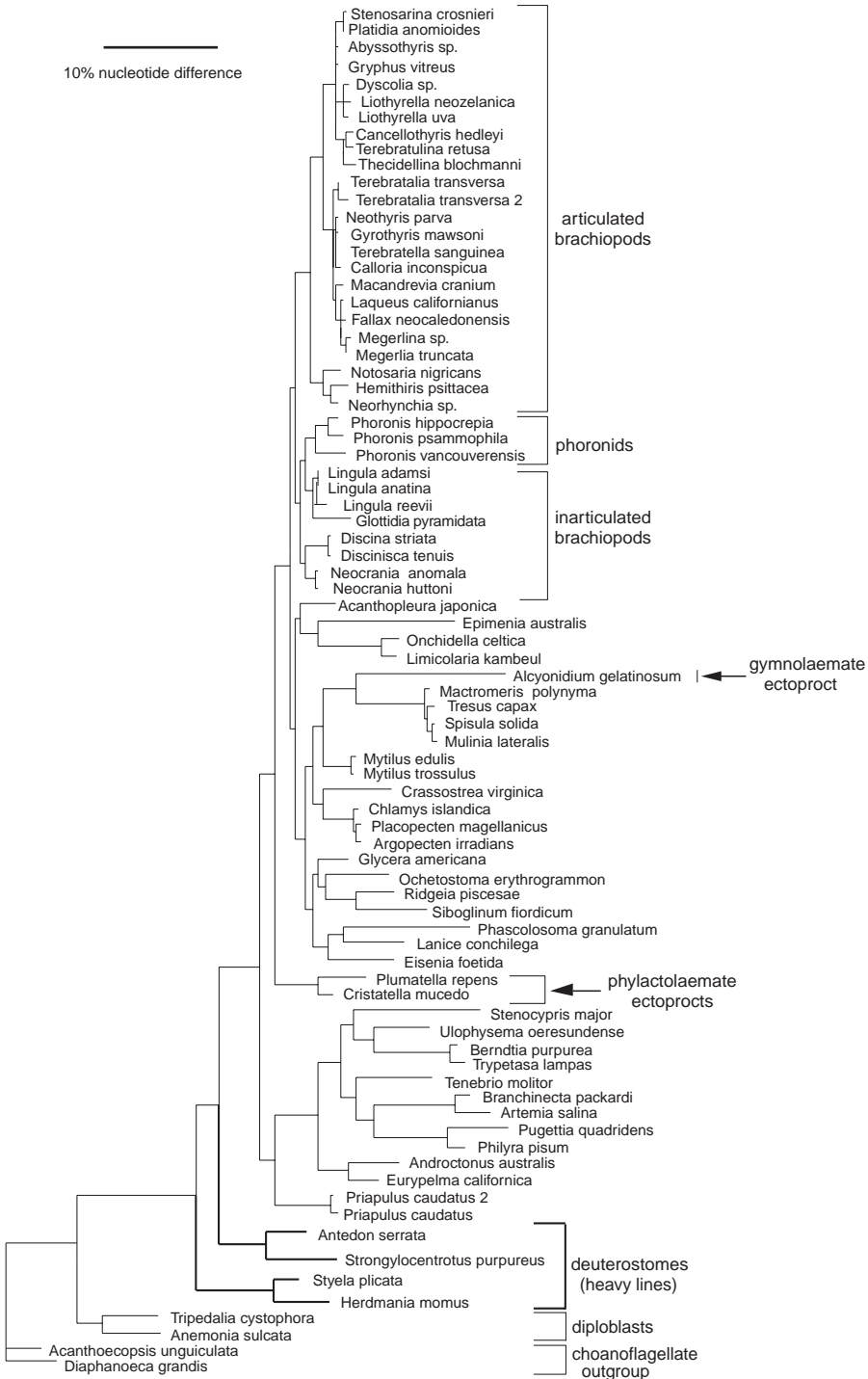


FIG. 182. For explanation, see facing page.

Another solution is to seek genomic synapomorphies such as mitochondrial genome rearrangements. Faster-evolving sequences cannot be used because they introduce excessive homoplasy and reach saturation. The second problem is that long branches may artificially cluster together. This can be alleviated by not relying completely on reconstruction methods most sensitive to this effect and by increasing the number of related taxa studied, thus subdividing long branches. The third problem is that ingroup phylogeny is not independent of the outgroup used. For the lophophorate phyla this is particularly awkward since there is no certain, independent basis on which to identify the most appropriate outgroup, which therefore has to be identified recursively from preliminary analysis of the same sequence data that will be used to determine phylogeny. This problem will be addressed below. Finally, all the reconstruction methods used here may also cluster sequences according to similarity of nucleotide composition, independently of sequence similarity. Since the SSU genes of brachiopods and phoronids are very similar in sequence and composition, this base composition effect is unlikely to mislead, but we have no objective assessment of its influence. The LogDet transformation (HUSON & WETZEL, 1994; LOCKHART & others, 1994) may eliminate compositional effects, but our results with this method are too preliminary to be described.

The earlier conclusion that lophophorates are protostomes (ISHIKAWA, 1977; FIELD & others, 1988) was recently confirmed by analysis of SSU sequences from single articulated and inarticulated brachiopods, a phoronid, and an ectoproct (HALANYCH & others, 1995). Since analyses of our more

extensive data agree entirely with this conclusion (Fig. 180–182), we will take this point as established. In contrast, the latter report (HALANYCH & others, 1995) also claimed that phoronids are the sister group of articulated brachiopods and that ectoprocts are the sister group of a clade comprising brachiopods, molluscs, and annelids. Our analyses disagree strongly with the former assignment; we find phoronids to be contained within a clade comprising inarticulated brachiopods, although their position within that clade remains uncertain. We are also uncertain about the position of the ectoprocts, and both issues are discussed below.

Selecting an Outgroup

Accepting that lophophorates are protostomes, there arises the important question of identifying the most appropriate outgroup with which to root the phylogenetic trees and thus to determine the apparent direction of evolution (HENNIG, 1966; FARRIS, 1972; DONOGHUE & CANTINO, 1984; MADDISON, DONOGHUE, & MADDISON, 1984; NIXON & CARPENTER, 1993; SMITH, 1994). Recent analyses of outgroup rooting (NIXON & CARPENTER, 1993; SMITH, 1994) stress the dangers of remote outgroups and lead to a preference for the closest outgroup, preferably the ingroup's sister group.

How can the ingroup's sister group be identified? Ideally, it would be identified by reference to independent evidence such as comparative zoology. But comparative zoology has decided that the lophophorates are deuterostomes (BRUSCA & BRUSCA, 1990; EERNISSE, ALBERT, & ANDERSON, 1992) in clear conflict with the molecular results (e.g., Fig. 180–182), so we must look elsewhere. No other, independent source of evidence

FIG. 182. High-level phylogenetic relationships of phoronids, ectoprocts, and brachiopods. Maximum-likelihood tree based on the same alignment used for the parsimony analysis in Figure 181. For list of organisms representing nonlophophorate, coelomate protostome taxa, see caption to Figure 180. The fastDNAMl program (OLSEN & others, 1994) was used with nucleotide frequencies estimated from the data (empirical frequencies) and with global branch exchange. Because this analysis took over 20 days full-time processing on a 70 MHz SUN Sparc5 workstation, no bootstrap analysis was done (new).



FIG. 183. Phylogenetic relationships of brachiopods, ectoprocts, phoronids, and other protostomes in an unrooted weighted parsimony tree based on the alignment of complete SSU sequences used for Figures 181 and 182 but with nonprotostomes omitted. The alignment comprised sequences from 72 protostome taxa and 2,098 sites. For list of organisms representing nonlophophorate, coelomate protostome taxa, see caption to Figure 180. This tree was one of three equally most parsimonious, RCI-weighted trees that differed only in arrangement of the shortest terminal (Continued on facing page.)

exists, however, and the best we can do is to base outgroup choice on phylogenetic analysis of a large number of available SSU sequences, confining our attention to protostomes so as to avoid the more remote outgroups and seeking as an outgroup the protostome sequence closest to brachiopods plus phoronids. This approach to outgroup rooting minimizes homoplasy, enables alignment of variable regions to be least ambiguous, and minimizes the need to exclude data (SMITH, 1994), in contrast with the approach using evolutionarily remote diploblasts as the outgroup (HALANYCH & others, 1995). We have therefore sought the outgroup in unrooted trees derived from an alignment of sequences from 24 articulated brachiopods, 8 inarticulated brachiopods, 3 phoronids, 3 ectoprocts, 14 molluscs, 12 arthropods, 3 annelids, 2 priapulans, and 1 each of echiuran, pogonophoran, sipunculan, and vestimentiferan, these being all the major protostome lineages from which complete SSU sequences are currently available. The resulting unrooted WP, ML, and NJ trees are presented in Figures 183–185.

Principal conclusions from Figures 183–185 are as follows.

1. All the new inarticulated brachiopod sequences cluster closely with the partial sequence from *Lingula reevii* (FIELD & others, 1988), and the phylogenetic positions of all other brachiopod sequences are consistent with their reputed brachiopod origin. None is an outright contaminant.

2. Brachiopods plus phoronids are monophyletic in all three trees.

3. The phylactolaemate ectoprocts are the sister group of brachiopods plus phoronids in the ML tree but are more distant in the WP and NJ trees.

4. The gymnolaemate ectoproct (*Alcyonidium*) uniformly appears as a long-branched sister group of eulamellibranch

molluscs and is distant from brachiopods plus phoronids. The *Alcyonidium* sequence, however, contains a number of unusual sequence motifs in generally conserved regions and may not be truly representative of gymnolaemates. Clearly, given the high taxonomic diversity of ectoprocts (HYMAN, 1959a), the limited species sample currently available, and the disagreement between reconstructions, it is premature to come to any firm conclusion about ectoproct relationships (*contra* HALANYCH & others, 1995); more data are required. It remains possible that ectoprocts may eventually prove to be a sister group of brachiopods plus phoronids.

5. Arthropods, priapulans, the echiuran, the sipunculan, and eulamellibranch molluscs are all distant from brachiopods plus phoronids and therefore are not appropriate outgroups.

6. Ectoprocts apart, the plausible sister groups of brachiopods plus phoronids lie among molluscs or alternatively molluscs and a wider group of taxa including annelids, but quantitative data are needed to determine their relative order of proximity to the ingroup.

Table 6 shows branch lengths extracted from the analyses that generated the trees of Figures 183–185 and list the five closest candidate outgroup taxa in order of proximity to brachiopods and phoronids (the ingroup). All three analyses agree in one respect: the chiton *Acanthopleura* is closest.

In addition, we performed equally weighted and RCI-reweighted (WP) analyses in which each of 22 diverse protostome sequences was used in turn to root a small, representative set of brachiopod plus phoronid sequences, noting the overall tree length and the retention index (RI) in each case. RI measures the proportion of the data that is explained by synapomorphy rather than homoplasy, the higher the better. Since

FIG. 183. *Continued from facing page.*

articulated brachiopod branches. It was based on 685 parsimony-informative sites. See caption to Figure 181 for heuristic search details. The branch-length scale is based on the trees obtained before reweighting and gives an approximate indication of the number of inferred nucleotide base substitutions along each branch (new).



FIG. 184. Phylogenetic relationships of brachiopods, ectoprocts, phoronids, and other protostomes in an unrooted maximum-likelihood tree based on the alignment of complete SSU sequences used for Figures 181 and 182 but with nonprotostomes omitted. The alignment comprised sequences from 72 protostome taxa and 2,098 sites. For list of organisms representing nonlophophorate, coelomate protostome taxa, see caption to Figure 180. This tree was computed using empirical nucleotide frequencies and global rearrangement. All nodes were statistically significant ($P < 0.01$) except for those bearing the shortest articulated brachiopod branches comprising the unresolved *Laqueus*, *Fallax*, *Megerlia* plus *Megerlina* node (new).

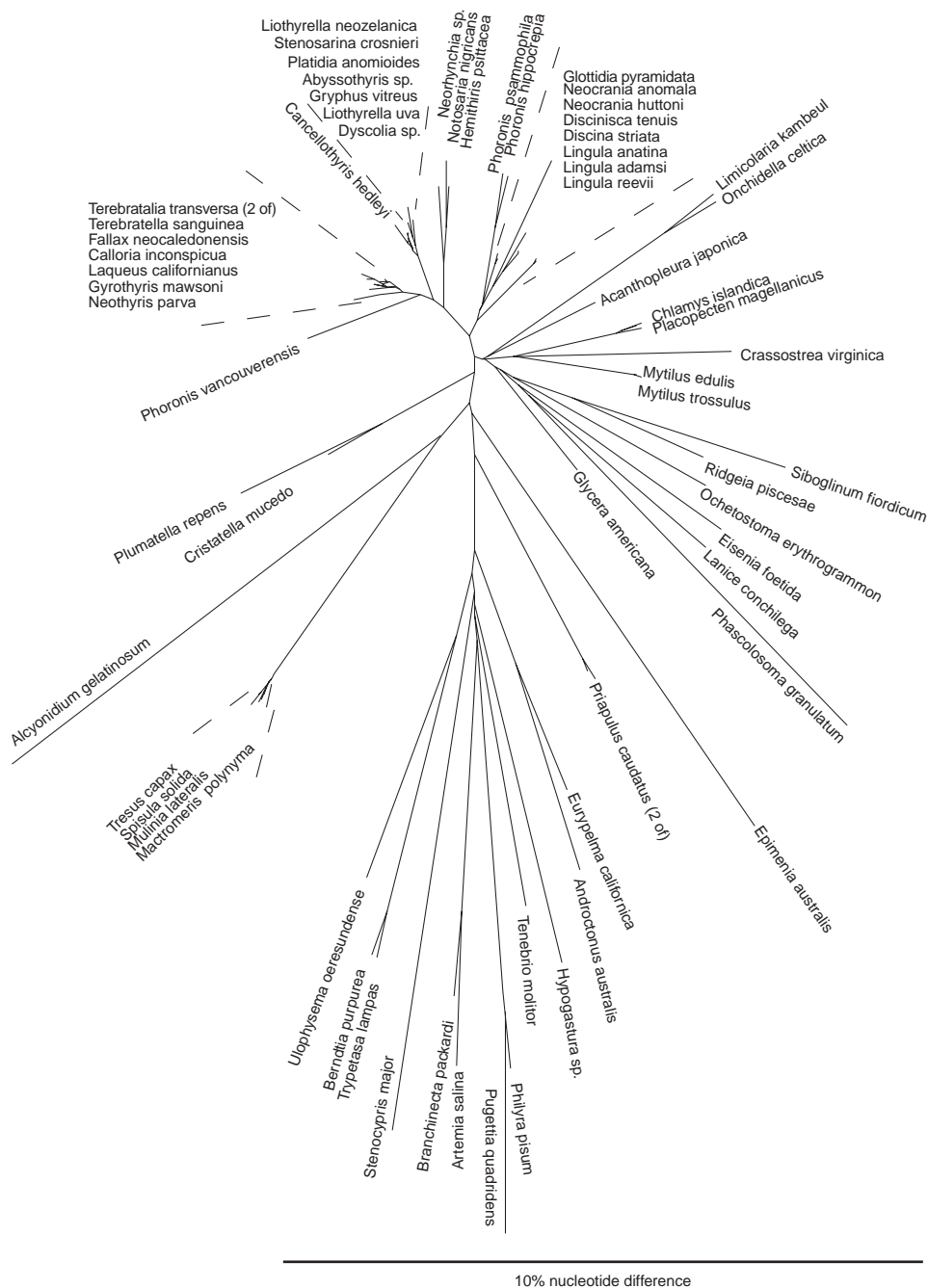


FIG. 185. Phylogenetic relationships of brachiopods, ectoprocts, phoronids, and other protostomes in an unrooted neighbor-joining tree based on the alignment of complete SSU sequences used for Figures 181 and 182 but with nonprotostomes omitted. The alignment comprised sequences from 72 protostome taxa and 2,098 sites. For list of organisms representing nonlophophorate, coelomate protostome taxa, see caption to Figure 180. This tree was based on a distance matrix calculated with the Kimura 2-parameter correction. Alternative correction algorithms and taxon-addition orders did not alter tree topology (new).

TABLE 6. Numerical parameters used to identify the closest outgroup. The methods of analysis used to obtain the parameters shown were also used (with addition of *a posteriori* parsimony character weighting) to construct Figures 183–188 (new).

Order ¹	Equally weighted parsimony			Maximum likelihood		Neighbor-joining	
	Taxon	Tree length ²	Retention index	Taxon	Nucleotide distance ³	Taxon	Nucleotide distance ⁴
1	<i>Acanthopleura</i>	495	0.801	<i>Acanthopleura</i>	0.0408	<i>Acanthopleura</i>	0.0605 ± 0.0009
2	<i>Chlamys</i>	496	0.802	<i>Glycera</i>	0.0550	<i>Glycera</i>	0.0622 ± 0.0009
3	<i>Mytilus</i>	507	0.793	<i>Chlamys</i>	0.0598	<i>Chlamys</i>	0.0681 ± 0.0014
4	<i>Cristatella</i>	509	0.790	<i>Cristatella</i>	0.0619	<i>Mytilus</i>	0.0686 ± 0.0010
5	<i>Glycera</i>	512	0.791	<i>Eisenia</i>	0.0943	<i>Cristatella</i>	0.0701 ± 0.0009

¹order of distance from ingroup; nearest = 1.

²overall tree length in a heuristic search, with characters equally weighted.

³distances estimated by summing branch lengths between the ingroup node and the outgroup terminal taxon. Each branch was shown as being significantly positive, $P < 0.01$, but confidence limits for the summed branch lengths cannot be stated. The ingroup node is the node in Figure 184 at which the branch carrying the inarticulate brachiopods joins the tree.

⁴nucleotide divergence between the outgroup and each ingroup taxon estimated using the Kimura 2-parameter correction and averaged over all ingroups ± standard error of mean.

the ingroup set was constant, tree length depended only on the length of the outgroup branch; and, hence, the shortest tree should identify the phenetically closest outgroup. Again, the tree rooted with *Acanthopleura* was the shortest by a small margin and gave the highest RI (details not shown). Thus, due to some combination of true phyletic position and similarity of evolutionary rate and of nucleotide composition, this chiton is the closest available outgroup for brachiopods and phoronids. While some of the 22 different outgroups yielded topologies showing less resolution, especially of the inarticulated brachiopod plus phoronid clade, none gave a radically different topology from that given by *Acanthopleura*.

The fact that outgroup selection may involve some subjectivity has long been recognized (DONOGHUE & CANTINO, 1984) and is inescapable when, as here, no independent evidence can be used to support outgroup choice. However, we have attempted to minimize the subjective element by basing choice of outgroup upon parameters estimated from the data. The need for selected outgroups arises not only from the theoretical considerations mentioned above but also from practical considerations: an alignment of approximately 80 SSU sequences causes computational difficulties.

The Phylogeny of Brachiopods and Phoronids Analyzed Using the Selected Outgroup

Figures 186–188 illustrate WP, ML, and NJ reconstructions using the selected outgroup, *Acanthopleura*, and lead to the following observations and conclusions.

1. Phoronids are either monophyletic, basal members of the inarticulated brachiopod clade (WP) or diphyletic with *Phoronis hippocrepi* and *P. psammophila* being the sister group of craniids and *P. vancouverensis* joining the base of the articulated brachiopods (ML and NJ with low bootstrap support). The association of *P. vancouverensis* with the articulated brachiopods has been reported elsewhere (HALANYCH & others, 1995).

Diphily of phoronids is biologically implausible and cannot be accepted, but the conflict is easily resolved by examination of the three phoronid sequences. Those of *Phoronis hippocrepi* and *P. psammophila* show no unusual features when compared with other protostomes, but the *P. vancouverensis* sequence (HALANYCH & others, 1995) lacks several nucleotides in otherwise highly conserved sites. More importantly, all three phoronid sequences share at least three variable-region motifs that are clear

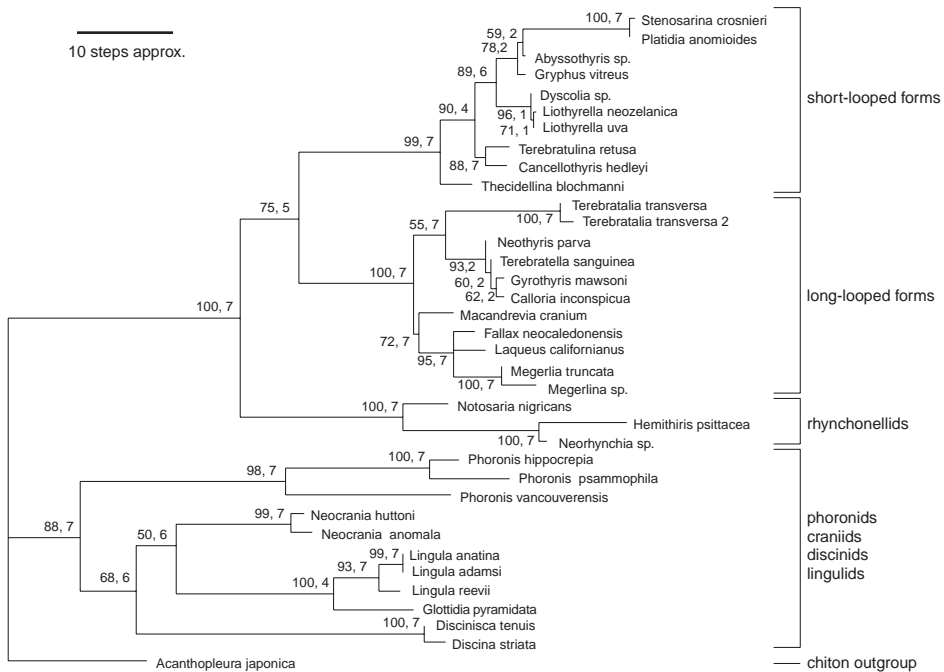


FIG. 186. Relationships of brachiopods and phoronids in phylogenetic trees rooted on the selected outgroup, *Acanthopleura*. This figure shows a weighted parsimony tree based on the alignment of complete SSU sequences used for Figures 181 and 182 but with ectoprocts, nonlophophorate protostomes, and nonprotostomes omitted. The alignment comprised 36 taxa and 1,813 sites, 198 of which were parsimony-informative. The skewness index of 10,000 random trees was $g_1 = -0.504$, suggesting that WP has an excellent chance of finding the true tree (HILLIS, HUELSENBECK, & CUNNINGHAM, 1994). Heuristic search found 36 equally most parsimonious trees of 495 steps, $RI = 0.801$. After three cycles of reweighting (base = 100) and heuristic search these were reduced to three trees of 20,355 weighted steps, $RI = 0.892$, differing only in topology at the unresolved *Laqueus*, *Fallax*, *Megerlia* plus *Megerlina* node, and one of these trees is shown. See caption to Figure 181 for search details. The numbers adjacent to each node are, first, the frequency with which that node appeared among 100 bootstrap replicates, and, second, the support index for that node (BREMER, 1988; KÄLLERSJÖ & others, 1992). Support indices were calculated as follows: after identifying the length of shortest RCI-weighted trees, a series of heuristic searches was conducted, keeping all trees longer than the shortest by graded proportions. The strict consensus of the trees at each increased length was then calculated, and the collapsed nodes in each consensus tree were identified. Tree length was increased in steps until the number of trees retained reached the level (> 4,000 trees) at which computer memory overflowed, when the search was abandoned. The corresponding support indices are given on a 7-point scale where 1 to 5 identify nodes that collapsed in trees longer than the minimal tree by 0.1 percent to 0.5 percent, 6 identifies nodes that collapsed after an 0.75 percent increase, and 7 identifies nodes that were still intact when the search was abandoned while searching for trees 1.0 percent longer than the minimal tree (new).

synapomorphies of phoronids alone. Since in Figure 186 the support index for the node uniting all three phoronids is relatively high (and this WP analysis is insensitive to apomorphy and plesiomorphy), we reject the suggestion that phoronids are most closely related to articulated brachiopods (HALANYCH & others, 1995); it must be erroneous (CONWAY MORRIS & others, 1996). This con-

clusion is further supported by the three analyses represented in Figures 180–182 and particularly by Figure 180, which is based on the least variable and hence most reliably aligned nucleotides and in which all three phoronids are again a monophyletic sister group of inarticulated brachiopods.

2. Two of the three reconstructions (Fig. 186, 188) agree in placing the origin of

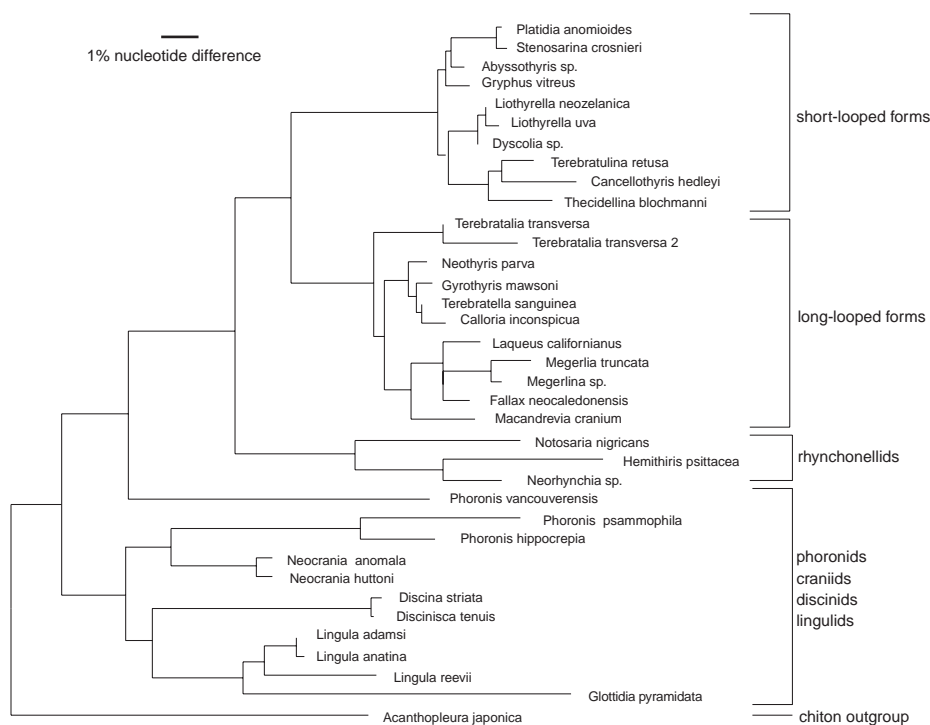


FIG. 187. Relationships of brachiopods and phoronids in phylogenetic trees rooted on the selected outgroup, *Acanthopleura*. This figure shows a maximum-likelihood tree based on the alignment of complete SSU sequences used for Figures 181 and 182 but with ectoprocts, nonlophophorate protostomes, and nonprotostomes omitted. The alignment comprised 36 taxa and 1,813 sites. This tree was computed using empirical nucleotide frequencies and global rearrangement. All nodes were statistically significant ($P < 0.01$) except for those leading to the shortest, articulated brachiopod branches comprising the unresolved *Laqueus*, *Fallax*, *Megerlia* plus *Megerlina* node. No bootstrap analysis was performed for computational reasons (new).

discinids before that of lingulids. The long branch and basal position of *Glottidia* among lingulids should be treated with reserve since this sequence (HALANYCH & others, 1995) lacks approximately 14 nucleotides in otherwise highly conserved positions.

3. The WP reconstruction (Fig. 186) joins the craniids and lingulids in a clade, but this has low bootstrap support, indicating that with more data the reconstructed topology might be altered.

4. Rhynchonellids are the sister group of all other articulated brachiopods.

5. Long-looped and short-looped articulated brachiopods are sister groups.

6. Long-looped articulated brachiopods are clearly monophyletic, and at least three subclades are recognized. *Terebratalia* represents either a basal, long-looped form (ML,

NJ) or is the sister group of the New Zealand terebratellids (WP). The latter are extremely closely related to one another, with *Neothyris* probably being basal. All three reconstructions (Fig. 186–188) agree that *Macandrevia* is the sister group of a morphologically diverse clade that includes kraussinids.

7. The morphological divergence that gave rise to the genus-level diversity of the New Zealand terebratellids has been accompanied by very little change in the 18S rRNA gene. An adequate molecular phylogeny of the long-looped articulated brachiopods must await results from a wider species sample and a faster-evolving gene.

8. Short-looped articulated brachiopods are clearly monophyletic, and at least four subclades are recognized. The thecideidine is unambiguously a short-looped articulated

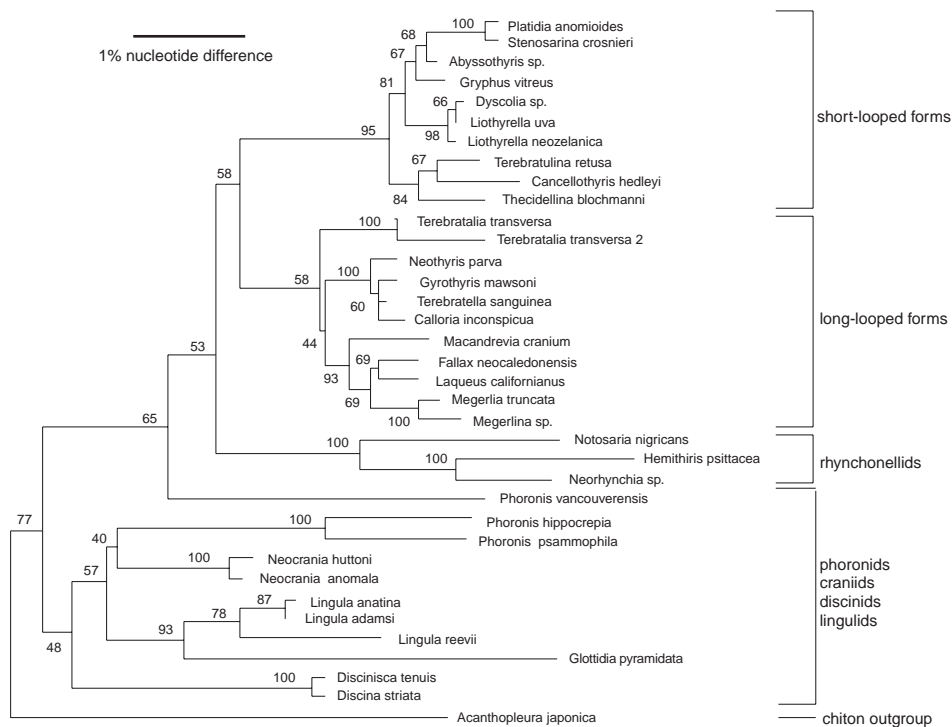


FIG. 188. Relationships of brachiopods and phoronids in phylogenetic trees rooted on the selected outgroup, *Acanthopleura*. This figure shows a neighbor-joining tree based on the alignment of complete SSU sequences used for Figures 181 and 182 but with ectoprocts, nonlophophorate protostomes, and nonprotostomes omitted. The alignment comprised 36 taxa and 1,813 sites. This tree is based on a distance matrix calculated with the Kimura 2-parameter correction. Alternative correction algorithms and taxon-addition orders did not alter tree topology. The numbers adjacent to each node are bootstrap frequencies (%) (new).

brachiopod, either basal (WP, strongly supported) or a sister group of cancellothyrids (ML, NJ). The cancellothyrid subclade shows weak affinity with the *Dyscolia-Liothyrella* subclade. Surprisingly, *Gryphus* is not most strongly associated with the *Dyscolia-Liothyrella* subclade. There is also a surprising association of the undoubted short-looped terebratulid *Stenosarina* with *Platidia* (the sample of which had an atypical history—see above). Some of these nodes, however, are not strongly supported, being based on very few differences. An adequate molecular phylogeny of the short-looped articulated brachiopods must await results from a wider species sample and a faster-evolving gene.

In summary, the topology of relationships among the articulated brachiopods is stable

with but minor differences in diverse phylogenetic reconstructions rooted with the closest sister group. It thus appears that the results are reliable and satisfy the aim of providing a first molecular phylogenetic framework for this clade. The topology of the inarticulated plus phoronid clade is less firm; phoronids are either the sister group of all inarticulated brachiopods or the sister group of craniids. The relative position of discinids, craniids, and lingulids is also unsettled. Nevertheless, the results unambiguously indicate that all three inarticulated brachiopod lineages belong together and, to that extent, also provide a secure, high-level framework for their phylogeny and classification.

Although the addition of sequence data from other genes and SSU sequences from

more terminal taxa may improve the robustness of the earliest branch points, an impractically large amount of such data may be required (PHILIPPE, CHENUIL, & ADOUTTE, 1994; RAFF, MARSHALL, & TURBEVILLE, 1994); and the most conclusive evidence will probably come not from additional sequence *per se* but from finding rare, qualitative evolutionary events such as insertions into conserved protein-coding genes or changes in mitochondrial gene order. Clearly, a fully satisfying reconstruction of the historical origins of the deep branches of the radiation that gave rise to the major protostome lineages will depend on the future accumulation of such new types of data. Similarly, a fuller molecular phylogeny of articulated brachiopods below the superfamily or family level will require sequence data from genes that evolve more rapidly than nuclear-encoded SSU.

IMPLICATIONS OF THE SSU rRNA GENE COMPARISON RESULTS FOR BRACHIOPOD SYSTEMATICS

It would be premature and inappropriate to make proposals for taxonomic revision on the basis of phylogenetic reconstructions from a single gene sequence, but it is appropriate to draw attention to the main implications for traditional, cladistic, and immunotaxonomic brachiopod systematics.

1. Regardless of how their embryology may be interpreted, brachiopods, phoronids, and ectoprocts belong in the clade that contains all undoubted protostomes, not in the clade of deuterostomes (BRUSCA & BRUSCA, 1990; NIELSEN, 1991, 1994, 1995; SCHRAM, 1991; EERNISSE, ALBERT, & ANDERSON, 1992; BACKELJAU, WINNEPENNINGCKX, & DE BRUYN, 1993). The deuterostome hypothesis of brachiopod, phoronid, and ectoproct affinities was also rejected earlier, when the SSU data included fewer sequences (FIELD & others, 1988; IRWIN, 1991; HALANYCH & others, 1995).

This result presents perhaps the sharpest conflict yet between molecules and morphol-

ogy (CONWAY MORRIS, 1995; GEE, 1995; PATTERSON, 1985), and it will be interesting to see which relationship will be supported by independent molecular data, such as that from mitochondrial genes.

2. The results are not sufficiently clear-cut to distinguish between alternative proposals for the relationships between discinids, lingulids, and craniids (ROWELL, 1982; GORJANSKY & POPOV, 1986; BASSETT & others, 1993; POPOV & others, 1993), but they are consistent with grouping all three inarticulated lineages into a single taxon and exclude the arrangement that unites craniids with articulated brachiopods (GORJANSKY & POPOV, 1986; BASSETT & others, 1993; POPOV & others, 1993).

3. Articulated and inarticulated brachiopods form a monophyletic group, within which articulated and inarticulated forms belong to separate clades; the traditional system of two brachiopod classes appears to be valid (but see next point below).

4. The results contradict the traditional status of the phoronids as a separate phylum and suggest that they should be included with all three lineages of inarticulated brachiopods in a new taxon, perhaps as a class. If the possible sister group relationship of phoronids and craniids is verified, a taxon comprising craniids plus phoronids may instead be called for, perhaps as a subclass.

5. Within the articulated brachiopods, rhynchonellids fully deserve their distinct taxonomic status.

6. Short-looped and long-looped articulated brachiopods (as so far analyzed) represent distinct clades, but articulated brachiopods such as *Platidia* (note caveat above) and *Megerlia* with atypical, incomplete loops may belong to either clade. Thus, a threefold division of the articulated brachiopods (rhynchonellids, short-looped forms, and long-looped forms), perhaps as orders, may be sufficient to reflect justly the extant sequence diversity. The thecideidines belong within the short-looped articulated brachiopods and are therefore unlikely to be descendants of spiriferids or strophomenids (WILLIAMS, 1973; BAKER, 1990). One tree raises

the possibility of a sister-group relationship between cancellothyrids and thecideidines, which seems not to have been previously considered (BAKER, 1990).

7. A taxonomic method using quantitative immunological cross reaction between shell antigens and antibodies has been described as a practical approach (COLLINS & others, 1988; COLLINS, CURRY, & others, 1991; COLLINS, MUYZER, CURRY, & others, 1991; CURRY, QUINN, & others, 1991; CURRY & others, 1993; ENDO & others, 1994), although this has been disputed (COHEN, 1992, 1994). Some specific immunotaxonomic proposals, such as the close clustering of *Terebratalia* and *Laqueus* or the grouping of *Macandrevia* relatively close to *Abyssothyris*, *Gryphus*, and *Liothyrella* are clearly inconsistent with our results.

FUTURE PROSPECTS

GENE EXPRESSION IN DEVELOPMENT AND DIFFERENTIATION

Recognition of homology is the fundamental task of comparative morphology, whether in the egg, the embryo, the larva, or the adult. It is a hazardous undertaking, exemplified by the long-standing uncertainty about whether brachiopods and other lophophorates are protostomes, deuterostomes, neither, or both, and by the uncertain homology of lophophores (NIELSEN, 1995 and references therein). The difficulty of correctly interpreting homology in developmental processes is highlighted by claims for the existence of three distinct methods of embryonic coelom formation in brachiopods (references cited by CHUANG, 1991), with different methods apparently being employed in two species of one genus. This divergence is inherently unlikely; developmental processes are not so plastic. It is more likely that traditional histological methods are too blunt a tool for the proper interpretation of such dynamic processes. Alternatively, if the multiple methods of coelom formation do occur, that process can have no value as a high-level phylogenetic character. Some implications of

lophophorates as protostomes in relation to the evolution of larval forms have been explored (STRATHMANN & EERNISSE, 1994).

The ultimate justification for postulated homology is the identification of orthologous evolutionary relationships between the ancestral and descendant genes that provide the necessary information for anatomy and development. Although this too is fraught with difficulty and largely awaits the future, it has a more objective basis than many anatomical interpretations (PATTERSON, 1985; WILLMER & HOLLAND, 1991). Since the expression of evolutionarily homologous genes has been discovered to underlie the establishment of the embryonic axis and segmentation in both insects and mammals (HOLLAND, 1992; KIMBLE, 1994; PATEL, 1994; SCOTT, 1994) and three of these genes have been found in a brachiopod (HOLLAND & HOGAN, 1986; HOLLAND, WILLIAMS, & LANFEAR, 1991), the scene is set for very desirable studies of gene expression in brachiopod embryonic development. Furthermore, a recent development even hints at the possibility of an assured supply of embryos (FREEMAN, 1994), a prerequisite for such work.

The wider paleontological context to which our results must be assimilated has been recently outlined (CONWAY MORRIS, 1994). In relation to the latter it is tempting to suggest that the brachiopod-like shells of halkieriids might indicate that the protostome radiation was indeed a matter of combinatorial mixing and matching of a limited number of developmental gene cassettes and might even lead us to invent an (unfashionably *ad hoc*) evolutionary scenario in which predatory selection pressure on diverse *Baupläne* originating by such "stochastic mosaicism" (SCHRAM, 1983, p. 337) favored sessile or infaunal halkieriid-like organisms with more shell and less body and thus led to the emergence of brachiopods. At least this scenario, in which the bivalve shells would both be dorsal but one would have reversed anterior-posterior polarity, might more easily account for the symmetry of the brachiopod shell and the recurved brachiopod,

ectoproct, and phoronid gut than any other yet proposed; and it makes testable predictions about the expression of embryonic axis-determining genes. A much more fully developed hypothesis in which halkieriids play a central part was published after the above was written (CONWAY MORRIS & PEEL, 1995). Neglecting compositional effects, the sequence similarity demonstrated here between brachiopods plus phoronids and a chiton could reflect a true sister-group relationship, a shared (low) rate of SSU sequence evolution, or convergence in the more rapidly evolving regions of this gene. The fact that chitons appear early in the fossil record (BENTON, 1993) is consistent with the possibility of their being a sister group. The possible relationships of chitons and halkieriids have been discussed (CONWAY MORRIS & PEEL, 1995).

YET MORE GENE SEQUENCE COMPARISONS

Given taxonomic overlap, molecular sequence data is additive (not addictive; it is hard and tedious work!). We can therefore look forward eventually to combining rRNA gene sequences with amino-acid or nucleotide sequences from, for example, highly conserved nuclear protein-coding genes, thus perhaps to resolve the most enigmatic and ancient evolutionary events. Furthermore, a total-evidence approach in which molecular and morphological character-state data are combined is possible (e.g., EERNISSE & KLUGE, 1993) and may prove informative, although it faces formidable character-weighting and polarization problems. Of more immediate value, the processes underlying speciation, especially population genetic structure, gene flow, and geographical isolation, can be addressed by judicious use of mitochondrial and nuclear gene sequences and other genetic markers (AVISE, 1994). The low dispersal potential of articulated brachiopods (but see PECK & ROBINSON, 1994), their endemism in oceanic provinces, and the existence of morphological variation between populations over shorter

distances (e.g., ALDRIDGE, 1981) suggest that they offer particularly favorable material for the analysis of genomic changes in evolution (WILSON, 1987; KNOWLTON, 1993) and might, if adequately sampled, provide paradigmatic material for the study of speciation (TEMPLETON, 1989). Preliminary evidence indicates, for example, that both DNA fingerprinting by the comparison of randomly amplified fragments and mitochondrial SSU rRNA gene sequences can be used successfully to resolve divergence between brachiopod individuals, populations, species, and genera (CARYL, 1992; S. STARK, C. THAYER, & B. COHEN, unpublished observations, 1993; B. COHEN & A. GAWTHROP, unpublished work, 1995); many golden opportunities lie ahead.

ACKNOWLEDGMENTS

We are grateful to the following individuals: Alwyn Williams for invaluable encouragement, support, and guidance; Moyra Cohen for help with collection of specimens and DNA preparation in New Zealand; Howard Brunton for identification of specimens; Jonathan Sheps and Mark Wilkinson for cladistic criticism; and Mary Burke for practical support. The work could not have proceeded without specimens collected, provided, or identified by C. Birkeland and G. Paulay, University of Guam, T. Cavalier-Smith and E. Chao, University of British Columbia; C. Duffy, Conservation Department, Picton; C. C. Emig, Station Marine d'Endoume, Marseille; B. Richer de Forges, ORSTOM, Noumea; H. G. Hansson, Tjaerno Marine Biology Laboratories, Stroemstad; N. Hiller, Rhodes University; B. Laurin, University of Bourgogne, Dijon; D. E. Lee, University of Otago; L. Lewis, Scripps Institution of Oceanography, La Jolla; D. I. McKinnon, University of Canterbury; L. Peck, British Antarctic Survey; S. A. Pedersen, University of Copenhagen; L. Singleton, New Zealand Oceanographic Institute, Wellington; R. Tarr, Sea Fisheries Research Institute, Capetown; C. T. Thayer

and M. C. Rhodes, University of Pennsylvania; A. Williams, University of Glasgow; Bamfield Marine Laboratory, University of British Columbia; Portobello Marine Laboratory, Otago University; Scottish Marine Biological Association, Dunstaffnage, Oban; Tasmanian Museum, Hobart; Western Australia Museum, Perth. B. Okamura and J. Vernon, Universities of Bristol and Oxford, respectively, kindly provided DNA from *Cristatella mucedo*. We apologize to anyone whose assistance may have been inadvertently overlooked.

SOURCES OF SEQUENCES

The following sequences were provided by their authors, to whom we are grateful for permission to use them in our analyses while they are still unpublished: *Alcyonidium gelatinosum*, *Eisenia foetida*, *Lanice conchilega*, *Ochetostoma erythrogrammon*, *Onchidella celtica*, *Phascolosoma granulatum*, *Ridgeia piscesae*, *Siboglinum fiordicum*, B. Winnepeninckx and R. De Wachter, University of Antwerp; *Epimania australis*, B. Runnegar, University of California; C. Harrison and C. M. Turbeville, Universities of Indiana and Michigan, respectively; *Glottidia pyramidata*, *Phoronis vancouverensis*, *Plumatella repens*, and *Terebratalia transversa* 2, K. Halanych, J. Bachelor, A. M. Aguinaldo, S. Liva, and D. M. Hillis, University of Texas, and J. A. Lake, University of California.

The following sequences were obtained in our own laboratory:

Abyssothyris sp., *Calloria inconspicua*, *Cancellothyris hedleyi*, *Cristatella mucedo*, *Discina striata*, *Discinisca tenuis*, *Dyscolia* sp., *Fallax neocaledonensis*, *Gryphus vitreus*, *Gyothyris mawsoni*, *Hemithiris psittacea*, *Laqueus californianus*, *Lingula adamsi*, *Lingula anatina*, *Liothyrella neozelanica*, *Liothyrella uva*, *Macandrevia cranium*, *Megerlia truncata*, *Megerlina* sp., *Neocrania anomala*, *Neocrania huttoni*, *Neorhynchia* sp., *Neothyris parva*, *Notosaria nigricans*, *Phoronis hippocrepia*, *Phoronis psammophila*, *Platidia anomioides*, *Priapulus caudatus*, *Stenosarina crosnieri*,

Terebratalia transversa, *Terebratella sanguinea*, *Terebratulina retusa*, and *Thecidellina blochmanni*. All these sequences will be deposited in GenBank (BENSON & others, 1994). DNA aliquots and associated brachiopod shells will be deposited in the Natural History Museum, London. Details of provenance and identification were published (COHEN, GAWTHROP, & CAVALIER-SMITH, in preparation). Copies of the sequence alignment will be available until approximately 1998 on magnetic disk or by FTP by contacting the senior author, e-mail address b.l.cohen@udcf.gla.ac.uk.

The following sequences were obtained from the Ribosomal Database Project electronic archive (MAIDAK & others, 1994) or from GenBank (BENSON & others, 1994): *Acanthoecopsis unguiculata*, *Acanthopleura japonica*, *Alligator mississippiensis*, *Androctonus australis*, *Anemonia sulcata*, *Antedon serrata*, *Argopecten irradians*, *Artemia salina*, *Berndtia purpurea*, *Branchinecta packardii*, *Branchiostoma floridae*, *Bufo valliceps*, *Caenorhabditis elegans*, *Callinectes sapidus*, *Chlamys islandica*, *Crassostrea virginica*, *Diaphanoeca grandis*, *Echinorhynchus cookei*, *Eurypelma californica*, *Fundulus heteroclitus*, *Gallus gallus*, *Glycera americana*, *Herdmania momus*, *Heterodon platyrhinus*, *Homo sapiens*, *Hypogastura* sp., *Lampetra aepyptera*, *Latimeria chalumnae*, *Limicolaria kambeul*, *Lingula reevii*, *Mactromeris polynyma*, *Microcionia prolifera*, *Mulinia lateralis*, *Mytilus edulis*, *Mytilus trossulus*, *Myxine glutinosa*, *Nematodirus battus*, *Notorhynchus cepedianus*, *Oryctolagus cuniculus*, *Petromyzon marinus*, *Philyra pisum*, *Placopecten magellanicus*, *Porocephalus crotali*, *Priapulus caudatus* 2, *Pugettia quadridens*, *Raninoides lousianensis*, *Rattus norvegicus*, *Rhinobatos lentiginosus*, *Scypha ciliata*, *Sebastolobus altivelis*, *Spisula solida*, *Squalus acanthias*, *Stenocypris major*, *Strongylocentrotus intermedius*, *Strongylocentrotus purpureus*, *Strongyloides stercoralis*, *Styela plicata*, *Tenebrio molitor*, *Tresus capax*, *Trichoplax adhaerens*, *Tripedalia cystophora*, *Typetasa lampas*, *Ulophysema oeresundense*, and *Xenopus laevis*.

PHYSIOLOGY

LLOYD S. PECK¹, MELISSA C. RHODES², GORDON B. CURRY³, and
ALAN D. ANSELL⁴

[¹British Antarctic Survey; ²Academy of Natural Sciences, Philadelphia, PA; ³University of Glasgow; ⁴Scottish Association for Marine Science]

INTRODUCTION

Prior to the publication of Part H, Brachiopoda, of the *Treatise on Invertebrate Paleontology* in 1965, very few studies dealing with aspects of the physiology of the brachiopods had been published. In that edition, RUDWICK was able to record much of what little information there was, including his own unpublished observations, in the chapter on ecology and paleoecology (1965a), which was later expanded elsewhere into a more comprehensive account (RUDWICK, 1970). Since that date, interest in living representatives of the Brachiopoda has increased, to a large extent as a result of desire by paleontologists for information that could help to interpret the life-styles and habits of fossil brachiopods. Much of the resultant information is discussed in a recent review of the biology of living brachiopods (JAMES & others, 1992), to which readers are referred for a more comprehensive bibliography.

A theme common to many of the recent studies and one of particular relevance to paleontological interpretation is that of scaling or allometry. Scaling concerns particularly the way in which physiological rates and other processes change as organisms grow (intraspecific), or how rates differ between species of differing maximum size (interspecific). Changes in scale, either by growth or through evolution of a larger or smaller body size, inevitably imply some compromises in form or function since not all morphological and functional parameters can increase in proportion while still maintaining the same functional relationships.

A review by LABARBERA (1986a) provided a useful introduction to the vast general literature available on allometric relationships. Following COCK (1966), he distinguished

three main categories of primary data in allometric studies—static, cross-sectional, and longitudinal, and four different levels of allometric analysis—ontogenetic, intraspecific, interspecific, and evolutionary. Most reported brachiopod studies are essentially intraspecific, although many authors make interspecific comparisons among groups of allometric exponents and coefficients derived for individual species. In most reported brachiopod studies, allometric analysis has been based on data measured for a group of individuals spanning the whole or part of the size range of the species, usually without the ages being specified or known. This common form of treatment is cross-sectional in COCK's classification (1966). Few sets of data in these brachiopod studies meet all of the criteria regarded as desirable by LABARBERA (1989) either in terms of the choice of variables used, the range of sizes included, or the rigor in choice or reporting of the statistical procedures used. Few reports include all the characteristics of the data or description of the techniques of analysis and results that are included in LABARBERA's (1989) Menu for Scaling Analyses. Finally, most of the studies report empirical relationships without attempting to test specific models derived from theoretical considerations of the relationships involved. A notable exception is the study by ACKERLY (1991, 1992) in which various parameters measured during rapid closure of the shell in articulated brachiopods were compared with values predicted from a theoretical model of the hydrodynamic forces involved. Despite these shortcomings, the variety of size-related data becoming available on many aspects of brachiopod function and physiology constitutes valuable source material for the paleontologist. As many as possible of these quantitative data are therefore summarized here,

although no attempt has been made to rework the original data to minimize the above criticisms.

SENSORY AND NEUROMUSCULAR PHYSIOLOGY AND BEHAVIOR

The sensory and behavioral capabilities of brachiopods are limited. The only sensory structures that have been described are the setae present in the larvae and around the mantle margin in the adult and the statocysts. Although responses to a variety of stimuli have been reported or implied, differentiated sensory structures concerned in such responses have not been identified.

The inarticulated brachiopods include both attached and free-living forms, the former including such species as *Neocrania anomala* (O. F. MÜLLER) in which the pedicle valve is cemented to a hard substratum, further restricting behavioral capabilities. In contrast, the free-living lingulids are the only group to have evolved an infaunal habit, and they have a range of physiological and behavioral features that adapt them for this mode of life. In particular, they are able to burrow into sediment, to maintain their position within the sediment, and to withdraw rapidly into the sediment in an escape response. During burrowing, the pedicle acts as a support or prop, while penetration is achieved by cyclical movements of the shell valves combined with action of the lateral setae. The detailed mechanism of burrowing has been well studied for a number of species (e.g., TRUEMAN & WONG, 1987; SAVAZZI, 1991; and review in JAMES & others, 1992). During burrowing the coelomic fluid functions as a hydrostatic skeleton facilitating movements of the valves and pedicle, and the lingulids thus differ from other brachiopods in which the coelom persists only as a fluid-transport system. In lingulids, the greatest pressures in the coelom coincide with shell opening during burrowing, indicating that thrust generated by the hydrostatic pressure is required to open the shell against the resistance of the sediment (Fig. 189).

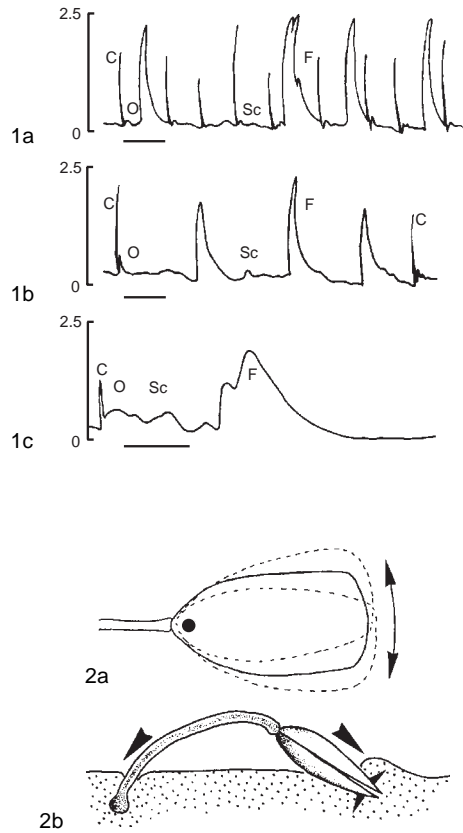


FIG. 189. 1a-c, Recordings of coelomic pressure (kPa) from the perivisceral coelom of *Lingula anatina* during the early stages of burrowing; recording for 1b follows immediately after 1a, showing closing (C), opening (O), scissors movements of the valves (Sc), and the application of greater force (F) to effect movement into the sand (time mark, one minute); 1c, as above; time mark, 10 seconds. 2a-b, Diagram of the ventral and dorsal valve of *Lingula anatina* showing movement of the valves during 2a, the scissor motion in burial; the principal pivotal area is represented by a dot; 2b, diagram of entry into the sand during high pressure pulse (large arrows) that forces valves and pedicle into the substratum with equal force and opens valve simultaneously (small arrows) (adapted from Trueman & Wong, 1987).

The articulated brachiopods comprise both attached forms and forms that may become unattached but rely on such passive adaptations as heavy shell thickening to resist physical stress. Activity in the articulated brachiopods is essentially restricted to opening and closing of the valves and, in the attached forms, rotation of the valves around

the pedicle. Rapid closure is accomplished by contraction of the adductor muscles, while opening results from the contraction of the opposing diductor muscles. Cycles of rapid adduction followed by slow abduction occur during normal activity and in response to various stimuli but show little clear rhythmicity (RUDWICK, 1962b; MCCAMMON, 1971). Prolonged shell closure in response to unfavorable conditions is possible and is maintained by contraction of the smooth muscle of the anterior pair of adductors.

Studies of the physiology of the muscle systems involved in these movements of the shell in articulated brachiopods, particularly by J. L. WILKENS and his co-workers (for references see JAMES & others, 1992), have shown that each of the opposing sets of muscles possess features consistent with its individual role. The smooth adductor muscles and the diductor muscles in particular exhibit unique characteristics. In the former, the tension generated in the muscle outlasts the initial neuronal stimulation, allowing the muscle to maintain tension for prolonged periods (WILKENS, 1987). This enables the smooth adductor muscles to eliminate slowly the shell gape remaining after contraction of the striated posterior adductor and to maintain shell closure. The diductor muscles exhibit the phenomenon of slip or slippage in which their tension drops abruptly to zero when they are subjected to vibration or stretching during contraction. This occurs naturally when contraction of the diductor muscles is opposed by the contraction of the striated adductor muscles. After slippage, tension begins to develop immediately but does so very slowly (WILKENS, 1978b). These properties of the diductor muscles allow the valves to be kept open at minimal metabolic cost while allowing for rapid closure in an emergency (ESHLEMAN & WILKENS, 1979a).

Rapid shell closure in the articulated brachiopods is subject to important hydrodynamic constraints related to expulsion of water from the shell. During closure, the principal hydrodynamic forces acting on the shell are inertial reactions, due to the accel-

eration of water, which dominate the kinematics of shell closure during the initial phases, and pressure forces, which develop as water is expelled from the shell and dominate the later phases of closure. ACKERLY (1991) developed a generalized hydrodynamic model that described the relative magnitude of these forces as functions of the shell's angular acceleration, velocity, and gape. Solutions of the general model predict how variables such as the closing speed and the mass flux of water depend on shell size, initial shell gape, and magnitude of the closing force. Measurements made from actual shell-closure events in *Terebratulina retusa* (LINNAEUS) and *Terebratalia transversa* (SOWERBY), recorded using electronic techniques and high-speed video cameras (Fig. 190), showed close agreement with the predictions of the hydrodynamic model, confirming that hydrodynamic reactions are a fundamental restraint on the closing mechanism (ACKERLY, 1992).

Allometric equations relating features of the kinematics of shell closure (maximum gape, closing velocity, closing time) and of muscle mechanics (moment arm length, muscle length, muscle cross-sectional area, muscle moment force, muscle force) to shell length of *Terebratulina retusa* and *Terebratalia transversa* are summarized in Table 7.

BODY SIZE AND COMPOSITION

RUDWICK (1970, p. 19) stated that "the shell of a brachiopod gives a misleading idea of the real size of the organism." This is because there is little tissue between the valves of a brachiopod shell, and much of the space enclosed by the valves, constituting the mantle cavity, can be viewed as part of the external environment. The problem of how big an animal is superficially appears to be a trivial question, but an organism's size affects almost all aspects of its physiology and ecology. The appropriate measure of size varies with the type of study being conducted and the questions being asked: taxonomists, for example, might be interested in linear

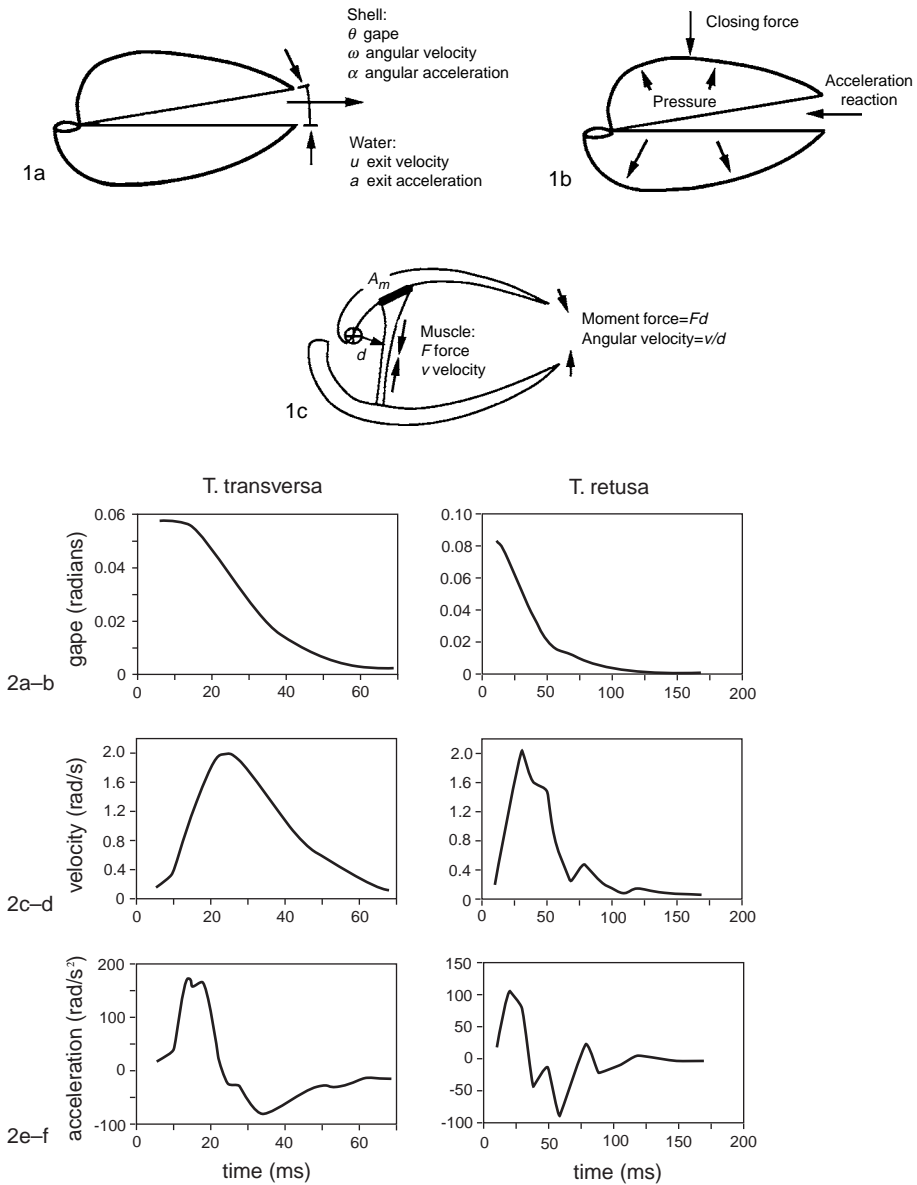


FIG. 190. 1a–c, Diagrams of the brachiopod shell showing 1a, the kinematic parameters, 1b, the forces involved in closure, and 1c, the quick adductor muscle position; A_m , cross sectional area of the muscle base; d , moment arm distance (Ackerly, 1991). 2a–f, Kinematic data for typical shell closing events in *Terebratalia transversa* and *Terebratulina retusa* showing 2a–b, the shell gape, 2c–d, angular velocity, and 2e–f, angular acceleration as functions of time (James & others, 1992; data from Ackerly, 1992).

dimensions or the ratios of linear dimensions of the shell or parts of the shell to give information on interpopulation or interspecies differences; ecologists might be concerned

with the volume of the animal to gain information about competitive interactions between species in terms of space occupied. Physiologists often need to know the

TABLE 7. Regression parameters from equations relating features of the muscle mechanics involved in shell closure to shell lengths (L , mm) for the articulated brachiopods *Terebratulina retusa* and *Terebratalia transversa*. Parameters are for the equation $\log_e y = a + b \log_e L$ and were fitted by reduced major axis techniques; CI , confidence interval; r^2 , coefficient of determination (adapted from Ackerly, 1992).

Species	Dependent variable (y)	Slope (b)	CI_{95}	r^2	Significant allometry ($P < 0.05$)
<i>T. retusa</i>	moment arm length (cm)	1.25	0.114	0.98	positive
	muscle area (cm ²)	2.59	0.73	0.90	-
	muscle force ($\times 10^{-2}$ N)	1.55	0.419	0.81	negative
	muscle length (cm)	1.03	0.349	0.86	-
	muscle moment ($\times 10^{-4}$ N.m)	2.72	0.553	0.94	-
<i>T. transversa</i>	moment arm length (cm)	0.968	0.562	0.66	-
	muscle area (cm ²)	3.04	1.34	0.81	-
	muscle length (cm)	1.37	0.622	0.84	-
	muscle moment ($\times 10^{-4}$ N.m)	3.33	0.107	0.998	positive

amount of organic material present, usually measured as ash-free dry mass (AFDM), while measurements of surface area of body tissues or structures may be important in understanding such processes as the rates of capture of particles by the filter-feeding apparatus or the rates of excretion of the end products of metabolism.

For most biological investigations of brachiopods, linear dimensions (shell length, breadth, and height) are measured, and length is usually used when comparisons with other parameters are made. As a consequence of allometry, ratios of linear dimensions have been shown to vary with size, for example, in the Antarctic brachiopod *Liothyrella uva* (BRODERIP) (PECK, CLARKE, & HOLMES, 1987a). This is a point of some significance to taxonomic studies, which may rely on such ratios for interspecific comparisons.

Mass is the next most common measurement of size taken in brachiopod studies. Here several different measures have been made. Tissue dry mass, which is the mass of soft tissue between the valves weighed after it has been dried to constant weight, has been used in investigations of respiration rate (SHUMWAY, 1982). Ash-free dry mass has been more commonly measured in physiological investigations of brachiopods, and this has also been separated in some cases into amounts present in the shell and in the

tissues (CURRY & ANSELL, 1986; PECK, CLARKE, & HOLMES, 1987a).

For the inarticulated brachiopod *Neocrania anomala*, the exponents in the allometric relationship between ash-free dry mass (AFDM) or dry mass (DM) and shell length are close to the value of 3 predicted by geometric isometry (Table 8).

For the articulated brachiopods measured, the exponents in these relationships are generally less than 3, with a mean of 2.71 ± 0.17 SD (Table 8; Fig. 191). Measured exponents in the relationship between AFDM of the tissues only (i.e., neglecting that component of the tissues contained in the caeca) vary between 2.36 and 3.48, with a mean of 2.95 ± 0.42 SD. In the Antarctic brachiopod *Liothyrella uva*, the exponent in these relationships varies systematically through the year, with midsummer exponents as low as 2.69 and late winter values as high as 3.23. Such changes result from differences between young and old individuals in their seasonal cycles of storage and utilization of resources for metabolism during winter and for reproduction. Higher values of the exponent are associated with periods when reserves have been used up and adults have not yet spawned, while lower exponents are found after spawning in the summer and during the period when overwintering reserves are high in all size classes (PECK & HOLMES, 1989b). In *L. uva* also, exponents

TABLE 8. Regression parameters from equations relating dry mass (*DM*, mg) or ash-free dry mass (*AFDM*, mg) to shell length (*L*, mm) for inarticulated (*Neocrania anomala*) and articulated (*Calloria inconspicua*, *Terebratulina retusa*, *Liothyrella uva*, *Liothyrella neozelanica*, *Neothyris lenticularis*, and *Notosaria nigricans*) brachiopods. Parameters are for the equation $\log_e y = a + b \log_e L$ and were fitted by least squares techniques. The suffixes *t* and *s* refer to measurements of internal tissue and shell respectively; where no suffix is given, data are for measurements of whole animal; *n*, sample size; r^2 , coefficient of determination; *SE*, standard error (see also Fig. 191; new).

Species	Dependent variable (y)	Intercept (a)	Slope (b)	SE _b	n	r ²	Source	Size range (mm)
Inarticulated								
<i>N. anomala</i>	DM	-2.12	2.91	-	39	0.95	CURRY & ANSELL (1986)	8–15
<i>N. anomala</i>	AFDM	-4.40	2.96	-	40	0.96	CURRY & ANSELL (1986)	8–15
<i>N. anomala</i>	AFDM(t)	-3.64	2.36	-	9	0.82	CURRY & ANSELL (1986)	8–15
Articulated (punctate)								
<i>C. inconspicua</i>	DM	-3.24	3.25	-	12	0.96	CURRY & ANSELL (1986)	
<i>C. inconspicua</i>	AFDM	-5.04	2.80	-	12	0.97	CURRY & ANSELL (1986)	
<i>C. inconspicua</i>	AFDM(t)	-6.07	2.97	-	12	0.91	CURRY & ANSELL (1986)	8–15
<i>T. retusa</i>	DM	-1.19	2.59	-	100	0.99	CURRY & ANSELL (1986)	8–15
<i>T. retusa</i>	AFDM	-4.22	2.62	-	100	0.98	CURRY & ANSELL (1986)	8–15
<i>T. retusa</i>	AFDM	-4.20	2.67	0.14	18	0.96	PECK & others (1989)	3.4–21.2
<i>T. retusa</i>	AFDM(t)	-4.44	2.55	-	9	0.94	CURRY & ANSELL (1986)	8–15
<i>L. uva</i>	AFDM	-5.22	2.97	0.07	37	0.98	PECK & HOLMES (1989a)	4.2–52.8
<i>L. neozelanica</i>	AFDM(t)	-7.87	3.25	0.12	25	0.91	PECK (1993)	8–50
<i>L. neozelanica</i>	DM(s)	-2.49	2.83	0.06	25	0.99	PECK (1993)	8–50
<i>N. lenticularis</i>	AFDM(t)	-6.17	3.08	0.22	24	0.90	PECK (1993)	8–40
<i>N. lenticularis</i>	DM(s)	-2.60	3.14	0.11	23	0.98	PECK (1993)	8–40
Articulated (impunctate)								
<i>N. nigricans</i>	AFDM(t)	-7.25	3.48	0.18	26	0.94	PECK (1993)	4–25
<i>N. nigricans</i>	DM(s)	-3.31	3.45	0.13	25	0.97	PECK (1993)	4–25

in the relationship between AFDM and length for adults may differ from those for juveniles at certain times of the year (PECK & HOLMES, 1989a) as a result of reproductive activity.

Measured exponents in the relationship between shell mass and shell length range from 2.83 for *Liothyrella neozelanica* (IHERING) to 3.45 for *Notosaria nigricans* (SOWERBY) with a mean of 3.14 ± 0.31 SD, indicating that there is no consistent pattern of positive or negative allometry (Fig. 191). Measured exponents in the relationship between tissue mass (but neglecting that component of the tissues contained in the caeca) and shell mass of the inarticulated brachiopod *Lingula anatina* LAMARCK (as *L. bancrofti* JOHNSON & HIRSCHFELD) and three species of articulated brachiopods are all less than the value of 1 predicted by geometrical isometry, with a mean of 0.82 ± 0.07 SD, indi-

cating that the mass of shell material increases more with age than the mass of internal tissues (Table 9).

Different internal tissues scale differently with brachiopod size. Exponents in the relationship between tissue AFDM and shell length vary not only between tissues, but also seasonally (Table 10). For the digestive gland, the exponent has low values throughout the year, ranging from 2.28 at the end of winter to 2.69 at the end of summer, significantly less than the value of 3 predicted by geometrical isometry. Values for the lophophore are also consistently and significantly less than 3. Exponents for the gonads, in contrast, are more variable, ranging from 2.34 in early summer to 6.21 in late summer.

Absolute amounts of tissue AFDM also vary seasonally in a consistent fashion (Fig. 192). In *Liothyrella uva* from the Antarctic, all tissues show a sharp increase in mass dur-

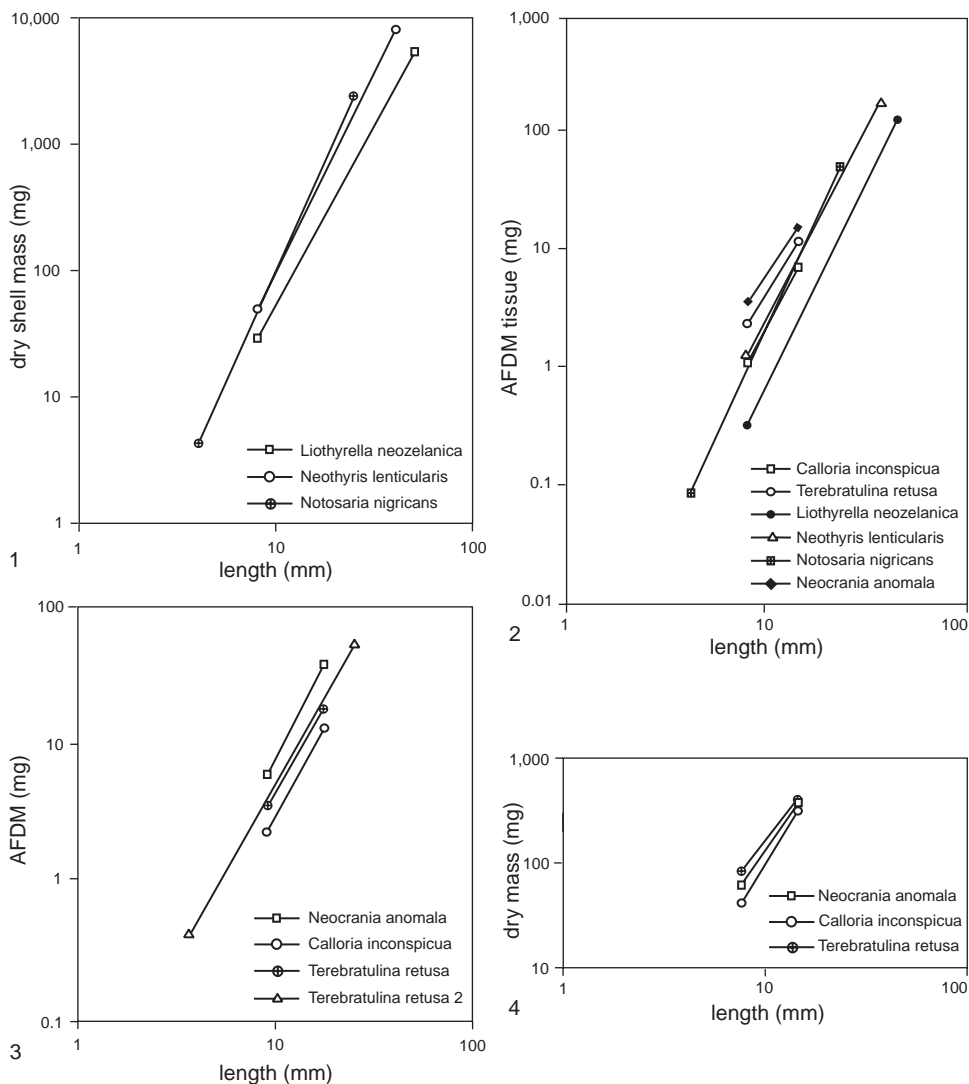


FIG. 191. Relationships between 1, \log_e dry shell mass (mg) and \log_e shell length (mm); 2, \log_e ash-free dry mass of tissues (AFDM tissue, mg) and \log_e shell length; 3, \log_e ash-free dry mass (AFDM, mg) and \log_e shell length; and 4, \log_e dry mass (mg) and \log_e shell length for inarticulated and articulated brachiopods. Parameters for each regression are shown in Table 8 (new).

ing the period of the summer phytoplankton bloom, the increases in the digestive gland and lophophore probably being related to raised activity levels associated with processing food. The AFDM of the gonad shows a cycle related to growth and proliferation of the gametes and subsequent spawning, while variations in shell AFDM reflect a combina-

tion of the storage of reserves for winter and reproductive events combined with the processing of those reserves by intracellular machinery in the caeca (PECK & HOLMES, 1989b; JAMES & others, 1992). Thus brachiopod tissue sizes and proportions change both as the animals grow and with seasonal events.

TABLE 9. Regression parameters from equations relating dry tissue mass ($DM(t)$, mg) to dry shell mass ($DM(s)$, mg) for inarticulated and articulated brachiopods. Parameters are for the equation $\log_e DM(t) = a + b \log_e DM(s)$ and were fitted by least squares techniques; n , sample size; r^2 , coefficient of determination (Shumway, 1982).

Species	Intercept (a)	Slope (b)	n	r^2	P (<)	Size range mg DM(s)
Inarticulated						
<i>Lingula bancroftii</i>	0.93	0.78	23	0.93	0.001	40–2,000
Articulated (punctate)						
<i>Neothyris lenticularis</i>	-2.26	0.75	18	0.82	0.001	1,100–12,000
<i>Calloria inconspicua</i>	-3.43	0.88	40	0.98	0.001	50–3,000
<i>Terebratella sanguinea</i>	-3.60	0.89	20	0.93	0.001	50–1,200

Articulated brachiopods generally have a lower overall organic content than many other marine benthic invertebrates, while inarticulated brachiopods do not (SHUMWAY, 1982; CURRY & ANSELL, 1986). The inarticulated brachiopod *Neocrania anomala* has a proportion of inorganic matter in its internal tissues (18.6 percent) similar to crustaceans, polychaetes, and bivalve and gastropod molluscs but a lower proportion than in sponges (PECK, 1993). Values for inorganic content of the internal tissues of articulated brachiopod species are generally about twice those of crustaceans, polychaetes, and molluscs and close to the inorganic contents of sponges. When the shell is also taken into account, 93.9 percent to 97.5 percent of the dry mass of the articulated brachiopods *Liothyrella neozelanica*, *Neothyris lenticularis* (DESHAYES), and *Notosaria nigricans* is found to be inorganic. These very high

values of inorganic content combined with the small amounts of internal tissue found in articulated brachiopod species have profound implications for potential predators (PECK, 1993).

A corollary of the low tissue mass in relation to volume enclosed between the valves in articulated brachiopods is that the size of the mantle cavity and the amount of water held in it is large. The exponent in the allometric relationship between the volume of the shell valves and shell length for *Liothyrella uva* is 2.77, a significant negative allometry (Table 11; PECK & HOLMES, 1989a). In contrast, the volume of the mantle cavity scales with an exponent of 3.34, showing significant positive allometry. The exponents in the relationships of internal tissues and of total animal volume with shell length are 3.06 and 3.12, respectively, and not significantly different from

TABLE 10. Exponents from regressions relating tissue ash-free dry mass ($AFDM$, mg) to shell length (L , mm) for the articulated brachiopod *Liothyrella uva* for six dates during the 1982–1983 austral summer. ANCOVA data test for significant variations in exponents among sampling periods, i.e., seasonal changes in the scaling of a given tissue. Exponents are values of b in the equation $\log_e AFDM = a + b \log_e L$; DG , digestive gland; GO , gonads; LO , lophophore; OT , other internal tissue; SH , shell; TOT , whole animal (adapted from Peck & Holmes, 1989a).

Tissue	1982		1983				ANCOVA	
	13 Sep	6 Nov	1 Dec	4 Jan	3 Feb	16 Feb	F	P (<)
DG	2.62	2.28	2.30	2.67	2.69	2.58	1.23	0.302
GO	4.36	2.83	2.34	3.86	6.21	3.49	7.00	0.001
LO	2.85	2.83	2.54	2.39	2.80	2.92	2.70	0.024
OT	2.97	3.24	2.83	2.84	3.01	3.03	0.76	0.597
SH	3.13	3.02	2.56	2.56	2.85	2.95	2.68	0.023
TOT	3.16	3.23	2.75	2.69	2.97	2.99	2.03	0.074

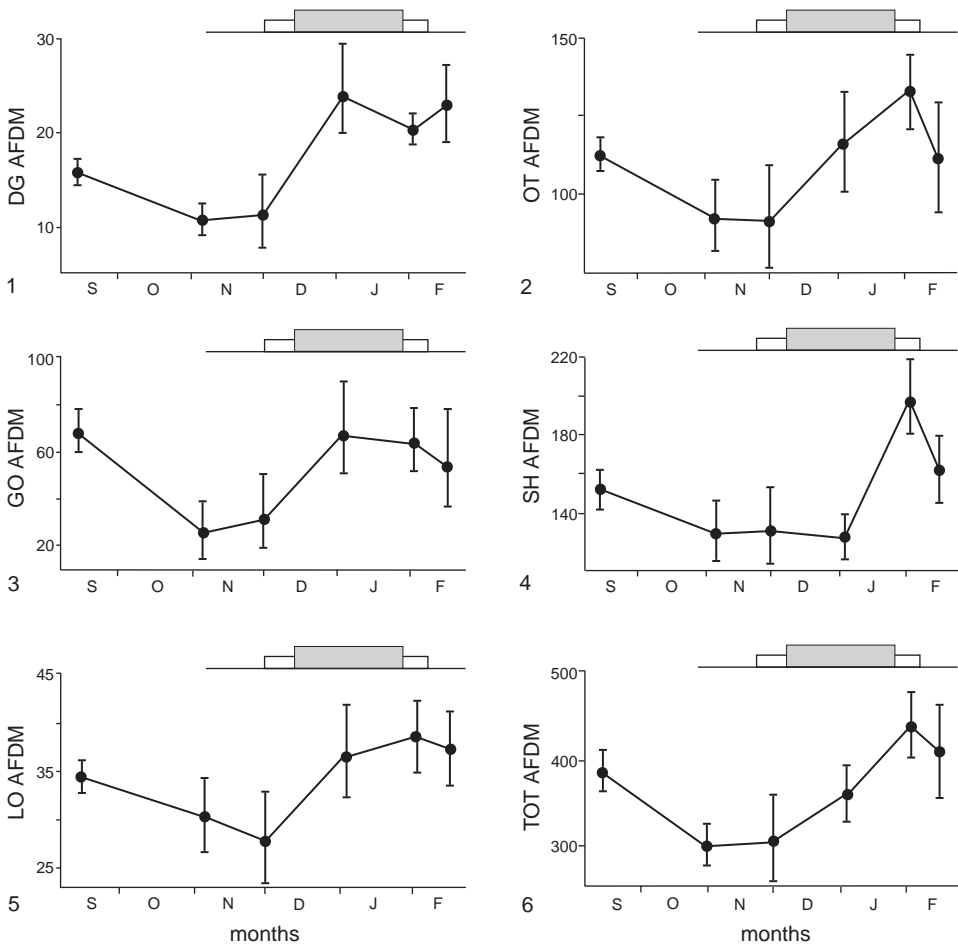


FIG. 192. 1–6, Seasonal variations in the ash-free dry mass (AFDM, mg) of the tissues of *Liothyrella uva* from Signy Island, Antarctica. Data are for a large adult (45 mm long) from the late winter through late summer of the 1982–1983 season. Points are means with ± 95 percent confidence intervals. Bars at the top of each graph show the duration and intensity of the phytoplankton bloom: *single line*, >1 mg chlorophyll/m³; *open box*, >5 mg chlorophyll/m³; *shaded box*, >10 mg chlorophyll/m³; *DG*, digestive gland; *GO*, gonads; *LO*, lophophore; *OT*, other internal tissues combined; *SH*, shell; *TOT*, total, or whole animal, values (adapted from Peck & Holmes, 1989b).

the value of 3 predicted by geometric isometry (Fig. 193). Thus, with increasing size, a progressively smaller proportion of the total volume is taken up by the shell valves, while relatively more is devoted to the mantle cavity.

The large volume of the mantle cavity may be an adaptation allowing for long periods of closure while utilizing the oxygen stored in the mantle cavity water (SHUMWAY, 1982) or may be a functional requirement set by the architecture of the lophophore.

Liothyrella uva continues to remove oxygen from water in the mantle cavity for around eight hours during enforced closure of the shell valves (PECK, MORRIS, & CLARKE, 1986a), which supports the former hypothesis. This may not be the sole factor in the evolution of large mantle cavities in articulated brachiopods, however. The architecture of the lophophore, consisting of unfused filaments, may dictate a need for a large mantle cavity for its efficient operation (PECK, 1992). PECK postulated that the resultant

TABLE 11. Regression parameters from equations relating shell valve volume ($V(s)$, cm^3), internal tissue volume ($V(t)$, cm^3), mantle cavity volume ($V(m)$, cm^3), and whole animal volume ($V(\text{tot})$) to shell length (L , mm) for the articulated brachiopod *Liothyrella uva*. Parameters are for the equation $\log_e y = a + b \log_e L$ and were fitted by least squares techniques. P values refer to differences between the slope and a value of 3 predicted by geometric isometry. Shell length ranged from 11.5 to 52.2 mm; n , sample size; r^2 , coefficient of determination; SE , standard error (see also Fig. 193; new).

Component	Intercept (a)	Slope (b)	SE_b	n	r^2	Significant allometry (P < 0.05)
V(s)	-9.84	2.77	0.075	45	0.97	negative
V(t)	-9.76	3.06	0.037	45	0.99	-
V(m)	-10.66	3.34	0.091	45	0.97	positive
V(tot)	-9.10	3.12	0.066	45	0.98	-

constraints have a profound influence on brachiopod lifestyles, resulting in low metabolic rates, which in turn contribute to the success of brachiopods in areas of low or highly seasonal food supply.

FEEDING

All brachiopods, both articulated and inarticulated, feed with the lophophore, a ciliated tentacular organ that occupies most of the volume in the mantle cavity. Although the lophophore occurs in a number of configurations, brachiopod species possessing different lophophore types feed in essentially the same manner. When the lophophore tentacles are fully extended for feeding and respiration, the mantle cavity is separated into inhalant and exhalant regions (Fig. 194). Weak, through-going currents are created by the lateral cilia of the tentacles, while the frontal cilia transport food particles along the length of the tentacle toward the brachial groove for transport to the mouth. Undesirable particles are eliminated by a variety of mechanisms (RUDWICK, 1970; THAYER, 1986a; JAMES & others, 1992). Mantle cilia assist in rejection and in the exchange of water through the mantle cavity (WESTBROEK, YANAGIDA, & ISA, 1980; THAYER, 1986a). Water movement through the mantle cavity is generally slow and laminar (Fig. 195), thus minimizing the energy dissipation involved in turbulent-flow regimes (LABARBERA, 1977, 1981, 1990).

The lophophore, in common with other filter-feeding structures, provides a large sur-

face area for the capture of particles suspended in the water being passed across it. As the lophophore is essentially an external surface providing an interface between the tissues and the outside environment, one might expect that its area would scale with exponents of 2 or 2/3 in allometric relationships with length or mass respectively. For

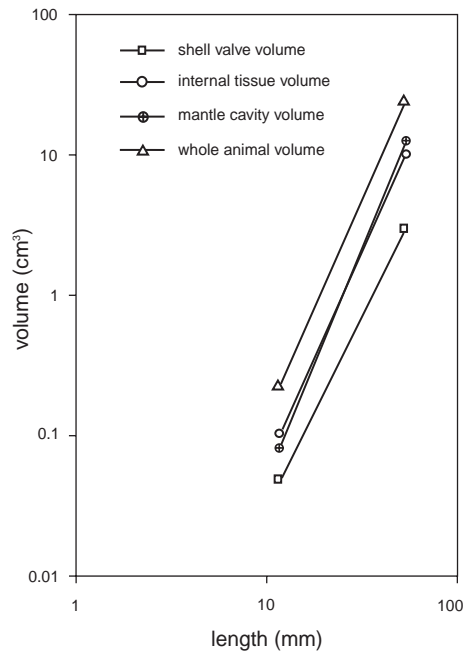


FIG. 193. Relationships of \log_e whole animal volume, \log_e shell valve volume, \log_e mantle cavity volume, and \log_e internal tissue volume (cm^3) with \log_e shell length (mm) for the articulated brachiopod *Liothyrella uva*. Parameters for each regression are shown in Table 11 (new).

two species of inarticulated brachiopods, *Neocrania californica* (BERRY) and *Discinisca strigata* (BRODERIP), measured values for the exponent in the allometric relationships of surface area of the lophophore with AFDM are close to 0.66 (Table 12; Fig. 196). Thus, for inarticulated brachiopods, lophophore area scales in a way that would be expected from a surface increasing in isometric proportion to shell length with growth. Measured values of the exponents in the allometric relationship between lophophore area and AFDM are greater than 0.66 for four species of articulated brachiopods, although for *Terebratalia transversa* and *Laqueus californianus* the difference from 0.66 was not significant. The mean value for the articulated brachiopods, however, is 0.712, indicating significant positive allometry. The mean value for these articulated brachiopods is significantly greater than that of the inarticulated brachiopods.

Epifaunal brachiopods are facultatively active suspension feeders (LABARBERA, 1977, 1981, 1984). They use metabolic energy to produce currents for feeding and respiration, but, when possible, they orient themselves to external water currents so that their ciliary pumping is augmented by the hydrodynamics of the ambient flow regime, and recirculation of previously filtered water is avoided. Some species such as *Terebratalia transversa*, do not reorient themselves after settlement of the larvae. Also such species as *Calloria inconspicua* and *Notosaria nigricans* live in dense, conspecific clusters, where the water pumped by one individual may include a significant component already filtered by closely neighboring individuals or epibionts, resulting in an increase in the total energy needed for pumping water to obtain food. There are no published studies on the hydrodynamics of infaunal inarticulated brachiopods.

Although the sources of nutrition used by brachiopods are still poorly understood for most species, there is little doubt that most of the energy needs of most species are supplied by particulate material filtered from the feeding current. This may include, in various

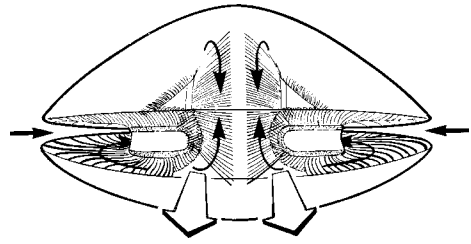


FIG. 194. Diagrammatic representation of the separation of incurrent (solid arrows) and excurrent water streams (open arrows) through the mantle cavity and lophophore of a typical plectolophous brachiopod (new).

proportions, phytoplankton, bacteria, organic detritus, or organic molecules adsorbed onto inorganic particles. Brachiopods are also able to absorb dissolved carbohydrates and amino acids directly from seawater, but the significance of this process as a source of energy has not been established (for references to nutritional sources, see JAMES & others, 1992).

Indirect evidence from measurements of particle-retention efficiencies suggests that brachiopods may fail to capture a large proportion of the suspended particles that are available to them in the water column (JAMES & others, 1992). Absolute particle-retention efficiency, defined as the number of suspended particles in a given size range captured by an organism during one traverse of the feeding structure, is difficult to measure directly without disturbing the animal. More commonly used, therefore, are relative retention efficiencies of differently sized particles, calculated as the percent retention of particles in a given size range relative to the retention efficiency of the most effectively retained size group of particles, taken as 100 percent (MOHLENBERG & RIISGARD, 1978). Particle-retention efficiency versus size has been studied in only three plectolophous articulated brachiopod species, *Terebratulina retusa* (JØRGENSEN & others, 1984), *Terebratulina septentrionalis*, and *Liothyrella uva* (M. RHODES, unpublished data, July, 1989; Newfoundland; December, 1994; Signy). For all the species studied, particles larger than 5 μm are captured more efficiently than smaller

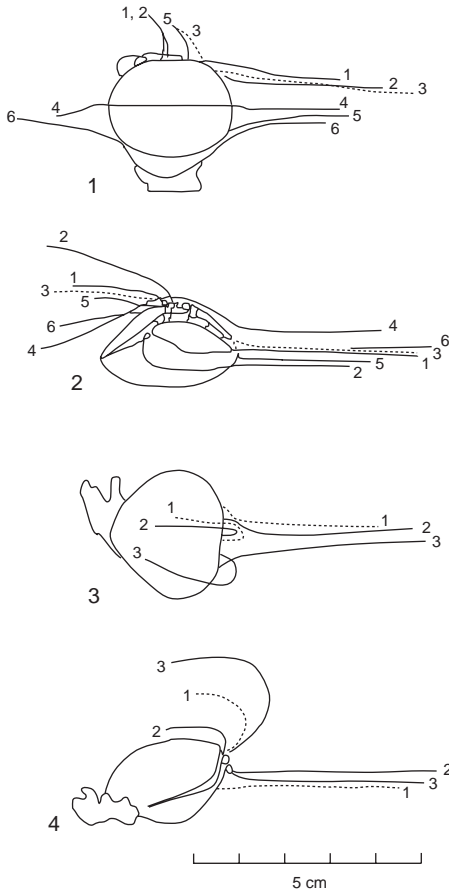


FIG. 195. Dye stream paths (indicated by *numbered lines*) around and through *Terebratalia transversa* in a 2 cm/s current (current flow is from right to left). 1–2, *Terebratalia* in the preferred orientation relative to the current direction; 3–4, *Terebratalia* in the least favorable orientation for normal flow through the lophophore. Regardless of orientation, the excurrent plume completely bypasses the shell and is never refiltered by the animal. Note that the water entering the anterioventral portion of the downstream incurrent gape (*lines 2 and 5*) passes very close to the dorsal valve and turns through 90° to enter the shell (LaBarbera, 1981).

particles. No comparable information is available for spirolophous articulated brachiopods or inarticulated brachiopods. Unlike bivalve molluscs, which frequently retain 100 percent of all particles above a given size range, articulated brachiopods retain at best only 68 percent of the particles passing through the lophophore (JØRGENSEN & oth-

ers, 1984). Direct observation of the plectolophous lophophore of undamaged *Terebratalia transversa*, using an endoscope with a high magnification zoom lens, showed that significant leakage of particles occurs through the lateral arms directly into the excurrent stream (THOMPSON, WARD, & RHODES, 1992).

The more efficient retention of larger-sized particles by articulated brachiopod species living in the photic zone (<200 m depth) is consistent with the sizes of particles found in their gut contents, where the most abundant particles are generally 5 to 10 µm in diameter and larger (SUCHANEK & LEVINTON, 1974; DOHERTY, 1976). The preponderance of small inorganic particles less than two microns in the guts of *Hemithiris psittacea* (GMELIN), *Terebratulina septentrionalis* (COUTHOUY), *Glaciarcularia spitzbergensis* (DAVIDSON), *Neothyris lenticularis* (DESHAYES), and *Abyssothyris wyvillei* (DAVIDSON) (MCCAMMON, 1969) probably reflects the presence of materials remaining in the gut after digestion.

Water exchange rates through brachiopods are extremely variable and are low relative to such other groups of marine invertebrates as bivalve molluscs or sponges (LABARBARA, 1981; RHODES & THOMPSON, 1992, 1993). In *Terebratulina septentrionalis*, flow rate varies considerably both for the same individual and between individuals of similar size (Fig. 197; MCCAMMON, 1971). Measured rates lie in the range of 0.05 to 0.75 cm/sec for individuals of 19.3 to 21.2 mm shell length. Exhalant flow of *Laqueus californianus* (KOCH), *Terebratulina unguicula* (CARPENTER), *Hemithiris psittacea* (GMELIN), and *Terebratalia transversa* (SOWERBY) (LABARBARA, 1977, 1981) has similarly low, variable, and intermittent rates. Measured mean excurrent rates range from a minimum of 0.2 cm/sec in *Hemithiris psittacea* of 7.9 to 19.8 mm length to a maximum of 1.41 cm/sec in *Terebratalia transversa* of 14.4 mm to 27.8 mm length.

Clearance rate is a measure of the rate at which a suspension feeder filters algae or par-

TABLE 12. Regression parameters from equations relating total lophophore area (LA , cm^2) and total ash-free dry mass ($AFDM$, mg) for inarticulated and articulated brachiopods. Parameters are for the equation $\log_e LA = a + b \log_e AFDM$ and were fitted by reduced major axis techniques; n , sample size; r^2 , coefficient of determination; SE_b , standard error (see also Fig. 196; adapted from LaBarbera, 1986b).

Species	Intercept (a)	Slope (b)	SE_b	r^2	n	Size range mg AFDM
Inarticulated						
<i>Neocrania californica</i>	-0.73	0.65	0.018	0.98	15	0.018–23
<i>Discinisca strigata</i>	-2.21	0.65	0.029	0.94	31	0.1–45
Articulated (punctate)						
<i>Terebratalia transversa</i>	-1.27	0.67	0.008	0.98	99	0.0018–>400
<i>Terebratulina unguicula</i>	-1.06	0.70	0.010	0.98	80	0.026–80
<i>Laqueus californianus</i>	-0.89	0.69	0.023	0.98	22	2.7–80
<i>Hemithiris psittacea</i>	-1.32	0.78	0.019	0.96	74	0.0045–60

ticles from the surrounding water. It thus reflects the ability to acquire food. Clearance rate is defined as the volume cleared per unit time, measured in liters per hour (l/h) or milliliters per hour (ml/h) (WIDDOWS,

1985). Clearance rates for the spirolophous articulated brachiopod *Hemithiris psittacea* and the plectolophous articulated brachiopods *Terebratulina septentrionalis*, *Neothyris lenticularis*, and *Liothyrella neozelanica* fed

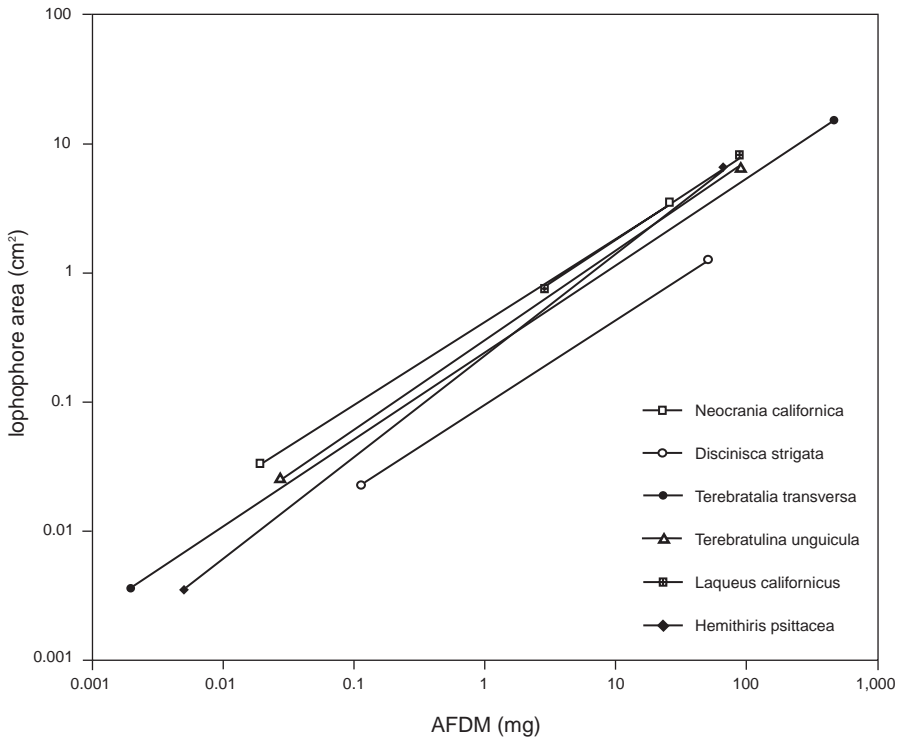


FIG. 196. Relationships between \log_e total lophophore area (cm^2) and \log_e total ash-free dry mass (AFDM, mg) of inarticulated and articulated brachiopods. Parameters for each regression are shown in Table 12 (new; data from LaBarbera, 1986b).

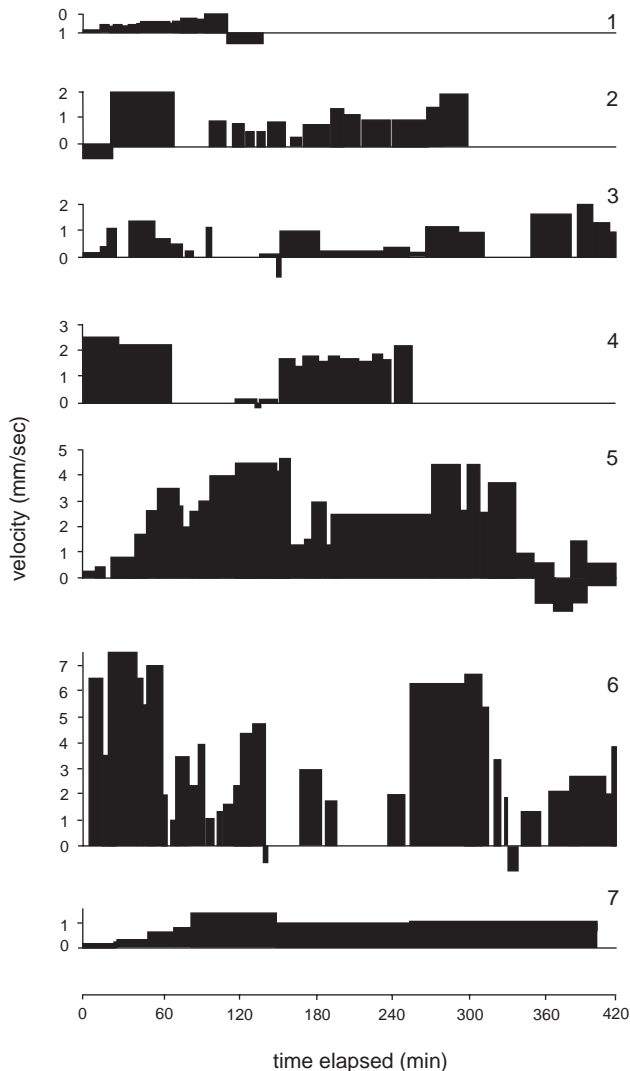


FIG. 197. Flow velocity in seven *Terebratulina septentrionalis* during the first seven hours of recording from a thermistor flow meter positioned in the incurrent flow. Maximum velocity of flow recorded during each cycle is plotted against time. Shell lengths of animals: 1, 19.4 mm; 2, 19.3 mm; 3, 12.7 mm; 4, 18.3 mm; 5, 16.0 mm; 6, 21.2 mm; 7, 14.8 mm (McCammon, 1971).

unicellular algae in controlled laboratory conditions (Table 13; Fig. 198; RHODES & THOMPSON, 1992, 1993), range from 22.0 ml/h for a 12.8 mg *Liothyrella neozelanica* to 1.20 l/h for a *Neothyris lenticularis* of 183 mg. Individuals have highly variable clearance rates; for example, recorded rates of one *Neothyris lenticularis* differed by a factor of seven to eight during repeated measurements

at ten-minute intervals. This variability is thus similar to that noted earlier for water pumping rates. No similar data are available for inarticulated brachiopods.

Exponents in the allometric relationship between clearance rate and ash-free dry mass (AFDM) range from 0.54 for *Terebratulina septentrionalis* to 0.62 for *Liothyrella neozelanica* (Table 13; Fig. 198; RHODES &

TABLE 13. Regression parameters from equations relating clearance rate (CR , ml/h) to ash-free dry mass ($AFDM$, mg) for articulated brachiopods. Parameters are for the equation $\log_e CR = a + b \log_e AFDM$ and were fitted by least squares technique. There is no significant correlation between CR and $AFDM$ for *T. septentrionalis* at an algal cell concentration of 11,000/ml, but the correlation is significant at 5,500 cells/ml; n , sample size; r^2 , coefficient of determination; SE , standard error (see also Fig. 198; adapted from Rhodes & Thompson, 1992, 1993).

Species	Concentration algal cells/ml	Intercept (a)	Slope (b)	SE_b	n	r^2	Size range mg AFDM
<i>Hemithiris psittacea</i>	11,000	3.43	0.61	0.108	24	0.59	11–44
<i>Terebratulina septentrionalis</i>	11,000	-	-	-	15	NS	32–102
<i>Terebratulina septentrionalis</i>	5,500	3.52	0.54	0.227	12	0.36	32–102
<i>Liothyrella neozelanica</i>	5,300	1.92	0.62	0.084	20	0.63	13–292
<i>Neothyris lenticularis</i>	5,300	3.57	0.56	0.111	19	0.72	39–251

THOMPSON, 1992, 1993). The measured exponents were all lower than 0.66 but not significantly so. However, the mean value of this exponent for articulated brachiopods was 0.583, suggesting slight negative allometry (RHODES & THOMPSON, 1992, 1993), and is close to but generally lower than the value of 0.66 that would be predicted if clearance increased isometrically with surface area. This contrasts with measured exponents in the relationships between lophophore surface area and tissue mass for plectolophes, which are generally higher than 0.66 (Table 12). Simple measures of lophophore area, however, do not take into account the pathways of particles in the feeding current, which may be equally important in predicting the effectiveness of suspension feeding. The lower exponents found for clearance rates suggest that not all areas of the lophophore are functionally equivalent. The tentacles of the median coil in two plectolophous species, *Terebratalia transversa* and *Terebratulina unguicula*, pump at only 60 percent the rate of the tentacles in the lateral arms (LABARBERA, 1981, 1986b). In *Terebratalia transversa*, however, most particles are captured in the median coil, while sorting and rejection are concentrated in the lateral arms (THOMPSON, WARD, & RHODES, 1992).

In the relationships between clearance rate and $AFDM$, scaling coefficients (intercepts), which measure the relative levels of activity of different species, range from 1.92 for

Liothyrella neozelanica to 3.57 for *Neothyris lenticularis* (Table 13). Comparisons between species, using clearance rates for individuals of 50, 100, and 350 mg $AFDM$, calculated using the relationships in Table 13, are summarized in Table 14. These rates are generally lower than those measured for other ecologically similar suspension feeders, such as bivalve molluscs, and are consistent with other evidence for overall low metabolic rates of brachiopods (JAMES & others, 1992).

Clearance rates of the plectolophous articulated brachiopods *Terebratulina septentrionalis* and *Neothyris lenticularis* are concentration dependent (Table 13–14; RHODES & THOMPSON, 1992, 1993), with low rates of clearance at high algal concentrations (10,500 to 12,600 cells/ml). In contrast, the spirolophous *Hemithiris psittacea* continues to clear algal cells effectively in algal concentrations of 10,500 to 12,600 cells per ml (Table 13–14).

There is little agreement whether brachiopods are selective feeders (JAMES & others, 1992), but sorting activity may be one reason for the reduced filtration rates of particles by plectolophes in high particle concentrations. Experimental evidence for the plectolophe *Terebratalia transversa* (RHODES & THAYER, 1991) suggests that articulated brachiopods can sort particles on the basis of specific gravity, shape, or charge. Sorting and rejection are useful adaptations in areas subject to high loads of suspended particulates but may involve extra expenditure of energy.

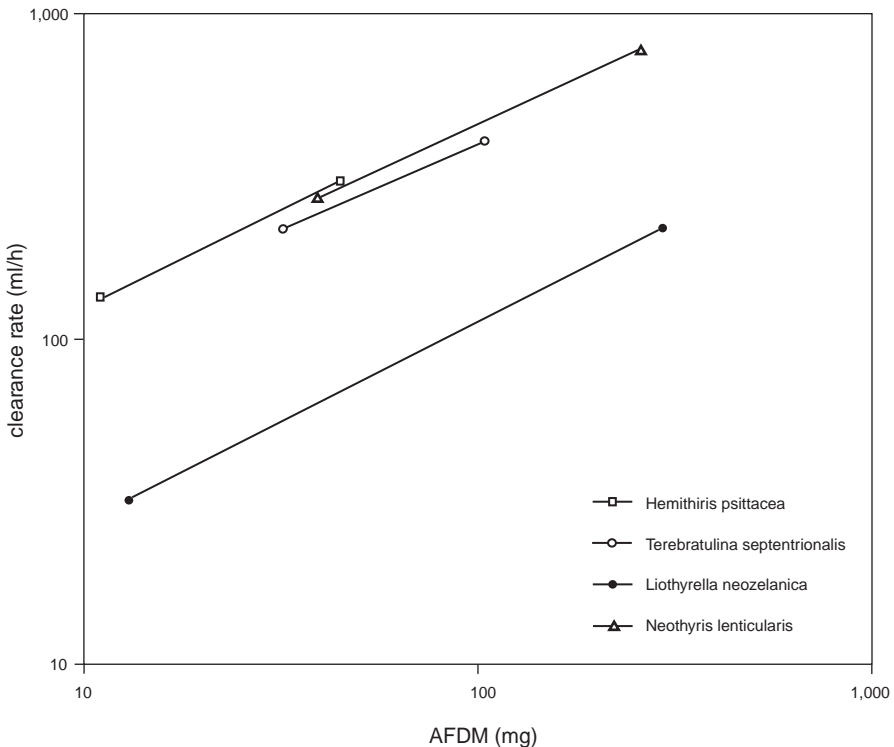


FIG. 198. Relationships between \log_e clearance rate (ml/h) and \log_e total ash-free dry mass (AFDM, mg) for articulated brachiopods. Parameters for each regression are shown in Table 13 (new; data from Rhodes & Thompson, 1992, 1993).

DIGESTION

Brachiopod digestive tracts have two basic configurations. Articulated brachiopods have a blind-ended gut, while inarticulated brachiopods have a separate anus. In both inarticulated and articulated brachiopods, the alimentary tract consists of pharynx, esophagus, stomach, digestive diverticula, and pylorus or intestine (STEELE-PETROVIC, 1976; MCCAMMON, 1981; review in JAMES & others, 1992). Epifaunal inarticulated brachiopods have a short, pouchlike intestine, while the infaunal lingulids have a long intestine (MCCAMMON, 1981). Articulated brachiopods eliminate feces by antiperistalsis through the mouth; inarticulated brachiopods, both epifaunal and infaunal, eliminate feces by peristalsis through the anus. Other than in this respect, the alimentary tracts of both articulated and inarticulated brachiopods are morphologically and histo-

logically similar (STEELE-PETROVIC, 1976; MCCAMMON, 1981).

Brachiopods combine both extracellular and intracellular digestion, depending on the type of material ingested (STEELE-PETROVIC, 1976; review in JAMES & others, 1992). Extracellular digestion and mechanical disruption resulting from contractions of the gut wall break particles down to a size ($<2 \mu\text{m}$) that the digestive cells can phagocytose (STEELE-PETROVIC, 1976).

The three inarticulated brachiopods *Terebratulina retusa*, *Gryphus vitreus* (BÖRN), and *Megerlia truncata* (LINNAEUS) and one inarticulated brachiopod, *Neocrania anomala*, for which digestive enzymes have been studied most comprehensively (D'HONDT, 1986) are closely similar in the distribution and level of activity of enzymes in the intestine and digestive gland; the only important difference noted was the strong activity of β -galactosidase in the inarticulated brachiopod

compared with the articulated brachiopods. Only acid phosphatase and N-acetyl- β -glucosaminidase showed greater activity in the intestine than in the digestive gland, indicating that only these enzymes are secreted throughout the gut. Most enzyme activities are located in the cells of the digestive gland, reflecting the important role of this organ in digestion and absorption in brachiopods (for review and full references, see JAMES & others, 1992).

RESPIRATION

Respiration refers to the processes involved in the uptake of oxygen by an organism from its proximate environment, the transportation of oxygen to the tissues, and its use as the final electron acceptor in energy-yielding, biochemical pathways. The rate of oxygen consumption (respiration rate) is often taken as a measure of metabolic rate but accurately represents rates of metabolic energy production only when no significant amounts of energy are being produced via anaerobic pathways.

Oxygen enters the body of an animal across soft tissue interfaces with the surrounding medium. These are often specially adapted areas (e.g., gills), where the integument is thin to facilitate the passage of molecules required for metabolism. Waste products of metabolic pathways, including carbon dioxide and nitrogenous wastes in the form of ammonia, urea, or amino nitrogen, may also pass out of the animal via these areas. In brachiopods the transport of oxygen into the body tissues takes place predominantly through the epithelia of the lophophore and mantle lobes. It has been suggested that, under specific conditions, oxygen may be removed from the surrounding seawater by caeca in punctate species (SHUMWAY, 1982). Physical barriers, however, make this unlikely. For example, in the terebratulides, the labyrinthine periostracum would be a formidable barrier even for the diffusion of oxygen, while in the thecideidines the caeca are separated from the subperiostracal cavities by many transverse partitions (A. WILLIAMS, personal communi-

TABLE 14. Comparison of clearance rates (ml/h) for similar-sized individuals of the articulated brachiopods *Hemithiris psittacea*, *Terebratulina septentrionalis*, *Liothyrella neozelanic*, and *Neothyris lenticularis* (new; data from Rhodes & Thompson, 1992, 1993).

Species	50 mg individual	100 mg individual	Cells/ml
<i>H. psittacea</i>	338	516*	11,000
<i>T. septentrionalis</i>	280	406	5,500
<i>L. neozelanic</i>	77	118	5,300
<i>N. lenticularis</i>	317	468	5,300

*extrapolation slightly beyond range of original data.

cation, 1994). The caeca should not be viewed as respiratory organs because they do not supply oxygen to the internal tissues (PECK, MORRIS, & CLARKE, 1986a, 1986b; JAMES & others, 1992).

Measured rates of oxygen consumption in brachiopods (Table 15–16) are generally low, consistent with the low rates of laminar flow through the brachiopod mantle cavity. They range from 0.1 to 0.9 times those of equivalently sized bivalve molluscs, with a mean value of around 0.5 (JAMES & others, 1992). Most published data on respiration are for articulated brachiopods; those for the inarticulated brachiopods *Lingula anatina* (as *L. bancrofti*) (SHUMWAY, 1982), *L. anatina* (as *L. reevii* DAVIDSON), and *Glottidia pyramidata* (STIMPSON) (HAMMEN, HANLON, & LUM, 1962; HAMMEN, 1969, 1971, 1977) are inconsistent and difficult to compare with the data for articulated brachiopods, partly because of the procedures adopted and partly because different bases were used for measurement of the size of the brachiopods (for detailed discussion see JAMES & others, 1992). At present, good assessments of the oxygen consumption of inarticulated brachiopods based on AFDM are not available.

Exponents in the allometric relationship between rates of oxygen consumption and AFDM or tissue dry weight range from 0.72 for *Terebratella sanguinea* (LEACH), *Laqueus californianus*, and *Liothyrella uva* to 1.00 for *Terebratulina retusa* (Table 15; Fig. 199). The average value of this exponent for the articulated brachiopods (0.78) is greater than the

TABLE 15. Regression parameters from equations relating oxygen consumption ($\dot{V}O_2$, $\mu\text{l O}_2/\text{h}$) with animal ash-free dry mass (AFDM, mg) for inarticulated and articulated brachiopods. Parameters are for the equation $\log_e \dot{V}O_2 = a + b \log_e \text{AFDM}$ and were fitted by least squares techniques after logarithmic transformation of the data. Coefficients in parentheses were fitted by reduced major axis techniques. Oxygen consumption measurements on brachiopods were also made by HAMMEN (1971) and THAYER (1986b), but it was not possible to extract relevant data from these sources; F, fed; n, sample size; r^2 , coefficient of determination; S, starved; SE, standard error (see also Fig. 199; new).

Species	Temp (°C)	Intercept (a)	Slope (b)	SE _b	r ²	n	Authority	Size range mg AFDM
Inarticulated								
<i>Lingula bancrofti</i>	10	-0.68	0.71	-	0.85	31	SHUMWAY (1982)	35–2,000
Articulated (punctate)								
<i>Neothyris lenticularis</i>	10	0.26	0.73	-	0.79	22	SHUMWAY (1982)	2–300
<i>Calloria inconspicua</i>	10	0.17	0.74	-	0.88	50	SHUMWAY (1982)	1.5–48
<i>Terebratalia sanguinea</i>	10	0.30	0.72	-	0.86	31	SHUMWAY (1982)	1.5–48
<i>Terebratalia transversa</i>	-	(0.40)	(0.73)	0.023	0.96	45	LABARBERA (1986b)	1–360
<i>Terebratulina unguicula</i>	-	(0.26)	(0.74)	0.026	0.96	34	LABARBERA (1986b)	3–60
<i>Laqueus californianus</i>	-	(0.02)	(0.77)	0.039	0.94	22	LABARBERA (1986b)	2.8–80
<i>Hemithiris psittacea</i>	-	(0.58)	(0.72)	0.028	0.96	33	LABARBERA (1986b)	0.38–80
<i>Terebratulina retusa</i>	5.8F	-0.24	0.95	0.089	0.88	24	PECK & others (1989)	38–450
<i>Terebratulina retusa</i>	10.7F	-2.41	0.97	0.055	0.88	45	PECK & others (1989)	5–520
<i>Terebratulina retusa</i>	5.6S	-2.70	1.00	0.055	0.88	46	PECK & others (1989)	12–450
<i>Liothyrella uva</i>	0	-2.16	0.72	0.028	0.88	105	PECK & others (1986)	0.32–660
<i>Liothyrella uva</i>	0	-2.30	0.80	0.033	0.92	45	PECK, CLARKE, & HOLMES (1987b)	1–610

value of 0.66 that would be predicted if oxygen consumption increased isometrically with surface area but close to the exponent of 0.75 commonly found in interspecific scaling comparisons of metabolic rate (see LABARBERA, 1986b).

Exponents in the relationships between rates of oxygen consumption and tissue weight (Table 15) are generally greater than the equivalent exponents for the relationships between particle clearance rates and tissue weight (Table 13). Similarly, when the relationships of rates of oxygen consumption to body mass are compared with those for lophophore surface area (Table 12), three plectolophes, *Terebratalia transversa*, *Terebratulina unguicula*, and *Laqueus californianus*, all have higher exponents for oxygen consumption than for lophophore area. For the spirolophe, *Hemithiris psittacea*, however, the reverse is the case. As the lophophore is the feeding organ, its area should limit the ability of the brachiopod to capture food particles. Thus, for plectolophes, there is an in-

creasing disparity between ability to obtain food and metabolic energy requirements, and this could limit the maximum attainable size. For spirolophes the limited data available would suggest that no such constraint applies. In this context, LABARBERA (1986b) pointed out that whenever a brachiopod clade has produced species of large size in the fossil record the lophophore was a spirolophe.

Even when the differences in scaling exponent among the relationships between rates of oxygen consumption and tissue mass are taken into account, considerable differences remain between rates for different brachiopod species and between rates measured under different conditions for the same species. Differences in the temperature at which the measurements were made account for part of this variation, but when the data are adjusted to allow for temperature differences between experiments (assuming a Q_{10} value of 2 where

$$Q_{10} = (V_2/V_1)^{10/(t_2-t_1)}$$

TABLE 16. Comparison of rates of oxygen consumption ($\dot{V}O_2$, $\mu\text{l/h}$) for similar-sized individuals of articulated brachiopods; F, fed; S, starved (new).

Species	Temp ($^{\circ}\text{C}$)	$\dot{V}O_2$ ($\mu\text{l/h}$)		Authority
		50 mg individual	100 mg individual	
<i>Neothyris lenticularis</i>	10	21.3	37.3	SHUMWAY (1982)
<i>Calloria inconspicua</i>	10	22.1	35.7	SHUMWAY (1982)
<i>Terebratella sanguinea</i>	10	20.3	37.1	SHUMWAY (1982)
<i>Terebratalia transversa</i>	-	26.0	42.9	LABARBERA (1986b)
<i>Terebratulina unguicula</i>	-	23.4	39.1	LABARBERA (1986b)
<i>Laqueus californianus</i>	-	21.1	35.4	LABARBERA (1986b)
<i>Hemithiris psittacea</i>	-	29.7	49.0	LABARBERA (1986b)
<i>Terebratulina retusa</i>	5.8F	3.6	7.1	PECK & others (1989)
<i>Terebratulina retusa</i>	10.7F	4.0	7.8	PECK & others (1989)
<i>Terebratulina retusa</i>	5.6S	3.4	6.7	PECK & others (1989)
<i>Liothyrella uva</i>	0	1.9	3.2	PECK & others (1986)
<i>Liothyrella uva</i>	0	2.3	4.0	PECK, CLARKE, & HOLMES (1987b)

and V_1 and V_2 are the respiration rates at the temperatures t_1 and t_2 respectively) the lowest and highest values recorded for articulated brachiopods are still different by a factor of five.

Rates of oxygen consumption of individual brachiopod species are influenced by other factors besides temperature. These include seasonal factors as metabolic rate in winter is usually lower than in summer even when temperatures are the same, or physiological states, such as reproductive or nutritional condition. The variation in measured rates may also reflect methodological differences among the different studies, in particular the influence of stirring of the experimental chambers (see JAMES & others, 1992). High values tend to be associated with experimental systems using oxygen electrodes and stirred water (SHUMWAY, 1982; LABARBERA, 1986b) and low values with still-water regimes using wet-chemical titration techniques (DOHERTY, 1976; PECK, CLARKE, & HOLMES, 1987b; PECK & others, 1989). Neither accurately reproduce the hydrodynamic conditions in which brachiopods normally live.

Rates of oxygen consumption in articulated brachiopods are relatively insensitive to temperature change. Q_{10} values are generally below 2 when brachiopods are held at temperatures within the range they normally experience (DOHERTY, 1976; SHUMWAY, 1982;

PECK, 1989; PECK & others, 1989). For *Calloria inconspicua* (SOWERBY), Q_{10} may be as low as 1.18 within the normal temperature range but greater than 4 when held below the normal temperature range (DOHERTY, 1976; SHUMWAY, 1982). The time course of temperature change affects the apparent effect of temperature on oxygen consumption. Acute (short-term) responses to temperature change in the Antarctic brachiopod *Liothyrella uva* gave Q_{10} values as high as 9.7, while for acclimated (longer-term) responses Q_{10} values were all less than 2 (PECK, 1989).

The rate of oxygen consumption is also affected by the oxygen tension in the surrounding sea water. The inarticulated brachiopod *Lingula anatina* and the articulated brachiopod *Calloria inconspicua* both show strong abilities to remove oxygen from water at low oxygen tension; *Neothyris lenticularis* is poor in this respect, and *Terebratella sanguinea* intermediate (Fig. 200; SHUMWAY, 1982). These different abilities reflect the likelihood in each case that the species would encounter conditions of low oxygen tension in its natural habitat. *Lingula anatina*, living in an infaunal habitat, is the most likely to regularly experience low oxygen tension in the surrounding water; *Calloria inconspicua*, living in fairly shallow areas, is likely to regularly experience low oxygen concentrations during some low tides; while *Neothyris*

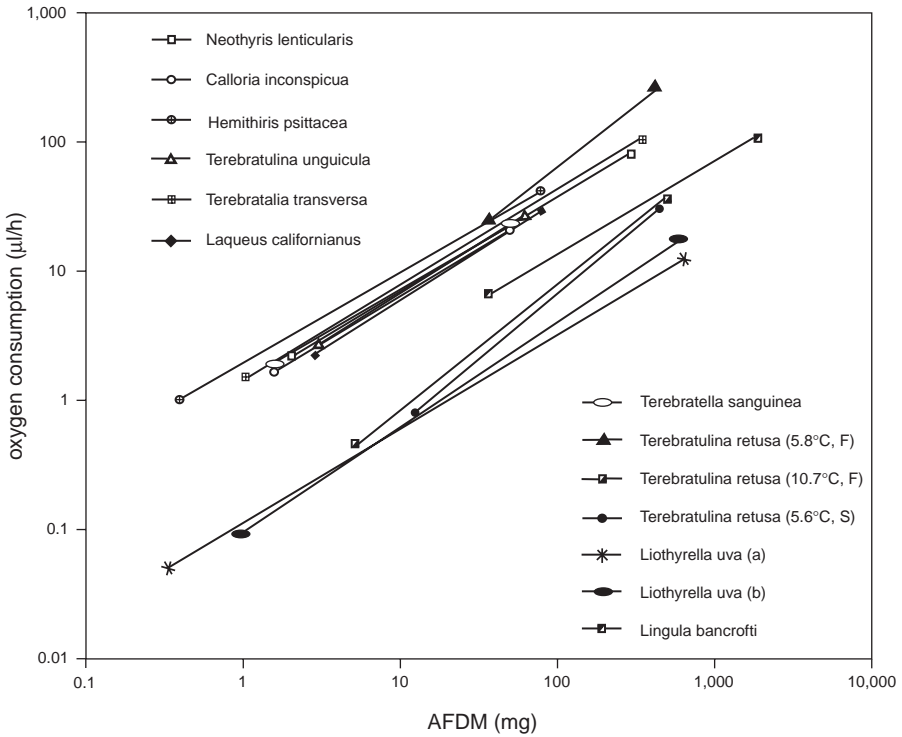


FIG. 199. Relationships between \log_e rate of oxygen consumption ($\mu\text{l/h}$) and \log_e animal ash-free dry mass (AFDM, mg) for inarticulated and articulated brachiopods. Parameters for each regression and the sources of the data are shown in Table 15; F, fed; S, starved (new).

lenticularis and *Terebratella sanguinea* both live in deeper-water environments where reduced oxygen regimes are unlikely. *Terebratalia transversa* from subtidal habitats near the San Juan Islands, Washington, USA, are capable of regulating the uptake of oxygen at constant rates down to levels of around 10 percent saturation ($0.5 \text{ cm}^3 \text{ O}_2/\text{l}$; THAYER, 1986b).

A further factor affecting rates of oxygen consumption is the nutritional state of the individual. In *Liothyrella uva* and *Terebratulina retusa*, feeding raises rates of oxygen consumption above starved or standard levels by between 20 and 25 percent (PECK & others, 1986, 1989; PECK, CLARKE, & HOLMES, 1987b). Starvation may reduce rates by more than 50 percent in *Liothyrella uva* (PECK, 1989) with reduction to these basal (standard) levels taking between 25 and 30 days to complete from the initiation of starvation. DOHERTY (1976) found no differ-

ence in the rates of oxygen consumption of *Calloria inconspicua* held at four different food concentrations, but with his experimental protocol it would not have been possible to detect changes of the order of 25 percent. The above studies do, however, show that the effects of feeding on respiration rate are low. There is no information on the effects of such other parameters as animal density, light regime, turbidity, or salinity on oxygen uptake in brachiopods.

Their low levels of respiration combined with the low tissue densities described earlier (p. 220) suggest that diffusion processes should be sufficient to supply oxygen to the tissues of articulated brachiopods. Calculations based on an equation derived by HARVEY (1928) indicate that diffusion could supply oxygen to the tissues over distances of around 2 mm, which is less than the average thickness of the mantle including the gonads (JAMES, ANSELL, & CURRY, 1991a). There is

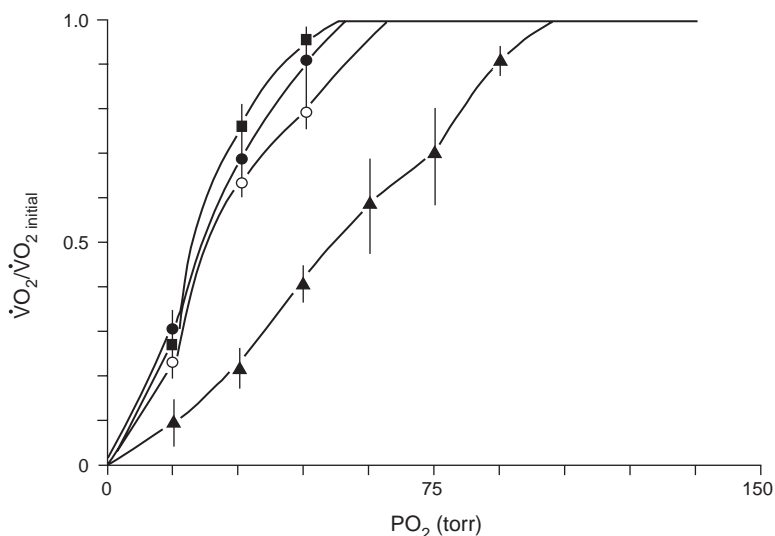


FIG. 200. The effect of declining oxygen tension on oxygen consumption in four species of brachiopods: *Calloria inconspicua* (●, sample size = 15), *Terebratella sanguinea* (○, sample size = 5), *Neothyris lenticularis* (▲, sample size = 5), *Lingula anatina* (as *L. bancrofti*) (■, sample size = 6). Initial $\dot{V}O_2$ (ml O_2 /h/g) values are set equal to 1.0 and all subsequent values are expressed as fractions of 1.0. Points on each line represent the mean with 95 percent confidence limits; experimental conditions: 10°C, 33.5 ppt salinity (Shumway, 1982).

thus little requirement for an efficient circulation to transport respiratory gases and waste products. The only brachiopod for which heart-beat rates have been measured, the articulated brachiopod *Liothyrella uva*, shows a rate of less than 1 beat per minute (average = 0.8 beats/min) at 0°C (BUCHAN, PECK, & TUBLITZ, 1988).

Respiratory pigments used to transport oxygen or to store oxygen within the body tissues have not been recorded in articulated brachiopods. The inarticulated brachiopod, *Lingula anatina* (as *L. unguis*), however, contains hemerythrin (KAWAGUTI, 1941), a nonheme, oxygen-carrying Fe-protein that is the rarest of the four respiratory pigments found in the metazoa. Hemerythrin from Japanese *L. anatina* consists of two different subunits, alpha and beta, that are present in equal amounts and have a molecular weight of approximately 12 kDa (SATAKE & others, 1990). In its natural state the molecule has an octameric structure, composed of four alpha helices and four beta helices. In *L. anatina*, both the alpha and beta subunits consist of 117 amino acids, and the primary sequence of both subunits has been deter-

mined (Figure 201; YANO, SATAKE, UENO, KONDO, & TSUGITA, 1991). Preliminary investigations have indicated that hemerythrin is also present in *Discina* and *Disciniscia* (M. CUSACK, personal communication, 1994). Further information on the distribution of respiratory pigments in brachiopods will require systematic biochemical and genetic investigations.

EXCRETION

Excretion is the process whereby waste products of metabolism, particularly nitrogenous waste, are removed from the body. In marine invertebrates, the main excretory product is ammonia. In brachiopods, metabolic end products are probably mainly excreted across the mantle and lophophore epithelia by diffusion. Brachiopods also have a single pair or, in a few exceptional cases, two pairs of metanephridia situated one on either side of the intestine, which may have some excretory function. The basic form of the nephridium is the same in all brachiopods: a funnel-shaped nephrostome opens into the coelomic cavity, then tapers to a nephridiopore, which opens to the mantle cavity.

	1	10	20	30	40
Lingula alpha	VKVPEPFAWN		ESFATSYKNI	DLEHRTLFGN	LFALSEFNTR
Lingula beta	MKIPVPYAWT		PDFKTTYENI	DSEHRTLFGN	LFALSEFNTR
	41	50	60	70	80
Lingula alpha	DQLLACKEVF		VMHFRDEQQG	MEKANYEHFE	EHRGIHEGFL
Lingula beta	HQLNAAIEVF		TLHFHDEQQG	MIRDNYVNTK	EHTDIHNGFM
	81	90	100	110	117
Lingula alpha	EKMGHWKAPV		AQKDIKFGME	WLVNHIPTED	FKYKGL
Lingula beta	DTMRGWQSPV		PQKALKDGME	WLVNHIPTED	FKYKGL

FIG. 201. Sequence data for hemerythrin from the inarticulated brachiopod *Lingula unguis* (YANO, SATAKE, UENO, KONDO, & TSUGITA, 1991). Hemerythrin contains two chains of amino acids designated alpha and beta, each composed of 117 amino acids. Single letters are standard abbreviations for individual amino acids in the sequence. The order of amino acids in the protein is determined by the DNA of the genes responsible for coding this protein (Yano, Satake, Ueno, Kondo, & Tsugita, 1991).

RUDWICK (1970) stated that excretory products were ingested by coelomocytes before being moved by ciliary currents to the nephridia. In the nephridia they are bound in mucus and then passed out of the nephridiopore. This view was probably based on the observations of HELLER (1931; reported in HYMAN, 1959b) of the fate of materials injected into the coelom of *Hemithiris psittacea* and *Terebratulina retusa*. It is likely that the role of the nephridia includes the removal of such foreign material as bacteria as well as infected or damaged brachiopod tissues. In general biologists now consider ejection of such solid products as elimination, along with the ejection of feces or pseudofeces, rather than excretion. The nephridia have a major role as the channel through which the eggs and sperm are discharged in spawning.

Of the nitrogen excreted by the inarticulated brachiopod *Lingula anatina* (as *L. reevii*), 94 percent is in the form of ammonia, the remaining 6 percent being amino acids (LUM & HAMMEN, 1964; HAMMEN, 1968). The other major end products excreted by marine invertebrates include urea, uric acid, amino acids, and purines (REGNAULT, 1987). Urea was not detected as a waste product by LUM and HAMMEN (1964), and other products were not investigated. There have been no further investigations using more reliable methods of analysis (see JAMES & others, 1992 for discussion) nor have the nitrogenous products excreted by articulated brachiopods been ex-

aminated, although they are generally assumed to be predominantly ammonia.

The 6 percent of nitrogen excreted as amino acids by *Lingula anatina* is a low percentage compared with data for molluscs (HAMMEN, 1968; BAYNE, WIDDOWS, & THOMPSON, 1976; BAYNE & NEWELL, 1983) or crustaceans (REGNAULT, 1987). Losses of amino acids may be due to leakage across membrane surfaces along concentration gradients, rather than active excretion. The articulated brachiopod *Calloria inconspicua* is capable of removing glutamic acid and glycine from seawater (DOHERTY, 1981) at rates that vary with animal size and nutritional state, temperature, and the concentration of amino acids in the seawater. The low rate of loss of amino acids by *Lingula*, therefore, probably reflects the ability of membrane pumps in the epithelia of the mantle and lophophore to actively transport amino acids and hence maintain the equilibrium. Tighter junctions between the cell membranes of these epithelia may also be involved. The loss of amino acids to the external medium represents a failure to use them metabolically to build proteins or to gain energy via deamination. The low rates of loss of amino acid by *L. anatina* may indicate that brachiopods are able to efficiently metabolize their nitrogenous energy reserves (JAMES & others, 1992).

Measured exponents in the allometric equations relating rates of ammonia excretion under different conditions to AFDM of *Terebratulina retusa* range from 0.84 to 1.28

TABLE 17. Regression parameters from equations relating rates of $\text{NH}_3\text{-N}$ excretion (E , $\mu\text{g}\cdot\text{atom NH}_3\text{-N/h}$) to ash-free dry mass ($AFDM$, g) for the articulated brachiopods *Terebratulina retusa* and *Liothyrella uva*. Parameters are for the equation $\log_e E = a + b \log_e AFDM$ and were fitted by least squares techniques; n , sample size; r^2 , coefficient of determination; SE , standard error (see also Fig. 202; new).

Species	Temp (°C)	Fed/Starved	Intercept (a)	Slope (b)	SE_b	r^2	n	Authority	Size range mg AFDM
<i>T. retusa</i>	5.6	Starved	-0.99	0.84	0.098	0.68	36	PECK & others (1989)	38–450
	5.8	Fed	-2.40	0.85	0.030	0.45	12	PECK & others (1989)	12–450
	10.7	Fed	0.06	1.28	0.279	0.45	8	PECK & others (1989)	5–520
<i>L. uva</i>	0	Starved	-1.71	0.76	0.042	0.81	78	PECK & others (1986)	0.77–580
	0	Fed	-1.23	0.86	0.040	0.94	45	PECK, CLARKE, & HOLMES (1987b)	1–610

(Table 17; Fig. 202). The differences between exponents are not significant, and the combined data give an exponent of 1.01 (PECK & HOLMES, 1989a). Exponents in this relationship for *Liothyrella uva* are 0.76 in winter conditions and 0.86 in summer conditions. No other comparable data are available for other articulated brachiopods or for inarticulated brachiopods.

Published rates of ammonia excretion by other brachiopods, for which only limited information is available, are compared with those for *T. retusa* in Table 18. If the values are adjusted to take account of temperature differences using a Q_{10} value of 2, the rate for the inarticulated brachiopod *Lingula anatina* is within the range of values for the articulated brachiopod *Terebratulina retusa*, while the results for *Liothyrella uva* were slightly higher than those for *Terebratulina retusa* on the same basis.

Rates of ammonia excretion are strongly dependent on the substrate being respired and the general level of metabolic rate. Excreted ammonia is almost wholly produced from the metabolism of proteins; and, if lipids and carbohydrates are used as the only metabolic energy sources, essentially no nitrogen will be excreted. *Terebratulina retusa* kept in conditions that simulate a winter regime (5.6°C; starved) have 29 percent higher rates of ammonia excretion than in summer conditions (10.7°C; fed). In intermediate conditions (5.8°C; fed) rates were 4.4 times lower than in the winter conditions (PECK & others, 1989). Similar seasonal effects are

seen in the Antarctic brachiopod *Liothyrella uva* where the rate of ammonia excretion is 21 percent higher in summer than in winter conditions (PECK & others, 1986; PECK, CLARKE, & HOLMES, 1987b).

The ratio of gram atoms of oxygen consumed to ammonia nitrogen excreted (O:N ratio) provides information on the importance of proteins that yield excreted nitrogen as fuel for metabolism compared to lipids and carbohydrates that yield no nitrogen. The minimum theoretical value of the O:N ratio should approach 7 when the sole metabolic substrate is protein (CONOVER & CORNER, 1968), although MAYZAUD (1973) showed that the ratio could be as low as 4 under some circumstances. O:N ratios of 20 to 30 are obtained when protein forms around 50 percent of the total metabolic substrates (IKEDA, 1974). Brachiopods generally have low values of O:N ratio (Table 19). In *Liothyrella uva*, protein is the dominant substrate under both winter and summer conditions. Protein levels in tissue also have large seasonal variations compared with very small fluctuations in lipids and carbohydrates (PECK & others, 1986; PECK, CLARKE, & HOLMES, 1987b).

In aquaria, *Terebratulina retusa* has O:N ratios of 16 in simulated summer conditions, 8 in winter conditions, and 42 in intermediate conditions (PECK & others, 1989), indicating that protein, almost solely, fuels metabolic costs in winter conditions and is still the dominant respiratory substrate in summer conditions. In intermediate conditions

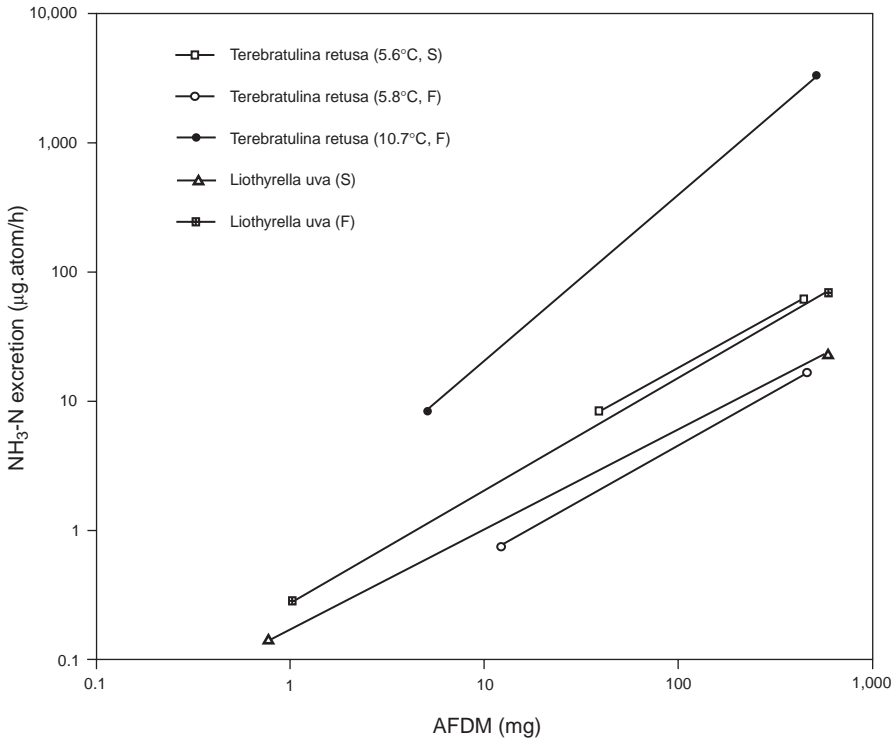


FIG. 202. Relationships between \log_e rate of ammonia excretion ($\text{NH}_3\text{-N}$ $\mu\text{g}/\text{h}$) with \log_e animal ash-free dry mass (AFDM, mg) of articulated brachiopods. Parameters for each regression and the sources of the data are shown in Table 17; F fed; S, starved (new).

Terebratulina retusa uses more lipids and carbohydrates than protein.

The exponents in the scaling relationships between rates of ammonia excretion and tissue weight (Table 17) are not significantly greater than the equivalent exponents for the relationships between rates of oxygen consumption and tissue weight (Table 15), indicating that O:N ratios and hence the proportions of different metabolic substrates used are not size dependent.

One should bear in mind when considering scaling studies of the types discussed above that many of the allometric relationships measured are the end products of evolutionary pressures on many underlying allometries. Metabolic scaling is a case in point, in that the metabolic rate of an organism is the sum of its various requirements for energy in the form of adenosine triphosphate (ATP) at a given time, including, for ex-

ample, the energy needed for muscular activity, fluid circulation, membrane transport, and osmotic balance. All of these have individual allometric relationships with size, and a rigidly mechanistic approach to the interpretation of the scaling of such complex parameters as metabolism may not always be appropriate.

METABOLIC PATHWAYS

The earliest investigations of metabolic pathways of brachiopods began in the late 1950s and were done by a group of workers led by C. S. HAMMEN (for detailed references see JAMES & others, 1992). Their work, motivated by the very long fossil record of the inarticulated brachiopods, involved mainly linguloids and included studies of aerobic, anaerobic, and nitrogen metabolism, all factors thought to be of importance to species living in infaunal habitats. Other published

TABLE 18. Comparison of rates of ammonia (NH₃-N) excretion by inarticulated and articulated brachiopods (adapted from James & others, 1992).

Species	AFDM (mg)	Temp (°C)	Fed/Starved	Rate $\mu\text{g. atom NH}_3\text{-N/day}$	Authority
Inarticulated					
<i>Lingula reevii</i>	3580.0 ^a	22–25.5	Starved	8.31	HAMMEN (1968)
Articulated					
<i>Terebratulina retusa</i>	572.8 ^b	5.6	Starved	5.59	PECK & others (1989)
	572.8 ^b	5.8	Fed	1.35	PECK & others (1989)
	572.8 ^b	10.7	Fed	12.48	PECK & others (1989)
	30.5 ^b	5.6	Starved	0.48	PECK & others (1989)
	30.5 ^b	5.8	Fed	0.11	PECK & others (1989)
	30.5 ^b	10.7	Fed	0.29	PECK & others (1989)
<i>Liothyrella uva</i>	30.5	0	Starved	0.30	PECK & others (1986)
	30.5	0	Fed	0.35	PECK, CLARKE, & HOLMES (1987b)

^amass quoted for *L. reevii* is mean of six individuals; ash-free dry mass (AFDM) calculated based on assumptions of 80% tissue water content and 20% dry tissue ash content.

^btwo sets of values are given for *T. retusa* to allow comparison with both inarticulated brachiopod *L. reevii* and articulated brachiopod *L. uva*.

studies of metabolic pathways include those of SCHEID and AWAPARA (1972), ZWAAN and others (1982), LIVINGSTONE (1983), and a group of papers on intermediary metabolism in the mantle of brachiopods in relation to shell growth and free amino acid utilization (HUGHES, ROSENBERG, & TKACHUCK, 1988; ROSENBERG, HUGHES, & TKACHUCK, 1988; TKACHUCK, ROSENBERG, & HUGHES, 1989).

The initial investigations focused on oxidative metabolism. *Lingula anatina* (as *L. reevii*) was shown to be capable of fixing carbon dioxide (HAMMEN & OSBORNE, 1959). In comparisons of enzyme activities and oxygen consumption rates between *L. anatina* and bivalve molluscs (HAMMEN, HANLON, & LUM, 1962), none of the enzyme activities compared were lower in the brachiopod, some (catalase and arginine deaminase) were within the range of those of the bivalves, and others (urease, carbonic anhydrase, succinic dehydrogenase, and arginase) were higher. HAMMEN, HANLON, and LUM (1962) concluded from these comparisons that there are no enzyme deficiencies in *L. anatina* and that the measured low rates of oxygen consumption for whole animals were due to control mechanisms (but see p. 229).

Studies of enzymes important in aerobic and anaerobic metabolic pathways were continued by HAMMEN and LUM (1966) and HAMMEN (1969). They measured activities of

the enzymes succinate dehydrogenase (SD) and fumarate reductase (FR) and the rates of pyruvate reduction (PR) and lactate oxidation (LD) for the inarticulated brachiopods *Lingula anatina* and *Glottidia pyramidata* and the articulated brachiopod *Terebratulina septentrionalis*; they then calculated the ratios FR:SD and PR:LD (Table 20; Fig. 203).

The ratio FR:SD is a measure of the strength of the reverse reaction rates, that is, reactions that should proceed in opposite directions during aerobiosis and anaerobiosis. It should be low in highly aerobic organisms and high in anaerobic species (SINGER, 1965; HOCHACHKA & SOMERO, 1973, 1984). Values of this ratio of less than 1 are low, while values greater than 4.5 are high in comparison with other marine invertebrates (HAMMEN, 1969). HAMMEN (1969) suggested that the values of 0.43 and 0.37 obtained for the inarticulated brachiopods indicate that they are rarely faced with conditions that require them to use anaerobic pathways but that the articulated brachiopod *Terebratulina septentrionalis* (collected from the intertidal environment) is highly adapted to anaerobic conditions, perhaps associated with the need to stay tightly closed during low tide to avoid desiccation. These results are not totally consistent with expectations based on the different life-styles of these brachiopods, as such infaunal species

TABLE 19. Comparison of oxygen to nitrogen ratios (O:N ratio) for articulated brachiopods; CI, confidence interval; n, sample size (new).

Species	Temp (°C)	Fed/Starved	O:N ratio	95% CI	n	Authority
<i>Liothyrella uva</i>	0.0	Starved	9.3	7.78, 11.01	78	PECK & others (1986)
<i>Liothyrella uva</i>	0.0	Fed	9.2	7.95, 10.70	45	PECK, CLARKE, & HOLMES (1987b)
<i>Terebratulina retusa</i>	10.7	Fed	16.3	9.1, 29.2	27	PECK & others (1989)
<i>Terebratulina retusa</i>	5.6	Starved	8.0	6.7, 9.7	39	PECK & others (1989)
<i>Terebratulina retusa</i>	5.8	Fed	42.4	23.9, 75.2	12	PECK & others (1989)

as *Lingula anatina* live in habitats where they would be expected to experience anaerobic conditions at regular intervals.

HAMMEN (1969) suggested that the PR:LD ratio could be used as an indication of whether a species is likely to produce the end products of glycolysis in the form of lactate, with a high ratio indicating that the end product was mainly lactate. He postulated that sedentary species would have low ratios and that the ratio would increase in proportion with the scope of the species for muscular activity. The values of 0.68 to 1.76 found for the brachiopods are among the lowest of any marine invertebrates. The articulated brachiopod *Laqueus californianus* has similarly low rates of pyruvate reduction (SCHEID & AWAPARA, 1972), but lactate oxidation in this species was too low to be detectable, so it was not possible to calculate a PR:LD ratio.

Brachiopods possess alternative anaerobic pathways as indicated by the presence of lactate, octopine, alanopine, and taurine dehydrogenases (LDH, ODH, ADH, and TDH) in brachiopod species (ZWAAN & others, 1982; LIVINGSTONE, 1983; DOUMEN &

ELLINGTON, 1987). A likely early primitive function of these opine pathways was to provide energy for burrowing (LIVINGSTONE, 1983); but other functions of the pathways have evolved, such as survival during or recovery from anoxia.

HAMMEN (1971, 1977) studied substrate specificity of lactate dehydrogenase in the inarticulated brachiopod *Glottidia pyramidata* and the articulated brachiopods *Notosaria nigricans*, *Calloria inconspicua*, and *Terebratulina septentrionalis*. With the exception of *T. septentrionalis*, all the brachiopods used only L-lactate; *T. septentrionalis* used L- and D-lactate at approximately equal rates. HAMMEN (1977) used the spread of the above data to suggest that brachiopods had a closer phylogenetic relationship to the deuterostomes (echinoderms and chordates) than to the other branch of the animal kingdom. This type of affinity study is now being done by analysis and sequencing of proteins and DNA, where the data are more robust and the conclusions drawn more specific.

In comparisons between the activities of enzymes involved in nitrogen metabolism in the inarticulated brachiopod *Lingula anatina*

TABLE 20. Enzyme activities and ratios of activities for inarticulated and articulated brachiopods; FR, fumarate reductase; LD, lactate dehydrogenase; PR, pyruvate reductase; SD, succinate dehydrogenase (adapted from Hammen, 1969).

Species	PR	LD	Enzyme activities (μ moles/min/g tissue wet mass)		SD	FR/SD
			PR/LD	FR		
Inarticulated						
<i>Lingula reeuii</i>	0.311	0.240	1.30	0.087	0.203	0.43
<i>Glottidia pyramidata</i>	0.494	0.280	1.76	0.053	0.142	0.37
Articulated						
<i>Terebratulina septentrionalis</i>	0.098	0.144	0.68	0.067	0.010	6.80

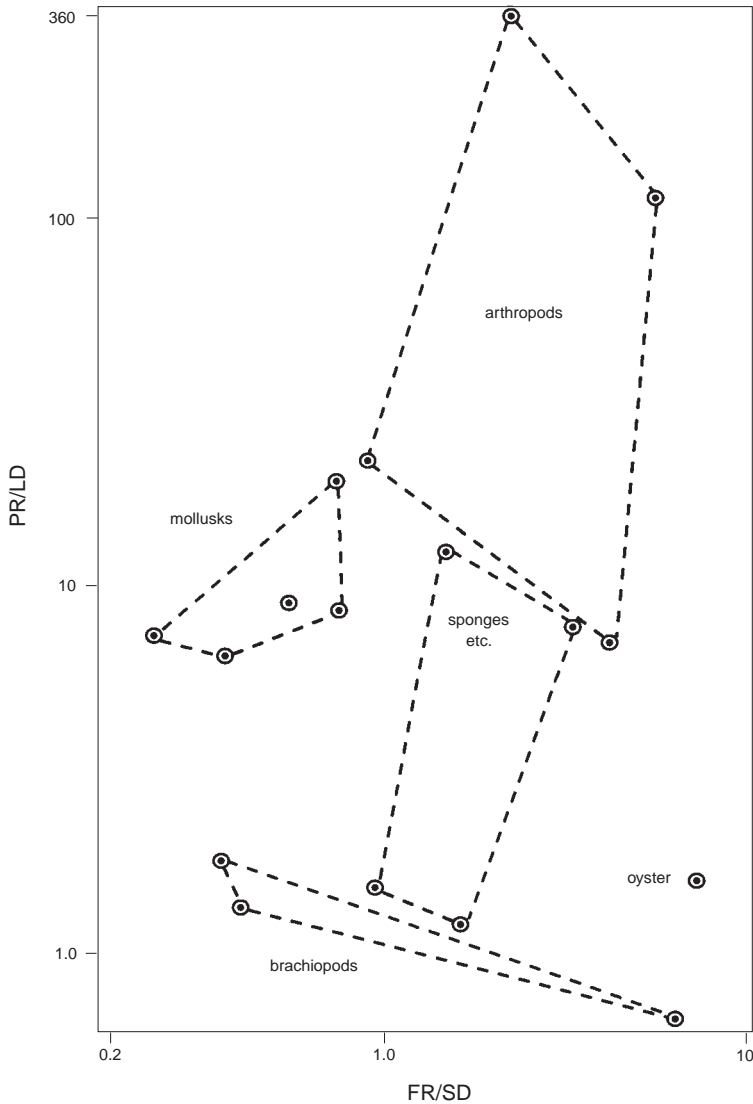


FIG. 203. Relationships between the ratios of rates of fumarate reductase (*FR*) to succinate dehydrogenase (*SD*) activity and the rates of pyruvate reduction (*PR*) to lactate oxidation (*LD*) for brachiopods compared to those of other groups of marine invertebrates (Hammen, 1971).

and those of several bivalve mollusks, aminotransferase activities were found to be lowest in the brachiopod (LUM & HAMMEN, 1964; HAMMEN, 1968).

None of these studies of enzyme activities provides data on the relationship between enzyme activities and dry tissue weight. Expressing results of such metabolic studies on a mass specific basis, for example, the

amount of activity per unit mass of tissue does not standardize the measured rates among larger or smaller individuals because metabolic rate rarely scales to body mass with an exponent of 1 (KLEIBER, 1947, 1965; HEMMINGSEN, 1960; SCHMIDT-NIELSEN, 1984; PANDIAN & VERNBERG, 1987). The mean value of 0.78 for the exponent in the relationship between rate of oxygen

consumption and body mass for brachiopods (see p. 229–230) implies that a doubling of body mass will be accompanied by only a 1.70 times increase in metabolic rate. Hence, a doubling of body mass might be expected to be accompanied by a 15 percent fall in enzyme activities expressed on a mass-specific basis. These problems should not, however, affect the ratios of activities discussed above, as these should be more independent of body size.

Isolated portions of mantle tissue from *Terebratalia transversa* were found to be capable of metabolizing 11 of 19 amino acids investigated by measurement of the evolution of carbon dioxide from radioactively labelled amino acids (TKACHUCK, ROSENBERG, & HUGHES, 1989). The most metabolically active amino acid was aspartate, which accounted for 52 percent of the total of 38 $\mu\text{mol/g/h}$ of carbon dioxide evolved. In comparison, in the bivalve *Chlamys hastata*, valine was the most metabolically active amino acid, accounting for 29 percent of the 138 $\mu\text{mol/g/h}$ of carbon dioxide produced.

The metabolic rate of mantle tissue, as assessed by measurement of the rates of use of ^{14}C -labelled carbohydrates, is low in *Terebratalia transversa* (HUGHES, ROSENBERG, & TKACHUCK, 1988; ROSENBERG, HUGHES, & TKACHUCK, 1988). The metabolic rate is 3.7 times greater in the leading marginal edge than in the midportion of the mantle. This compares with a ratio of 1.8:1 in the mantle of the bivalve *Chlamys hastata*. Lengthy periods of anoxia result in a decrease in glucose metabolism in *T. transversa*, and, since the decrease is larger in the leading marginal edge than elsewhere, this results in a fall in the ratio of metabolic rates between sites to 1:1. Organic acids could not be detected in the tissues during these periods of exposure to anoxia (ROSENBERG, HUGHES, & TKACHUCK, 1988), probably because of the very low metabolic rates and not an absence of these end products of anaerobic metabolism. HUGHES, ROSENBERG, and TKACHUCK (1988) thought that periods of alternating aerobic and anaerobic metabolism in mantle tissues might result in cycles of deposition and re-

sorption of calcium carbonate in the shell, with the carbonate being used to buffer the acids produced during anaerobiosis. The same hypothesis was proposed by LUTZ and RHOADS (1977) to explain growth bands in the shells of bivalve molluscs.

More recently, ROSENBERG and HUGHES (1991) have consolidated their earlier work and extended the theory of shell growth and composition being controlled by mantle metabolic rates. This theory contrasts with the generally accepted model that the orientation of the marginal mantle along the commissure is the determinant of shell growth and form (HUXLEY, 1932; WILLIAMS, 1966, 1968a). Part of the mantle-metabolism theory suggests that shell curvature is dictated by the size of the gradient in metabolic rate from the anterior leading edge of the mantle to areas away from the shell edge. Higher shell curvature is thought to be produced by larger gradients in mantle metabolic rate. ROSENBERG, HUGHES, and TKACHUCK (1988) claimed that the deposition of shell material away from the leading edge lends support to their hypothesis. They also concluded that calcium-rich areas of shell were energetically less costly to produce than matrix-rich areas or parts of the shell that are rich in minor elements, which supports the general hypothesis for costs of calcium-carbonate shell production formalized by PALMER (1981, 1983). ROSENBERG and HUGHES (1991) suggested that this was of great significance for paleobiological studies, which could potentially gain much from information on variations in skeletal composition within and between populations of brachiopods and through ontogeny.

ENERGY PARTITIONING

Brachiopods have long been characterized as having low levels of activity. SHIPLEY and MACBRIDE (1920, p. 374) described “the fixed Brachiopod, whose strength is to sit still and sweep little particles of food towards its mouth . . .” This, with the observation that there was relatively little tissue between the shell valves of articulated brachiopods (HYMAN, 1959b; RUDWICK, 1970), com-

bined to produce the impression that brachiopods had low energy requirements compared with many other marine invertebrates.

Many of the more recent studies of aspects of brachiopod physiology have provided results that strengthen this concept. Ratios of enzyme activities indicative of low levels of muscular activity (HAMMEN, 1969), the long period needed for the diductor muscle to reach tetanus (WILKENS, 1978b), the ability of some articulated brachiopods to facilitate water movement through the mantle cavity by orienting to ambient seawater currents (LABARBERA, 1978), the observation that water flow through the mantle cavity is laminar and speeds of water movement low (LABARBERA, 1981), the low rates of oxygen consumption (SHUMWAY, 1982; PECK, MORRIS, & CLARKE, 1986a; PECK & others, 1986, 1989; THAYER, 1986b; PECK, CLARKE, & HOLMES, 1987b; CURRY & others, 1989) and heartbeat (BUCHAN, PECK, & TUBLITZ, 1988), and the relatively reduced feeding abilities (RHODES & THOMPSON, 1992) have all been proposed to be energy-saving adaptations or indicative that brachiopods have low energy requirements. More recently the concept of an overall, low-energy life-style for brachiopods has been developed (CURRY & others, 1989; PECK & others, 1989; THAYER & ALLMON, 1990). The available evidence for and implications of such a strategy were discussed in detail by JAMES and others (1992). Advantages include an enhanced ability to survive in areas where food supplies are low or highly seasonal, since low metabolic rates require smaller reserves for maintenance through periods of food limitation.

A full assessment of an organism's energy strategy requires quantitative data that can be used to compile a full budget of acquisition and subsequent partitioning of acquired energy between different activities. This is expressed in the energy budget equation:

$$C = F + P_g + P_r + R + U + M$$

where C is food consumed, F is feces produced, P_g is somatic production, P_r is reproductive production, R is respiratory costs, U is excretory losses, and M is mucus produced, all expressed in energy units

(BRANCH, 1981; modified from WINBERG, 1956 and RICKER, 1971). The mucus term is often ignored in energetic studies but may be very important, for example, where mucus is used extensively in particle rejection mechanisms, as it is in brachiopods living in turbid areas (RHODES & THAYER, 1991).

Equivalent budgets may also be assessed in terms of biomass, organic carbon, or nitrogen. How closely such budgets balance is not merely an indication of how well the individual parameters have been measured; there can be short-term imbalances in the equation, where seasonal effects are important or individuals are unusually active. Full assessments must therefore take into account longer-term balances between periods of net gain and periods of net loss, in which storage tissues may be implicated.

There are no species of brachiopod for which all the necessary data to compile an energy budget have been collected, and for some of the necessary parameters, such as energy lost in feces and mucous production, there are no published data at all. Data on mucous production are likely to be of less importance to the production of a general energy budget for brachiopods, as mucus appears to be produced only under specific conditions of high turbidity. Measurement of fecal losses, on the other hand, are crucially necessary for the estimation of the amount of energy actually absorbed and hence available to fuel other physiological functions.

On the consumption side of the budget, information on filtration and clearance rates for *Neothyris lenticularis* (RHODES, 1990; JAMES & others, 1992; RHODES & THOMPSON, 1992) may be used to calculate food consumption rates with different concentrations of algal cells in the water. For example, *N. lenticularis* of 200 mg AFDM has a clearance rate of 690 cm³/h, which converts to a food-consumption rate of around 1,000 algal cells/sec. When feeding on the alga *Dunaliella primolecta*, which has an organic content of 95 pg AFDM per cell, of which 19 percent is lipid (I. LAING, personal communication, 1993), this represents 3.6 mg

AFDM of algae/h, or 79 J/h (1.9 kJ/day) using appropriate energy conversion factors (SCHMIDT-NIELSEN, 1979).

Problems remain, however, in interpreting such data in energetic assessments, as articulated brachiopods cease feeding when the blind-ending gut is full. Useful estimates of consumption therefore require assessments of the proportion of time spent in feeding. Similar needs for estimates of the time spent in other activities affect other components of the budget, but no data on which to base such estimates of activity time budgets are available for brachiopods.

Assessments of growth rates for *Terebratulina retusa* in natural populations (COLLINS, 1991) provide an estimate of somatic production (P_g). Between the ages of one and six years (approximately 2 mm to 17 mm in length), *T. retusa* grow at a rate of 2.5 mm per year. This converts to a growth rate of 48 mg AFDM per year for a 10 mm length brachiopod (65 mg total body AFDM) using data relating AFDM to shell length (CURRY & ANSELL, 1986). This is equivalent to 0.26 mg AFDM day, assuming a growing season of six months or 0.18 mg AFDM/day, with a nine-month growing season, which converts to 2.2 and 3.2 J/day using a conversion factor from AFDM to energy content of 12.2 kJ/g AFDM (PECK, 1993).

Similar calculations are possible for the energy requirements of reproductive growth (P_r). The difference in AFDM between empty and full gonads of large adult (45 mm

in length) *Liothyrella uva* is some 50 mg (PECK & HOLMES, 1989b). Build up of gonads occurs over a three-month period, indicating an increase of about 0.5 mg AFDM per day, or 70 J/day, using a conversion factor of 2.66 kJ/g AFDM for gonad tissues (L. S. PECK, unpublished data, 1992).

More extensive and better data are available on respiratory costs (R). Oxygen-consumption rates calculated for an individual of 50 mg AFDM from the data summarized in Table 15 range from 1.9 to 29.7 $\mu\text{l/h}$ (Table 16). Using an appropriate oxycaloric coefficient (18.8 kJ/l oxygen) based on the assumption that protein is a major respiratory substrate (see p. 235) provides an estimate of respiratory costs ranging from 0.9 to 13.4 J/day.

Estimates of excretory losses (U) based on nitrogen excreted as ammonia (Table 17–18) range from 0.11 to 12.48 $\mu\text{mol/day}$, equivalent to 3.2×10^{-5} to 3.6×10^{-3} J/day using a conversion factor of 288 J/mol ammonia (BRAFIELD & SOLOMON, 1972).

Clearly all these calculations have large errors associated with them, and to carry this exercise to the stage of comparing the relative effort or the levels of resource allocation to various components of the energy budget would not be appropriate. Before it will be possible to assess accurately the energy strategies of brachiopods and to identify which components of their energy budgets may be constrained to low levels, much more quantitative data suitable for incorporation into the calculation of energy budgets is needed.

SHELL BIOCHEMISTRY

MAGGIE CUSACK¹, DEREK WALTON², and GORDON B. CURRY¹

[¹University of Glasgow; ²University of Derby, U.K.]

INTRODUCTION

GENERAL

The paired valves of the brachiopod shell are among the earliest examples of biomineralization. As with all biominerals, brachiopod valves contain organic molecules as well as the obvious inorganic components since organic material is essential for the formation of biominerals. Therefore, it is important to examine both the organic and the inorganic components of brachiopod shells with a view to understanding the formation of the valves. As well as playing an active role in the process of biomineralization, organic molecules are also potentially informative to those interested in the evolution of the brachiopods and the phylogenetic relationships between taxa. The mineral components of brachiopod valves were comprehensively identified in the 1965 *Treatise on Invertebrate Paleontology* (MOORE, 1965). Since that time, more information has become available regarding the components and the structure of the inorganic phase (see the following section of this chapter, below, and the chapter on shell structure, p. 367–320). Regarding the organic components, a wealth of information has been added to that discussed in the 1965 *Treatise*.

In brief, the valves of articulated brachiopods are composed of calcium carbonate in the form of low-magnesium calcite (JOPE, 1965) with proteins (in some instances, carotenoproteins), lipids, and carbohydrates. Inarticulated brachiopods possess valves of a carbonate fluorapatite at least crystallographically similar to francolite (WATABE & PAN, 1984) in association with proteins, chitin, glycosaminoglycans, and, for *Lingula*, collagen (WILLIAMS, CUSACK, & MACKAY, 1994). Brachiopods with phosphatic valves contain high levels of organic material, while those with carbonate valves contain much

lower levels (Table 21). The pioneering work on the analysis of proteins and amino acids of brachiopod valves was done by JOPE, who demonstrated the taxonomic value of molecular information from brachiopod shell material (JOPE, 1965, 1967a, 1967b, 1969a, 1969b, 1973, 1977, 1979, 1980, 1986).

INORGANIC COMPONENTS OF BRACHIOPOD VALVES

The division of brachiopods into articulated and inarticulated kinds is based on shell morphology and generally coincides with the nature of the inorganic component of the valves. The articulated species possess carbonate valves of stable, low-magnesium calcite (JOPE, 1965), while the inarticulated brachiopods possess phosphatic valves in the form of apatite (McCONNELL, 1963). The exceptions to this pattern are the craniids, which, although lacking shell articulation, have carbonate shells. There is debate about whether the craniids should be classified on the basis of shell mineralogy (BASSETT & others, 1993; POPOV & others, 1993) or absence of articulation (CARLSON, 1993a).

Calcium carbonate comprises 94.6 to 98.6 percent of the inorganic material of articulated brachiopod valves and 87.8 to 88.6 percent of the craniids (JOPE, 1971). Magnesium, as a carbonate, comprises 0.4 to 1.4 percent of the articulated shells and 8.6 percent of craniid valves. Sodium is present in small amounts, and manganese and copper occur in trace amounts in *Terebratulina retusa*.

The unusual occurrence of phosphate in an exoskeleton has prompted several studies of the inorganic components of inarticulated brachiopod valves. Calcium phosphate comprises 74.7 to 93.7 percent of the inorganic component of lingulid valves and 75.2 percent in *Discinisca* (JOPE, 1971). Magnesium

TABLE 21. Quantity of organic material in brachiopod valves (new; data from Curry & Ansell, 1986; Curry & others, 1989).

Genus	mg/g	% organic by weight
<i>Calloria</i>	23.65	2.3
<i>Dallina</i>	10.00	1.0
<i>Gryphus</i>	4.76	0.5
<i>Macandrawia</i>	8.13	0.8
<i>Neocrania</i>	44.77	4.5
<i>Notosaria</i>	46.60	4.6
<i>Terebratulina</i>	30.19	3.0
<i>Lingula</i>	295.73	29.6

also occurs as 0.6 to 3 percent of the inorganic components of the lingulid valves and 6.7 percent in *Discinisca*. The apatite of inarticulated brachiopod valves was described as the carbonate fluorapatite francolite (McCONNELL, 1963; IWATA, 1981). Since those reports, the mineral of the valves of *Lingula* and *Glottidia* has been described as a carbonate containing fluorapatite similar to francolite with no other mineral phase present, i.e., no separate carbonate phase (WATABE & PAN, 1984; LEGEROS & others, 1985). Carbonate integration is analogous with other biological apatites (LEGEROS & others, 1985). The apatite of *Glottidia* and *Lingula* differs principally in the carbonate content. WATABE and PAN (1984) reported carbonate levels of 2.2 wt percent in *Lingula* and 3.6 wt percent in *Glottidia* while LEGEROS and others (1985) reported slightly lower levels for *Lingula* (1.8 wt percent). The higher carbonate level in *Glottidia* accounts for the lower crystallinity (LEGEROS & others, 1985). Integral fluorine increases crystallinity and stability of apatites, but for both *Lingula* and *Glottidia*, fluorine levels are equal. Fluorine accounts for 1.64 wt percent of whole *Glottidia* valves and about 2.58 wt percent of calcified layers (WATABE & PAN, 1984). Calcium and fluorine are localized in mineralized layers in *Lingula* and *Glottidia* valves at a constant F:Ca ratio of 0.033 ± 0.002 . In 1991, IJIMA (IJIMA, KAMEMIZU, & others, 1991) confirmed the carbonate apatite nature of the valves of *Lingula anatina* and *Lingula shantoungensis* and reported the

presence of chlorine as well as fluorine. IJIMA and others (1991) used pyrolysis to characterize the apatite of the two species of *Lingula* and demonstrated that the structural water of *Lingula* apatite is loosely bound such that it is lost at lower temperatures than that in tooth enamel. The c-axis of apatite and the fiber axis of β -chitin are parallel and coincident with the growth direction of the *Lingula* shell (IJIMA & MORIWAKI, 1990; IJIMA, MORIWAKI, & KUBOKI, 1991).

PAN and WATABE (1988a) examined the uptake and transportation of calcium and phosphorus in *Glottidia pyramidata*. Calcium ions are taken up from seawater primarily by the lophophore, move through the coelomic fluid, are concentrated in the mantle, and are eventually deposited in the inner shell layer. Calcium is deposited in the shell at a rate of 12×10^{-2} μg per mg of shell weight per hour. This rate is similar to that for the bivalve *Argopecten*. Calcium uptake and deposition in *Glottidia* occurs three hundred times faster than phosphorus uptake, indicating that phosphorus is unlikely to be obtained directly from seawater and more likely to be obtained indirectly from food (PAN & WATABE, 1988a).

ORGANIC COMPONENTS OF BRACHIOPOD VALVES

A consistently high proportion of total organic mass is contained in brachiopod valves (CURRY & others, 1989). On average, 40 to 50 percent of the total organic mass of both articulated and inarticulated brachiopods is in the shell (CURRY & ANSELL, 1986; CURRY & others, 1989). Such a high percentage has implications for the predation of brachiopods, because the nutrient yield to predators varies significantly depending on whether the shell is crushed and ingested or only body tissues are consumed (CURRY & ANSELL, 1986; CURRY & others, 1989; PECK, 1993). The proportion of tissue present in the shell varies seasonally in *Liothyrella uva* from the Antarctic. This variation, from 36.3 percent in winter to 46.0 percent in summer, may result from the seasonal availability of

nutrients in the Antarctic (CURRY & others, 1989). Comparable data for other brachiopods are not available, but it is reasonable to assume that the percentage of total tissue mass in the shells of other taxa will also vary seasonally in response to variations in the availability of nutrients.

The organic molecules isolated from brachiopod valves and discussed in this chapter are proteins, carotenoproteins, amino acids, lipids, carbohydrates, chitin, and glycosaminoglycans (GAGs). Proteins and nucleic acids (DNA and RNA) are the most information rich of the biopolymers. To date, there have been no reports of nucleic acids within brachiopod valves although the isolation of DNA from a range of biominerals in other phyla, both recent and fossil, suggests that brachiopod valves will also contain DNA. Analysis of any possible DNA from brachiopod valves depends on knowledge of the brachiopod genome (see section on the brachiopod genome for information, p. 189–211). Proteins are built up of long chains of amino acids, and the order of amino acids in the polypeptide chain (the primary sequence) is of great value in phylogenetic studies. Information on brachiopod shell proteins will follow in the section on proteins, and the section on amino acids in brachiopod valves discusses the use of amino acid composition *per se* as a taxonomic indicator.

INTRACRYSTALLINE ORGANIC MOLECULES

In calcitic articulated brachiopods, organic molecules are located both within the calcitic fibers (intracrystalline) and between the fibers (intercrystalline). The entombment of organic material within the secondary layer calcitic fibers protects it from contamination and even degradation. Since the calcitic fibers are essentially closed systems, any degradation occurs *in situ*, and the residues can be employed in taxonomic analyses. Thus, organic material trapped within single crystals during biomineralization offers the best hope for the study of ancient fossil mol-

ecules (TOWE, 1980; COLLINS, MUYZER, CURRY, & others, 1991; CURRY, CUSACK, WALTON, & others, 1991). COLLINS (COLLINS, MUYZER, CURRY, & others, 1991) estimated that intracrystalline organic material accounts for 0.03 percent of the weight of the articulated brachiopod valve. The phosphatic valves of inarticulated brachiopods do not contain structures analogous to the calcitic fibers of the articulated brachiopods. Although the methods for the extraction of organic molecules from inarticulated brachiopod valves are not as well established as those for the articulated valves, the same principles apply in that the organic material associated most intimately with the mineral should be the most reliable source of indigenous material and the most likely source of preserved material in fossil samples.

AMINO ACIDS IN BRACHIOPOD VALVES

GENERAL

Amino acids are ubiquitous, both as the monomeric units of proteins and in the free (uncombined) state. The use of such molecules in paleontological analysis must recognize this ubiquity to ensure that the amino acid record obtained for a sample represents the actual composition, as opposed to any diagenetic or environmental overprint. While the primary sequence of a protein provides a high level of taxonomic and evolutionary information, the amino acid composition alone may also reflect the taxonomy of the organism (CORNISH-BOWDEN, 1983). Amino acid analysis requires much smaller amounts of shell material than protein sequencing; 10 mg is sufficient for several analyses. Such information, while not as powerful as the primary sequence, is easier to gain and is particularly important in the fossil record, where the peptide bonds that bind the amino acids are largely degraded.

Shell proteins and their associated amino acids have been studied by JOPE in continuation of her research for the first edition of the *Treatise* (JOPE, 1967a, 1967b, 1969b,

1973, 1979). This work examined both intra- and intercrystalline amino acids and has remained the primary source for data on amino acids of brachiopod shells. Since 1988, the focus of research has changed toward intracrystalline proteins. There are broad similarities between the nature of the inter- and intracrystalline fractions, although they differ in their composition, possibly indicating a difference in the function of the proteins.

Most of the common protein-forming amino acids are found within brachiopod valves, although in this discussion, tryptophan, methionine, and cysteine are not considered due to their variable destruction during the hydrolysis procedure (e.g., HEINRIKSON & MEREDITH, 1984). Histidine was not quantified from intracrystalline sites.

INARTICULATED BRACHIOPODS

Intercrystalline Amino Acids of Recent Brachiopods

Inarticulated brachiopods (e.g., of *Lingula* sp.) contain quantitatively more amino acid (25 percent of shell weight; JOPE, 1967a) within their shell (in the form of protein) than articulated brachiopods (0.5 percent of shell weight; JOPE, 1967a). The group is represented by shells of *Neocrania anomala* (MÜLLER), *Discina striata* (SCHUMACHER), *Lingula anatina* (LAMARCK), and *Lingula* sp., which generally contain lower relative concentrations of glycine (e.g., *L. anatina*, 15 percent; *Laqueus californicus*, 20 percent) and higher concentrations of alanine (up to four times; e.g., *L. anatina*, 20 percent; *Laqueus californicus*, 5 percent) than articulated shells (JOPE, 1967a; KOLESNIKOV & PROSOROVSKAYA, 1986). Hydroxyproline, probably indicating the presence of collagen, has been detected in the organophosphatic *L. anatina* (approximately 6 percent) and *D. striata* (approximately 14 percent; JOPE, 1967a; KOLESNIKOV & PROSOROVSKAYA, 1986). It has not been detected in any carbonate-shelled species, including the craniides. Hydroxyproline represents one-third of the amino acid

residues present in collagen. Estimation of the abundance of hydroxyproline will therefore give an indication of the amount of collagen present within the shell.

The anomalous taxonomic position of the craniides is reinforced through amino acid taxonomy (JOPE, 1967a). The shells of this group have relatively high glycine and low alanine, indicating similarity with the articulated brachiopods, but they also contain the amino sugar glucosamine, indicating allegiance with other inarticulated species. The craniid shell has characteristically high aspartic acid and serine, in contrast with all the other brachiopods, confirming the anomalous position of the group.

Paracrystalline Amino Acids of Recent Brachiopods

Organic material is extracted for paracrystalline material as it is for intracrystalline material of articulated brachiopods (CUSACK & others, 1992). The term paracrystalline or mineral-associated material is more accurate for inarticulated brachiopods since they lack the protein-containing mineral fibers of the articulated brachiopods. In *Discinisca tenuis* the most abundant peptide-bound paracrystalline amino acids are glycine, alanine, aspartic acid, and glutamic acid, all at about 13 percent. In *Glottidia pyramidata*, aspartic acid is the most abundant amino acid at 15 percent, followed by glycine at 14 percent, and arginine at 11 percent.

Intercrystalline Amino Acids of Fossil Brachiopods

JOPE (1969b) published the only study of the amino acid composition of fossil inarticulated brachiopods, studying *Petrocrania scabiosa* (HALL), *Orbiculoidea forbesi* (DAVIDSON), and *Lingula* sp. Amino acids recovered from the proteinaceous compounds remaining after demineralization differed proportionally from those of the nearest living relatives. Comparisons cannot be directly made, as figures are given as relative rather than actual abundance. Any de-

composition of amino acids over time will alter the relative abundance of the molecules and therefore minimize the level of the signal recovered.

Paracrystalline Amino Acids of Fossil Brachiopods

There is no published information on the amino acid composition of this fraction from fossil inarticulated species.

ARTICULATED BRACHIOPODS

Intercrystalline Amino Acids of Recent Brachiopods

Examination of the intercrystalline fraction has proceeded with amino acid taxonomy in mind, concentrating on the proteins recovered after demineralization in the form of the intercrystalline protein web. Articulated brachiopods are represented by *Neothyris* sp., *Laqueus californicus* (KOCH), *Terebratella* sp., *Terebratalia transversa* (SOWERBY), *Macandrevia cranium* (MÜLLER), *Terebratulina* sp., *Hemithiris psittacea* (GMELIN), and *Notosaria nigricans* (SOWERBY) (JOPE, 1967a); and *Neothyris lenticularis* (DESHAYES), *Terebratulina* sp., and *Hemithiris psittacea* (GMELIN) (KOLESNIKOV & PROSOVSKAYA, 1986).

Glycine (up to 40 percent) is the most abundant of the amino acids present in the intercrystalline fraction, followed by alanine (up to 14 percent). The acidic amino acids, aspartic and glutamic acid, which are abundant within the shells of molluscs (WEINER, 1983), are of generally low relative abundance in brachiopods (up to 12 percent and 8 percent respectively), possibly indicating a difference in function of the proteins from the two phyla. No hydroxyproline was detected, indicating that no collagen is present.

Taxonomy based on amino acid composition within articulated shells shows an ordinal level of separation, with the Terebratulida having lower acidic to basic ratios than the Rhynchonellida (1.3 to 1.9 as opposed to 2.3 to 2.5; JOPE, 1967a). Familial separation may also be possible through differences in the

relative abundance of amino acids (e.g., higher alanine in the Terebratellidae), although there are as yet insufficient analyses to test the separation of groups below this level. Initial conclusions tend to reinforce the morphological classification of these groups, although much further work will be required before a full assessment of the usefulness of this technique in taxonomy is possible.

Intracrystalline Amino Acids of Recent Brachiopods

Recent brachiopod shells contain appreciable amounts of intracrystalline amino acid, ranging between 70 and 800 ng/mg, most (generally >90 percent) of which is contained within proteins while the organism is living. Detailed analyses of the abundance of intracrystalline amino acids are available only for a limited but increasing number of samples of the orders Rhynchonellida and Terebratulida (CURRY, CUSACK, ENDO, & others, 1991; CURRY, CUSACK, WALTON, & others, 1991; AL-RIKABI, 1992; WALTON, CUSACK, & CURRY, 1993), outlined below.

The intracrystalline amino acid compositions so far reported account for between 30 and 40 percent of the total amino acid present throughout the shell, excluding body tissue, and comprise 0.007 to 0.08 percent of the total mass of the shell. The absolute and relative abundance of intracrystalline amino acids varies taxonomically, reflecting variation in the number of types or sizes of the proteins present within the shell (WALTON, CUSACK, & CURRY, 1993).

Rhynchonellide brachiopods are represented by *Notosaria nigricans* (SOWERBY) and contain the highest concentrations of intracrystalline amino acid so far recorded. These shells are especially rich in the acidic molecule aspartic acid (214.52 mg/g; 36.94 mol percent) and in glycine (218.20 mg/g; 37.57 mol percent). Rhynchonellides also have a somewhat different organic matrix, and shell biomolecules are more resistant to the effects of oxidation by sodium hypochlorite. This may be related to the hard and soft

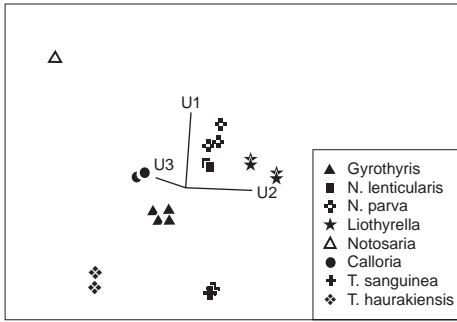


FIG. 204. Graph of the first three principal components of the relative proportion data for amino acids from recent brachiopods (complete organic extract). Note close groupings of the related species (e.g., members of the *Neothyris* genus) and the distance of more distantly related species (e.g., *Notosaria*) (new).

protein layers discussed by JOPE (1967a) for intercrystalline molecules.

Terebratulide brachiopods (represented by *Neothyris lenticularis* (DESHAYES), *Neothyris parva* (COOPER), *Calloria inconspicua* (SOWERBY), *Terebratella sanguinea* (LEACH), *Terebratella haurakiensis* (ALLAN), *Liothyrella neozelanica* (THOMSON), and *Gyrothyris mawsoni* (THOMSON) are all generally characterized by high concentrations of glycine (up to 55 percent), proline (up to 9 percent), and alanine (up to 8 percent). High concentrations of glycine and proline may reflect the conformation of the included protein; such amino acids are common in tightly folded proteins.

The information derived from the amino acids for taxonomic purposes is difficult to assimilate objectively from the raw data alone: the information is contained within up to 17 variables. Several investigations have used factor and principal component analysis (PCA) to differentiate between species (DEGENS, SPENCER, & PARKER, 1967; KING & HARE, 1972; HAUGEN, SEJRUP, & VOGT, 1989), although as yet this has only once been applied to brachiopods (Fig. 204; WALTON, CUSACK, & CURRY, 1993). Scatter plots and three-axis plots allow the variation summarized in the principal components to be observed directly. Brachiopods that are closely related should have fewer differences in the abundance of amino acids and there-

fore should have less variation. This may be observed in Figure 204, where rhychnonellide brachiopods plot at a distance from terebratulides. Within the terebratulide genus *Neothyris*, two species investigated plot closely together. This contrasts with the situation in *Terebratella* where two species studied are widely separated on the basis of their amino acid compositions. Further research is necessary to explore the taxonomic value of such results.

Intercrystalline Amino Acids of Fossil Brachiopods

Amino acids have been extracted from intercrystalline sites in brachiopod shells as old as Silurian and have been compared with those in recent brachiopods from similar sites in a number of studies (JOPE, 1977, 1980; KOLESNIKOV & PROSOROVSKAYA, 1986). Comparisons of the amino acid composition allowed some phylogenetic interpretation (to the class level), which generally confirm the morphological discrimination. Amino acid compositions from fossil articulated brachiopods show marked differences from their nearest living relatives, probably resulting from the diagenetic alteration of the proteins, although this has not been quantified.

Articulated brachiopods are represented by *Camarotechia* sp., *Epithyris oxonica* (ARKELL), *Globirhynchia suboboleta* (DAVIDSON), *Loboiodothyris kakardinensis* (MOISSEEV), and *Gusarella gusarensis* (MOISSEEV). All samples released amino acids only on hydrolysis, indicating the presence of acid labile bonds. In all instances the soluble proteins analyzed for recent shells had been lost through the action of migrating fluids, and thus two different sets of proteins have been sampled, probably accounting for the marked differences in the amino acid compositions of the two fractions. In addition, all free amino acids (those formed through the degradation of peptide bonds) have been lost. Intercrystalline amino acids from fossil samples appear not to contain much phylogenetic information.

The composition of each of the five samples is markedly different from that of their nearest recent relatives. Of particular note in the work of both JOPE (1967b) and KOLESNIKOV and PROSOROVSKAYA (1986) are the raised levels of serine and glutamic acid in the fossil samples, which contrast strongly with the data from the intracrystalline sites (see below). Serine is a common, natural contaminant, and thus the raised levels of this amino acid might indicate some contamination of the sample from extraneous sources (e.g., ORÓ & SKEWES, 1965; WALTON & CURRY, 1991). Intercrystalline amino acids from fossil samples appear not to contain significant amounts of phylogenetic information.

Intracrystalline Amino Acids of Fossil Shells

Amino acids and paleoproteins have been sampled from several genera of brachiopods ranging in age from 0.12 to 2.6 Ma (WALTON, 1992). Compared to those of recent samples, both the relative and absolute abundances of the molecules are altered, sometimes dramatically. Although such differences in amino acid composition could be due to either genetic or diagenetic change, the most notable effect is likely to be the degradation during diagenesis of the structure of the proteins and amino acids that were originally present within the shell. The peptide bond (linking the amino acids) is the most unstable part of the protein structure, and the cleavage of this bond, by hydrolysis,

is the first step in the degradation of the protein (HARE & MITTERER, 1969; VAN KLEEF, DE JONG, & HOENDERS, 1975). In the intracrystalline proteins of brachiopods, this process is extremely rapid. By the time the valve is 0.12 Ma old, more than 60 percent of the total amino acid that remains is present in the free state (WALTON, 1992). Such observations indicate that perfect protein preservation within the shell is not likely; peptide bonds are degraded, and only the free amino acids survive, which remain trapped within the biocrystal. In intercrystalline sites, it is possible that these will be lost through leaching from the shell matrix. The degradation products of the proteins may be directly sampled from intracrystalline sites.

Individual amino acids vary in their stability toward oxygen and water (Fig. 205). Once free from the relative protection of the protein structure, amino acids will themselves degrade at a rate dependent on their stability and ambient temperatures and the time they are exposed to these conditions. The molecules present within the shell form a complex mixture of preserved short chains of paleoprotein-peptide, released (free) amino acids, and the variously degraded remains of amino acids.

The most common amino acids found in fossils are glycine, alanine, aspartic acid and glutamic acid. They are present in absolute abundances that generally reflect their original proportions; for example, glycine remains the most abundant amino acid but decreases in concentration from 76 ng/mg to

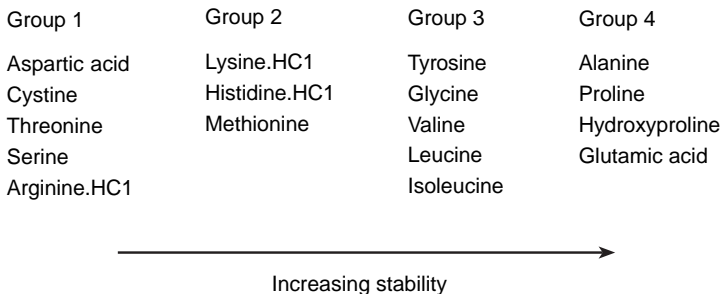


FIG. 205. Relative stability of the amino acids determined by pyrolysis experiments (new; data from Vallentyne, 1964).

31 ng/mg over a 2.2 Ma time interval (WALTON, 1992). The exception is alanine, which increases greatly in concentration in young fossil samples. This increase is due to the diagenetic production of alanine during the decomposition of serine (BADA & others, 1978) and possibly of phenylalanine and tyrosine (WALTON, 1992).

Glutamic acid is preserved in the fossil record by conversion of the released biomolecule to its lactam pyroglutamic acid (WILSON & CANNON, 1937). In fossil samples this has a dramatic effect. First, lactam may only form after natural hydrolysis has taken place so that its formation is evidence of cleavage of the peptide bond on either side of a particular glutamic acid residue. Second, the formation of the lactam releases a molecule of water, allowing further degradation of the protein. Third, this is a method whereby much of the original amino acid may be preserved: the lactam reverts to glutamic acid on hydrolysis and thus a large proportion of the original amino acid is preserved.

Further protein diagenesis accelerates degradation of the molecules with individual amino acids undergoing irreversible degradation. Such degradation rapidly reduces the level of taxonomic information, which may be revealed through the amino acid record. For example, a well-documented degradation pathway is the degradation of the hydroxy amino acids serine and threonine (BADA & others, 1978), whereby a number of products may be derived from the amino acid parent molecules, including other proteinaceous amino acids.

Such amino acids that are readily degraded as arginine, threonine, and serine quickly become unavailable for taxonomic differentiation. In *Calloria inconspicua* for example, serine drops from 7 ng/mg to 0.8 ng/mg, arginine from 6.7 ng/mg to 0, and threonine from 3.7 ng/mg to 0 over 2.2 Ma (WALTON, 1992). It is likely that reduction in the specificity of the PCA calculations is due to this information loss. In any local sedimentary succession, however, it is likely that samples have been subjected to a simi-

lar thermal history, and the level of organic degradation is likely to be the same for different fossil species. Coeval species from different localities cannot accurately be compared using PCA unless corrections can be made to diagenetic effects on the proportions of the amino acids.

Shells of terebratulides and rhynchonellides from the Plio-Pleistocene South Wanganui basin of New Zealand have been analyzed using PCA by WALTON (1992), and a trend has been observed in the information recovered by this technique. In the youngest fossil samples, there is good separation between the species, with out-groups of molluscs included to demonstrate that the amino acid signal had not homogenized. Progressively older samples move closer together within the dimensions defined by the principal components (Fig. 206–207). This indicates how decomposition of susceptible amino acids at various sites within an organism might preclude discrimination. A basic taxonomic distinction can still be derived to the ordinal level although how much this discrimination is affected by diagenesis is not yet known. Such analyses may provide some preliminary evidence for the use of amino acids as taxonomic indicators in the fossil record.

PROTEINS

GENERAL

Proteins are highly information-rich molecules since the order of amino acids in the polypeptide chain, the primary sequence, relates to the order of nucleotide bases within the genome. By characterizing the proteins, it should be possible to comment on the relationships between brachiopod species at a molecular level. Attempts to obtain phylogenetic information from shell proteins have led to a range of approaches being employed. Some studies (CURRY, CUSACK, ENDO, & others, 1991; CURRY, CUSACK, WALTON, & others, 1991; CUSACK & others, 1992) extract only intracrystalline material, while others extract all of the soluble protein from within the valves (JOPE, 1965, 1967a, 1967b,

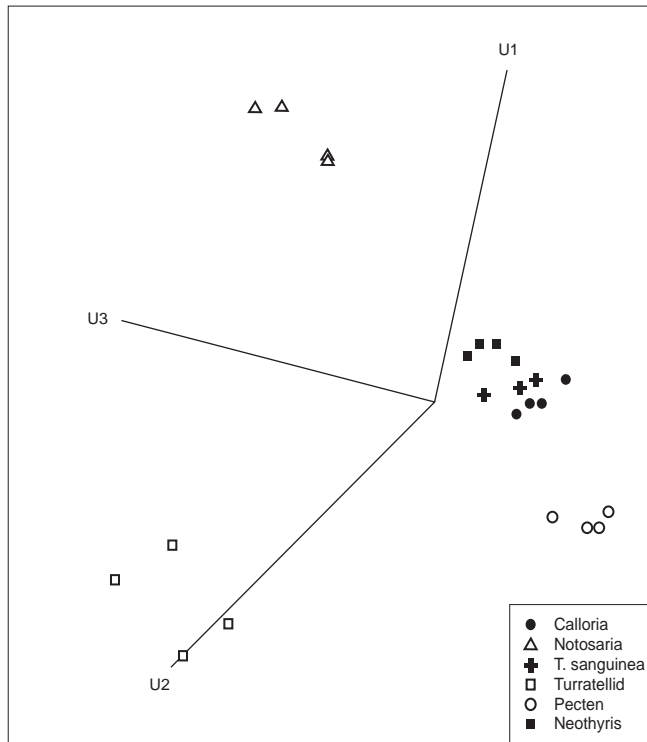


FIG. 206. Graph of the three principal components calculated for the reactive proportions of amino acids from the Tainui shell bed. Separation of the species is at the subordinal level; although the *Terebratulida* plot close together, they may still be separated (new).

1969b, 1973, 1979). In addition, in some instances, proteins are extracted and then purified to homogeneity to allow characterization of individual protein species (JOPE, 1969a, 1969b) and determination of primary sequences (CURRY, CUSACK, ENDO, & others, 1991; CURRY, CUSACK, WALTON, & others, 1991; CUSACK & others, 1992); other studies have analyzed the total protein fraction (JOPE, 1965, 1967a, 1967b).

PROTEINS OF ARTICULATED BRACHIOPODS

Proteins are extracted from the mineral of the articulated brachiopods by chelating the calcium of the calcite with ethane diamine tetra acetic acid (EDTA) (CUSACK & others, 1992). Dissolution of the mineral is effected after the intercrystalline proteinaceous material has been destroyed by oxidation with sodium hypochlorite, ensuring that only

proteins within the mineral are isolated. EDTA is removed and the sample concentrated using the Minitan tangential-flow filtration system fitted with filters of 10 kDa molecular weight cutoff. This cutoff depends on the conformation of the protein, and, therefore, some molecules smaller than 10 kDa will be retained.

Typically, a final volume of 2 ml concentrated extract is obtained from 100 g of shell. The proteins extracted from the valves are then separated by sodium dodecyl sulphate polyacrylamide gel electrophoresis (SDS PAGE). The separated proteins are revealed by staining with Coomassie Brilliant Blue R250, and the molecular weight of each protein is estimated. Samples for SDS PAGE are generally 10 μ l from the 2 ml extract, approximately equivalent to the extract from 0.5 g of shell material. Proteins can be either fixed and stained in the gel using Coomassie

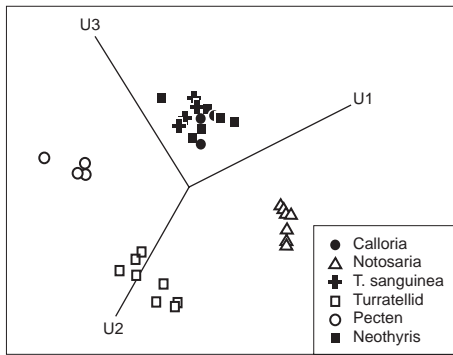


FIG. 207. Graph of the three principal components calculated for the relative proportions of amino acids from the Kupe Formation. Separation of the species is at the ordinal level with *Notosaria* samples plotting away from the rest of the samples, although the *Terebratulida* plot close together (new).

or electroblotted onto ProBlott™ membrane and revealed on the membrane, again with Coomassie. Immobilizing the protein mixture on the membrane provides a stable record of the protein samples, and the amino acid composition and N-terminal sequence can be determined from the immobilized proteins. The articulated brachiopods included in this study and their collection localities are listed in Table 22.

SDS PAGE analyses of the intracrystalline proteins of the above articulated brachiopods are presented in Figures 208 to 213, and a summary of the number and size of intracrystalline proteins is presented in Table 23.

T. retusa appears to contain three intracrystalline proteins (Fig. 208). The major protein, of molecular weight 44 kDa, may be further fractionated to two protein bands on extended electrophoresis (Julie LAING, personal communication, 1995). In addition, highly concentrated extracts obtained using

filters with 5 kDa cutoff indicate that other protein species, in addition to those of 18 and 79 kDa, are also present (Julie LAING, personal communication, 1995). *C. inconspicua* contains three proteins of molecular weights 6.5, 16, and 49 kDa (Fig. 209). In Figure 210 the four proteins of *N. lenticularis* are evident. These proteins are of the same molecular weight as those from *C. inconspicua* with an additional 20 kDa protein. The mixture of intracrystalline proteins from *T. sanguinea* comprises two major proteins of 6.5 and 49 kDa molecular weight as well as three minor proteins of 10, 16, and 20 kDa (Fig. 211). The three proteins of *T. coreanica* are of similar molecular weight (Fig. 212) to those of *C. inconspicua* (Fig. 209). *L. rubellus* contains three major proteins of 6.5, 10, and 50 kDa molecular weight as well as a minor protein of 47 kDa (Fig. 213).

Carotenoproteins

CUSACK and others (1992) demonstrated the presence of carotenoprotein in three species of terebratulid brachiopods. These pigmented brachiopods are *Neothyris lenticularis*, *Calloria inconspicua*, and *Terebratella sanguinea*. The pigmentation in all three species results from a carotenoid bound to the 6.5 kDa protein. The N-terminal sequence of this 6.5 kDa protein has been determined from these three New Zealand brachiopods with red valves (Fig. 214).

The low level of carotenoprotein (27.22, 41.11, and 47.58 ng/g shell in *N. lenticularis*, *C. inconspicua*, and *T. sanguinea* respectively) precluded the extraction of the carotenoid directly from purified carotenoprotein for identification, and so carotenoid was extracted from whole valves. The pig-

TABLE 22. Species and localities used in SDS PAGE analysis of intracrystalline proteins of valves of articulated brachiopods (new).

Brachiopod	Locality
<i>Terebratulina retusa</i> (LEACH)	Kerrera Sound, Scotland
<i>Calloria inconspicua</i> (SOWERBY)	Portobello Caves, New Zealand
<i>Neothyris lenticularis</i> (DESHAYES)	Paterson Inlet, Stewart Island, New Zealand
<i>Terebratella sanguinea</i> (LEACH)	Paterson Inlet, Stewart Island, New Zealand
<i>Terebratalia coreanica</i> (ADAMS & REEVE)	Oki Island, Shimane, Japan
<i>Laqueus rubellus</i> (SOWERBY)	Jogashima, Sagami Bay, Japan

ment could not be extracted from finely powdered shells using cold or warm organic solvents such as methanol, ethanol, acetone, or dichloromethane (CLEGG, 1993). Demineralization of the shell with EDTA resulted in the release of the pigment indicating an intimate association between the carotenoprotein and the mineral. The red pigment was extracted using the acetone-diethyl ether method of POWLS and BRITTON (1976). Two carotenoids are present in the valves, canthaxanthin, and the tentatively identified mono-acetylenic analogue of astaxanthin, according to the standard color test of DUNNING (1963), solubility in organic solvents, co-chromatography with pure carotenoid standards, β -carotene and canthaxanthin, and mass spectroscopy. The total amount of carotenoid in the valves is 0.76 μg , 1 μg , and 0.81 $\mu\text{g/g}$ shell for *N. lenticularis*, *C. inconspicua*, and *T. sanguinea*, respectively (CLEGG, 1993). It is not known which of the two carotenoids is attached to the 6.5 kDa protein.

PROTEINS OF INARTICULATED BRACHIOPODS

The inarticulated brachiopods (and localities) included in this study are presented in Table 24. A summary of the number and size of mineral-associated proteins in the inarticulated brachiopod valves is given in Table 25.

The molecular components of *Lingula anatina* (LAMARCK) have been studied more extensively than any other species of inarticulated brachiopod. JOPE (1973) extracted three proteins from the valves of *Lingula*

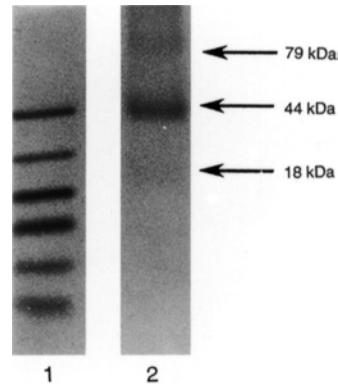


FIG. 208. Separation of intracrystalline proteins of *Terebratulina retusa* by SDS PAGE in a 15 percent polyacrylamide gel according to the method of SCHÄGGER and VON JÄGGER (1987). Proteins were fixed and revealed using Coomassie Brilliant Blue R250 stain. Lane 1 contains protein standards of the following molecular weight: 45 kDa, 29 kDa, 18 kDa, 15 kDa, 6 kDa, and 3 kDa. Lane 2 contains the intracrystalline protein extract (new).

anatina. TUROSS and FISHER (1989) used guanidine to extract nonmineral-associated protein, which they described as analogous to those extracted by JOPE in 1973. TUROSS and FISHER (1989) also used EDTA to extract mineral-associated proteins from *Lingula anatina* valves; and the extract was dominated by a 43 kDa protein, which they suggested may play a role in the control of the formation of the mineral phase. TUROSS and HARE (1990) reestimated the molecular weight of this protein as 40 kDa and, using a polyclonal antibody generated against the protein, demonstrated that the protein can

TABLE 23. Estimated molecular weight of intracrystalline proteins of articulated brachiopod valves as determined by SDS PAGE (see Fig. 208–213; see Fig. 214 for N-terminal sequence) (new).

Brachiopod	Number	Protein	
		Major	Minor
<i>Terebratulina retusa</i> (LEACH)	3	44,	79, 18
<i>Calloria inconspicua</i> (SOWERBY)	3	6.5*, 16, 49	
<i>Neothyris lenticularis</i> (DESHAYES)	4	6.5*, 16, 20, 49	
<i>Terebratella sanguinea</i> (LEACH)	5	6.5*, 49	10, 16, 20
<i>Terebratalia coreanica</i> (ADAMS & REEVE)	3	6.5, 16, 49	
<i>Laqueus rubellus</i> (SOWERBY)	4	6.5, 10, 50	47

*carotenoprotein.

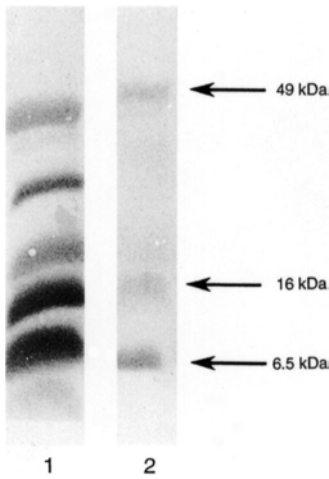


FIG. 209. Separation of intracrystalline proteins of *Calloria inconspicua* by SDS PAGE as described in the caption of Figure 208. Following SDS PAGE, the proteins were electroblotted onto ProBlott™ membrane and revealed using Coomassie Blue staining (new).

be detected in fossil *Lingula*. WILLIAMS, CUSACK, and MACKAY (1994) extracted all of the soluble protein from *Lingula anatina* valves; at least ten proteins were identified in the 6 to 50 kDa molecular weight range (Fig. 215) with the major protein of molecu-

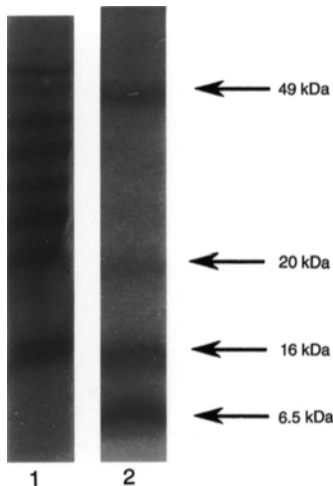


FIG. 210. Separation of intracrystalline proteins of *Neothyris lenticularis* by SDS PAGE as described in the caption of Figure 208. The molecular weights of the standard protein in Lane 1 are 66 kDa, 45 kDa, 36 kDa, 29 kDa, 24 kDa, 20 kDa, and 14.2 kDa (new).

lar weight 36 kDa likely to be that described by TUROSS and FISHER (1989) as 43 kDa and as 40 kDa by TUROSS and HARE (1990). In each case the molecular weight of the protein was assessed by SDS PAGE, which provides only an estimate of molecular weight.

Clean, powdered valves of *Glottidia pyramidata* were incubated with an aqueous solution of sodium hypochlorite to destroy the exposed organic material. Following removal of the sodium hypochlorite, the mineral phase was dissolved using EDTA to release the organic material more intimately associated with the mineral. *G. pyramidata* valves contain five, mineral-associated proteins of estimated molecular weights 28, 35, 52, 62, and 144 kDa (Fig. 216). In addition to these distinct bands, there are two diffuse bands in the 8 and 17 kDa molecular weight range, which may be glycosylated proteins.

Powdered valves of *Discinisca tenuis* were demineralized after incubation with hypochlorite or phosphate buffer. The proteins extracted after treatment with hypochlorite are those more closely associated with the mineral. Three mineral-associated proteins of molecular weight 6, 9, and 14 kDa are evident (Fig. 217). Bleach treatment removes the large range of higher molecular weight proteins found in unbleached samples. In addition, the 6 kDa protein is present in higher levels in the extract that has not been bleached, indicating that the bleach treatment may also destroy some of the mineral-associated protein.

Although *Neocrania anomala* lacks articulation, the valves are calcitic, and the proteins were extracted from the valves as for the articulated, calcitic brachiopods (CUSACK & others, 1992). One major protein, of molecular weight 40 kDa, is evident; there appears to be a minor protein of molecular weight 44 kDa as well as a protein of 8 kDa (Fig. 218).

Collagen

JOPE (1967a) detected the modified amino acid hydroxyproline in the shell of the phosphatic, inarticulated brachiopods *Lingula anatina* and *Discinisca striata*, while it was

absent from the nine species of carbonate brachiopods in her survey, including the inarticulated carbonate brachiopod *Neocrania anomala*. Although hydroxyproline is considered indicative of collagen, JOPE did not present direct evidence of the presence of collagen in the phosphatic valves other than to mention the unpublished work of OWEN, who detected fibrous, collagen-like structures in the valves of *Discina striata*. These fibers, however, lacked the characteristic banding periodicity of collagen fibers. JOPE (1967a, 1973) also reported insufficient levels of glycine, since glycine makes up one-third of the total amino acids in collagen. TUROSS and FISHER (1989) confirmed the presence of hydroxyproline in *Lingula anatina*, although no collagen was extracted. WILLIAMS, CUSACK, and MACKAY (1994) clearly demonstrated the presence of fibrillar collagen with a banding periodicity of 45 nm in the body platform of *Lingula anatina* valves.

Biological systems generally employ one of the three, major molecular systems in skeletal support: the cellulose system so widely present in plants, the collagenous system common in animals, and the chitinous system. Chitin often occurs in fungal cell walls, replacing cellulose, but chitin is best known for its occurrence in the cuticle of arthropods (RUDALL, 1969). It is intriguing that *Lingula* valves should possess collagen as well as chitin (see section on chitin, p. 260, for more information). The presence of collagen in a phosphatic, biomineralized system, the *Lingula* valve, is analogous with the composition of vertebrate bone.

LIPIDS IN BRACHIOPOD VALVES

GENERAL

The presence of lipids in brachiopod valves was first described by JOPE (1965) from recent brachiopod valves. Within shells generally, the organic matter is predominantly proteinaceous, but small amounts of lipids, pigments, and polysaccharides also occur (HARE, 1962). Analysis of the organic

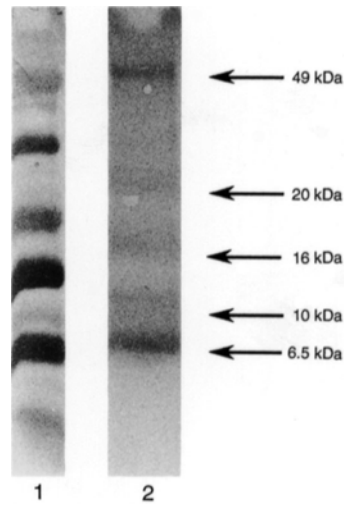


FIG. 211. Separation of intracrystalline proteins of *Terebratella sanguinea* by SDS PAGE as described in the caption of Figure 208. Following SDS PAGE, the proteins were electroblotted onto ProBlott™ membrane and revealed using Coomassie Blue staining (new).

components of brachiopod valves has tended to concentrate on proteins and amino acids since such molecules yield taxonomic information. Lipids, however, have a greater preservation potential than proteins due to their low solubility in water (EGLINTON & LOGAN,

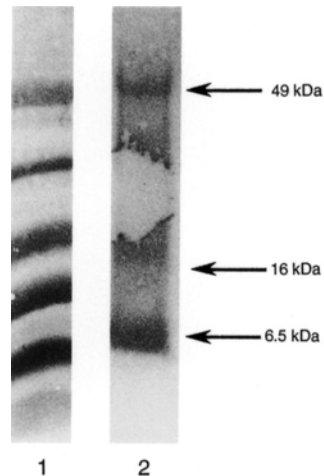


FIG. 212. Separation of intracrystalline proteins of *Terebratalia coreanica* by SDS PAGE as described in the caption of Figure 208. Following SDS PAGE, the proteins were electroblotted onto ProBlott™ membrane and revealed using Coomassie Blue staining (new).

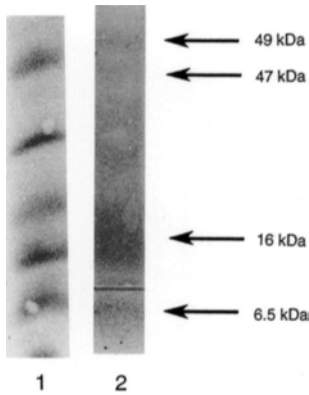


FIG. 213. Separation of intracrystalline proteins of *Laqueus rubellus* by SDS PAGE as described in the caption of Figure 208. Following SDS PAGE, the proteins were electroblotted onto ProBlott™ membrane and revealed using Coomassie Blue staining (new).

1991). Although diagenesis may alter the lipids especially by the hydrogenation of double bonds, aromatization of rings, or loss of such functional groups as hydroxyl groups, the carbon skeleton is retained such that an unequivocal link can be made with a known biological molecule (EGLINTON & LOGAN, 1991).

Lipids in Living Brachiopods

JOPE (1971) estimated that lipids comprise 5 percent of the total organic material in the valves of the rhynchonellides *Notosaria* and *Hemithiris*, 40 percent of which are neutral lipids, chiefly cholesterol or its ester and 60 percent polar lipids. The polar lipids contain a high proportion of phosphatidylethanolamine, phosphatidylserine, and small amounts of phosphatidylcholine, phospho-

	10	20		
<i>N. lenticularis</i>	GWEQL	PYATM	ISKTS	NA_KP
<i>C. inconspicua</i>	GWEQL	PYATM	ISKTS	QAKNP
<i>T. sanguinea</i>	GWEYL	PYASM	ISKTS	QADNP

FIG. 214. N-terminal amino acid sequence of the 6.5 kDa protein from *N. lenticularis*, *C. inconspicua*, and *T. sanguinea*. The sequence is presented using the one-letter code for amino acids. Those amino acid residues that are identical in all three proteins are presented in bold to highlight the high degree of sequence similarity (new).

inositide, and sphingomyelin. In the terebratulides, the proportion is 30 percent neutral and 70 percent polar lipids.

CLEGG (1993) isolated three fractions of lipids from the brachiopod valve: intercrystalline free lipids (IFL), intracrystalline free lipids (FIL), and bound intracrystalline lipids (BIL), that is, lipids bound to crystals. The lipids were isolated and characterized using GC-MS from the valves of living *Neothyris lenticularis* (DESHAYES), *Calloria inconspicua* (SOWERBY), and *Terebratella sanguinea* (LEACH). The identity and quantity of intercrystalline free lipids (IFL) from shells of living *N. lenticularis*, *C. inconspicua*, and *T. sanguinea* are presented in Table 26.

C. inconspicua contains a higher concentration of sterols (19.86 $\mu\text{g/g}$) than *N. lenticularis* (10.16 $\mu\text{g/g}$) and *T. sanguinea* (17.18 $\mu\text{g/g}$). Cholest-5-en-3 β -ol was the dominant sterol for all three species but particularly for *C. inconspicua*, representing more than 50 percent of the sterol composition. *C. inconspicua* contains the highest percentage of C₂₇ sterols, 59.3 percent, compared with 54.3 percent and 50 percent for *N. lenticularis* and *T. sanguinea*, respectively. C₂₈ sterols, however, constituted 39.6 percent of the total sterols in *T. sanguinea* compared with 33.2 percent and 29 percent in *N. lenticularis* and *C. inconspicua*. *n*-C₂₈ alcohol was found in *N. lenticularis* and *C. inconspicua*.

The identity and quantity of intracrystalline free lipids (FIL) from shells of living *N. lenticularis* and *T. sanguinea* are presented in Table 27.

T. sanguinea contains the highest concentration of fatty acids in the FIL fraction (1.73 $\mu\text{g/g}$) compared with 1.54 $\mu\text{g/g}$ for *N. lenticularis*. C_{16:0} is the dominant fatty acid in both species. C_{12:0} and C_{18:0} are the second most abundant fatty acids of *T. sanguinea* and *N. lenticularis*, respectively. In both species there is a dominance of even-numbered fatty acids. The identity and quantity of intracrystalline, crystal-bound fatty acids and *n*-alcohols from shells of living *N. lenticularis*, *C. inconspicua*, and *T. sanguinea* are presented in Table 28.

C. inconspicua contains the highest concentration of fatty acids and *n*-alcohols (23.62 µg/g) in the BIL fraction, while *N. lenticularis* contains 9.82 µg/g and *T. sanguinea* contains 18.77 µg/g. There is a dominance of even-numbered fatty acids in the three species. The BIL fraction contains the highest concentration of lipids compared with the FIL and IFL fractions of the three species studied. C_{16:0} fatty acid is the dominant compound in the BIL fraction. *T. sanguinea* contains the highest concentration of unsaturated fatty acids in the BIL fraction (6.06 µg/g) in comparison with *C. inconspicua* (3.21 µg/g) and *N. lenticularis* (2.85 µg/g).

Lipids in Recent Brachiopods

CLEGG (1993) examined the lipids in the shells of recent *N. lenticularis* dredged from Otago Head Peninsula, South Island, New Zealand, and *C. inconspicua* and *Notosaria nigricans* (SOWERBY) that were washed up on the seashore. No estimate of age of the shells was available. No lipids could be extracted from the IFL fraction of recent *N. lenticularis*, *C. inconspicua*, and *N. nigricans*. Lipids could not be extracted from the FIL fraction of *N. nigricans*. The quantities of fatty acids in the FIL fraction of *C. inconspicua* and *N. lenticularis* are presented in Table 29.

Recent *N. lenticularis* contains a greater concentration of fatty acids in the FIL fraction (0.41 µg/g) than *C. inconspicua* (0.06 µg/g). Polyunsaturated fatty acid C_{20:2} and monounsaturated fatty acid C_{20:1} do not occur in recent *N. lenticularis* but do occur in the FIL fraction of living *N. lenticularis*. Odd-numbered fatty acids did not occur in the FIL fraction of *C. inconspicua*. Recent *N. lenticularis* has decreased saturated fatty acids but not unsaturated fatty acids.

The lipids of the BIL fraction of *N. nigricans* are nonvolatile and not amenable to GC analysis. Recent *N. lenticularis* contains a higher concentration of lipids (3.65 µg/g) in the BIL fraction than recent *C. inconspicua* (2.11 µg/g). This is the reverse of

TABLE 24. Species and localities used in SDS PAGE analysis of mineral-associated proteins of valves of inarticulated brachiopods (new).

Brachiopod	Locality
<i>Lingula anatina</i> (LAMARCK)	Ariake Bay, Japan
<i>Glottidia pyramidata</i> (STIMPSON)	Panacea, Florida
<i>Discinisca tenuis</i> (SOWERBY)	Swapokmund, Namibia
<i>Neocrania anomala</i> (MÜLLER)	Kerrera Sound, Scotland

the situation in living shells, where *C. inconspicua* contains more than twice the amount of lipids in the BIL fraction than *N. lenticularis*. All of the fatty acids in the BIL fraction decreased in concentration from living to dead recent shells, especially for *C. inconspicua*. Saturated fatty acids decrease more rapidly in the FIL fraction than in the BIL fraction of *N. lenticularis*.

Lipids in Fossil Brachiopods

Lipids from fossil brachiopods have been analyzed by THOMPSON and CREATH (1966), IVANOV and STOYANOVA (1972), IVANOV, STOYANOVA, and DASKALOV (1975), and STOYANOVA (1984). THOMPSON and CREATH (1966) examined the lipids in the atrypidine brachiopods *Atrypa spinosa* (Devonian) and the orthidine *Platystrophia* sp. (Ordovician), which contained 6.8 µg/g and 7.5 µg/g respectively of C₁ to C₅, low-molecular-weight

TABLE 25. Estimated molecular weight of mineral-associated proteins of inarticulated brachiopod valves as determined by SDS PAGE (see Fig. 215–218). Values in parentheses represent diffuse bands that may be glycosylated (new).

Brachiopod	Protein	
	Number	Molecular weight (kDa)
<i>Lingula anatina</i> (LAMARCK)	10	6–50
<i>Glottidia pyramidata</i> (STIMPSON)	7	28, 35, 52, 62, 144 (8, 17)
<i>Discinisca tenuis</i> (SOWERBY)	3	6, 9, 14
<i>Neocrania anomala</i> (MÜLLER)	3	8, 40, 44

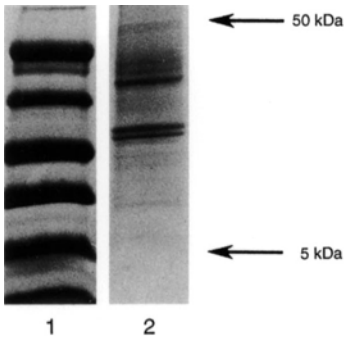


FIG. 215. Separation of paracrystalline proteins from *Lingula anatina* valves by SDS PAGE as described in the caption of Figure 208 (new).

hydrocarbons. IVANOV and STOYANOVA (1972) analyzed an unspecified brachiopod species (Devonian) that contained a homologous series of normal alkanes from n -C₁₄ to n -C₃₅. They also reported branched (unspecified) and normal fatty acids from C₁₄ to C₂₆ from an unknown brachiopod species of Devonian age. C_{16:0} and C_{18:0} were present in the highest proportions. STOYANOVA (1984) studied in detail the normal alkanes and normal fatty acids in *Atrypa reticularis* (Upper Silurian), *Sieberella sieberi* (Lower Devonian), *Spirifer elegans* (Middle Devonian), *Marginifera* sp. (Upper Per-

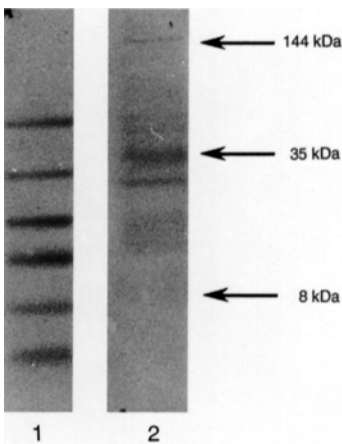


FIG. 216. Separation of paracrystalline proteins from *Glottidia pyramidata* valves by SDS PAGE as described in the caption of Figure 208 (new).

mian), and *Productus horides* (Upper Permian). The survey revealed a trend of increasing amounts of alkanes and decreasing levels of fatty acids with increasing age of the fossil.

These studies did not distinguish between intercrystalline and intracrystalline lipids. CLEGG (1993) analyzed fossil brachiopod shells to compare the lipids of the shells of living brachiopods with those from the corresponding fossil ancestors. The fossil samples included in the survey are presented in Table 30.

Fossil terebratulides were analyzed as well as a specimen of chonetidine *Daviesiella llan-gollensis* (Carboniferous) from northern Wales to assess the long-term survival of lipids. Alcohols n -C₂₂₋₃₀ are an important component of the IFL fraction of the fossil samples, particularly n -C₂₂ and n -C₂₈ alcohols. Identification of the compounds in the FIL fraction of the fossil samples was not possible due to the very low level of purified compounds. Only the tentative identification of the fatty acids in the FIL fraction of the *Neothyris* sp. was possible (Table 31). Samples of *Neothyris* sp. analyzed were from the Kupe shell bed (0.45 Ma), Waipuru shell bed (1.49 Ma), and the Wairarapa Formation (1.47 to 1.7 Ma).

All three samples contained very low levels of fatty acids. C_{16:0} is the dominant fatty acid in the FIL fraction of *Neothyris* from the Kupe shell bed, while samples from Waipuru and Wairarapa contained C_{14:0} and C_{16:0} as the most abundant fatty acids. The quantities of lipid components from the BIL fraction of fossil brachiopods are presented in Table 32. The dominant class of lipids in the BIL fraction of all the fossils examined are the fatty acids. *Neothyris* sp. (Rapanui Formation, 0.12 Ma and Waipipi, 2.65 Ma) and *C. inconspicua* (Kupe shell bed, 0.45 Ma) do not contain unsaturated fatty acids. Analysis of the lipids in the BIL fraction of three different genera from the Kupe shell bed, *Neothyris* sp., *T. sanguinea*, and *C. inconspicua*, revealed differences in the lipid composition that are likely to be important at the generic

level since the samples are all from the same locality. *C. inconspicua* contains the greatest range of lipids. The concentration of $C_{16:0}$ fatty acid in *C. inconspicua* was more than twice that of *T. sanguinea*. *C. inconspicua* contains no unsaturated fatty acids in the BIL fraction. *Neothyris* sp. contains the highest amount of $C_{14:0}$ and $C_{18:0}$ fatty acids. The BIL fraction of *Neothyris* sp. also contains C_{21} , C_{24} , C_{26} α -hydroxy fatty acids and C_{22} ω -hydroxy fatty acids, which are not present in the BIL fraction of *C. inconspicua* and *T. sanguinea*. *C. inconspicua* contains $C_{19:0}$ and $C_{30:0}$ fatty acids that are not present in *Neothyris* sp. and *T. sanguinea*. C_{14} β -hydroxy fatty acid present in *T. sanguinea* is not present in the BIL fraction of *Neothyris* sp. or *C. inconspicua*. The major similarity between the three species is the dominance of saturated fatty acids.

The dominant constituent of the BIL fraction from *Neothyris* sp. and *T. sanguinea* from Waipipi (2.5 Ma) are saturated fatty acids. *T. sanguinea* contains a higher concentration of $C_{14:0}$, $C_{15:0}$, $C_{16:0}$, $C_{17:0}$, $C_{18:0}$, $C_{19:0}$, $C_{22:0}$, and $C_{23:0}$, while *Neothyris* sp. contains a higher concentration of $C_{24:0}$, $C_{26:0}$, and $C_{28:0}$ fatty acids. *T. sanguinea* contains a large amount of C_{22} ω -hydroxy fatty acid (0.38 $\mu\text{g/g}$) as well as α -hydroxy fatty acids, neither of which occurs in *Neothyris* sp., although C_{13} β -hydroxy fatty acid is present in *Neothyris* sp.

The Carboniferous brachiopod *Daviesiella llangollensis* did not yield an insoluble fraction, and, therefore, it was not possible to compare the BIL fraction with that of the New Zealand fossils. The dominant compounds present in the IFL fraction are squalene, pristane, and phytane, indicating postdepositional ingress. The FIL fraction contains a homologous series of *n*-alkanes, *n*- C_{24} being the most abundant. There is a dominance of even *n*-alkanes. The presence of pristane and phytane in the FIL fraction indicates some postdepositional ingress.

The living brachiopods contain the highest concentration and range of lipids with a significant reduction for recent and fossil

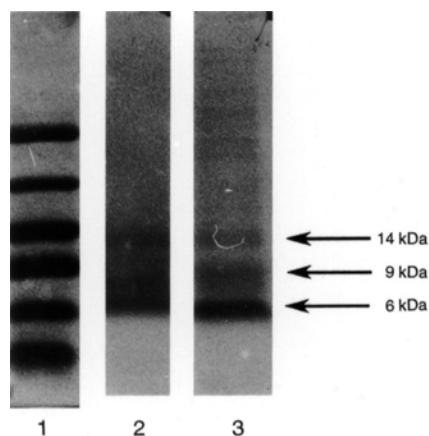


FIG. 217. Separation of proteins from *Disciniscia tenuis* valves by SDS PAGE as described in the caption of Figure 208. Lane 1 contains proteins of known molecular weight (see caption of Figure 208). The sample in lane 2 has been treated with sodium hypochlorite before EDTA dissolution while the sample in lane 3 has not (new).

shells for both the free and unbound fractions. Although lipids have been isolated and characterized from living, recent, and fossil brachiopod valves, the source or role of these lipids is unknown. The epithelial cells of the mantle are the most likely source of the lipids, which may be important for biomineralization or may simply be trapped during deposition of the shell.

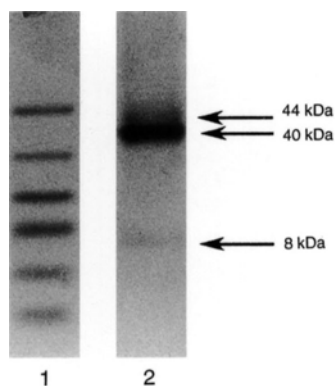


FIG. 218. Separation of mineral-associated proteins from *Neocrania anomala* valves by SDS PAGE as described in the caption of Figure 208 (new).

TABLE 26. The intercrystalline free lipids of *N. lenticularis*, *C. inconspicua*, and *T. sanguinea* as identified by GC-MS (new; data from Clegg, 1993).

Compound	<i>N. lenticularis</i>	<i>C. inconspicua</i>	<i>T. sanguinea</i>
	µg/g	µg/g	µg/g
24-norcholesta-5, 22E-dien-3β-ol	0.52	0.80	0.72
24-methyl-27-norcholesta-5,22-dien-3β-ol	0.25	0.28	0.54
cholesta-5,22E-dien-3β-ol	1.08	1.30	2.06
cholesta-5-en-3β-ol	4.19	10.20	5.99
<i>n</i> -C ₂₈ alcohol	0.60	0.26	0.00
24-methylcholesta-5,22E-dien-3β-ol	1.48	2.99	2.33
24-methylcholesta-5,24(28)-dien-3β-ol	1.89	2.77	4.47
24-ethylcholesta-5,22E-dien-3β-ol	0.16	0.54	0.26
24-ethylcholesta-5-en-3β-ol	0.59	0.98	0.81

CARBOHYDRATES IN BRACHIOPOD VALVES

GENERAL

Carbohydrates are important biomolecules, since they are formed during photosynthesis and are thus the first intermediate in the incorporation of carbon, hydrogen, and oxygen into living matter. Commonly known as sugars, carbohydrates can occur as monosaccharides, oligosaccharides (2 to 10 monosaccharides), or polysaccharides (larger polymer carbohydrates). Carbohydrates occur in biominerals, including brachiopod valves (JOPE, 1965), although very little work has been done to characterize these molecules. BORMAN and others (1987) described methylated and dimethylated monosaccharides in the calcite of the coccolith *Emiliana huxleyi*, while neutral sugars were extracted from *Mercenaria mercenaria* (CRENSHAW, 1972). COLLINS, CURRY, and others (1991) detected neutral sugars in the EDTA-soluble fraction of recent *Neothyris lenticularis* by colorimetric assays using sulphuric acid and phenol. They also used immunological techniques to demonstrate the presence of carbohydrates in Pleistocene *Neothyris* sp. (Kupe shell bed, 0.45 Ma) using periodate oxidation to remove carbohydrate moieties. Neutral polysaccharides occur in the primary layer of *Glottidia pyramidata* valves (PAN & WATABE, 1988b) as well as the periostracum (PAN & WATABE, 1989).

TABLE 27. Free intracrystalline fatty acids from valves of *N. lenticularis* and *T. sanguinea* as identified by GC-MS (new; data from Clegg, 1993).

Fatty acid	<i>N. lenticularis</i>	<i>T. sanguinea</i>
	µg/g	µg/g
C _{12:0}	0.16	0.18
C _{13:0}	0.00	0.02
C _{14:0}	0.08	0.14
C _{15:0}	0.04	0.04
C _{16:1}	0.03	0.05
C _{16:0}	0.83	1.10
C _{17:0}	0.04	0.02
C _{18:1}	0.02	0.02
C _{18:0}	0.04	0.05
C _{18:0}	0.25	0.11
C _{20:2}	0.02	0.00
C _{20:1}	0.03	0.00

Chitin

The monomer of the polysaccharide chitin, the amino sugar N-acetyl glucosamine, has been detected in the phosphatic valves of *Lingula anatina*, *Discina striata*, and, intriguingly, the carbonate valves of *Neocrania anomala* (JOPE, 1967a). X-ray diffraction has demonstrated that chitin in *Lingula* valves is in the β-form, i.e., the polysaccharide chains are parallel (DWELTZ, 1961; IJIMA, MORIWAKI, & KUBOKI, 1991b). The fiber axis of β-chitin is coincident with the *c*-axis of apatite and parallel with the growth direction of the valves of *Lingula anatina* (KELLY, OLIVER, & PAUTARD, 1965) and *Lingula shantoungensis* (IJIMA &

TABLE 28. The intracrystalline crystal-bound fatty acids and *n*-alcohols of *N. lenticularis*, *C. inconspicua*, and *T. sanguinea* as identified by GC-MS; measurements are $\mu\text{g/g}$ (new; data from Clegg, 1993).

Compound	<i>Neothyris lenticularis</i>	<i>Calloria inconspicua</i>	<i>Terebratella sanguinea</i>
C _{12:0}	0.07	0.51	0.14
C _{13:0}	0.01	0.14	0.07
C _{14:0}	0.13	0.79	0.15
C ₁₂ β -hydroxy	0.00	0.96	0.00
C _{15:0} <i>iso</i>	0.00	0.30	0.00
C ₁₃ β -hydroxy	0.00	0.25	0.00
C _{15:0} normal	0.09	0.17	0.14
C ₁₃ β -hydroxy	0.00	0.42	0.00
C _{16:1}	0.23	0.70	0.36
C _{16:0}	3.85	6.06	6.26
<i>n</i> -C ₁₆ alcohol	0.05	0.16	0.16
C _{17:0} <i>iso</i>	0.10	2.40	0.18
C _{17:0}	0.26	1.77	0.55
C _{18:1}	0.13	0.48	0.12
C _{18:1}	0.21	0.47	0.28
C _{18:0}	1.48	3.26	2.22
<i>n</i> -C ₁₈ alcohol	0.06	0.98	0.24
C _{19:0}	0.05	0.14	0.12
C ₁₇ β -hydroxy	0.00	0.26	0.00
C ₂₀ polyunsaturated	0.09	0.00	0.13
C _{20:2}	0.65	0.33	1.36
C _{20:1}	1.27	1.13	3.08
C _{20:0}	0.07	0.57	0.00
C ₁₈ α -hydroxy	0.00	0.00	0.19
C _{21:0}	0.06	0.10	0.13
C _{22:2}	0.27	0.10	0.73
C _{22:0}	0.31	0.35	0.47
C _{23:0}	0.00	0.24	0.00
C ₂₁ α -hydroxy	0.09	0.10	0.44
C _{24:0}	0.06	0.25	0.00
C ₂₂ α -hydroxy	0.06	0.00	0.90
C ₂₂ ω -hydroxy	0.06	0.23	0.00
C ₂₃ α -hydroxy	0.11	0.00	0.24
C ₂₄ α -hydroxy	0.00	0.00	0.11
Total	9.82	23.62	18.77

others, 1988; IJIMA & MORIWAKI, 1990; IJIMA, MORIWAKI, & KUBOKI, 1991).

Glycosaminoglycans (GAGs)

GAGs occur in the valves of *Glottidia pyramidata* (WATABE & PAN, 1984) where they are associated with the apatitic mineral (PAN & WATABE, 1988b). Alcian blue staining of sections of *Lingula anatina* valves indicates the pervasive presence of acidic

TABLE 29. Fatty acids in the FIL fraction of *C. inconspicua* and *N. lenticularis* as determined by GC-MS (new; data from Clegg, 1993).

Fatty acid	<i>C. inconspicua</i> $\mu\text{g/g}$	<i>N. lenticularis</i> $\mu\text{g/g}$
C _{14:0}	0.01	0.03
C _{15:0}	0.00	0.02
C _{16:1}	0.04	0.04
C _{16:0}	0.00	0.19
C _{17:0}	0.00	0.02
C _{18:1}	0.00	0.03
C _{18:0}	0.01	0.08

GAGs (WILLIAMS, CUSACK, & MACKAY, 1994). TANAKA, ANNO, and SENO (1982) described a novel GAG from the pedicle of *Lingula anatina*. The GAG is sulphated and contains equimolar amounts of galactose and *N*-acetylgalactosamine. The carbohydrate is linked to the peptide portion through the *O*-glycosyl bond between threonine and *N*-acetylgalactosamine. TANAKA, ANNO, and SENO (1982) named this GAG lingulin sulfate.

Carbohydrates in Fossil Brachiopods

CLEGG (1993) analyzed in a preliminary way the carbohydrates in the EDTA-insoluble residue of *Neothyris* sp. from the Kupe shell bed (0.45 Ma). Table 33 lists the quantities and types of carbohydrate present. No amino sugars were detected. No recent material was analyzed.

IMMUNOLOGY OF BRACHIOPOD SHELL MACROMOLECULES

Immunological methods have been used to estimate the degree of biochemical similarity between biomolecules extracted from the shells of a wide range of brachiopods. These data are available predominantly for extant species, but the use of antibodies has also been extended to a number of fossil taxa. In all cases the antibodies have been prepared against intracrystalline biomolecules, as the extraction procedure excludes intercrystalline biomolecules.

TABLE 30. Identity and locality of fossil samples included in the survey of CLEGG, 1993 (new).

Age (Ma)	Taxa	Stratigraphical age	Location
0.12	<i>Neothyris</i> sp.	Rapanui	Castlecliff, N. Island
0.45	<i>Neothyris</i> sp.	Kupe shell bed	Castlecliff, N. Island
0.45	<i>T. sanguinea</i>	Kupe shell bed	Castlecliff, N. Island
0.45	<i>C. inconspicua</i>	Kupe shell bed	Castlecliff, N. Island
1.49	<i>Neothyris</i> sp.	Waipuru shell bed	Turakina Point, N. Island
1.47–1.7	<i>Neothyris</i> sp.	Wairarapa	The Reef, Castlepoint, N. Island
2.0	<i>Neothyris</i> sp.	Hautawa shell bed	Castlecliff, N. Island
2.2	<i>Neothyris</i> sp.	Parihauhau shell bed	Castlecliff, N. Island
2.5	<i>Neothyris</i> sp.	Waipipi	Castlecliff, N. Island
2.5	<i>T. sanguinea</i>	Waipipi	Castlecliff, N. Island
2.65	<i>Neothyris</i> sp.	Waipipi	Wapukura, N. Island
15	<i>Pachymagas</i> sp.	Gee Greensand	Old Rifle Butts, S. Island
23	<i>Pachymagas</i> sp.	Otekaike limestone	Trig Z, S. Island
300	<i>D. llangollensis</i>	Pen-yr-hendlas	Holywell, North Wales*

*all other localities in New Zealand.

VARIATION OF SKELETAL MACROMOLECULES IN RECENT BRACHIOPODS

A total of 26 different antibodies has been prepared against macromolecules extracted from brachiopod shells. Extraction of these macromolecules was achieved by powdering the shells, removing the intercrystalline material, and then releasing the intracrystalline organic material by etching the shells with EDTA. Antibodies were then prepared against bulk extracts from each taxon for which sufficient quantities of shell were available. Measurements of immunological cross-reactivity and hence overall biochemical similarity were determined using enzyme-linked immuno-sorbent assay using a fluorescent substrate (FELISA). The nature of the antigens detected by the antibodies is unknown, although it has been suggested that both proteins and carbohydrates are involved (COLLINS, CURRY, & others, 1991). Full descriptions of the techniques used are given in the references cited below. These antibodies were subsequently used in a range of experiments to assess the degree of biochemical similarity between representatives of approximately half of the total present-day brachiopod fauna.

The first immunological study utilized three antibodies, and the results suggested that the long-established subdivision of the

largest living extant brachiopod order (the Terebratulida) into short- and long-looped groups was an oversimplification (COLLINS & others, 1988). Subsequently a larger number of antibodies was prepared, initially against nine brachiopod genera (COLLINS, MUYZER, CURRY, & others, 1991) and then against eleven genera (CURRY, QUINN, & others, 1991). The availability of these additional antibodies allowed the calculation of immunological distances between major brachiopod groups. The data from these investigations were assessed by a variety of different clustering methods, and the resulting dendrograms and cluster diagrams confirm the earlier results and provide strong evidence for a primary three-fold subdivision of the living terebratulids, with the cancellothyridoids

TABLE 31. Fatty acids in the FIL fraction of fossil *Neothyris* sp. Fatty acids identified by the retention times of the trimethyl silyl ethers (new; data from Clegg, 1993).

Fatty acid	Kupe shell bed µg/g	Waipuru shell bed µg/g	Wairarapa formation µg/g
C _{12:0}	0.003	0.002	0.00
C _{13:0}	0.01	0.004	0.00
C _{14:0}	0.03	0.005	0.002
C _{15:0}	0.015	0.00	0.001
C _{16:0}	0.04	0.005	0.002
C _{18:0}	0.003	0.001	0.001

TABLE 32. Amount of lipids (*mg/g*) in BIL fraction of fossil brachiopods; *A*, Rapanui *Neothyris* sp. (0.12 Ma); *B*, Kupe *Neothyris* sp. (0.45 Ma); *C*, Kupe *T. sanguinea* (0.45 Ma); *D*, Kupe *Calloria inconspicua* (0.45 Ma); *E*, Waipuru *Neothyris* sp. (1.49 Ma); *F*, Wairarapa *Neothyris* sp. (1.47–1.7 Ma); *G*, Hautawa *Neothyris* sp. (2.0 Ma); *H*, Parihauhau *Neothyris* sp. (2.2 Ma); *I*, Upper Waipipi *Neothyris* sp. (2.5 Ma); *J*, Upper Waipipi *T. sanguinea* (2.5 Ma); *K*, Lower Waipipi *Neothyris* sp. (2.65 Ma); *L*, Gee Greensand *Pachymagas* sp. (15 Ma); *M*, Otekaike Limestone *Pachymagas* sp. (23 Ma); *ND*, not determined (new; data from Clegg, 1993).

	A	B	C	D	E	F	G	H	I	J	K	L	M
C _{12:0} fatty acid	0.02	0.03	0.06	0.04	0.01	0.01	0.06	0.03	0.03	0.03	0.15	ND	ND
C _{13:0} fatty acid	ND	0.10	0.01	0.02	0.05	0.05	ND	0.08	0.01	ND	0.15	ND	ND
C _{14:0} fatty acid	0.07	0.20	0.08	0.13	0.24	0.22	0.14	0.33	0.09	0.12	0.48	0.07	0.04
C _{15:0} iso fatty acid	0.01	0.01	0.01	0.03	ND	ND	0.01	ND	ND	ND	ND	ND	ND
C _{15:0} fatty acid	0.05	0.06	0.03	0.08	0.06	0.05	0.07	0.09	0.04	0.06	0.09	0.03	0.02
C ₁₃ β-hydroxy fatty acid	ND	0.04	0.04	0.06	0.07	0.08	ND	0.05	0.01	ND	ND	ND	ND
C _{16:1} fatty acid	ND	0.06	0.02	ND	0.09	0.05	0.03	0.05	0.06	0.08	ND	0.03	0.03
C _{16:0} fatty acid	0.55	0.65	0.54	1.09	0.60	0.70	0.52	0.61	0.41	0.64	1.16	0.44	0.37
C _{17:0} iso fatty acid	0.01	0.02	0.03	ND	0.02	0.02	ND	ND	ND	ND	ND	ND	ND
C _{17:0} fatty acid	0.02	0.03	0.01	0.03	0.04	0.03	0.04	0.04	0.03	0.05	0.05	0.03	0.03
C _{18:1} fatty acid	ND	0.07	0.01	ND	0.06	0.03	0.01	0.03	0.04	0.20	ND	0.16	0.08
C _{18:1} fatty acid	ND	ND	0.01	ND	0.01	0.02	0.04	0.01	ND	ND	ND	0.06	0.01
C _{18:0} fatty acid	0.10	0.24	0.07	0.11	0.19	0.21	0.13	0.23	0.14	0.24	0.39	0.20	0.16
C _{13:0} hydroxy fatty acid	ND	ND	0.02	ND	ND	ND	ND	ND	ND	ND	ND	ND	ND
C _{19:0} fatty acid	ND	ND	ND	0.01	ND	ND	ND	0.01	ND	0.01	ND	0.01	0.02
C _{20:0} fatty acid	0.01	0.03	0.06	0.09	0.02	0.02	0.03	0.02	0.03	0.06	0.05	0.04	0.03
C _{21:0} fatty acid	0.04	0.01	0.01	0.01	0.01	0.01	0.01	0.01	ND	0.02	ND	0.01	0.01
C _{22:0} fatty acid	0.02	0.03	0.02	0.08	0.02	0.01	0.05	0.02	0.02	0.07	0.02	0.05	0.04
C _{23:0} fatty acid	0.01	0.01	ND	0.02	0.01	ND	0.01	0.01	0.01	0.02	ND	0.01	0.01
C ₂₁ α-hydroxy fatty acid	ND	0.01	ND	ND	ND	0.01	ND	ND	ND	0.02	ND	0.02	0.01
C _{24:0} fatty acid	0.02	0.01	0.03	0.05	0.01	0.01	0.03	0.01	0.03	0.01	0.02	0.02	0.01
C ₂₂ hydroxy fatty acid	ND	0.16	ND	ND	0.08	0.07	ND	ND	ND	0.38	ND	0.21	0.03
C ₂₄ α-hydroxy fatty acid	ND	0.04	ND	ND	0.02	0.01	ND	ND	ND	0.05	ND	0.05	0.03
C _{26:0} fatty acid	ND	ND	0.02	0.10	ND	ND	0.01	0.04	0.01	ND	ND	ND	ND
C ₂₆ α-hydroxy fatty acid	ND	0.02	ND	ND	0.01	0.01	ND	ND	ND	0.06	ND	0.04	0.02
C ₂₈ fatty acid	ND	ND	0.01	0.05	ND	ND	0.01	ND	0.01	ND	ND	ND	ND
C _{30:0} fatty acid	ND	ND	ND	0.02	ND	ND	ND	ND	ND	ND	ND	ND	ND
C _{32:0} fatty acid	ND	ND	ND	ND	ND	ND	ND	ND	ND	ND	ND	ND	ND

plotting separately from the long-looped terebratelloids and predominantly short-looped terebratuloids (Fig. 219–220).

Immunological techniques were also used to investigate the extent of biochemical similarity between skeletal biomolecules from twelve species and one subspecies of *Terebratulina* (ENDO & CURRY, 1991). These species were collected from worldwide localities, and, where possible, morphometric analysis allowed an integrated molecular and morphological investigation of their relationships. The immunological results revealed two main clusters of *Terebratulina* species (ENDO & CURRY, 1991). These clusters are

not determined geographically or ecologically, because both Japanese and North Atlantic species of the genus appear in the two subclusters. It has been suggested that these two subclusters reflect a major vicariance event during the evolution of the genus, possibly representing an older group of species and a more recently evolved group that has also undergone considerable geographic dispersal. In addition it was discovered that two sympatric Japanese species were morphologically indistinguishable and very closely related at the molecular level and, hence, are best considered as synonymous (ENDO & CURRY, 1991). The morphometric analysis

TABLE 33. Sugars in EDTA-insoluble fraction of *Neothyris* sp. (Kupe, 0.45 Ma) (new; data from Clegg, 1993).

Sugar	mg/g	% of total
Rhamnose	0.001	0.79
Fucose	0.001	0.79
Ribose	0.006	4.76
Arabinose	0.002	1.59
Xylose	0.008	6.35
Mannose	0.005	3.97
Galactose	0.003	2.38
Glucose	0.1	79.37

also revealed ecophenotypic differences in the species surveyed, with clear differentiation apparent between species with heavy shells and small pedicle forams and those with light shells and large pedicle forams (ENDO & CURRY, 1991). The former association of characters is usually taken to indicate a tendency toward a free-lying mode of life, while the latter suggest a more pedicle-dependent life habit.

The most unexpected result of the immunological investigation was the clustering of the long-looped kraussinid genera with the short-looped terebratulids (Fig. 219), and several other anomalous relationships (Fig. 220) were revealed by an investigation of immunological responses in a wide range of other brachiopod taxa for which reciprocal data are not yet available (CURRY, QUINN, & others, 1991). Such results point to a level of biochemical similarity between these taxa that would not be expected, which warrants further investigation.

At higher taxonomic levels, the pattern of immunological cross-reactivity proved to be entirely consistent with the traditional view of brachiopod evolution based on shell morphology and the fossil record. Thus representatives of different orders were strongly separated by immunology, indicating that there was considerable biochemical differentiation between groups that last shared a common ancestor as far back as the Paleozoic Era.

ENDO and others (1994) extended the range of the immunological survey to investigate 44 species from the most abundant,

extant brachiopod order, the terebratulides. This study confirmed and reinforced the conclusions of the previous studies and identified four groups of terebratulid taxa that were consistently differentiated on the basis of shell biochemistry. ENDO and others (1994) demonstrated that these four groups were also distinct morphologically and, from detailed consideration of the morphology and stratigraphic distribution of fossil terebratulid brachiopods, proposed a reconstruction of evolutionary history that was consistent with the immunological data (Fig. 221).

The advantage of the immunological approach is that it can be applied to small fragments of shell, even those that have been

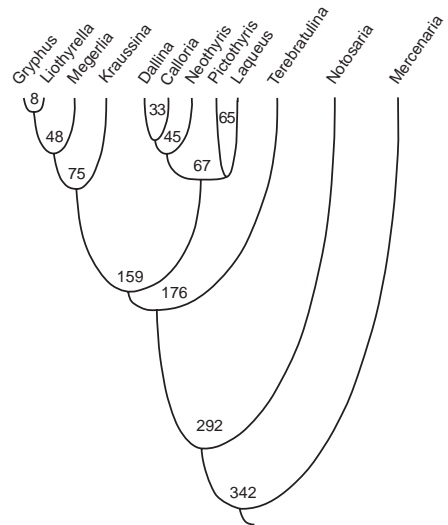


FIG. 219. UPGMA (unweighted pair-group method using arithmetic averages) dendrogram based on immunological distance data for the following brachiopod genera: *Gryphus vitreus* (BÖRN), Mediterranean Sea; *Liothyrella neozelanica* (THOMSON), New Zealand; *Megerlia truncata* (GMELIN), Mediterranean Sea; *Kraussina rubra* (PALLAS), South Africa; *Dallina septigera* (LOVEN), Scotland; *Calloria inconspicua* (SOWERBY), New Zealand; *Neothyris lenticularis* (DESHAYES), New Zealand; *Pictothyris picta* (DILLWYN), Japan; *Laqueus rubellus* (SOWERBY), Japan; *Terebratulina retusa* (LINNAEUS), Scotland; *Notosaria nigricans* (SOWERBY), New Zealand; and the bivalve *Mercenaria* as an outgroup. The numbers are immunological distances (Curry, Quinn, & others, 1991).

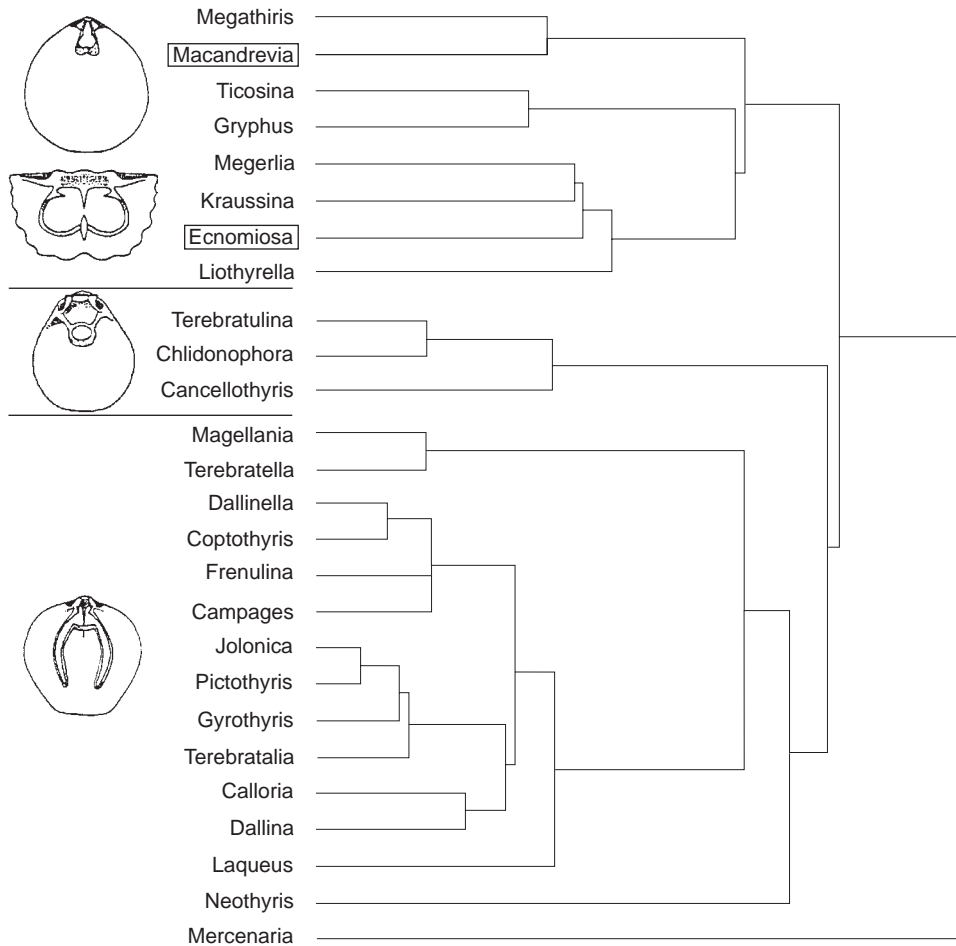


FIG. 220. Single-linkage cluster analysis of 25 terebratuloid brachiopods with the three major groups outlined and represented by stylized loop sketches. The anomalous positions of *Macandrevia* and *Ecnomiosa* (i.e., long-looped genera clustering with short-looped stocks) are indicated by boxes; the bivalve *Mercenaria* is included as the outgroup (Curry, Quinn, & others, 1991).

stored in museum collections. Consequently a large number of taxa could be included in this study, many more than could have been included in a survey using any other molecular method. The main disadvantage is that, for taxonomic purposes, the resolution of immunological data is lower than some of the other available techniques. For the shell macromolecules of brachiopods, immunological techniques appear to be most effective at the generic level and above, although species-level discrimination was possible in

the long-lived genus *Terebratulina* (ENDO & CURRY, 1991).

APPLICATION OF IMMUNOLOGY TO FOSSIL BRACHIOPODS

Immunological techniques applied to fossil brachiopods have provided unequivocal evidence of the survival of antigenic determinants in brachiopod shells over 2 million years old (COLLINS, CURRY, & others, 1991; COLLINS, MUYZER, WESTBROEK, & others, 1991). The immunological approach was

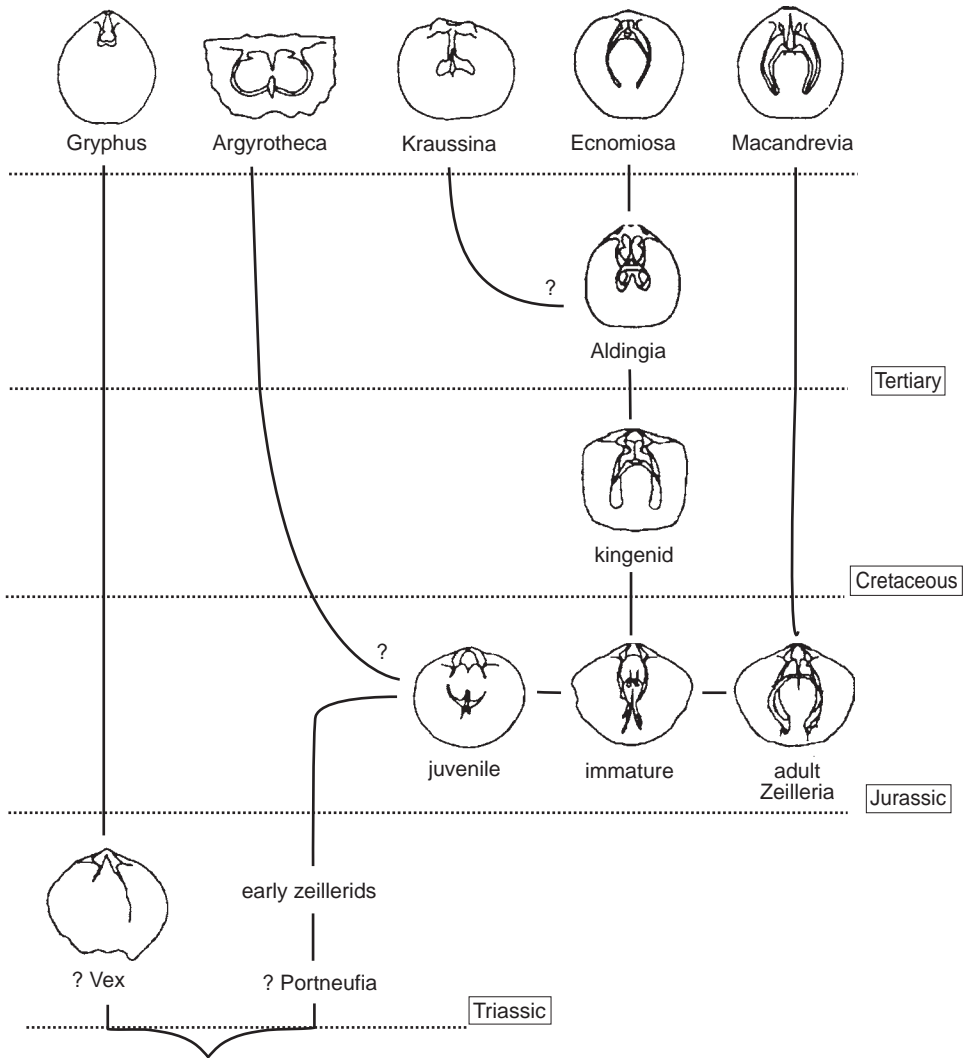


FIG. 221. A possible terebratulide phylogeny, based on immunological data (Endo & others, 1994).

also applied to investigate the biochemical similarity between extant taxa and a related, extinct Pleistocene brachiopod from Japan (ENDO, 1992). The technique allowed the

extinct taxon to be linked to one of four extant species of *Terebratulina*. This relationship was not evident from morphology alone.

SHELL STRUCTURE

ALWYN WILLIAMS

[University of Glasgow]

INTRODUCTION

The integument of the living brachiopod consists of the epidermis and all surface layers secreted by it, the most striking of which is the biomineralized shell. The main constituents of the shell are aggregations of biominerals (with intracrystalline proteins) and their matrices or membranes, which are composed of glycosaminoglycans (GAGs), proteins, and chitin. So far as we know, only the biominerals and a few stable polymers, like collagen, normally survive fossilization in a recognizable state. Even so, there are two

advantages to considering the skeletal successions of extinct groups in conjunction with those of living species. First, biominerals are the main components of the subperiostacal shell of all brachiopods and largely determine its structural frame (fabric). These biomineralized successions are invariably secreted in a well-stratified order and, under favorable conditions, have been preserved more or less in the original state throughout the skeletal fossil record. Second, the fabric of all brachiopod shells conforms to a standard stratiform succession (Fig. 222). This consists of a periostracum underlain by

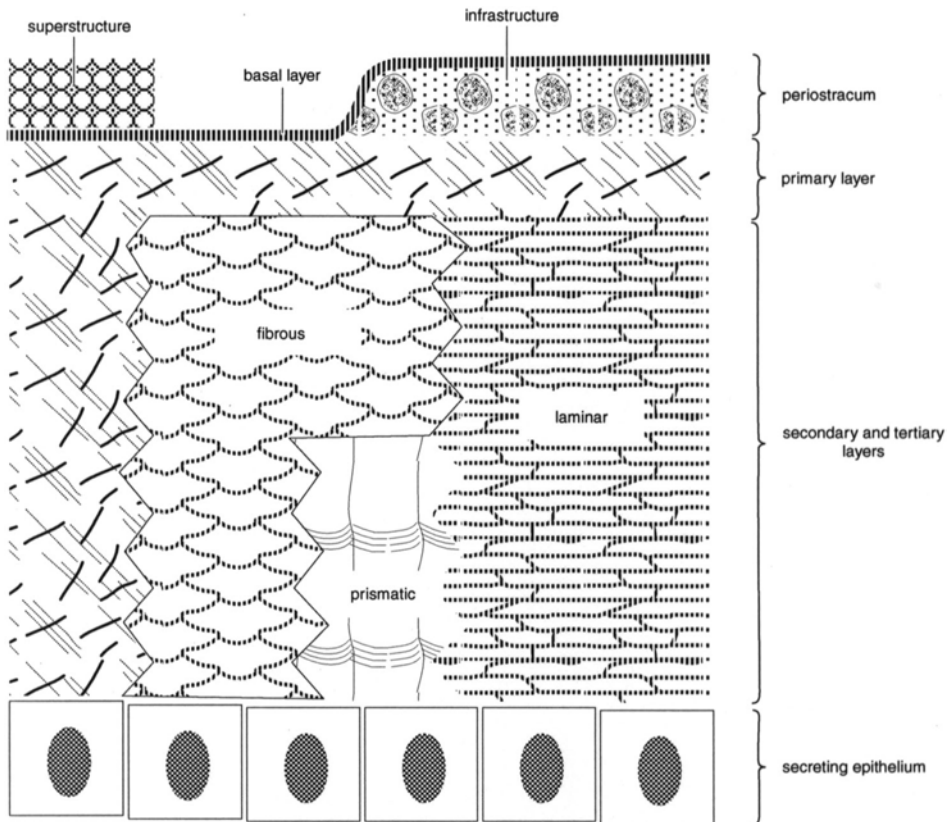


FIG. 222. Stylized representation in the form of a chronostratigraphic succession of the main components of the integument of calcitic-shelled brachiopods (new).

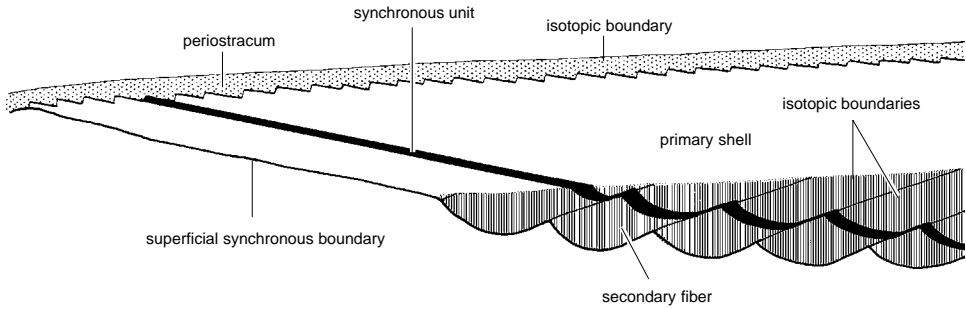


FIG. 223. Stylized medial longitudinal section of the valve edge of a young rhynchonellide, *Notosaria nigricans* (SOWERBY), showing the relationship between various isotopic and synchronous surfaces (Williams, 1971a).

biomineralized primary, secondary, and tertiary layers, of which only the periostracum and the primary layer are always present, the secondary layer being almost entirely absent in living thecideidines and the tertiary layer mainly restricted to a minority of living and fossil species (Fig. 222).

The standard succession of the brachiopod shell reflects the inherent homogeneity of the fabric of each layer, which forms an isotopic unit (WESTBROEK, 1967). The isotopic interfaces bounding such layers are quite different from surfaces of active shell deposition or resorption, which are isochronous

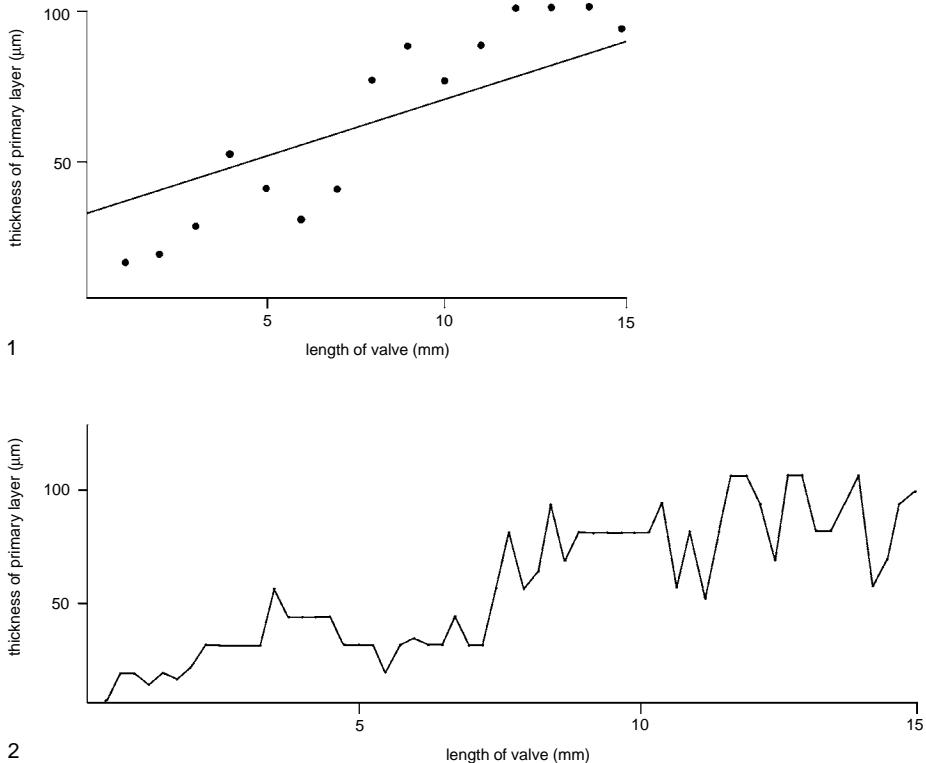


FIG. 224. Maximum thickness of the primary shell, 1, per mm and 2, per 0.25 mm, measured along a medial section of a dorsal valve of the rhynchonellide *Notosaria nigricans* (SOWERBY) (Williams, 1971a).

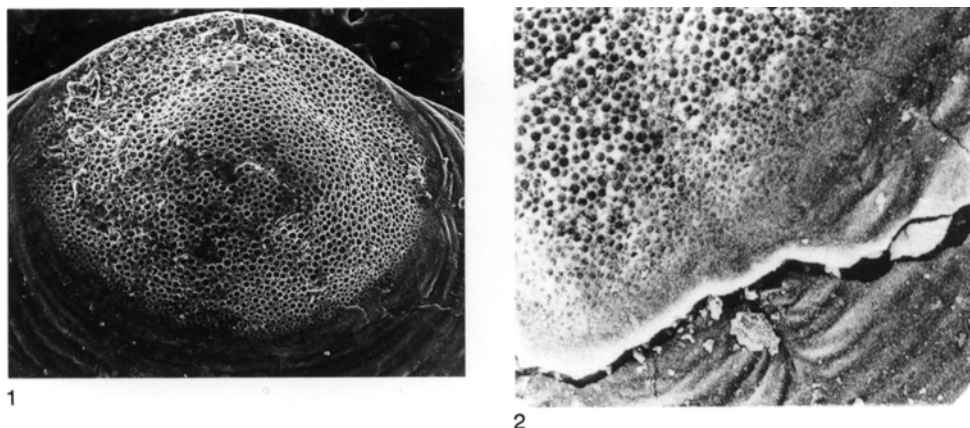


FIG. 225. Pitted larval shells of acrotretooids; 1, dorsal valve of *Scaphelasma mica* POPOV indented by hemispherical pits, $\times 43$ (new); 2, diminution and loss of hemispherical pits toward the margin of a dorsal larval shell of *Angulotreta postapicalis* PALMER, $\times 516$ (Williams & Holmer, 1992).

and anisotropic (WILLIAMS, 1971a) as is illustrated by the entire shell interior at the moment of death (superficial synchronous boundary; Fig. 223). With respect to cumulative growth, the primary layer differs from other biomineralized isotopic units in being subject only to incremental increases in thickness from umbo to anterior margin (Fig. 224). In a dorsal valve of *Notosaria* 15.5 mm long, periodic retraction of the outer mantle lobe continually reduced the primary layer to negligible thicknesses. Even so the maximum thicknesses of the primary layer increased steadily from the umbo by about $12\ \mu\text{m}$ per mm of surface length (WILLIAMS, 1971a). The primary layer of organophosphatic brachiopods is also fairly constant in thickness. In a dorsal valve of *Lingula*, the thickness of the primary layer ranged from 31 to $46\ \mu\text{m}$ (mean of $40\ \mu\text{m}$) for 15 measurements along half of a transverse section through the midregion (WILLIAMS, CUSACK, & MACKAY, 1994).

PERIOSTRACA

Periostraca have rarely been found in the fossilized state. The most remarkable preservation so far reported is the organic cover of a Late Cretaceous species of the terebratulid *Sellithyris* (GASPARD, 1982). Sufficient fabric

has survived to confirm that the *Sellithyris* periostracum was openly vesicular like that of its living relative *Liothyrella* (WILLIAMS & MACKAY, 1978). More commonly, however, features that are feasibly interpreted as casts of periostraca ornament the shell exteriors of fossil and living species.

Larval shells of acrotretooids are indented by hemispherical or flat-bottomed, circular pits (Fig. 225) ranging from $250\ \text{nm}$ to more than $5\ \mu\text{m}$ in diameter and varying in distribution from hexagonal, close packing in two sizes (*Torynelasma*) to less regular arrangements with overlapping pit boundaries (*Opsiconidion*). The pits are like negatives of bubble rafts or of the labyrinthine superstructure of terebratuloid periostraca (WILLIAMS, 1968b). They have therefore been interpreted (Fig. 226) as impressions of vesicular periostraca cast in polymerizing primary layers (BIERNAT & WILLIAMS, 1970; POPOV, ZEJINA, & NOLVAK, 1982). This would require the accumulation of vesicles infrastructurally beneath the basal layer in a succession homologous with that of *Notosaria*. Their absence from the adult shell of acrotretooids has been attributed to the post-larval secretion of a rapidly thickening, inner bounding membrane, which would have blanketed the vesicular microtopography of

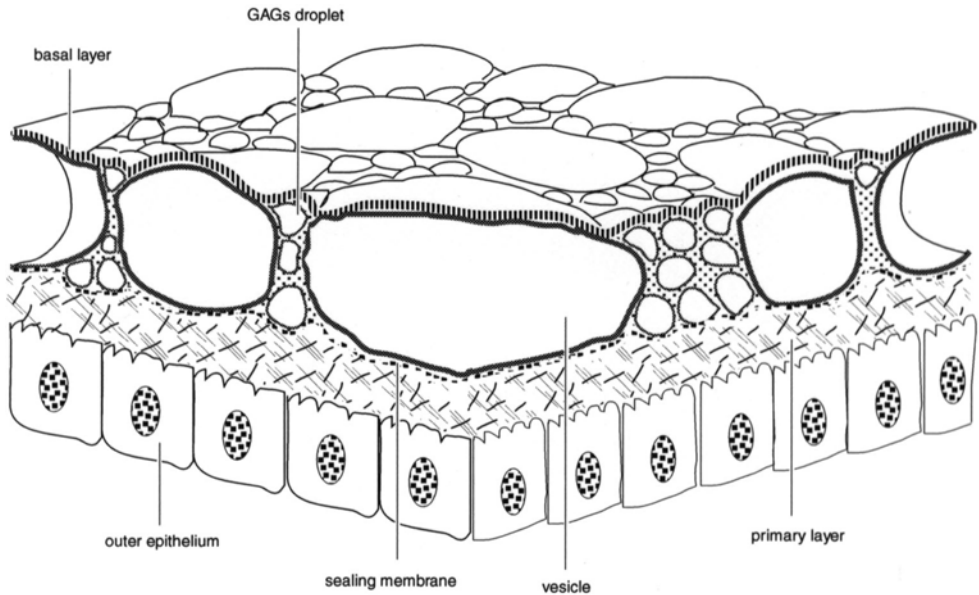


FIG. 226. Diagrammatic restoration of the acrotretoid periostracum to show its inferred relationship with the apatitic primary layer (new).

the mature periostracum (WILLIAMS & HOLMER, 1992). This is consistent with the casts of hemispherical vesicles becoming smaller and shallower toward the margin of the larval shell (Fig. 225).

An alternative interpretation of the flat-bottomed, overlapping pits, such as those of *Opsiconidion*, is that they were formed by selective resorption of successive laminae composing the larval shell (LUDVIGSEN, 1974; VON BITTER & LUDVIGSEN, 1979). This explanation is unlikely for two reasons (Fig. 227). First, surfaces undergoing biogenic resorption become pitted with irregular depressions with frayed, not sharp, edges. Second, pits that overlap like craters on biogenic surfaces do not necessarily constitute chronological successions, an essential criterion of selective resorption. Vesicles in a terebratelloid periostracum can vary from spherical bodies up to 2 μm in diameter to flattened disks no more than 250 nm thick, which are commonly stacked against one another. The overlapping arrangement of

similar bodies in an acrotretoid periostracum would therefore indicate the way they were packed during exocytosis and not their relative ages.

Pits, interpreted as casts of periostracal vesicles, also indent the postlarval shells of other extinct organophosphatic brachiopods, including the linguloid *Rowellecta* (HOLMER, 1989) and the discinoid *Orbiculoidea* (WILLIAMS & CURRY, 1991). In the latter genus they form closely packed, concentric bands becoming segregated distally into radial sets, with up to 8 pits in a row, which periodically dichotomize. The association of these radially aligned sets of pits with microscopic isoclinal folds with radial axial traces suggests that their disposition was determined by the distribution of setae at the mantle edge (Fig. 228).

Another kind of cast, found on the external surfaces of brachiopod shells, is that of the microtopography of the inner periostracal surface, which serves as a seeding substrate for the primary layer (Fig. 229). In

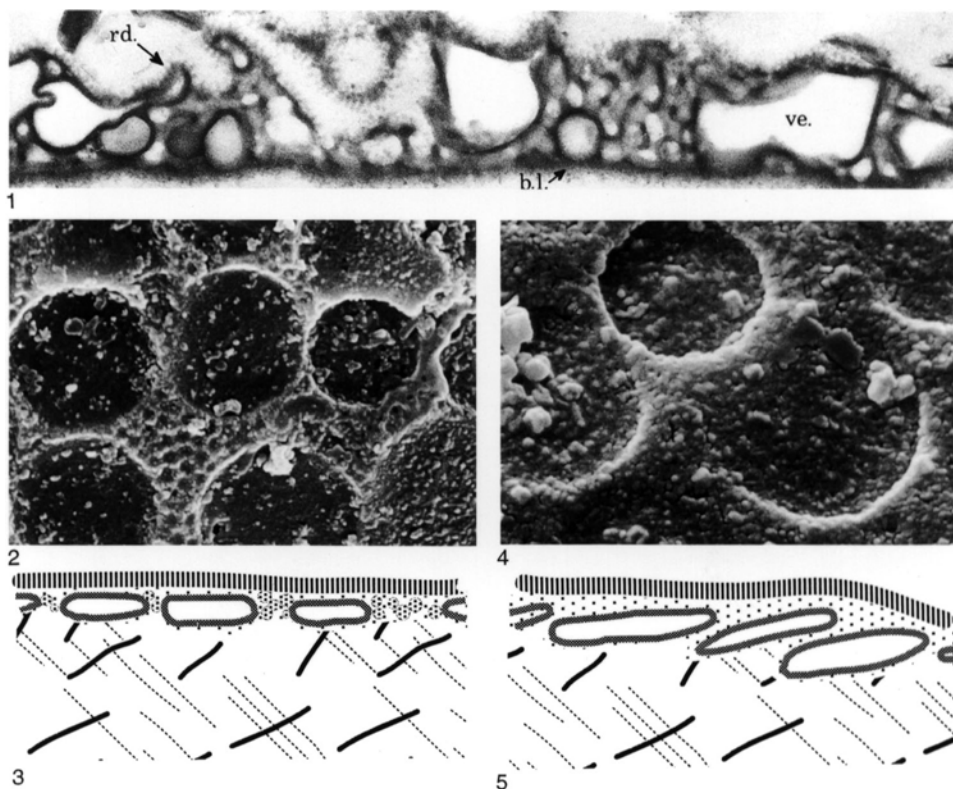


FIG. 227. Comparison of sections of the reconstructed periostracum (3, 5) of the acrotretoid *Opsiconidion aldridgei* (COCKS), as inferred from the surface of the dorsal larval shell (2, 4), $\times 4,000$, with a section of the periostracum of the terebratulide *Magellania australis* (QUOY & GAUMARD) (1) showing the basal layer (b.l.) surmounted by vesicles (ve.) and proteinaceous rods (rd.), $\times 36,000$ (new).

terebratelloids calcitic rhombs may accrete on the basal layer of the periostracum simultaneously with the continuing exudation of proteinaceous ridges along intercellular spaces of the secreting epithelium. Consequently molds of vesicular cell outlines are commonly found on the external, primary calcitic shell surface when stripped of periostracum (WILLIAMS & MACKAY, 1978). Molds originating in the same way and delineating elongate, parallel-sided vesicular cells also occur sporadically on acrotretoid shell surfaces (WILLIAMS & HOLMER, 1992). Vesicular cell outlines are probably sporadically but widely preserved on the surfaces of brachiopod shells throughout the Phanerozoic.

PRIMARY LAYER

Differences in the composition of the primary layers of organophosphatic and calcitic brachiopods are responsible for striking dissimilarities in their fabrics. There are also compositional differences among species within these two groups. Thus the proportion of finely granular apatite present in the primary layer of living organophosphatic species is greater in discinids than in lingulids; but the matrix, which is mainly GAGs, determines those characteristics of greatest morphological interest. Accordingly, irrespective of the levels of concentration of the dispersed apatite, the layer acts as a

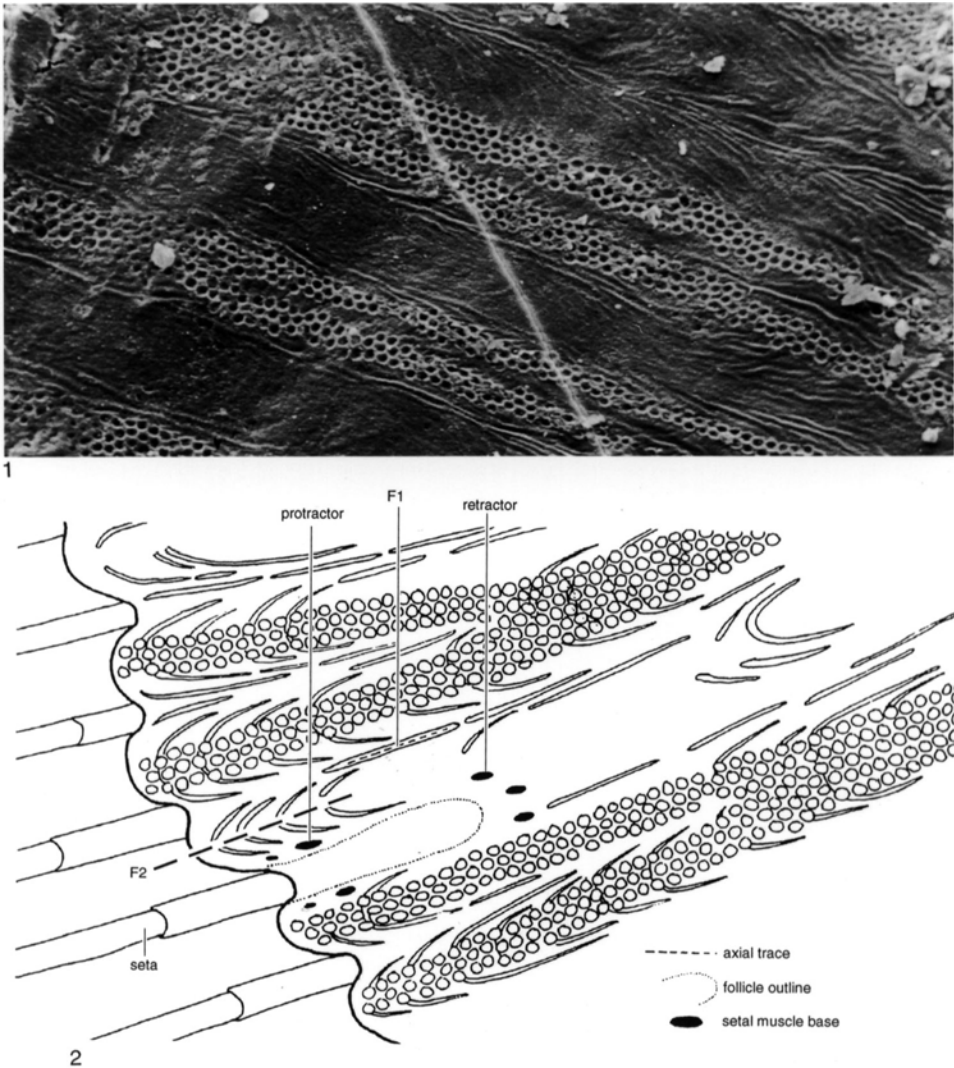


FIG. 228. 1, Radial arrays of pits on the surface of a dorsal valve ($\times 570$) of the discinoid *Orbiculoidea nitida* (PHILLIPS) and 2, their inferred relationship in life with setae and their principal muscle systems at the mantle edge (Williams & Curry, 1991).

flexible, plastic body that polymerizes slowly enough to preserve not only impressions of the overlying periostracum but also microscopic fold systems resulting from stress fields operating at the shell margin. These include the differential pull at sites along the outer mantle lobe by protractor and flexor muscles activating setae and the variation in rates of secretion of the periostracum relative to the migration of associated vesicular cells.

Stress fields set up by setae are believed to be responsible for deforming concentric folds of primary shell (fila) into sets of discrete arcs (drapes) (Fig. 230–231; WILLIAMS & HOLMER, 1992), while complex fold systems, found on the surfaces of many well-preserved fossil and living shells, represent the latter (Fig. 232).

The primary layer of calcareous-shelled brachiopods is essentially a brittle crystalline

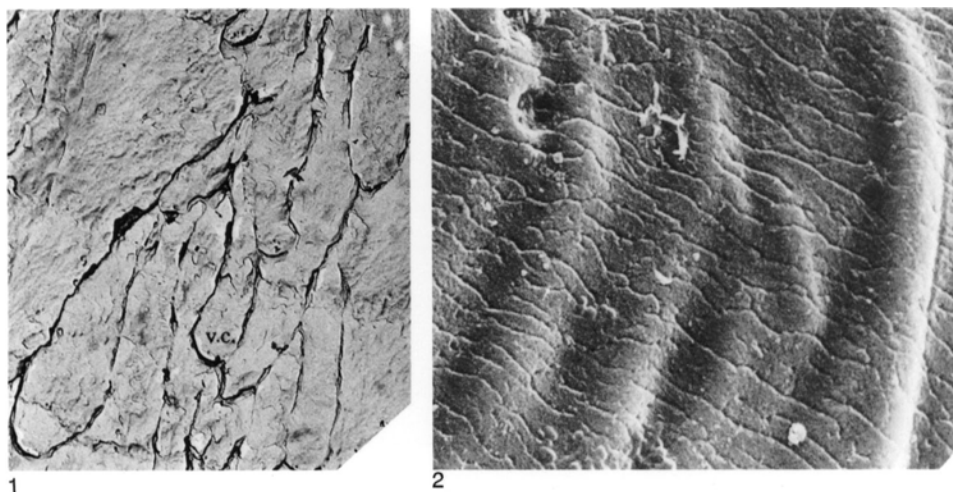


FIG. 229. Vesicular cell (*v.c.*) casts on primary shell surfaces; 1, external surface of the terebratulide *Calloria inconspicua* (SOWERBY), $\times 7,100$ (Williams & Mackay, 1978); 2, external surface of the acrotretoid *Prototreta* sp., $\times 2,050$ (Williams & Holmer, 1992).

medium, and its fabric is normally finely granular or acicular (Fig. 233; WILLIAMS, 1968a, 1973; MACKINNON & WILLIAMS, 1974), although it can also be sporadically tabular or lenticular with aggregates of crystallites up to $2\ \mu\text{m}$ in size as in *Neocrania* (WILLIAMS & WRIGHT, 1970). Even so, radial sections of the layer commonly show synchronous shell units as a distinct banding inclined at acute angles to the primary-

secondary isotopic interface. Such bands are traces of old depositional surfaces and are parallel with the section of the superficial synchronous boundary, on which the outer face of the outer mantle lobe rests (WILLIAMS, 1971a; GASPARD, 1991).

The nature of these surfaces is well shown by sections of valves of living thecideidines, which are composed almost entirely of primary shell (Fig. 233). In *Thecidellina* the

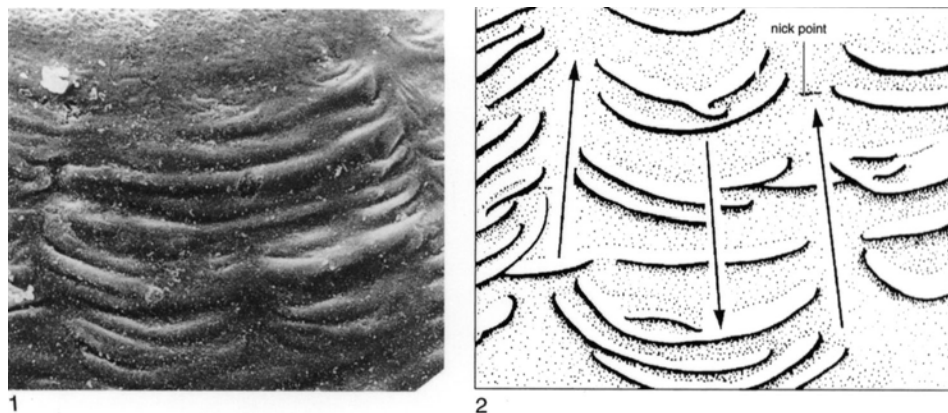


FIG. 230. 1, Discrete folds interrupting fila on the external surface of the dorsal valve of the acrotretoid *Angulotreta triangulatus* PALMER, $\times 700$; 2, diagram of the inferred stress couples responsible for the folds, $\times 700$ (Williams & Holmer, 1992).

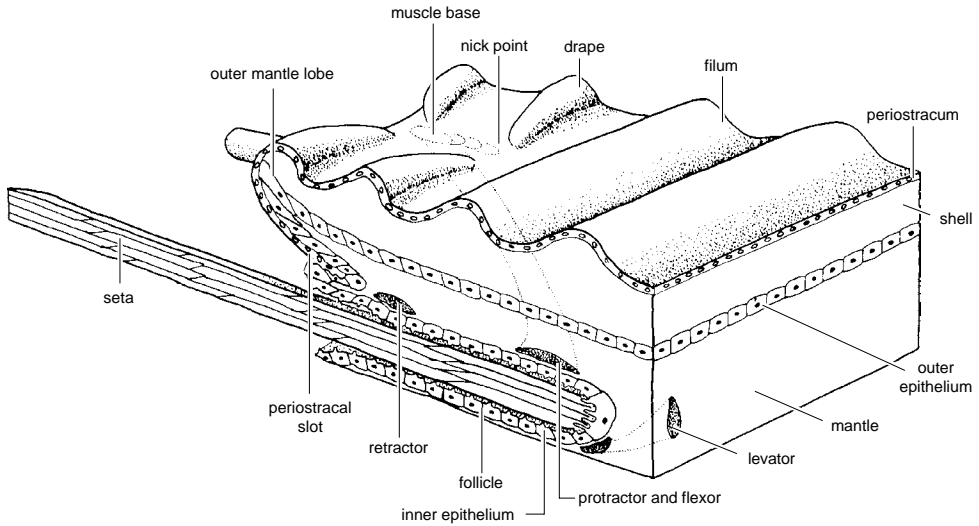


FIG. 231. Inferred structure of the outer mantle lobe of a living acrotretoid in relation to the shell, a follicle, and the muscles controlling the seta; all features are assumed to have been arranged as in *Lingula* (Williams & Holmer, 1992).

basic constituents are calcitic crystallites between 250 and 400 nm thick and up to 15 μm long with rhombic or scalenohedral ter-

minal faces, which tend initially to be disposed as overlapping rows. As the shell thickens, crystallites frequently amalgamate into

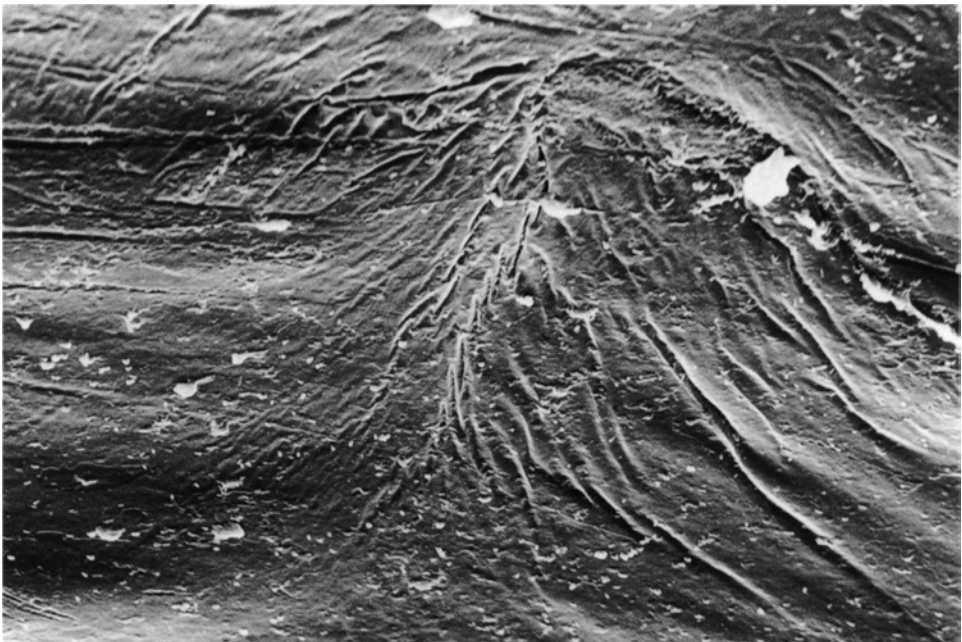


FIG. 232. Isoclinal folds affecting the periostracum and primary layer of *Glottidia pyramidata* (STIMPSON); the folds close in a posteromedian direction, $\times 140$ (new).

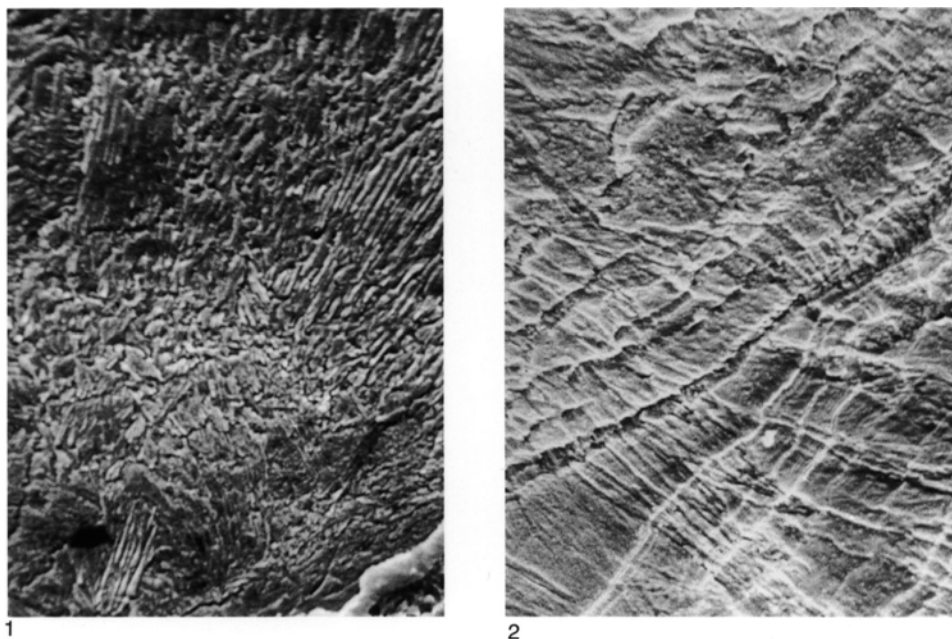


FIG. 233. The ultrastructural fabric of the primary layer; 1, etched section of the ventral valve of *Neocrania anomala* (MÜLLER) with periostracum and underlying substrate in bottom right-hand corner, $\times 2,400$ (new); 2, etched section of the dorsal valve of *Thecidellina barretti* (DAVIDSON) showing a transgression of one set of growth bands over another, $\times 1,300$ (Williams, 1973).

impersistent lenticular blades or mosaics, but the overall fabric is that of acicular crystallites in epitaxial continuity even across transgressive growth surfaces. The microtopography of this primary fabric of *Thecidellina* consists of tubercles up to $30\ \mu\text{m}$ high, made up of crystallites that are disposed normal to the outer surface and closely packed groups of rhombs composed of acicular crystallites aligned parallel with cleavage planes (Fig. 234).

Despite the fact that any biomineralized succession always includes a first-formed layer secreted on an external organic substrate (periostracum), such a primary layer is not always found in fossilized shells. Comprehensive studies have confirmed its existence in most of the early brachiopod stem groups (WILLIAMS, 1968a; HOLMER, 1989) but occasionally only with great difficulty for two reasons. First, the biomineralized primary layer may have been so thin and of such an open microtexture in the original

state as to facilitate replacement by entombing rock matrix (WILLIAMS, 1970a). Second, the primary layer of organophosphatic fossil species may have been largely organic (as in some living *Lingula anatina*) and therefore subject to prediagenetic degradation. The sporadic occurrence of the primary layer in some linguloid species described by HOLMER (1989) may be evidence of this circumstance.

SECONDARY LAYER

The secondary layer is the most variable succession of the brachiopod shell within as well as among species groups. Six different kinds of fabrics are already known with two being characteristic of wholly extinct groups, and more are expected to be discovered as study of early Paleozoic stocks progresses. The three fabrics of the organophosphatic brachiopods are inherently the most diverse but are more obviously related to one another than to those of calcitic brachiopods, which are less variable in composition.

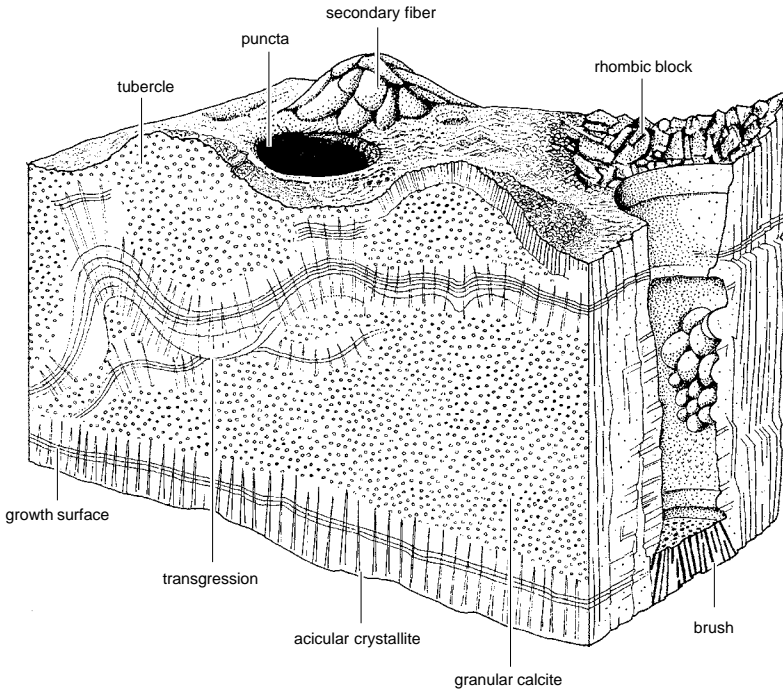


FIG. 234. Diagrammatic view of a sectioned block of *Thecidellina* shell showing some of the microtopographic and fabric features, approximately $\times 640$ (Williams, 1973).

ORGANOPHOSPHATIC LAMINATION

The compositional and structural diversity of the secondary organophosphatic shell is well displayed in living lingulids. In *Lingula*, four constituents identifiable at ultrastructural level (Fig. 235)—apatitic granules, chitinous strands, fibrillar collagens, and all-pervading GAGs—are assembled into a succession of isotopic and isochronic laminae with thicknesses measured in microns compared with areas frequently of several square millimeters (Fig. 236). Compact laminae composed of closely packed spheroidal aggregates of apatitic granules (spherules) are succeeded by botryoidal or walled laminae, in which apatitic aggregates form botryoidal masses or vertical walls in a GAGs matrix, or by rod and plate laminae with apatitic rods accreting into anastomosing ridges disposed transversely on the body platform and radi-

ally in peripheral regions (Fig. 235, 237). Membranous laminae in GAGs can occur throughout the succession, while stratified laminae, characterized by gently inclined, alternating organic and apatitic units, each about $1 \mu\text{m}$ thick, are especially well developed at the junction with the primary layer.

These laminae can pass laterally from one kind to another. Even so, they usually group into well-defined rhythmic sets passing gradually from a mainly apatitic lamina to a terminating membrane(s) that is a substrate for the next set. The laminar fabric of living *Lingula* is also characteristic of fossil lingulids (CUSACK & WILLIAMS, 1996).

The fabric of *Glottidia*, however, is distinguishable from that of *Lingula* in including laminae consisting of regular arrays of rods (baculi) coated with spherular apatite that commonly subtend acute angles with one another and are generally inclined at high

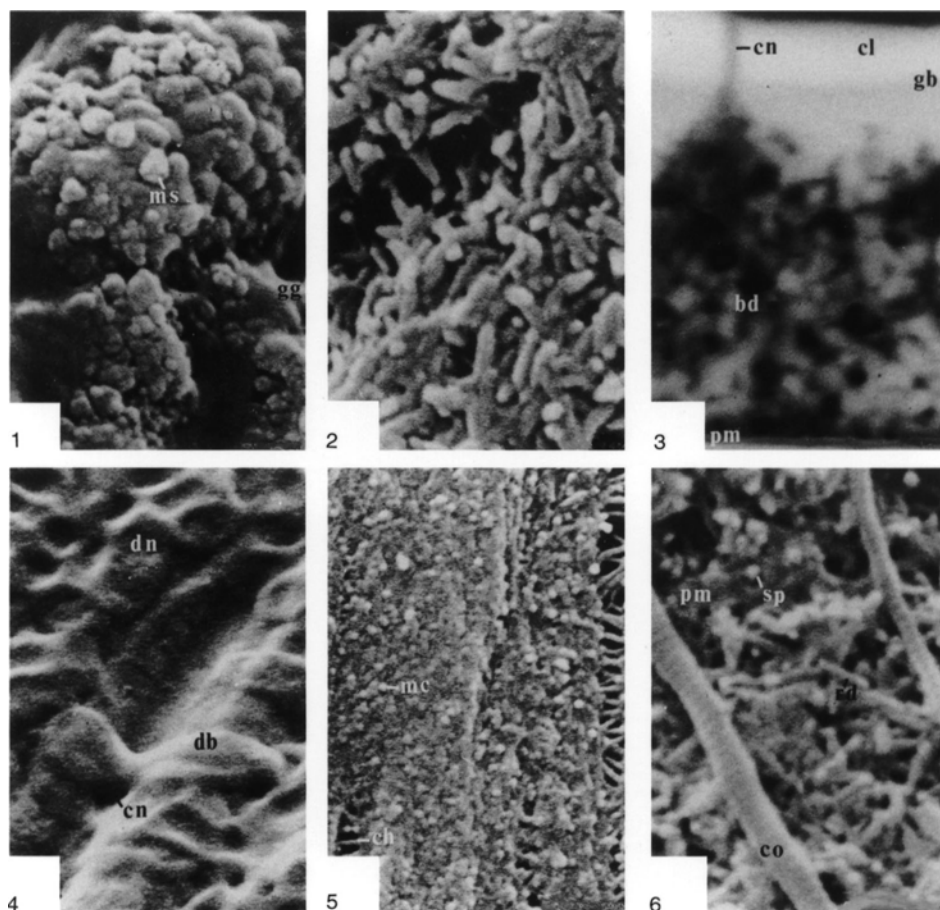


FIG. 235. The ultrastructure of the main constituents of the shell of *Lingula anatina* LAMARCK; 1, botryoidal aggregates of apatitic mosaics (*ms*) in a matrix of GAGs (*gg*), $\times 11,552$; 2, rods and mosaics of apatite, $\times 11,552$; 3, back-scattered electron micrograph of a lamina showing a rhythmic unit of secretion from a predominantly apatitic base (*cl*) of packed mosaics (*white band* at top of micrograph), penetrated by the organic contents of a canal (*cn*) and terminated by a boundary (*gb*) marking the onset of GAGs secretion through a zone of dispersed mosaics and rods (*bd*) to an organic lamina (*pm*; *black band* at bottom), $\times 4,043$; 4, residual GAGs with contraction depressions (*dn*) and discoidal bodies (*db*) on ridges of apatite with a canal (*cn*), $\times 8,056$; 5, chitinous fibers (*ch*) coated with apatitic mosaics (*mc*), exposed in tension cracks, $\times 8,664$; 6, collagen fibrils (*co*) associated with apatitic rods (*rd*) and spherules (*sp*) in a muscle scar membrane (*pm*), $\times 20,216$ (Williams, Cusack, & Mackay, 1994).

angles to the surfaces of bounding laminae (Fig. 238.1). A baculate lamina appears to have been a primitive fabric as it has been found in such Ordovician linguloids as *Ungula* and *Pseudolingula* (HOLMER, 1989).

The discinid secondary fabric, as typified by that of *Discina*, differs from that of lingulids mainly in the higher biomineral con-

tent (Fig. 239). As a result, compact laminae are usually about twice as thick (6 to 7 μm) as those of *Lingula*; and the botryoidal and walled laminae of *Lingula* are normally represented by poorly bedded (rubbly) successions of mosaics and lenticles up to 2 to 3 μm in lateral spread. Stratified laminae, however, are present immediately below the primary

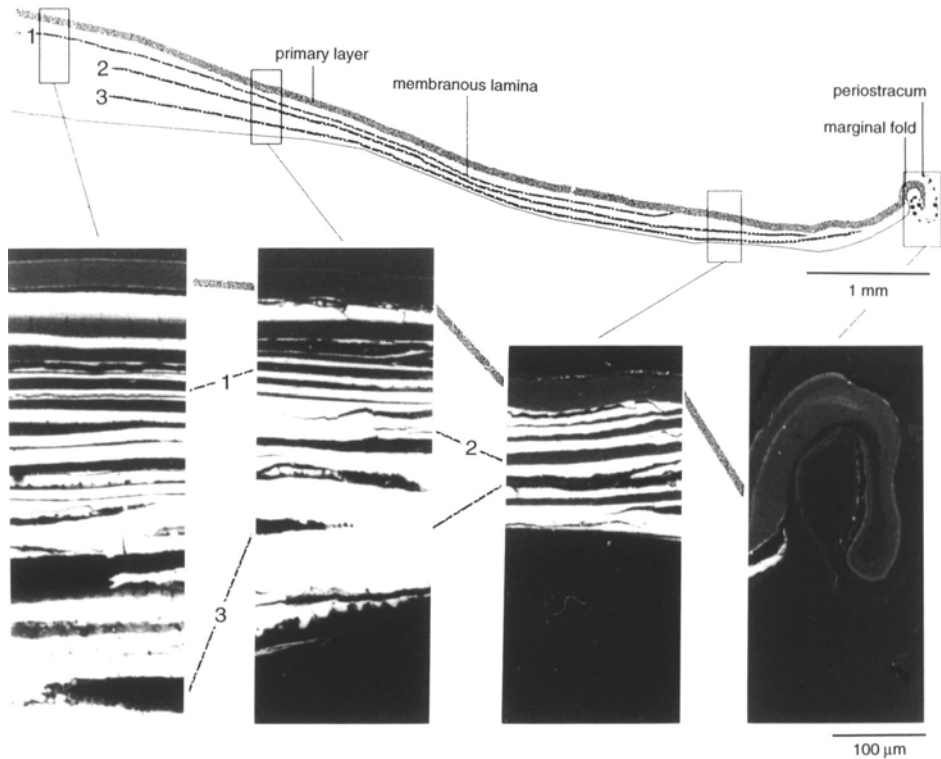


FIG. 236. Back-scattered electron micrographs of the successions at four indicated traverses of a transverse section of half of a valve of *Lingula anatina* LAMARCK showing variations in the apatitic content (white) and in three numbered prominent organic laminar sets (black) (Williams, Cusack, & Mackay, 1994).

layer, and baculate laminae are as well developed as they are in *Glottidia*, confirming the early phylogenetic origin of this fabric (WILLIAMS, MACKAY, & CUSACK, 1992)

The most extraordinary secondary fabric yet found is that of the lower Paleozoic acrotretoids (Fig. 240; POULSEN, 1971; HOLMER, 1989). The secondary shell consists of an overlapping stack of laminae, each of which can normally be traced throughout the skeletal succession internal of its subcircular junction with the primary layer. Each lamina is separated from its neighbors by a continuous, slotlike space (presumably the site of a membranous sheet) and consists of a pair of granular, apatitic lamellae (Fig. 241). The lamellae, which are contiguous medially, open up outwardly to form a wedgelike laminar margin enclosing variably developed spaces. In some acrotretoids, the

apatitic walls of these spaces are studded with domes (Fig. 240.3) and connected by apatitic columns (Fig. 240.1–240.2) with hollow cores (columnar laminae). In others, the spaces are divided into boxlike compartments by vertical partitions of apatite (Fig. 240.4) with narrow (200 nm) medial spaces (camerate laminae). These medial spaces coincide with intercellular spaces found in the primary layer and are assumed to have been occupied by membranes in life. In determining how spaces with domes and columns and membrane-covered empty boxes of apatite originate, it has to be assumed that in life the spaces were filled with discrete bodies of granular apatite in a GAGs matrix; and this apatitic mesh contributed to the biomineralized coats of camerate membranous partitions and organic strands that formed the substrates for domes and columns (Fig. 241).

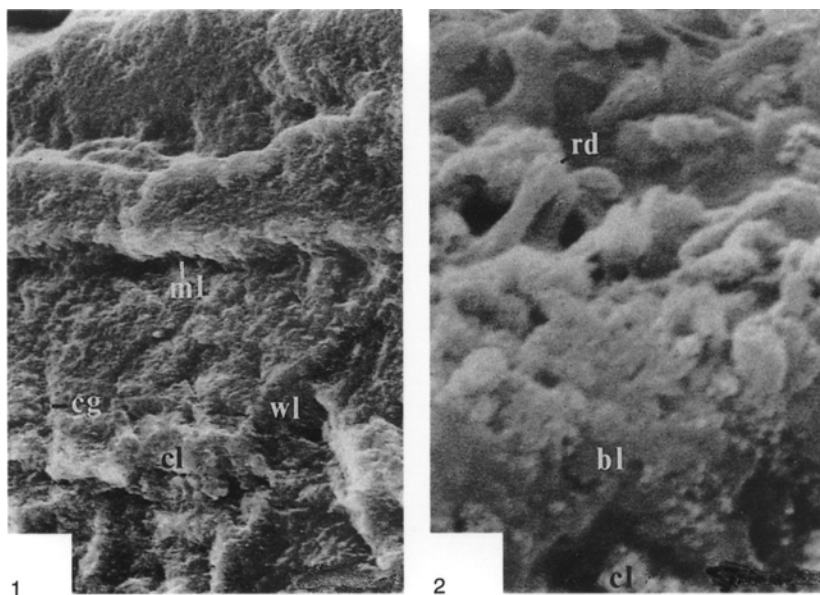


FIG. 237. Sections of the shell of *Lingula anatina* (LAMARCK) showing rhythmic laminar sets; 1, three cleaved (*cg*) sets, each consisting of a compact lamina (*cl*) passing into a walled lamina (*wl*) and a capping membranous lamina (*ml*), $\times 1,300$; 2, compact lamina (*cl*) passing through a botryoid (*bl*) into a lamina of rods and plates (*rd*) embedded in GAGs, $\times 14,000$ (Williams, Cusack, & Mackay, 1994).

The secondary fabric of the problematic organophosphatic paterinides is also anomalous although more readily interpretable

(POPOV & USHATINSKAYA, 1987). The secondary layer, which constitutes the sole succession of the genera described (*Cryptotreta*,

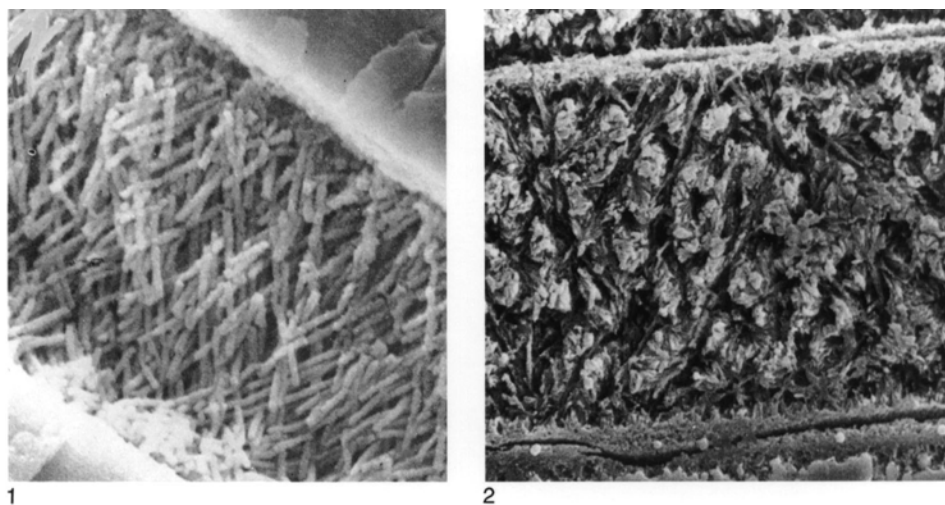


FIG. 238. Sections of linguloid shells showing the disposition of baculi between compact laminae; 1, recent *Glottidia pyramidata* (STIMPSON), $\times 2,200$ (Iwata, 1982); 2, Early Ordovician *Ungula ingraca* (EICHWALD), $\times 3,300$ (Holmer, 1989).

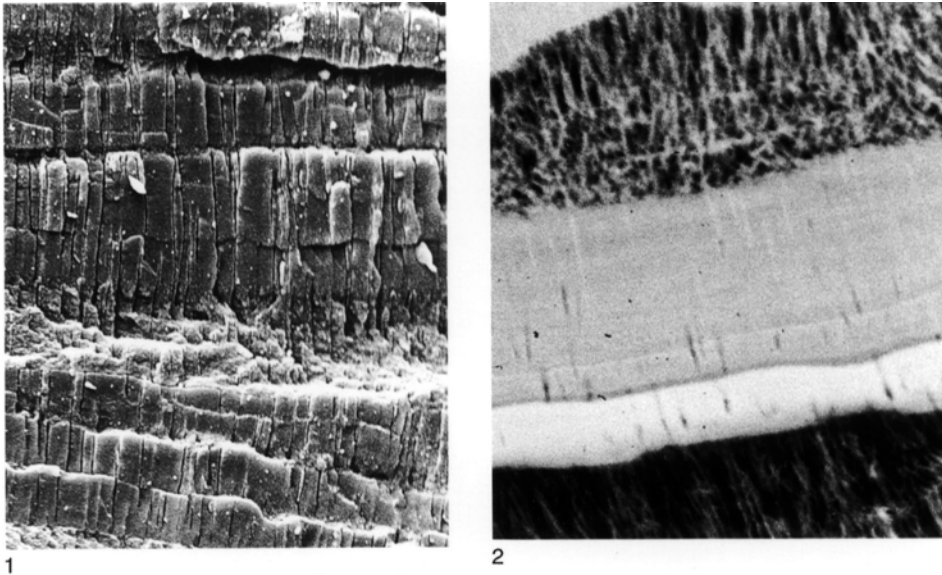


FIG. 239. Sections of the shell of *Discina striata* (SCHUMACHER); 1, SEM showing thick apatitic laminae seamed by canals with rubbly laminae in midsection indicative of discrete apatitic components including baculi, $\times 720$; 2, back-scattered electron micrograph of compact laminae (white) between baculate laminae (vertically striped), $\times 1,260$ (new).

Micromitra), consists of almost horizontal laminae up to 40 μm thick, composed of hexagonal, closely packed vertical prisms about 7 to 8 μm thick. In *Dictyonina*, the laminar microtexture is known to be spherular in aggregates up to 1 μm across (WILLIAMS, MACKAY, & CUSACK, 1992). If the apatitic prisms with their surrounds were secreted by cuboidal epithelium (POPOV & USHATINSKAYA, 1987), one can also assume that the primary layer, which together with the periostracum would have been exuded by elongate vesicular cells of the outer mantle lobe, consisted mainly of GAGs and would not have been preserved. In such a setting the paterinide prismatic fabric would have been analogous with that of the terebratulid tertiary layer.

CALCITIC FABRICS

The three kinds of secondary fabric found in calcitic-shelled brachiopods differ not only in their structure but also in their relative importance within the phylum as a whole. A fibrous fabric has always been the

dominant feature of articulated shells except possibly during the Permo-Carboniferous when the cross-bladed, laminar strophomenides (*s.l.*) attained the peak of their diversity. In comparison with these major groups, the inarticulated calcitic species characterized by tabular laminae had a relatively modest distribution in the lower Paleozoic but, unlike the strophomenides, they survive to the present day and their living representative, *Neocrania*, furnishes an insight into laminar secretion.

CALCITIC FIBERS

The fabric of a fibrous, secondary shell is unmistakable in surface view and in section (WILLIAMS, 1966, 1968a, 1971b). On the internal surfaces of a valve, the transition from primary to secondary fabric is relatively sudden. In *Notosaria*, for example, the radial distance between the first traces of the arcuate fronts of newly formed fibers and fully developed ones is less than 20 μm . As the secondary shell thickens, these discrete patches of calcite (about 10 μm across) with

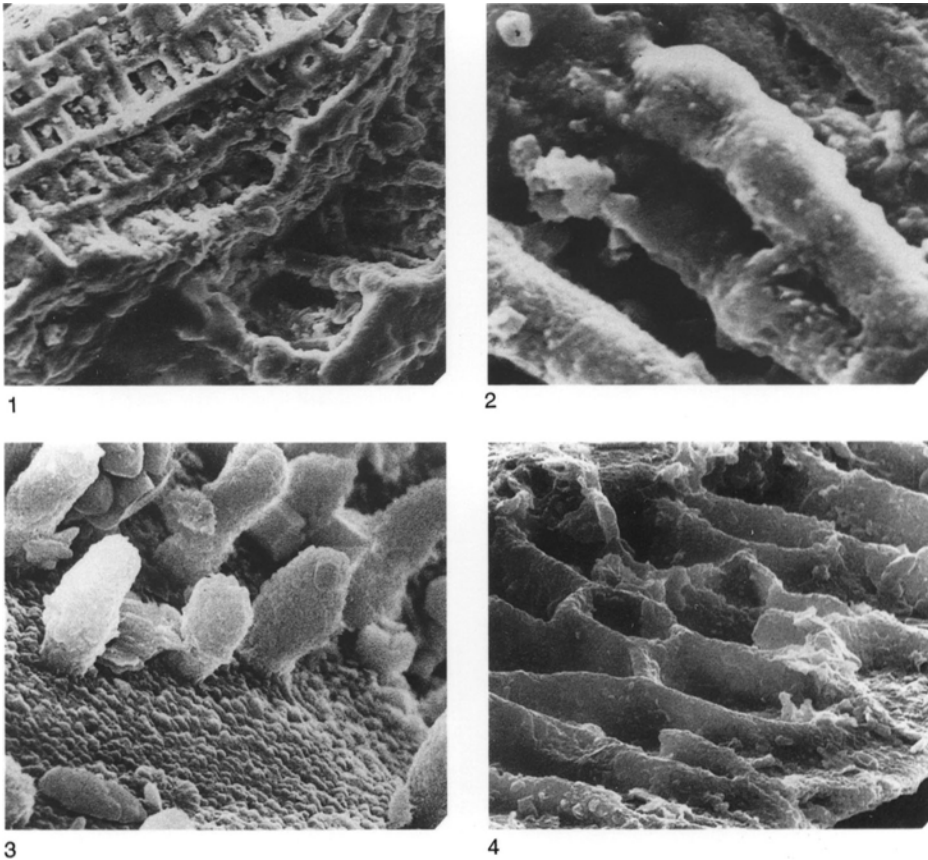


FIG. 240. Columnar and camerate fabric structures in acrotretoid secondary shell; 1, general view of a columnar laminate succession, $\times 710$, with 2, details of columns, $\times 3,000$, and 3, of domes in a section of a ventral valve of *Angulotreta postapicalis* PALMER, $\times 4,100$; 4, internal margin of a dorsal valve of *Hisingerella tenuis* showing the disposition of partitions in a camerate lamina, $\times 2,200$ (Williams & Holmer, 1992).

their surrounding membranes become elongated into fibers ensheathed in proteinaceous sheets. In this way the internal surface of secondary shell is fashioned into a distinctive mosaic that is really a protein-calcite cast of the secreting plasmalemmas of outer epithelium (Fig. 242).

The mosaic has a discernible lineation reflecting the incremental growth relationship of fibers that can be graphically represented by plotting the long axes of exposed parts of fibers (keels) as growth vectors. The resultant growth maps are informative (Fig. 243–244). For example, they show that extensions of fibers normal to the edges of convex valves

are only characteristic of a narrow peripheral zone. Inwardly the terminal faces of fibers become reoriented more or less parallel to the valve margin. Accordingly, each fiber tends to grow in a spiral arc directed clockwise in the right half of a valve and counterclockwise in the left half (WILLIAMS, 1968a; BAKER, 1970b). Modifications of this pattern, the characteristic trace (WILLIAMS, 1971a), include the formation of microscopic whorls, in which individual fibers can be bent into open spirals (see Fig. 274). Such configurations can be regarded as solid-state summaries of the dynamics of epithelial migration during shell growth as each traces

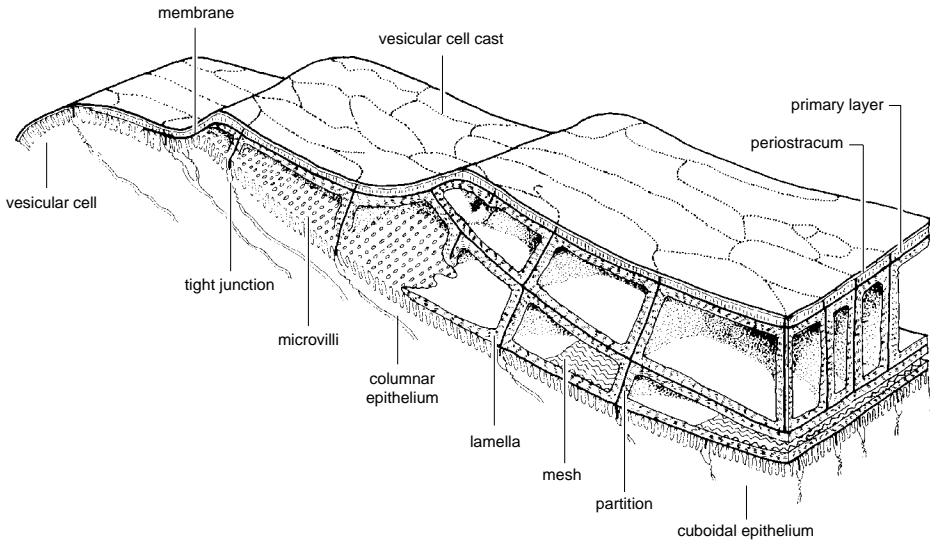


FIG. 241. Inferred relationships between the mantle and its outer lobe and the valve margin of the acrotretoid *Hisingerella* in life (Williams & Holmer, 1992).

successive loci of a secretory cell. All internal outgrowths of secondary shell result from accelerated rates of secretion and are built up of fibers lengthened and reoriented in this way.

Differential growth of the fibrous secondary shell is facilitated by the mode of stacking of the fibers (Fig. 242). Fibers within their membranous sheaths remain segregated from one another throughout life and interlock to achieve the best possible fit without impeding localized variations in growth. The arrangement is best understood in terms of shape of the fibers. In medial longitudinal section, fibers appear as blades that gradually become wider toward their terminal faces in phase with the increasing size of the maturing cells secreting them. The fibers are initially inclined outward at about 10° to the isotopic interface with the primary layer but may become reoriented with further growth. In contrast to this relatively simple longitudinal profile, cross sections of a typical fiber show that it is bounded by an inner, keeled surface that is flatly to roundly concave outward and an outer surface made up of two lateral arcs and a medial saddle, all also con-

cave outwardly. This profile corresponds to the topography of the mosaic. The inner surface with its keel represents the terminal face of the fiber and its exposed posterior trail respectively, while the outer lateral areas rest on the two adjacent halves of fibers in the immediately younger row, and the saddle accommodates the keel of the next younger fiber. During the growth of a fiber, its transverse outline also changes and usually flattens as it enlarges laterally. A composite picture of these changes is provided by any transverse section of a secondary layer.

A fibrous fabric is invariably characteristic of the secondary shell of living rhynchonellids and terebratulides and is well developed in earliest known genera, such as the Devonian *Mutationella* and the Ordovician *Rostricellula*, respectively. It is also the standard fabric for all spire-bearing brachiopods, pentamerides, and most orthides (Fig. 245; WILLIAMS, 1968a). Even the problematic dictyonellidines have been shown to have some fibrous secondary shell (WRIGHT, 1981).

The secondary fibrous layer is, of course, variably developed in all groups; but no such changes are so spectacular as the neotenous

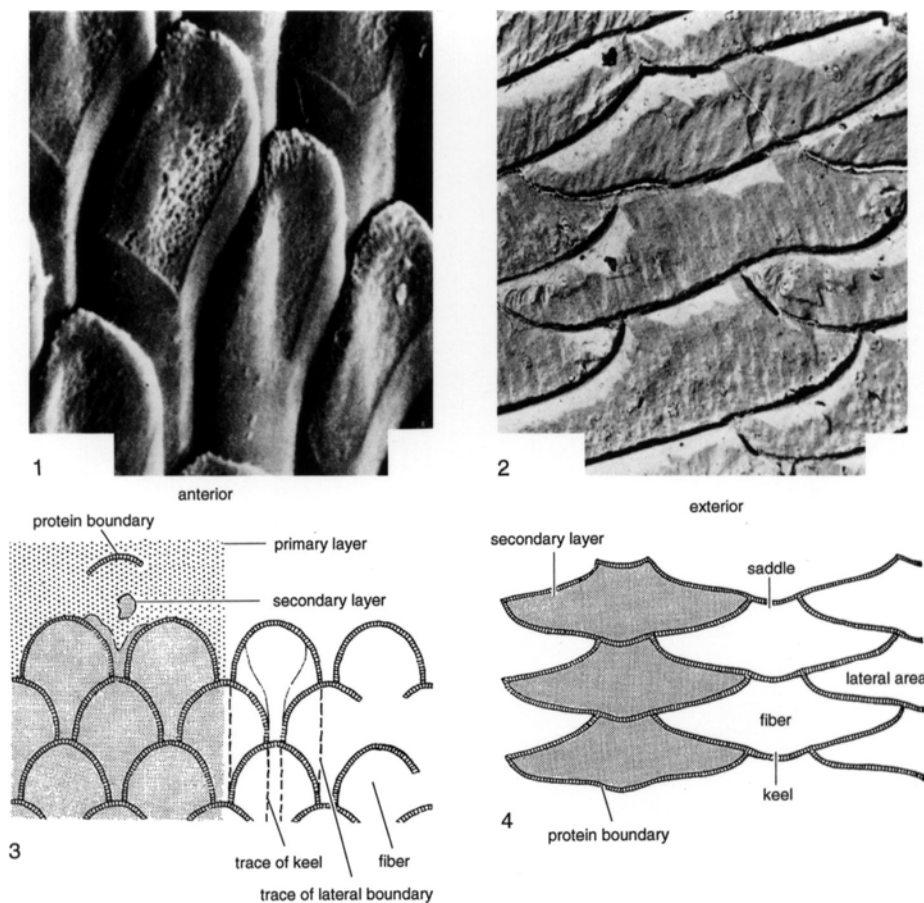


FIG. 242. Mosaic of the fibrous secondary shell of the rhynchonellide *Notosaria nigricans* (SOWERBY); 1, terminal faces of fibers exposed in the floor of a valve, $\times 2,000$; 2, transverse section of orthodoxy stacked fibers, $\times 4,000$ (Williams, 1968d); 3–4, morphology of terminal faces and transverse sections respectively of orthodoxy stacked fibers (Williams, 1966).

reduction of the layer in the thecideidines (Fig. 246; WILLIAMS, 1973; BAKER, 1991). Such early Mesozoic thecideidines as *Davidsonella* and *Moorellina* have continuous layers of fibrous secondary shell. Post-Jurassic members of all lineages, however, were affected by a heterochronous, progressive loss of secondary shell so that, in living *Thecidellina* and *Lacazella*, orthodoxy stacked fibers are restricted to the teeth and additionally occur in the sockets and as microscopic patches on internal tubercles of the former genus. On the other hand, the shell contin-

ues to thicken throughout life so that the acicular and granular calcite of the primary layer is seamed with growth banding bearing frequent signs of interrupted accretion or absorption and widely distributed microscopic features like tubercles and closely packed rhombic blocks on mature internal surfaces.

During the evolution of the fibrous secondary sheet, fibers have varied in shape from large rods with lenticular cross sections of the spiriferide *Koninckina* to broad, flat structures commonly interleaved with lenses

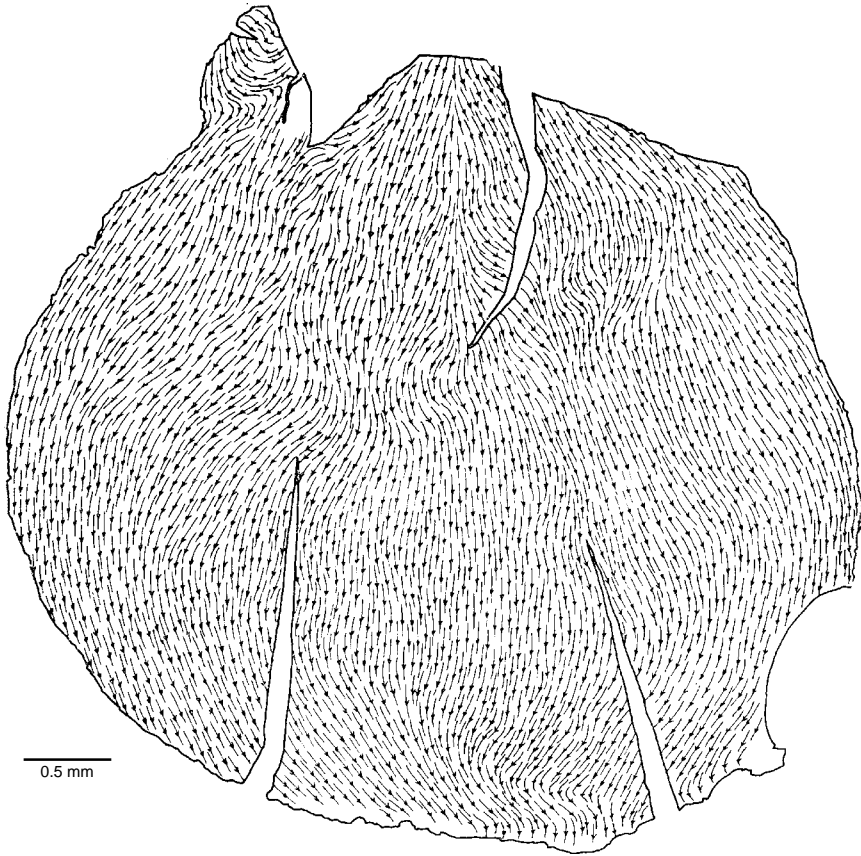


FIG. 243. Growth map of the mosaic of the dorsal valve of the rhynchonellide *Notosaria nigricans* (SOWERBY), using the long axes of exposed fibers as vectors of growth (Williams, 1968a).

of prismatic calcite as in pentameroids and many spire-bearing species. Yet there is no doubt that this fabric was typical of some of the oldest-known calcitic brachiopods like *Nisusia* and *Kotujella* (WILLIAMS, 1968c) and was the dominant fabric among articulated brachiopods.

CALCITIC TABULAR LAMINATION

The secondary fabric of the remaining articulated brachiopods, the extinct billingelloids and strophomenides, is more easily interpreted if that of the living inarticulated calcitic brachiopod *Neocrania* is considered first.

The secondary shell of *Neocrania* has a laminar fabric, seen in section as a succession

of calcitic plates (Fig. 247.1) separated from one another by interconnected proteinaceous membranes. On the internal surface of a valve, the laminae are seen as overlapping tablets that are rarely perfectly rhombohedral (Fig. 247.2). They normally occur as single or double screw dislocations with fine growth banding on the tablet faces. The banding registers the incremental (possibly diurnal) growth of tablets recording, for example, sudden increases in corner angles from 75° to 135° or 150° so that extra hexagonal and dihexagonal edges are added by spiral growth to impart a subrounded outline to large laminae. If adjacent nuclei are crystallographically aligned, they may amalgamate into a composite tablet with a common

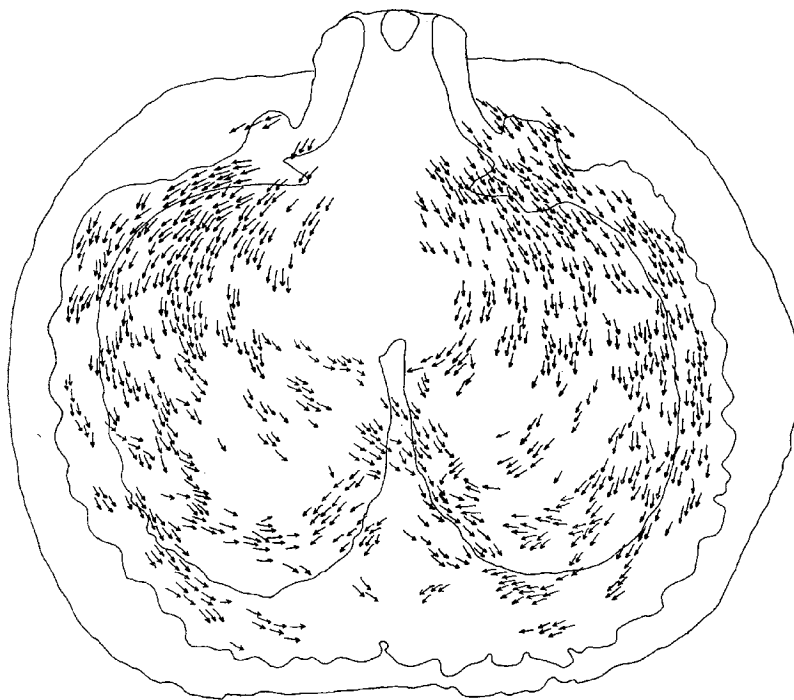


FIG. 244. Reconstruction of the secondary growth mosaic of the thecideidine *Moorellina granulosa* (MOORE), plotted from 25 superimposed peels (Baker, 1970a).

accretionary border. More usually, laminae are not aligned, and the junctions between neighboring units persist as cracks or notches. Where the edges of three or more laminae meet, triangular or trapezoidal enclosures occur.

Two constraints must be taken into account when considering how such a laminar shell is deposited as an alternating succession of tablets and membranes. First, discrete biomineral tablets require an organic substrate on which to seed and expand. Second, as nearly all tablets are affected by screw dislocation, they grow spirally by calcitic accretion along dislocation edges. Consequently as a calcitic lamina undergoes lateral accretion, it simultaneously presents an expanding inner surface for settlement by proteins, which polymerize into a new membrane. But the lamina is normally part of an expanding helicoid spiral so that its newly accumulating proteinaceous coat is also part of one con-

tinuous strip rotating just behind the dislocation front around the helicoid axis. Hence, the membrane acts as a cover for one calcite surface and a foundation for a later-forming calcitic tablet in the manner shown in Figure 248 (WILLIAMS, 1970b).

Secondary shell deposition in *Neocrania*, therefore, involves simultaneous secretion of protein and calcite by outer epithelium at different levels within a laminar succession. In effect, the succession thickens and expands laterally by spiral growth, which is a continuous, not an episodic, process. Spiral growth of this kind also affords sufficient biomineral continuity between levels within a shell succession to ensure a general crystallographic alignment (epitaxy) even when intervening proteinaceous membranes are imperforate.

This secondary laminar fabric of tablets is characteristic of all cranioids although it is variably developed in the ventral valve, by

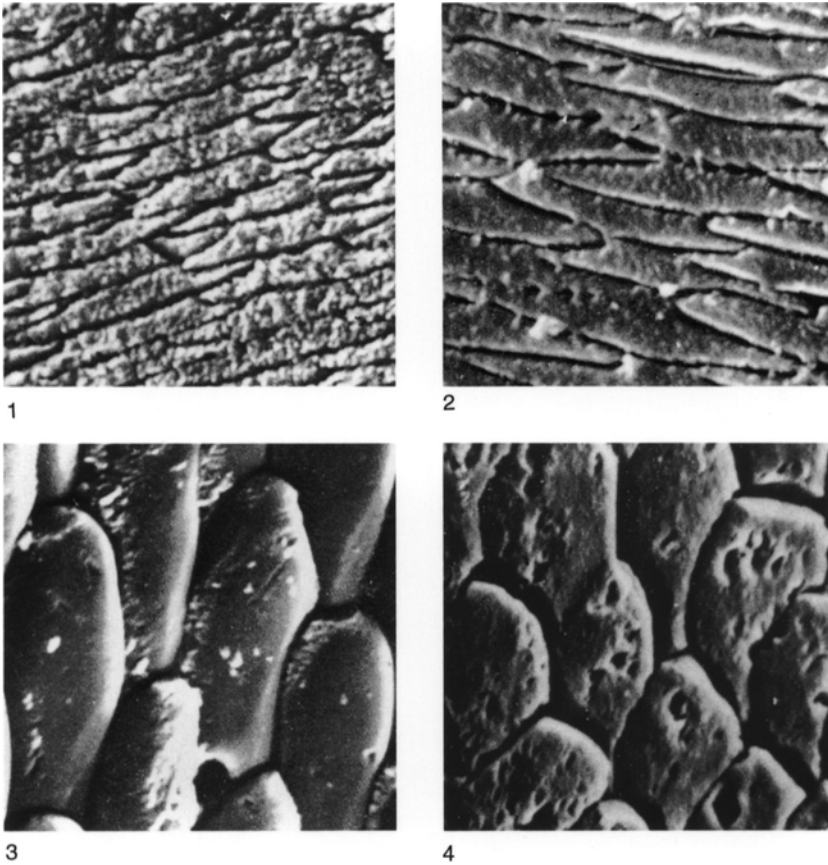


FIG. 245. Sections and internal surface views of the fibrous secondary shell of articulated brachiopods; 1, Ordovician rhynchonellide *Rostricellula lapworthi* (DAVIDSON), $\times 2,600$; 2, late Silurian terebratulide *Mutationella podolica* (SIEMIRADZKI), $\times 2,700$; 3, Jurassic spiriferide *Spiriferina walcotti* (SOWERBY), $\times 1,300$; 4, Pennsylvanian enteletoid *Rhipidomella* sp., $\times 1,300$ (Williams, 1971b).

which all but the oldest cranioids are cemented to the substrate. Indeed the ventral valve is commonly represented only by primary shell, and even this biomineralized layer may be absent as in species of *Craniscus*. Primary and secondary fabrics, however, were developed in both valves of the oldest known cranioid, the Ordovician unattached *Pseudocrania* (WILLIAMS & WRIGHT, 1970).

Two other inarticulated groups have calcitic shells with well-developed primary and secondary layers (WILLIAMS & WRIGHT, 1970). The fabric of the craniopoid second-

ary shell, as typified by a mid-Silurian species of *Craniops*, is finely and regularly laminar with units about 300 nm thick (Fig. 249). The succession is so like that of Paleozoic cranioids as to make it likely that the craniopoid laminae were also tablets interleaved with interconnected membranes.

The secondary layer of the obolellide *Trematobolus*, on the other hand, is more coarsely and irregularly laminar with lenticular units (folii) up to 500 nm thick and 10 μm across (Fig. 249). The fabric is further complicated by the presence of regularly dis-

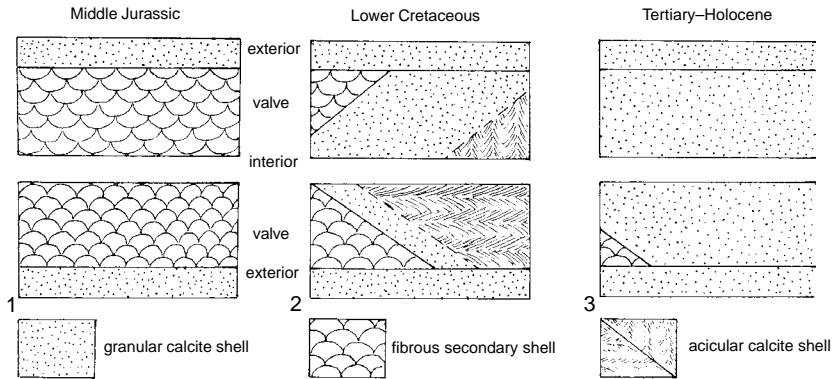


FIG. 246. Selected chronological states in the evolution of thecideidine shell structure; 1, *Moorellina* with a continuous fibrous secondary shell in both valves; 2, *Thecidiopsis* with a reduced fibrous secondary shell and well-developed acicular crystallites associated with the primary granular fabric; 3, *Lacazella* with vestigial fibrous secondary shell on teeth and inner socket ridges (adapted from Baker, 1990).

tributed hemispherical nodules of coarsely crystalline calcite up to 40 μm across and convex externally. Nodules also occur in the cranioid secondary shell, but they are convex internally and more readily identifiable as temporary muscle bases. On balance, the obolellide secondary folii were probably ensheathed in membranes and more like fibers than laminae in origin.

CALCITIC CROSS-BLADED LAMINATION

The laminar secondary fabric of the strophomenides (*s.l.*) and billingselloids is not tabular in the cranioid style. The basic unit is a long, lath- or blade-shaped crystal-lite of variable length (but commonly traceable for more than 100 μm) and with a width

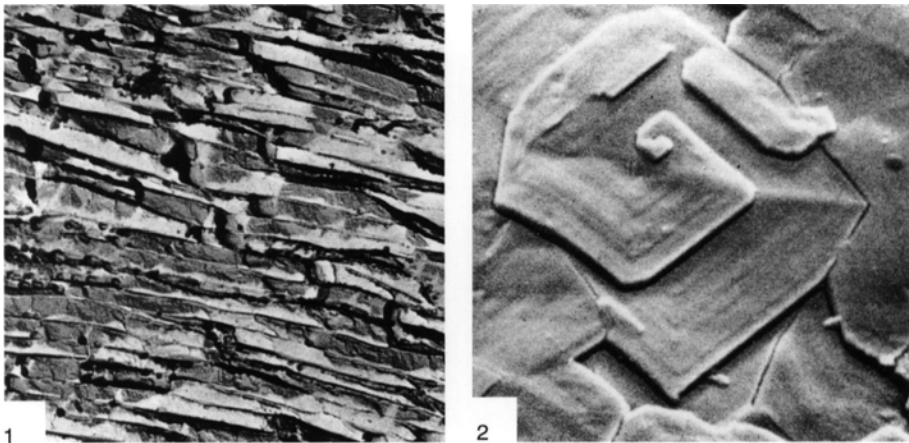


FIG. 247. The laminar secondary shell of living *Neocrania anomala* (MÜLLER); 1, section of a succession of laminae with acutely triangular and trapezoidal outlines representing different aspects of spiral growth, $\times 7,000$; 2, internal surface of a dorsal valve showing three successive laminae of a single spiral growth unit with concentric growth bands, $\times 5,900$ (Williams, 1970b).

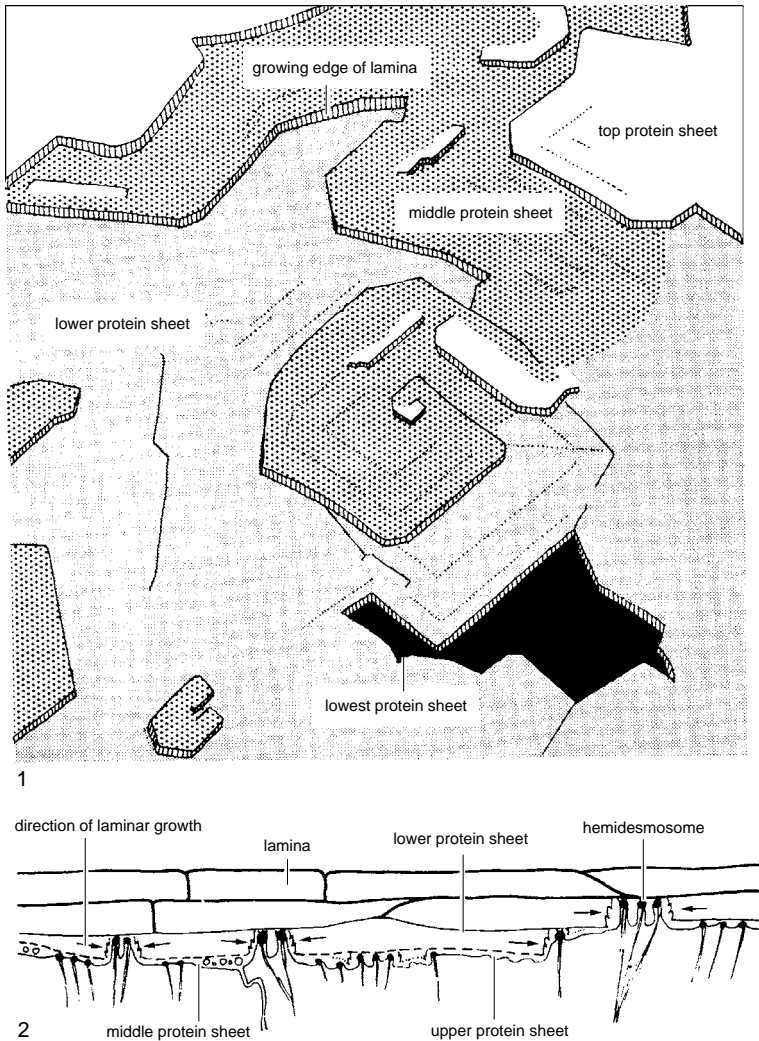


FIG. 248. Stylized reconstruction of several laminae, shown in Figure 247.2, in association with their proteinaceous covers as seen on the internal surface of the dorsal valve (1), together with the inferred relationship with secreting outer epithelium (2) (Williams, 1970b).

ranging from 2 μm to 6 μm and a thickness from about 100 nm to 500 nm (WILLIAMS, 1970a). Each lamina consists of a set of contiguously aligned blades with their lateral junctions in various stages of amalgamation (Fig. 250). Accordingly, although traces of these junctions on a laminar surface are normally parallel with one another, they vary from breaks cutting through the lamina (Fig.

250.1–250.2) to faint ridges on the inner surfaces (Fig. 250.3). Such traces of blade sets may be disposed at acute angles to one another in successive laminae (the cross-bladed fabric of ARMSTRONG, 1969) and act as optical diffraction gratings to give the nacreous sheen of loosely foliated shells like those of *Pholidostrophia* (TOWE & HARPER, 1966). The other noteworthy feature of

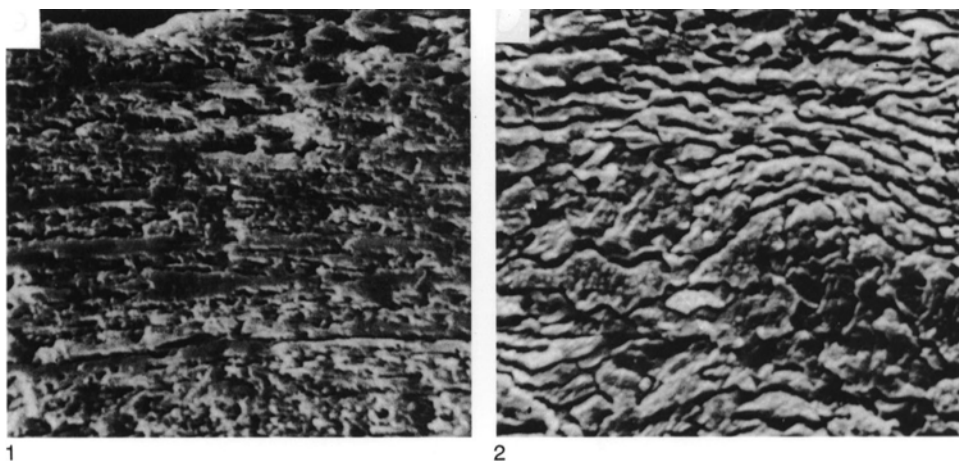


FIG. 249. Sections of the calcitic secondary shell of inarticulated brachiopods; 1, ventral valve of the craniopoid *Craniops implicata* (SOWERBY) showing the laminar structure of the secondary shell, $\times 1,140$; 2, *Trematobolus pristinus bicostatus* GORYANSKY with a coarse and irregularly laminar (foliated) secondary shell, $\times 2,280$ (Williams & Wright, 1970).

cross-bladed lamination is that even in such later-appearing groups as the productidines and orthotetidines, the external surfaces of blades, which are normally flat, may be gently convex with rounded or obtusely planar slopes (crested laminae) and appear to terminate in scalenohedral faces as opposed to the rhombohedral edges of flat blades (Fig. 251).

The recovery of amino acids from strophomenide shells by JOPE (1965) suggests that cross-bladed laminae were associated with proteinaceous membranes. The disposition of the calcitic components also suggests that the membranes were interleaved with laminae, comparable in that respect with cranioid secondary successions. However, it seems unlikely that the well-ordered blades of the strophomenide laminar fabric grew by screw dislocation. A more feasible assumption is that the growth of this kind of lamina involved simultaneous deposition of protein and calcite on the surfaces and along the rhombohedral edges (or scalenohedral faces) respectively of blade sets (Fig. 251). This is confirmed by the disposition of growth banding in individual blades, which is transverse to the long axes of the blades and parallel to their edges (Fig.

250.2–250.3). With respect to the origin of the cross-bladed laminar fabric, the nature of the secondary shell of two early Paleozoic groups has to be taken into account.

The orthidine *Billingsella* has a well-developed, albeit recrystallized, primary layer underlain by a secondary shell composed of parallel-sided laminae about $1\ \mu\text{m}$ thick. The laminae are composed of blades that can be up to $35\ \mu\text{m}$ wide, presumably recrystallized, amalgamated sets of four or five laths (Fig. 252).

The strophomenide plectambonitoids, on the other hand, have a fibrous secondary shell (Fig. 252–253). This anomalous condition is all the more intriguing in that typical chonetidines, which are likely to have evolved from the plectambonitoids, have a secondary shell with a cross-bladed laminar fabric. In this context it is noteworthy that plectambonitoid aegiromenines like *Aegiromena* and contemporaneous chonetidines (*Strophochonetes*), which are morphologically alike except for the presence of hinge-spines in the latter stock, have a similar secondary shell fabric (Fig. 253). In *Aegiromena* orthodoxly stacked fibers dominate the outer secondary shell fabric, but internally the

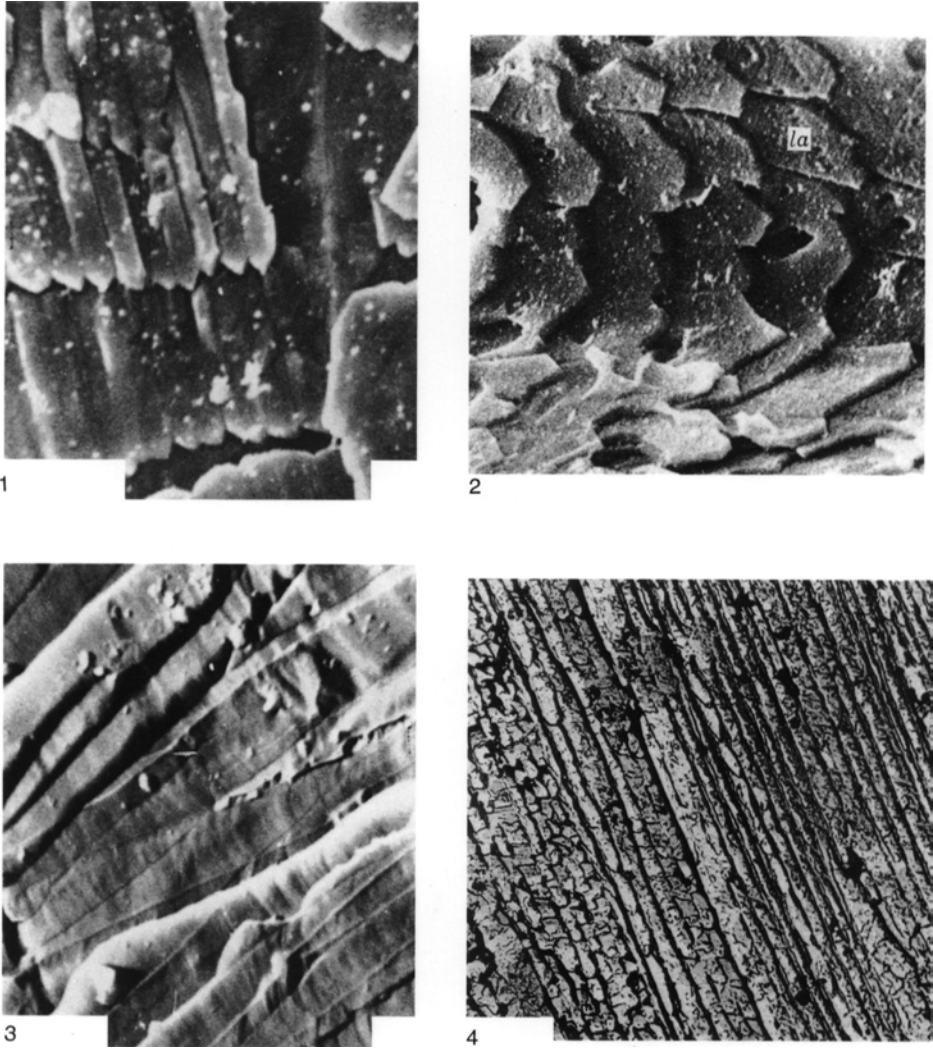


FIG. 250. The cross-bladed laminar secondary shell of strophomenoides; 1, contiguous laths in various stages of amalgamation to form laminae in a fracture surface of the ventral valve of the orthotetidine *Gacella insolita* WILLIAMS, $\times 2,600$ (Williams, 1970a); 2, internal surface of a ventral valve of the orthotetidine *Schellwienella* cf. *aspis* (SMYTHE) showing the overlapping arrangement of laminae composed of laths (*la*) along their terminal faces, $\times 2,800$ (Williams, 1973); 3, cross-bladed laminae composed of amalgamated laths in a fracture surface of a ventral valve of the strophomenoid *Strophomena oklahomensis* COOPER, $\times 2,600$ (Williams, 1970a); 4, section of a cross-bladed laminar succession in a valve of the stropheodontoid *Pholidostrophia* cf. *geniculata* IMBRIE, $\times 2,500$ (Williams, 1968a).

fibers (about $14 \mu\text{m}$ wide) are lathlike and typically flattened in cross section with their edges commonly overlapping. In *Strophochonetes*, the basic constituents of the second-

ary shell are also lath-shaped (6 to $10 \mu\text{m}$ wide) and overlap like those of *Aegiromena* or lie in contiguity without lateral fusion. These discrete laths are the dominant fabric of Sil-

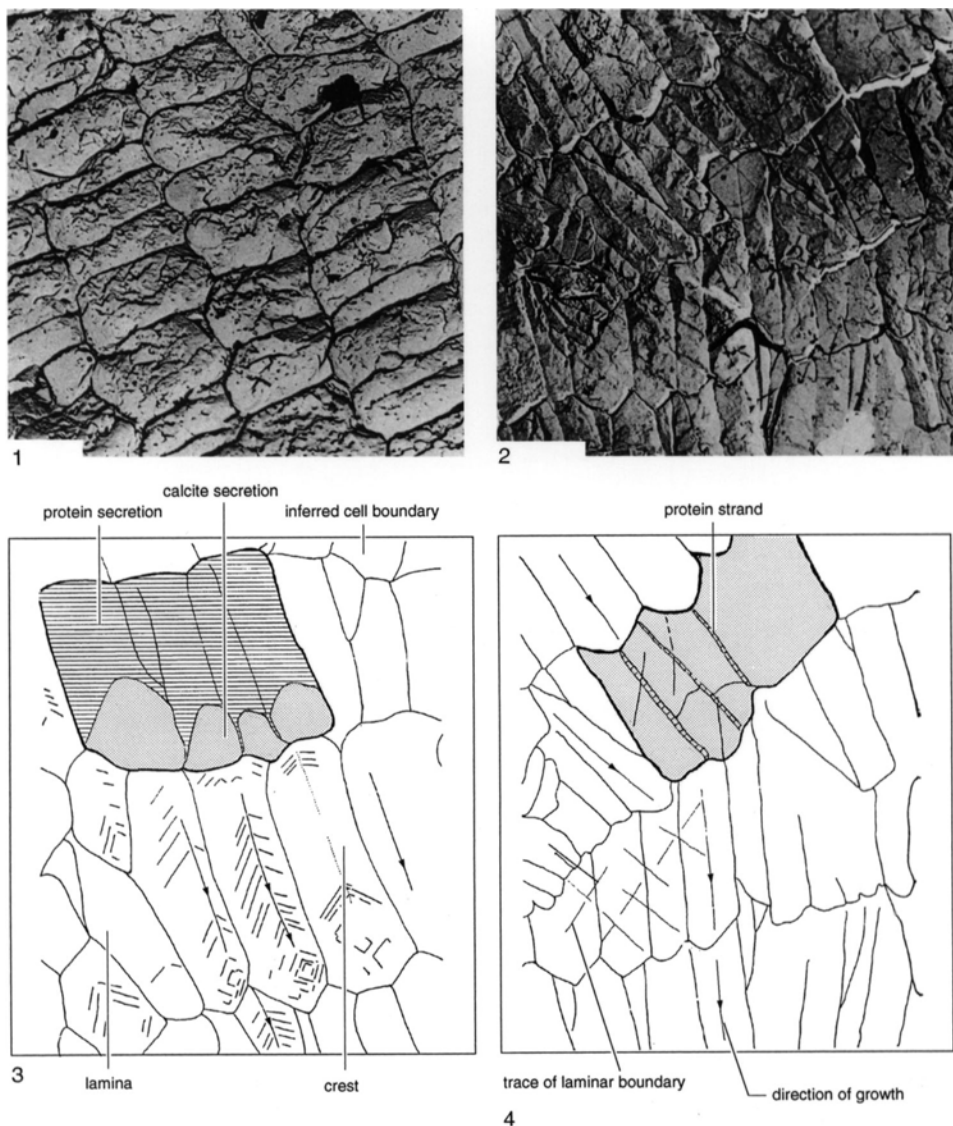


FIG. 251. Mosaics on the internal surfaces of valves with cross-bladed laminae and their inferred relationships with interleaved proteinaceous membranes and secreting outer epithelium; 1, 3, angular ridges along terminal faces giving rise to crested laminae, $\times 2,500$; 2, 4, flat terminal faces of typical, cross-bladed laminae, $\times 2,500$.

Both sets of terminal faces in a dorsal valve of the productidine *Juresania* sp. (Williams, 1968a).

urian chonetidines. They were not fully fused into laminae sheets until the Devonian and did not become wholly cross-bladed until the Carboniferous (BRUNTON, 1972).

The ancestry of cross-bladed lamination is clearly complicated. There are good morphological grounds for assuming a close affinity between *Billingsella* and the

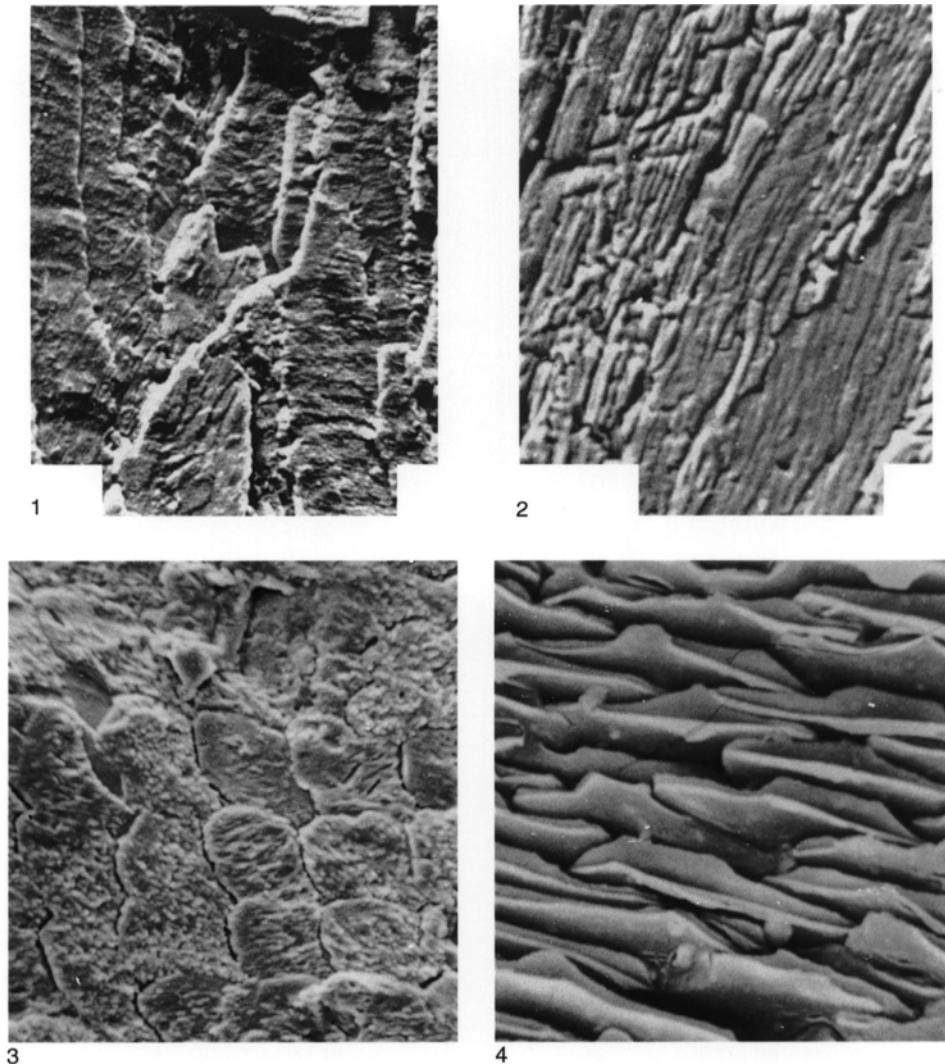


FIG. 252. Secondary shell fabrics; 1, fracture surface ($\times 1,700$) and 2, section ($\times 800$) of the laminar shell of the orthide *Billingsella lindströmi* (LINNARSSON) (Williams, 1970a); 3, internal surface ($\times 600$) and 4, section ($\times 830$) of the pseudopunctate fibrous shell of the plectambonitoid *Sowerbyella variabilis* COOPER (new).

impunctate, early orthotetidines and triplesiidines and to a lesser extent between *Billingsella* and the pseudopunctate early strophomenoids. There are equally good grounds for believing that plectambonitoids and strophomenoids are more closely related to each other than to any other known

brachiopod stock. The conclusion, therefore, is that the cross-bladed laminar fabric is homoplastic with billingselloids and chonetidines originating in late Precambrian and Late Ordovician times respectively and the strophomenoids possibly in the Early Ordovician from plectambonitoids (WILLIAMS,

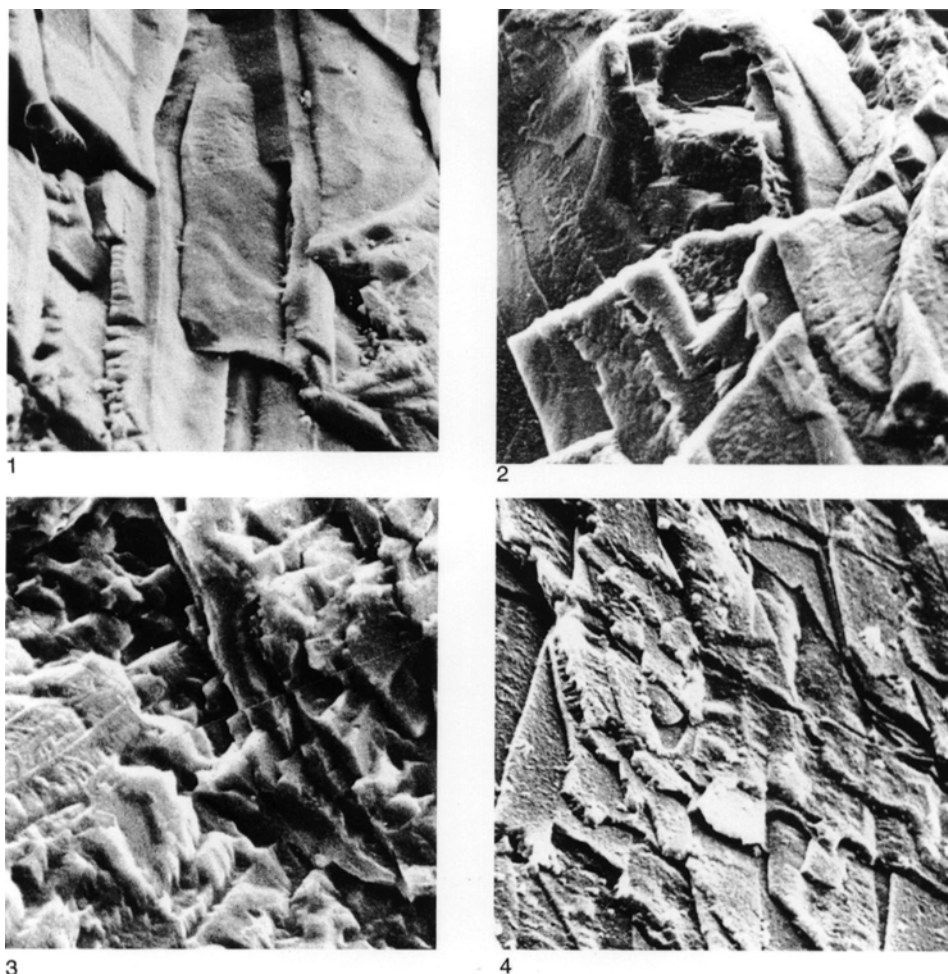


FIG. 253. Secondary shell fabrics; 1, orthodoxy stacked, flattened fibers in the outer part of the secondary succession of the plectambonitoid *Aegiromena aquila* (BARRANDE), $\times 1,200$; 2, flattened fibers forming laminae sheets around a taleola in the middle part of the secondary succession of *Aegiromena aquila*, $\times 1,100$; 3, flattened fibers forming laminae sheets in the secondary succession of the chonetidine *Strophochonetes primigenius* (TWEHNOFEL), $\times 1,000$; 4, secondary laminae of chonetidine *Rugochonetes silleesi* BRUNTON, $\times 2,100$ (Brunton, 1972).

1970a). In any event, it seems likely that a fibrous shell was ancestral to a cross-bladed laminae one.

TERTIARY LAYER

The term tertiary is given to a continuous layer of shell that is sufficiently different from the overlying secondary succession to

have been deposited by outer epithelium with a distinctive secretory regime. There is a continuity in secretion from the periostracum to the tertiary layer, which suggests that differences in the successions reflect physiological changes in the secretory regimes of distinctive outer epithelia (Fig. 254). Thus in such living terebratulids as

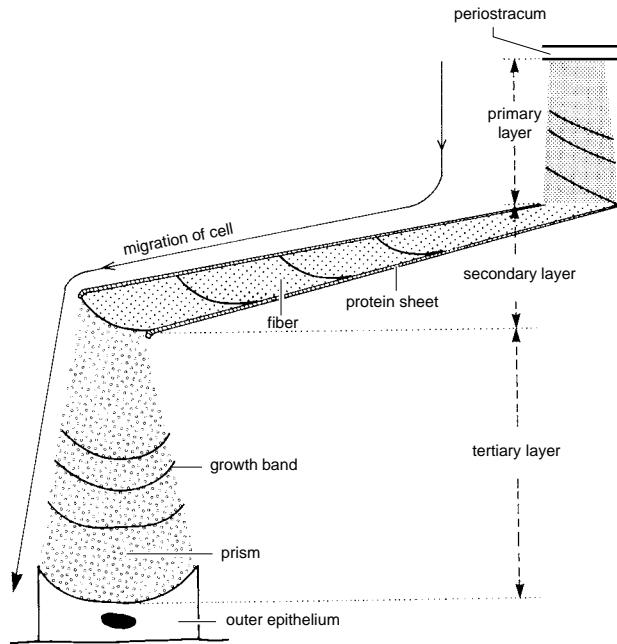


FIG. 254. Diagrammatic longitudinal section of integument of the terebratulide *Liothyrella* showing the migration of an outer epithelial cell during its secretion of succeeding biomineral components (Williams, 1990).

Gryphus and *Liothyrella*, prismatic calcite forms a continuous tertiary layer immediately distinguishable from the overlying fibrous secondary shell (MACKINNON & WILLIAMS, 1974). The origin of the tertiary layer has been traced in *Gryphus*. In the transitional zone, a flat-lying fiber becomes transformed by a lateral spreading of its terminal face, which is then extended vertically by accretion into a prism, normally corrugated by strong growth banding (Fig. 255). The prisms are discrete units, up to 20 μm thick. They have interlocking boundaries but are not separated from one another by extensions of the proteinaceous membranes enshathing the fibers. The amalgamation of prisms, therefore, may be inhibited by sheets of water-soluble polymers or by crystallographic nonalignment of contiguous prisms. This change in cell secretion must be reversible to account for interdigitations of fibrous and prismatic fabrics along the interface between the secondary and tertiary layers of *Liothyrella* (Fig. 255.2).

The terebratulid tertiary layer was acquired gerontomorphically by the group as a whole, but no chronostratigraphic order has yet been discerned in its phylogeny. Isolated lenses of prismatic calcite are common in the fibrous prismatic shell of fossil terebratulids and may have been precursory to the development of a continuous tertiary layer within the stocks concerned. A tertiary layer has also been identified in Mesozoic megathyrids and terebratellids, which confirms the homoplastic origin of this prismatic fabric even within an ordinal group of brachiopods (SMIRNOVA & POPIEL-BARCZYK, 1991).

Lenses of prismatic calcite also commonly occur within the fibrous secondary shell of many pentamerides and spire-bearing brachiopods. A fully developed, prismatic tertiary layer is found in the koninckinoids and reticularioids and in some atrypoids, athyroids, and pentameroids and must have evolved repeatedly.

So far as is known, a tertiary layer, as here defined, is rare in organophosphatic

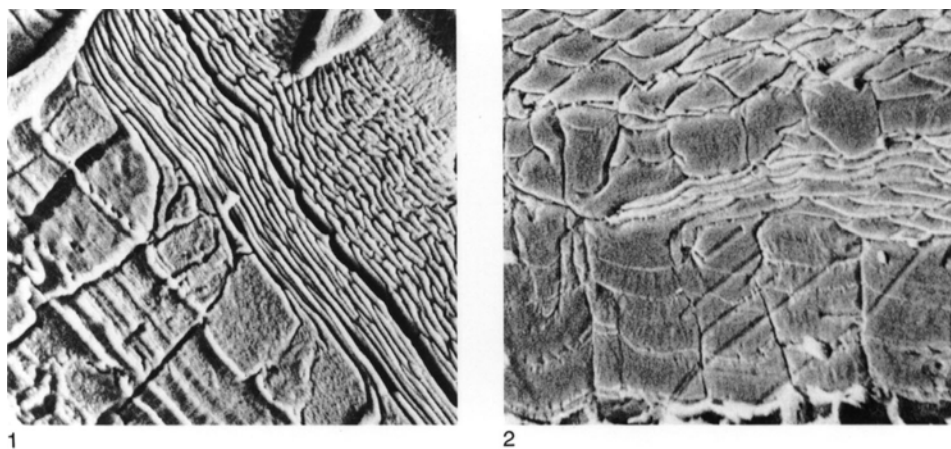


FIG. 255. Secondary and tertiary shell fabrics; 1, fibrous secondary layer passing into prismatic tertiary layer (bottom left of micrograph) of a dorsal valve of the terebratulid *Gryphus vitreus* (BÖRN), $\times 565$; 2, relationship between the tertiary layer and an earlier-formed lens of prismatic calcite enclosed by secondary fibers in the dorsal valve of *Liothyrella neozelanica* THOMSON, $\times 1,175$ (MacKinnon & Williams, 1974).

brachiopods. HOLMER (1989) described a continuous tertiary layer of columnar laminae succeeding a camerate secondary shell in such acrotretoids as *Acrotreta* and *Torynelasma*. This distinction in fabric is enhanced by the transgressive encroachment of the horizontal tertiary columnar laminae across the wedge-shaped sectors of the secondary camerate laminae. Similar structural discontinuities affect shell successions of *Ephippelasma* and *Biernatia*, which consist entirely of columnar laminae. However, they do not alone signify a basic distinction between secondary and tertiary layers (WILLIAMS & HOLMER, 1992).

SHELL PERFORATIONS

Conspicuous features of the fabric of many brachiopod shells are caused by persistent extensions or localized attachments of the mantle. The consequential microscopic perforations or protuberances are common features of extinct and living brachiopods and have developed in many different ways. In general, however, shells that are permeated by canals are referred to as punctate, and stratified fabric penetrated by them is deflected as perforated cones pointing externally. Shells with protuberances formed

within evaginations of the mantle are pseudopunctate when stratified fabric is puckered into cone-in-cone microstructures pointing internally. Shell fabric that is free of all such complications is described as impunctate.

PUNCTAE

There are three kinds of perforations (see Fig. 261)—endopunctae, punctae (*s.s.*), and canals—all of which are developed in living species. Endopunctae permeate terebratulides and thecideidines and, as described in the section on anatomy (p. 33), accommodate caecal extensions of the entire outer epithelium, which act as storage centers for the mantle. Endopunctae are relatively large canals, although they vary greatly in maximum diameter from about $5\ \mu\text{m}$ in *Terebratulina* to $20\ \mu\text{m}$ in *Macandrevia* (OWEN & WILLIAMS, 1969) or as much as $40\ \mu\text{m}$ in megathyrids (SMIRNOVA & POPIEL-BARCZYK, 1991). An endopuncta is usually funnel-shaped in longitudinal section with the maximum diameter just proximal of the distal, perforated canopy of primary shell ($1\ \mu\text{m}$ and $7\ \mu\text{m}$ thick in *Macandrevia* and *Thecidellina* respectively) separating the caecum from the periostracum (Fig. 256). The

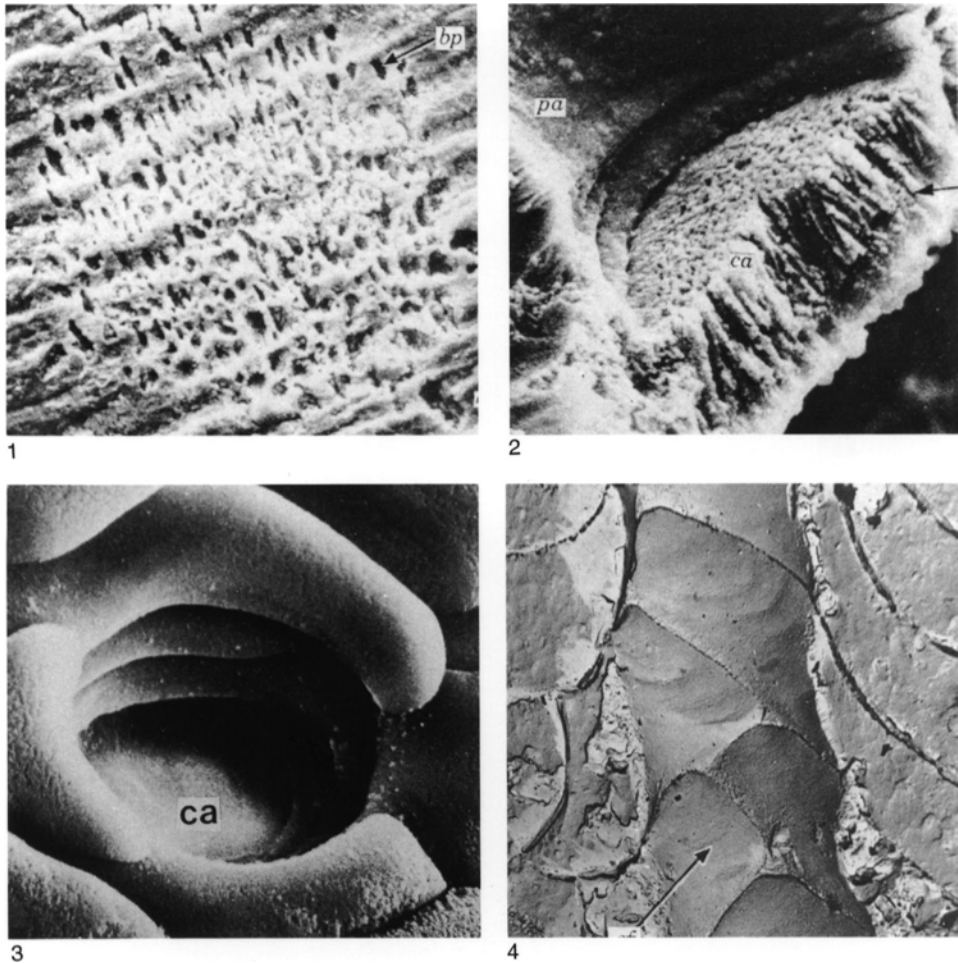


FIG. 256. Endopuncta; 1, perforations of the brush (*bp*) seen externally ($\times 1,400$) and 2, as perforations and canals (*arrow*; $\times 3,000$) in the fracture section of the canopy (*ca*) of an endopuncta (*pa*) of *Lacazella mediterranea* (Risso) (Williams, 1973); 3, disposition of fibers defining an endopuncta and its canopy floor (*ca*) near the primary-secondary shell junction of the terebratulid *Liothyrella neozelanica* THOMSON, $\times 2,800$ (Williams, 1990); 4, resin cast of endopuncta of *Calloria inconspicua* (SOWERBY) showing the overlap of fibers (*arrow*) in the wall, $\times 5,000$ (Owen & Williams, 1969).

narrowing of an endopuncta proximally is the result of the thickening of the secondary shell relative to the growth of a constant number of caecal peripheral cells, which become very attenuated (Fig. 257.2). With respect to its morphology, the definitive feature of an endopuncta is its perforated canopy. This is a calcitic cast of the microvillous plasmalemmas by which several storage

cells become temporarily attached to the periostracum during their differentiation into a caecum at the outer mantle lobe (STRICKER & REED, 1985b). The perforated canopy is assumed to be a unique feature of the brachiopod shell (WILLIAMS, 1973) and, therefore, a reliable guide to the close affinities of various stocks with punctae capped by such a structure.

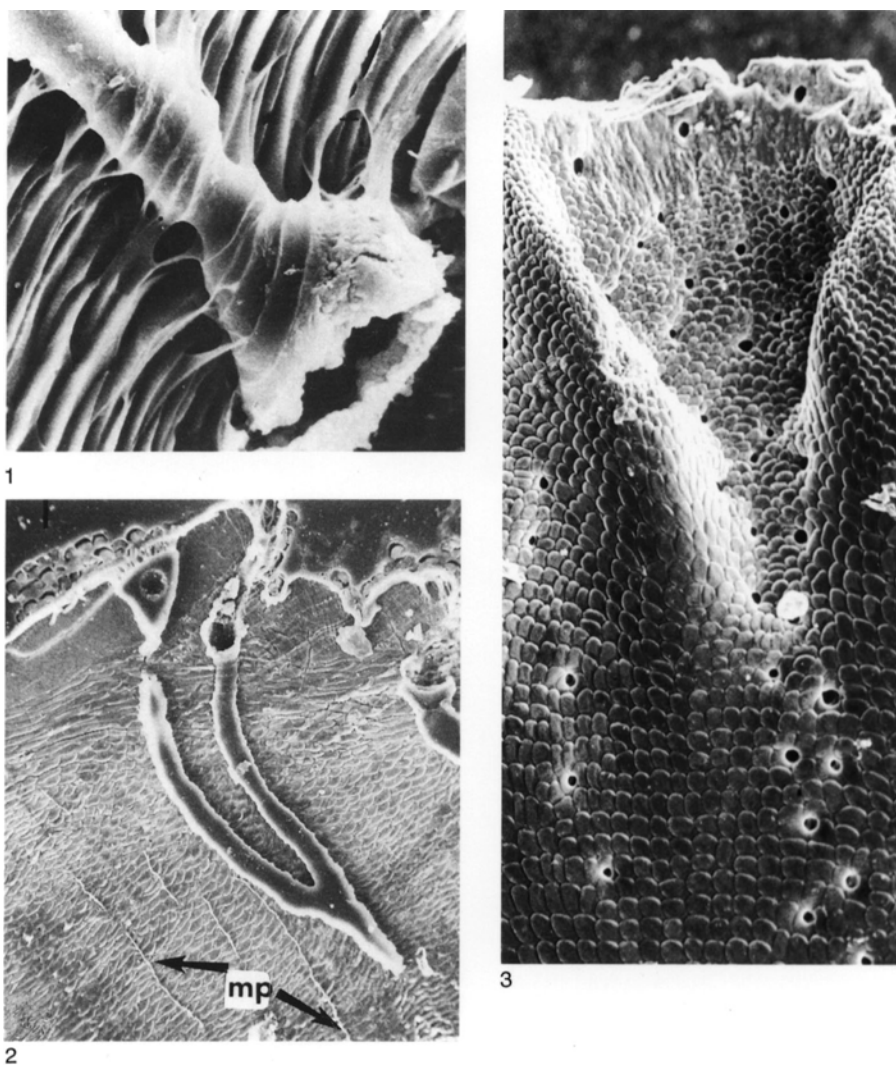


FIG. 257. Terebratulide punctation; 1, fracture section of *Macandrevia africana* COOPER showing the typical outline of caecum associated with membranes of the secondary shell, $\times 2,000$; 2, section of *Megerlia truncata* (LINNÉ) showing branched punctae (filled with resin) and micropunctae (*mp*), $\times 350$ (Gaspard, 1990); 3, interior of the dorsal valve of *Terebratulina retusa* (LINN.) showing how the more numerous, regularly spaced endopunctae at the valve margin converge, as a result of secondary fibrous shell thickening, to form a smaller number of radially distributed bases, $\times 200$ (new).

The distribution densities of endopunctae within the shell of living species are variable, but the pattern of distribution is essentially regular, as would be expected of features originating at the growing edge of a valve. The pattern is likely to be a mixture of hex-

agonal close packing (COWEN, 1966) and alternations in concentric rows (KEMEZYS, 1965) as was shown by BAKER (1970b) for the thecideidine *Moorellina* (Fig. 258). In *Thecidellina*, unbranched endopuncta (25 μm in maximum diameter) are arranged at

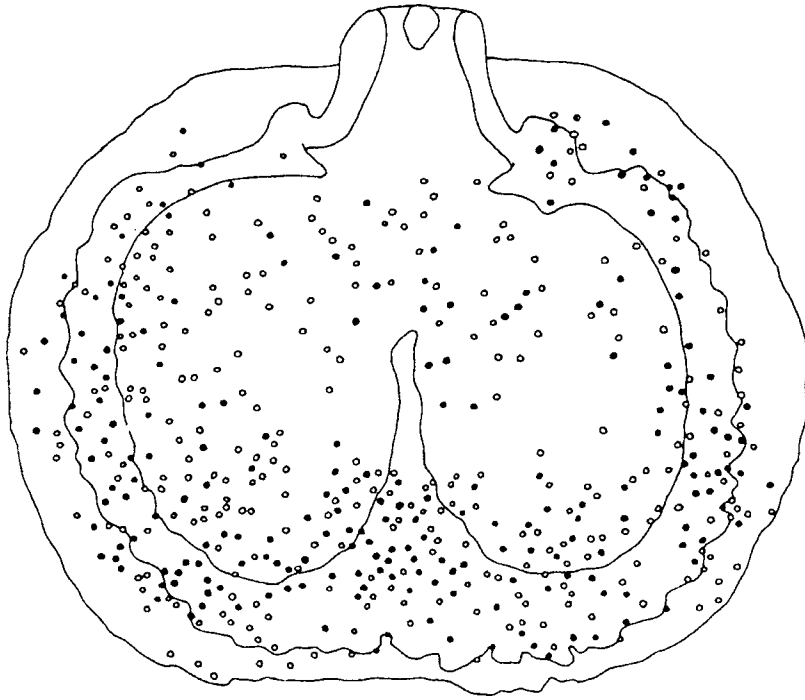


FIG. 258. Plot of endopunctae identified during horizontal serial sectioning of a dorsal valve of the thecideidine *Moorellina granulosa* (MOORE); closed circles, persistent punctae; open circles, impersistent punctae (Baker, 1970a).

intervals of about 45 μm in a dominantly hexagonal, close-packing pattern (WILLIAMS, 1973). This pattern is also the standard arrangement for terebratulides although it can be greatly modified by differential growth in such genera as *Terebratulina* where endopunctae are more densely distributed in radial sectors corresponding to the crests of ribs (Fig. 257). However, some indication of frequency differences even in regular, closely packed arrays is given by counts in the evenly contoured, median sector of the dorsal valve of *Magellania* where the frequency of endopunctae in quadrants with radii of 1 mm varied from 80 to 125 within 7 mm of the umbo (WILLIAMS & ROWELL, 1965b, p. 69).

Shell thickening and the microtopography of the external surface as well as the density of distribution and size of endopunctae determine whether endopunctae become branched in the manner shown in Figure 257.2. Endopunctae branch freely by con-

verging to share a common, attenuated stalk of outer epithelium, which is pinched up from the mantle by deposition of the surrounding secondary shell. This accounts for the relatively few, radially arranged internal openings of endopunctae compared with the greater number of their more widely dispersed distal heads in *Terebratulina* (Fig. 257.3). Such differences in the density distributions of punctae in outer and inner successions of strongly ribbed shells are clearly evident in the enteletoid *Dicoelosia* (WRIGHT, 1966). In this stock, the distal ends of punctae, which lie normal to the sharply folded surfaces of the strong ribs, were quickly coalesced by shell thickening into a smaller number of more openly distributed trunks in simulation of the arborescent canal system of the inarticulated craniids.

Endopunctae are characteristic of all terebratulides throughout their geological history. They also permeate the shells of theci-

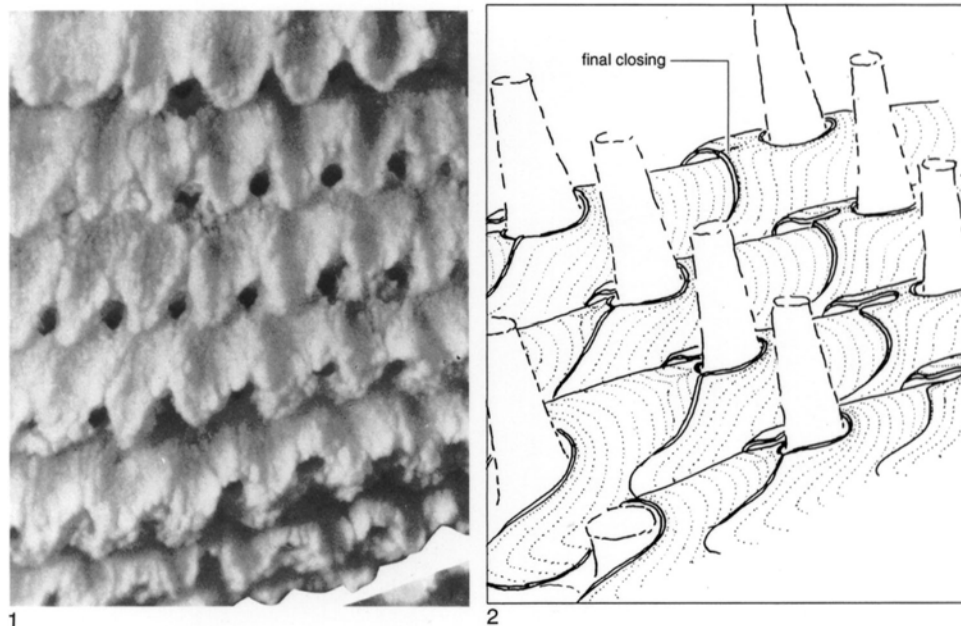


FIG. 259. Punctuation in the atrypidine *P. (Punctatrypa) naliukini* HAVLIČEK from the Lower Devonian Zlichov Limestones, Czech Republic; 1, fenestrae within the lamella on the exterior of a ventral valve, $\times 30$; 2, fenestrae interpreted as perforations accommodating setae (adapted from Wang, Copper, & Rong, 1983).

deidines but are sporadically suppressed as in the adult shell of *Bifolium* (BAKER & LAURIE, 1978). Endopunctae with perforated canopies have also been found in Jurassic spiriferinoids (MACKINNON, 1971). This suggests that the thecideidines, terebratulides, and some endopunctate spiriferides are monophyletic with a stem group of pre-Devonian age, a phylogeny supported by other, morphological considerations (WILLIAMS, 1973).

This phylogenetic relationship, however, does not necessarily support an assumption that punctae found in other spire-bearing brachiopods accommodated caeca with retractable apical microvilli. The fibrous secondary layer of *Punctatrypa* is pierced by very coarse, unbranched canals (fenestrae) that can also breach overlapping lamellae of primary shell (Fig. 259). Fenestrae that are up to 80 μm in diameter have been interpreted as having accommodated erect setae around the bases of which lamellae were secreted eventually to form a complete ring of pri-

mary shell by fusion of crenulations of the outer mantle lobe during forward growth (WANG, COPPER, & RONG, 1983).

This interpretation cannot be correct as setae (and their follicles) have always lain internal of the entire outer mantle lobe and, therefore, could not have been incorporated as appendages of the mantle itself. However, the persistence of fenestrae as canals suggests that they contained, temporarily at least, papillose outgrowths of the mantle. Moreover, the forward growth of lamellae to form by fusion complete, circular enclosures delineating fenestrae at the external surface indicate that these holes were filled in life with organic material. (There are no signs of perforated canopies or recrystallized primary shell.) Such material would have had to serve as a protective cover to any mantle extensions within the underlying canals. An obvious possibility is that the holes were filled with plugs of thickened periostracum, comparable with those closing the distal

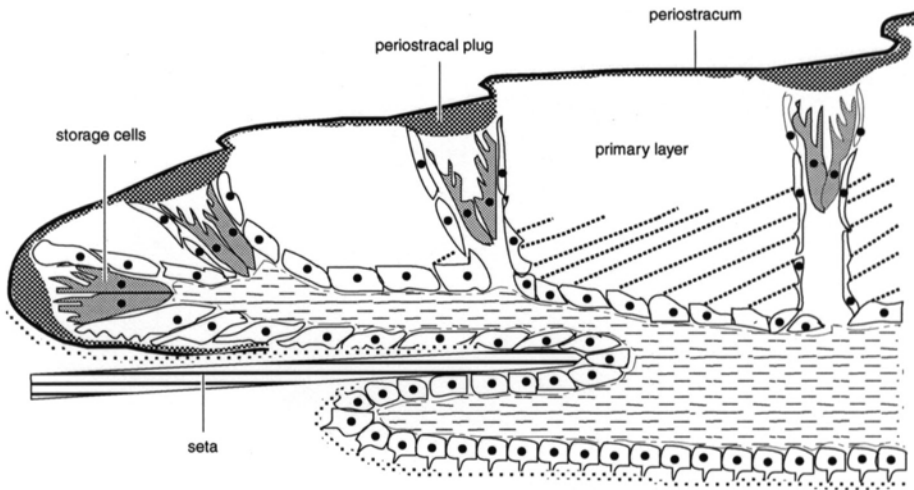


FIG. 260. Punctuation in the atrypidine *P. (Punctatrypa) naliwkini* HAVLIČEK interpreted as repositories for storage cells, capped by plugs of infrastructural periostracum (new).

apertures of punctae in the cyclostomate bryozoan *Crisidia* (WILLIAMS, 1984), and were, therefore, true punctae (Fig. 260). It is noteworthy that living rhynchonellides, like *Notosaria*, differ from contemporaneous terebratulides in having a greatly thickened infrastructure of GAGs underlying the basal layer of the periostracum.

There is even a form of endopunctuation that is not homologous with that of the terebratulides. The fibrous, secondary shells of the Carboniferous rhynchonellides, the Rhynchoporidae, are permeated by canals that do not penetrate the primary layer (Fig. 261). In *Tretorhynchia*, the canals, which are about 20 μm in diameter, end blindly just below a primary layer at least 30 μm thick (BRUNTON, 1971). The primary shell has been recrystallized, but there are no signs of perforations of any kind emanating from the distal ends of the canals. In any event, any organic contents of such endopunctae would not have been differentiated at the outer mantle lobe and could not have been more than columnar protuberances of outer epithelium. The rhynchonellide endopuncta was a short-lived phylogenetic novelty that may well be unique to the order.

The precise nature of punctuation in orthide enteletidines is also unknown. Enteletidine shells are always permeated by punctae (Fig. 262), which usually fall within the same size range and commonly have the same disposition and funnel-shaped outline as terebratulide endopunctae. However, no perforated canopies have yet been found in enteletidines, and they are best referred to as punctae although their presence throughout the primary layer precludes any homology with rhynchonellide endopunctae.

The nature of dictyonellidine punctuation is even more controversial. The network of rhombohedral to hexagonal ridges on the shell surface of *Dictyonella* itself normally defines deep cavities that connect with the interior by narrow canals. These composite structures have been interpreted as gross caeca; but the absence of such cavities in other genera has suggested that they were lined with periostracum and the caeca confined to the narrow proximal part of the structure (WILLIAMS, 1968a). However, it has now been shown (WRIGHT, 1981) that the pits of well-preserved *Dictyonella* are quite shallow, and their floors can be penetrated by up to nine fine canals. This suggests that the

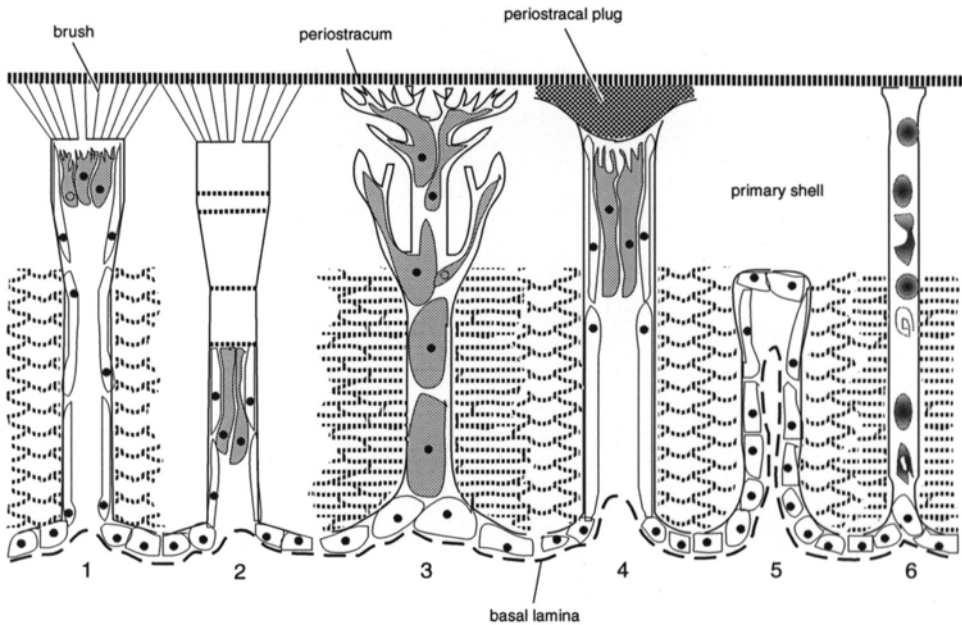


FIG. 261. Perforations of the brachiopod shell; 1–2, canopied endopunctae with storage cells hanging distally in lumen or restricted to proximal locations by proteinaceous partitions in terebratulides and thecideidines respectively; 3, branched puncta of cranioids perforating the entire shell, with storage cells throughout; 4, puncta of atrypide punctatrypids interpreted as having been plugged distally by a swelling of the infrastructural layer of the periostracum; 5, endopuncta of the rhynchonellide rhynchoporids interpreted as originating at the primary-secondary shell boundary and therefore filled with cylindroid infolds of outer epithelium; 6, canals of lingulids and discinids containing no extensions of the mantle, only secreted bodies (new).

canals contained branches of mantle outgrowths that converged centrally into large nodes more or less below the surface pits and that would form cavities in fossilized shells. The craniid puncta with its distal canopy of fine branches is a reasonably close model.

The many-branched canal systems of living *Neocrania* are certainly punctate in the strict sense as they terminate distally as finely divided branches more or less contiguous with the inner surface of the periostracum, to which they are connected by fibrils (Fig. 263). The fine branches are mainly restricted to the primary layer where they form a flat-topped arborescent zone because they coalesce within 50 μm of the periostracum into a series of relatively widely spaced trunks that, in turn, converge as the secondary shell thickens. Like terebratulide endopunctae, the canals accommodate storage outgrowths

of the mantle, and the finest terminal branches (tubules) may indeed be long microvilli. Apart from having originated at the outer mantle lobe, however, they have little in common with endopunctae, must have evolved independently, and have always been characteristic of cranioids except for their suppression in the cemented ventral valve of the Paleozoic *Petrocrania* (Fig. 264).

Petrocrania, incidentally, is well known as a fossil that reproduced topographic details of its substrate on the external surface of the dorsal valve. The Ordovician *P. scabiosa*, which frequently settled on the strophomenide *Rafinesquina*, replicated the parvicostellate ornamentation of that stock with remarkable clarity. Three factors promoted such mimicry. First, the ventral valve was thin and lacked any thickened margin that would have elevated the dorsal mantle edge

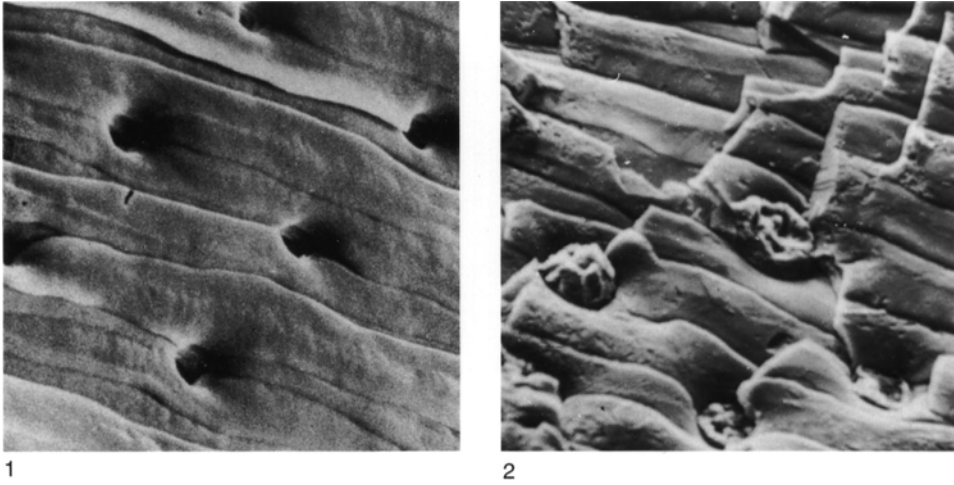


FIG. 262. Endopunctuation in internal fracture surfaces showing the similarity between the endopunctate fibrous secondary shell of 1, *Liothyrella neozelanica* THOMSON, $\times 1,600$ (Williams, 1990) and 2, of the enteletoid *Rhipidomella* sp., $\times 630$ (new).

above the substrate. Second, the dorsal valve invariably overlapped the margin of the ventral valve. Third, in the absence of setae the subperiostracal layer at the margin of the

dorsal valve must have constantly polymerized to form a cast of the substrate, over which it expanded (Fig. 264; WILLIAMS & WRIGHT, 1970).

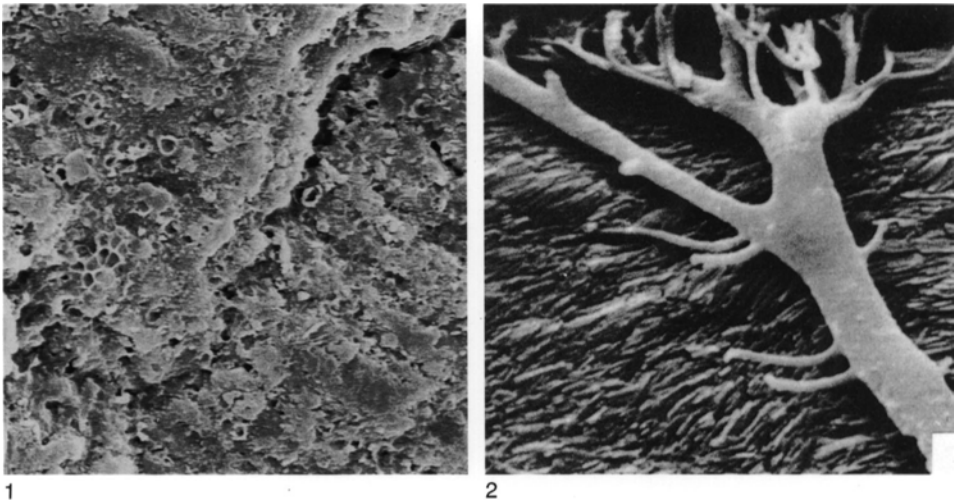


FIG. 263. Punctuation of the cranioid *Neocrania anomala* (MÜLLER); 1, external surface of the primary shell of a dorsal valve showing perforations (many with thickened organic surrounds) of the terminal branches of punctae, $\times 1,050$ (new); 2, section of the primary layer of a dorsal valve showing the main branches and tubules of a puncta filled with resin, $\times 2,600$ (Williams & Wright, 1970).

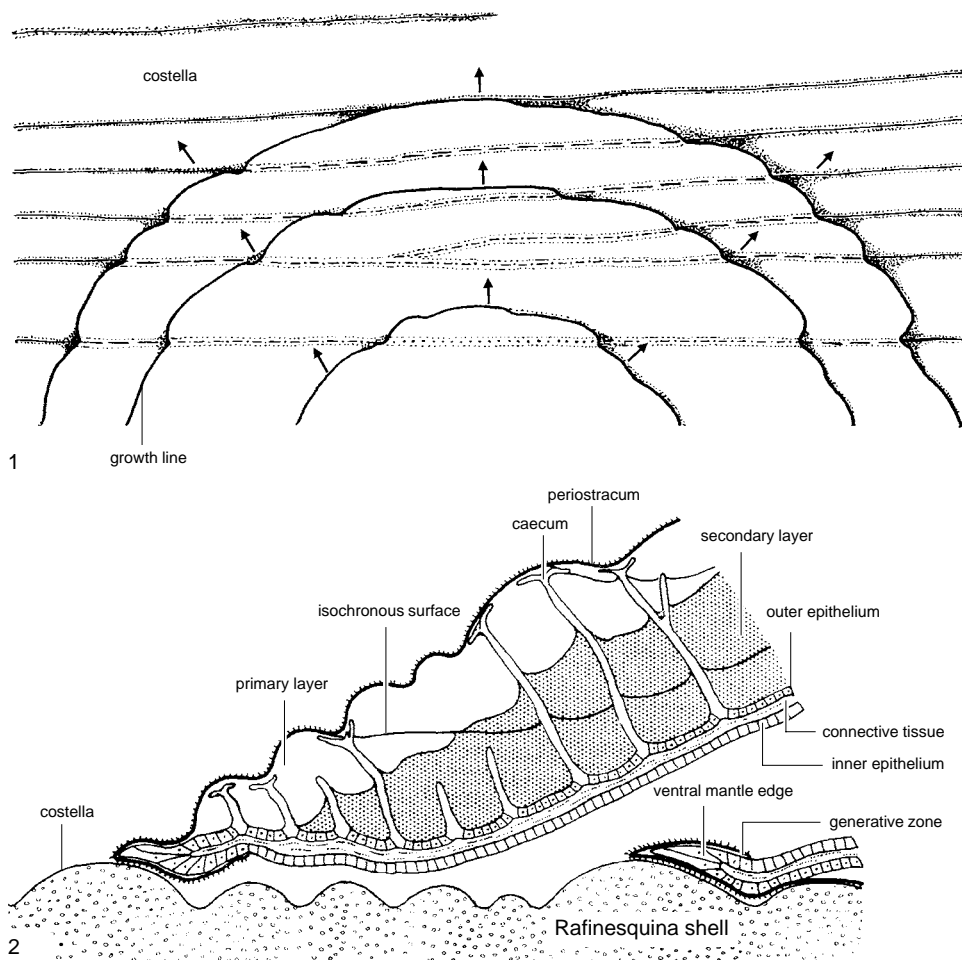
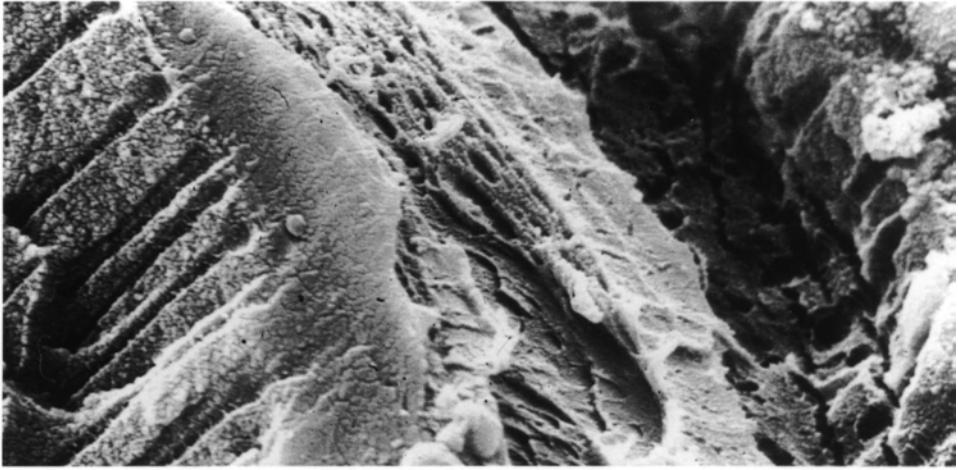


FIG. 264. 1, Stylized external view and 2, longitudinal section of the edge of the dorsal valve of the cranioid *Petrocrania scabiosa* (HALL) showing how details of substrate topography are reproduced on the dorsal external surface (Williams & Wright, 1970).

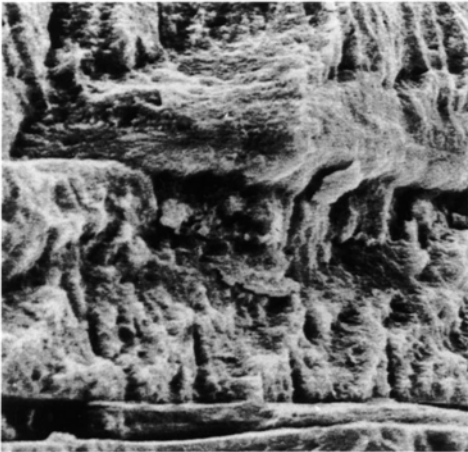
CANALS

The canals permeating the organo-phosphatic shell of living lingulids and discinids are fundamentally different from the punctation of calcitic-shelled brachiopods (Fig. 265.1–265.2). They are significantly finer with diameters ranging between 300 nm and 500 nm for *Discina* (WILLIAMS, MACKAY, & CUSACK, 1992) and between 180 nm and 850 nm (with bimodal peaks at 530 nm and 740 nm) for *Lingula*

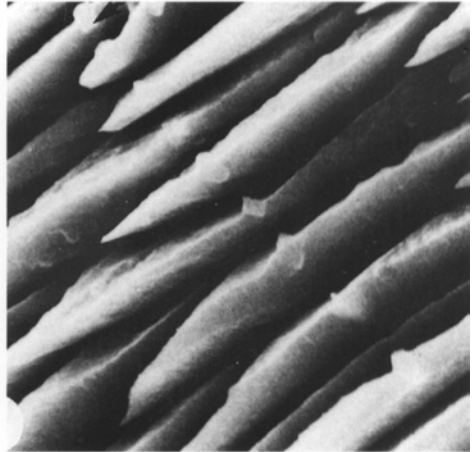
(WILLIAMS, CUSACK, & MACKAY, 1994). They contain only exocytosed materials and short extensions of apical plasmalemmas; and, although they are sporadically associated with recumbent cylindroid extensions and chambers several microns high, the protuberances of outer epithelium contained within these structures are not charged with storage vesicles as are caeca. Canals terminate with slightly expanded, flattened heads at the interface between the organic primary and biomineralized secondary layers of *Lingula*



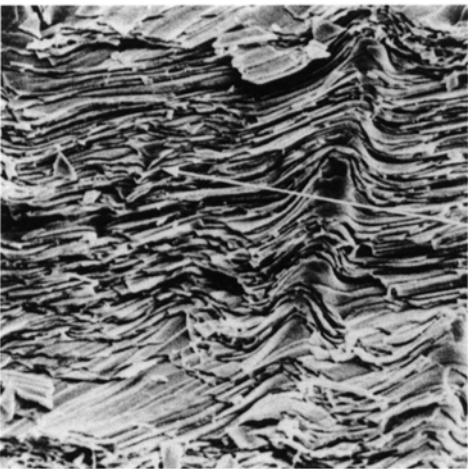
1



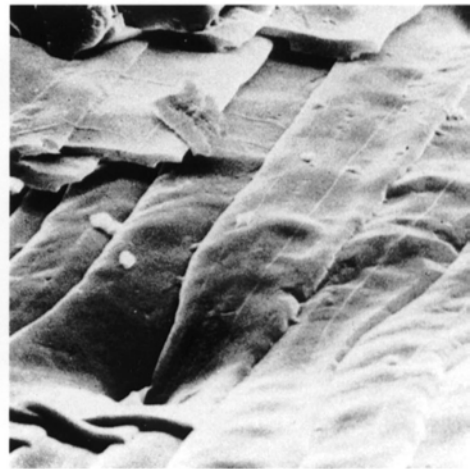
2



3



4



5

FIG. 265. For explanation, see facing page of Kansas Paleontological Institute

and in the narrow subperiostracal zone of GAGs terminating the mainly biomineralized primary layer of *Discina*. They are seldom (if ever) continuous throughout the secondary layer, as they are frequently interrupted especially, but not invariably, at intercalations of membranous laminae within successions. Canals also branch and, although they tend to be radially arranged at least in *Lingula*, the spacing can vary from 1 μm to 16 μm .

It is possible that this fine, canaliculate system is widely but sporadically developed among extinct organophosphatic groups. Thus they are found in acrotretoids but not in related spinose siphonotretoids (BIERNAT & WILLIAMS, 1971). However, the shell fabric of early Paleozoic stocks has not yet been comprehensively subjected to such studies as would reveal the existence and nature of these microscopic structures.

The only perforations in calcitic shells that are fine enough to be compared with lingulid canals are those found in late Mesozoic to recent endopunctate terebratulides and rarely in Silurian pseudopunctate plectambonitidines. The terebratulide micropunctae (GASPARD, 1978, 1982; SMIRNOVA & POPIEL-BARCZYK, 1991) occur in varying densities in terebratulids (Fig. 265.3), megalthyrids, kraussinids, and some living terebratulids and range in diameter from 200 nm to 4 μm , significantly less than the 10 μm to 20 μm diameters of coexisting endopunctae. There is, however, some doubt about their true nature. Many figured micropunctae may vertically penetrate several fibers and their membranous sheaths without causing displacement of their biomineral-organic interfaces. If such canals represented the trails of impersistent strands secreted by outer epithelium, they would have been

aligned with the long axes of fibers. Their vertical attitude should indicate that they originated at the outer mantle lobe and persisted in such a way as to cause thickening secondary shell to grow around them as it does around caeca. This is not so, and it is likely that at least some of the micropunctae are postmortem burrows of microorganisms comparable with those found by GASPARD (1989) infesting shells of recent terebratulids. The micropunctae of *Eoplectodonta*, on the other hand, are delineated by outwardly conical deflections of flattened, secondary fibers (BRUNTON, 1972) and are canaliculate (Fig. 265.4–265.5) although they have been formed like extropunctae.

PSEUDOPUNCTATION

Pseudopunctuation is preeminently characteristic of the strophomenide shell. Even with a low-power light microscope, the secondary fabric of the great majority of strophomenides is clearly seen to be sharply crenulated by tight microscopic deflections. Yet pseudopunctuation, initially interpreted as calcified punctuation (CARPENTER, 1851), was not understood until it was shown to be conical puckerings of the shell fabric, which normally contain indigenous rods of calcite (taleolae) (KOZLOWSKI, 1929; WILLIAMS, 1956).

In its typical form, a pseudopuncta consists of a slightly arcuate, anteriorly inclined trail of cone-in-cone deflections affecting the entire secondary laminar (or fibrous) fabric and emerging at the internal surface of the valve as a tubercle (Fig. 266.1–266.2). The arcuate trace and inclination of a pseudopuncta are growth effects resulting from the mantle having been pushed outward radially in response to the thickening of the secondary shell and the marginal expansion of the

FIG. 265. Various fine perforations of the brachiopod shell; 1, section across the interface between shell and mantle (top right-hand corner) of critical-point dried dorsal valve of the discinoid *Discina striata* (SCHUMACHER) showing the disposition of canals with exposed bases perforating stratified laminae, $\times 6,000$; 2, fracture section of the shell of *Lingula anatina* (LAMARCK) showing canals impersistently crossing laminae, $\times 1,400$ (new); 3, etched, resin-impregnated section of the secondary shell of *Sellithyris cenomanensis* GASPARD showing a micropuncta perforating a succession of fibers, $\times 4,000$ (Gaspard, 1990); 4–5, exfoliated internal surfaces of the secondary shell of the Silurian *Eoplectodonta transversalis* (WAHLENBERG) showing 4, a general view of a micropuncta (at tip of white arrow), $\times 250$ and 5, a detail of the surface showing the externally deflected conical surround of a micropuncta, $\times 1,200$

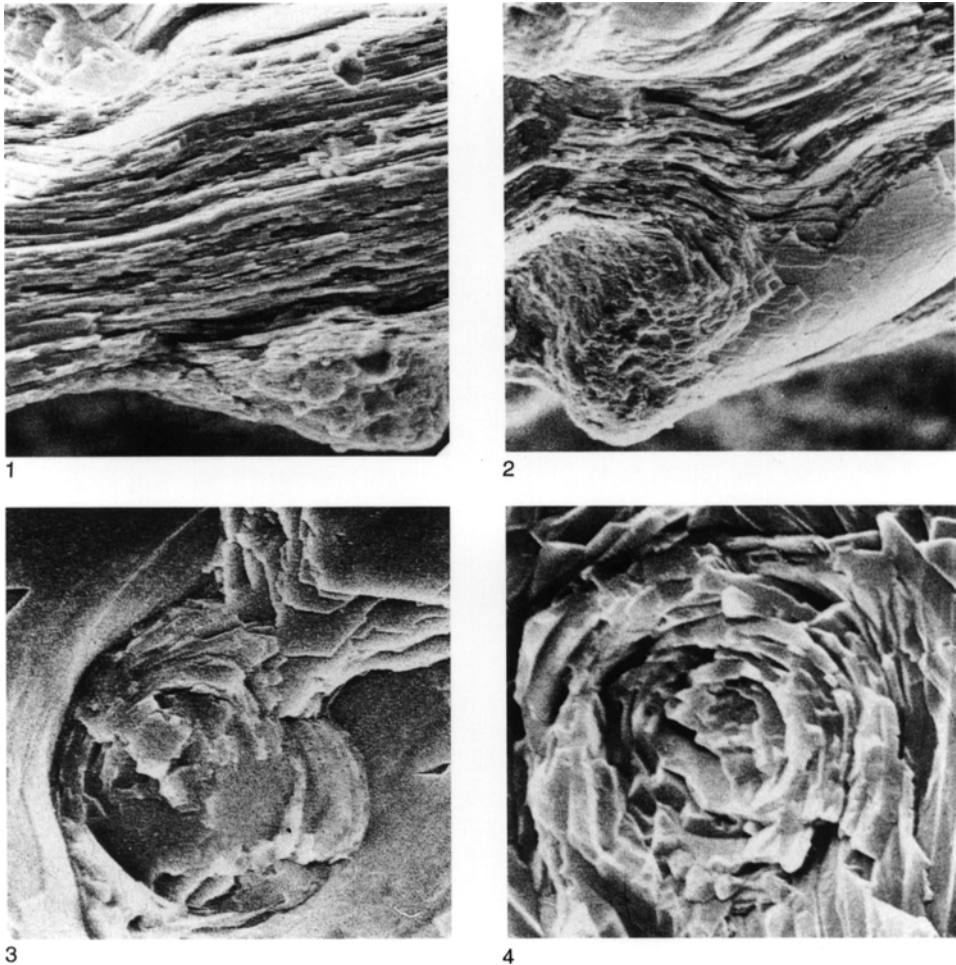


FIG. 266. Pseudopunctation in the laminar secondary shell of strophomenids; 1–3, fracture sections and internal fracture surface of a ventral valve of the orthotetidine *Apsocalymma sibielli* McINTOSH showing 1–2, the pseudopunctae indenting laminar surfaces and forming tubercles toward the tops and bottoms of micrographs, respectively, $\times 370$, $\times 570$, and 3, an external view of a pseudopunctate core of obliquely and spirally arranged laminae, $\times 1,500$; 4, detail of a pseudopunctate core of spirally inclined laminae in ventral valve of *Strophomena planumbona* (HALL), $\times 3,000$ (Williams & Brunton, 1993).

valve. Consequently a pseudopuncta is characteristically asymmetrical in longitudinal section with constituent laminae (or fibers) of the secondary shell deflected inwardly and inclined along the anterior and posterior sides of the pseudopuncta at narrowly and widely acute angles respectively. Pseudopunctae are usually hexagonally closely packed in varying densities (between 25 to

30 per mm^2 in orthotetids) and vary greatly in diameter as measured across all deflected laminae (or fibers) involved in their definition (rosettes).

There are two kinds of pseudopunctae (WILLIAMS & ROWELL, 1965b; MANANKOV, 1979). In orthotetidines and early strophomenoids, pseudopunctae consist exclusively of rosettes of conically disposed laminae. In

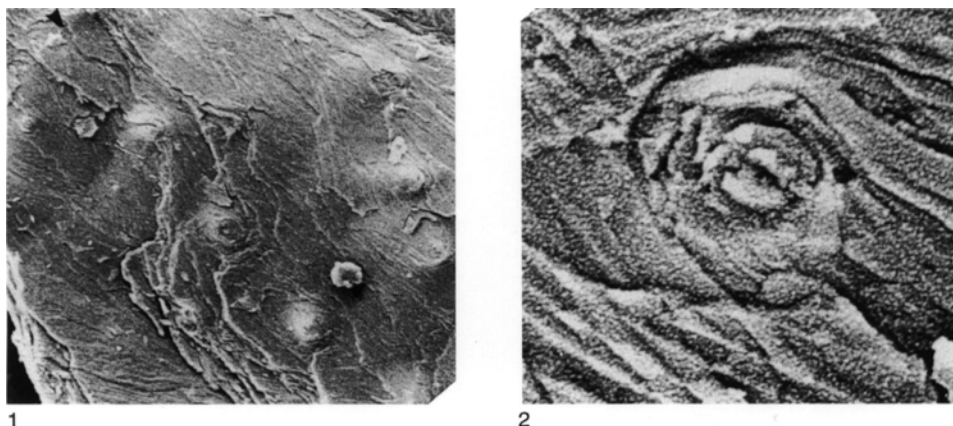


FIG. 267. Origin of orthotetidine pseudopunctation; 1, general view (X170) and 2, detail (X2,340) of internal surface of a fragment of the secondary shell of *Fardenia scotica* LAMONT showing incipient pseudopunctae breaking through cross-bladed laminae in spirally disposed arrangements (Williams & Brunton, 1993).

orthotetids up to 20 or so laminae can form a concentric layering (up to 50 μm across) with gently convex tops (tubercle) around a core (about 20 μm) of solid calcite or of tilted fragments of discrete laminae sets (Fig. 266.3). Well-preserved tubercles are completely covered by domed laminae that seem to have been unbroken in the original state. Arrays of these domed cones have been traced throughout shells along sinuous paths about 40 μm wide with cores consisting of amalgamated domes of successive laminae cones. The pseudopunctae of Ordovician strophomenoids (Fig. 266.4) are identical in structure with tilted blocks of laminae forming cores that, in *Rafinesquina*, can be 50 μm in diameter within rosettes about three times as big. Differentially preserved exteriors of *Strophomena*, which has radially disposed rosettes about 40 μm in diameter, reveal the nature of the first-formed parts of pseudopunctae. Interspatial depressions and pseudopunctate cores aligned within them are lined with granular primary shell, while cores of pseudopunctae exposed in the exfoliated crests of costellae consist of obliquely stacked, laminar blocks. In effect strophomenid pseudopunctae originated on a thin primary layer, probably in the same manner

as those of *Fardenia* (WILLIAMS & BRUNTON, 1993).

The cross-bladed, laminar fabric of the Ordovician orthotetidine *Fardenia* is impunctate; but exceptionally shallow immature pseudopunctae develop (Fig. 267). The rosettes of these pseudopunctae are seldom more than 40 μm across with cores (about 10 μm in diameter) encircled by fewer than seven laminae. The core of one immature pseudopuncta was composed of two spirally continuous laminae inclined toward a central slit. The most likely way for this arrangement to have arisen would have been for a cell about 5 μm across to have started secreting on an interlaminar membrane fibrillar proteins (or filaments) connected by hemidesmosomes and to have continued to do so at a faster rate than the deposition of laminae by surrounding cells. These rapidly lengthening filaments would, in turn, have caused adjacent cells to secrete laminae in a steeply inclined coil around the strands to form the biomineralized core of the growing pseudopuncta (Fig. 268). From time to time the process would have been brought to a halt by cessation of secretion of the strand. This would account for tubercles being capped by entire as well as perforated domes and would

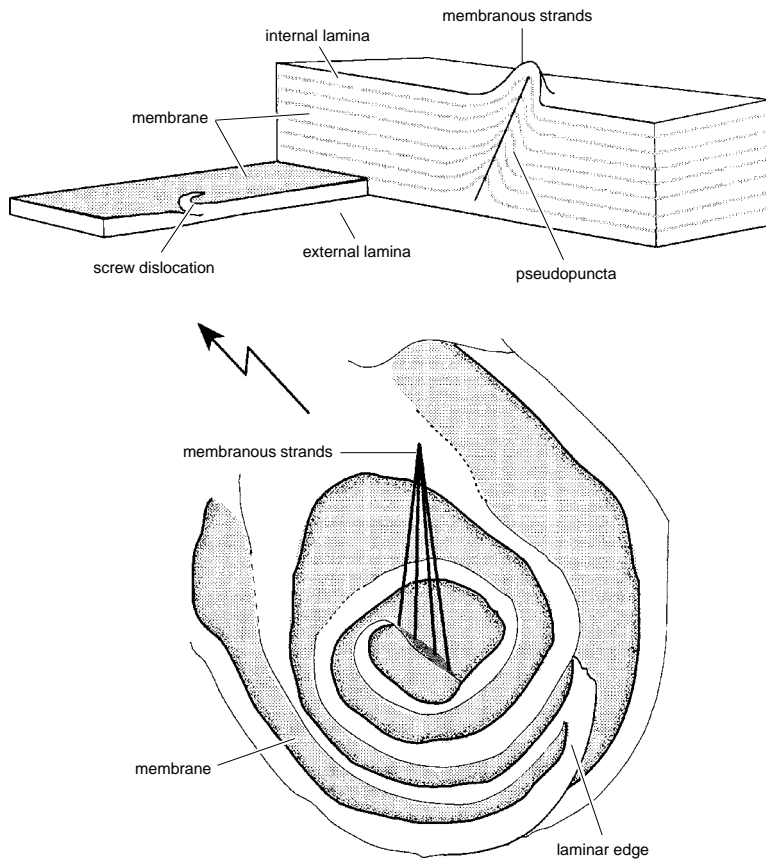


FIG. 268. Diagrammatic reconstruction of the origin and essential structure of a pseudopuncta, based on those found on internal laminae of *Fardenia scotica* LAMONT (see also Fig. 267) (Williams & Brunton, 1993).

not have precluded the growth of succeeding pseudopunctae on the same sites and at new loci.

The other kind of pseudopuncta, which is characteristic of plectambonitoids (Fig. 269.1), chonetidines, productidines, and oldhaminidines (Fig. 269.2), and such strophomenoids as leptaenids (Fig. 270) and stropheodontids, has a distinctive rod of calcite (taleola) at the core of a tubercle with a rosette of conically disposed laminae (or fibers in plectambonitoids). Thus the pseudopunctae of the Carboniferous leptaenid *Leptagonia* (Fig. 270) consist of rosettes of inwardly inclined laminae 75 μm or more in diameter grouped around taleolae (up to 30

μm across). A taleola is fully developed and differentiated from the fabric of its host shell when first formed, and its distinctiveness is further emphasized by the way its surface is a calcified patina that is sharply separated from the surrounding laminae. The most striking difference, however, between taleolae and the laminar infills of orthotetid pseudopunctae is brought out by the porous structure of etched taleolae. The pits of this porous fabric are commonly delineated by rhombohedral planes but are clearly part of an interlacing series of canals (up to 300 nm in diameter) permeating the entire structure. This suggests that a taleola, *in vivo*, consisted of a calcitic mesh permeated by intercon-

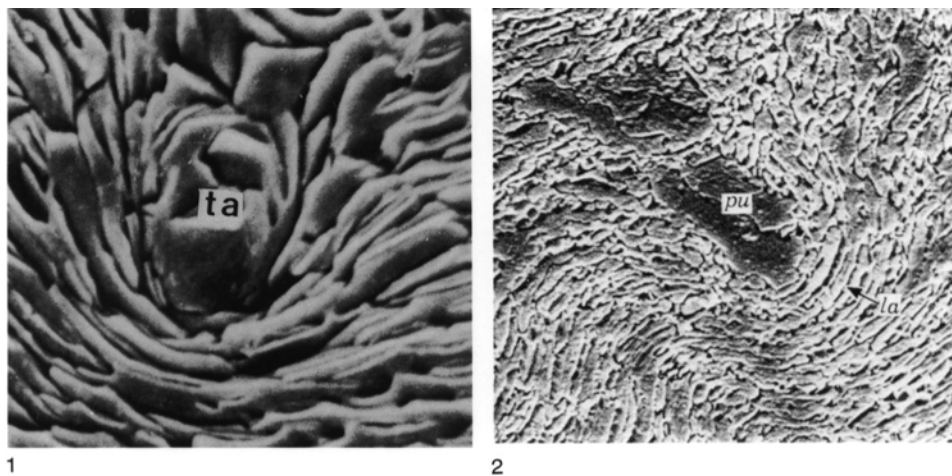


FIG. 269. Pseudopunctation in shell sections; 1, transverse view of a taleola (*ta*) within the fibrous secondary shell of the plectambonitoid *Sowerbyella variabilis* COOPER, $\times 1,400$ (Williams, 1990); 2, outwardly directed pseudopuncta (*pu*) in a laminar (*la*), secondary shelled dorsal valve of the lyttonioid (oldhaminidine) *Leptodus* cf. *richthofeni* KAYSER, $\times 1,200$ (Williams, 1973).

nected tunnels that were filled with organic materials and that it was probably bounded by a membrane continuous with those between the calcitic components of the laminar succession (WILLIAMS & BRUNTON, 1993).

The phylogenetic relationship between pseudopunctae with or without taleolae has yet to be determined. Both kinds have been reported in the same shells of many species. But in view of the subtle, albeit fundamental, difference between taleolar and amalgamated laminar cores there is abundant opportunity for misidentification. Pseudopunctae lacking taleolae are certainly homoplastic, having appeared independently on at least three occasions among the gonambonitoids, early strophomenoids, and orthotetidines. This is not surprising if such pseudopunctae represented spiral perpetuations of screw dislocations on sheeted secondary shell. However, pseudopunctae with taleolae also appear to be homoplastic, for even if the chonetidines and productidines inherited their taleolar shells from a plectambonitoid stem group, leptaenids and stropheodontids are unlikely to have derived their taleolae from the same source.

This potential for microtextural homoplasy is endorsed by the extraordinary condition of the shell of orthotetidine schuchertelloids (Fig. 271.3–271.4), the fabric of which is crenulated by arrays of asymmetrical, conical deflections invariably pointing externally (THOMAS, 1958). In *Schuchertella* and *Streptorhynchus*, these externally directed deflections (extropunctae) (WILLIAMS & BRUNTON, 1993) are densely arranged more or less radially at about 150 per mm^2 . On internal, exfoliated surfaces, mature extropunctae form shallow craters about 50 μm in diameter bounded by up to ten laminar sets arranged concentrically around elliptical cores (4 to 5 μm in maximum diameter) and usually with a medial slot. Exceptionally a single lamina lines part of the crater sides and merges with the core as a spirally twisted band with a medial slot. On exfoliated external surfaces extropunctae occur as low domes up to 30 μm across that consist of successions of curved laminae in rosettes surrounding cores of oblique or twisted plates, some with medial slots.

The laminar cores of extropunctae preclude any homology with punctae like those

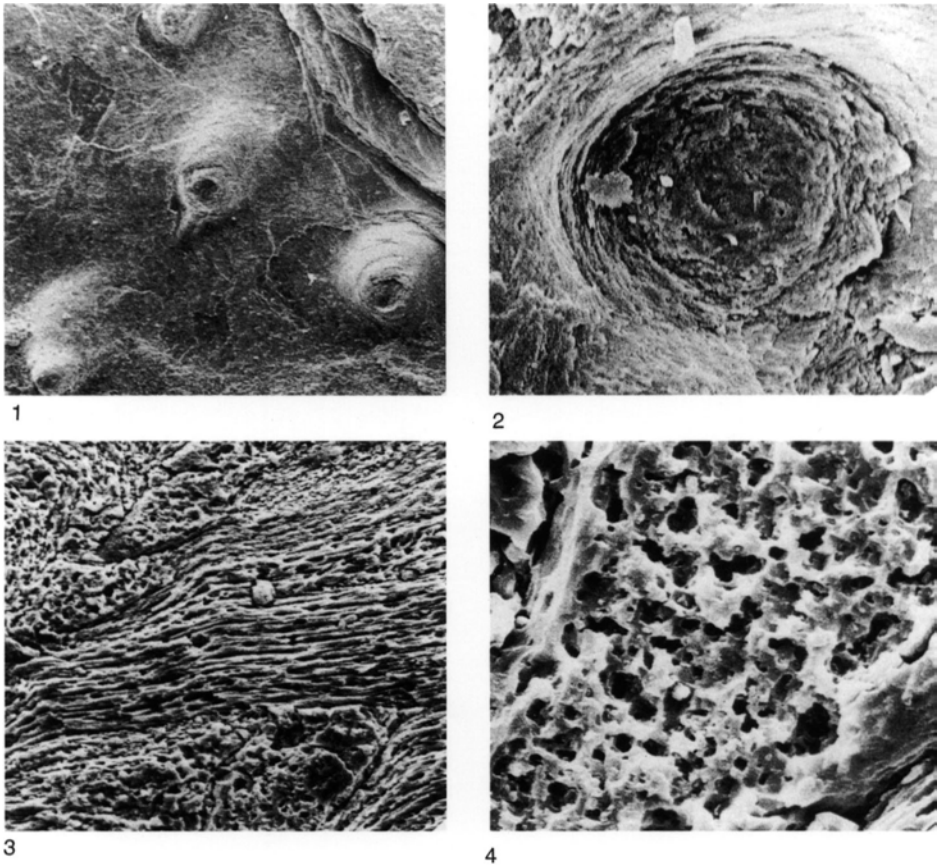


FIG. 270. Pseudopunctuation in the leptaenid *Leptagonia caledonica* BRAND; 1, general view of tubercles with taleolar cores on internal surface of ventral valve, $\times 85$; 2, external view of transverse fracture section of pseudopuncta with roughened, pock-marked surface to taleolar core, $\times 400$; 3, general view and 4, detail of section of a ventral valve showing disposition of laminae around taleolae (exterior toward the top), fully developed taleolar base secreted unconformably on horizontal laminae (bottom right-hand corner of 3), $\times 350$, and canal system within taleola of 4, $\times 1,450$ (Williams & Brunton, 1993).

in the laminar-shelled craniids, but they are much the same as those of pseudopunctae lacking taleolae. Accordingly the reversed orientation of deflection of the rosettes could be attributed to different rates of secretion of the organic components of the cores. More slowly growing so-called keratin filaments may have been the dominant constituent in extropunctae compared with rapidly secreted strands of proteinaceous membranes in pseudopunctae.

The function of pseudopunctae (with or without taleolae) and extropunctae is con-

tentious. Internal tubercles or indentations associated with all three kinds of conical deflections of shell fabric can be partly or entirely capped by laminae (or fibers) that signalled a termination of the growth of these structures. Pseudopunctae and extropunctae, however, can normally be traced through a shell and show little or no branching. This and the prospect that taleolae had an organocalcitic composition comparable with that of muscle scar bases affirm the view that the main function of both kinds of pseudopunctae and extropunctae was to pro-

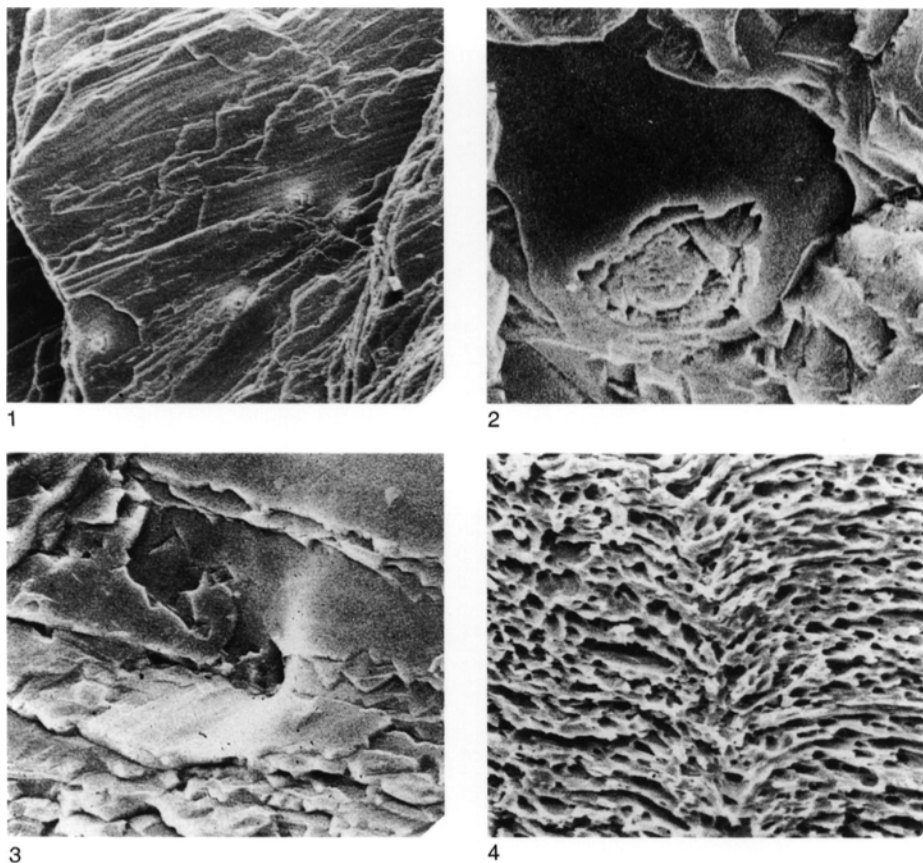


FIG. 271. Extropunctation in the orthotetidine *Schuchertella lens* (WHITE); 1, external surface of fragment of laminar secondary shell in general view, $\times 230$, and 2, in detail to show an extropuncta, $\times 2,100$; 3, internal surface of laminar secondary shell showing the conical depression of an extropuncta delineated by spirally disposed laminae, $\times 980$; 4, etched section of a dorsal valve with conical deflections of an extropuncta directed toward the exterior below the lower edge of the micrograph, $\times 470$ (Williams & Brunton, 1993).

vide holdfasts (Fig. 272) for mantle filaments (WILLIAMS, 1956) with rosettes, irrespective of the direction of deflection, additionally acting as rivets joining finely sheeted successions as friable as those of the stropheodontid *Pholidostrophia* (WILLIAMS, 1953). It has also been suggested that tubercles, especially those with taleolar cores, were the bases of transmantle muscle fibers operating fimbriae that sieved and conducted the flow of water in the mantle cavity (GRANT, 1968; MANANKOV, 1979). In view of the strongly ciliated nature of the inner epithelium lining the mantle cavities of all living brachiopods,

fimbriae would seem to be superfluous to the hydrodynamic requirements of stropheomenides. Indeed, the internal development of pseudopunctae in some stocks seems to confirm this conclusion.

Acceleration in the apical growth of pseudopunctae continually resulted in the prolongation of their tubercles into sharp cones or even spines (endospines) on the valve interiors. They are especially well developed in productidines and are commonly disposed in fringes along subperipheral rims where they could have functioned as straining or filtering systems (see Fig. 308).

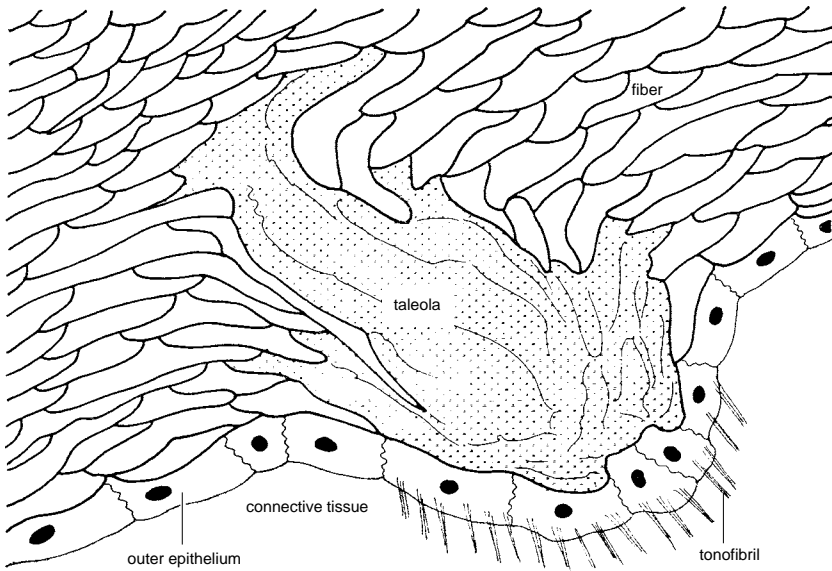


FIG. 272. Stylized oblique longitudinal section of a taleola deflecting the fiber of the secondary shell of the plectambonitoid *Sowerbyella* and showing its inferred relationship with secreting outer epithelium (Williams, 1968a).

The most extraordinary development of endospines, however, is found in productidine richthofenioids. In this group, the lidlike dorsal valve lies well within a sub-peripheral ring of endospines in the ventral valve, which grew centripetally. In many species these spines branched and amalgamated to form a complete net (coscinidium) over the opening of the ventral valve and may even have been elaborated into a regular honeycombed meshwork forming a high dome (*Sextropoma*). Such structures must have been enclosed in mantle (Fig. 273) so that a net would have been formed by the fusion of outer epithelium along zones of contiguity between converging struts. In this arrangement the inner epithelium would have been the outermost coat of the coscinidium and would, therefore, have been more exposed to the environment than it would have as a lining of the mantle cavity. However, judging from the mantle edge of such living brachiopods as *Terebratulina* and *Lingula*, the inner epithelium of a coscinidium was probably equipped with strongly developed cilia (which would have facilitated the circulation of sea water in the shell) and pro-

tected by a thick glycocalyx with a bounding pellicle.

INTERNAL TUBERCLES

Internal tubercles secreted within evaginations of the outer epithelium and serving as attachment sites for soft parts occur in other articulated brachiopods, notably the thecideidines and terebratulides. However, microscopic whorls of fibers are common features of the secondary layer of many species (Fig. 274.1) and are probably precursory to tubercles, like those found in the thecideidine *Bactrynum* (Fig. 274.2).

The infrastructure of thecideidine tubercles is much like that of pseudopunctae. In the Jurassic *Mimikonstantia*, which has a sheet of secondary shell, tubercles of the dorsal valve are composed of inwardly directed rosettes of fibers with cylindroid cores indistinguishable from the fabric of the primary layer, from which they arise more or less vertically (Fig. 274–275). Tubercles of the ventral valve, on the other hand, lie almost parallel with the internal surface and also have granular cores (Fig. 276; BAKER & ELSTON, 1984). In *Thecospira* no structural

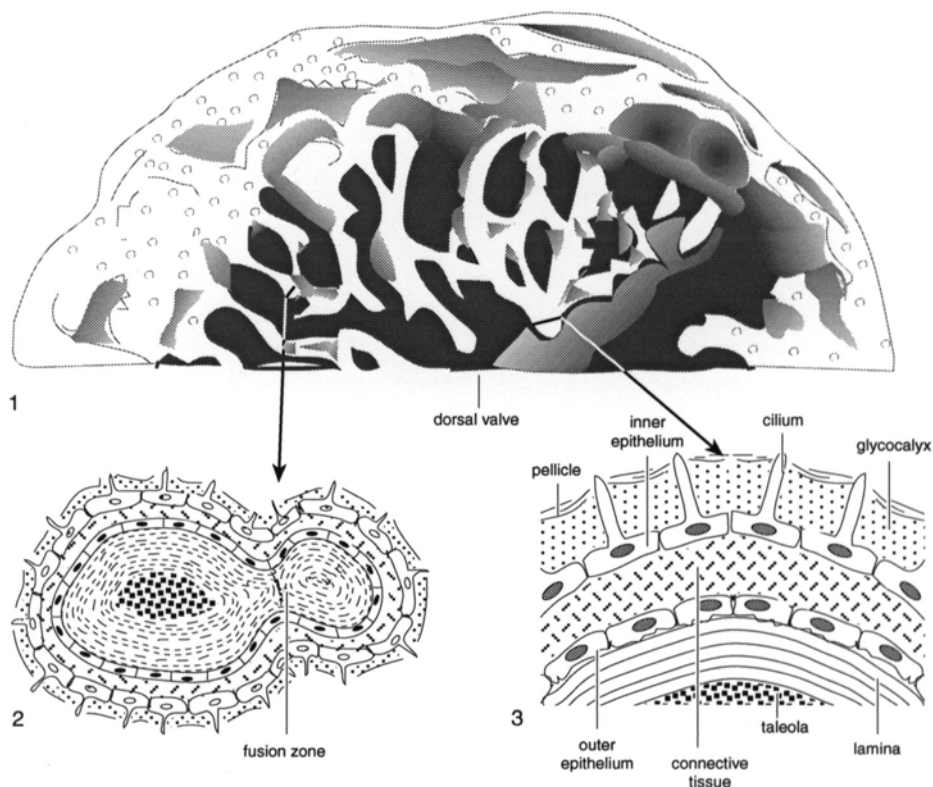


FIG. 273. Richthofenioid coscinidium; 1, diagrammatic external view of part of a coscinidium of *Cyclacantharia* COOPER & GRANT, approximately $\times 4.6$; 2, inferred fusion of endospine (with taleolar core) and a lateral branch of an adjacent endospine; 3, transverse section through the inferred mantle cover of a main strut (with taleolar core) (new).

differentiation of tubercles has been reported (BENIGNI & FERLIGA, 1988). All tubercles of both valves have well-developed cores (about $50\ \mu\text{m}$ in diameter) enclosed by rosettes of fibers of the secondary shell, which are deflected inwardly. The cores are composed of irregular calcite crystals with no preferred orientation. They are continuous with a primary layer of the same fabric, which has probably been affected by recrystallization. Some parts of cores appear to incorporate bits of contiguous fibers and, in that respect, are unlike true taleolae.

Thecideidine tubercles are structurally and functionally different from strophomenide pseudopunctae in several respects. In particular, tubercles are not uniformly distributed over valve interiors but are mainly concentrated within subperipheral rims of

valves where they support mantle margins. Accordingly, at those stages in shell growth entailing migration of the shell and mantle margins, mature tubercles undergo resorption (WILLIAMS, 1968a; BAKER, 1970a). Moreover the development of nonfibrous cores in tubercles is essentially an early stage in the neotenus shedding of a fibrous secondary shell. In living *Thecidellina*, with nothing more than vestiges of secondary shell, tubercles are composed almost entirely of splayed acicular crystallites of calcite (Fig. 275.2) and are only morphologically distinguishable from the rest of the primary shell, as any associated secondary fibers are restricted to small groups of 20 or so capping some tubercles (WILLIAMS, 1973).

The internal tubercles of terebratelloid kraussinids and megathyrids are homologous

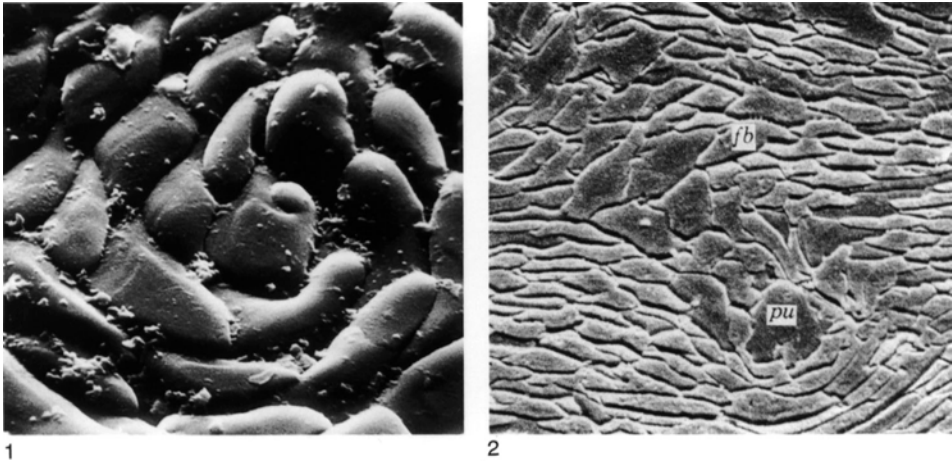


FIG. 274. Internal microstructures; 1, whorl of fibers on the internal surface of the secondary shell of the rhynchonellide *Hemithiris psittacea* (GMELIN), $\times 1,200$ (new); 2, tubercle (*pu*) in the fibrous (*fb*) secondary shell of a ventral valve of the thecideidine *Bactrynum emmrichii* (GÜMBEL), $\times 1,100$ (Williams, 1973).

with thecideidine thecospiroids. They consist of inwardly deflected rosettes of fibers that may exceed $100\ \mu\text{m}$ in diameter. Fibers may become larger at the cores of tubercles and may even be replaced locally by a crystalline fabric (SMIRNOVA & POPIEL-BARCZYK, 1991). Like thecideidine tubercles, they are mainly concentrated as subperipheral rims

and are also subject to resorption during the outward migration of the shell and mantle margins.

SHELL DAMAGE AND REPAIR

Apart from changes arising from the normal processes of secretion and growth, the brachiopod shell can also record permanent

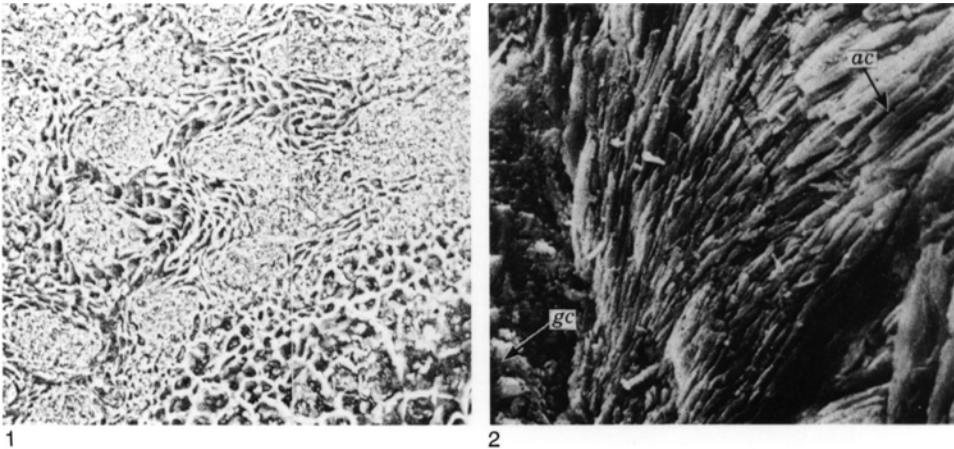


FIG. 275. Thecideidine tubercles; 1, section of the subperipheral rim of *Mimikonstantia sculpta* BAKER & ELSTON showing transverse sections of tubercles of granular primary shell associated with secondary fibrous shell, $\times 250$ (Baker & Elston, 1984); 2, fractured edge of dorsal valve of *Thecidellina barretti* (DAVIDSON) showing acicular crystallites (*ac*) and granular calcite (*gc*) within a tubercle of primary shell, $\times 1,400$ (Williams, 1973).

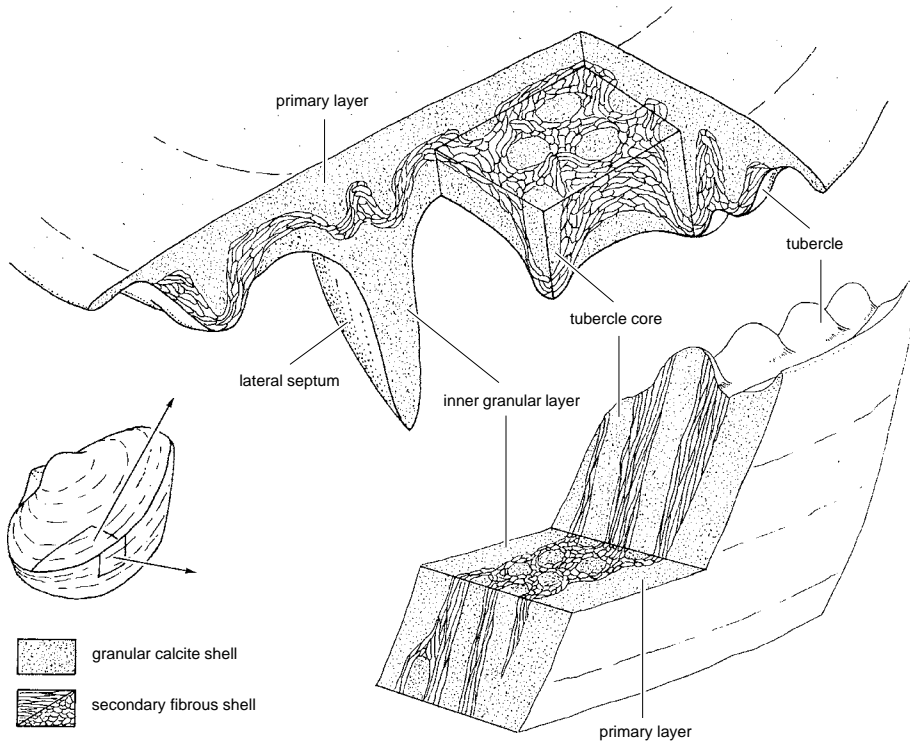


FIG. 276. Diagrammatic reconstruction of the shell microstructure of the thecideid *Mimikonstantia sculpta* BAKER & ELSTON showing the disposition of tubercles in the dorsal valve (top) and in the ventral valve (bottom right) (Baker & Elston, 1984).

damage from an extraneous source such as fractures and other malformations on surfaces and within the fabrics of fossil and living shells. Repair involves reversions or accelerations in the secretory regimes of mantles, which themselves are usually undergoing regeneration. A higher organic content renders organophosphatic shells more plastic than the brittle calcitic shells, and this difference is evident even in damage by fracture. A repaired zone of damage extended for about 200 μm on the surface of a valve of the Cambrian acrotretoid *Protoretta*. Within this zone two sets of slitlike indentations disrupted ten fila. One set of gashes is feasibly interpreted as a fracture in the living shell, the other, an en echelon set, as tension gashes (Fig. 277). Both sets are consistent with having been formed in a lateral shear zone, parallel with the trace of tissue undergoing repair. Some of

the tension gashes are associated with minute folds superimposed on fila. The folds are also consistent with the assumed stress fields but could not have been formed in brittle shells (WILLIAMS & HOLMER, 1992).

The sequence of repair of fractures in organophosphatic shells that are deep enough to expose the underlying outer epithelium has been described for living *Glottidia* (PAN & WATABE, 1989). Within the fracture zone, any shell debris is phagocytized by amoebocytes and partly released into a mantle canal(s). Concurrently the cuboidal epithelial cells at the fracture site become columnar and assume the characteristics of vesicular cells secreting periostracum at the outer mantle lobe. At the fracture site, the reverted cells secrete a sheetlike pellicle covering the exterior and then an inner layer that, in due course, differentiates into a normal

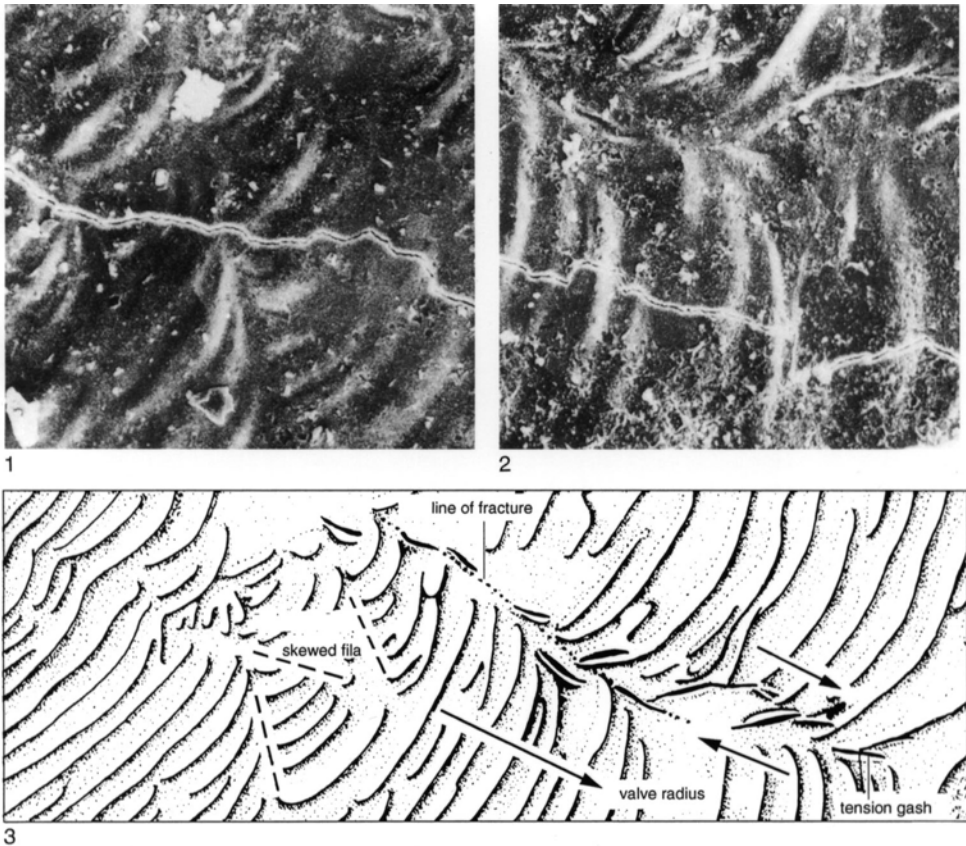


FIG. 277. Repaired shell of the acrotretoid *Prototreta* sp.; 1–2, malformed drapes of fila on the exterior of a dorsal valve with tension gashes and associated minor folding, $\times 350$ and approximately $\times 350$; 3, reconstruction of the line of fracture induced by the inferred stress couple, $\times 350$ (Williams & Holmer, 1992).

periostracum. Within 90 days of fracture the cells revert once more to a cuboidal shape and start secreting a biomineralized primary layer followed by inner secondary shell.

The nature and repair of fractures at the surfaces of brittle calcitic shells are better understood in relation to disruptions of radial ornamentation in finely costellate shells like that of the strophomenid *Rafinesquina* (WILLIAMS & ROWELL, 1965b, p. 74). When injury to part of the mantle edge was severe enough to impede forward growth, the space anterior to the zone of damage became constricted and was ultimately sealed off by the encroachment and fusion of the flanking unaffected parts, which thereby restored a fully functional and continuous mantle edge. Such encroachment involved an abnormal

proliferation of tissue toward the area of injury, as is shown by the increased number of costellae given off to converge in that direction. Concomitantly, the space immediately in front of the damaged part of the mantle edge became closed by outer epithelium, which originated behind the flanking parts of the mantle edge as they moved forward and was responsible for the deposition of unribbed shell, presumably beneath a newly secreted cover of periostracum in a sequence like that effecting repair of the *Glottidia* shell (Fig. 278).

The sequence of repair of damaged fabric of calcitic shells can be determined by studying the effects of mantle retraction, which may be periodic and genetically controlled or randomly induced by extraneous agencies.

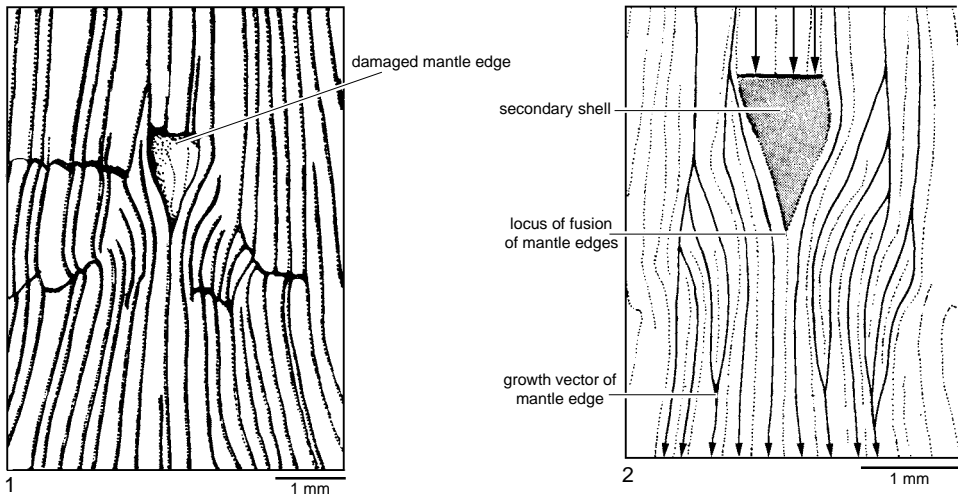


FIG. 278. Shell repair in the strophomenide *Rafinesquina nasuta* (CONRAD) showing 1, inferred relationships of area of repair, with 2, undamaged growing mantle edges (Williams & Rowell, 1965b).

The former are responsible for surface ornamentation and are not considered in this section. The latter can cause disruptions of the secondary shell, which trigger a distinctive sequence of secretory repair (WILLIAMS, 1971a).

In the living, impunctate rhynchonellide *Notosaria*, a violent retraction of the mantle

causes an abrupt termination of all secretion within the affected part of the shell (Fig. 279–280). As soon as retreat (regression) has ended, selective deposition begins. Cells must readjust to resume secretion at new sites because those parts of apical plasmalemmas responsible for carbonate secretion start depositing calcitic pads in continuity

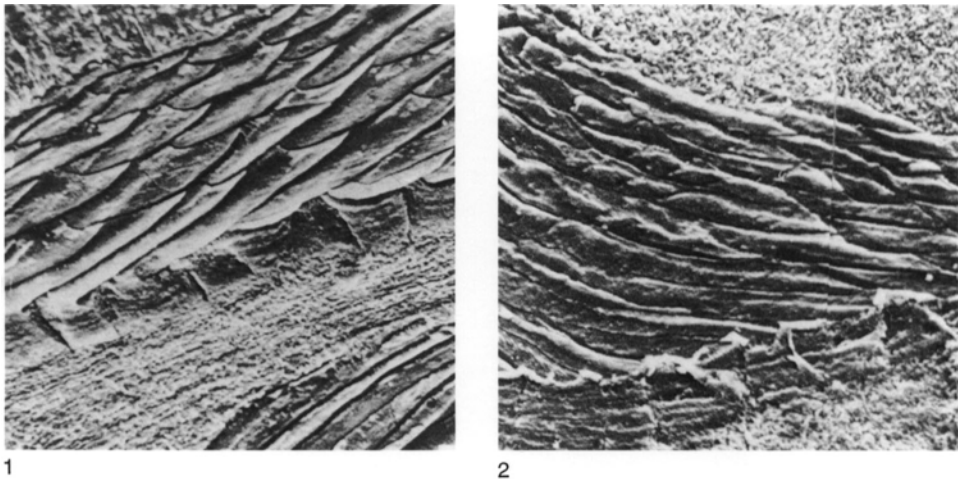


FIG. 279. Shell repair in fibrous-shelled brachiopods; 1–2, general views of regressed successions of fibrous secondary shell, showing primary layer and calcitic pads underlying the normal succession (upper part of 1), of primary and secondary shell in sections of 1, the rhynchonellide *Notosaria nigricans* (SOWERBY), $\times 1,300$ and of 2, the terebratelloid *Magasella sanguinea* (LEACH) with a proteinaceous layer marking the regressive interface, $\times 1,100$ (Williams, 1971a).

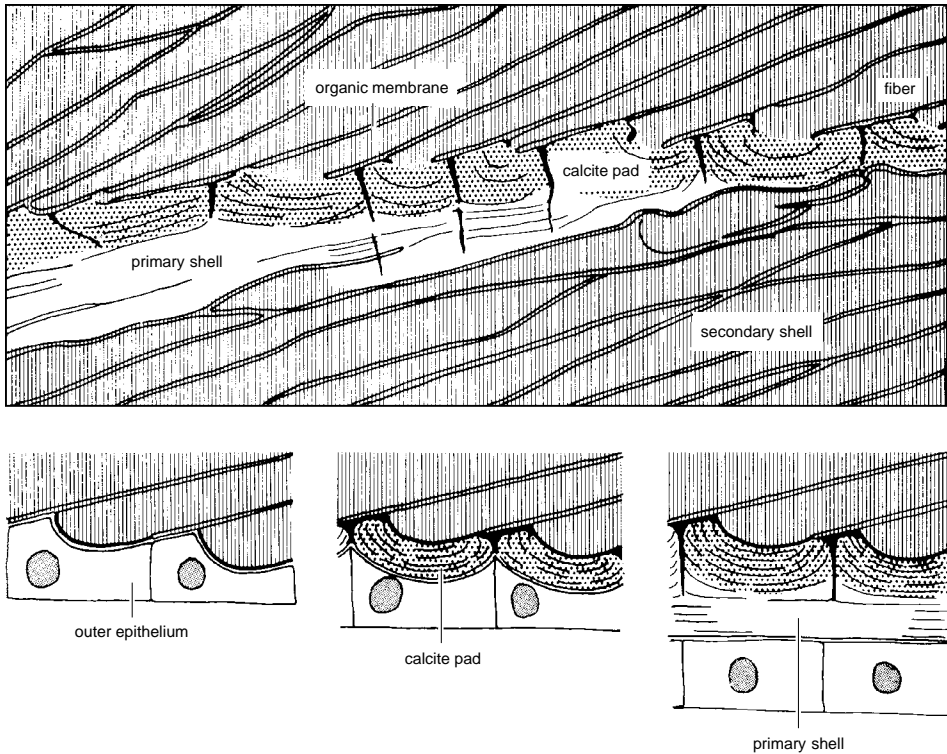


FIG. 280. Stylized tracing of shell succession of the rhynchonellide *Notosaria nigricans* (SOWERBY) shown in Figure 279.1 indicating the nature of a regression and the inferred relationships of retracted outer epithelium resuming secretion (Williams, 1971a).

with terminal faces of different fibers from those secreted by them before regression. Over a period of about two weeks, the pads form a continuous layer about $5\ \mu\text{m}$ thick, interrupted by narrow, vertical slots corresponding to intercellular spaces.

This layer of pads is secreted by all outer epithelial cells that had been brought into juxtaposition with the secondary shell surface irrespective of the phase of the secretory regime they were in prior to retraction. Thus cells of the outer surface of the outer mantle lobe, which normally deposit primary shell, secrete pads indistinguishable from those laid down by secondary outer epithelium. Once

the pads have been deposited, however, cells revert to their respective secretory regimes at the point where they left off; and the normal processes of shell secretion and growth are brought back into play. In this way impersistent bands of secondary fiber (false mosaics of BRUNTON, 1969) become intercalated within shell successions (Fig. 281).

Retraction of the mantle in endopunctate shells differs from that of the impunctate *Notosaria* in only one respect. In *Magasella*, which can be heavily ruttured with depositional breaks penetrating deep into the secondary layer, a proteinaceous membrane (Fig. 279.2) is secreted on the surface of re-

gression, which subsequently becomes the seeding sheet for the foundation layer of calcitic pads marking the first stage in recovery (transgression). This membrane cuts across punctae indicating that caeca are withdrawn during retraction. It would, therefore, not be surprising to find that caeca can get trapped along the regressive interface between the old surface and the newly formed shell and are eventually pinched out, so that punctal heads in the immediate vicinity of retraction surfaces within the living shell could be emptied of caeca by the processes of mantle transgression.

The frequency of damaged shells in fossil faunas varies among the main groups of articulated brachiopods. The proportions of shells with repaired breaks, represented in assemblages from Ordovician to Tertiary in age vary from 13 percent for strophomenides to just 1 percent for rhynchonellides (ALEXANDER, 1986). This discrepancy can be attributed to a number of factors. The likelihood, however, is that the laminar shells of strophomenides (especially those without taleolae) were more friable than the orthodoxly stacked fibrous ones of rhynchonellides. Yet it is also likely that, when crushed, fibrous shells would have cleaved more easily and lethally than those composed of cross-bladed laminae, which would have behaved like plywood. Consequently the proportions of lethally damaged shells among rhynchonellides could have been significantly greater than among the strophomenides. Even so, regeneration of the brachiopod shell seems to have been a more common feature of the organophosphatic and laminar calcitic brachiopods than of fibrous groups.

Koskinoid perforations of the shells of some extinct brachiopods are appropriately described in conclusion to this section as they are widely believed to have accommo-

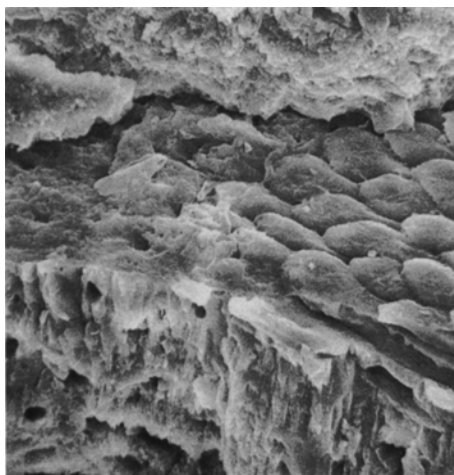


FIG. 281. Fracture surface of the shell of the recent rhynchonellide *Hemithiris psittacea* (GMELIN) showing a layer of secondary fibers (false mosaic) intercalated between primary layer above and below, $\times 1,100$ (Brunton, 1969).

dated extensions of soft parts. The ventral valves of the atrypidine *Uncites* and of many orthotetidines are penetrated by microscopic tunnels (koskinoid perforations). The perforations tend to concentrate in the umbonal regions; and, since perforated species invariably lacked functional pedicle openings, they have been interpreted as byssuslike threads (JUX & STRAUCH, 1966), distal branches of internal pedicles (SCHUMANN, 1969; MARTINEZ-CHACON & GARCIA-ALCADE, 1978), or attachment fibrils secreted by papillae of outer epithelium, which first made the tunnels by shell resorption (GRANT, 1980).

The perforations are usually orthogonal to the shell and occur as close clusters of almost perfectly circular, transverse sections on laminar surfaces without any deflection or general disturbance of the laminae themselves in the manner characteristic of the fabric of shell growing around a persistent

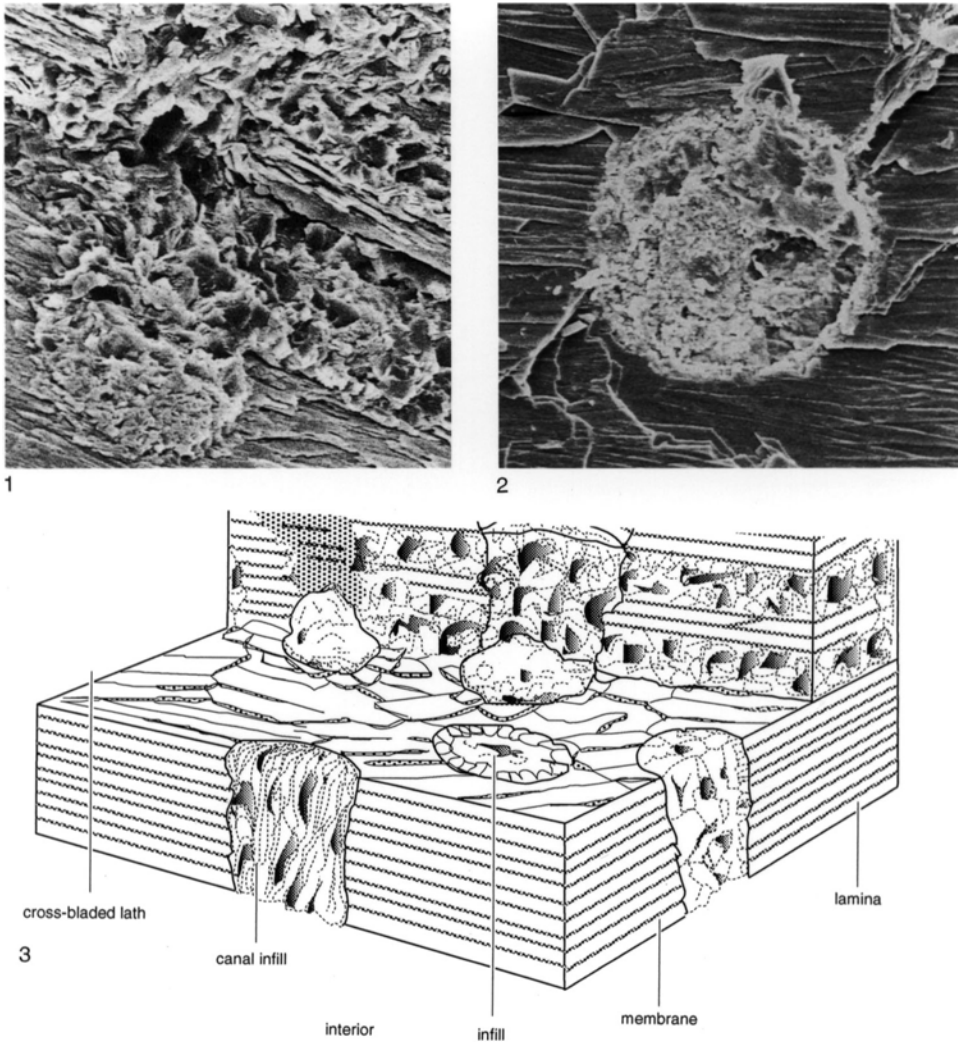


FIG. 282. Koskinoid perforations; 1, fracture section of ventral valve of Carboniferous *Brochocarina trearnensis* MCINTOSH showing circular infill representing tunnel in bottom left-hand corner connecting with rubbly infill representing two lateral galleries separated by shelf of laminae that has been penetrated by a perforation in the top left-hand quarter, $\times 475$ (Williams & Brunton, 1993); 2, fracture surface of ventral valve of Permian *Streptorhynchus pelicanensis* FLETCHER showing a perforation tunneled through the secondary laminae, which are undisturbed up to the rubbly periphery of the tunnel, $\times 300$ (new); 3, diagrammatic representation of koskinoid perforations based on those found in *B. trearnensis* (Williams & Brunton, 1993).

extension of the soft parts (Fig. 282). The tunnels vary in diameter from just over 10 μm to about 70 μm in some orthotetroids and schuchertelloids. Their walls are relatively smooth and sharply distinguishable from any infill and are rarely associated with horizontal galleries containing the same infill. There

are no known means of having tunnels so neatly drilled and then occupied by extensions of the mantle (or rudimentary pedicle); and koskinoid perforations are more reasonably explained as having been made by burrowing parasites (THOMAS, 1958; WILLIAMS & BRUNTON, 1993).

MORPHOLOGY

ALWYN WILLIAMS¹, C. HOWARD C. BRUNTON², and DAVID I. MACKINNON³

[¹University of Glasgow; ²The Natural History Museum, London; ³University of Canterbury, New Zealand]

SHELL FORM

The brachiopod shell, which is normally bilaterally symmetrical about the longitudinal median plane (plane of symmetry), consists of two dissimilar valves and is oriented according to the growth and disposition of the soft parts. That region of the shell from which the pedicle emerges and which normally represents the first-formed part of each valve is posterior so that the median portions at the opposite ends of the shell margin constitute the anterior (Fig. 283). The valve that accommodates most, if not all, of the pedicle is referred to as the **ventral valve**; it is typically larger than the opposing **dorsal valve**. These terms are preferred to pedicle and brachial respectively as they describe the orientation of the shell relative to the body axis and facilitate reference to the disposition of its various features. Dimensions indicating shell size, outline, and profile are conventionally taken in the manner shown in Figure 283.

The growth of the brachiopod valve, subsequent to the secretion of the protogulum, may proceed in three different ways (Fig. 284; THOMSON, 1927). In such inarticulated brachiopods as discinids, deposition continues around the entire margin of the protogulum, which, as a result of this holoperipheral growth, maintains a position more or less at the center of the adult valve (Fig. 284.1a–b). In other inarticulated species like the lingulids, although the posterior margin is thickened by some growth, nearly all the new shell is added to the lateral and anterior margins (hemiperipheral growth) so that the protogulum remains in a posteromedian position (Fig. 284.3a–b). The third type of growth affecting inarticulated forms (e.g., some acrotretoids), mixoperipheral, is a variant of holoperipheral growth in which the posterior surface of a valve is inclined ante-

riorly toward the other valve (Fig. 284.2a–b). Such a surface has been called a palintrope (THOMSON, 1927), but the term has limited use in this context because changes in growth directions, involving transitions between holoperipheral and mixoperipheral patterns, are common among brachiopods.

Mixoperipheral growth is preeminently characteristic of articulated brachiopods (Fig. 284.2a–b), especially in the definition in both valves of a planar or curved triangular area (**cardinal area**) subtended between each apex and the posterior ends of the lateral margins (cardinal extremities) (Fig. 283). The growth of the cardinal area is controlled at its free edge (posterior margin). In many genera the posterior margin is parallel to the hinge axis (i.e., the line about which the valves rotate during opening or closing of the shell) and forms a true hinge line, the growing edge of the posterior margin of the two valves being identical in extent. Shells in which both conditions are fulfilled are referred to as strophic (Fig. 285; RUDWICK, 1959) and the cardinal areas of these shells are referred to as **interareas**. The ventral interarea of such shells is commonly larger than the dorsal and both may be variously inclined relative to the surface containing the boundary line (commisure) between the anterior and lateral margins of the valves (Fig. 283). As can be seen in Figure 285.3, the disposition of interareas relative to the plane of commissure (the normal plane of RUDWICK, 1959) may vary by more than 180°. The most common attitude adopted by the ventral and dorsal interareas is apsacline and anacline, respectively, and the rarest conditions are probably the procline and hypercline, which represent aspects of holoperipheral growth. Among wide-hinged orthides, strophomenides, and spiriferides, the interareas form obtuse-angled triangles; but extreme lateral reduction of the hinge

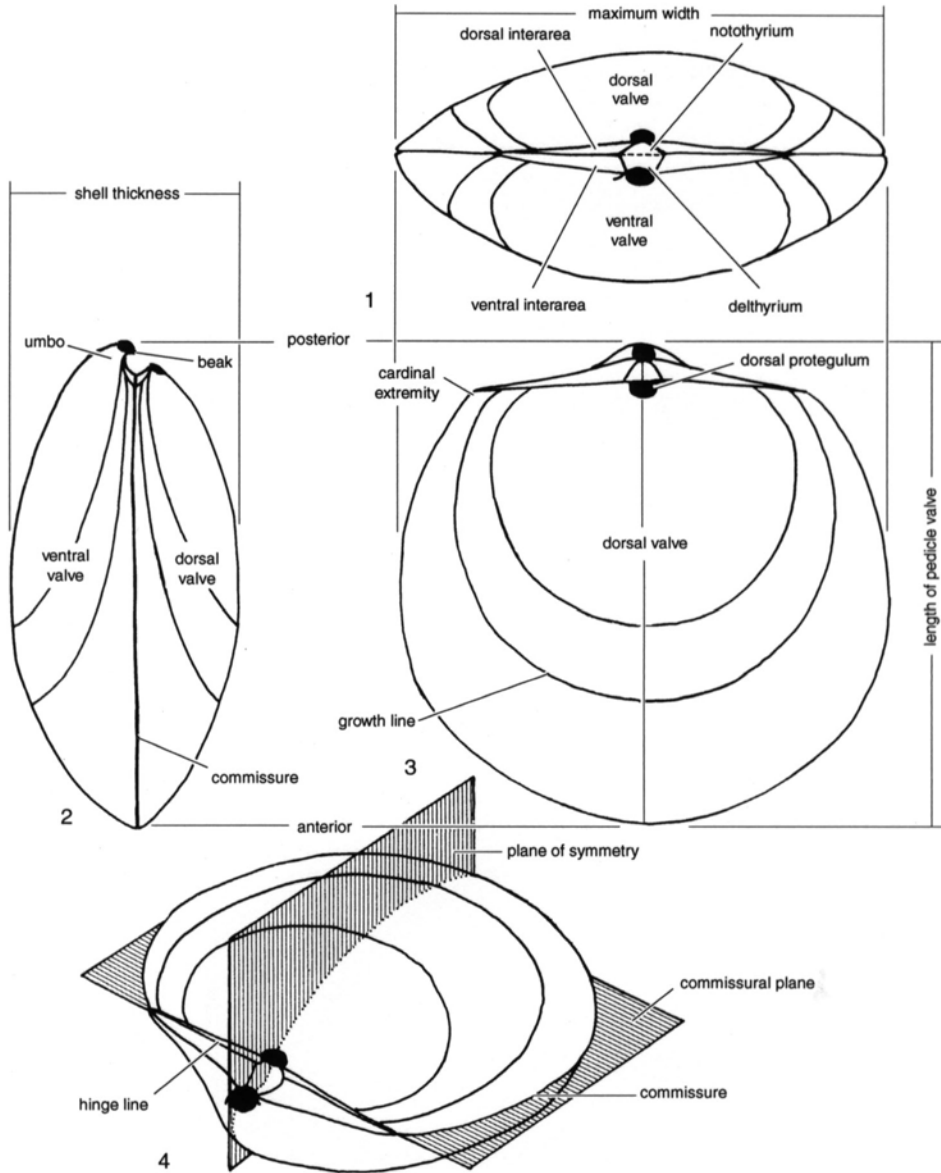


FIG. 283. External features of generalized enteletoid brachiopod seen in 1, posterior, 2, left lateral, 3, dorsal, and 4, dorsolateral views (Williams & Rowell, 1965b).

line led to rostrate shells like *Perditocardinia*, in which the apical angle of the interareas is narrowly acute. A conical ventral valve, due to excessive forward growth of its interarea, is characteristic of a number of genera (e.g., *Onychotreta*, *Scacchinella*, *Syringothyris*), whereas a suppression of forward growth, as

in productoids, led to linear interareas and hemiperipheral expansion of the dorsal valve.

Rostrate shells are also characteristic of astrophic (nonstrophic) terebratulides, rhynchonellides, and atrypoids, in which homologues of the interareas are greatly reduced or absent and homologues of the hinge lines are

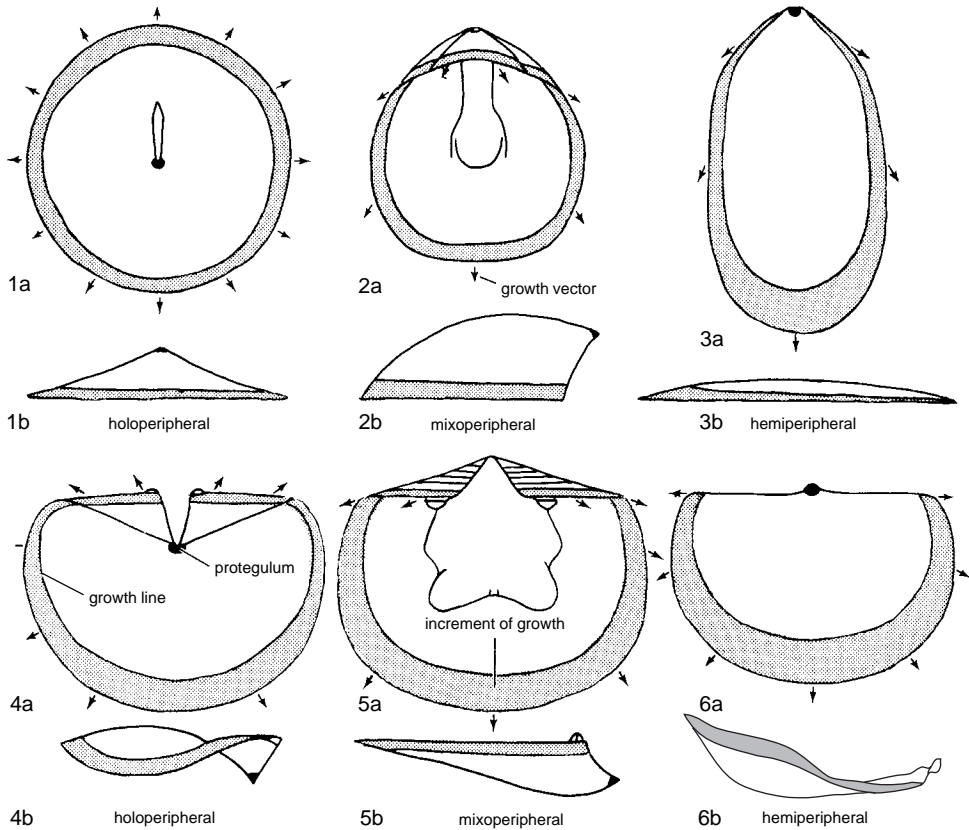


FIG. 284. Nature of shell growth as typified by holoperipheral increase in ventral valves in ventral and lateral views of 1, *Orbiculoidea* and 4, *Plaesiomys*; mixoperipheral increase in ventral valves in dorsal and lateral views of 2, *Apsotreta* and 5, *Dinorthis*; and hemiperipheral increase in dorsal valves in dorsal and lateral views of 3, *Lingula* and 6, *Productus* (adapted from Williams & Rowell, 1965b).

short and curved, so that their traces intersect only the hinge axis (Fig. 285). RUDWICK (1959) used the terms "palintrope" and "cardinal margin" to distinguish these vestiges from the well-developed interareas and hinge lines, respectively, of strophic shells. This distinction may seem academic, because the free edge of the dorsal umbo, which protrudes into the delthyrial cavity of the ventral valve of the astrophic shell (i.e., most of the cardinal margin as understood by RUDWICK, 1959), is no more an integral part of the hinge line than are the notothyrial edges of a strophic dorsal valve. However, if reference is made exclusively to those posterior surfaces and edges lateral of the points of

articulation (i.e., to the arcs underlain by fused mantle lobes), the differences described by RUDWICK (1959) are valid.

Irrespective of the different types of growth, the protegula and larval shells occupy the apices (or beaks) of the valves, and the region immediately around the apex is referred to as the **umbo** (Fig. 283). The attitude of the ventral beak can vary from being in the commissural plane (straight) to a dorsally directed inclination of up to 150° to that plane (strongly curved). Typically the cardinal areas of articulated brachiopods, immediately beneath apices of the valves, are notched by a pair of triangular openings—the **delthyrium** of the ventral valve, which

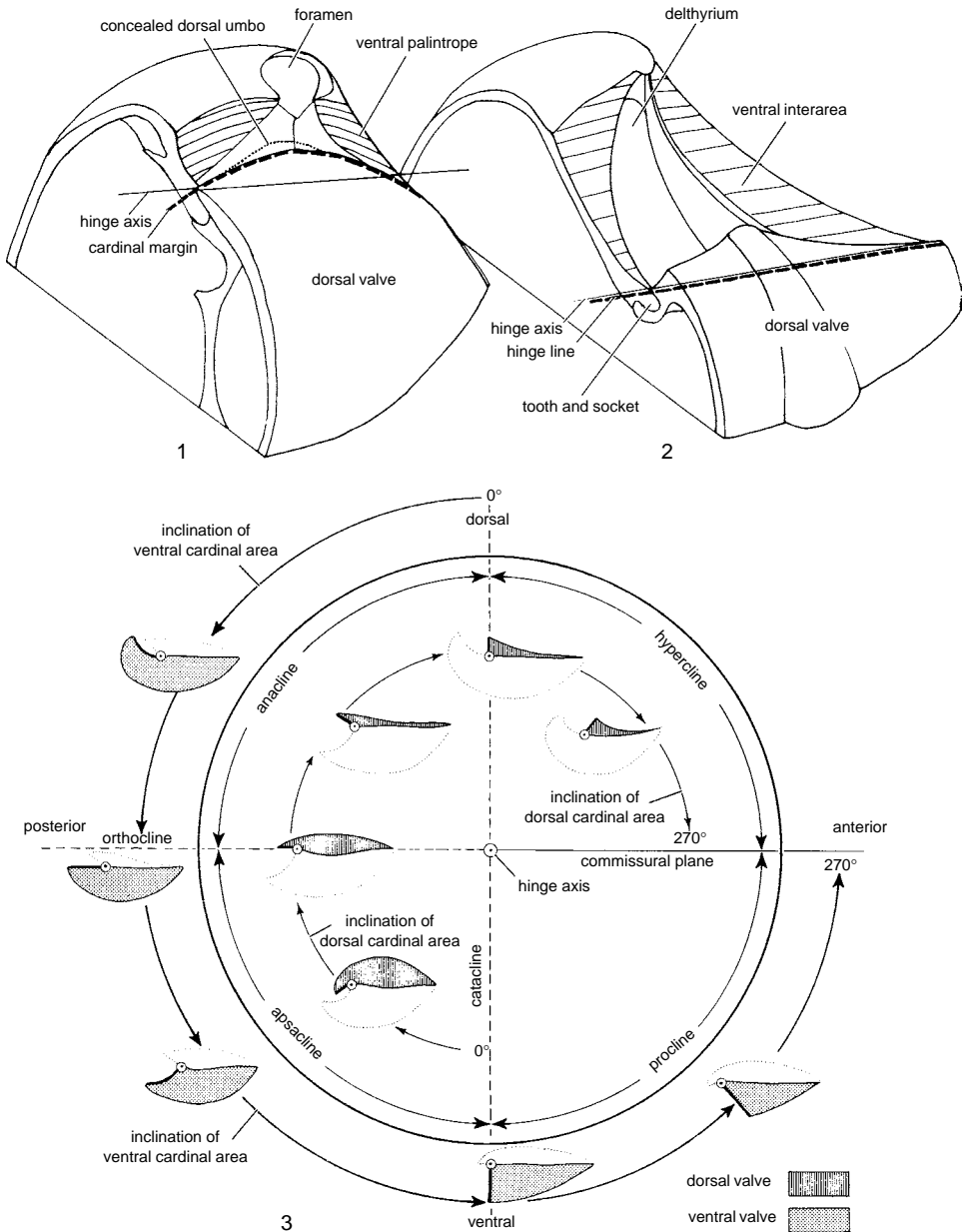


FIG. 285. Posteromedian regions of 1, astrophic (nonstrophic) and 2, strophic shells, with 3, a chart showing the various attitudes of cardinal areas about the hinge axis relative to the commissural plane (Williams & Rowell, 1965b).

normally accommodates the pedicle, and the **notothyrium** of the dorsal valve, which usually is filled with the attachment base (cardinal process) for the dorsal ends of the diductor muscles (Fig. 283). Both of these

openings may be partially or completely covered by shell outgrowths, as described below.

The posterior surface of the inarticulated valve may be completely unmodified and comparable with the anterior and lateral

slopes, as in the majority of cranioids (Fig. 286.1). More commonly some differentiation occurs, especially in the ventral valve. The simplest modification is some form of opening such as a notch or a slit for the pedicle as in discinids (Fig. 286.2), while a flattened surface (**pseudointerarea**) on the posterior margin of either valve is characteristic of many groups (Fig. 286.3–286.5). Thus, in the paterinides the pseudointerarea of the ventral valve consists of a pair of flattened triangular areas (**propareas**) marked off from the posterolateral regions of the valve by a break in slope and separated by the delthyrium partly covered by a homeodeltidium. The ventral pseudointerarea of linguloids, in contrast, is approximately orthocline in disposition and the two triangular propareas flank a pedicle groove. These basic patterns, with minor modifications, also occur in other inarticulated groups and can involve the posterior margin of the dorsal valve. An orthocline or anacline dorsal pseudointerarea, which may be divided medially as in many acrotretoids, is commonly developed, although other, less complex modifications may occur.

The protegula of living and extinct brachiopods suggest that in both transverse and longitudinal profiles the unspecialized shape of the adult shell is biconvex (Fig. 287). Ideally, then, there are three components of growth relative to the median and commissural planes of the shell, and vectors of growth, traced on the shell surface from the protegular node, may be resolved according to these axes. They are an anterior component parallel with the intersection of both planes, a ventral or dorsal one normal to the commissural plane, and a lateral one normal to the median plane. In general, the ventral valve is not only larger in outline but also deeper than the dorsal valve, although every conceivable variation in this relationship was attained during brachiopod evolution. Thus among the strophomenidines, chonetidines, and productidines, the more usual adult profile was concavoconvex, that is, with a dorsal valve becoming concave beyond the

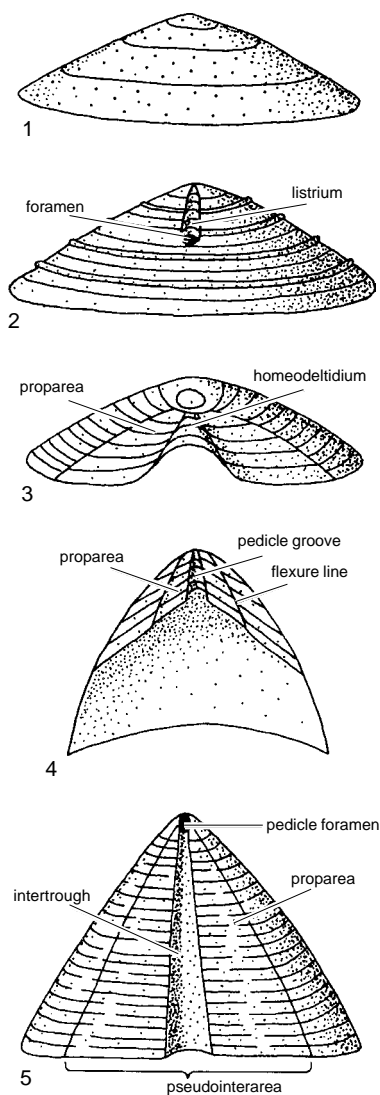


FIG. 286. Modifications of posterior sector of ventral valve of some inarticulated brachiopods; 1, cranioid (*Pseudocrania*); 2, discinoid (*Orbiculoidea*); 3, paterinide (*Paterina*); 4, linguloid (*Lingulella*); 5, acrotretoid (*Prototreta*) (Williams & Rowell, 1965b).

protegular node and the ventral valve continuing its initial convexity (Fig. 287.5). A reversal in growth direction was also common, so that the biconvexity of the protegulum was modified to a concavoconvex relationship in young shells, which in turn gave way to a convexoconcave attitude

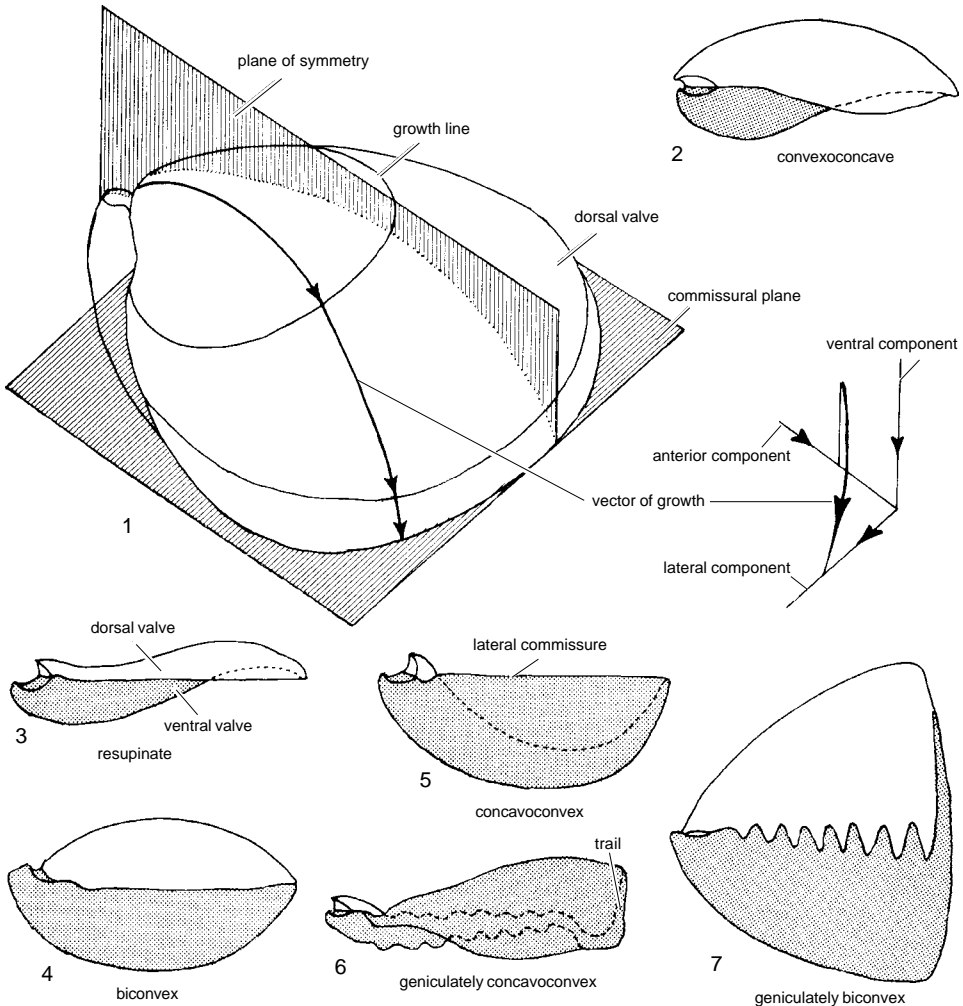


FIG. 287. 1, Components of growth in brachiopod shells, with 2–7, illustrations of various types of lateral profiles; the growth line marks the course of a growth band; the vector of growth traces a growth zone (Williams & Rowell, 1965b).

during adult stages of growth. This type of growth is known as **resupination** (Fig. 287.3). Such reversals in direction of growth were also accentuated by an angular deflection of one or both valves (**geniculation**) due to a marked reduction or cessation of the radial components of growth. Such deflections are directed either toward the other valve (e.g., *Enantiosphen*, *Sphaerirhynchia*) (Fig. 287.7), or in the same direction to define a corpus, commonly with an internal confining ridge (submarginal ridge) and a

trail (Fig. 287.6). The corpus is that part of the shell occupied by the body and lophophore; it does not include narrowly separated peripheral areas such as the ears and trails of many strophomenides or the flanges of many athyridines. Trails may be directed dorsally or ventrally and may even reverse direction as in leptaenids and some productidines.

A common modification of the profile of inarticulated brachiopods is the development of a conical valve. Both valves of *Orbiculoidea* may be subconical but it is more

usual for only one valve to become conical, such as in the acrotretid ventral valve and the discinid dorsal valve. This profile is very much less common in the articulated brachiopods, the most spectacular being the cone-shaped ventral valve of *Richthofenia*, which encloses a sunken, subcircular dorsal valve.

The brachiopod outline varies greatly, apart from the more orthodox transversely semi-oval, subcircular, elongately oval, and subtriangular appearance of wide- to short-hinged shells. Some of the more bizarre forms include the saucerlike, incurved, or conical ventral valve of the oldhaminidines, with a highly lobed dorsal structure that may have consisted of a vestigial dorsal valve and a large internal plate supporting the lophophore, and the tubelike ventral valve of the productidine *Proboscidella* and the terebratulide *Pygope*, pierced subcentrally by a hole that was sealed off by anteromedian fusion of a deeply indented (emarginate) anterior margin. Both outline and profile of the shell may be considerably modified by radially disposed deformations that display a variety of form and amplitude. The major, radial elevations of the valve surface are **folds** and the complementary major depressions are **sulci**. These broad deformations grade down into minor features (costae, costellae) that are produced in a comparable manner but are normally regarded as part of the ornament and as such are discussed in detail below.

In terms of their effect on the commissure, folds and sulci fall into two broad groups, and it is apparent that the deformations of these two groups arose in different ways (RUDWICK, 1959). In one group, the folds and sulci are developed opposite each other in the two valves (**opposite folding**), a fold being opposed to a fold and the commissure remaining straight (rectimarginate) (Fig. 288). These deformations may be regarded as being produced by localized anomalies of the radial growth component, which is the vector sum of the anterior and lateral components. Since the commissure is not deflected, such deformations do not involve

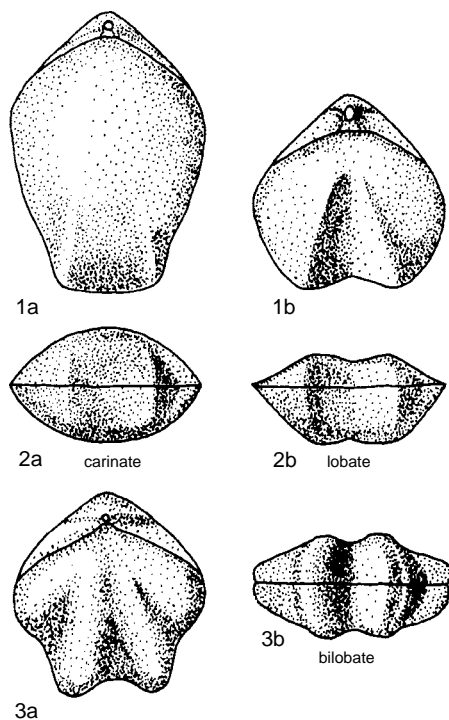


FIG. 288. Opposite folding; 1–3, dorsal and anterior views of designated types (adapted from Williams & Rowell, 1965b).

anomalies in the vertical component. Deformations produced in this way have their maximum expression when the valve is strongly convex.

In the second group, the folds and sulci are complementary to one another (alternate folding), a fold in one valve being opposed by a sulcus in the other, and the commissure becomes correspondingly undulated by deflections directed dorsally (plicae) and ventrally (sulci). The more common commissural shapes are shown in Figure 289; but these are not necessarily constant throughout ontogeny because, during growth, a median sulcus may be replaced by a fold and vice versa. Deformations of the alternate type commonly involve localized anomalies of the vertical growth component either acting alone or in conjunction with localized anomalies of the radial component. If the anomalies are entirely in the vertical

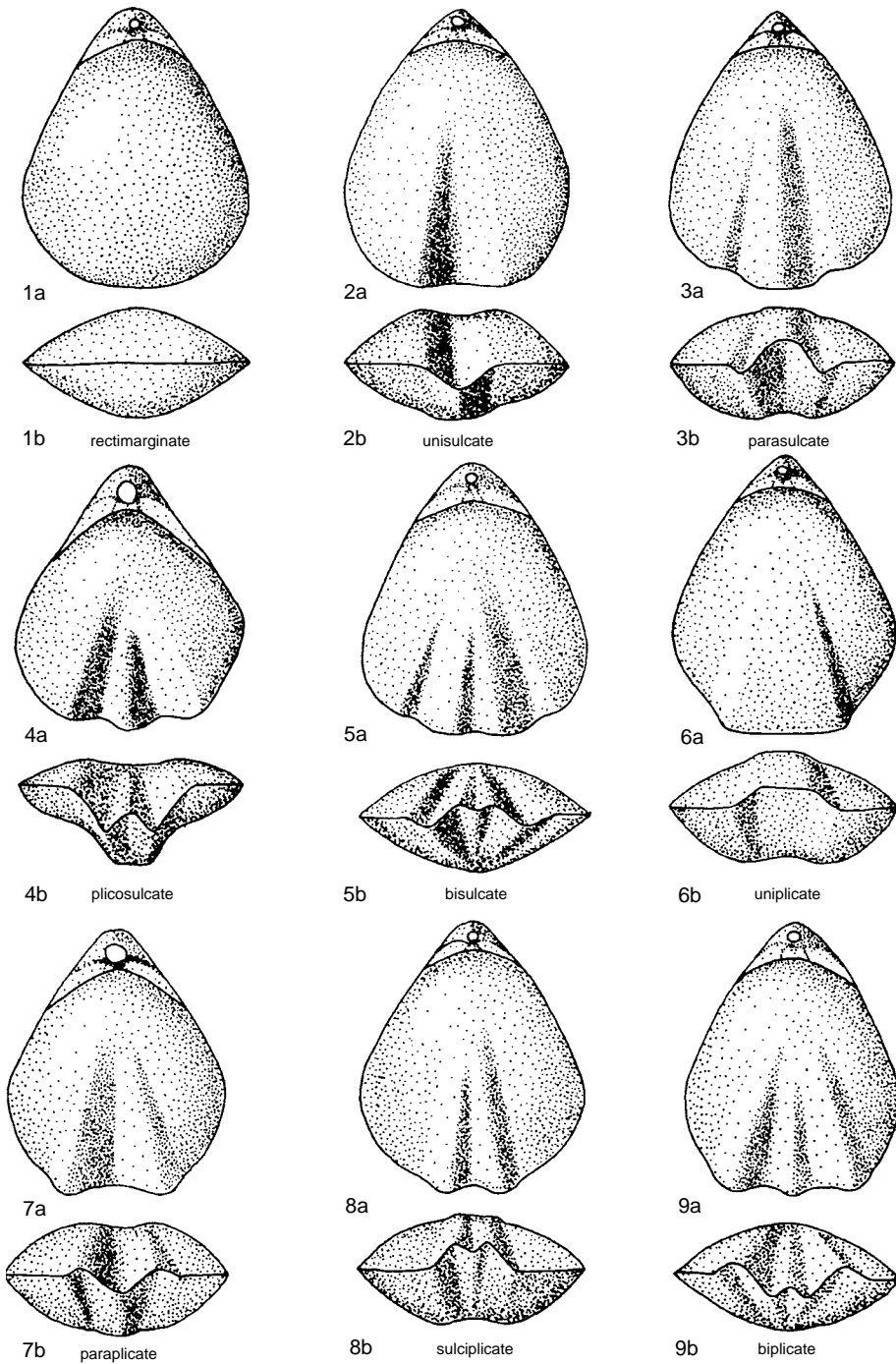


FIG. 289. Types of alternate folding; 1, rectimarginate; 2–5, forms of folding that are basically sulcate; 6–9, forms of folding that are basically plicate (adapted from Williams & Rowell, 1965b). [Note: this figure was corrected from version in Volume 1.]

component, the deformations will have their maximum expression on a plane valve and be less conspicuous on a highly convex one.

ORNAMENTATION

The ornamentation of the brachiopod shell has been defined as any regularly occurring outgrowth, deflection, or nonpathological interruption in growth found on the outer shell surface (WILLIAMS & ROWELL, 1965b; WILLIAMS & others, 1965). This definition covers most of the so-called growth lines on the shell surface even though they generally represent phenotypically controlled changes or breaks in secretion. Such growth lines are not always easily distinguishable from some variants of concentric ornamentation, which are genetically controlled. In effect there are several kinds of breaks or gradient changes posing as growth lines in the conventional sense on the surfaces of brachiopod shells (HILLER, 1988; GASPARD, 1989), and distinguishing them from one another largely depends on being able to gauge their effects on the fabric of the host integument.

Changes in the shell fabric of these concentric microstructures are determined by the mobility of the outer mantle lobe as well as the specificity of its secretory regime. Any temporary retraction or advance of the lobe that does not lead to permanent impairment of shell growth has to satisfy two criteria: no surface of shell accretion is ever exposed by mantle retraction, and organic substrates are always available for biomineral deposition during mantle advance. In typical sequences, illustrated by the impunctate rhychonellide *Notosaria*, a smooth retraction of the outer mantle lobe does not inhibit continuing secretion so that, for example, a resultant ledge of primary shell is covered by a folded sheet of entire periostracum (reflection). A rapid retraction of the outer mantle lobe, on the other hand, is accompanied by the simultaneous secretion of a new outer bounding membrane, which acts as a wrapping to the inner edge of the primary layer (regression)

(Fig. 290). The wrapping is probably proteinaceous and acts as a sealant as well as an organic slide for the regression. When re-advance of the outer lobe takes place (transgression), the wrapping serves as a substrate on which cells apparently restart secretion at that phase of the regime where they left off. Accordingly new primary shell is seeded on that part of the wrapping covering the old layer, the inner bounding membrane of the periostracum on that part of the wrapping coating the inner zones of the periostracum, and so on (WILLIAMS, 1971a).

The distinctiveness of the fabric associated with mantle reflection, regression, and transgression helps to identify three different kinds of growth lines. Growth banding, which is measured in nanometers, may be seen on external shell surfaces (Fig. 291.1) but is as clearly and, indeed, more frequently displayed in sections of the shell (Fig. 291.2–291.4). Banding represents rhythmic, usually diurnal, changes in the rate of shell secretion (or in the proportion of biomineral and organic constituents) and is an expression of momentary growth (RUDWICK, 1959; WESTBROEK, 1967). Any surface relief caused by growth banding is never more than small changes in gradient.

Growth banding may be interspersed with periodic sets of accentuated growth lines consisting of undercut microscopic ridges, which are usually measured in microns. Their inner sides (as well as their outer ones) are covered by an entire periostracum, which has been smoothly retracted. These concentric microstructures may even have been secreted slowly enough to be isoclinal folds (with cores of primary shell about axial planes inclined posteromedially). Such growth reflections are likely to represent seasonal changes in the environment.

Growth disturbances are induced by a sudden, traumatic interference with shell growth, which stimulates a rapid retraction of the lobe and even of the contiguous zone of the mantle proper so that the proteinaceous sheet secreted during regression may

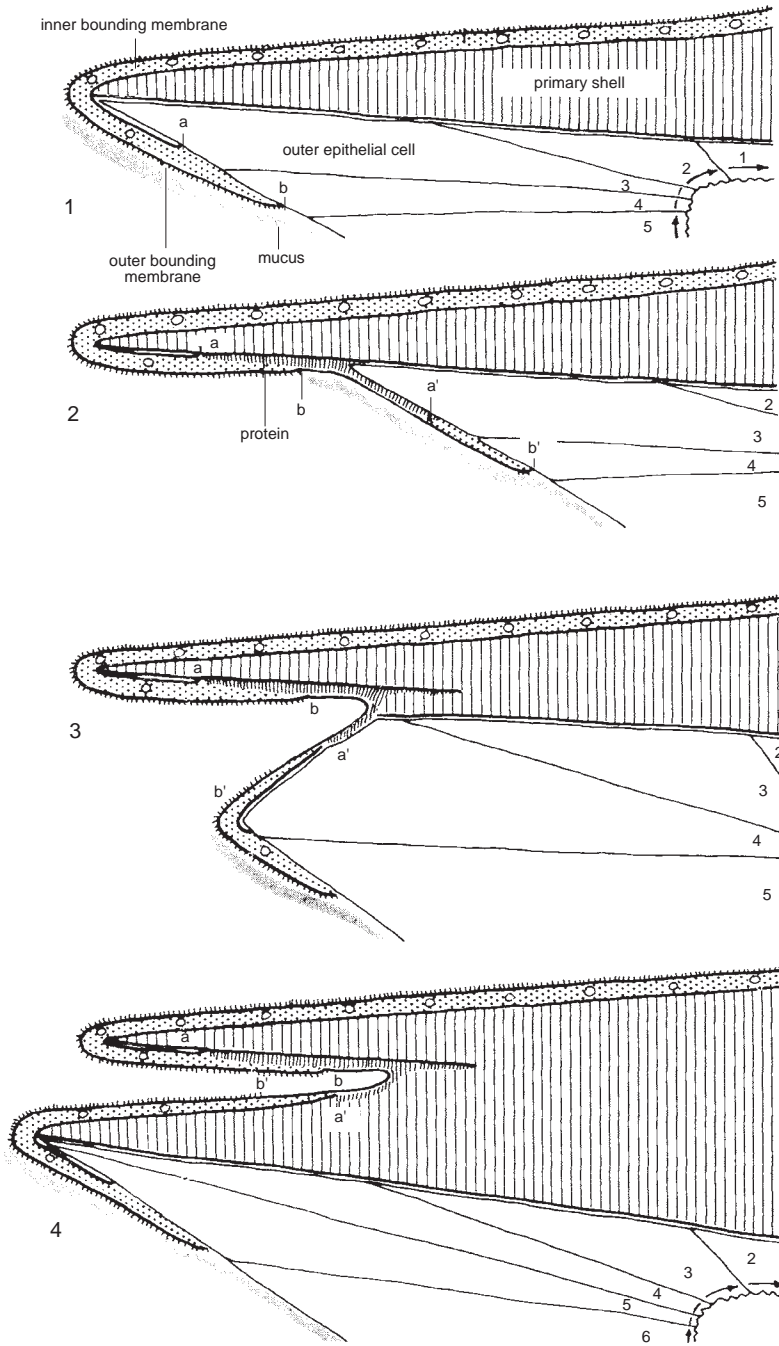
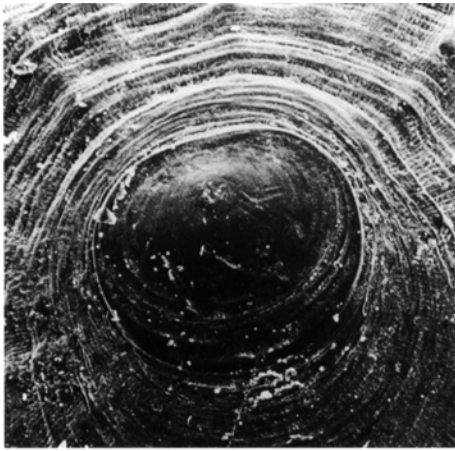
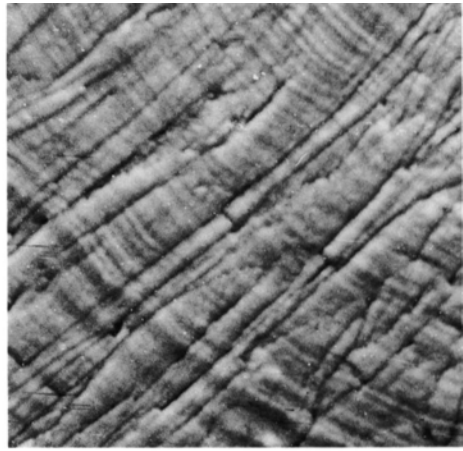


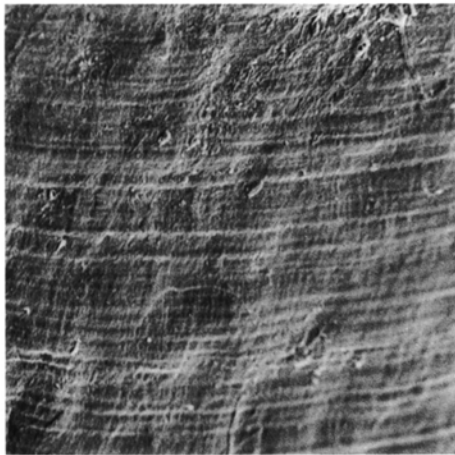
FIG. 290. Formation of a regression (a-a') in the periostracum of recent *Notosaria nigricans* (SOWERBY), shown embedded in primary shell in 4; 1, sudden retraction of the outer mantle lobe from its normal depositional attitude and 2, the concomitant secretion of the outer bounding membrane and a sealing proteinaceous layer before 3, forward movement of the lobe and the resumption of normal deposition (Williams, 1971a).



1



2



3



4

FIG. 291. Features of incremental growth; 1, growth disturbance marking the junction of the central, dark, larval shell and surrounding juvenile shell (with growth banding) of the dorsal valve of recent *Discina striata* (SCHUMACHER), $\times 80$; 2, etched section showing growth banding in the primary shell of recent *Lacazella mediterranea* (RISSO), $\times 2,600$; 3, growth banding on exterior of recent *Calloria inconspicua* (SOWERBY), $\times 235$; 4, growth banding on the laminar lamellae of the Ordovician *Strophomena oklahomensis* COOPER, $\times 2,600$ (new).

intrude deeply into the secondary shell. These concentric growth disturbances are randomly distributed on the shell surface as they are the effects of such haphazard extraneous factors as predatory attacks and storms.

All three kinds of growth lines are frequently seen on the surfaces of mature shells and may be confused with genetically controlled, concentric microstructures. Thus the

junctions between juvenile and larval or protegular shells on the external surfaces of organophosphatic and articulated brachiopods respectively are normally marked by gradient changes and undercut ledges. In living discinids, the larval shell is bounded by a concentric, low, rounded ridge, the rim of the larval halo (CHUANG, 1977). A similar, raised rim commonly delineates the larval shells of fossil lingulides and acrotretides

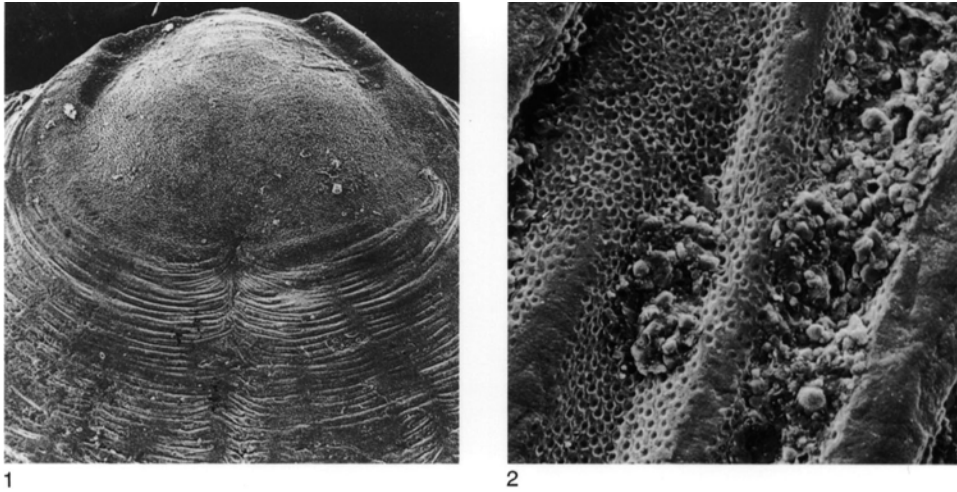


FIG. 292. Concentric microornamentation; 1, fila deformed into sets of discrete, outwardly convex arcs, and separated from the larval shell by a zone of disturbance on the dorsal valve of an Ordovician acrotretoid sp., $\times 180$ (Williams & Holmer, 1992); 2, detail of fila bearing the cast of a vesicular periostracum on the dorsal valve of the Carboniferous *Orbiculoidea nitida* (PHILLIPS), $\times 420$ (new).

(HOLMER, 1989; WILLIAMS & HOLMER, 1992), and a change of gradient also occurs at the junction between the protegulum and juvenile shell of articulated brachiopods (STRICKER & REED, 1985b). These raised rims are frequently thrown into relief by the outer perimeter of undercut ledges representing growth disturbances (Fig. 291.1). The rims have been attributed to changes in the rate of shell secretion of differing components (and a consequential imperfect amalgamation of fabric) attending the change to a sedentary mode of life.

Periodically occurring ridges of a comparable nature to the raised rim of the larval shell form a fine concentric ornament (fila), especially on organophosphatic shells (Fig. 292). In acrotretoids, for example, fila resemble parallel-sided anticlines with rounded crests overturned toward the valve margin and may be up to $8\ \mu\text{m}$ or more in wavelength (WILLIAMS & HOLMER, 1992). In fossil discinids, like *Orbiculoidea*, fila commonly have a greater wavelength (up to $30\ \mu\text{m}$) but are similar in structure.

All such fila have been deformed by stresses demonstrably set up within the periostracum. They must, therefore, have

originated as regular folds in a periostracum being secreted on the outer mantle lobe. These would have been homologous with the imperistent periclinal folds (Fig. 293) developed around the hinge of the marginal fold of the shell of living *Lingula* (WILLIAMS, CUSACK, & MACKAY, 1994). Such folds are filled in by the primary layer and do not affect the secondary shell. The infill of fila would also have been part of the primary layer but with a particular consistency. It would have been sufficiently fine to act as a mold mixture for structures smaller than one micron and, when first secreted, sufficiently plastic to register small-scale folding, presumably preserved by polymerization of the infill. These criteria suggest that the first-formed biomineral coat was a cohesive paste of fine apatitic crystals suspended in a glycosaminoglycans (GAGs) matrix (WILLIAMS & CURRY, 1991).

Acrotretoid fila anastomose and may become isolated as imperistent undulations. These are indistinguishable from a much coarser, oblique, or concentric wrinkling of the shell surface (rugation) (Fig. 294). Rugae are especially characteristic of the strophomenides (*s.l.*) with wavelengths varying from

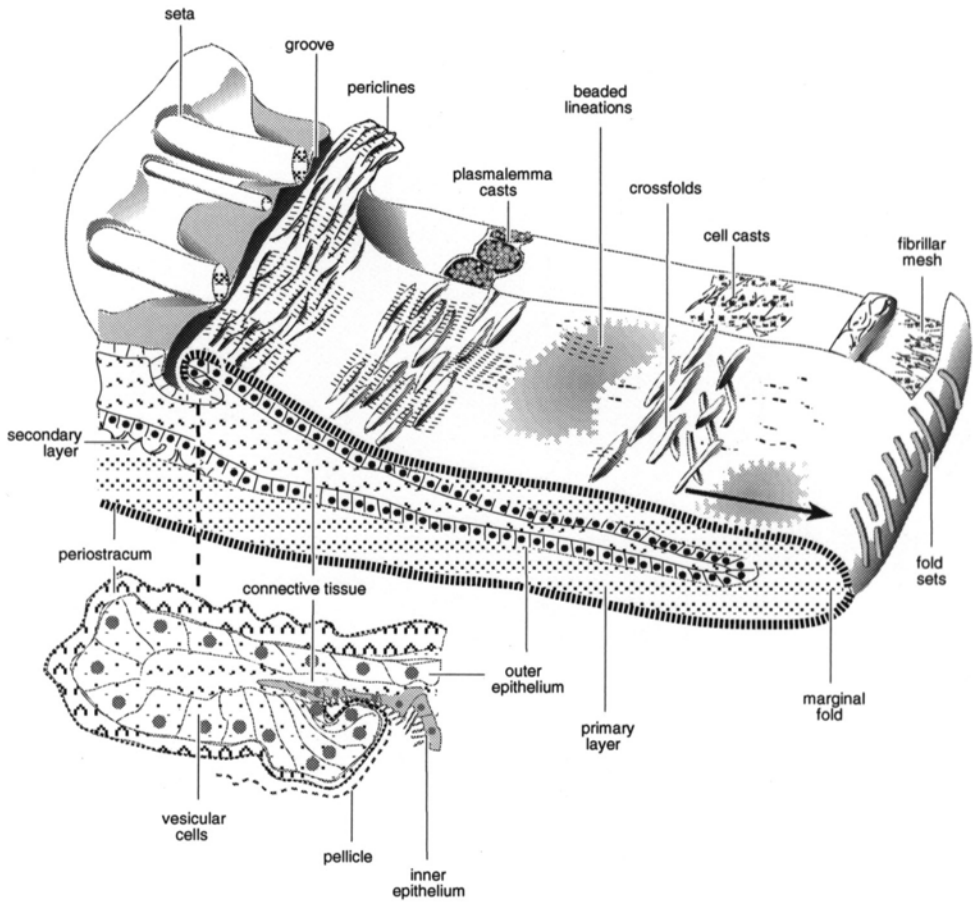


FIG. 293. Stylized block section of the marginal fold of *Lingula anatina* LAMARCK showing the relationship of an expanding mantle and a variously folded integument, unrolling in the direction of the arrow; enlargement of the periostracal lobe in the bottom left hand corner (Williams, Cusack, & Mackay, 1994).

about 100 μm (in plectambonitoids) to more than 3 mm in some productoids. Rugae of the coarser range of wavelength are also known rarely in other groups like pentamerides (*Kulumbella*). Rugae may be continuous and concentric, as in *Leptaena*, where they are precursory to the formation of the trail, which may be regarded, in that genus, as an indefinite continuation of the outer face of the last-formed ruga. Rugae may also be impermanent and oblique as in those of *Sowerbyella*. Rarely, as in *Ptychoglyptus*, the rugae are concentrically disposed but so interrupted at their junctions with the more accentuated elements of radial ornamentation that they are broken up into

a series of chevronlike or oblique strips. Exceptionally, two or more sets of oblique rugae may develop, intersecting at obtuse or acute angles (e.g., *Bellimurina*, *Kulumbella*).

Rugae were probably formed by deflection of the mantle edge through an arc of 180° along an axis that was disposed in any direction except that of the radial vector relative to the mantle margin (radial deflections give rise to such features as ribs and folds). The concentric arrangement of *Leptaena* was the simplest condition as it involved a simultaneous deflection of the growing mantle edges along the entire commissure anterior to the hinge line. An obliquely disposed ruga arose through a localized deflection of the mantle

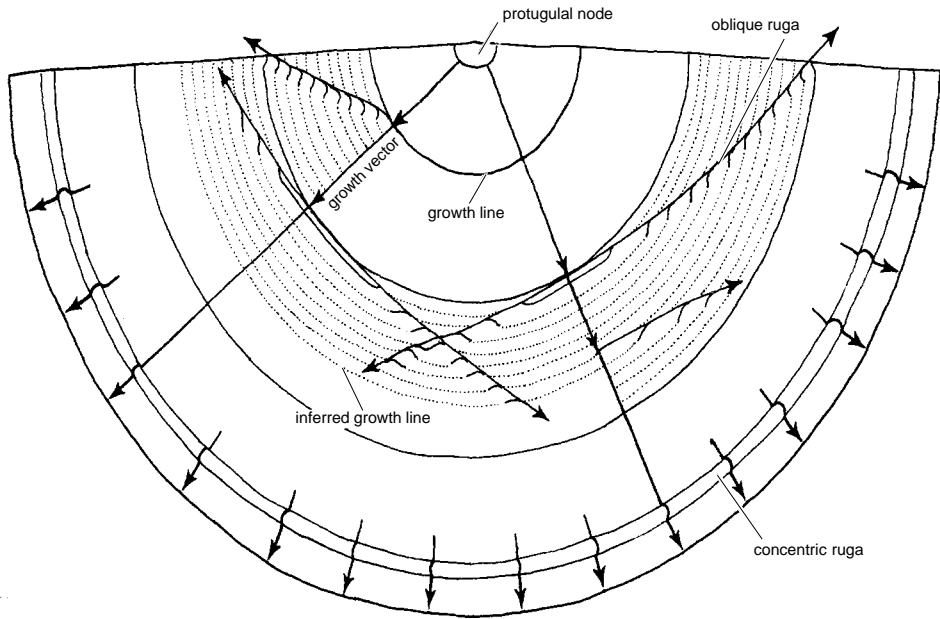


FIG. 294. Diagrammatic illustration of the nature and origin of oblique and concentric rugation (adapted from Williams & Rowell, 1965b).

edges at any point along the margins; and during subsequent growth the deflection was transmitted laterally either in one or both directions along axes traced out by the rugae in a full-grown shell. In the Carboniferous productidine *Vitilipproductus*, a quincuncial cross-rugation arose from a bilaterally symmetrical intersection of rugae, obtusely disposed in more or less paired sets along the hinge line on either side of the umbonal region (BRUNTON & MUNDY, 1988). In either manner, two or more sets of rugae may have developed a complicated pattern of intersections.

An interesting aspect of the assumed homology between rugae and fila is that rugae would have originated as folds of the periostracum around the outer mantle lobe. The folds would have been filled with secreted materials containing enough GAGs to polymerize into perfect casts. This mainly organic subperiostracal infill would have been unlike the almost pure calcitic composition of the primary layer of other articulated brachiopods, which may account for the

difficulty in identifying a primary layer in strophomenide shells.

Other kinds of regularly spaced, concentric outgrowths on the shell exterior (lamellae and imbricae) may be composed of secondary as well as primary shell but invariably involve periodic buckling or retraction of the outer mantle lobe. The fine lamellae of many strophomenides (Fig. 295) are regularly spaced overfolds (at intervals of 80 μm to 100 μm and with wavelengths of about 20 μm in the orthotetidine *Xystostrophia*). In most other brachiopod groups (including productidines), lamellae can be extravagantly developed as variably inclined, skirtlike sheets that may be differentially extended as spinose, open tubes along the crests of ribs as in *Glyptorthis* and *Acanthobasilola* (HILLER, 1988). Regularly spaced lamellae of *Athyris* can extend forward as recurved microfrills more than 300 μm long (Fig. 296.1). They are composed of secondary as well as primary shell and are associated with strongly developed regression surfaces. It is believed that microfrills, when newly formed at the shell

margin, acted as baffle chambers for excess detritus in the feeding currents of the mantle cavities of living specimens (ALVAREZ, BRIME, & CURRY, 1987). Other athyridines, like *Pachyplax* (ALVAREZ & BRUNTON, 1990), are ornamented by very coarse lamellae that are composed of a succession of flattened secondary fibers underlying a granular primary layer and are two to four times as thick as the principal secondary succession of the shell (Fig. 296.2). These thick lamellae are homologous with the concentric, knobby protuberances (comae) that give *Bimuria* its gnarled appearance (Fig. 296.3). Regression surfaces are well developed, and the backward-curving comae secreted on them are composed of fibers that become flattened distally into laths forming laminar sheets, which presumably represent an extensively developed primary layer (WILLIAMS, 1970a).

All radial ornamentation (ribs) is due to a persistent or impersistent deflection of the mantle edges along vectors radiating from the junction between the neanic and brephic shell (protegular node) or the margin of the larval shell, so that every variety of size and shape can be found (Fig. 297). The basic element is a well-defined elevation of the shell surface, triangular to rounded in transverse section and of variable amplitude and wave length, which normally arises at the protegular node and almost invariably extends to the margins of adult shells. Such a feature is known as a *costa*, whereas a *costella*, which may be of comparable thickness and shape, does not arise at the margin of the brephic shell but by branching from or intercalating between costae at any state during subsequent growth. Defining the terms according to the point of origin of the features precludes their arbitrary use to imply a relative coarseness in texture, which is better expressed as a frequency count for a standard arc at a stipulated distance from the beak. In some species (e.g., triplesoids and rynchonellides), the radial ornamentation may first appear along an arc of growth well beyond the protegular node, and this pattern is referred to as delayed costation or delayed

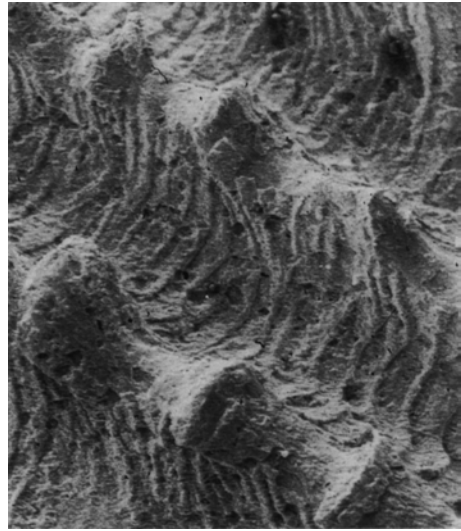


FIG. 295. Finely lamellose, parvicostellate exterior of the Middle Devonian *Xystostrophia umbulacrum* (SCHLOTHEIM) with shell margin to the right of the micrograph, $\times 55$ (new).

costellation if first or higher orders of costellae are involved. Certain brachiopods, especially strophomenides, are characterized by a finely textured ornamentation consisting of costae and several orders of costellae, all of which arise by intercalation. This pattern is usually referred to as **parvicostellate** (as opposed to **ramicostellate**, which implies an origin solely by branching, as in most orthoids); and when the costae and certain costellae are accentuated to segregate the ornamentation into a series of sectors, the condition is referred to as **unequally parvicostellate**. When the costellate and ramicostellate patterns are so evenly divided as to give an appearance of a uniformly fine ornamentation they are referred to as **multicostellate** (e.g., *Schizophoria*), whereas the segregation of these patterns into conspicuous bundles is called **fascicostellation** (e.g., *Fascicostella*).

The relative origins of costellae in ramicostellate patterns are stable enough to be used for taxonomic purposes. Several attempts have been made to devise a reliable notation. The most effective is that of

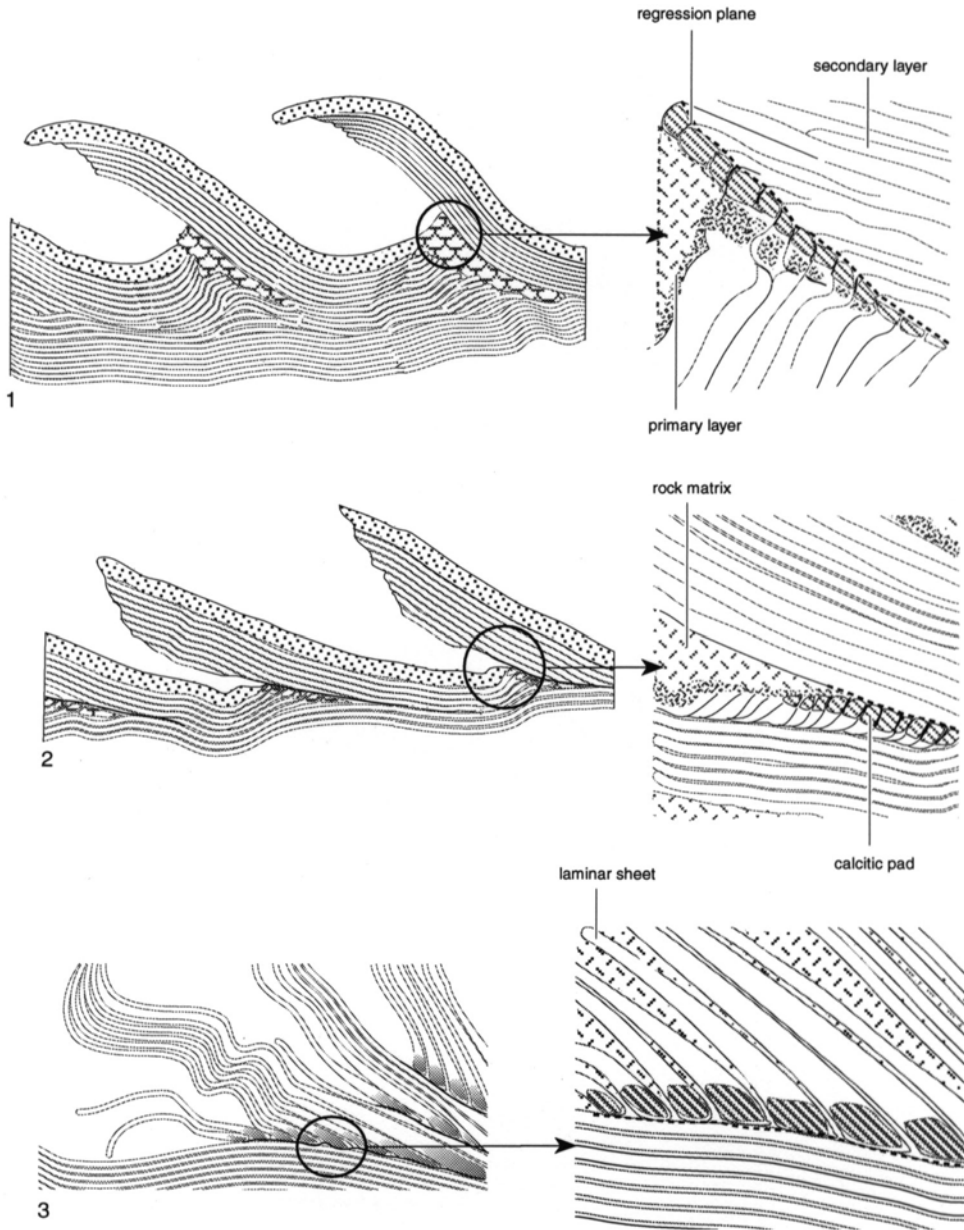


FIG. 296. Stylized structure of the lamellae of Devonian athyrids; 1, *Athyris campomanesi* (VERNEUIL & ARCHIAC) (adapted from Alvarez, Brime, & Curry, 1987); 2, *Pachyplax elongata* ALVAREZ & BRUNTON (Alvarez & Brunton, 1990); 3, comae of the Ordovician plectambonitoid *Bimuria* cf. *buttsi* COOPER. Detailed drawings to the right approximately $\times 500$, $\times 200$, and $\times 400$ respectively (new).

BANCROFT (1945). Costae originating at the protogular node of the right half of the dorsal valve are termed primaries (Fig. 297) and are numbered 1, 2, 3, and so on, primary 1

(which in the enteletoids arises from the very tip of primary 2) being nearest the median line and primary 4 farthest away. Secondary costellae, which split off from the primaries,

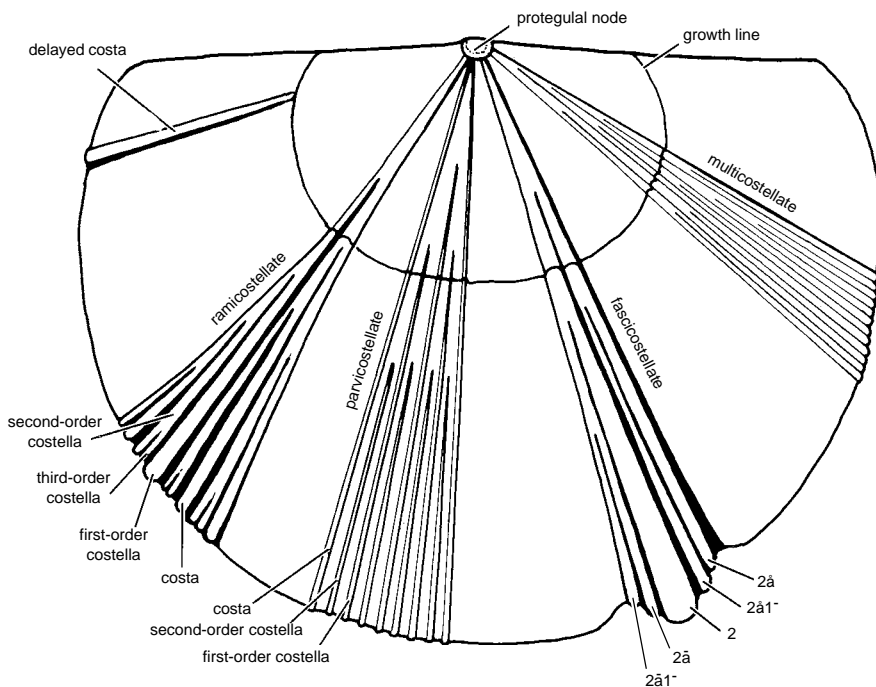


FIG. 297. Diagrammatic illustration of the more important types of brachiopod radial ornamentation; the notation for the order and direction of rib branching in the fascicostellate pattern is explained in the text (adapted from Williams & Rowell, 1965b).

are labelled *a*, *b*, *c*, and so on, *a* being the earliest to split off, *b* the next, and so on. Tertiary costellae, which branch from secondaries, are numbered in the same manner as the primaries; and for ribs of higher orders the numerals continue to alternate with the letters so that *1a1a* represents the earliest costella on the earliest tertiary on the earliest secondary on the first primary. Whether a costella branches toward the inside (i.e., toward the median line) or toward the outside of the parent is also important, and the superscript symbols “-” and “o” are used to denote inner and outer branches, respectively, so that $2\hat{a}1^-$ represents a costella arising on the inner side of the first outer branch of the second primary.

There is a correlation between the profile of a valve and the branching of costellae in that ribs tend to split off downslope (WILLIAMS & WRIGHT, 1963). Yet the variability of a complex ramicostellate pattern can be expressed in terms of the earlier branching of

about 10 costellae relative to 10 others (WILLIAMS, 1974) and appears to have the statistical validity of a genotypic character facies. The Bancroft notation has also been used to characterize the ribbing patterns of the Upper Ordovician *Diceromyonia* simply in terms of modal sectors (MACOMBER & MACOMBER, 1983). These sectors are composed of all ribs occurring in more than 50 percent of the valves irrespective of their order of branching from primary costae. This method is an alternative approach but is deficient in not taking into account valve size and in eschewing statistical controls. Other ribbing systems used to delineate suprageneric groupings of ramicostellate brachiopods, such as that used by KEMEZYS (1968) for enteletidines, have yet to be subjected to rigorous statistical controls.

The costellate radial ornamentation of some extinct brachiopods is probably related to the distribution of setae along the mantle edge (see chapter on shell structure, p. 272)

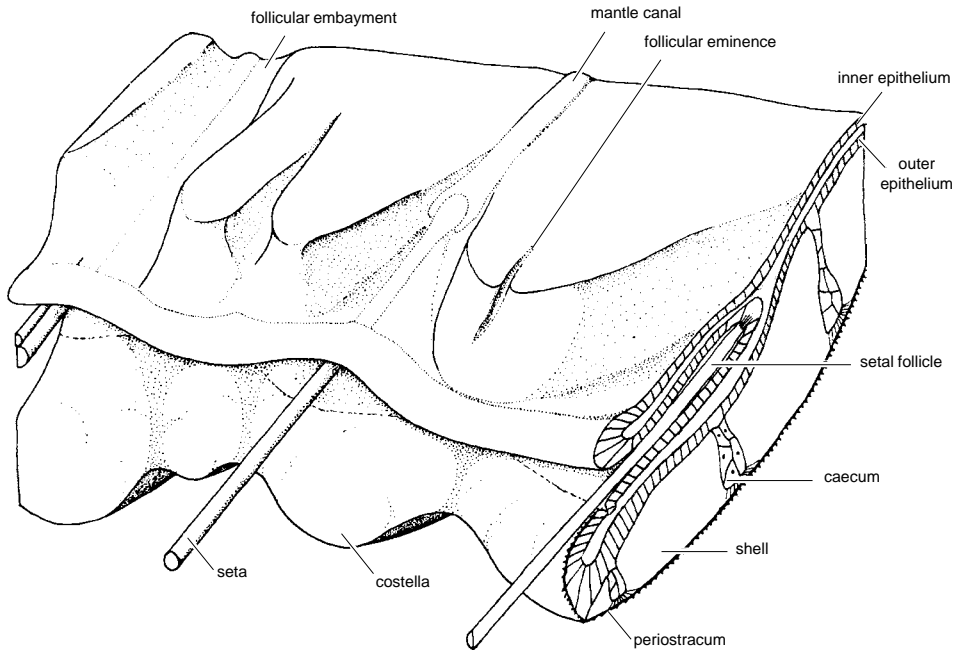


FIG. 298. Inferred relationship between the mantle edge and the shell margin of a typical, finely costellate, endopunctate articulated brachiopod (Williams & Rowell, 1965b).

as is characteristic of such living brachiopods as *Terebratulina* (compare Fig. 298). Along the edge of the *Terebratulina* valve, the secondary shell layer is not uniformly distributed, for it is indented by a series of V-shaped embayments underlying the crests of fully formed ribs and pointing posteriorly. Each embayment accommodates a follicle containing one or two setae or, more rarely, two follicles separated by a narrow ridge. The interspace of two adjacent ribs mutually coincides with a V-shaped eminence on the internal surface of the valve, pointing outwardly but ending abruptly just inside the zone of the valve edge, which is occupied by the mantle lobes. As the shell grows, each eminence develops a slight median furrow that begins to widen and deepen into an embayment, later to be occupied by a new follicle. Fully developed follicles appear relatively suddenly along the mantle edges of dissected specimens. However, the morphology of the shell margin suggests that they are first differentiated within the mantle groove

when the eminence, corresponding to the intercostellate spaces on the outer surface, is first indented by a median furrow. This occurs just before a new costella, containing the developing embayment, branches off from its parent. When the *Terebratulina* shell is closed, the crenulated commissures of the valves interlock in such a way that the eminences of one valve fit into the embayments of the other valve. The edges of both valves, corresponding to the zone of the mantle lobes, remain slightly parted and parallel to each other and thus facilitate the continuous deposition of the shell, as well as the movements of the setae, which protrude between each costella and the complementary eminence of the other valve.

The setal arrangement in *Terebratulina* with its well-developed intercostellate spaces is quite distinct from that of *Hemithiris*, which is ornamented by low-rounded ribs separated by linear interspaces. In the latter genus the follicles occur at regular intervals along the mantle edge, irrespective of exter-

nal ornamentation; and, apart from a marginal occurrence of slight ridges corresponding with the interspaces, there is no differentiation of the internal edges of the shell. This lack of setal indentations on the internal surfaces is also true of smooth shells like *Macandrevia* and of the coarsely costellate *Terebratalia* in which the radial ornamentation may be regarded as a superimposed crenulation of the commissure not affecting the distribution of setae.

The morphology of the inner marginal edge of costellate fossil shells, such as those of enteletoids, is so like that of *Terebratulina* that a similar arrangement of setae probably obtained (Fig. 298). A comparable pattern was also characteristic of costate orthidines (*Hesperorthis*, *Plaesiomys*, and *Orthambonites*) (Fig. 299.1). In such stocks as these, the costae are represented internally by grooves and the interspaces by V-shaped or bluntly rounded eminences indented by a median furrow that is shallower than the groove but almost as long. Judging from comparisons with living brachiopods and the impressions of peripheral branches of the mantle canals on the interiors of fossil shells like *Cyrtionella* (ÖPIK, 1934), it is feasible to assume that follicles occupied at least the median furrows. The arrangements in other costellate orthidines and clitambonitidines seem to have been more primitive in that no well-differentiated eminences, coincident with intercostellate spaces, were developed; and it seems likely that follicles occupied short grooves corresponding to the crests of the costellae. The absence of distinct grooving at the inner margins of adult shells of *Atrypa* suggests that, as in *Hemithiris*, there was no relationship between the incidence of setae and costellae in fossil species with this style of radial ornamentation. *Enteletes*, *Meekella*, and other brachiopods with strong costae superimposed upon a finely costellate ornamentation probably possessed a follicular distribution unaffected by the coarser ribbing, as in *Terebratalia*.

In contrast, the parvicostellate ornamentation of the strophomenides may well have

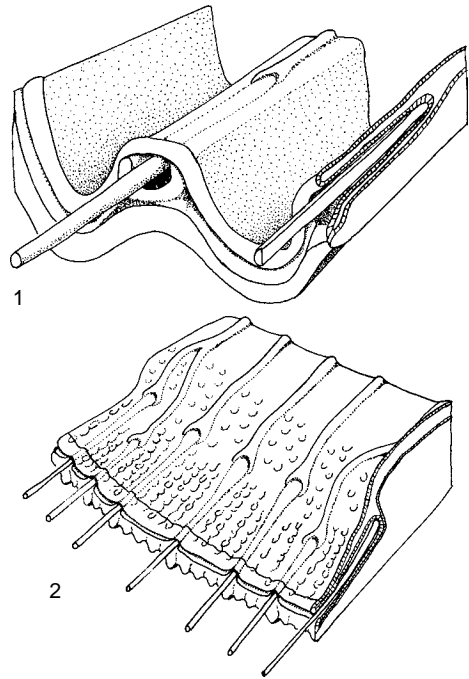


FIG. 299. Inferred relationship between the mantle edge and the shell margin of 1, *Hesperorthis* and 2, *Sowerbyella* (Williams & Rowell, 1965b).

reflected a high density of setae at the shell margin. In *Sowerbyella*, for example, deeply incised, short grooves, each ending posteriorly as a pit in the peripheral rims of secondary shell, occur at regular intervals along the lateral and anterior margins (Fig. 299.2). These grooves probably contained follicles. They underlie the crests of all costae and older generations of costellae and are separated from each other by low, flat, rectangular-ended eminences that correspond to as many as five or six younger costellae. Here and there slight pits and furrows indent the eminences and probably represent the early development of follicular grooves. Thus, at any one stage of growth, setae protruded from beneath about one-quarter of the costellae.

Some rhynchonellides (*Sphaerirhynchia*), which are highly globose as adults and develop a vertical zone formed when anterior and lateral growth is in abeyance, show an

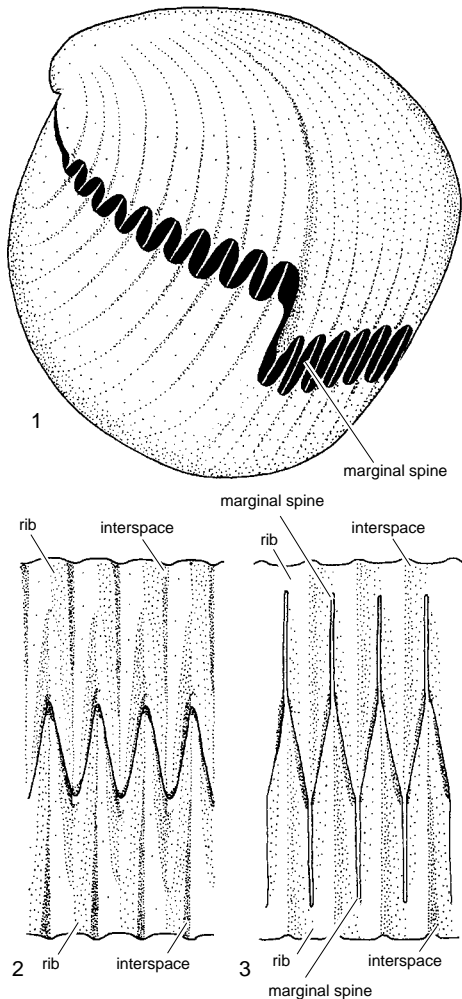


FIG. 300. Marginal spines forming a denticulate commissure of *Sphaerirhynchia*; 1, oblique anterolateral view of open shell showing grille formed by spines; 2, detail of part of anterior commissure, viewed externally; 3, detail of part of anterior commissure, viewed internally, showing relationship of spines and interspaces (Williams & Rowell, 1965b).

unusual modification of the anterior and lateral margins of the valves. The interspaces between costae or costellae are elongated to form long, slender marginal spines that lie against the inner surface of the costae or costellae involved in the vertical zone of the opposing valve. Conceivably, these spines had some protective function when the shell

was open, as they form a regular grille across the gape (Fig. 300; SCHMIDT, 1937).

The postlarval shell of *Discina* is parvicostellate but the valve margins, as those of other recent organophosphatic discinids and lingulids, are free of any grooves to accommodate setae, which are strongly developed in all stocks. In these brachiopods, the edge of a valve is a relatively wide marginal fold (see Fig. 293) of periostracum and a mainly organic primary layer, which together form an elastic cushion for the setae. Even in extinct organophosphatic species, the only traces yet found of a radial ornamentation, which may have been related to setal fringes, are those characteristic of some Paleozoic acrotretides and paterinides. As has been shown in the section on the shell structure of the brachiopod (p. 272), the impersistent radial distributions of dichotomizing arrays of surface pits in *Orbiculoidea* and of sets of nickpoints interrupting the fila of acrotretoids could have been induced by sets of muscles controlling marginal setae (WILLIAMS & HOLMER, 1992). Only the cranioids, which actually lack setae, have grooved internal valve margins (Fig. 301). In the dorsal valve of *Neocrania*, radial grooves and ridges, superficially similar to the eminences and furrows of *Terebratulina* but very much finer (with wavelengths of about 20 μm), are associated with the development of punctation. The punctae are located in the grooves, which increase in number distally by dichotomy of the ridges and become buried proximally in thickened concentric bands of secondary shell. This grooved margin corresponds to the gentler outer slope of the tuberculate subperipheral rim of the ventral valve, which is irregularly channelled. The apposition of these fine structures along the shell margins probably provides *Neocrania* with a crude sieve leading into the mantle cavity.

The brachiopod shell may also be finely to coarsely ornamented by superficial pits (exopunctae) or by outgrowths generally referred to as granules, tubercles, or spines. Superficial perforations are normally limited

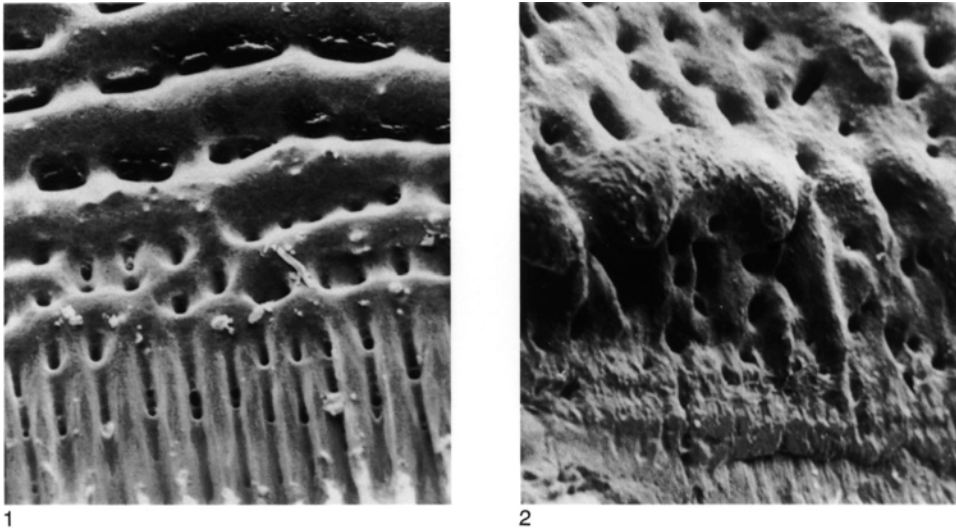


FIG. 301. The internal shell margins (along lower edges of micrographs) of recent *Neocrania anomala* (MÜLLER) showing 1, the radial grooves of the dorsal valve, $\times 140$, and 2, the channelled subperipheral rim of the ventral valve, $\times 70$ (new).

to the primary layer and, even when extending into the secondary layer, never penetrate the entire shell. WRIGHT (1981) has distinguished several types of superficial pits, although not all of them are distinctive enough to merit terminological recognition.

Shallow pits are found in widely different brachiopods. They are usually arranged radially as in the enteletoid *Saukrodictya* or in offsetting radiating rows culminating in hexagonal close packing (*Dictyonella*). In general, they tend to be symmetrical and evenly developed, as in the discinoid *Trematis*; but the outer rim may be subdued to give parabolic structures as in the rhynchonellide *Porostictia*.

Even more distinctive pits are relatively deep cylindroid perforations, which give rise to the hollow costellae (aditicles) of orthides, as in the impunctate orthoids (*Doleroides*, *Plaesiomya*) and punctate enteletoids (*Rhipidomella*). Hollow costellae have been interpreted (WILLIAMS & ROWELL, 1965b; WILLIAMS & others, 1965) as incipient spines that were formed by a regularly occurring, inward sag of the mantle edge away from the sharply rounded arches of the

principal ribs, while deposition continued and ultimately sealed off the reentrant as a short, oblique cylindrical hollow (Fig. 302). More recently, it has been shown that the sequence of sealing off hollow costellae can be followed at the internal margins of valves where they start as embayments, as in those widely interpreted to be sites of setal follicles (WRIGHT, 1981). It is, therefore, likely that hollow costellae housed setae in their early stages of formation. It is unlikely, however, that the setae persisted to become encased in shell, as they are an integral part of the inner epithelium; and it seems topologically impossible for setae and their lubricating and secreting coats of inner and follicular epithelium to become embedded in a continuously advancing outer mantle lobe without causing major aberrations in shell secretion. The hollow costellae are, therefore, best interpreted as temporary containers of setae that migrated with the advancing mantle edges.

Other smaller, highly inclined pits found perforating the ribs of such orthides as *Plectorthis* and *Paurorthis* are true exopunctae in probably having contained isolated bits of vesicular cells or periostracal plugs as

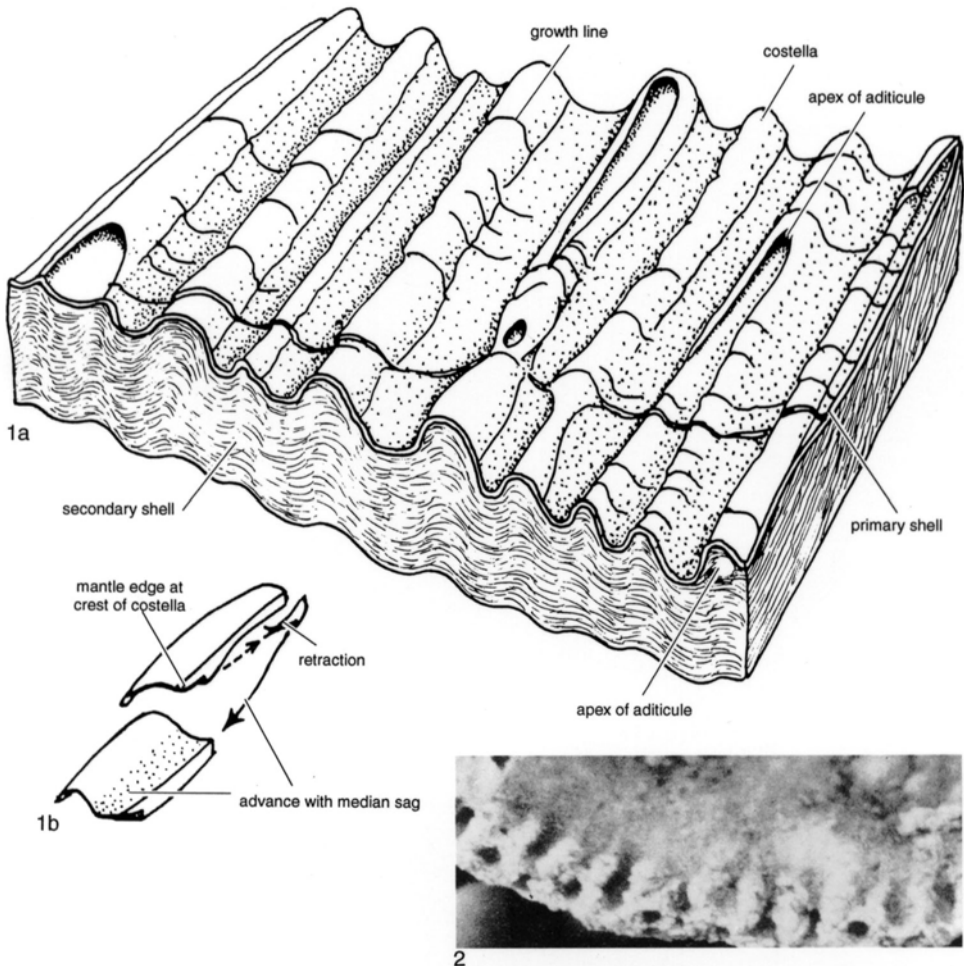


FIG. 302. Growth of hollow costellae (aditicles); *1a*, part of ventral valve of Ordovician *Plaesiomys subquadrata* (HALL) showing the nature of hollow costellae and *1b*, the inferred path of the mantle edge during the formation of an aditicle (Williams & Rowell, 1965b); *2*, internal margin of dorsal valve of Permian *Rhipidomella hessensis* KING showing stages in the sealing off of foliolar embayments to form aditicles, $\times 15$ (Wright, 1981).

envisaged in *Punctatrypa* (Fig. 260). There is little possibility of these perforations having accommodated sensory bristles as such structures would have to have been secreted by lobate cells on the basal layer of the periostracum.

The ornamental outgrowths on the external surfaces of brachiopod valves may be nothing more than nodes of excessive shell secretion in the form of fine granules and larger tubercles at the intersections of concentric fila or lamellae and rib crests (see Fig.

297). These range from the solid hooked spines of the terebratulide *Dictyothyris* (Fig. 303) to the densely distributed granules of the orthide *Platystrophia* and the lingulide *Lingulasma*.

Such excrescences are especially characteristic of many spire bearers, and recent studies (GOURVENNEC, 1987, 1989) have shown that their formation involves a distinctive secretory regime (Fig. 304). In such groups the fine ornamentation consists of capillae, which are disposed radially (the eospirifid

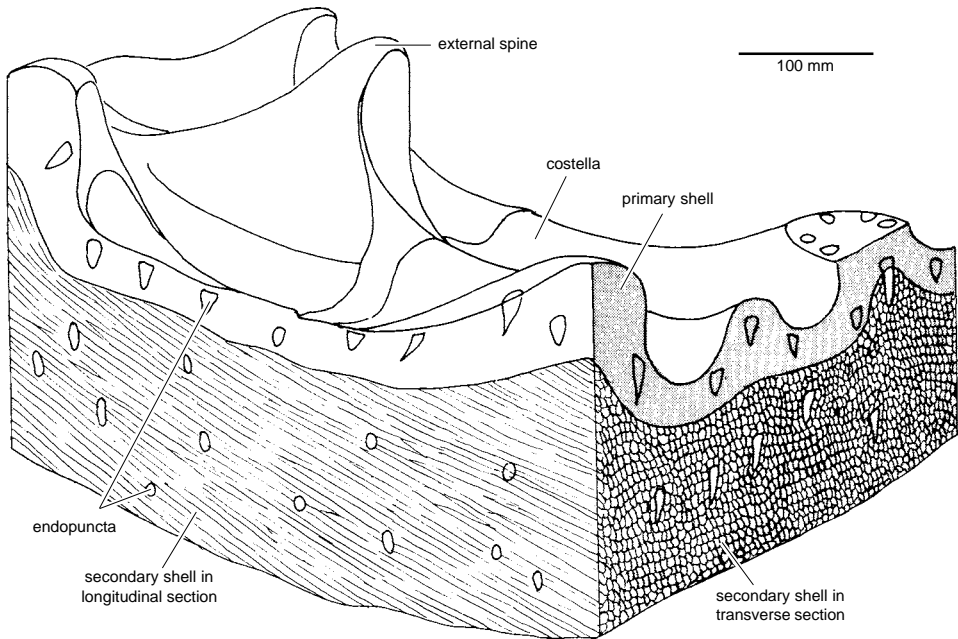


FIG. 303. Block section of ventral valve of Jurassic *Dictyothyris coarctata* (PARKINSON) showing the relationships of external spines with primary and secondary shell layers (Williams & Rowell, 1965b).

type) or pseudoradially (the delthyrid type) when they arise by intercalation in intercostal grooves and diverge onto the flanking costal crests (Fig. 305). Pseudoradial capillae may be superficial (*Maurispirifer*) or variably embedded in the lamellae of the primary layer and can be prolonged as spines (*Paraspirifer*). The spines can be quadrangular in transverse section and deeply grooved (*Elisia*) and are feasibly interpreted as having been secreted by fingerlike extensions of the outer mantle lobe (GOURVENNEC, 1987).

The microscopic spines of ambocoeliids are also outgrowths of the primary layer (BALINSKI, 1975) and can be exaggerated by differential weathering. They may contain impermanent canals like the **double-barrelled spines** of *Phricodothyris* (GEORGE, 1932a), but they are not continuous with perforations of the secondary shell (Fig. 306).

GOURVENNEC and MÉLOU (1990) have recently claimed that the microspinose frills of the well-developed lamellae of such orthides as *Ptychopleurella* are proof of the descent of

the microspinose spiriferides from such stocks. The development of frilled lamellae, however, probably in relation to marginal setae, is likely to be as recurrent a theme in brachiopod evolution as any other morphological feature.

The hollow productidine, chonetidine, rhynchonellide, and siphonotretoid spines, which also opened into the shell interior, were formed in a different way from spiriferide spines. Many of these spines must have continued to increase in length throughout the life of the animal and bear growth banding consistent with deposition by discrete generative zones (RACHEBOEUF, 1973). Such increments, however, could have been added only at the distal ends (intussusceptive growth), which must have been occupied by persistent generative tips capable of proliferating outer epithelium to line the lengthening axial canals and thereby maintain the processes of shell secretion (WILLIAMS, 1956). Since all spines were first differentiated at the shell margin, it is likely

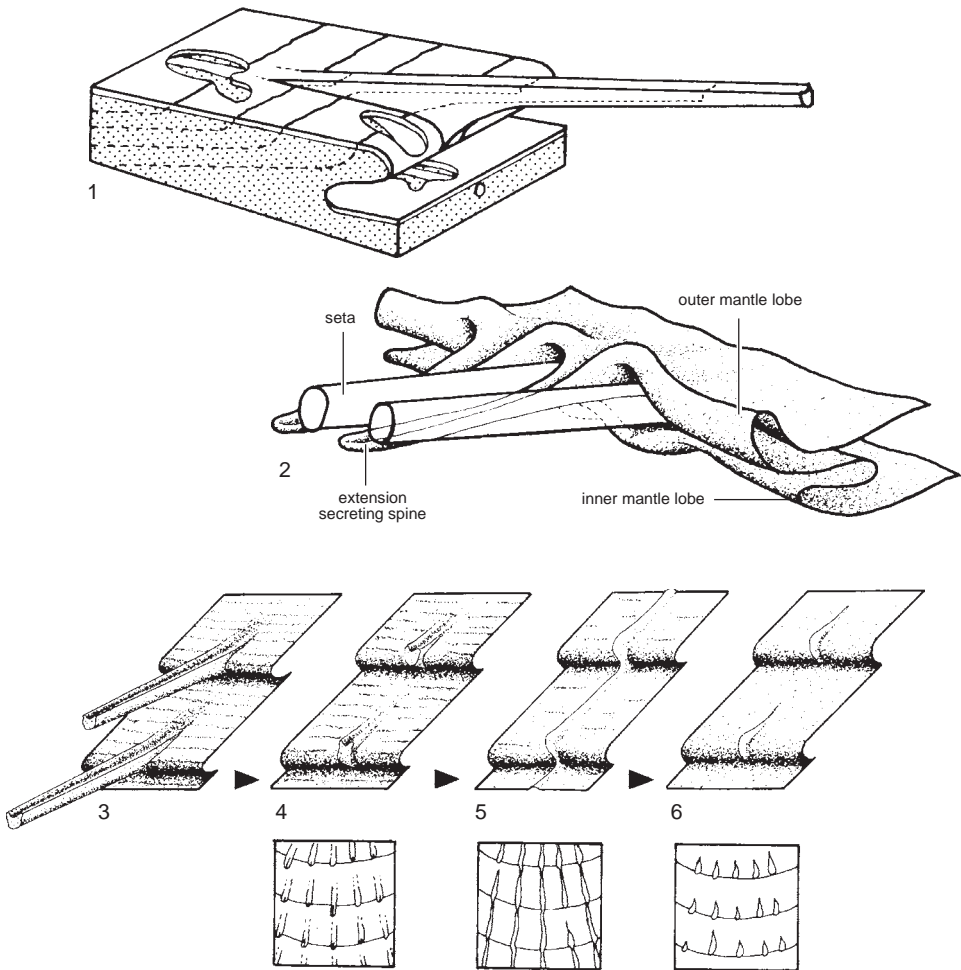


FIG. 304. Growth of delthyrid spines; 1, stages in the emergence of a spine (shown by *dotted lines* within the stippled layer of secondary shell) and 2, idealized reconstruction of the secreting mantle (shell and spines removed); 3–6, stages in the weathering of the shell surface, leading to the development of teardrop-shaped granules on worn filia (Gourvenec, 1987).

that the tips were actually isolated bits of the vesicular cells of outer mantle lobes that retained the generative properties of that part of the mantle. Such vesicular cells would continue to secrete the basal layer (and any infrastructure) of the periostracum; and it is feasible that the periostracal caps of some kinds of spines remained sufficiently sticky to attach the animal to the substrate. These epithelial evaginations were commonly sealed off by later deposition, especially in the body cavity, in which event growth of the

spines ceased and the axial canals end blindly within the secondary shell layer.

The simplest hollow spines (Fig. 307) are those of the rhynchonellide *Acanthothiris* (RUDWICK, 1965b) and the finer of two distinct sets of the siphonotretide *Siphonotreta* (BIERNAT & WILLIAMS, 1971). These prostrate or tangential spines, which can be many millimeters long, are radially disposed and variously arranged in concentric zones of high density. Inward of the valve margin, they invariably become sealed by secondary

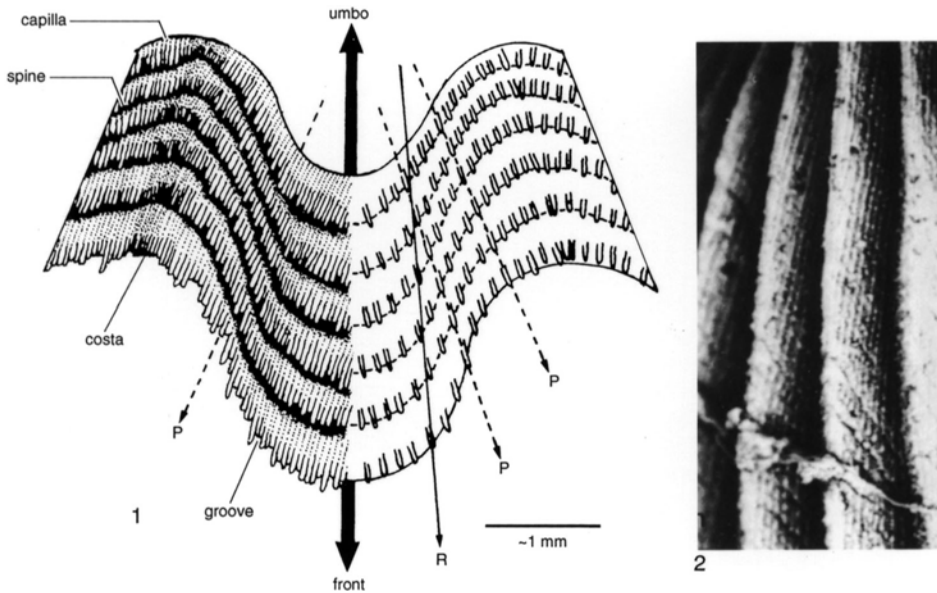


FIG. 305. Orientation of delthyrid-type, pseudoradial capillae; 1, capillae diverge from the bottom of the intercostal grooves toward the costal crests in line with a pseudoradial direction (*P* with dashed line) and not a radial one (*R* with solid line); 2, shell surface of Devonian *Adolfia* sp. showing the pseudoradial disposition of capillae, magnification about twice that of diagram (Gourvenec, 1989).

shell (unlike the coarser set in *Siphonotreta*, which remained open throughout life). Around the valve margins the fine spines interdigitate to form a grille that probably protected the commissural gape from extraneous objects (RUDWICK, 1965b; BIERNAT & WILLIAMS, 1971) and the shell surface from widespread colonization by cementing benthos. RUDWICK also concluded that such spines acted as sensory mechanisms, which hardly seems possible for mantle extensions that were completely enclosed in calcitic tubes with periostracal caps.

The spines of productidine brachiopods, which exceptionally exceed 20 cm in length, are much more diversified in form and function, even on individual shells. Some sets of spines (including arrays of strainer endospines on subperipheral rims) acted as external and internal grilles (Fig. 308; SHIELLS, 1968); others formed prostrate mats over external surfaces and probably protected the animals against predators as well as infestation by cementing benthos. Shells were also

supported by symmetrically placed, strutlike, halteroid spines; but the most spectacular kind of support was that afforded by dense entanglements of rhizoid spines and clasping or attachment spines. The ability of these spines to converge and encircle cylindrical objects suggests a cementing capability like that of the craniid ventral valve. It is, therefore, possible that the generative tips of

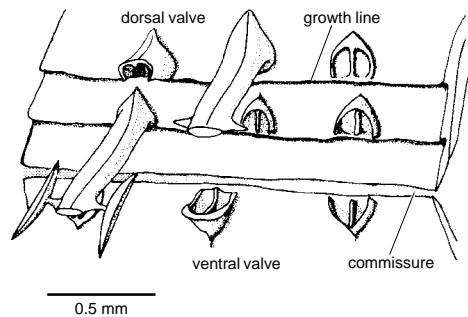


FIG. 306. Double-barreled spines of Carboniferous *Phricodothyris* sp. (Williams & Rowell, 1965b).

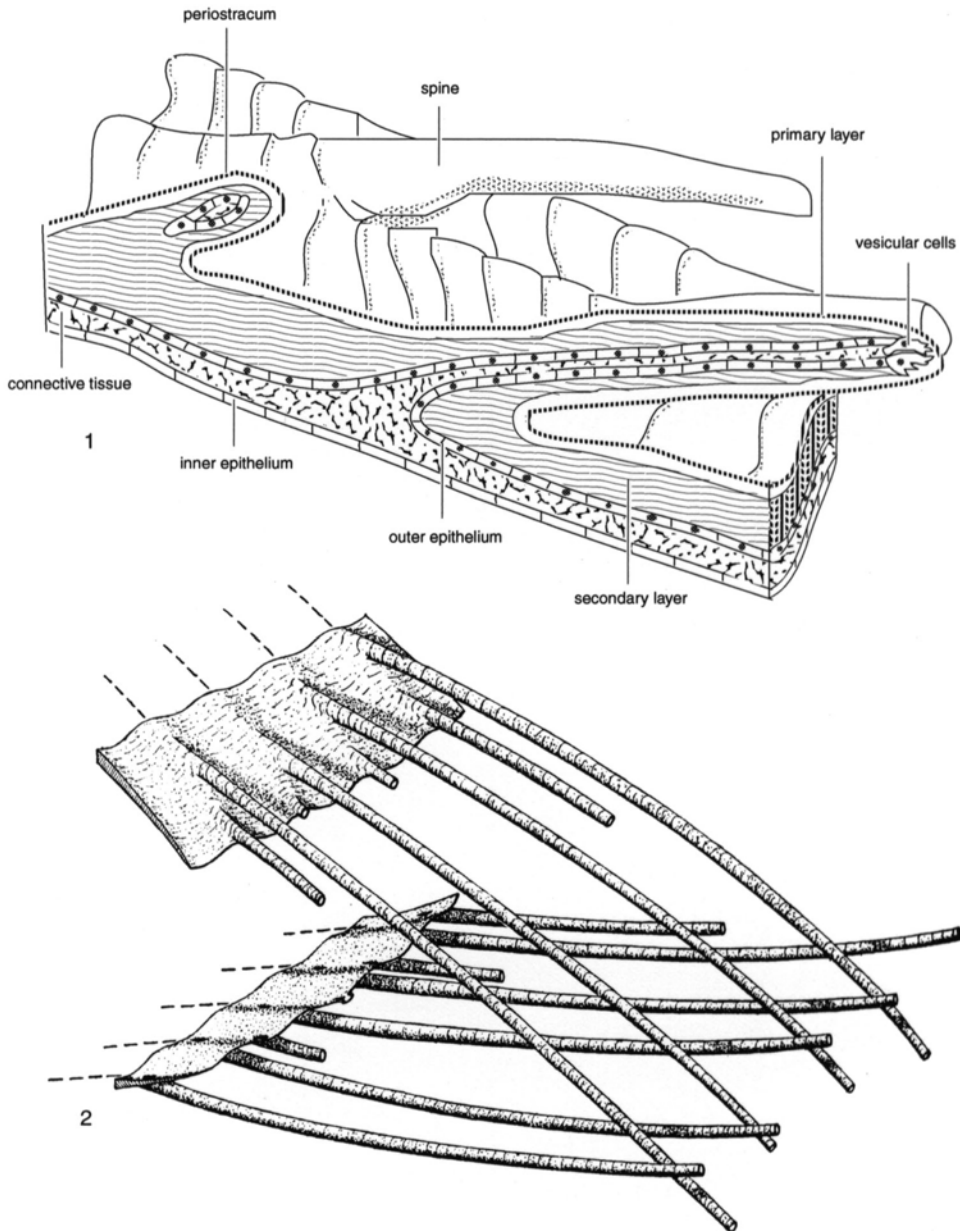


FIG. 307. The spines of Jurassic *Acanthothiris spinosa* (LINNÉ); 1, reconstruction showing relationship between mantle and calcareous spines (Williams & Rowell, 1965b); 2, reconstruction of parts of the valve edges, gapping as in life and showing how a grille of spines forms across the aperture (adapted from Rudwick, 1965b).

rhizoid and clasping spines exuded copious quantities of GAGs that cemented the periostracal coats of the spines to any contiguous object (Fig. 309). The first-formed bio-

mineralized layers lining the extending periostracal sheaths would also have been secreted as a mixture of GAGs and calcitic granules, which polymerized as a plastic layer

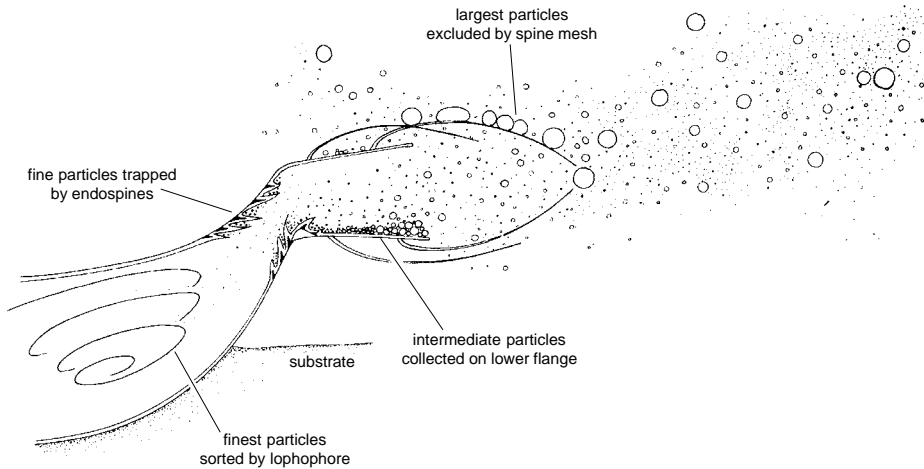


FIG. 308. The inferred filtering system of Carboniferous *Kochiproductus coronus* SHIELLS; the shell is shown partly buried in substrate with the gape of the valves facing a cross flow of detritus of various sizes; the productide lophophore was probably more like a schizolophe than a spirolophe (Shiells, 1968).

to account for the molding of spines to the contours of their substrates.

MODIFICATIONS OF PEDICLE OPENING

The anatomy of the pedicle and its cytological relationship with the mantle have been described, but its nature and disposition (as well as its absence) profoundly affect shell morphology in many ways. In particular, the opening in the shell for the emergence of the pedicle can vary greatly and is best described according to the degree of specialization of the organ during brachiopod evolution.

The simplest pedicle openings are found in organophosphatic brachiopods. In living lingulids the ventral pseudointerarea is indented medially by a pedicle groove that is lined by a strip of ventral outer epithelium sharing an arcuate junction with the circular base of pedicle epithelium (Fig. 310.3). The flanking propleareas and the entire pseudointerarea of the dorsal valve are secreted by the outer lobes along the posterior segments of the ventral and dorsal mantles respectively. This relationship was typical of lingulides throughout the geological record although

the pseudointerareas of early Paleozoic forms were better developed and the grooves more deeply indented (ROWELL, 1977).

The larval pedicle of the living discinoid *Pelagodiscus* (ASHWORTH, 1915) appears to develop, like that of *Lingula*, from the inner epithelial layer of the posteromedian sector of the ventral mantle (Fig. 39). However, a section of the mature pedicle of *Discinisca*, figured by BLOCHMANN (1900), showed a setal groove separating the inner epithelium of the posterior body wall from an outer mantle lobe, which secretes the posterior arc of the pedicle cuticle (Fig. 311). Accordingly, if this setal groove is the circumferential boundary between the ventral mantle and the body wall, the discinoid pedicle lies wholly within the outer layer of the ventral mantle and not just contiguous with it as in *Lingula*. Even so, this posteromedial strip of ventral outer mantle lobe seems never to have developed into an active site of integumental secretion during discinoid evolution. The postlarval, ventral valve of the early Paleozoic *Trematis*, which grew holoperipherally, was indented by a variably shaped pedicle notch so that no shell was secreted on the dorsal side of the pedicle along the mantle edge flanking the setal groove. In

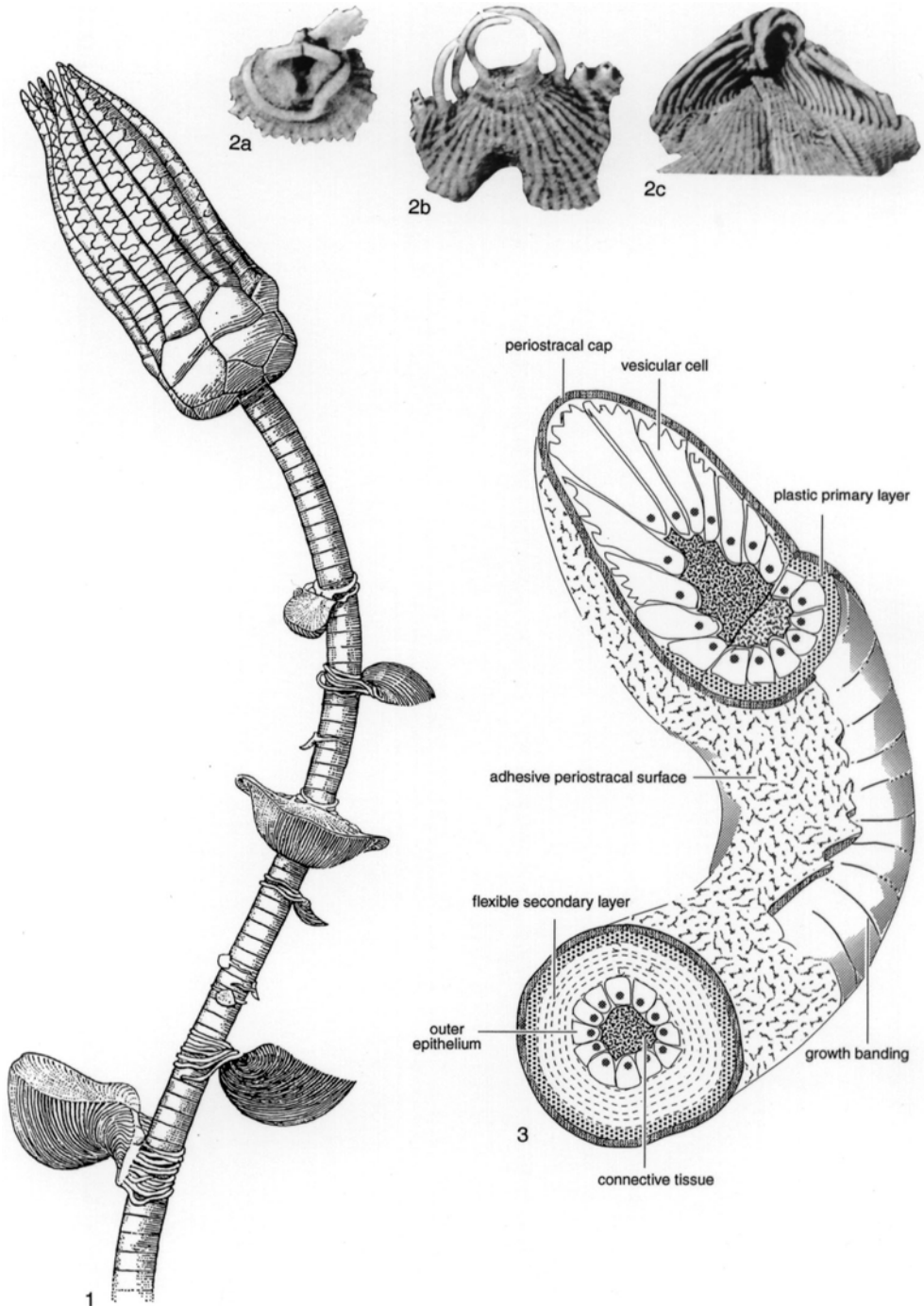


FIG. 309. Attachment spines of the Permian *Linoproductus*; 1, reconstruction of generalized crinoid and attached shells of *Linoproductus angustus* KING in various stages of growth; 2a–c, three stages in the development of the attaching cardinal spines of *L. angustus*, X3, X3, X1 (Grant, 1963); 3, inferred structure and composition of an attaching spine in relation to the mantle of living *Linoproductus* (new).

other mature discinoids, this notch is closed toward the valve margin by a strip of periostracum in living *Discinisca* or by a fully developed shell succession as in recent *Discina* and Paleozoic *Orbiculoidea* (Fig. 310.1). Such closure, however, is effected by the convergent growth of the posterolateral sectors of the ventral outer mantle lobe, which surround the pedicle base and fuse dorso-medially in the manner of deltidial plates of articulated brachiopods.

In some discinoids, migration of the pedicle has led to the enlargement of the opening toward the apex of the valve, which is commonly filled by a plate (listrium) growing posteriorly and secreted by the anterior part of the junction of the pedicle and outer epithelia. The free margin of the listrium in *Orbiculoidea* projects internally as a pedicle tube lying against the previously formed shell of the posteromedian part of the ventral valve (Fig. 310.1). The discinoid pedicle also leaves traces of its presence on the external surface of the ventral valve. The pedicle opening of some living and many extinct discinoids is contained within an elongately oval depression marking the external attachment area of an expanded pedicle.

The relationship of the pedicle to its putative opening in the remaining, wholly extinct organophosphatic brachiopods, the acrotretides and siphonotretides, is speculative. The pedicle openings of these groups are usually identified and interpreted in terms of the differentiation of the pedicle of living organophosphatic species, but there is a fundamental difference in the origin of the organ, at least compared with that of *Lingula*. In all siphonotretides and most acrotretides, the larval ventral valve, normally between 100 and 300 μm in length, is pierced more or less centrally by a foramen that is widely accepted as having accommodated the larval pedicle (Fig. 312). This suggests that the pedicle of these extinct organophosphatic stocks was an evagination of ectoderm that became the outer epithelium responsible for the secretion of the shell, and not an evagination of the inner epithelium as in *Lingula*. The pedicle of acrotretides and

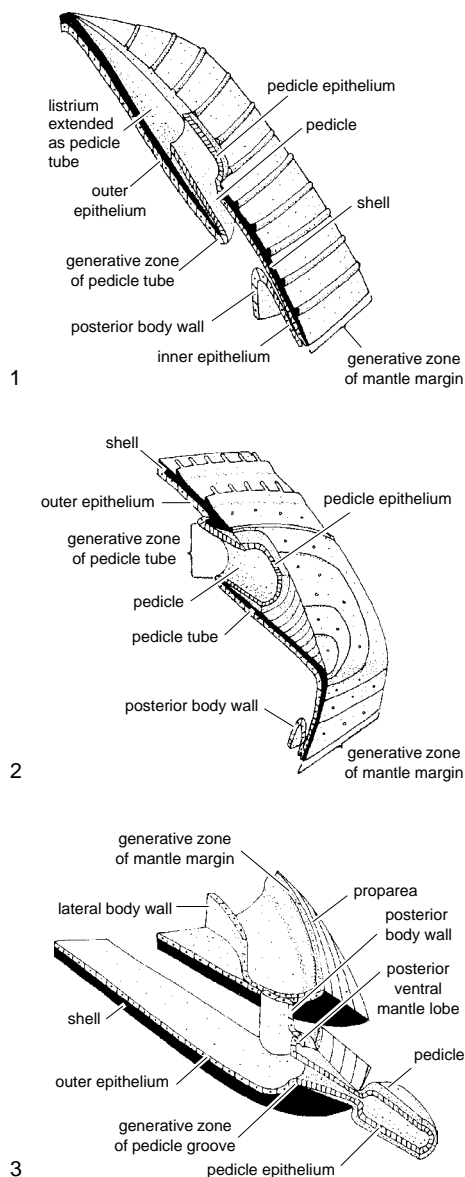


FIG. 310. Stylized reconstruction of posterior part of ventral valve with longitudinal section showing inferred epithelium-and-shell relations in 1, *Orbiculoidea* and 2, *Multispinula*, both viewed externally; 3, observed epithelium-and-shell relations in *Lingula*, viewed internally (Williams & Rowell, 1965b).

siphonotretides, therefore, could have been very different in its morphology and function from that of lingulides. In particular the pedicle of these extinct groups was probably a variably developed organ of adhesion with

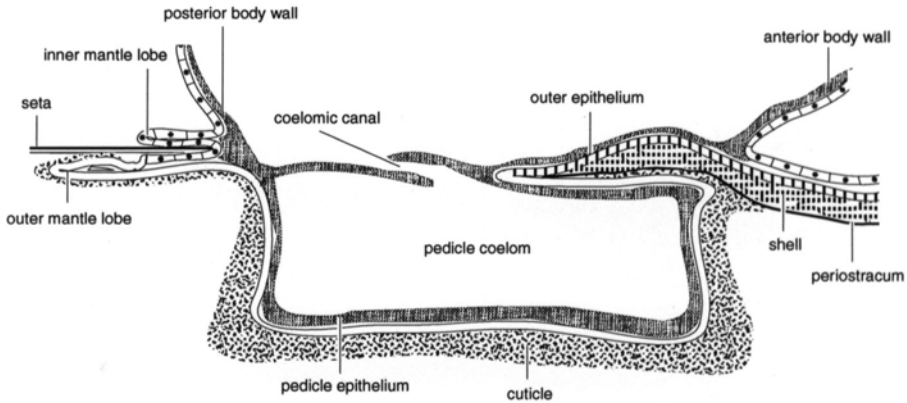


FIG. 311. Differentiation of epithelia associated with the pedicle of recent *Disciniscia lamellosa* (BRODERIP) (adapted from Blochmann, 1900).

a cuticle closely related in composition to the periostracum and with a potential for atrophy as well as resorption of an organophosphatic shell. Whether such a pedicle was homologous with that of living discinids is presently undeterminable. On the basis of BLOCHMANN'S (1900) interpretation of the mature discinid pedicle, it is possible that it, too, arose by differentiation of larval outer epithelium, although by changes in the vesicular cells of the outer mantle lobe.

Among the siphonotretides, the ventral pseudointerarea is always entire, and the foramen can be minute and plugged in maturity as in *Acanthambonia* or greatly enlarged anteriorly by resorption as a narrowly triangular opening restricted posteriorly by a plate (*Schizambon*) or pedicle tube (*Multispinula*) (Fig. 310.2). CHUANG (1971) has contended that the perforate valves of *Schizambon* and acrotretides are dorsal and that the foramina were for exhalant currents. This interpretation is contrary to brachiopod functional morphology in general and is untenable (ROWELL, 1977).

In most adult acrotretoids, the posterior margins of the ventral valves are entire and commonly flattened to produce strongly developed pseudointerareas. Entirely biomineralized posterior margins are also characteristic of their perforate larval valves except in two groups within this superfamily (Fig. 313). In maturing *Curticia*, the pedicle mi-

grated posterodorsally and the posterior margin of the ventral valve was breached by resorption to form a triangular pedicle opening. In *Scaphelasma*, however, the larval ventral valve was not perforated by a foramen; instead the posteromedian margin was indented by a pedicle notch, and shell secretion did not delineate a foramen until the brephic or neanic growth stages (HOLMER, 1989). In contrast, the related, cemented acrotretoid *Eoconulus* has a swelling (bullae) that is perforated by a pair of lateral aper-

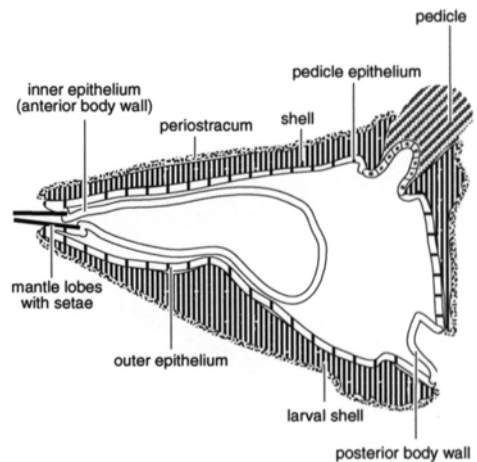


FIG. 312. Inferred distribution of the inner, outer, and pedicle epithelia in a longitudinal section of a typical juvenile acrotretoid (*Torynelasma*) shell, about $\times 150$ (new).

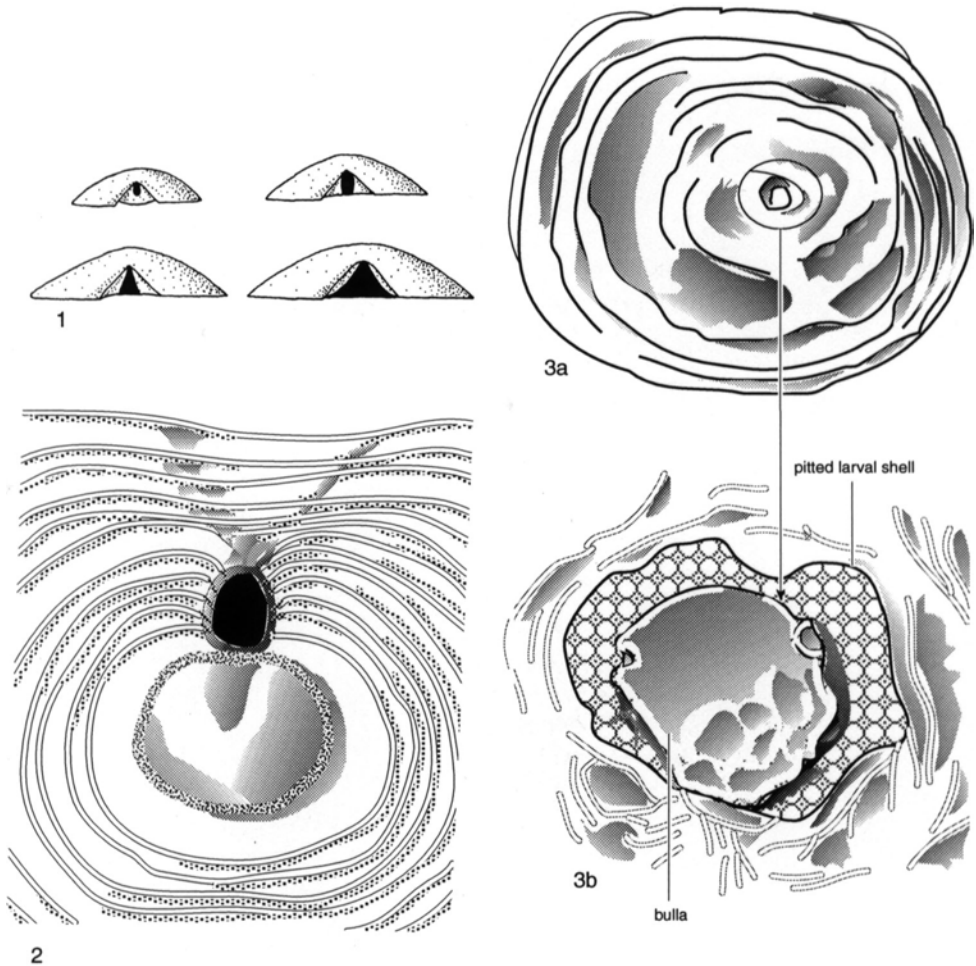


FIG. 313. Acrotreoid pedicle openings; 1, growth series of the Cambrian *Curticia minuta* BELL (beginning with the youngest ventral valve known, 1.1 mm wide, in the top left-hand corner) showing an increasingly triangular pedicle opening breaching the posterior margin of the enlarging ventral valve (Williams & Rowell, 1965b); 2, the closure of the pedicle opening during the growth of the Ordovician *Scapelasma* sp., $\times 125$; 3a, external view of the ventral valve of the Ordovician *Eocomulus* cf. *semiregularis* BIERNAT, $\times 125$, and 3b, a detail of the central region of the valve showing the bulla in relation to the pitted larval shell, $\times 700$ (adapted from Holmer, 1989).

tures and that generally has the appearance of having been a cast of sporadic clusters of vesicles; it is connected to the pitted larval plate by a constricted neck. The bulla has been interpreted as a protegulum (HOLMER, 1989); and this is borne out by the fact that similar swellings, in various stages of collapse, occur at the centers of the larval valves of living *Discinisca*.

The pedicle opening of the related botsfordioids is also fashioned differently from the typical acrotreoid foramen. In *Bots-*

fordia, the posterior margin of the larval ventral valve is indented by a triangular pedicle notch that persisted in maturity (Fig. 314.3), while in *Acrothele* rapid secretion along the posteromedian sector of the mantle gave rise to an entire ventral pseudointerarea restricting the foramen (Fig. 314.1–314.2). It is not known whether the growth of an entire pseudointerarea in such botsfordioids as *Acrothele* is homologous with the mineralized dorsal margins closing discinoid pedicle openings.

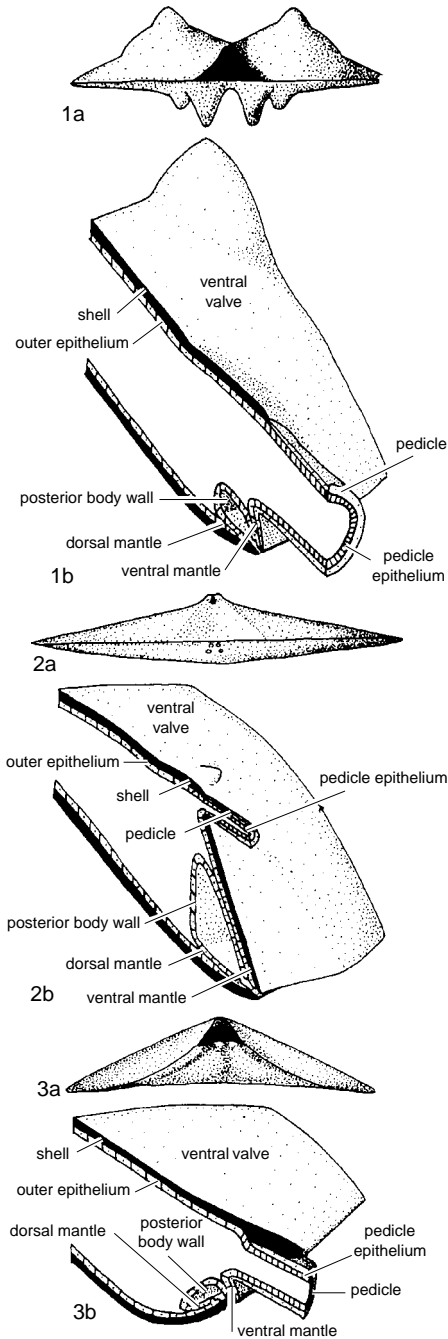


FIG. 314. Posterior views of shell and stylized reconstructions with longitudinal median section of posterior part of shell showing inferred epithelium-and-shell relations of 1, young *Acrothele*, 2, adult *Acrothele*, and 3, adult *Botsfordia* (anterior body wall omitted) (Williams & Rowell, 1965b).

In retrospect, the inferred shift in the acrotretide larval pedicle from its presumed normal position at the center of a shell undergoing holoperipheral growth is greater than that of the pedicle rudiment of articulated brachiopods, but it affects only a minority of species. The posterior slope of the acrotretide ventral valve is usually slightly indented or raised medially (intertrough, deltoid pseudointerarea). These features seem not to have reflected the disposition of the pedicle, which lay ventral of their growing edge. Indeed in most acrotretides, there was very limited posterior migration of the pedicle opening, which is usually located near the apex of the valve and which may be prolonged internally by a differential thickening (apical process) secreted by outer epithelium at its junction with pedicle epithelium.

The remaining organophosphatic brachiopods, the paterinides, are unique in having an imperforate shell with features normally associated with a supra-apical foramen as in the articulated strophomenides. These structures are the posteromedian, externally convex **homeodeltidium**, and **homeochilidium** of the ventral and dorsal valves respectively. It is usually supposed that the pedicle emerged between these two plates, which would then be the homologues of the pedicle collar and an exaggerated antigyidium of living rhynchonellides. It is less likely that no pedicle developed, at least in postlarval stages, and that the median gape between the plates was underlain by inner epithelium of the posterior body wall (Fig. 315; WILLIAMS & ROWELL, 1965b, p. 90).

The variability in the position of the pedicle opening is also characteristic of the oldest, carbonate-shelled, inarticulated obolellides. The opening may be represented by a posteromedian groove in the ventral pseudointerarea (*Obolella*), an apical foramen, or a triangular resorption slot well forward of the beak of the ventral valve (*Trematobolus*). The remaining inarticulated, carbonate-shelled brachiopods lacked pedicles, and the only evident morphologi-

cal effects are the absence of perforations and the distortion of the shell dependent on whether the animal was free-living or cemented. The development of living *Neocrania*, however, has some bearing on the nature of the acrotretide pedicle. The attachment area of a fully grown larva of *Neocrania* is a relatively thin patch of epithelium charged with electron-dense material (NIELSEN, 1991). This patch is central to a shell that is secreted holoperipherally during postlarval growth and probably had as its plesiomorphy an atrophied holdfast acting as a pedicle such as one would expect to have existed in the earliest craniids, as in the free-living *Pseudocrania*.

The morphological relationship between the pedicle and shell of living articulated rhynchonellides and terebratulides is superficially reminiscent of that of inarticulated species, but the development and role of both hard and soft parts are fundamentally different. The manner in which the sub-circular junction between the outer and pedicle epithelia is shared by the unmodified pedicle openings (the ventral **delthyrium** and the dorsal **notothyrium**) has already been described in the section on anatomy (p. 49), as has the replacement of the posterior body wall in these astrothic, tightly articulated shells by a strip of fused ventral and dorsal mantle lobes (p. 47). This basic arrangement is usually modified by the growth of plates that further confines the pedicle, as is well shown in mature *Notosaria* and *Liothyrella* (WILLIAMS & HEWITT, 1977).

The circumferential expansion of the junction occurs only at its intersection with the strip of fused mantle lobes, which are responsible for the growth of the cardinal margins of both valves (Fig. 316). As expansion takes place with a simultaneous increase in length, especially of the ventral cardinal margin, the junction migrates into the delthyrial cavity across the secondary fibers, which become realigned. This surface of inward migration is normally coated with a thin carbonate film and sealed by a proteinaceous membrane, both being secreted by the

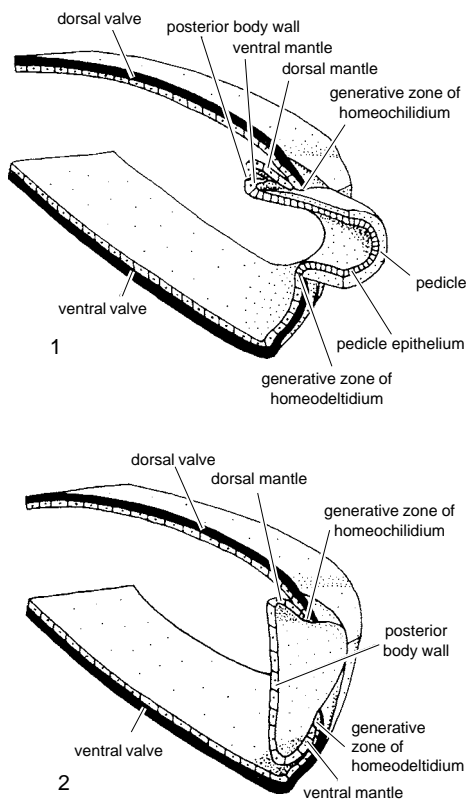


FIG. 315. Stylized reconstruction (with median longitudinal section) of posterior part of paterinide showing alternative interpretations of epithelium-and-shell relations (anterior body wall omitted); 1, inferred to possess pedicle; 2, inferred to lack pedicle (Williams & Rowell, 1965b).

retreating outer epithelium forming the outer rim of the junction. The membrane acts as a bonding sheet for a cuticular fold secreted by the pedicle epithelium at the inner rim of the junction. This entire zone constitutes the **pedicle collar** of the ventral valve. A similar succession, on a more modest scale, usually marks the retreat of the junction across the antigyidium within the notothyrium of the dorsal valve. With further expansion of the apertures, the ventral outer mantle lobes begin to grow postero-medially away from the fused strip at its two intersections with the pedicle-outer epithelial junction and secrete a pair of tetrahedral

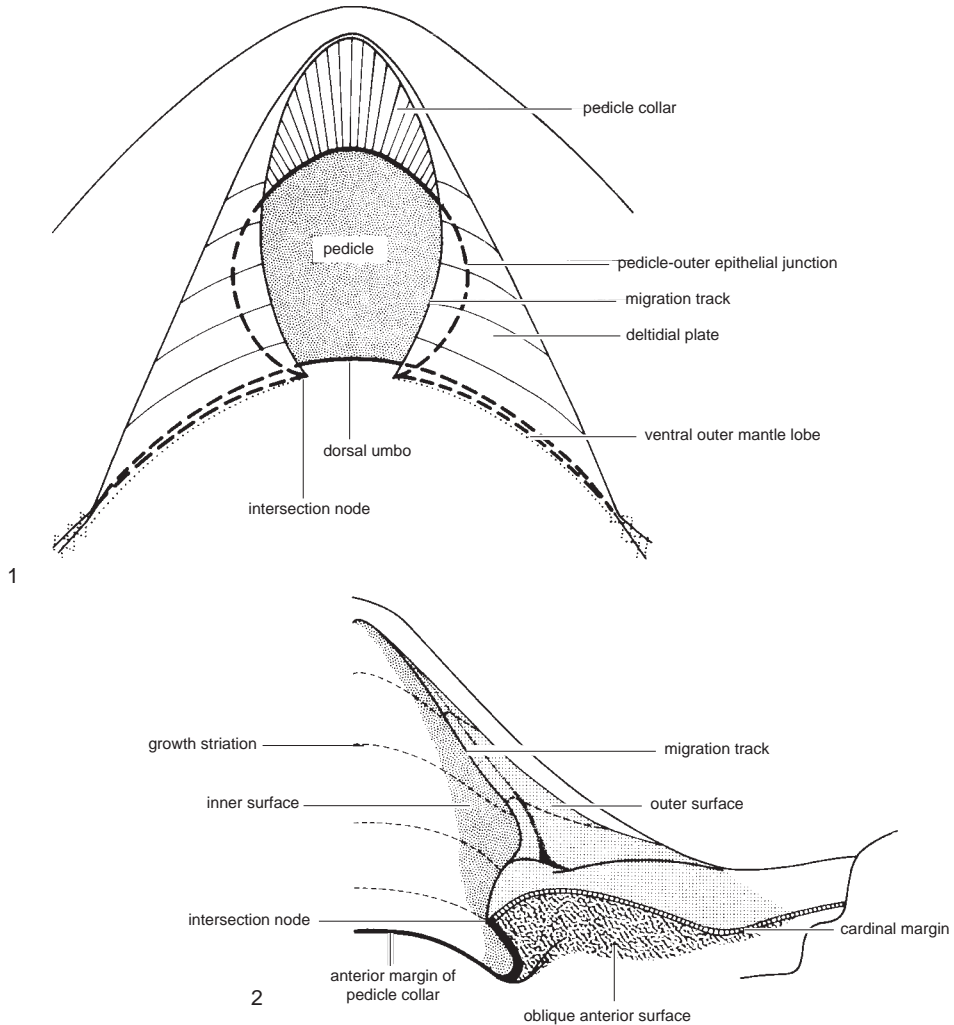


FIG. 316. Diagrammatic dorsal view of the pedicle opening of a mature *Notosaria nigricans* (SOWERBY) showing the relationship of the deltidial plates to 1, the pedicle-outer epithelial junction and 2, the surfaces defining a deltidial plate (Williams & Hewitt, 1977).

structures, the deltidial plates. Each plate is bounded by an outer surface of primary shell, an inner surface of pedicle collar, and an oblique anterior surface of secondary fibers.

The deltidial plates can extend medially only because they grow dorsally above the umbo of the dorsal valve. Further growth leads to a median conjunction of deltidial plates (deltidium). In such stocks as *Liothyrella*, a median fusion of the paired ventral

mantle lobes then takes place to form a continuous structure (symphytium) across the dorsal edge of the delthyrial area (Fig. 317). The term henidium has been coined for a symphytium that bears no sign of a median fusion of deltidial plates.

Within the limits imposed by this sequence of growth of delthyrial and noto-
thyrial biomineralized parts, the morphology of the pedicle opening in astrophic shells can vary. In rostrate shells with the dorsal sectors

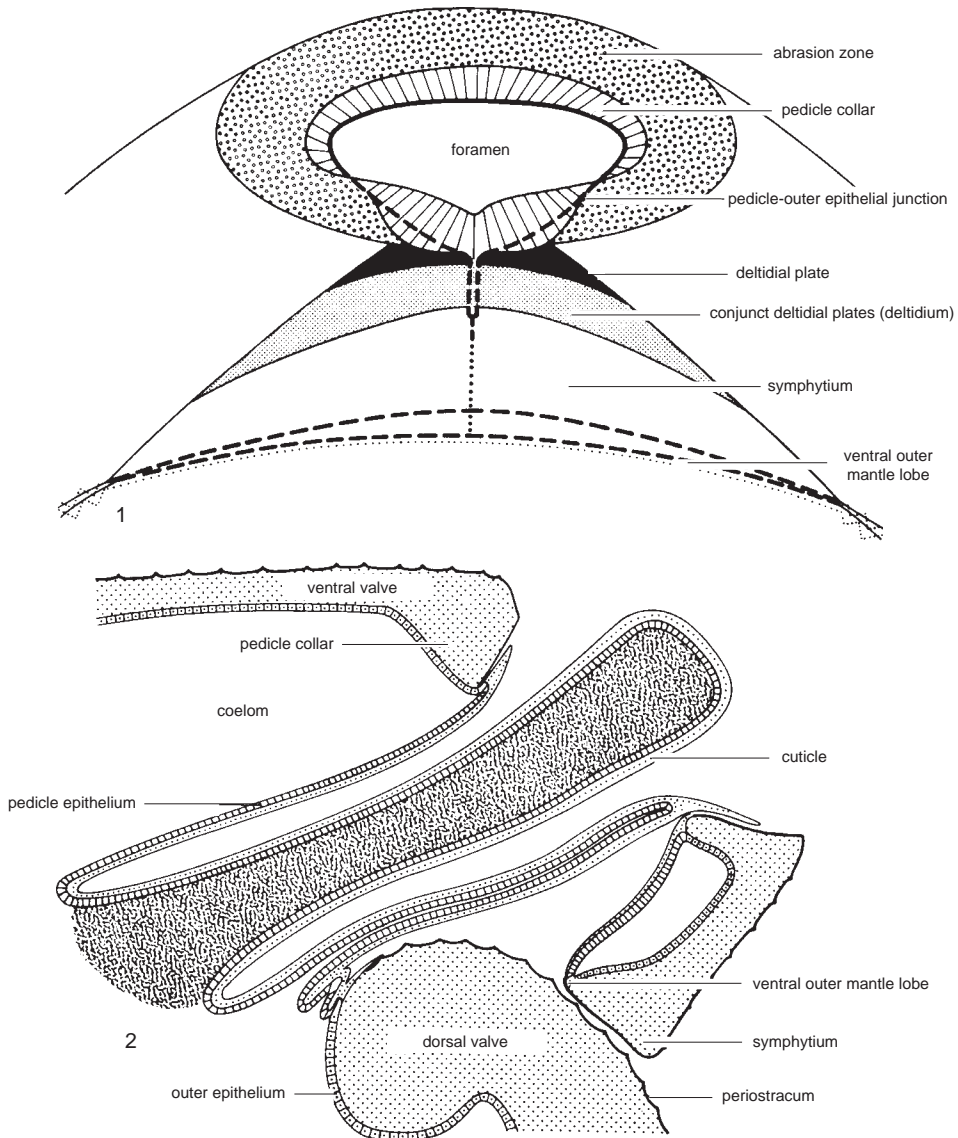


FIG. 317. 1, Diagrammatic dorsal view and 2, section of the symphytium with pedicle of a mature *Liothyrella uva* (BRODERIP) showing the relationship of the symphytium with the deltidium composed of conjunct deltidial plates (Williams & Hewitt, 1977).

of the pedicle zone not projecting beyond the hinge axis (e.g., *Terebratulina*), the plates remain discrete, flanking the dorsal sheet of pedicle epithelium. In other species, the growth of the dorsal umbo into the ventral valve facilitates the development of deltidia and symphytia. The position of the foramen

relative to the deltidium and ventral beak can also vary through migration, and a number of terms are in general use to indicate its location (Fig. 318).

The open delthyrium and notothyrium are typical of most orthidines, enteletidines, and pentamerides (Fig. 319.3); and it is

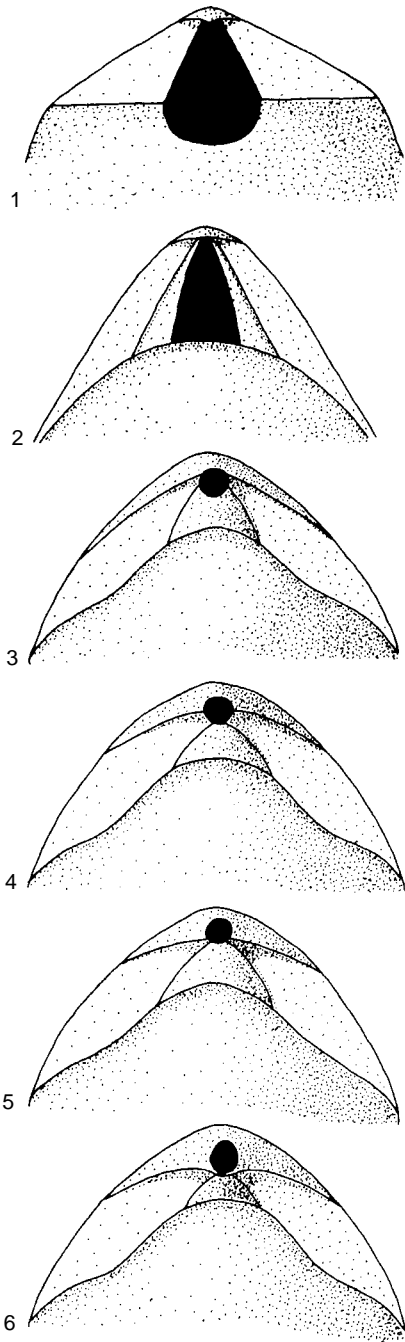


FIG. 318. Position of the pedicle opening relative to the beak ridges of some articulated brachiopods; 1, amphithyrid; 2, hypothyrid; 3, submesothyrid; 4, mesothyrid; 5, permesothyrid; 6, epithyrid (adapted from Williams & Rowell, 1965b).

likely that the junction between the pedicle and outer epithelia in these groups coincided with the boundaries of the diamond-shaped aperture subtended by these structures. Some modifications did occur. The pedicle collar (also known as the pedicle or apical plate) was commonly but variably developed by retreat of the ventral edge of the junction. Deltidial plates, fusing to form a deltidium or **notodeltidium** (COOPER, 1955), developed independently in *Barbarorthis* and *Phragmophora*. The unmodified notothyrial edges must also have acted as attachment surfaces for the pedicle-outer epithelial junction, in the same way as those of the delthyrium, so that lateral or apical extensions of them (the so-called **chilidial plates** and **chilidium** of *Hesperorthis*, *Nicolella*, *Valcourea*, and other genera) would have been secreted like deltidia. It is, however, probable that the pedicle apparatus of these Paleozoic groups differed from that of the rhyononellides, spire-bearers, and terebratulides in lacking any well-developed pedicle capsule. As will be discussed later, this assumption is based on differences in the distribution of ventral muscle fields.

Spire-bearing brachiopods display a greater variation in delthyrial modification as a result of repeated atrophy of the pedicle and the common, extravagant development of the ventral interarea. Cementation of the ventral valve occurred in such widely differing stocks as *Davidsonia* and *Thecospira* (and also in the presumed direct descendants, the thecideidines). In these forms the delthyrial cover is a solid structure as it is in species that lost their pedicles early in ontogeny. This was so in *Bittnerula*, which additionally developed attachment or stabilizing spines on the deltidium within 5 mm of the beak (COWEN & RUDWICK, 1970). Deltidial plates and conjunct deltidia are also found. The subcentrally developed foramen in the delthyrial cover of *Cyrtina*, for example, was probably formed by the secretion of an apically situated deltidial arch, like that found in *Eospirifer*, and a dorsally located symphytium homologous with that of *Liothyrella*.

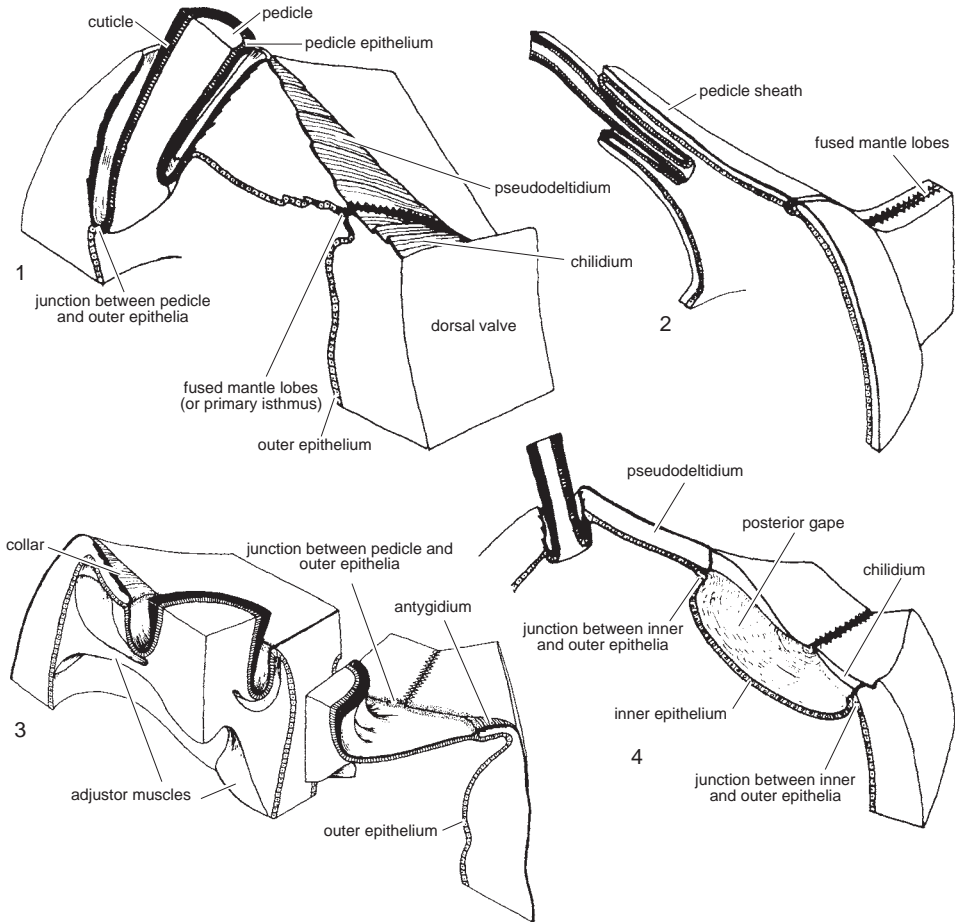


FIG. 319. Inferred relationships between the pedicle and pedicle opening; 1, adult *Leptaena*; 2, young *Coolinia*; 3, adult *Hesperorthis*; and 4, adult *Nisusia* (adapted from Williams & Rowell, 1965b).

The most intriguing structures found in the spiriferides, however, are the **stegidia** of the pyramidal *Syringothyris* and *Sphenothyris* (COOPER, 1954) and the stegidial plates of the alate *Mucrospirifer* (COWEN, 1968).

In *Mucrospirifer*, the delthyrium is filled by two discrete mineralized plates (Fig. 320.2–320.3). The ventral plate fits into the apical part of the delthyrium and consists of a succession of laminae such that the first formed is the smallest, external unit and the last to be secreted is the largest, innermost unit. It is assumed that these laminae were initially deposited around a pedicle that had more or less atrophied when the innermost

layer was secreted. The more dorsal plate fits into the open end of the delthyrium and overlaps onto the notothyrial sector of the dorsal valve. It, too, consists of a succession of thin laminae that are not single units but medially conjunct above the cardinal process.

The syringothyrid stegidium is essentially the same as the ventral stegidial plates of *Mucrospirifer*; and a rarely preserved set of laminae, fitting into the dorsal concavity of the stegidium and capping the cardinal process of *Syringospira* (COOPER, 1954), could well be homologized with the mucrospiriferid dorsal plates (Fig. 320.1). These

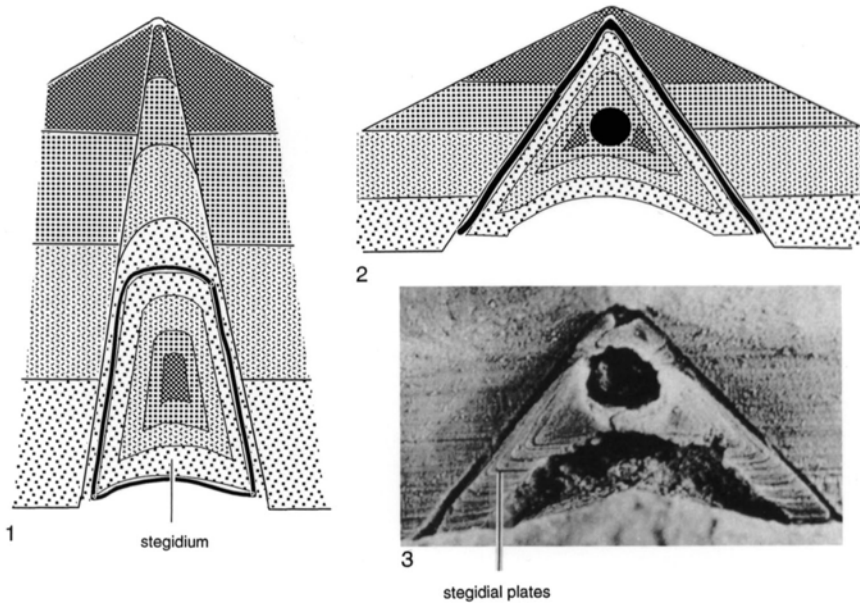


FIG. 320. Inferred growth of the stegidium of a 1, Devonian *Syringospira* and 2–3, Devonian *Mucrospirifer* with the first-formed layers of these structures and the apical regions of the ventral areas, into which they originally fitted, shown in the *darkest shade* of ornamentation to indicate successive growth stages (3, $\times 15$) (adapted from Cowen, 1968).

structures, however, have been differently interpreted as having been secreted in stages by the outer epithelium forming the rim of the junction with pedicle epithelium, which decreased in circumference concomitant with the atrophy of the pedicle.

The mode of secretion described here for the stegidial plates is now preferred for two reasons (COWEN, 1968). First, stegidial plates are complete; and second, they consist of stacked laminae composed exclusively of secondary shell. Neither criterion would hold if the plates had been deposited by outer epithelium peripheral to a reducing junction with pedicle epithelium. COWEN'S interpretation, however, poses a formidable problem in attempting to explain biomineral deposition at the sites postulated by him, without invoking a new secretory regime. A third kind of shell has been reported only once during embryological studies of brachiopods. Interestingly, this was in reference to the presence of a chitinous plate on the caudal segment of the embryo of the thecideidine *Lacazella*,

which is assumed to have had a spire-bearing ancestor (KOVALEVSKIY, 1874).

The covers of the delthyrium and notothyrium of the strophomenides, referred to respectively as **pseudodeltidium** and **chilidium**, were deposited in a fundamentally different way (Fig. 319.1–319.2). The larval shells of a sufficient number and variety of species are now well enough known to conclude that the junction between the outer and pedicle epithelia was restricted throughout growth to the ventral valve. In such larval shells the pedicle opening occurs suprapically (ARBER, 1942) within the ventral valve and is commonly enclosed in a high calcitic ring (pedicle sheath). The pedicle junction, therefore, must have lain within the edge of the sheath, so that the pseudodeltidium, lying dorsal of it, was an integral part of the interarea; and its development was not dependent upon the presence of the pedicle but on secretion of its dorsal edge by an outer lobe of outer epithelium. The deposition of the chilidium must have been con-

trolled in the same manner by outer epithelium as were the entire margins of both valves, a condition comparable with that determining the growth of some inarticulated shells (acrotretides).

In early strophomenides, as well as billingelloids and kutorginides, which also possess pseudodeltidia and variably developed chilidia, the pseudodeltidium is not flush with the hinge line but concave to it; and, although the chilidium may protrude into this space, it is not entirely filled so that a well-defined posteromedian gap commonly persists. Previously it has been contended that the gap could have been closed internally by either a strip of periostracum secreted by a zone of fused mantle lobes, as in living articulated brachiopods, or a strip of inner epithelium homologous with the posterior body wall of inarticulated species (WILLIAMS & ROWELL, 1965b, p. 88). The first explanation, however, is unlikely for two reasons. First, the phylogeny of the strophomenides (*s.l.*) appears generally to preclude fusion of the mantle lobes along the cardinal margins; indeed, in some of the more aberrant groups, as the richthofenioids and the lytonioids, such a fusion would have been impossible. Second, there is good reason for believing that the anus opened into the postromedian gap of the *Nisusia* shell (ROWELL & CARUSO, 1985) and could only have perforated a posterior body wall (Fig. 319.4).

As to the nature of the pedicle itself, it was seldom strongly developed. In many leptaenids, for example, the foramen may be enlarged by resorption or completely plugged with secondary shell in adults from the same population. Indeed the pedicle atrophied at some time or other in most stocks during their evolution. It must, therefore, have been more akin, in its embryonic differentiation, to the attachment area of *Neocrania* than to the organ rudiments of living organophosphatic and articulated brachiopods. In particular, it was primarily differentiated as an adhesive pad, around which the larval ventral valve was secreted holoperi-

pherally as a funnel-shaped receptacle closed by a lidlike dorsal valve. This structural relationship was especially characteristic of the ventral valve of productidines and strophalosiidines, which frequently bore a cicatrix of attachment.

Despite the lack of information about the development of the delthyrial cover in triple-siidines, it is likely that it, too, was homologous with the strophomenide pseudodeltidium, for the presence of an inner calcareous pedicle tube can only be explained on this assumption. The evidence for a close affinity between the strophomenides and the clitambonitidines is equivocal. The so-called pseudodeltidium of the latter is frequently pierced by an apical rather than a supra-apical foramen and did not develop at all in some forms such as *Apatomella*.

Finally, the elongate, subtriangular apertures perforating the ventral valves of a few extinct obscure groups, as the dictyonellidines and chileoids, have no parallel among better-known stocks, extinct or living; and the nature of their organic cover is entirely conjectural. The apertural boundaries are not smooth (YOUNG, 1884), as they would have been had they been fashioned along a persistent epithelial junction. One can, therefore, assume that they are roughened as a result of resorption and postmortem fracture. The aperture is overlain by an internal plate (colleplax), from which it is separated by a narrow space. The external surface of the colleplax, that seen through the aperture, is relatively smooth, while its internal surface bears scars and evidently served as a platform for the attachment of the adductor muscles as it is flanked by flabellate diductor scars on the valve floor (COOPER, 1952).

This kind of aperture has been variously described, mainly as pedicle openings (COOPER & GRANT, 1974) or even for the intake and expulsion of seawater (POPOV & TIKHONOV, 1990). The most feasible interpretation, however, is that the aperture was covered by a tissue coated with adhesive polymers (WRIGHT, 1981). The structure would not have been a pedicle in the sense of

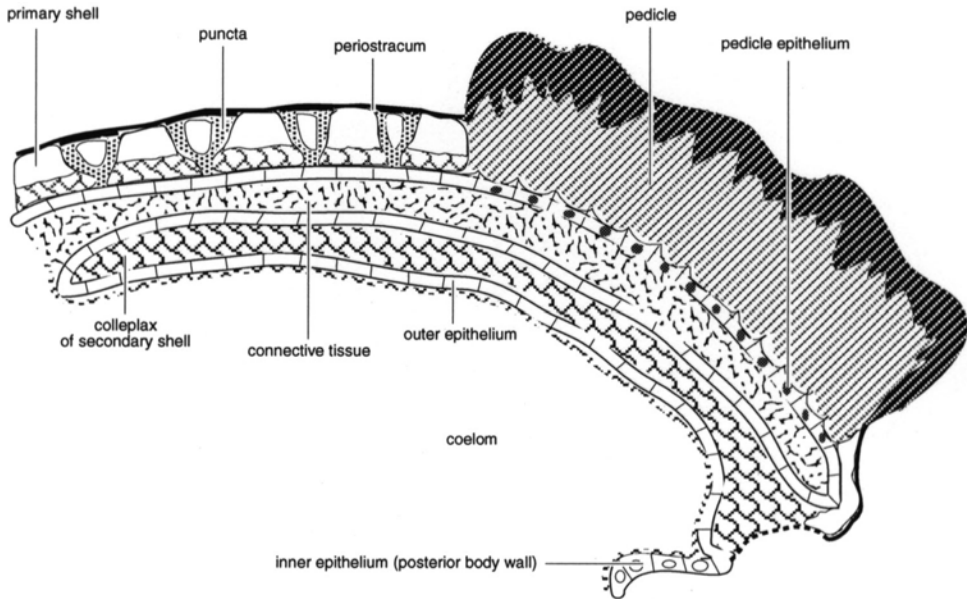


FIG. 321. Inferred relationship of the pedicle of the Silurian *Dictyonella* to the mantle lining the shell and investing the colleplax (adapted from Wright, 1981).

having afforded the animal an axis on which to rotate (Fig. 321). There are no markings that could reasonably represent the bases of adjustor muscles focused on the space between the aperture and the **colleplax**, while the narrowness of the space itself indicated that the adhering structure was essentially superficial. It must have been relatively large, however, and high enough to fill the aperture and to maintain distortion-free shells well above the substrate. In effect the structure could have been a cuticular pad, thick enough to persist some time after death and to have broken free of the shell by volumetric change.

ARTICULATION

The articulated brachiopods are preeminently characterized by a pair of hinge **teeth** in the ventral valve that fit into a pair of **dental sockets** in the dorsal valve (Fig. 322). In four-day-old specimens of *Terebratalia transversa*, STRICKER and REED (1985b) reported the initial appearance of teeth composed of finely granular calcite, with the differentiation of sockets evident in eleven-day-old specimens. After growth for

23 days each tooth had become transformed into a tight cluster of secondary layer fibers, similar in appearance, but much less numerous than in adults. The growth tracks of the teeth invariably define the margins of the delthyrium, so that they protrude from beneath the ventral cardinal area on either side of the delthyrium or its cover. Two distinct kinds of teeth have been described in articulated brachiopods (Fig. 322.1–322.2; JAANUSSON, 1971). They are either simple, knoblike **deltidodont teeth**, which grew solely by shell accretion, or they are hook-shaped **cyrtomatodont teeth** whose more elaborate curved form involved partial posterior resorption of earlier formed shell. Deltidodont teeth had their origin in the mid-Cambrian and are generally characteristic of extinct, strophic-hinged groups, but the latter occur in some spire-bearers and in fossil and living rhynchonellides, terebratulides, and thecideidines. JAANUSSON (1971) drew a clear taxonomic distinction between these two types of dentition. The cyrtomatodont style, which holds the two valves together while modifying its detailed morphology during growth, allows greater variability

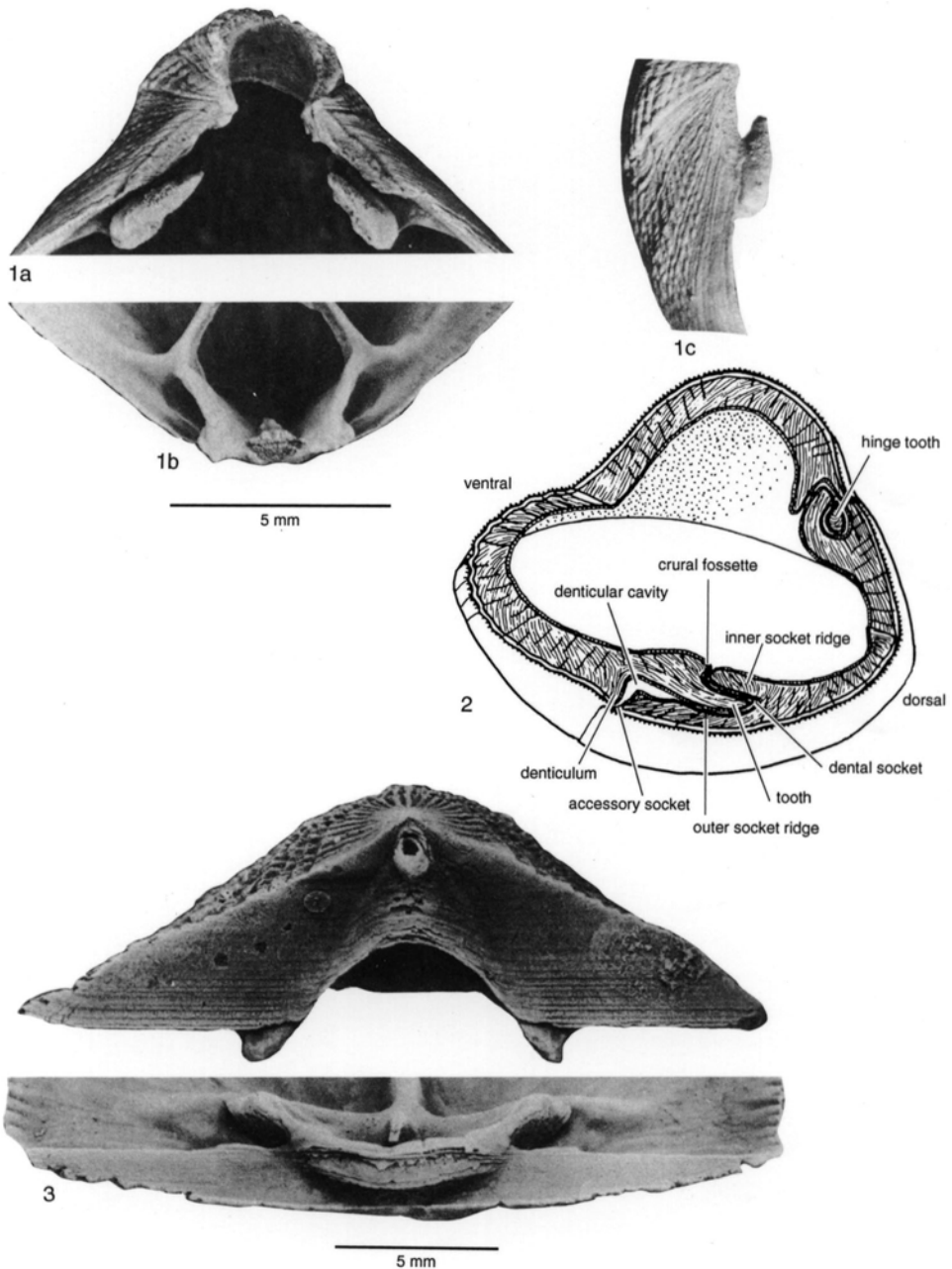


FIG. 322. 1–3. Articular features; 1a–c, cyrtomatodont *Terebratulina retusa* (LINNAEUS), recent, showing separated ventral and dorsal valves and a lateral view (Jaanusson, 1971); 2, *T. retusa* umbonal region seen in transverse and submedian sections (Williams & Rowell, 1965b); 3, deltidiodont *Clitambonites squamatus* (PAHLEN), Middle Ordovician, Estonia, showing separated ventral and dorsal valves (Jaanusson, 1971).

in hinge shape and function. A clear transformation, however, from deltidiodont to cyrtomatodont, possibly seen in the penta-

merides, is not evident in the view of CARLSON (1993b). Although she demonstrated (1989) that the ability of brachiopods

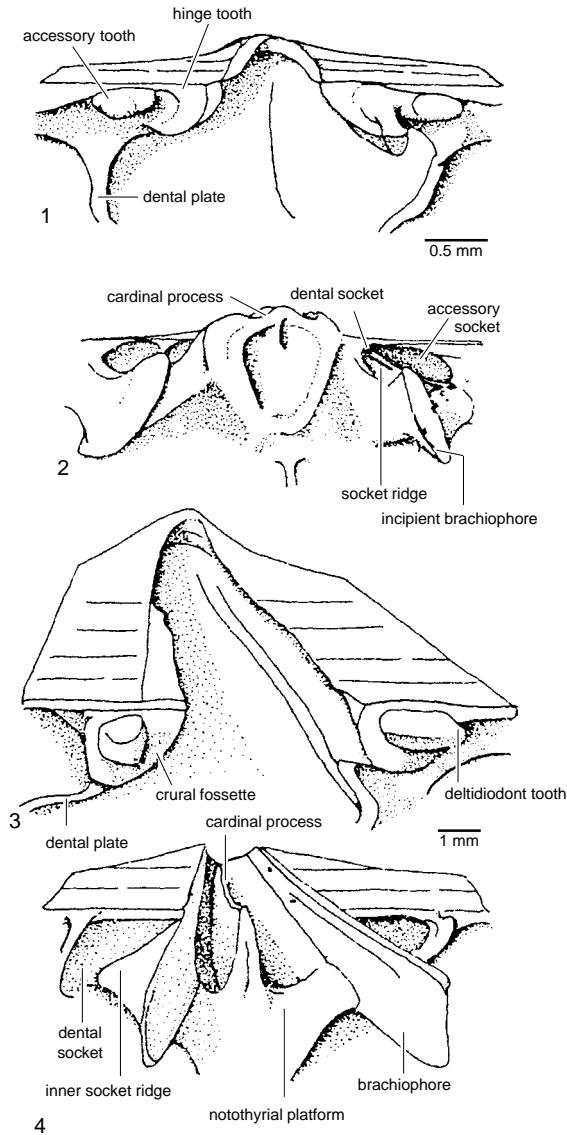


FIG. 323. 1–2, Articulating outgrowths of *Leptellina tennesseensis* ULRICH & COOPER and 3–4, *Hesperorthis australis* COOPER, Middle Ordovician, USA (adapted from Williams & Rowell, 1965b).

to resorb shell was not a prerequisite of cyrtomatodont articulation, it is undeniable that cyrtomatodont teeth are typical of the major groups in which shell resorption also plays important roles in the growth of spiral and loop-shaped brachia.

Teeth are varied in cross section and are commonly supported by a pair of variably disposed plates also built up exclusively of

secondary shell and known as **dental plates** (Fig. 323.1, 323.3). Dental plates in some spiriferides have been differentiated into two parts: **dental flanges**, which directly support the teeth, and ventral **adminicula** (BROWN, 1953) that connect these to the valve floor. Some authors follow BROWN (1953) in also recognizing dorsal adminicula, which connect crural bases to the dorsal valve floor, as

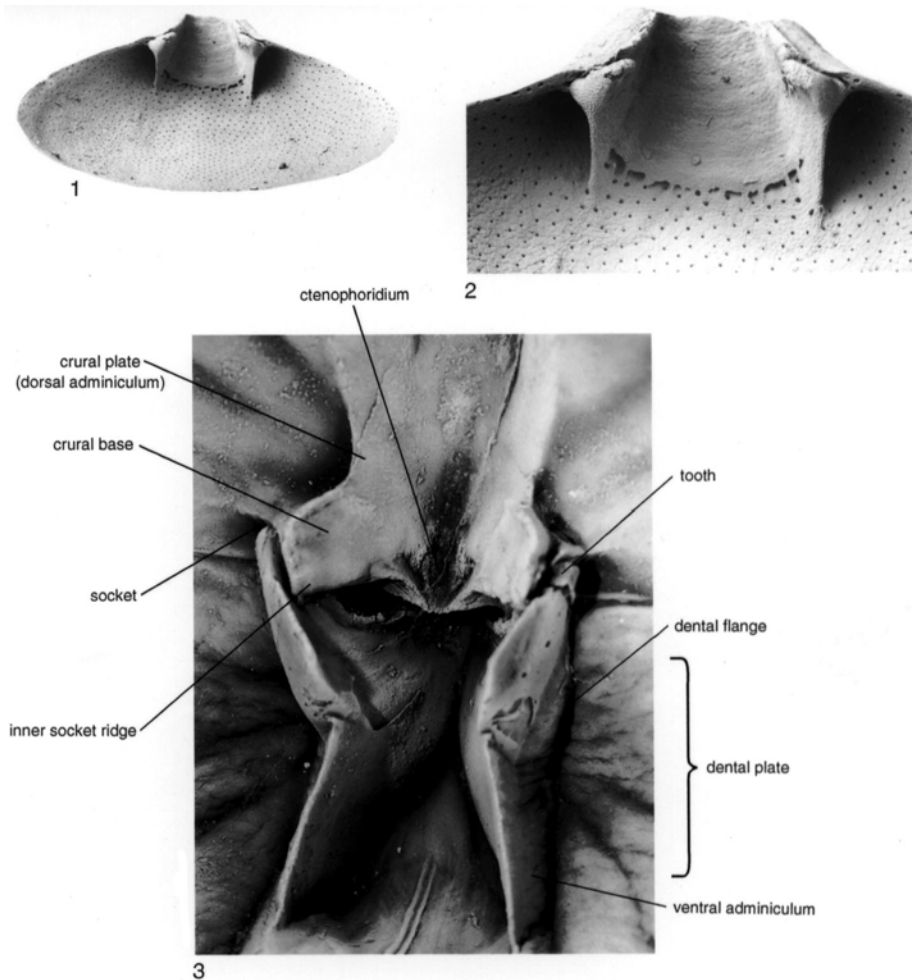


FIG. 324. Dental plates in *Fallax dalliniformis* ATKINS; 1, general view, SEM, $\times 12.5$; 2, detail of dental plates and pedicle collar, SEM, $\times 30$ (new); 3, latex replica of articulatory structures in *Tomiopsis*, Permian, Australia, showing the relationships between the supporting structures for teeth and crura, $\times 3$ (new).

do the better-known crural plates (Fig. 324). The dorsal surface of the tooth may be blunt or sharp, smooth or crenulated, and further complicated by minor grooves and apophyses, which fit snugly with complementary features associated with the socket. The **crural fossette** is perhaps the most common of these minor modifications (Fig. 323.3). It consists of a groove located on the inner (anteromedian) side of the tooth and accommodates the ventral surface of the inner socket ridge. A more unusual arrangement, which is especially characteristic of the

plectambonitoids, involves the growth of a pair of **accessory teeth** lateral to the teeth bordering the delthyrium and separated by a pair of deep grooves (Fig. 323.1; ÖPIK, 1930). Two pairs of sockets are found in the ventral valve, one on either side of the socket ridges, the posterior surfaces of which fit into the grooves between the teeth.

It is inevitable that, since the tooth and socket are fashioned from secondary shell, the former is commonly separated from the valve margin by a groove that receives the variably thickened or undercut dorsal margin

forming the posterior edge of the socket. A number of conflicting terms have been used to describe this relationship, but the following selections seem to be the most appropriate, although they do not necessarily have historical precedence. Thus **denticulum** (MUIR-WOOD, 1934) may be used for the posterior edge of the ventral valve margin (e.g., *Digonella*) or of the **symphytium** (e.g., *Laqueus*). For the prominence of secondary shell along the posterior edge of the socket, the term outer socket ridge affords the best description, while the grooves accommodating the denticulum and outer socket ridge are best referred to as **accessory socket** and **denticular cavity** (Fig. 322.2).

The teeth may be supplemented or, rarely, replaced by a series of smaller protuberances extending lateral to the teeth and in a complementary arrangement along the posterior margin of both valves. In spiriferides, such **denticles** are small crenulations of primary and adjacent secondary shell underlying the interareas (Fig. 325.4–325.5), as are the denticles found in many plectambonitoids except that each of them appears to have been built up around a taleola (Fig. 325.3). The strophodontoid denticulation, in contrast, arises only after the fusion of widely divergent, platelike teeth and dental plates, following the posterior migration of the latter, although in this group too, the denticles contain taleolae (Fig. 325.1–325.2; WILLIAMS, 1953). The denticulation of the chonetoid *Eodevonaria* and the strophalosioid *Ctenalosisia* appears to be most closely related in development to that of the strophodontoids (MUIR-WOOD & COOPER, 1960).

Although all Early to Late Devonian productides have teeth and sockets, the productidines lost them entirely after the late Famennian. Articulation for most productidines relied upon the large, posteriorly projecting cardinal process extending into the confined ventral umbonal cavity. Not only did the cardinal process provide the simple lever system and muscle attachment necessary to open the shell, but also the location pin preventing lateral or rotational move-

ment between the valves. Location and articulation of the valves was further aided by ridges close to the hinge lines fitting against slight depressions on the opposite valve (Fig. 326.1) and by the close fit of most dorsal valves within the more strongly convex ventral valve. By contrast, the articulation of many richthofeniids was by knobs (or **tegula**) at the positions of the ears on a narrow dorsal hinge fitting into weak pits in the ventral valve (Fig. 326.2).

Systems of articulation using thickened surfaces at the posterior margins are seen in such Lower Cambrian brachiopods as *Nisusia*, in which a thickened edge of the pseudodeltidium fits against shallow grooves in the dorsal valve, which can be identified as sockets and inner socket ridges; but no true teeth are present.

Early Cambrian calcareous-shelled brachiopods usually have strophic shells with a variety of articulatory structures (POPOV, 1992); only chileides and some of the earliest Cambrian obolellides lack any form of articulation. The posterior margin of such early obolellides as *Obolella* and *Magnicanalis* is similar to that of chileides, with a ventral interarea and narrow delthyrium, but with a narrower and low dorsal pseudo-interarea. In other Early Cambrian obolellides such as *Bicea*, *Alisina*, *Siberia*, or *Trematobolus* (Fig. 327.3), however, there are small teeth on the lateral sides of the delthyrium and shallow sockets on the posterolateral sides of the low notothyrial platform. In *Bicia* the teeth are composed partly of primary shell (USHATINSKAYA, 1988), but in other obolellide genera they are composed entirely of secondary shell, lack supporting structures, and have no inner socket ridges. In the obolellide suborder Naukatidina the teeth are situated on an **anteris** (Fig. 327.4), forming an arcuate thickening of secondary shell anterior to the delthyrium.

A different pattern of articulation is known in the Kutorginida, including nisusiids, all of which have strophic shells and well-defined interareas on both valves. In the Lower Cambrian *Kutorgina* there are deep

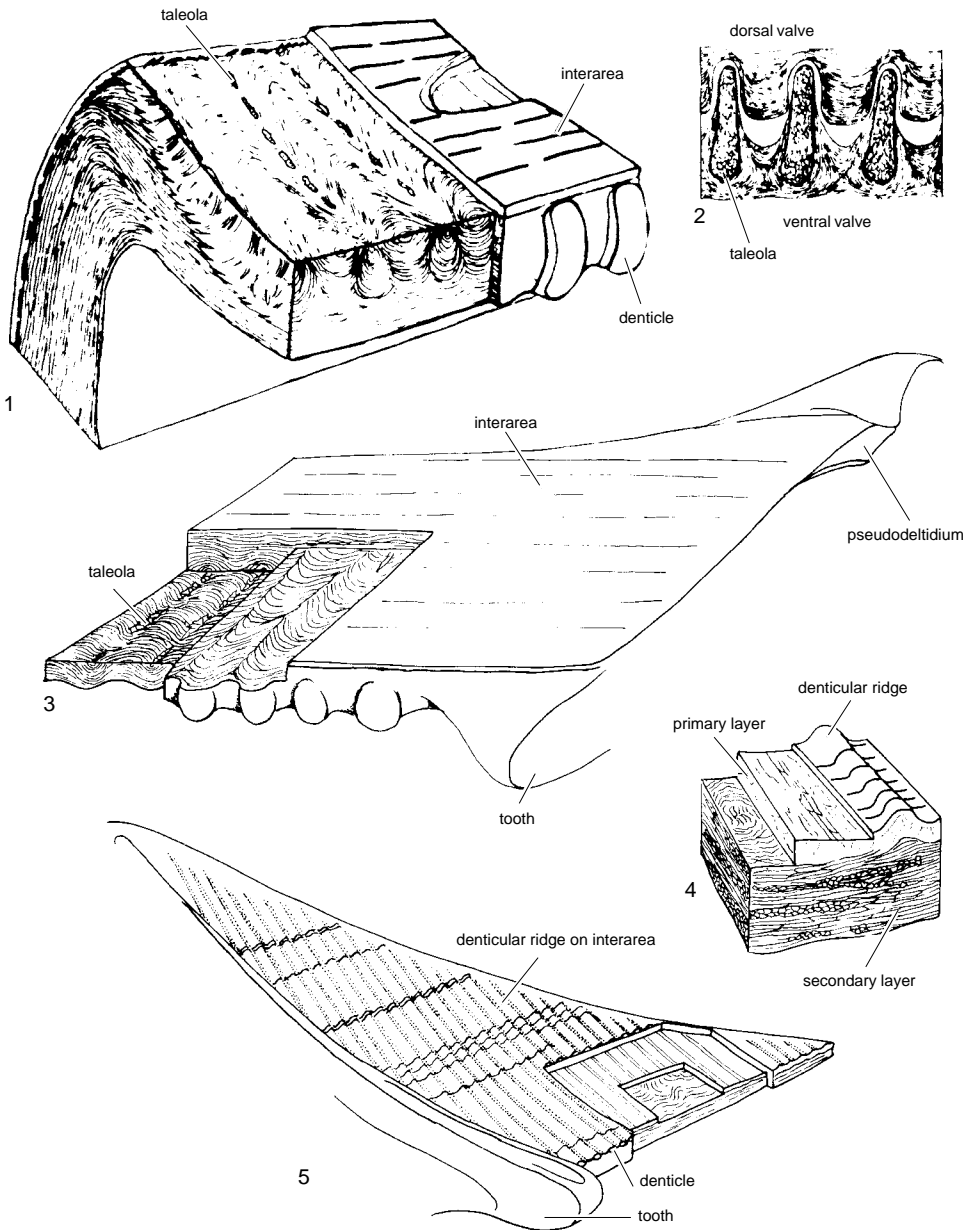


FIG. 325. Stylized denticular structures in 1, *Pholidostrophia* sp., Middle Devonian, USA; 2, *Plectodonta transversalis* WAHLENBERG, Middle Silurian, England (adapted from Williams, 1953); 3, a plectambonitacean; and 4–5, a spiriferid (adapted from Williams & Rowell, 1965b).

furrows lateral to a broad pseudodeltidium and triangular dorsal propleareas that fit into the furrows (Fig. 327.1; POPOV & TIKHONOV, 1990). This pattern of articulation is

modified in nisusiids, as in *Nisusia* and *Narynella*, in which furrows and ridges are present along the inner sides of the ventral propleareas, lateral to the pseudodeltidium,

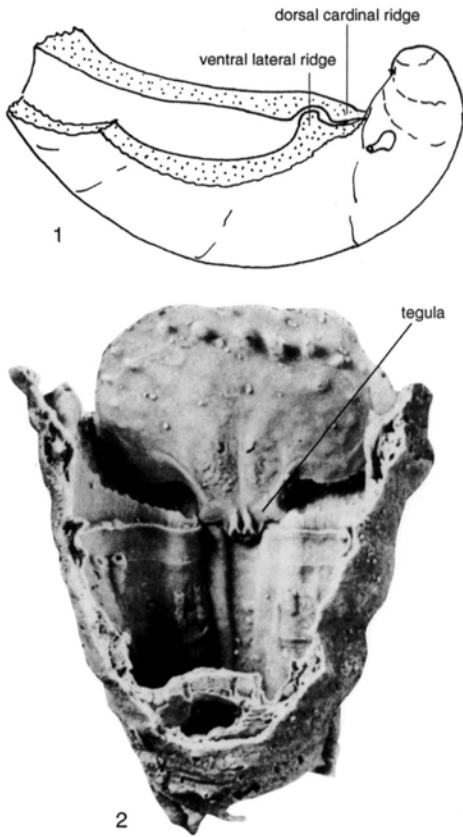


FIG. 326. 1, Articulating hinge ridges in oblique lateral view of a submedian section of *Argentiproductus margaritaceus* (PHILLIPS), Lower Carboniferous, northern Wales (new); 2, *Cyclacantharia kingorum* COOPER & GRANT, in the open position showing the articulating tegula on the dorsal valve hinge line fitting depressions at the hinge line of the ventral corpus, Upper Permian, Texas, $\times 2$ (adapted from Cooper & Grant, 1975).

which articulate with sockets, bounded by inner socket ridges originating on the inner sides of the dorsal propleas (Fig. 327.2). These paired sockets and ridges are functionally comparable with those of orthides but are probably not homologous and differ in being formed of primary plus secondary shell (ROWELL & CARUSO, 1985).

A similar type of articulation developed independently in the craniformean trimerellides (NORFORD & STEELE, 1969; GORJANSKY & POPOV, 1985, 1986). Most trimerellide genera, such as *Dinobolus*, *Eodinobolus*,

Monomerella, and *Trimerella*, have cardinalia with a median hinge plate that fits into the cardinal socket of the ventral valve (Fig. 328). The axis of rotation is along the outer sides of the ventral propleas. The concave **homeodeltidium** of trimerellides did not originate only as a cover to the pedicle opening but also as a means of restricting lateral movement of the dorsal valve.

A simple articulatory structure occurs in some lingulites. For example, in the Late Cambrian acrotretid genus *Linnarssonella* the dorsal pseudointerarea has distinctive grooves that may have functioned as simple sockets fitting with ridges on the ventral pseudointerarea and may have restricted relative movement and sliding of the valves. There are similar structures on the dorsal propleas of some acrotretides within the Torynelasmatinae, and a similar feature is present in the obolid *Dicellomus*. All these articulatory structures in lingulites and acrotretides, however, are only analogous to true sockets because they developed on the shell surface and not as modifications of the inner shell layers.

The ridges defining the sockets in the dorsal valve of toothed articulated brachiopods are part of structural modifications of varying complexity found in the dorsal umbo and collectively referred to as the **cardinalia**. The several pieces comprising the cardinalia are composed of secondary shell and provide vital structures, even from the earliest growth stages. Apart from defining the sockets (allowing articulation between the valves), the cardinalia afford attachment areas for musculature and even include the bases of processes giving support to the lophophore. This diversity of function has naturally given rise to a wide variety of features (Fig. 329–330), and since combinations of them tend to be characteristic of major taxa, complicated terminologies, frequently incompatible with one another, have grown up for each taxon. In living brachiopods the importance of articulation is clearly expressed by the presence of well-differentiated teeth and sockets, even

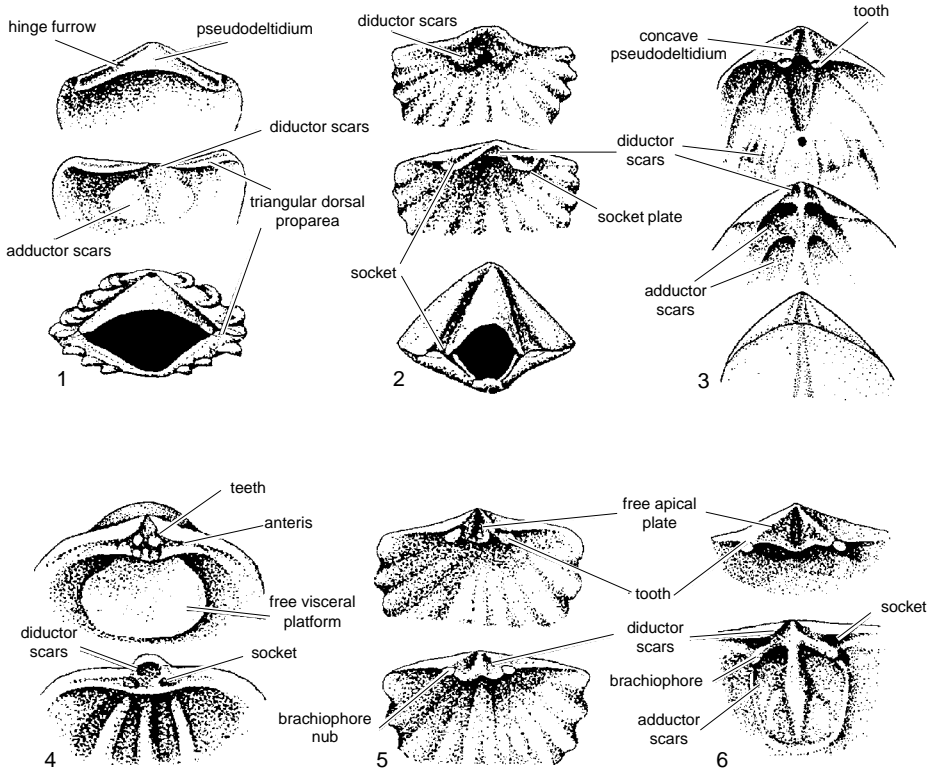


FIG. 327. Articulation of various groups of brachiopods lacking a well-developed tooth-and-socket hinge mechanism; 1, *Kutorgina*; 2, *Nisusia*; 3, *Trematobolus*; 4, *Oina*; 5, *Glyptoria*; 6, *Arctohedra* (adapted from Popov, 1992).

in the smallest of shells (STRICKER & REED, 1985b). When shells are still only a few millimeters long, crura start to grow from the prominent, inner socket ridges and soon support the body wall in the mouth region of the lophophore. Thus in the ontogeny of living specimens as well as in the evolution of articulated brachiopods, the lophophore-supported structures had origins intimately associated with the inner socket ridges.

Another generality in the emended terminology is that a structure connecting some part of the cardinalia to the valve floor, with cavities remaining between it and the valve wall, is called a plate, while a shell thickening, representing the growth trace of a structures, is called a base (as in crural bases). In view of the above the terminology of the cardinalia has been rationalized as compared

to that of the 1965 edition (Fig. 331). Previously used, but discarded, terms are listed as synonyms in the glossary of morphological terms (p. 423–440).

An important element in the dorsal valve cardinalia is a medially situated structure (**cardinal process**), which is developed as the attachment area for the dorsal ends of the diductor muscles. This feature is more conveniently dealt with when considering the shell modifications resulting from the insertion of muscles concerned with relative movements of valves (see section on musculature, p. 385).

True deltidiodont teeth fitting well-developed sockets with inner ridges first appeared in the mid-Cambrian orthides and pentamerides (POPOV, 1992). In mid-Cambrian and later orthides (Fig. 329.1),

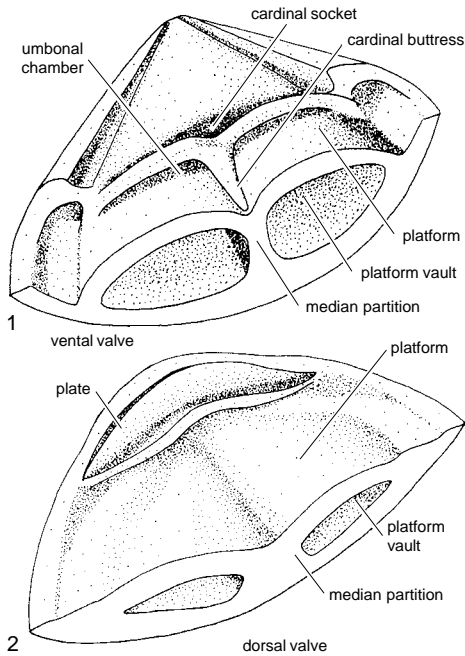


FIG. 328. Morphology of posterior region of 1, ventral valve and 2, dorsal valve of *Dinobolus* (Williams & Rowell, 1965b).

a pair of widely divergent ridges act as inner walls to sockets that are excavated within the secondary shell, uniting the ridges with the edge of the dorsal interarea. Medially, the proximal ends of these socket ridges may be encased by lateral extensions of a low-lying deposit of secondary shell that forms the floor of the notothyrium (**notothyrial platform**). These socket ridges have been called **brachiophores** in the belief that prolongations of their distal (anteroventral) edges gave support to the lophophore. Such processes, however, are unknown in early protorthoids, in which the plates do not extend beyond the lateral edges of the sockets, and are only rarely developed incipiently among the strophomenoids and clitambonitoids; and even in later orthoids it is questionable whether they extend sufficiently anteroventrally to reach the inferred position of the anterior body wall. In all, it seems preferable to use the term **inner socket ridge** for widely divergent structures of limited

extension like those of the billingselloids, strophomenoids, as well as in all other groups (Fig. 329.2; WILLIAMS, 1953). Certainly an exclusive function of articulation may be inferred for the socket ridges of strophodontids although they became vestigial or even disappeared subsequent to the loss of teeth in members of that family (WILLIAMS, 1953).

The orthoid arrangement represents a significant advance in that the shell outgrowths (commonly in the past called brachiophores) associated with the ventromedian limits of the socket ridges were rotated to point anterolaterally and were also prolonged as blade-shaped or rodlike processes beyond the limits of the sockets (SCHUCHERT & COOPER, 1932). Thus disposed, they probably performed the function of the crura in more recent groups. However, in view of the functional uncertainty of these structures in stratigraphically older taxa, the term brachiophore remains appropriate in those species. Disposed as previously described, the brachiophores are free of the posterior margin and in many orthoids (e.g., *Hesperorthis*) are supported by a well-developed notothyrial platform (Fig. 329.4). The sockets are grooves in a thick, secondary shell deposit between the socket ridges and the posterior margin; but in other orthoids the development of a pair of lateral umbonal cavities within the shell thickening underlying the sockets may lead to the differentiation ventrally and medially of **fulcral** and **socket plates** respectively (Fig. 332). The forward growth of brachiophores (or **crural bases**) and their anterior processes, as in most enteletoids and many orthoids, was accompanied by the forward growth of support plates reaching the floor of the dorsal valve. These plates, which can include those called socket plates, may be disposed at varying angles to the median plane of symmetry and have been called supporting plates only when they converge toward the dorsal median ridge. It seems best, however, to refer to them as **brachiophore plates**, irrespective of

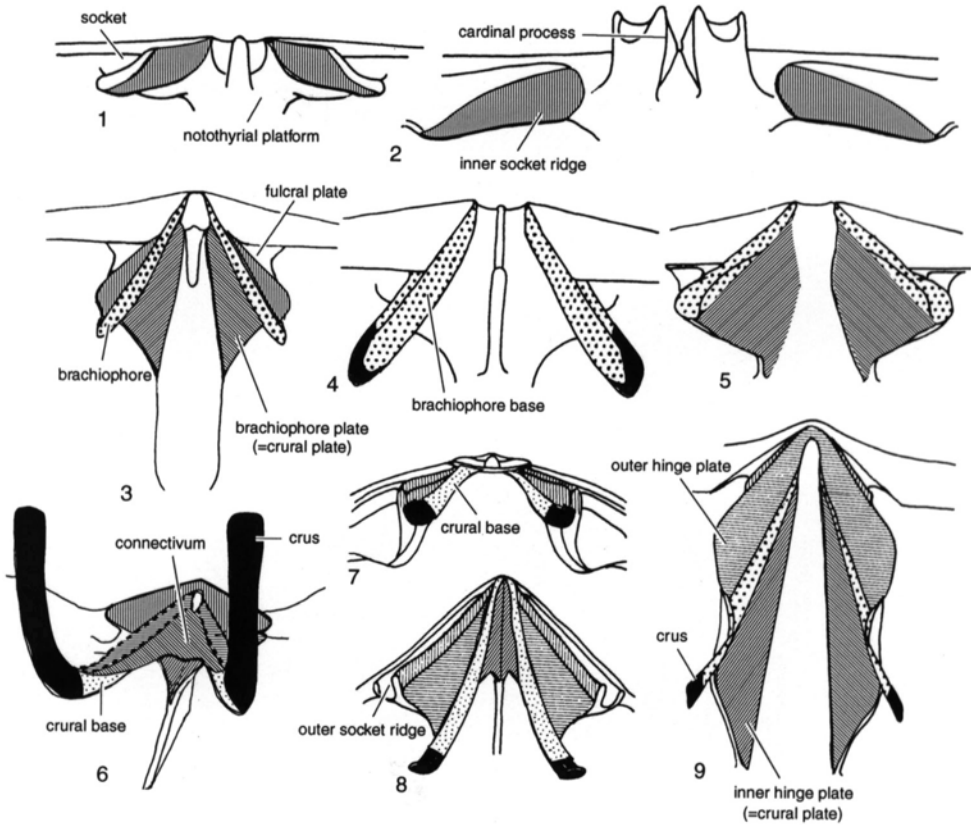


FIG. 329. Cardinalia of 1, *Billingsella*; 2, *Strophomena*; 3, *Dalmanella*; 4, *Hesperorthis*; 5, *Imbricatia* (adapted from Williams & Rowell, 1965b); 6, a Devonian rhynchonellid (adapted from Johnson & Westbroek, 1971); 7, *Notosaria*; 8, a camarotoechiid; and 9, *Gypidula*, all ventral views; *vertical lines*, inner socket ridge; *horizontal lines*, outer hinge plate; *diagonal lines*, inner hinge plate, brachiophore plate, or crural plate; *dots*, brachiophore or crural base; *solid black*, crus (adapted from Williams & Rowell, 1965b).

inclination (WILLIAMS & WRIGHT, 1963) and to think of them as homologues of crural plates in more recent taxa.

It is significant that the ventral adjustor scars are first indisputably identified in the orthoids and enteletoids, and judging from anatomical reconstruction, the only sites for the attachment of the dorsal adjustor muscles were the inner faces of their well-developed brachiophores (WILLIAMS & WRIGHT, 1963). This is exactly the situation seen in living species, where pedicle adjustor muscle scars are distinguished before diductor muscle scars. Initially, dorsal adjustor muscles are situated between the inner

socket ridges, but commonly they spread during ontogeny onto variously disposed hinge plates as these grew.

The cardinalia of early porambonitoids consist essentially of socket ridges and brachiophores (ULRICH & COOPER, 1938) with plates variably convergent onto the floor of the valve (Fig. 329.5). The protruding brachiophores (called brachiophore processes in some literature) may be negligible in the older stocks but were very well developed in such younger forms as *Camerella*, where they deserve the name crura. Furthermore, a raised ridge is commonly found standing above the posterior edge of the

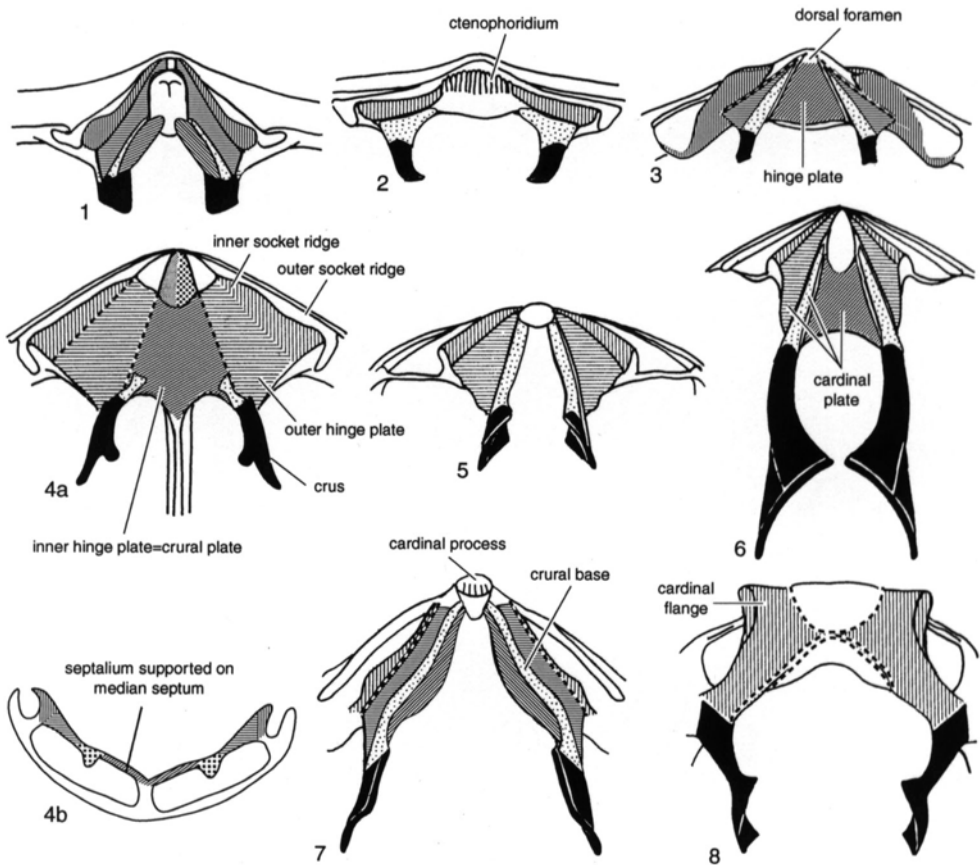


FIG. 330. Cardinalia of 1, *Crenspirifer*; 2, *Neospirifer*; 3, young *Cleiothyridina*; 4a, b, *Laqueus*; 5, *Dallithyris*; 6, *Nanothyris*; 7, *Terebratula*; and 8, *Terebratulina*; all ventral views except 4b (new), which is a transverse section showing the septalium; vertical lines, inner socket ridge; horizontal lines, outer hinge plate; diagonal lines, inner hinge plate, brachiophore plate, or crural plate; dots, brachiophore or crural base; solid black, crus (adapted from Williams & Rowell, 1965b).

brachiophore (or crural base) but intervening between it and the concave socket floor or fulcral plate. Theoretically at least, this ridge could have arisen either as an upgrowth along the contact between the fulcral plate and the brachiophore (or crural base) or within the fulcral plate as an inner restriction to a small posterolateral socket. These arrangements, however, are reminiscent of the patterns characteristic of many spiriferoids and rhynchonelloids, respectively. In both conditions, the raised ridge is at least analogous with the rhynchonelloid inner socket ridge, and that part of the socket, which now intervenes between the inner socket ridge

and the brachiophore, is homologous with the outer hinge plate, thus justifying the term crural base for the brachiophore (Fig. 329.6–329.7). One other modification is noteworthy. In camerellids, for example, the brachiophore plates converge toward the floor of the valves, either uniting with or fusing to form a median septum. This structure has been referred to as a cruralium, but since it did not contain the dorsal ends of the adductor muscles, it is more correctly termed a **septalium** (Fig. 330).

The use of an entirely different terminology for the pentameroid cardinalia is not a reflection of any radical departure from the

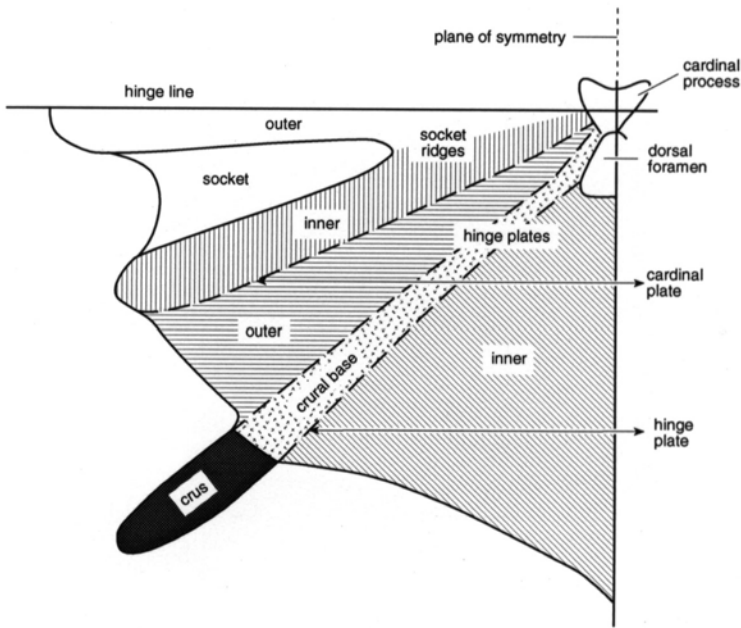


FIG. 331. Schematic view showing relationships of structures within the cardinalia of articulated brachiopods (new).

morphology of ancestral groups but of historical precedent. In general, the cardinalia are only better developed, or, as with the homologues of the brachiophore plates, are only differently disposed. Nonetheless the extended crus of the pentameroids has been known as the brachial process, the brachiophore plate or crural plate as the outer plate, and the outer hinge plate (with or without modification like the inner socket ridge) as the inner plate (Fig. 329.9; ST. JOSEPH, 1938). Such terminology is so divorced from that employed for other groups that it should be discarded in favor of the more unified terminology presented here and seen, for example, in the rhynchonelloid cardinalia.

In the remaining groups of articulated brachiopods some sort of calcareous support to the lophophore was almost invariably developed, so that greatly prolonged homologues of the brachiophores and their processes of the early Paleozoic brachiopods are the **crura**, which form important elements of the cardinalia. The crura, which are commonly strongly curved, divergent apophyses extending anteroventrally, are known in liv-

ing brachiopods to pass forward on either side of the esophagus to make contact with the anterior body wall and posterior part of the lophophore on either side of the mouth; and it is highly probable that all processes so named in fossil rhynchonellides, in terebratulides, and in many spire-bearing brachiopods performed a similar function. Only rarely, as in *Enteletes* and *Skenidioides*, were brachiophores known to be sufficiently prolonged and suitably disposed to give support to the lophophore (WILLIAMS, 1956). The crura, therefore, represent an important advance in brachiopod organization and are associated with other features of the cardinalia that are distinctive enough to warrant an elaboration of the terminology used for the more primitive groups. The rhynchonellide crura were commonly supported by a pair of plates (**crural plates**) that converged to form a septalium (Fig. 329.6–329.7). In some Paleozoic rhynchonelloids another pair of plates grew from the median sides of the crural bases to fully or partially cover the septalium ventrally. These have been called inner hinge plates or the **connectivum**

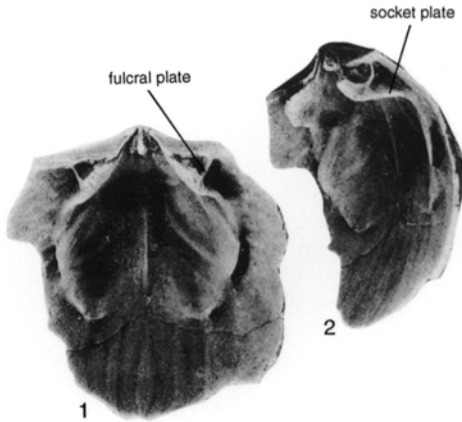


FIG. 332. Dorsal valve interior views of *Schizophoria iowensis* (HALL), Upper Devonian, Iowa, USA, showing socket structures, $\times 2$ (Schuchert & Cooper, 1932).

(HAVLIČEK, 1961), but the former have well-defined different positions in Mesozoic and recent terebratulides, so it is recommended that the description cover plates or term connectivum be used (Fig. 329.6).

The cardinalia of Paleozoic terebratulides (CLOUD, 1942) are very much like those of the rhynchonellides, although the crural plates defining the septalium may be sub-parallel, as in *Nanothyris* (Fig. 330.6), or convergent, as in *Globithyris*. The **inner hinge plates** are normally well developed and, together with the posterior faces of the crura and the **outer hinge plates**, constitute the **cardinal plate** (Fig. 330.6). The simplest arrangement found in post-Paleozoic terebratulides is that found in *Terebratulina* (Fig. 330.8), which consists of crura arising directly from high inner socket ridges. In other terebratulides like *Dallithyris*, outer hinge plates are differentiated (Fig. 330.5); and in a minority like *Terebratula*, a pair of discrete inner hinge plates were also developed (Fig. 330.7). The cardinalia of *Laqueus*, in contrast, include a pair of plates arising inside the crural bases and converging on to the dorsal median septum, forming a septalium. In the past, these have been called inner hinge plates, crural plates, or septalial plates. However, new studies of the early ontogenetic development of the cardinalia in very

young *Laqueus* clearly indicate that the inner plates appear initially prior to the crura in association with the dorsal pedicle adjustor musculature and thus are more appropriately referred to as inner hinge plates.

The cardinalia of many spire-bearing brachiopods, especially the spiriferide and atrypide stocks, are reminiscent of *Terebratulina* in that the crura arose directly from well-developed inner socket ridges (e.g., *Neospirifer*, Fig. 330.2). Less commonly, thin strips representing outer hinge plates (e.g., *Plectatrypa*), crural bases, and inner hinge plates (e.g., *Crenispirifer*, Fig. 330.1) were developed. Among *Athyris* and its allies (like *Cleiothyridina*), the inner hinge plates are commonly fused to form a median horizontal **hinge plate**, subtended between the inner sides of the crural bases or a **cardinal plate** between prominent inner socket ridges (Fig. 330.3). In earlier athyridides these undifferentiated hinge or cardinal plates are commonly penetrated posteromedially by a canal, the **dorsal foramen**, connecting the dorsal umbonal cavity to the ventral surface of the plate (see Fig. 359.1). In more recent examples this foramen is absent, and the cardinal plate is bounded posteromedially by ridges that, in some genera, aided articulation by curving posteroventrally into the ventral umbo. In still younger athyridides these ridges, called **cardinal flanges**, became serrated by diductor myophores, simulating, in some genera, a true cardinal process (see section on musculature, p. 396).

BRACHIDIA

The cardinalia of many articulated brachiopods are also connected with spirally coiled ribbons (**spiralia**) or calcareous **loops** (Fig. 333–334). The spiralia and loops are greatly variable in form and attitude and, indeed, may have arisen in different ways. Nonetheless, two aspects of their growth and disposition seem to have been common to all. First, they represent outgrowths from the crura, extending well into the mantle cavity and, like the crura, were contained in sheaths of outer epithelium responsible for their

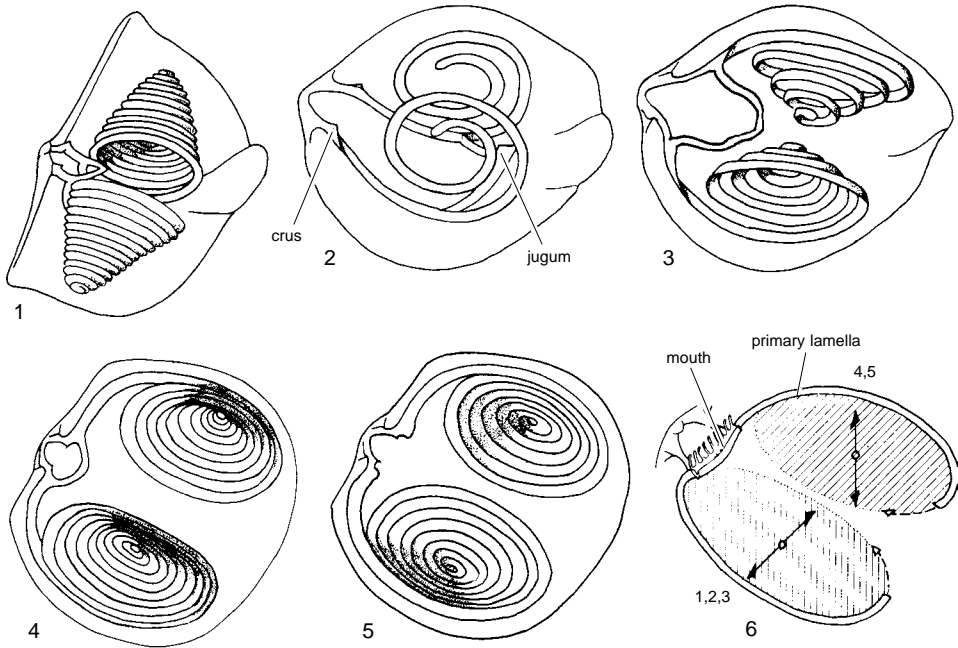


FIG. 333. Stylized representation of various attitudes adopted by primary lamellae of the spiralia relative to planes parallel with the plane of symmetry, as in 1, a spiriferid, 2, *Protozyga*, 3, a zygospirid; or parallel with the commissural plane (with apices of spiralia directed ventrally) as in 4, a koninckinid, or 5, an atrypid (with apices dorsally directed); 6, general diagram of the crus and primary lamellae showing the orientations of the previous representations (adapted from Williams & Rowell, 1965b).

growth and enlargement by controlled processes of secretion and resorption (WILLIAMS, 1956, 1968a; MACKINNON, 1991; MACKAY & others, 1994). Second, although the loops grew independently of the lophophores, in living terebratulides they are intimately associated with that organ, and the disposition of both loops and spires in extinct stocks suggests that they performed a similar function of support.

As far as is known from the development of spiralia in a few species (BEECHER & CLARKE, 1889), the first structure was an elongately oval loop formed by the anteromedian fusion of a pair of curved prongs extending from the crura. Thereafter, through a process of differential secretion and resorption, the anterior part of the loop became truncated to form a band (**jugum**) with a pair of short projections at the anterolateral corners (Fig. 335). These prolongations represent the beginnings of the first

pair of coils (**primary lamellae**) of the spiralia.

Succeeding coils of the spiralia may be oriented to take up almost any attitude within the mantle cavity, but all of them are variations of five basic dispositions (Fig. 333). In most Atrypida, which include the geologically oldest spire bearers, the apices of spiralia were directed medially or dorso-medially but occasionally were planispiral parallel to the median plane. In most Spiriferida and Athyridida, the apices of the spiralia were laterally directed, but in Suessioidea and Koninckinoidea they were ventrally directed. Although laterally directed spiralia predominate in both the Spiriferida and Athyridida, the angular relationships between the crura and primary lamellae are markedly different in the two orders. In spiriferides, as well as in early atrypides such as *Protozyga*, the primary lamellae grew as direct extensions of the

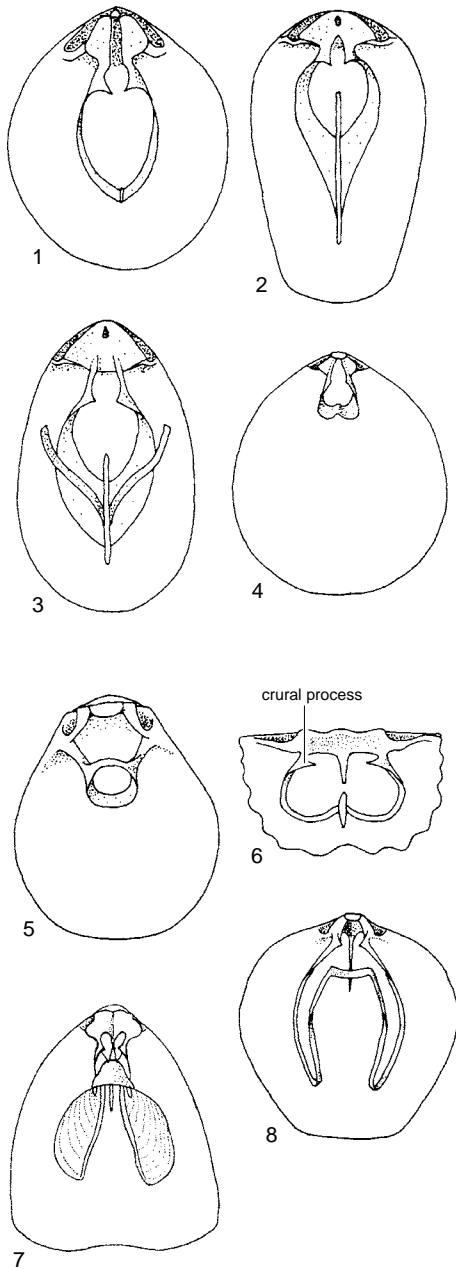


FIG. 334. Some loop forms in the Terebratulida; 1, *Centronella*; 2, *Rensselaeria* (Cloud, 1942); 3, *Gefonia* (Stehli, 1956); 4, *Gryphus*; 5, *Terebratulina* (Williams & Rowell, 1965b); 6, *Argyrotheca*; 7, *Campages* (adapted from Thomson, 1927); 8, *Magellania* (Williams & Rowell, 1965b).

anteriorly directed crura (Fig. 333.2); in athyridides the initial growth direction of primary lamellae was posterior (Fig. 336), in precisely the opposite direction from that of the crura.

The jugum is unknown in a number of spire-bearing brachiopods. In many poorly investigated stocks the absence could well be ascribed to the breakage of such a delicate structure during burial of the shell. In others, its absence may have been due to resorption, which is known partially to have affected the juga of some adult Spiriferida and Atrypida. In a few stocks, like *Cyclospira*, however, no jugum has been found in well-preserved adult shells, suggesting that the spiralia developed directly from the crura and not by modification of a loop (COPPER, 1965, 1986). Furthermore, COPPER (1986) has argued that in the earliest atrypides of Late Ordovician age, the spiralia evolved without the development of a jugum and that this structure is only found in some later stocks. By the Silurian, the **jugal processes** in many atrypoids became divided. The relationship of the spiralia to the crura in atrypides may also differ from other spire bearers. COPPER (1986) suggested, for atrypides, that the lack of continuous skeletal connection between crura and spiralia allowed the spiralia some freedom of movement within the mantle cavity. COPPER's contention (1965) that generation of the spiralia may have occurred at this proximal position of the crura has been contested by MACKINNON (1991), who advocated expansion of the spiralia by generative zones at the leading edges of each spirulum. In Athyridida, by contrast, development and elaboration of the jugum was widespread. Here the jugum consists of a pair of **lateral jugal branches** that arose near the middle of the dorsal limb of the primary lamella and extend ventromedially or anteromedially, until they unite in a V- or U-shaped jugal arch (ALVAREZ, 1990). Commonly the leading edge of the jugal arch is extended anteriorly as a prominent, anteriorly spinose jugal saddle, while the posterior

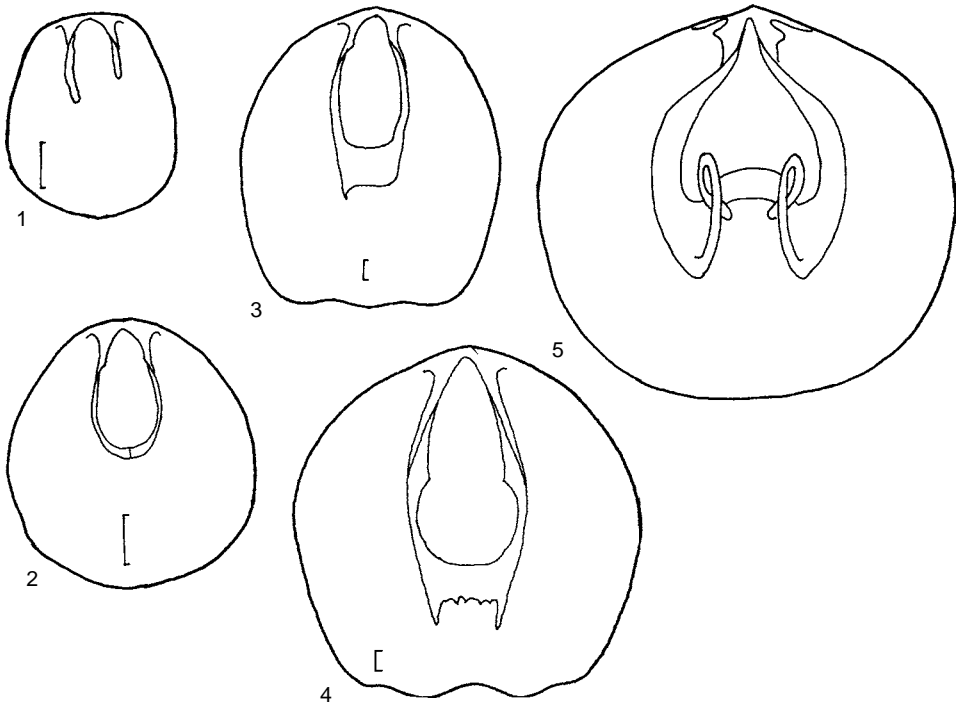


FIG. 335. Growth of the brachidial apparatus of *Protozygia*; 1–4, *P. elongata* COOPER; scale bars: 0.1 mm (adapted from Williams & Wright, 1961); 5, *P. exigua* (HALL) with adult loop (adapted from Copper, 1986).

edge of the jugal arch tapers and bends sharply to become a thin, posteromedially directed process, the **jugal stem**. In a number of stocks bifurcation of the jugal stem gave rise to a pair of arcs (**arms of the jugum**) lateral to the primary lamellae. In some Meristellidae, strongly arcuate jugal bifurcations became reunited with either the jugum or jugal stem to form a pair of jugal loops. In *Athyris* and related genera, the arms of the jugum were further extended as narrow curved blades (**accessory lamellae**) running adjacent to the primary lamellae for about half a coil (Fig. 336). In certain other, unrelated genera (e.g., *Kayseria*, *Diplospirella*, and *Koninckina*) the accessory lamellae continued to grow into a pair of spires coextensive with the entire primary spirillum.

The relationship of the inferred lophophore to the calcareous spirillum and its functional morphology have been the subject

of debate. The simple spirolophe coincident with the spiralia, as advocated by RUDWICK (1960), may not be true for all genera. If the paired generative zones of the early schizolophe were retained medially on the jugum, which must have been their original position, the growth of the primary lamellae would have been accompanied by an antero-lateral lobation of the lophophore to fit around the peripheries of the calcareous ribbons (WILLIAMS, 1956). In these circumstances the double lophophore (**deuterolophe**) borne by the spiralia would have been homologous with the side arm of *Terebratulina* (Fig. 337.4; WILLIAMS & WRIGHT, 1961). In the athyridides ALVAREZ and BRUNTON (1990) suggested that the migration of the generative zones from the jugum posterolaterally formed the accessory lamellae while, anteriorly, the deuterolophe continued to grow on the apical sides of the

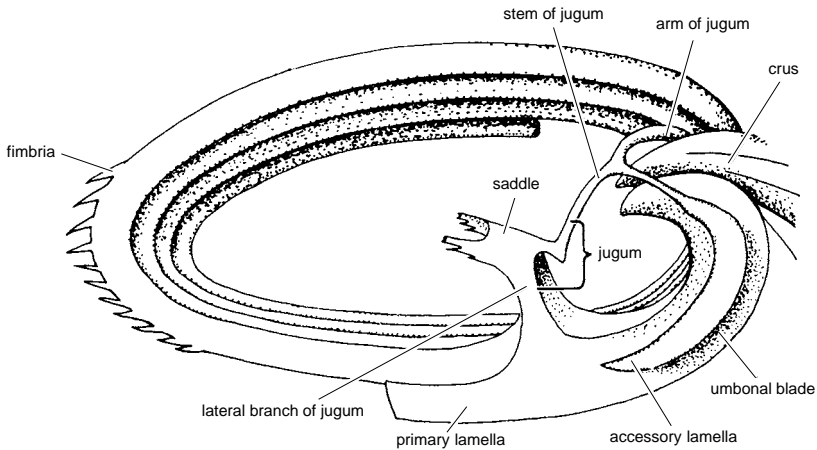


FIG. 336. Structure of spirialium in an athyridid (Hall & Clarke, 1894–1895).

developing spirialium. The demonstration by MACKINNON (1974, 1991) that the shell structure of spiralia in many spiriferides and atrypidides differs from that of athyridides indicates that there may well have been fundamental differences in the dispositions of their lophophores. CAMPBELL and CHATTERTON (1979) reviewed the discussion on spiralia and their inferred lophophore reconstructions in a detailed study of *Coelospira*. Its double spires, which do not connect with the crura, and unusual jugal apparatus were thought to have supported a double lophophore with the jugum secreted by epithelium from both valves, allowing some adjustment of the lophophore position while the shell was open.

Calcareous ribbons composed of secondary shell and brachiostest (MACKAY and others, 1994) may also extend from the distal ends of crura to form a closed structure known as the **loop**, which is especially characteristic of the Terebratulida. The loop varies greatly, not only in form but also in origin and growth; yet it gives support to a plectolophous lophophore in the great majority of living adult terebratulides, an association that also probably applied to most fossil members of the group. Depending on whether support for both the side arms and the central coil of the plectolophe is provided by a narrow and twisted calcareous ribbon (MACKAY and others, 1994) or by a spicular

meshwork, the terebratulide brachidium may be broadly categorized as either long-looped or short-looped. In the past, it was customary to apply to mainly long-looped terebratulides an extensive loop terminology based on genera considered to be closely related phylogenetically that purported to illustrate various stages of loop development in particular stocks (e.g., THOMSON, 1927; MUIR-WOOD, 1934; ELLIOTT, 1953; COOPER, 1956; STEHLI, 1956). By the mid-1970s at least ten stocks had been given their own set of terms (DAGYS, 1974). In order to overcome the difficulties in dealing with the plethora of taxon-based terminology, which has, at times, been based on incomplete sequences of loop development, a more recently proposed descriptive scheme (RICHARDSON, 1975), somewhat emended and expanded, is introduced herein.

The simplest loop arrangement is found in Paleozoic terebratulides such as *Centrorella* (Fig. 334.1) and consists of a pair of gently curved **descending lamellae** that unite anteriorly and tend to form a broad-pointed blade, the **echmidium**. This is the **acuminate loop**, which was probably associated with a trocholophe or early schizolophe. Such a loop persisted in some adult shells with little modification, apart from enlargement of the outer edge and resorption along the inner edge, as in *Rensellandia*, with or without peripheral spines (e.g., *Stringocephalus*); how-

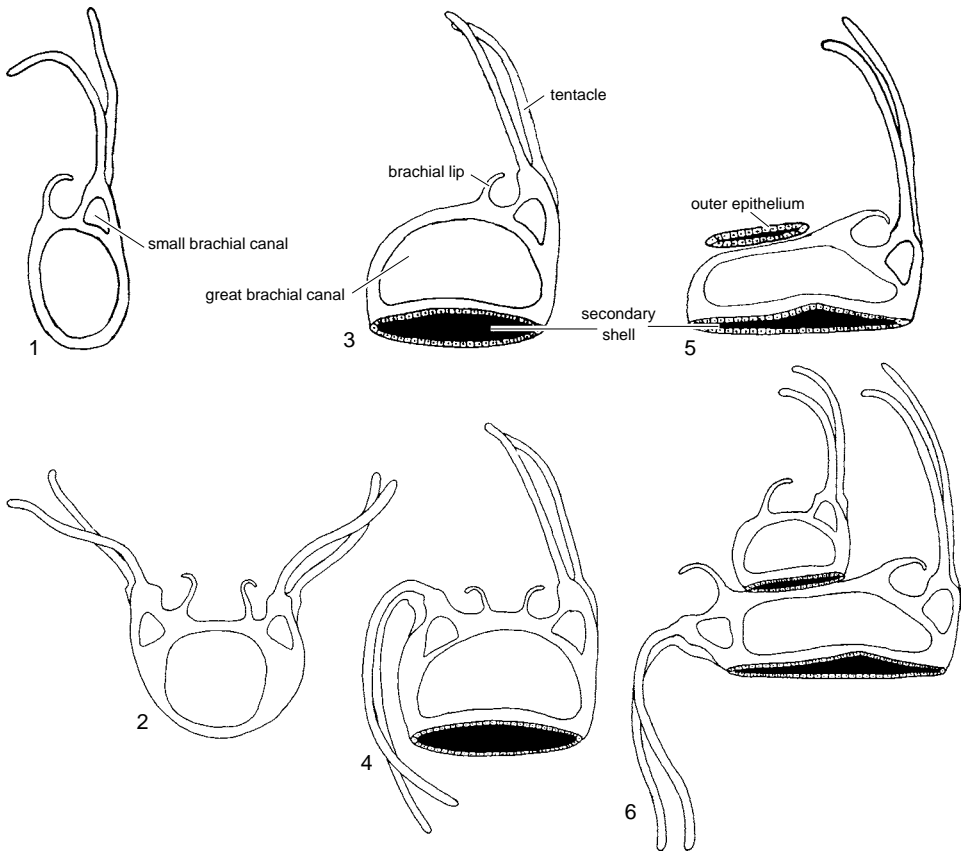


FIG. 337. Diagrammatic cross sections of lophophore of 1, *Notosaria* and 2, side arm of *Terebratulina* with inferred lophophore restorations of 3–4, spiriferoids and 5–6, athyridoids, according to whether they should be homologized with 1 (as in 3 and 5) or with 2 (as in 4 and 6) (adapted from Williams & Rowell, 1965b).

ever, in a number of Paleozoic and Mesozoic terebratulides, a ventrally projecting median plate (vertical plate) developed normal to the echmidium (e.g., *Rensselaeria*, Fig. 334.2). Accelerated growth in the anterolateral parts of a juvenile, acuminate loop (with or without a vertical plate) gave rise, in the adult stage of many Paleozoic terebratulides (e.g., *Dielasma* and *Cranaena*), to a **deltiform loop** (Fig. 338). This subtriangular form of loop, consisting of two short, divergent descending lamellae with distal extremities united by an undulating transverse band, is typical also of many post-Paleozoic, short-looped brachiopods and is very similar to that partly supporting a plectolophous lophophore in living *Gryphus*. In such late Paleozoic dielasmatoids as *Labaia* and *Gefonia*, the ventral edge of

the vertical plate split into a pair of slender, sharply recurved lamellae that, unlike the **ascending lamellae** of post-Paleozoic, long-looped forms, were not posteriorly united by a transverse band. In *Cryptacanthia* and related stocks (COOPER, 1957; COOPER & GRANT, 1976), however, the echmidium (without a vertical plate) was the site of differential secretion and resorption of a juvenile acuminate loop that gave rise, ultimately, to a **teloform loop** (Fig. 338) consisting of long, gently curved descending lamellae and reflected ascending lamellae united by a transverse band. The teloform loop of *Cryptacanthia* and its allies is comparable to that supporting a plectolophous lophophore of many recent terebratulidines but fashioned in an entirely different way.

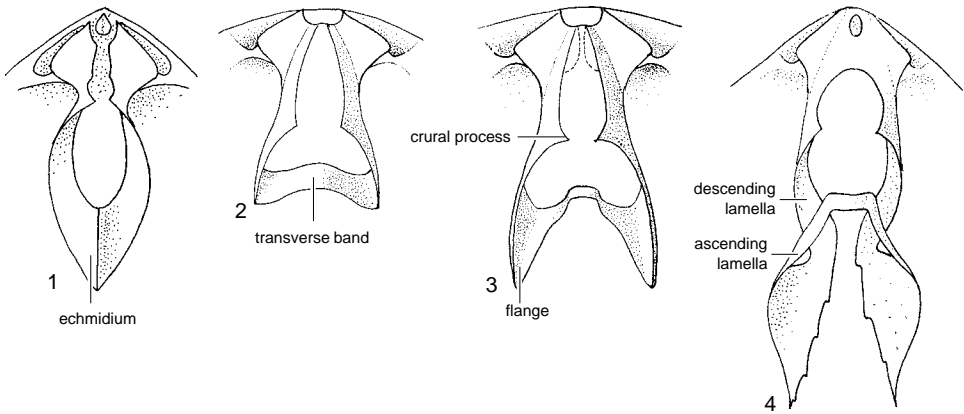


FIG. 338. Terebratulide loop types; 1, acuminate loop of *Centronella* (adapted from Stehli, 1965); 2, deltiform loop typical of many short-looped Terebratuloidea; 3, long-flanged deltiform loop typical of Lobothyroidea (adapted from Cooper, 1983); 4, teloform loop of *Cryptacanthia* (adapted from Cooper, 1957).

Unlike their Paleozoic antecedents, growth of a teloform loop in most post-Paleozoic terebratulides is linked with the development of a **septal pillar**, which first makes its appearance as a high columnar or platelike outgrowth from the dorsal valve floor. During the ontogeny of many long-looped taxa, the ventral or posteroventral edge of the septal pillar undergoes cleavage to form first a shallow groove and then an inverted, variably compressed cone or hood. By means of localized resorption in the vicinity of the dorsally directed apex of the hood and secretion of new shell around its ventrally facing rim, the hood is transformed into a ring, representing the rudiments of the ascending lamellae and transverse band. At about the same time as the appearance of the hood, descending branches appear as prolongations growing anteriorly from the crura to meet and fuse with either the septal pillar or a pair of posteriorly directed outgrowths. From such beginnings, the development of a teloform loop may involve any one of a number of complex series of metamorphoses; these are more fully discussed and illustrated in the systematic volume dealing with the terebratulides (Part H(R), vol. 4, in preparation).

Although many long-looped taxa utilize a septal pillar during various complex loop metamorphoses, similarly complex loop sequences have been recorded in several species

of Mesozoic Loboithyroidea that, as adults, exhibit essentially a deltiform loop with extremely prominent, long-flanged, anterolateral extremities (Fig. 338). In forms such as *Viligothyris* and *Taimyrothyris*, juvenile phases of loop development involve the growth of ascending elements such as a hood and ring, not on a septal pillar but on a vertical plate supported only by descending lamellae (DAGYS, 1968, 1972). In many short looped terebratuloids, support for the side arms and central coil of the plectolphe is provided by a dense, interlocking

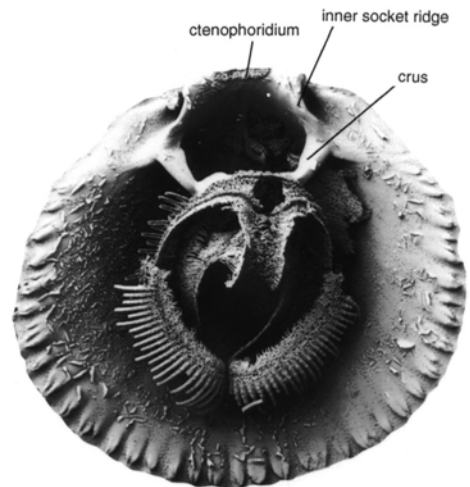
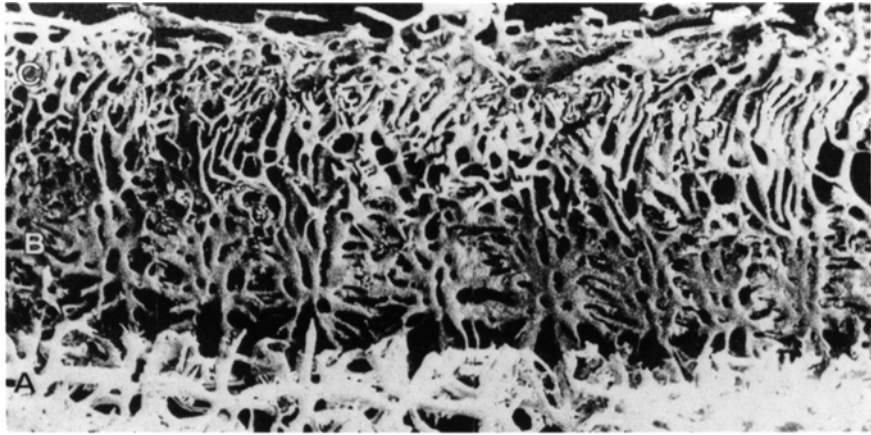


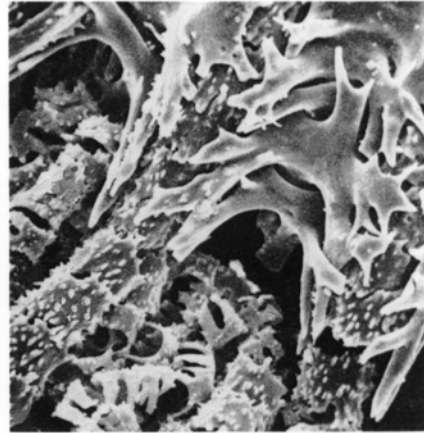
FIG. 339. *Terebratulina unguicula* (CARPENTER), recent, Puget Sound, USA, showing the nearly complete spiculation of the lophophore, SEM, $\times 7.5$ (new).



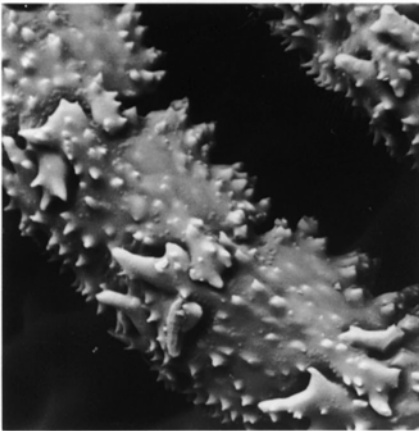
1



2



3



4



5

FIG. 340. Spicules within the lophophores of terebratulides; 1, *Terebratulina retusa* (LINNAEUS), recent, SEM, $\times 65.8$; 2, *Megerlia truncata* (LINNAEUS), recent, showing spicules in the tentacles, SEM, $\times 130$; 3, *Platidia anomioides* (SCACCHI & PHILIPPI), showing spicules in the tentacles and separating their bases within the lophophore arm, SEM, $\times 253.8$ (Schumann, 1973); 4–5, *Leptothyrella incerta* (DAVIDSON), recent, Gulf of Gascoigne, showing articulation between the tentacle spicules, allowing inward flexing, SEM, $\times 103.4$, and 5, view including arm spicules, SEM, $\times 26.3$ (new).



FIG. 341. Dorsal valve interior of *Spondylospira lewesensis* (LEES), Triassic, central Peru, showing the brachidial net. A broken crus shows on the right, $\times 7$ (SANDY, 1994).

meshwork of **spicules** (e.g., *Terebratulina*, Fig. 339), which is only rarely preserved in fossils (STEINICH, 1965; SURLYK, 1972; BRUNTON & HILLER, 1990). Spicules are highly variable in form and size and in some genera (e.g., *Terebratulina*, *Platidia*, and *Megerlia*) extend into the brachial tentacles (Fig. 340; SCHUMANN, 1973). Body wall and brachial arm spiculation is particularly strongly developed in platidioids and cancellothyridids but meager or absent in zeillerioids, laqueoids, and some terebratelloids. There is, however, insufficient information on the distribution, nature, and growth of spiculation in living genera.

A structure loosely connected with the lophophore is the **brachidial net** (SANDY & LANGENKAMP, 1992), first noted by COOPER (1942) in the Late Triassic *Spondylospira*, and well illustrated by SANDY (1994; Fig. 341). This calcareous netlike structure unites the crura and crural processes (or jugum) to the dorsal valve floor, in so doing surrounding the inferred body cavity, as if by a heavily mineralized, body-wall spiculation. Anteromedially and ventrally, between the crural processes, a gap probably accommodated the mouth and esophagus leading posteriorly from the lophophore. Another structure in a similar but median position in several genera of the Neospiriferinae has been described by COOPER and GRANT (1976) as a **buccal plate**. This is a bilaterally symmetrical, stellate, concave posterodorsally, five- to seven-rayed,

perforate plate medially positioned between the spiralia (Fig. 342). These plates were commonly lost from the insides of silicified specimens as they were digested by acid from the rock, and it seems, therefore, they were not fixed in place; in consequence their true position is conjectural. The nature of the plates is indicative of their being formed within the anterior body wall, and thus they may have aided support of the lophophore in the mouth region.

Apart from the terebratuloids and immature spiriferoids, loops are found only in the somewhat problematical pentameroid? *Enantiosphen* and the enteletoid? *Tropidoleptus* (Fig. 343; WILLIAMS & WRIGHT, 1961). The bilobate loop of the former seems to have developed by accelerated, anterolateral growth as well as general enlargement (with resorption) from a young, subcircular structure and may have supported a modified schizolophe. The growth of the *Tropidoleptus* loop, on the other hand, was dependent on the development of a dorsal median septum. The inferred arrangement seems to have been like that of terebratelloids, and it may have supported a plectolophe, especially if spirolophes were restricted to the spiriferides (*s.l.*), as seems likely.

The interiors of the dorsal valves of many thecideidines exhibit a variety of patterns of grooves, ridges, and tubercles that correspond with the configuration of an associated **schizolophous** or **ptycholophous** lophophore (BAKER, 1990). During the early phases of thecideidine evolution in the Triassic Period, some particularly novel forms of brachidial structures have been recorded (DAGYS, 1974). Spiralia with V-shaped cross sections and ventrally directed apices, found in *Thecospira* and *Thecospiropsis*, provide undisputable evidence of spirolophous lophophores in those genera. On the other hand, the disposition of lamellar and septal outgrowths in the dorsal valves of *Pamirotheca*, *Hungaritheca*, and *Thecospirella* suggest that in those taxa a plain or modified schizolophe prevailed (DAGYS, 1974). Brachidial development in post-Triassic thecideidines seems to have proceeded along

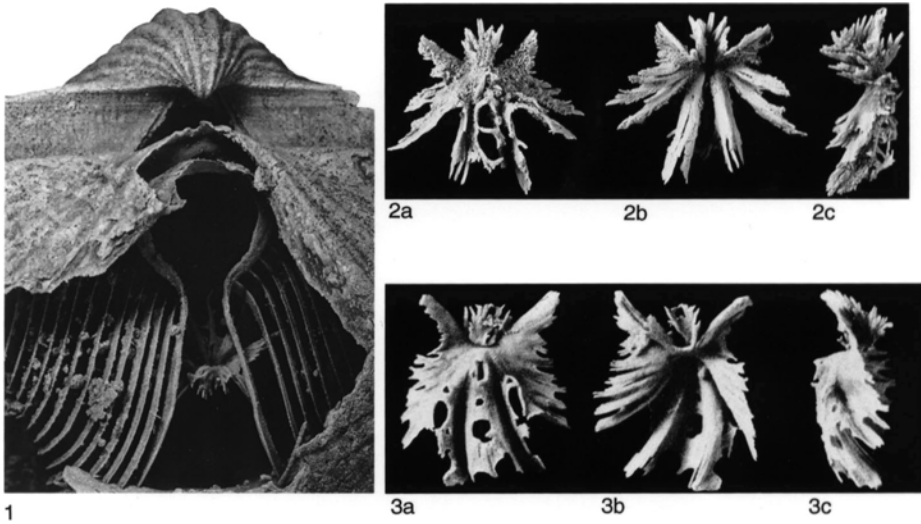


FIG. 342. 1, Buccal plate, possibly *in situ* between the spiralia of a *Neospirifer* species, Permian, Texas, USA, $\times 2.5$; 2a–c, anterior, posterior, and lateral views of isolated plates, $\times 3$; 3a–c, anterior, posterior, and lateral views of isolated plates, $\times 3$ (Cooper & Grant, 1976).

two main lines, reflecting differentiation of schizolophous and ptycholophous stocks (BAKER, 1990).

Despite the lack of structures comparable with crura, some internal features of the dorsal valves of plectambonitoids, strophomenides, chonetidines, productines, and strophalosiidines seem also to have functioned as supports to the lophophore (WILLIAMS, 1956). Among the plectambonitoids, a variably elevated, semicircular, medially divided disc (**brachial platform**), like that of *Leptelina*, is commonly present and may be interpreted as having borne a schizolophous lophophore (Fig. 344.1). The deeply divided, elongately oval platform of *Bimuria* or the pair of long, U-shaped sets of ridges of the strophomenoid *Christiania* must have functioned in a similar way; although like the divergent oval areas of the sowerbyellids, which are not only bounded submedially by ridges but also divided by a pair of divergent lateral septa, the structures (**bema**) may have supported a lobate trocholophe rather than a ptycholophe (Fig. 344.2). Indeed, attached and modified trocholophes or schizolophes seem to have been the more likely kind of plectambonitoid lophophore. Some strophomenoids, most chonetidines, and other early

productides are characterized by a pair of ridges arising between the posterior and anterior pair of dorsal adductor scars (**anderidia**) while in other productides recurring ridges define a pair of anterolateral areas commonly occupied by a smooth, raised mound of secondary shell. These features are called **brachial ridges** in the belief that they gave support to the dorsal epithelium, from which hung the lophophore. They are exceptionally associated with subconical impressions directed ventrally, which might represent differential thickening to accommodate the median parts of the lophophore (e.g., *Levitusia*, *Gigantoproductus*). The evidence indicates a schizolophe or simple ptycholophe for most taxa in these groups (Fig. 345). There is evidence in the Permian among some aulostegids, however, for a calcified falafer brachidium (GRANT, 1972) supporting a multilobed ptycholophe (Fig. 345.2) of the type suggested by GRANT (1972) as being typical of all productides having a deep **corpus** cavity (see also the section on Productida in the systematic volume Part H(R), volume 2, in preparation). The extreme lobate brachiophore of lytonniids can be seen as an exaggerated growth and reorientation of the above falafer type in response to their

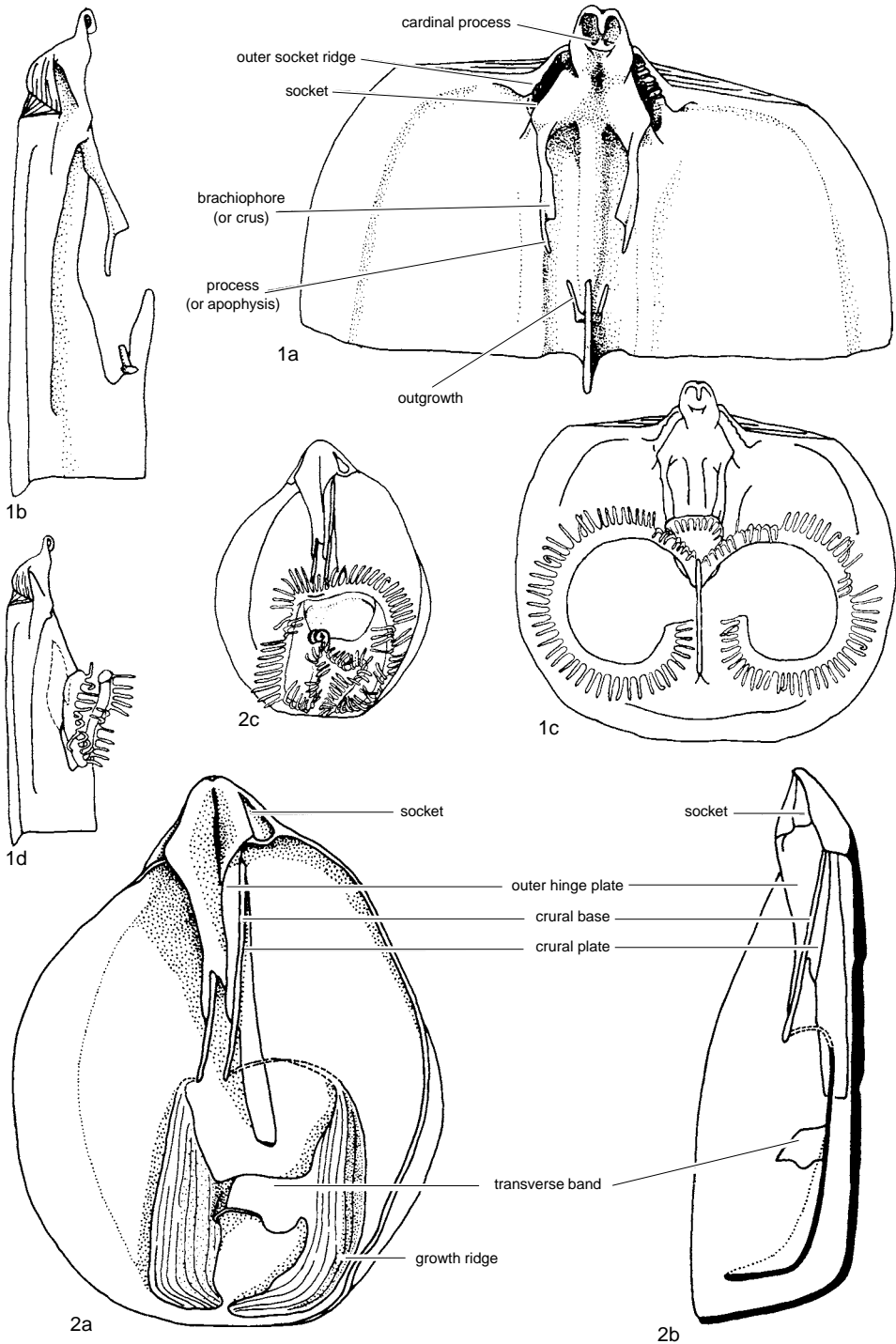


FIG. 343. Internal morphology of dorsal valve in 1a, ventral and 1b, lateral views of *Tropidoleptus carinatus* CONRAD, Middle Devonian, USA with 1c-d, inferred restoration of lophophore in ventral and lateral views; and of dorsal valve in 2a, ventral and 2b, lateral views of *Enantiosphen vicaryi* (DAVIDSON), Middle Devonian, England, with 2c, inferred restoration of lophophore in ventral view (adapted from Williams & Wright, 1961).

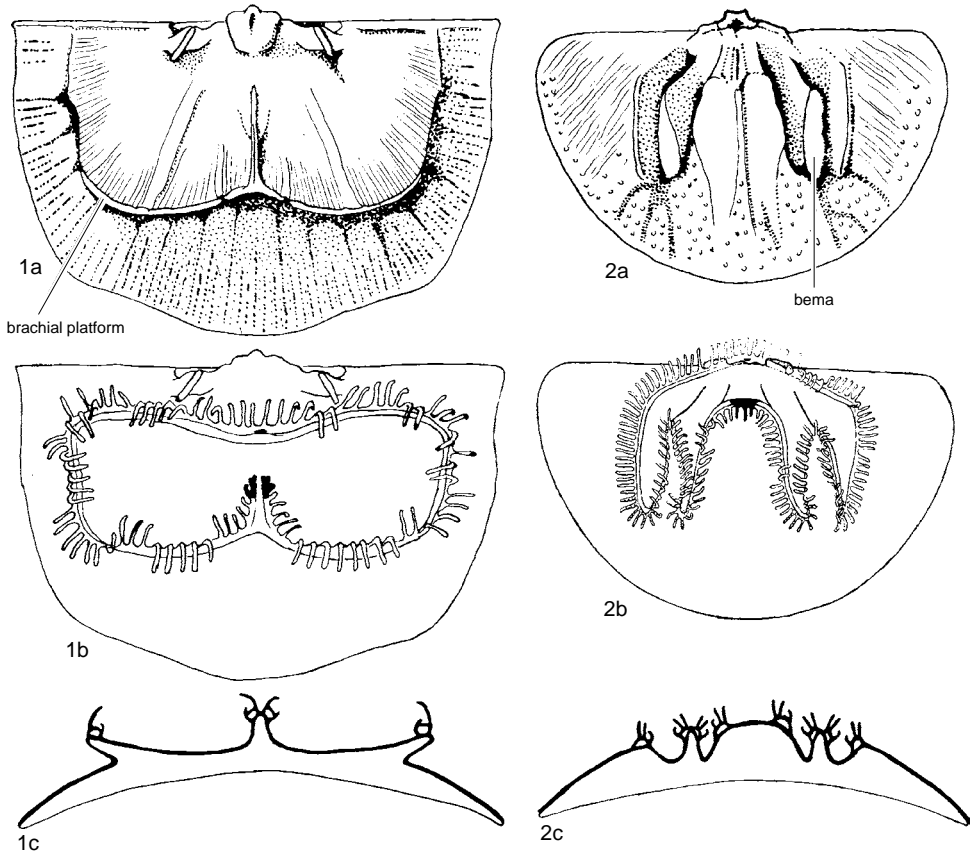


FIG. 344. Internal morphology of the dorsal valve in the plectambonitoids 1, *Leptellina* and 2, *Eoplectodonta*; 1a, 2a, internal view, with an internal reconstruction of the lophophore in 1b, 2b, ventral, and 1c, 2c, transverse sectional views; dotted segments of lophophore are inferred as raised above the valve floor; generative regions are in black (adapted from Williams & Rowell, 1965b).

oysterlike life habit (GRANT, 1972). A variation on the usual schizolophous situation in chonetidines was suggested by RACHEBOEUF and COPPER (1990) in a Late Ordovician example of *Archeochonetes* in which they found a gamma-shaped structure with a median lobe arching anteriorly around the dorsal median septum. They interpreted this as a remnant indication of the lophophore, which they termed a mesolophe, and suggested it might have been present in many chonetidines; but its growth remains difficult to envisage.

It has also been suggested that the brachial ridges may represent traces of the mantle-canal system, such as sites of gonocoels, mainly because they commonly arise from

the dorsal muscle field in a position occupied by the *vascula myaria* of orthoides and strophomenoides (MUIR-WOOD & COOPER, 1960). The mantle canal systems of the productines are unknown, but traces of radiating peripheral canals seen in *Peniculauris* terminate abruptly against the well-developed brachial ridges. Generally the role of brachial ridges as part of the mantle canal system is now rejected.

Among inarticulated brachiopods there are no prolongations of the shell that indisputably functioned as lophophore supports, but projections from the dorsal valves of acrotetide genera may have given support to the lophophore and anterior body wall. This would appear to be the most probable

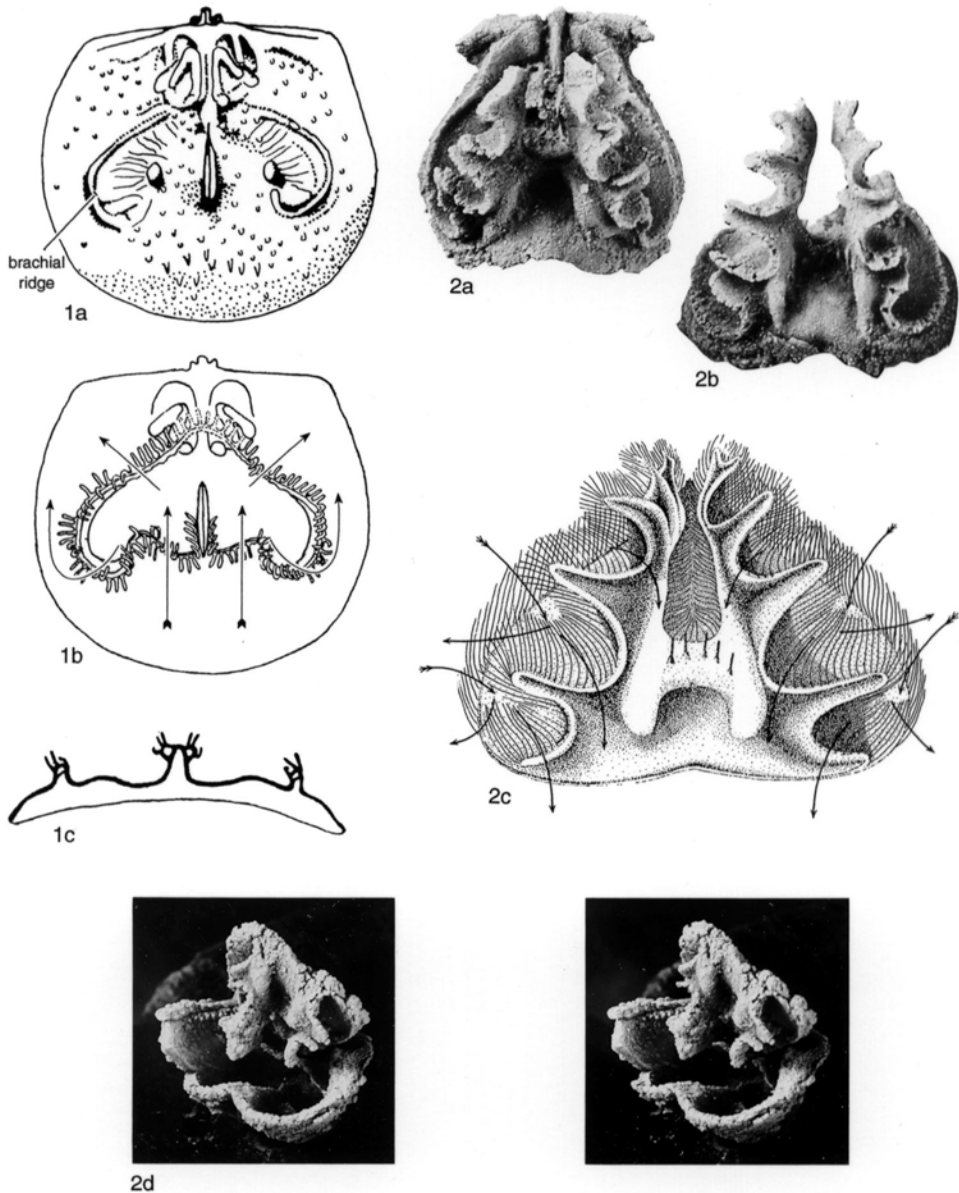


FIG. 345. Inferred dorsal features in productides; *1a-c*, productidine *Pugilis* with the inferred lophophore viewed ventrally and in transverse sections (adapted from Williams & Rowell, 1965b); *2a-d*, the alustegoid *Falafer epidetus* GRANT, Permian, Greece, viewed *2a*, ventrally, $\times 8$; *2b*, anteroventrally, $\times 8$; *2c*, inferred ptycholophe reconstruction; feathered arrows indicate incurrents; and *2d*, complete shell widely open, stereopair, $\times 6$ (Grant, 1972).

function of these saddle-shaped plates of *Ephippelasma* (COOPER, 1956) and *Numericoma* (see HOLMER, 1989), which arise from a relatively narrow base slightly behind the center of the valve and expand

ventrally and anteriorly to terminate in a number of slender projections (Fig. 346). These projections are disposed with a crude symmetry about the median plane, and their tips roughly fall on an imaginary surface that

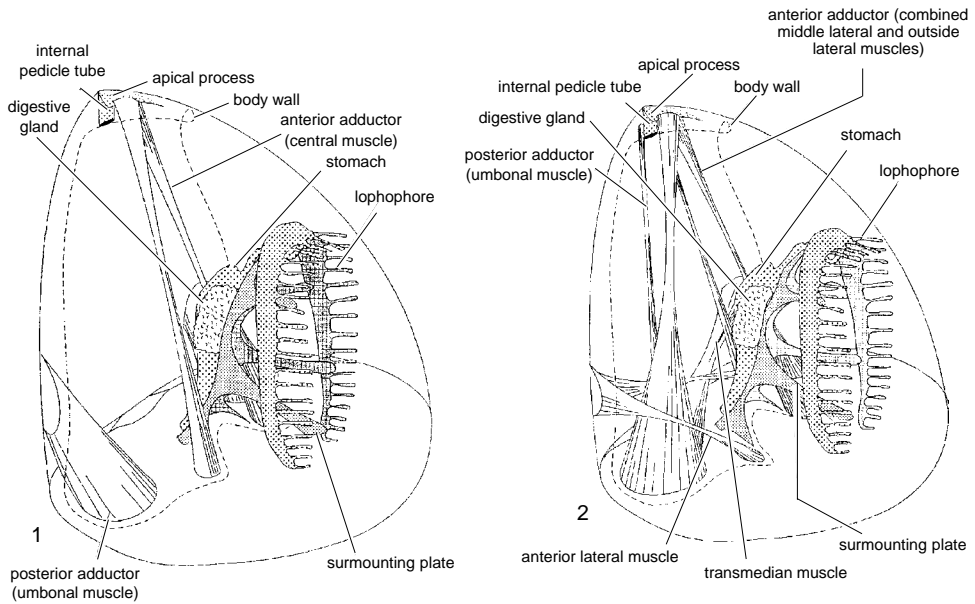


FIG. 346. Stylized reconstructions of *Ehippelasma* with inferred location of lophophore, muscles, and alimentary canal; shell treated as transparent; 1, adapted from Williams and Rowell (1965b) assuming a cranioid relationship; 2, with the lingulide relationship of POPOV, 1992 (new).

is inclined posteroventrally to make a high angle with the plane of commissure. The mouth in *Ehippelasma* presumably lay in the plane of symmetry, as in all recent brachiopods, and must have opened along the crest line of the median plate or ventrally of this line. All adult individuals of *Ehippelasma* are small enough to suggest that their lophophores were probably trocholophous or schizolophous, and if the tips of the projections from the median plate touched the anterior part of the body wall, the limited mantle cavity could conveniently have accommodated a trocholophe (or schizolophe) only when the organ was oriented approximately parallel with the plane defined by the tips of the projections. In this attitude, the median projection could have supported the lophophore immediately dorsal of the mouth, with the laterally placed prongs embedded in the posterior arcs of the trocholophous ring on either side of the mouth.

Many other acrotretid genera have a thin, bladelike median septum, usually subtriangular in lateral profile and attached basally

along its length to the dorsal valve. The posteroventral edge of the median septum is commonly unmodified, but it may bear variously disposed transverse plates (the **surmounting plate**). In *Torynelasma* this is a slender, ventrally concave, triangular plate; in *Biernatia* it is a ventrally convex plate (Fig. 347), or it may be narrowly expanded and digitate in a plane more or less normal to the septum as in *Angulotreta* or *Prototreta*. In all these forms, the medially situated mouth must have lain on or ventral of the free edge of the septum, which dorsally may have supported the generative tips of a trocholophe or schizolophe. The modifications on the posteroventral edge of the septum, however, are generally too narrow to have given much support to the lophophoral arcs lateral of the mouth.

MUSCULATURE

The muscles of most articulated brachiopods consist of two sets passing between the valves (**diductors, adductors**) and another two sets controlling the pedicle (**ventral and dorsal adjustors**). Distinct impressions

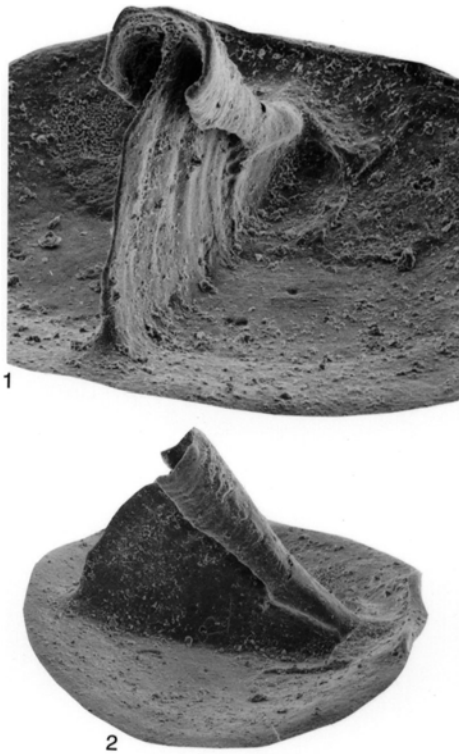


FIG. 347. Dorsal valve interior of the acrotretide *Brernatia holmi* HOLMER, Middle Ordovician, Sweden, showing the median septum with its posteroventrally convex surmounting plate in 1, oblique anterior (SEM, $\times 105$), and 2, lateral (SEM, $\times 70$) views (Holmer, 1989).

(**muscle scars**) commonly mark the sites of muscle bases on the interiors of both valves. Such impressions are formed as a result of modifications in the fine structure and secretory behavior of localized areas of shell-secreting outer epithelium to which the muscles became attached (WILLIAMS, 1968a; WILLIAMS & WRIGHT, 1970; MACKINNON, 1977). The microscopic shell structure of muscle scars is commonly so distinct that it is best regarded as a localized development of an additional shell layer, for which KRANS (1965) introduced the term **myotest**. During ontogeny, muscle bases (with the exception of the posteromedially located dorsal diductor attachment scar) generally migrate anteriorly more rapidly than the underlying epithelium. Thus, in radial section, myotest can be traced posteriorly, becoming buried by

the overlap of normal secondary shell more recently secreted in that part of the shell located behind the muscle field. In the ventral valve, all muscle scars tend to be grouped together to form a muscle field, which is ideally differentiated into a median adductor muscle scar contained posteriorly by two incomplete arcs of inner diductors and outer adjustors (Fig. 348.1b, 2b, 3b). The attachment areas in the dorsal valve, however, are generally much more scattered (Fig. 348.1a, 2a, 3a). The adductor field commonly consists of an anterior and a posterior pair of scars, with one of each pair discernible on either side of the median line and well forward of the cardinalia, which accommodated both the dorsal adjustors and dorsal ends of the diductors (Fig. 349), usually along the inner faces of the hinge plates (or brachio-phores) and on a posteromedian outgrowth of secondary shell (cardinal process), respectively.

Muscle scars can vary not only in their relative position but also in the clarity of their impression. They may be deeply inserted, raised above the general level of the valve floor, or even greatly elevated on elaborate platforms. The definition of muscle scars in brachiopod shells is normally a function of age, so that the ultimate area of attachment attained in adult stages of growth is much more easily seen than the impressions in young or immature valves. This clarity is due mainly to differential secretion involving greater organic and less mineral secretion, which results in a change in the texture of that part of the secondary layer affording attachment (Fig. 350; MACKINNON, 1977). As a consequence, muscle marks are commonly sunk below the level of adjacent shell. Indeed, even when the entire muscle field is raised above the valve floor on thick deposits of secondary shell, the marks themselves may be deeply impressed on the platform. Such impressions usually included a variable number of striplike indentations or **muscle tracks** disposed parallel with the adjacent boundaries of the muscle scars, which represent the course of migration for the muscle bases during growth of the shell.

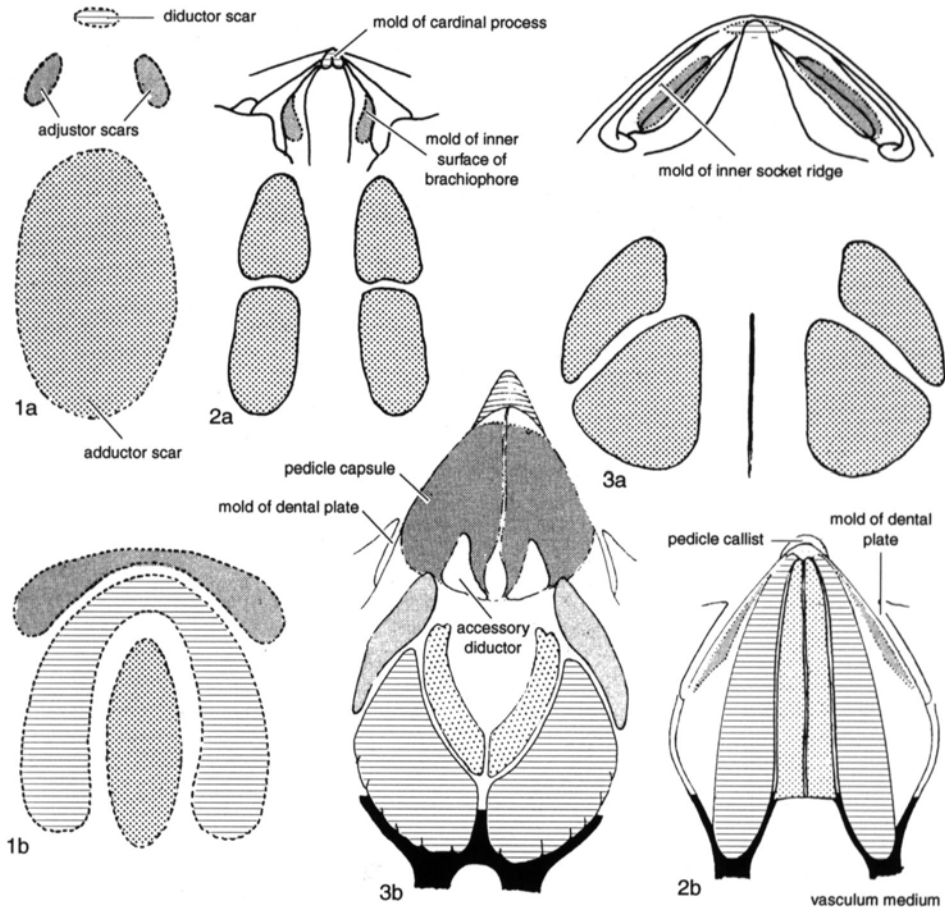


FIG. 348. Diagrammatic representation of principal muscle marks in *1a*, dorsal and *1b*, ventral interiors with examples of corresponding actual scars seen in *2a–b*, *Dalmanella watti* (BANCROFT), Middle Ordovician, England, and *3a–b*, *Hemithiris psittacea* (GMELIN), recent (adapted from Williams & Rowell, 1965b).

The migration of muscle bases can involve two aspects of growth. First, the proportions of the field relative to those of the valve may remain constant, or they may undergo changes at any stage in growth by an accelerated expansion in size of either the valve or the muscle field. Greatly extended and splayed impressions (**flabellate muscle scars**) are commonly found in the adult ventral valves of many stocks and usually result from an acceleration in the spread of the muscle bases. Second, irrespective of any changes in relative growth rates, there is always an absolute increase in the area occupied by the muscle bases, which may be greater along some vectors than others, so that the outline

of the muscle marks may change significantly during growth. Even examination of muscle scars with a relatively low-powered microscope can reveal the type of modifications to the shell mosaic described by WILLIAMS and WRIGHT (1970), MACKINNON and WILLIAMS (1974) or MACKINNON (1977).

The growth and distribution of platforms and apophyses to accommodate the various sets of muscles controlling shell movement are related to both the function and grouping of the muscles. The ventral muscle field tends to be located posteriorly of the transverse midline and, apart from details of outline, its relative size probably does not vary greatly throughout most articulated

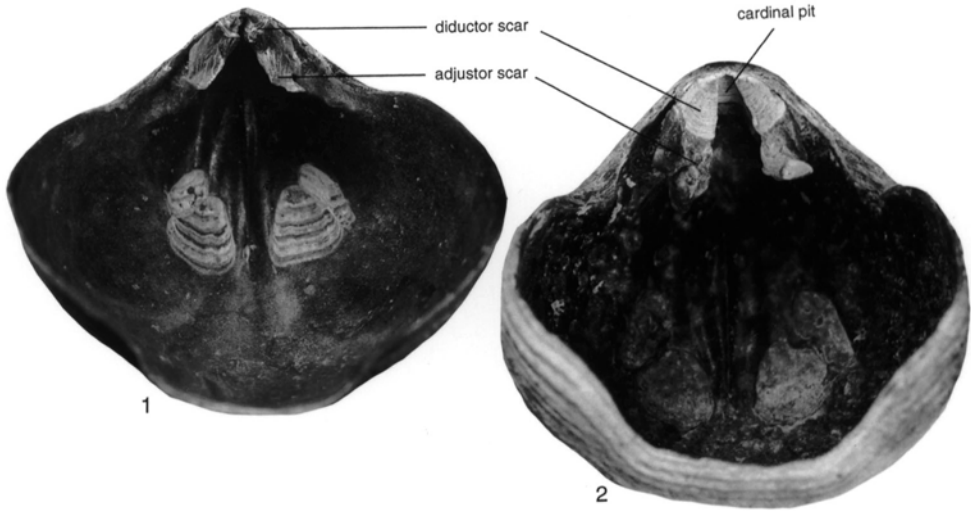


FIG. 349. Dorsal valve interiors of *Hemithiris psittacea* (GMELIN), recent, Tromso and Labrador, showing divided pair of adductor scars on valve floor; diductor scars posteromedially (especially in 2) and dorsal adjustor scars on the crural bases, $\times 3$ (new).

brachiopods. An important difference, however, is noted in location of the field within the valve, since those of rhynchonelloids, spiriferoids, and terebratuloids are well forward of the umbonal chamber that accommodated the pedicle base, whereas the orthoid, strophomenoid, and porambonitoid fields typically occupied all available wall space within the delthyrial chamber and usually did not extend very much forward of it (Fig. 348.2b,3b; WILLIAMS & WRIGHT, 1963). One of the consequences of this posterior location in the older brachiopods is that the dental plates commonly afforded attachment for the ventral adjustors and, by convergence toward each other, for an increasing area of the ventral diductor and adductor bases as well. Convergent dental plates that united with each other in such a way as to elevate the entire ventral muscle field above the floor of the pedicle valve constitute a **spondylium** (Fig. 351).

The spondylium is preeminently characteristic of the clitambonitoids, pentameroids, and stenoscismatoids; but it is also found in other unrelated stocks such as the orthoid *Skenidioides*, some orthotetoids, for example, *Ombonia*, and the stringocephaloid *Amphi-*

genia. A complicated terminology, partly reflecting this diversity of origin, is now used to indicate various stages in spondylial development. KOZŁOWSKI (1929) named the slightly convergent dental plates that grew directly from the floor of the ventral valves of some porambonitaceans, like *Huenella*, the **spondylium discretum**. This arrangement is, however, identical with that of most orthoids, and the term is acceptable only where clear evidence indicates that such a disposition was precursory to growth of a spondylium. Structures involving discrete dental plates are also known as **pseudospondylia** (SCHUCHERT & COOPER, 1932) if the anterior part of the ventral muscle field is elevated on an undercut callosity, which may be prolonged anteromedially as a ridge (Fig. 352). Pseudospondylia have frequently been designated sessile spondylia, but it is preferable to restrict the use of this latter term, with its implications of a true spondylial relationship, to structures formed by dental plates that unite with each other on the floor of the ventral valve (e.g., *Sicelia*).

Spondylia formed by the convergence of dental plates above the floors of adult valves may be free of septal support, as in *Protorthis*

and *Holorhynchus*, and presumably represent an anteromedian growth from a juvenile sessile spondylium. More commonly the spondylium is supported by a median septum or ridge of variable length. KOZŁOWSKI (1929) distinguished between two types of septal support. In the **spondylium simplex** of *Skenidioides*, for example, the median septum consists of secondary calcite disposed in such a way as to suggest the incremental growth of a single structure. A low elevation of secondary shell commonly trailed anteriorly from the septum along the floor of the valve and became buried during the subsequent thickening and forward growth of the entire apparatus so that anterior sections of the adult spondylium simplex appear to show a dichotomy in the ventral end of the septum (Fig. 351.1). KOZŁOWSKI (1929) believed that this kind of arrangement evolved by the elevation of the entire pseudospondylium above the floor of the valve rather than by a convergence of dental plates. In contrast, a thin plate of prismatic calcite (intraseptal lamella) appeared invariably to occupy the median plane of the septum supporting the pentameroid **spondylium duplex**. Its presence led KOZŁOWSKI (1929) to conclude that such a septum was formed by the incomplete fusion of the dental plates (Fig. 351.2). He also assumed that the spondylium duplex was derived from the spondylium discretum by the convergence of the ventral parts of the dental plates toward each other.

The differences between the spondylia simplex and duplex may not be as fundamental as is generally believed (WILLIAMS & WRIGHT, 1961). The intraseptal lamella has been described as having an enlarged base at the junction of the septum with the spondylium and as thinning toward the floor of the valve, a disposition that is compatible with the prevalent interpretation of its origin. But ST. JOSEPH (1938) and AMSDEN (1953) have observed that the dorsal end of the intraseptal lamella can be continuous with extensive deposits of prismatic calcite lining the spondylium. Moreover, serial sections show that in at least some pentameroid

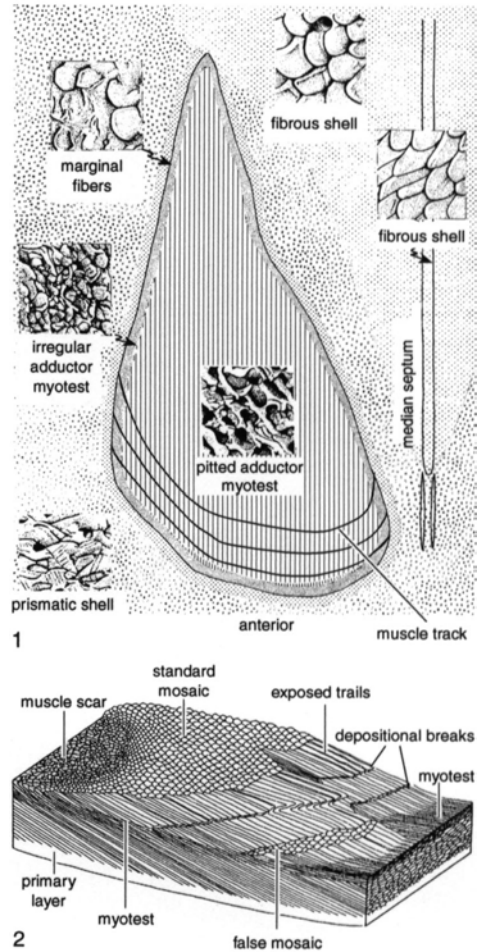


FIG. 350. Muscle scar morphology; 1, diagrammatic representation of a dorsal adductor muscle scar in *Liothyrella* showing variations in the shell fabrics of the myotest and surrounding mosaic. In this genus secondary shell built the median septum on the right and tertiary prismatic shell surrounds the scar (MacKinnon & Williams, 1974); 2, stylized block diagram of part of a dorsal valve of *Notosaria* exfoliated posterior to the adductor muscle scar (on left) and sectioned radially (adapted from MacKinnon, 1977).

genera (e.g., *Pentamerella* and *Gypidula*) the prismatic calcite along the median plane of the septum is disposed more like a series of disconnected lenticles than a continuous sheet and in some planes of section is no more concentrated medially than elsewhere throughout the septum or spondylium (Fig. 351.2b). The distinctiveness of the spondylium duplex may therefore have resulted

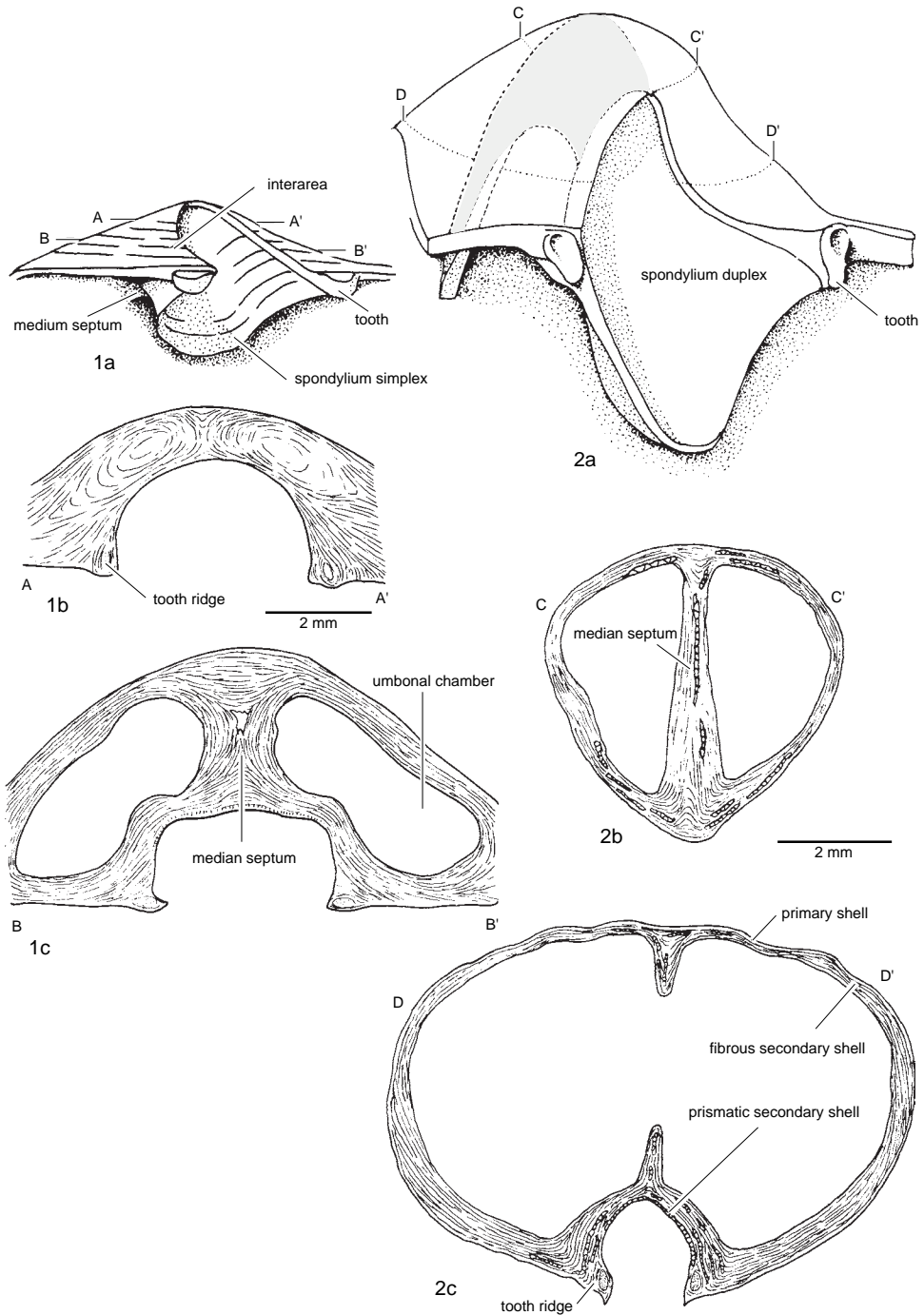


FIG. 351. Ventral valve showing 1, spondylium simplex of *Skenidioides craigensis* REED, Middle Ordovician, Scotland, and 2, spondylium duplex of *Gypidula dudleyensis* SCHUCHERT, Upper Silurian (Wenlock), England; 1a, oblique view showing location of transverse sections (1b-c); 2a, oblique transparent view showing position of median septum and location of transverse sections (2b-c) (adapted from Williams & Rowell, 1965b).

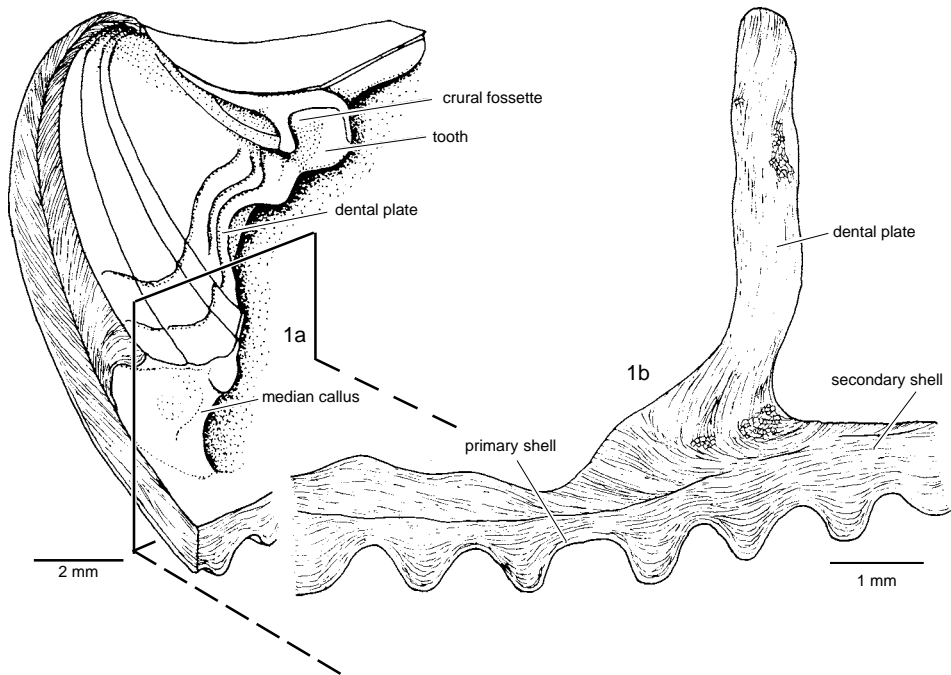


FIG. 352. *1a*, Structure of pseudospondylium of *Glossorthis tacens* ÖPIK, Middle Ordovician, USSR, with plane of transverse section showing *1b*, relationship between dental plate and floor of ventral valve (adapted from Williams & Rowell, 1965b).

from the secretory activities of the outer epithelium of the pentameroids, which, unlike that of the skenidiids, was capable of depositing prismatic calcite (WILLIAMS, 1956), and not from an imperfect fusion of dental plates. This interpretation would account for a more random distribution of the two different types of spondylia than was formerly believed possible, for a spondylium simplex has been identified in the syntrophiids and a spondylium duplex in the stenoscismatoids and camerellids. The spondylium of *Amphigenia* is truly duplex in that the dental plates are seen to unite into a median septum (BOUCOT, 1959).

Complications also arise in the use of the term **spondylium triplex** (ÖPIK, 1934) for an apparatus with a variably developed trisepate support that is especially characteristic of some gonambonitoids (Fig. 353). In some genera the underlying median and lateral (or accessory) septa were fashioned during early stages of growth by a pair of subconical hol-

lows that developed between the floor of the valve and a sessile spondylium as it diverged in an anterolateral direction. In *Antigonambonites*, at least, the lateral septa acted as posterior partitions between the *vascula media* and *vascula genitalia* of the ventral mantle so that their growth may have been conditioned by the relationship between the ventral mantle canals and the body cavity. The term may therefore be used for the spondylia of some porambonitoids, as for *Tetralobula*, in which accessory septa, posteriorly underlying the spondylium, are also lateral boundaries to the ventral *vascula media*. It has been used but is less appropriate, except in a strictly morphological sense, for the structure found in *Polytoechia*, which appears to consist of a pair of subparallel dental plates containing a pseudospondylial platform elevated on a median septum.

The apparatus found in the pedicle valve of *Cyrtina* (Fig. 354) is not a spondylium in the sense that its posterior elements gave

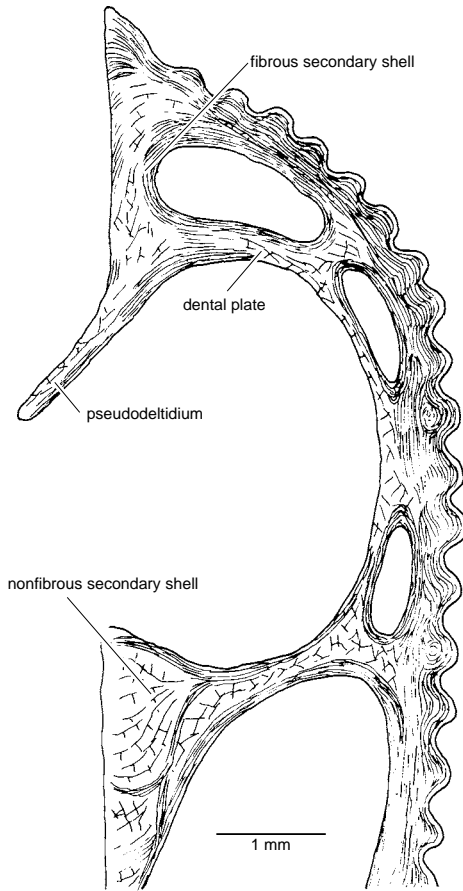


FIG. 353. Section through spondylium triplex of ventral valve of *Antigonambonites planus* (PANDER), Lower Ordovician, Baltic (Williams & Rowell, 1965b).

support to the entire ventral muscle field. It consists of a long, high, bladelike median septum to which the short, convergent, dental plates are ankylosed just below the posterior edge. A pair of lateral struts is subtended between the inner surfaces of the dental plates and the posteriorly protruding part of the median septum to define an anteriorly widening, medially positioned tube (**tichorhinum**) that is suboval in section and extends from the umbo to the dorsal edge of the median septum. The tichorhinum is actually a chamber within a larger one, bounded by an arched deltidium and the dental plates that must have contained the

pedicle. Given this likely location for the pedicle, the ventral adjustor muscles would have attached to the troughlike dental plates and the dorsal adjustor muscles to the crural bases. Most probably the main adductor muscles would have attached to the anterior part of the tichorhinum and the diductors to the lower anteroventral sides of the median septum (Fig. 354.2), where MACKINNON (1974) recognized the presence of myotest (Fig. 354.3). This interpretation does, however, raise a possible functional problem because the adductor and diductor muscle would have crossed close together. With respect to their convergence into a median septum well posterior of the ventral muscle field, the dental plates are like the short, dental ridges of some orthotetoids (e.g., *Orthotetes*), which also form a small chamber that has been incorrectly called a spondylium.

Quite possibly, the **syrix** of *Syringothyris* (Fig. 355) may have performed the same function as the tichorhinum, that is, as the attachment site of the ventral adductor muscles, except that the tubular syrix was attached to the ventral surface of a sunken delthyrial plate rather than to the postero-dorsal edge of a median septum, as is the tichorhinum of *Cyrtina*. The sunken plate (**delthyrial plate**) within the delthyrium to which the syrix is attached is probably homologous with the pedicle collar and would thus have lain anteroventrally to the pedicle or its remnant. This interpretation is consistent with the pattern of paired diductor muscle impressions only on the floor of the ventral valve, the closed ventral end of the syrix, and the sporadic development of a deltidium or stegidium posterior of the sunken plate.

One other type of muscle platform developed among such spire-bearing brachiopods (HALL & CLARKE, 1894–1895) as *Merista* and its allies (Fig. 356). It consists of a transverse partition (**shoe-lifter process**) extending across the posterior part of the ventral valve to define an open, hemipyramidal chamber (**cella**). The process was formed by deposition of secondary shell within an in-

fold of outer epithelium elevated above the floor of the ventral valve even in early stages of growth so that in some genera (e.g., *Aulidospira*) the dental plates encroached forward over the inner surfaces of the partitions. A similar structure, which bears a strong median septum, is found in *Parenteleles*. The term has also been extended to similarly shaped structures in dorsal valves, where it is bisected by the dorsal median septum, as in the meristellid *Rowleyella*.

The dispersion of the attachment areas of the diductor and adductor muscles within the dorsal valve has led to independently derived modifications of the dorsal interior. In general, the former are inserted near or at the notothyrial apex and posterior of the articulatory fulcral points to provide a third-order lever, and the latter are positioned sub-medially on the valve floor and well forward of the hinging mechanism. Ideally, both muscle sets are attached symmetrically about the median plane, the diductors to a pair of small bases and the adductors to two pairs of relatively large scars (Fig. 348.1a,2a,3a); this symmetry of insertion has led to many morphological changes, especially around the dorsal beak.

The dorsal attachment of the diductor muscles was commonly onto some form of boss or projection from the inside of the dorsal valve beak. Since DAVIDSON'S use of the term in 1853, these structures have generally been called the **cardinal process** in whatever groups of brachiopods they occur, and the term remains in general use. Recent studies indicate, however, that there are at least two different forms of cardinal processes. The first and geologically earlier, seen typically in orthides and strophomenides *s.l.*, is a structure with radially disposed ridges bordering and separating a pair of laterally adjacent diductor scars. In more advanced forms the diductor attachment sites became raised on a **shaft** with the muscles inserted into crenulated grooves (**myophores**) at the distally lobed head of the cardinal process (e.g., *Dalmanella*, Fig. 357.4). The second style of cardinal process growth is seen in

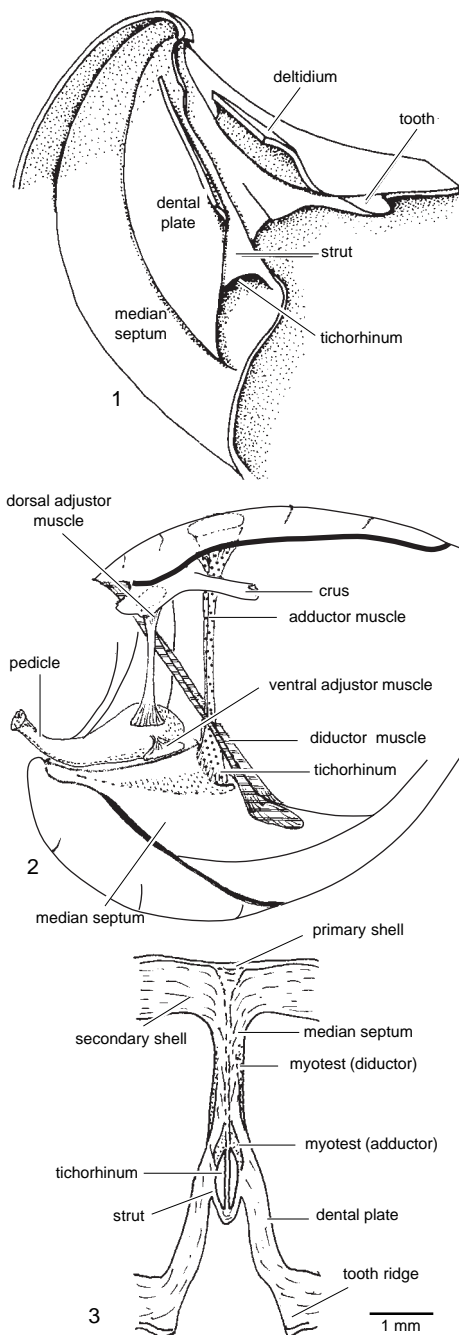


FIG. 354. 1, Tichorhinum in the spondylium of *Cyrtina hibernica* BRUNTON, Lower Carboniferous, north Ireland (Williams & Rowell, 1965b); 2, inferred disposition of the pedicle and muscles (new); 3, transverse section showing tichorhinum of *Cyrtina* sp., Middle Devonian, USA (adapted from Williams & Rowell, 1965b).

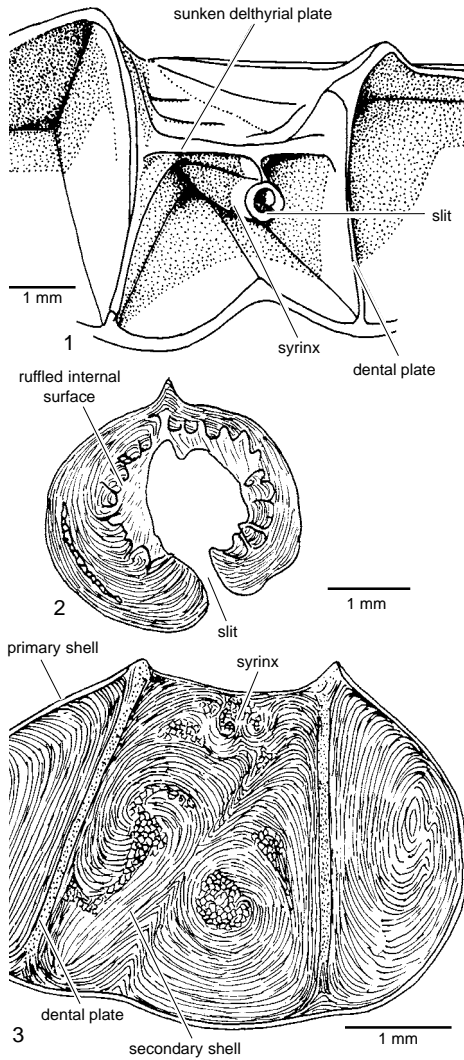


FIG. 355. 1, Ventral interior of *Syringothyris cuspidata exoleta* NORTH, Lower Carboniferous, England, with 2, transverse sections of free dorsal end of syrx and 3, of apex (Williams & Rowell, 1965b).

many spiriferides, athyridines, atrypides, rhynchonellides, and terebratulides and includes the **ctenophoridium** (Fig. 358) and **cardinal flanges** (Fig. 359). The former may be within the dorsal beak or, as is common with the latter, elevated above the valve floor on ridges or plates, dorsal to which are cavities, and attached laterally to the inner socket ridges. They are discussed further below.

Orthides and strophomenides have cardinal processes in which the dorsal diductor bases commonly remain separated so that the muscle scars are paired and bordered laterally and medially by ridges. Throughout life the muscle bases remained in a posteromedian position and tended to become elevated onto protruding structures that became bilobed in many groups. There is considerable variation in these cardinal processes, depending on the degree of development of the ridges bordering the paired muscle bases and the elevation of the bases above the valve floor. In early orthoids the notothyrial platform thickened to raise the diductor muscles above the valve floor, and accelerated deposition of fibrous secondary layer by the outer epithelium between the paired muscle bases commonly produced variably defined median ridges separating the two scars. In some the median ridge itself became the seat of muscle attachment, as in some orthoids, enteletoids, and some early rhynchonellides (e.g., *Orthorhynchula*; Fig. 360.2–360.3). In others this median ridge or the closely positioned muscle scars themselves became elevated and differentiated into a proximal shaft and distal lobed head, which was crenulated to increase the areas of muscle attachment at the myophores, as in many productides (Fig. 361.2). In *Resserella* each of the two myophore lobes is bordered by low ridges of smooth shell, acting as boundaries to the crenulated muscle scars (Fig. 357.3). The development of cardinal process shafts and bilobed myophores is most prominently seen in strophomenates, especially some orthotetines and the Productida, in which there is great variation. In some strophomenates, in which there is a dorsal interarea and a well-separated bilobed cardinal process, the median ridge on the notothyrial platform was retained in support of the chilidium, as in the orthotetidine *Schuchertella*. The diversity of form results from differences in the extent of growth of the shaft and from the growth or absence of the ridges separating the muscle bases medially or enclosing them laterally. To differentiate the main bilobed

structure from these ridges, the latter have been designated by the suffix -fid. A single median ridge on the cardinal process, normally separating the muscles, is termed unifid, a pair of lateral bounding ridges is termed bifid, a median ridge plus paired bounding ridges is termed trifid, and a median ridge plus paired bounding ridges plus paired lateral bounding ridges is termed quadrifid (BRUNTON, 1966). Ontogenetic and evolutionary changes from one condition to another led to adults of some species having a bilobed, trifid cardinal process through the median fusion of the paired median ridges of an earlier quadrifid stage of development, as in *Pugilis* (361.2). In other productides, such as *Echinoconchus*, and in the enteletoid *Paucicrura* (Fig. 361.5) the muscles spread medially onto the ridge and almost united into a single myophore, but commonly in productides the diductor bases were confined within myophore clefts with roughened surfaces.

Apart from unusual orthides, or in the triplesiods with their grotesquely exaggerated bilobed processes (Fig. 357.2) and the orthidiellids with their trifid structures formed by the outgrowth of high inner socket ridges with diductor scars between them and separated by a median ridge (Fig. 361.4), the plectambonitoids display an unusual variation on the cardinal process theme. Some of these genera have rudimentary diductor attachment structures with the scars on a slightly elevated notothyrial platform; some developed simple ridges separating the diductor muscle bases, while others developed a raised notothyrium with a small cavity below creating an overhanging cardinal process, which was characteristically trifid, as in some sowerbyellids (Fig. 361.1). In the dorsal valve of *Bilobia*, on the other hand, a basically trifid arrangement became secondarily bilobed by the development of a cleft in the high median crest (ÖPIK, 1933); and in *Anoptambonites* the cardinal process consists of a median ridge and up to six, lower, lateral ridges simulating the transverse comb of many spiriferoids (WILLIAMS, 1962). Although the cardinal processes of many

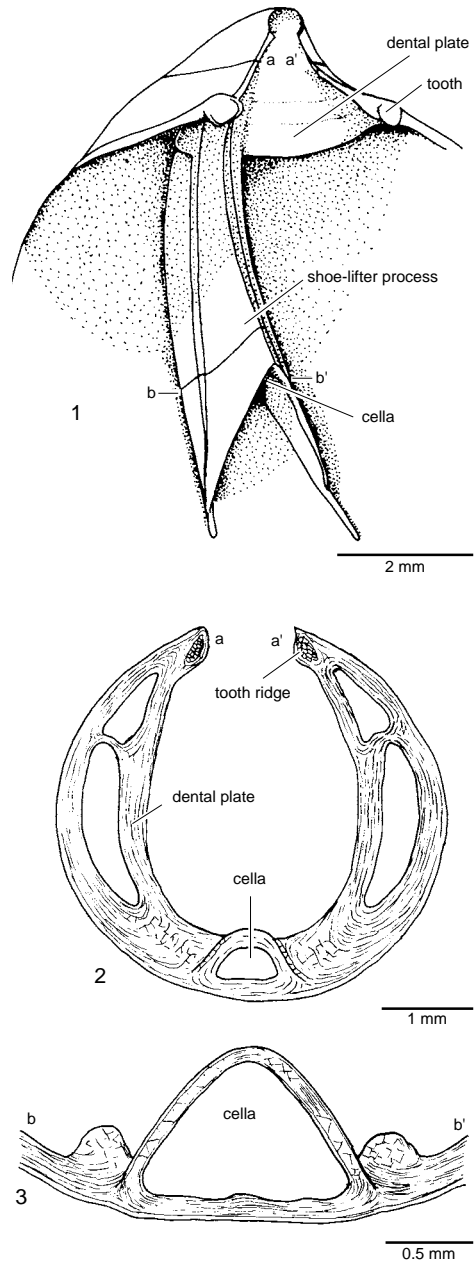


FIG. 356. Ventral valve of *Merista tennesseensis* HALL & CLARKE, Middle Silurian, USA, showing shoe-lifter process; 1, oblique view showing location of 2–3, transverse sections (adapted from Williams & Rowell, 1965b).

plectambonitoids resemble, to some extent, the elevated diductor attachments of the cardinal flange condition, their paired diductor

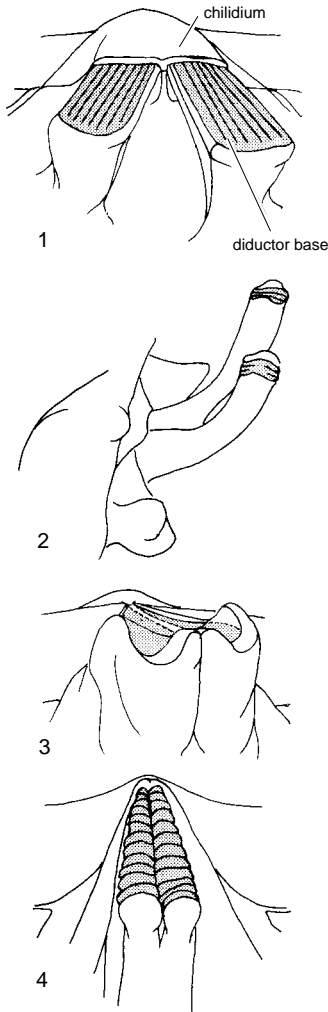


FIG. 357. Various types of bilobed cardinal processes; 1, *Rafinesquina*; 2, *Oxoplica*; 3, *Resserella* (weakly fused bilobed producing a trifold cardinal process); 4, *Dalmanella* (adapted from Williams & Rowell, 1965b).

scars and traces of their myophores from their origins close to the ventral beak and anteriorly across the cardinal process confirms their basic style of cardinal processes.

Another style of cardinal process, seen in many spire bearers, rhynchonellides, and terebratulides, is where the dorsal ends of the diductor muscles commonly produce a single attachment scar with no median separating structure. In the least elaborate taxa, the site of dorsal diductor muscle attachment occupies a shallow posteromedian depression

or shallow **cardinal pit** at the dorsal umbo, but in others the muscle bases tend to encroach more widely onto a variety of structures in the cardinalia, such as the posteromedian ends of the inner socket ridges or the crural bases, as in *Hemithiris* (Fig. 349). In some fossil taxa an undifferentiated horizontal plate, the **cardinal plate**, extended between the inner socket ridges; in others a more restricted **hinge plate** partly or completely filled the gap between the crural bases. To maintain posteromedian attachment of the dorsal diductors on the valve floor, both types of plates incorporated a hole or **dorsal foramen** (Fig. 362) that would have allowed the muscles to pass from the dorsal beak to the ventral valve floor. In others the muscle bases spread onto prominent ridges at the beak, such as the ctenophoridium of many spiriferides or onto reduced cardinal plates, in some producing structures resembling a bilobed style of cardinal process, as in the cardinal flanges of athyridids (Fig. 359.2). Cardinal flanges are best seen in athyridids where the dorsal ends of the diductor muscles in juvenile and stratigraphically older species were inserted onto the beak floor. In stratigraphically younger species the dorsal foramen, which earlier was functional, became blocked by secondary shell, and the muscles became attached to the posterior edge of the cardinal plate. Here exaggerated growth of the posterior ends of the inner socket ridges gave rise to more substantial cardinal flanges, to which the diductor muscles became attached. These flanges, well developed in the genus *Pachyplax* (Fig. 359.1), were serrated in a manner characteristic of a myophore. In other athyridids, such as *Cleiothyridina* or Permian *Composita* (Fig. 359.2), the muscle bases spread onto reduced and much thickened cardinal plates, while in others the diductor scars produced shallow serrated pits on the cardinal plate. ALVAREZ and BRUNTON (1990) pointed out that this growth in athyridids was similar to that seen during the ontogeny of the recent *Eohemithiris* in which the diductor muscles spread from the juvenile median position onto the posterior ends of

the crural bases and reduced inner hinge plates.

In some retzioids (e.g., *Nucleospira*), a juvenile median ridge grew ventroposteriorly into a hooklike structure extending into the ventral umbo (Fig. 363.1). This resembles a small version of the bilobed cardinal process of orthotetid meekellids, but is built of medially united cardinal flanges. Unlike the bilobed cardinal process of strophomenates, which preserves growth traces of the myophores on the external (posterior) surfaces (Fig. 364), the retzioid structure is smooth as if secreted by conventional epithelium during growth. The myophores, being restricted to the distal tips, leave no growth traces (Fig. 363.2). This exaggerated cardinal flange has been called a cardinal process by some and a cardinal plate by others, but it cannot be the latter because the myophores, being distally positioned, would be in an impossible position at the anterior end of a more normally disposed cardinal plate.

No elaborate dorsal diductor attachment structure is known among the Pentamerida. In some Cambrian genera there is a small median ridge, probably separating the diductor bases; in later genera there is a lack of any positive structure, and the diductor bases probably formed a single median scar, as seen in more recent rhynchonellids. In early rhynchonellids there is no elaborate diductor attachment structure, but in some

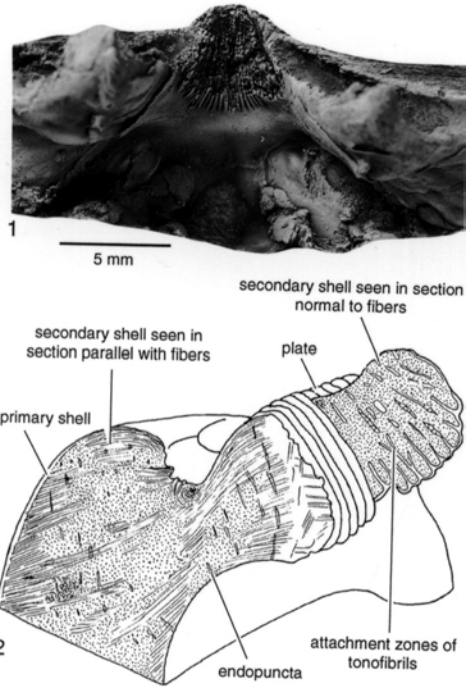


FIG. 358. Cardinal process, of ctenophoridium type; 1, *Fusispirifer* sp., Permian, Tasmania, with a sessile cardinal process (new); 2, *Terebratalia transversa* (SOWERBY) in median and tangential sections showing associated shell structure (Williams & Rowell, 1965b).

a median ridge became enlarged into a bosslike structure, as in *Clarkeia*, and some genera developed a posterior, transverse structure resembling the ctenophoridium of some spiriferides (e.g., *Hypothyridina*).

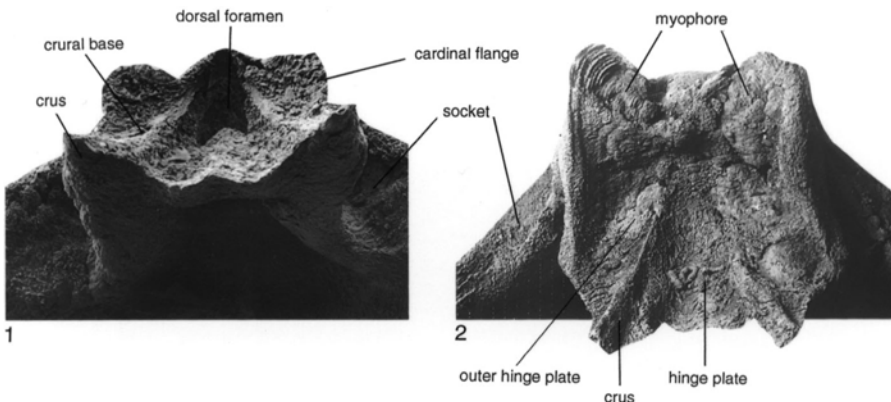


FIG. 359. Internal views of cardinalia in 1, *Pachyplax gyralea* ALVAREZ & BRUNTON, Lower Devonian, Spain, $\times 30$ (Alvarez & Brunton, 1990) and 2, *Composita crassa* COOPER & GRANT, Middle Permian, Texas, USA, $\times 10$ (new).

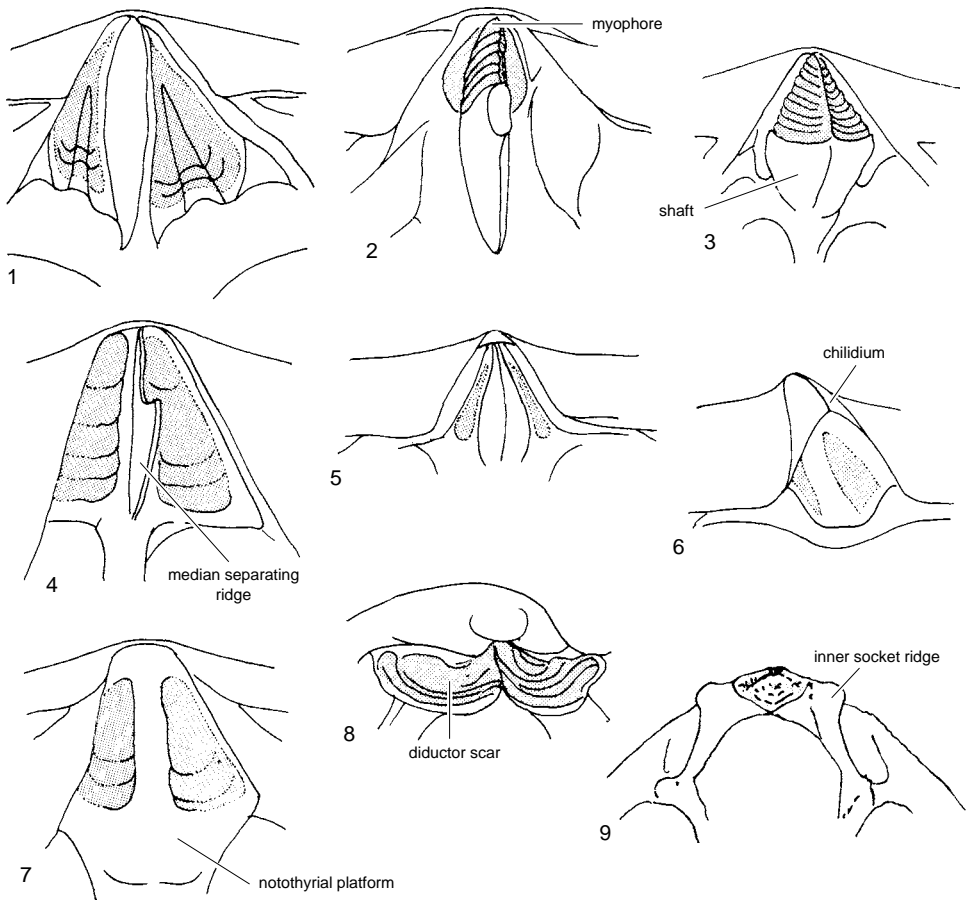


FIG. 360. Various types of cardinal processes; 1, development of subsidiary ridges flanking median ridge of *Glossorthis*; differentiation of myophore and shaft in 2, *Hebertella* and 3, *Dinorthis*; simple partition of 4, *Glyptorthis* and 5, *Bimuria*; diductor scars on notothyrial platform with no enclosing ridges of 6, *Leptella* and 7, *Nothorthis*; and transverse and elevated muscle scars utilizing crural bases and inner socket ridges in 8, *Notosaria* (adapted from Williams & Rowell, 1965b) and 9, *Terebratulina* (new).

During the Mesozoic and up to recent times rhynchonellides generally failed to develop strong diductor attachments, retaining a median diductor pit flanked by scars extending onto the crural bases (Fig. 349).

The early terebratulides tend to display diductor attachment characters similar to those of athyridides with a dorsal foramen, and in stringocephaloid genera, with strongly developed ventral umbones, the cardinal process grew posteroventrally in an exaggerated fashion like those of some retzioids. Because of the ventral median sep-

tum in these terebratulides, however, the myophores divided so as to simulate the bilobed cardinal process of triplesioids. Genera with hinge plates bearing a dorsal foramen continued to the close of the Paleozoic after which the dorsal diductor scars were commonly spread onto the more median structures of the cardinalia. The distinctly knoblike structures associated with the cardinal processes of many adult species, such as *Chatwinothyris* or *Neothyris*, result from differential, posterior, shell thickening and weighting that accompanied a tendency to a

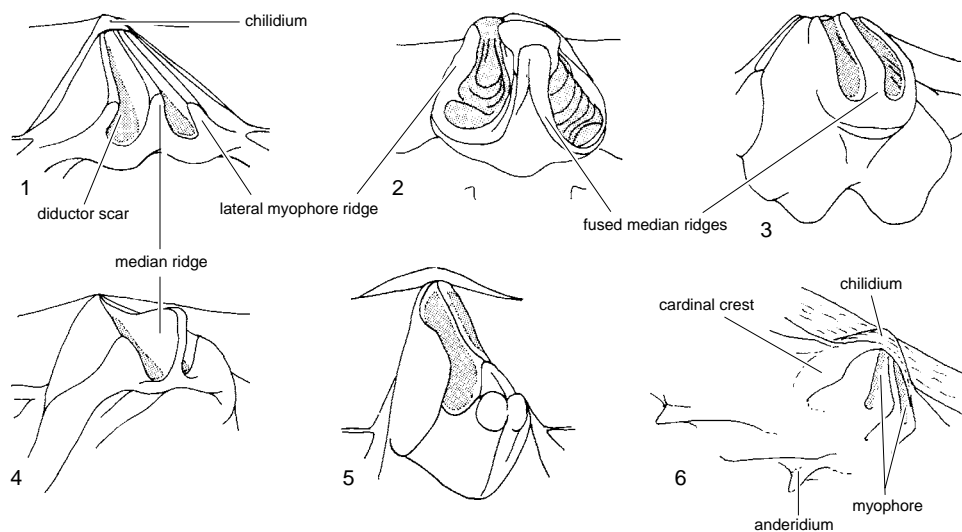


FIG. 361. Various types of trifold cardinal processes; 1, *Sowerbyella*; 2, *Pugilis* viewed posteriorly; 3, *Prionothisyris*; 4, *Orthidiella*; 5, *Paucicrura* (Williams & Rowell, 1965b); 6, a chonetoid (new).

freeliving mode of life. Again, in genera with elongate or strongly inflated ventral umbos the cardinal process extended posteriorly carrying the diductor bases into the ventral valve, but in no instance did these structures preserve the trace of the myophores on their dorsal surfaces as they would have if originating like the cardinal processes of strophomenides. The same is true of recent thecideioids, in which the diductors attached to the inner surface of ventrally or posteriorly facing distal ends of enlarged and unified cardinal flanges, lying between the inner socket ridges. Again this structure resembles a strophomenate cardinal process from the inner side, but externally it is smooth, and the muscle bases leave no scars on the external surface of the structure.

The attachment areas of the dorsal ends of the adductor muscles normally consist of two pairs of scars impressed on the floor of the dorsal valve at a variable distance anterior of the cardinalia. The scars may differ in size and arrangement, but they are commonly disposed in the median area of the valve with the posterior pair flanking the more closely placed anterior pair (Fig. 348.3a). Modification by differential secretion of secondary

calcite is minor except for the deposition of a median ridge that normally extends anteriorly from the vicinity of the cardinalia to separate the right and left set of adductor impressions (**myophragm**). The muscle field may, however, be raised above the floor of the valve in a number of different ways that deserve a brief review.

The best-known elevated structure for the reception of the dorsal adductor bases is the **cruralium**, which, like its ventral



FIG. 362. Cardinalia of *Cleiothyridina seriata* GRANT, Permian, Thailand, showing exaggerated inner socket ridges and dorsal foramen enlarged posteriorly by action of diductor muscles, $\times 7$ (new).

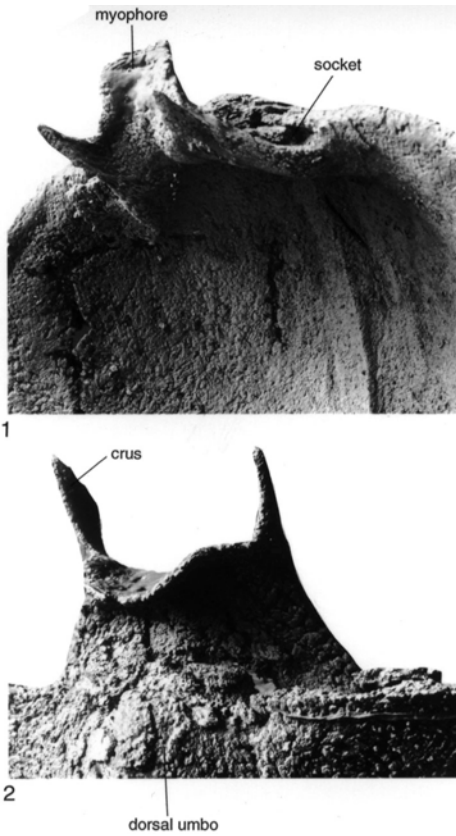


FIG. 363. Cardinalia of *Nucleospira carlukensis* (DAVIDSON), Lower Carboniferous, Ireland, viewed 1, internally (SEM, $\times 27$) and 2, externally (SEM, $\times 34$). The myophore is confined to the cardinal process tip and leaves no trace externally (new).

counterpart, the spondylium, is especially characteristic of the pentameroids (KOZŁOWSKI, 1929). It was formed by the forward growth of the inner hinge plates underlying the base of the brachiophores to receive part or all of the adductor muscle field. The plates may be subparallel to divergent (e.g., *Pentamerus*) or variably convergent (e.g., *Gypidula*, Fig. 365) so that they grew forward along the floor of the valve independently of each other to enclose a strip of the valve floor. Alternatively, they may converge to unite with each other at their junction with the valve floor, with the sessile cruralium of *Barrandella*, or above the valve floor to which they are joined by a median septum. The median septum of *Sieberella* is reported to have been developed indepen-

dently of the plates, but in some species of *Pentamerella* it is known to have been formed by the ankylosis of the converging plates.

The term cruralium has been used for structures that may have originated in the same way as those characteristic of the pentameroids but that could not have given support to the dorsal adductor field. The elevated troughs found in the dorsal valves of the syntrophiids and parastrophinids (Fig. 366) or of the skenidiids and *Kaysarella*, for example, were formed by the convergence of the brachiophore bases onto the valve floor or a median septum, but they all lie well posterior of the adductor scars and are more like septalia than cruralia, as originally understood by HALL and CLARKE (1894–1895). Moreover, although the spoonlike apparatus in the dorsal valve of stenoscismatoids gives support to the dorsal adductor muscles, its growth around a high median septum was independent of the crura, and it is more appropriately called a **camarophorium** or **torynidium** (Fig. 367; COOPER, 1956). The **spyridium** of *Spyridiophora* (COOPER & STEHLI, 1955) and some aulostegids also supported the dorsal adductor muscles but did so on the transversely flattened posteroventral surfaces of a pair of subparallel plates that grew vertically from the floor of the

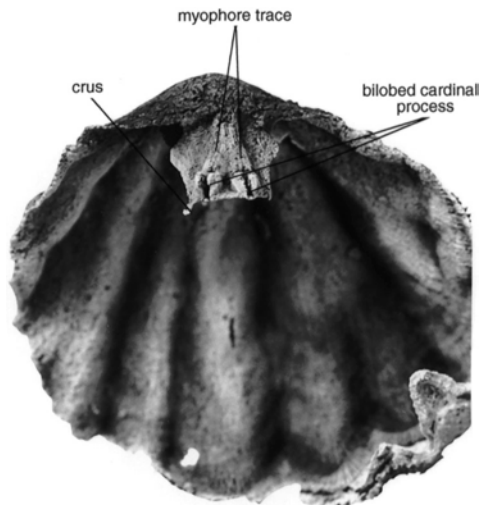


FIG. 364. Cardinalia of *Meekella*, Permian, Texas, viewed posteroventrally showing growth traces of myophores on cardinal process shaft ($\times 216$) (new).

dorsal valve on either side of a low median septum (Fig. 368.1). These plates are quite different in disposition from the **braceplates** (WILLIAMS, 1953) of such strophodontids as *Douvillina* (Fig. 369), which grew antero-medially of the adductor field and are more likely to have given support to the median segment of the lophophore on either side of the mouth. In contrast, the apparatus subtended between the brachiophores and median septum of *Mystrophora* (COOPER, 1955) accommodated the dorsal adductor bases and is correctly called a cruralium.

Articulated brachiopods developed pedicle adjustor muscles from an early age, commonly producing scars that were visible before the scars of the diductor muscles. The dorsal adjustor muscles are situated on the posterior ends of the crural bases or on the inner hinge plates. During growth these scars moved forward so that in adult specimens they occupy the anterior regions of the inner hinge plates. The muscles commonly acted to rotate the shell relative to the attached pedicle. In some genera these plates united medially, forming a troughlike **septalium** that, in some, is supported on a median septum (Fig. 330.4), while in others it is sessile, resting directly on the valve floor, and in some it is unsupported. If the united inner hinge plates are unsupported, flat and medially undifferentiated between the crural bases, they are called a hinge plate (Fig. 330.3). Although the septalium commonly accommodated adjustor muscles and provided the base from which the cardinal process developed, it did not accommodate dorsal adductor muscles. For this reason septalia generally do not extend forward of crural bases, as do cruralia. A distinctive functional variation in the positioning and style of dorsal adjustor muscle scars has been described by MINEUR and RICHARDSON (1984) and RICHARDSON (1991). Posteriorly thick-shelled terebratulides, such as the Anakineticinae, living in shallow-water sands, have long, thin, and mobile pedicles to which the dorsal adjustor muscles tend to be attached close to the cardinal process, leaving small, distinctive scars. This relatively posterior position allows the pedicle the maximum

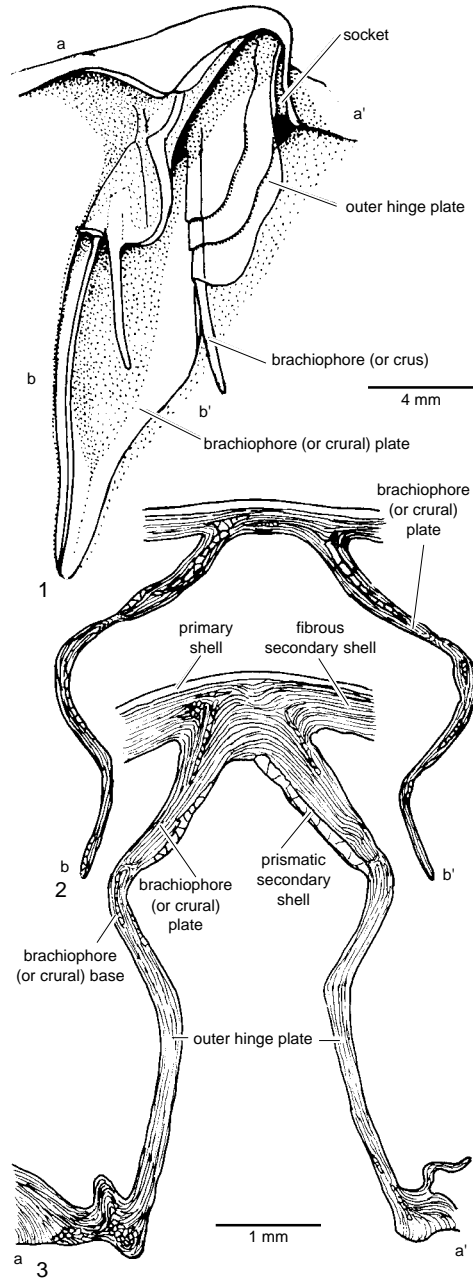


FIG. 365. Parts of dorsal valves of *Gypidula*; 1, *G.* sp., Middle Devonian, USA, with convergent brachiophore plates simulating sessile cruralium; 2-3, transverse sections of *G. dudleyensis* SCHUCHERT, Upper Silurian (Wenlock), England, in planes indicated on 1 (adapted from Williams & Rowell, 1965b).

extension and withdrawal movement, which aids the specimen in shifting its position in

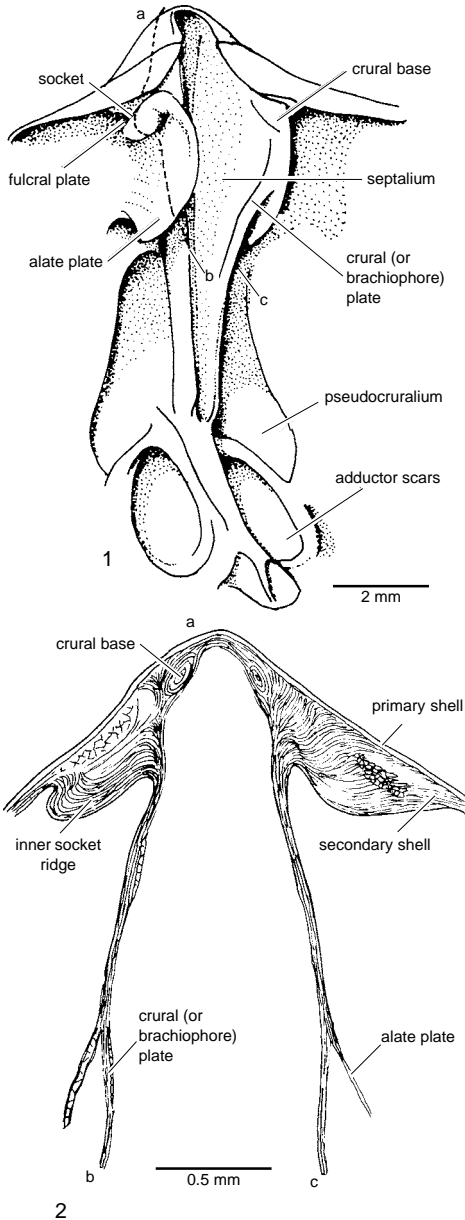


FIG. 366. Part of dorsal valve of *Anastrophia* sp., Middle Silurian, England, showing 1, cardinalia relative to dorsal adductor field, and 2, oblique section along line indicated in 1 (adapted from Williams & Rowell, 1965b).

In the ecologically similar Tertiary to recent terebratulide subfamily, the Bouchardiinae, the living type genus, *Bouchardia*, has been recognized as distinctive since being

established by DAVIDSON in 1850. They also live in shallow water on coarse-grained sediments off the southeastern coast of South America (MANCENIDO & GRIFFIN, 1988). These shells are unique in having such highly and extensively thickened valves posteriorly, especially the cardinalia, that they completely fill the posterior internal space other than for muscle grooves and a central tunnel accommodating the pedicle (Fig. 370.3–370.4). Despite the high-energy environment of this genus, the pedicle adjustor muscles are reduced to a small, ventral pair attached immediately posterior to the ventral, centrally placed adductor scars. This reduction is related to the trend, suggested by RUDWICK (1970) and RICHARDSON (1973), of the activity of the reduced pedicle being correlated with increased weight of the posterior portion of the shell. The most obvious feature of *Bouchardia* is the dorsal, inverted V-shaped muscle scar. This represents the apical area of true muscle attachment (cardinal process) plus paired anterior grooves, in which the muscles were confined as they traversed the thickened posterior region. Anteriorly these grooves project from the anterior face of the massive cardinalia (**hinge platform**) (Fig. 370.2, 370.4). The diductor muscles become fan-shaped anteriorly and attached ventrally to poorly differentiated, widespread scars anterolateral to the adductor scars (Fig. 370.1).

In some genera (e.g., *Hypsomyonia*), the growth of a high, dorsal median septum was accompanied by the elevation of the anterior boundaries to the dorsal adductor field above the floor of the valve. KOZŁOWSKI (1929) has proposed the term pseudocruralium for this kind of structure, but it hardly seems necessary to distinguish it from raised, callus rims of secondary calcite that commonly define the limits of the scars. In other genera, high median septa, commonly in ventral valves, include areas of **myotest**, as in *Cyrtina*, indicating that muscles attached to their sides (Fig. 354.3). The term myophragm has been used in these situations as well as for low ridges dividing muscle scars.

Apart from septa that clearly played a part in accommodating muscle bases, found in either valve, a few articulated brachiopods (e.g., *Phragmorthis*, *Skenidioides*, and *Mystrophora*) were equipped with septa that stood so high above the floor of the dorsal valve as to divide the mantle cavity into two compartments (Fig. 371). A septum of this kind usually rises steeply to its apex along its posterior edge, whereas the anteroventral edge tends to fall away more gently in a curve conforming to the anteromedian longitudinal profile of the pedicle valve. This characteristic profile and the closeness of the fit with the ventral valve, when the shell was closed, suggest that the septum was associated with the lophophore. It is unlikely, however, that the septum gave support to the lophophore, although it may have assisted in the separation of the left and right halves of that organ during its schizolophous growth, in a manner reminiscent of comparable outgrowths in the dorsal valves of terebratelloids. Transverse partitions, again unrelated to the insertion of muscle bases, are also found in the ventral valves of such independent stocks as richthofeniids (MUIR-WOOD & COOPER, 1960), scacchinellids (WILLIAMS, 1953), and *Syringospira* (COOPER, 1954) (in which they are known as **blisters**). All shells with these **cystose** structures have deep, conical or subpyramidal ventral valves that must have grown at a faster rate than the enlargement of the contained soft parts so that the viscera migrated continually dorsally (Fig. 372). The formation of these blisters must have involved the movement of the brachiopod's body away from its shelly floor, aided by the secretion of a thin organic layer allowing uncoupling of the epithelium from the skeletal material, as in the process of mantle regression. This movement left a space across which the outer epithelium secreted a new organic membrane that acted as the seeding surface for a new shell partition and creation of a new blister (Fig. 372).

Muscle scars and, more rarely, muscle tracks are developed in the inarticulated brachiopods and are impressed on the inner

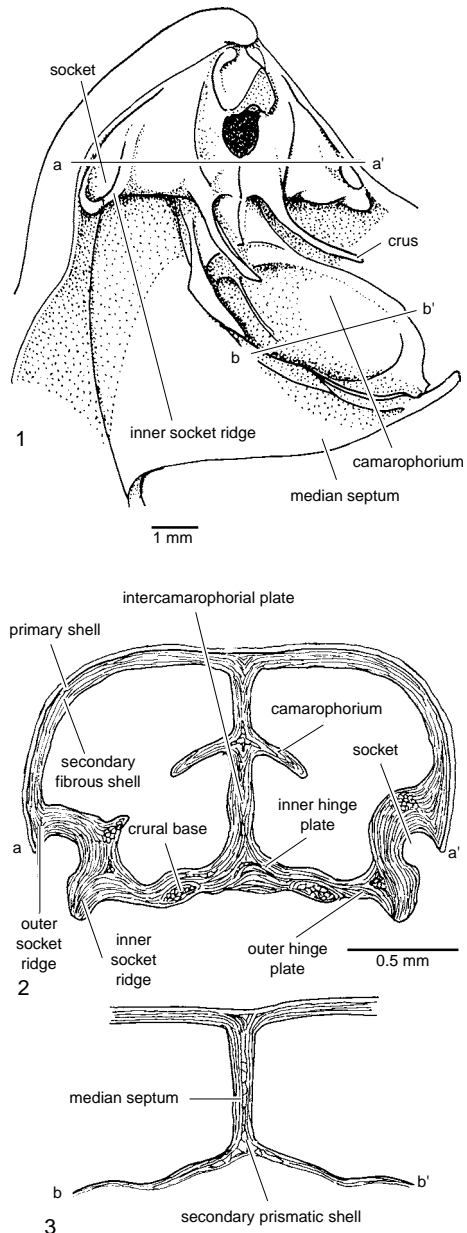


FIG. 367. 1, Camarophorium of *Stenosisma* sp., Middle Permian, USA; 2–3, transverse sections of camarophorium of *Stenosisma* sp., Upper Devonian, USA, with approximate location of cuts indicated on 1 (adapted from Williams & Rowell, 1965b).

surface of the valves by differential secretion of the outer epithelium associated with the muscle bases, and in this sense they are

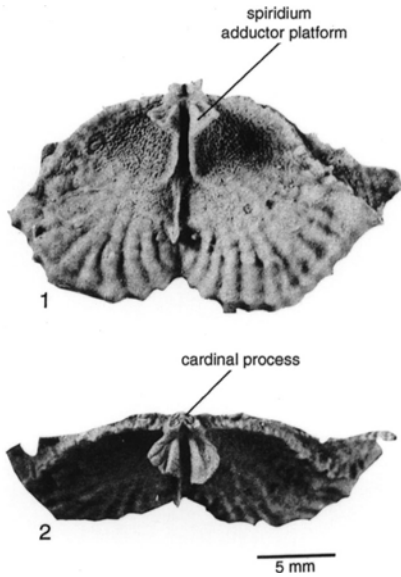


FIG. 368. *Spiridiophora reticulata* (R. E. KING), Lower Permian, Texas, USA, showing the spiridium viewed 1, ventrally and 2, posteroventrally (Cooper & Grant, 1975).

closely comparable with the scars and tracks of the articulated brachiopods. Commonly this differential secretion merely involves a reduced rate of deposition of shell material, the shell underlying the muscle scars being similar in structure and composition to the remainder of the valve. Within the inarticulated brachiopod groups the numbers of muscles and their scars are variable, unlike the regularity of scars in the articulated groups.

Physiological changes of the epithelium at the base of the muscles may, however, be pronounced, as in *Neocrania*, where the modified epithelium is responsible for the deposition of calcite intracellularly, in marked contrast to the extracellular secretion that characterizes the rest of the outer epithelium. In fossil cranioids, from the time of *Pseudocrania* in the Early Ordovician, muscle scars are commonly well preserved and similar to those of recent *Neocrania* (Fig. 373) in being distributed peripherally within the body cavity as two paired muscle fields in each valve. In recent species the paired ad-

ductors pass more or less directly between the valves, and they have been considered homologous with the adductor muscles of discinids and lingulids. Indeed it is possible that their musculature represents the primitive state for all stocks, the earliest known craniopsid-like brachiopod, *Heliomedusa* from the Early Cambrian apparently having a similar muscle pattern (JIN & WANG, 1992). Other aspects of craniid musculature are more unusual; the **oblique lateral** muscles in *Neocrania* are attached close to the posterior adductors in the ventral valve, but they are not attached to the dorsal valve but to the anterior body wall (see section on anatomy, Fig. 84). All known fossil craniids have similar oblique lateral muscle scars, unique to the group. GORJANSKY and POPOV (1986) suggested they might have acted as a type of diductor muscle by creating hydrostatic pressure in the body cavity; unlike recent lingulids, *Neocrania* does not have a well-developed musculature in the body wall and thus probably cannot open its shell as described by TRUEMAN and WONG (1987). The **internal oblique** muscles of craniids are

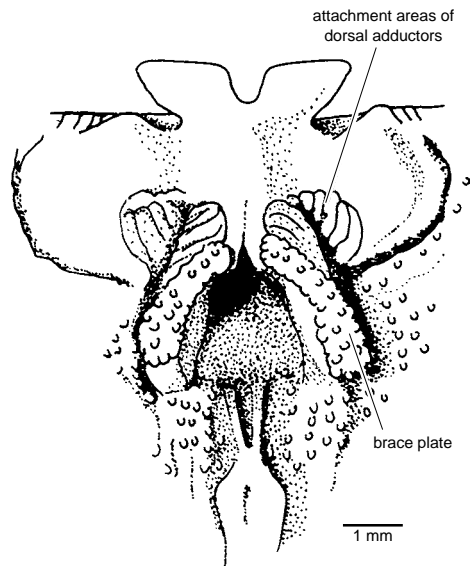


FIG. 369. Representation of brace plates in *Douvillina*, based on *D. arcuata* (HALL), Upper Devonian, USA (Williams & Rowell, 1965b).

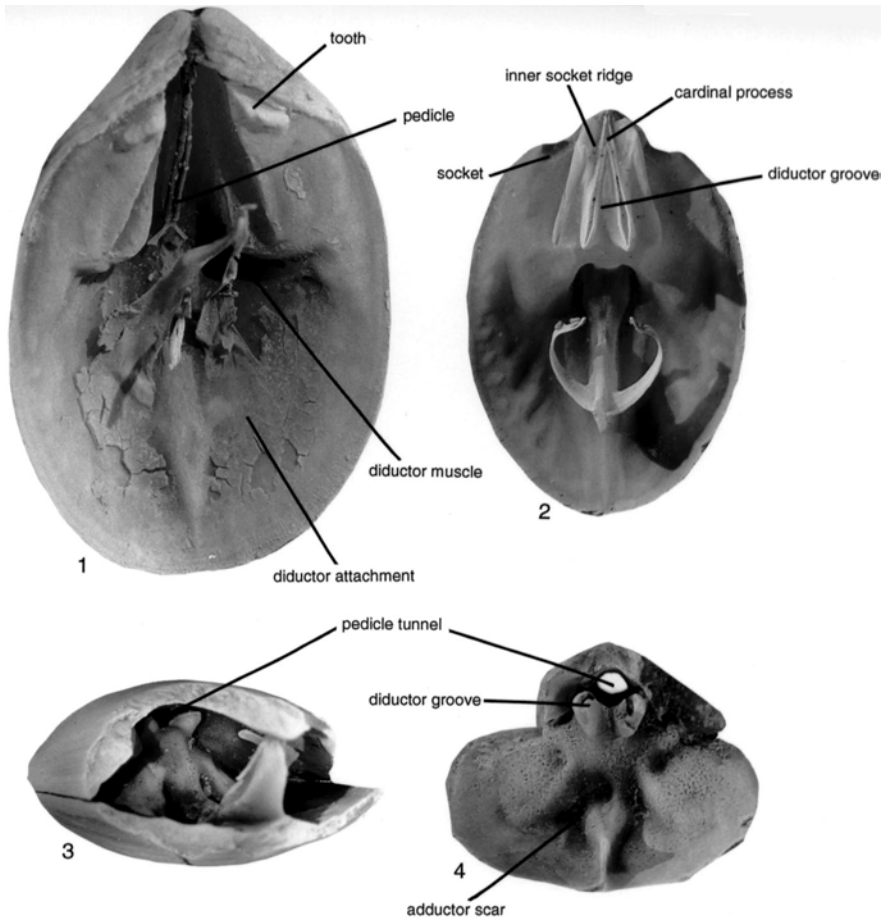


FIG. 370. *Bouchardia* specimens; 1–3, *B. rosea* (MAWE), recent, Rio de Janeiro; 4, *B. antarctica* BUCKMAN, Eocene, Seymour Island, Antarctica; 1, ventral valve interior of a dry specimen retaining muscles, $\times 5$; 2, dorsal valve interior of a cleaned specimen, $\times 4$; 3, oblique anterior view of a cleaned, articulated specimen showing the massively thickened cardinalia, $\times 4$; 4, anterior view of the posterior region of an articulated specimen, $\times 3$ (new).

the only oblique muscles comparable with those of lingulids and discinids; they are attached to the anteromedian region of ventral valves and close to the posterior adductors in the posterolateral region of the dorsal valve. Craniids also have a unique, unpaired **median muscle** controlling the position of the anus and several other muscles associated with the lophophore, all of which are also commonly preserved as scars in fossils.

The musculature of the extinct craniopsids and trimerellids has commonly been compared with that of lingulids, but

GORJANSKY and POPOV (1985) interpreted the preserved muscle scars in these two groups by comparison with the craniids. Craniopsids (Fig. 374.1) have an unpaired median muscle scar posteriorly in both valves, comparable to that of craniids. In addition there are three paired dorsal and four ventral muscle scars comparable with the anterior and posterior adductors, oblique lateral, and the **brachial protractor muscles** of craniids (Fig. 374).

Muscle scars of trimerellids are more unusual, being different from those of lingulids (NORFORD & STEELE, 1969). All trimerellids

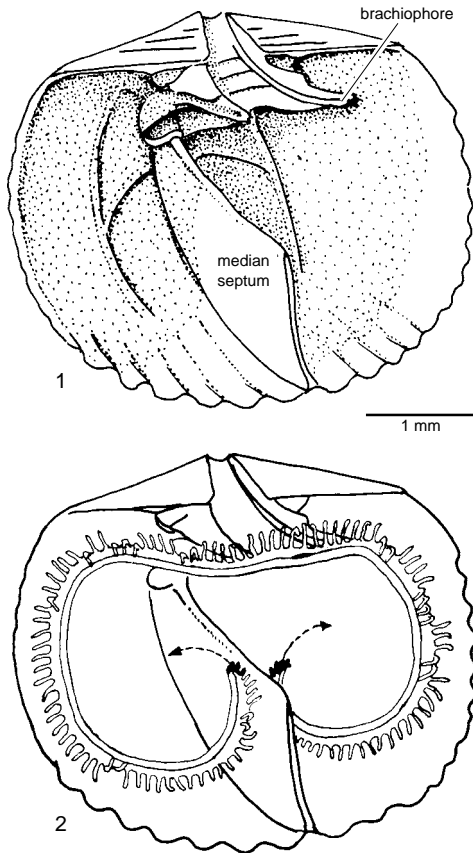


FIG. 371. 1, Dorsal interior of *Phragmorthis* sp. cf. *P. butsi* COOPER, Middle Ordovician, Scotland, with 2, inferred disposition of lophophore about median septum (adapted from Williams & Rowell, 1965b).

have scars of two paired adductors, but some genera (*Palaeotrimerella* and *Eodinobolus*) have posterior diductor scars that might have worked posterior to the axis of rotation (Fig. 374; NORFORD & STEELE, 1969; GORJANSKY & POPOV, 1985, 1986), more as in the articulated brachiopods. In younger forms like *Trimerella* (Fig. 375), muscle platforms are hollow anteriorly and are elevated high above the valve floor, being supported medially by a **median partition** that projects in front of the platform and divides the cavity beneath it into two subtubular vaults. The entire platform was invested in and secreted by outer epithelium. During the earlier stages of growth of the animal, the front edge of the platform and the median partition grew an-

teriorly, and the posterior ends of the vaults were progressively infilled with shell material secreted by the infolds of epithelium lining them.

Calcareous-shelled members of the Obolllida include genera lacking articulatory structures (*Obollla*) as well as those with primitive structures (*Alisina*, *Trematobolus*, and *Oina*), but the muscle scars are invariably comparable to those of true articulated brachiopods (Fig. 376); they preserve scars of paired anterior and posterior adductors commonly forming a quadripartite muscle field in the dorsal valve.

In phosphatic-shelled brachiopods muscle scars are also produced by differential secretion of the outer epithelium between the muscle bases and the shell. This process includes not only differential rates of deposition but also changes in the relative amounts of organic and mineral components in the shell material underlying the muscles. The muscles in the two recent groups, the Linguloida and the Discinoida, can be divided into **dermal**, adductor, and oblique muscles (see section on anatomy, p. 83). The dermal muscles in both groups are probably responsible for the hydraulic opening of the shell, although this is only confirmed experimentally in the lingulids (TRUEMAN & WONG, 1987). Recent discinids have paired posterior adductors, which are probable homologues of the unpaired umbonal muscle in recent lingulids, and paired anterior adductors are apparently the equivalent of lingulid central muscles (see section on anatomy, Fig. 83). The scars of these muscles are commonly well preserved, even in their earliest known fossils, but in the early Paleozoic Obolllidae the scars of the umbonal muscles are paired (MICKWITZ, 1896; POPOV, 1992), which indicates that this type of musculature is primitive for lingulids and discinids, while the unpaired umbonal muscles appeared comparatively late in lingulid evolution, in the late Paleozoic and only in the Lingulidae.

In recent lingulids and discinids the oblique muscles control rotation and sliding of the valves; there are four pairs of these

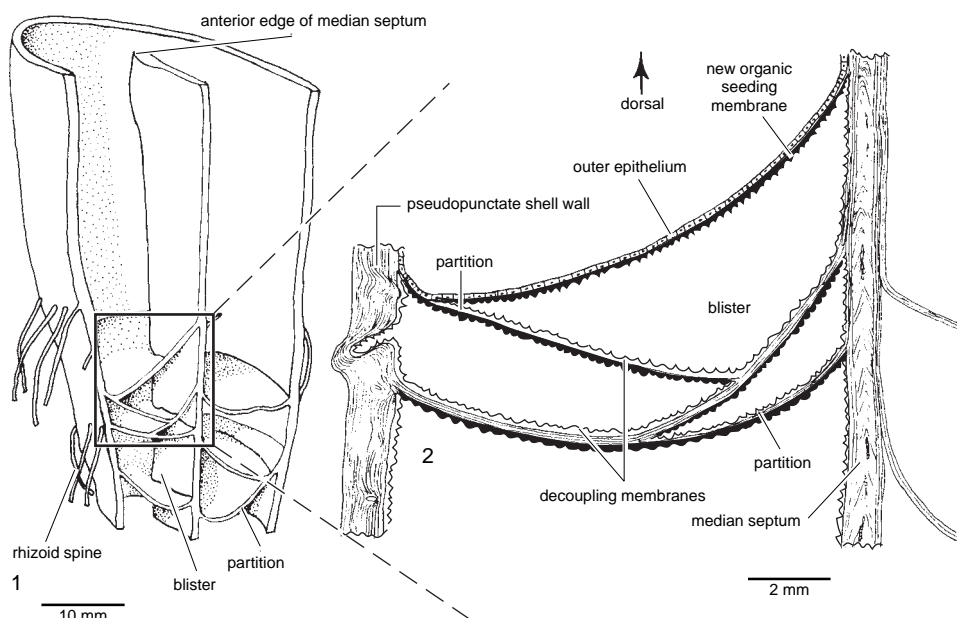


FIG. 372. 1, Ventral valve of *Scacchinella americana* STEHLI, Lower Permian, USA, cut parallel with and anterior to interarea; 2, section showing inferred relationship between transverse partitions and outer epithelium (adapted from Williams & Rowell, 1965b).

muscles in the Lingulida and three in the Discinida. The largest oblique muscles, the **transmedian**, are asymmetrically situated in recent Lingulidae, a position unique to this family. Scars indicating an identical type of asymmetry are recorded in Lingulidae as old as the Mesozoic (EGOROV & POPOV, 1990; BIERNAT & EMIG, 1993), and this type of musculature may be an adaptation to a more active, burrowing mode of life. In general oblique muscles are poorly defined in fossil representatives.

Apart from the Lingulidae, all known lingulides had symmetrical musculature that appears to have been conservative and almost identical to the pattern in obolides like *Oepikites*, *Obolus*, and *Ungula* (POPOV, 1992); it consists of four, major muscle fields (Fig. 377): (1) an umbonal field with paired **umbonal muscle** scars in both valves; (2) ventral **transmedian** and **anterior lateral** scars and dorsal transmedian, **outside lateral** and **middle lateral** scars in posterolateral muscle fields invariably placed posterolateral to the *vascula lateralia* in both valves; (3)

ventral middle lateral and **central muscle** scars and dorsal central scars antero-central to the *vascula lateralia* in both valves; and (4) the dorsal **anterior lateral muscle** field situated in the narrow, central, anterior projection of the dorsal body cavity.

The acrotretoid muscle system is reduced, as compared to the lingulides, and each valve of most species (including *Acrotreta*) has the following three muscle fields (Fig. 378): (1) a thickened field (**median buttress**) with one or two scars posteromedially in the dorsal valve and a field with two small scars (apical pits) directly lateral to the pedicle opening in the ventral valve; (2) a large, usually thickened, posterolateral field (**cardinal muscle** scars) in both valves; and (3) a small dorsal field with **antero-central** scars placed directly lateral to the median septum and an equally small, but strongly raised scar on the **apical process**, just anterior to the pedicle opening.

The muscle system of acrotretides has been poorly understood, and it is difficult to homologize their muscles with lingulides. WILLIAMS and ROWELL (1965b) compared

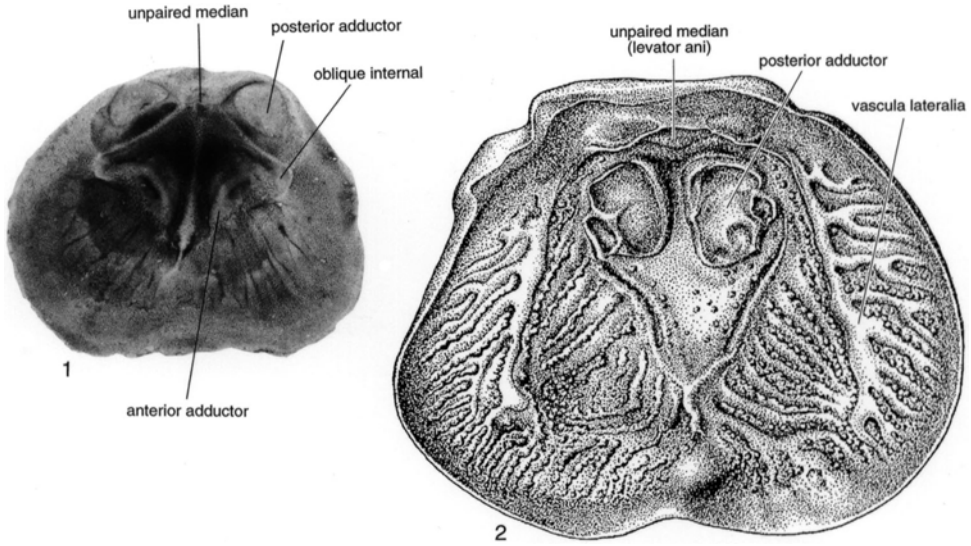


FIG. 373. 1, *Neocrania anomala* (MÜLLER); dorsal valve interior showing main muscle scars, recent, west coast of Sweden, $\times 6$; 2, *Petrocrania* sp.; dorsal valve interior (anterior adductor scars are not preserved), Silurian (Wenlock), Gotland, Sweden, $\times 6$ (new).

the inferred muscle system with discinoid or cranioid systems, suggesting that the large, posteriormost scars in each valve accommodated a pair of cardinal (umbonal) muscles; that the apical process, near the pedicle foramen, was the attachment for a pair of anterocentral muscles that attached dorsally close to the median septum (surmounting plate); and that these were equivalent to the posterior and anterior adductors respectively of cranioids (Fig. 346.1). POPOV (1992), however, has shown that the musculature is closer to that of lingulids (Fig. 346.2), the group from which he thought the acrotretides were derived. POPOV's (1992) interpretation necessitates the attachment of muscles within the apical pit and on the apical process of the ventral valve and the attachment of several muscles to some of the dorsal scars (Fig. 346.2).

The siphonotretoid muscle system is not well studied, although one pair of relatively large scars may be definitely recognized in each valve. According to HAVLIČEK (1982), some well-preserved *Siphonobolus* specimens have a full set of scars closely similar to those of Paleozoic obolides.

The internal morphology of the Paterinida, unfortunately, is only imperfectly known for a limited number of genera. Impressions on the internal surface of the shell

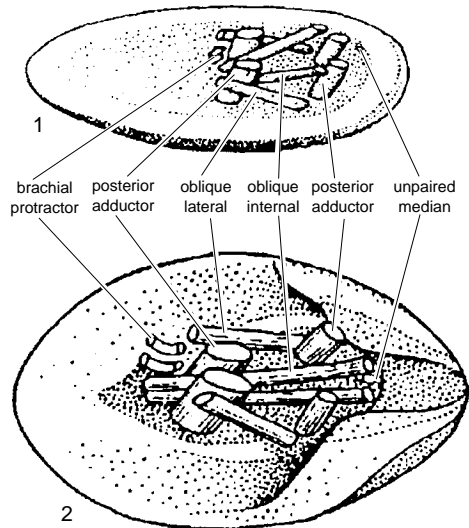


FIG. 374. Stylized reconstructions of muscle systems of 1, *Craniops* and 2, *Eodinobolus* (adapted from Gorjansky & Popov, 1985).

are very delicate, and it is difficult to be confident of their origin; but what are seemingly muscle tracks suggest that the musculature of this order differed considerably from that of the remainder of the inarticulated brachiopods (see Fig. 383). All of the scars recognized produce narrowly triangular tracks radiating from the apex. In the ventral valve two such tracks diverge slightly anteriorly, terminating near the center of the valve, whereas in the dorsal valve there are seemingly two pairs of tracks, one pair diverging anterolaterally and a second pair forming a single, medially located depression. The location of these tracks, if they are correctly

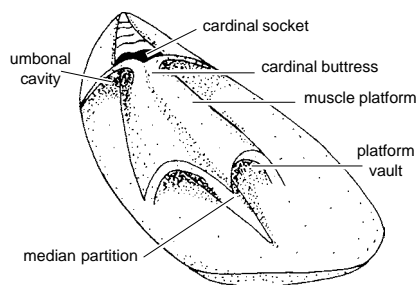


FIG. 375. Morphology of ventral valve of *Trimerella* (Williams & Rowell, 1965b).

interpreted as muscular in origin, in some ways is more reminiscent of the muscle system of articulated brachiopods.

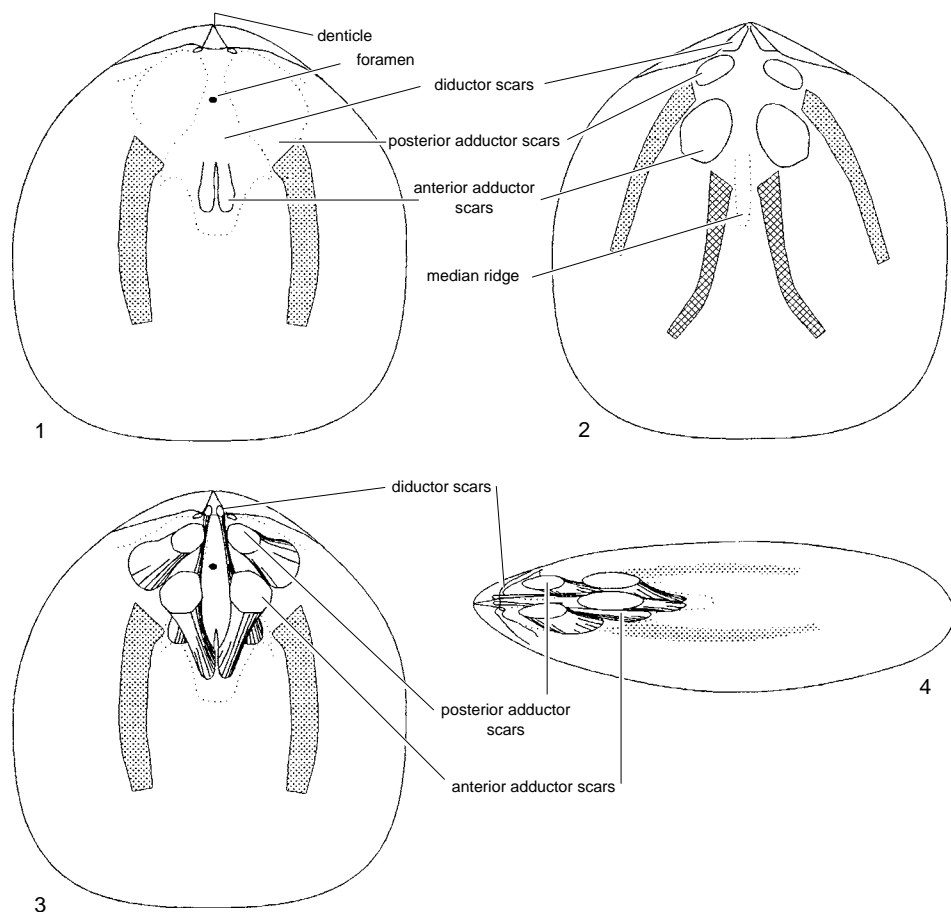


FIG. 376. 1–2, Muscle scars and 3–4, inferred musculature in the obolellide *Trematobolus*, based on *T. pristinus bicostatus* GORJANSKY, Lower Cambrian, north-central Siberia; 1, ventral valve interior; 2, dorsal valve interior; 3–4, inferred musculature viewed dorsally and laterally (new).

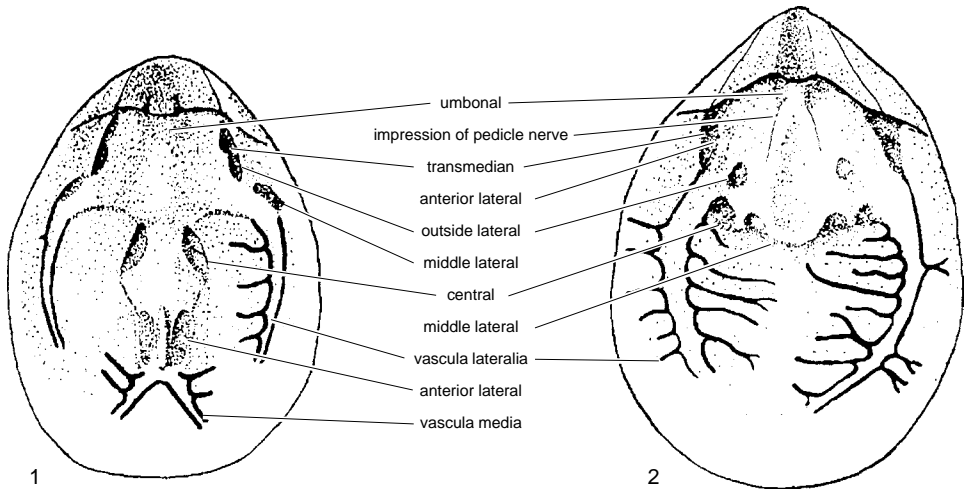


FIG. 377. Morphology of dorsal and ventral valves of *Oepikites*, showing muscle scars and mantle canals (new).

MANTLE CANAL SYSTEMS

The system of canals that pervaded the mantles of fossil brachiopods may be reconstructed by deciphering impressions on the interiors of both valves. These impressions consist of grooves or ridges, more or less symmetrically disposed on either side of the longitudinal midline, which are commonly seen to originate in the vicinity of the muscle scars. Many were differentially secreted by strips of outer epithelium, arching the canals, which deposited shell at a slower or, less commonly, faster rate than over the mantle generally. Larger, canal-like grooves may also truncate smaller ones, suggesting that they were caused by resorption (ROBERTS, 1968).

The fine distal branches of all canals, terminating just within the shell margins, are known to connect with setal follicles in living brachiopods. The disposition of impressions of terminal branches relative to grooves and eminences along the internal margins of fossil shells suggests that this arrangement always has obtained.

Interpretable patterns are rare and in general are more likely to be found not only in gerontic specimens but also, for some obscure reason, in older stocks (e.g., orthides, strophomenides, and porambonitoids); and it is symptomatic of this geological circumstance that the first analytic study of the patterns was prepared by ÖPIK (1934). He showed that arrangements deduced from a

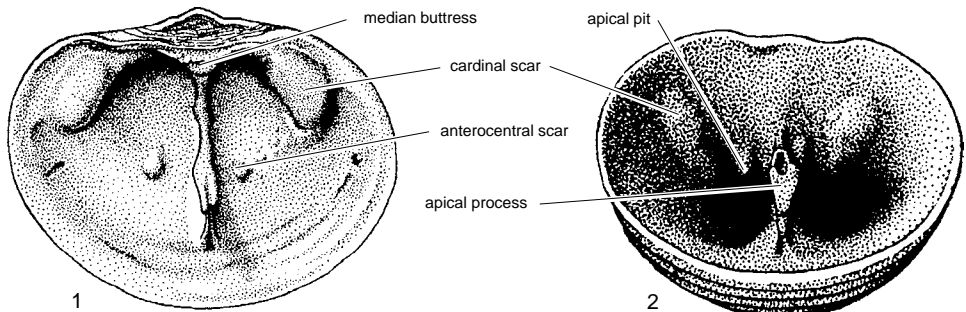


FIG. 378. Morphology of dorsal and ventral valves of *Ceratreta* (Holmer & Popov, 1990).

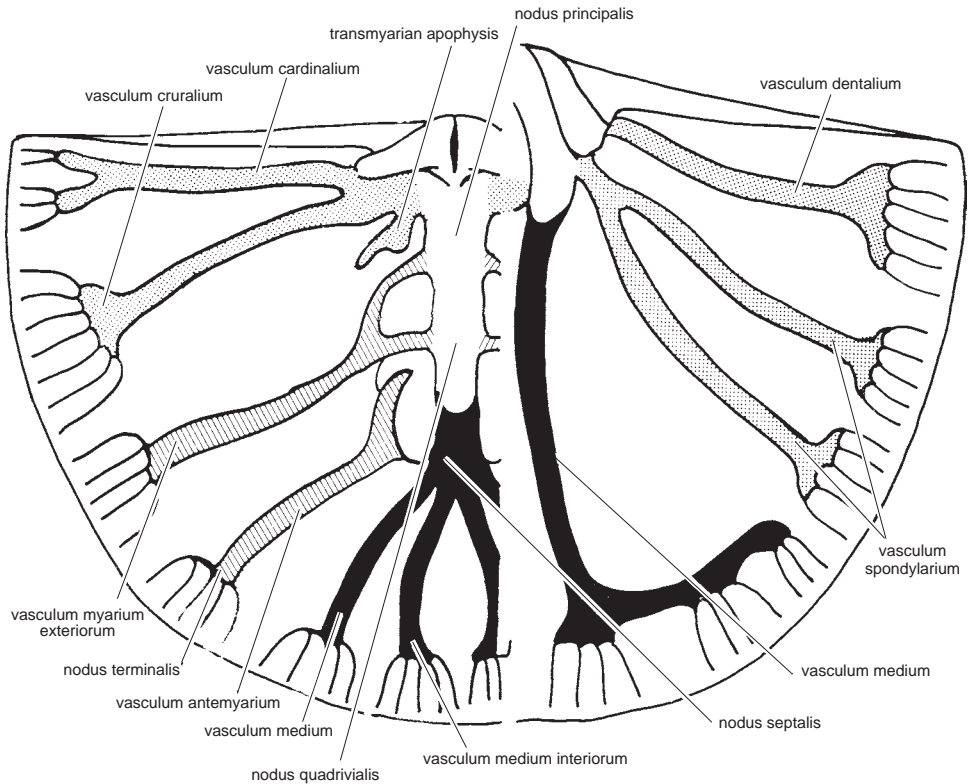


FIG. 379. Idealized canal systems in dorsal (to left) and ventral (to right) valves of primitive articulated brachiopod, especially to illustrate terminology used by ÖPIK (1934) (Williams & Rowell, 1965b).

study of the clitambonitoids were sufficiently consistent to merit a special terminology (Fig. 379). Some of the terms have been proposed for details of canal intersections or locations within what must have been the body cavity and the terms are not important in any comparative survey. But having regard for what is now known of the patterns in fossil and living shells, all canals can ultimately be related to three principal pairs of extensions of the body cavity into the mantles (WILLIAMS, 1956). They are the *vascula media*, which arise anteromedially of the muscle fields; the *vascula myaria*, which originate between or within muscle bases and which are unequivocally identifiable mainly in association with the dorsal adductor scars; and the *vascula genitalia*, which normally occupy the posterolateral areas of the mantles. These last vary from peripheral

branches given off from pouches within the mantles that contain the gonads (gonocoels) to a complex of branches, including, according to ÖPIK's terminology, combinations of *vascula dentalia* and *myaria* (or *spondylaria*) and of *vascula cardinalia* and *cruralia* in the ventral and dorsal mantles, respectively. In shells of adults, however, they are always associated with the gonads, which may occur elsewhere within mantle canals but are invariably present in the posterolateral areas.

A survey of the known patterns of articulated brachiopods shows that they can be assigned to a few standard types, which were probably derived from those characteristic of Cambrian shells. Thus, in *Billingsella* (Fig. 380.7), circulation within the ventral mantle was apparently effected by a pair of *vascula media* that curved arcuately within the shell margin and presumably served the peripheral

mantle lobes and their setae. After allowing for the different distributions of muscle bases, this arrangement is not far removed from that of living *Lingula*. But the ventral mantle of *Billingsella* also contained a pair of pouchlike sinuses lying wholly posterior to the arcuate *vascula media*, which were probably homologous with similarly disposed gonocoels of *Hemithiris*; this entire pattern is referred to as the saccate condition (WILLIAMS, 1956). The projection of the gonads into the mantle is rare among inarticulated brachiopods but has always been characteristic of the articulated brachiopods.

The beginning of a profound modification of the saccate condition is seen in impressions on the ventral interior of *Finkelnburgia* (Fig. 380.8). The gonocoels projected laterally almost as far as the mantle edge (digitate condition) and must have served not only as sexual receptacles but also as circulatory channels because the lateral arcs of the *vascula media* were correspondingly reduced. In most younger stocks, this tendency is carried to conclusion. The *vascula media* became greatly abbreviated, although never entirely suppressed, while the *vascula genitalia*, which originated as a pair of gonocoels, also became the dominant circulatory canals. In *Palaeostrophomena* the gonocoels are still pouchlike but gave rise to a series of canals (lemniscate condition) (Fig. 380.2); and in *Clitambonites* the pouches were entirely replaced by radially disposed *vascula genitalia* (pinnate condition) that presumably contained gonadal cords (Fig. 380.6).

Despite a basic difference in arrangement, the dorsal mantle canal systems underwent the same kind of changes as those described for the ventral mantle. In *Billingsella* and *Finkelnburgia*, digitate gonocoels were well developed, but the *vascula media* far less so than those of the ventral mantle because a third pair of primary canals appeared laterally between the posterior and anterior adductors (*vascula myaria*) (Fig. 380.7–380.8). These are probably best interpreted as prin-

cipal branches of the *vascula media*, with which they enveloped the submedian anterior adductor scars in such a way as to suggest that the muscles were responsible for a premature branching of what were really a pair of median canals.

Such digitate patterns as these did not represent the most primitive system. The dorsal mantle of some Cambrian forms, possibly stocks like *Eoorthis*, in which the patterns were not impressed on the shells, must have been saccate because a pair of pouchlike gonocoels were certainly typical of many Ordovician brachiopods (e.g., *Strophomena*, *Leptaena*, and *Orthostrophia*) (Fig. 380.1, 380.3, 380.5), while the peripheral extensions of the other canals (especially the *vascula myaria*) to cover the entire margin suggest that they alone were responsible for circulation in the mantle (inequidistributate condition). More commonly, the digitate, lemniscate (e.g., *Palaeostrophomena*) or pinnate (e.g., *Clitambonites*) patterns prevailed, and the *vascula genitalia* also assisted in circulation (equidistributate condition). ÖPIK (1934) figured a very instructive variation within the species *Cyrtototella kukersiana*. In one specimen, the entire posterolateral periphery of the mantle was served by arcuate *vascula myaria*, while the lemniscate *vascula genitalia* were limited within the arc. In another, the peripheral arcs of the *vascula myaria* were abbreviated and the posterolateral mantle margin, for about one-third its length, was pervaded by *vascula genitalia*. The same degree of variation probably obtained in the basically saccate to lemniscate dorsal mantle of *Nicolella actoniae* (Fig. 381.1; WILLIAMS, 1963).

It is now evident that, although these different patterns are well defined, they constitute morphological grades that were attained during the development of many independent stocks. The post-Cambrian orthoids tended to retain a saccate ventral mantle, although, as in the orthoids, plaesiomyids, and plectorthids, the arcs to the *vascula media*

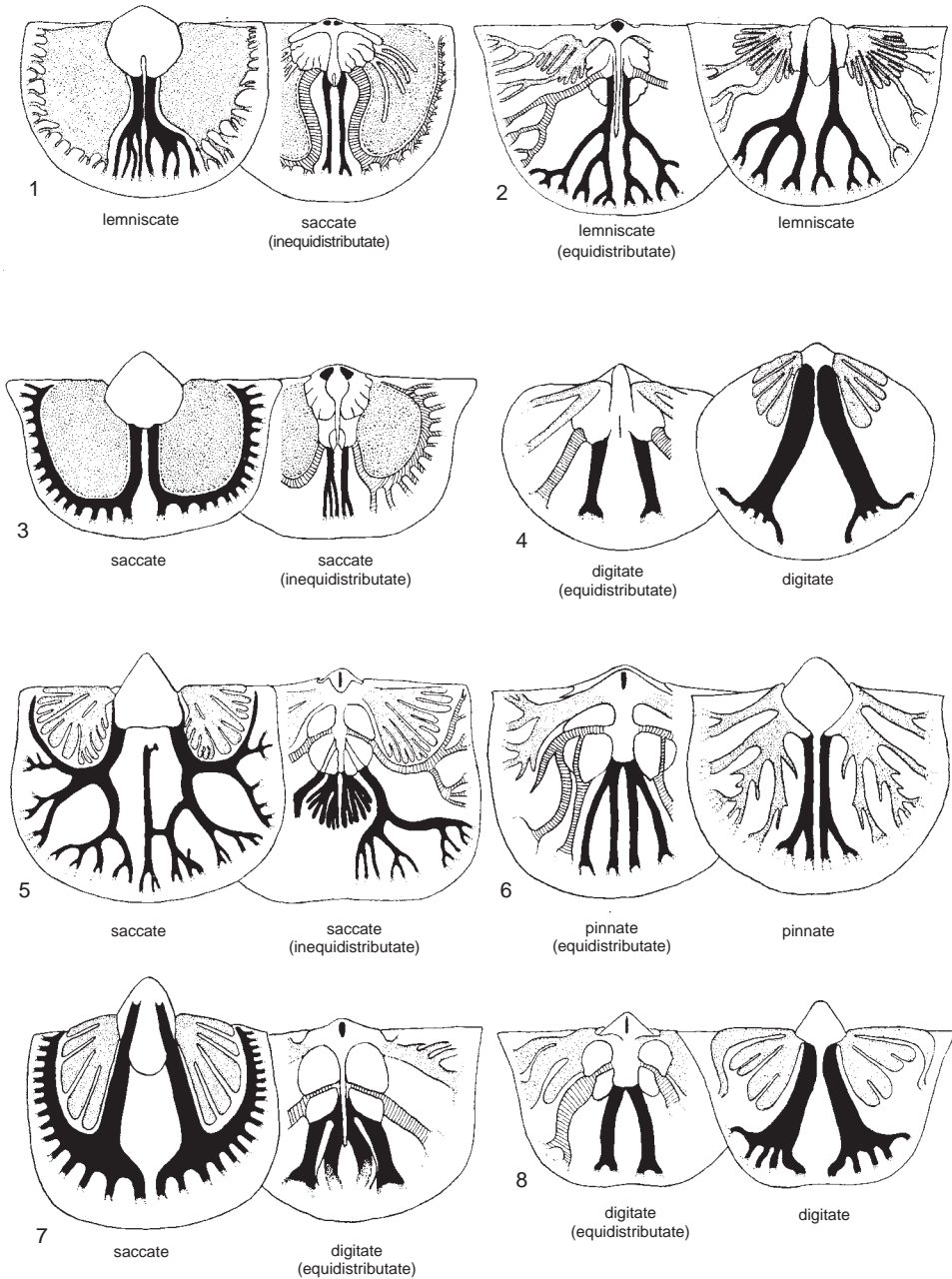


FIG. 380. Mantle canal systems of 1, *Strophomena*; 2, *Palaeostrophomena*; 3, *Leptaena*; 4, *Tetralobula*; 5, *Orthostrophia*; 6, *Clitambonites*; 7, *Billingsella*; 8, *Finkelburgia*; in each example dorsal valve is inner figure and ventral valve is outer; *vascula media* in solid black; gonadal sacs and *vascula genitalia* stippled; *vascula myaria* ornamented by closely spaced lines (Williams, 1956).

developed in the posterior part of the mantle and served the mantle edge by giving rise to a series of long, radiating branches, while the small posterolateral gonocoels were supplemented by subsidiary median ones. The most radical departure from this condition is found in *Dolerorthis*. In later species of this genus, the ventral pattern was orthodoxly saccate, but that of the dorsal mantle consisted of greatly branched *vascula media* with complete lateral arcs and pouchlike gonocoels; the *vascula myaria* do not appear to have developed (apocopate condition) (Fig. 381.5). This simple arrangement seems to represent a degeneration from an equidistributate lemniscate pattern, as is seen in some Ordovician species (Fig. 381.6).

The triplesioids and clitambonitoids, which are contemporaries of the orthoids, are lemniscate and pinnate, respectively. The enteletoids are also predominantly lemniscate in both valves, but the saccate condition was characteristic of the ventral mantle of *Paurorthis*. ROBERTS (1968) has shown that, during the ontogeny of the lemniscate mantle canal system of *Schizophoria*, the *vascula genitalia* became interconnected by small branches with *vascula media* and *vascula myaria* in the manner described for the orthoids *Cyrtanotella* and *Nicolella*.

Reconstructions of the strophomenoid and plectambonitoid mantles show a similar drift away from the primitive saccate condition. A few genera (e.g., *Titanambonites*) possessed saccate ventral mantles, but in both groups the lemniscate (or pinnate) condition was more usual (e.g., *Strophomena*, *Palaestrophomena*, *Sowerbyella*) (Fig. 380.1–380.2; 381.8). The effects of sexual maturity can be seen in species of *Leptellina*. The basic ventral pattern is saccate, but the distension of the gonocoels became so great in some valves that they became amalgamated with the lateral arcs of the *vascula media* to simulate a lemniscate condition. Indeed, this process of capture, presumably involving replacement of connective tissue by embayments of ciliated epithelium, may have been the main mode of development.

The dorsal mantle systems of these groups are not well known. Among plectambonitoids, the lemniscate equidistributate pattern of *Palaestrophomena* and the pinnate inequidistributate patterns of *Plectodonta* and *Sampo* seem to be dominant; and this conclusion may also be true for the strophomenoids, although in *Leptaena* and *Strophomena* the dorsal mantles were essentially saccate (Fig. 380.1, 380.3).

The pattern of other groups (e.g., orthotetoids, spiriferides, and pentameroids) is rarely preserved, and those of the chonetoids and productoids is largely unknown except for traces of *vascula media* belonging to what was possibly a lemniscate ventral mantle of *Rugosochonetes* (MUIR-WOOD, 1962). The orthotetidine *Floweria* rarely shows impressions of patterns suggestive of expanded lemniscate (or pinnate) *vascula genitalia* and abbreviated median and submedian canals in both valves.

The patterns of atrypoids are indifferently preserved, but if *Atrypa* is representative, the mantle canal systems developed in members of the superfamily constituted an interesting modification (Fig. 382). The distribution of impressions of discrete muscle attachments in the shell interior suggests that the gonads occupied most of the disrupted mantles of both valves in adult specimens, although the courses of the principal canals can still be made out. VANDERCAMMEN and LAMBIOTTE (1962) have plotted these for *Desquamatia* but have also included patterns within the body cavity that were not canals but sites of unmodified outer epithelium within the muscle fields and sporadically on the valve floor (P. COPPER, personal communication, 1993). Ignoring these, the *vascula media* were poorly developed in the ventral mantle to give a modified saccate condition and were somewhat reduced in the dorsal mantle where the *vascula myaria* and *vascula genitalia* were about equally developed (modified digitate condition). In contrast, a pinnate condition with destructive, narrow, radiating primary canals was probably the prevalent type of atrypoids (Fig. 381.9–381.10) and

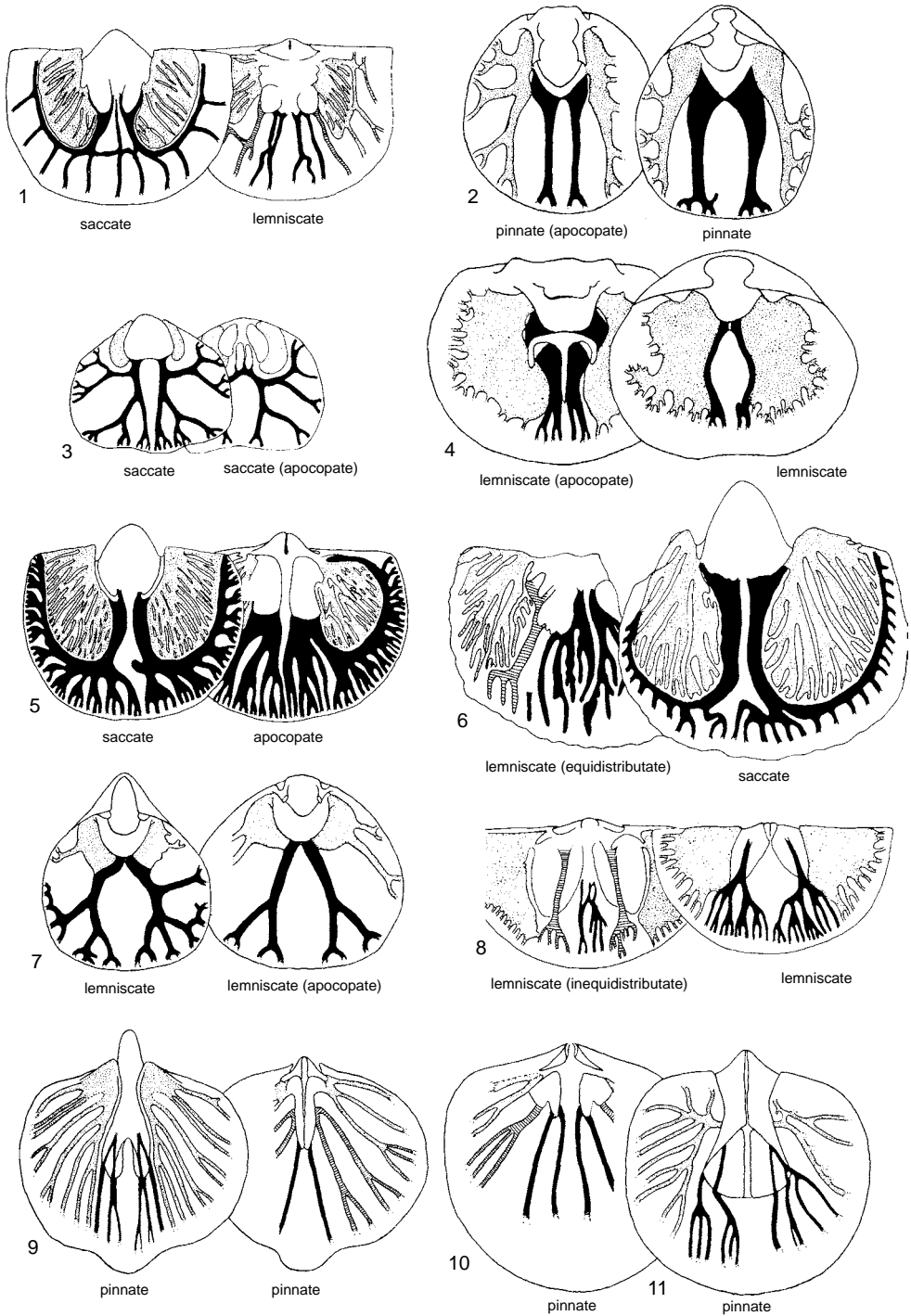


FIG. 381. Mantle canal systems of 1, *Nicolella*; 2, *Macandrevia*; 3, *Uncinulus*; 4, *Megerlina*; 5–6, *Dolerorthis*; 7, *Notosaria*; 8, *Sowerbyella*; 9, *Athyris*; 10, *Coelospira*; 11, *Meristina*; arrangement and shading as in Figure 380 (Williams & Rowell, 1965b).

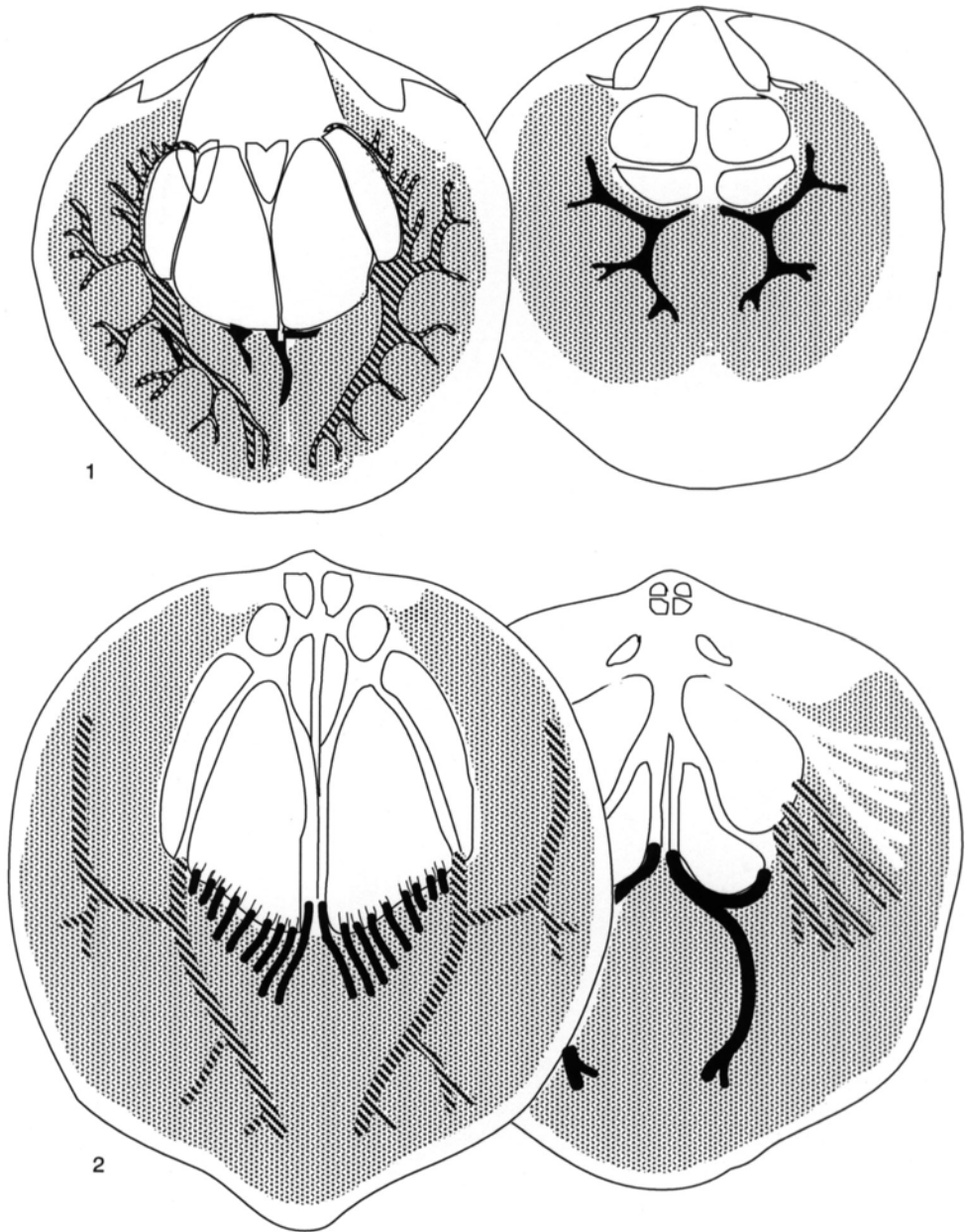


FIG. 382. Mantle canal systems of sexually mature atrypidines, as typified by 1, *Atrypa reticularis* LINNÉ and 2, *Desquamatia* sp. (original drawing by P. Copper and Vandercammen & Lambiotte, 1962).

was also possibly the representative pattern of the spiriferoids among which traces of a pinnate arrangement can rarely be found, especially as impressions of the ventral mantle.

The two remaining major groups, the rhynchonellides and terebratulides, are represented by living species, the canal systems of which can be studied by injection preparations of the mantles. Both are unusual in

that the pattern for the dorsal mantle is and almost invariably was apocapate. Yet it is fairly certain that the rhynchonellide arrangement was independently derived from a saccate or lemniscate condition and the terebratulide from a radial pinnate pattern.

Two contrasting patterns exist among recent rhynchonellides. The gonocoels in both mantles of *Hemithiris* are pouchlike and conform to the saccate condition, while those of *Notosaria* give off branches peripherally in the lemniscate manner (Fig. 381.7). Both of these patterns occur in fossil forms. *Sphaerirhynchia*, *Fitzroyella*, and *Uncinulus* (Fig. 381.3) are saccate and *Leiorhynchus* is lemniscate, but whether they constitute two persistently independent groups or whether the saccate stocks continually replenished the lemniscate ones is unknown. The latter conclusion is more likely, because impressions on the interiors of *Pugnax* may show a saccate condition or one in which the gonocoels may have enlarged sufficiently to rupture into the lateral arcs of the *vascula media* and capture them.

In modern terebratulides, the *vascula media* are subordinate to the lemniscate or pinnate *vascula genitalia*, and this relationship seems not to have varied greatly throughout their history. Even in Devonian times, when the terebratulides first emerged as significant members of the brachiopod phylum, the pattern of such living stocks as *Macandrevia* (Fig. 381.2) was already characteristic of stringocephaloids (CLOUD, 1942). A few genera (e.g., *Meganteris*, *Cranaena*) displayed the impressions of three or even four pairs of narrow sinuses radiating from the muscle scars of each valve in a manner reminiscent of the athyridoids. It is possible, then, that the characteristic dorsal pattern was derived from a pinnate condition by atrophy of the *vascula myaria*. In some modern terebratuloids (e.g., *Laqueus*, *Macandrevia*, and *Pumilus*) gonadal cords also occur in the *vascula media*, and in some respects this development may be regarded as the climax of anatomical reorganization that began with the formation of the gonocoel in the mantle.

It is not unique, however; the ventral mantle of *Plaesiomys* and the dorsal mantle of *Orthostrophia* possessed a pair of subsidiary saccate gonocoels situated anteromedially between the *vascula media*; and, in view of the poor data on mantle canal systems generally, it may well have been characteristic of other groups unrelated to the terebratulides.

The mantle canal pattern of inarticulated brachiopods is basically simpler than that of articulated species. Commonly, there is also some difference in function of the canals, for only in the Craniidae (see Fig. 387) are the gonads known to be partially inserted into them; in all other recent inarticulated brachiopods the gonads are confined to the body cavity, and the canals have primarily a circulatory function.

There is, however, a striking anomaly in the mantle canal systems (and musculature) of the early Paleozoic organophosphatic Paterinida (Fig. 383). LAURIE (1987) has shown that arcuate *vascula media* were present in the mantles of both valves as were pouchlike *vascula genitalia*, especially in the ventral valve. Such patterns are indeed best described as either saccate or saccate (possible apocapate) for the ventral and dorsal valves respectively and are orthide rather than lingulide in arrangement.

The mantle canal system of most of the organophosphate-shelled species consists of a single pair of main trunks in the ventral mantle (*vascula lateralia*) and two pairs in the dorsal mantle, one pair (*vascula lateralia*) occupying a similar position to the single pair in the ventral mantle and a second pair projecting from the body cavity near the midline of the valve. This latter pair may be termed the *vascula media*, but whether they are strictly homologous with the *vascula media* of articulated brachiopods is a matter of opinion. It is also impossible to assert that the *vascula lateralia* are the homologues of the *vascula myaria* or *genitalia* of articulated species, although they are likely to be so as they arise in a comparable position.

This basic pattern of one ventral and two dorsal pairs of canals is commonly developed

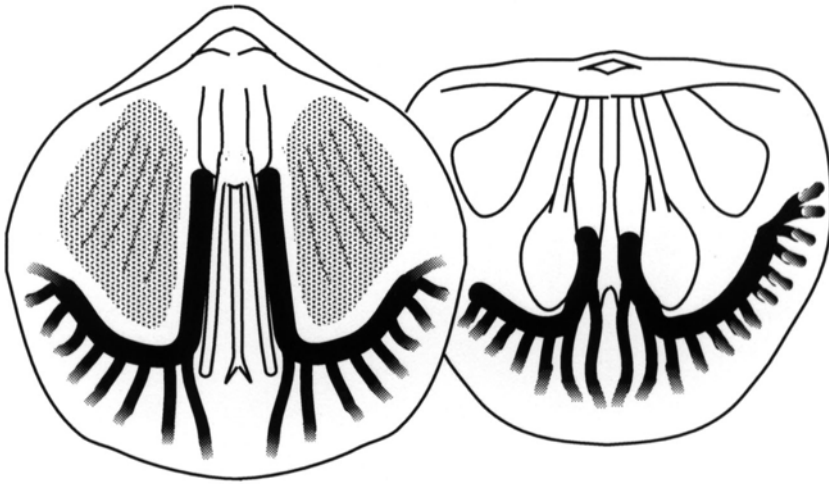


FIG. 383. Mantle canal systems of *Paterina* with ventral valve on the left and dorsal valve on the right; *vascula media* in black; gonadal sacs stippled (adapted from Laurie, 1987).

in lower Paleozoic lingulides. The ventral *vascula lateralia* curve forward from a lateral position on the anterior body wall, subparallel with the shell margin; the dorsal *vascula lateralia* are similarly disposed, and the *vascula media* diverge anteriorly from near the anterior lateral muscles. In obolids (*Oepikites*) and elkaniids (*Broeggeria*) (Fig. 384.1, 384.5) numerous minor canals branch from either side of the main trunks, and they and their distributaries permeate much of the mantle. These small branches are rarely seen in fossil forms, but it is reasonable to assume their presence in most lingulides. The branches from the principal canals are relatively minor; the *vascula lateralia*, in particular, extend forward without any major dichotomy or bifurcation (baculate condition).

The seemingly fundamental pattern of a pair of baculate *vascula lateralia* in each valve with a pair of *vascula media* in the dorsal mantle is also characteristic of many of the older lingulides including the paterulids (*Paterula*) and zhanatellids (*Zhanatella*) (Fig. 384.3–384.4) as well as the elkaniids and obolids.

In the lingulids and pseudolingulids (*Pseudolingula*), however, the mantle canal systems are fundamentally different (Fig. 384.2, 384.6) as is well shown in recent *Glottidia* and *Lingula*. In these groups, the dorsal *vascula media* are not developed and the *vascula lateralia* in both valves divide immediately after leaving the body cavity (bifurcate condition) or could well have done so as in *Pseudolingula*. Thereafter, the smaller branch of each main canal extends posteriorly to supply the mantle lateral of the lateral body wall, while the larger branches pass anteriorly and converge toward the midline of the valve. From these principal branches minor canals are given off comparable to those of elkaniids and obolids. The bifurcation of each of the *vascula lateralia* into anterior and posterior branches is not solely a function of the form of the shell, for in the obolids *Barroisella* and *Langella*, genera very similar in outline to recent *Lingula*, the *vascula lateralia* arise in a similar position but are comparable in form to those of other obolids. The bifurcation of these canals in recent lingulids appears to be more closely related to their relatively anterior origin and

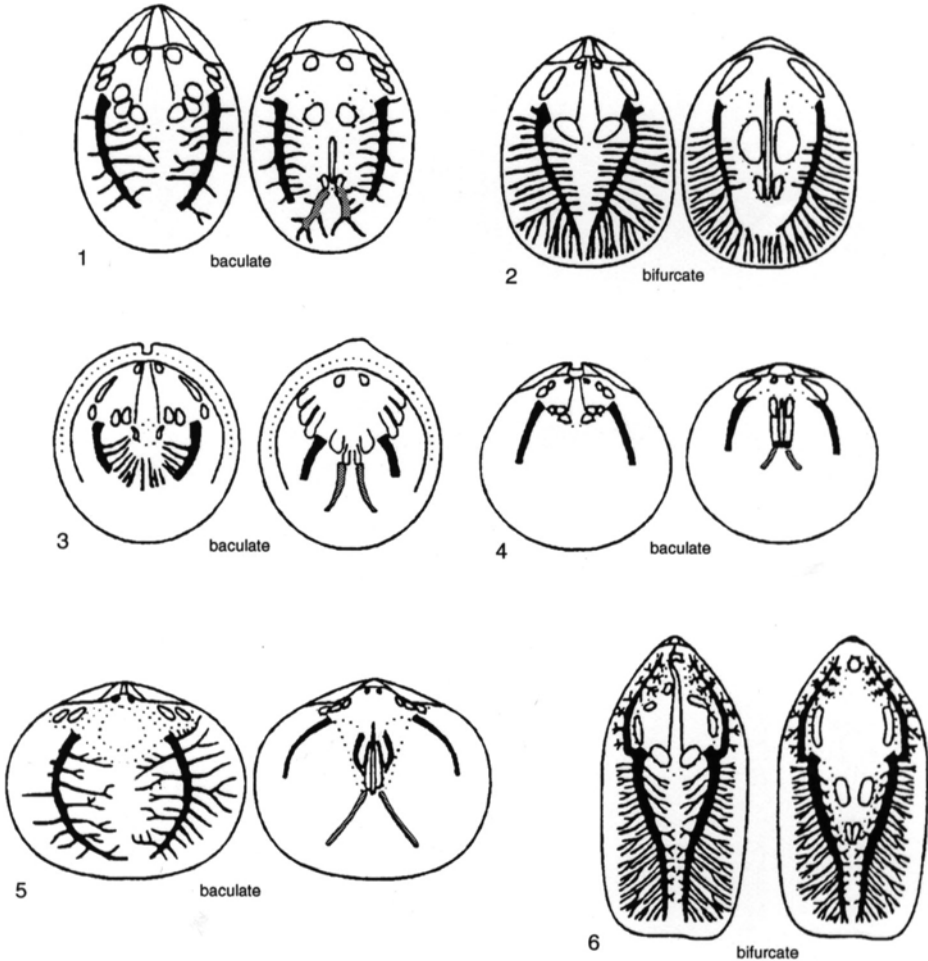


FIG. 384. Mantle canal systems of representative organophosphatic inarticulated brachiopods (lingulides); 1, *Oepikites*; 2, *Pseudolingula*; 3, *Paterula*; 4, *Zhanatella*; 5, *Broeggeria*; 6, *Lingula*; ventral valve on left, dorsal valve on right; *vascula lateralia* in black; *vascula media* in gray (original drawings by L. E. Holmer & L. Popov).

to the attenuated outline of the posterior part of the body cavity. Both these factors combine to produce a comparatively large area of mantle posterolateral of the body cavity, which, if it is to be supplied by the existing vascular system, necessitates a relatively large, posteriorly directed branch from the *vascula lateralia*. The absence of the dorsal *vascula media* is more difficult to explain. It is not directly a consequence of the considerable forward extension of the body cavity,

for in several Paleozoic lingulides, particularly the obolid *Schmidites*, the limit of the anterior body wall was placed relatively farther forward than that of *Lingula*, yet they still developed *vascula media*. The respiratory function of the dorsal *vascula media* of Paleozoic lingulides is performed in modern lingulides by the anterior branches of the *vascula lateralia*, which converge medially.

A similar bifurcate condition of the ventral *vascula lateralia* has also arisen

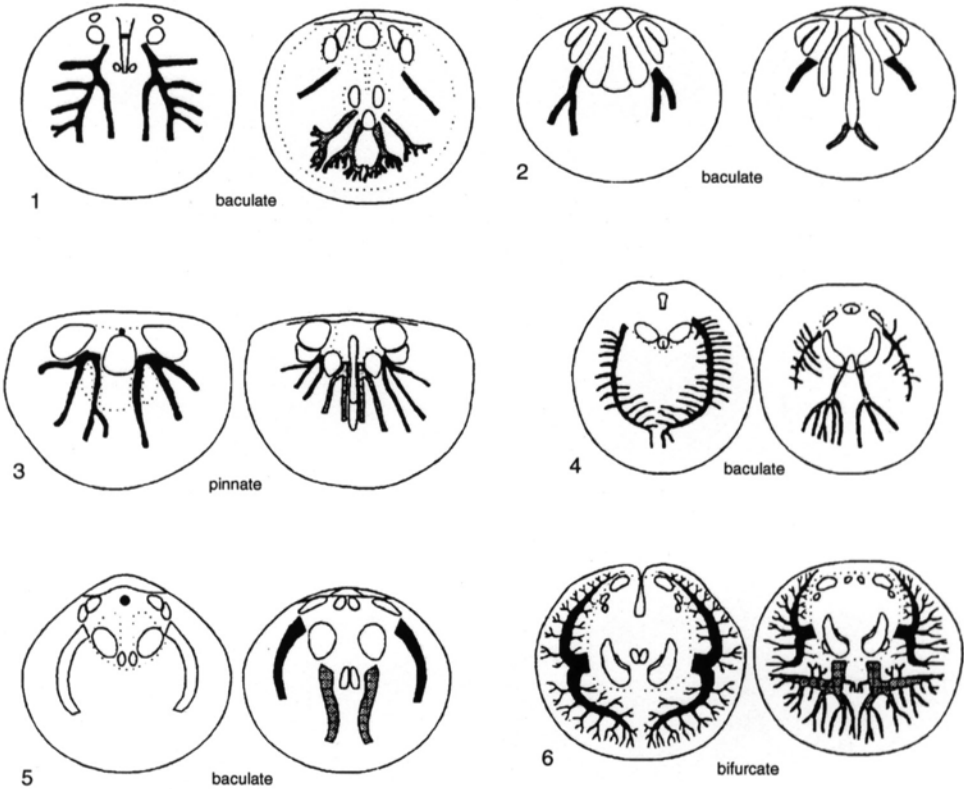


FIG. 385. Mantle canal systems of representative organophosphatic inarticulated brachiopods (discinides, siphonotretides, and acrotretides); 1, *Orbihele*; 2, *Botsfordia*; 3, *Cyrtontreta*; 4, *Lochkothele*; 5, *Schizambon*; 6, *Discinisca*; ventral valve on left, dorsal valve on right; *vascula lateralia* in black; *vascula media* in gray (original drawings by L. E. Holmer & L. Popov).

independently in living discinides but with the dorsal *vascula media* expanded to serve the anterior half of the dorsal mantle (Fig. 385). The older Paleozoic discinides, as the orbiculoid *Lochkothele*, had baculate mantle systems (Fig. 385.4) that, however, could easily have been transformed into the bifurcate condition. The dorsal *vascula media* were also relatively more important among acrotretides, especially the later botsfordiids (*Orbihele*). Indeed in acrotretoids (*Cyrtontreta*), the *vascula lateralia* of both valves rapidly branch into a number of subequal, radially disposed canals (pinnate condition) (Fig. 385.3). Although this branching commonly produced in the ventral mantle medially situated canals whose position is similar to that of the dorsal *vascula media*, they may be regarded as branches of the *vascula lateralia*,

since true *vascula media* are otherwise unknown in the pedicle valve of inarticulated brachiopods.

The mantle canal systems of the carbonate-shelled inarticulated brachiopods show some interesting variations (Fig. 386–387). The baculate condition (Fig. 386.3–386.4) seems to have been wholly characteristic of the Cambrian obolellides (*Obolella*, *Trematobolus*) and of the oldest craniide, the Ordovician *Pseudocrania* (Fig. 387.3) although, with the main branches of both the *vascula media* and *lateralia* giving rise to second-order distributaries marginally, the craniide canal systems simulate the pinnate condition. Subsequently, however, the canals of the dorsal mantle seem to have undergone extreme changes with the suppression of the *vascula lateralia* in living *Neocrania* and of

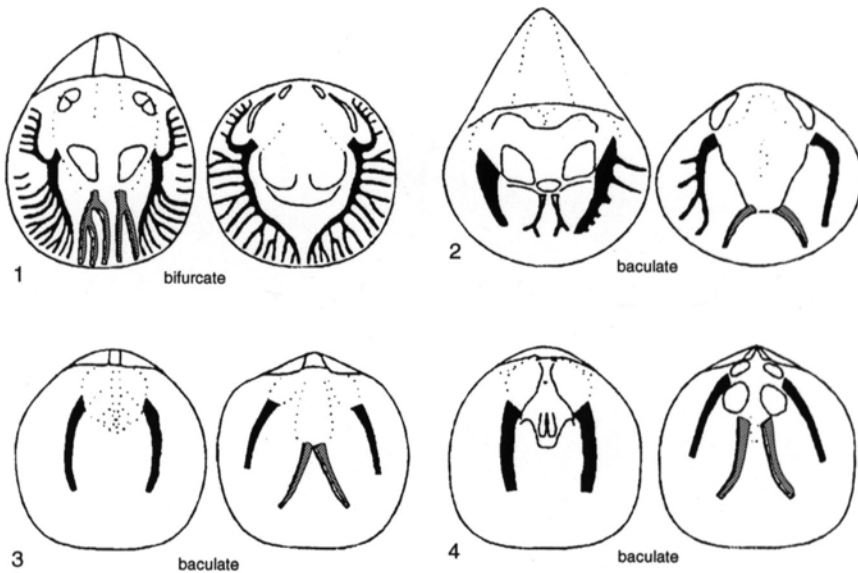


FIG. 386. Mantle canal systems of representative carbonate-shelled inarticulated brachiopods (obolellides, trimerellides); 1, *Palaeotrimerella*; 2, *Monomerella*; 3, *Obolella*; 4, *Trematobolus*; ventral valve on left, dorsal valve on right; *vascula lateralia* in black; *vascula media* in gray (original drawings by L. E. Holmer & L. Popov).

the *vascula media* in *Petrocrania*; these atrophies were accompanied by a compensatory enlargement of the remaining network of canals (Fig. 387.1–387.2). Yet the mantle ca-

nal system that most diverged from the basic baculate condition of inarticulated brachiopods is that of the carbonate-shelled trimerellides (Fig. 386.1–386.2). In this

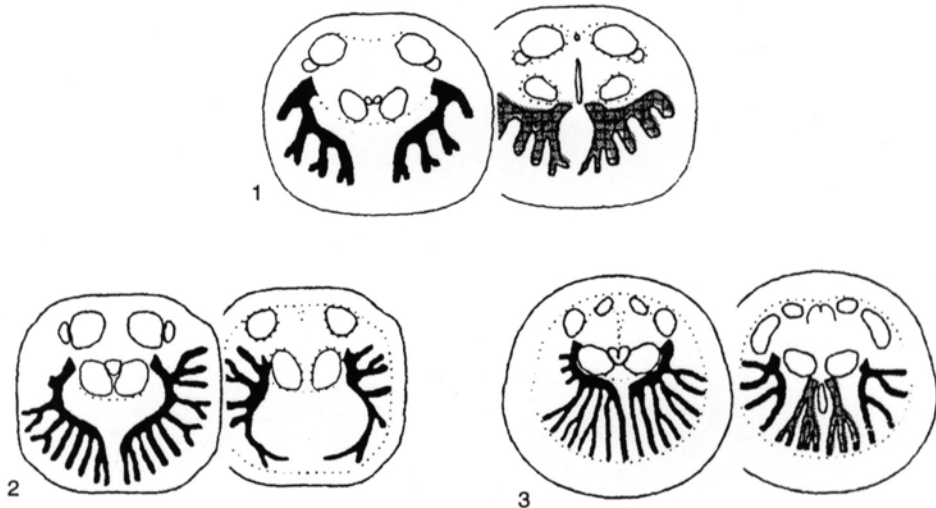


FIG. 387. Mantle canal systems of three genera selected to show the diversity attained during the evolution of craniid brachiopods; 1, *Neocrania*; 2, *Petrocrania*; 3, *Pseudocrania*; ventral valve on left, dorsal valve on right; *vascula lateralia* in black; *vascula media* in gray (original drawings by L. E. Holmer & L. Popov).

lower Paleozoic group the main submedial trunks of the *vascula media* were fully developed in the ventral mantle but only variably so in the dorsal one. Moreover, both main mantle canal patterns characterizing inartic-

ulated brachiopods as a whole are found in this order: the baculate condition in such forms as *Monomerella* and *Gasconsia* and the bifurcate condition in *Palaeotrimerella*.

MORPHOLOGICAL AND ANATOMICAL TERMS APPLIED TO BRACHIOPODS

ALWYN WILLIAMS¹ and C. HOWARD C. BRUNTON²

with contributions from other contributors to this revision of Part H,
Brachiopoda

¹University of Glasgow; ²The Natural History Museum, London

The following glossary consists of terms used in a distinctive way to describe brachiopod shells and to define the biology of the phylum as a whole. Anatomical terms defined herein are restricted to those used for soft parts that directly affect shell morphology.

All terms given in boldface in the glossary are used throughout the text in the way they have been defined. Those that can normally be used for any taxon, at least to class level within the phylum, are printed in capitals (for example, ADDUCTOR MUSCLES). Those that describe a feature generally specific to a particular taxonomic group(s) are printed in lower case letters (for example, accessory adductor scars).

Terms printed in plain style do not merit formal recognition that would restrict their use to a singular feature, for example, flange (of a crus); the term flange is currently used in morphological descriptions of several unrelated features.

Terms in italics (for example, *accessory denticles*) are considered by most or all of the contributors to be obsolete. They have been listed and, where necessary, defined so that future researchers with the aid of the glossary can consult older literature without being misled by outmoded terminology. Their continued use by brachiopod workers is not recommended.

GLOSSARY OF MORPHOLOGICAL AND SELECTED ANATOMICAL TERMS

accessory adductor scars. Pair of muscle scars in ventral valve of daviesiellids lying anterior to principal adductor impressions, interpreted as ancillary adductor bases.

accessory dental sockets (of orthidines). See denticular cavities.

accessory denticles. See denticles.

accessory diductor muscles. Pair of muscles branching posteroventrally from main diductor muscles and inserted in ventral valve posterior to adductor bases (Fig. 348).

accessory lamellae. Pair of lamellae developed from arms of jugum and coiled parallel to main lamellae of spiralia (Fig. 336).

accessory septum. Used informally for any septum ancillary to others. See anderidia.

accessory socket. Outer part of divided dental socket of plectambonitoids (Fig. 322–323); also used for depression in outer socket ridge.

accessory tooth. Articulating process flanking hinge tooth of plectambonitoids and fitting into accessory socket in dorsal valve (Fig. 323).

acuminate (loop). Phase in loop development with laterally bowed, descending lamellae extending from crura but otherwise unsupported and uniting anteromedially to form an echmidium (Fig. 334.1, 338.1).

adductor dividing ridges. See anderidia.

ADDUCTOR MUSCLES. Muscles that contract to close shell. In articulated brachiopods two adductor muscles, each divided dorsally, are commonly present to produce single pair of scars located between diductor impressions in ventral valve and two pairs (anterior, posterior) in dorsal valve. In inarticulated brachiopods two pairs of adductor muscles (anterior, posterior) are commonly present, passing almost directly dorsoventrally between valves (Fig. 348). See central muscles, umbonal muscles.

adductor pits. Pair of depressions indenting anterior face of notothyrial platform of some orthides for attachment of posterior adductor muscles.

aditicle. Gently inclined, coarse exopuncta; allegedly contained seta (Fig. 302).

ADJUSTOR MUSCLES. Two pairs of muscles in many articulated brachiopods moving pedicle or shell and arising from proximal end of pedicle to attach posterolaterally of diductors in the ventral valve (pedicle adjustors) and on hinge plates or floor of dorsal valve behind posterior adductors (brachial adjustors) (Fig. 348–349).

adminicula (sing., **adminiculum**). Paired subvertical plates situated umbonally in either valve and extending from valve floor to ventral edges of dental flanges (ventral adminicula) or to dorsal edges of crural bases (dorsal adminicula; however, see crural plates) (Fig. 324.3).

- alae.** Winglike extensions at cardinal extremities. See ears.
- alate plate.** Flaplike extension of secondary shell arising from lateral surface of brachiophore plate in porambonitoids (Fig. 366).
- alternate folding.** Deflection of shell surface in which fold of one valve is opposed by sulcus of other (Fig. 289).
- alveolus.** See cardinal process pit.
- amphithyrid** (foramen). Pedicle opening shared by delthyrium and notch in beak of dorsal valve (Fig. 318).
- anacline.** See inclination of cardinal area or of pseudointerarea (Fig. 285).
- ancillary strut.** Secondary shell material deposited between brachiophore base and median ridge in some orthides.
- anderidia** (sing., **anderidium**). Paired ridges in some strophomenides, situated posterolaterally of median plane of dorsal valve, of increasing elevation or projecting anterolaterally (Fig. 361).
- angle of spines.** External angle subtended by chonetoid external hinge spines with posterior margin of ventral valve, measured in plane parallel with plane of commissure.
- annular** (loop). Phase of loop development with a ring formed by resorption of the posterior apex of the hood. The attachments of the ring and descending lamellae are separate and the descending lamellae are usually complete.
- ANTERIOR.** Direction in plane of symmetry or parallel to it away from pedicle and toward mantle cavity (Fig. 283).
- anterior lateral (oblique) muscles.** Pair of muscles in some lingulids originating on ventral valve posterolateral to central muscles, converging dorsally to their insertions anteriorly on dorsal valve (Fig. 346.2).
- anteris.** Arcuate plate of secondary shell underlying hinge teeth in some Early Cambrian articulated brachiopods (Fig. 327.4).
- antiplicate** (folding). See plicate.
- antron.** Triangular to elongate groove variably developed between cardinal process buttress plates and brevisseptum in some productides. See cardinal process buttress plates.
- antygidium.** Low, platelike ridge of shell near beak of dorsal valve, covered externally by cuticle and deposited during ventral migration of junction of pedicle epithelium with outer epithelium (Fig. 319.3).
- anvil-type fiber.** A fiber of the secondary shell with the convex surfaces of the anvil-like cross section facing the valve interior (Fig. 242).
- apex.** First-formed part of valve around which shell has grown subsequently (term usually restricted to valves having this point placed centrally or subcentrally).
- apical angle.** Angle subtended by umbonal slopes at umbo.
- apical callosity.** See pedicle callist; for inarticulated brachiopods, see apical process.
- apical cavity.** Undivided space beneath umbo in either valve. See delthyrial chamber, notothyrial chamber.
- apical plate.** Dorsally enlarged pedicle collar partly closing apex of delthyrium.
- apical process.** Variably shaped protuberance in umbonal region of ventral valve of some acrotretoids, which probably served as a muscle platform and may have contained a pedicle tube (Fig. 346, 378).
- apiculate** (beak). Beak of ventral valve with a subapical hypothyrid or amphithyrid foramen.
- apocopate** (mantle canal). Dorsal, mantle-canal system with single pair of canals in addition to *vascula genitalia* (Fig. 381).
- apsacline.** See inclination of cardinal area or of pseudointerarea (Fig. 285).
- arcuiform** (crura). Crura hammer shaped in cross section, with arcuate heads concave toward each other.
- area.** See cardinal area.
- areola.** See planareas.
- arms.** See brachia.
- arms of jugum.** Processes arising by bifurcation of distal end of jugal stem, which may become extended into accessory lamellae (Fig. 336). See jugal stem, jugal processes.
- arrugia.** Highly inclined, fine exopuncta; allegedly contained chitinous bristle.
- ARTICULATION.** Interlocking of two valves by projections along their posterior margins; commonly effected in articulated brachiopods by two ventral teeth fitting sockets of dorsal valve but may be assisted or replaced by other projections and complementary pits (Fig. 322).
- ascending lamellae** (of loop). Paired ventral elements of long terebrateloid loop continuous anteriorly with ventrally recurved descending lamellae and joined posteriorly by transverse band (Fig. 338).
- astrophic.** Shell with posterior margin not parallel with hinge axis (Fig. 285).
- attrite** (foramen). Ends of beak ridges worn away.
- aulacoterma.** Thickening on inside wall of richthofeniid ventral valve against which dorsal valve rests when shell is closed.
- auriculate** (foramen). Opening bounded by deltidial plates bearing external rims or winglike extensions.
- axial** (loop). Phase of loop development with a vertical plate (Paleozoic forms) or septal pillar (post-Paleozoic forms); descending lamellae complete in Paleozoic forms, rudimentary in most post-Paleozoic forms.
- baculi** (sing., baculum). Microscopic apatitic rods forming a criss-cross array in an organic matrix in linguloid and discinoid shells (Fig. 238).
- baculate condition** (mantle canal). *Vascula lateralia* lacking major dichotomy or bifurcation (Fig. 384).
- band.** A distinguishable increment of growth on a shell. See transverse band.
- base of brachial process.** Proximal part of pentameroid brachial process attached dorsally to outer plate and ventrally to inner plate; homologue of base of brachiophore crus (Fig. 365).
- BEAK.** Extremity of umbo, commonly pointed (Fig. 283).
- beak angle.** Angle subtended between commissural plane at the hinge axis and line bisecting beak of

- astrophic ventral valve as seen in lateral profile; defined as straight (beak angle, 0 to 20°), inclined (20° to 30°), suberect (30° to 70°), erect (70° to 90°), incurved (more than 90°); corresponds to orthocline-anacline condition of strophic shells (Fig. 285).
- beak ridges.** More or less angular linear shell elevations extending from each side of umbo so as to delimit all or most of cardinal area.
- bema.** Raised area of secondary shell originating near anterior ends of inner socket ridges in some plectambonitoids; may be elevated marginally or divided by radial ridges (Fig. 344.2).
- biconvex.** Both valves convex (Fig. 283).
- bifurcate (loop).** Lophophore support in form of Y-shaped median septum (characteristic of Kraussinidae).
- bifurcate condition (mantle canal).** *Vascula lateralia* split into anterior and posterior branches immediately beyond point of leaving body cavity.
- bilacunar (loop).** Long reflected loop, typical of adult *Kingena* and related genera, with a lacuna in the dorsal segment of each ascending lamellae defining a pair of mediovertical connecting bands extending between the median septum and transverse band; descending lamellae still united to the median septum.
- bilateral (loop).** Long reflected loop, typical of adult *Laqueus* and related genera, with two pairs of connecting bands, lateral and lateroventral.
- bilobate (folding).** Opposite folding with well-developed median sulci flanked by variably developed carinae (Fig. 288.3).
- biplicate (folding).** Alternate folding with pair of submedian folds in dorsal valve separated by sulcus containing smaller median fold (Fig. 289).
- biseptum.** Double septum in ventral valve formed by union of dental plates.
- bisulcate.** Alternate folding resembling parasulcate condition but with median fold of dorsal valve indented by median sulcus (Fig. 289).
- blister.** Space and enclosing curved partition of secondary shell in umbonal and delthyrial chambers of some spiriferides, productides, and pentamerides; formed by sporadically migrating outer epithelium (Fig. 372).
- BODY CAVITY.** Principal part of coelomic space, situated posteriorly, bounded by body wall and containing alimentary tract, nephridia, and other organs (Fig. 1).
- braceplates.** Narrowly diverging septa extending anteriorly of dorsal adductor muscle scars in some strophodontids (Fig. 369).
- BRACHIA (sing., BRACHIUM).** Two armlike projections from either side of mouth segment of lophophore, variably disposed but symmetrically placed about mouth (Fig. 1).
- brachial base.** See inner socket ridge.
- brachial branches.** Narrow elevations of secondary shell within brachial ridges and converging anteromedially.
- brachial cavity.** See mantle cavity.
- brachial lamellae.** Calcareous support for lophophore.
- See brachidium and brachial platform.
- brachial loop.** See loop.
- brachial muscles.** Muscles in small brachial canal of inarticulate genera, arising from connective tissue at proximal ends of canals extending along their length.
- brachial plate.** One of pair of subvertical plates constituting pentameroid cardinalia and including inner plate, base of brachial process, and outer plate.
- brachial platform.** Raised area of secondary shell originating near alae in dorsal valves of some plectambonitoids that may be elevated marginally (Fig. 344).
- brachial process.** Anteriorly directed blade or rodlike projection from pentameroid cardinalia; comparable with crus.
- brachial protractor muscles.** Pair of muscles in craniids that assists movements of lophophore, located anteromedially on dorsal valve (Fig. 374).
- brachial retractor muscles.** Pair of small muscles in dorsal valve of discinids and craniids, located lateral to anterior adductor muscles.
- brachial ridges.** Paired narrow elevations of secondary shell extending laterally or anteriorly as open loops from dorsal adductor muscle field of some articulated brachiopods (Fig. 345).
- brachial valve.** See dorsal valve.
- brachidial net.** Calcareous netlike structure uniting the crura and jugum to the floor of the dorsal valve (Fig. 341).
- brachidium.** Calcareous support for lophophore in form of loop or spires.
- BRACHIOPHORES.** Blades of secondary shell projecting from either side of notothyrium and forming or in close association with inner socket ridges (Fig. 329).
- brachiophore bases.** See brachiophore plate.
- brachiophore plates.** Basal (dorsal) parts of brachiophores that join floor of valve (Fig. 329, 365).
- brachiophore process.** See brachiophore.
- brachiophore support.** See brachiophore plates.
- brachiotest.** Thin, granular layer overlain by secondary fibers in calcareous ribbons (lamella) of loops and spiralia; secreted by densely filamentous, outer epithelium (Fig. 29).
- breadth.** See width.
- brephic.** Juvenile stage in shell development following secretion of protegulum; best seen on ribbed valves where it can be distinguished from protegulum by presence of growth lines and from neanic shells by absence of radial ornament.
- brevisseptum.** Dorsal median septum not fused posteriorly with cardinal process.
- bridge.** Posteromedian part of marginal flange of thecideoid dorsal valve free of valve floor.
- brush.** Many fine radiating tubular extensions of proteinaceous membrane, which permeate a thin canopy of primary shell separating periostracum from distal head of caecum of terebratulides, thecideidines, and spiriferides (Fig. 31).
- buccal plate.** Small, variously shaped, but bilaterally symmetrical, posteriorly concave plates, normally loose within complete shells of spiriferids, but

- exceptionally placed posteromedially between spiralia and close to jugal processes; possibly discrete supporting piece for the mouth region of the lophophore (Fig. 342).
- buttress plates.* See cardinal process buttress plates.
- caecum** (pl., caeca). Papillose outgrowth of mantle occupying a puncta and connecting with periostracum either by a brush as in articulated brachiopods or by fibrillar strands as in cranioids (Fig. 31).
- calcareoconeous.* See chitinophosphatic.
- calcariform** (crura). Falciform crura said to be distinguishable by dorsally directed process at distal end of each crus.
- callist.* See pedicle callist.
- callus.** Any excessive thickening of shell located on valve floor (Fig. 352).
- camarophorium.** Spoon-shaped, adductor-bearing platform in stenoscismatoid dorsal valve supported by median septum (Fig. 367).
- camerate.** Acrotretoid shell fabric of discrete apatitic lamellae connected by perpendicular walls forming polygonal chambers (Fig. 241).
- campagiform* (loop). Growth stage of loop of certain terebratulides marked by proportionally large funnel-shaped ascending elements without lateral lacunae. See diploform.
- campagiform hood.* Large, commonly funnel-shaped structure without lateral lacunae, with descending branches attached to median septum by transverse processes.
- canal** (shell). Fine perforation of organophosphatic shell not penetrating primary layer and partly occupied by secreting plasmalemma (and exuded bodies) of outer epithelium (Fig. 261).
- canaliform** (crura). Variant of raduliform type, folded longitudinally in form of dorsally facing channel or gutter.
- capilla** (pl., capillae). Very fine radial ridge on outer surface of shell. See costa.
- capsular muscles.* Longitudinal fibers in connective tissue of pedicle of articulated brachiopods; may be attached to floor of ventral valve.
- cardinal angle.** Angle between hinge line and posterolateral margins of shell.
- cardinal area.** Posterior sector of valve of articulated brachiopods exclusive of delthyrium or notothyrium (may be interarea, planarea, or palintrope) (Fig. 285).
- cardinal buttress.** Vertical plate or ridge supporting cardinal socket in some trimerelloids dividing cavity beneath beak into two umbonal chambers (Fig. 375).
- cardinal crests.** Paired ridges originating near apex of notothyrium, below chilidium and flanking cardinal process of chonetidines (equivalent to the chilidial crests of some authors) (Fig. 361).
- cardinal extension.* Thecideidine cardinal process.
- cardinal extremities.** Lateral terminations of posterior margin (Fig. 283).
- cardinal facet.* See cardinal socket.
- cardinal flanges.** Variably disposed posteroventral extensions of inner socket ridges or cardinal plate protruding into ventral umbo; in some taxa becoming thickened and serrated ventrally to accommodate diductor muscle bases (Fig. 359).
- CARDINALIA.** Structures of secondary shell in posteromedian region of dorsal valve, associated with articulation, support of lophophore, and muscle attachment; include, for example, cardinal process, socket ridges, crural bases, and their accessory plates (Fig. 329–331, 359).
- cardinal margin.** Curved posterior margin of shell, homologous with hinge line of strophic shells but not coincident with hinge axis (Fig. 285).
- cardinal muscle scar.** Posterolaterally placed muscle scars in acrotretoids and obolellides (Fig. 378).
- cardinal pit.** Depression between inner socket ridges accommodating cardinal process and diductor muscle bases as in some rhynchonellides (Fig. 349).
- cardinal plate.** Plate extending across posterior end of dorsal valve, consisting laterally of outer hinge plates and medially of either conjunct inner hinge plates or single plate, commonly perforated posteriorly by dorsal foramen (Fig. 331, 362).
- CARDINAL PROCESS.** Blade or variably shaped boss of secondary shell situated medially in posterior end of dorsal valve and serving for separation or attachment of paired diductor muscles (Fig. 357–364). See also cardinal flanges, ctenophoridium, myophore.
- cardinal process buttress plates.* Two vertical converging, parallel, or diverging plates extending anteriorly from cardinal process to enclose space and, in some productidines, uniting with brevisseptum.
- cardinal process cowl.** Proximal cover directed umbonally on triplesoid cardinal process.
- cardinal process hood.* See cardinal process cowl.
- cardinal process lobes.** Projections forming all or part of cardinal process and bearing muscle bases or myophore (Fig. 357, 360).
- cardinal process pit.** Pit at internal base of cardinal process in some plectambonitoids, chonetoids, and productoids.
- cardinal process shaft.** Ridge- or stalklike proximal part of cardinal process (Fig. 360).
- cardinal ridge.** Thickened ridge confined to hinge lines of some productidines, aiding in articulation of shell (Fig. 326).
- cardinal socket.** Transverse depression on posterior margin of trimerelloid ventral valve that receives plate or tooth of dorsal valve (Fig. 375).
- carina.** Major angular elevation of valve surface, externally convex in transverse profile and radial in disposition.
- carinate** (of folding). Opposite folding characterized by incipient lateral carinae but without median sulci (Fig. 288). See also rectimarginate.
- catacline.** See inclination of cardinal area or of pseudointerarea (Fig. 285).
- cella.** Any chamber contained between floor of valve and elevated muscle-bearing platform; best known

- as inverted V-shaped chamber beneath shoe-lifter process (Fig. 356).
- central muscles.** Anteriorly or medially placed pair of muscles in lingulides, originating on ventral valve and passing anterodorsally to dorsal valve (Fig. 346.1).
- centronellid stage* (of folding). See unisulcate.
- centronelliform* (loop). Simple lanceolate loop suspended free of valve floor, commonly bearing vertical median plate in addition to echmidium. See acuminate and axial.
- cheniothyrid stage* (of folding). See lobate stage.
- chilidial crests.* See cardinal crests.
- CHILIDIAL PLATES.** Pair of posterior platelike extensions of notothyrial walls, commonly forming lateral boundaries of cardinal process.
- CHILIDIUM.** Crescentic plate covering apex of notothyrium, commonly convex externally and extending for variable distances ventrally over proximal end of cardinal process and chilidial plates when present (Fig. 319, 357, 361).
- chilidonophorid* (loop). Short loop with converging but not fused crural processes, and transverse band not well differentiated from descending branches.
- chitinophosphatic** (shell). Consisting dominantly of some form of calcium phosphate and chitin (hexosamine) with various proteins.
- cicatrix** (of attachment). Scar on ventral umbo or umbonal region, representing place of cementation of shell to substrate.
- ciliform** (crura). Variant of raduliform type; flattened in plane of commissure, forming direct prolongations of horizontal hinge plates, then turning parallel to plane of symmetry as slightly crescentic blades.
- cinctid stage* (of folding). See opposite folding.
- cincture.** External concentric furrow in either valve of some productoids, corresponding to internal shell deflection or thickening.
- circinate* (lophophore). Distally coiling spirolophore.
- cirri socles.* See spicules.
- clavicular plates.* See cardinal crests.
- colleplax.** Triangular umbonal plate in dictyonellidines exposed externally by resorption of ventral umbo (Fig. 321).
- columnar** (shell). Acrotretoid shell fabric of discrete apatitic lamellae connected by microscopic perpendicular columns (Fig. 240).
- coma** (pl., **comae**). Concentrically disposed impermanent and irregular protuberance composed of primary and secondary shell on external shell surface of some plectambonitoids (Fig. 295).
- commissural plane.** Plane containing cardinal margin and either commissure of rectimarginate shell or points on anterior commissure midway between crests of folds in both valves (Fig. 283).
- COMMISSURE.** Line of junction between edges or margins of valves (Fig. 283).
- concaconvex** (shell). Dorsal valve concave; ventral valve convex (Fig. 287).
- conjoint deltidial plates.** Deltidial plates in contact anterodorsally of pedicle.
- connecting band** (of loop). Band of terebratellide long loop connecting ascending lamellae to each other (transverse band), descending lamellae to median septum (lateral connecting band), and descending lamellae to ascending lamellae (vertical connecting band) (Fig. 338).
- connectivum.** Medially united plates extending from crural bases to cover septalium ventrally (Fig. 329).
- convexoconcave** (shell). Dorsal valve convex; ventral valve concave (Fig. 287.2).
- convexoplane** (shell). Dorsal valve convex; ventral valve plane.
- corpus.** Shell enclosing principal part of body cavity and mantle cavity, excluding peripheral extensions of shell such as trails or flanges (see section on Productida in systematic volume Part H(R), volume 2, in preparation).
- coscinidium.** Reticulate extension of inner secondary shell over aperture of conicoventral valve of richthofenioids (Fig. 273).
- COSTA** (pl., **COSTAE**). First-formed radial ridge on external surface of shell most commonly originating at the junction between the brephic and neanic shell (Fig. 297). [Also but ambiguously used for any coarse rib, without reference to origin. **Costella** is a fine rib, and **capilla** a very fine rib. This usage gives no indication of the nature of radial ornamentation and any quantitative definitions, related to the incidence of ribs at the margins of shell irrespective of their sizes, are of no value. Thus in brachiopods ornamented by ribs that increase in wave length during growth, shells of the same species could be described as capillate, costellate, or costate according to their size.]
- costate.** Shell radially ornamented exclusively by costae.
- COSTELLA** (pl., **COSTELLAE**). Radial ridge on external surface of shell originating later than costa by bifurcation of existing costa or costella or by intercalation between earlier-formed ribs (Fig. 297).
- costellate.** Shell radially ornamented by costae and costellae.
- cowl.** Anterodorsally growing shell producing conical shape of holoperipheral ventral valve of lyttoniids.
- crenulations.* See denticles.
- crescent.* Site of cardinal socket of trimerelloids.
- cristae.* See socket ridges.
- crossed-bladed structure.** Sheets of parallel aggregations of laths or blades oriented in different directions in adjacent sheets and in parts of same sheet of a laminar shell succession, for example, secondary layer of most strophomenides (Fig. 251).
- crown of crescent.* See crescent.
- CRURA** (sing., **CRUS**). Paired processes extending from cardinalia or septum to give support to posterior end of lophophore; distal ends may also be prolonged into primary lamellae of spire or descending lamellae of loop (Fig. 329–331).
- crural band.** Ribbon of secondary shell joining crural processes ventrally.

crural bases. Parts of crura united to hinge plates or socket plates and separating inner and outer hinge plates when present (Fig. 329–331).

crural fossette. Cavity on inner face of tooth receiving posteroventral edge of brachiophore or crural plate when valves are closed (Fig. 322).

crural hooks. Hooklike ends of crura facing a matching set of curved primary lamellae of the spirulum.

cruralium. Spoon-shaped structure of dorsal valve formed by dorsal union of pentameroid, ambo-coeliidid, or some meristellid brachiophore plates (or homologues) and bearing adductor muscles (Fig. 365).

cruralium discretum. Paired outer plates attached independently of each other to floor of pentameroid dorsal valve to enclose dorsal adductor field.

crural keel. Dorsal extension of crus beyond junction with flange.

crural lobe. Strongly developed, posteroventrally elevated inner socket ridge in atrypoids and some athyroids.

crural plate. Plate extending from inner edge of outer hinge plate or crural base to floor of dorsal valve; may fuse medially with counterpart to form septalium. See septalial plate (Fig. 329–330).

crural pit. Cavity near floor of dorsal valve separating brachiophore plate and fulcral plate in some orthides.

crural point. See crural process.

crural process. Pointed part of crus directed obliquely inward and ventrally (Fig. 334).

crural trough. See septalium.

CRUS. See CRURA.

cryptacanthiiform (loop). Long, reflected loop unsupported by median septum with descending lamellae anterolaterally divergent but still fused postero-medially. See diploform.

cryptonelliform (loop). Long, reflected loop unsupported in adults by median septum and having narrow transverse band. See teloform.

ctenophoridium. Cardinal process with radially striated myophore not elevated on a shaft but commonly on an elevated transverse ridge (Fig. 358).

cupulate (loop). Phase of loop development with a hood on either vertical plate or septal pillar. Descending lamellae complete in Paleozoic forms, commonly incomplete in post-Paleozoic forms.

curvature of beak. Curvature of beak toward the opposing valve. See beak angle.

curvilinear (length or width). A dimension measured along the external curvature of a valve.

cuticle. Organic cover of pedicle; secreted by pedicle epithelium.

cyclothyrid (foramen). See auriculate.

cyncephalous (folding). Sharply folded dorsal valve.

cyrtomatodont. Knoblike or hook-shaped hinge teeth developed by differential secretion and resorption of secondary shell (Fig. 322.1).

cyrtomorph. Chonetid hinge spines curving medially or laterally but remaining close to commissural plane.

cystose (shell). Valves containing blisters of secondary shell (Fig. 372).

dalliniform (loop). Loop arrangement typical of adult *Dallina* in which long descending lamellae recurve into ascending lamellae that meet in transverse band, all free of the valve floor. See teloform.

delayed costation (or **costellation**). Ribbing that first arises in postneanic stages of shell growth. See costa (or costella) (Fig. 297).

deltarium discretum. Thickened edge of delthyrium.

delthyrial angle. Angle subtended by margins of delthyrium.

delthyrial callosity. See pedicle callist.

delthyrial carinae. See teeth ridges.

delthyrial cavity. See delthyrial chamber.

delthyrial chamber. Cavity beneath umbo of ventral valve bounded by dental plates, if present, or by posterolateral shell walls, if dental plates absent.

delthyrial foramen. Foramen in young shells.

delthyrial plate. Plate within delthyrial chamber of some spiriferides, extending variable distance from apex between dental plates (probably homologue of pedicle collar) (Fig. 355.1).

DELTHYRIUM. Median triangular or subtriangular aperture bisecting ventral cardinal area or pseudo-interarea, commonly serving as pedicle opening (Fig. 283).

deltidial cover. Externally concave plate in some pentameroids closing posterior end of delthyrium (probably homologue of pedicle collar).

deltidial grooves. Lines delimiting thecideidine pseudodeltidium in species with this structure not flush with ventral area.

DELTIDIAL PLATES. Two plates growing medially from margins of delthyrium, partly or completely closing it (Fig. 316).

deltidial ridges. Two narrowly triangular ridges separating homeodeltidium and propareas of trimerelloids.

deltidodont. Simple hinge teeth developed by distal accretion of secondary shell (Fig. 322).

deltidium. Cover of delthyrium formed by conjunct deltidial plates; line of junction of plates visible (Fig. 317).

deltiform (loop). Terminal loop phase typical of many short-looped terebratulides with a variably disposed transverse band extending between the distal ends of two relatively short, divergent, descending lamellae.

dental cavity. Anteriorly expanding cavity, presumably occupied by evagination of outer epithelium secreting the tooth of some atrypoids.

dental flange. Internal border and buttress to delthyrium and teeth in spiriferides, not extending to valve floor (Fig. 324). See adminicula.

dental lamellae. See dental plates.

DENTAL PLATES. Variably disposed plates of secondary shell underlying hinge teeth and extending to floor of ventral valve (Fig. 323).

DENTAL SOCKETS. Excavations in posterior margin of dorsal valve for reception of hinge teeth (Fig. 323).

dental valve. See ventral valve.

denticles. Small, protruding ridges that alternate with complementary sockets located along cardinal mar-

- gin or hinge line of both valves; also small processes on posterior surfaces of dental sockets fitting into accessory sockets in hinge teeth (Fig. 325).
- denticular cavities*. Pair of grooves on outer side of teeth that receives projections from outer socket ridges (Fig. 322).
- denticular plates**. Pair of obtusely triangular plates lateral to delthyrium, bearing denticles and fused with dental plates, developed in strophodontids.
- denticulated cardinal margin**. Posterior margin of both valves bearing denticles, fitting into complementary sockets.
- denticulated commissure**. Zigzag commissure due to interfingering of angular ribs (Fig. 300).
- denticulum** (pl., *denticula*). Small toothlike termination of cardinal area, usually in ventral valve, commonly articulating with accessory socket in outer socket ridge (Fig. 322).
- dentifer*. Vestigial brachiophore in some orthotetidines. See brachiophore.
- depth*. See thickness.
- descending branches*. See descending lamellae.
- descending lamellae**. Paired dorsal elements of loop extending anteriorly from crura and recurved ventrally at anterior ends (Fig. 338).
- deuterolophe**. Spirally coiled part of lophophore bearing double brachial fold and double row of paired tentacular appendages, homologous with side arms of plectolophe (Fig. 337.2, 337.4–337.6).
- diaphragm**. Extension of visceral disk, commonly as marginal ridge, of productide and strophomenide dorsal valve maintaining a close fit with ventral valve and usually associated with trails.
- dictyothridid stage* (of folding). See parasulcate.
- DIDUCTOR MUSCLES**. Muscles serving to open valves of articulated brachiopods, commonly consisting of two pairs attached to dorsal valve immediately anterior to beak, usually to cardinal process; principal pair commonly inserted in ventral valve on either side of adductor muscles and accessory pair posterior to them (Fig. 348).
- digitate** (brachidium). Thecideoid brachidium with brachial branches extending inward from marginal flange.
- digitate** (mantle canal). Posterior part of *vascula genitalia* projecting laterally nearly to mantle margin, with corresponding abbreviation of *vascula myaria* (Fig. 379–380).
- diploform** (loop). Phase of loop development, typical of adult *Campages*, with adjacent ascending and descending elements fused, well developed, and free of the septum except at their posterior extremities (Fig. 334).
- disjunct deltidial plates**. Plates not in contact anterodorsally of pedicle.
- divaricator muscles*. See diductor muscles.
- divided hinge plates. Plates not united medially.
- DORSAL**. Direction toward dorsal valve.
- dorsal adjutor muscles*. See adjutor muscles.
- dorsal adminicula. See adminicula.
- dorsal denticulum*. See outer socket ridge.
- dorsal foramen**. Posteriorly located perforation of cardinal plate which may encroach on beak of dorsal valve (Fig. 359).
- DORSAL VALVE**. Valve that invariably contains any skeletal support for lophophore and never wholly accommodates pedicle; commonly smaller than ventral valve and with distinctive muscle-scar pattern (Fig. 283).
- dorsibiconvex**. Dorsal valve more convex than ventral valve.
- dorsiconvex*. See dorsibiconvex.
- dotted brachial ridges*. Ridges of thecideoid brachidium represented by rows of small, separate pustules.
- double-barrelled spine**. External spine of primary shell having oval to subquadrangular cross section and commonly barbed, bearing variably closed suture on commissural surface and, at least proximally, a median partition so that spine scars are bipartite (Fig. 306).
- double deltidial plates. Pair of deltidial plates, each of which is seen in certain transverse sections to consist either of two parallel plates or of one plate nearer hinge line, buttressed by another disposed at angle to it.
- double median septum*. More or less elevated median plate in pentameride dorsal valve formed by union of two septal plates.
- dyscolioid stage* (of lophophore). Probably a trocholophe.
- ear**. Flattened or pointed cardinal extremity of shell subtended between hinge line and lateral commissure usually distinct from corpus (Fig. 283).
- ear baffle. Ridge differentiating ear from corpus in some productides.
- echmidium**. Spear-shaped plate formed during ontogeny of loop of Paleozoic terebratulides by fusion of anterior ends of descending lamellae (Fig. 338).
- elytridium. Narrowly convex, puckered cover of delthyrium in aulostegids. See pseudodeltidium.
- emarginate**. Median segment of anterior commissure deflected posteriorly (Fig. 288.2a, 288.3a).
- emarginatura**. Median semicircular opening bisecting apical region of the ventral valve of some oboloids.
- endopuncta** (pl., *endopunctae*). Perforation of shell separated from periostracum on external surface by sievelike canopy of primary shell; occupied by caecum as in terebratulides, thecideidines, and spiriferides; also used for perforations ending within the primary layer of some rhynchonellides (Fig. 31).
- endopunctum* (pl., *endopuncta*). See endopuncta.
- endospines**. Fine, solid or hollow, short spines on interior of shell.
- entering valve*. See dorsal valve.
- ephebic*. Mature.
- episculate* (folding). See bisulcate.
- epithyrid** (foramen). Pedicle opening wholly within ventral umbo and ventral from beak ridges (Fig. 318).
- equidistribute** (mantle canal). *Vascula genitalia*, *vascula myaria*, and *vascula media* all well developed and contributing to mantle canal circulation (Fig. 381).
- erect beak**. See beak angle.
- erect spines**. Spines projecting at high angle (more than 70°) from shell surface.
- erisma* (pl., *erismata*). Plate supporting cardinal process

- and brachiophore of orthotetidines. See socket plates.
- euseptoidum*. See myophragm.
- euseptum*. See septum.
- everted stage* (of folding). See uniplicate.
- exopuncta** (pl., **exopunctae**). Perforation of external shell surface commonly restricted to primary layer and never penetrating to internal surface.
- exopunctum* (pl., *exopuncta*). See exopuncta.
- extremities*. See cardinal extremities.
- extropuncta** (pl., **extropunctae**). Microscopic, asymmetrical, conical deflection of laminae of secondary shell invariably pointing externally, characteristic of orthotetidine schuchertellids (Fig. 271).
- falciform** (crura). Crura arising on dorsal side of hinge plates and projecting into dorsal valve as broad, bladelike processes.
- false cardinal area*. Previously used for any poorly defined cardinal area or pseudointerarea.
- false pedicle groove*. See intertrough.
- fascicostellate**. Ornament of costae and costellae arranged into bundles (Fig. 297).
- fastigium*. Dorsal radial fold resulting from commissural flexure in many spiriferides.
- fenestrae** (sing., **fenestra**). Concentrically aligned, orthogonal openings in anterior part of punctatrypid shells, extending from interior through primary layer to exterior; closed posteriorly by shell secretion (Fig. 259–260).
- fibrous layer**. See secondary layer; term commonly used as alternative for secondary layer of articulated brachiopods when exclusively composed of calcitic rods (fibers) with lenticular or anvil-like cross sections (Fig. 242).
- filum** (pl., **fila**). Fine concentric ridge of variable persistence ornamenting external surface of shell (Fig. 292).
- fimbria** (pl., **fimbriae**). Spinelike projection from spiralia or jugum; also used for spinose projection on margin of growth lamella, as in *Spinilingula* (Fig. 336).
- flange** (of cardinal plate). See cardinal flange.
- flange** (of corpus). Peripheral shell beyond corpus as trails in productids or shell extensions in athyrids. See frill.
- flange** (of crus). Lateral projection from crus formed by anterior extension of part of outer hinge plate adjacent to crural base.
- flange** (dyscolliid). Incurved lateral and anterior margins of both valves.
- flanges** (septal, of loop). Pair of small, laterally projecting flanges that appears very early in loop ontogeny on the posteroventral edge of the septal pillar of laqueoids and some platidioids.
- flanks*. See lateral slopes.
- flap*. See posterior flap.
- flexure line**. Line extending from beak to anterior border of both ventral propareas in some linguloids, marked by deflection of growth lines (Fig. 286).
- FOLD**. Major elevation of valve surface, externally convex in transverse profile and radial from umbo (Fig. 288–289).
- foramen**. See pedicle foramen; term commonly used with this meaning (Fig. 285).
- foraminal sheath*. See pedicle sheath.
- foraminal tube*. See pedicle tube.
- free (brachiopod). Animal not attached to substrate.
- free spondylium**. Spondylium unsupported by septum.
- frenuliniform* (loop). Growth stage of loop characterized by a lacuna in each ascending lamella. See bilacunar.
- frill**. Relatively large growth lamella projecting well beyond general contour of valve, deposited by margin of highly retractile mantle.
- fulcral plate**. Small plate raised above floor of dorsal valve extending between posterior margin and brachiophore plate or inner socket ridge and socket plate and forming floor of socket (Fig. 332).
- furrow*. See interspace.
- fused hinge plates**. Hinge plates joined together along midline with no development of septalium (Fig. 330.3).
- gape**. Anterior and lateral opening of shell (Fig. 1).
- gastrothyrid* (foramen). Pedicle opening limited to ventral valve.
- geniculate**. Abrupt and more or less persistent change in direction of valve growth producing angular to sharply rounded bend in lateral profile (Fig. 287).
- geniculated spines**. Chonetid hinge spines, commonly cyrtomorph, bending along their length.
- genital area**. Part of shell known to be or inferred to have been overlain by gonocoel.
- genital markings**. Radial ridges or pits on inside of shell within genital area.
- ginglymus**. Secondarily developed, heavily thickened hinge line especially characteristic of ventral valves of some productides, externally resembling interarea.
- glossothyropsiform* (glossothyropsidiform) (loop). Long reflected loop, unsupported by median septum, bearing two broad ascending elements joined by wide transverse band. See teliform.
- glotta* (pl., *glottae*). See squama.
- granule*. See tubercle.
- growth lamella**. Concentric outgrowth of shell deposited by retractile mantle margin; smaller than frill (Fig. 295–296).
- growth line**. Concentric line on outer surface of shell formed when forward growth of shell temporarily ceased (Fig. 290–291, 294).
- gusset**. Plate uniting brachiophore to cardinal process shaft of orthotetidines; homologue of inner hinge plate.
- gutter**. Marginal anteroventral recurvature of trail of one or both valves.
- halteroid spines**. Long, straight, external hollow spines, symmetrically developed as strutlike supports on productide ventral valve.
- hamiform** (crura). Crura straight, in plane of commissure and slightly compressed; variant of falciform crura.
- haptoid** (loop). Phase of loop development with anterior fusion of ascending and descending elements and their accompanying separation from the vertical plate or septal pillar. Posterior sections of the ascending and descending elements still separately attached to vertical plate or septal pillar.
- HEIGHT**. In biconvex, planoconvex, and convexo-

- plane shells, height equals thickness, being the maximum dimension normal to length and width; in concavoconvex and convexoconcave shells, height is maximum distance measured normal to length in plane of symmetry between shell and line joining beak and anterior margin (Fig. 283).
- helicophores*. See *crura*.
- hemiperipheral growth**. New shell material added anteriorly and laterally but not posteriorly (Fig. 284).
- hemispondylium**. Two small plates within thecideoid ventral umbo, usually free of valve floor and side walls but commonly supported by median septum and bearing median adductor muscles.
- hemisyrix**. Conical chamber extending medially along floor of clitambonitoid spondylium and delineated posteriorly by pair of discrete lateral ridges.
- hemisyrix ridge*. Ridge forming posterolateral boundary of hemisyrix.
- hemithyrid stage* (of shell structure). See *impunctate*.
- henidium**. Symphytium that loses line of junction during late stages of growth.
- hinge*. Often used loosely for either hinge line or cardinal margin.
- hinge area*. See *cardinal area*.
- hinge axis**. Line joining points of articulation about which valves rotate when opening and closing (Fig. 285).
- hinge line**. Straight posterior margin of shell parallel with hinge axis; previously used as synonym of cardinal margin (Fig. 285).
- hinge notch**. Notch at lateral margin of pentameroid delthyrium accommodating posterior side only of hinge tooth.
- hinge plate**. Medially undifferentiated plate between crural bases. See *inner hinge plates*, *outer hinge plates* (Fig. 331).
- hinge platform**. Solid secondary shell platform extending between socket ridges of terebratulide cardinalia (Fig. 370).
- hinge projections*. Projections of fused inner socket ridges and crural bases, visible externally posterior to dorsal umbo. See *cardinal flanges*.
- hinge socket*. See *dental socket*.
- hinge spines**. Hollow spines developed in chonetoids in row along posterior margin of ventral interarea on either side of umbo and continuous with cylindrical, hollow, commonly deflected passageways through interarea, often called roots of spines. Also used for spines at hinge line in productidines.
- HINGE TEETH**. Two principal articulating processes situated at anterolateral margins of delthyrium and articulating with dental sockets in dorsal valve (Fig. 322). See *cyrtomatodont* and *deltidodont*.
- hinge trough*. See *septalium* (in sessile form).
- hinge width**. Lateral extent of hinge line.
- holcothyrid stage* (of folding). See *paraplicate*.
- hollow ribs**. Marginally facing openings on ribs of some orthides and strophomenides (Fig. 302).
- holoperipheral growth**. Increase in valve size all around margins, in posterior as well as anterior and lateral directions (Fig. 284).
- homeochilidium**. Externally convex triangular plate closing almost all or only apical part of notothyrium in paterinides; spelled *homoeochilidium* by some authors (Fig. 315).
- homeodeltidium**. Externally convex triangular plate closing almost all or only apical part of delthyrium in paterinides; spelled *homoeodeltidium* by some authors (Fig. 286).
- hood**. Conical structure arising at posteroventral edge of septal pillar, or vertical plate on echmidium, representing rudiment of ascending elements of loop.
- hypercline**. See *inclination of cardinal area* or of *pseudointerarea* (Fig. 285).
- hypothyrid** (foramen). Pedicle opening located below or on dorsal side of beak ridges with umbo intact (Fig. 318).
- imbricate** (ornament). Strong, regular, overlapping growth lamellae.
- impunctate** (shell). Shell lacking punctae, pseudopunctae, or canals of any kind.
- inclination of cardinal area or of pseudointerarea**. Commonly used terms to describe the condition of either valve based on convention of viewing specimen in lateral profile with beaks to left and dorsal valve uppermost, referring cardinal area to its position within one of four quadrants defined by commissure plane and plane normal to it and symmetry plane, touching base of cardinal areas (Fig. 285). Cardinal area lying on continuation of commissure plane is **orthocline**. Moving clockwise, cardinal area in first quadrant (top left) is weakly to strongly **anacline**; in second quadrant (top right) weakly to strongly **hypercline**. Moving counterclockwise from orthocline position, cardinal area lying in bottom left quadrant is weakly to strongly **apsacline**; at 90° to orthocline it is **catacline**; and continuing counterclockwise into bottom right quadrant cardinal area is weakly to strongly **procline** (Fig. 285).
- inclined beak*. See *beak angle*.
- incurved beak*. See *beak angle*.
- inequidistribute** (mantle canal). *Vascula genitalia* of dorsal mantle saccate and contributing little to canal circulation (Fig. 380).
- inner carbonate layer*. See *secondary layer*.
- inner hinge plates**. Pair of subhorizontal or concave plates in cardinalia located medially of crural bases and fused laterally with them (Fig. 330–331). See *cardinal plate*, *hinge plate*, *crural plate*.
- inner plates*. Pair of subvertical plates in cardinalia of some pentameroids lying on ventral side of base of brachial process and fused dorsally with it; homologue of outer hinge plates. See *brachiophore plates* for orthides.
- inner socket ridge**. Ridge of secondary shell commonly overhanging dental socket and forming its inner or anterior margin (Fig. 329–331).
- interarea**. Posterior sector of shell with growing edge at hinge line; also, more commonly used for any plane or curved surface lying between beak and posterior margin of valve and bisected by delthyrium or notothyrium (Fig. 285).
- intercalary lamellae**. See *accessory lamellae*.
- intercalation**. Costella arising by insertion between costae or costellae, not by bifurcation of existing costa or costella (Fig. 297).
- intercamarophrial plate**. Short, low median septum on posterior midline of camarophorium in

- stenoscismatoids, extending to underside of hinge plate but independent of median septum duplex (Fig. 367).
- interconnecting bands*. See connecting bands.
- intercostal sulci*. See interspace.
- internal oblique muscles**. Pair of muscles in some inarticulated brachiopods originating on ventral valve between anterior adductors and passing posterolaterally to insertions on dorsal valve located anterolaterally of posterior adductor muscles (Fig. 374).
- interridge*. Median external ridge in pedicle pseudo-interarea of some acrotretoids.
- interspace**. Flat or externally concave sectors of shell between adjacent costae or costellae (Fig. 298, 300).
- intertext* (folding). See alternate folding.
- intertrough**. Median, narrowly triangular furrow dividing pseudointerarea of ventral valve of some acrotretoids (Fig. 286).
- intraplicate* (folding). See plicosulcate.
- intraseptal lamella**. Sheet of prismatic calcite of varying persistency found in median septum of spondylium duplex (Fig. 351.2b).
- inverted stage* (of folding). See sulcate.
- isemeniform* (loop). See diploform.
- jugal processes**. Pair of discrete, ventromedially directed lamellae arising from primary lamellae of spiralia.
- jugal stem**. Ventroposteriorly directed continuation of jugum which, by bifurcation, may give rise to accessory lamellae posteriorly (Fig. 336).
- JUGUM**. Medially placed structure of secondary shell connecting two primary lamellae of spiralia; also junction between descending lamellae in loop of *Cryptacanthia* (Fig. 336).
- kingeniform* (loop). Long reflected loop, typical of adult *Kingenia* and related genera, with descending lamellae united to median septum, and ascending lamellae supported by mediovertical connecting bands also converging on median septum. See bilacunar.
- koskinoid perforations**. Clusters of fine perforations penetrating the ventral valves, especially in the beak region, of many orthotetoids and *Uncites* (Fig. 282).
- labiate** (foramen). Exaggerated marginate foramen in which dorsal edge is prolonged and liplike.
- lacuna*. Aperture in hood.
- lamella**. Sheetlike extension of primary and even underlying secondary shell deposited by retractile mantle margin on external shell surface (see growth lamella); also used for calcareous ribbon comprising spirulum and coiled extension from arm of jugum.
- lamellar layer. See primary layer, secondary layer.
- lamina**. Parallel-sided, thin mineral constituents of a shell succession, normally ensheathed in membranes and consisting of tablets, plates, or blades in various stages of amalgamation (Fig. 247).
- laqueiform* (loop). Long reflected loop with laterovertical connecting bands connecting ascending and descending lamellae, and lateral connecting bands extending between descending lamellae and median septum. See bilateral.
- lateral adductor muscles**. Paired muscles in theci-
- deidines attached posterolaterally in ventral valve and on either side of cardinal process of brachial valves.
- lateral areas. Ventral palintrope on either side of delthyrial structures.
- lateral branch** (of jugum). Part of jugum continuous with primary lamella (Fig. 336).
- lateral cavities*. See umbonal chambers.
- lateral connecting bands**. See connecting bands.
- lateral oblique muscles**, also **oblique lateral muscles**. Paired muscles in some inarticulated brachiopods, originating on ventral valve anterolaterally of posterior adductor muscles and passing anterodorsally to insertions either on dorsal valve and anterior body wall against anterior adductors (discinids) or entirely on anterior body wall (craniids) (Fig. 374).
- lateral ridges. Ridges of secondary shell common in productines, extending laterally from cardinal process or ventral beak, diverging from posterior margin toward ears or lateral margins.
- lateral septa*. See anderidia.
- lateral slopes. Valve surfaces on either side of median sector of shell.
- laterovertical** (loop). Long reflected loop, typical of adult *Pictothyris*, with laterovertical connecting bands only.
- leiolophid stage* (of lophophore). Rudimentary lophophore ring, before development of tentacular appendages.
- lemniscate** (mantle canal). Saclike gonocoel giving rise to branches that extend to posterolateral margins with corresponding peripheral reduction of *vascula media* and *vascula myaria* (Fig. 380).
- LENGTH** (of valve). Distance from most posterior point of valve (normally umbo) to farthest point on anterior margin measured on commissural plane in plane of symmetry or parallel with it (Fig. 283).
- lenticular stage* (of folding). Both valves gently and subequally biconvex, anterior margin rectimarginate.
- ligate stage* (of folding). See lobate.
- limbus**. Flattened inner margin of inarticulate valve.
- linguiform extension**. Anterior tongue-shaped extension of either valve.
- liothyridid stage* (of folding). See lenticular stage.
- lirae*. Fine concentric or radial ridges and grooves.
- listrium**. Plate in some discinids closing anterior end of pedicle opening that has migrated posteriorly (Fig. 286).
- lobate** (of folding). Opposite folding with single sinus in one valve opposed by single sulcus in other; commissure rectimarginate (Fig. 288).
- longitudinal axis**. Intersection of planes of commissure and symmetry (Fig. 283).
- long loop. See loop.
- LOOP**. Support for lophophore composed of secondary shell and brachiotest extending anteriorly from crura as closed apparatus that may be short (centronellidines, terebratulidines) or long (terebratulidines) or a derivative of one of these forms (Fig. 338).
- lophidium**. Inverted V-shaped projection of median posterior part of dorsal valve or of external face of

- cardinal process, helping to close gap in delthyrium in some aulostegoids.
- LOPHOPHORE.** Feeding and respiratory organ with tentacles, symmetrically disposed around mouth, typically suspended from anterior body wall but may be attached to dorsal mantle; occupies mantle cavity (Fig. 1).
- lophophore platform.* See brachial platform.
- lophrothyrid stage* (of folding). See uniplicate.
- magadiform* (loop). See diploform.
- magadiniiform* (loop). See annular.
- magaselliiform* (loop). See haptoid.
- magellanian stage* (of shell). See endopuncta.
- magellaniiform* (loop). Type of free terebratellide loop consisting of long descending lamellae recurved into ascending lamellae that meet in transverse band. See teloform.
- magelliiform* (loop). See haptoid.
- main flanks.* See lateral slopes.
- maniculiform** (crura). Derived from raduliform type, with handlike processes at end of straight, ventrally directed crura.
- MANTLE.** Prolongation of body wall as fold of ectodermal epithelium (Fig. 1).
- MANTLE CANALS.** Flattened, tubelike extensions of body cavity into mantle (Fig. 379).
- MANTLE CAVITY.** Anterior space between valves bounded by mantle and anterior body wall and containing lophophore (Fig. 1).
- mantle papilla. See caecum.
- mantle sinus. See mantle canal.
- margin** (of valve). Edge of valve.
- marginal flange* (of shell). See geniculate.
- marginal flange* (of thecideoid dorsal valve). See subperipheral rim.
- marginal ridge. See subperipheral rim.
- marginal spines.** Long, slender prolongations of interspaces between ribs of rhynchonellides lying against inner surface of opposing valve when shell is shut and forming grille when shell is open (Fig. 300); also used for spinose extensions of growth lamellae.
- marginate* (foramen). Pedicle foramen with thickened margin.
- marsupial notch.** Small double notch or perforation in ventral edge of brachial bridge in some adult female thecideoids marking passage of two specialized posteriorly directed filaments to which embryos are attached.
- median.** In plane of shell symmetry (Fig. 283).
- median buttress.** Knoblike projection at posterior end of dorsal median septum in some acrotretoids, which may have been the site of attachment of umbonal muscle (Fig. 378).
- median partition.** Median septum supporting anterior part of trimerelloid muscle platform and dividing cavity beneath platform into two vaults (Fig. 375).
- median plane.** See plane of symmetry (Fig. 283).
- mediotest.** Variably persistent, granular sheet occurring medially in platelike structures of fibrous secondary shell.
- mediovertical** (loop). Long reflected loop, typical of adult *Ecnomiosa* with a pair of mediovertical connecting bands extending from the median septum to the transverse band.
- megathyrid* (posterior margin). Posterior margin long and straight.
- megerliiform* (loop). Loop of kraussinids with descending lamellae united to anterior projections of Y-shaped median septum; extremities of median septum also united by narrow transverse band. See mediovertical.
- mergiform** (crura). Variant of raduliform type with long, closely parallel crura arising directly from swollen edge of dorsal median septum.
- mesothyrid** (foramen). Pedicle opening located partly in ventral umbo and partly in delthyrium; beak ridges appearing to bisect foramen (Fig. 318).
- metacarinata stage* (of folding). See bilobate.
- micropuncta** (pl., **micropunctae**). Perforation of calcitic shell, too fine to contain caecum but possibly extension of secreting plasmalemma (Fig. 265).
- middle lateral muscles.** Pair of muscles in some lingulides originating on ventral valve between central muscles and diverging slightly posteriorly before insertion on dorsal valve (Fig. 377).
- mixoperipheral growth.** Differs from holoperipheral growth in that posterior sector of valve increases in size anteriorly and toward other valve (Fig. 284).
- monticules. See tubercle.
- monticulus. Narrow median fold of the pseudodeltidium of orthotetidines and triple-siindines.
- mosaic.** Pattern on interior of valve formed by outlines of adjacent fibers of secondary shell layer (Fig. 242).
- mouth segment** (of lophophore). Median part of lophophore containing mouth; attached to anterior body wall and bearing single row of paired or unpaired tentacles.
- mucronate** (cardinal margin). Cardinal extremities extended into sharp points.
- muehlfeldtiiform* (loop). See mediovertical.
- multicostellate.** Costellae increasing in number by bifurcation or intercalation but not varying greatly in size (Fig. 297).
- muscle area.** See muscle field.
- muscle-bounding ridge.** Elevation composed of secondary shell bounding part of muscle field.
- muscle field.** Area of valve in which muscle scars are concentrated.
- muscle impression.** Marks of muscle attachment.
- muscle platform.** Solid or undercut elevation of shell to which muscles are attached (Fig. 375).
- MUSCLE SCAR.** More or less well-defined impression or elevation on valve representing final site of attachment of muscle (Fig. 350).
- muscle track.** Path of successive muscle impressions formed by migration of muscle base during growth (Fig. 350).
- myocoelidium.** Chamber similar to spondylium but not formed by dental plates, serving for attachment of muscles as in richthofeniids.
- myophore.** Differentiated site of diductor muscle attachment on cardinal process, consisting of ridged myotest (Fig. 357, 360).
- myophragm.** Ridge or septum of secondary shell

- dividing paired muscle scars that may encroach on its sides.
- myotest.** Muscle scar shell usually bearing impressions of the secretory cuboidal epithelium associated with the attached bases of muscle systems; commonly granular in texture and pitted by resorption in carbonate shells (Fig. 350).
- mystrochial plates.** Pair of small plates buttressing spondylium posterolaterally, as in *Amphigenia* and some meristids.
- neanic.** Youthful phase, immediately following brephic stage of shell development, at which generic characters of shell begin to be apparent.
- nearly straight beak.** See beak angles.
- neponic.** See brephic.
- neural valve.** See ventral valve.
- node.** Thickened junction of rib and lamella, frequently accentuated by growth line. Any thickening at a junction between converging apophyses.
- nodus** (*principalis, quadrivalis, septalis, terminalis*). Point of divergence of branches in mantle canal system (Fig. 379).
- nonintertext** (folding). Type of folding in which sulcus or carina of one valve is opposed by plane valve.
- nonstrophic** (shell). See astrophic.
- norellid stage** (of folding). See unisulcate.
- notodeltidium.** Plate completely filling delthyrium, formed by fusion of deltidial plates with eventual plugging of pedicle foramen by posterior retreat of junction between pedicle epithelium and outer epithelium.
- notothyrial cavity.** See notothyrial chamber.
- notothyrial chamber.** Cavity in umbo of dorsal valve corresponding to delthyrial chamber of ventral valve, bounded laterally by inner socket ridges, brachiophore plates (or homologues), or by posterolateral shell walls if brachiophore bases absent.
- notothyrial platform.** Umbonal thickening of floor of dorsal valve between inner socket ridges, brachiophore, or crural plates (Fig. 323.4, 329).
- notothyrid** (foramen). Pedicle opening in dorsal valve, a condition never completely attained.
- NOTOTHYRIUM.** Median subtriangular opening bisecting dorsal cardinal area or pseudointerarea (Fig. 283).
- oblique lateral muscles.** See lateral oblique muscles.
- oblique muscles.** Variable sets of muscles in inarticulated brachiopods responsible for rotational and longitudinal movements of valves (Fig. 374).
- occlusor muscle.** See adductor muscle.
- oligopalmate.** Mantle canal system with two pairs of principal canals in each mantle.
- opercular.** Lidlike valve.
- opposite folding.** Folding in which fold or sulcus in one valve is opposed by fold or sulcus in other; commissure remaining rectimarginate (Fig. 288).
- ornament.** Any regularly occurring outgrowth, deflection or nonpathological interruption in growth (other than growth lines) found on outer shell surface.
- ornithellid stage** (of folding). See carinate.
- orthocline.** See inclination of cardinal area or of pseudointerarea (Fig. 285).
- orthoconate.** Brachia coiled parallel with plane of commissure.
- orthomorph.** Chonetoid hinge spines remaining straight, perpendicular, oblique, or parallel to hinge line.
- outer carbonate layer.** See primary layer.
- outer epithelium.** Ectodermal epithelium underlying shell and responsible for its secretion (Fig. 3).
- outer hinge plates.** Pair of concave or subhorizontal plates in cardinalia separating inner socket ridges and crural bases (Fig. 329–331).
- outer mantle lobe.** Outer peripheral part of mantle, separated by mantle groove from inner lobe; in articulated brachiopods responsible for secretion of periostracum and part or all of primary shell layer (Fig. 3).
- outer plates.** Pair of subvertical plates in pentameroid cardinalia with ventral surface fused to base of brachial process and dorsal edge attached to floor of valve or rarely, septal plate; homologue of crural plates or inner hinge plates (Fig. 329.9).
- outer socket ridge.** Low ridge bounding dental socket on outer lateral or posterior side of dorsal valve (Fig. 322, 331).
- outside lateral muscles.** Pair of muscles in some lingulides that originates on ventral valve lateral of centrals and extends posteriorly to insertions behind middle lateral muscles on dorsal valve (Fig. 377).
- ovarian impression.** See genital marking.
- ovarian marking.** See genital marking.
- palintrope.** Originally used for morphologically posterior sector of either valve that was reflexed to grow anteriorly (mixoperipheral growth); more recently used for curved surface of shell, bounded by beak ridges and cardinal margin of astrophic shells (differs from planarea in being curved in all directions) (Fig. 285).
- pallial caecum.** See caecum.
- pallial lobe.** See mantle.
- pallial markings.** See vascular markings.
- pallial sinus.** See mantle canal.
- pallium.** See mantle.
- papillae.** See endospines.
- paraendopunctae.** See extropunctae.
- parallel.** Hinge spines of chonetoids bending sharply laterally to become parallel with posterior margin of ventral valve.
- paraplicate** (folding). Alternate folding in which two folds in dorsal valve bound median sulcus (Fig. 289).
- parasulcate** (folding). Alternate folding in which dorsal sulcus bears strong median fold (Fig. 289).
- parathyridium.** Deep, pouchlike indentation of shell on either side of beak, formed by medially directed depression or flexure of posterolateral shell surface of both valves, particularly dorsal (e.g., *Cardinaria*).
- parvicostellate.** Costellae numerous, arising entirely by intercalation between widely spaced costae (Fig. 297).
- paucicostate.** Costae distant from umbo and few.
- paucicostellate.** Costae and costellae distant and few.

paucispinose. Very few spines.

PEDICLE. Variably developed, cuticle-covered, stalklike appendage commonly protruding from ventral valve that adjusts position of shell relative to external environment (Fig. 1).

pedicle callist. Localized thickening of secondary shell layer in apex of ventral valve representing track of anterior migration of junction between pedicle epithelium and outer epithelium (Fig. 348).

pedicle capsule. Cylindroid infold of pedicle epithelium and cuticle accommodating the proximal bulbous end of the pedicle of articulated brachiopods (Fig. 1).

pedicle collar. Complete or partial, ringlike thickening of inner surface of ventral beak; continuous laterally with internal surface of deltidial plates; sessile, with septal support, or free anteriorly and secreted by anteriorly migrating outer epithelium at its junction with pedicle epithelium (Fig. 316).

pedicle epithelium. Ectodermal epithelium investing pedicle (Fig. 2).

PEDICLE FORAMEN. Subcircular to circular perforation of shell through which pedicle passes (Fig. 317).

pedicle fulcrum. Pair of subparallel plates median to dental plates in ventral umbo of some early athyridines.

pedicle furrow. External plate extending anteriorly from beak to pedicle foramen in some siphonotretoids and obolellides.

pedicle groove. Subtriangular groove dividing ventral pseudointerarea medially and affording passage for pedicle in many lingulides (Fig. 286).

pedicle muscles. Muscles associated with pedicle; external to pedicle in articulated brachiopods (adjustor and median pedicle muscles); internal in inarticulated brachiopods.

pedicle muscle scar. Scar of attachment on ventral valve of longitudinal fibrils in connective tissue of pedicle of articulated brachiopods.

pedicle notch. Small, subtriangular depression, posteromedially placed on limbus of paterulids, probably functioning as pedicle groove.

pedicle opening. Variably shaped aperture in shell through which pedicle emerges.

pedicle plate. Tongue-shaped shelly deposit inside labiate foramen.

pedicle sheath. Externally directed tube projecting posteroventrally from pedicle umbo, probably enclosing pedicle in young stages of development of some shells with supra-apical pedicle opening (Fig. 319).

pedicle tube. Internally directed tube of secondary shell continuous with margin of pedicle foramen and enclosing proximal part of pedicle (Fig. 310). pedicle valve. See ventral valve.

peduncle. See pedicle.

perideltidial area. Discrete part of perideltidium.

perideltidial line. Break of slope marking outer boundary of perideltidial area.

perideltidium. Pair of slightly raised triangular parts of interarea flanking pseudodeltidium or lateral to it and characterized by vertical striae in addition to

horizontal growth lines parallel to posterior margin; characteristic of orthotetidines.

periostracal pad. Thickened band of periostracum covering cardinal areas and spun out by fused mantle lobes along posterior margin of some articulated brachiopods (Fig. 44).

periostracum. Organic external layer of shell secreted by the outer mantle lobe beneath an impersistent film of glycosaminoglycans and acting as the seeding sheet for the primary mineralized shell (Fig. 2).

permesothyrid (foramen). Pedicle opening located mostly within ventral umbo (Fig. 318).

pinnate (mantle canal). *Vascula genitalia* or *vascula lateralia* consisting exclusively of radially disposed canals (Fig. 381).

planareas. Two flattened areas developed, one on either side of posterior part of shell, more or less perpendicular to commissural plane; single median interarea may be much reduced or absent.

plane commissure. See rectimarginate.

plane of symmetry. Plane bisecting shell symmetrically (Fig. 283).

planoconvex. Dorsal valve flat; ventral valve convex. plate (trimerellids). Single transverse, platelike projection from cardinal margin of dorsal valve articulating with cardinal socket of ventral valve (Fig. 375). platform. Relatively broad, solid, or undercut elevation of inner surface of valve, commonly bearing muscles (Fig. 368, 375).

platform (of Orthidina). See notothyrial platform, notothyrial chamber.

platform line. Side bounding notothyrial chamber.

platform vaults. Two cavities beneath platform in some trimerelloids, separated by median partition (Fig. 375).

platidiiform (loop). Loop consisting of descending lamellae from cardinalia to median septum occasionally with only rudimentary outgrowths from distal end of septum analogous to ascending lamellae. See axial.

plectolophe. Lophophore in which each brachium consists of U-shaped side arm bearing double row of paired tentacles but terminating distally in medially placed planospire normal to commissural plane and bearing single row of paired tentacles (Fig. 114).

plectolophus (noun). See plectolophe.

pleuromal plates. Pair of plates in posterior part of delthyrial cavity of some spiriferides immediately internal to dental plates; probably merely later infilling of delthyrial cavity.

plica. Major undulation of commissure, reflected on shell interior, with crest directed dorsally; commonly but not invariably associated with dorsal fold and ventral sulcus.

plication. See plica.

pliciligate stage (of folding). See parasulcate.

plicosulcate. Alternate folding in which dorsal sulcus bears small median fold (Fig. 289).

polypalmate. Mantle canal system with more than four principal canals in each mantle.

pore. See puncta.

POSTERIOR. Direction in plane of symmetry or

- parallel to it toward pedicle and away from mantle cavity (Fig. 283).
- posterior flap.** Reflexed to anteriorly directed extension of lytoniid ventral valve lying dorsal to at least posteromedian part of dorsal valve.
- posterior margin.** Posterior part of junction between edges of valves; may be hinge line or cardinal margin (Fig. 285).
- posterior oblique muscles.** Pair of muscles in discinoids originating posterolaterally on ventral valve and converging dorsally to insertions on dorsal valve between posterior adductors; equivalent to oblique internals (Fig. 374).
- precampagiform flange.* See septal flange.
- precampagiform hood.* See hood.
- prefalcifer* (crura). See hamiform.
- pre-ismeniform* (loop). See diploform.
- premagadiniform* (loop). One of the early stages of terebratellid loop development marked by growth of descending branches from both cardinalia and median septum and their completion and by the appearance of tiny hood developing into ring on septum. See cucullate and annular.
- prepygites stages* (of folding). See plicosulcate.
- presocket line.* Anterior or anterolateral side of triangular slot produced by brachiophore plate (and falcral plate if present) in internal mold of orthides.
- primary lamella.** First half whorl of each spirulum distal from its attachment to crus (Fig. 336).
- PRIMARY LAYER** (of shell). Outer, mineralized shell layer immediately beneath periostracum, deposited by vesicular cells of outer mantle lobe (Fig. 11).
- prismatic shell.** Band or continuous layer of polygonal columns of calcite disposed normal to the shell surface. See tertiary layer.
- procline.** See inclination of cardinal area or of pseudo-interarea (Fig. 285).
- prodeltidium.* So-called third plate; at one time thought to be developed in earlier embryonic growth of atrematous, neotrematous, and protrematous species (BEECHER, 1891, 1892), subsequently becoming more or less attached to either dorsal (atrematous) or ventral valve.
- promontorium** (pl., **promontoria**). Shelflike structure extending laterally from lateral sloping face of cardinal process; homologue of inner socket ridges in some orthotetidines.
- PROPAREAS.** Pair of subtriangular halves of pseudo-interarea divided medially by various structures (e.g., homeodeltidium, intertrough, and pedicle groove) of inarticulated brachiopods (Fig. 286, 327.1).
- propuncta* (pl., *propunctae*). See pseudopunctum (proposed for deflections without taleolae).
- prosocket ridge.* See socket ridge.
- prostrate spines.** Usually straight spines that lie prone on shell surface of some productides.
- protegular node.** Apical portion of adult shell, commonly raised, representing site of protegulum and later growth up to neanic stage (Fig. 297).
- protegulum.** First-formed shell of periostracum and mineralized lining secreted simultaneously by both mantles (Fig. 283).
- protractor muscles.* See outside lateral muscles, middle lateral muscles in inarticulated brachiopods; also used for longitudinal fibrils attached to setae and those in the connective tissue of pedicle of articulated brachiopods. See pedicle muscle scar.
- pseudoarea.* See pseudo-interarea.
- pseudobranch plate.* Tuberculate ridges bearing dorsal adductor muscles.
- pseudochilidium.* See chilidium.
- pseudocruralium.** Callus of secondary shell bearing dorsal adductor impressions and elevated anteriorly above floor of valve (Fig. 366).
- PSEUDODELTIDIUM.** Single, convex, or flat plate affording variably complete cover of delthyrium but invariably closing apical angle when foramen is supra-apical or absent and always dorsally enclosing apical foramen (Fig. 319; 327.1, 327.3; 353).
- PSEUDOINTERAREA.** Somewhat flattened, posterior sector of shell of some inarticulated brachiopods secreted by posterior sector of mantle not fused with that of opposite valve (Fig. 286).
- pseudopedicle collar.* Sessile pedicle collar.
- pseudopedicle groove.* See intertrough.
- pseudopuncta** (pl., **pseudopunctae**). Conical deflection of secondary shell, with or without taleola, pointing inwardly and commonly anteriorly to appear on internal surface of valve as tubercle (Fig. 267–269).
- pseudopunctum* (pl., *pseudopuncta*). See pseudopuncta.
- pseudoresupinate.* Convexoconca shell.
- pseudosocket.* See secondary sockets.
- pseudospondylium.** Cup-shaped chamber accommodating ventral muscle field and comprising undercut callus of secondary shell contained between discrete dental plates (Fig. 352).
- pseudoteeth.* See secondary teeth.
- pseudotellae.* Pair of external projections resembling tellae but produced by dorsal migration of pedicle cutting labiate foramen, not beak ridges.
- ptycholophe.** Lophophore with brachia folded into one or more lobes in addition to median indentation (Fig. 115).
- ptycholphus* (noun). See ptycholophe.
- puncta** (pl., **punctae**). Perforation penetrating shell to connect with periostracum and occupied by caecum as in cranioids; any perforation apparently penetrating fossil shell and large enough to accommodate caecum (Fig. 261).
- punctum* (pl., *puncta*). See puncta.
- pygoid* (loop). Short, ringlike loop with slightly arched transverse band. See deltidium.
- quadruplicate (folding). Having four anterior folds and three intervening sulci.
- raduliform** (crura). Hook-shaped or rodlike crura that arise on ventral side of hinge plate and project toward ventral valve.
- ramicostellate.** Costellae numerous, arising entirely by branching (Fig. 297).
- ramulus** (pl., **ramuli**). Folds developed on lateral walls of longitudinally divided dorsal median septum in thecideids.
- receiving valve.* See ventral valve.
- rectimarginate.** Having planar anterior commissure (Fig. 289).
- recumbent spines.** Slightly curved spines extending at

- angle of less than 45° to shell surface.
- reflexed interarea*. Hypercline dorsal interarea.
- remigrant* (foramen). Pedicle opening that tends to move dorsally after initially migrating toward ventral beak.
- resupinate**. Reversal in relative convexity of post-brephic shells with convex ventral valve that becomes concave and with concave dorsal valve that becomes convex during successive adult stages of growth (Fig. 287).
- reticulate** (ornament). Subrectangular patterns on shell exterior, commonly involving nodelike enlargements formed by intersection of concentric and radial elements of ornament.
- retractor muscles*. See anterior lateral oblique muscles.
- rhizoid spines**. Spines of productides resembling rootlets, serving for attachment either by cementation to substrate or by entanglement.
- rhynchonellid stage* (of folding). See uniplicate.
- ribs**. Any ornament of radial ridges.
- ridge**. Relatively long narrow elevation of secondary shell, indicated to variable depth within underlying floor of valve by low, wide deflections of the skeletal fabric normal to long axis of ridge.
- rinned* (foramen). See auriculate.
- ring**. Precursor to ascending elements of terebratellide loop arising from resorption of hood apex, consisting of thin circular ribbon; narrow ventrally and broadening dorsally to its attachment on septal pillar.
- rostellum**. Low projection between anterior adductor muscle scars of ventral valve of some cranioids to which internal oblique muscles are attached.
- rostral callosity*. See delthyrial plate.
- rostrate**. With prominent beak of ventral valve projecting over narrow cardinal margin.
- rostrum*. Beak of articulated brachiopods. See beak.
- rostrum**. Elevation of secondary shell on inner surface of dorsal valve of some cranioids in front of anterior adductor muscles, consisting of pair of low club-shaped protuberances forming seat of attachment for brachial protractor muscles.
- RUGA** (pl., **RUGAE**). Concentric or oblique wrinkling of external shell surface (Fig. 294).
- saccate** (mantle canal). *Vascula genitalia* pouchlike, without terminal branches, not extending to anterolateral periphery of mantle, functioning primarily as gonocoels (Fig. 381).
- saddle**. Median arched part of jugum between stem and lateral branches (Fig. 336).
- scar**. See muscle scar (Fig. 348–350).
- scar of pedicle attachment*. See pedicle muscle scar.
- schizolophe**. Lophophore indented anteromedially to define pair of brachia, each bearing row of paired tentacles, at least distally (Fig. 112–114).
- schizolophus* (noun). See schizolophe.
- SECONDARY LAYER** (of shell). Shell deposited by a layer of outer epithelium within the circumferential lobes of the mantle and consisting of fibers or laminae ensheathed in interconnecting membranes (Fig. 5, 222).
- secondary pseudointerea**. Flat, undivided pseudointerea, lacking flexure lines and developing after origin of pedicle foramen in some lingulides.
- secondary sockets**. Pair of small depressions immediately posterodorsal of cardinal process lobes receiving secondary teeth.
- secondary teeth**. Pair of dorsally directed projections from ventral process fitting into secondary sockets of strophodontid dorsal valve.
- septal pillar**. High, brachial septum anterior to cardinalia, formed early in development of terebratelloid loop.
- septal plates**. Two plates that fuse to form duplex median septum in dorsal valve of some pentamerides and bearing outer plates on their ventral surfaces. See also septal plates, below.
- septal plates*. Various parts of cardinalia. See crural plates, hinge plates. See also septal plates, above.
- septalial plates*. Crural plates forming floor of septalium and united with earlier formed part of median septum.
- septalium**. Troughlike structure of dorsal valve between crural bases, consisting of crural plates (or homologues) fused medially and usually supported by median septum, but may be unsupported or sessile; does not carry adductor muscles (Fig. 330.4). See crural plates.
- septiform (crura)**. Crura having form of septa that descend directly from brachial side of hinge plates to floor of dorsal valve.
- septule**. Small elongate tubercle within strophomenide valves. See also accessory septa.
- septum** (pl., **septa**). Relatively long, narrow elevation of secondary shell, commonly bladellike; indicated within underlying floor of valve by persistent high, narrow deflections of shell fabric originating near primary layer (Fig. 354).
- sessile cruralium**. Cruralium united with floor of dorsal valve without intervention of supporting median septum.
- sessile spondylium**. Spondylium united with floor of ventral valve without intervention of supporting median septum.
- seta** (pl., **setae**). Chitinous bristle arising from invaginated follicle along mantle grooves and commonly protruded beyond shell margin (Fig. 48).
- shaft**. See cardinal process shaft.
- shell mosaic**. See mosaic.
- shell space**. Cavity enclosed by conjoined valves.
- shoe-lifter process**. Arched platform of secondary shell attached posteriorly and laterally to floor of either valve but sharply elevated and free medially; in ventral valve, bearing part of ventral muscle field and lying between or supporting dental plates; in dorsal valve bisected by median septum (Fig. 356).
- short loop**. See loop.
- sinus**. Major undulation of commissure with crest directed ventrally, commonly but not invariably associated with ventral fold and dorsal sulcus; also used irrespective of commissure, as a synonym of sulcus.
- siphonothyrid* (foramen). Pedicle foramen continued internally as tube made up of exaggerated pedicle collar.
- socket line*. Posterior side of triangular slot in internal molds of orthide brachiopods produced by brachiophore base (and fulcral plates if present) and bounding impression of socket.

socket plate (of orthides). See fulcral plate.

socket plates. Pair of plates supporting inner socket ridges, attached to cardinal process, and resting on floor of dorsal valve of orthotetoids and some orthoids; also pair of plates defining sockets of atrypid dorsal valve, confined by inner socket ridges medially and normally supported by thickened shell deposit (Fig. 332).

socket ridges. Linear elevations of secondary shell extending laterally from cardinal process and bounding anteromedian margin of dental sockets. See also inner socket ridge and outer socket ridge (Fig. 323, 331).

sockets. See dental sockets.

socket valve. See dorsal valve.

spicules. Small irregular bodies of calcite secreted by scleroblasts within connective tissue of mantle and lophophore (Fig. 53, 339–340).

spine. Solid or hollow, cylindrical, parallelepipedic, or, less commonly, elongate triangular projections from external shell surface or anterior margin (Fig. 304, 307).

spine apertures. Internal opening of spine bases.

spine ridge. Ridgelike radial trace of prostrate spine on shell exterior.

spinule bases or apertures. See hollow ribs.

spinules. Spines of small diameter and approximately 1 or 2 mm in length in chonetoids.

spinuliform (crura). Variant of raduliform type, but with crura laterally compressed.

SPIRALIA (sing., SPIRALIUM). Pair of spirally coiled lamellae composed of secondary shell and supporting lophophore (Fig. 333, 336).

spires. See spiralia.

spiriferid stage (of posterior margin). Long, straight posterior margin.

spirolophe. Lophophore in which brachia are spirally coiled and bear single row of paired tentacles (Fig. 113).

spplanchnocoel. See body cavity.

spondylial cavity. Space enclosed by posterior part of spondylium and purported to be bounded by spondylial lining.

spondylial lining. Thin prismatic layer of tertiary shell forming more or less continuous veneer on dorsal surface of pentameroid spondylium and entire deltidial cover.

spondylium. Trough-shaped or spoonlike apparatus composed of dental plates in various stages of coalescence, usually with median septum, accommodating ventral muscle field (Fig. 354).

spondylium discretum. Muscle-bearing chamber formed by slight convergence of dental plates that are attached separately to floor of valve.

spondylium duplex. Spondylium formed by convergence of dental plates and supported by variably developed median septum arising from floor of ventral valve (Fig. 351.2).

spondylium pseudotriplex. See spondylium triplex.

spondylium simplex. Spondylium formed by convergence and growth of dental plates and supported by variably developed simple ventral median septum or ridge (Fig. 351.1).

spondylium triplex. Spondylium supported by median septum and two lateral septa as in *Polytoechia* (Fig. 353).

spondyloid (dental plates). Basal inner surfaces of dental plates thickened and coalesced to simulate spondylium.

spyridium. Cuplike apparatus affording attachment for dorsal adductors and consisting of variably fused pair of subtriangular platforms elevated on subjacent ridges (Fig. 368).

squama (pl., *squamae*). Small arc of posterolateral margin of dorsal valve, especially of rhynchonellides, overlapping complementary arc (glotta) of ventral margin.

squamose. Growth lamellae having irregular and ragged margin.

stalk. See pedicle.

stegidium. Convex plate or series of imbricate concentric plates closing gap between delthyrial plate and spiriferide dorsal valve consisting of series of concentric layers deposited by outer epithelium associated with atrophying pedicle migrating dorsally (Fig. 320).

stolidium. Thin, marginal, short to long frill protruding at distinct angle to main contour of one or both valves of adult stenoscismatoids.

straight beak. See beak angle.

strainer spines. See endospines.

strangulate (of folding). See lobate.

striae. Fine grooves or incisions.

strophic (shell). Shell with true hinge line coincident with hinge axis (Fig. 285).

subdelthyrial plate. See delthyrial plate.

suberect (beak). See beak angle.

suberect spines. Spines inclined to shell surface at angles between 45° to 75°.

subhypothyrid (foramen). Foramen occupying apex of delthyrium as in atrypids.

subintertext folding. See alternate folding.

submarginal ridge (of productids). Thickening of either valve anterolaterally bordering corpus cavity.

submegathyrid (posterior margin). Posterior margin approximately straight and slightly less than maximum width of shell.

submesothyrid (foramen). Pedicle opening located partly in ventral umbo but mainly in delthyrium (Fig. 318).

subperipheral rim. Elevation of secondary shell concentric to and within margin of valve.

subplectolophous (lophophore). See plectolophe.

subspondylial chambers. See umbonal chambers.

subvertebratulid (posterior margin). Posterior margin considerably less than maximum width of shell but not strongly curved.

sulcate (folding). See unisulcate.

sulcificate (folding). Form of alternate folding with dorsal valve bearing median fold indented by shallow median sulcus (Fig. 289).

SULCUS. Major depression of valve surface, externally concave in transverse profile and radial from umbo.

supporting plates. See brachiophore plates.

supporting septum (of hemispondylium). Median septum attached to floor of thecideoid ventral valve

and supporting concave plates of hemispondylium.
supra-apical foramen. Pedicle foramen initially located in ventral umbo away from apex of delthyrium (Fig. 319.2).

surmounting plate. Variably developed platform along posteroventral margin of dorsal median septum of some acrotretoids (Fig. 346–347).

symbolothyrid (pedicle opening). Pedicle opening shared by both valves.

symphytium. Deltidial plates fused dorsally or anteriorly from pedicle foramen and retaining only weak median line of junction (Fig. 317).

syndeltarium. See deltidial cover.

syrix. Tube of secondary shell medially located on ventral side of delthyrial plate and split along its ventroanterior surface (Fig. 355).

tabella (pl., *tabellae*). See adminicula.

taleola (pl., *taleolae*). Porous cylinder of granular calcite in axial region of many pseudopunctae (Fig. 269–270).

taxolophous lophophore. Rudimentary lophophore with tentacles not completely encircling mouth.

teeth. See hinge teeth.

teeth ridges. Linear elevations bounding delthyrium laterally, representing growth track of hinge teeth and commonly forming low elevations on internal surface of cardinal area in absence of dental plates (Fig. 351.1b,2c).

tegula. Articulating knobs on dorsal hinge line of richthofeniids (Fig. 326.2).

tela (sing., *tela*). Pair of pointed terminations of beak ridges projecting into and beyond pedicle opening, formed by apical migration of pedicle.

teleoform (loop). Long reflected loop, typical of adult stage of various remotely related long-looped stocks (e.g., *Macandrevia*, *Magellania*), with loop free of septum (Fig. 338.4).

terebrataliiform (loop). Long reflected loop typical of *Terebratalia* and related genera, with lateral connecting bands extending between descending lamellae and median septum. See trabecular.

terebreatelliform (loop). Long reflected terebratellid loop with lateral connecting bands uniting descending lamellae to median septum; morphologically similar to terebrataliiform loop, but deriving from dissimilar loop ontogeny. See trabecular.

terebatulid (posterior margin). Strongly curved posterior margin much less than maximum width of shell.

terebatulid stage (of folding). See sulcificate.

terebatuliform (loop). Short, typically U- or W-shaped loop found in most terebratuloids. See deltidform.

terebatuliniiform (loop). Short (deltiform) loop in which crural processes are fused medially to complete ringlike structure.

TERTIARY LAYER (of shell). Continuous layer of prismatic shell secreted by outer epithelium within margin of secondary layer and in internal succession to that layer (Fig. 254–255).

THICKNESS. Maximum dimension between valve exteriors normal to length and width (Fig. 283).

tichorhinum. Small, suboval chamber, with or without median partition, formed by medially directed

struts arising from dental plates converging onto median septum in spiriferide ventral valve; possibly accommodated base of adductor muscles (Fig. 354). tongue. See linguiform extension.

torynidium. See camarophorium.

trabecular (loop). Long reflected loop, typical of adult state of several remotely related long looped stocks (e.g., *Terebratalia*, *Calloria*), with lateral connecting bands extending between descending lamellae and median septum.

track. See muscle track.

trail. Subparallel extensions normally of both valves anterior to corpus and commonly resulting in a geniculate shell profile (Fig. 287.6).

transmedian muscles. Pair of muscles in some lingulides anterior to umbonal muscle; one muscle originating on left side of ventral valve rising dorsally to be inserted on right side of dorsal valve; second muscle originating on right side of ventral valve and inserted on left side of dorsal (Fig. 346.2, 377).

transmuscle septa. Assemblage of narrow elevations comprising one median and two pairs of diverging laterals associated with strophomenoid dorsal adductor field.

transverse band. Lamella joining posterior ends of ascending lamella of loop (Fig. 338).

transverse delthyrial plate. See delthyrial plate.

transverse plate (of spiriferides). See delthyrial plate.

transverse plate (of stringocephaloid loop). See echmidium.

trocholophe. Lophophore disposed as ring surrounding mouth, bearing either single row of unpaired (or more rarely double row of paired) tentacles (Fig. 112–114).

trocholophus (noun). See trocholophe.

tropoconate. Brachia coiled parallel with plane of symmetry.

trough. See septalium.

truncate (beak). Ventral umbo of articulated brachiopods with beak abraded due to pedicle movement and foramen in transapical position (submesothyrid, mesothyrid, permesothyrid, and epithyrid).

tubercle. Any fine, low, rounded protuberance on either surface of valve, irrespective of origin (Fig. 274).

UMBO (pl., **UMBONES**). Apical portion of either valve containing beak (Fig. 283).

umbonal angle. See apical angle.

umbonal blade. Part of primary lamella of spirarium extending from lateral branch of jugum to distal end of crus (Fig. 336).

umbonal chambers. Pair of posterolaterally located cavities in either valve; in ventral valve bounded by dental plates (cardinal buttresses in trimerelloids) and shell walls; in dorsal valve limited medially by crural plates (or homologues) and shell walls (Fig. 351).

umbonal muscle. Single muscle occurring in some lingulides, thought to be homologous with posterior adductors; consists of two bundles of fibers posteriorly and slightly asymmetrically placed (Fig. 346.1).

umbonal slopes. Region of shell surface adjacent to umbo.

- uniplicate** (folding). Form of alternate folding with ventral valve bearing median sulcus and anterior commissure median plica (Fig. 289).
- uniseptum*. See septum.
- unisulcate** (folding). Form of alternate folding with dorsal valve bearing median sulcus and anterior commissure median sinus (Fig. 289).
- unpaired median muscle scar*. See pedicle muscle scar.
- vallum**. Wall of secondary shell surrounding body and mantle cavities in lytoniid valves.
- varix* (pl., varices). See growth line.
- vascula** (sing., vasculum). Any identifiable branches of mantle canal system (Fig. 379).
- vascula - antemyaria, arcuata, cardinalia, cruralia, dentalia, media exteriora, media interiora, myaria ventri, spondyliaria, terminalia*. Finely divided components of mantle canal.
- vascula genitalia**. Mantle canals of articulated brachiopods that contain gonads; may consist of *vascula dentalia* and *vascula spondyliaria* in ventral valve and *vascula cruralia* and *vascula cardinalia*, if developed, in dorsal valve (Fig. 379).
- vascula intermyaria**. Posteromedian parts of *vascula myaria*, segments passing between anterior and posterior adductor scars, distal continuations of which form *vascula myaria exteriora*.
- vascula lateralia**. Laterally located pair of mantle canals developed in both valves of inarticulated brachiopods (Fig. 384).
- vascula media**. Pair of mantle canals in either valve, medially located, projecting anteriorly from body wall (Fig. 379).
- vascula myaria**. Simple or branched pair of mantle canals arising between anterior and posterior adductor muscle scars of dorsal valve of some articulated brachiopods (Fig. 379).
- vascular markings*. Impressions of mantle canals on shell interior.
- vascular ridges*. See vascular markings.
- vascular sinus*. See mantle canal.
- vascular trunk*. Any major branch of mantle canal system.
- venter*. Median region of productoid shell between lateral slopes.
- VENTRAL**. Direction toward ventral valve from dorsal valve.
- ventral adjustor muscles**. See adjustor muscles.
- ventral adminicula**. See adminicula.
- ventral biplicate* (folding). See biplicate.
- ventral dental socket*. See denticular cavities.
- ventral process**. Median callus of secondary shell underlying pseudodeltidium and projecting dorsally to fit between lobes of cardinal process.
- VENTRAL VALVE**. Valve through which pedicle commonly emerges, usually larger than dorsal valve and invariably containing teeth when present (Fig. 283).
- ventribiconvex**. Both valves convex, ventral valve more strongly so than dorsal.
- vertical connecting bands**. See connecting bands.
- vertical plate** (of terebratulides). Plate of secondary shell more or less in plane of symmetry and borne on echmidium.
- vertical zone**. Part of valve secreted normal to commissure plane.
- vestibule**. Subcylindrical prolongation of ventral valve dorsal of dorsal valve.
- virgate*. Straight and erect.
- visceral area**. Part of shell enclosing body cavity.
- visceral cavity*. See body cavity.
- visceral disk**. Part of shell posterior to origin of trails.
- visceral foramen*. See dorsal foramen.
- WIDTH**. Maximum dimension normal to plane of symmetry (Fig. 283).
- xenidium*. See pseudodeltidium.
- zeilleriid* (loop). Long reflected loop, not attached to dorsal septum in adult. See teloform.
- zeilleriid stage* (of folding). See bilobate.
- zygidium**. Collarlike structure uniting lateral ridges on posterodorsal side of cardinal process and fitting within ventral umbo of some productides.
- zygolophe**. Lophophore in which each brachium consists of straight or crescentic side arm bearing two rows of paired tentacles (Fig. 114).
- zygolophus* (noun). See zygolophe.

ECOLOGY OF ARTICULATED BRACHIOPODS

JOYCE R. RICHARDSON

[Museum of Victoria, Australia]

Living articulated brachiopods are notably uniform in appearance and function. The soft parts are enclosed within two valves, one of which is almost invariably beaked. They are suspension feeders with separate sexes; they produce larvae; and they lead a solitary, nonsocial existence. Substrate relationships are governed by the pedicle system, which, with the beak, is present in all living adults except for the members of one order, the Spiriferida. The presence or absence of the pedicle system is correlated with differences in the morphological diversity of living and fossil faunas. Recent articulated brachiopods have little diversity, while the greater diversity of shape in fossil assemblages is derived from forms in which the pedicle is presumed to have been absent and in which substrate relationships are governed by the shell in place of the pedicle system.

All articulated brachiopods are marine, most occupying the waters of the continental shelves and bathyal slopes. Some extend into or are exclusive to abyssal depths; few species are found intertidally; and none is known to be restricted to this zone.

The geographical distribution of living species is correlated at the family level (see section on the biogeography of articulated brachiopods, p. 464), a difference first noted by BEECHER (1892), who differentiated austral and boreal faunas on the mode of the development of their loops. BEECHER's austral fauna consists of those members of the family Terebratulidae that are found in the higher latitudes of the southern hemisphere. From the Oligocene onward they have formed the greatest proportion of fossil brachiopods found in South America, Antarctica, Australia, and New Zealand. They are no less common in modern seas as has been described for Antarctica and the South Pacific (FOSTER, 1974, 1989), South America (MCCAMMON, 1970, 1973; COOPER, 1973, 1982), the subantarctic waters of the Indian

and Atlantic oceans (COOPER, 1981, 1982), New Zealand, and Australia (RICHARDSON, 1981c, 1987). These terebratulids from southern waters are a prime source of most new information on ecology since they are abundant, diverse, and accessible.

SUBSTRATE RELATIONSHIPS

The concept of articulated brachiopods as a sedentary group has undergone a radical change in the past two decades, which is one consequence of the opportunities scuba has given for the direct study of those species that occupy benthic sediments. The common notion of articulated brachiopods as a group with a uniform life-style has been replaced by one of variable substrate relationships that includes both sedentary and active species. Although the pedicle has been generally considered to be an organ for attachment, its function is more closely comparable with an appendage than with a stalk; i.e., it adjusts the position of the organism relative to its external environment. Adjustments in position for life on different types of surfaces require different actions, and the structure of the pedicle is modified for a range of different life-styles. In this respect, it is analogous with the single foot of a mollusc but is morphologically less variable.

All observations of living articulated brachiopods show that movements are directed toward the maintenance of a stable position at the water-substrate interface, an essential requirement for suspension feeders. The pedicle system is adapted in a variety of ways to fulfill this need, and adaptations differ with the energy of the environment, as the pedicles of *Parakinetica stewarti* and *Abyssothyris wyvillei* illustrate. The pedicle of *P. stewarti* is free, and its ratcheting action prevents burial by shifting bryozoan sands in a tidal environment (Fig. 388). The pedicle of *A. wyvillei* tethers the organism to foraminiferal sands, an environment in which

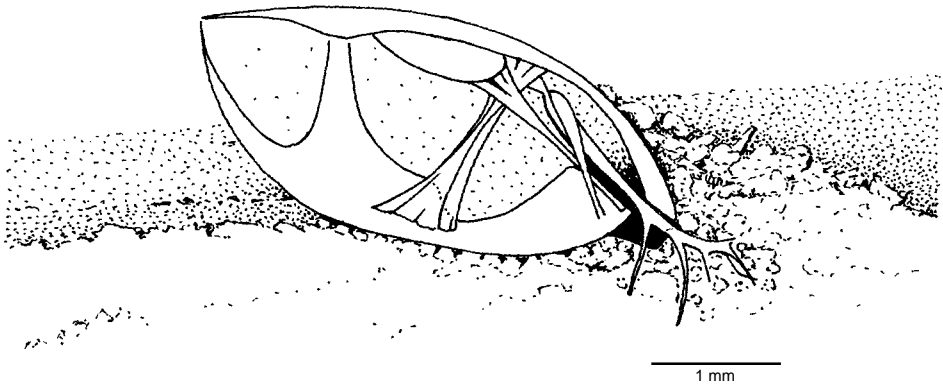


FIG. 388. *Parakinetica stewarti*; western Bass Strait, Australia, fine bryozoan sand, 82 m; the larval substrate is outgrown early in development, and the ratchetlike action of a free pedicle with long, blind processes moves the organism upward and forward to maintain a position at the water-sediment interface. Differential thickening and muscle extent limit the space available within the mantle cavity, which houses an annular loop (new).

movement of the organism may be unnecessary because water and sediment at abyssal depths move very little (Fig. 389). Studies show that the muscles of abyssal species do little more than hold the valves in position, probably constantly open at the sediment-water interface.

The concept of the pedicle as a stalk and anchor developed as a result of the difficulties in observing living articulated brachiopods except for those found on rocks and reefs in shallow water. These are now known to be specialized for that type of habitat. In environments of this type articulated brachiopods follow a sedentary existence, with the pedicle functioning as an organ for attachment to the substrate. As a consequence, the presence of a pedicle was regarded as a sign of attachment, and foramen size was thought to be correlated with strength of attachment. Dredged collections tended to confirm these assumptions because the individuals of some species that were retrieved had pieces of the substrate adhering to the tip of the pedicle.

The principal benefit derived from the study of species from shelf sediments has been to clarify the role that the substrate bonded to the pedicle plays in the life of different brachiopods, that is, the substrate on which the larvae settled. For example, differences in life-style can be observed among

individuals of a number of shoreline species that have been defined as generalists. Some are fixed to rock faces; others lie freely on the sea floor with those components characteristic of the sediment cover adhering to the tip of the pedicle. This pattern of distribution shows, in the first place, that larval settlement is random with respect to grain size of the substrate and, second, that substrate is used for anchorage in one environment but not in others.

These differences in the substrate relationships of individuals within a species are a consequence of the relationship between the pedicle system, shell, and bonded substrate. The pedicle muscles lie between the proximal tip of the pedicle and the inner surfaces of the valves. The distal tip of the pedicle is bonded with substrate, and, since that junction is immovable, the two function as one unit. Such stimuli as sediment on the valve surfaces cause contractions of the pedicle muscles. The response differs, however, according to the mass of substrate bonded with the pedicle tip. Contractions of the muscles cause rotation either of the shell in those individuals bonded to large masses or of the pedicle in those bonded to small masses (Fig. 390).

This mechanism of movement means that the behavior of individuals of generalist spe-

cies is flexible and highly idiosyncratic. Those larvae that settle on a stable rock surface will, as adults, follow a sedentary life-style. Other larvae may settle on substrates made of particles that either have less mass than the adult will have or those that are apt to disintegrate, for example, the empty shell of a brachiopod or mollusc. In such instances, a free life-style will follow a sedentary phase. In other words, the life-style of generalist species is governed by the life history of the substrate.

Given these attributes, it may be seen that, while generalist species (which invariably retain the larvae's substrate) have been described as permanently attached, only those individuals bonded with large masses are also sedentary. Furthermore, the retention of substrates that differ in mass means that for free individuals the bonded and underlying substrates differ, whereas they are the same for sedentary individuals. Sedentary and free individuals also differ in visible movement. Contractions of the dorsal adjustor muscles of sedentary individuals twist the shell; the ventral adjustors pull the shell closer to the substrate. The same contractions by free individuals twist and withdraw the pedicle. These movements of the pedicle cause reactive movements of the shell, and together they maintain the position of a buoyant body at the surface of an inert medium. Although the movements of these individuals may seem undirected, they are effective because they prevent the accumulation of loose sediment on the top and sides of the shell.

Movements of either or both shell and pedicle prevent burial by dislodging sediment from the surfaces of the valve, and, as a result, maintain the position at the water-sediment interface. The movements generated by contractions of the pedicle muscles are, of course, augmented by the adductors and diductors, which open and close the shell; and they not only prevent the build up of sediment but inhibit overgrowth by colonial sponges and ascidians.

The differentiation of species as generalists is based on their ecology, generalists hav-

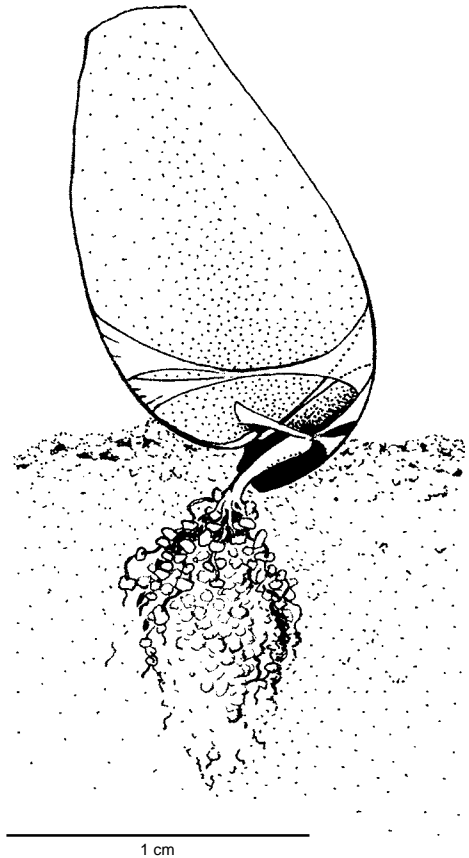


FIG. 389. *Abyssothyris wyvillei*; Tasman Sea, foraminifer sand, 1,463 m; the pedicle is used for tethering and is variable in length and in the number of distal processes that extend from the shaft. In the individual illustrated, each process is bonded with a foraminiferum (new).

ing the capacity to occupy the widest range of substrates on which they may live as sedentary or free forms and at any orientation. Other species are consistent in orientation (with either dorsal or ventral valve uppermost) and in life habit (either sedentary or free) and are morphologically adapted to either hard or soft substrates. As a general rule, species adapted to hard surfaces are sedentary, and those adapted to soft surfaces are free-living forms that may be either active or inactive. The pedicle system of inactive or free-lying forms is reduced or atrophied as in *Neothyris lenticularis* (Fig. 391.2). Active species possess either a free or bonded

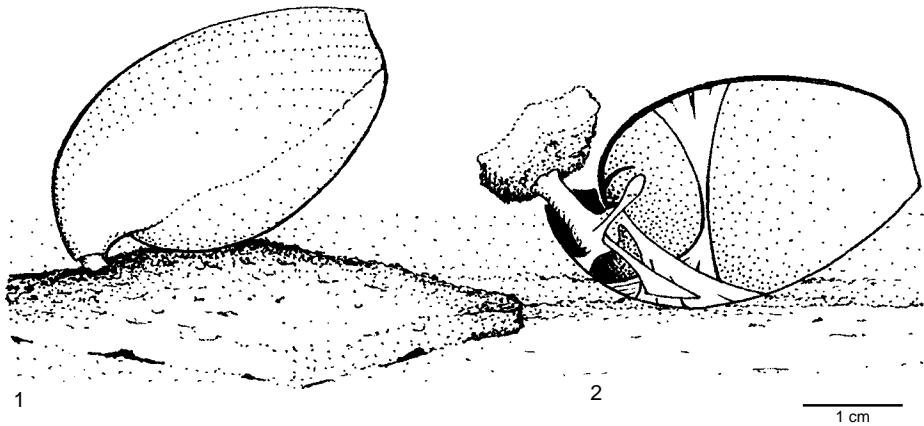


FIG. 390. *Magasella sanguinea*; the larval substrate is retained throughout the life of the individual; contraction of the dorsal adjustor muscles causes rotation of either 1, the shell or 2, the pedicle according to the mass of substrate bonded to the pedicle. Free individuals may lie on either the dorsal or ventral valve (new).

pedicle, with ratcheting movements being characteristic of the former (*Anakinetica*, *Parakinetica*, *Bouchardia*) and twisting movements of the latter (*Neothyris compressa*).

GENERALIST SPECIES

Generalist species may be found on an apparently unlimited range of substrates and in low- to high-energy regimes (Fig. 392). Highest population densities occur around shorelines where rocky surfaces are adjacent to gravel, sand, or mud. Both sedentary and free populations have been observed for the antipodean members of the Terebratellinae, *Magellania flavescens*, *Calloria inconspicua*, and *Magasella sanguinea*, and RICHARDSON (1994) inferred that they are also characteristic of *Laqueus californianus*, species of *Terebratalia* from the northwestern and northeastern Pacific, and species of *Magellania* from the Ross Sea shelf of Antarctica.

The pedicle of a terebratelloidean generalist is squat and cylindrical with its distal tip bonded closely with a substrate (Fig. 390). Pedicle muscles are stout and are clearly defined. Free individuals have no preferred orientation and may lie on either the dorsal or ventral valve. All are biconvex without differential thickening and with a short rostrate beak, submesothyrid to mesothyrid foramina, and moderate size ranging approxi-

mately from 28 to 40 mm. They vary in shape according to life-style and the energy of the environment occupied (ALDRIDGE, 1981; STEWART, 1981) with the morphological variants of *Terebratalia transversa* differentiated as spirifer, atrypa, and terebratula types (SCHUMANN, 1991). The most extensively documented taxa are the New Zealand terebratellid *Magasella sanguinea* (RICHARDSON & MINEUR, 1981; FOSTER, 1989) and the northwestern American laqueid *Terebratalia transversa* (HERTLEIN & GRANT, 1944; MATTOX, 1955; BERNARD, 1972), which show considerable conformity in distribution with substrate and in morphological character.

While members of superfamilies other than the Terebratelloidea are similar in their adaptations for hard and soft surfaces (see below), generalists of these superfamilies are either less common or are not accessible for study. The only member of the Terebratuloidea described with free and sedentary populations is *Terebratulina septentrionalis* (CURRY, 1981). No recent member of the Rhynchonelloidea is known with generalist characters, but older taxa, for example, the Lower Devonian *Pachyplax gyralea*, resemble modern terebratelloids in those morphological features linked with substrate relationships (ALVAREZ & BRUNTON, 1990).

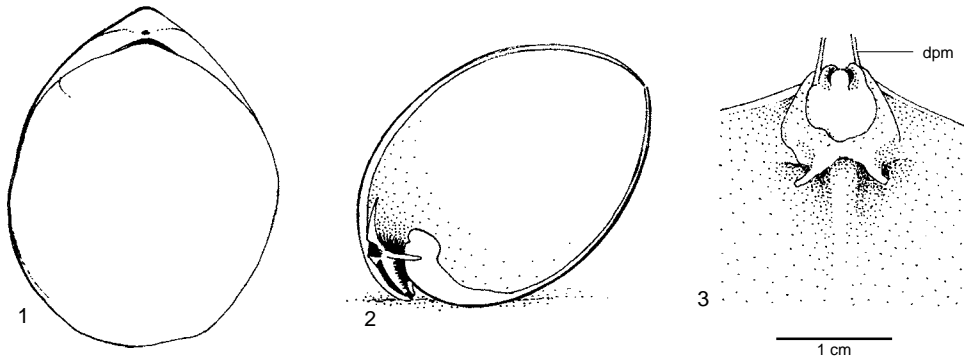


FIG. 391. 1–3, *Neothyris lenticularis*; Port Pegasus, Stewart Island, New Zealand, mud, 18 m; a free-lying and immobile species in which the pedicle system is atrophied and any action of the dorsal adjurator muscles is prevented by thickening of the cardinal process; *dpm*, dorsal pedicle muscle (new).

Because the pedicle system and associated characters of generalist species give individuals the physical means of occupying a wide range of substrates, they also have the capacity to live in areas in which substrates are less variable than those around shorelines. For example, the bryozoan sands of the Australian shelf contain populations of anakinetinids, a group highly adapted to this medium. The generalist species *Magellania flavescens* occurs most commonly in the inlets around the Australian coast. Individuals may also be collected from the middle shelf but only as sedentary forms bonded with local reefs and outcrops on the shelf. The absence of any free-lying individuals on the sediments illustrates that in areas of high energy the limited movements possible with the pedicle system make maintenance of a surface position difficult. The sedentary individuals collected are invariably stunted.

ADAPTATIONS FOR SOFT SURFACES

The diversity of life-styles possible with two variables, substrate and the pedicle system, can be illustrated clearly in those species that are specialized to varying degrees for soft surfaces. Species may be tethered or free and, if free, active or inactive. The larvae's substrate is retained in tethered forms and in some free and active species such as *Neothyris compressa* (Fig. 393; RICHARDSON, 1981d). It

is outgrown in other free and active forms (*Anakinetica* and *Bouchardia*) and in free but inactive species (*Eobemithiris*). That the larvae's substrate is not lost but actively outgrown can be seen during growth of the pedicle as described for *Anakinetica cumingi* (RICHARDSON, 1987).

Apparently progressive stages in the occupation of soft sediments are evident in terebratelline species. One group (*Magellania venosa*, *Terebratella dorsata*, and species of *Aerothyris*) dredged from varied shelf sediments is similar to generalists in morphological character and in the retention of substrate. They appear to differ only in the presence of differential thickening in some individuals and populations. Differential thickening is not a variable character in *Gryphus vitreus* (BRUNTON, 1988) or in species of *Neothyris*, *Gyrothyris* (FOSTER, 1974), and *Pictothyris* (ENDO, 1987); and its distribution in these genera gives an orientation with the dorsal valve lying next to the substrate. Species of *Neothyris* are all free, but they differ in extent of activity; and these differences are evident in the outgrowth or retention of the larvae's substrate (Fig. 391–392). In this genus retention indicates some activity, and outgrowth indicates inactivity. *Neothyris lenticularis* is widely distributed geographically; it occupies varied sediments, the pedicle system is reduced in size, and retention of the larvae's substrate is variable. The larvae's

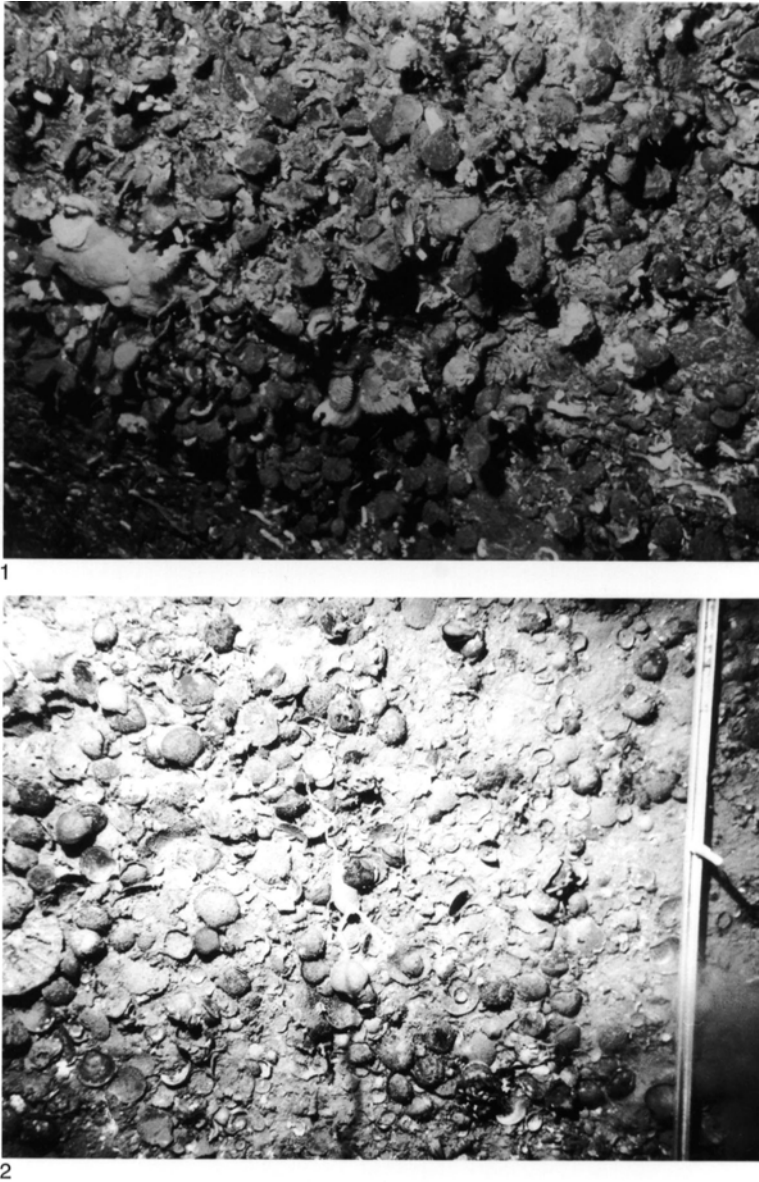


FIG. 392. *Magasella sanguinea*; a species with the physical capacity to live on a wide range of substrates and with no apparent physiological barrier to the occupation of environments ranging from mud to rock walls; 1, rock face, Cunaris Sound, New Zealand, 25 m; sedentary individuals covered with coralline algae, $\times 1.16$; 2, Paterson Inlet, Stewart Island, New Zealand; free individuals on coarse sand and shell, 38 m, $\times 1.18$; 3, Crail Bay, Marlborough Sounds, New Zealand; sedentary individuals fixed to a horse mussel, free individuals on mud, $\times 2.22$; 4, *Xenophora neozelanica* as substrate, $\times 2.78$ (new).

substrate is invariably outgrown in populations from muddy inlets, whereas it tends to be retained in those found on shell gravel, although weak activity is indicated by reduc-

tion of the areas of attachment (by differential thickening) of the pedicle muscles. *Neothyris compressa* has been collected only from sediments of shell grit and gravel in areas



3



4

FIG. 392 (continued). *For explanation, see facing page.*

with strong tidal currents. The larvae's substrate is invariably retained, and movements of the pedicle stabilize the position of individuals, preventing dispersal and disorienta-

tion in strong current regimes. The life-style of *Gryphus vitreus* is similar (EMIG, 1987).

Similarly, a group of anakineticines varies in degree of specificity for occupation of

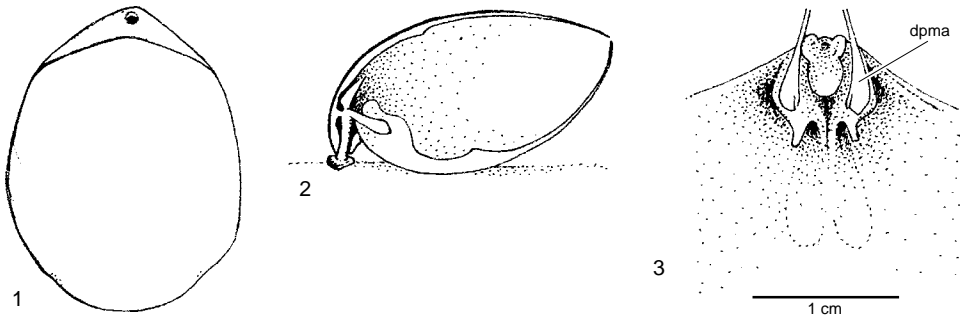


FIG. 393. 1–3, *Neothyris compressa*; Stephens Island, New Zealand, shell grit and gravel, 19 m; a free-living, active species that retains the larval substrate and is oriented with the dorsal valve and beak next to the underlying substrate; *dpma*, dorsal pedicle muscle anterior attachments (new).

Australian bryozoan sands (RICHARDSON, 1987). Some, *Magadinella mineuri* for example, retain the substrate, and movements of the pedicle give the capacity to maintain or regain positions at the sediment-water interface. In other anakinetines (*Anakinetica* and *Parakinetica*) the larvae's substrate is outgrown early in ontogeny, and the ratcheting action of a free and active pedicle gives individuals the capacity to surface. The pedicle differs in the length and spacing of its processes for life in coarse (*Anakinetica*) or fine sands (*Parakinetica*). This type of pedicle also occurs in *Bouchardia rosea*, a Brazilian species also from bryozoan sands (TOMMASI, 1970a; MANCENIDO & GRIFFIN, 1988).

Similar adaptations of the pedicle for life in such abyssal sediments as foraminiferal oozes may be seen in genera from all superfamilies: *Cryptopora* (Rhynchonelloidea), *Chlidinophora* (Cancellothyroidea), *Abyssothyris* (Terebratuloidea), and *Phaneropora* (Terebratelloidea). In general, the pedicle is frayed in appearance with rootlets from its end penetrating shells or fragments. Considerable intraspecific variation is evident in pedicle length, however, and also in number of rootlets in these species (Fig. 394). Individuals of *Abyssothyris wyvillei* have been collected with a short pedicle bonded to a manganese nodule, while others are extensively frayed with each rootlet terminating in the shells of foraminifera. Movement of individuals would be unlikely in view of the state and size of muscles, and it appears that in life

the pedicle sat vertically in the sediment with the shell lying open at the sediment-water interface.

Gwynia capsula is the only interstitial species known (SWEDMARK, 1971), a permanent member of the fauna of shell and sand debris. The shell is tiny with a diameter of 1 mm, and the pedicle adheres to the sand grains on which the larvae settle.

ADAPTATIONS FOR HARD SUBSTRATES

Notosaria nigricans is adapted for sedentary life. The attachment area of the pedicle is large and irregular (Fig. 395.2), and it may differ in size among individuals. Unlike the pedicles of most other species, it cannot be withdrawn or covered by the shell; and the exposed parts are heavily chitinized. The position of the dorsal pedicle muscles relative to the pedicle shows that tilting but not rotation of the shell is possible (RICHARDSON, 1981b). The beak of *N. nigricans* is apicate and the foramen hypothryid.

A trend toward the loss of movement is also evident in sedentary and pediculate species from hard surfaces, which are most commonly represented by members of the Platididae, Megathyrididae, and Kraussinidae. In these species the pedicle and pedicle muscles are not clearly differentiated, and together they function as one contractile unit. Therefore movements generated by the pedicle system are restricted to raising and lowering the shell, and the capacity to twist the shell

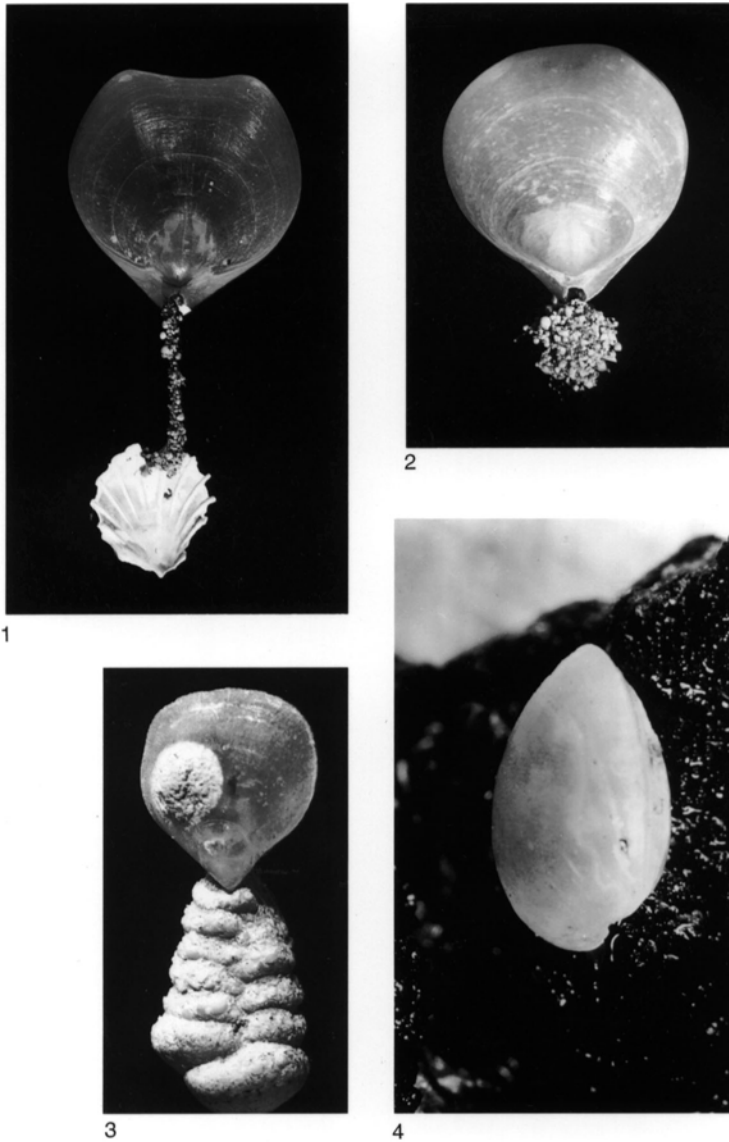


FIG. 394. *Abyssothyris wyvillei*, found throughout the Pacific; individuals collected in the Tasman Sea and bonded with 1–3, shell fragments and foraminifera at 1,463 m, $\times 4.42$; 4, a manganese nodule from 4,548 to 4,714 m, $\times 4.42$ (new).

has been lost. A nonrostrate beak and amphithyrid foramen are associated with pedicle systems of this type.

Thecideidines are the only living articulated brachiopods known in which the pedicle is lost following larval settlement and in which the shell of the adult is fixed directly to the substrate. As a consequence,

shell movements other than opening and closing are not possible (Fig. 395.4).

ORIENTATION

The positions of individuals relative to the substrate differ with morphological character. The substrate relationships of generalists are variable; that is, they have the capacity to

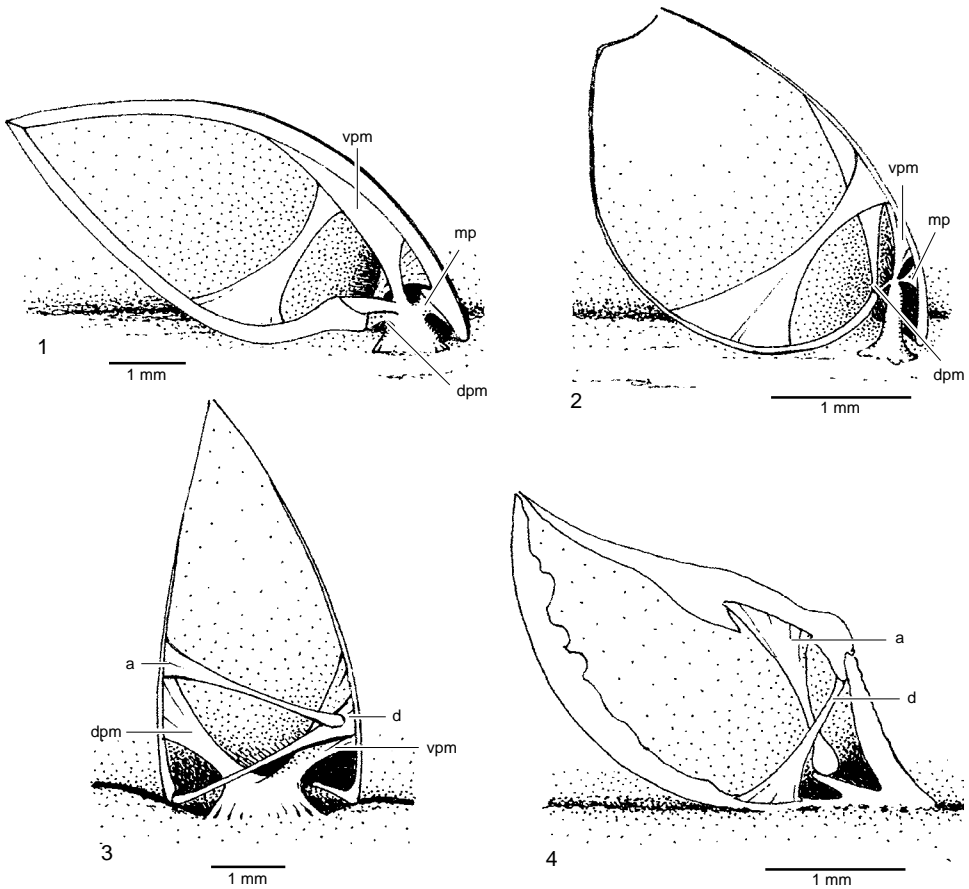


FIG. 395. Species adapted for a sedentary life on hard substrates. The pedicle system is absent in the adult of *Thecidellina maxilla*, and the ventral valve is cemented to the substrate. The other three species possess a nonrostrate beak and vary in the degree of differentiation of the pedicle and its muscles. The absence of a sharp distinction between muscles and pedicle is associated with movement restricted to tilting and raising the shell and the absence of twisting movements of the shell; 1, *Megerlina lamarckiana*; intertidal, Port Jackson, Australia; 2, *Notosaria nigricans*; Paterson Inlet, Stewart Island, New Zealand, 10 m; 3, *Argyrotheca johnsoni*; Discovery Bay, Jamaica, 29 m; 4, *Thecidellina maxilla*; off Murray Island, Torres Strait, Australia, 15 m; a, adductor muscle; d, diductor muscle; dpm, dorsal pedicle muscle; mp, median pedicle muscle; vpm, ventral pedicle muscle (new).

live fixed to a rock face or to lie freely on the sea floor, resting on either valve (Fig. 390, 393). It is a characteristic of nongeneralist species that substrate relationships are constant; and, with the exception of some species of *Argyrotheca*, the dorsal valve lies next to the substrate whether species are sedentary or free and whether individuals hang grape-like (Fig. 396–397) from the substrate (*Liothyrella neozelanica*) or hug the substrate (*Magasella sanguinea*). Although *L. neozelanica* and *M. sanguinea* are respectively uni-

plicate and sulcate, this difference in orientation means that the curvature of the anterior commissure appears to be the same in a frontal, *in situ* view of individuals of each species. Some species of *Argyrotheca* (Fig. 395.3) are fixed with the anterior-posterior axis at right angles to the substrate (COOPER, 1977; ASGAARD & STENTOFT, 1984).

The orientation of free-lying and free-living species is effected by thickening, which is distributed so that the individual lies in a stable position with the ventral valve upper-

most, with the beak lying next to the substrate, and with the anterior end elevated above the surface.

Laboratory studies by LABARBERA (1977) suggested that some orientations of the shell assist pumping by the lophophore. ESHLEMAN and WILKENS (1979b) also noted that among *in situ* sedentary populations of *Terebratalia transversa*, 70 percent of individuals were consistently oriented relative to the current, with the anteroposterior axis of the shell lying nearly at right angles to the ambient current. Other *in situ* studies (RICHARDSON, 1981d; EMIG, 1987) have shown that active orientation with the current occurs in exclusively free-lying or free-living species that are, therefore, differentially thickened. In these examples, the anteroposterior axis commonly lays parallel to the current (Fig. 398). Active orientation has not been observed in free populations of generalist species or of exclusively sedentary forms. The orientation of individuals in crowded and clustered populations appears to be quite random, and individuals in the populations observed showed no reorientation in response to currents (Fig. 399). It is possible therefore that stability may be of greater importance in determining orientation than the direction of water flow.

DISTRIBUTION

The role played by abiotic factors in the distribution of articulated brachiopods is difficult to assess given that current strength, salinity, light, and temperature are rarely if ever recorded. Some data of this nature are available for *Terebratulina septentrionalis* and *T. retusa* but from only one part of the range of each species, and both are widely distributed geographically. Therefore information is not available on the range of salinity and temperature that can be tolerated. Experimental laboratory work is of questionable value since articulated brachiopods have the capacity to survive for periods in excess of one year in seawater and in the absence of a food supply. No records exist of breeding in captivity, but artificial insemination has

made studies of larval development possible (LONG, 1964; WEBB, LOGAN, & NOBLE, 1976; STRICKER & REED, 1985a). The role of environmental parameters, however, can be assessed from other sources: from the geographic and bathymetric ranges of species, from the occurrence of species in areas in which physical factors differ (tidal and sheltered environments) and in which they may fluctuate (fiords), and from the character of those areas in which densities are greatest.

The extent of the geographic and bathymetric ranges of many species is notable; for example, *Macandrevia americana* occurs in the eastern Pacific between San Diego, California, and the Antarctic at depths of 112 to 4,066 m; *Platidia anomioides* is found in the Mediterranean Sea and the Atlantic, southern Indian, and South Pacific oceans from 18 to 2,190 m (FOSTER, 1989). Such tolerance of differences in latitude and depth suggests that consequential factors such as temperature and food supply are unlikely to limit distribution. Furthermore, of those species cited as temperature limited, factors other than temperature may account for distribution. For example, collections of *Frenulina sanguinolenta* are only from shallow waters (30 to 92 m) of the Pacific Ocean (35°S to 20°N), and the species is cited as temperature limited. Since the patchy color pattern of the species indicates adaptation for coral-reef environments, however, substrate may be the limiting factor. *F. sanguinolenta* is the only articulated brachiopod collected so far from Australia's Great Barrier Reef.

In general most species show a considerable bathymetric range (ZEZINA, 1985; LOGAN, 1993), but inhabitants of the intertidal zone are rare, and the members of those species collected littorally are far more abundant in subtidal waters. In shallow, subtidal waters, articulated brachiopods occur only in such cryptic habitats as under surfaces and in crevices. Individuals have been found on upper surfaces at depths greater than 40 m in the Mediterranean Sea (LOGAN, 1979), below 25 m in Canada's Bay of Fundy (NOBLE, LOGAN, & WEBB, 1976), and below 73 m in



FIG. 396. *Liothyrella neozelanica*; Long Sound, Preservation Inlet, New Zealand, 20 m; population on granite wall, $\times 2$ (new).

the Caribbean Sea (COOPER, 1977). These differing values suggest that light intensity may differ in each of the areas. The intensity of light is low in the saline waters of New Zealand fiords, and articulated brachiopods are found from depths of 6 m, i.e., immediately below the thermocline separating a thin layer of cold, brackish water from warmer, underlying saline water. These records and larval preferences for areas of settlement in poor light all indicate that light intensity plays a role in distribution.

Fiords are areas of particular value in the study of those physical factors that influence distribution because of the environmental restraints in fiords, that is, an association in shallow water of rock substrates and unidirectional currents of low velocity. The subtidal walls below the thermocline provide continuous, vertical change in light intensity on the same kind of granite substrate with

little variation in salinity, in the observed strength and direction of water movement, in temperature, or in the amount of suspended material in the water. Articulated brachiopods have been recorded from two fiords in British Columbia (MCDANIEL, 1973; TUNNICLIFFE, 1981), Norway's Trondhjem Fjord (NORMAN, 1893), all of New Zealand's fiords (RICHARDSON, 1981c), and Chilean fiords. The New Zealand fiords contain species of all brachiopod genera described from New Zealand waters, species of *Neocrania*, *Notosaria*, *Liothyrella*, *Terebratulina*, *Platidia*, *Pumilus*, *Amphithyris*, *Calloria*, *Magasella*, and *Neothyris*; and most occur in great abundance. With the exception of *Neothyris lenticularis*, all species from the fiords are either generalists or are species adapted to hard substrates. *N. lenticularis*, the only free-living form, is found on a shallow, sandy spit (20 m) in the Long Sound fiord.

Unlike fiords studied in other parts of the world, in New Zealand fiords the halocline was present in all seasons during a five-year-long survey. In those fiords studied in the northern hemisphere (PEDERSEN, 1978), the halocline breaks down during the summer and so facilitates the renewal of saline waters by winds and tides. Periodic breakdown of the halocline means loss of protection from light and water movement for varying periods of two to three months and may be one of the factors responsible for differences evident between fiord-basin faunas of New Zealand and British Columbia. Typical algae-dominated, shallow-water assemblages occur above 30 m in Saanich Inlet, British Columbia; in New Zealand they are found only above the halocline breakdown of 4 to 5 m. In addition, the articulated brachiopod fauna of Saanich Inlet is less varied and abundant than that of New Zealand's fiords, which resulted from the difference in the stocks available in southern and northern waters for recolonization at the end of the last ice age.

The difficulty in defining the impact of different physical factors is well illustrated by the distribution of articulated brachiopods in New Zealand and South Africa. They dominate the rich, rock-wall life of fiords; and their abundance suggests that the degree of shelter found in these enclaves provides optimum conditions. Although all 14 New Zealand fiords appear to provide similar conditions, occurrences of species vary. All species occur within the Long Sound fiord; the others differ such that one species may dominate and others may be rare or absent. Furthermore, some of the rock-wall species occur on the sea floor of Foveaux Strait, an area with strong tidal flow separating the South Island of New Zealand from Stewart Island. The inlets of Stewart Island also contain rich populations of *Calloria*, *Magasella*, *Neothyris*, *Notosaria*, and *Liothyrella* that occur in various current regimes and with free-lying and free-living forms on a variety of sediments.

In South Africa distribution appears to be influenced by two major oceanographic sys-

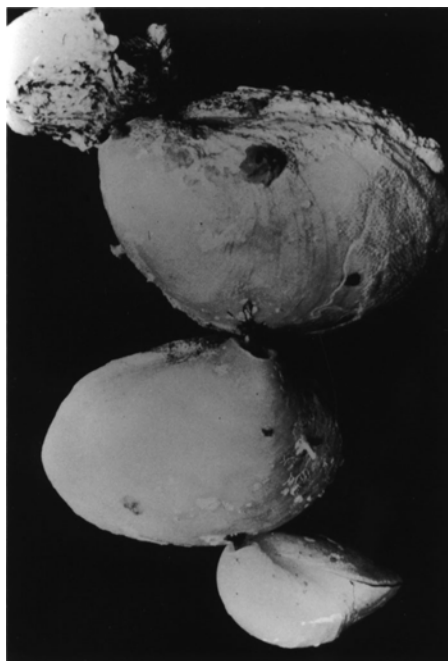


FIG. 397. *Liothyrella neozelanica*; Long Sound, Preservation Inlet, New Zealand, 20 m; three individuals of different age illustrating the orientation characteristic of the species, i.e., suspended from the substrate, $\times 1.28$ (new).

tems (ZEZINA, 1987; HILLER, 1991). The warm Mozambique and Agulhas currents flow southwestward along the east coast, and the west coast is washed by the north-flowing waters of the cold Bengula system. Some species occur around the entire coastline; others are restricted to one or another of the coasts. Given the depth ranges of the species, it seems likely that the differences in geographical distribution are not associated with water temperature but with larval dispersal from different areas.

In the Mediterranean Sea, studies using submersibles showed an association between the densities of benthic populations and current velocity (EMIG, 1987, 1989c). Populations of *Gryphus vitreus* were recorded on detrital sand of the bathyal slope at depths of 103 m to 260 m with highest densities (700 to 800 m^2) occurring in an area in which the current velocity was 1.5 to 3



FIG. 398. *Neothyris lenticularis*; Paterson Inlet, Stewart Island, New Zealand, shell gravel, 42 m; free individuals oriented with the anterior-posterior axis parallel to ambient current (4.5 km/hr at time of sampling), $\times 26$; arrow indicates direction of bottom current (new).

km/hr. A similar correlation of population density with current strength has been noted for the free-lying form *Neothyris lenticularis* in an inlet within which both substrate and energy regimes differ (RICHARDSON, 1981d).

Similarities have been noted in faunas from the Caribbean Sea and adjacent waters (COOPER, 1977; ASGAARD & STENTOFT, 1984; LOGAN, 1990), the Mediterranean Sea (LOGAN, 1979; BRUNTON, 1988; ASGAARD & BROMLEY, 1991), mid-Pacific atolls (GRANT, 1987), and the Red Sea (JACKSON, GOREAU, & HARTMAN, 1971). Brachiopods from rocky substrates and coral reefs in these areas are commonly members of the Thecideoidea, Kraussinidae, Platidiidae, and Megathyrididae. These suites of brachiopods appear to be characteristic of shallower waters in low latitude regions. Many of the individual species they contain, however, are not restricted in distribution; for example, *Cryptopora gnomon* occurs from 76°N (Franz Joseph Land) to 51°S (Falkland Islands) at depths ranging from 300 to 4,060 m; *Pla-*

tidia anomiooides occurs at from 18 to 2,190 m in the Mediterranean Sea, West Indies, Atlantic, southern Indian, and South Pacific oceans. Furthermore, they are all small forms adapted for a sedentary existence, and the presence of reefs in the areas in which they are most commonly found may be a factor in their distribution.

Cold-water coral banks also provide a substrate for brachiopods (TEICHERT, 1958; LOGAN, 1979). The branching calcareous skeletons of species of *Lophelia*, *Madrepora*, *Styaster*, and *Allopora*, together with the smaller scleractinians with which they are associated, provide a rigid, sediment-bonding framework that furnishes an environment for an abundant benthic fauna. The minimum depth of these banks has been recorded as 56 m, but they are more common at 182 to 274 m, and living *Lophelia* have been recorded from 914 m. Coral banks have been described from Norwegian and western European waters and from the Mediterranean Sea, and coral-brachiopod associations



FIG. 399. Varied orientation of sedentary individuals in 1, populations of *Calloria inconspicua* and *Notosaria nigricans*, Port Pegasus, Stewart Island, New Zealand, 15 m, $\times 1.2$; 2, cluster of living individuals from the floor of Paterson Inlet, Stewart Island, New Zealand at 27 m; cluster made up of one individual of *Neothyris lenticularis*, six of *Terebratella sanguinea*, and three of *Calloria inconspicua*, $\times 66$ (new).

are known from deep water south of both New Zealand and Australia.

The substrate occupied may provide one of the best guides from which to evaluate factors that govern distribution. For example, the Australian species *Aulites brazieri* occupies a wide range in latitude (23° to 39° S), longitude (113° to 154° E), and depth (40 to 250 m) but is found only in bryozoan

sands and fixed to the undersides of the free-living bryozoan species *Selenaria maculata* and *Lunulites capulus* (RICHARDSON, 1987). In contrast, such generalist species as *Magasella sanguinea* and *Terebratalia transversa* may be bonded to substrates of any size and composition, and the free-living populations of these species can live on sediments of any type and therefore in a wide range of energy

regimes. *Magasella sanguinea* is the dominant brachiopod on the walls of the New Zealand fiord, George Sound, and on the muddy sediments of Paterson Inlet. These distributions together with the comparative anatomy of the pedicle system (RICHARDSON, 1981b) indicate, first, that no apparent physiological barrier exists to the occupation of a wide range of regimes (RICHARDSON, 1981a) and, second, that the range of habitats occupied is correlated with pedicle type and associated characters (RICHARDSON & MINEUR, 1981). Some types of pedicle systems give species the capacity to colonize and survive as adults in or on a wide range of substrates, while others restrict them to specific types or ranges of substrate.

Substrate is also considered to be a factor in the predominance of small taxa in abyssal environments (FOSTER, 1989). A survey of South Pacific localities showed that populations collected from areas with numerous, hard surfaces contained large individuals, whereas populations in areas with few, hard objects contained individuals of small size. This conclusion was drawn from work on living populations and accords with that drawn from studies of Cretaceous brachiopods from the Danish chalk (SURLYK, 1972), in which the lack of surface area of hard substrates limited populations. Variations in substrate type appear to determine the assemblages found in different zones of the Mediterranean Sea (LOGAN, 1979) and the Caribbean Sea (ASGAARD & STENTOFT, 1984). The presence of suitable substrate is considered to be the most important factor controlling the distribution of *Terebratulina septentrionalis* (NOBLE, LOGAN, & WEBB, 1976) and, along with pedicle type, the distribution of *Terebratulina retusa* (CURRY, 1982) since the pedicle of the latter species is considered to give the capacity to colonize a wide range of substrates.

Known factors that limit the distribution of articulated brachiopods are therefore the capacity to disperse and the nature of the

pedicle system, i.e., whether it is adapted to substrates of a particular type. The patterns of settlement and survival in New Zealand's Paterson Inlet illustrate the latter point. Paterson Inlet contains four species, all of which settle at random on surfaces of any size and composition (RICHARDSON, 1981d). Only the generalists *Magasella sanguinea* and *Calloria inconspicua* survive as adults on the larvae's substrates of any grain size. One species (*Notosaria nigricans*) is restricted to coarse-grained or stable substrates; the other (*Neothyris lenticularis*) is confined to fine-grained substrates. This pattern also suggests that any preferences for substrate that have been recorded for species are unlikely to be larval preferences but reflect the requirements of the morphology that is expressed as development proceeds. Within the range of substrates for which species are adapted, greatest densities occur in areas in which light intensity is low.

Such other physical factors as depth, temperature, and energy of the water have not yet been shown to limit distribution, as is evident from what is known of the distributions of some species. For example, *Liothyrella neozelanica* has been collected from rock surfaces in New Zealand in two of ten fiords, in one of the two straits that separate the three islands, in one of the three inlets studied around Stewart Island, and from the Chatham Rise. If it were possible to establish why the species is not present in Paterson Inlet, which is dominated by articulated brachiopods, or in Foveaux Strait, then it might be possible to gain further insight into the role of physical factors in distribution.

In contrast with the predominately shallow-water studies outlined above, examination of brachiopod distribution in deeper waters (ZEZINA, 1985) has led to the conclusion that the diversity of articulated brachiopods is higher in the bathyal than in sublittoral and abyssal zones and that this can be attributed to a guaranteed food supply and biotopic variability in this region.

DEMOGRAPHY

Articulated brachiopods are seasonal breeders with determinate growth and variable recruitment. They produce lecithotropic eggs and brood larvae through all developmental stages prior to settlement. The strong correlation between densities of recruits and residents in populations (DOHERTY, 1979; NOBLE & LOGAN, 1981) is an indication of the limited capacity for dispersal of articulated brachiopod larvae.

Some insight into the physical and biological factors that control population structure has been derived from size-frequency distributions when these distributions have been related to recruitment, longevity, and mortality. Most population studies recorded before 1979 were those of species from the littoral zone (PERCIVAL, 1944; RUDWICK, 1962b; PAINE, 1969; RICKWOOD, 1977; THAYER, 1977; LEE, 1978), a zone rarely colonized by living species or represented in fossil collections. Size-frequency distributions constructed from dredged collections of four species from the San Juan Islands, Washington (THAYER, 1975), indicated episodic recruitment at irregular intervals.

Studies of subtidal populations in different geographic areas of both Canada and New Zealand are of particular interest. All areas studied had optimal conditions for brachiopods as was shown by high population densities. All were studied by scuba, and samples were taken from more than one locality in each area. Populations of *Terebratulina septentrionalis* had high juvenile peaks in populations from both the Bay of Fundy (Fig. 400; NOBLE & LOGAN, 1981) and the Gulf of Maine (Fig. 401; WITMAN & COOPER, 1983). The Gulf of Maine populations were collected from the same depth (33 m) and from adjacent but different habitats: upper rock surfaces and rock wall. Although both populations were dominated by juveniles, adult modes occurred at different shell lengths in each—at 14 to 15 mm in the

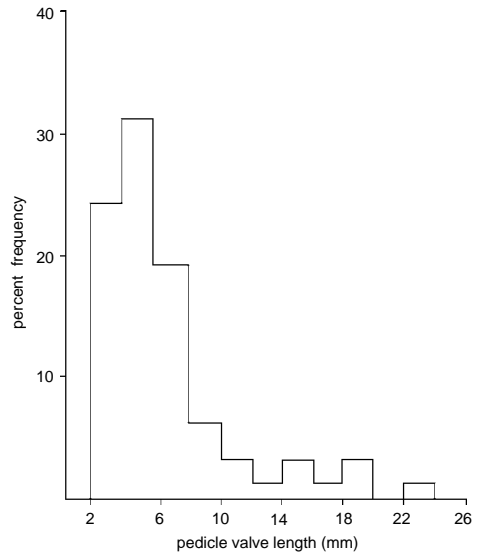


FIG. 400. Size-frequency histogram of living population of *Terebratulina septentrionalis* from the cave at Simpson's Island; $n = 103$ (Noble & Logan, 1981).

population from rock surfaces and at 19 to 20 mm in that from the rock wall. It was presumed (WITMAN & COOPER, 1983) that the shorter life span of rock-surface brachiopods could be attributed to predation by cod, which ingested the substrates to which the brachiopods were attached, especially tubicolous polychaetes and red algae that are absent from the rock-wall habitat.

The subtidal populations of *Calloria inconspicua* studied in northern New Zealand at monthly intervals for one year (Fig. 402; DOHERTY, 1979) were either bimodal or left-skewed (dominated by adults), a pattern attributed to the high rate of attrition of postlarval stages and to seasonal recruitment. The structure of hard-bottom, subtidal populations of *C. inconspicua* was recorded from southern New Zealand in one summer and compared with intertidal and soft-bottom, benthic populations in the same area (Fig. 403; STEWART, 1981). Size-frequency histograms were distinctive for the three habitats. Intertidal populations were

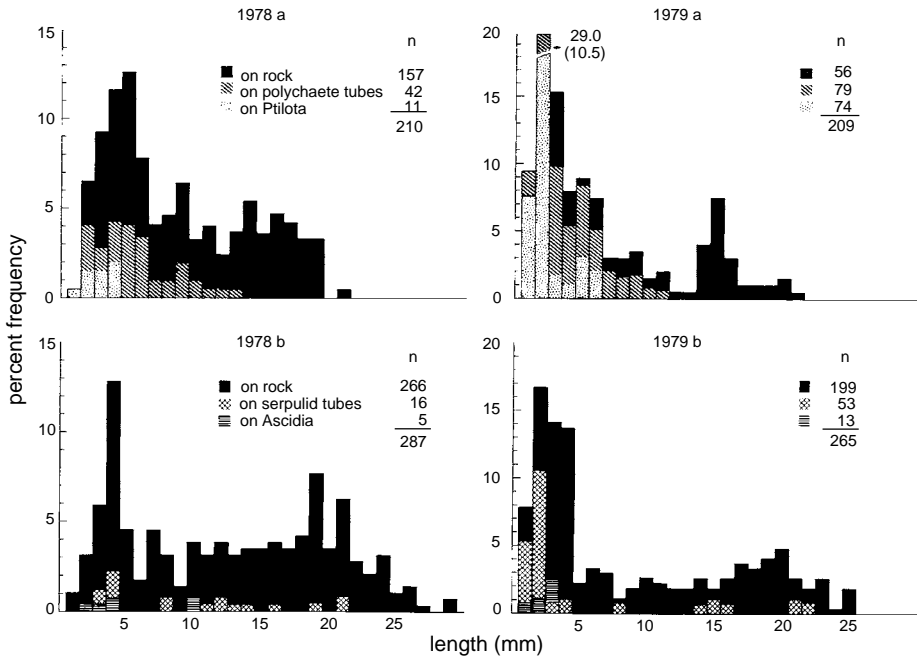


FIG. 401. Substratum specific size-frequency distributions of *Terebratulina septentrionalis* collected by airlift sampling in 1, upper rock surface and 2, rock wall habitats during 1978 and 1979; in upper surface habitats, diagonally hatched bars represent brachiopods attached to sandy polychaete tubes; dotted bars refer to individuals attached to *Ptilota serrata*; in rock wall habitats brachiopods attached to calcareous serpulid tubes (crosshatched bars) and to *Ascidia callosa* (horizontally hatched bars); black bars represent brachiopods attached directly to rock; note the restricted size range (1 to 13 mm) of brachiopods on polychaete tubes and *Ptilota* in upper rock surface habitats (Witman & Cooper, 1983).

right-skewed; subtidal ones were also right-skewed but with an adult mode varying in prominence with depth. Benthic populations were bimodal, and the same pattern was evident in benthic populations of *Magasella sanguinea* and *Neothyris lenticularis* from the same area (Paterson Inlet). *N. lenticularis* is an exclusively free-living and benthic form; *M. sanguinea* and *C. inconspicua* are opportunistic species with the capacity to settle and survive on substrates of any size. While the larvae of *N. lenticularis* also settle on any available substrate, adults can function only if bonded to small fragments that they frequently outgrow. Shell shape, thickening, and pedicle-system structure of this species preclude a mechanically stable position on coarse substrates.

CURRY (1982; Fig. 404; Table 34) examined the structure of populations of *Terebra-*

tulina retusa from a depth of 200 m from Scotland's Firth of Lorne, but he did not state whether mature individuals were fixed and sedentary or were free (with only a small mass of substrate bonded to the pedicle). He attributed the bimodality shown in histograms to biannual spawning periods assumed to be late spring and autumn. A subsequent study of *Terebratulina retusa* (COLLINS, 1991) from the same area included benthic specimens that permitted an extension of the growth-rate curve from a logarithmic to a sigmoidal shape and implied that conditions for rapid, early growth may be more favorable in shallow than in deep water. The New Zealand species *Notosaria nigricans* and *Calloria inconspicua*, however, had slower rates of growth in intertidal than in subtidal habitats; and the subtidal and benthic species *Magasella sanguinea* and *Neo-*

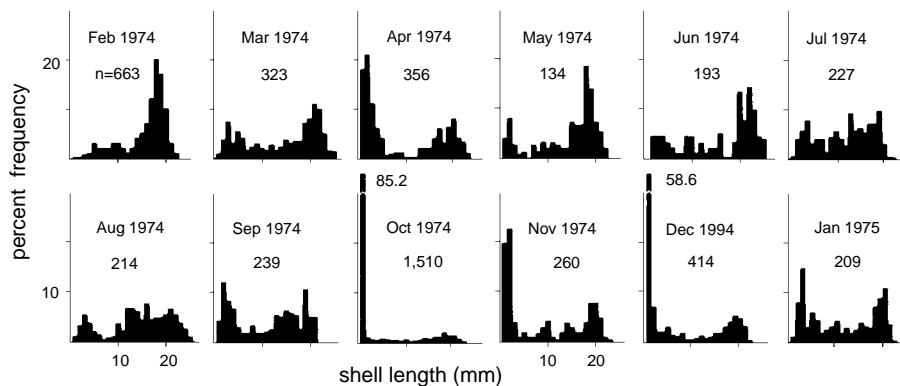


FIG. 402. *Calloria inconspicua*; size-frequency distributions from monthly sampling of the canyon population; area of samples: February, 0.25 m²; November, 150 cm²; all others, 625 cm² (Doherty, 1979).

thyris lenticularis grew rapidly initially (STEWART, 1981).

Spawning periods have been determined in most instances from the preponderance of postlarval stages in size-frequency distributions, and observations of the spontaneous release of larvae from the female have been rare. The linkage of spawning time with any physical factor is difficult given the times of the year recorded from different geographical regions and the differences of seasons from the two hemispheres. Spawning of subtidal populations of *Calloria inconspicua* from northern New Zealand was observed in September (DOHERTY, 1979), in May in intertidal populations from the mid-eastern coast (PERCIVAL, 1944), and in July in subtidal populations from the middle to southern west coast. Spawning of *Magasella sanguinea*, *Neothyris lenticularis*, *N. compressa*, and *Notosaria nigricans* during mid-July was also observed; but only some stages in the development in the latter have been documented (HOVERD, 1985). In the northern hemisphere, *Terebratulina septentrionalis* is presumed to spawn between May and August (MORSE, 1873; NOBLE, LOGAN, & WEBB, 1976; WEBB, LOGAN, & NOBLE, 1976); and an estimate of dates of settlement of *Terebratulina retusa* indicated spawning periods in spring and autumn (CURRY, 1982; COLLINS, 1991). Mediterranean species of *Argyrotheca* are thought to spawn late in the

year with the possibility of a further spawning period in early summer (ASGAARD & BROMLEY, 1991). A further factor to take into account in any attempt to reconcile the differences in spawning periods is that ripe gonads occur in most specimens of *Terebratulina septentrionalis* in every month of the year with larvae present within the females from December to April (WEBB, LOGAN, & NOBLE, 1976). Ripe gonads were also present in February in those New Zealand species that were observed to spawn during July (TORTELL, 1981).

In general, size-frequency distributions show that intertidal populations are not as heavily skewed toward large individuals as are subtidal populations, which may indicate a shorter life expectancy or slower rates of growth. The main cause of death of *Calloria inconspicua* from subtidal populations on rock walls was thought to be old age (DOHERTY, 1979), and survivorship curves of both this species and *Magasella sanguinea* from soft surfaces show relatively constant mortality rates in the adult size ranges.

The high mortality of juveniles shown in size-frequency distributions has been attributed to overcrowding, grazing, and overgrowth. Size-frequency distributions of individuals bonded to rock and associated with conspecifics have shown that the latter group have a shorter life expectancy as adults. The need to be wary in drawing conclusions from

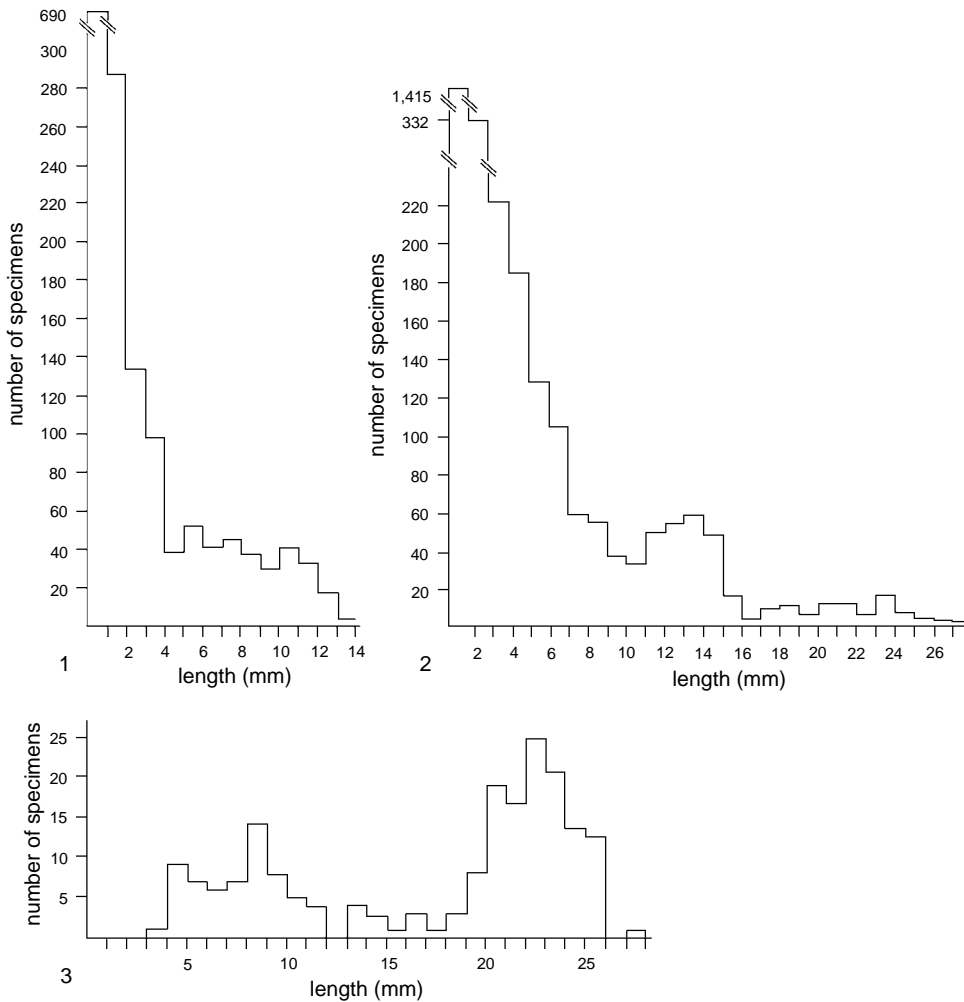


FIG. 403. Length-frequency histograms of populations of *Calloria inconspicua*; all stations in Paterson Inlet, Stewart Island, New Zealand; 1, live population, station K1019, intertidal, $n = 1,553$; 2, live population, station K993, rock slope, subtidal at 7 m; $n = 2,894$; 3, live population, station K989, floor of muddy sand, benthic at 22 m; $n = 194$ (Stewart, 1981).

size-frequency distributions only, however, has been graphically illustrated by the effect on the population structure of two adjoining populations of *Terebratulina septentrionalis* as a result of fish predation of the underlying animal substrate of one of those populations (WITMAN & COOPER, 1983).

PREDATION AND PARASITISM

Significant levels of predation, parasitic infection, or disease have not been reported

for articulated brachiopods. Predators are probably limited by the fact that most living articulated brachiopods contain an internal skeleton or spicules, that biomass is slight, and that the shell invariably encloses all soft parts with the occasional exception of the distal portion of the pedicle. This section of the pedicle is covered with a thick coat of chitin in those species in which it is exposed, for example in *Notosaria nigricans*, in living anakinetinids, and in such terebratellids as *Liothyrella notorcadensis* and *Magellania flavescens* in which the pedicle varies in length,

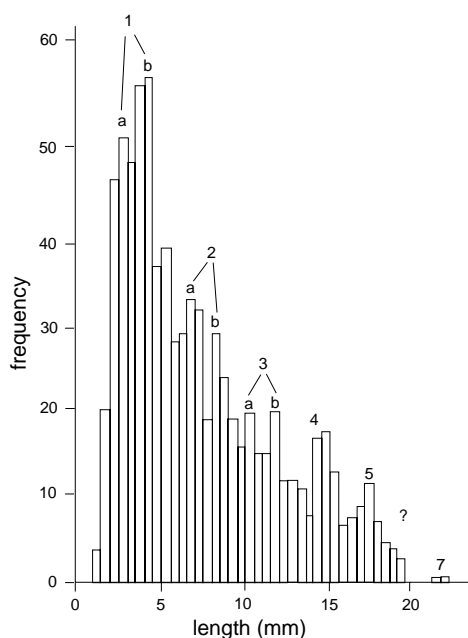


FIG. 404. Length-frequency histogram of *Terebratulina retusa*, from the Firth of Lorne, 22 March 1977 sample (ZB3727–ZB3736; see Table 34 for analysis); 1a, b, 2a, b, etc., settlement cohorts; n = 811 (Curry, 1982).

The principal impact of other organisms appears to be drilling by carnivorous gastropods and grazing pressure on juvenile populations either directly by echinoderms and chitons or indirectly as a consequence of those sites chosen by larva for attachment. In some areas colonized by *Calloria inconspicua*, overgrowth by an encrusting sponge had smothered young but not adult individuals, which were protected by the capacity of sedentary individuals to twist the shell from side to side and moderately high elevation of the feeding aperture above the substrate (DOHERTY, 1979).

Studies of *Terebratulina septentrionalis* from upper rock surfaces and lower rock walls of the Gulf of Maine, Canada, demonstrated that juveniles were taken by cod from only the upper rock surfaces (WITMAN & COOPER, 1983). Selective indices showed that the cod feed preferentially on tube-dwelling polychaetes, which, along with red algae, are the principal substratum of brachiopods on upper rock surfaces and which are absent from the lower rock walls,

TABLE 34. Analysis of the 22 March 1977 length-frequency histogram (see Fig. 404). All measurements are in mm (adapted from Curry, 1982).

Annual increment	Peak	Biannual increment	Date of settlement	Year/Class
4	2.75	1.5	Autumn 1976	1a
	4.25		Spring 1976	1b
4	6.75	1.5	Autumn 1975	2a
3.5	8.25		Spring 1975	2b
3.5	10.25	1.5	Autumn 1974	3a
3	11.75		Spring 1974	3b
2.5	14.75		1973	4
2.5	17.25		1972	5
2.5	19.75		1971	6
1.75	21.50		1970	7

Fishermen from Paterson Inlet, New Zealand, have noted the presence of small terebratellids in the guts of bottom-feeding fish. It is probable, however, that since the species are dominant members of the benthos in this inlet, they would have been engulfed with other material.

Brachiopods in both the Gulf of Maine and Paterson Inlet have been extensively studied using scuba. Occasional instances of asteroids feeding on adult brachiopods have been observed in the Gulf of Maine and once in Paterson Inlet (Fig. 405). Predation by asteroids on subtidal populations of *Terebratalia transversa* in Puget Sound has also been recorded (MAUZEY, BIRKELAND, & DAYTON, 1968).

Drill holes in the shells of terebratuloid species have been recorded from Canadian inlets (NOBLE & LOGAN, 1981; WITMAN & COOPER, 1983), the Caribbean Sea (LOGAN, 1990), the Mediterranean Sea (LABARBERA, 1977), the Sea of Alboran (TADDEI RUGGIERO, 1991), and New Zealand (STEWART, 1981). In most instances drill holes occur in the posterior half of the shell. The size and shape of these holes are like those made by carnivorous gastropods; they are circular and tapered with an outer diameter ranging from 0.45 to 1.05 mm (WITMAN & COOPER, 1983). An example of microborings in the shell of *Magasella sanguinea* is presumed to have been caused by boring fungi and is of interest because the borings do not penetrate

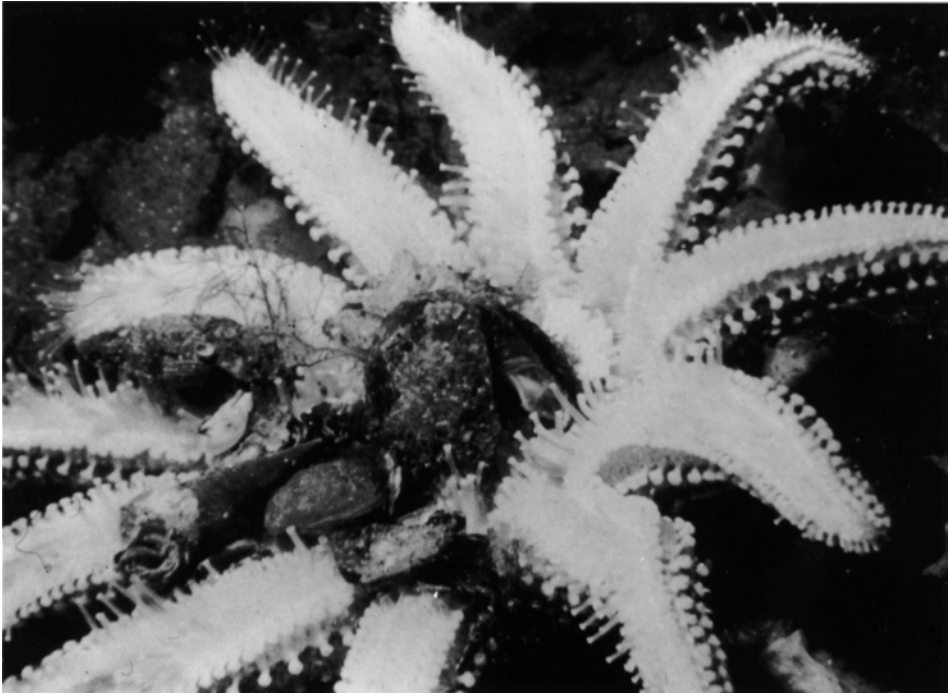


FIG. 405. *Magasella sanguinea* with predator *Coscinasterias calamaria*, $\times 63$ (new).

areas of the shell that overlie the caecae (CURRY, 1983).

An association of the amphipod *Aristias neglectus* with two brachiopod species, *Macandrevia cranium* and *Terebratulina retusa*, has been recorded from Swedish and Norwegian waters (VADER, 1970). An am-

phipod was found in the mantle cavity of one individual; other amphipods were obtained from the rinsing of samples, so the nature of the association is unknown. Another amphipod was associated with an unnamed brachiopod species from the Indian Ocean (WALKER, 1909).

BIOGEOGRAPHY OF ARTICULATED BRACHIOPODS

JOYCE R. RICHARDSON

[Museum of Victoria, Australia]

Fundamental differences in larval type indicate that patterns and paths of distribution differ for inarticulated and articulated brachiopods. The planktotrophic larvae of the inarticulated brachiopods are globally distributed and result in the absence of endemic genera. In contrast, the larvae of articulated brachiopods are nonplanktotrophic and short-lived, and faunas of articulated brachiopods have major differences both between widely separated areas (austral and boreal zones) and narrowly separated areas (Japan and China). Some of these differences in geographical distribution can be accounted for with the knowledge of living species, both from their capacity to disperse and colonize and from factors that may limit distribution.

FACTORS GOVERNING DISTRIBUTION

Distribution is concerned with both the means and pathways of distribution and so requires knowledge of the capacity for dispersal of both the larva and the adult and of their capacity for colonization.

Field studies of articulated brachiopod species indicate that the larvae are brooded, either within pouches or in the lophophore. Pouches have been described for *Lacazella mediterranea* (LACAZE-DUTHIERS, 1861), *Gwynia capsula* (SWEDMARK, 1971), and *Argyrotheca cordata* and *A. cuneata* (ATKINS, 1960a). Brooding within the lophophore has been described for *Pumilus antiquatus* (RICKWOOD, 1968), *Hemithiris psittacea* (LONG, 1964), *Notosaria nigricans* (HOVERD, 1985), *Calloria inconspicua* (DOHERTY, 1979), *Terebratulina septentrionalis* (WEBB, LOGAN, & NOBLE, 1976), and *T. unguicula* (LONG, 1964). The free-swimming phase of the larvae is brief, and laboratory studies indicate that settlement occurs between one hour and one to two days. Patterns of settlement are

consistent with limited dispersal (NOBLE, LOGAN, & WEBB, 1976; WEBB, LOGAN, & NOBLE, 1976; DOHERTY, 1979; CURRY, 1982), and the density of recruits is positively correlated with the density of residents. The diversity of sites of settlement is shown in the nature of substrates bonded with the pedicle in those individuals that retain the larval substrate in adult life. Strong preferences have been recorded for settlement on conspecifics, however.

The extent of dispersal is also correlated with adult life-style (see section on ecology of articulated brachiopods, p. 441–462). With the exception of exclusively sedentary forms, all other species possess some capacity to move in relation to their external surroundings. Movements appear to be limited to those that maintain an individual's position at the sediment-water interface, i.e., those that shed sediment from the surfaces of the valves and so prevent burial. Therefore the direction of movement in soft sediments tends to be vertical rather than horizontal except for species of *Parakinetica*, which display some capacity for horizontal progression. The influence of currents and the mobility of sediments must also be taken into account for free-lying and free-living species and for interstitial species that would behave as grains of sand and so move with the sediment. Articulated brachiopods have also been found fixed to the valves of vagile sea scallops in Canada (LOGAN, NOBLE, & WEBB, 1975) and New Zealand (ALLAN, 1937). In New Zealand they also commonly occur on such gastropods as *Astraea* and *Xenophora* (Fig. 392.4).

As reviewed in the section on the ecology of articulated brachiopods (p. 441–462), it is difficult to assess the role of physical factors in distribution because of the lack of data. At present there is no direct evidence to show that depth, temperature, latitude, or energy of the water limit distribution. The

distribution of living species is most closely related to morphology, that is, whether it is adapted to a specific range or type of substrate. Species differ, therefore, in their capacity to colonize different substrates. Having no specific requirements, generalists can colonize substrates of any size and composition and, consequently, are less affected by those environmental events that result in changes of the substrate. Generalists occur in greatest abundance in shoreline areas where settlement surfaces range in size from rock faces to the components of sea floor sediments. In these areas since life-style is governed by the mass of substrate used for settlement (see section on ecology of articulated brachiopods, p. 441), substrate relationships are varied, i.e., the life-style of an individual may be sedentary or free or a combination of both. The capacity for colonization is related to degree of specialization since specialists can colonize only those substrates for which they are morphologically adapted. For example, *Neothyris lenticularis* has the capacity to live on sediments ranging from muddy sand to gravel, whereas *Parakinetica mineuri* is specific to fine, bryozoan sands. The pedicle systems of such exclusively sedentary forms as *Platidia*, *Megerlina*, and *Kraussina* can function only if bonded to substrates in which the substrate is of greater mass than the individual. Hence generalist species possess a greater capacity for colonization and can spread around shorelines and onto shelf sediments. They are restricted in their dispersal only by the length of time spent in the larval stage.

DISTRIBUTION OF FAMILIES

Differences in taxonomic philosophies (FOSTER, 1989) and difficulties in sampling present considerable problems in biogeographic analyses. The common range of depth of articulated brachiopods is down to 600 m, and littoral species are rare. Difficulties in tracing relationships are well illustrated by the families of micromorphs: Platidiidae, Kraussinidae, and Megathyrididae. These so-called neotenous forms are grouped together on the basis of size in com-

bination with lack of development of the cardinalia and loop that is characteristic of other members of the Terebratelloidea. Relationships between the genera within each family, however, are unknown. Similarly the neotenous origin and masking effects of convergent evolution combine to obscure lines of descent within the Thecideoidea (BAKER, 1990).

Despite such problems, however, the predominance of families in some areas is quite clear. Austral and boreal families were first differentiated by the mode of development of the loop (BEECHER, 1892). At present, three broad, regional patterns can be recognized.

1. The southern area includes Australia, New Zealand, South America, the southern Indian Ocean, and circumpolar southern seas and is occupied by representatives of all superfamilies and families belonging to the Rhynchonelloidea, Terebratuloidea, Cancellothyroidea, Thecideoidea, and Terebratelloidea.

2. The northern Pacific region has representatives of all families except the Terebratellidae and most members of the Laqueidae.

3. The northern area (Atlantic, Mediterranean Sea, North Sea, and circumpolar northern seas) has representatives of all families except the terebratellids and the laqueids, with the exception of one species in the Gulf of Mexico (*Ecnomiosa gerda*).

Therefore, the family Terebratellidae is exclusive to the southern sector; the Laqueidae is a predominately northern Pacific group, while families of the Rhynchonelloidea, Terebratuloidea, and Cancellothyroidea and the families Macandreviidae, Dallinidae, Kraussinidae, and Platidiidae are worldwide in distribution.

Except for the high latitudes of the southern hemisphere, articulated brachiopods are not a common constituent of grab or dredge hauls, and their abundance in southern waters is due to the presence of members of two terebratellid subfamilies, the Anakinetiinae and the Terebratellinae.

Those families that are restricted in distribution with either geography, time, depth,

or substrate provide some insight into paths of dispersal. Few data can be obtained from the families that appear to be unlimited in distribution and in which genera contain species from widely separated geographical areas. Accordingly the following account excludes those families contained in the Rhynchonelloidea, Terebratuloidea, and Cancellothyroidea.

TEREBRATELLIDAE

The family Terebratellidae, in particular the subfamily Terebratellinae, gives the best basis for analysis because more information is available about its members than for any other group of living articulated brachiopods. It is also the group in which taxonomy causes few problems, first because the Terebratellinae contains polytypic species accessible to study in one geographical area and second because the variability of populations has been studied in many parts of the range of each species (McCAMMON & BUCHSBAUM, 1968; McCAMMON, 1970; FOSTER, 1974, 1989; ALDRIDGE, 1981, 1991; COOPER, 1981, 1982; STEWART, 1975, 1981). This means that distribution can be analyzed from populations and species rather than from genera, which in most other articulated families include species from widely separated geographical areas (Fig. 406).

The subfamily Terebratellinae contains 20 genera, five from the Tertiary and recent, seven from the Tertiary alone, and eight restricted to the recent. They are confined to the southern hemisphere between the Antarctic shoreline and a latitude of approximately 35°S and exist in very large numbers in areas shallower than 1,000 m; for example, species of *Magellania* are the most prominent on the entire Antarctic shelf (FOSTER, 1974), and species of *Neothyris*, *Magasella*, and *Calloria* are dominant forms in a number of fiords and inlets in southern New Zealand (RICHARDSON, 1981c). Most of the Antarctic species are found at all depths (100 to 1,000 m) of the Ross Sea shelf (FOSTER, 1974) and of the New Zealand shelves and neighboring rises (Chatham Rise and Campbell Plateau) that rarely exceed depths of 400

m. The South American species *Magellania venosa* is most common at shelf depths of approximately 300 m but has been recorded from 5 to 1,900 m (FOSTER, 1989) and is the only terebratelline species known from a slope.

All living terebratelline species (19 species belonging to 13 genera) have been collected from a variety of shelf sediments including gravels, coarse and fine sands, and muds. Individuals of the same species may also be found on subtidal rocks, while rare occurrences in the littoral zone are known for only two species, *Magellania flavescens* and *Calloria inconspicua*. Although *Magellania flavescens* is found in shallow water throughout southern Australia, intertidal populations have been found at only one site.

The kind of substrate occupied, morphological character, and life-style of terebratellines are strongly correlated. Species with populations living on both hard and soft surfaces are generalists and follow a sedentary or free existence (see section on the ecology of articulated brachiopods: substrate relationships, p. 441). Species exclusive to unconsolidated sediments are free living or free lying, and no terebratelline species has been described that is exclusively sedentary, i.e., restricted, like micromorphs and the rhynchonellid *Notosaria nigricans*, to coarse-grained or stable substrates. Australian and New Zealand terebratellines can be studied directly, but South American, subantarctic, and Antarctic species are known only from dredged collections. Most of these species appear to be generalists judging from morphology, from the nature and size of material adhering to the pedicle, and from the nature of the sediment. *Terebratella dorsata* and species of *Aerothyris* are generalists with the exception of one feature, differential thickening. Free-living and free-lying taxa are invariably thickened. Species observed to have the capacity to follow both sedentary and free modes of life are invariably not thickened. The variability of this character in *T. dorsata* and in *Aerothyris* indicates a trend, if not already established, toward a free life-style. An opposite trend toward a sedentary

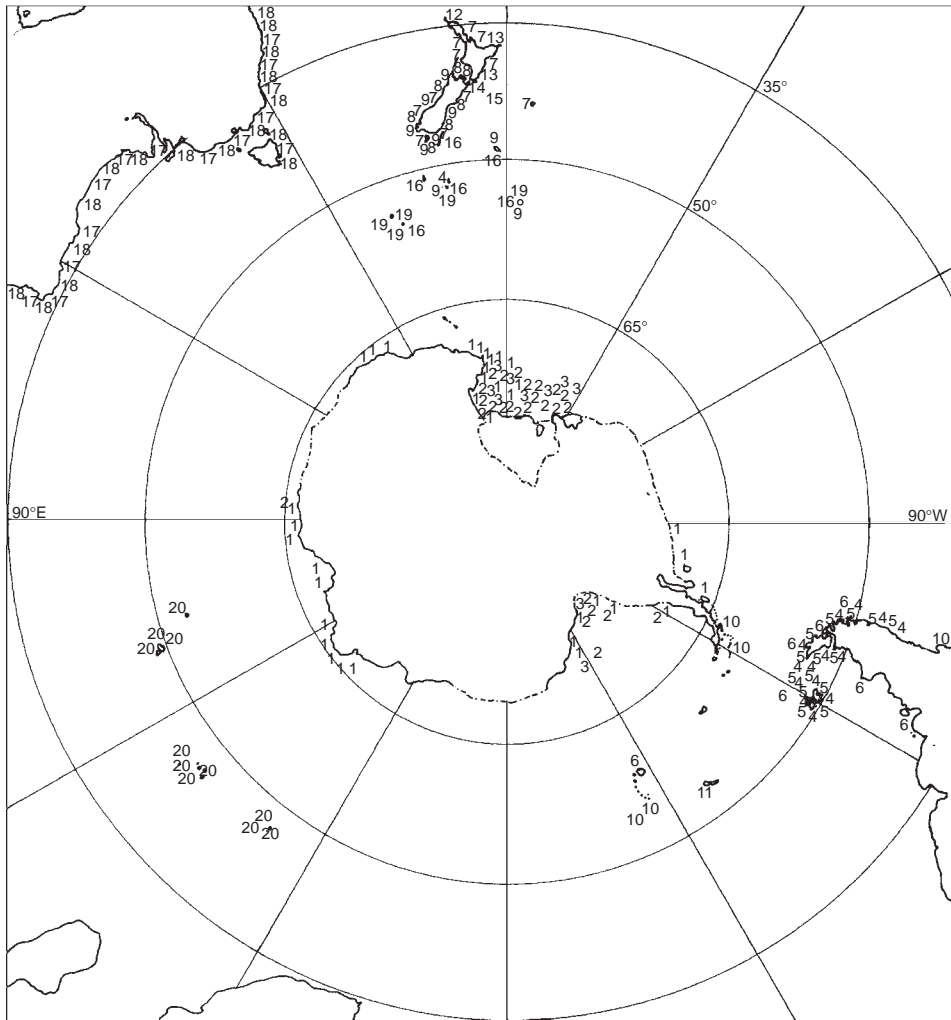


FIG. 406. Distribution of the species of the subfamily Terebratellinae from the records of COOPER (1973, 1981, 1982), COOPER and DOHERTY (1993), FOSTER (1974, 1989), McCAMMON (1973), and RICHARDSON (1981c); 1, *Magellania joubini*; 2, *Magellania fragilis*; 3, *Fosteria spinosa*; 4, *Terebratella dorsata*; 5, *Magellania venosa*; 6, *Aneboconcha obscura*; 7, *Calloria inconspicua*; 8, *Magasella sanguinea*; 9, *Neothyris lenticularis*; 10, *Syntomaria curiosa*; 11, *Dyscritosia secreta*; 12, *Calloria variegata*; 13, *Magasella haurakiensis*; 14, *Neothyris compressa*; 15, *Neothyris dawsoni*; 16, *Gyrothyris mawsoni*; 17, *Magellania flavescens*; 18, *Jaffaia jaffaensis*; 19, *Aerothyris macquariensis*; 20, *Aerothyris kerguelensis* (new).

life on hard surfaces may be inferred from the distribution of species of *Calloria*. *C. inconspicua* is found on surfaces of all types but more commonly on rocky substrates. The populations from rocky intertidal and shallow subtidal habitats differ from benthic populations in the mean size and shape of individuals. Sedentary individuals are smaller and less convex and appear to be stunted (STEWART, 1981). A new variegated

species has been collected only from rocky substrates (COOPER & DOHERTY, 1993) and closely resembles *C. inconspicua* from the same type of habitat except in the color patterns of the shell.

Members of the other southern terebratellid subfamilies, Anakineticinae and Bouchardiinae, are all specific to bryozoan sands and are smooth, free-living forms with little variability in the shape and size of spe-

cies (RICHARDSON, 1987). In comparison, terebratelline species show little specialization in life-style and substrate occupied. They vary in shape, size, and ornamentation, and relationships within the subfamily provide some insight into its origins. The difficulties all workers (ALLAN, 1949; FOSTER, 1974; COOPER, 1981; RICHARDSON, 1994) have experienced in separating the nonspecialist members of the subfamily is an indicator of the close relationship between species now attributed to *Aerothyris*, *Aneboconcha*, *Calloria*, *Dyscritosia*, *Fosteria*, *Magasella*, *Magellania*, *Syntomaria*, and *Terebratella*. These similarities are the result of relatedness, not of convergence, because they occur in sets of characters that appear to be unrelated to the environment, including the shape of the cardinal process, presence of a hinge plate, and position of the beak ridge. The most specialized terebratellines are the species included in *Neothyris* and *Gyrothyris*. They occupy soft sediments but not, as in the Anakineticinae, of a particular size range or composition and are considered to have evolved from *Magasella*-like ancestors (THOMSON, 1927), i.e., from more generalist stocks. Similar relationships occur within Australian terebratellines: such free-living forms as *Victorothyris* appear to have been derived from *Magellania*-type stock (RICHARDSON, 1980).

Members of the Terebratellidae have occupied shorelines and shelves throughout the Tertiary. Forms not confined to a specific substrate (*Calloria*, *Magasella*, *Magellania*, and *Terebratella*) are found from Eocene and later strata of Australia and New Zealand and from Oligocene and Miocene strata in Antarctica. The occurrence of shelf forms can be correlated with the Tertiary history of different areas. The New Zealand record shows that the sediment changes that accompanied Miocene regressions led to the extinction of all substrate-specific terebratelline (*Waiparia*, *Stethothyris*, and *Pachymagas*) and anakineticine (*Rhizothyris* and *Magadina*) genera. Species of *Neothyris* are found in a variety of originally soft sediments only from the Pliocene and Pleistocene periods (ALLAN,

1960; NEALL, 1972). Australian Tertiary deposits consist almost exclusively of originally soft sediments, and there is an almost continuous record of anakineticines from the Eocene. Unlike in New Zealand, the deposits of shelly limestones that are similar to those occupied by modern, rocky-shoreline assemblages are not found in Australia. Species with nonspecialist characters occur in Australian Eocene deposits, while those terebratellines specialized to varying degrees for limestones (*Austrothyris*, *Cudmorella*, *Stethothyris*, and *Victorothyris*) are found in Oligocene and Miocene rocks and were lost during Miocene regressions. The only living terebratellines found in Australian waters are *Magellania flavescens* and *Jaffaia jaffaensis*.

Distributions of fossil taxa indicate that, in Australia and New Zealand at least, nonspecialist forms have occupied shoreline habitats since the Eocene and were apparently unaffected by the lowering of sea level at the end of the Miocene. At this time all terebratellines and anakineticines that were specialized for life on the shelf, occurring in greensands, calcarenites, and calcilitites, were lost in New Zealand. In Australia, only terebratellines in calcilitites became extinct. The persistence of the anakineticines in calcarenites throughout the Cenozoic may be attributed to the areal extent of the calcarenites and to their position on the shelf. Calcarenites now cover the middle and outer shelves, whereas extinct terebratellines have been collected from deposits that formed the floor of former inlets, the Murray and Gippsland basins.

LAQUEIDAE

The family Laqueidae contains 13 living genera, most of which are found around the North Pacific rim. *Coptothyris*, *Jolonica*, and *Pictothyris* occur in Japan only. *Terebratalia* and *Laqueus* occur between California and Japan, and *Tythothyris* and *Simplicithyris* are found in the northwestern Pacific. *Frenulina* occurs in the central Pacific (southern China Sea, Philippines, Indonesia, and Hawaii), in Australia, and in the western Indian Ocean. One species of *Ecnomiosa* is recorded from

the Gulf of Mexico and another from South Crozet Island in the southern Indian Ocean, while *Compsoria* occurs in the eastern Indian Ocean and off Mozambique.

Two groups of genera, therefore, differ in area of distribution: those from the North Pacific are considered as one section of the family (HATAI, 1940), while *Ecnomiosa*, *Frenulina*, and *Compsoria* are found in the central and southern Pacific and the eastern and southern Indian Ocean. With respect to fossil occurrences, most members of the northern group are represented in Tertiary and Quaternary deposits of the areas they now occupy. *Frenulina* is found in the Australian Miocene to Pliocene, and *Ecnomiosa* is related to Australian stock from the Cretaceous (*Kingena*) and Miocene (*Paral dingia*). *Aldingia willemoesi* was recorded from Australian seas (THOMSON, 1927) but is unknown in any Australian collections. The existence of natural seaways across parts of Columbia, Panama, and Costa Rica afforded free communication between the Pacific and the Caribbean Sea or western Atlantic up to the end of the Miocene or Pliocene and may account for the presence of *Ecnomiosa gerda* in the Gulf of Mexico.

Laqueidae is unknown from northern or southern circumpolar seas, from the Atlantic, or from abyssal sediments.

Shell color patterns and associations with coral reefs indicate that *Frenulina* is probably exclusive to shallow, coralline substrates. *Pictothyris picta* and all Japanese species of *Laqueus* except *L. blanfordi* and *L. quadratus* are differentially thickened forms and have been retrieved from sands at depths of approximately 100 m off the coast of Japan (ENDO, 1987). Both sedentary and free populations of *Laqueus californianus* (BERNARD, 1972; ASGAARD & BROMLEY, 1991) and of species of *Terebratalia* (DU BOIS, 1916; RICHARDSON, STEWART, & XIXING, 1989; SCHUMANN, 1991) have been described.

DALLINIDAE

The Dallinidae is a family of which little is known of habitat, life-style, or morpho-

logical variability. Species have been collected from bottom sediments; but the species of only one genus, *Nipponithyris*, are differentially thickened, an indicator of a free mode of life. The genera included in the family differ in cardinalia and in the presence or absence of dental plates, leading to the conclusion that the family is made up of distinct stocks.

One genus, *Dallina*, contains species from the Pacific, Antarctic, and the North to South Atlantic oceans. Fossil representatives from the Eocene and later times are as widely distributed as those from the recent and have been collected in Italy, Japan, Norway, New Hebrides, and Fiji. *Fallax* contains two species that are difficult to separate (FOSTER, 1974), one from the northeastern Atlantic (from 686 to 1,408 m) and the other from the southwestern Pacific (2,285 to 2,342 m); and the genus has been recorded from the Pliocene of Sicily. Both *Campages* and *Nipponithyris* are found in the Miocene of Japan. In modern seas *Nipponithyris* occurs in New Caledonia and Japan, and *Campages* is found in Japan, Australia, and the Philippines. *Glaciarcula* with two species occurs in the northern circumpolar region and in the Pleistocene of Scandinavia.

MACANDREVIIDAE

The family Macandreviidae, with a single exception, contains abyssal species that occur in greatest numbers in the northwestern Atlantic region. *Diestothyris* contains 1 and *Macandrevia* contains 11 recent species. *D. frontalis* has been collected in the North Pacific from depths of 0 to 435 m and has also been described from the Miocene of Alaska and Japan. Other species of the genus are known from the Miocene of Canada and the Pliocene and Pleistocene of the Kamchatka Peninsula and Japan.

In modern seas *Macandrevia* is recorded almost exclusively from abyssal waters (COOPER, 1975). One species (*M. cranium*) is found from 9 to 2,492 m. *M. americana* occurs from 112 to 4,066 m, and *M. tenera* is found from 207 to 2,652 m. Other species occur at depths that exceed 2,000 m.

Species have been described from Atlantic, Mediterranean, Antarctic, and eastern Pacific waters. The wide geographical distribution of species is noteworthy; for example, *M. americana* has been recorded from San Diego, California, south to Antarctica and the southernmost South Atlantic. Fossil members of the genus have been collected from Quaternary deposits of Norway, Sweden, and Italy. The shell is unthickened in all forms except for one unnamed species collected from a rock near hydrothermal vents of the western Pacific at 2,700 m.

MEGATHYRIDIDAE

Members of the three genera attributed to the Megathyrididae are found principally in European and West Indian waters. They are small, sedentary forms commonly bonded so closely with the substrate that the beak and parts of the dorsal valve are misshapen and worn. They have been collected from cryptic habitats in shallow water but are not restricted in depth.

Gwynia is known from the Pleistocene of Norway and the one living species is found along the coasts of the United Kingdom, France, and the Netherlands from 15 to 46 m (BRUNTON & CURRY, 1979). It has also been recorded from north of the Azores at 4,060 m (FISCHER & OEHLERT, 1892). Species of *Megathiris* have been described from the Mediterranean Sea, eastern Atlantic, and South Africa; and fossil species are known from the European Late Cretaceous to Pliocene.

Argyrotheca contains 22 named and 6 unnamed living species from the West Indies (COOPER, 1977; ASGAARD & STENTOFT, 1984), Mediterranean Sea (LOGAN, 1979; BRUNTON, 1988), Red Sea (JACKSON, GOREAU, & HARTMAN, 1971), southeastern North Atlantic (LOGAN, 1983), Mozambique Channel (ZEZINA, 1987), South Africa, Australia, and eastern and western Pacific (GRANT, 1987). *Argyrothecans* are common from Tertiary deposits in Europe, United States, West Indies, Peru, Mexico, and Europe; and *Argyrotheca* is 1 of only 3 articulated brachiopod genera that crossed the

Cretaceous-Tertiary boundary (COOPER, 1988). Most species occupy cryptic habitats in shallow-water, but many have a considerable depth range. For example, *A. barrettiana* has been collected from 1,473 m (COOPER, 1977).

KRAUSSINIDAE

Kraussina contains five species from South Africa with a depth range of 18 to 366 m (HILLER, 1991); one of these species is also found in the southeastern North Atlantic (LOGAN, 1983). Most species of *Megerlina* have been collected from low tide to 274 m in South Africa, southern Indian Ocean, and Australia. Fossils of either genus are unknown.

Megerlia has been described from the European Miocene and, in recent seas, from South Africa, southeastern North Atlantic, Mediterranean Sea, West Indies, southern Indian Ocean, Red Sea, and Australia. *Pumilus* is found in shallow water in New Zealand.

PLATIDIIDAE

Like the families Megathyrididae and Kraussinidae, platidiids are small, sedentary forms requiring a hard, stable surface for permanent attachment. *Platidia* is considered to contain three species (FOSTER, 1989), one from the Gulf of Mexico (*P. clepsydra*) and one from the Mediterranean Sea, the southeastern North Atlantic, the West Indies, and Argentina (*P. davidsoni*). *P. anomioides*, the third, is the only species in Tertiary rocks and is almost worldwide in distribution throughout the Cenozoic.

Amphithyris contains three species, two from New Zealand and one from the Ross Sea (Antarctica). Three species have also been assigned to *Annuloplatidia* from different regions of the Pacific Ocean. One, *A. indopacifica*, has a depth range of 370 to 5,800 m (ZEZINA, 1985).

THECIDELLINIDAE AND THECIDEIDAE

Thecideidine brachiopods are uniform in life-style, habitat occupied, and morphology

and are restricted in depth and to latitudes lower than 35 degrees.

Thecidellina is the only living member of the Thecidellinidae, and *Lacazella* and *Pajaudina* are the only living Thecideidae. They are also the only living taxa in which the pedicle is absent in adults that are sessile forms cemented to substrates. Living specimens have been collected from cryptic, reef habitats and from depths of 5 to 176 m. The latitudinal range of the group is from 20°S in Australia to 35°N in the Mediterranean Sea.

Thecidellina has been described from the western and central Pacific Ocean, the Caribbean Sea, and the Indian Ocean, with fossils collected from the Eocene and Miocene of the Gulf and Atlantic coasts of the United States, the Eocene of the west coast of the United States, the Eocene of France, and the Miocene of the Pacific Ocean (COOPER, 1977). *Pajaudina* is found in the southeastern North Atlantic, and species of *Lacazella* occur in the Mediterranean Sea, southeastern North Atlantic, Indian Ocean, and Caribbean Sea. Fossil *Lacazella* occur in Eocene to Miocene deposits of Cuba and in Eocene deposits of the Gulf and Atlantic coasts of the United States.

FAMILY ORIGINS AND PATHS OF DISPERSAL

Examination of the distribution of different families shows clear linkages between the age of a family and some aspects of composition and distribution. Older families are cosmopolitan. As a rule members do not occur in abundance, but they do occupy slopes and the abyss. The youngest families are restricted in distribution. They may occur in abundance at the shoreline and on shelves but are not found on slopes or in the abyss. Families of the Rhynchonelloidea, Cancellothyroidea, and Terebratuloidea were all more common in past eras. Numbers of genera in the Rhynchonelloidea, for example, declined from 113 in the Jurassic to 17 in the recent. The Terebratuloidea declined in numbers from 136 to 19 in the same periods (COOPER, 1988). Age, together

with sparse occurrence and cosmopolitan distribution, means that the present composition of these superfamilies is unrepresentative of the past diversity and distribution: they are relict groups that have shown no evidence of diversification at least since the Jurassic. Therefore relationships between species and genera would be difficult if not impossible to determine. As a consequence, the present composition and distribution of nonterebratelloid families can provide little information on the origins and paths of dispersal of articulated brachiopods.

Terebratelloid families are also cosmopolitan except for the southern Terebratellidae and northern members of the family Laqueidae. The Terebratellidae and Laqueidae are presumed to be the youngest articulated brachiopod families, and in modern seas they appear to be as common as or more common than in the Tertiary. Also, unlike other families, polytypic genera may be found in the same geographical area. Therefore, they provide the most reliable sources from which to speculate on origins of modern articulated brachiopod assemblages and paths of dispersal.

Terebratellids and laqueids are consistent in patterns of distribution with the nature of species, i.e., generalist species are most abundant in areas in which substrates available for settlement vary in mass, and these patterns of living faunas conform with those from Tertiary deposits. Species not specific to a particular substrate are widely distributed both geographically and with respect to substrate and are variable in such characters linked with the environment as differential thickening, beak shape, size, and shape. Species specialized for shelf sediments may be more limited in distribution and are less variable morphologically, both distribution and variability being related to degree of specialization. Japanese and New Zealand seas contain members of most living families, but the major components of articulated brachiopod faunas of the Cenozoic are members respectively of the Terebrataliidae (Laqueidae) and the Terebratellinae (Terebratellidae if Tertiary forms are included). In both areas, general-

ist species of *Terebratalia* and *Magasella* are widespread on shorelines and shelves, and species of *Coptothyris* (NOMURA & HATAI, 1936), *Dallinella* (THOMSON, 1927), and *Neothyris* (RICHARDSON, 1994) adapted to shelf sediments are endemic and are considered to have been derived from the generalist stocks found in these areas.

The differences in the patterns of distribution of the Laqueidae (in Japan) and Terebratellidae (in New Zealand) from those of other articulated brachiopod families may be attributed to differences in the opportunities for colonization. One reason for the absence of any evidence of diversification in older families since the end of the Jurassic (COOPER, 1988) could be the absence of those substrates that existing faunas have the capacity to colonize. For example, members of the Bouchardiinae and Anakineticinae are found on bryozoan sands off Brazil and Australia, the only areas in which these sands are common and which members of the subfamilies are specialized to occupy. Their specificity for this kind of sediment and a short larval life mean that transoceanic dispersal was not possible.

The contrast between Japanese and Chinese articulated brachiopod faunas provides good evidence that transoceanic migration is an unlikely means of dispersal and that species differ in capacities for colonization. The Cenozoic Japanese fauna is abundant (50 species in 18 genera) and consists of a major component of endemic terebratelloid genera and a lesser component of genera belonging to older cosmopolitan families (HATAI, 1940). In contrast only four living species (*Terebratalia coreanica*, *Campages mariae*, *Terebratulina hataiana*, and *Frenulina sanguinolenta*) occur in Chinese waters; none is endemic, and no articulated brachiopods are known from the Chinese Tertiary (RICHARDSON, STEWART, & XIXING, 1989). *Terebratalia coreanica* is a generalist species common around the shorelines and shelves of Japan and Korea. *Campages mariae* has been collected from shelf sediments around Japan and is not known to be specific to any particular grain size or composition. *Terebra-*

tulina hataiana has been collected from sandy sediments of the South China Sea and has also been described from seas around the Philippine Islands. *Frenulina sanguinolenta* is widely distributed in low to mid-latitudes of the Indo-Pacific and has been collected from coral reefs around islands in the South China Sea. Thus Japan and China, although near neighbors, provide the strongest contrast between a rich, indigenous fauna and a sparse, immigrant fauna.

Differences in the faunal composition of other neighboring areas also contribute to an understanding of factors governing geographic distribution. The living faunas off Australia and New Zealand are dominated by terebratellids but by members of different subfamilies, the Anakineticinae in Australia and the Terebratellinae in New Zealand. This is one consequence of differences in the stability of the two areas during the Tertiary, which has resulted in different shelf sediments in modern seas. Anakineticines are adapted for life in either greensands or bryozoan sands, and the stability of the Australian continent has meant that a shelf cover of the sands has been maintained from at least the Eocene. Anakineticines were also common in the greensand sandstones and bryozoan sandstone of the New Zealand Oligocene and Miocene but became extinct before the end of the Miocene. These two kinds of sand now support different terebratellid faunas— anakineticines in Australia's bryozoan sands and terebratellines in the New Zealand terrigenous sediments. Hence the Australian fauna has been unchanged throughout the Cenozoic, whereas the present New Zealand shelf fauna is of relatively recent, Pliocene origin.

The endemic nature of the terebratellid faunas around Australia, New Zealand, and other southern land masses led earlier workers (BLOCHMANN, 1908; THOMSON, 1918; ALLAN, 1963) to the conclusion that their probable source of origin was Gondwana and that pre-Tertiary land bridges would have provided routes for the dispersal of ancestral forms. Plate tectonics, of course, has provided the means of distribution without

the need to postulate land bridges. It seems unlikely that the patterns of distribution of terebratellid brachiopods in earlier periods would differ appreciably from those evident throughout the Cenozoic. Therefore in the absence of evidence to the contrary, it is safe to surmise that the shorelines and shelf of Gondwana were occupied by generalist species and by species specialized to varying degrees for life on the shelf. With the break up of the continent their survival would have been inversely correlated with the extent of loss or change of substrate. Differences in the requirements of generalists and specialists mean that generalists are more likely to survive periods of environmental change as illustrated by the extinction of all taxa specialized for shelf sediments during periods of instability in the New Zealand Miocene.

The break up of Gondwana and the differential survival of species account for the present distribution in which generalists and near-generalists occur around southern, Gondwana-derived land masses except for South Africa. The only specialists that occur in Tertiary deposits of both Australia and New Zealand are three conspecifics, one cancellothyrid and two terebratellid species, all of which were adapted for life in carbonate sands. The presence of these conspecifics indicates that they evolved before the break up of Gondwana and that parts of the Gondwana shelf contributed to the shelves of Australia and New Zealand. Any transoceanic dispersal between Australia and New Zealand is precluded by length of larval life and by the absence of carbonate sands bridging the Australian and New Zealand shelves. All other specialists found in southern latitudes are endemics; i.e., they evolved in the area they now occupy and are more likely to have been derived from nonspecialist or generalist stock of that area, not from species with similar adaptations from a different geographical area. For example, studies of growth stages show that species of *Neothyris* and *Victorothyris* are more closely related respectively to species of *Magasella* and to *Magellania* than to any other species. The absence of any member of the Terebratellidae

from the Cenozoic of South Africa suggests that those sections of the Gondwana shoreline and shelf that contained members of the family did not contribute to the southern part of Africa.

The similarities in the distribution of the Terebratellidae and northern Laqueidae suggest that processes of diversification were similar and that they occurred in different areas. Laqueid generalists are found around the shorelines of the northern Pacific, and diversification of this stock has resulted in species specialized for different shelf sediments, for example those in Japan and California. Generalist species of the Terebratellinae occur around Gondwana-derived land masses, and genera specialized for life in shelf sediments are endemic to Australia, New Zealand, and South America. Although other families are not restricted in distribution, fossil occurrences together with preponderances of living faunas indicate the centers from which each group may have originated and dispersed. For example, the family Kraussinidae is a predominately South African family (HILLER, 1991). The family Megathyrididae is found principally in European and West Indian waters, and living species shared between these two areas (LOGAN, 1993) and in the fossil record (ELLIOTT, 1951; COOPER, 1977) have led workers to conclude that at some time in the past the coasts were close together. Given the age of articulated brachiopod families and the difficulties of transoceanic travel, vicariance seems to be the principal means of distribution; i.e., the diversification of most families occurred during periods when shorelines were close together. In addition it seems that, with the obvious exception of substrate-specific taxa, the extent of geographic and bathymetric distribution may be correlated with age of families rather than a consequence of inherent limiting factors. The present restriction of the Terebratellinae to high latitudes and to waters exceeding depths of 1,000 m may be an indicator not of a preference for cold water but a consequence of relatively recent origin and slow rates of dispersal.

ECOLOGY OF INARTICULATED BRACHIOPODS

CHRISTIAN C. EMIG

[Centre d'Océanologie de Marseille]

INTRODUCTION

Living inarticulated brachiopods are a highly diversified group. All are marine, with most species extending from the littoral waters to the bathyal zone. Only one species reaches abyssal depths, and none is restricted to the intertidal zone. Among the living brachiopods, the lingulides, which have been most extensively studied, are the only well-known group.

Both living lingulide genera, *Lingula* and *Glottidia*, are the sole extant representatives of a Paleozoic inarticulated group that have evolved an infaunal habit. They have a range of morphological, physiological, and behavioral features that have adapted them for an endobiont mode of life that has remained remarkably constant at least since the early Paleozoic. The lingulide group shares many features that are characteristic of this mode of life including a shell shape that is oblong oval or rectangular in outline with straight, lateral, subparallel to parallel margins and an anterior margin that is straight to slightly concave for burrowing; a complex muscle system that operates the inarticulated valves; a mantle margin and its setae that serve several basic purposes; and a pedicle that anchors the animal at the bottom of the burrow and shifts the position of the shell. Such characteristics can be considered as plesiomorphic among the Brachiopoda.

The ecological requirements of inarticulated brachiopods indicate the need for a life-history approach that emphasizes aspects of populations rather than individuals because many such factors as reproduction, survivorship, dispersion, and evolution depend on populations. Accordingly there is no single factor that determines the occupancy of a niche by a population and that is always directly related to the biocoenosis in which the population is living. Those requirements

need to be analyzed carefully at the population level before using them to interpret species and genera.

Assemblages with lingulides are routinely interpreted as indicating intertidal, brackish, and warm conditions, but the evidence for such assumptions is mainly anecdotal. In fact, formation of lingulide fossil beds generally occurred during drastic to catastrophic ecological changes.

BEHAVIOR

INFAUNAL PATTERN: LINGULIDAE

Burrows

Lingulides live in a vertical burrow in a soft substrate. Their burrow has two parts (Fig. 407): the upper part, oval in section, about two-thirds of the total length of the burrow, in which the shell moves along a single plane, and the cylindrical lower part in which only the pedicle moves (EMIG, 1981b, 1982). In a homogenous fine sand the length of the whole burrow is about ten times the length of the shell (Fig. 407), but it can be reduced when the coarse fraction increases at depth in the sediment or when a hard layer occurs (EMIG, 1982). In tropical areas, a layer formed by pieces of coral and pebbles or by shell fragments often limits the thickness of the sandy sheet to about 15 to 20 cm. The pedicle is anchored within this coarse layer, and the detrital mass of the bulb is less than that of individuals living in thick, sandy sediment. The extension of the pedicle can reach a length 20 times that of the shell to compensate for sedimentation (EMIG, 1983a). Fossil burrows with lingulide shells *in situ* show the same structure (Fig. 407). Thus when determining the relationship of the burrow to the length of the shell, the compaction of the sand layer can be estimated at about one-third (EMIG & others, 1978; EMIG, 1982).

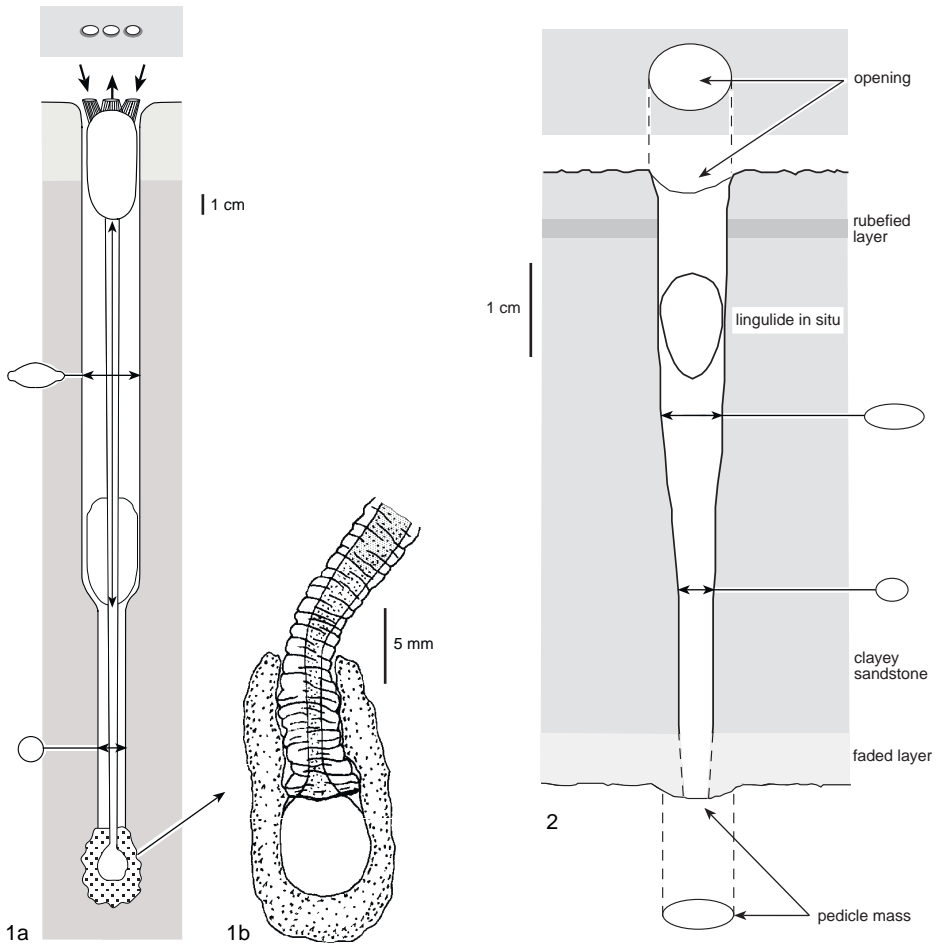


FIG. 407. *1a*, Longitudinal section of a burrow of a living lingulide with the shell in normal position and retracted (and *1b*, detailed pedicle mass); and *2*, of a fossil lingulide (Triassic of Vosges Mountains; Emig & others, 1978).

The walls of the burrow are lined with mucus secreted by the edges of the mantle and the pedicle (EMIG, 1982). The mucous layer binds the walls and lubricates the movements of the animal in its burrow. Only the distal bulb of the pedicle, surrounded by a mass of sand and various detrital particles agglutinated by the bulb's sticky mucous secretion, is firmly anchored into the substratum at the bottom of the burrow (Fig. 407). The size of this mass depends upon characteristics of the sediment. Functioning like the ampulla in the Phoronida, the distal bulb of the lingulides is able, by turgescence un-

der coelomic pressure, to reinforce the anchoring in the substratum and is enhanced by crenulation of the pedicle bulb.

The lingulides often live in sediment that is in a reducing environment below the upper 2 to 5 centimeters, but the peripheral substrate, which is up to 1 to 2 mm thick along the burrow walls, is oxygenated by continuously renewed water in the burrow (Fig. 407).

Continuous filtering indicates that the normal position of the lingulide shell is at the top of the burrow (EMIG, 1982). To maintain this position (Fig. 408), a weak

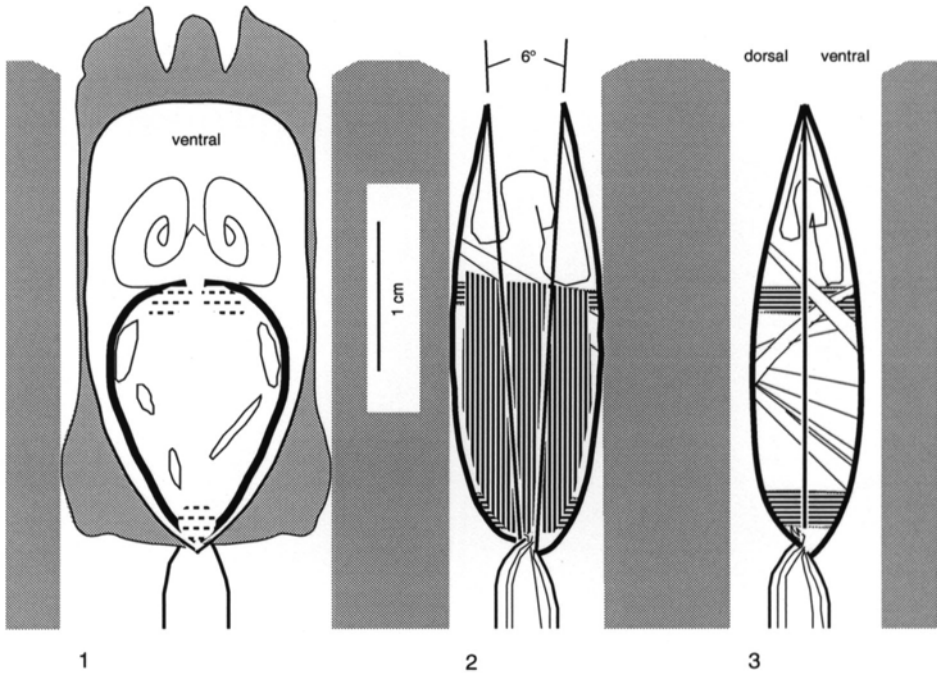


FIG. 408. Longitudinal section of a lingulide in its burrow; 1, ventral side showing the mantle setae length; 2, normal position (lateral view) by contraction of the lateral muscles; 3, quick valve closure by contraction of the anterior and posterior adductor muscles, first step of the escape reflex (new).

contraction of the lateral body muscle layer produces a hydrostatic pressure on the body's coelomic cavity; the body volume is shifted posteriorly and laterally; the valves gape about 6° to rest against the lateral burrow walls, which act as supports; and the lophophore extends to become functional within an enlarged pallial cavity. The normal life position is static and can be maintained without much effort. The pedicle plays no role in the maintenance of this position. Occasional scissorlike movements of the valves assist in maintenance of the burrow (Fig. 409).

Coarser or muddier substrates are less well suited for providing stable burrow walls. Consequently, the animal is unable to live or to survive in sediment that is too coarse or too muddy, contrary to general assumptions about habitats of lingulides. Thus living lingulides have rarely been found in muddy sediments with a fine fraction ($< 63 \mu\text{m}$) higher than 35 to 40 percent because in such

fluid sediments the walls, even when bonded by mucous secretion, inadequately support the shell in its normal filtering position (EMIG, 1983a).

At the surface of the sediment, three characteristic pseudosiphons indicate the presence of a lingulide in normal, life position (Fig. 407–408, 410; Table 35). They are shaped by the highly specialized anterior setae of the mantle. At the level of the shortest setae, the anterior mantle margin of each valve develops an epidermal crest. These come into contact with each other and induce tilting and interlacing of the setae borne by the crests. Simultaneously the longest setae, which can be as long as a third of the shell length, remain vertical (Fig. 408). The central aperture is exhalant, while the two lateral apertures are inhalant. The exhalant and inhalant water streams are completely separated by the mantle crests and internally by tentacle tips without any mixing of the flows. The diameter of setae varies

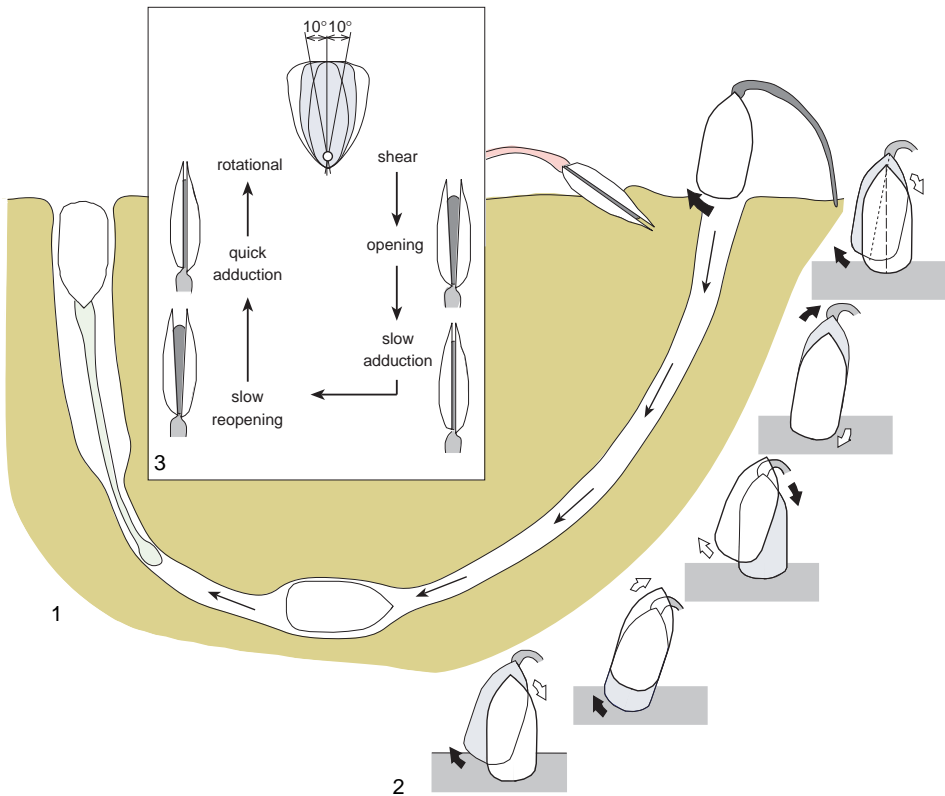


FIG. 409. 1, U-shaped reburrowing by *Glottidia* (Emig & others, 1978); 2, sequence of the scissors burrowing movements of *G. pyramidata* (Thayer & Steele-Petrovic, 1975); 3, patterns in the burrowing sequence of *Lingula anatina* (Savazzi, 1991).

from 15 to 60 μm , and they occur at intervals of 15 to 30 μm so that they exclude large particles from the pallial cavity. Contrary to general assumptions (PAINE, 1970; THAYER & STEELE-PETROVIC, 1975), the absence of lingu-
 gulides from mud is not related to clogging of the lophophoral cavity by fine particles. In a turbid water mass, fine particles may be retained in large masses by the mucus on the setae of the pseudosiphons and do not enter the pallial cavity but are flushed out periodically by scissorlike movements of the shell (EMIG, 1983a).

No orientation related to current direction has been observed (WORCESTER, 1969; EMIG, 1981b) because the strong, jetlike, exhalant current precludes possible recycling by the inhalant currents. A turn of the shell plane of about 25 to 30° from the near-bottom cur-

rent direction appears to be sufficient to avoid recycling (Fig. 410).

Shell Movements and Burrowing

Shell movements and burrowing behavior are similar in both extant lingu-
 gulide genera, *Lingula* and *Glottidia* (YATSU, 1902b; THAYER & STEELE-PETROVIC, 1975; EMIG, 1981b, 1982, 1983b; TRUEMAN & WONG, 1987; SAVAZZI, 1991), and have probably been practiced by oblong or rectangular lingu-
 guloides since early Paleozoic times (EMIG, 1984b; SAVAZZI, 1991).

Opening and slow closing movements (Fig. 408–409) of the valves are governed by fluctuations in pressure within the meta-
 coelomic body cavity and are generated by contraction of the lateral muscle layers of the body, which are composed of circulo-

TABLE 35. Summary of the two adult lophophore types in living inarticulated brachiopods in relation to the number of inhalant (*in*) and exhalant (*ex*) compartments and apertures in the shell and shell orientation in or on substratum (new).

Taxa	Genera	Species	Shell orientation	Schizolophe <i>of Pelagodiscus atlanticus</i>	Spirolophe
Lingulides	2	12	shell vertical	-	2 in + 1 ex ¹
Craniids	4	19	dorsal valve above, ventral valve below	-	2 in + 1 ex ¹
Discinids	1	1	dorsal valve above, ventral valve below	1 in + 2 ex	
	3	11	dorsal valve above, ventral valve below	-	1 in + 2 ex

¹in these groups, there are two small additional exhalant apertures behind the shell.

longitudinal fibers. This body cavity functions as a single, fluid-filled chamber, although partially divided by a gastroparietal band and, with the coelomic canal of the pedicle, acts as a fluid reservoir in the hydraulic system. This system that opens the valves performs the same function as the elastic hinge ligament of the molluscs and the diductor muscles of articulated brachiopods. Quick closure is obtained by the contraction of the anterior and posterior adductor muscles. Scissorlike movements of the valves occur by contraction of the well-developed, oblique muscles. This complex body musculature sustains the unique, infaunal mode of life of these brachiopods.

When a lingulide is on a sandy substrate, fluctuations in pressure within the coelomic body and pedicle cavities open and close the valve. When the lingulide starts to burrow (Fig. 409), the pedicle stiffens with its distal bulb pressing downward to prop up the valves, thereby bringing the anterior margins of the valves into contact with the sediment. Penetration takes place by means of a combination of scissorlike movements of the valves and ejection of water from them that loosen the sand prior to a downward movement of the shell and an upward transportation of mucous-bound sand by the lateral setae of the mantle.

The typical burrowing sequence consists of the following phases (Fig. 409). First, scissorlike movements occur by oscillatory rotation of the valves about an axis passing dorsoventrally through the posterior shell; the movements coincide with small, pressure

pulses and, although the shell is moderately gaping, the setae, which prevent sediment particles from entering the mantle cavity, aid in the burrowing process. A complete rotation takes five to eight seconds. Second, there is a slow opening of the valve of one to five seconds in duration, followed by a short pause (up to three seconds). Third, a slow closure and then reopening of the valves are followed by a quick contraction of the adductor muscles that forces water jets into the surrounding sediment. Fourth, there is a pause of variable length.

Progression into the sand coincides with large pressure pulses and is facilitated by the secretion of a large amount of mucus. Contrary to popular belief, the lingulide pedicle is not used for burrowing; it is unable to dig into the sediment. Instead it acts as a support or prop while repeated scissorlike movements, shell closure with water injection, and shell openings accompanied by pressure pulses result in successively deeper penetration. Burrowing follows a semicircular course, the radius of which probably depends on shell size. The animal burrows obliquely downward to a depth that has not yet been established in natural conditions, then curves upward and burrows vertically until it reaches the surface of the sediment. Pedicle anchoring following burial is achieved by mucoadhesion of sand and various particles. Some fossil U-shaped burrows could be related to reburrowing features (EMIG & others, 1978). While reentering the sediment the animal is extremely susceptible to predation.

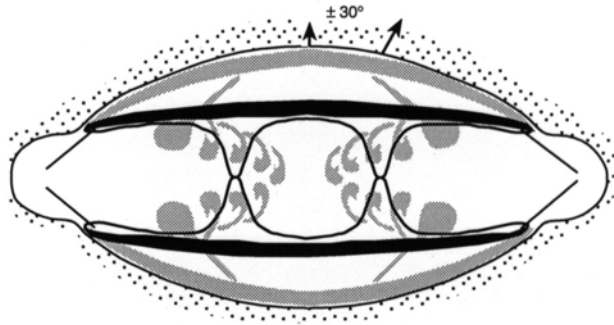


FIG. 410. Composite of two transverse sections of a lingulide in its burrow, one section at the level of the anterior mantle margin showing the epidermal crests and inhalant and exhalant opening (shown in *heavy lines*), the other at the level of the lophophore (*shaded in gray*) (adapted from Emig, 1982).

Burrowing is faster in small individuals than in larger ones, and failure to reburrow increases in *Lingula* with shell lengths exceeding 1.7 to 2 cm (MORSE, 1902; AWATI & KSHIRSAGAR, 1957; WORCESTER, 1969; EMIG, 1981b, 1982, 1983a; HAMMOND, 1983; SAVAZZI, 1991). Reburrowing could be interpreted as a size-related process, but such a performance seems to vary between geographic populations, as contradicting accounts have shown (EMIG, 1983a; SAVAZZI, 1991). In experimental conditions the burrowing speed is always five to ten times faster than in natural conditions (Table 36). Upward burrowing is essential for the survival of the lingulides and can be accelerated to compensate for sedimentation above their burrows, perhaps a response to the increase of the sediment pressure (Table 36). A rapid influx of coarse sediment, which is not typical of the environments of lingulides, however, may occur during high-energy events (HAMMOND, 1983). The nature of the sediment has a direct influence on burrowing capability, which is about twice as fast in a sandy substrate as in coarser sediment (particles > 2 mm). In experimental conditions *Lingula anatina* was able to burrow upward in coarse sediment but was unable to construct a stable burrow and finally emerged onto the sediment surface, often after autotomy of its pedicle. The results are indecisive under natural conditions (EMIG, 1983a), but the temperature seems to have no influence on the burrowing speed. *Glottidia* is unable

to dig in such coarse sediments (THAYER & STEELE-PETROVIC, 1975; CULTER, 1979).

During rapid experimental sedimentation, autotomy of the pedicle occurs when accumulation exceeds the pedicle extension. A new pedicle is regenerated in four to eight weeks in *Lingula*, but individuals without a pedicle maintain their filtering position with difficulty and generally emerge onto the sediment surface. Any damage to the pedicle always impairs burrowing as it precludes the use of the coelom as a hydraulic system. *L. reevii* is able to move pebbles of several centimeters in diameter that happen to lie on top of its burrow (EMIG, 1981b).

Retraction into the Burrow

Rapid retraction into the burrow is an escape reflex (FRANÇOIS, 1891; MORSE, 1902) that is well known in almost all animals that live in burrows or tubes. This protective reaction in response to unfavorable circumstances in the external environment is accompanied by the rapid closure of the shell. This response by the lingulides is elicited by tactile stimulations of the anterior marginal setae (MORSE, 1902; TRUEMAN & WONG, 1987), by an organism moving over the sediment surface, or by a shadow falling on the brachiopod (EMIG, 1981b). Such stimuli result in a quick closure of the shell with expulsion of water combined with contraction of the pedicle muscle, and the animal withdraws quite quickly into the burrow. If the disturbance continues the animal generally

TABLE 36. Experimental and *in situ* (measurements in italics) burrowing conditions (data from *a*, Emig, 1981b; *b*, Emig, 1983a; *c*, Hammond, 1983; *d*, Paine, 1963; Thayer & Steele-Petrovic, 1975; *e*, Worcester, 1969). Mean burrowing speed is given in parentheses (new).

	<i>L. anatina</i> (b)	<i>L. reevei</i> (a, e)	<i>G. pyramidata</i> (d)
Burrowing speed in normal conditions (cm/h)			
experimental	0.5–1.7 (0.9)	0.2–2.5 (0.75)	0.67–2.7
<i>in situ</i>	<i>0.08–0.21</i>	<i>0.21–0.75</i>	<i>< 0.67–2.7</i>
Mean upward speed (cm/h) during experimental sedimentation			
Thickness of sediment	b c	e	d
10 cm	(0.11) (0.45)	-	(1.3)
15 cm	-	(0.14), (1.07)	-
20 cm	(0.13) (0.58)	-	(0.33)
30 cm	(0.18) -	(0.38)	(0.40)

retracts 1 to 3 cm from the surface into the lower section of the upper part of the burrow. During retraction the upper part (0.5 to 1 cm) of the burrow collapses and is obturated by sand grains, although in compact sand the burrow remains open (EMIG, 1981b, 1982).

At the end of a disturbance, the lingulide is elevated by scissorlike and small opening movements of the shell combined with the action of the setae and copious mucous secretion, all of which restore the upper part of the burrow. During retraction and reextension, the coelomic pedicle canal functions as a hydrostatic skeleton combined with the contractions of the pedicle muscle and coelomic pressures in the body.

In intertidal environments, the lingulide retracts into the burrow during low tide. It follows the water level down and then moves upward again with the advancing tide (CHUANG, 1956, 1961; EMIG & others, 1978).

EPIFAUNAL PATTERN: DISCINIDAE AND CRANIIDAE

The other extant inarticulated brachiopods are epifaunal, attached either by a fixation organ (discinids) or by cementation to some hard substrate (craniids). The ventral valve is always oriented toward the substratum, a feature that the discinids and craniids share with the articulated thecideidines, which is related to the orientation of the

larva during settlement. All discinids are attached by a highly muscular pedicle to hard substrates except for *Pelagodiscus*, which is closely fixed to the hard substrate by means of its two main vertical body muscles. The pedicle is very short, and the shell is held near the substratum. Among living inarticulated brachiopods only the pedicle of the discinids has a dual function. It acts as an anchor, and it supports the weight of the shell and holds it in relative position to the substrate (Fig. 411.2).

The craniids, which are cemented by the entire surface of the ventral valve to a hard substrate, lack a pedicle; the larvae settle with the posterior end expanded along the substrate and secreting the ventral valve, which is cemented to the substrate. This ventral valve is variably calcified in *Neocrania* species and has a calcified, alveolate structure in *Neoancistrocrania norfolki*.

As in lingulides, the strong adductor muscles of discinids and craniids close the shell, which is opened mainly or exclusively by hydrostatic mechanisms with longitudinal and outer body muscles working against the pressure of the coelomic fluid. The setae of the mantle edges of the discinids are as highly specialized as those of lingulides. They have tactile sensitivity, resulting in a protective closure of the shell, which is accompanied by the contraction of the pedicle drawing the shell near the substratum. The craniids have no setae.

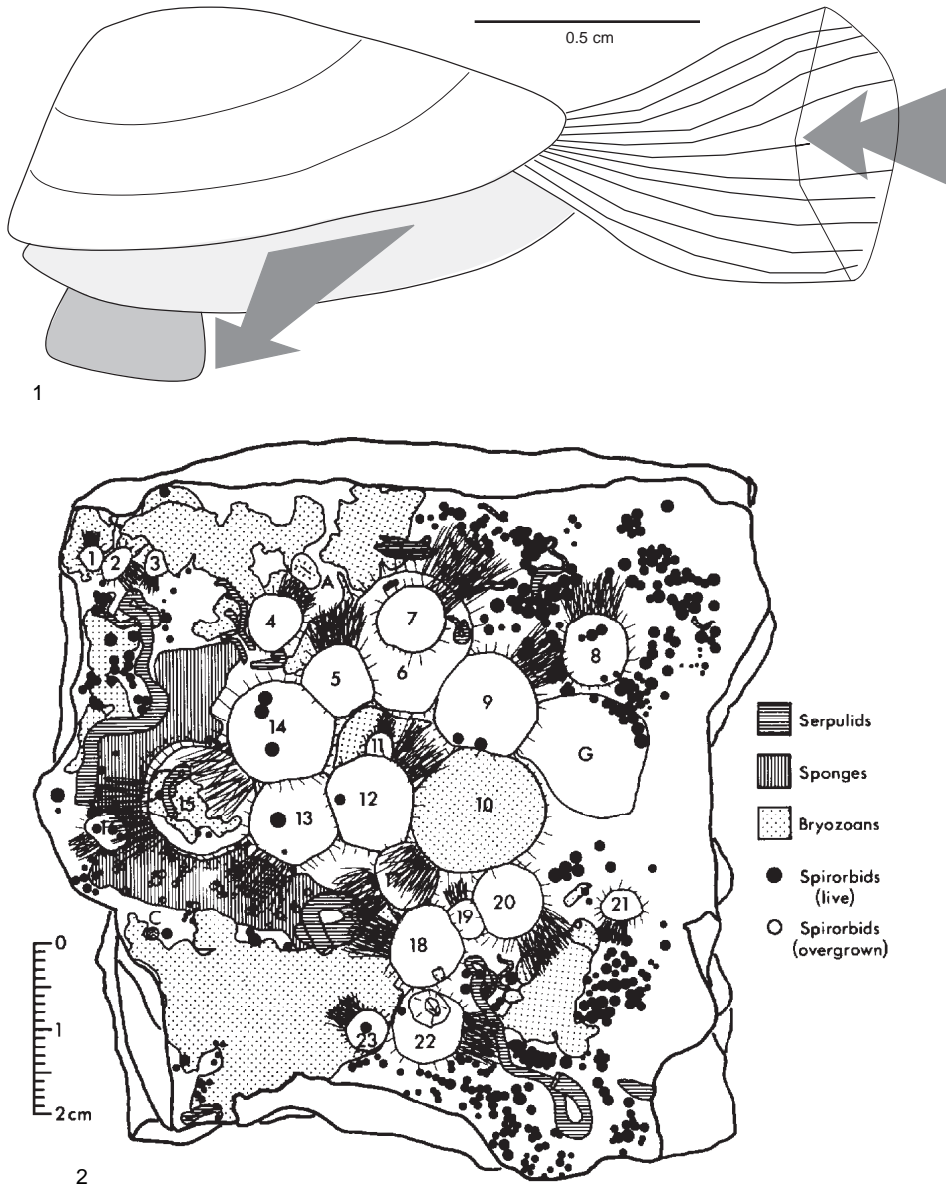


FIG. 411. 1, Live *Discradisca strigata* in pumping position, the anterior setae interlocked to form a functional siphon; arrows indicate in- and outcurrent directions (adapted from LaBarbera, 1985); 2, faunal distribution on a rocky substrate. All *D. strigata* are numbered; number 6 bears a *D. strigata* (number 7) and number 22 bears a barnacle; A, anemone; C, solitary coral; G, gastropod (LaBarbera, 1985).

The shells of discinids and craniids gape quite widely at the anterior edge and more narrowly at the posterior margin. A copious, median, inhalant flow enters the shell ante-

riorly and exits through two, posterolateral, exhalant gapes (Table 35; PAINE, 1962b; LABARBERA, 1985; EMIG, 1992). Another disposition for craniids is that two inhalant cur-

rents flow in at the anterolateral margins, while one main exhalant current flows out at the anteromedian edge; additional exhalant currents occur at the posterolateral margins (CHUANG, 1974).

In discinids the densely packed setae of the anterior mantle margin function as an incurrent siphon (Fig. 411.1). These anterior setae can be nearly three times as long as the diameter of the shell, while the length of the setae diminishes rapidly toward the posterior end (MORSE, 1902). Discinids orient the lophophore relative to the current (LABARBERA, 1985); but *Pelagodiscus*, because of the nature of its attachment, probably undergoes a small degree of reorientation against the current. In the cemented craniids the orientation may depend on the larval settlement under the influence of the prevailing bottom current, with adjustments at that stage so that the anterior region faces the local flow direction.

Discradisca strigata has a characteristic behavior pattern (LABARBERA, 1985). At irregular intervals or when disturbed, the valves nearly close, and the dorsal valve rotates clockwise and counterclockwise through an arc of 60 to 120°. This movement rubs the lateral setae of the dorsal valve over and past the ventral setae. The setal siphon is disturbed by this movement but remains potent. When the dorsal valve returns to its normal alignment with the ventral valve, their margins clamp together tightly and both valves rotate as a unit through an arc of 60 to 150°. On returning to a resting position, the margins of the valves remain clamped tightly to the substrate, but within several minutes at most the shell returns to a position slightly elevated above the substrate and the valves slowly reopen. The subcentral foramen of discinids affords greater protection for the pedicle than the posterior opening of articulated brachiopods and ensures that the entire shell margin, including regions adjacent to the pedicle, sweeps through a sizeable arc when the animal rotates, thus inhibiting growth of epifauna at a greater distance from the shell.

LIFE SPAN

The longevity of lingulides based on the length of the shell is a matter of conjecture. The life spans of *Lingula anatina* and *L. reevii* have been recently estimated theoretically from five to eight years, while *Glottidia pyramidata* is said to live from 14 months to less than two years (Fig. 412; MORSE, 1902; PAINE, 1963; CULTER, 1979). Shell growth in *Lingula anatina* and *L. reevii* decreases linearly with increasing size (WORCESTER, 1969; MAHAJAN & JOSHI, 1983). *L. anatina* attains a length of 25.6, 36.8, and 47.6 mm at the age of one, two, and three years respectively (Fig. 412); consequently the theoretical life span appears to be six to seven years. Two previous shell growth curves have been established for *Lingula reevii* in Hawaii (WORCESTER, 1969) and for *Lingula anatina* in Australia (Fig. 412; KENCHINGTON & HAMMOND, 1978). Growth in a population in a restricted area, however, is directly related to such local environmental factors as water characteristics, disturbances, nature of the substrate, and nutrients. These time-dependent variations can affect the metabolism of the animal and consequently retard or favor growth, although the shell grows continuously throughout its life. Consequently, individuals of equal shell length may differ in age, sexual maturity, and longevity (CHUANG, 1961; PAINE, 1963; WORCESTER, 1969; C. EMIG, personal unpublished data, 1983).

There are few data on the life spans of other inarticulated brachiopods. Populations of *Discradisca strigata* (LABARBERA, 1985) take more than 10 years to become stabilized. The three to six growth rings in the shell of *Pelagodiscus atlanticus* may be interpreted as evidence of a life span of three to six years. However, shells from the continental slope have a greater length and a narrower relative width and a smoother, less crenulated periostracum than those from the abyssal plain (ZEZINA, 1981). These differences seem to be the results of such environmental factors as temperature variations (2.65 to 3.07°C on the slope, 2.2 to 2.35°C in the

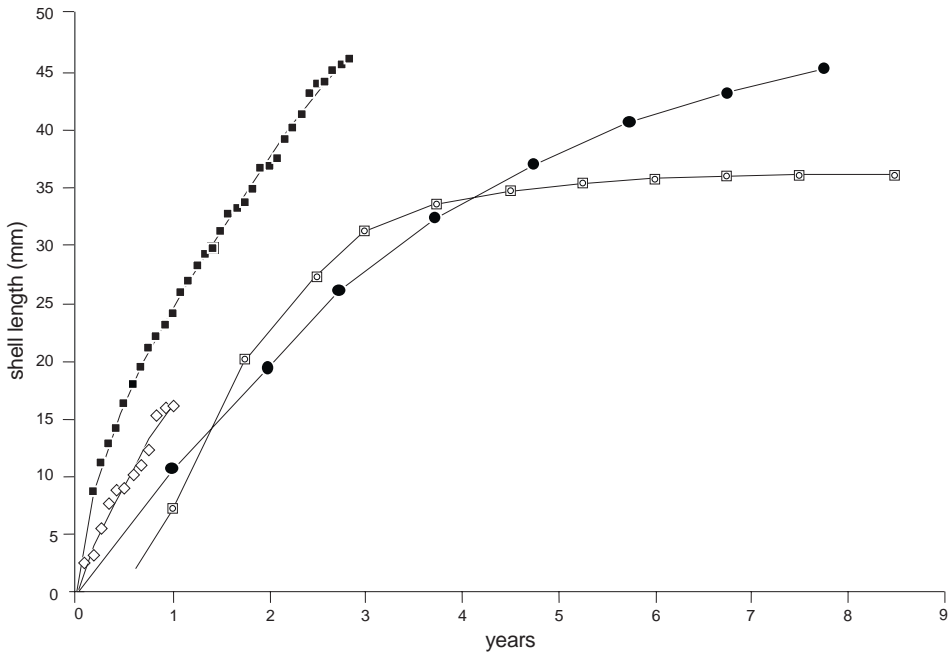


FIG. 412. Growth curves of various lingulide species; ■, *Lingula anatina* (data from Mahajan & Joshi, 1983); ●, *Lingula anatina* (data from Kenchington & Hammond, 1978); □, *Lingula reevii* (data from Worcester, 1969); ◇, *Glottidia pyramidata* (data from Culter, 1979) (new).

plain) and food supply. Presumably these factors control the growth rate more effectively on the slope than on the abyssal plain (ZEZINA, 1981). *Neocrania anomala* lived for 14 months in aquaria at normal laboratory light and without changing the water (JUBIN, 1886).

ECOLOGY

ABIOTIC FACTORS

Substrates

Soft substrates: Lingulidae.—Lingulides live in compact and stable sediments under the influence of moderate, near-bottom currents (PAINE, 1970; EMIG, 1984a). The two preferred substrates are either well-sorted, fine- to very fine-grained sand and clayey sand (in which the 90 to 250 μm fraction comprises more than 50 to 60 percent) and coarse sand grains in a fine-grained or very fine-grained sandy matrix. The sediment can be further stabilized by marine phanerogams

or mangrove tree roots. The grain-size fraction that is transported by saltation (about 90 to 220 μm) and generally associated with the traction-load fraction (> 600 μm) determines lingulide distribution. Where the traction fraction (about 220 to 600 μm) or the suspension fractions (< 90 μm) increase in the sediment relative to the saltation fraction, lingulide density decreases rapidly. The distribution of lingulides in deeper waters sometimes depends on the presence of Quaternary littoral sands, as in New Caledonia. From the few available data, the organic content of substrates containing *Lingula* is rather low (one to four percent) (EMIG & LEOEFF, 1978; BARON, CLAVIER, & THOMASSIN, 1993). Nevertheless, other ecological features affect the distribution and may be even more important.

Hard substrates: Discinidae and Craniidae.—Discinids attached to various rocky surfaces and to mollusc fragments occur singly or in clusters of many individuals, for ex-

ample, *Discinisca lamellosa*, *D. laevis*, and *Discradisca strigata*. The last species forms clusters of more than 12 individuals separated by less than 2 mm, while solitary individuals are uncommon (LABARBERA, 1985).

Pelagodiscus atlanticus is found attached to rocks ranging in size from pebbles to boulders (FOSTER, 1974) and is sometimes found on bivalve shells (*Vesicomya*, *Bathyarca*), brachiopod shells (COOPER, 1975), scaphopod shells, whale bones, and manganese nodules (ZEZINA, 1981). *P. atlanticus* occurs in deep-sea areas where fine-grained substrates accumulate slowly; both factors appear to limit the distribution of this species (ZEZINA, 1961).

Neocrania species show a wide depth tolerance and a preference for flat, hard surfaces on which they generally grow in clusters. In shallow water *Neocrania* occurs attached to the undersides or sheltered sides of rocky surfaces, including areas of bare rock, substrates coated with coralline algae, and submarine caves. In deeper water, individuals occur on rocks, ranging from pebble to boulder size, shells, hard skeletons of other invertebrates, various hard fragments, and, more rarely, on other brachiopod shells (ROWELL, 1960; BERNARD, 1972; FOSTER, 1974; BRUNTON & CURRY, 1979; LOGAN, 1979; LEE, 1987). *Neocrania* larvae settle on hard substrates where the sedimentation rate is very low and often colonize substrates that are swept by strong currents reaching 3 to 5 km/h (ROWELL, 1960; FOSTER, 1974; LEE, 1987), but they do not occur in more strongly current-swept environments more frequently than other brachiopods. The external shape and height of the craniid shell vary greatly in response to the contours of the substrate to which they are attached (FOSTER, 1974; LOGAN, 1979; LEE, 1987).

Craniscus has been recorded from Japan on various kinds of substrates from sandy mud to rocky bottoms.

Salinity

At present, all inarticulated brachiopods live in seawater of normal salinity; and, be-

cause all are typically quite intolerant of lower salinity, none is adapted to brackish-water or freshwater conditions. Accordingly lingulides actually live in biotopes in normal-marine salinities but are capable of osmotic response to stresses of strong salinity variations, particularly at low tide in the intertidal zone when freshwater input occurs (HAMMEN & LUM, 1977). The salinity range of the populations of a species depends on the geography of its habitat. Yet populations can survive a greater range of salinity than that occurring in its normal environmental conditions. The presence in a deltaic environment does not, therefore, imply that the lingulides constantly live under reduced or highly fluctuating salinities (EMIG, 1981a, 1986). Mean salinities during annual variations as low as 20‰ are exceptionally reported in lingulide environments. Actually lingulides are not tolerant of extremely low salinity except for brief periods, generally less than 24 hours. The lowest limit is about 16 to 18‰, which is not exceptional in comparison to bivalve molluscs (HAMMEN & LUM, 1977).

Temperature

Previously regarded as the limiting factor of the latitudinal extension of the lingulides, the range of temperature tolerance is highly variable among populations; and a population of a given area is generally unable to survive temperature variations, especially low temperatures, larger than those occurring in natural conditions. The salinity or temperature range under which an indigenous population normally lives can be lethal for another population adapted to a different range of conditions. *Lingula anatina* is a good example as is illustrated by comparing the reaction of three populations that are widely dispersed (Table 37; EMIG, 1986, 1988). Neither of the populations from northern Japan and New Caledonia could survive at salinities higher than 40 to 50‰. In northern Japan (EMIG, 1983a) and China (LEROY, 1936) the temperatures remain below 5°C for three months and below 11°C for more

TABLE 37. Annual variations of temperature, salinity, and the bathymetric range of *Lingula anatina* in three locations (Emig, 1988).

	Temperature (°C)	Salinity (g/l)	Depth (m)
Persian Gulf	15–40	55–60	6–16
New Caledonia*	18–30	15–25	intertidal (to 67)
Northern Japan	1–22	28–30	5–18

*lethal conditions at <15 °C and salinity of >40 g/l.

than six months, while populations from New Caledonia that experience experimental temperatures below 15 to 17°C undergo a lethal, irreversible retraction of the mantle.

The onset of breeding and the length of the spawning season of lingulides depend mainly on water temperature and latitudinal and seasonal effects. They vary from a 1.5-month period in midsummer in temperate waters (northern Japan, Virginia) and a five- to nine-month period between late spring and late autumn in warm temperate waters to year-round breeding in tropical waters (southern Florida, Singapore, Burma, and India) if temperatures do not drop below 26 to 27°C.

There are no data on temperature requirements of the discinids except that *Pelagodiscus* is more abundant in the deep sea at temperatures below 3.5°C.

Neocrania species tolerate a wide annual range of temperature related to their geographic and bathymetric distribution, from -2° to 1.5°C for *N. lecointei* (FOSTER, 1974), 14 to 21°C for *N. huttoni* (LEE, 1987), and about 26 to 28°C for species living in equatorial waters. *N. anomala*, which is distributed between 30° to 60°N in the Atlantic Ocean and Mediterranean Sea, has a wide temperature tolerance. The almost complete absence of calcite in the pedicle valve of several species of *Neocrania* does not represent an adaptation to very cold water (FOSTER, 1974). The temperature range of the biotopes of *Craniscus* is from 2 to 18°C.

Oxygen

Lingulides are able to survive temporarily in poorly oxygenated waters because of the

presence of hemerythrin within the coelomocytes (YATSU, 1902b; HAMMEN, HANLON, & LUM, 1962; WORCESTER, 1969). Hemerythrin, however, seems to be used as a store under anoxic conditions or during cessation of respiration, such as may occur intertidally when the burrow is exposed and is part of the oxygen-transporting function in lingulides. Data on the rates of oxygen consumption are available only for lingulides but are difficult to compare because they are based on either total-animal wet weight (HAMMEN, HANLON, & LUM, 1962) or on dry mass of tissue (SHUMWAY, 1982). *Lingula reevii* and *Glottidia pyramidata* have higher rates of oxygen consumption than the articulated *Terebratulina septentrionalis* by a factor of two to nine, and the activity of metabolically important enzymes, such as succinate dehydrogenase, is up to 20 times higher (HAMMEN & LUM, 1977; HAMMOND, 1983). On the other hand, the oxygen consumption rate of *Lingula anatina* is about 2.5 times lower than in three articulated species (SHUMWAY, 1982).

The redox layer, which often occurs some 2 to 5 cm below the sediment-water interface, does not signify a low oxygen concentration in the surrounding water mass, even in the burrow. Such anaerobic conditions as red tides can be responsible for a mass mortality. Although *Glottidia pyramidata* was one of the five species of 22 species surviving such events that temporarily lowered the mean density of the population from 42 to 13 individuals per square meter, two years later this density had risen to 1,332 individuals per square meter (SIMON & DAUER, 1977). Individuals of *Glottidia* are probably able to resist short-term anoxic events because they bear mantle papillae over the secondary mantle canals in the pallial cavity. The papillae allow an increase of the respiratory and nutritional exchanges. On the other hand, the volume of the lophophoral cavity in *Glottidia* is less than that of *Lingula*. In the same way *Lingula anatina* is more resistant to stress from loss of oxygen than bivalves collected from the same locality (ROBERTSON, 1989).

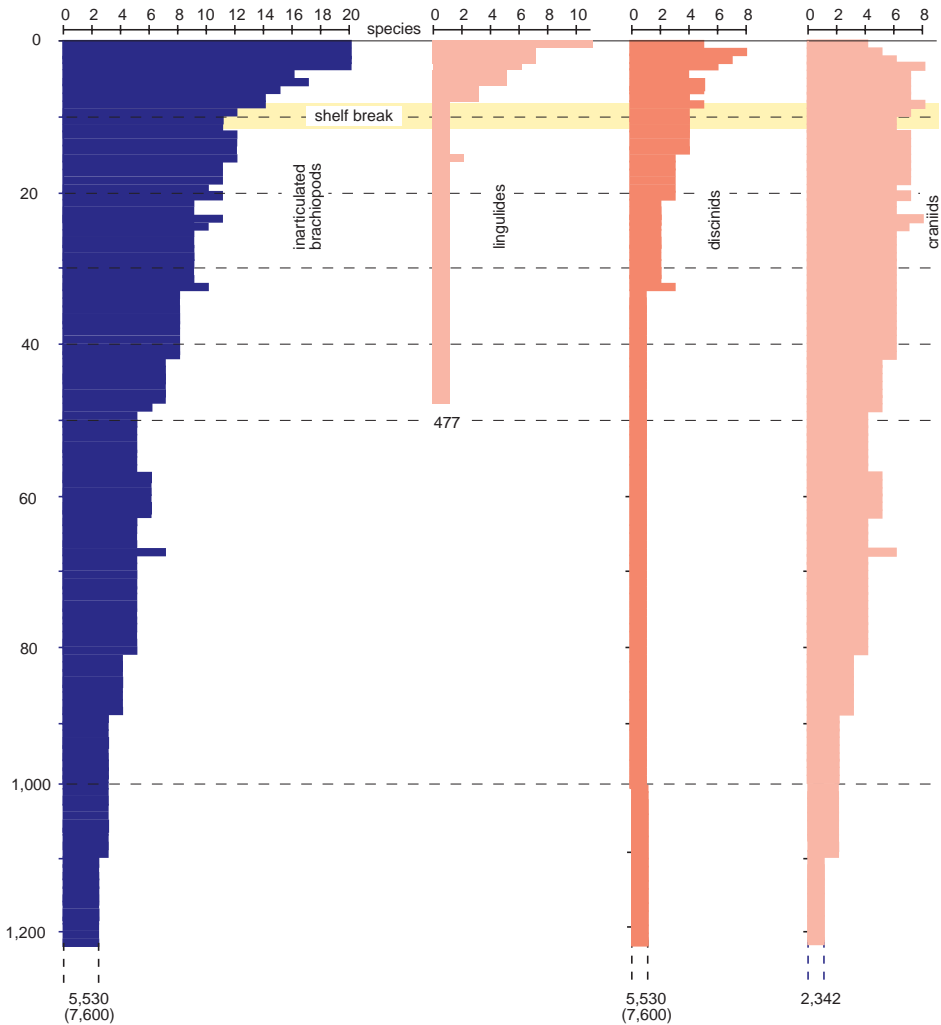


FIG. 413. Bathymetric distribution of the living inarticulated species; numbers at bottom indicate deepest recorded living specimens; those in parentheses indicated deepest recorded empty shells (new).

Depth and density

Many living inarticulated species extend through a remarkable depth range from littoral waters into the bathyal zone (ranging from the shelf break, generally about 100 m, to 3,000 m) down to about 500 m on the slope (Fig. 413). Only *Pelagodiscus atlanticus* occurs at abyssal depths, i.e., in the zone ranging from 3,000 to 6,000 m. Inarticulated brachiopods seem not to have migrated into deeper water in the course of time and cannot be used as indicators of

depth. More than 40 percent of inarticulated brachiopods, mainly lingulide and discinid species, occur between 0 and 60 m depth; and more than 40 percent of the craniids occur between 20 to 420 m.

The optimum environment for living *Lingula* and *Glottidia* species is not intertidal, although 11 of the 12 species of lingulides have been recorded in the intertidal zone (PAINE, 1970; EMIG, 1984a) and in the infralittoral zone from 1 to 2 m to about 20 m. The maximum recorded density of *Lingula reevii* is 500 individuals per square

meter (WORCESTER, 1969); that of *L. anatina* is 864 individuals per square meter (KENCHINGTON & HAMMOND, 1978). *Glottidia pyramidata* reaches concentrations of more than 8,000 individuals per square meter in Florida (CULTER, 1979), and *G. albida* shows a density peak of more than 500 individuals per square meter in depths of 22 to 47 m off the coast of California (JONES & BARNARD, 1963).

Pelagodiscus atlanticus, one of the deepest-water brachiopods, has been recorded throughout the bathyal and abyssal zones with one-third of the occurrences being at depths of more than 4,000 m (ZEZINA, 1961) and only a few of the records of its occurrence being from less than 1,000 m (ZEZINA, 1975). Its density may reach up to 480 individuals per square meter at the foot of seamounts and up to 76 individuals per square meter at 1,500 to 2,000 m in Antarctic waters (ZEZINA, 1961). On the marginal ridge of the Kurile-Kamchatka trench, however, a eutrophic area with a rich food supply and rather active currents, the density of 12 individuals per square meter is comparable to that in the tropical oligotrophic parts of the ocean (ZEZINA, 1981). The other species of discinids are mainly restricted to the continental shelves. Four of the 12 species of discinids have been recorded in the intertidal zone, although all of them are more abundant below the low-tide level or subtidally (Fig. 413).

The craniids extend from shallow waters to the bathyal zone and appear as a deeper-water group among the inarticulated brachiopods. Densities of *N. anomala* up to 500 individuals per square meter have been recorded on small, flat, hard surfaces at various depths between 10 and 200 m. *N. lecointei* has been found alive only on the seaward edge of the continental shelf in the Ross Sea, which belongs presently to the bathyal zone, between approximately 450 and 650 m, where it is the dominant brachiopod with up to 46 individuals per square meter (FOSTER, 1974).

Other Factors

As suspension feeders, brachiopods require good circulation of the water. Seawater constituents also play a role in the ecological requirements. Some are used for formation of the shell and their rate of assimilation may have a direct influence on growth of the shell. Calcium ions, which are taken up from the seawater primarily by the lophophore, move through the coelomic system into the mantle and are eventually deposited in the inner layer of the shell. Yet the major source of inorganic phosphate for shell formation in *Glottidia pyramidata* is likely to be food and not seawater (PAN & WATABE, 1988a).

On the Florida coast, *Glottidia pyramidata*, together with the lancelet *Branchiostoma caribbaeum*, are sensitive to deterioration of water quality and, thus, are used as indicator organisms of unspoiled areas and uncontaminated waters in determining suitability for fishing.

Taphonomy

Recent ecological statements on taphonomic conditions of living lingulides (EMIG, 1986, 1990) have been corroborated by re-interpretations of fossil beds (Fig. 414). The natural death of the lingulides leads to the extrusion of the animal from its burrow (WORCESTER, 1969; EMIG, 1986). The valves become separated, and the organic matrix degrades rapidly due to hydrolysis, microorganisms, and mechanical abrasion. The thin, fragile, chitinophosphatic valves are reduced to unrecognizable fragments, the deterioration occurring from the margins to the central portion of the valve; and in general after two or three weeks the valves have completely disappeared from the sediment (EMIG, 1983a, 1990). This explains why only a catastrophic event, occurring over some days, is the most significant source of mortality with respect to preservation of the shell and ultimate fossilization because there is little potential for fossilization in normal environments (EMIG, 1986). Consequently,

fossil lingulides are not indicators of their biotopes but of drastic environmental changes that led to their burial.

Fossilization can occur either *in situ* in life position, for example, in conditions of rapid temperature decrease, salinity increase, desiccation, emersion of the substratum or drop of sea level, or very fine sedimentation; or it can occur as flat-lying disarticulated valves, for example, after prolonged reduction of salinity, coarse-grained sedimentation, and storms (EMIG, 1986). Data obtained for living species obviously apply to the interpretation of fossils (EMIG, 1986). Nevertheless survivorship under abnormal conditions can vary according to the geographical population and depends also on the synergy of the applicable environmental factors on a given population.

When salinity increases to 40 to 50‰, the death of populations occurs in burrows in a few days. Osmotic pressure empties the animal of its coelomic fluid, and the pedicle becomes detached from the shell. When the salinity decreases below 16 to 18‰, death occurs in one day to several weeks and quickens with lowering salinity, although the salinity of interstitial water remains high for several days. Individuals leave their burrows as their bodies swell under osmotic pressure, and pedicles become limp or detached. The putrefaction of the soft body causes separation of the valves, which are then spread over the sediment surface. Shells rarely float, but it has been reported (EMIG, 1981b). At a salinity of 18‰, the initial body weight increases by 3.3 percent in three hours; at 5‰, it increases by 3.8 percent in one hour. Weight then remains constant for about two hours followed by another weight increase that is lethal (HAMMEN & LUM, 1977). Reduced salinities in rapid transition are tolerated, for example, during tidal cycles in estuarine or deltaic environments where the salinity can drop to less than 10‰. Several observations have reported high mortality after heavy rains of two to three days' duration causing nearby rivers to flood (PAINE,

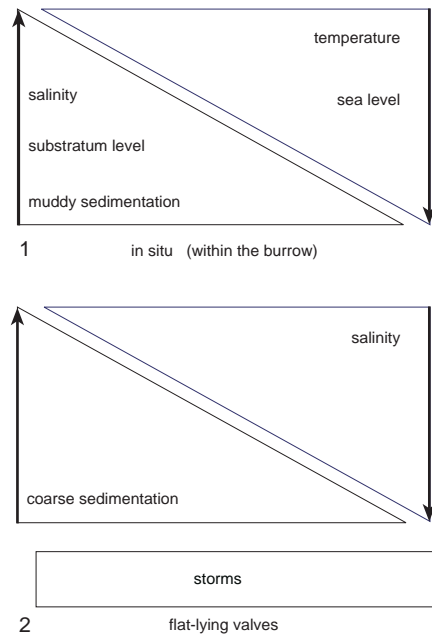


FIG. 414. Diagram summarizing the effects of abiotic factors that may induce lingulide fossilization (new).

1963; SOOTA & REDDY, 1976; EMIG, 1986, and personal observations, 1983). Nevertheless from experimental results the duration of survivorship to low salinity is variable among species. At a salinity of 15‰, *Lingula anatina* in Queensland (Australia) resists longer than *Lingula reevii* in Hawaii, while *Glottidia pyramidata* in Florida has a greater survivorship than populations of *Lingula*.

During an exceptional storm often associated with heavy rains, the sediment is churned up, and the lingulides are washed onto the shoreline and may form shell masses up to 75 cm high (RAMAMOORTHY, VENKATARAMANUJAM, & SRIKRISHNADHAS, 1973; HAMMOND, 1983; EMIG, 1986).

When the sea level drops through tectonism, regression, or high sedimentation, the animal retreats with the water level until it reaches the bottom of its burrow where death occurs in about three days.

Experiments on *Lingula anatina* in New Caledonia with decreasing temperatures

show that below 15 to 17°C (the lowest temperature in natural conditions is 18 to 19°C) individuals go down to and remain at the bottom of their burrows. At 6 to 10°C an irreversible retraction of the mantle occurs over several millimeters from the shell margins leading to death within one to three weeks because the lingulides are unable to form their pseudosiphons, and, consequently, the pallial water streams are highly perturbed (C. EMIG, personal unpublished data, 1983). Mantle regression has been observed in both inarticulated and articulated brachiopods, but a factor specifically responsible for this regression is identified for the first time herein.

When the temperature drops below 10°C in Florida, *Glottidia pyramidata* does not respond to any stimuli, although slow warming after three days at low temperature produced signs of activity at 12°C (PAINE, 1963).

Muddy sediment with more than 35 to 40 percent of very fine fraction (< 50 µm) deposited over original sandy bottoms leads to the death of lingulides within their burrows in several weeks. A lingulide can maintain only sporadically its normal position before collapsing into the sandy layer, and this generally leads to death by debilitation. This observation is of paleoecological importance. When lingulide valves occur at the bottom of a shale overlying a sandstone, the sandstone unit is the normal substrate of the lingulides that are sometimes fossilized within their burrows. The shale cannot be interpreted as the normal substrate for lingulides but as a deposit of muddy sedimentation that was responsible for the death of the lingulide population. Conversely, coarse sedimentation (> 0.5 mm) leads to the emerging of the lingulides at the sediment surface and finally lying on the surface.

The shallow-water species *Discinisca tenuis* occurs intertidally at a few localities. It is known in the Walvis Bay area (Namibia) where large deposits formed by huge numbers of shells are washed up onto the beach. Its occurrence along the Namibian coast is linked to the existence of the Benguela up-

welling system. Such deposits totally dominate the littoral sediment (HILLER, 1993). A correspondence is suggested with the Estonian Lower Ordovician obolid conglomerates, which are likely to have formed under similar conditions of upwelling.

BIOTIC FACTORS

Nutritional sources

Sources of nutrition are known for only a few lingulide species. The type and abundance of ingested particles as well as the importance of direct absorption of nutrients depend on such factors as season, depth, and geographic area. Analyses of gut contents of *Lingula reevii* from Hawaii (EMIG, 1981b) show the presence of two types of food: a vegetal fraction, mainly phytoplanktonic and consisting of diatoms, peridinians, and filamentous algae, and an animal fraction, mainly from the superficial meiobenthos and macrobenthos, i.e., foraminifers, rotifers, polychaetes, oligochaetes, and copepods. Both fractions are mixed with a constant amount of sedimentary particles of 2 to 3 µm and various organic detritus (e.g., spicules and spines). *Glottidia pyramidata* ingests particles smaller than 125 µm in diameter, including sand grains and various vegetal and animal matter, *Coscinidiscus*, gastropod veligers, nauplii, and even *Glottidia* eggs (PAINE, 1963). Food particles from the sediment-water interface may be readily resuspended by tidal or bottom currents or waves, by arm shaking of ophiurians, or by holothurians.

Direct absorption of dissolved nutrients is known to occur in the lophophorates. The lophophore in lingulides (STORCH & WELSCH, 1976) appears to be able to absorb directly dissolved organic matter from seawater. There is also evidence that digestion occurs in the lophophore, attested to by the presence within the tentacles of alkaline phosphatase and three esterases (STORCH & WELSCH, 1976). Like the phoronids, lingulides are able to live in aquaria for some weeks without having the water changed. *Glottidia pyramidata* can be maintained at

least three months under starvation conditions without apparent loss of vitality (PAINE, 1963).

The body weight of *Lingula anatina* varies from 0.13 g for a shell length of 1.35 cm to 5.19 g for a shell length of 4.25 cm. (The mean value is 2.24 g for a length of 3.19 cm; n=346; KAWAGUTI, 1943.) The body weight, like the shell height, increases more rapidly than the shell length. The weight:length ratio of *Glottidia pyramidata* changes at a length of approximately 8 mm corresponding to the development of gonads (PAINE, 1963). In *Lingula* this development occurs at a shell length of 1.5 to 2 cm.

Predation

Lingulides are eaten by such crustaceans as hermit, stone, and portunid crabs, crangonids, stomatopods, shrimps, and amphipods (PAINE, 1963; WORCESTER, 1969; CULTER, 1979; EMIG & VARGAS, 1990). The asteroid *Luidia clathrata* is an important predator of *Glottidia pyramidata*. Forty-three percent of the *Luidia* collected contained *Glottidia* shells with little selectivity for size for shells less than 1 cm long, suggesting that larger individuals may withdraw too deeply into the sediment to be preyed upon. Other echinoderms are also reported as predators, such as the ophiuroid *Amphipholis germinata* and the echinoid *Encope stokessi* (EMIG & VARGAS, 1990). Gastropods (mainly naticids and muricids) are only occasional predators of lingulides, but bored valves can represent up to 14 percent of the valves recovered from the sediment (PAINE, 1963). Dead shells of craniids are sometimes drilled by gastropods (LEE, 1987).

Lingula parva has been recorded during the dry period (March to September 1953) along the Sierra Leone and Nigerian coasts in the stomachs of several demersal fishes (LONGHURST, 1958; ONYIA, 1973). Several tens of *Glottidia pyramidata* shells have been recorded in stomachs of sturgeons and various rays along the Florida coast. The mud flats inhabited by *Glottidia audebarti* are visited seasonally by migratory birds, and at least 13 species were observed foraging at low

tide (VARGAS, 1988); stomach contents of the willet *Catoptrophorus semipalmatus* but more frequently the short-billed dowitcher *Limnodromus griseus* revealed that *G. audebarti* is an important food item. *Catoptrophorus semipalmatus* and the fish *Symphurus plagiusa* are known predators of *Glottidia pyramidata*, which is their main source of food (PAINE, 1963). People also eat *Lingula anatina* and *L. rostrum* on almost all the western Pacific islands from Japan to New Caledonia.

Parasites

Unencysted metacercariae of trematodes of the subfamily Gymnophallinae (usually one to three in an individual) have been seasonally recorded around the nephrostomes and in the gonads of *Glottidia pyramidata*, mainly at the end of summer and in autumn. The infestations can reach 68 percent of the population. These parasites can reduce or destroy the gonads and have a secondary influence on the digestive glands and mantle canals (PAINE, 1962a, 1963). Adult parasites are likely to occur in avian predators of *G. pyramidata*. The occurrence of two species of poecilostomatoid copepods, *Parostrincola lingulae* and *Panjakus platygyrae*, associated with *Lingula anatina* has been reported from Hong Kong (HULMES & BOXSHALL, 1988). Zooxanthellae are abundant within the digestive gland of *Lingula* (KIRTISINGHE, 1949), and monocystid protozoa have been reported in *Neocrania*.

FAUNAL RELATIONSHIPS

Communities

Soft-substrate communities.—By their general characteristics, lingulides are nearly stable in their evolutionary state. They present all the features of a dominant group within a community (EMIG, 1989a): low growth rate, uniformity of shape, larger size than the other members of the community, long life span, low recruitment potential, generally just higher than the population replacement (K-demography), and long geological range. Such characteristics allow high

biomass to develop related to the available energy and result in an excellent ability to integrate and conserve energy. Such a dominant group generally shows plesiomorphic characters compared to other taxa.

Few lingulide communities have been studied. Data on the macrobenthic fauna are given in Tables 38 and 39. *Lingula anatina* has been investigated in the Mutsu Bay (northern Japan) in fine sands and muddy sands from 4 to 18 m depth (TSUCHIYA & EMIG, 1983); on the west coast of Korea in a tidal flat of silty sands from -2.5 to 2.3 m (AN & KOH, 1992) where the number of species collected monthly varies from 28 to 41; in Taiwan in a tidal flat of fine, sandy mud (DÖRJES, 1978); in Phuket Island (Thailand) in front of a mangrove in an intertidal, large, bay-shaped, fine-sand flat dominated by molluscs, mainly the gastropod *Cerithidea cingulata*, where the other most abundant animals are the fiddler crab *Uca lactea* and the sipunculid *Phascolosoma arcuatum* (FRITH, TANTANASIRIWONG, & BHATIA, 1976). In New Caledonia in association with the seaweed *Halodule* on coarse sands the macrofauna is dominated respectively by *Lingula anatina*, molluscs (mainly the bivalve *Gafrarium tumidum* and a gastropod *Cerithium* sp.), and polychaetes (mainly *Caulleriella* sp.) (BARON, CLAVIER, & THOMASSIN, 1993). *Glottidia audebarti* recorded in Costa Rica (VARGAS, 1988; EMIG & VARGAS, 1990) in mud flats exposed only at a tide level below 0.1 m has an associated macrofauna composed mainly of deposit feeders; the meiofauna comprises 88 percent nematodes, 6 percent foraminifers, and 3 percent ostracodes. *Glottidia pyramidata* occurs in Sapelo Island (Georgia, USA) in the *Moira-atrops* community located between 10 and 13 m depth in coarse, relict sand dominated by polychaetes followed in importance by crustaceans, but the fauna shows a generally low density (DÖRJES, 1977). In Winyah Bay (South Carolina, USA) it occurs in medium- to fine-grained sands from 6 to 11 m

(DOLAH & others, 1984). Near Charleston Harbor (Florida, USA) it is present in coarse to fine sands from 8 to 17 m (DOLAH, CALDER, & KNOTT, 1983) with the highest density being at 17 m. In Tampa Bay (Florida, USA) the reestablishment of a benthic community following natural defaunation by red tide has been studied in an intertidal sand flat (SIMON & DAUER, 1977).

The associated fauna of other locations is briefly listed here. On the western Korean coast *Lingula anatina* occurs in sand to sandy mud flats with many other such endobiotic species as polychaetes, crabs, and molluscs, which are dominant quantitatively (FREY & others, 1987). In a New Hebridian mangrove community *L. anatina* occurs seaward of the *Rhizophora* zone dominated by gastropods and crabs (MARSHALL & MEDWAY, 1976). On the western African coast *L. parva* occurs in the *Venus* community, particularly at the *Venus-Amphioplus* transition (LONGHURST, 1958). In the Ebrié Lagoon (Ivory Coast) *L. parva* occurs in a shallow, sandy substrate in the *Corbula trigona* community in which the main species are 12 polychaetes, 9 gastropods, 14 bivalves (dominant), and 10 crustaceans (ZABI, 1984). In Ambon, *L. rostrum* occurs midlittorally seaward of a mangrove stand and on a sandy beach located between the ocypodid zone and the clypeasterid zone (EMIG & CALS, 1979). In a benthic survey on the eastern coast of India (BHAVANARAYANA, 1975) a *Lingula-Solen* zone was reported, almost exclusively populated by both taxa in considerable numbers. Off the Californian coast, *Glottidia albida* occurs at high density in the *Amphioplus* community inhabiting a compact, fine, sandy substrate although it has also been recorded in several other communities, including the *Listrolobus*, *Amphioda*, *Nothria*, and *Tellina* communities (JONES & BARNARD, 1963). In Mission Bay (San Diego, California), *G. albida* occurs with a macrofauna dominated by 65 percent polychaetes, 15 percent

TABLE 38. Richness and percentage of the species of the main taxonomic groups present in various communities in which lingulides occur. The results presented have been calculated from the data given by the cited authors (new).

Location	Polychaetes		Mollusks		Crustaceans		Echinoderms		Others		Lingulide species		Total n
	n	%	n	%	n	%	n	%	n	%	n		
Japan ¹⁰	15-29	39-59	5-12	12-27	3-9	8-21	1-6	3-15	0-4	0-7		<i>L. anatina</i>	30-46
Korea ¹	8-17	39-47	3-14	18-34	4-7	16-29	0-3	0-8	0-1	0-3		<i>L. anatina</i>	17-43
Taiwan ⁵	8	31	7	27	6	23	1	4	3	12		<i>L. anatina</i>	26
Thailand ⁷	9	30	8	27	7	23	-	-	5	20		<i>L. anatina</i>	30
New Caledonia ²	38	45	25	29	12	14	3	4	7	8		<i>L. anatina</i>	85
Western Africa ⁸	38	19	54	28	57	29	27	14	19	10		<i>L. parva</i>	195
Costa Rica ^{6,11}	30-38	38-41	15-18	19	21-25	27	-	-	12-13	13-16		<i>G. audebari</i>	79-93
Georgia ⁴	15-31	38-56	3-18	11-38	5-9	11-19	1-2	4	3-5	6-7		<i>G. pyramidata</i>	27-55
S. Carolina ⁴	-	40-45	-	20-21	-	21-23	2	2	-	12-14		<i>G. pyramidata</i>	37-193
S. Carolina ³	31-88	43-60	9-31	12-29	12-42	22-32	1-7	2-5	-	-		<i>G. pyramidata</i>	54-155
Florida ⁹	32	39	22	27	19	23	-	-	10	12		<i>G. pyramidata</i>	83

¹AN & KOH, 1992; ²BARON, CLAVIER, & THOMASSIN, 1993; ³DOLAH, CALDER, & KNOTT, 1983; ⁴DORRIS, 1977; ⁵DORRIS, 1978; ⁶EMIG & VARGAS, 1990; ⁷FRITH, TANTANASIRWONG, & BHARTIA, 1976; ⁸LONGHURST, 1958; ⁹SIMON & DAUER, 1977; ¹⁰TSUCHIYA & EMIG, 1983; ¹¹VARGAS, 1988.

TABLE 39. Densities per square meter and percentage of the individuals of the main taxonomic groups present in various communities in which lingulides occur. The results presented have been calculated from the data given by the cited authors (new).

Location	Polychaetes		Mollusks		Crustaceans		Echinoderms		Others		Lingulides		Total n
	n	%	n	%	n	%	n	%	n	%	n		
Japan ⁹	195-910	45-77	35-150	3-12	5-230	4-27	5-185	1-26	0-80	0-10		55-150	455-1,195
Korea ¹	8-39	1-49	12-7,000	14-99	2-20	1-6	0-14	0-12	0-9	0-6		1-66	79-7,100
Taiwan ⁵	580	46	340	27	285	23	20	2	15	1		15	1,255
Thailand ⁷	14	9	103	62	27	16	-	-	21	13		1	166
New Caledonia ²	98	22	130	29	29	7	39	9	152	33		151	448
Costa Rica ^{6,10}	-	33-55	-	5-12	-	29-47	-	-	-	4-15		17	3,700-41,000
S. Carolina ⁴	-	15-32	-	24-45	-	5-19	-	1-3	-	22-35		100	438-6,240
S. Carolina ³	308-2,378	27-64	70-424	3-30	98-1,522	5-32	4-48	1-3	158-207	67-53		2-48	1,070-5,132
Florida ^{8,11}	231-868	7-37	4-50	1-4	64-7,877	3-89	-	-	80-261	2-13		50-1,178	646-8,850
Florida ^{8,12}	(336)	(5)	(2,478)	(38)	(2,181)	(34)	-	-	(1,501)	(23)		1,332	(6,496)

¹AN & KOH, 1992; ²BARON, CLAVIER, & THOMASSIN, 1993; ³DOLAH, CALDER, & KNOTT, 1983; ⁴DORRIS, 1977; ⁵DORRIS, 1978; ⁶EMIG & VARGAS, 1990; ⁷FRITH, TANTANASIRWONG, & BHARTIA, 1976; ⁸SIMON & DAUER, 1977; ⁹TSUCHIYA & EMIG, 1983; ¹⁰VARGAS, 1988; ¹¹total data from one area of Florida; ¹²mean data from a different area of Florida.

molluscs, and 11 percent crustaceans, with mean density from 621 to 1,874 individuals per square meter (DEXTER, 1983). On the coasts of Florida, *Glottidia pyramidata* is often associated with the lancelet *Branchiostoma caribbaeum*, polychaetes, cumaceans, and amphipods; and its biomass, which has a mean value of 35 percent, can reach up to 75 percent of the total biomass of the benthic invertebrates. *G. pyramidata* occurs also in the biocoenosis of well-sorted, fine sands with the phoronid *Phoronis psammophila* (PAINE, 1963; EMIG, 1983b).

The associated fauna within a given community seems to play a minor role in lingulide distribution (EMIG, 1984a). Nevertheless, when the density of *Lingula* increases there is a small decrease in the total number of species with an increase of the total number of individuals; when the density of *Glottidia* increases the total number of species and individuals tends to increase. Comparisons of the distribution of the major groups (Table 38–39) with the increase of density of lingulides show in western Korea that polychaetes (number of species and individuals) and crustaceans (number of species) tend to decrease, while echinoderms, mainly suspension feeders, tend to increase or to appear; in the Mutsu Bay, polychaetes, the dominant group, molluscs, and crustaceans tend to decrease; with the muddy fraction increasing with the depth there is a general decrease in the fauna. Near Charleston Harbor the number of individuals of molluscs and the number of individuals and species of polychaetes tend to increase, while on the southwestern coast of Florida opposite variations of the densities have been observed over a year between polychaetes, crustaceans, and *Glottidia*.

Polychaetes are generally the dominant group in numbers of individuals and species followed by molluscs or crustaceans (see Table 38–39). The presence of molluscs is not fundamentally related to the distribution of lingulides (BABIN & others, 1992). Another important feature is the large number of species and individuals of the associated fauna (Table 38–39), which should be taken

into account when analyzing taphonomic factors to explain the poor, associated fauna found in paleocommunities or when speculating about diversity of the fossils. In fossil assemblages lingulides are often the only fossils found, indicating either that other kinds of organisms were not preserved or that the biocoenosis was oligotypical (EMIG, 1989a). The occurrence of such a monospecific assemblage of fossils requires an extensive analysis of the environmental constraints and of the characters of the occurring species to identify any patterns of the original community. The oligotypical biocoenosis presents one or several of the following characteristics: low-energy input resulting from the effects of climatic factors, extreme harshness due to edaphic factors reducing the physiology of the individuals, or high daily or seasonal variations of the edaphic and climatic factors. Thus the biocoenosis is characterized by high dominance in faunal and environmental features and develops conservatism with highly reduced capacity for organisms to evolve.

Hard-substrate communities.—In the deep parts of the slope in the Antarctic regions (FOSTER, 1974), *Pelagodiscus atlanticus* is associated with a very meager fauna. In the lagoonal complex of Cananéia, Brazil (TOMMASI, 1970b), *Disciniscia* sp. has been recorded at 6 and 8 m depth on a rocky-sand bottom with the following macrofauna: polychaetes respectively 600 and 60 individuals per square meter (10 and 18 percent of the fauna), molluscs 1,170 and 30 (19 and 9 percent), decapods 380 and 150 (6 and 46 percent), amphipods 2,900 and 0 (47 percent), others 1,080 and 70 (18 and 21 percent), and *Disciniscia* 10 and 20 (0.2 and 6 percent). In the Bahia Concepción, Chile, *Disciniscia lamellosa* occurs in the intertidal zone with a meager fauna of one cnidarian, one nemertine, two molluscs, two polychaetes, and one to three crustaceans (URIBE & LARRAIN, 1992). In Baja, California, *Disciniscia strigata* lives under cobbles and small boulders, patchily distributed on an extensive sandy beach and extending down to the low-water mark (PAINE, 1962b) where it is

associated with sponges, gastropods, and bivalves. The fractional area covered by epifauna averaged 49 percent, and free space ranged from 32 to 74 percent on a rock area from 21 to 116 cm²: *D. strigata* covered 2 to 26 percent of the surface, bryozoans 5 to 38 percent, serpulids 2.5 to 29 percent, spirorbids 0.01 to 7.3 percent, and sponges 0.5 to 8.2 percent.

Neocrania anomala is recorded in shallow waters under rocky surfaces together with a sciaphilic fauna. It also occurs deeper in the sublittoral zone with a fauna dominated by sponges, cnidarians, spirorbid worms, and bryozoans, and on the continental slope below 100 m on smooth, fine-grained, hard substrate to large rocks, particularly within the community dominated by the brachiopod *Gryphus vitreus*. *N. anomala* is also recorded in Scottish lochs with hydroids, sponges, chitons, foraminifers, and molluscs (CURRY, 1982) and in the Strait of Messina between 80 and 200 m under conditions where there are bottom currents where the macrofauna is dominated by anthozoans (eight species), bryozoans (31 species), annelids (14 species), molluscs (20 species), crustaceans (5 species), and echinoderms (2 species) (DI GERONIMO & FREDJ, 1987). *Neocrania huttoni* forms part of a distinctive rocky substrate community with calcareous algae, sponges, serpulids, ascidians, bivalves, barnacles, and bryozoans including a variety of filter feeders (LEE, 1987). *N. lecointei* is associated with a varied fauna that includes corals, polychaetes, ophiuroids, bryozoans, and ascidians (FOSTER, 1974). *N. pourtalesi* occurs not uncommonly throughout some communities of cryptic habitats of coral reefs, where brachiopods and sponges are the dominant taxa (JACKSON, GOREAU, & HARTMAN, 1971). *Craniscus* occurs in Japan with an associated fauna that comprises mainly molluscs and two articulated brachiopod species, *Dallina* and *Terebratulina* (HATAI, 1940).

Population structure

Because the distribution of lingulides is controlled by environmental factors, annual

fluctuations in density are highly variable even within a restricted geographic area. Episodic failure of recruitment observed in lingulide populations can be related to such causes as protracted breeding season, bad environmental conditions for settlement, food supply, and interactions with the surrounding fauna including predation.

Some authors (PAINE, 1970; KENCHINGTON & HAMMOND, 1978) have raised the question of unidentified factors affecting the absence of lingulides in apparently suitable sediments. Actually the distribution of lingulides is restricted within the limits of the biocoenosis in which a lingulide species is living, even if preferred substrates occur beyond the limits of the community (EMIG, 1984a, and personal unpublished data, 1983).

Shell epibionts

Epibionts preferentially settle on the hard substrate provided by the brachiopod shell. According to the infaunal habit of lingulides, almost all epibionts are restricted to the anterior margins of the valves because only these margins are accessible and are not disturbed during withdrawal into the burrow. Cyanobacteria, however, frequently extend to the umbonal region along the margins.

In one locality the following macroorganisms were recorded from 5,000 *Lingula* shells (WORCESTER, 1969): 10 occurrences of algae, 14 anemone *Aptasia*, many bryozoans, 2 polychaetes, 6 barnacles, 1 amphipod and, on 16 percent of the shells, the limpet *Cruciblum spinosum*. From a large list of epibionts (represented by two algal divisions and six animal phyla) on the shells of *Lingula anatina* and *L. reevii* (HAMMOND, 1984), the most commonly recorded taxa are cyanobacteria (frequency up to 30 percent), polychaetes (frequency up to 45 percent), barnacles (frequency up to 20 percent), limpets (frequency up to 16 percent), bryozoans (frequency up to 11 percent), and traces of the attachment of the egg cases of gastropods or the byssal threads of mussels (frequency up to 29 percent). In only ten percent of the infested *Lingula* were both valves affected.

Algae, specifically *Enteromorpha* sp., established itself only on those valves that had regeneration scars (PAINE, 1963). The hydroid Campanulatiidae *Clytia* can occur on up to 20 percent of lingulide individuals with a shell length exceeding 1.4 mm.

An unidentified leptocean bivalve (perhaps *Euciroa*) is found byssally attached to the shell of *Lingula anatina* (SAVAZZI, 1991) in densities of up to nine individuals per shell. The posterior region of the bivalve shell is oriented upward, located at the anterior margin near the exhalant currents of the brachiopod. The bivalve progressively migrates upward as is shown by a trail of byssal filaments left along their paths to compensate for growth of the *Lingula* shell. The bivalve feeds on feces of *L. anatina*. Lingulides were found to carry gastropods near the anterior margin. Egg capsules of gastropods occurred seasonally on the anterior margins of the valves of lingulides; up to 45 *Nassarius* and up to 5 *Olivella* egg capsules were found on a single individual of *Glottidia pyramidata*.

Epibionts like the worm *Polydora* or the mollusc *Brachiodontes* may benefit from lingulide inhalant currents, but their presence can have detrimental effects by causing distortion of the shell of the host (PAINE, 1963; HAMMOND, 1984). The number of worms on a valve varies from one to six, with a typical number of three or four while the number of small *Brachiodontes* may be as many as five.

Among the craniids, *Neocrania* shells frequently bear encrusting organisms including bryozoans, serpulids, barnacles, calcareous algae, and sponges. Most valves carry more than one epibiont, and the percentage of the cover can reach 95 percent.

In some specimens of *Discradisca laevis*, great numbers of full-grown Pedicellinae adhered to the long, barbed setae (DAVIDSON, 1880). One-third of the *Discradisca* shells (17 percent of the total valve area) bore epizoans, primarily bryozoans and spirorbids, and occasional other *Discradisca*, serpulids, and small sponges.

Competitive interactions

Mechanisms of competitive interaction are likely to be characteristic of the discinids and may have been important in ensuring the success of the living genera since their earliest known occurrence in the Triassic (ROWELL, 1961). The only work that has addressed the competitive abilities of inarticulated brachiopods deals with *Discradisca strigata*, which invariably wins competitive interactions for space with other sessile epifauna (LABARBERA, 1985). One such competitive interaction is metamorphosis on the surface of bryozoan colonies facilitated by a reversal of the flow patterns and the possession of a functional anterior siphon that allows juveniles to draw water from above the bryozoan's lophophores, so that mature individuals eventually usurp the space occupied by the colony. Another interaction is maintenance of a pool of particle-depleted water around most of the shell of larger juveniles and adults, which probably inhibits encroachment by bryozoans and sponges. In addition, abrasion of underlying calcareous epifauna by the harder phosphatic shell occurs, which erodes these faunal elements to the level of the substrate. Numerous eroded epizoans occur under the ventral valves of *Discradisca* although no abrasion of the valves themselves was seen. The edge of these valves probably abrades neighboring organisms during rotation of the shell even of juveniles, and it is probably made more effective by the simultaneous sweep of lateral setae that mechanically damage the tissues of surrounding sponges and bryozoans.

Three of these mechanisms are not available to articulated brachiopods, and the fourth is apparently not exploited, which may explain differences in competitive abilities between inarticulated and articulated brachiopods. Numerous examples of apparent spatial competition between *D. strigata* and other epifauna, particularly sponges and bryozoans, have been recorded (LABARBERA, 1985); but this species was spatially dominant on only 3 of the 11 rocks investigated,

even though it dominates in competitive interactions; and no individual appeared to be in any danger of overgrowth. In discinids the foramen, which is more centrally located than in articulated brachiopods, affords greater protection for the pedicle and ensures

that the entire shell margin, including regions adjacent to the pedicle, sweeps through a sizeable arc when the animal rotates. This inhibits growth of epifauna at a greater distance from the shell than is possible for articulated species.

BIOGEOGRAPHY OF INARTICULATED BRACHIOPODS

CHRISTIAN C. EMIG

[Centre d'Océanologie de Marseille]

INTRODUCTION

The distribution of the inarticulated brachiopods is largely controlled by environmental factors (see chapter on ecology of inarticulated brachiopods, p. 473–495). Most of the inarticulated genera have broad geographic distributions on which the dispersal potential of the larvae has had only a small influence; lingulides and discinids have planktotrophic larvae, while craniids have short-lived, lecithotrophic larvae. The differences between species in their ecological requirements are more related to their ability to settle, which is induced by biotic or abiotic factors of the biocoenosis to which the species belongs. All adult inarticulated brachiopods are exclusively sedentary.

PATTERNS IN DISTRIBUTION

Because the biogeographic analyses of the inarticulated taxa, especially discinids and craniids, cannot presently be based on infra-generic and subtle ecological distinctions or broad geographic records, this account will be limited to the distribution of the genera. Many published records are deficient in precise information on the biogeography and ecology of species. Sampling inarticulated brachiopods at depths beyond the range of scuba may also present a misleading picture of brachiopod distribution and abundance. The use of submersibles provides reliable information only on large species that can be observed directly or by video. Another factor that introduces bias is the propensity of craniids and discinids to settle on more or less extensive, hard substrates that are difficult to investigate with traditional oceanographic sampling gear. Furthermore, the attention paid to brachiopods in benthic studies and during oceanographic cruises is frequently perfunctory so that large gaps

persist in our knowledge of the distribution and ecology of inarticulated species.

Populations of inarticulated species undergo seasonal to continuous recruitment depending on their latitudinal distribution. The early, shelled larvae of the lingulides are common members of the tropical plankton. A *Lingula* female can spawn 28,000 oocytes over a six-month period, and a *Glottidia* female may produce 130,000 ova over a four-month period. The duration of the planktonic stage of lingulide larvae varies from 3 to 6 weeks (CHUANG, 1959a; PAINE, 1963).

Discinid larvae, at least *Discinisca* itself, are also planktotrophic and acquire valves only in late stages (CHUANG, 1977). Discinid larvae have been reported from marine plankton from the water surface to depths of 3,000 m, sometimes at great distances from the shore (HELMCKE, 1940; ODHNER, 1960; CHUANG, 1977). Larvae of *Discinisca* have been recorded from littoral waters down to 350 m, while discinid larvae recorded from deep waters belong probably to *Pelagodiscus atlanticus*. For example, *Pelagodiscus* larvae have been collected with a calculated density of 2 to 3.5 larvae per 1,000 m³ (MILEIKOVSKY, 1970) between depths of 500 and 2,000 m in the northwestern Pacific Ocean. Postlarval specimens dredged from great depths (2,700 to 3,200 m) indicate that *Pelagodiscus* larvae become sedentary at different valve sizes.

The lecithotrophic larva of *Neocrania anomala*, the only craniid species in which development has been studied (NIELSEN, 1991), has a short swimming stage of about four to six days before settlement. Hydrodynamic conditions that occur in the biotope of *N. anomala* (EMIG, 1989b) can disperse larvae over several hundred kilometers during this short stage. Hence, the gregarious pattern of *Neocrania* species must be related to an environmental factor that attracts and

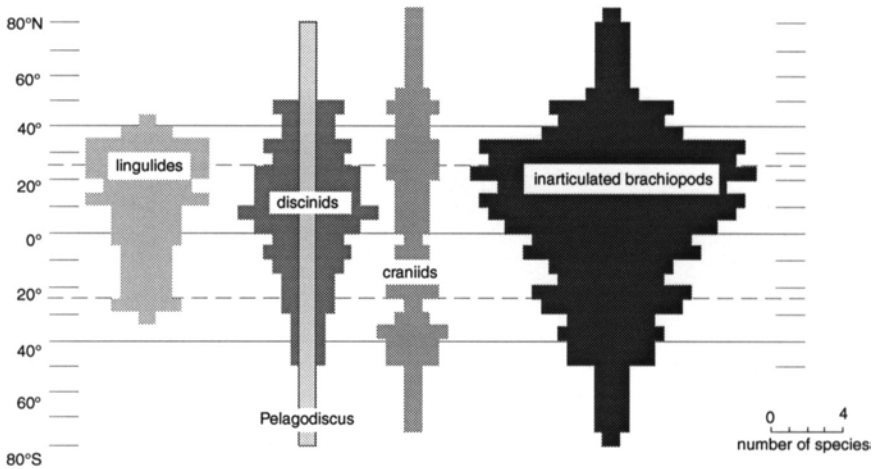


FIG. 415. Latitudinal distribution of inarticulated brachiopods (new).

induces larval settlement close to the adult forms, not to the short swimming stage of the larvae.

The upper and lower limits of tolerance to such factors as temperature, salinity, and depth have been used generally to explain the range of geographic distribution of the species. As stated in the section on the ecology of inarticulated brachiopods (Table 37, p. 484), however, such tolerances can vary subtly even among populations and have to be analyzed carefully before being used to explain the biogeographic distribution of higher taxa.

DISTRIBUTION OF FAMILIES AND GENERA

The three extant inarticulated families have a worldwide distribution. The Lingulidae are dominant in tropical and subtropical areas; the Discinidae occur mainly in intertropical areas; the Craniidae are widely distributed from northern to southern high latitudes, into which the discinid *Pelagodiscus* also extends (Fig. 415). The latitudinal dis-

tribution of inarticulated taxa can be globally related to their bathymetric extension (see Fig. 413) although more constraints are involved than the temperature, pressure, and dynamics of seawater.

Most inarticulated genera are cosmopolitan (Fig. 416) and were common in past eras. Indeed among living brachiopod families only the Lingulidae, Discinidae, and Craniidae can be traced back to the early Paleozoic. The radiations of the inarticulated species and genera represented in recent marine faunas (Table 40) are related to geological events. Most genera began their development in the Cenozoic with the global biotope changes marking the end of the Cretaceous crisis, at the end of the Paleogene threshold, and during the Neogene as a result of changes in the circulation of the ocean waters that allowed the development of deep-sea species.

LINGULIDAE

Living Lingulidae belong to two genera: *Lingula* (seven species), which is worldwide in distribution, except along the coasts of

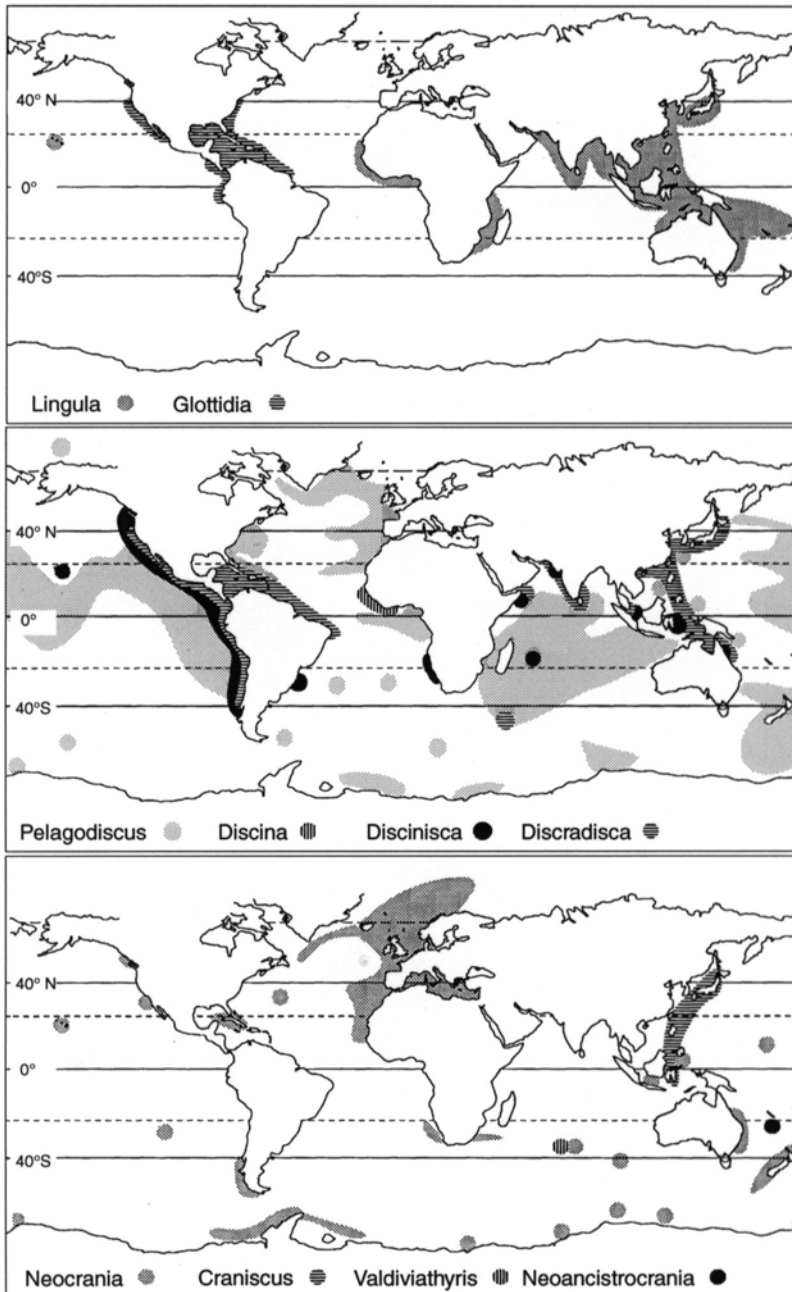


FIG. 416. Geographic distribution of inarticulated brachiopod genera (new).

TABLE 40. First geological record of the inarticulated genera represented in present marine faunas (new).

	Lingulidae	Discinidae	Craniidae
Triassic		<i>Discinisca</i>	
Upper Jurassic			<i>Craniscus</i>
Paleocene	<i>Lingula?</i> <i>Glottidia?</i>	<i>Discradisca</i>	
Eocene			<i>Neocrania</i>
Miocene		<i>Pelagodiscus</i>	
Holocene		<i>Discina</i>	<i>Valdiviathyris?</i> <i>Neoancistrocrania</i>

America, where *Glottidia* (five species) occurs exclusively (Fig. 416). Large variations in edaphic factors during the late Mesozoic (EMIG, 1984b; BIERNAT & EMIG, 1993) are probably responsible for the radiation of both genera. *Glottidia* may have originated on the western coast of North and Central America and *Lingula* possibly in the islands of the western Pacific. Their latitudinal distribution occurs within the 40° belt from temperate to equatorial areas (Fig. 417), and their bathymetric distribution is restricted to the continental shelf except for *Glottidia albidia*, which extends onto the upper part of the bathyal slope. Such a geographic distribution appears to be a consequence of the opening of the Atlantic Ocean and of the Paleocene-Eocene extension of the tropical-subtropical belt to about 45° latitude, with optimal conditions for the development of new temperate marine biotopes with good prospects for speciation. Yet the distribution of the lingulides appears rather similar at least since the early Paleozoic when taking into account the paleolatitudinal positions in correlation with temperatures of water masses.

DISCINIDAE

Pelagodiscus atlanticus occurs worldwide in deep water in the bathyal and abyssal zones and is undoubtedly the most widespread brachiopod species geographically and bathymetrically (Fig. 416–417). *Discinisca* (four species) and *Discradisca* (six species) have a warm-temperate to tropical, cosmo-

politan distribution and extend mainly over the continental shelf. *Discina striata* has a restricted distribution in the intertropical zone of the western coast of Africa.

CRANIIDAE

Neocrania (13 species) has a worldwide distribution (Fig. 416). Its latitudinal range is as wide as that of *Pelagodiscus*, but its bathymetric distribution is from shallow waters of the continental shelf to about 1,000 m depth on the bathyal slope (Fig. 417). Only one species, *Neocrania lecointei*, is recorded in the deeper parts of the bathyal zone (to 2,342 m). The two other genera have restricted distributions. *Craniscus japonicus* occurs in the western Pacific from 23 to 885 m, while *Valdiviathyris quenstedti* is known from a single location at 672 m. *Neoancistrocrania norfolki* has been collected in two locations of the South Pacific Ocean at 233 and 250 m depth.

All three inarticulated brachiopod families are of ancient stocks and are fairly cosmopolitan in distribution, extending from the shoreline to the bathyal depths. Most species have a distribution restricted to the 45° latitudinal belt and occur on the continental shelf from intertidal to a depth of about 100 m. Species extending to latitudes higher than 45° occur also in the bathyal zone (between about 100 and 3,000 m). Their bathymetric extent, however, is limited mainly to the upper bathyal part (to 1,000 m). Only *Pelagodiscus atlanticus*, one of the most recent species, is widespread in the abyssal zone (3,000 to 6,000 m). Species of the two monospecific genera *Discina striata* and *Valdiviathyris quenstedti* and also *Neoancistrocrania norfolki*, which is said to be recent as well, have a restricted geographic and bathymetric distribution (Fig. 416–417).

In contrast to the lingulides, speculating on the origins and paths of dispersal of the discinids and craniids is difficult. The present distribution of inarticulated taxa cannot be explained as the consequence of their age or their dispersal rate as suggested for the taxa of articulated brachiopods. The

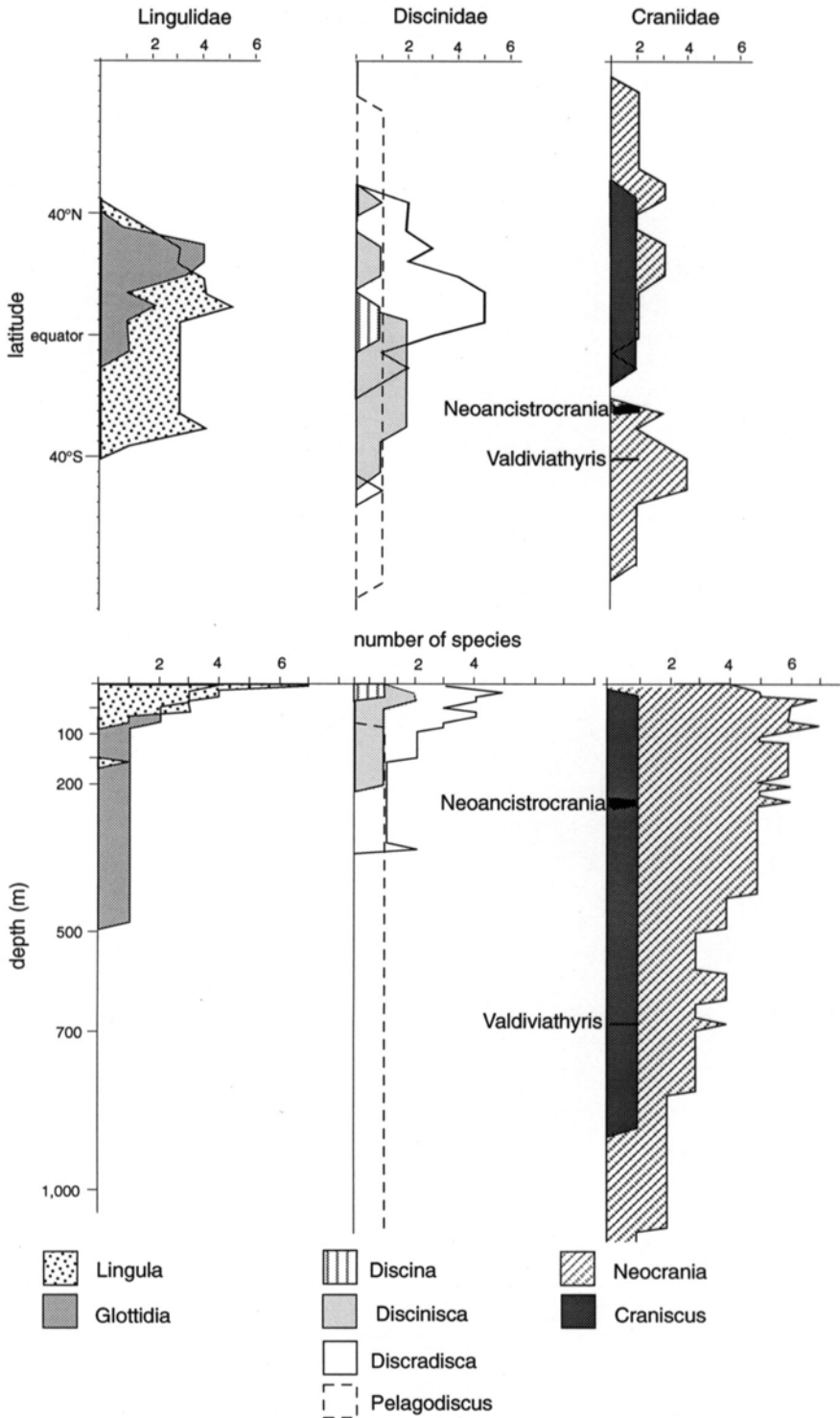


FIG. 417. Latitudinal and bathymetric extension of inarticulated brachiopod genera (new).

diversification of the genera and the long geological history of species are relevant to our understanding of the extent of the geographic and bathymetric distribution of inarticulated brachiopods. As ZEZINA (1970) previously stated the reasons for the biogeography of supraspecific brachiopod taxa are elusive.

REFERENCES

- Ackerly, Spafford. 1991. Hydrodynamics of rapid shell closure in articulate brachiopods. *Journal of Experimental Biology* 156:287–314.
- . 1992. Rapid shell closure in the brachiopods *Terebratulina retusa* and *Terebratalia transversa*. *Journal of the Marine Biological Association of the United Kingdom* 72:579–598.
- Adoutte, André, & H. Philippe. 1993. The major lines of metazoan evolution: summary of traditional evidence and lessons from ribosomal RNA sequence analysis. In Y. Pichon, ed., *Comparative Molecular Neurobiology*. Birkhauser. Basel. p. 1–30.
- Afzelius, B. A. 1979. Sperm structure in relation to phylogeny in the lower Metazoa. In D. W. Fawcett & J. M. Bedford, eds., *The Spermatozoon. Maturation, Motility, Surface Properties and Comparative Aspects*. Urban and Schwarzenberg. Baltimore. p. 243–251.
- Afzelius, B. A., & M. Ferraguti. 1978. Fine structure of brachiopod spermatozoa. *Journal of Ultrastructural Research* 63:308–315.
- Afzelius, B. A., & H. Mohri. 1966. Mitochondria respiring without exogenous substrate. A study of aged sea urchin spermatozoa. *Experimental Cell Research* 42:11–17.
- Aldridge, A. E. 1981. Intraspecific variation of shape and size in subtidal populations of two recent New Zealand articulate brachiopods. *New Zealand Journal of Zoology* 8:169–174.
- . 1991. Shape variation of *Neothyris* (Brachiopoda, Terebratellinae). In D. I. MacKinnon, D. E. Lee, & J. D. Campbell, eds., *Brachiopods Through Time, Proceedings of the 2nd International Brachiopod Congress, University of Otago, Dunedin, New Zealand, 1990*. Balkema. Rotterdam. p. 115–122.
- Alexander, R. R. 1986. Frequency of sublethal shell-breakage in articulate brachiopod assemblages through geologic time. In P. R. Rachebœuf & C. C. Emig, eds., *Les Brachiopodes Fossiles et Actuels, Actes du 1er Congrès International sur les Brachiopodes, Brest 1985*. Biostratigraphie du Paléozoïque 4. p. 159–166, pl. 1.
- Allan, R. S. 1937. On a neglected factor in brachiopod migration. *Records of the Canterbury Museum* 4:157–165.
- . 1949. Notes on a comparison of the Tertiary and recent Brachiopoda of New Zealand and South America. *Transactions of the Royal Society of New Zealand* 77:288–289.
- . 1960. The succession of Tertiary brachiopod faunas in New Zealand. *Records of the Canterbury Museum* 7:233–268.
- . 1963. On the evidence of Austral Tertiary and recent brachiopods on Antarctic biogeography. In *Proceedings of the 10th Science Congress of the Pacific Science Congress, University of Hawaii, Honolulu*. Bishop Museum Press. Honolulu. p. 451–454.
- Al-Rikabi, Ikbāl. 1992. A molecular approach to palaeontology: Biochemical method applications of brachiopod proteins. Master of Science thesis, University of Glasgow. 116 p.
- Alvarez, Fernando. 1990. Devonian athyrid brachiopods from the Cantabrian Zone (N.W. Spain). *Biostratigraphie du Paléozoïque* 11:311 p., 30 pl.
- Alvarez, Fernando, Covadonga Brime, & G. B. Curry. 1987. Growth and function of the micro-frills present on the Devonian brachiopod *Athyris campomanesi* (Verneuil & Archiac). *Transactions of the Royal Society of Edinburgh* 78:65–72.
- Alvarez, Fernando, & C. H. C. Brunton. 1990. The shell-structure, growth and functional morphology of some Lower Devonian athyrids from northwest Spain. *Lethaia* 23(2):117–131, 12 fig.
- Amsden, T. W. 1953. Some notes on the Pentameracea, including a description of one new genus and one new subfamily. *Washington Academy of Sciences, Journal* 43(5):137–147, 7 fig.
- An, S., & C. H. Koh. 1992. Environments and distribution of benthic animals on the Mangyung-Dongjin tidal flat, west coast of Korea. *Journal of the Oceanological Society of Korea* 27(1):78–90.
- In Korean.
- Arber, M. A. 1942. The pseudodeltidium of the strophomenid brachiopods. *Geological Magazine* 79:170–187.
- Armstrong, J. 1969. The cross-bladed fabrics of the shells of *Terrakea solida* (Etheridge and Dun) and *Streptorhynchus pelicanensis* Fletcher. *Palaeontology* 12:310–320.
- Asgaard, Ulla, & R. G. Bromley. 1991. Colonization by micromorph brachiopods in the shallow subtidal of the eastern Mediterranean Sea. In D. I. MacKinnon, D. E. Lee, & J. D. Campbell, eds., *Brachiopods Through Time, Proceedings of the 2nd International Brachiopod Congress, University of Otago, Dunedin, New Zealand, 1990*. Balkema. Rotterdam. p. 261–264.
- Asgaard, Ulla, & N. Stenfort. 1984. Recent micromorph brachiopods from Barbados; palaeoecological and evolutionary implications. *Géobios, Mémoire spécial* 8:29–37, pl. 1–2.
- Ashworth, J. H. 1915. On larvae of *Lingula* and *Pelagodiscus* (Disciniscia). *Transactions of the Royal Society of Edinburgh* 51:45–69, pl. 4–5.
- Atkins, Dorothy. 1956. Ciliary feeding mechanisms of brachiopods. *Nature* 177:706.
- . 1958. A new species and genus of Kraussinidae (Brachiopoda) with a note on feeding. *Proceedings of the Zoological Society of London* 131:559–581.
- . 1959. The growth stages of the lophophore of the brachiopods *Platidia davidsoni* (Eudes Des-Longchamps) and *P. anomioides* (Phillipi), with notes on the feeding mechanism. *Journal of the Marine Biological Association of the United Kingdom* 38:103–132.
- . 1960a. A new brachiopod from the Western Approaches, and the growth stages of the lophophore. *Journal of the Marine Biological Association of the United Kingdom* 39:71–89, fig. 1–14, pl. 1.
- . 1960b. The ciliary feeding mechanism of the

- Megathyridae (Brachiopoda), and the growth stages of the lophophore. *Journal of the Marine Biological Association of the United Kingdom* 39:459–479.
- . 1961a. A note on the growth stages and structure of the adult lophophore of the brachiopod *Terebratella (Waltonia) inconspicua* (G. B. Sowerby). *Proceedings of the Zoological Society of London* 136:255–271.
- . 1961b. The growth stage of the adult structure of the lophophore of the brachiopod *Megerlia truncata* (L.) and *M. echinata* (Fischer & Oelhart). *Journal of the Marine Biological Association of the United Kingdom* 41:95–111.
- . 1963. Notes on the lophophore and gut of the brachiopod *Tegulorhynchia nigricans* (G. B. Sowerby). *Proceedings of the Zoological Society of London* 140:15–24.
- Atkins, Dorothy, & M. J. S. Rudwick. 1962. The lophophore and ciliary feeding mechanism of the brachiopod *Crania anomala* (Müller). *Journal of the Marine Biological Association of the United Kingdom* 42:469–480.
- Avise, J. C. 1994. *Molecular markers, natural history and evolution*. Chapman & Hall. New York & London. 511 p.
- Awati, P. R., & G. R. Kshirsagar. 1957. *Lingula* from western coast of India. *Zoological Memoirs of the University of Bombay* 4:1–87.
- Ayala, F. J., J. W. Valentine, T. E. DeLaca, & G. S. Zumwalt. 1975. Genetic variability of the Antarctic brachiopod *Liothyrella notorcadensis* and its bearing on mass extinction hypotheses. *Journal of Paleontology* 49:1–9.
- Babin, C., J. H. Delance, C. C. Emig, & P. R. Racheboeuf. 1992. Brachiopodes et Mollusques Bivalves: concurrence ou indifférence? *Géobios, Mémoire spécial* 14:35–44.
- Bäckeljaug, T., B. Winnepeninckx, & L. De Bruyn. 1993. Cladistic analysis of metazoan relationships: a reappraisal. *Cladistics* 9:167–181.
- Bada, J. L., M. Y. Shou, E. H. Man, & R. A. Schroeder. 1978. Decomposition of hydroxy amino acids in foraminifera tests; kinetics, mechanism and geochronological implications. *Earth and Planetary Science Letters* 41:67–76.
- Baker, P. G. 1970a. Significance of the punctuation mosaic of the Jurassic thecidellinid brachiopod *Moorellina*. *Geological Magazine* 107:105–113.
- . 1970b. The growth and shell microstructure of the thecideacean brachiopod *Moorellina granulosa* (Moore) from the Middle Jurassic of England. *Palaeontology* 13:76–99.
- . 1990. The classification, origin and phylogeny of the thecideidine brachiopods. *Palaeontology* 33(1):175–191, 3 fig.
- . 1991. Morphology and shell microstructure of Cretaceous thecideidine brachiopods and their bearing on thecideidine phylogeny. *Palaeontology* 34:815–836.
- Baker, P. G., & D. G. Elston. 1984. A new polyseptate thecideacean brachiopod from the middle Jurassic of the Cotswolds, England. *Palaeontology* 27:777–791.
- Baker, P. G., & K. Laurie. 1978. Revision of the Aptian thecideidine brachiopods of the Faringdon sponge gravels. *Palaeontology* 21:555–570.
- Balakirev, E. S., & G. P. Manchenko. 1985. High levels of allozymic variation in brachiopod *Coptothyris grayii* and *Ascidia Halocynthia aurantium*. *Genetika* 21:239–244.
- Balinski, Andrzej. 1975. Secondary changes in microornamentation of some Devonian ambocoeliid brachiopods. *Palaeontology* 18:179–189.
- Bancroft, B. B. 1945. The brachiopod zonal indices of the stages Costonian–Onnian in Britain. *Journal of Paleontology* 19:181–252, pl. 22–38.
- Baron, J., J. Clavier, & B. A. Thomassin. 1993. Structure and temporal fluctuations of two intertidal seagrass-bed communities in New Caledonia (SW Pacific Ocean). *Marine Biology* 117:139–144.
- Bassett, M. G., L. E. Holmer, L. E. Popov, & John Laurie. 1993. Phylogenetic analysis and classification of the Brachiopoda—reply and comments. *Lethaia* 26:385–386.
- Bayne, B. L., & R. C. Newell. 1983. Physiological energetics of marine molluscs. In A. S. M. Saleuddin & K. M. Wilbur, eds., *The Mollusca*, Vol. 4. Academic Press. New York. p. 407–515.
- Bayne, B. L., J. Widdows, & R. J. Thompson. 1976. *Physiological integrations*. In B. L. Bayne, ed., *Marine Mussels: Their Ecology and Physiology*. Cambridge University Press. Cambridge. p. 261–291.
- Beecher, C. E. 1891. Development of the Brachiopoda. Part I. Introduction. *American Journal of Science (series 3)* 41:343–357.
- . 1892. Development of the Brachiopoda. Part II. Classification of the stages of growth and decline. *American Journal of Science (series 3)* 44:133–155.
- . 1897. Morphology of the brachia. *Bulletin of the United States Geological Survey* 87:105–112.
- Beecher, C. E., & J. M. Clarke. 1889. The development of some Silurian Brachiopoda. *New York State Museum Memoir* 1(1):1–95, pl. 1–8.
- Bemmelen, J. F. van. 1883. Untersuchungen über den anatomischen und histologischen Bau der Brachiopoda Testicardina. *Jena. Zeitschrift für Naturwissenschaften* 16:88–161.
- Benigni, Chiara, & Carla Ferluga. 1988. Carniana *Thecospiridae* (Brachiopoda) from San Cassiano Formation (Cortina d'Ampezzo, Italy). *Rivista Italiana di Paleontologia* 94:515–560.
- Benson, D. A., M. Boguski, D. L. Lipman, & J. Ostell. 1994. GenBank. *Nucleic Acids Research* 22:3441–3444.
- Benton, M. J., ed. 1993. *The Fossil Record 2*. Chapman & Hall. London. 845 p.
- Bernard, F. R. 1972. The living Brachiopoda of British Columbia. *Syesis* 5:73–82.
- Beyer, H. G. 1886. A study of the structure of *Lingula (Glottidia) pyramidata* Stim. (Dall). *Studies from the Biology Laboratory, Johns Hopkins University* 3:227–265.
- Bhavanarayana, P. V. 1975. Some observations on the benthic faunal distribution in the Kakinada Bay. In R. Natarajan, ed., *Recent Researches in Estuarine*

- Biology. Hindustan Publishing Co. Dehli. p. 146–150.
- Biernat, Gertrude, & C. C. Emig. 1993. Anatomical distinctions of Mesozoic lingulide brachiopods. *Acta Palaeontologica Polonica* 38(1/2):1–20, 8 fig.
- Biernat, Gertrude, & Alwyn Williams. 1970. Ultrastructure of the protegulum of some acrotretide brachiopods. *Palaeontology* 13:491–502.
- . 1971. Shell structure of the siphonotretacean Brachiopoda. *Palaeontology* 14:423–430.
- Bitter, P. H. von, & R. Ludvigsen. 1979. Formation and function of protingular pitting in some North American acrotretid brachiopods. *Palaeontology* 22:705–720.
- Blochmann, F. 1892. Untersuchungen über den Bau der Brachiopoden. I. Die Anatomie von *Crania anomala* (Müller). Jena. Gustav Fischer. p. 1–65.
- . 1898. Die larve von *Discinisca* (Die Muellersche Brachiopodenlarve). *Zoologische Jahrbücher Abteilungen Anatomie und Ontogenie der Tiere* 11:417–426.
- . 1900. Untersuchungen über den Bau der Brachiopoden. I. Die Anatomie von *Crania anomala* O.F.M. (1892). II. Die Anatomie von *Discinisca lamellosa* (Broderip) und *Lingula anatina* (Bruguière). Gustav Fischer. Jena. p. 1–124.
- . 1906. Neue Brachiopoden der Valdivia- und Gaussexpeditionen. *Zoologischer Anzeiger* 30:690–702.
- . 1908. Zur Systematik und geographischen Verbreitung der Brachiopoden. *Zeitschrift für wissenschaftliche Zoologie* 90:596–644, pl. 36–40.
- Boore, J. L., & W. M. Brown. 1994. Complete DNA sequence of the mitochondrial genome of the black chiton, *Katharina tunicata*. *Genetics* 138:423–443.
- Borman, A. H., E. W. de Jong, R. Thierry, P. Westbroek, & L. Bosch. 1987. Coccolith-associated polysaccharides from cells of *Emiliania huxleyi* (Haptophyceae). *Journal of Phycology* 23:118–123.
- Bosi Vanni, M. R., & A. M. Simonetta. 1967. Contributo alla conoscenza dell'anatomia ed isologia di *Muehlfedria disculus* (Pallas) 1766 (Brachiopoda, Testicardines). Gli apparati lofoforale, digerente, nefridiale e riproduttore. *Societa Toscana di Scienze Naturali, Memorie (series B)* 74B:21–34.
- Boucot, A. J. 1959. Brachiopods of the lower Devonian rocks at Highland Mills, New York. *Journal of Paleontology* 33(5):727–769, 5 fig., pl. 90–103.
- Bozzo, M. G., R. Bargalló, M. Durfort, R. Fontarnau, & J. López-Camps. 1983. Ultraestructura de la cubierta de oóbits de *Terebratula vitrea* (Brachiopoda: Testicardina). *Butlletí de la Institució Catalana d'Història Natural* 49 (Secció de Zoologia, 5):13–18, fig. 1–11.
- Brafield, A. E., & D. J. Solomon. 1972. Oxycaloric coefficients for animals respiring nitrogenous substrates. *Comparative Biochemistry and Physiology* 43A:837–841.
- Branch, G. M. 1981. The biology of limpets: physical factors, energy flow and ecological interactions. *Oceanography and Marine Biology: An Annual Review* 19:235–380.
- Bremer, K. 1988. The limits of amino acid sequence data in angiosperm phylogenetic reconstruction. *Evolution* 42:795–803.
- Britten, R. J., & E. H. Davidson. 1971. Repetitive and non-repetitive DNA sequences and a speculation on the origins of evolutionary novelty. *Journal of Molecular Evolution* 46:111–133.
- Britten, R. J., & D. E. Kohne. 1968. Repeated sequences in DNA. *Science* 161:529–540.
- Bromley, R. G., & Finn Surlyk. 1973. Borings produced by brachiopod pedicles, fossil and recent. *Lethaia* 6:349–365.
- Brooks, W. K. 1879. The development of *Lingula* and the systematic position of the Brachiopoda. Johns Hopkins University, Chesapeake Zoology Laboratory, Scientific Results of the Session of 1878:34–112.
- Brown, I. A. 1953. *Martinopsis* Waagen from the Salt Range, India. *Journal and Proceedings of the Royal Society of New South Wales* 86:100–107, 3 fig., pl. 9.
- Brunton, C. H. C. 1966. Silicified productoids from the Visean of County Fermanagh. *British Museum (Natural History) Bulletin (Geology)* 12(5):175–243, pl. 1–19.
- . 1969. Electron microscopic studies of growth margins of articulate brachiopods. *Zeitschrift für Sellforsch* 100:189–200.
- . 1971. An endopunctate rhynchonellid brachiopod from the Viséan of Belgium and Britain. *Palaeontology* 14:95–106.
- . 1972. The shell structure of chonetacean brachiopods and their ancestors. *Bulletin of the British Museum of Natural History (Geology)* 21:1–26.
- . 1988. Some brachiopods from the eastern Mediterranean Sea. *Israel Journal of Zoology* 35:151–169.
- Brunton, C. H. C., & G. B. Curry. 1979. British brachiopods. Synopses of the British fauna (new series) 17:64 p., 30 fig.
- Brunton, C. H. C., & Norton Hiller. 1990. Late Cainozoic brachiopods from the coast of Namaqualand, South Africa. *Palaeontology* 33(2):313–342, 11 fig.
- Brunton, C. H. C., & D. J. C. Mundy. 1988. Strophalosiacean and aulostegacean productoids (Brachiopoda) from the Craven Reef Belt (late Viséan) of North Yorkshire. *Proceedings of the Yorkshire Geological Society* 47:55–88.
- Brusca, R. C., & G. J. Brusca. 1990. Invertebrates. Sinauer Associates, Inc. Sunderland, Massachusetts. 922 p.
- Buchan, P., L. S. Peck, & N. Tublitz. 1988. A light, portable apparatus for the assessment of invertebrate heart beat rate. *Journal of Experimental Biology* 136:495–498.
- Bullivant, J. S. 1968. The method of feeding of lophophorates (Bryozoa, Phoronida, Brachiopods). *New Zealand Journal of Marine and Freshwater Research* 2:135–146.
- Bulman, O. M. B. 1939. Muscle systems of some inarticulate brachiopods. *Geological Magazine* 76:434–444.
- Campbell, K. S. W., & B. D. E. Chatterton. 1979. *Coelospira*: do its double spires imply a double

- lophophore? *Alcheringa* 3:209–223, fig. 1–7.
- Carlson, S. J. 1989. The articulate brachiopod hinge mechanism: morphological and functional variation. *Paleobiology* 15(4):364–386, 13 fig.
- . 1993a. Investigating brachiopod phylogeny and classification—response to Popov *et al.* 1993. *Lethaia* 26:383–384.
- . 1993b. Phylogeny and evolution of “pentameride” brachiopods. *Palaeontology* 36(4):807–837, 10 fig.
- Carpenter, W. B. 1851. On the intimate structure of shells of Brachiopoda. In T. Davidson, *British Fossil Brachiopoda*. Monograph of the Palaeontographical Society 1:22–40.
- Carter, J. L., J. G. Johnson, R. Gourvenec, & H.-F. Hou. 1994. A revised classification of the spiriferid brachiopods. *Annals of the Carnegie Museum* 63:327–374.
- Caryl, Anthony. 1992. DNA fingerprinting of brachiopod DNA. Unpublished Honours Bachelor of Science thesis. University of Glasgow. 37 p.
- Chuang, S. H. 1956. The ciliary feeding mechanisms of *Lingula unguis* (L.) (Brachiopoda). *Proceedings of the Zoological Society of London* 127(2):167–189.
- . 1959a. The breeding season of the brachiopod *Lingula unguis* (L.). *Biological Bulletin, Marine Biology Laboratory, Woods Hole, Massachusetts* 117(2):202–207.
- . 1959b. The structure and function of the alimentary canal in *Lingula unguis* (L.) Brachiopoda. *Proceedings of the Zoological Society of London* 132:283–311.
- . 1960. An anatomical, histological and histochemical study of the gut of the brachiopod *Crania anomala*. *Quarterly Journal of Microscopical Science* 101:9–18.
- . 1961. Growth of the postlarval shell in *Lingula unguis* (L.) (Brachiopoda). *Proceedings of the Zoological Society of London* 137(2):299–310.
- . 1968. The larvae of a discinid (Inarticulata, Brachiopoda). *Biological Bulletin* 135:263–272.
- . 1971. New interpretation of the morphology of *Schizambon australis* Ulrich and Cooper (Ordovician siphonotretid inarticulate brachiopod). *Journal of Paleontology* 45:824–832.
- . 1973. The inarticulate brachiopod larvae of the International Indian Ocean Expedition. *Journal of the Marine Biological Association of India* 15:538–544.
- . 1974. Observations on the ciliary feeding mechanisms of the brachiopod *Crania anomala*. *Journal of the Zoological Society of London* 173:441–449.
- . 1977. Larval development in *Discinisca* (inarticulate brachiopod). *American Zoologist* 17:39–53.
- . 1983a. Brachiopoda. In K. G. Adiyodi & R. G. Adiyodi, eds., *Reproductive Biology of Invertebrates*. Oogenesis, Oviposition and Oosorption, Vol. I. John Wiley and Sons Ltd. p. 571–584.
- . 1983b. Brachiopoda. In K. G. Adiyodi & R. G. Adiyodi, eds., *Reproductive Biology of Invertebrates*. Spermatogenesis and Sperm Function, Vol. II. John Wiley and Sons Ltd. p. 517–530.
- . 1990. Brachiopoda. In K. G. Adiyodi & R. G. Adiyodi, eds., *Reproductive Biology of Invertebrates*. Fertilisation, Development and Parental Care, Vol. VI. John Wiley and Sons Ltd. p. 211–254.
- . 1991. Common and evolutionary features of recent brachiopods and their bearing on the relationship between, and the monophyletic origin of, the inarticulates and the articulates. In D. I. MacKinnon, D. E. Lee, & J. D. Campbell, eds., *Brachiopods Through Time*, Proceedings of the 2nd International Brachiopod Congress, University of Otago, Dunedin, New Zealand, 1990. Balkema, Rotterdam. p. 11–14.
- Clegg, H. 1993. Biomolecules in recent and fossil articulate brachiopods. Ph.D. thesis. University of Newcastle Upon Tyne. 246 p.
- Cloud, P. E. Jr. 1942. Terebratuloid Brachiopoda of the Silurian and Devonian. *Geological Society of America Special Paper* 38:1–182, pl. 1–26.
- . 1948. Notes on recent brachiopods. *American Journal of Science* 246:241–250.
- Cock, A. G. 1966. Genetical aspects of metrical growth and form in animals. *Quarterly Review of Biology* 41:131–190.
- Cohen, B. L. 1992. Utility of molecular phylogenetic methods: a critique of immuno-taxonomy. *Lethaia* 24:441–442.
- . 1994. Immuno-taxonomy and the reconstruction of brachiopod phylogeny. *Palaeontology* 37:907–911.
- Cohen, B. L., Peter Balfe, Moyra Cohen, & G. B. Curry. 1991. Molecular evolution and morphological speciation in North Atlantic brachiopods (*Terebratulina* spp.). *Canadian Journal of Zoology* 69:2903–2911.
- . 1993. Molecular and morphometric variation in European populations of the articulate brachiopod *Terebratulina retusa*. *Marine Biology* 115:105–111.
- Cohen, B. L., Peter Balfe, & G. B. Curry. 1986. Genetics of the brachiopod *Terebratulina*. In P. R. Rachebœuf & C. C. Emig, eds., *Les Brachiopodes Fossiles et Actuels, Actes du 1er Congrès International sur les Brachiopodes*, Brest 1985. *Biostratigraphie du Paléozoïque* 4. p. 55–63.
- Cohen, B. L., A. B. Gawthrop, & T. Cavalier-Smith. In preparation. Phylogeny of lophophorates, especially brachiopods, based on nuclear-encoded SSU rRNA gene sequences.
- Collins, M. J. 1991. Growth rate and substrate-related mortality of a benthic brachiopod population. *Lethaia* 24:1–11.
- Collins, M. J., G. B. Curry, G. Muzer, R. Quinn, S. Xu, P. Westbroek, & S. Ewing. 1991. Immunological investigations of relationships within the terebratulid brachiopods. *Palaeontology* 34:785–796.
- Collins, M. J., G. B. Curry, R. Quinn, G. Muzer, T. Zomerdijk, & P. Westbroek. 1988. Sero-taxonomy of skeletal macromolecules in living terebratulid brachiopods. *Historical Biology* 1:207–224.
- Collins, M. J., G. Muzer, G. B. Curry, P. Sandberg, & P. Westbroek. 1991. Macromolecules in brachiopod

- shells: characterisation and diagenesis. *Lethaia* 24:387–397.
- Collins, M. J., G. Muyzer, P. Westbroek, G. B. Curry, P. A. Sandberg, S. J. Xu, R. Quinn, & D. I. MacKinnon. 1991. Preservation of fossil biopolymeric structures: conclusive immunological evidence. *Geochimica et Cosmochimica Acta* 55:2253–2257.
- Conklin, E. G. 1902. The embryology of a brachiopod, *Terebratulina septentrionalis* Couthouy. Proceedings of the American Philosophical Society 41:41–76.
- Conover, R. J., & E. D. S. Corner. 1968. Respiration and nitrogen excretion by some marine zooplankton in relation to their life cycles. *Journal of the Marine Biological Association of the United Kingdom* 48:49–75.
- Conway Morris, Simon. 1994. Why molecular biology needs palaeontology. In M. Akam, P. Holland, P. Ingham, & G. Wray, eds., *The Evolution of Developmental Mechanisms*. Development, 1994 Supplement. Company of Biologists. Cambridge. p. 1–13.
- . 1995. Nailing the lophophorates. *Nature* 375:365–366.
- Conway, Morris, Simon, B. L. Cohen, A. B. Gawthrop, T. Cavalier-Smith, & B. Winnepeinninckx. 1996. Lophophorate phylogeny. *Science* 272:282.
- Conway Morris, Simon, & J. S. Peel. 1995. Articulated halkieriids from the Lower Cambrian of north Greenland and their role in early protostome evolution. *Philosophical Transactions of the Royal Society (series B)* 347:305–358.
- Cooper, G. A. 1942. New genera of North American brachiopods. *Washington Academy of Sciences Journal* 32(8):228–235.
- . 1952. Unusual specimens of the brachiopod family Isogrammidae. *Journal of Paleontology* 26:113–119, pl. 21–23.
- . 1954. Unusual Devonian brachiopods. *Journal of Paleontology* 28:325–332, 5 fig., pl. 36–37.
- . 1955. New genera of middle Paleozoic brachiopods. *Journal of Paleontology* 29:45–63, pl. 11–14.
- . 1956. New Pennsylvanian brachiopods. *Journal of Paleontology* 30:521–530, pl. 61.
- . 1957. Loop development of the Pennsylvanian terebratuloid *Cryptacanthia*. *Smithsonian Miscellaneous Collection* 134(3):1–18, pl. 1–2.
- . 1973. Vema's Brachiopoda (recent). *Smithsonian Contributions to Paleobiology* 17:1–51.
- . 1975. Brachiopods from west African waters with examples of collateral evolution. *Journal of Paleontology* 49:911–927, fig. 1–7, pl. 1–4.
- . 1977. Brachiopods from the Caribbean Sea and adjacent waters. *Studies in Tropical Oceanography Miami* 14. Rosenstiel School of Marine and Atmospheric Science. University of Miami Press. 212 p., 6 fig., 35 pl.
- . 1981. Brachiopods from the southern Indian Ocean. *Smithsonian Contributions to Paleobiology* 43:1–93, fig. 1–30, pl. 1–14.
- . 1982. New Brachiopoda from the southern hemisphere and *Cryptopora* from Oregon (recent). *Smithsonian Contributions to Paleobiology* 41:1–43, fig. 1–4, pl. 1–7.
- . 1983. The Terebratulacea (Brachiopoda), Triassic to recent: A study of the brachidia (loops). *Smithsonian Contributions to Paleobiology* 50:1–445, 17 fig., 77 pl., 86 tables.
- . 1988. Some Tertiary brachiopods of the east coast of the United States. *Smithsonian Contributions to Paleobiology* 64:1–45.
- Cooper, G. A., & P. J. Doherty. 1993. *Calloria variegata*, a new recent species of brachiopod (Articulata: Terebratulida) from northern New Zealand. *Journal of the Royal Society of New Zealand* 23:271–281.
- Cooper, G. A., & R. E. Grant. 1974. Permian brachiopods of West Texas, II. *Smithsonian Contributions to Paleobiology* 15:233–793.
- . 1975. Permian brachiopods of West Texas, III. *Smithsonian Contributions to Paleobiology* 19:795–1298, pl. 192–502.
- . 1976. Permian brachiopods of West Texas, IV. *Smithsonian Contributions to Paleobiology* 21:1923–2285, pl. 503–662.
- Cooper, G. A., & F. G. Stehli. 1955. New genera of Permian brachiopods from West Texas. *Journal of Paleontology* 29:469–474, pl. 52–54.
- Copper, Paul. 1965. A new Middle Devonian atrypid brachiopod from the Eifel, Germany. *Senckenbergiana Lethaea* 46(4/6):309–325, 13 fig., pl. 27.
- . 1986. Evolution of the earliest smooth spire-bearing Atrypoids (Brachiopoda: Lissatrypidae, Ordovician–Silurian). *Palaeontology* 29(4):827–866, pl. 73–75.
- Cornish-Bowden, A. 1983. Relating proteins by amino acid composition. *Methods in Enzymology* 91:60–75.
- Cowen, R. 1966. The distribution of punctae on the brachiopod shell. *Geological Magazine* 103:269–275.
- . 1968. A new type of delthyrial cover in the Devonian brachiopod *Mucrospirifer*. *Palaeontology* 11:317–327, pl. 63–64.
- Cowen, R., & M. J. S. Rudwick. 1970. Deltidial spines in the Triassic brachiopod *Bittnerula*. *Palaeontologische Zhurnal* 44:82–85, pl. 9.
- Crenshaw, M. A. 1972. The soluble matrix from *Mercenaria mercenaria* shell. *Biom mineralization* 6:6–11.
- Culter, J. M. 1979. A population study of the inarticulate brachiopod *Glottidia pyramidata* (Stimpson). Unpublished master of science thesis. University of South Florida. Tampa. 53 p.
- . 1980. The occurrence of hermaphrodites of the inarticulate brachiopod *Glottidia pyramidata*. *Florida Scientist* 43(1):20.
- Culter, J. M., & J. L. Simon. 1987. Sex ratios and the occurrence of hermaphrodites in the inarticulate brachiopod, *Glottidia pyramidata* (Stimpson) in Tampa Bay, Florida. *Bulletin of Marine Science of the Gulf and Caribbean* 40:193–197.
- Curry, G. B. 1981. Variable pedicle morphology in a population of the recent brachiopod *Terebratulina septentrionalis*. *Lethaia* 14:9–20.
- . 1982. Ecology and population structure of the

- recent brachiopod *Terebratulina retusa* from Scotland. *Palaeontology* 25(2):227–246.
- . 1983. Microborings in recent brachiopods and the functions of caeca. *Lethaia* 16:119–127.
- Curry, G. B., & A. D. Ansell. 1986. Tissue mass in living brachiopods. In P. R. Rachebœuf & C. C. Emig, eds., *Les Brachiopodes Fossiles et Actuels, Actes du 1er Congrès International sur les Brachiopodes*, Brest 1985. *Biostratigraphie du Paléozoïque* 4. p. 231–241.
- Curry, G. B., A. D. Ansell, Mark James, & L. S. Peck. 1989. Physiological constraints on living and fossil brachiopods. *Transactions of the Royal Society of Edinburgh, Earth Sciences* 80:255–262.
- Curry, G. B., Maggie Cusack, Kazuyoshi Endo, Derek Walton, & R. Quinn. 1991. Intracrystalline molecules from brachiopod shells. In S. Suga & H. Nakahara, eds., *Mechanisms and Phylogeny of Mineralization in Biological Systems*. Springer-Verlag. Tokyo. p. 35–40.
- Curry, G. B., Maggie Cusack, Derek Walton, Kazuyoshi Endo, H. Clegg, G. Abbott, & H. Armstrong. 1991. Biogeochemistry of brachiopod intracrystalline molecules. *Philosophical Transactions of the Royal Society of London* 333B:359–366.
- Curry, G. B., R. Quinn, M. J. Collins, Kazuyoshi Endo, S. Ewing, G. Muyzer, & P. Westbroek. 1991. Immunological responses from brachiopod skeletal macromolecules; a new technique for assessing taxonomic relationships using shells. *Lethaia* 24:399–407.
- . 1993. Molecules and morphology—the practical approach. *Lethaia* 26:5–6.
- Cusack, Maggie, G. B. Curry, H. Clegg, & G. Abbott. 1992. An intracrystalline chromoprotein from red brachiopod shells: implications for the process of biomineralisation. *Comparative Biochemistry and Physiology* 102B:93–95.
- Cusack, Maggie, & Alwyn Williams. 1996. Chemostructural degradation of Carboniferous lingulid shells. *Philosophical Transactions of the Royal Society of London* B351:33–49.
- Dagys, A. S. 1968. Jurskiye i rannemelovye brachiopody Severa Sibiri [Jurassic and Early Cretaceous brachiopods from northern Siberia]. *Akademia Nauk SSSR Sibiroskoe Otdelenie Geologii I Geofiziki (IGIG) Trudy* [Institute of Geology and Geophysics, Academy of Sciences of the USSR, Siberian Branch, Transactions] 41:167 p., 81 fig., 26 pl.
- . 1972. Postembrional'noye razvitiye brakhidiya pozdnepaleozoyskikh i rannemezozoykskikh Terebratulida [Postembryonic development of the brachidium of late Paleozoic and early Mesozoic terebratulids]. In A. S. Dagys & A. B. Ivanovskii, eds., *Morphologicheskkiye i filogeneticheskkiye voprosy paleontologii* [Morphological and Phylogenetic Questions of Paleontology]. *Akademia Nauk SSSR Sibiroskoe Otdelenie Institut Geologii I Geofiziki (IGIG) Trudy* [Institute of Geology and Geophysics, Academy of Sciences of the USSR, Siberian Branch, Transactions] 112:22–58, fig. 1–28.
- . 1974. Triasovye brachiopody (morfologiya, sistema, filogeniya, stratigraficheskoye znachenie i biogeografiya) [Triassic Brachiopoda (morphology, systematics, phylogeny, stratigraphic distribution, and biogeography)]. *Akademia Nauk SSSR Sibiroskoe Otdelenie Institut Geologii I Geofiziki (IGIG) Trudy* [Institute of Geology and Geophysics, Academy of Sciences of the USSR, Siberian Branch, Transactions] 214:386 p., 171 fig., 49 pl.
- Darwin, Charles. 1859a. *On the Origin of Species*. 1st edition. John Murray. London. 490 p.
- . 1859b. On the origin of the species by means of natural selection or the preservation of favoured races in the struggle for life. The Folio Society edition (1990). 298 p.
- Davidson, Thomas. 1850. Sur quelques Brachiopodes nouveaux ou peu connus. *Bulletin de la Société Géologique de France (série 2)* 8:62–74, 1 pl.
- . 1853. A Monograph of the British fossil Brachiopoda (Volume 1: General introduction). *Palaeontographical Society (London) Monograph* 7:1–136, pl. 1–9.
- . 1880. Report on the Brachiopoda dredged by the HMS *Challenger* during the years 1873–1876. *Report of the Scientific Results of the Voyage of HMS Challenger* 1(1):1–67, pl. 1–4.
- Davis, C. C. 1949. Observations of plankton taken in marine waters of Florida in 1947 and 1948. *Quarterly Journal of the Florida Academy of Science* 11:67–103.
- Degens, E. T., D. W. Spencer, & R. H. Parker. 1967. Paleobiochemistry of molluscan shell proteins. *Comparative Biochemistry and Physiology* 20:553–579.
- Devereaux, P., P. Haeberli, & O. Smithies. 1984. A comprehensive set of sequence analysis programs for the VAX. *Nucleic Acids Research* 12:387–395.
- Dexter, D. M. 1983. Soft bottom infaunal communities in Mission Bay. *California Fish Game* 69(1):5–17.
- Di Geronimo, I., & G. Fredj. 1987. Les fonds à *Errina aspera* et *Pachylasma giganteum*. *Documents et Travaux de l'Institut de Géologie "Albert de Lapparent"* (Paris) 11:243–247.
- Doherty, P. J. 1976. Aspects of the feeding ecology of the subtidal brachiopod, *Terebratella inconspicua* (Sowerby, 1846). Master of Science Thesis. Department of Zoology, University of Auckland. 183 p.
- . 1979. A demographic study of a subtidal population of the New Zealand articulate brachiopod *Terebratella inconspicua*. *Marine Biology* 52:331–342.
- . 1981. The contribution of dissolved amino acids to the nutrition of brachiopods. *New Zealand Journal of Zoology* 8:183–188.
- Dolah, R. F. van., D. R. Calder, & D. M. Knott. 1983. Assessment of the benthic macrofauna in an ocean disposal area near Charleston, South Carolina. Technical Report, South Carolina Marine Resource Center 56:1–97.
- Dolah, R. F. van., D. M. Knott, E. L. Wenner, T. D. Mathews, & M. P. Katuna. 1984. Benthic studies and sedimentological studies of the Georgetown

- ocean dredged material disposal site. Technical Report, South Carolina Marine Resource Center 59:1–97.
- Donoghue, M. J., & P. D. Cantino. 1984. The logic and limitations of the outgroup substitution approach to cladistic analysis. *Systematic Botany* 9:192–202.
- Dörjes, J. 1977. Marine macrobenthic communities of the Sapelo island, Georgia region. In B. C. Coull, ed., *Ecology of Marine Benthos*. University of South Carolina Press, Columbia, Belle W. Baruch Library in Marine Science 6:399–421.
- . 1978. Sedimentology and faunistics of tidal flats in Taiwan. II. Faunistic and ichnocoenotic studies. *Senckenbergiana Maritima* 10(1/3):85–115.
- Doumen, C., & W. R. Ellington. 1987. Isolation and characterization of a taurine-specific opine dehydrogenase from the pedicles of the brachiopod, *Glottidia pyramidata*. *Journal of Experimental Zoology* 243:25–31.
- Du Bois, H. M. 1916. Variation induced in brachiopods by environmental conditions. *Publications of the Puget Sound Marine Station* 1:177–183.
- Dunning, H. N. 1963. Geochemistry of organic pigments: carotenoids. In I. A. Berger, ed., *Organic Geochemistry*. Macmillan, New York, p. 367–430.
- Dwartz, N. E. 1961. The structure of β -chitin. *Biochimica et Biophysica Acta* 51:283–294.
- Eernisse, D. J., J. S. Albert, & F. E. Anderson. 1992. Annelida and arthropoda are not sister taxa: a phylogenetic analysis of spiralian metazoan morphology. *Systematic Biology* 41:305–330.
- Eernisse, D. J., & A. G. Kluge. 1993. Taxonomic congruence versus total evidence and amniote phylogeny inferred from fossils, molecules and morphology. *Molecular Biology and Evolution* 10:1170–1195.
- Eglinton, G., & G. A. Logan. 1991. Molecular preservation. *Philosophical Transactions of the Royal Society of London* 333B:315–328.
- Egorov, A. N., & L. Ye. Popov. 1990. Novyi rod Lingulid iz niznepermiskikh otlozhenii Sibroskoi Platformy [A new lingulid genus from the Early Permian deposits of the Siberian Platform]. *Paleontologicheskii Zhurnal* 1990(4):111–115, fig. 1–3.
- Eichler, P. 1911. Die Brachiopoden der deutschen Südpolar-Expedition 1901 bis 1903. *Deutsche Südpolar-Expedition 1901–1903 (series 12) Zoologie* 4:381–401.
- Ekman, T. 1896. Beiträge zur Kenntnis des Steiles der Brachiopoden. *Zeitschrift für Wissenschaftliche Zoologie* 62:169–249.
- Elliott, G. F. 1951. On the geographical distribution of terebrateloid brachiopods. *Annals and Magazine of Natural History (series 12)* 5:305–333.
- . 1953. Brachial development and evolution in terebrateloid brachiopods. *Cambridge Philosophical Society Biological Reviews* 28:261–279, 9 fig.
- Emig, C. C. 1976. Le lophophore-structure significative des Lophophorates (Brachiopoda, Bryozoa, Phoronida). *Zoologica Scripta* 5:133–137.
- . 1981a. Implications de données récentes sur les lingules actuelles dans les interprétations paléocéologiques. *Lethaia* 14(2):151–156.
- . 1981b. Observations sur l'écologie de *Lingula reevii* Davidson (Brachiopoda: Inarticulata). *Journal of Experimental Marine Biology and Ecology* 52(1):47–61.
- . 1982. Terrier et position des lingules (brachiopodes, inarticulés). *Bulletin de la Société Zoologique de France* 107(2):185–194.
- . 1983a. Comportement expérimental de *Lingula anatina* (brachiopode, inarticulé) dans divers substrats meubles (Baie de Mutsu, Japon). *Marine Biology* 75(2/3):207–213.
- . 1983b. Taxonomie du genre *Glottidia* (brachiopodes inarticulés). *Bulletin du Museum National d'Histoire Naturelle de Paris (série 4) 5(secteur 4; no. 2):469–489*.
- . 1984a. Importance du sédiment dans la distribution des lingules (brachiopodes, inarticulés). *Lethaia* 17:115–123.
- . 1984b. Pourquoi les lingules (brachiopodes, inarticulés) ont survécu à la transition Secondaire-Tertiaire. *Bulletin de la Commission des Travaux historiques et scientifiques, Section Sciences* 6:87–94.
- . 1986. Conditions de fossilisation du genre *Lingula* (Brachiopoda) et implications paléocéologiques. *Palaeogeography, Palaeoclimatology, Palaeoecology* 53:245–253.
- . 1987. Offshore brachiopods investigated by submersible. *Journal of Experimental Marine Biology and Ecology* 108:261–273.
- . 1988. Les brachiopodes actuels sont-ils des indicateurs (paléo) bathymétriques? *Géologie Méditerranéenne* 15(1):65–71.
- . 1989a. Les lingules fossiles, représentants d'écosystèmes oligotypiques? *Atti 3° Simposio di Ecologia e Paleocologia delle Comunità bentoniche, Catania* 1985:117–121.
- . 1989b. Distribution bathymétrique et spatiale des populations de *Gryphus vitreus* (brachiopode) sur la marge continentale (Nord-Ouest Méditerranée). *Oceanologica Acta* 12(2):205–209.
- . 1989c. Distributional patterns along the Mediterranean continental margin (upper bathyal) using *Gryphus vitreus* (Brachiopoda) densities. *Palaeogeography, Palaeoclimatology, Palaeoecology* 71:253–256.
- . 1990. Examples of post-mortality alteration in recent brachiopod shells and (paleo) ecological consequences. *Marine Biology* 104:233–238.
- . 1992. Functional disposition of the lophophore in living Brachiopoda. *Lethaia* 25:291–302.
- Emig, C. C., & P. Cals. 1979. Lingules d'Amboine, *Lingula reevii* Davidson et *Lingula rostrum* (Shaw), données écologiques et taxonomiques concernant les problèmes de spéciation et de répartition. *Cahiers de l'Indo-pacifique* 2:153–164.
- Emig, C. C., J. C. Gall, D. Pajaud, & J. C. Plaziat. 1978. Réflexions critiques sur l'écologie et la systématique des Lingules actuelles et fossiles. *Géobios* 11(5):573–609.

- Emig, C. C., & P. LeLoeuff. 1978. Description de *Lingula parva* Smith (Brachiopoda, Inarticulata), récoltée en Côte d'Ivoire avec quelques remarques sur l'écologie de l'espèce. *Téthys* 8(3):271–274.
- Emig, C. C., & J. A. Vargas. 1990. Notes on *Glottidia audebarti* (Broderip) (Brachiopoda, Lingulidae) from the Gulf of Nicoya, Costa Rica. *Revista de Biología Tropical* 38(2A):251–258.
- Endo, Kazuyoshi. 1987. Life habit and relative growth of some laqueid brachiopods from Japan. *Transactions and Proceedings of the Palaeontological Society of Japan (new series)* 147:180–194.
- . 1992. Molecular systematics of recent and Pleistocene brachiopods. Ph.D. thesis. University of Glasgow. 208 p.
- Endo, Kazuyoshi, & G. B. Curry. 1991. Molecular and morphological taxonomy of a recent brachiopod genus *Terebratulina*. In D. I. MacKinnon, D. E. Lee, & J. D. Campbell, eds., *Brachiopods Through Time*, Proceedings of the 2nd International Brachiopod Congress, University of Otago, Dunedin, New Zealand, 1990. Balkema. Rotterdam. p. 101–108.
- Endo, Kazuyoshi, G. B. Curry, R. Quinn, M. J. Collins, G. Muyzer, & P. Westbroek. 1994. Re-interpretation of terebratulide phylogeny based on immunological data. *Palaeontology* 37:349–373, fig. 1–10.
- Erdmann, V. A., J. Wolters, E. Huysmans, & R. De Wachter. 1985. Collection of published 5S, 5.8S and 4.5S ribosomal RNA sequences. *Nucleic Acids Research* 13:r105–r153.
- Eshleman, W. P., & J. L. Wilkens. 1979a. Actinomysin ATPase activities in the brachiopod *Terebratalia transversa*. *Canadian Journal of Zoology* 57:1944–1949, fig. 1–3.
- . 1979b. Brachiopod orientation to current direction and substrate position (*Terebratalia transversa*). *Canadian Journal of Zoology* 57:2079–2082, fig. 1.
- Eshleman, W. P., J. L. Wilkens, & M. J. Cavey. 1982. Electrophoretic and electron microscopic examination of the adductor and diductor muscles of an articulate brachiopod, *Terebratalia transversa*. *Canadian Journal of Zoology* 60:550–559, fig. 1–5.
- Farris, J. S. 1972. Outgroups and parsimony. *Systematic Zoology* 31:328–334.
- Felsenstein, Joseph. 1993. PHYLIP (Phylogeny Inference Package). Computer program distributed by the author. Department of Genetics, University of Washington. Seattle, Washington.
- Field, Katherine, G. Olsen, D. J. Lane, S. J. Giovannoni, M. T. Ghiselin, E. C. Raff, N. R. Pace, & R. A. Raff. 1988. Molecular phylogeny of the animal kingdom. *Science* 239:748–753.
- Fischer, P., & D.-P. Oehlert. 1892. Brachiopodes de l'Atlantique Nord. *Resultats des Campagnes Scientifiques du Prince de Monaco* 3:1–30.
- Flower, N. E., & C. R. Green. 1982. A new type of gap junction in the phylum Brachiopoda. *Cell and Tissue Research* 227:231–234.
- Folmer, O., M. Black, W. Hoeh, R. Lutz, & R. Vrijenhoek. 1994. DNA primers for amplification of mitochondrial cytochrome c oxidase subunit I from diverse metazoan invertebrates. *Molecular Marine Biology and Biotechnology* 3:294–299.
- Foster, M. W. 1974. Recent Antarctic and subantarctic brachiopods. *Antarctic Research Series* 21:1–189.
- . 1989. Brachiopods from the extreme South Pacific and adjacent waters. *Journal of Paleontology* 63:268–301.
- Fouke, B.W. 1986. The functional significance of spicule-reinforced connective tissues in *Terebratulina unguicula* (Carpenter). In P. R. Rachebœuf & C. C. Emig, eds., *Les Brachiopodes Fossiles et Actuels*, Actes du 1er Congrès International sur les Brachiopodes, Brest 1985. *Biostratigraphie du Paléozoïque* 4. p. 271–279, fig. 1–4.
- François, P. 1891. Choses de Nouméa. II. Observations biologiques sur la lingule. *Archives de Zoologie expérimentale et générale* (2)9:229–245.
- Franzen, Åke. 1956. On spermiogenesis, morphology of the spermatozoon, and biology of fertilization among invertebrates. *Zoologiska Bidrag från Uppsala* 31:355–482.
- . 1969. On the larval development and metamorphosis in *Terebratulina*, Brachiopoda. *Zoologiska Bidrag från Uppsala* 38:155–174.
- . 1982. Ultrastructure of spermatids and spermatozoa in three polychaetes with modified biology of reproduction: *Autolytus* sp., *Chitinopoma serrula* and *Capitella capitata*. *International Journal of Invertebrate Reproduction* 5:185–200.
- . 1987. Spermatogenesis. In A. C. Giese, J. S. Pearse, & V. B. Pearse, eds., *Reproduction of Marine Invertebrates*. Volume 9. General aspects: seeking unity in diversity. Blackwell Scientific Publications. California. p. 1–47.
- Freeman, Gary. 1994. The endocrine pathway responsible for oocyte maturation in the inarticulate brachiopod *Glottidia*. *Biological Bulletin* 186:263–270.
- Frey, R. W., J. S. Hong, J. D. Howard, B. K. Park, & S. J. Han. 1987. Zonation of benthos on a macrotidal flat, Inchon, Korea. *Senckenbergiana Maritima* 19(5/6):295–329.
- Frith, D. W., R. Tantanasiwong, & O. Bhatia. 1976. Zonation of macrofauna on a mangrove shore, Phuket island. *Phuket Marine Biological Center Research Bulletin* 10:1–37.
- Gaspard, Danièle. 1978. Biominéralisation chez les brachiopodes articulés—microstructure et formation de la coquille. *Annales de Paléontologie* 64:1–25.
- . 1982. Microstructure de térébratules bipsées (Brachiopodes) du Cénomaniens de la Sarthe (France). Affinités d'une des formes avec le genre *Selliithyris* Midd. *Annales de Paléontologie (Vertébrés-Invertébrés)* 68(1):1–14, 3 pl.
- . 1986. Aspects figurés de la biominéralisation unités de base de la sécrétion carbonatée chez les Terebratulida actuels. In P. R. Rachebœuf & C. C. Emig, eds., *Les Brachiopodes Fossiles et Actuels*, Actes du 1er Congrès International sur les Brachiopodes, Brest 1985. *Biostratigraphie du Paléozoïque* 4. p. 77–83.
- . 1989. Quelques aspects de la biodégradation

- des coquilles de brachiopodes; conséquences sur leur fossilisation. Bulletin de la Société Géologique de France 6:1207–1216.
- . 1990. Diagenetic modifications of shell microstructure in the Terebratulida (Brachiopoda, Articulata) II. In J. G. Carter, ed., *Skeletal Biomineralization: Patterns, Processes and Evolutionary Trends*, Volume 1. Van Nostrand Reinhold. New York. p. 53–56.
- . 1991. Growth stages in articulate brachiopod shells and their relation to biomineralization. In D. I. MacKinnon, D. E. Lee, & J. D. Campbell, eds., *Brachiopods Through Time*, Proceedings of the 2nd International Brachiopod Congress, University of Otago, Dunedin, New Zealand, 1990. Balkema. Rotterdam. p. 167–174.
- Gee, Henry. 1995. Lophophorates prove likewise variable. *Nature* 374:493.
- George, T. N. 1932a. *Ambocoelia* Hall and certain similar British Spiriferidae. Geological Society of London, Quarterly Journal 87:30–61, pl. 3–5.
- . 1932b. The British Carboniferous reticulate Spiriferidae. Geological Society of London, Quarterly Journal 88:516–575, pl. 31–35.
- Ghiselin, M. T. 1988. The origin of molluscs in the light of molecular evidence. In P. H. Harvey & L. Partridge, eds., *Oxford Surveys in Evolutionary Biology*. Oxford University Press. Oxford. p. 66–95.
- Giese, A. C., J. S. Pearse, & V. B. Pearse. 1987. *Reproduction of Marine Invertebrates*. Volume 9. General aspects: seeking unity in diversity. Blackwell Scientific Publications. California. 712 p.
- Gilmour, T. H. J. 1978. Ciliation and function of the food-collecting and waste-rejecting organs of the lophophorates. *Canadian Journal of Zoology* 56:2142–2155.
- . 1981. Food-collecting and waste-rejecting mechanisms in *Glottidia pyramidata* and the persistence of lingulean brachiopods in the fossil record. *Canadian Journal of Zoology* 59:1539–1547.
- Golding, G. B., & R. S. Gupta. 1994. Protein-based phylogenies support a chimeric origin for the eukaryotic genome. *Molecular Biology and Evolution* 12:1–6.
- Gorjansky, V. Iu. [see also Gorjansky, W. Ju.], & L. E. Popov. 1985. Morphologiya, systematicheskoe polozhenie i proiskhozhdenie bezzamkovykh brachiopod s karbonatnoi rakovinoi [Morphology, systematic position and origin of inarticulate brachiopods with a carbonate shell]. *Paleontologicheskii Zhurnal* 1985(3):3–14, 5 fig., pl. 1.
- Gorjansky, W. Ju. [see also Gorjansky, V. Iu.], & L. Ye. Popov. 1986. On the origin and systematic position of the calcareous-shelled inarticulate brachiopods. *Lethaia* 19:233–240, fig. 1–3.
- Gourvenec, Rémy. 1987. Morphologie des épines chez les brachiopodes Delthyrididae. *Lethaia* 20:21–31.
- . 1989. Radial microornament in spiriferid brachiopods and paleogeographical implications. *Lethaia* 22:405–411.
- Gourvenec, Rémy, & Michel Mélou. 1990. Découverte d'un cas d'ornementation épineuse chez les Orthida (Brachiopoda). *Compte-Rendus de l'Académie des Sciences de Paris* 311(II):1273–1277.
- Grant, R. E. 1963. Unusual attachment of a Permian linoproductid brachiopod. *Journal of Paleontology* 37:134–140, 1 fig., pl. 19.
- . 1968. Structural adaptation in two Permian brachiopod genera, Salt Range, West Pakistan. *Journal of Paleontology* 42:1–32.
- . 1972. The lophophore and feeding mechanism of the Productina (Brachiopoda). *Journal of Paleontology* 46:213–248, pl. 1–9.
- . 1980. Koskinoid perforations in brachiopod shells: function and mode of formation. *Lethaia* 13:313–319.
- . 1987. Brachiopods of Enewetak Atoll. In D. M. Devaney & others, eds., *The Natural History of Enewetak Atoll*, vol. 2. Office of Scientific and Technical Information, U. S. Department of Energy. Oak Ridge, Tennessee. p. 77–84.
- Gratiot, M. P. 1860. Études anatomiques sur la *Lingule anatine* (L. *anatina* Lam.). *Journal de Conchyliologie* 4:49–172.
- Gustus, R. M., & R. A. Cloney. 1972. Ultrastructural similarities between setae of brachiopods and polychaetes. *Acta Zoologica* 53:229–233.
- Halanych, K. M. 1991. 5S ribosomal RNA sequences inappropriate for phylogenetic reconstruction. *Molecular Biology and Evolution* 8:249–253.
- Halanych, K. M., J. D. Bacheller, A. M. A. Aguinaldo, S. M. Liva, D. M. Hillis, & J. A. Lake. 1995. Evidence from 18S ribosomal DNA that the lophophorates are protostome animals. *Science* 267:1641–1643.
- Hall, J., & J. M. Clarke. 1892–1894. An introduction to the study of the genera of Palaeozoic Brachiopoda. New York Geological Survey 8. Pt. 1(1892):i–xvi, 1–367, pl. 1–20; Pt. 2: i–xvi, 1–394, pl. 21–84.
- . 1894–1895. An introduction to the study of the Brachiopoda intended as a Handbook for the use of Students. New York State Geologist Annual Report for 1891 (1894):134–300, pl. 1–22; continuation (pt. 2) New York State Geologist Annual Report for 1893 (1894) [1895]:751–943, pl. 23–54.
- Hammen, C. S. 1968. Aminotransferase activities and amino acid excretion of bivalve molluscs and brachiopods. *Comparative Biochemistry and Physiology* 26:697–705.
- . 1969. Lactate and succinate oxidoreductases in marine invertebrates. *Marine Biology* 4:233–238.
- . 1971. Metabolism of brachiopods and bivalve molluscs. In R. Alvarado, E. Gadea, & A. de Haro, eds., *Actas del I Simposio Internacional de Zooflogenia*, Salamanca, 1969, Acta Salmanticensia, Ciencias 36:471–478.
- . 1977. Brachiopod metabolism and enzymes. *American Zoologist* 17:141–147.
- Hammen, C. S., & R. C. Bullock. 1991. Opine oxidoreductases in brachiopods, bryozoans, phoronids and molluscs. *Biochemical Systematics and Ecology* 19:263–269.

- Hammen, C. S., D. P. Hanlon, & S. C. Lum. 1962. Oxidative metabolism of *Lingula*. Comparative Biochemistry and Physiology 5:185–192.
- Hammen, C. S., & S. C. Lum. 1966. Fumarate reductase and succinate dehydrogenase activities in bivalve mollusks and brachiopods. Comparative Biochemistry and Physiology 19:775–781.
- . 1977. Salinity tolerance and pedicle regeneration of *Lingula*. Journal of Paleontology 51:548–551.
- Hammen, C. S., & P. J. Osborne. 1959. Carbon dioxide fixation in marine invertebrates: a survey of major phyla. Science 130:1409–1410.
- Hammond, L. S. 1980. The larvae of a discinid (Brachiopoda, Inarticulata) from inshore waters near Townsville, Australia, with revised identifications of previous records. Journal of Natural History 14:647–661.
- . 1982. Breeding season, larval development and dispersal of *Lingula anatina* (Brachiopoda, inarticulata) from Townsville, Australia. Journal of Zoology, London 198:183–196.
- . 1983. Experimental studies of salinity tolerance, burrowing behavior and pedicle regeneration in *Lingula anatina* (Brachiopoda, Inarticulata). Journal of Paleontology 57:1311–1316.
- . 1984. Epibioti from the valves of recent *Lingula* (Brachiopoda). Journal of Paleontology 58:1528–1531.
- Hammond, L. S., & I. R. Poiner. 1984. Genetic structure of three populations of the “living fossil” brachiopod *Lingula* from Queensland, Australia. Lethaia 17:139–143.
- Hancock, A. 1859. On the organisation of the Brachiopoda. Philosophical Transactions of the Royal Society 148:791–869.
- Hare, P. E. 1962. The amino acid composition of the organic matrix of some recent and fossil shells of some west coast species of *Mytilus*. Ph.D. thesis. California Institute of Technology.
- Hare, P. E., & R. M. Mitterer. 1969. Laboratory simulation of amino acid diagenesis in fossils. Carnegie Institute of Washington Yearbook 67:205–208.
- Haro, A. de. 1963. Estructura y anatomia comparadas des las gonadas y pedunculo des los Braquiópodos testicardinos. Publicaciones del Instituto de Biología Aplicada, Barcelona 35:97–117.
- Harvey, E. N. 1928. The oxygen consumption of luminous bacteria. Journal of General Physiology 11:469–475.
- Hatai, K. M. 1940. The Cenozoic Brachiopoda of Japan. Science Reports of the Tohoku Imperial University, Sendai, Japan (second series, Geology) 20:1–413, pl. 1–12.
- Haugen, J.-E., H.-P. Sejrup, & N. B. Vogt. 1989. Chemotaxonomy of Quaternary benthic foraminifera using amino acids. Journal of Foraminiferal Research 19:38–51.
- Havličěk, Vladimir. 1961. Rhynchonelloidea des Bohemischen aelteren palaeozoikums (Brachiopoda). Ustredni Ustav Geologicky Rozpravy 27:211 p., 27 pl.
- . 1982. Lingulacea, Paterinacea and Siphonotretacea (Brachiopoda) in the Lower Ordovician sequence of Bohemia. Sbornik Geologických ved (Paleontologie) 25:9–82, 16 fig., pl. 1–16.
- Hay-Schmidt, A. 1992. Ultrastructure and immunocytochemistry of the nervous system of the larvae of *Lingula anatina* and *Glottidia* sp. (Brachiopoda). Zoomorphology 112:189–205.
- Heinrikson, R. L., & S. C. Meredith. 1984. Amino acid analysis by reverse-phase high-performance liquid chromatography: precolumn derivatization with phenylisothiocyanate. Analytical Biochemistry 136:65–74.
- Heller, M. 1931. Exkretorische Tätigkeit der Brachiopoden. Zeitschrift für Morphologie und Oekologie der Tiere 24:238–258.
- Helmcke, J. G. 1940. Die Brachiopoden der deutschen Tiefsee-Expedition. Wissenschaftliche Ergebnisse der deutschen Tiefsee-Expedition auf dem Dampfer “Valdivia” 1898–1899. G. Fischer Verlag, 1932–1940. Jena. Wissenschaftliche Ergebnisse der deutschen Tiefsee-Expedition 24(3):217–316.
- Hemmingsen, A. M. 1960. Energy metabolism as related to body size and respiratory surfaces and its evolution. Report to the Steno Memorial Hospital 9:7–110.
- Hennig, Willi. 1966. Phylogenetic Systematics. University of Illinois Press. Urbana. 263 p.
- Hertlein, L. G., & U. S. Grant IV. 1944. The Cenozoic Brachiopoda of western North America. Publications of the University of California at Los Angeles in Mathematical and Physical Sciences 3:236 p., pl. 1–21.
- Hiller, Norton. 1988. The development of growth lines on articulate brachiopods. Lethaia 21:177–188.
- . 1991. The southern African recent brachiopod fauna. In D. I. MacKinnon, D. E. Lee, & J. D. Campbell, eds., Brachiopods Through Time, Proceedings of the 2nd International Brachiopod Congress, University of Otago, Dunedin, New Zealand, 1990. Balkema. Rotterdam. p. 439–445.
- . 1993. A modern analogue of the Lower Ordovician *Obolus* conglomerate of Estonia. Geological Magazine 130(2):265–267.
- Hillis, D. M., & M. T. Dixon. 1991. Ribosomal DNA: molecular evolution and phylogenetic inference. Quarterly Review of Biology 66:411–453.
- Hillis, D. M., J. P. Huelsenbeck, & C. W. Cunningham. 1994. Application and accuracy of molecular phylogenies. Science 264:671–677.
- Hillis, D. M., & D. Moritz. 1990. Molecular Systematics. Sinauer Associates, Inc. Sunderland, Massachusetts. 588 p.
- Hirai, E., & T. Fukushi. 1960. The development of two species of lamp shells, *Terebratalia coreanica* and *Coptothyris grayi*. Bulletin of the Ashamushi Marine Biological Station 10:77–80.
- Hochachka, P. W., & G. H. Somero. 1973. Strategies of Biochemical Adaptation. W. B. Saunders Company. Philadelphia. 358 p.
- . 1984. Biochemical Adaptation. Princeton University Press. Princeton. 480 p.
- Holland, P. W. H. 1992. Homeobox genes in vertebrate evolution. BioEssays 14:267–273.

- Holland, P. W. H., & B. L. M. Hogan. 1986. Phylogenetic distribution of Antennapedia-like homeoboxes. *Nature* 321:251–253.
- Holland, P. W. H., N. A. Williams, & J. Lanfear. 1991. Cloning of segment polarity gene homologues from the unsegmented brachiopod *Terebratulina retusa* (Linnaeus). *Federation of European Biochemical Societies Letters* 291:211–213.
- Holmer, L. E. 1989. Middle Ordovician phosphatic inarticulate brachiopods from Västergötland and Dalarna, Sweden. *Fossils and Strata* 26:1–172, 118 fig.
- Holmer, L. E., & L. Ye. Popov. 1990. The Acrotretacean brachiopod *Ceratreta tanneri* (Metzger) from the Upper Cambrian of Baltoscandia. *Geologiska Foreningens i Stockholm Forhandlingar* 112(3):249–263.
- d'Hondt, Jean-Loup. 1986. Étude de l'intestin et de la glande digestive de *Terebratulina retusa* (L.) (Brachiopode). IV. Comparaison avec les activités enzymatiques d'autres brachiopodes du même biotope. In P. R. Rachebœuf & C. C. Emig, eds., *Les Brachiopodes Fossiles et Actuels*, Actes du 1er Congrès International sur les Brachiopodes, Brest 1985. *Biostratigraphie du Paléozoïque* 4. p. 301–305.
- d'Hondt, Jean-Loup, & E. Boucaud-Camou. 1982. Étude l'intestin et de la glande digestive de la *Terebratulina retusa* (L.) (Brachiopode). Ultrastructure et recherche d'activités amylasiques et protéasiques. *Bulletin de la Société Zoologique de France* 107(2):207–216.
- Hori, H., B. L. Lim, T. Ohama, T. Kumazaki, & S. Osawa. 1985. Evolution of organisms deduced from 5S rRNA sequences, p. 369–384. In T. Ohta & A. Aoki, eds., *Population Genetics and Molecular Evolution*. Springer. Berlin. 503 p.
- Hori, H., & S. Osawa. 1986. Evolutionary change in 5S rRNA secondary structure and a phylogenetic tree of 352 5S rRNA species. *BioSystems* 19:163–172.
- Hoverd, W. A. 1985. Histological and ultrastructural observations of the lophophore and larvae of the brachiopod, *Notosaria nigricans* (Sowerby, 1846). *Journal of Natural History* 19:831–850.
- . 1986. The adult lophophore of *Notosaria nigricans* (Brachiopoda). In P. R. Rachebœuf & C. C. Emig, eds., *Les Brachiopodes Fossiles et Actuels*, Actes du 1er Congrès International sur les Brachiopodes, Brest 1985. *Biostratigraphie du Paléozoïque* 4. p. 307–312.
- Huelsenbeck, J. P. 1995. Performance of phylogenetic methods in simulation. *Systematic Biology* 44:17–48.
- Hughes, W. W., G. D. Rosenberg, & R. D. Tkachuck. 1988. Growth increments in the shell of the living brachiopod *Terebratalia transversa*. *Marine Biology* 98:511–518.
- Hulmes, A. G., & G. A. Boxshall. 1988. Peocilostome copepods associated with bivalve molluscs and a brachiopod at Hong-Kong. *Journal of Natural History* 22(2):537–544.
- Huson, D. H., & R. Wetzell. 1994. SplitsTree 1.0: Computer program distributed by the authors. Mathematics Department, University of Bielefeld, Germany. Bielefeld.
- Huxley, J. S. 1932. *Problems of Relative Growth*. The Dial Press. New York. 244 p.
- Hyman, L. H. 1959a. *The Invertebrates: Smaller Coelomate Groups*. Chaetognatha, Hemichordata, Pogonophora, Phoronida, Ectoprocta, Brachiopoda, Sipunculida, the Coelomate Bilateria, Vol. 5. McGraw-Hill. New York, London, Toronto. viii + 783 p., fig. 1–240.
- . 1959b. The Lophophorate Coelomates—Phylum Brachiopoda. In L. H. Hyman, *The Invertebrates: Smaller Coelomate Groups*. McGraw-Hill. New York, London, Toronto. p. 228–609.
- Iijima, M., T. Hiroko, M. Yutaka, & K. Yoshinori. 1991. Difference of the organic component between the mineralized and the non-mineralized layers of *Lingula* shell. *Comparative Biochemistry and Physiology* 98A:379–382.
- Iijima, M., H. Kamemizu, N. Wakamatsu, T. Goto, & Y. Moriwaki. 1991. Thermal decomposition of *Lingula* shell apatite. *Calcified Tissue International* 49:128–133.
- Iijima, M., & Y. Moriwaki. 1990. Orientation of apatite and organic matrix in *Lingula unguis* shell. *Calcified Tissue International* 47:237–242.
- Iijima, M., Y. Moriwaki, Y. Doi, & Y. Kuboki. 1988. The orientation of apatite crystals in *Lingula unguis* shell. *Japanese Journal of Oral Biology* 30:20–30.
- Iijima, M., Y. Moriwaki, & Y. Kuboki. 1991. Orientation of apatite and the organic matrix in *Lingula* shells, p. 433–437. In S. Suga & H. Nakahara, eds., *Mechanisms and Phylogeny of Mineralization of Biological Systems*. Springer-Verlag. Tokyo.
- Ikeda, T. 1974. Nutritional ecology of marine zooplankton. *Memoirs of the Faculty of Fisheries, Hokkaido University* 21:19–112.
- Irwin, D. H. 1991. Metazoan phylogeny and the Cambrian radiation. *Trends in Ecology and Evolution* 6:131–134.
- Ishikawa, Hajime. 1977. Comparative studies on the thermal stability of animal ribosomal RNAs: V. Tentaculata (Phoronids, moss-animals and lampshells). *Comparative Biochemistry and Physiology* 57B:9–14.
- Ivanov, C. P., & R. Z. Stoyanova. 1972. Aliphatic hydrocarbons in fossils of Mesozoic belemnites. *Comptes-Rendus de l'Académie Bulgare des Sciences* 25(5):637–639.
- Ivanov, C. P., R. Z. Stoyanova, & C. P. Daskalov. 1975. Content and composition of higher fatty acids in fossils of Mesozoic belemnites. *Comptes-Rendus de l'Académie Bulgare des Sciences* 28(7):935–938.
- Iwata, K. 1981. Ultrastructure and mineralization of the shell of *Lingula unguis* Linné (Inarticulate Brachiopod). *Journal of the Faculty of Science of Hokkaido University (series IV)* 20(1):35–65.
- . 1982. Ultrastructure and calcification of the shells in inarticulate brachiopods Part 2. Ultrastructure of the shells of *Glottidia* and *Disciniscia*. *Journal of the Geological Society of Japan* 88:957–966, 5 pl.
- Jaanusson, Valdar. 1971. Evolution of the brachiopod hinge. In J. T. Dutro, Jr., ed., *Paleozoic Perspectives*:

- A Paleontological Tribute to G. Arthur Cooper. Smithsonian Contributions to Paleobiology 3:33–46, 6 fig., pl. 1–2.
- Jackson, J. B., T. F. Goreau, & W. D. Hartman. 1971. Recent brachiopod-coraline sponge communities and their paleoecological significance. *Science* 173:623–625.
- Jacobs, H. T., P. Balfe, B. L. Cohen, A. Farquharson, & L. Comito. 1988. Phylogenetic implications of genome rearrangement and sequence evolution in echinoderm mitochondrial DNA. In C. R. C. Paul & A. B. Smith, eds., *Echinoderm Phylogeny and Evolutionary Biology*. Clarendon Press. Oxford. p. 121–137.
- Jaeger, J. A., D. H. Turner, & M. Zuker. 1989a. Improved predictions of secondary structure for RNA. *Proceedings of the National Academy of Sciences, USA* 86:7706–7710.
- . 1989b. Predicting optimal and suboptimal secondary structure for RNA. *Methods in Enzymology* 183:281–306.
- James, M. A., A. D. Ansell, & G. B. Curry. 1991a. Reproductive cycle of the brachiopod *Terebratulina retusa* on the west coast of Scotland. *Marine Biology* 109:441–451.
- . 1991b. Functional morphology of the gonads of the articulate brachiopod *Terebratulina retusa*. *Marine Biology* 111:401–410.
- . 1991c. Oogenesis in the articulate brachiopod *Terebratulina retusa*. *Marine Biology* 111:411–423.
- James, M. A., A. D. Ansell, M. J. Collins, G. B. Curry, L. S. Peck, & M. C. Rhodes. 1992. Biology of living brachiopods. *Advances in Marine Biology* 28:175–387.
- Jin, Yu-gan, & Hua-yu Wang. 1992. Revision of the Lower Cambrian brachiopod *Heliomedusa* Sun & Hou, 1987. *Lethaia* 25(1):35–49, fig. 1–14.
- Johnson, J. G., & P. Westbrook. 1971. *Cardinalia* terminology in rhynchonellid brachiopods. *Geological Society of America Bulletin* 82:1699–1702.
- Jones, G. J., & J. L. Barnard. 1963. The distribution and abundance of the inarticulate brachiopod *Glottidia albida* (Hinds) on the mainland of southern California. *Pacific Naturalist* 4(2):27–52.
- Jope, H. M. 1965. Composition of brachiopod shell. In R. C. Moore, ed., *Treatise on Invertebrate Paleontology*. Part H, Brachiopoda. Geological Society of America & University of Kansas Press. New York & Lawrence. p. 156–164.
- . 1967a. The protein of brachiopod shell. I. Amino acid composition and implied protein taxonomy. *Comparative Biochemistry and Physiology* 20:593–600.
- . 1967b. The protein of brachiopod shell. II. Shell protein from fossil articulate: amino acid composition. *Comparative Biochemistry and Physiology* 20:601–605.
- . 1969a. The protein of brachiopod shell. III. Comparison with structural protein of soft tissue. *Comparative Biochemistry and Physiology* 30:209–224.
- . 1969b. The protein of the brachiopod shell. IV. Shell protein from fossil inarticulates: amino acid composition and disc electrophoresis of fossil articulate shell protein. *Comparative Biochemistry and Physiology* 30:225–232.
- . 1971. Constituents of brachiopod shells. In M. Florin & E. H. Stotz, eds., *Comprehensive Biochemistry*. Elsevier. Amsterdam. p. 749–784.
- . 1973. The protein of brachiopod shell. V. N-terminal end groups. *Comparative Biochemistry and Physiology* 45B:17–24.
- . 1977. Brachiopod shell proteins: their function and taxonomic significance. *American Zoologist* 17:133–140.
- . 1979. The protein of brachiopod shell. VI. C-terminal end groups and sodium dodecylsulphate-polyacrylamide gel electrophoresis: molecular constitution and structure of the protein. *Comparative Biochemistry and Physiology* 63B:163–173.
- . 1980. Phylogenetic information from fossil brachiopods. In P. E. Hare, T. C. Hoering, & K. J. King, eds., *Biogeochemistry of Amino Acids*. John Wiley & Sons. New York. p. 83–94.
- . 1986. Evolution of the Brachiopoda: the molecular approach. In P. R. Racheboeuf & C. C. Emig, eds., *Les Brachiopodes Fossiles et Actuels, Actes du 1er Congrès International sur les Brachiopodes*, Brest 1985. *Biostratigraphie du Paléozoïque* 4. p. 103–111.
- Jørgensen, C. B. 1981. A hydromechanical principle for particle retention in *Mytilus edulis* and other ciliary suspension feeders. *Marine Biology* 61:277–282.
- Jørgensen, C. B., T. Kjørboe, F. Mohlenberg, & H. U. Riisgard. 1984. Ciliary and mucus-net filter feeding, with special reference to fluid mechanical characteristics. *Marine Ecology Progress Series* 15:283–292.
- Joshi, J. G., & B. Sullivan. 1973. Isolation and preliminary characterisation of haemerythrin for *Lingula unguis*. *Comparative Biochemistry and Physiology* 44B:857–867.
- Joubin, L. 1886. Recherches sur l'anatomie des brachiopodes inarticulés. *Archives de Zoologie Expérimentale et Générale (série 2)* 4:161–303.
- Jux, U., & F. Strauch. 1966. Die mitteldevonische Brachiopoden-Gattung *Uncites* de France 1825. *Palaeontographica* 56:176–222.
- Källersjö, M., J. S. Farris, A. G. Kluge, & C. Bult. 1992. Skewness and permutation. *Cladistics* 8:275–287.
- Karlin, S., & A. M. Campbell. 1994. Which bacterium is the ancestor of the animal mitochondrial genome? *Proceedings of the National Academy of Sciences, USA* 91:12842–12846.
- Kawaguti, S. 1941. Hemerythrin found in the blood of *Lingula*. *Memoirs of the Faculty of Science and Agriculture, Taihoku Imperial University, Formosa (Zoology, Number 12)* 23:95–98.
- . 1943. A biometrical study on *Lingula unguis* (Linné). *Venus* 12(3/4):171–182.
- In Japanese.
- Kelly, P. G., P. T. P. Oliver, & F. G. E. Pautard. 1965. The shell of *Lingula unguis*. In *Proceedings of the*

- Second European Symposium on Calcified Tissue. Liège, Belgium. p. 337–345.
- Kemczyns, K. J. 1965. Significance of punctae and pustules in brachiopods. *Geological Magazine* 102:315–324.
- . 1968. Arrangements of costellae, setae and vascula in entelesteacian brachiopods. *Journal of Paleontology* 42:88–93, 1 fig.
- Kenchington, R. A., & L. S. Hammond. 1978. Population structure, growth and distribution of *Lingula anatina* (Brachiopoda) in Queensland, Australia. *Journal of Zoology* 184:63–81.
- Kimble, J. 1994. An ancient molecular mechanism for establishing embryonic polarity? *Science* 266:577–578.
- King, K., Jr., & P. E. Hare. 1972. Amino acid composition of the test as a taxonomic character for living and fossil planktonic foraminifera. *Micropaleontology* 18:285–293.
- Kirtsinghe, P. 1949. Unicellular algae in association with invertebrates. *Nature* 164:970.
- Kleiber, M. 1947. Body size and metabolic rate. *Physiological Reviews* 27:511–541.
- . 1965. Metabolic body size. In K. L. Blaxter, ed., *Energy Metabolism*. Proceedings of the 3rd Symposium, Troon, Scotland. Academic Press. London. p. 427–435.
- Klippenstein, G. L. 1980. Structural aspects of haemerythrin and myohaemerythrin. *American Zoologist* 20:39–51.
- Kniprath, E. 1975. Das Wachstum des Mantels von *Lymnaea stagnalis* (Gastropoda). *Cytobiologie* 10:260–267.
- Knowlton, N. 1993. Sibling species in the sea. *Annual Review of Ecology and Systematics* 24:189–216.
- Kolesnikov, C. M., & E. L. Prosorovskaya. 1986. Biochemical investigation of Jurassic and recent brachiopod shells. In P. R. Rachebœuf & C. C. Emig, eds., *Les Brachiopodes Fossiles et Actuels*, Actes du 1er Congrès International sur les Brachiopodes, Brest 1985. *Biostratigraphie du Paléozoïque* 4. p. 113–119.
- Komiya, H., N. Shimizu, M. Kawakami, & S. Takemura. 1980. Nucleotide sequence of 5S ribosomal RNA from *Lingula anatina*. *Journal of Biochemistry* 88:1449–1456.
- Kovalevskiy, A. O. 1874. Nablyudeniya Nad Razvitiem Brachiopoda [On the development of the Brachiopoda]. *Izvestiya Obschestvo Liubiteley Estestvoznaniya, Anthropologii i Etnografii* [Proceedings of the Imperial Society for Natural Science, Anthropology, and Ethnology, Moscow] 14:1–40, pl. 1–5.
- In Russian.
- . 1883. Observations sur le développement des brachiopodes, Analyse par Oehlert et Deniker. *Archives de Zoologie Expérimentale et Générale* (series 2) 1:57–76.
- Kozłowski, Roman. 1929. Les brachiopodes gothlandiens de la Podolie polonaise. *Palaeontologia Polonica* 1:1–254, pl. 1–12.
- Krans, Th. F. 1965. Études morphologiques de quelques spirifères Dévonien de la Chaîne Cantabrique (Espagne). *Leidse Geologische Mededelingen* 33:73–148, 71 fig., pl. 1–16.
- Kuga, Hiroto, & Akira Matsuno. 1988. Ultrastructural investigations on the anterior adductor muscle of a brachiopod, *Lingula unguis*. *Cell Structure and Function* 13:271–279.
- Kume, M. 1956. The spawning of *Lingula*. *Natural Science Report of Ochanomizu University, Tokyo* 6:215–223.
- Kume, M., & K. Dan. 1968. *Invertebrate Embryology*. Nolit Publishing House. Belgrade. 605 p.
- LaBarbera, Michael. 1977. Brachiopod orientation to water movement. I. Theory, laboratory behavior and field observation. *Paleobiology* 3:270–287.
- . 1978. Brachiopod orientation to water movement: functional morphology. *Lethaia* 11:67–79.
- . 1981. Water flow patterns in and around three species of articulate brachiopods. *Journal of Experimental Marine Biology and Ecology* 55:185–206.
- . 1984. Feeding currents and particle capture mechanisms in suspension feeding animals. *American Zoologist* 24:71–84.
- . 1985. Mechanisms of spatial competition of *Disciniscia strigata* (Inarticulata: Brachiopoda) in the intertidal of Panama. *Biological Bulletin* 168(1):91–105.
- . 1986a. The evolution and ecology of body size. In D. M. Raup & D. Jablonski, eds., *Patterns and Processes of Life, Dahlem Konferenzen*. Springer-Verlag, Berlin, Heidelberg. p. 69–98.
- . 1986b. Brachiopod lophophores: functional diversity and scaling. In P. R. Rachebœuf & C. C. Emig, eds., *Les Brachiopodes Fossiles et Actuels*, Actes du 1er Congrès International sur les Brachiopodes, Brest 1985. *Biostratigraphie du Paléozoïque* 4. p. 313–321.
- . 1989. Analyzing body size as a factor in ecology and evolution. *Annual Review of Ecology and Systematics* 20:97–117.
- . 1990. Principles of design of fluid transport systems in zoology. *Science* 249:992–1000.
- Lacaze-Duthiers, F. J. H. de. 1861. *Histoire naturelle des Brachiopodes vivantes de la Méditerranée*. Iie Monographie. Histoire naturelle de la Thécide (*Thecidium mediterraneum*). *Annales des sciences naturelles Zoologie* (série 4) 15:259–330.
- Lankester, E. R. 1873. Summary of zoological observations made at Naples in the winter of 1871–1872. *Annals and Magazine of Natural History* (series 4) 11:81.
- Laurie, John. 1987. The musculature and vascular systems of two species of Cambrian Paterinide (Brachiopoda). *Bureau of Mineral Resources Journal of Australian Geology and Geophysics* 10:261–265.
- Law, R. H., & C. W. Thayer. 1991. Articulate fecundity in the Phanerozoic: Steady state or what? In D. I. MacKinnon, D. E. Lee, & J. D. Campbell, eds., *Brachiopods Through Time*, Proceedings of the 2nd International Brachiopod Congress, University of Otago, Dunedin, New Zealand, 1990. Balkema. Rotterdam. p. 183–190.

- Lee, D. E. 1978. Aspects of the ecology and paleoecology of the brachiopod *Notosaria nigricans* (Sowerby). *Journal of the Royal Society of New Zealand* 8:395–417.
- . 1987. Cenozoic and recent inarticulate brachiopods of New Zealand: *Discina*, *Pelagodiscus* and *Neocrania*. *Journal of the Royal Society of New Zealand* 17(1):49–72.
- LeGeros, R. Z., C.-M. Pan, S. Suga, & Norimitsu Watabe. 1985. Crystallo-chemical properties of apatite in atremate brachiopod shells. *Calcified Tissue International* 37:98–100.
- Leroy, P. 1936. "*Lingula anatina*" Lamarck (1809) dans les mers froides de Chine. *Bulletin de la Société des Sciences de Nancy* 5:121–124.
- Livingstone, A. 1983. Invertebrate and vertebrate pathways of anaerobic metabolism: evolutionary considerations. *Journal of the Geological Society of London* 140:27–37.
- Livingstone, D. R., A. De Zwann, M. Leopold, & E. Marteljn. 1983. Studies on the phylogenetic distribution of pyruvate oxidoreductases. *Biochemical Systematics and Ecology* 11:415–425.
- Lockhart, P. J., M. A. Steel, M. D. Hendy, & D. Penney. 1994. Recovering evolutionary trees under a more realistic model of sequence evolution. *Molecular Biology and Evolution* 11:605–612.
- Logan, Alan. 1979. The recent Brachiopoda of the Mediterranean Sea. *Bulletin de l'Institut Océanographique de Monaco* 72(1434):1–112, 10 pl.
- . 1983. Brachiopoda collected by CANCEP 1-111 expeditions to the south-east North Atlantic. 1976–1978. *Zoologische Mededelingen* 57:165–189, 1 pl.
- . 1988. A new thecideid genus and species (Brachiopoda, recent) from the southeast North Atlantic. *Journal of Paleontology* 62:546–551.
- . 1990. Recent Brachiopoda from the Snellius and Luymes expeditions to the Surinam-Guyana Shelf, Bonaire-Curacao, and Saba Bank, Caribbean Sea, 1966 and 1969–1972. *Zoologische Mededelingen* 63:123–136.
- . 1993. Recent brachiopods from the Canarian-Cape Verdean region: diversity, biogeographic affinities, bathymetric range and life habits. *Courier Forschungs-Institut Senckenberg, Frankfurt-am-Main* 159:229–233.
- Logan, Alan, J. P. A. Noble, & G. R. Webb. 1975. An unusual attachment of a recent brachiopod, Bay of Fundy, Canada. *Journal of Paleontology* 49:557–558.
- Long, J. A. 1964. The embryology of three species representing three superfamilies of articulate Brachiopoda. Unpublished Ph.D. thesis. University of Washington. Seattle. 184 p.
- Long, J. A., & S. A. Stricker. 1991. Brachiopoda. In A. Geise, J. S. Pearce, & V. B. Pearce, eds., *Reproduction of Marine Invertebrates*, Vol. 6. Blackwell Scientific. California. p. 47–84.
- Longhurst, A. R. 1958. An ecological survey of the west African marine benthos. Colonial Office Fishery Publications 11:1–102.
- Ludvigsen, R. 1974. A new Devonian acrotretid (Brachiopoda, Inarticulata) with unique protegular ultrastructure. *Neues Jahrbuch für Geologie und Palaeontologie, Monatshefte* 3:133–148.
- Lum, S. C., & C. S. Hammen. 1964. Ammonia excretion in *Lingula*. *Comparative Biochemistry and Physiology* 12:185–190.
- Lutz, R. A., & D. C. Rhoads. 1977. Anaerobiosis and a theory of growth line formation. *Science* 198:1222–1227.
- Mackay, Sarah, & R. A. Hewitt. 1978. Ultrastructural studies on the brachiopod pedicle. *Lethaia* 11: 331–339.
- Mackay, Sarah, D. I. MacKinnon, & Alwyn Williams. 1994. Ultrastructure of the loop of terebratulide brachiopods. *Lethaia* 26:367–378.
- MacKinnon, D. I. 1971. Perforate canopies to canals in the shells of fossil Brachiopoda. *Lethaia* 4:321–325.
- . 1974. The shell structure of spiriferide Brachiopoda. *British Museum (Natural History) Bulletin (Geology)* 25(3):189–261, 27 fig., pl. 1–32.
- . 1977. The formation of muscle scars in articulate brachiopods. *Philosophical Transactions of the Royal Society of London (series B, Biological Sciences)* 280(970):1–27, 86 fig., pl. 1–11.
- . 1991. A fresh look at growth of spiral brachidia. In D. I. MacKinnon, D. E. Lee, & J. D. Campbell, eds., *Brachiopods Through Time*, Proceedings of the 2nd International Brachiopod Congress, University of Otago, Dunedin, New Zealand, 1990. Balkema. Rotterdam. p. 147–153, 6 fig.
- MacKinnon, D. I., & Alwyn Williams. 1974. Shell structure of terebratulid brachiopods. *Palaeontology* 17(1):179–202, 3 fig., pl. 21–27.
- Macomber, R. W., & Lenore Macomber. 1983. Ribbing patterns in the brachiopod *Diceromyonia*. *Lethaia* 16:25–37.
- Maddison, W. P., M. J. Donoghue, & D. R. Maddison. 1984. Outgroup analysis and parsimony. *Systematic Zoology* 33:83–103.
- Mahajan, S. N., & M. C. Joshi. 1983. Age and shell growth in *Lingula anatina* (Lam.). *Indian Journal of Marine Sciences* 12:120–121.
- Maidak, B. L., N. Larsen, M. J. McCaughey, R. Overbeek, G. L. Olsen, K. Fogel, J. Blandy, & C. R. Woese. 1994. The ribosomal database project. *Nucleic Acids Research* 22:3485–3487.
- Malakhov, V. V. 1976. Certain stages of embryogenesis in *Cnismatocentrum sakhalienis parvum* (Brachiopoda, Testicardines) and the problem of evolution of the way of origin of coelomic mesoderm. *Zoologicheskii Zhurnal* 55:66–75.
- Manankov, I. N. 1979. Pseudopunctae in strophomenids. *Paleontological Journal* 3:332–338.
- Translation of O psevdoporakh strofomenid. *Paleontologicheskii Zhurnal* 3(13):72–78.
- Mancenido, M. O., & Miguel Griffin. 1988. Distribution and palaeoenvironmental significance of the genus *Bouchardia* (Brachiopoda, Terebratellidina): its bearing on the Cenozoic evolution of the South Atlantic. *Revista Brasileira de Geociencias* 18(2):201–211, pl. 1.
- Mano, R. 1960. On the metamorphosis of the brachiopod *Frenulina sanguinolenta* (Gmelin). *Bulletin of*

- the Marine Biological Station of Asamushi 10:171–175.
- Marshall, A. G., & L. Medway. 1976. A mangrove community in the New Hebrides, southwest Pacific. *Biological Journal of the Linnean Society* 8:319–336.
- Martinez-Chacon, M. L., & J. L. Garcia-Alcalde. 1978. La genesis del koskinoide en braquiopodos articulados. *Revista de la Facultad de Ciencias, Universidad de Oviedo* 17–19:261–279.
- Mattox, M. T. 1955. Observations on the brachiopod communities near Santa Catalina. *In Essays in the Natural Sciences in Honor of Captain Allan Hancock*. University of Southern California Press. Los Angeles. p. 73–86.
- Mauzey, K. P., C. Birkeland, & P. K. Dayton. 1968. Feeding behaviour of asteroids and escape responses of their prey in the Puget Sound region. *Ecology* 49:603–619.
- Mayzaud, P. 1973. Respiration and nitrogen excretion of zooplankton II. Studies of the metabolic characteristics of starved animals. *Marine Biology* 21:19–28.
- McCammon, H. M. 1965. Filtering currents in brachiopods measured with a thermistor flowmeter. *Ocean Science Engineering* 2:772–779.
- . 1969. The food of articulate brachiopods. *Journal of Paleontology* 43:976–985.
- . 1970. Variation in recent brachiopod populations. *Bulletin of the Geological Institutions of the University of Uppsala (new series)* 2:41–48.
- . 1971. Behaviour in the brachiopod *Terebratulina septentrionalis* (Couthouy). *Journal of Experimental Marine Biology and Ecology* 6:35–45.
- . 1973. The ecology of *Magellania venosa*, an articulate brachiopod. *Journal of Paleontology* 47:266–278.
- . 1981. Physiology of the brachiopod digestive system. *In* T. W. Broadhead, ed., *Lophophorates, Notes for a Short Course*. University of Tennessee Department of Geological Sciences, Studies in Geology 5:170–204.
- McCammon, H., & R. Buchsbaum. 1968. Size and shape variation of three recent brachiopods from the Strait of Magellan. *Antarctic Research Series* 2:215–225.
- McCammon, H. M., & W. A. Reynolds. 1976. Experimental evidence for direct nutrient assimilation by the lophophore of articulate brachiopods. *Marine Biology* 34:41–51.
- McConnell, D. 1963. Inorganic constituents in the shell of the living brachiopod *Lingula*. *Geological Society of America Bulletin* 74:363–364.
- McCrary, J. 1860. On the *Lingula pyramidata* described by Mr. W. Stimpson. *American Journal of Science Arts (series 2)* 30:157–158.
- McDaniel, N. G. 1973. A survey of the benthic macroinvertebrate fauna and solid pollutants in Howe Sound. Fisheries Board of Canada, Technical Report 385:1–64.
- Mickwitz, August. 1896. Über die Brachiopodengattung *Obolus* Eichwald. *Académie Impériale des Sciences de St. Petersburg, Mémoires (série 8)* 4(2):215 p., 7 fig., 3 pl.
- Mileikovsky, S. A. 1970. Distribution of pelagic larvae of bottom invertebrates in Kurile-Kamtchatka area. *In* V. G. Bogorov, ed., *Fauna of the Kurile-Kamtchatka Trench and Its Environment*. Nauka. Moscow. p. 124–143.
- In Russian, translated in English.
- Mineur, R. J., & J. R. Richardson. 1984. Free and mobile brachiopods from New Zealand Oligocene deposits and Australian waters. *Alcheringa* 8(3–4):327–334, fig. 1–5.
- Mohlenberg, F., & H. U. Riisgard. 1978. Efficiency of particle retention in 13 species of suspension feeding bivalves. *Ophelia* 14:239–246.
- Moore, R. C., ed. 1965. *Treatise on Invertebrate Paleontology*. Part H, Brachiopoda. The Geological Society of America & The University of Kansas Press. New York & Lawrence. xxxii + 927 p., 746 fig.
- Morse, E. S. 1873. Embryology of *Terebratulina*. *Memoirs of the Boston Society of Natural History* 2:249–264, pl. 8–9.
- . 1902. Observations on living Brachiopoda. *Memoirs of the Boston Society of Natural History* 5(8):313–386.
- Morton, J. E. 1960. The functions of the gut in ciliary feeders. *Biological Reviews* 35:92–140.
- Muir-Wood, H. M. 1934. On the internal structure of some Mesozoic Brachiopoda. *Royal Society of London Philosophical Transactions (series B)* 223:511–567, pl. 62–63.
- . 1962. On the morphology and classification of the brachiopod suborder Chonetoida. *British Museum (Natural History)*, monograph. viii + 132 p., 24 fig., 16 pl.
- . 1965. Mesozoic and Cenozoic Terebratulidina. *In* R. C. Moore, ed., *Treatise on Invertebrate Paleontology*. Part H, Brachiopoda. Geological Society of America & University of Kansas Press. Boulder & Lawrence. p. 762–816, fig. 622–695.
- Muir-Wood, H. M., & G. A. Cooper. 1960. Morphology, classification and life habits of the Productoida (Brachiopoda). *Geological Society of America Memoir* 81:477 p., 135 pl.
- Muir-Wood, H. M., G. F. Elliott, & Kotora Hatai. 1965. Mesozoic and Cenozoic Terebratellidina. *In* R. C. Moore, ed., *Treatise on Invertebrate Paleontology*. Part H, Brachiopoda. Geological Society of America & University of Kansas Press. Boulder & Lawrence. p. 816–857, fig. 696–741.
- Müller, F. 1860. Beschreibung einer Brachiopoden Larva. *Archives für Anatomie und Physiologie*:72–79.
- Neall, V. E. 1972. Systematics of the endemic New Zealand brachiopod *Neothyris*. *Journal of the Royal Society of New Zealand* 2:229–247.
- Negri, A., G. Tedeschi, F. Bonomi, J.-H. Zhang, & D. M. Kirtz. 1994. Amino-acid sequences of the alpha- and beta-subunits of hemerythrin from *Lingula reevii*. *Biochimica et Biophysica Acta* 1208:277–285.
- Nekvasilova, O., & D. Pajaud. 1969. Le mode de fixation chez *Bifolium lacazelliforme* Elliot (Thecideidae Gray, Brachiopodes) au substrat. *Casopis pro*

- Mineralogii a geologii 14:323–330.
- Nielsen, Claus. 1987. The structure and function of metazoan ciliary bands and their phylogenetic significance. *Acta Zoologica* 68(4):205–262.
- . 1991. The development of the brachiopod *Crania (Neocrania) anomala* (O. F. Müller) and its phylogenetic significance. *Acta Zoologica* 72:7–28.
- . 1994. Larval and adult characters in animal phylogeny. *American Zoologist* 34:492–501.
- . 1995. *Animal Evolution: Interrelationships of the Living Phyla*. Oxford University Press. Oxford. 467 p.
- Nixon, K. C., & J. M. Carpenter. 1993. On outgroups. *Cladistics* 9:413–426.
- Noble, J. P. A., & A. Logan. 1981. Size-frequency distributions and taphonomy of brachiopods: a recent model. *Palaeogeography, Palaeoclimatology, Palaeoecology* 36:87–105.
- Noble, J. P. A., A. Logan, & G. R. Webb. 1976. The recent *Terebratulina* community in the rocky subtidal zone of the Bay of Fundy, Canada. *Lethaia* 9:1–17.
- Nomura, S., & K. M. Hatai. 1936. A note on *Coptothyris grayi* (Davidson). *Saito Ho-on Kai Museum Research Bulletin* 10:209–217.
- Norford, B. S., & H. M. Steele. 1969. The Ordovician trimerellid brachiopod *Eodinobolus* from southeast Ontario. *Palaeontology* 12(1):161–171, pl. 32–33.
- Norman, A. M. 1893. A month on the Trondhjem. *Annals and Magazine of Natural History (series 6)* 12:340–367.
- Odhner, N. H. 1960. Brachiopoda. Report of the Swedish Deep-Sea Expedition 2(4):23.
- Ohue, T. 1937. On the coelomic corpuscles in the body fluid of some invertebrates VIII. Supplementary note on the formed elements in the coelomic fluid of some Brachiopoda. *Scientific Reports of Tohoku University (series 4, Biology)* 11:231–238.
- Olsen, G. J., H. Matsuda, R. Hagstrom, & R. Overbeek. 1994. fastDNAm1: a tool for construction of phylogenetic trees of DNA sequences using maximum likelihood. *Computer Applications in the Biological Sciences* 10:41–48.
- Onyia, A. D. 1973. Contribution to the food and feeding habit of the threadfin *Galeoides decadactylus*. *Marine Biology* 22(4):371–378.
- Õpik, A. A. 1930. Brachiopoda protremata der estlandischen Ordovizischen kukruse-stufe. *Tartu Ulikooli Geoloogia-Instituudi Toimestused Acta et Commentationes Universitatis Tartuensis* 17:1–261, pl. 1–22.
- . 1933. Über die Plectamboniten. *Tartu Ulikooli Geoloogia-Instituudi Toimestused Acta et Commentationes Universitatis Tartuensis* 28:1–79, 6 fig., pl. 1–12.
- . 1934. Über die Klitamboniten. *Tartu Ulikooli Geoloogia-Instituudi Toimestused Acta et Commentationes Universitatis Tartuensis* 39:1–239, 55 fig., pl. 1–48.
- Oró, J. & H. B. Skewes. 1965. Free amino acids on human fingertips: the question of contamination in microanalysis. *Nature* 207:1042–1045.
- Owen, G., & Alwyn Williams. 1969. The caecum of articulate Brachiopoda. *Proceedings of the Royal Society of London (series B)* 172:187–201.
- Paine, R. T. 1962a. Ecological notes on a gymnophalline *Metacercaria* from the brachiopod *Glottidia pyramidata*. *Journal of Parasitology* 48(3):509.
- . 1962b. Filter-feeding pattern and local distribution of the brachiopod *Disciniscia strigata*. *Biological Bulletin* 123:597–604.
- . 1963. Ecology of the brachiopod *Glottidia pyramidata*. *Ecological Monographs* 33:187–213.
- . 1969. Growth and size distribution of the brachiopod *Terebratalia transversa* Sowerby. *Pacific Science* 23:337–343.
- . 1970. The sediment occupied by recent lingulid brachiopods and some paleoecological implications. *Palaeogeography, Palaeoclimatology, Palaeoecology* 7:21–31.
- Palmer, A. R. 1981. Do carbonate skeletons limit the rate of body growth? *Nature* 292:150–152.
- . 1983. Relative cost of producing skeletal organic matrix versus calcification: evidence from marine gastropods. *Marine Biology* 75:287–292.
- Pan, C.-M., & Norimitsu Watabe. 1988a. Uptake and transport of shell minerals in *Glottidia pyramidata* Stimpson (Brachiopoda: Inarticulata). *Journal of Experimental Marine Biology and Ecology* 118:257–268, fig. 1–14.
- . 1988b. Shell growth of *Glottidia pyramidata* Stimpson (Brachiopoda: Inarticulata). *Journal of Experimental Marine Biology and Ecology* 119:43–53, fig. 1–21.
- . 1989. Periostracum formation and shell regeneration in the lingulid *Glottidia pyramidata* (Brachiopoda: Inarticulata). *Transactions of the American Microscopical Society* 108(3):283–289.
- Pandian, T. J., & F. J. Vernberg. 1987. *Animal Energetics, Volume 2, Bivalvia through Reptilia*. Academic Press. San Diego. 631 p.
- Patel, N. H. 1994. Developmental evolution: insights from studies of insect segmentation. *Science* 266:581–590.
- Patterson, Colin. 1985. Introduction. *In* C. Patterson, ed., *Molecules and Morphology in Evolution. Third International Congress of Systematic & Evolutionary Biology, University of Sussex, July 1985*. Cambridge University Press. p. 1–22.
- . 1989. Phylogenetic relations of major groups: conclusions and prospects. *In* B. Fernholm, K. Bremer, & H. Jörnvall, eds., *The Hierarchy of Life: Molecules and Morphology in Phylogenetic Analysis. Proceedings from Nobel Symposium 70, 1988*. Elsevier. Amsterdam. p. 471–488.
- Peck, L. S. 1989. Temperature and basal metabolism in two Antarctic marine herbivores. *Journal of Experimental Marine Biology and Ecology* 127:1–12.
- . 1992. Body volumes and internal space constraints in articulate brachiopods. *Lethaia* 25:383–390.
- . 1993. The tissues of articulate brachiopods and their value to predators. *Philosophical Transac-*

- tions of the Royal Society of London (series B) 339:17–32.
- Peck, L. S., A. Clarke, & L. J. Holmes. 1987a. Size, shape and the distribution of organic matter in the recent Antarctic brachiopod *Liothyrella uva*. *Lethaia* 20:33–40.
- . 1987b. Summer metabolism and seasonal changes in biochemical composition of the Antarctic brachiopod *Liothyrella uva* (Broderip, 1833). *Journal of Experimental Marine Biology and Ecology* 114:85–97.
- Peck, L. S., G. B. Curry, A. D. Ansell, & Mark James. 1989. Temperature and starvation effects on the metabolism of the brachiopod *Terebratulina retusa* (L.). *Historical Biology* 2:101–110.
- Peck, L. S., & L. J. Holmes. 1989a. Scaling patterns in the Antarctic brachiopod *Liothyrella uva* (Broderip, 1833). *Journal of Experimental Marine Biology and Ecology* 133:141–150, fig. 1–3.
- . 1989b. Seasonal and ontogenetic changes in tissue size in the Antarctic brachiopod *Liothyrella uva* (Broderip, 1833). *Journal of Experimental Marine Biology and Ecology* 134:25–36, fig. 1–2.
- Peck, L. S., D. J. Morris, & Andrew Clarke. 1986a. Oxygen consumption and the role of caeca in the recent Antarctic brachiopod *Liothyrella uva notorcadensis* (Jackson, 1912). In P. R. Racheboeuf & C. C. Emig, eds., *Les Brachiopodes Fossiles et Actuels, Actes du 1er Congrès International sur les Brachiopodes*, Brest 1985. *Biostratigraphie du Paléozoïque* 4. p. 349–355.
- . 1986b. The caeca of punctate brachiopods: a respiring tissue not a respiratory organ. *Lethaia* 19:232, fig. 1.
- Peck, L. S., D. J. Morris, A. Clarke, & L. J. Holmes. 1986. Oxygen consumption and nitrogen excretion in the Antarctic brachiopod *Liothyrella uva* (Jackson, 1912) under simulated winter conditions. *Journal of Experimental Marine Biology and Ecology* 104:203–213.
- Peck, L. S., & K. Robinson. 1994. Pelagic larval development in the brooding Antarctic brachiopod *Liothyrella uva*. *Marine Biology* 120:279–286.
- Pedersen, Fl. Bo. 1978. A brief review of present theories of fjord dynamics. In C. J. Nihoul, ed., *Hydrodynamics of Estuaries and Fjords*. Elsevier Scientific Publishing Company. Amsterdam. p. 407–422.
- Percival, E. 1944. A contribution to the life-history of the brachiopod *Terebratella inconspicua* Sowerby. *Transactions of the Royal Society of New Zealand* 74:1–23, pl. 1–7.
- . 1960. A contribution to the life history of the brachiopod *Tegulorhynchia nigricans*. *Quarterly Journal of Microscopical Science* 101:439–457.
- Philippe, Hervé, A. Chenail, & A. Adoutte. 1994. Can the Cambrian explosion be inferred through molecular phylogeny? In M. Akam, P. Holland, P. Ingham, & G. Wray, eds., *The Evolution of Developmental Mechanisms*. Development, 1994 Supplement. Company of Biologists. Cambridge. p. 15–25.
- Plenk, H. 1913. Die Entwicklung von *Cistella (Argiope) neopolitana*. *Arbeiten aus dem Zoologischen Institute der Universitaet Wien und der Zoologischen Station in Triest*, Wien 20:93–108.
- Popov, L. Ye. 1992. The Cambrian radiation of brachiopods. *Topics in Geobiology* 10:399–423, 6 fig.
- Popov, L. Ye., M. G. Bassett, L. E. Holmer, & J. Laurie. 1993. Phylogenetic analysis of higher taxa of Brachiopoda. *Lethaia* 26:1–5.
- Popov, L. Ye., & Yu. A. Tikhonov. 1990. Rannekembriiskie brachiopody iz iuzhnoi Kirgizii [Early Cambrian brachiopods from south Kirgizii]. *Paleontologicheskii Zhurnal* 1990(3):33–44, 2 fig., pl. 3–4.
- Popov, L. Ye., & G. T. Ushatinskaya. 1987. Novyye dannyye o mikrostrukture rakoviny bezzamkovykh brachiopod otrjada Paterinida [New data on the microstructure of the shell in inarticulate brachiopods of the Order Paterinida]. *Doklady Akademii Nauk Soyuzsa Sovetskikh Sotsialisticheskikh Republik [Academy of Sciences of the USSR, Reports]* 293(5):1228–1230.
- Popov, L. Ye., O. N. Zezina, & J. Nolvak. 1982. Mikrostruktura apikal'noy chasti rakoviny bezzamkovykh brachiopod i eye paleoecologicheskoye znachenie [Microstructure of the apical part of the shell in inarticulate brachiopods and its paleoecological significance]. *Byulletin' Moskovskogo obshchestva ispytatelej prirody, otdel biologicheskij [Moscow Society of Natural History, Branch of Biology, Bulletin]* 87:94–104.
- Poulsen, V. 1971. Notes on an Ordovician acrotretacean brachiopod from the Oslo region. *Bulletin of the Geological Society of Denmark* 20:265–278.
- Powls, R., & G. Britton. 1976. A carotenoprotein violaxanthin, isolated from *scenedesmus obliquus* D3. *Biochimica et Biophysica Acta* 453:270–276.
- Prenant, M. 1928. Notes histologiques sur *Terebratulina caput-serpentis* L. *Bulletin de la Société Zoologique de France* 59:113–125.
- Pross, A. 1980. Untersuchungen zur Gliederung von *Lingula anatina* (Brachiopoda). *Archimerie bei Brachiopoden*. *Zoologische Jahrbücher, abteilung für Anatomie und Ontogenie der Tiere* 103:250–263.
- Punin, M. Y., & M. V. Filatov. 1980. The epithelium organisation in the digestive gland of the articulate brachiopod *Hemithyris psittacea*. *Citologija* 22(3):277–286.
- In Russian.
- Racheboeuf, P. R. 1973. Données nouvelles sur le développement des épines chez certains Brachiopods Chonetacea du Massif Armoricain. *Comptes-Rendus de l'Académie des Sciences de Paris* 277(D):1741–1744.
- Racheboeuf, P. R., & Paul Copper. 1990. The mesolophe, a new lophophore type for chonetacean brachiopods. *Lethaia* 23(4):341–346, 5 fig.
- Raff, R. A., C. R. Marshall, & J. M. Turbeville. 1994. Using DNA sequences to unravel the Cambrian

- radiation of the animal phyla. *Annual Review of Ecology and Systematics* 25:351–375.
- Ramamoorthi, K., K. Venkataramanujam, & B. Srikrishnadhas. 1973. Mass mortality of *Lingula anatina* (Lam.) (Brachiopoda) in Porto-Novo waters, S. India. *Current Science* 42(8):285–286.
- Rand, D. M. 1993. Endotherms, ectotherms and mitochondrial genome-size variation. *Journal of Molecular Evolution* 37:281–295.
- Reed, C. G. 1987. Phylum Brachiopoda Coast. In M. Strathmann, ed., *Reproduction and Development of Marine Invertebrates of the Northern Pacific*. University of Washington Press. Seattle. p. 486–493.
- Reed, C. G., & R. A. Cloney. 1977. Brachiopod tentacles: ultrastructure and functional significance of the connective tissue and myoepithelial cells in Terebratalia. *Cell and Tissue Research* 185:17–42.
- Regnault, M. 1987. Nitrogen excretion in marine and fresh-water Crustacea. *Biological Reviews* 62:1–24.
- Reynolds, W. A., & H. M. McCammon. 1977. Aspects of the functional morphology of the lophophore in articulate brachiopods. *American Zoologist* 17:121–132.
- Rhodes, M. C. 1990. Extinction patterns and comparative physiology of brachiopods and bivalves. Ph.D. thesis, Department of Geology, University of Pennsylvania. Philadelphia. 152 p.
- Rhodes, M. C., & C. W. Thayer. 1991. Effects of turbidity on suspension feeding: Are brachiopods better than bivalves? In D. I. MacKinnon, D. E. Lee, & J. D. Campbell, eds., *Brachiopods Through Time*, Proceedings of the 2nd International Brachiopod Congress, University of Otago, Dunedin, New Zealand, 1990. Balkema. Rotterdam. p. 191–196.
- Rhodes, M. C., & R. J. Thompson. 1992. Clearance rate of the articulate brachiopod *Neothyris lenticularis* (Deshayes, 1839). *Journal of Experimental Marine Biology and Ecology* 163:77–89.
- . 1993. Comparative physiology of suspension feeding in living brachiopods and bivalves: evolutionary implications. *Paleobiology* 19:322–334.
- Richards, J. R. 1952. The ciliary feeding mechanism of *Neothyris lenticularis* (Deshayes). *Journal of Morphology* 90:65–91, fig. 1–6.
- Richardson, J. R. 1973. Studies on Australian Cainozoic Brachiopods 3. The subfamily Bouchardiinae (Terebratellidae). *Royal Society of Victoria Proceedings* 86(1):127–132, pl. 7.
- . 1975. Loop development and the classification of terebratellacean brachiopods. *Palaeontology* 18(2):285–314, 4 fig., pl. 44.
- . 1979. Pedicle structure of articulate brachiopods. *Journal of the Royal Society of New Zealand* 9:415–436.
- . 1980. Studies on Australian Cainozoic brachiopods 5. The genera *Victorithyris* Allan and *Diedrothyris* nov. *Memoirs of the National Museum of Victoria* 41:43–52.
- . 1981a. Brachiopods in mud: resolution of a dilemma. *Science* 211:1161–1163.
- . 1981b. Brachiopods and pedicles. *Paleobiology* 7:87–95.
- . 1981c. Recent brachiopods from New Zealand. *New Zealand Journal of Zoology* 8:133–248.
- . 1981d. Distribution and orientation of six articulate species from New Zealand. *New Zealand Journal of Zoology* 8:189–196.
- . 1986. Brachiopods. *Scientific American* 254:100–106.
- . 1987. Brachiopods from carbonate sands of the Australian shelf. *Proceedings of the Royal Society of Victoria* 99:37–50.
- . 1991. Australasian Tertiary Brachiopoda. The subfamily Anakineticinae nov. *Proceedings of the Royal Society of Victoria* 103(1):29–45, fig. 1–5.
- . 1994. Origins and dispersal of a brachiopod family—the systematics, biogeography and evolution of the Family Terebratellidae. *Proceedings of the Royal Society of Victoria* 106:17–29.
- Richardson, J. R., & R. J. Mineur. 1981. Differentiation of species of *Terebratella* (Brachiopoda: Terebratellinae). *New Zealand Journal of Zoology* 8:163–168.
- Richardson, J. R., I. R. Stewart, & Liu Xixing. 1989. Brachiopods from Chinese Seas. *Chinese Journal of Oceanology and Limnology* 7:211–219, pl. 1–4.
- Richardson, J. R., & J. E. Watson. 1975. Form and function in a recent free living brachiopod *Magadina cumingi*. *Paleobiology* 1:379–387.
- Ricker, W. E. 1971. Methods for assessment of fish production in fresh waters. I. B. P. Handbook No. 3. Blackwell Scientific Publications. Oxford & Edinburgh, United Kingdom. 326 p.
- Rickwood, A. E. 1968. A contribution to the life history and biology of the brachiopod *Pumilus antiquatus* Atkins. *Transactions of the Royal Society of New Zealand (Zoology)* 10:163–182, 10 fig.
- . 1977. Age, growth and shape of the intertidal brachiopod *Waltonia inconspicua* Sowerby, from New Zealand. *American Zoologist* 17:63–73, fig. 1–9.
- Roberts, John. 1968. Mantle canal patterns in *Schizophoria* (Brachiopoda) from the Lower Carboniferous of New South Wales. *Palaeontology* 11(3):389–405, pl. 74–75.
- Robertson, J. D. 1989. Physiological constraints upon marine organisms. *Transactions of the Royal Society of Edinburgh, Earth Sciences* 80:225–234.
- Rokop, F. J. 1977. Seasonal reproduction of the brachiopod *Frieleia halli* and the scaphopod *Cadulus californicus* at bathyal depths in the deep sea. *Marine Biology* 43:237–246.
- Rong, J.-Y., & L. R. M. Cocks. 1994. True *Strophomena* and a revision of the classification and evolution of strophomenoid and “strophodontoid” brachiopods. *Palaeontology* 37:651–694.
- Rosenburg, G. D., & W. W. Hughes. 1991. A metabolic model for the determination of shell composition in the bivalve mollusc, *Mytilus edulis*. *Lethaia* 24:83–96.
- Rosenberg, G. D., W. W. Hughes, & R. D. Tkachuck. 1988. Intermediatory metabolism and shell growth in the brachiopod *Terebratalia transversa*. *Lethaia* 21:219–230.
- Rouse, G. W., & B. G. M. Jamieson. 1987. An ultra-

- structural study of the spermatozoa of polychaetes *Eurythoe complanata* (Amphinomidae), *Clymnella* sp. and *Micromaldane* sp. (Maldanidae), with definition of sperm types in relation to reproductive biology. *Journal of Submicroscopic Cytology* 19:573–584.
- Rowell, A. J. 1960. Some early stages in the development of the brachiopod *Crania anomala* (O. F. Müller). *Annals and Magazine of Natural History* (series 13) 3:35–52.
- . 1961. Inhalant and exhalant feeding current systems in recent brachiopods. *Geological Magazine* 98(3):261–263.
- . 1977. Valve orientation and functional morphology of the foramen of some siphonoretacean and acrotretacean brachiopods. *Lethaia* 10:43–50.
- . 1982. The monophyletic origin of the Brachiopoda. *Lethaia* 15:299–307.
- Rowell, A. J., & N. E. Caruso. 1985. The evolutionary significance of *Nisusia sulcata*, an early articulate brachiopod. *Journal of Paleontology* 59:1227–1242, fig. 1–9.
- Rowley, A. F., & P. J. Hayward. 1985. Blood cells and coelomocytes of the inarticulate brachiopod *Lingula anatina*. *Journal of Zoology, London (series A)* 205:9–18.
- Rubenstein, D. I., & M. A. R. Koehl. 1977. The mechanisms of filter feeding: some theoretical considerations. *American Naturalist* 111:981–994.
- Rudall, K. M. 1955. The distribution of collagen and chitin. Symposium of the Society for Experimental Biology 9:49–71.
- . 1969. Chitin and its association with other molecules. *Journal of Polymer Science (Part C)* 28:83–102.
- Rudwick, M. J. S. 1959. The growth and form of brachiopod shells. *Geological Magazine* 94:1–24.
- . 1960. The feeding mechanisms of spire-bearing fossil Brachiopoda. *Geological Magazine* 97:369–383, 8 fig.
- . 1961. 'Quick' and 'catch' adductor muscles in brachiopods. *Nature* 191:1021.
- . 1962a. Filter feeding mechanisms in some brachiopods from New Zealand. *Journal of the Linnean Society, Zoology* 44:592–615.
- . 1962b. Notes on the ecology of brachiopods in New Zealand. *Transactions of the Royal Society of New Zealand, Zoology* 1:327–335.
- . 1965a. Ecology and paleoecology. In R. C. Moore, ed., *Treatise on Invertebrate Paleontology. Part H, Brachiopoda*. Geological Society of America & University of Kansas Press. New York & Lawrence. p. 199–214.
- . 1965b. Sensory spines in the Jurassic brachiopod *Acanthothiris*. *Palaeontology* 8:604–617, pl. 84–87.
- . 1970. *Living and Fossil Brachiopods*. Hutchinson and Co. Ltd. London. 199 p., 99 fig.
- Runnegar, B., A. Scheltema, L. Jackson, M. Jebb, J. McC. Turbeville, & C. R. Marshall. In preparation. A molecular test of the hypothesis that Aplacophora are progenetic aculifera.
- Russell, G. R., & J. H. Subak-Sharpe. 1977. Similarity of the general designs of protochordates and invertebrates. *Nature* 266:533–535.
- Sandy, M. R. 1994. Triassic–Jurassic articulate brachiopods from the Pucará group, central Peru, and description of the brachidial net in the spiriferid *Spondylospira*. *Palaeontographica A233:99–126*.
- Sandy, M. R., & M. R. Langenkamp. 1992. The brachidial net—a unique internal support structure in the Brachiopoda? *Geological Society of America, Abstracts with Programs (Boulder)* 24(7):A226.
- Sass, D. B., E. A. Monroe, & D. T. Gerace. 1965. Shell structure of recent articulate Brachiopoda. *Science* 149:181–182.
- Satake, K., M. Yugi, M. Kamo, H. Kihara, & A. Tsugita. 1990. Hemerythrin from *Lingula unguis* consists of two different subunits, alpha and beta. *Protein Sequences and Data Analysis* 3:1–5.
- Savazzi, E. 1991. Burrowing in the inarticulate brachiopod *Lingula anatina*. *Palaeogeography, Palaeoclimatology, Palaeoecology* 85:101–106.
- Sawada, N. 1973. Electron microscope studies on gametogenesis in *Lingula unguis*. *Zoological Magazine* 82:178–188.
- Schaeffer, C. 1926. Untersuchungen zur vergleichenden Anatomie und Histologie der Brachiopodengattung *Lingula*. *Acta Zoologica, Stockholm* 7:329–402.
- Schägger, H., & G. Von Jagow. 1987. Tricine-sodium dodecyl sulfate-polyacrylamide gel electrophoresis for the separation of proteins in the range from 1 to 100 kDa. *Analytical Biochemistry* 166:368–379.
- Scheid, M. J., & J. Awapara. 1972. Stereospecificity of some invertebrate lactic dehydrogenases. *Comparative Biochemistry and Physiology* 43B:619–626.
- Scheul, H. 1978. Secretory functions of egg cortical granules in fertilisation and development. A critical review. *Gamete Research* 1:299–382.
- Schmidt, Herta. 1937. Zur Morphogenie der Rhynchonelliden. *Senckenbergiana* 19:22–60, fig. 1–56.
- Schmidt-Nielsen, K. 1979. *Animal Physiology: Adaptation and environment*, second edition. Cambridge University Press. Cambridge. 560 p.
- . 1984. *Scaling: Why is animal size so important?* Cambridge University Press. Cambridge. 241 p.
- Schram, F. R. 1983. Method and madness in phylogeny. In F. R. Schram, ed., *Crustacean Issues I: Crustacean Phylogeny*. Balkema. Amsterdam. p. 331–350.
- . 1991. Cladistic analysis of metazoan phyla and the placement of fossil problematica. In A. M. Simonetta & Simon Conway Morris, eds., *The Early Evolution of the Metazoa and the Significance of Problematic Taxa*. Cambridge University Press. Cambridge. p. 35–46.
- Schuchert, Charles, & G. A. Cooper. 1932. Brachiopod genera of the suborders Orthoidea and Pentamerioidea. *Peabody Museum of Natural History Memoir* 49(1):1–270, pl. 1–29.
- Schulgin, M. A. 1885. *Argiope kowalewskii* (ein Beitrag zur Kenntniss der Brachiopoden). *Zeitschrift für wissenschaftliche Zoologie* 41:116–141.
- Schumann, Dietrich. 1969. "Byssus" - artige

- Stielmuskel - Konvergenzen bei artikulaten Brachiopoden. Neues Jahrbuch für Geologie und Paläontologie, Abhandlungen 133:199–210.
- . 1970. Inäquivalver Schalenbau bei *Crania anomala*. *Lethaia* 3:413–421.
- . 1973. Mesodermale Endoskelette terebratulider Brachiopoden. I. Paläontologische Zeitschrift 47(1–2):77–103, 10 fig., pl. 12–15.
- . 1991. Hydrodynamic influences in brachiopod shell morphology of *Terebratalia transversa* (Sowerby) from the San Juan Islands, USA. In D. I. MacKinnon, D. E. Lee, & J. D. Campbell, eds., *Brachiopods Through Time*, Proceedings of the 2nd International Brachiopod Congress, University of Otago, Dunedin, New Zealand, 1990. Balkema. Rotterdam. p. 265–272.
- Scott, M. P. 1994. Intimations of a creature. *Cell* 79:1121–1124.
- Senn, E. 1934. Die Geschlechtsuerhaeltnisse der Brachiopoden im besonderen die Spermato—und Oogenese der *Lingula*. *Acta Zoologica* 15:1–154.
- Sewell, R. B. S. 1912. Note on the development of the larva of *Lingula*. *Records of the Indian Museum* 7:88–90.
- Shiells, K. A. G. 1968. *Kochiproductus coronus* sp. nov. from the Scottish Viséan and a possible mechanical advantage of its flange structure. *Transactions of the Royal Society of Edinburgh* 67:477–510, 20 fig., 1 pl.
- Shimizu, N., & K-I. Miura. 1972. Studies on nucleic acids of living fossils. I. Isolation and characterization of DNA and some RNA components from the brachiopod *Lingula*. *Animal ribosomes: Experimental studies of the last five years*. MSS Information Corporation. New York. p. 19–25.
- Shiple, A. E. 1883. On the structure and development of *Argiope*. *Zoologie Stazione Neapoli, Mitteilungen* 4:494–520.
- Shiple, A. E., & E. W. MacBride. 1920. *Zoology*. 4th edition. Cambridge University Press. Cambridge. 752 p.
- Short, G., & S. L. Tamm. 1991. On the nature of paddle cilia and discocilia. *Biological Bulletin, Marine Biological Laboratory, Woods Hole, Massachusetts* 180:466–474.
- Shumway, S. E. 1982. Oxygen consumption in brachiopods and the possible role of punctae. *Journal of Experimental Marine Biology and Ecology* 58:207–220.
- Simon, J. L., & D. M. Dauer. 1977. Reestablishment of a benthic community following natural defaunation. In B. C. Coull, ed., *Ecology of Marine Benthos*. University of South Carolina Press, Columbia, Belle W. Baruch Library in Marine Science 6:139–154.
- Singer, T. P. 1965. Comparative biochemistry of succinate dehydrogenase: forms and functions. In T. E. King, H. S. Mason, & M. Morrison, eds., *Oxidases and Related Redox Systems*. Wiley. New York. p. 448–481.
- Smirnova, T. N., & E. Popiel-Barczyk. 1991. Characteristics of the shell ultrastructure in Terebratellacea. In D. I. MacKinnon, D. E. Lee, & J. D. Campbell, eds., *Brachiopods Through Time*, Proceedings of the 2nd International Brachiopod Congress, University of Otago, Dunedin, New Zealand, 1990. Balkema. Rotterdam. p. 159–165.
- Smith, A. B. 1994. Rooting molecular trees: problems and strategies. *Biological Journal of the Linnean Society* 51:279–292.
- Smith, M. J., A. Arndt, S. Gorski, & E. Fajber. 1993. The phylogeny of echinoderm classes based on mitochondrial gene arrangements. *Journal of Molecular Evolution* 36:545–554.
- Soota, T. D., & K. N. Reddy. 1976. On the distribution and habitat of the brachiopod *Lingula* in India. *Newsletter of the Zoological Survey of India* 2(6):235–237.
- Steele, K. P., K. E. Holsinger, R. K. Jansen, & D. W. Taylor. 1991. Assessing the reliability of 5S rRNA sequence data for phylogenetic analysis in green plants. *Molecular Biology and Evolution* 8:240–248.
- Steele-Petrovic, H. M. 1976. Brachiopod food and feeding processes. *Palaeontology* 19:417–436.
- Stehli, F. G. 1956. Evolution of the loop and lophophore in terebratuloid brachiopods. *Evolution* 10:187–200, 9 fig.
- . 1965. Paleozoic Terebratulida. In R. C. Moore, ed., *Treatise on Invertebrate Paleontology*. Part H, Brachiopoda. Geological Society of America & University of Kansas Press. New York & Lawrence. p. 730–762, fig. 594–621.
- Steinich, G. 1965. Die artikulaten Brachiopoden der ruegener Schreibkreide (Unter-Maastricht). *Geologische und Palaeontologische Abhandlungen (Abt. A)* 2:220 p., 21 pl.
- Stewart, I. R. 1975. Morphological variation within the recent brachiopod genus *Magellania*. Unpublished thesis submitted for Geology Fellowship Diploma. Royal Melbourne Institute of Technology. 13 p.
- . 1981. Population structure of articulate brachiopod species from soft and hard substrates. *New Zealand Journal of Zoology* 8:197–208.
- St. Joseph, J. K. S. 1938. The Pentameracea of the Oslo region. *Norsk Geologisk Tidsskrift* 17:255–336, pl. 1–8.
- Storch, Volker, & Ulrich Welsch. 1972. Über Bau und Entstehung der Mantelrandstacheln von *Lingula unguis* L. (Brachiopoda). *Zeitschrift für Wissenschaftliche Zoologie (Leipzig)* 183:181–189.
- . 1974. Epitheliomuscular cells in *Lingula unguis* (Brachiopoda) and *Branchiostoma lanceolatum* (Acrania). *Cell and Tissue Research* 154:543–545.
- . 1975. Elektronenmikroskopische und enzym-histochemische Untersuchungen über die Mitteldarmdrüse von *Lingula unguis* L. (Brachiopoda). *Zoologische Jahrbücher, abteilung für Anatomie und Ontogenie der Tiere* 94:441–452.
- . 1976. Elektronenmikroskopische und enzym-histochemische Untersuchungen über Lophophor und Tentakeln von *Lingula unguis* L. (Brachiopoda). *Zoologische Jahrbücher, abteilung für Anatomie und Ontogenie der Tiere* 96:225–237.
- Stoyanova, R. Z. 1984. Alkane and fatty acid content and composition in Palaeozoic Brachiopoda fossils. *Comptes-rendus de l'Académie Bulgare des Sci-*

- ences 37(6):771–774.
- Strathmann, R. R. 1973. Function of lateral cilia in suspension feeding of lophophorates (Brachiopoda, Phoronida, Ectoprocta). *Marine Biology* 23:129–136.
- Strathmann, R. R., & D. J. Eernisse. 1994. What molecular phylogenies tell us about the evolution of larval forms. *American Zoologist* 34:502–512.
- Stricker, S. A., & C. G. Reed. 1985a. The ontogeny of shell secretion in *Terebratalia transversa* (Brachiopoda, Articulata). I. Development of the mantle. *Journal of Morphology* 183:233–250.
- . 1985b. The ontogeny of shell secretion in *Terebratalia transversa* (Brachiopoda, Articulata). II. Formation of the protegulum and juvenile shell. *Journal of Morphology* 183:251–271, fig. 1–45.
- . 1985c. Development of the pedicle in the articulate brachiopod *Terebratalia transversa* (Brachiopoda, Terebratulida). *Zoomorphology* 105:253–264.
- Suchanek, T. H., & J. Levinton. 1974. Articulate brachiopod food. *Journal of Paleontology* 48:1–5.
- Summers, R. G. 1970. The fine structure of the spermatozoon of *Penmaria tiarella* (Coelenterata). *Journal of Morphology* 131:117–130.
- Sundarsan, D. 1968. Brachiopod larvae from the west coast of India. Proceedings of the Indian Academy of Science (section B) 68:59–68.
- . 1970. On a lingulid larva from Coondapur (Mysore State), India. *Journal of the Marine Biological Association of India* 12:97–99.
- Surlyk, Finn. 1972. Morphological adaptations and population structures of the Danish chalk brachiopods (Maastrichtian, Upper Cretaceous). Kongelige Danske Videnskabernes Selskab, Biologiske Skrifter 19(2):2–57, 24 fig., pl. 1–5.
- Swedmark, B. 1967. *Gwynia capsula* (Jeffreys), an articulate brachiopod with brood protection. *Nature* 213:1151–1152.
- . 1971. A review of Gastropoda, Brachiopoda, and Echinodermata. *Smithsonian Contributions to Zoology* 76:41–45.
- Swofford, D. L. 1993. PAUP: phylogenetic analysis using parsimony. Computer program distributed by the author. Smithsonian Institution. Washington, D.C.
- Taddei Ruggiero, E. 1991. A study of damage evidence in brachiopod shells. In D. I. MacKinnon, D. E. Lee, & J. D. Campbell, eds., *Brachiopods Through Time*, Proceedings of the 2nd International Brachiopod Congress, University of Otago, Dunedin, New Zealand, 1990. Balkema. Rotterdam. p. 203–210.
- Tanaka, S., K. Anno, & N. Seno. 1982. A novel sulfated glycosaminoglycan, lingulin sulfate, composed of galactose and N-acetylgalactosamine from *Lingula unguis*. *Biochimica et Biophysica Acta* 704:549–551.
- Teichert, Curt. 1958. Cold and deep-water coral banks. *Bulletin of the American Association of Petroleum Geologists* 42:1064–1082.
- Templeton, Alan. 1989. The meaning of species and speciation: a genetic perspective. In D. Otte & J. A. Endler, eds., *Speciation and Its Consequences*. Sinauer Associates, Inc. Sunderland, Massachusetts. p. 3–27.
- Thayer, C. W. 1975. Size-frequency and population structure of brachiopods. *Palaeogeography, Palaeoclimatology, Palaeoecology* 17:139–148.
- . 1977. Recruitment, growth, and mortality of a living articulate brachiopod, with implications for the interpretation of survivorship curves. *Paleobiology* 3:98–109.
- . 1986a. Are brachiopods better than bivalves? Mechanisms of turbidity tolerance in articulate and their interaction with feeding in articulate. *Paleobiology* 12:161–174.
- . 1986b. Respiration and the function of brachiopod punctae. *Lethaia* 19:23–31.
- Thayer, C. W., & R. A. Allmon. 1990. Evolutionary refugia? Oligotrophic marine caves of Micronesia. Abstract. Fourth International Congress of Systematic and Evolutionary Biology. p. A323.
- Thayer, C. W., & H. M. Steele-Petrovic. 1975. Burrowing of the lingulid brachiopod *Glottidia pyramidata*: its ecologic and palaeoecologic significance. *Lethaia* 8:209–221.
- Thomas, G. A. 1958. The Permian Orthotetacea of Western Australia. Bureau of Mineral Resources, Geology and Geophysics, Bulletin 39:1–159.
- Thompson, R. R., & W. B. Creath. 1966. Low molecular weight hydrocarbons in recent and fossil shells. *Geochimica et Cosmochimica Acta* 30:1137–1152.
- Thompson, R. J., E. Ward, & M. C. Rhodes. 1992. *In vivo* observations of feeding in an articulate brachiopod. Abstract. Annual Marine Benthic Ecology Meeting, Newport, RI, March 1992.
- Thomson, J. A. 1918. Brachiopoda. Australasian Antarctic Expedition, 1911–1914, Scientific Reports (series C) 4:1–76, pl. 15–18.
- . 1927. Brachiopod morphology and genera (recent and Tertiary). New Zealand Board of Science and Art, Manual 7:338 p., 103 fig., 2 pl.
- Tkachuck, R. D., G. D. Rosenberg, & W. W. Hughes. 1989. Utilization of free amino acids by mantle tissue in the brachiopod *Terebratalia transversa* and the bivalve mollusc, *Chlamys hastata*. *Comparative Biochemistry and Physiology* 92B:747–750.
- Tommasi, L. R. 1970a. Sôbre o braquiopode *Bouhardia rosea* (Mawe, 1823). *Boletim do Instituto Oceanografico, Sao Paulo* 19:33–42.
- . 1970b. Observações sôbre a fauna benthico do complexo estuarino-lagunar de Cananéia. *Boletim do Instituto Oceanografico, Sao Paulo* 19(1):43–56.
- Tortell, P. 1981. Notes on the reproductive biology of brachiopods from southern New Zealand. *New Zealand Journal of Zoology* 8:175–182.
- Towe, K. M. 1980. Preserved organic ultrastructure: an unreliable indicator for paleozoic amino acid biogeochemistry. In P. E. Hare, T. C. Hoering, & K. J. King, eds., *Biogeochemistry of Amino Acids*. John Wiley & Sons. New York. p. 65–74.
- Towe, K. M., & C. W. Harper, Jr. 1966. Pholidostrophiid brachiopods: origin of the nacreous lustre. *Science* 154:153–155.
- Trueman, E. R., & T. M. Wong. 1987. The role of the

- coelom as a hydrostatic skeleton in lingulid brachiopods. *Journal of Zoology* 213(2):221–232, 3 fig.
- Tsuchiya, M., & C. C. Emig. 1983. Macrobenitic assemblages in a habitat of the recent lingulid brachiopod *Lingula anatina* Lamarck at Asamushi, Northern Japan. *Bulletin of the Marine Biological Station of Asamushi, Tohoku University* 17(3):141–157.
- Tunncliffe, Verena. 1981. High species diversity and abundance of the epibenthic community in an oxygen-deficient basin. *Nature* 294:354–356.
- Turoso, Noreen, & L. W. Fisher. 1989. The proteins in the shell of *Lingula*. In R. E. Crick, ed., *Origin, Evolution, and Modern Aspects of Biomineralization in Plants and Animals*. Plenum Press. New York. p. 325–328.
- Turoso, Noreen, & P. E. Hare. 1990. A 40 kDa protein in modern and fossil *Lingula*. In *The Sixth International Symposium on Biomineralization, Conference Abstracts*. Kyoritsu Shuppan Co. Ltd. Tokyo, Japan. p. 76.
- Ulrich, E. O., & G. A. Cooper. 1938. Ozarkian and Canadian Brachiopoda. *Geological Society of America Special Paper* 13:viii + 323 p., 14 fig., 58 pl.
- Uribe, M. E., & A. P. Larrain. 1992. Estudios biológicos en el enteropneusto *Ptychodera flava* Eschscholtz, 1825, de Bahía Concepción, Chile. I: Aspectos morfológicos y ecológicos. *Gayana, Zoología* 56(3–4):141–180.
- Ushatinskaya, G. T. 1988. Obolellidy (Brachiopody) s zamkovym sochleneniyem stvorok iz nizhnego kembriia Zabaikal'ia [Obolellids (Brachiopoda) with a hinge from the Lower Cambrian of the Transbaikal area]. *Paleontologicheskii Zhurnal* 1988(1):34–39, 1 fig., pl. 3–4.
- Vader, W. 1970. The amphipod, *Aristias neglectus* Hansen, found in association with brachiopods. *Sarsia* 43:13–14.
- Valentine, J. W., & F. J. Ayala. 1975. Genetic variation in *Freileia halli*, a deep sea brachiopod. *Deep-Sea Research* 22:37–44.
- Vallentyne, J. R. 1964. Biogeochemistry of organic matter II: Thermal reaction kinetics and transformation products of amino compounds. *Geochimica et Cosmochimica Acta* 32:1353–1356.
- Vandercammen, A., & M. Lambiotte. 1962. Observations sur les sarcoglyphes dans *Atrypa reticularis* (C. Linné, 1767). *Bulletin de l'Institut Royal des Sciences Naturelles de Belgique, Bruxelles* 38:1–15, pl. 1.
- Van Kleef, F. S. M., W. W. de Jong, & H. J. Hoenders. 1975. Stepwise degradation of the eye lens protein α -crystallin in aging. *Nature* 258:264–266.
- Vargas, J. A. 1988. Community structure of macrobenthos and the results of macropredator exclusion on a tropical intertidal mud flat. *Revista de Biología Tropical* 36(2A):287–308.
- Walker, A. O. 1909. Amphipoda Gammaridea from the Indian Ocean, British East Africa, and the Red Sea. *Transactions of the Linnean Society of London (series 2, Zoology)* 12:323–344, pl. 42–43.
- Walton, Derek. 1992. Biogeochemistry of brachiopod intracrystalline proteins and amino acids. Ph.D. thesis. University of Glasgow. 237 p.
- Walton, Derek, & G. B. Curry. 1991. Amino acids from fossils, facies and fingers. *Palaeontology* 34:851–858.
- Walton, Derek, Maggie Cusack, & G. B. Curry. 1993. Implications of the amino acid composition of recent New Zealand brachiopods. *Palaeontology* 36:883–896.
- Wang, Yu, Paul Copper, & Jia-Yu Rong. 1983. Distribution and morphology of the Devonian brachiopod *Punctatrypa*. *Journal of Paleontology* 57:1067–1089, 11 fig.
- Watabe, Norimitsu, & C.-M. Pan. 1984. Phosphatic shell formation in atremate brachiopods. *American Zoologist* 24:977–985.
- Webb, G. R., A. Logan, & J. P. A. Noble. 1976. Occurrence and significance of brooded larva in a recent brachiopod, Bay of Fundy, Canada. *Journal of Paleontology* 50:869–871.
- Weiner, S. 1983. Mollusk shell formation: isolation of two organic matrix proteins associated with calcite deposition in the bivalve *Mytilus californianus*. *Biochemistry* 22:4139–4145.
- Westbroek, Peter. 1967. Morphological observations with systematic implications on some Palaeozoic Rhynchonellida from Europe, with special emphasis on the Uncinulidae. Thesis. Leidse Geologische Mededelingen 41:1–82, 14 pl.
- Westbroek, Peter, J. Yanagida, & Y. Isa. 1980. Functional morphology of brachiopod and coral skeletal structures supporting ciliated epithelia. *Paleobiology* 6:313–330.
- Widdows, J. 1985. Physiological procedures. In B. L. Bayne, ed., *The Effects of Stress and Pollution on Marine Animals*. Praeger Scientific. New York. p. 161–178.
- Wilkins, J. L. 1978a. Adductor muscles of brachiopods: activation and contraction. *Canadian Journal of Zoology* 56:315–323.
- . 1978b. Diductor muscles of brachiopods: activation and very slow contraction. *Canadian Journal of Zoology* 56:324–332.
- . 1987. Tonic free maintenance after the decay of active state in brachiopod smooth adductor muscle. *Journal of Comparative Physiology (series B)* 157:651–658.
- Williams, Alwyn. 1953. North American stropheodontids: their morphology and systematics. *Geological Society of America Memoir* 56:67 p., 13 pl.
- . 1956. The calcareous shell of the Brachiopoda and its importance to their classification. *Biological Reviews* 31:243–287, fig. 1–7.
- . 1957. Evolutionary rates of brachiopods. *Geological Magazine* 94:201–211.
- . 1962. The Barr and lower Ardmillian series (Caradoc) of the Girvan district, southwest Ayrshire, with descriptions of the Brachiopoda. *Geological Society of London Memoir* 3:267 p., 25 pl.
- . 1963. The Caradocian brachiopod faunas of the Bala District, Merionethshire. *Bulletin of the British Museum (Natural History) Geology, Lon-*

- don 8:327–471, 13 fig., 16 pl.
- . 1965. Stratigraphic Distribution. In R. C. Moore, ed., *Treatise on Invertebrate Paleontology*. Part H, Brachiopoda. Geological Society of America & University of Kansas Press. New York & Lawrence. p. 237–250, fig. 148–154.
- . 1966. Growth and structure of the shell of living articulate brachiopods. *Nature* 211:1146–1148.
- . 1968a. Evolution of the shell structure of articulate brachiopods. *Special Papers in Palaeontology* 2:1–55, 27 fig., 24 pl.
- . 1968b. Significance of the structure of the brachiopod periostracum. *Nature* 218:551–554.
- . 1968c. Shell structure of the billingsellacean brachiopods. *Palaeontology* 11:486–490.
- . 1968d. A history of skeletal secretion among articulate brachiopods. *Lethaia* 1:268–287.
- . 1970a. Origin of laminar-shelled articulate brachiopods. *Lethaia* 3:329–342.
- . 1970b. Spiral growth of the laminar shell of the Brachiopod *Crania*. *Calcified Tissue Research* 6:11–19.
- . 1971a. Comments on the growth of the shell of articulate brachiopods. In J. Thomas Dutro, Jr., ed., *Paleozoic Perspectives: A Paleontological Tribute to G. Arthur Cooper*. Smithsonian Contributions to Paleobiology 3:47–67.
- . 1971b. Scanning electron microscopy of the calcareous skeleton of fossil and living Brachiopoda. In V. H. Heywood, ed., *Scanning Electron Microscopy. Systematic and Evolutionary Applications*. Academic Press. London & New York. p. 37–66.
- . 1973. The secretion and structural evolution of the shell of the thecideidine brachiopods. *Philosophical Transactions of the Royal Society of London (series B)* 264:439–478.
- . 1974. Ordovician Brachiopoda from the Shelve District, Shropshire. *Bulletin of the British Museum (Natural History) Geology, Supplement* 11:1–163, 11 fig., 28 pl.
- . 1977. Differentiation and growth of the brachiopod mantle. *American Zoologist* 17:107–120.
- . 1984. Lophophorates. In J. Bereiter-Hahn, A. G. Matolsky, & K. S. Richards, eds., *Biology of the Integument, Volume 1, Invertebrates*. Springer-Verlag, Berlin, Germany. p. 728–745.
- . 1990. Biomineralization in the lophophorates. In J. G. Carter, ed., *Skeletal Biomineralization: Patterns, Processes and Evolutionary Trends*. Volume I & II. Van Nostrand Reinhold. New York. p. 67–82.
- Williams, Alwyn, & C. H. C. Brunton. 1993. Role of shell structure in the classification of the orthoretidine brachiopods. *Palaeontology* 36:931–966.
- Williams, Alwyn, S. J. Carlson, C. H. C. Brunton, L. E. Holmer, & L. E. Popov. 1996. A supra-ordinal classification of the Brachiopoda. *Philosophical Transactions of the Royal Society of London B351*:1171–1193.
- Williams, Alwyn, & G. B. Curry. 1991. The micro-architecture of some acrotretide brachiopods. In D. I. MacKinnon, D. E. Lee, & J. D. Campbell, eds., *Brachiopods Through Time*, Proceedings of the 2nd International Brachiopod Congress, University of Otago, Dunedin, New Zealand, 1990. Balkema. Rotterdam. p. 133–140, fig. 1–4.
- Williams, Alwyn, Maggie Cusack, & Sarah Mackay. 1994. Collagenous chitinophosphatic shell of the brachiopod *Lingula*. *Philosophical Transactions of the Royal Society of London (series B)* 346:223–266.
- Williams, Alwyn, & R. A. Hewitt. 1977. The delthyrial covers of some living brachiopods. *Proceedings of the Royal Society of London (series B)* 197:105–129, pl. 1–7.
- Williams, Alwyn, & L. E. Holmer. 1992. Ornamentation and shell structure of acrotretoid brachiopods. *Palaeontology* 35:657–692.
- Williams, Alwyn, & Sarah Mackay. 1978. Secretion and ultrastructure of the periostracum of some terebratulide brachiopods. *Proceedings of the Royal Society of London (series B)* 202:191–209.
- . 1979. Differentiation of the brachiopod periostracum. *Palaeontology* 22:721–736.
- Williams, Alwyn, Sarah Mackay, & Maggie Cusack. 1992. Structure of the organo-phosphatic shell of the brachiopod *Disciniscia*. *Philosophical Transactions of the Royal Society of London (series B)* 337:83–104.
- Williams, Alwyn, & A. J. Rowell. 1965a. Brachiopod anatomy. In R. C. Moore, ed., *Treatise on Invertebrate Paleontology*. Part H, Brachiopoda. Geological Society of America & University of Kansas Press. New York & Lawrence. p. 1–58.
- . 1965b. Morphology. In R. C. Moore, ed., *Treatise on Invertebrate Paleontology*. Part H, Brachiopoda. Geological Society of America & University of Kansas Press. New York & Lawrence. p. 57–138, fig. 59–138.
- Williams, Alwyn, A. J. Rowell, D. V. Ager, G. F. Elliott, R. E. Grant, H. M. Muir-Wood, & F. G. Stehli. 1965. Morphological terms applied to Brachiopods. In R. C. Moore, ed., *Treatise on Invertebrate Paleontology*. Part H, Brachiopoda. Geological Society of America & University of Kansas Press. New York & Lawrence. p. 139–155.
- Williams, Alwyn, & A. D. Wright. 1961. The origin of the loop in articulate brachiopods. *Palaeontology* 4:149–176, fig. 1–13.
- . 1963. The classification of the “*Orthis testudinaria* Dalman” group of brachiopods. *Journal of Paleontology* 37:1–32, fig. 1–10, pl. 1–2.
- . 1965. Orthida. In R. C. Moore, ed., *Treatise on Invertebrate Paleontology*. Part H, Brachiopoda. Geological Society of America & University of Kansas Press. New York & Lawrence. p. 299–359, fig. 188–228.
- . 1970. Shell structure of the Craniacea and other calcareous inarticulate brachiopods. *Special Papers in Palaeontology* 7:1–51, 15 pl.
- Willmer, P. G., & P. W. H. Holland. 1991. Modern approaches to metazoan relationships. *Journal of Zoology* 224:689–694.
- Wilson, G. D. F. 1987. Speciation in the deep sea. *Annual Review of Ecology and Systematics* 18:185–207.

- Wilson, H., & R. K. Cannon. 1937. The glutamic acid-pyrrolidone carboxylic acid system. *Journal of Biological Chemistry* 119:309–331.
- Winberg, G. G. 1956. Rate of metabolism and food requirements of fishes. *Trudy Belorusskogo gosudarstvennogo universiteta Minske*. 253 p.
Translated from Russian by Fisheries Research Board of Canada, Translation Series 194, 1960.
- Winnepenninckx, B., T. Backeljau, & R. De Wachter. 1995. Phylogeny of protostome worms derived from 18S rRNA sequences. *Molecular Biology and Evolution* 12:641–649.
- Wisely, B. 1969. Preferential settlement in concavities (rugophilic behaviour) by larvae of the brachiopod *Waltonia inconspicua* (Sowerby, 1846). *New Zealand Journal of Marine and Freshwater Research* 3:237–280.
- Witman, J. D., & R. A. Cooper. 1983. Disturbance and contrasting patterns of population structure in the brachiopod *Terebratulina septentrionalis* (Couthouy) from two subtidal habits. *Journal of Experimental Marine Biology and Ecology* 73:57–79.
- Worcester, W. 1969. On *Lingula reevii*. Unpublished Master of Science thesis. University of Hawaii. 49 p.
- Wourms, J. S. 1987. Oogenesis, p. 49–187. *In* A. C. Giese, J. S. Pearse, & V. B. Pearse, eds., *Reproduction of Marine Invertebrates*. Volume 9. General aspects: seeking unity in diversity. Blackwell Scientific Publications. California. 712 p.
- Wright, A. D. 1966. The shell punctation of *Dicoelosia biloba* (Linnaeus). *Geologiska Foreningens I Stockholm Forhandlingar* 87:548–556.
- . 1981. The external surface of *Dictyonella* and of other pitted brachiopods. *Palaeontology* 24:443–481, pl. 62–71.
- Yamada, M. 1956. Notes on discinid larvae (Brachiopoda) from Osyuro, West coast of Hokkaido. *Annotated Zoology of Japan* 29:165–167.
- Yano, Hiroyuki, K. Satake, Y. Ueno, K. Kondo, & A. Tsugita. 1991. Amino acid sequence of the haemerythrin α subunit from *Lingula unguis*. *Journal of Biochemistry* 110:376–380.
- Yano, Hiroyuki, K. Satake, Y. Ueno, & A. Tsugita. 1991. The amino acid sequence of the β chain of hemerythrin from *Lingula unguis*. *Protein Sequences and Data Analysis* 4:87–91.
- Yatsu, Naukidé. 1902a. On the development of *Lingula anatina*. *Journal of the College of Science, Imperial University, Tokyo, Japan* 17(4):1–112, pl. 1–8.
- . 1902b. On the habits of the Japanese *Lingula*. *Annotationes Zoologicae Japonenses* 4(2):61–67.
- Young, J. 1884. Notes on the shell structure of *Eichwaldia capewelli*. *Geological Magazine* 1(series 3):214–218.
- Zabi, S. G. 1984. Rôle de la biomasse dans la détermination de l'“importance value” pour la mise en évidence des unités de peuplements benthiques en Lagune Ebrié (Côte d'Ivoire). *Documents Scientifiques du Centre de Recherches Océanographiques, Abidjan* 15(1/2):55–87.
- Zeina, O. N. 1961. Distribution of the deepwater brachiopod *Pelagodiscus atlanticus* (King). *Okeanology* 5(2):354–358.
In Russian.
- . 1970. Brachiopod distribution in the recent ocean with reference to problems of zoogeographic zoning. *Paleontologicheskii Zhurnal* 2:3–17.
In Russian.
- . 1975. Deep-sea brachiopods from the south-east Pacific and Scotia Sea. *Trudy Instituta Okeanologii* 103:247–258.
In Russian.
- . 1981. Recent deep-sea Brachiopoda from the western Pacific. *Galathea Report* 15:7–20.
- . 1985. Sovremennye brachiopody i problemy batial noi zony okeana [Living brachiopods and problems of the north bathyal oceans]. *Nauka*. Moscow. 247 p.
- . 1987. Brachiopods collected by BENTHEDI-Cruise in the Mozambique Channel. *Bulletin du Muséum Nationale d'Histoire naturelle de Paris (série 4)* 9:551–563.
- Zhang, J-H., & D. M. Kurtz. 1991. Two distinct subunits of hemerythrin from the brachiopod *Lingula reevii*: an apparent requirement for cooperativity in oxygen binding. *Biochemistry* 30:9121–9125.
- Zittel, K. A. von. 1880. *Handbuch der Palaeontologie*, Vol. 1, No. 4. R. Oldenbourg. München & Leipzig. p. 641–722.
- Zuckerandl, Emil, & L. Pauling. 1965. Molecules as documents of evolutionary history. *Journal of Theoretical Biology* 8:357–366.
- Zuker, Michael. 1989. On finding all suboptimal foldings of an RNA molecule. *Science* 244:48–52.
- Zwaan, A. de, M. Leopold, E. Marteyn, & D. R. Livingstone. 1982. Phylogenetic distribution of pyruvate oxidoreductases, arginine kinase and aminotransferases. *In* A. D. F. Addink & N. Spronk, eds., *Exogenous and Endogenous Influences on Metabolic and Neural Control*, Volume 2. Pergamon Press. Oxford. p. 136–137.

INDEX

- abduction 75
Abyssothyris 209, 448
 A. elongata 134
 A. sp. 211
 A. wyvillei 224, 441, 443, 449
Acanthambonia 350
Acanthobasiliola 334
Acanthocopsis unguiculata 211
Acanthopleura 201, 204, 205,
 206, 207
 A. japonica 195, 211
Acanthothiris 344
acinus (pl., acini) 84, 85, 91, 92,
 93, 94, 96
acrosome 133
Acrothele 351
Acrotreta 295, 407
activity,
 carbohydrase 94
adduction 75
adductor,
 posterior 79, 83
adminiculum 362
 dorsal 362
Aegiromena 289, 290
 A. aquila 293
Aerothyris 445, 465, 467
 A. kerguelensis 466
 A. macquariensis 466
AFDM (ash-free dry mass) 217,
 218, 219, 220, 221, 223, 225,
 227, 228, 229, 230, 235, 236,
 242
Alcyonidium 201
 A. gelatinosum 211
Aldingia 266
 A. willemoesi 468
Alisina 364, 406
Alligator mississippiensis 211
allometry 213
allozyme 192
amino acid 243, 245, 246, 247,
 248, 249, 250, 252, 254, 255
amoebocyte 74, 79, 105
Amphigenia 388
Amphithyris 113, 452, 469
ampula,
 gill 71
Anakinetica 68, 444, 445, 448
 A. cumingi 66, 445
Anastrophia 402
anderidia 381
Androctonus australis 195, 211
Aneboconcha 467
 A. obscura 466
Anemonia sulcata 211
Angulotreta 385
 A. postapicalis 269, 281
 A. triangulatus 273
annelid 201
Annuloplatidia 469
 A. indopacifica 469
Anoptambonites 395
Antedon serrata 211
anterior 364
Antigonambonites 391
 A. planus 392
antigyidium 352, 353
antiperistalsis 94, 95
anus 84, 85, 89, 166, 171, 185,
 186
apatite 243, 244
apparatus,
 brachial 159
 fiber-anchoring 134
approach,
 total-evidence 210
Apsocalymma shiellsi 306
Apsotreta 323
arch,
 jugal 374, 375
archenteron 153, 157, 159, 165,
 171
Archeochonetes 383
Arctohedra 367
area,
 cardinal 321, 360
Argentiproductus margaritaceus
 366
Argopecten 244
 A. irradians 195, 211
Argulus nobilis 195
Argyrotheca 90, 102, 113, 117,
 125, 126, 127, 148, 173, 174,
 175, 176, 177, 178, 187, 266,
 374, 459, 469
 A. baretii 134
 A. barrettiana 469
 A. cistellula 64
 A. cordata 151, 160, 165, 463
 A. cuneata 137, 151, 160, 463
 A. jacksoni 151, 158, 160
 A. johnsoni 134, 450
 A. sp. 158
arm,
 side 375
arm-sinus 159
arrangement,
 setal 338
Artemia salina 195, 211
arthropod 201
ash-free dry mass (AFDM) 217,
 218, 219, 220, 221, 223, 225,
 227, 228, 229, 230, 235, 236,
 242
astrophic (nonstrophic)
 terebratulides, rhynchonellides,
 and atrypoids 322
Athyris 334, 372, 375, 415
 A. campanesi 336
Atrypa 339, 414
 A. reticularis 258, 416
 A. spinosa 257
Aulidospira 393
Aulites brazieri 455
Austrothyris 467
autophagy 104
axis,
 brachial 113
 hinge 321, 355
axoneme 135
Bactrynum 312
 B. emmrichii 314
baculum 26, 27, 276, 279, 280
band,
 growth 17, 273, 275, 294,
 326, 329
 gastroparietal 70, 84, 87, 96,
 125, 128, 129
 ileoparietal 70, 72, 84, 96,
 128, 129
 transverse 377, 378
Barbarorthis 356
Barrandella 400
Barrosella 418
base 367
 crural 367, 368, 370, 372,
 396, 398, 401
 muscle 386, 387, 396, 403
Baupläne 209
beak 323
behavior 124, 125, 175, 178, 214
 larval 175
Bellimurina 333
bema 381
Berndtia purpurea 195, 211
Bernoulli's principle 117
Bicea 364
Biernatia 295, 385
 B. holmi 386
bifid 395
Bifolium 299
Billingsella 289, 292, 369, 411,
 412, 413
 B. lindströmi 292
Bilobia 395
Bimuria 335, 381, 398
 B. cf. buttsi 336
biomineralization 192
Bittnerula 356
blastocoel 157, 160, 163
blastomere 157, 160, 164
blastopore 153, 154, 157, 160,
 164, 165, 171, 186
blastula 155, 157, 160, 163, 164
 coeloblastula 153

- blister 403
blood 73
body,
 polar 154, 155, 156, 163
 spindle 73, 74
bootstrap 195, 197, 199, 205
botryoid 279
Botsfordia 351, 420
Bouchardia 402, 405, 444, 445
 B. antarctica 405
 B. rosea 448
braceplate 401
brachidium 98, 110, 376
 falafer 381
 short-looped 376
brachiophore 368, 369, 370, 381,
 386, 400
brachiopod,
 articulated 7, 60, 158, 207
 free-spawning 160
 gonochoristic 126, 151, 160
 nonplanktotrophic 463
 short-looped articulated 206,
 208, 377
 threefold division of the
 articulated 208
brachiotest 32, 376
brachium (pl., brachia) 84, 98,
 100, 102, 103, 105, 113, 115,
 183
 spiral 114
branch,
 descending 378
 lateral jugal 374
 long 199
Branchinecta packardi 195, 211
Branchiostoma floridae 211
Brochocarina trearnensis 320
Broeggeria 418, 419
brush 33
buccal plate 380
bud,
 pedicle 168
Bufo valliceps 211
bulb,
 pedicle 64, 65
bulla 350, 351
bundle,
 setal 165, 176
burrow 473, 474, 475, 477, 479,
 487, 488
burrowing 214
buttress,
 median 407
caecum (pl., caeca) 33, 34, 299,
 300, 303, 305, 319
Caenorhabditis elegans 211
calcite 243, 251
 prismatic 294, 295
Callinectes sapidus 195, 211
Calloria 9, 12, 14, 15, 16, 17, 32,
 95, 123, 124, 131, 132, 133,
 135, 136, 137, 139, 143, 146,
 148, 151, 154, 155, 156, 165,
 173, 177, 178, 182, 183, 186,
 251, 252, 452, 453, 264, 465,
 467
 C. inconspicua 10, 11, 12, 21,
 36, 38, 39, 40, 79, 80, 95,
 115, 117, 126, 134, 140,
 142, 144, 153, 156, 159,
 160, 211, 218, 219, 220,
 223, 230, 231, 232, 234,
 238, 248, 250, 252, 253,
 254, 256, 260, 261, 262,
 263, 264, 273, 296, 331,
 444, 455, 456, 457, 458,
 459, 460, 461, 463, 465,
 466
 C. variegata 466
 camarophorium 400
 Camarotechia sp. 248
 Camerella 369
 Campages 68, 265, 374, 468
 C. mariae 471
 canal 30, 33, 35, 36, 280, 295,
 303
 alimentary 93, 123, 171
 brachial 100, 110, 159, 168
 coelomic 71, 98
 great brachial 98
 mantle 9, 127, 128, 133
 small brachial 72, 99
 cancellothyrid 209
 Cancellothyris 67, 68, 265
 C. hedleyi 211
 canopy 33, 295, 296
 capilla 342, 343
 capillary 110
 capsule,
 follicular 139, 146, 151
 pedicle 64, 66, 356
 capture,
 particle 118
 carbohydrate 243, 245, 260, 261,
 262
 carbonate 243, 244, 255
 cardinalia 366, 367, 371, 386,
 398, 399, 402
 carotenoid 252, 253
 carotenoprotein 245, 252
 cartilage,
 hyaline 106
 catecholamine 122, 127
 cavity,
 coelomic 7, 61
 denticular 364
 mantle (brachial) 7, 46, 98,
 372, 403
 pedicle 61
 perivisceral 69
 umbonal 364, 368
 cell,
 accessory 137, 139, 140, 145,
 155
 basophil-like 93
 blood 73, 77
 ciliated coelomic (peritoneal)
 110
 coelomic epithelial 136
 core 33
 digestive 94
 follicular 136, 139, 145, 148,
 150, 152, 155, 156
 germ 136
 glandular 92
 intraepidermal 105
 intra-epithelial 104
 laterofrontal 106
 lobate 9, 12, 15, 16, 40
 mesenchyme 159
 microvillous epithelial 103
 mold of vesicular 271
 monociliated epithelial 104
 mucous (glandular) 91, 96,
 105
 musculoepithelial 91
 myoepithelial 77, 81, 82, 83,
 89, 103, 106, 110
 nurse 137, 145, 148
 nutritive 146, 150
 outer epithelial 19, 23, 30, 31,
 41, 318
 peripheral 33
 primary germ 135
 secretory 98, 104, 105
 smooth adductor 88
 smooth myoepithelial 90, 108,
 110
 squamous smooth myoepithe-
 lial 110
 striated adductor 88
 striated myoepithelial 90, 110
 vesicular 9, 12, 15, 41, 42,
 271, 272, 344, 350
 cella 392
 Centronella 374, 376, 378
 Ceratretra 410
 chamber,
 brood 148, 160
 delthyrial 388
 exhalant 119
 channel 110
 character,
 morphological 465
 character-weighting 210
 Chatwinothyris 398
 chilidium 356, 358, 359, 394
 chitin 243, 244, 245, 255, 260
 chiton 201, 210
 Chlamys 204
 C. islandica 195, 211
 Chludinophora 265, 448
 C. chuni 67
 C. incerta 67
 Christiania 381
 chromosome 189
 brachiopod 190
 cilia,
 apical 173
 Clarkeia 397

- classification 191
 cleavage 157, 160
 Cleiothyridina 370, 372
 C. seriata 399
 Clitambonites 412, 413
 C. squamatus 361
 closure,
 shell 215, 217
 coeloblastula 157
 coelomocyte 73, 74, 105, 155
 Coelospira 415
 coil,
 median 115
 plane-spiral median 115
 collagen 243, 247, 254, 255
 collar,
 pedicle 352, 353, 356, 392
 colleplax 359, 360
 colonization 464
 commissure 8, 321, 338
 component,
 principal 248, 252
 Composita 396
 C. crassa 397
 composition,
 base 191
 Compsoria 468
 connectivum 371, 372
 conspecifics 472
 consumption,
 oxygen 229, 230, 231, 232,
 233, 241
 Coptothyris 156, 165, 173, 178,
 265, 467, 471
 C. grayii 120, 154, 158
 core,
 taleolar 311
 corpus 326, 381
 coscinidium 312
 costa 327, 335, 336, 339, 340
 costella 327, 335, 338, 339, 340
 hollow 341
 Cranaena 377, 417
 Crania (Neocrania) anomala 191
C. californica 114
C. pourtelesi 114
 craniid 207, 208
 Craniops 408
 C. implicata 289
Craniscus 286, 483, 484, 493,
 499, 500, 501
Craniscus japonicus 500
Crassostrea virginica 195, 211
Crenispirifer 370, 372
 Cristatella 204
 C. mucedo 211
 cross reaction,
 immunological 209
 cruralium 370, 399, 400, 401
 sessile 400
 crus (pl., crura) 367, 369, 371,
 372, 374, 378, 380, 381
 Cryptacanthia 377, 378
 Cryptopora 448
 C. gnomon 67, 454
 Cryptotreta 279
 Ctenalosis 364
 ctenophoridium 394, 396, 397
 Cudmorella 467
 current 116
 exhalant 119
 feeding 125
 rejection 119
 Curticia 350
 cuticle 61, 62, 350
 pedicle 41, 46, 49, 347
 Cyclacantharia 313
 C. kingorum 366
 cycle,
 diploid life 189, 190
 haploid life 189, 190
 life 189, 190
 reproductive 158
 Cyrtina 356, 391, 392, 393, 402
 C. hibernica 393
 cyrtomatodont 360, 362
 Cyrtoneella 339
 Cyrtoneotella 414
 C. kukersiana 412
 Cyrtoneotreta 420
 cytokinesis 132

 Dallina 265, 468, 493
 D. septigera 137, 139, 264
 D. sp. 158
 Dallinella 265, 471
 Dallithyris 370, 372
 Dalmanella 369, 393, 396
 D. watsii 387
 Davidsonella 283
 Davidsonia 356
 Daviesiella llangollensis 258, 259,
 262
 degradation 245, 248, 249, 250
 delthyrium 353, 355, 358, 360,
 363, 364
 deltidodont 367
 deltidium 50, 354, 355, 356
 denticle 364
 denticulum 364
 deoxyribose nucleic acid (DNA)
 189
 depth 464
 Desquamatia 414, 416
 deuterolophe 375
 deuterostome 154, 199, 208, 209
 Deuterostomia 151
 development 168, 180
 lecithotrophic larval 179
Diaphanoeca grandis 211
Dicellomus 366
Diceromyonia 337
Dicoelosia 298
Dictyonella 300, 341, 360
Dictyothyris 342
 D. coarctata 343
Dielasma 377
Diestothyris 468
 D. frontalis 468
 digestion 91, 94, 228
 extracellular 94
 intracellular 94
Digonella 364
 dimorphism,
 sexual 126
Dinobolus 366, 368
Dinorthis 323, 398
 diploblast 201
Diplospirella 375
Discina 25, 28, 29, 37, 38, 44,
 53, 54, 55, 114, 233, 277, 303,
 340, 349, 499, 500, 501
 D. striata 17, 26, 27, 53, 211,
 246, 255, 260, 280, 305,
 331, 500
 discinid 207, 208
Discinisca 10, 24, 25, 44, 45, 61,
 63, 68, 70, 71, 73, 79, 84, 85,
 87, 92, 100, 114, 115, 122,
 123, 136, 168, 172, 176, 179,
 183, 233, 243, 244, 347, 349,
 351, 420, 483, 488, 492, 497,
 499, 500, 501
 D. laevis 129, 171
 D. lamellosa 74, 121, 128, 170
 D. sp. 158, 159
 D. striata 254
 D. strigata 223, 225
 D. tenuis 211, 246, 254, 257,
 259
Discradisca 480, 481, 492, 494,
 499, 500, 501
 dispersal 457, 463, 464, 465, 470,
 472
 distance,
 nucleotide 204
 distribution,
 geographical 441, 451, 463
 size-frequency 457, 459, 460
 disturbance,
 growth 329, 331
 diversification 472
 diverticulum,
 digestive 84, 85, 90, 91, 93,
 94, 95, 96, 97, 98, 99, 167,
 169, 171, 185, 186
 division,
 meiotic 132, 156
 DNA (deoxyribose nucleic acid)
 189
 fingerprinting 210
Doleroides 341
Dolerorthis 414, 415
Douvillina 401, 404
 D. arcuata 404
 drape 272
 duplication,
 gene 192
Dyscolia 102, 112
 D. sp. 211
Dyscritosia 467
 D. secreta 466

- ear 364
 Echinoconchus 395
 Echinorhinus cookei 211
 echiuran 201
 echmidium 376, 377
 eclosion 153
 Ecnomiosa 265, 266, 467, 468
 E. gerda 464, 468
 ectoderm 153
 ectoproct 195, 197, 199, 203
 gymnolaemate 201
 phylactolaemate 201
 efficiency,
 particle-retention 223
 egg 132, 135, 160
 Eisenia foetida 195, 211
 Elisia 343
 emboly 153
 embryo 120, 153, 154, 166
 embryology 151, 208
 Emiliania huxleyi 260
 Enantiosphen 326, 380
 E. vicaryi 382
 endemicity 210
 endemics 472
 endoderm 153, 171
 endopuncta 295, 296, 297, 298,
 299, 300, 318
 endospine 311, 312
 Enteleter 339, 371
 enterocoel 165
 enterocoely 154, 163
 entrainment,
 viscous 117
 enzyme,
 activity 237, 238, 239, 240,
 241
 digestive 228
 Eoconulus 350
 Eodevonaria 364
 Eodinobolus 366, 406, 408
 Eohemithiris 396, 445
 Eoorthis 412
 Eopectodonta 305, 383
 E. transversalis 305
 Eospirifer 356
 Ehippelasma 295, 384, 385
 epidermis,
 tentacular 103
 Epimienia australis 195, 211
 epistome 159, 183, 186
 epitaxy 275, 285
 epithelium 8, 403
 coelomic 8, 61
 germinal 128, 129, 131
 inner 9, 19, 44, 45, 50, 312,
 352
 outer 9, 18, 24, 30, 32, 40, 44,
 45, 48, 49, 281, 293, 300,
 312, 316, 347, 349, 350,
 352, 356, 358, 372, 386
 pedicle 9, 44, 45, 61, 62, 63,
 64, 347, 352, 353, 355, 358
 pyloric 92
 Epithyris oxonica 248
 erythrocyte 73, 74, 77
 esophagus 84, 85, 89, 93, 94, 100,
 101, 121, 159, 167, 186, 371
 Eucalathis murrayi 67
 Eurypelma californica 195, 211
 exchange,
 gaseous 104
 excretion 233, 237
 ammonia 234, 235, 236, 237
 nitrogen 116
 expression,
 differential gene 192
 expuncta 340, 341
 extension,
 caecal 295
 extropuncta 305, 309, 310, 311
 eyespot 125, 170, 171, 172, 173

 face,
 terminal 18, 282, 294, 318
 factor,
 abiotic 451
 physical 452, 453, 456
 falafer 381
 Falafer epidelus 384
 Fallax 71, 75, 202, 205, 206, 468
 F. dalliniformis 126, 363
 F. neocaledonensis 211
 family,
 gene 192
 Fardenia 307
 F. scotica 307, 308
 Fascicostella 335
 feces 94, 116
 fecundity 151
 feeding 116, 117, 118, 222
 fenestra 299
 fertilization 144, 153, 154, 155,
 176, 177
 fiber 18, 32, 280, 282, 283, 284,
 293, 294, 295, 318
 collagen 106, 108
 muscle 75, 110, 167
 nerve 107, 125, 131, 132, 174
 rosette of 312
 secondary 354
 unsheathed nerve 123
 field,
 myofilament 83
 filum 272, 273, 316, 332, 340,
 342
 filament,
 acrosome 156
 Finkelnburgia 412, 413
 Fitzroyella 417
 flange,
 cardinal 372, 394, 395, 396,
 397, 399
 dental 362
 flexor 272
 setal 58
 flow,
 exhalant 98, 118
 gene 189, 210
 inhalant 98, 118
 laminar 116
 turbulent 116
 water 116
 Floweria 414
 fluid,
 coelomic 61, 71, 131
 extrapallial 26
 fluorapatite,
 carbonate 243, 244
 FMRFamide 127
 fold,
 brachial 183
 folding,
 alternate 327
 folium 286, 287
 follicle 42, 50, 51, 52, 53, 56, 57,
 299, 338, 339
 setal 71
 foramen 349, 350, 351, 352, 355,
 356, 359
 dorsal 372, 396, 398
 supra-apical 352
 force,
 London-van der Waals 119
 form,
 long-looped 206, 208, 376,
 377
 formation,
 coelom 209
 fossette,
 crural 363
 Fosteria 467
 F. spinosa 466
 francolite 243, 244
 Frenulina 135, 136, 137, 146,
 176, 177, 182, 186, 265, 468
 F. sanguinolenta 134, 146,
 158, 160, 173, 451, 471
 frequency,
 nearest-neighbor base doublet
 191
 Frieleia halli 134, 158, 160
 Fundulus heteroclitus 211
 funnel,
 nephridial 146
 Fusispirifer 397

 Gacella insolita 290
 GAGs (glycosaminoglycans) 243,
 245, 261
 Gallus gallus 211
 gamete 144, 178
 gametogenesis 145, 190

- ganglion 121, 167
 apical 122, 127
 subenteric 105, 121, 122, 123
 supraenteric 121, 122
 ventral 122, 126, 127
- gap,
 neurological 123
- gape 7
- gastrula 153, 159
- gastrulation 153, 157, 160, 163,
 164, 175
- Gefonia 374, 377
- gene 189
 embryonic axis-determining
 210
 mitochondrial SSU (12S) 193
 mitochondrial LSU (16S) 193
- genealogy 191
- genetics,
 population 192
- generalist 442, 443, 444, 445,
 452, 455
- genetic,
 information 189
 marker 189
- genome 189, 191
 complexity 189, 190
 mitochondrial (mtDNA) 189,
 190
 nuclear 189
- Gigantoproductus 381
- Glaciarcua 468
G. spitzbergensis 224
- Globirhynchia subobsoleta 248
- Globithyris 372
- Glossorthis 398
G. tacens 391
- Glottidia 12, 24, 25, 40, 44, 61,
 62, 63, 64, 65, 69, 71, 72, 76,
 77, 104, 106, 119, 121, 122,
 125, 147, 157, 166, 170, 179,
 183, 206, 244, 276, 278, 315,
 316, 418, 473, 476, 478, 481,
 482, 484, 485, 486, 487, 488,
 489, 490, 492, 494, 497, 499,
 500, 501
G.? 500
G. albida 130, 500
G. pyramidata 14, 17, 47, 56,
 61, 103, 127, 130, 152,
 158, 160, 180, 190, 211,
 229, 237, 238, 244, 246,
 254, 257, 258, 260, 261,
 274, 279, 476, 479
- Glycera 204
G. americana 195, 211
- glycosaminoglycans (GAGs) 243,
 245, 261
- Glyptoria 367
- Glyptorthis 334, 398
- gonad 126, 128, 129
 hermaphroditic 132, 140
- Gondwana 471, 472
- Goniobrochus 112
- gonocoel 411, 412, 417
- gonoduct 95
- granule 24, 26, 29, 276, 340, 342
 cortical 143, 145, 146, 148,
 150, 152
 pigment 125, 173, 174
 yolk 136
- grille 340, 345
- groove,
 brachial 84, 101, 105, 183
 brachial food 93, 98
 food 108, 118
 pedicle 347
 periostracal 14, 45
 setal 347
- group,
 monophyletic 201, 208
 sister 191
 sister, relationship of phoronids
 and craniids 208
- growth,
 hemiperipheral 321
 holoperipheral 321, 352, 359
 intussusceptive 343
 line 329
 mixoperipheral 321
 spiral 23, 285, 287
- Gryphus 21, 50, 59, 117, 121,
 143, 207, 209, 265, 266, 294,
 374, 377, 493
G. sp. 158
G. vitreus 11, 120, 123, 139,
 160, 211, 228, 264, 265,
 266, 295, 445, 447, 453
- Gusarella gusarensis 248
- gut 90, 91, 93, 166, 173, 175,
 184, 186
- gutter,
 brachial 115
- Gwynia 16, 112, 469
G. capsula 12, 67, 120, 148,
 160, 178, 448, 463
- Gypidula 369, 389, 400, 401
G. dudleyensis 390, 401
- Gyrothyris 265, 445, 467
G. mawsoni 134, 211, 248,
 466
- halkieriid 209, 210
- halo 331
- hatching 153, 154, 159, 164
- heart 72, 130
- Hebertella 398
- Heliomedusa 404
- hemerythrin 73, 192, 233, 234
- Hemithyris 70, 75, 90, 91, 92,
 108, 110, 117, 120, 154, 156,
 163, 173, 177, 178, 186, 256,
 338, 339, 396, 412, 417
- H. psittacea* 64, 93, 103, 134,
 144, 148, 154, 158, 160,
 180, 211, 224, 225, 227,
 228, 229, 230, 231, 232,
 234, 247, 314, 319, 387,
 388, 463
H. sp. 160
- hemostasis 74
- Herdmania momus 211
- heredity,
 mechanism of 189
- hermaphrodite 126, 160
- hermaphroditism 151
- Hesperorthis 339, 356, 368, 369
H. australis 362
- Heterodon platyrhinos 211
- heterophagy 104
- hinge 364
- Hisingerella 282
H. tenuis 281
- Holorhynchus 389
- homeochilidium 352
- homeodeltidium 325, 352, 366
- Homo sapiens 211
- homology 209
- homoplasmy 191, 199
- Huenella 388
- Hungaritheca 380
- hydrodynamics 117
- Hypogastura sp. 211
- hypothesis,
 molecular-clock 193
- Hypothyridina 397
- Hypsomyonia 402
- identity,
 amino-acid 192
- Imbricatia 369
- immunology 261, 265
- immunotaxonomy 209
- index,
 retention (RI) 201, 204
 support 205
- infrastructure 16
- ingroup 199
- insemination,
 artificial 451
- intensity,
 light 452, 456
- interarea 321, 322, 356, 364, 368,
 394
- intercrystalline 245, 246, 247,
 248, 249, 251, 256, 258, 260,
 261
- interspace 339, 340
- intestine 84, 89, 90, 93, 166, 167,
 171, 185
- intracrystalline 245, 246, 247,
 249, 250, 252, 253, 254, 255,
 256, 258, 260, 261

- isolation,
geographical 210
- Jaffaia jaffaensis 466, 467
- Jolonica 265, 467
- jugum 373, 374, 380
arm of the 375
- junction 124
myoneural 106, 125
septate 124
- Juresania 291
- juvenile 154, 168, 182, 183, 186
- Kaysrerella 400
- Kayseria 375
- Kingena 46
- kingenid 266
- Kirtisinghe 489
- Koninckina 375
- Kotujella 284
- Kraussina 265, 266, 464, 469
K. rubra 264
- krassinid 206
- Kulumbella 333
- Kutorgina 364, 367
- Lacazella 19, 59, 82, 90, 113,
120, 126, 137, 148, 151, 160,
165, 173, 174, 177, 187, 283,
287, 358, 470
L. mediterranea 33, 126, 127,
151, 160, 163, 178, 296,
331, 463
- lamella 334, 335, 342, 343
accessory 375
ascending 377, 378
descending 376, 377
primary 373
- lamina 23, 26, 276
botryoidal 30, 277
camerate 278, 295
columnar 278, 295
compact 30, 276, 277, 279,
280
crested 289
genital 128, 129, 130, 131,
132, 135, 136, 137, 139,
141
intra-septal 389
tubular 284, 285, 286
- lamination,
cross-bladed 287, 288, 289,
291, 293
tabular 284
- Lampetra aeopyptera 211
- Langella 418
- Lanice conchilega 195, 211
- Laqueus 50, 104, 105, 108, 117,
118, 119, 202, 205, 206, 209,
265, 364, 370, 372, 417, 467
L. blanfordi 468
L. californianus 116, 134, 160,
211, 223, 224, 225, 229,
230, 231, 232, 238, 444,
468
- L. californicus 103, 246, 247
- L. quadratus 468
- L. rubellus 252, 253, 256, 264
- larva 120, 124, 125, 126, 127,
151, 153, 154, 163, 164, 169,
173
brooded 158, 463
drift 179
free-swimming 160, 166, 176
lecithotrophic 151, 160, 179,
184
planktotrophic 122, 151, 160,
178, 463
- Latimeria chalumnae 211
- lattice,
genital 133
- layer 14
basal 14, 16
chitin 24
primary 22, 26, 268, 269, 270,
271, 272, 275, 276, 300,
332, 335, 340, 341
primary shell 17, 343
secondary shell 18, 22, 26,
268, 275, 276, 278, 282,
285, 286, 289, 294, 318,
332, 334, 335, 338, 339,
340, 341, 344, 362, 364,
376
tertiary 21, 268, 293, 294, 295
- Leiorhynchus 417
- Leptaena 333, 412, 413, 414
- Leptagonia 308
L. caledonica 310
- Leptella 398
- Leptellina 381, 383, 414
L. tennesseensis 362
- Leptodus cf. richthofeni 309
- Leptothyrella 114
L. incerta 379
- Levitusia 381
- life,
planktonic 169
- life-style 443, 465
- Limicolaria kambeul 195, 211
- line,
hinge 321, 322
- Lingula 10, 24, 25, 28, 29, 36,
37, 44, 45, 50, 51, 54, 55, 56,
57, 61, 62, 69, 72, 73, 76, 77,
80, 81, 82, 83, 85, 87, 91, 92,
93, 94, 100, 105, 110, 123,
125, 130, 132, 133, 134, 135,
136, 137, 139, 146, 147, 155,
156, 157, 166, 170, 171, 172,
179, 183, 186, 190, 192, 193,
243, 244, 246, 255, 260, 269,
274, 276, 303, 312, 323, 332,
347, 349, 412, 418, 419, 473,
476, 478, 479, 481, 482, 483,
484, 485, 487, 488, 489, 490,
492, 493, 494, 497, 498, 499,
501
L.? 500
L. adamsi 109, 110, 111, 112, 113, 114, 115, 116, 117, 118, 119, 120, 121, 122, 123, 124, 125, 126, 127, 128, 129, 130, 131, 132, 133, 134, 135, 136, 137, 138, 139, 140, 141, 142, 143, 144, 145, 146, 147, 148, 149, 150, 151, 152, 153, 154, 155, 156, 157, 158, 159, 160, 161, 162, 163, 164, 165, 166, 167, 168, 169, 170, 171, 172, 173, 174, 175, 176, 177, 178, 179, 180, 181, 182, 183, 184, 185, 186, 187, 188, 189, 190, 191, 192, 193, 194, 195, 196, 197, 198, 199, 200, 201, 202, 203, 204, 205, 206, 207, 208, 209, 210, 211, 212, 213, 214, 215, 216, 217, 218, 219, 220, 221, 222, 223, 224, 225, 226, 227, 228, 229, 230, 231, 232, 233, 234, 235, 236, 237, 238, 239, 240, 241, 242, 243, 244, 245, 246, 247, 248, 249, 250, 251, 252, 253, 254, 255, 256, 257, 258, 259, 260, 261, 262, 263, 264, 265, 266, 267, 268, 269, 270, 271, 272, 273, 274, 275, 276, 277, 278, 279, 280, 281, 282, 283, 284, 285, 286, 287, 288, 289, 290, 291, 292, 293, 294, 295, 296, 297, 298, 299, 300, 301, 302, 303, 304, 305, 306, 307, 308, 309, 310, 311, 312, 313, 314, 315, 316, 317, 318, 319, 320, 321, 322, 323, 324, 325, 326, 327, 328, 329, 330, 331, 332, 333, 334, 335, 336, 337, 338, 339, 340, 341, 342, 343, 344, 345, 346, 347, 348, 349, 350, 351, 352, 353, 354, 355, 356, 357, 358, 359, 360, 361, 362, 363, 364, 365, 366, 367, 368, 369, 370, 371, 372, 373, 374, 375, 376, 377, 378, 379, 380, 381, 382, 383, 384, 385, 386, 387, 388, 389, 390, 391, 392, 393, 394, 395, 396, 397, 398, 399, 400, 401, 402, 403, 404, 405, 406, 407, 408, 409, 410, 411, 412, 413, 414, 415, 416, 417, 418, 419, 420, 421, 422, 423, 424, 425, 426, 427, 428, 429, 430, 431, 432, 433, 434, 435, 436, 437, 438, 439, 440, 441, 442, 443, 444, 445, 446, 447, 448, 449, 450, 451, 452, 453, 454, 455, 456, 457, 458, 459, 460, 461, 462, 463, 464, 465, 466, 467, 468, 469, 470, 471, 472, 473, 474, 475, 476, 477, 478, 479, 480, 481, 482, 483, 484, 485, 486, 487, 488, 489, 490, 491, 492, 493, 494, 495, 496, 497, 498, 499, 500, 501, 502, 503, 504, 505, 506, 507, 508, 509, 510, 511, 512, 513, 514, 515, 516, 517, 518, 519, 520, 521, 522, 523, 524, 525, 526, 527, 528, 529, 530, 531, 532, 533, 534, 535, 536, 537, 538, 539, 540, 541, 542, 543, 544, 545, 546, 547, 548, 549, 550, 551, 552, 553, 554, 555, 556, 557, 558, 559, 560, 561, 562, 563, 564, 565, 566, 567, 568, 569, 570, 571, 572, 573, 574, 575, 576, 577, 578, 579, 580, 581, 582, 583, 584, 585, 586, 587, 588, 589, 590, 591, 592, 593, 594, 595, 596, 597, 598, 599, 600, 601, 602, 603, 604, 605, 606, 607, 608, 609, 610, 611, 612, 613, 614, 615, 616, 617, 618, 619, 620, 621, 622, 623, 624, 625, 626, 627, 628, 629, 630, 631, 632, 633, 634, 635, 636, 637, 638, 639, 640, 641, 642, 643, 644, 645, 646, 647, 648, 649, 650, 651, 652, 653, 654, 655, 656, 657, 658, 659, 660, 661, 662, 663, 664, 665, 666, 667, 668, 669, 670, 671, 672, 673, 674, 675, 676, 677, 678, 679, 680, 681, 682, 683, 684, 685, 686, 687, 688, 689, 690, 691, 692, 693, 694, 695, 696, 697, 698, 699, 700, 701, 702, 703, 704, 705, 706, 707, 708, 709, 710, 711, 712, 713, 714, 715, 716, 717, 718, 719, 720, 721, 722, 723, 724, 725, 726, 727, 728, 729, 730, 731, 732, 733, 734, 735, 736, 737, 738, 739, 740, 741, 742, 743, 744, 745, 746, 747, 748, 749, 750, 751, 752, 753, 754, 755, 756, 757, 758, 759, 760, 761, 762, 763, 764, 765, 766, 767, 768, 769, 770, 771, 772, 773, 774, 775, 776, 777, 778, 779, 780, 781, 782, 783, 784, 785, 786, 787, 788, 789, 790, 791, 792, 793, 794, 795, 796, 797, 798, 799, 800, 801, 802, 803, 804, 805, 806, 807, 808, 809, 810, 811, 812, 813, 814, 815, 816, 817, 818, 819, 820, 821, 822, 823, 824, 825, 826, 827, 828, 829, 830, 831, 832, 833, 834, 835, 836, 837, 838, 839, 840, 841, 842, 843, 844, 845, 846, 847, 848, 849, 850, 851, 852, 853, 854, 855, 856, 857, 858, 859, 860, 861, 862, 863, 864, 865, 866, 867, 868, 869, 870, 871, 872, 873, 874, 875, 876, 877, 878, 879, 880, 881, 882, 883, 884, 885, 886, 887, 888, 889, 890, 891, 892, 893, 894, 895, 896, 897, 898, 899, 900, 901, 902, 903, 904, 905, 906, 907, 908, 909, 910, 911, 912, 913, 914, 915, 916, 917, 918, 919, 920, 921, 922, 923, 924, 925, 926, 927, 928, 929, 930, 931, 932, 933, 934, 935, 936, 937, 938, 939, 940, 941, 942, 943, 944, 945, 946, 947, 948, 949, 950, 951, 952, 953, 954, 955, 956, 957, 958, 959, 960, 961, 962, 963, 964, 965, 966, 967, 968, 969, 970, 971, 972, 973, 974, 975, 976, 977, 978, 979, 980, 981, 982, 983, 984, 985, 986, 987, 988, 989, 990, 991, 992, 993, 994, 995, 996, 997, 998, 999, 1000
- L. anatina 15, 25, 28, 29, 30,
31, 32, 44, 46, 58, 61, 69,
74, 77, 79, 87, 95, 96, 97,
98, 99, 100, 103, 108, 111,
120, 121, 122, 127, 129,
138, 141, 143, 144, 150,
152, 158, 159, 160, 161,
163, 169, 184, 211, 214,
229, 231, 233, 234, 235,
237, 238, 244, 246, 253,
254, 255, 257, 258, 260,
261, 275, 277, 278, 279,
305, 333, 476, 482, 486
- L. bancrofti 220, 229, 230,
232
- L. reevii 201, 211, 237, 238,
482
- L. shantoungensis 244, 260
- L. unguis 233, 234
- L. unguis (= anatina) 192
- Lingulasma 342
- Lingulella 325
- lingulid 207, 208
- Linnarssonella 366
- Liothyrella 15, 21, 31, 50, 68, 72,
120, 209, 265, 269, 294, 353,
354, 356, 389
- L. antarctica 160
- L. blochmanni 134
- L. neozelanica 11, 22, 117,
134, 159, 211, 218, 219,
220, 225, 226, 227, 228,
229, 248, 264, 295, 296,
302, 450, 452, 453, 456
- L. notorcadensis 134, 460
- L. sp. 159
- L. uva 177, 211, 217, 218,
220, 221, 222, 223, 229,
230, 231, 232, 233, 235,
236, 237, 238, 242, 244
- L. uva antarctica 148, 177
- lip,
brachial 98, 100, 102, 105,
121, 177
- lipid 243, 245, 255, 256, 257,
258, 259, 260
- listrium 349
- liver 84
- lobe,
anterior 157, 182
azygous 187
inner 10
inner mantle 47
mantle 165, 168, 174, 182,
353, 412
outer mantle 12, 47, 282, 299,
305, 315, 332, 334, 347,
349, 350
pedicle 168, 174, 181
- Loboidothyris kakardinensis 248
- Lochkothele 420
- loop 372, 373, 376
acuminate 376, 377
deltiform 377, 378
retiform 377, 378

- lophophorate 192, 197
 lophophore 7, 58, 72, 98, 103,
 104, 105, 108, 111, 112, 113,
 116, 118, 121, 147, 157, 159,
 166, 168, 171, 177, 183, 184,
 186, 188, 222, 223, 224, 225,
 366, 367, 368, 371, 375, 380,
 381, 383, 385, 401, 403, 405
 brooding in the 120, 160
 homology of 209
 ptycholophous 380
 schizolophous 380, 385
 trocholophous 104, 385
 Lymnaea 39

 Macandrevia 71, 94, 100, 137,
 206, 209, 265, 266, 295, 339,
 415, 417, 468
 M. africana 297
 M. americana 451, 468, 469
 M. cranium 38, 64, 67, 134,
 137, 211, 247, 462, 468
 M. tenera 468
 Mactromeris polynyma 195, 211
 Magadina 67, 467
 M. flavescens 66
 Magadinella mineuri 448
 Magasella 58, 318, 452, 453, 465,
 467, 471, 472
 M. haurakiensis 466
 M. sanguinea 317, 444, 446,
 450, 455, 456, 458, 459,
 461, 466
 Magellania 67, 68, 71, 91, 265,
 298, 374, 465, 466, 472
 M. australis 124, 134, 271
 M. flavescens 444, 445, 460,
 465, 466, 467
 M. fragilis 466
 M. joubini 466
 M. venosa 445, 466
 Magnicanalis 364
 mantle 7, 38, 39, 58
 ventral 168, 171
 margin,
 cardinal 323, 353
 Marginifera sp. 258
 mass,
 botryoidal 29, 276
 material,
 storage 108
 mating,
 random 190
 matrix,
 distance 197
 hyaline 106
 metachromatic 106
 Maurispirifer 343
 mechanism,
 rejection 120
 Meekella 339, 400
 Meganteris 417
 Megathiris 113, 117, 265, 469
 M. detruncata 116, 160
 Megerlia 59, 202, 205, 206, 208,
 380, 265, 469
 M. truncata 60, 211, 228, 264,
 297, 379
 Megerlina 68, 202, 205, 206, 415,
 464, 469
 M. lamarckiana 450
 M. sp. 211
 meiosis 132, 190
 membrane,
 fertilization 143, 154, 156,
 160, 166
 fertilization (vitelline) 153
 inner mantle 130, 136
 mantle 134
 Mercenaria 264, 265
 M. mercenaria 260
 Merista 392
 M. tennesseensis 395
 Meristina 415
 mesentery 69
 mesocoelom 98
 mesoderm 153, 171
 mesolophe 383
 mesosoma 98
 metamorphosis 164, 165, 175,
 179, 182, 183, 186
 metanephridiopore 177
 metanephridium 70, 72, 73, 95,
 96, 97, 101, 129, 146, 148,
 167, 171, 175, 186
 metapase 154, 156
 method,
 maximum-likelihood (ML)
 197, 204
 Microcionia prolifera 211
 Micromitra 280
 micromorph 464
 micropuncta 305
 migration,
 transoceanic 471
 Mimikonstantia 312
 M. sculpta 314, 315
 mollusc 201
 eulamelibranch 201
 Monomerella 366, 421, 422
 Moorellina 283, 287, 297
 M. granulosa 285, 298
 morphology 191
 comparative 209
 spermatozoan 144
 mosaic 26, 29, 282, 283, 284, 285
 false 318, 319
 secondary layer 281
 mosaicism,
 stochastic 209
 motion,
 pendular 94
 mouth 84, 93, 98, 101, 186
 embryonic 159
 movement 441, 442, 443, 445,
 448, 463
 conveyor-belt 41
 mtDNA (mitochondrial genome)
 189, 190
 Mucrospirifer 357
- Mulinia lateralis 195, 211
 Multispinula 350
 muscle 408
 accessory diductor 76
 adductor 75, 76, 79, 80, 122,
 124, 359, 385, 386, 388,
 392, 393, 399, 400, 406,
 408
 adductor (occluser) 75
 adjustor 66, 67, 68, 75, 360,
 369, 392
 anterior adductor 80, 81, 83,
 100, 122, 125, 185
 anal 185
 anterior occluser 167
 anterocentral 408
 brachial 100
 brachial elevator 100
 brachial protractor 100, 405
 brachial retractor 100
 cardinal 407, 408
 catch (adductor) 83
 central 77, 407
 dermal 84, 406
 diductor 75, 76, 80, 88, 215,
 324, 367, 369, 385, 386,
 388, 392, 393, 394, 395,
 398, 401, 406
 diductor (divaricator) 75
 dorsal 167
 dorsal adjustor 385, 401
 esophageal 90
 internal oblique 167, 404
 lophophore elevator 76
 lophophore protractor 76, 185
 lophophore retractor 76, 183
 median 405
 median pedicle 68
 middle lateral 77, 407
 oblique 76, 77, 79, 84, 407
 oblique external 167
 oblique internal 79
 oblique lateral 79, 404
 oblique longitudinal 168
 outside lateral 77, 407
 pedicle 61, 66
 pedicle adjustor 182, 369, 372,
 401, 402
 pedicle (peduncular) 75
 posterior oblique 79
 principal valve 75
 quick (adductor) 83
 retractor 58
 smooth adductor 80, 215
 smooth (opaque) 80
 striated 80
 striated (translucent) 80
 transmedian 77, 407
 umbonal 77, 83, 406, 407
 unpaired posterior occluser
 168
 ventral 167
 ventral adjustor 76, 385, 388
 musculature 171, 184

- musculus, 452, 454, 456, 458, 464, 466
 brachialis 122
 lophophoralis 122
 occludens anterior 125
 Mutationella 282
 M. podolica 286
 myoepithelium 75, 83, 110
 myofilament 80, 81, 82, 88, 110
 myophore 372, 393, 394, 396, 397, 399
 myophragm 399, 402
 myotest 31, 386, 402
 Mystrophora 401, 403
 Mytilus 204
 M. edulis 195, 211
 M. trossulus 195, 211
 Myxine glutinosa 211

 N-terminal sequence 252, 253
 Nanothyris 370, 372
 Narynella 365
 necrosis 146
 Nematodirus battus 211
 Neoancistrocrania 479, 499, 500
 N. norfolki 500
 Neocrania 22, 31, 54, 70, 72, 73, 79, 85, 87, 89, 92, 94, 100, 110, 122, 123, 125, 130, 131, 133, 134, 135, 136, 137, 151, 153, 155, 163, 168, 171, 175, 178, 179, 181, 182, 184, 186, 273, 280, 284, 285, 301, 340, 353, 359, 404, 420, 421, 452, 479, 482, 483, 484, 489, 493, 494, 497, 499, 500, 501
 N. anomala 23, 35, 42, 43, 48, 55, 74, 105, 120, 121, 128, 130, 134, 138, 143, 144, 152, 158, 160, 161, 166, 172, 180, 185, 211, 214, 217, 218, 219, 220, 228, 246, 254, 255, 257, 259, 260, 275, 287, 302, 341, 408, 486
 N. californica 160, 223, 225
 N. huttoni 211
 N. leccointei 486, 500
 Neorhynchia profunda 134
N. sp. 211
 Neospirifer 370, 372, 381
 Neothyris 55, 206, 248, 251, 252, 258, 262, 263, 264, 265, 398, 452, 453, 465, 467, 471, 472
 N. compressa 445, 446, 448, 459, 466
 N. dawsoni 466
 N. lenticularis 134, 159, 160, 218, 219, 220, 224, 225, 226, 227, 228, 229, 230, 231, 232, 233, 241, 247, 248, 252, 253, 254, 256, 260, 261, 264, 443, 445,
- 452, 454, 456, 458, 464, 466
 N. parva 211, 248
 N. sp. 247, 258, 260, 261
 nephridiopore 95, 146
 nephridium 233, 234
 nephrostome 96, 98, 100, 102
 nerve 103, 105
 accessory and lower brachial 105
 basiepithelial 106
 brachial 122
 circumenteric 121, 122
 dorsal lophophore 122
 lateral 123
 mantle 122, 128
 marginal 123
 peritoneal 106, 125
 sensory 124
 net,
 brachidial 380
 neuron 91, 123
 neuropeptide 122
 neurophil 127
 neurotransmitter 122
 Nicolella 356, 414, 415
 N. actoniae 412
 Nipponithyris 468
 Nisusia 364, 365, 367
 notation 335, 337
 Nothorthis 398
 Notorhynchus cepedianus 211
 Notosaria 16, 17, 18, 21, 49, 50, 54, 55, 58, 66, 68, 69, 71, 75, 91, 93, 104, 105, 108, 110, 116, 120, 132, 133, 135, 136, 137, 139, 143, 148, 163, 165, 173, 174, 176, 177, 187, 248, 251, 252, 256, 269, 280, 317, 329, 353, 369, 377, 389, 398, 415, 417, 452, 453
 N. nigricans 18, 19, 51, 52, 57, 103, 114, 117, 122, 126, 134, 141, 144, 153, 159, 160, 211, 218, 219, 220, 223, 238, 247, 257, 264, 268, 283, 284, 317, 318, 330, 448, 450, 455, 456, 458, 459, 460, 463, 465
 notothyrium 324, 353, 355, 358, 368
 Nucleospira 397
 N. carlukensis 400
 nucleus,
 quantity of DNA per 189
 Numericoma 384

 O:N ratio 235, 236, 238
 Obolella 352, 364, 406, 420, 421
 Obolus 407
 ocellum (pl., ocelli) 125, 173

 Ochetostoma erythrogrammon 195, 211
 Oepikites 407, 410, 418, 419
 Oina 367, 406
 Ombonia 388
 Onchidella celtica 195, 211
 ontogeny 135, 369
 Onychotreta 322
 Onyia 489
 oocyte 135, 136, 137, 139, 143, 145, 147, 148, 150, 152, 153, 156
 primary 136, 154
 vitellogenic 131, 135, 137, 155
 oogensis 146, 190
 oogonia 131
 primary 136
 secondary 136
 oolemma 137, 140, 152
 ooplasm 145
 oosorption 74
 Opsiconidion 269
 O. aldrigei 271
 Orbiculoidea 62, 270, 323, 325, 326, 332, 340, 349
 O. forbesi 246
 O. mediorhenana 63
 O. nitida 272, 332
 Orbithele 420
 order,
 gene 190
 organ,
 excretory 70, 186
 feeding 116
 sense 124
 organogenesis 186
 orientation 443, 445, 450, 451
 origin 467, 470, 472
 ornamentation,
 concentric 329
 radial 335
 Orthambonites 339
 Orthidiella 399
 Orthorhynchula 394
 Orthostrophia 412, 413, 417
 Orthotetes 392
 Oryctolagus cuniculus 211
 outgroup 199
 selected 205, 206, 207
 ovary 134, 136, 137, 138
 ovum (pl., ova) 146, 163, 177
 Oxoplica 396

 Pachymagas 262, 263, 467
 Pachyplax 335, 396
 P. elongata 336
 P. gyralea 397, 444
 pad,
 calcite 317, 318, 319
 Pajaudina 59, 113, 470
 P. atlantica 60
 Palaeostrophomena 412, 413, 414

- Palaeotrimerella 406, 421, 422
 palintrope 321, 323
 Pamirotheca 380
 papilla 150
 holdfast 65
 paracrystalline 246, 247, 258
 Parakinetica 444, 448, 463
 P. mineuri 464
 P. stewarti 441, 442
 Paralindingia 468
 paralogy 192
 paramyosin 81, 83
 Paraspirifer 343
 Parenteletes 393
 partition,
 median 406
 Paterina 325, 418
 Paterula 418, 419
 pathway,
 metabolic 236, 237
 pattern,
 regional 464
 Paucicrura 395, 399
 Paurorthis 341
 PCA 250
 PCR (polymerase chain reaction)
 191, 193
 Pecten 251, 252
 pedicle 7, 41, 43, 49, 60, 62, 64,
 65, 66, 67, 75, 83, 122, 124,
 165, 168, 169, 179, 182, 183,
 186, 321, 325, 347, 349, 352,
 353, 356, 358, 402
 median 67
 Pelagodiscus 55, 113, 114, 171,
 173, 174, 179, 183, 347, 476,
 479, 481, 483, 484, 485, 486,
 492, 497, 498, 499, 500, 501
 P. atlanticus 166, 170, 477,
 500
 P. sp. 159
 pellet,
 fecal 95
 Penicularis 383
 Pentamerella 389, 400
 Pentamerus 400
 Perditocardinia 322
 perforation,
 koskinoid 319
 period,
 spawning 458, 459
 periostracum 12, 14, 15, 34, 36,
 46, 48, 49, 185, 267, 269, 270,
 271, 272, 275, 295, 301, 316,
 329, 332, 342, 344, 349, 350
 peristalsis 93, 94
 Petrocrania 301, 408, 421
 P. scabiosa 246, 301, 303
 Petromyzon marinus 211
 phagocyte 91, 94, 145, 155
 phagocytosis 93, 131
 Phaneropora 448
 pharynx 84, 93, 100, 123
 of Calloria 132
 Phascolosoma granulatum 195,
 211
 phase,
 planktonic larval 175
 Phylira pisum 195, 211
 Pholidostrophia 288, 311, 365
 P. cf. genticulata 290
 phoronid 195, 197, 199, 203,
 205, 206, 207, 208, 210
 diphyly of 204
 Phoronis hippocrepeia 204, 211
P. psammophila 204, 211
P. vancouverensis 204, 211
 phosphate 243
 photosensitivity 125
 phototaxis 175, 176
 Phragmophora 356
 Phragmorthis sp. cf. *P. buttsi* 403,
 406
 Phricodothyris 343
 phylum 208
 physiology 213
 Pictothyris 265, 445, 467
 P. picta 264, 468
 pillar,
 septal 378
 pinocytosis 93
 pit 341
 apical 407, 408
 cardinal 396
 larval shell 269
 post-larval shell 270, 341
 Placopecten magellanicus 195,
 211
 Plaesiomys 323, 339, 341, 417
 P. subquadrata 342
 plate 367
 brachiophore 368, 371
 cardinal 372, 396, 397
 cover 372
 crural 363, 369, 371, 372
 delthyrial 392
 deltidial 50, 354, 356
 dental 362, 364, 388, 389, 393
 fulcral 368, 370
 hinge 372, 386, 396, 398, 401
 inner 371
 inner hinge 372, 400, 401
 outer hinge 370, 371, 372
 socket 368
 surmounting 385, 408
 plate tectonics 471
 platform,
 brachial 381
 hinge 402
 muscle 406
 notothyrial 364, 368, 394, 395
 Platidia 59, 76, 207, 208, 380,
 452, 464, 469
 P. annulata 82
 P. anomioides 60, 195, 211,
 379, 451, 454, 469
 P. clepsydra 469
 P. davidsoni 126, 469
 P. spp. 158
 Platystrophia 257, 342
 Plectatrypa 372
 Plectodonta 414
 P. transversalis 365
 plectolophe 104, 115, 376, 380
 Plectorthis 341
 plexus,
 nerve 123
 Plumatella repens 211
 polarity,
 evolutionary 191
 polarization 210
 pole,
 blastoporal 160
 polychaete 192
 polymerase chain reaction (PCR)
 191, 193
 Polytoechia 391
 populations 190
 morphological variation
 between 210
 Porocephalus crotali 195, 211
 Porostictia 341
 Portneufia? 266
 postlarva 154
 potential,
 dispersal 210
 pouch,
 brachial 100
 predation 457, 461
 pressure,
 hydrostatic 98
 priapulans 192, 201
Priapulus caudatus 195, 211
 Prionoathyris 399
 prism 21
 Proboscidella 327
 process,
 apical 407, 408
 brachial 371
 cardinal 76, 324, 364, 367,
 372, 386, 393, 396, 397,
 398, 399
 crural 380
 jugal 374
 shoe-lifter 392
 product,
 gene 189
 waste 98, 116
 Productus 323
 P. horides 258
 pronucleus 157
 proparea 325, 365, 366
 prophase 136, 154
 protegulum 160, 166, 169, 183,
 186, 321, 323, 325, 332
 cuticle 157

- protein 189, 191, 243, 245, 246,
247, 248, 249, 250, 251, 252,
253, 254, 255, 256, 262
- Protorthis 388
- protostome 154, 192, 193, 203,
208, 209
- Protostomia 151
- Prototreta 273, 315, 316, 325,
385
- Protozyga 373, 375
 P. elongata 375
 P. exigua 375
- protractor 58, 272
- Pseudocrania 286, 325, 353, 404,
420, 421
- pseudocruralium 402
- pseudodeltidium 358, 359, 364,
365
- pseudointerarea 325, 350, 351,
352, 366
- Pseudolingula 277, 418, 419
- pseudopuncta 305, 306, 307, 308,
309, 310, 311, 313
- pseudosiphon 115
- pseudospondylium 388, 389
- Ptychoglyptus 333
- ptycholophe 113, 116, 381
- Ptychopleurella 343
- Pugettia quadridens 195, 211
- Pugilis 384, 395, 399
- Pugnax 417
- Pumilus 71, 100, 113, 120, 148,
173, 177, 178, 417, 452, 469
 P. antiquatus 126, 159, 160,
165
- pump,
 ciliary 116, 117
- puncta 33, 34, 300, 309, 319
- Punctatrypa 299, 342
 P. (Punctatrypa) nalivkini 299,
300
- Pygope 327
- pylorus 84, 85, 89, 90, 91, 93, 95,
186
- quadrid 395
- Rafinesquina 301, 307, 316, 396
 R. nasuta 317
- range,
 bathymetric 451
- Raninoides lousianensis 195, 211
- rate,
 clearance 224, 225, 226, 227,
228, 229
 oxygen-consumption 242
 water exchange 224
- ratio,
 sex 126
- Rattus norvegicus 211
- record,
 fossil 191
- reflection,
 growth 329
- reflex,
 shadow 124
- relationship,
 orthologous evolutionary 209
- substrate 441, 442, 450, 464
- Renssellandia 376
- Rensselaeria 374, 377
- reserve,
 yolk 141
- respiration 118
- response,
 immune 74
- Resserella 394, 396
- retraction 329, 334
- Rhinobatos lentiginosus 211
- Rhipidomella 286, 302, 341
 R. hessensis 342
- Rhizothyris 467
- rhynchonellid 206, 208
- RI (retention index) 201, 204
- ribose nucleic acid (RNA) 189,
192, 193
- ribosomal RNA (rRNA) 192, 193
 large nuclear-encoded, subunit
 (28S or LSU) 193
 small subunit (SSU) 193
 5S sequence 192, 193
 18S sequence 193
- Richthofenia 327
- ridge,
 brachial 159, 163, 381
 brachial arm 159
 inner socket 363, 364, 367,
368, 369, 370, 371, 372,
395, 396, 399
 laterofrontal epidermal 106
 socket 364, 369
- Ridgeia piscesae 195, 211
- RNA (ribose nucleic acid) 189,
192, 193
- rootlet 62, 65
 pedicle 63, 64
- rosette 306, 307, 308, 309, 310,
311, 313, 314
- Rostricellula 282
 R. lapworthi 286
- Rowellella 270
- Rowleyella 393
- rRNA (ribosomal RNA) 192, 193
 large nuclear-encoded, subunit
 (28S or LSU) 193
 small subunit (SSU) 193
 5S sequence 192, 193
 18S sequence 193
- rudiment,
 mantle 61
 pedicle 60
- ruga 332, 333
- Rugochonetes silleesi 293
- Rugosochonetes 414
- sac,
 coelomic 163, 184
 setal 171
- saddle,
 jugal 374
- sand,
 bryozoan 442
- saturation 199
- Saukrodictya 341
- Scacchinella 322
 S. americana 407
- scaling 213
 lophophore 112
- Scaphelasma 350
 S. mica 269
- scar,
 adjustor 369
 anterior lateral 407
 anterocentral 407
 diductor 359
 flabellate muscle 387
 muscle 75, 386, 387, 403, 404
- Schellwienella 290
- Schizambon 350, 420
- schizocoely 154, 157, 163
- schizolophe 113, 114, 115, 168,
177, 183, 375, 376, 381
- Schizophoria 335, 414
 S. iowensis 372
- Schmidites 419
- Schuchertella 309, 394
 S. lens 311
- scleroblast 12, 58, 59, 98
- Scypha ciliata 211
- Sebastolobus altivelis 211
- selection,
 particle 125
 substrate 178
- Selliathyris 269
 S. cenomanensis 305
- sensitivity 124
- septalium 370, 371, 372, 401
- septum (pl., septa),
 lateral 113
 median 370, 380, 400
- sequence,
 amino-acid 191, 192
 DNA 190
 nuclear-encoded SSU 197
 primary 245, 250, 251
 protein amino-acid 191
 repetitive 190
 repetitive nuclear 190
- serotonin 122, 126
- seta 42, 44, 50, 51, 52, 53, 54,
55, 56, 114, 115, 125, 130,
168, 169, 171, 174, 186, 272,
299, 302, 339, 341, 412
 chitinous 125
 embryonic 170
- setoblast 50, 51, 130
- settlement 125, 154, 164, 169,

- 171, 175, 179, 182, 184, 463
Sextropoma 312
 shaft 393
 sheath,
 membranous 18, 21
 pedicle 358
 sheet,
 pedicle 42
 shell 170, 185, 321
 astrophic 353
 fibrous secondary 289
 foliated secondary 289
 larval 163, 166
 primary 24, 286, 299, 318,
 334, 354, 364
 pseudopunctate 295
 punctate 295
 strophic 321, 360, 364
Siberia 364
Siboglinum fiordicum 195, 211
Sicelia 388
Sieberella 400
 S. sieberi 258
Simplicithyris 113, 467
Siphonobolus 408
Siphonotreta 344
 sipunculan 192, 201
 size,
 mitochondrial genome 190
 skeleton,
 hydrostatic 98, 113
Skenidioides 371, 388, 389, 403
 S. craigensis 390
 slot,
 periostacral 12, 14
 socket 363, 364, 366, 367, 368
 accessory 364
 cardinal 366
 dental 360
 sorting,
 particle, and rejection 119
Sowerbyella 312, 333, 339, 399,
 414, 415
 S. variabilis 292, 309
 space,
 periesophageal 100
 spawning 131, 145, 147, 155
 speciation 210
 species,
 adapted to hard substrates 452
 brooding 148
 interstitial 448
 sperm 132, 141, 145, 156, 157
 spermatid 132, 133
 spermatocyte 133
 primary 132
 secondary 132
 spermatogenesis 132
 spermatogonia 131, 132
 spermatozoa 131, 132, 133, 139,
 143, 156
 spermiogenesis 133
Sphaerirhynchia 326, 339, 340,
 417
Sphenothyris 357
 spherule 26, 29, 276
 spicule 12, 19, 58, 59, 98, 100,
 110, 380
 spine 340, 342, 343, 344, 346,
 347
 attachment 345
 clasping 346
 marginal 340
 spirillum 372, 373, 374, 375,
 376, 380
 planispiral apex of 373
Spirifer elegans 258
 spiriferid 208
Spiriferina walcotti 286
spirolophe 100, 113, 114, 184,
 186, 375, 380
Spisula solida 195, 211
 S. solidissima 195
 spondylium 391, 400
 sessile 389, 391
 spondylium,
 discretum 388
 duplex 389
 simplex 389
 triplex 391
Spondylospira 380
 S. lewesensis 380
Spyridiophora 400
 S. reticulata 404
 spyridium 400
Squalus acanthias 211
 stage,
 developmental 166
 free-swimming 171
 statocyst 125, 166, 167, 169, 170,
 171
 statolith 125
 stegidium 357, 358, 392
 stem,
 jugal 375
Stenocypris major 195, 211
Stenosarina 207
 S. crosnieri 211
Stenoscisma 403
Stethothyris 467
 stimulus 124
 stomach 84, 85, 89, 90, 91, 95,
 159, 167
 posterior 89
 stomodaemum 159, 186, 187
 strategy,
 reproductive 160, 161
 spawning and reproductive
 146
Streptorhynchus 309
 S. pelicanensis 320
Stringocephalus 376
Strongylocentrotus intermedius
 211
S. purpureus 211
Strongyloides stercoralis 211
Strophochonetes 289, 290
 S. primigenius 293
Strophomena 307, 369, 412, 413,
 414
 S. oklahomensis 290, 331
 S. planumbona 306
 strophomenid 208
 structure,
 cystose 403
 population 457
 population genetic 210
Styela plicata 211
 subclade,
 Dyscolia-Liothyrella 207
 substrate 169, 455, 456, 465
 succession,
 stratiform 267
 superstructure 15, 16
 survivorship 459
 symphytium 50, 355, 364
 synapse 106
Syntomaria 467
 S. curiosa 466
Syringospira 357, 403
Syringothyris 322, 357, 392
 S. cuspidata exoleta 394
 syrinx 392
 system,
 canal 37
 central nervous 120
 circulatory 69
 conveyor-belt 40
 current 113, 114, 120
 digestive 84, 170
 immune 146
 muscular 75, 169
 nervous 106, 121, 124, 125,
 128, 129
 pedicle 441, 442, 443, 445,
 449, 450, 456
 vascular (circulatory) 71, 130
Taimyothyris 378
taleola 305, 308, 309, 310, 312,
 364
 taxolophe 186
 tooth 32, 360, 364, 366
 regula 364
 tendon 80
Tenebrio molitor 195, 211
 tentacle 101, 102, 103, 106, 107,
 108
 ablabial (outer) 98, 106, 120
 adlabial (inner) 98, 106
 brachial 380
 filament or cirri 98
 inner (adlabial) 120
 median 159, 163, 171, 183
 tentacular canal 99, 110
 trochlophous 104

- Terebratalia 15, 16, 31, 41, 50,
52, 53, 71, 72, 80, 81, 82, 83,
103, 104, 106, 108, 110, 125,
137, 155, 156, 163, 176, 183,
206, 209, 265, 339, 444, 468,
471
T. coreanica 154, 156, 158,
165, 173, 178, 252, 253,
252, 255, 471
T. transversa 41, 64, 66, 68,
81, 88, 89, 103, 107, 108,
111, 116, 117, 120, 134,
136, 144, 153, 154, 158,
160, 163, 164, 172, 173,
174, 176, 178, 180, 182,
183, 186, 211, 215, 216,
217, 223, 224, 225, 230,
231, 232, 240, 247, 360,
397, 444, 451, 455, 461
Terebratella 68, 91, 93, 124, 139,
143, 248, 265, 467
T. dorsata 134, 445, 465, 466
T. haurakiensis 248
T. sanguinea 133, 134, 144,
159, 160, 211, 220, 229,
230, 231, 233, 248, 251,
252, 253, 255, 256, 258,
260, 261, 262, 263
T. sp. 247
terebratellid,
New Zealand 206
Terebratula 370, 372
Terebratulida 251, 252
Terebratulina 7, 15, 50, 52, 58,
59, 61, 63, 64, 65, 75, 91, 92,
93, 108, 110, 117, 125, 130,
132, 134, 135, 136, 137, 139,
146, 155, 156, 263, 265, 266,
295, 298, 312, 338, 339, 340,
355, 370, 372, 374, 375, 377,
380, 398, 452, 484, 493
T. hataiana 471
T. inconspicua 233
T. retusa 12, 59, 60, 62, 64,
101, 102, 104, 133, 134,
135, 136, 138, 142, 143,
144, 145, 147, 151, 152,
153, 154, 158, 160, 161,
164, 165, 173, 174, 175,
176, 177, 180, 181, 182,
186, 191, 211, 215, 216,
217, 218, 219, 223, 228,
229, 230, 231, 232, 234,
235, 236, 237, 238, 242,
243, 252, 253, 264, 297,
361, 379, 451, 456, 458,
459, 461, 462
T. septentrionalis 65, 148, 151,
153, 154, 155, 160, 163,
165, 173, 177, 178, 223,
224, 225, 226, 227, 228,
229, 237, 238, 444, 451,
456, 457, 458, 459, 460,
461, 463
T. sp. 158, 247
T. unguicula 116, 120, 144,
148, 151, 156, 160, 163,
165, 173, 177, 180, 224,
225, 230, 231, 232, 378,
463
T. unguis 158
testis 74, 126, 136, 138
tetanus 83
Tetralobula 391, 413
Thaumatosis 113
thecideidine 206, 208, 209
Thecidellina 19, 31, 47, 104, 113,
151, 177, 273, 276, 283, 295,
297, 313, 470
T. barretti 21, 22, 33, 50, 158,
160, 275, 314
T. blochmanni 211
T. congregata 158
T. maxilla 450
Thecidiopsis 287
Thecospira 312, 356, 380
Thecospirella 380
Thecospiropsis 380
tichorhinum 392
Ticosina 265
tissue,
connective 10, 58, 61, 62, 64,
108, 110
necrotic 145
Titanambonites 414
Tomiopsis 363
tonofibril 75
tooth 363
accessory 363
complementary, and socket 8
deltiodont 360
hinge 360
Torynelasma 269, 295, 385
transformation,
character-state 191
transmission,
matrilineal 190
track,
muscle 386, 403, 409
tree,
gene 197
maximum-likelihood 199, 202,
206
neighbor-joining 195, 197,
203, 204, 207
parsimony 197, 200, 204
phylogenetic 205
species 197
unrooted 200, 202, 203
weighted 205
Trematis 341, 347
Trematobolus 286, 352, 364, 367,
406, 409, 420, 421
T. pristinus 289
T. pristinus bicostatus 289
Tresus capax 195, 211
Tretorhynchia 300
Trichoplax adhaerens 211
trifid 395
Trimerella 366, 406, 409
Tripedalia cystophora 211
trochlophoe 101, 102, 112, 114,
115, 159, 166, 170, 183, 187,
188, 376
trophocyte 74, 145
Tropidoleptus 380
T. carinatus 382
Trypetasa lampas 195
tubercle 19, 283, 305, 307, 308,
311, 312, 313, 314, 340, 342
turratellid 251, 252
Typetasa lampas 211
Tythothyris 467
Ulophysema oeresundense 195,
211
umbo 166, 323, 355, 366, 372
Uncinulus 415, 417
Uncites 319
Ungula 277, 407
U. ingrica 279
unifid 395
unit,
isotopic 268
uptake,
oxygen 116
Valcourea 356
Valdiviathyris 499
V.?: 500
V. quenstedti 500
valve 321
variation,
intraspecific 448
vascula,
genitalia 12, 71, 75, 127, 130,
131, 135, 145, 391, 411,
412, 413, 414, 417
lateralia 70, 407, 417, 418,
419, 420
media 70, 71, 75, 128, 391,
411, 412, 413, 414, 417,
418, 419, 420, 421, 422
myaria 383, 411, 412, 413,
414, 417
ventilation 98
vesicle,
germinal 154
vessel,
blood 69, 71, 72, 89, 110,

- 111, 137, 139, 144
- tentacular blood (channel) 77,
110, 111
- Vex? 266
- vicariance 472
- Victorithyris 467, 472
- Viligothyris 378
- vitellogenesis 136, 137, 145
 - follicular 137
 - mixed 139, 147
 - nutritive 137, 147
- Vitiliprductus 334
- Waiparia 467
- wall,
 - anterior body 7
 - body 367, 368, 383
 - posterior body 41, 44, 60, 359
- waste,
 - metabolic 174
- Xenopus laevis 211
- Xystostrophia 334
 - X. umbulacrum 335
- yolk 131, 143
- Zhanatella 418, 419
- zone,
 - collagenous 12
- zonulae adhaerens 83, 107
- zygophe 115
- zygote 157